Veterinary Diagnostic Imaging

THE HORSE

Charles S. Farrow







MOSBY
ELSEVIER

MOSBY
ELSEVIER

11830 Westline Industrial Drive
St. Louis, Missouri 63146

VETERINARY DIAGNOSTIC IMAGING: THE HORSE
ISBN 13 978-0-323-01206-5
ISBN 10 0-323-01206-X
Copyright © 2006, Mosby Inc.

All rights reserved. No part of this publication may be reproduced or transmitted in any form or by any means, electronic or mechanical, including photocopying, recording, or any information storage and retrieval system, without permission in writing from the publisher. Permissions may be sought directly from Elsevier's Health Sciences Rights Department in Philadelphia, PA, USA: phone: (+1) 215 239 3804, fax: (+1) 215 239 3805, e-mail: healthpermissions@elsevier.com. You may also complete your request on-line via the Elsevier homepage (http://www.elsevier.com), by selecting 'Customer Support' and then 'Obtaining Permissions.'

NOTICE

Knowledge and best practice in this field are constantly changing. As new research and experience broaden our knowledge, changes in practice, treatment, and drug therapy may become necessary or appropriate. Readers are advised to check the most current information provided (i) on procedures featured or (ii) by the manufacturer of each product to be administered, to verify the recommended dose or formula, the method and duration of administration, and contraindications. It is the responsibility of the practitioner, relying on their own experience and knowledge of the patient, to make diagnoses, to determine dosages and the best treatment for each individual patient, and to take all appropriate safety precautions. To the fullest extent of the law, neither the Publisher nor the Editor/Authors assumes any liability for any injury and/or damage to persons or property arising out of or related to any use of the material contained in this book.

International Standard Book Number 0-323-01206-X

Publishing Director: Linda Duncan
Acquisitions Editor: Liz Fathman
Senior Developmental Editor: Jolynn Gower
Publishing Services Manager: Pat Joiner
Senior Project Manager: Rachel E. Dowell
Designer: Amy Buxton

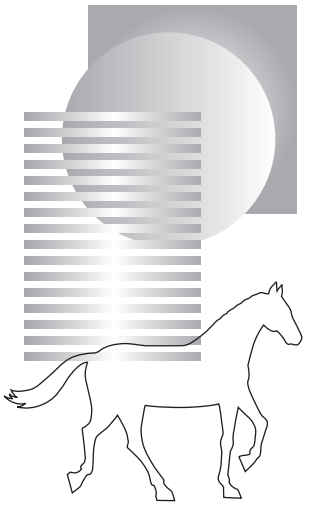
Printed in the United States of America
Last digit is the print number: 9 8 7 6 5 4 3 2 1

Working together to grow
libraries in developing countries
www.elsevier.com | www.bookaid.org | www.sabre.org
ELSEVIER BOOK AID International Sabre Foundation

To Col. Robert Morgan, USAFR, Ret. (1918–2004)
Pilot of the *Memphis Belle* and the *Dauntless Dotty*—
a true American hero.



About This Book



Successful diagnostic medical imaging, equine and otherwise, depends on 2 things: *image quality* and *diagnostic ability.* It is the latter skill that I hope to enhance with this book.

DIAGNOSTIC SUCCESS BEGINS WITH A QUALITY IMAGE

Image quality has been defined in a variety of ways, but can be distilled down to two essential ingredients, *contrast* and *clarity. Contrast* means that a portion of a particular image differs sufficiently from its background that it can be recognized as such. Without contrast a lesion remains camouflaged, defying detection. But contrast alone is not enough. A lesion must also possess sufficient *clarity* of size, shape, position, and density—so-called *disease indicators*—to be recognized or looked up subsequently in an appropriate reference source.

NOVICE VERSUS EXPERT STRATEGIES

Novices are rightfully taught to carefully scrutinize each and every medical image without bias or expectation and then to render a diagnosis based on probability. Experienced medical imagists, on the other hand, typically employ a more efficient *where and what* approach to film reading, a form of intuitive diagnosis common to most medical specialties. Using the where and what stratagem, the experienced film reader considers the historical and clinical features of a particular case, and then, based on past experience, looks first at one or more high-yield areas of the image for specific disease indicators. Of course the entire film will eventually be examined thoroughly, but it is the initial directed search that distinguishes the experienced from the inexperienced. It is this latter expert skill, use of the where and what approach, that I hope to impart to the readers of this book.

To further augment the reference value of this text, I have included contextual normals, numerous anatomical specimens, a wide spectrum of disease variation and degree of involvement, and a generous number of combined orientation and close-up views.

CONTEXTUAL NORMALS AND ANATOMIC SPECIMENS

Colleagues and students alike have told me repeatedly that normal radiographs are the most useful when displayed next to or nearby case example. On consideration, this makes perfect sense, given the subtleties of radiographic diagnosis, the anatomic nature of medical imaging, and the inherently comparative nature of the diagnostic process.

Over the years I have accumulated a number of anatomic specimens, bones and dried tendons for the most part, which I have used countless times while trying to figure out one radiographic problem or another. I have photographed these specimens and added them to the most appropriate portions of the text, where I believe they should prove most useful.

FULL DISEASE SPECTRUMS AND ORIENTATION/DETAIL CASE EXAMPLES

As in *Volume I, The Dog and Cat,* I have done my utmost to provide as many examples of each disease as possible, ranging from the barely perceptible to the obviously diseased, eschewing the more traditional approach of simply displaying one or two classics. Although of undeniable teaching value, classic examples are seen only occasionally, with less fully featured cases being the rule.

Likewise I incorporated a combination of orientation and close-up views for as many cases as possible in ensure that the reader fully appreciates the nuances of each lesion, seemingly small features that often pay big diagnostic dividends.

ORGANIZATION AND CREDIT

Organization

This textbook on equine medical imaging is organized in a traditional anatomic fashion. There are 7 sections: (1) Extremities, (2) Skull, Face, Jaws, and Cranium, (3) Throat and Neck, (4) Spine, (5) Thorax, (6) Hear, and (7) Abdomen. Within these sections are 44 individual chapters covering not only various body regions but important related subjects as well. For example, in the extremital section there is a chapter on maturity, immaturity, and dysmaturity, to include a discussion on the limitations and necessity of radiometrics. Another chapter in the same section deals with fracture healing and bone remodeling.

I have also attempted to introduce the concept of anatomic-radiologic correlation by beginning many chapters with a brief list of *anatomic facts*. Hopefully, these condensed info-packets will serve both to whet the reader's intellectual appetite and provide an anatomic framework on which to consider the related clinical material.

Credit

As with the initial volume in this series, *The Dog and Cat,* I have done my utmost to fully credit those whose original observations comprise the fabric of this work. Specifically, I have acknowledged these individuals both contextually and at the conclusion of each chapter so that the reader may fully appreciate their important contributions to the field of medical imaging. My apologies if I have inadvertently omitted anyone.

Charles S. Farrow

Acknowledgments

As with any project of this size, much effort is required by a large number of people. However, among this company are two exceptional individuals worthy of special recognition: Jolynn Gower, Senior Development Editor, and Rachel Dowell, Senior Project Manager. A writer couldn't hope for two more competent or understanding collaborators.

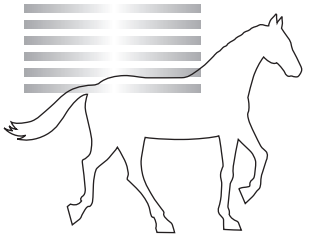
I asked Jolynn and Rachel for pictures of themselves, believing this would be a fitting tribute, but in their modesty they declined. Instead, they suggested I use a photograph of an animal, which I hope they find satisfactory.

Charles S. Farrow



SECTION I

The Extremities



Chapter 1

Skeletal Maturity, Immaturity, and Dysmaturity

NEWBORN VERSUS ADULT BONES

The bones of the newborn foal differ dramatically from those of the adult horse. Specifically, they are smaller, smoother, and generally rounder (Figure 1-1). Many are composed of multiple parts, the result of as yet unfused, secondary growth centers (Figure 1-2). Seen radiographically, the joint spaces of foals—in reality composed mostly of cartilage—appear disproportionately wide compared with those of adults (Figure 1-3). The outer perimeter of some secondary growth centers appears abnormally roughened and in places incomplete, falsely suggesting infection or osteochondritis (Figure 1-4). Some bones, as yet unossified, are invisible altogether.

Growth Plates, Cutback Zones, and Tubulation

A long bone (and some short bones) grows longitudinally from either end, although not always equally. Cartilaginous growth plates, or *physes,* continuously produce the new bone required for axial development: first as a living and later as dead, cartilaginous scaffolding; then as an area of disorganized, roughened new bone; and finally as a structurally refined cortex and medulla—a process that continues until maturation is complete.

The metaphysis of an immature long bone can appear quite rough and irregular compared with the adjacent shaft (Figure 1-5), inviting misdiagnoses such as fracture, infection, or osteochondritis. Such concern is usually unwarranted, however, as a comparison image of the opposite metaphysis will readily reveal. This temporarily roughened area is termed the *cutback zone*, or simply, the *cutback.*

The cutback zone is the place in the bone, situated on the metaphyseal side of the growth plate between the shaft and the epiphyses, where the bone changes from wide and rough to smooth and narrow, an organizational process termed *tubulation* (Figure 1-6). Cutback zones are for the most part quite variable but typically are most pronounced during the first few months of skeletal development.

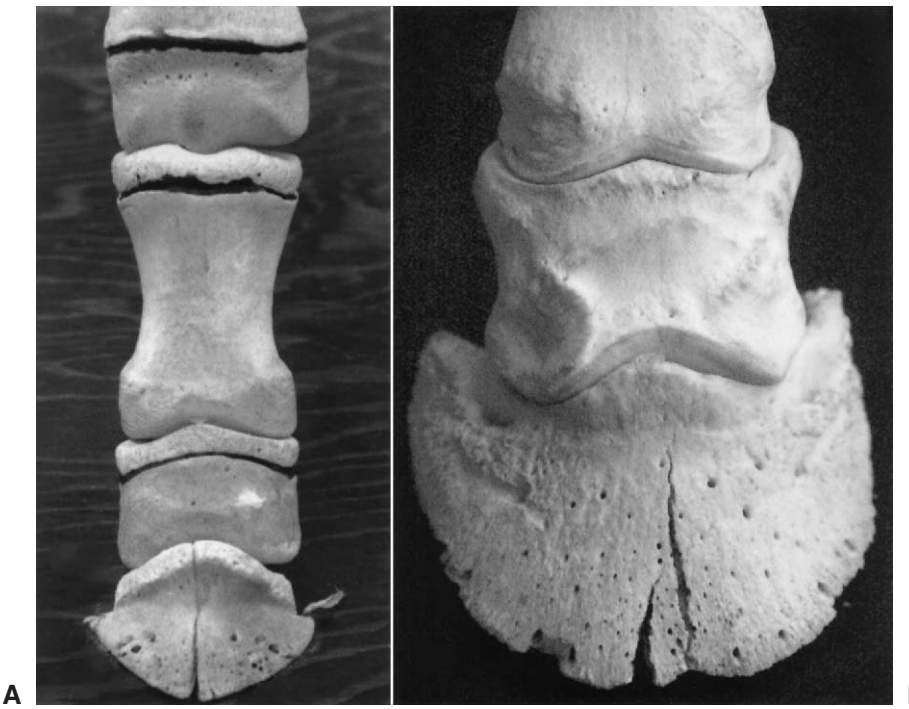


Figure 1-1 • Bones of a young foal's distal forelimb **(A)** compared with those of an adult horse **(B).** The bones of the foal are smaller, smoother, and rounder than those of an adult and contain numerous unfused epiphyses and open growth plates (simulated with black acrylic). Specimen preparation resulted in distal phalangeal splitting.



Figure 1-2 • Bones of a young foal's stifle as seen in lateral **(A)** and frontal **(B)** perspectives show separate ossification centers for the (1) distal femoral epiphysis, (2) proximal tibial epiphysis, and (3) tibial tuberosity. Growth plates are simulated with black acrylic.

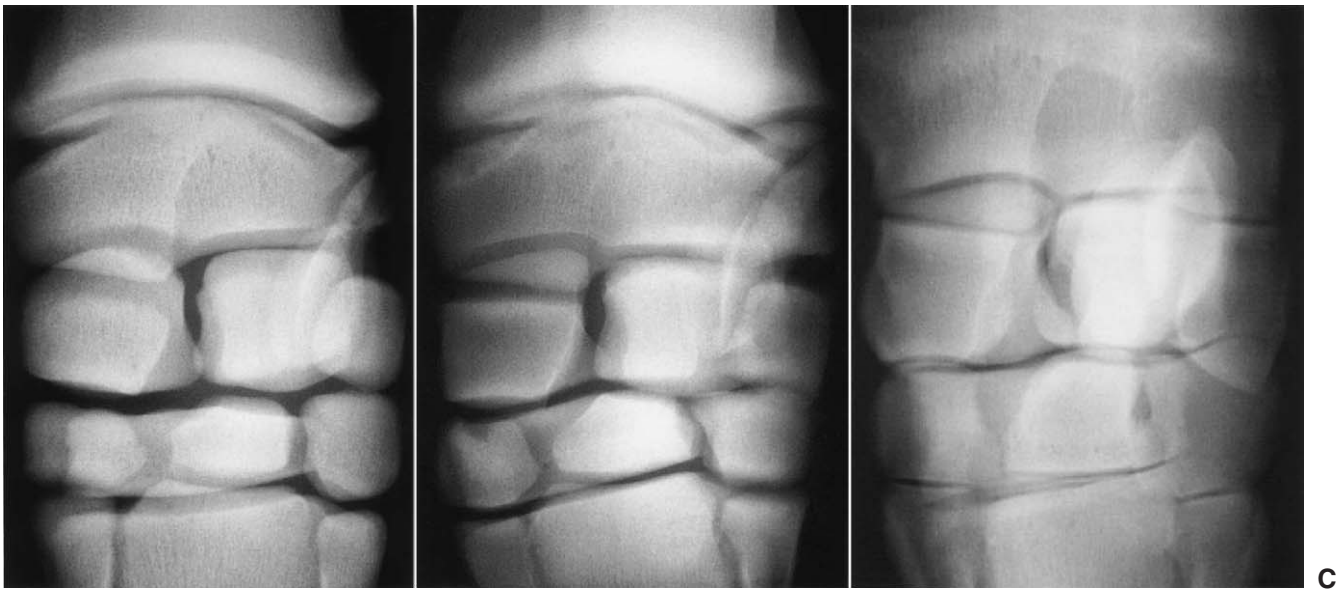


Figure 1-3 • Comparative differences in carpal cartilage spaces as a function of age: newborn foal **(A),** 2-month-old foal **(B),** and adult horse **(C).**

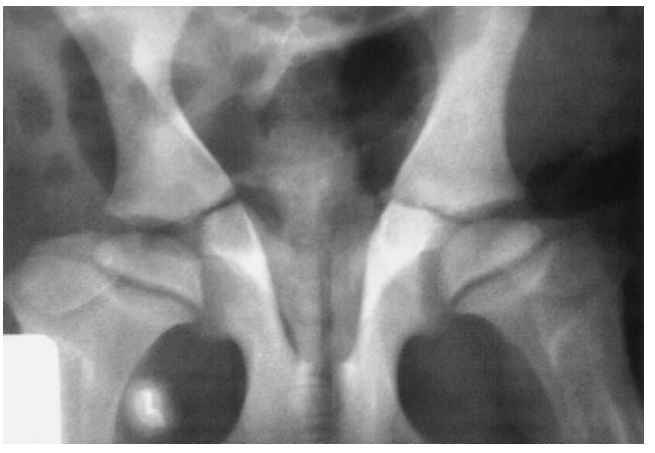


Figure 1-4 • Close-up ventrodorsal view of the hips of a young foal show typically roughened femoral head and greater trochanter bilaterally, a normal variant in immature horses.



Figure 1-5 • Close-up view of the distal tibia of a foal shows roughing and flaring on the metaphyseal side of the growth plate, a normal but temporary finding termed the *cutback zone.*

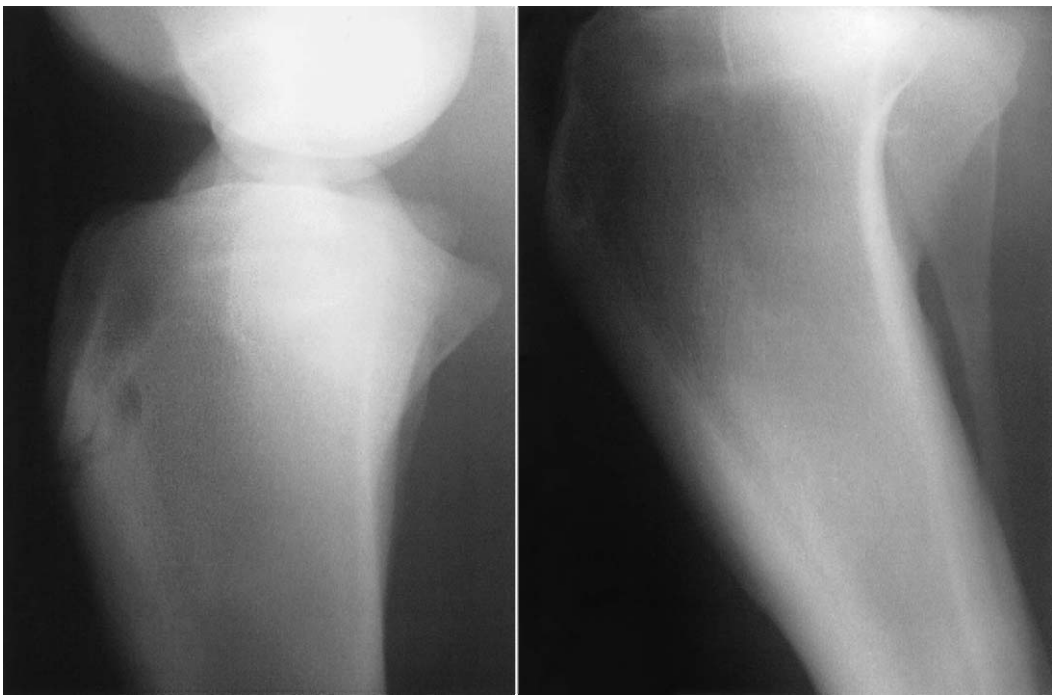


Figure 1-6 • Close-up, lateral views of the proximal tibial growth plate before **(A)** and after **(B)** closure showing the process of long bone tubulation, a process by which a roughened, structurally undifferentiated metaphysis smoothes, narrows, and eventually develops a discrete cortex and medulla.

Separate Ossification Centers (Secondary, Accessory Growth Centers)

Appearance and Disappearance. Most secondary ossification centers are radiographically evident at birth and then gradually disappear as they become incorporated into the parent bone, a process termed *fusion*. From a practical perspective, the presence (or absence) of separate ossification centers enables one to estimate the age of an immature horse (assuming the precise date of birth is not known).

Smallwood and colleagues described the xeroradiographic appearance of the growth plates of the distal forelimb of the foal from birth to 6 months of age (Table 1-1).[1] In a companion article, Metcalf and coworkers described the scintigraphic appearance of the distal forelimb growth plates over the same period of development, with the aim of establishing normal comparisons.[2]

Because hard, highly concussive-type running and jumping can potentially injure growth plates, or more specifically their circulation, most trainers eschew such training until certain *sentinel growth plates*, most often those found in the distal radii, have fully closed (Figure 1-7).

Because of their relatively weak cartilaginous attachment, accessory growth centers are subject to avulsion-type fractures, injuries that in some instances may be so subtle that only a comparison radiograph of the opposite leg will confirm their existence.

Table 1–1 • XEROGRAPHICALLY OBSERVED APPEARANCE AND DISAPPEARANCE OF DISTAL FORELIMB GROWTH PLATES IN FOALS FROM BIRTH TO 6 MONTHS OF AGE

First radiographic appearance of distal epiphyseal ossification in metacarpal 2 and metacarpal 4 (extremely variable)	4-38 wk
First radiographic appearance of the crena	4-22 wk
Closure of the proximal growth plate of P2	18-30 wk
Closure of the proximal growth plate of P1	22-38 wk
Closure of the distal growth plate of MC3	18-38 wk

Ossification Fronts. Growth of the normal epiphyses is outward, increasing in volume while preserving shape. Epiphyseal ossification follows suit but in a somewhat uneven, random fashion. The result is that for a few weeks during early development, the condylar-type epiphyses, such as those found on the proximal and distal humerus and distal femur, may assume a distinctive, serrated appearance that resembles some forms of osteochondritis and osteomyelitis (Figure 1-8). Adams and Thilstead illustrated this phenomenon in their description of the radiographic appearance of the developing equine stifle from birth to 6 months of age.[3]

This is a normal, transient variation, typically found bilaterally, and termed an *ossification front*. Where

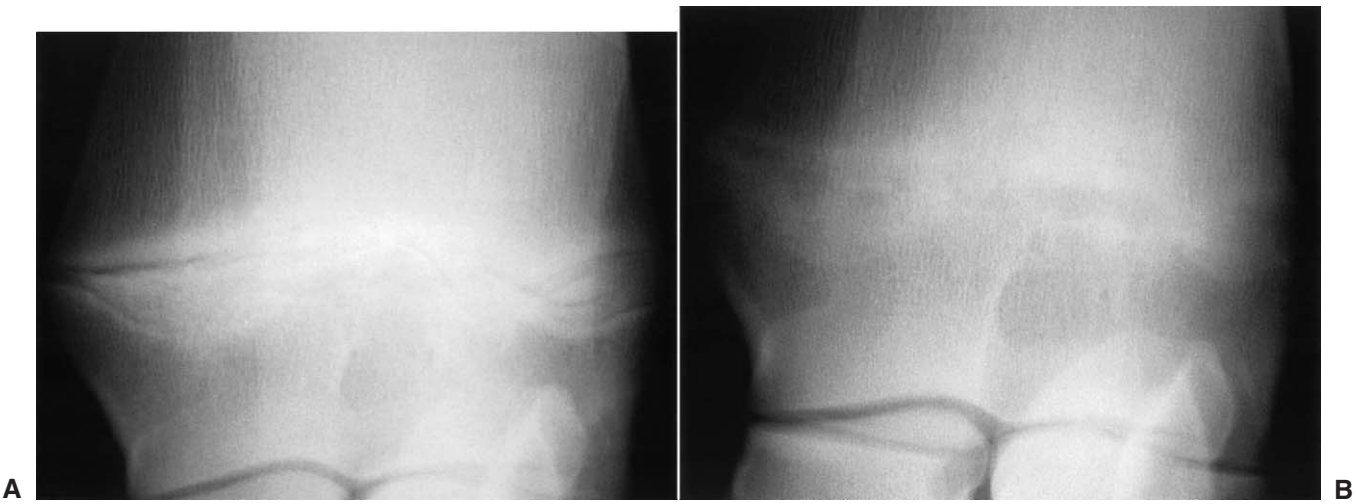


Figure 1-7 • Close-up, fully open **(A)** and nearly closed **(B)** distal radial growth plates.

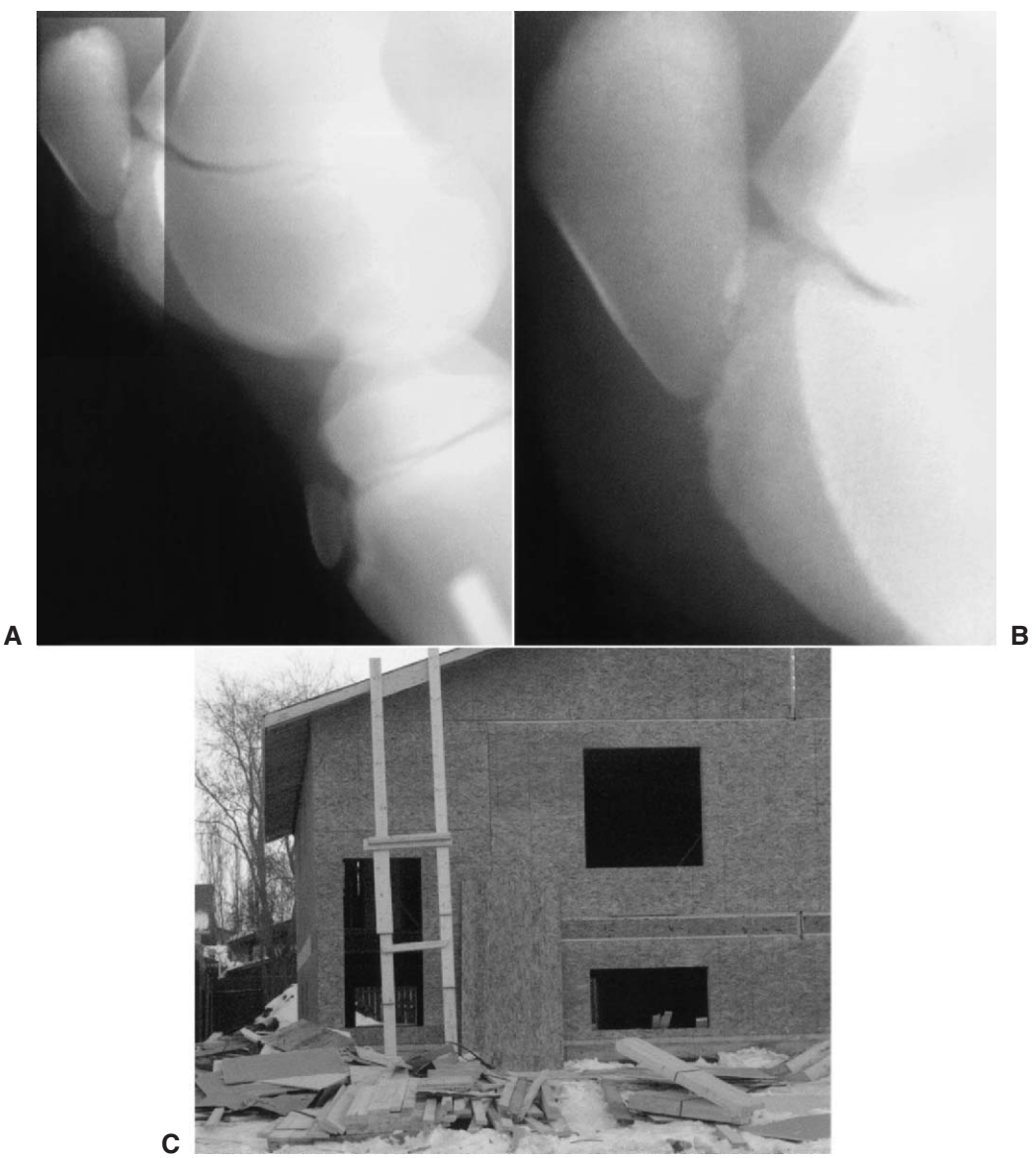


Figure 1-8 • Lateral **(A)** and lateral close-up **(B)** views of a foal stifle show distinctive serration of the proximal edge of the medial trochlear ridge *(emphasis zone),* a normal developmental phenomenon termed an *ossification front,* which can be likened to the foundation of a construction project **(C)** insofar as it will eventually be cleaned up.



Figure 1-9 • Close-up view of a foal's coxal joint shows an epiphysis, the femoral head, and an apophysis, the greater trochanter, both of which are currently unfused.

diagnostic uncertainty exists, a 2- to 4-week progress check usually reveals a more uniform bone density and smoothing of the perimeter. Examination of the contralateral limb can be of some value but is not foolproof because osteochondritis is often bilateral, whereas hematogenous osteomyelitis may or may not be.

▮▮▮ EPIPHYSEAL AND APOPHYSEAL DEVELOPMENT

Epiphysis

The normal development of most epiphyses (Figure 1-9, *A*) depends on a number of factors, but none is more important than their relationship to the opposing joint surface. To develop properly, an epiphysis must be regularly and intermittently *compressed* by the opposing epiphysis, ensuring adequate synovial perfusion of the articular cartilage, which also functions as a template for epiphyseal growth. If not adequately compressed, an epiphysis will become stunted and deformed.

Apophysis

An apophysis (Figure 1-9, *B*), on the other hand, depends on intermittent *traction,* not on compression as with epiphyses. If traction is insufficient, as with a displaced apophyseal fracture or tendon severance, the apophysis will not develop fully but will appear small and rounded compared with the normal opposite side.

Consequences of Abnormal Epiphyseal or Apophyseal Development

Hypoplastic, deformed epiphyses or apophyses may or may not lead to pain and disability. Factors that affect the outcome of such injuries include the following:

- When in the development of a particular bone and joint the injury occurs
- The magnitude and duration of the injury
- Success or failure of attempted repair (if any)
- Accommodation and adaptation by the other elements of the injured joint (including associated soft tissues such as muscle, tendon, and ligaments)
- Whether or not arthritis develops

Epiphyseal Closure

Myers and Emmerson radiographically monitored the growth plates of two Arabian foals, a colt and a filly, from birth to 3 years of age; their graphic results were published in *Veterinary Radiology*.[4] Surprisingly, relatively few such studies have been performed, especially considering the recent emphasis on equine sports medicine, the equine "athlete," and the well-publicized adverse effects of premature sprint and endurance training on the immature equine skeleton.

Epiphysitis

The term *epiphysitis* is often ambiguous and sometimes misleading. Brown and MacCallum declared it a misnomer, saying that it implied *epiphyseal* rather than *growth plate* inflammation.[5] Rooney contends that epiphyseal compression resulting in injury to the metaphyseal vasculature is likely an important factor in the development of epiphysitis. Hintz and Schryver suggest a nutritional link, whereas Fretz and others have focused on thyroid dysfunction.[6]

Radiologic Findings. Sherrod described the badly deformed hind fetlock joints of a 3-month-old Arabian foal with epiphysitis as resembling an hourglass because of the large amount of new bone surrounding the distal metatarsal growth plate.[7] Figure 1-10 shows three cases of such a deformity.

▮▮▮ RADIOLOGIC ESTIMATION OF LONG-BONE GROWTH

Campbell and Lee described an experimental method for radiographically estimating the growth rate of long bones in foals.[8] In this technique, small-diameter Steinmann pins are inserted into the midshaft of the

long bones being studied (cortex to cortex); these pins serve as radio-opaque markers. The foals used in the study were then periodically radiographed until skeletal development was complete. Bone length was compared with pin position to determine the relative contribution made by the growth plates at either end. The broader purpose of the study was to determine the optimal age for the surgical correction of debilitating limb deformities.

Long-bone growth in ponies was similar to that described in other farm animals, with the exception of the femur. No growth spurts or lags were observed. The relative contributions to bone length made by the proximal and distal epiphyses for the long bones studied are listed in Table 1-2.

▮▮▮ CONCEPTS OF THE CARTILAGE SPACE AND TEMPORARY VOLUME LOSS

The radiographically transparent area between two or more articulating bones (Figure 1-11) is simplistically termed the *joint space,* but in reality it is far more than a mere void. This so-called joint space is actually filled almost entirely with articular cartilage, leaving room for only a thin film of intervening synovial fluid in a living animal. Even a prepared teaching specimen reveals only a small volume of synovial fluid separating a comparatively large amount of articular cartilage (Figure 1-12).

Recognition of the fact that joint spaces are probably better conceived of as *cartilage spaces* is both diagnostically and prognostically useful. For example, if in the radiographic examination of a lame horse one or more joint spaces appear narrowed and no additional bony abnormalities are present, the most probable explanation is that the articular cartilage in question has undergone a *temporary volume loss* related to the animal's lameness rather than actual destruction (Figure 1-13). In most instances, a subsequent return to normal once the lameness has resolved will confirm the highly labile nature of the cartilage space.

Conversely, if a joint space appears widened, especially in a young foal, fluid distension secondary to an infection is more likely (Figure 1-14). In older foals, additional possible explanations are warranted, including traumatic dislocation, posttraumatic hemarthrosis, and synovitis secondary to fragmenting osteochondritis.

▮▮▮ PREMATURITY, IMMATURITY, "DYSMATURITY": ARE THEY READILY DISTINGUISHABLE CONDITIONS?

Differentiating the bones of a premature, immature, and "dysmature" foal may be difficult or impossible because of their many radiographic similarities. For example, the bones of a premature foal are small, rounded, sometimes tapered, and often roughly marginated, but so are those of an immature foal; the major difference between the two is that the premature foal has had insufficient time to develop, whereas the immature individual did not develop in sufficient time.

The bones of the "dysmature" foal, presumably full term, also appear underdeveloped in a manner similar to that described in the premature and immature foals. However, in some instances, foals with *hyperplastic goiter,* for example, the carpal bones may be composed almost entirely of cartilage, with only a few spicules of centrally located bone representing the normally well-ossified nucleus.[9]

A Simplified Diagnostic Strategy

How then can premature, immature, and "dysmature" foals be distinguished from one another radiographically? My suggestion is first to simplify the selection process by eliminating one of the alternatives: dysmaturity. At best, the term is ambiguous, and at worst, it lacks widespread medical acceptance.

Next assess the part or parts in question. Take the carpus, for example. Are the individual carpal bones normal in size, shape, contour, density, and position? Is the distal radial growth plate abnormal? Is there abnormal curvature? Is the opposite carpus affected? And, most important, when was the mare bred?

Prematurity. If a foal was born prematurely and the carpal bones appear radiographically abnormal, my recommendation is initially to attribute their appearance to incomplete skeletal development resulting from prematurity.

Immaturity. If the foal was carried to full term and the carpal bones appear radiographically abnormal, their appearance can be attributed to immaturity resulting from a specific cause, if known; otherwise, their appearance can be attributed to immaturity (cause or causes unknown).

Bones of the Immature Carpus and Tarsus. Key radiographic features of carpal or tarsal bone immaturity include the following:

- Diminished size relative to a normal foal of comparable age
- Rounded versus normally squared corners
- Abnormally tapered profile
- Increased number of visible vascular canals causing increased porosity
- One or more fringed margins
- Perimeter defects
- Diminished size
- Fragmentation, extrusion, or overt fracture

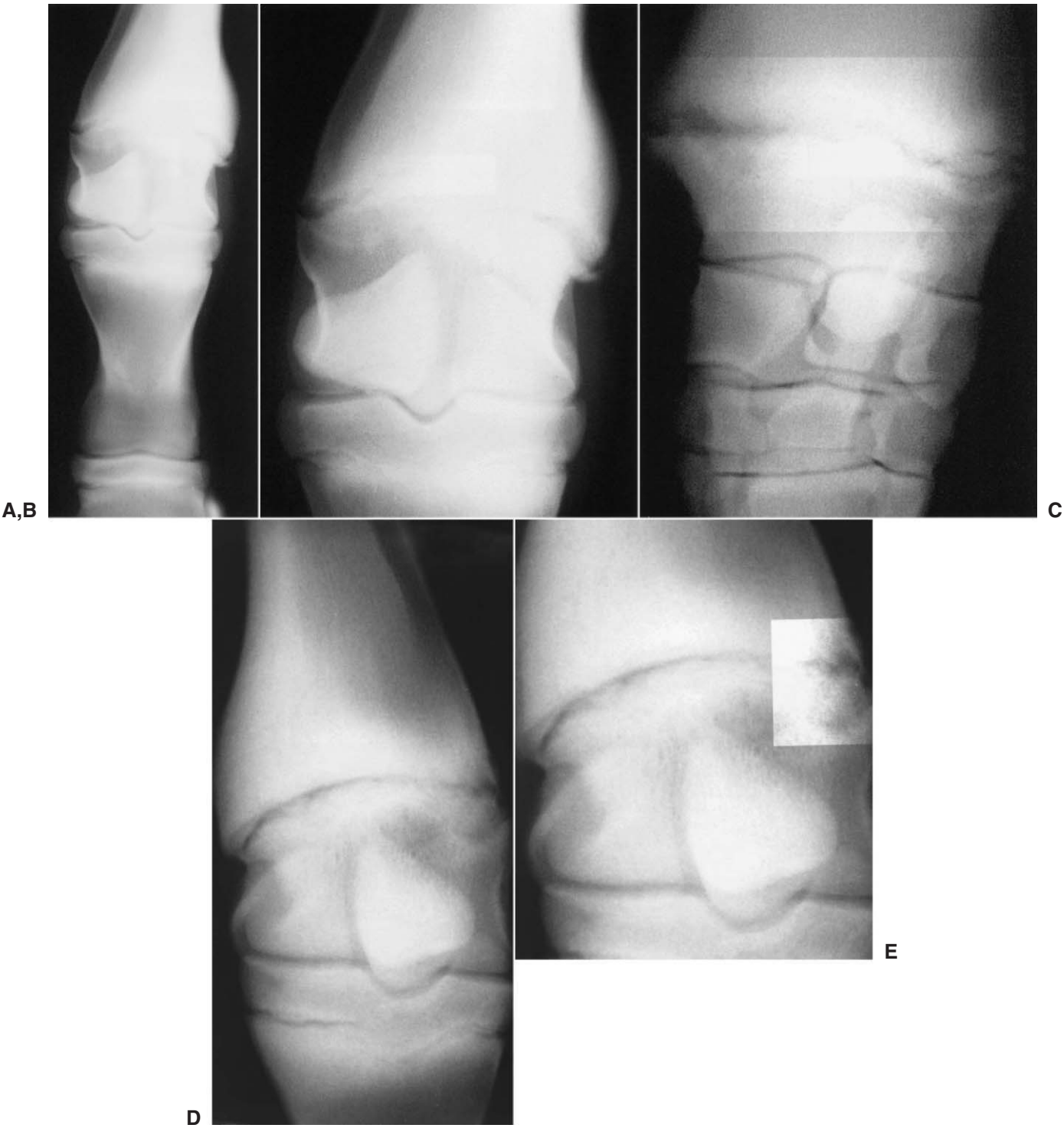


Figure 1-10 • Epiphysitis (three cases). Case 1: Orientation **(A)** and close-up dorsoplantar **(B)** views of the fetlock of young colt with epiphysitis show an hourglass shape as described by Sherrod (see text for details). Case 2: Close-up craniocaudal view of abnormally flared distal radial metaphysis **(C),** caused by epiphysitis. Case 3: Orientation **(D)** and close-up **(E)** views of the fetlock of a 6-month-old colt with epiphysitis.



Figure 1-11 • So-called pastern and coffin "joint spaces," seen in this close-up lateral radiograph as thick translucent bands situated between bone ends, are in fact composed mostly of cartilage, not space.

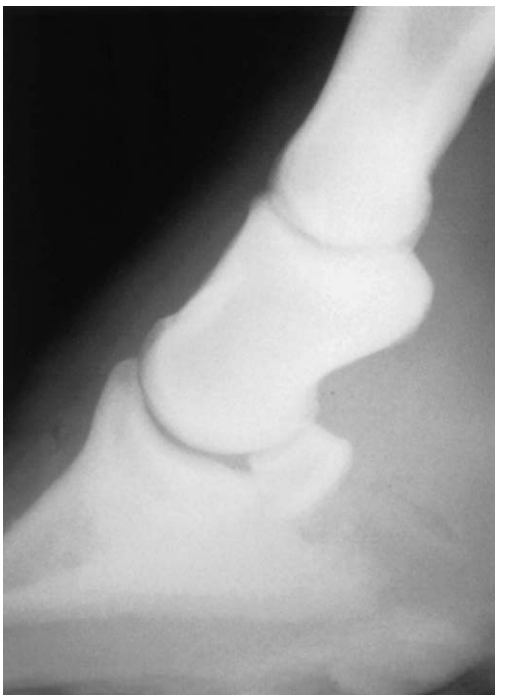


Figure 1-13 • Lateral view of equine foot shows *temporary* narrowing of the pastern and coffin joints resulting from disuse following a sole abscess.

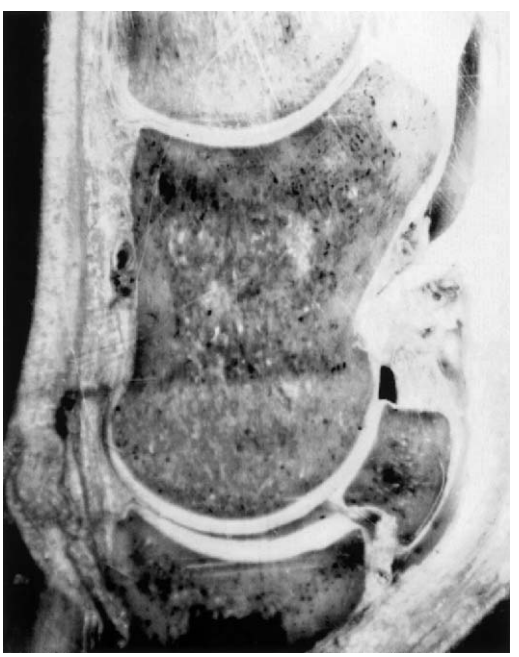


Figure 1-12 • Midsagittal section of the pastern and coffin joints of an adult horse (lateral perspective) shows clearly that most of the joint is composed of articular cartilage with comparatively little intervening space.



Figure 1-14 • Dorsopalmar view of the foot of a horse shows asymmetric widening of the distal interphalangeal joint caused by infection.

Table 1–2 • RELATIVE CONTRIBUTIONS OF PROXIMAL AND DISTAL EPIPHYSES TO LONG BONE LENGTH

	Proximal Growth Plate (%)	Distal Growth Plate (%)
Humerus	75	25
Radius	37	63
Femur	55	45
Tibia	55	45

- Poor calcification
- Abnormal attitude or position

Many of these radiographic features are exemplified in Figures 1-15 to 1-17.

Skeletal Ossification Index. Adams and Thilstead proposed a radiographic classification for evaluating the carpi and tarsi of newborn foals (defined as 2 weeks old or younger), terming it a *skeletal ossification index*.[3] The scheme contains four categories or grades, three of which are used to describe abnormal-appearing carpal and tarsal bones and one to describe the norm (Table 1-3).

Radiographic and Sonographic Monitoring of Tarsal Ossification in Immature Foals. Ruohoniemi and coworkers reported the use of ultrasound and radiography to monitor the progress of tarsal ossification in three premature foals (foals with a gestation period of 320 days or less).[10] Clearly, radiography is the superior method of imaging the tarsal interior, with sonography providing little more than a glimpse of the accessible surface contours, which in immature foals appear uneven owing to the mix of cartilage and bone.

Prognosis for Foals Born With Incompletely Ossified Tarsal Bones. As mentioned elsewhere, my experience with foals born with incompletely ossified tarsal bones is that they often resemble a severe case of bone spavin by the time they become skeletally mature. Some are sound, but most are not. I have yet to see a legitimate racehorse with this condition, so I cannot comment on how well they compete. I have seen adult Mexican mules with this problem that apparently serve as effective pack animals.

Dutton and co-workers studied 22 immature foals with incomplete ossification of their tarsal bones, not surprisingly concluding that those foals with overt collapse of the third tarsal bone had a poorer prognosis than those that did not.[11] They divided their radiographic material into two groups—types I and II according to lesion severity, with particular emphasis on the degree of mineral deficiency and the presence and amount of third tarsal bone collapse (less than or greater than 30%). This scheme appears too broad and imprecise to warrant numeric description, which implies quantitative rather than qualitative assessment, and it would better (and more simply) be described as mild, moderate, or severe.

▮▮▮ ABNORMAL LIMB CURVATURE AND ANGULATION (ANGULAR LIMB DEFORMITY)

Valgus Versus Varus

The terms *valgus* and *varus* have been the subject of literary debate and frequent fodder for letters to the editor.[12] A valgus deformity is one in which the *interior angle* of the joint, as viewed frontally, is *greater than 180 degrees* (Figure 1-18). Conversely, a varus deformity is one in which the *interior angle*, viewed frontally, is *less than 180 degrees* (Figure 1-19). Horse owners often refer to these conditions simply as *bowlegged* (carpi bent inwardly) and *knock-kneed* (carpi bent outwardly). The colloquial term for combined valgus and varus deformities is *windswept* (Figure 1-20).

Axial Rotation: The Overlooked Consideration

Little or no attention has been directed to the problem of axial rotation as it pertains to foals with angular limb deformities, although nearly all foals with carpal valgus also have outward angular rotation. One means of estimating the amount of axial rotation in the carpus and metacarpus is to compare the relative positions of the third metacarpal nutrient foramen as seen in the combined and individual carpal views (Figure 1-21). A more immediate but less accurate assessment is possible by merely observing the amount of carpal misalignment in the combined view because this projection is standardized to the midsagittal plane of the animal's torso, whereas the individual frontal views are only rough estimates.

▮▮▮ LIMITATIONS AND NECESSITY OF DIAGNOSTIC RADIOMETRICS

Intersecting Lines to Determine the Source of Carpal Angulation: Are They Necessary?

In my opinion, the use of intersecting lines to establish "fault" in foals with angular limb deformities is unnecessary and, worse, smacks of pseudoscience. The term *pivot point*, used to describe the place in the bone or joint where the radial and metacarpal midlines intersect, is also misleading because it falsely implies the use of biomechanics.[13]

In most cases, merely examining a 7-×-17 craniocaudal view of the affected leg, centered on the carpus,



Figure 1-15 • One-month-old foal with a carpus of an animal half its age. Lateral close-up **(A)** and ultra-close-up **(B)** views of immature carpus show severe fringeing of proximal and caudoventral margins of third carpal bone. Craniocaudal close-up **(C)** and ultra-close-up **(D)** views show an undersized styloid and increased porosity and rounding of the carpal bones.

is usually sufficient to incriminate either the distal radius or carpal bones or, alternatively, the associated soft tissues. Where there is uncertainty regarding the source of angulation based on conventional film viewing, holding the radiograph horizontally, just below eye level, offers a different perspective that may prove diagnostic.[14]

Carpal Radiometrics, Postural Variation, and Patience

In my experience, carpal radiometrics are often inaccurate. The problem as I see it is that foals assume a wide variety of postures while being radiographed, especially when being forcefully restrained. It therefore follows that the degree of carpal angulation must also vary, and accordingly single radiographs may overestimate or underestimate the mean angulation, sometimes by 50% or more.

Given the physical difficulty in restraining most foals (and often their mothers), making a large series of carpal images to ensure a representative sample from which to measure is probably impractical; however, there is an alternative solution: Do not immediately start handling the foal, but instead observe it closely, especially the way it prefers to stand. When the

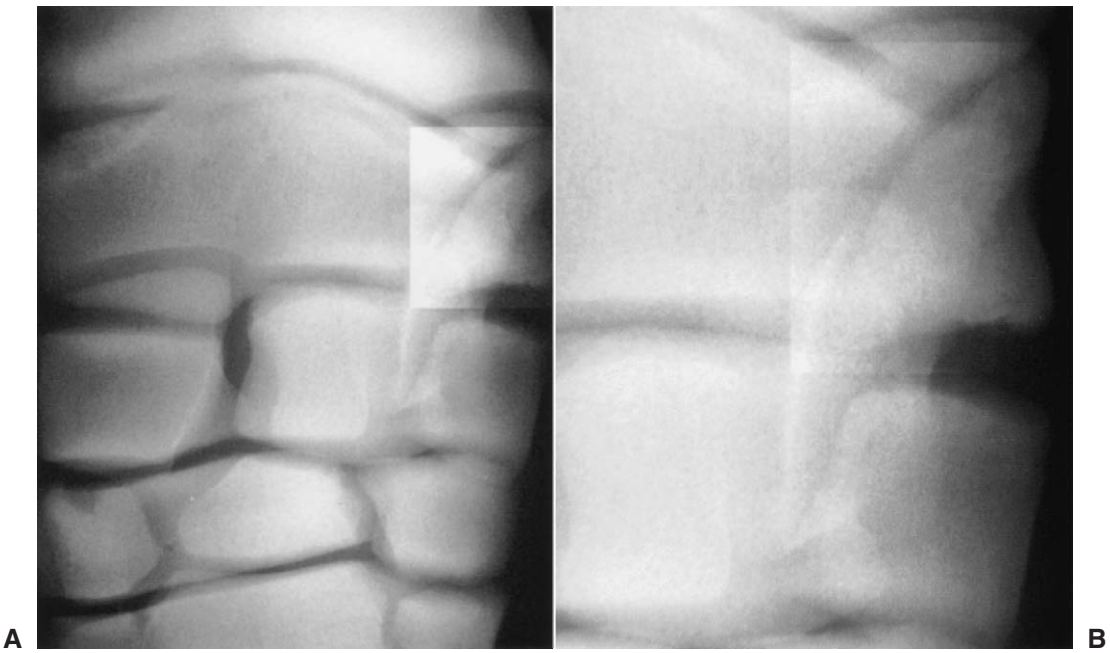


Figure 1-16 • Close-up craniocaudal **(A)** and ultra-close-up **(B)** views of the carpus of a normal 52-day-old foal show the styloid process (vestigial distal ulna) as a separate ossification center, which will eventually fuse with the adjacent physis, completing the formation of the distal radius.

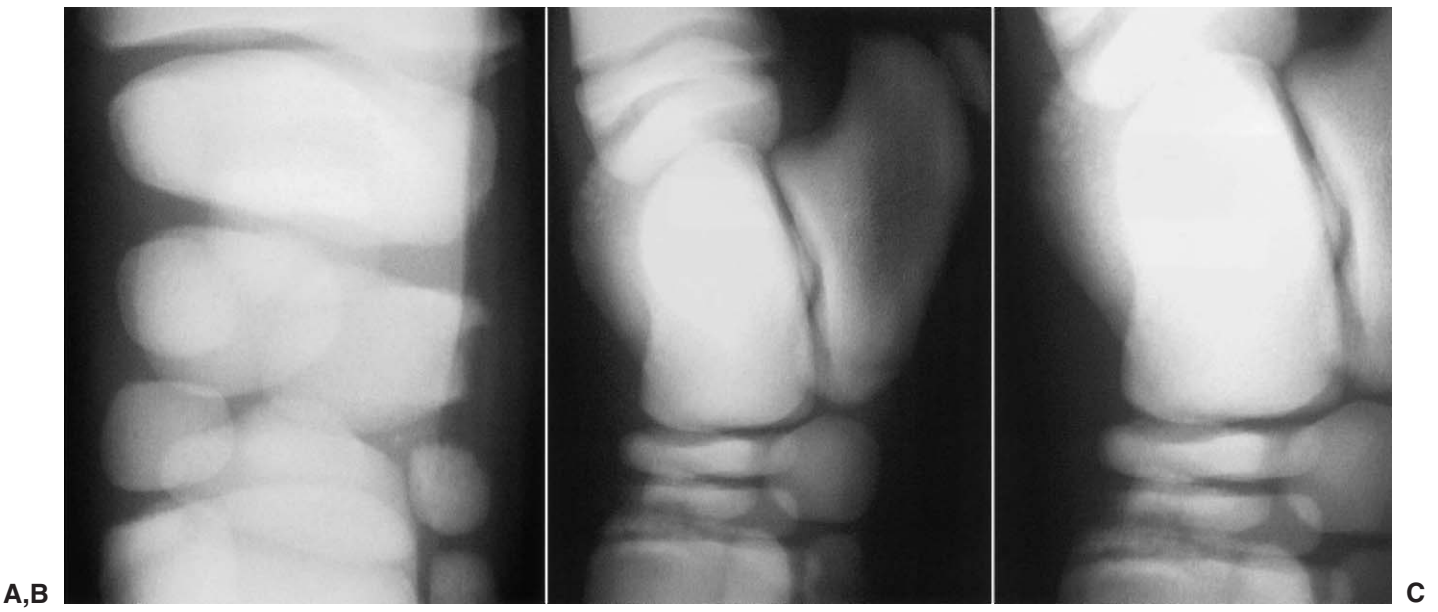


Figure 1-17 • Three-week-old Quarter Horse colt with immature carpal and tarsal bones. Close-up craniocaudal oblique view **(A)** of carpus shows (1) fringeing of the proximal border of the second carpal bone, (2) a defective radial carpal bone, and (3) generalized hypoplasia. Lateral **(B)** and close-up lateral **(C)** views of the tarsus show (1) marked talar fringeing and distortion, (2) marginal rounding, (3) poor mineralization, (4) diminished size, and (5) an unfused proximal metatarsal epiphysis.

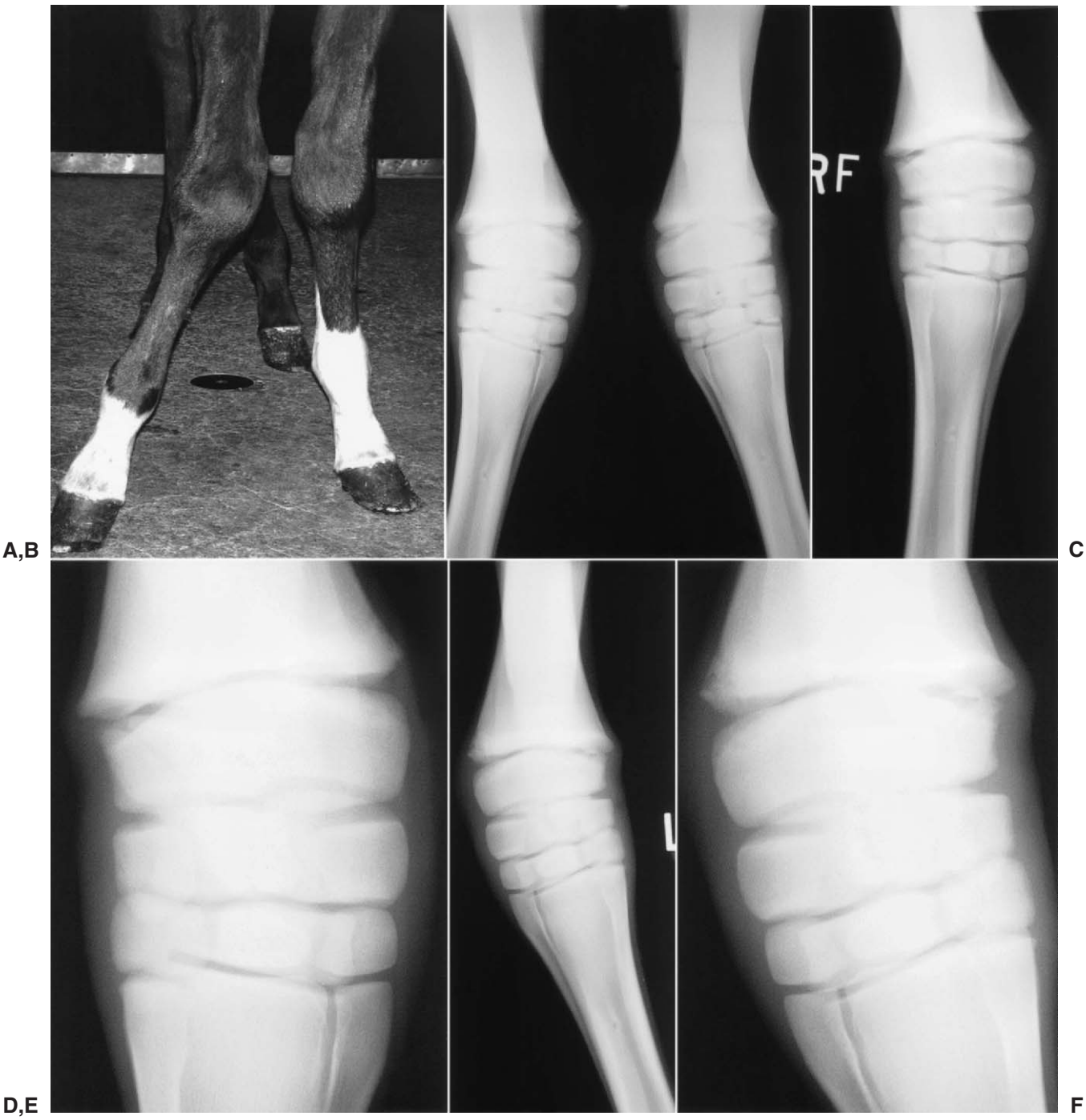


Figure 1-18 • Frontal view **(A)** of lower forelimbs of foal with bilateral valgus deformities. Combined craniocaudal **(B),** right craniocaudal **(C),** right craniocaudal close-up **(D),** left craniocaudal **(E),** and left craniocaudal close-up **(F)** views of the carpi show bilateral distal radial curvature resulting in valgus deformities. Note the disparity between the way the foal's right leg appears in the photograph and its radiographic appearance.



Figure 1-19 • Frontal **(A)** and close-up frontal **(B)** views of a young foal with left-sided varus deformity at the levels of the metacarpus and fetlock. Craniocaudal radiograph **(C)** of the left carpus shows an overly straight, outwardly canted distal radius and carpus with varus curvature.

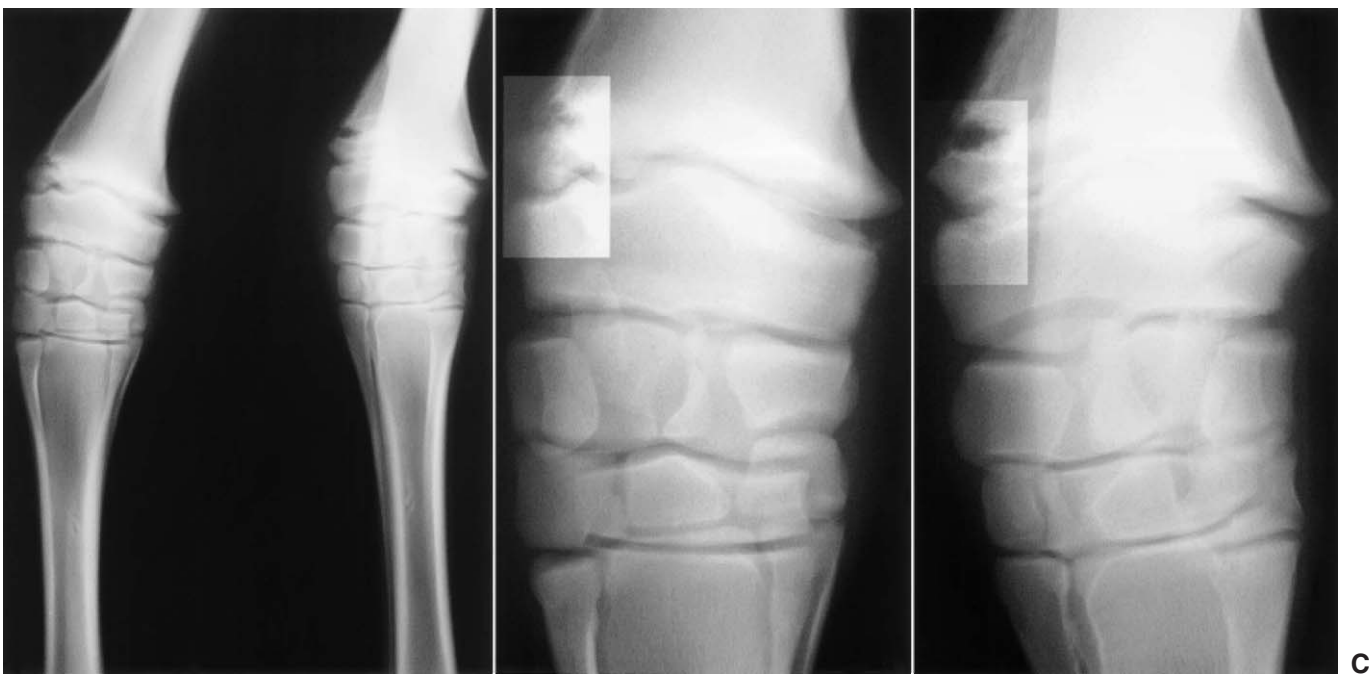
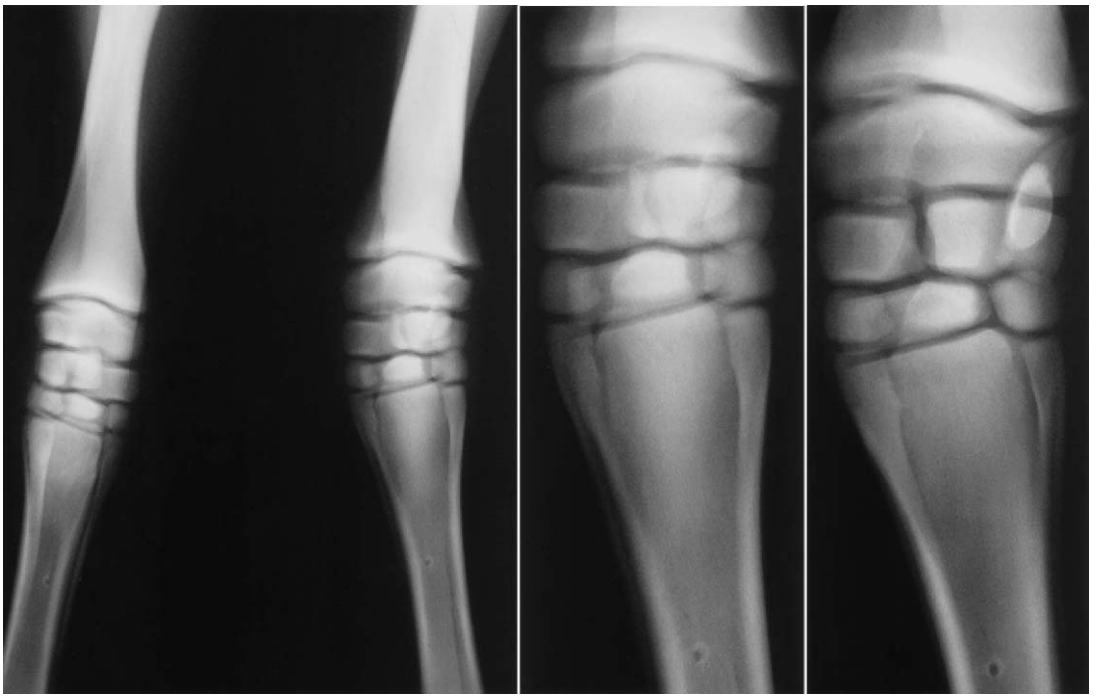


Figure 1-20 • Windswept foal. Combined craniocaudal **(A),** right craniocaudal close-up **(B),** and left craniocaudal close-up **(C)** views show right-sided valgus and left-sided varus limb deformities. Emphasis zones in the close-up views show prominent distraction defects in both distal radial metaphyses.



A,B **C**

Figure 1-21 • A, Combined craniocaudal view of the distal forelimbs of a foal with uneven radial growth causing an inward curvature of the left carpus. **B,** Careful study of the spatial arrangement of the bones of the left carpus reveals extensive overlap, the result of axial rotation, a common but infrequently mentioned sequela to uneven distal radial growth in foals. **C,** A second craniocaudal projection made from the *estimated* front of the carpus, as opposed to the midsagittal plane of the animal used in the combined view, shows how the carpus should appear.

Table 1–3 • CARPAL AND TARSAL OSSIFICATION INDEX FOR NEWBORN FOALS

Grade	Description
1 (abnormal)	Unossified carpal or tarsal bones.
2 (abnormal)	Partial ossification of carpal and tarsal bones. Open proximal 3rd metacarpal or metatarsal growth plates. Absent or only faintly visible lateral styloid process, and tibial malleoli.
3 (abnormal)	All carpal or tarsal bones mineralized, but with abnormally rounded corners, and relatively wide cartilage spaces. Distinct styloid and malleoli. Closed proximal 3rd metacarpal or metatarsal growth plates
4 (normal)	Carpal and tarsal bones fully mineralized with square corners resembling an adult. Cartilage spaces normal for a young immature animal. Closed metacarpal and metatarsal physes.

image is firmly fixed in mind, radiograph the foal once it has assumed this position. If any doubt exists as to whether or not the assumed position was representative, repeat the examination and compare it with the original. If they are similar, proceed with the analysis; if not, make a third film, which will usually serve as a capable tiebreaker.

The preceding advice is predicated on *patience:* patience in taking the time to observe the foal's preferred stance carefully, before beginning the radiographic examination, that is, patience in waiting until the foal is in the desired predetermined position, before making the film. Finally, one needs to have the patience to repeat nonrepresentative or ambiguous images.

▮▮▮ STANDARD AND SUPPLEMENTED ANGULAR LIMB DEFORMITY SERIES

The standard angular limb deformity series consists of two to four views, depending on personal preference. I prefer five views: frontal projections of each leg centered on the carpus, including as much of the radius and metacarpus as possible; lateral views of each carpus; and, most important, a full-length frontal view of both carpi and metacarpi side-by-side (the *Nancy view*). In my opinion the last projection is the most diagnostic because it employs a constant plane of reference, the horse's torso, and allows assessment of both angular and torsional deformities.

Combined Carpal View (Nancy View)

I first began making combined carpal views—a standing projection centered on a pair of intersecting lines

passing vertically through the pectoral muscles and horizontally through the carpi—in the early 1980s. I named the projection after one of the radiology technicians, Nancy (thus called the Nancy view). Figures 1-22 and 1-23 show two normal variants of the combined projection, and Figure 1-24 shows an animal with a unilateral varus angulation.

Recumbent Views

Occasionally a foal is so wild that it is impossible to restrain, and when it is drugged sufficiently to control it is not able to stand. Recumbent projections can be used under such circumstances, but only for anatomic assessment because angular assessment will be inaccurate (Figure 1-25).

▮▮▮ CAUSES OF ABNORMAL LIMB CURVATURE IN FOALS

Joint "Laxity"

The term *laxity*, as used in radiographic diagnosis, is often ambiguous but generally caries a negative connotation of looseness or a lack of tightness. At least one canine hip registry arduously avoids the term *dysplasia* (and its attendant diagnostic commitment), substituting in its place the word *laxity.* A number of persuasive arguments can be made against the use of this term, most focusing on its highly inferential nature.

Opponents of using the term have challenged supporters to prove their case with stress radiography, a position I strongly support. An increased distance between two or more bones in a particular joint does not, in my opinion, constitute prima facie evidence of excessive mobility or looseness, nor does such an observation warrant a prediction of future osteoarthritis.

Foals whose carpi are bowed as a result of capsular or intercarpal ligament weakness typically show valgus deformities centered on the midcarpus, with a relatively straight radius and metacarpus. Many fully resolve in a month or two, with or without casts (Figure 1-26).

Uneven Distal Radial Growth

Valgus deformities in young foals are most often attributed to unequal distal radial growth. Typically the medial side of the radial growth plate outgrows the lateral side, although exactly how this comes about is not known. It may be that growth on the medial side of the physis is accelerated or, alternatively, that growth on the lateral side is retarded or even ceases altogether for a time. In any event, the result is that the

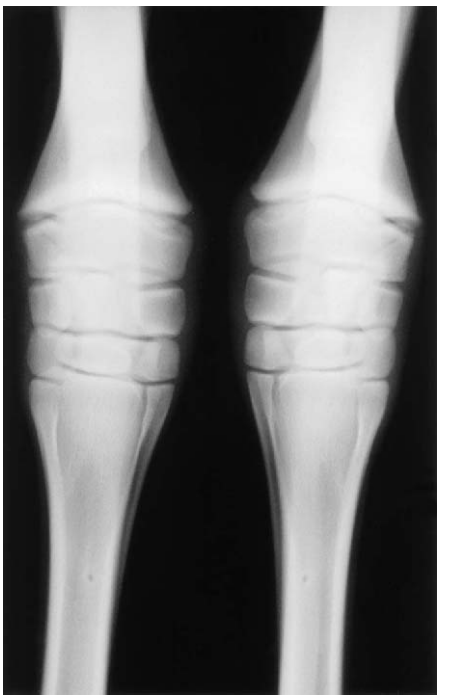


Figure 1-22 • Combined craniocaudal view of the carpi of a normal foal shows a narrow-based stance.



Figure 1-23 • Subsequent combined craniocaudal view of foal shown in Figure 1-22 now shows a wide-based stance, illustrating the postural variation often observed in young foals.

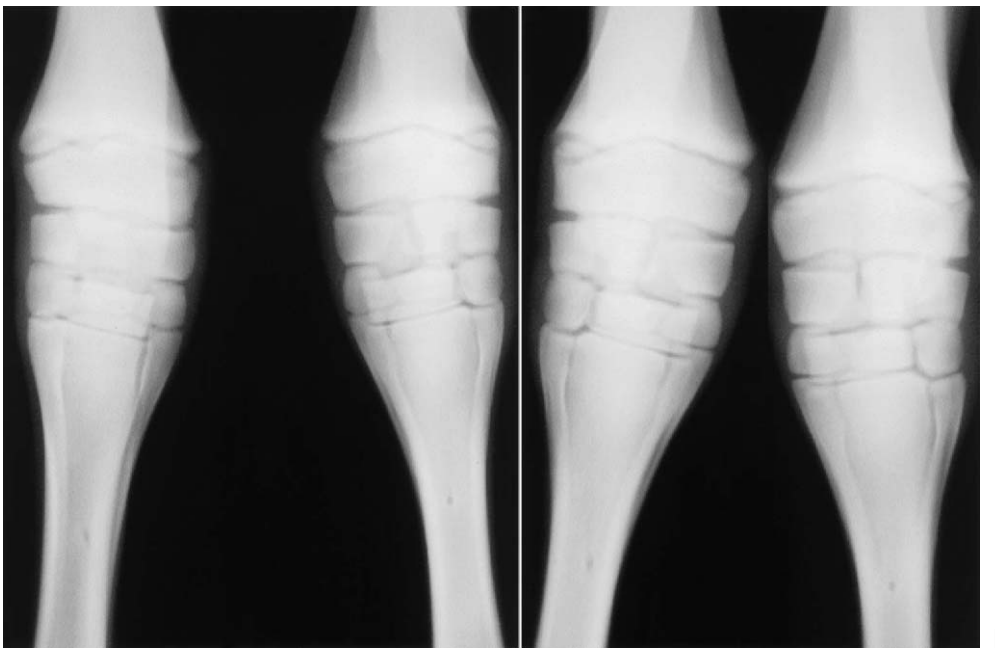


Figure 1-24 • Mild valgus angulation of the right carpus of a foal, as demonstrated in a combined craniocaudal view **(A)** compared with individual views of the carpi pictured side-by-side **(B).**

bones of the carpus, along with the underlying metacarpus, are deflected laterally, creating an abnormal inward bending of the carpus (Figure 1-27).

Hypoplastic, Dysplastic, and Fractured Carpal or Tarsal Bones

In my experience, carpal and tarsal hypoplasia is the most common misdiagnosis made in foals. Insofar as I can determine, the principal reason for this error is a failure to differentiate between projectional variation and pathology. To explain: A crooked-legged foal is radiographed to assess both the degree of angulation and its probable cause. As I mentioned previously in this chapter, most foals with angular deformities also have torsional rotation, which together result in a wide variety of carpal projections. It is these *unfamiliar projections* of normal bones that are often misinterpreted as deformed carpal or tarsal bones.

Theoretically, grossly undermineralized carpal or tarsal bones may not be able to bear the weight of a young foal without being fractured or crushed. Likewise, a bone structurally weakened by infection or avascular necrosis might also be expected to break under similar circumstances; but the reality appears to be that most such structural failings are due to osteochondritis, in which a wide variety of lesions have been described (Figure 1-28).

▮▮▮ POSTOPERATIVE RADIOGRAPHIC EVALUATION OF ANGULAR LIMB DEFORMITIES IN FOALS

Congenitally Contracted and Hyperextended Tendons

Etiology. The precise cause or causes of congenital lower-limb contraction and hyperextension in foals is not known. Most hypotheses about contracted tendons focus on the somewhat overly simplistic view that during development, a small uterus, a large foal, or a combination of these two will lead to fetal malpositioning and reduced movement, causing tendon or ligament dysplasia or both.[15] Various hypotheses that attempt to explain tendon abnormalities in newborn foals are listed in Box 1-1.

Even less is known about the cause or causes of hyperextended tendons in newborn foals. Because lower limb hyperextension is often found in premature or stunted individuals, their tendinous weakness is often attributed to incomplete or abnormal development.

Most foals with mild to moderate digital hyperextension become normal in 2 to 3 weeks, often with no more than routine exercise. In severe cases, avulsion-type, apical or basilar sesamoid fractures may occur following release from close confinement.

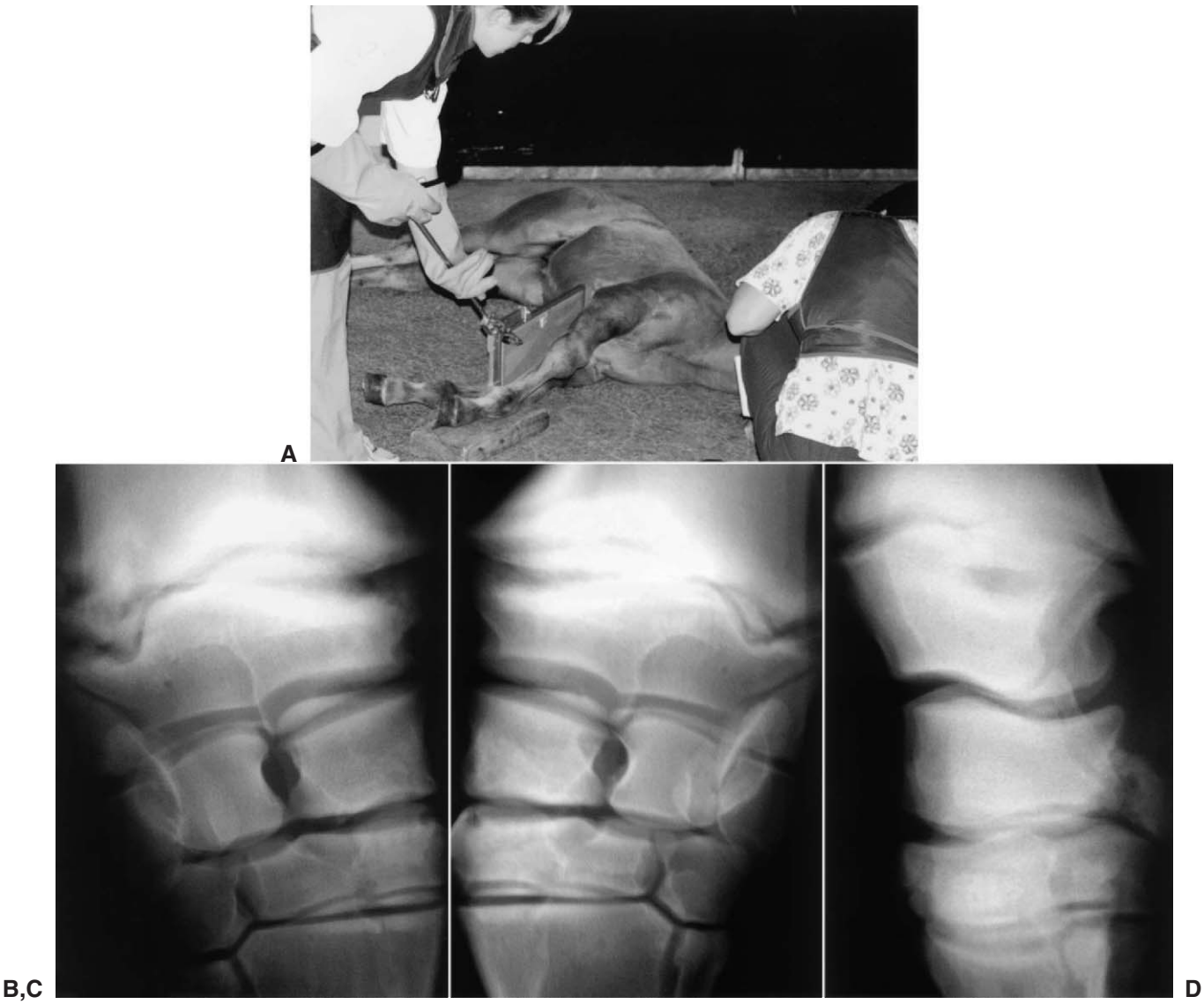


Figure 1-25 • Picture of a heavily sedated foal having its right carpal region radiographed while recumbent **(A).** Close-up, right craniocaudal **(B),** left craniocaudal **(C),** and right lateral **(D)** views show (1) severe deformity and uneven calcification of the distal radial epiphyses, (2) bilateral metaphyseal distraction defects, and (3) multiple radiolucent defects in the perimeters of many of the carpal bones.

▮▮▮ SPECIFIC CONTRACTURES

Distal Interphalangeal Joint

Forelimb distal interphalangeal contractures are more common than hindlimb contractures. Severely affected feet typically assume a distinctly curled appearance so that the dorsal surface of the hoof lies nearly parallel to the ground.

Fetlock Joint

Forelimb and hindlimb fetlock contractures occur with equal frequency and can be either bilateral or unilateral. In the case of the former, one limb is often worse than the other. Typically the long pastern appears nearly vertical, and the foot is curled awkwardly backward. Differentially a ruptured common digital extensor tendon may result in a similar appearance.

Carpus

Congenital carpal contracture is usually bilateral, often unequal in severity, and can cause mechanical dystocia. Serious contractures may flex the carpi to the extent that walking, or even standing, is impossible. Some foals with carpal contracture have a fluctuant swelling over the dorsolateral aspect of the carpus and also may knuckle at the fetlock. Rupture of the common digital extensor tendon can produce similar findings.

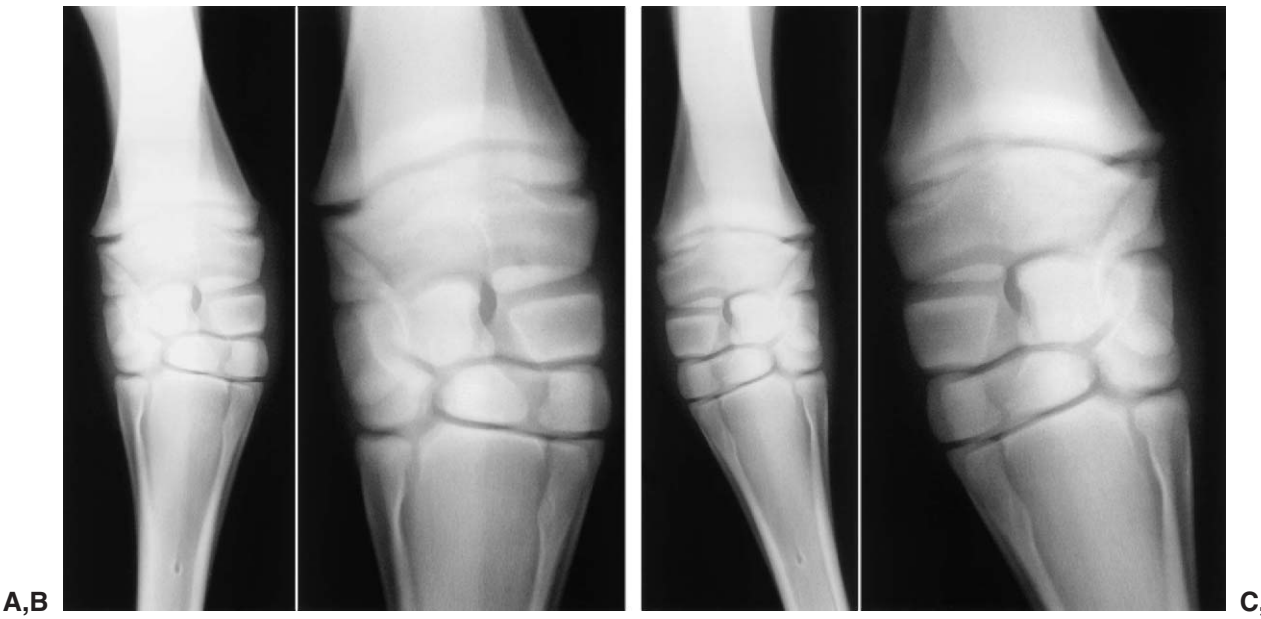


Figure 1-26 • Orientation and close-up views of the right **(A, B)** and left **(C, D)** carpi of a crooked-legged foal show that the abnormal curvature is most likely the result of weak intercarpal ligaments. This foal's carpi became radiographically normal within a month.

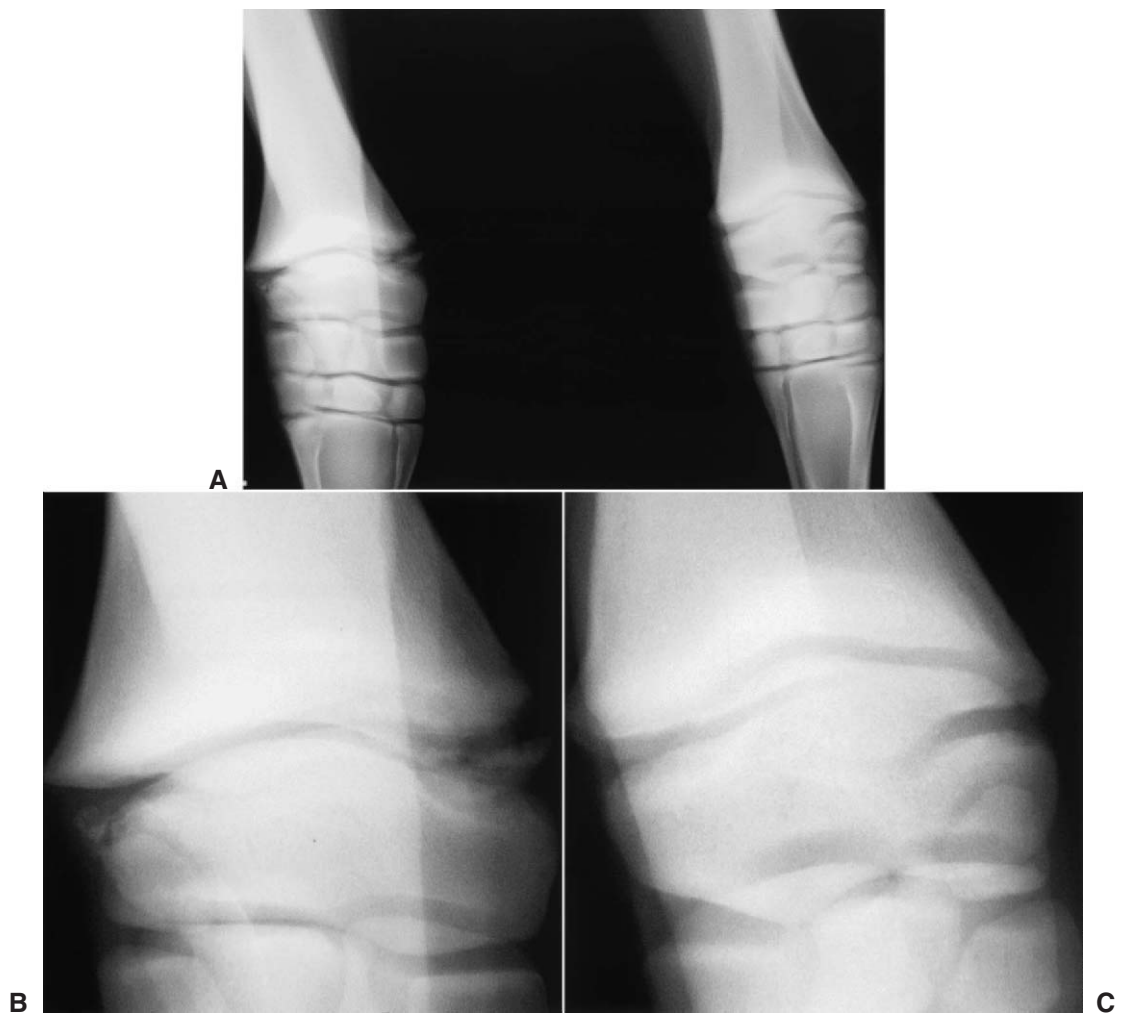


Figure 1-27 • Combined craniocaudal **(A)** and ultra-close-up craniocaudal **(B, C)** views of the carpi of a windswept foal show distraction defects and pseudofractures on either side of the right distal radial growth plate. The valgus curvature on the right appears to be due to uneven radial growth; the canted varus deformity on the left is probably a postural adaptation.

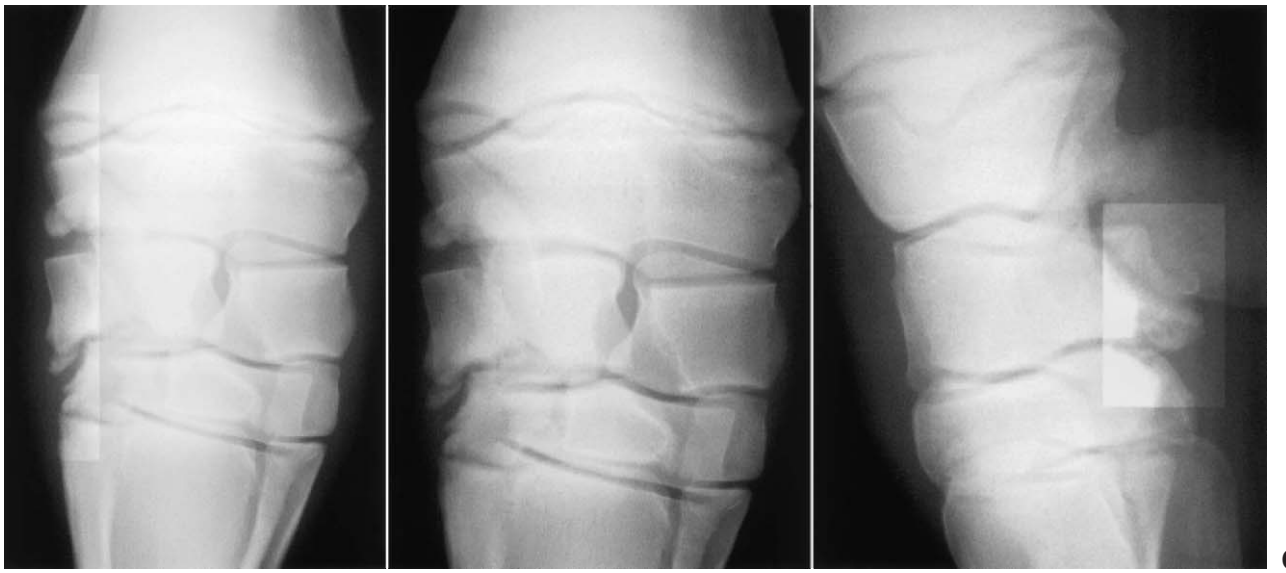


Figure 1-28 • Osteochondritis: craniocaudal **(A),** close-up craniocaudal **(B),** and close-up lateral **(C)** views of the right carpus show fragmentation of the styloid process, ulnar carpal, and fourth carpal bone, all on their lateral aspects. In addition, the ulnar and fourth carpal bones are hypoplastic, deformed, and subluxated, with the latter accounting for the foal's valgus deformity. The left carpus showed similar but less pronounced changes.

Tarsus

Congenital tarsal contracture is rare. In one reported case by Trout and Lohse, a severe unilateral contraction of the peroneus tertius was successfully treated using a combination of transection and physiotherapy.[16]

Hemi-Circumferential Periosteal Transection and Elevation

Read and co-workers showed that for foals with moderate experimentally induced valgus deformities of the carpus, stall confinement and hoof trimming are as effective as hemi-circumferential periosteal transection and elevation in straightening the leg.[17]

Osteopetrosis

Berry and co-workers reported the radiologic, subgross, and histologic appearance of osteopetrosis in two newborn Peruvian Paso foals.[18] On presentation, the foals were dyspneic, unable to rise, and had brachygnathia. Abnormal laboratory findings included anemia, hypogammaglobulinemia, and increased alkaline phosphatase.

Various long bones, the skull, and the cervical spinal region showed increased medullary opacity, making it impossible to distinguish a discrete cortex or medulla. Some of the diseased long bones exhibited a distinctive hourglass appearance, the result of asymmetric, tapered endosteal bone deposition. The described abnormalities were similar to those described in children with a lethal form of autosomal-recessive osteopetrosis.

Box 1-1
Theories on Contracted Tendons and Ligaments in Newborn Foals

Fetal malpositioning and stasis secondary to uterine overcrowding
Maternal exposure to influenza virus during pregnancy.
Maternal consumption of locoweed or hybrid Sudan grasses during pregnancy
Goiter
Unspecified "neuromuscular disorders"
Unspecified "heritable defect"

Osteochondritis (Osteochondrosis)

The subject of osteochondritis (or osteochondrosis) will be treated contextually in this book, in other words, in the appropriate sections. A few osteochondritis facts seem appropriate at this junction of the book, however:

- Osteochondrosis, osteochondritis dissecans, and subchondral bone cysts all appear to be part of the same disease.[19]
- Osteochondritis of horses, dogs, pigs, and poultry appears to be the same disease in all these animals.
- Osteochondritis occurs in young, rapidly growing animals.
- Osteochondritis is at its most basic level a failure of enchondral ossification.
- Mineral and vitamin supplementation probably plays a minor role at most in the development of osteochondritis in animals.
- Osteochondritis is almost certainly heritable.

Zinc-Induced Osteochondrosis

Environmental zinc pollution, which interferes with copper metabolism, was reported to cause generalized osteochondrosis in a pair of foals born near a zinc smelter. The animals also suffered from nephrocalcinosis and osteoporosis attributed to cadmium toxicosis from the same source. Radiographs of the midlimb and lower-limb bones of the affected foals showed an uneven loss of subchondral bone, decreased and disoriented metaphyseal trabeculation, and cortical thinning. The authors noted that even if such smelting operations were halted, or their toxic emissions quelled, the surrounding soil and associated vegetation would remain contaminated for hundreds of years.[20]

Fluoride Osteosclerosis

Stevenson and Watson described the radiographic appearance of fluoride osteosclerosis in humans.[21]

▮▮▮ JUVENILE BONE TUMORS

Multiple Hereditary Exostoses

Hanselka and co-workers reported the clinical, gross, radiographic, and histologic appearance of multiple cartilaginous exostoses (scapula, radius, ulna, ribs) in a 1.5-year-old Appaloosa stallion.[22] Shupe and coworkers compared the clinicopathologic features of hereditary multiple exostoses in horses with those found in humans.[23] They also reported the effect that excessive dietary fluoride had on the composition of equine bone tumors.[24]

Generally, multiple hereditary exostoses are ascribed to one of three causes, although no one is certain:

1. Small bits of cartilage are pinched off the periphery of the growth plate and carried along as the bone grows longitudinally, eventually forming the nidus for localized new bone formation.
2. Small cartilaginous rests located in the osteogenic layer of the periosteum rather than the growth plate are awakened, giving rise to a localized new bone deposit.
3. Inappropriate localized new bone formation occurs from the unrestricted perimeter of the growth plate, which is then carried to the metaphyseal region of the bone.

Radiographically, individual cartilaginous exostoses have no single characteristic appearance. Most resemble old periosteal lacerations; but, unlike deep wounds, they lack associated skin blemishes. Individual bone deposits may be narrow-based and conical or spikelike or, alternatively, smoothly marginated, low mounds. Most exostoses are located in the metaphysis or distal shaft of the bone. Rib lesions closely resemble heavily callused rib fractures with highly variable sizes and shapes. Scapular lesions appear somewhat differently from long bone lesions, usually being ridgelike and almost always located proximally.

Polydactylism

Behrens and co-workers described polydactylism in three foals.[25] They used a simplified classification, which I have modified slightly, dividing polydactyly into three subtypes:

1. *Teratogenic polydactyly*. Characterized by splitting, displacement, or dispersion of the basipodal elements of the embryo
2. *Developmental polydactyly*. Also termed atavistic polydactyly
3. *Heritable polydactyly*. Usually bilateral with an extra digit located on the medial aspect of the forelimb

References

1. Smallwood JE, Albright SM, et al: A xeroradiographic study of the developing equine foredigit and metacarpal phalangeal region from birth to six months of age, *Vet Radiol* 30:98, 1989.
2. Metcalf MR, Sellett LC, et al: A scintigraphic characterization of the equine foredigit and metacarpal phalangeal region from birth to six months of age, *Vet Radiol* 30:111, 1989.
3. Adams WM, Thilstead JP: Radiographic appearance of the equine stifle from birth to 6 months, *Vet Radiol* 26:126, 1985.
4. Myers VS, Emmerson MA: The age and manner of epiphyseal closure in the forelegs of two Arabian foals, *Vet Radiol* 12:39, 1966.
5. Brown MP, MacCallum FJ: Observations on growth plates in limbs of foals, *Vet Rec* 98:443, 1976.
6. Hintz HF, Schryver HF: Nutrition and bone development in horses, *J Am Vet Med Assoc* 168:39, 1976.
7. Sherrod WW: Epiphysitis in foals, *Vet Med Small Anim Clin* 701443, 1975.
8. Campbell JR, Lee R: Radiological estimation of differential growth rates of the long bones of foals, *Equine Vet J* 13:247, 1981.
9. McLaughlin BG, Doige CE: Congenital musculoskeletal lesions and hyperplastic goiter in foals, *Can Vet J* 22:130, 1981.
10. Ruohoniemi M, Hilden L, et al: Monitoring the progression of tarsal ossification with ultrasonography and radiography in three immature foals, *Vet Radiol Ultrasound* 36:402, 1995.
11. Dutton DM, Watkins JP, et al: Incomplete ossification of the tarsal bones in foals (1988-1996), *J Am Vet Med Assoc* 213:1590, 1998.
12. Fretz PB, Pharr JW, et al: Letters, *J Am Vet Med Assoc* 181:636, 1982.
13. Pharr JW, Fretz PB: Radiographic findings in foals with angular limb deformities, *J Am Vet Med Assoc* 179:812, 1981.
14. Morgan JP: Personal communication. 1974.
15. Embertson RM: Congenital abnormalities of tendons and ligaments, *Vet Clin N Am (Equine Pract) Tendon & Ligament Injuries* I 10:351, 1994.

16. Trout DR, Lohse CL: Anatomy and therapeutic resection of the peroneus tertius muscle in a foal, *J Am Vet Med Assoc* 179:247, 1981.
17. Read EK, Read M, et al: Effect of hemi-circumferential periosteal transection and elevation in foals with experimentally induced angular limb deformities, *J Am Vet Med Assoc* 221:536, 2002.
18. Berry CR, House JK, et al: Radiographic and pathologic features of osteopetrosis in two Peruvian Paso foals, *Vet Radiol Ultrasound* 35:355, 1994.
19. Trotter GW, McIlwraith CW: Osteochondritis dissecans and subchondral cystic lesions and their relationship to osteochondrosis in the horse, *Equine Vet Sci* 5:1157, 1981.
20. Gunson DE, Kowalczyk DF, et al: Environmental zinc and cadmium pollution associated with generalized osteochondrosis, osteoporosis, and nephrocalcinosis in horses, *J Am Vet Med Assoc* 180:295, 1982.
21. Stevenson DA, Watson AR: Roentgenologic findings in fluoride osteosclerosis, *Arch Indust Hyg* 21:340, 1960.
22. Hanselka DV, Roberts RE, et al: Equine multiple cartilaginous exostoses, *Vet Med Small Anim Clin* 69:979, 1974.
23. Shupe JL, Leone NC, et al: Hereditary multiple exostoses: clinicopathologic features of a comparative study in horses and man, *Am J Vet Res* 40:751, 1979.
24. Shupe JL, Eanes ED, Leone NC: Effect of excessive exposure to sodium fluoride on composition and crystallinity of equine bone tumors, *Am J Vet Res* 42:1040, 1981.
25. Behrens E, Donawick WJ, Raker CW: Polydactyly in a foal, *J Am Vet Med Assoc* 174:266, 1979.

Chapter 2

Fracture Healing and Other Forms of Bone Remodeling

ASSESSING FRACTURE HEALING

Few would quarrel with the proposition that *anatomic restoration* is the radiographic hallmark of fracture healing, but is this goal realistic when assessing fractures? Of course not. Full restoration may require months or even years to complete, and who would monitor the radiographic progress of an uncomplicated fracture for that long? So what is a practical objective in evaluating fracture healing, and how can it be determined radiographically?

Before going further with this train of thought, some background information is necessary; namely, what are the expectations for any individual fracture: how long will it take to heal or, in the medical parlance of the day, what is the expected outcome?

Determinants of Fracture Healing

The following factors influence fracture healing:

- The severity of the fracture
- Which bone is fractured
- Where in a particular bone the fracture occurs
- Whether or not the fracture is fresh
- Whether or not the fracture is open
- The age of the horse
- Whether any other serious injuries or preexisting disease are present
- How the fracture is repaired
- The skill of the surgeon
- The quality of the aftercare

Fracture Severity. Generally, comminuted and multiple fractures require more time to heal than simple two-piece fractures, assuming equal degrees of reduction and stabilization. The greater the degree of fragment displacement, the greater the amount of secondary muscle and vascular damage—both important factors in callus formation.

Fracture Location. Fractures that occur at the distal end of long bones often cannot be compressed because there is insufficient room for a bone plate and screws. Distal limb fractures are also surrounded by less muscle than proximal fractures and thus have less potential collateral circulation and soft-tissue support.

Fracture Age. Fresh fractures are easier to work with, and the surrounding muscles, nerves, lymphatics, and vasculature are in better condition. Subacute fractures are not only often overridden but are beginning to form a primitive callus, which, along with lacerated and bruised muscles, makes fragment manipulation very difficult. Unstabilized limb fractures move regularly, leading to varying degrees of secondary fragmentation, especially at the ends of the damaged bones. A similar fate awaits horses that must be transported more than a short distance to the hospital, so-called *transport fractures.*

Open Fractures. Open fractures (also termed *compound fractures*) are often infected and as such carry a greater potential for nonunion than closed fractures.

Age of the Horse. In people, pets, and cattle, the young heal more rapidly and with fewer complications than do the old. Thus foals, yearlings, and young adults usually heal more rapidly than older horses, assuming a comparable degree of injury and similar treatment.

Concomitant Injury. Concomitant injuries place an additional demand on the body's resources, especially the immune system, compromising healing to varying extents.

Method of Repair. All things equal, a plated fracture will heal more rapidly and with less callus than one that is pinned.

Surgical Skill. The skill of the surgeon may be the single most important variable in predicting the outcome of orthopedic procedures.



Figure 2-1 • Radiographs of a horse that stepped in a hole and dislocated its pastern joint approximately a year ago. The animal is now mildly to moderately lame, especially after exercise. Close-up lateral **(A)** and dorsopalmar **(B)** views of the pastern joint show advanced osteoarthritic remodeling as evidenced by (1) symmetric periarticular and extraarticular new bone deposition, (2) a narrowed cartilage space, and (3) subchondral sclerosis. Similar views **(C, D)** of the opposite normal pastern are provided for comparison.



Figure 2-2 • Radiographs of a horse that completely severed its flexor tendons 2 to 3 years previously. As a result, both proximal sesamoids are severely deformed, as seen in close-up dorsopalmar **(A),** true lateral **(B),** lateral oblique **(C),** and medial oblique **(D)** views, resembling what is often observed following displaced apical or body fractures. Adaptive remodeling of this sort is rarely documented radiographically because many horses with such injuries are destroyed.

Postoperative Aftercare. The type, amount, and quality of postsurgical aftercare strongly influence healing time. This is especially true of physiotherapy.

▮▮▮ BONE GRAFTS

Although it is theoretically possible radiographically to identify and monitor the progress of autogenous cancellous bone grafts, in fact, such exercises prove futile more often than not.[1] On the other hand, crushed and stave-type cortical bone grafts can usually be readily recognized. Examples of short- and long-term fracture healing are presented in the chapters that follow.

▮▮▮ BONE REMODELING

Exercise Induced

Sprint and endurance training in racehorses causes varying degrees of bone remodeling, typically taking the form of increased radiographic density and

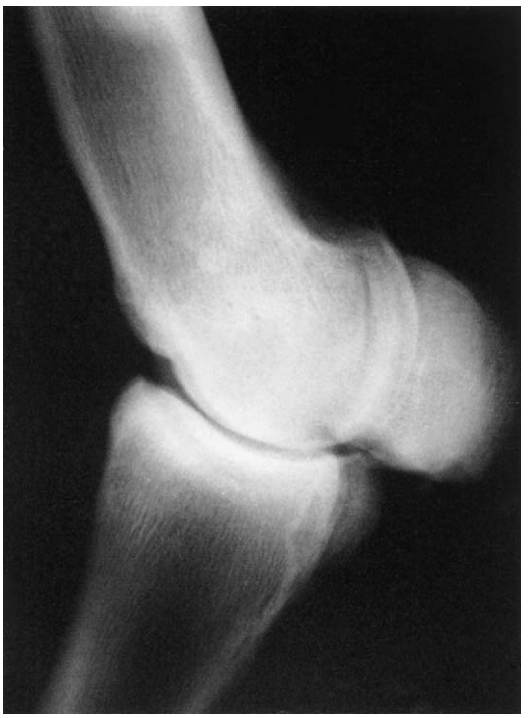


Figure 2-3 • Lateral view of the fetlock of a horse that completely severed its right front flexor tendons 20 years ago. As a result, the metacarpal condyle has "drifted" toward the palmar aspect of the proximal phalanx, which now has a flatter articular surface, to better match the dorsal half of the overlying condyle, with which it now articulates. For their part, the sesamoids are fully (and for the most part) articulating with the palmar aspect of the canon bone, accommodating its forward inclination and the hyperflexed attitude of the fetlock. The flattened mound of new bone on the dorsal surface of the distal metacarpal metaphysis and a similar deposit on the underlying phalanx are impingement exostoses, a consequence of one surface striking the other.



A **B**

Figure 2-4 • A, What makes the previous case (Figure 2-3) an even better example of remodeling are the secondary changes to the opposite fetlock, which in many respects are more pronounced than those in the injured limb. Note the greater degree of hyperextension, and the extensive dystrophic calcification in the suspensory field. **B,** A normal lateral view is provided for comparison.

increased scintigraphic uptake. The most commonly affected bones in the horse are the third carpal, proximal sesamoids, and distal metacarpus/metatarsus.[2] The described bony alterations are often quite subtle, requiring technically comparable, high-quality, serial examinations to appreciate any radiographic differences.

Traumatically Induced

Perhaps the best and most obvious example of skeletal remodeling is the fracture callus. Take the case of a simple two-piece distal extremity fracture treated with a cast. The ends of the broken bone are first physiologically fixed by a combination of clot and connective tissue, the so-called *soft callus.* Then, through a surprisingly sophisticated process, the soft callus is transformed into a lump of very primitive bone, which not only joins but also immobilizes the fracture fragments. The process of remodeling begins shortly thereafter.

Thought of most simply, fracture remodeling is a restorative process. Seemingly, the broken bone is attempting, not just to repair itself, but ideally to regain fully its original appearance: a normal cortex, a normal medulla, a normal length and width, and no deformity. Like any restoration, the process of fracture healing is often slow and sometimes tedious, a little bit of bone added here, a little bit subtracted there. In most instances, however, the bone succeeds in its restorative efforts, so much so that some months later it may be difficult or impossible to identify the original injury.

Accommodative

Remodeling may take another form, one predicated on the concept of *accommodation.* A good example of accommodative remodeling is the sprain-fracture-dislocation. In this often painful and debilitating injury, one or more joint surfaces are often fractured, producing large gaps in the articular cartilage and subchondral bone, which fill eventually with new bone, a sort of interior callus. The result is incongruency, one joint surface no longer matching the other.

Triggered by an articular mismatch, and to a lesser extent by any associated instability, each of the involved bone surfaces, injured and uninjured alike, attempts to reach an anatomic accommodation through the process of remodeling. In other words, each surface tries to match that of the other, although usually not with the usual accoutrements of a normal joint, such as articular cartilage.

Accommodative remodeling also can occur in uninjured parts, especially joints in the opposite leg. Secondary remodeling is induced by a variety of biomechanical factors but most importantly by a combination of overwork and overload. Examples of primary and secondary accommodative remodeling are shown in Figures 2-1 to 2-4.

References

1. Kold SE, Hickman J, Melson F: Qualitative aspects of the incorporation of equine cancellous bone grafts, *Equine Vet J* 19:111, 1987.
2. Ehrlich PJ, Dohoo IR, O'Callaghan MW: Results of bone scintigraphy in racing standard bred horses: 64 cases (1992-1994), *J Am Vet Med Assoc* 215:982, 1999.

Chapter 3

The Foot

THE STANDARD FOOT SERIES

Conventional Radiography

The standard foot series typically consists of two views*: a frontal view (high-coronary, 65- to 70-degree dorsopalmar/dorsoplantar) and a lateral (lateral-to-medial) view centered as closely as possible on the center of P3 (Figures 3-1 and 3-2). Often studies of this type are of a survey nature, where there is no certain diagnosis other than a suspicion that the foot is responsible for the animal's lameness. In most instances a fracture or an infection is being sought. Areas of potential pathology are listed in Table 3-1.

Some General Considerations on Other Means of Medical Imaging

Computed Radiography: An Alternate Form of X-Ray Imaging. The foot as well as other parts of the skeleton can also be imaged using *computed radiography* (CR), in many respects a superior form of imaging compared with conventional radiography, but also a very expensive one. Briefly, CR, as its name indicates, converts penetrated x-rays into numeric data that can be manipulated by a computer to improve image contrast; enhance edges; and brighten, darken, and enlarge areas of interest, much like the immensely popular desktop computer program *PhotoShop*. As an added benefit, lossless digital images can be readily deployed to both intranets and the Internet, greatly reducing the *time-to-view* waiting period for those requesting the examinations.

Advantages of Computed Radiography. Roberts and Graham described the specific advantages of CR for equine medical imaging (Box 3-1).[1]

*In light of the increasing complexity—and in my opinion, unwieldiness—of current radiographic terminology often used in publication, I have chosen to use classic descriptors that we routinely employ in our hospital when discussing radiographs. I hope no one takes offense.

Xerography. Smallwood and Holladay reported the normal xerographic appearance of the equine digit and fetlock.[2] Xerography is now used almost exclusively for teaching radiographic anatomy.

Ultrasound. Busoni and Denoix reported the normal sonographic appearance of what they termed the *podotrochlear apparatus*, in three cadaver limbs and five living animals.[3] Sonograms were obtained through the sulcus of the frog and correlated with sagittal and transverse tissue slices comparable to the scan planes. The technique proved capable of displaying the following anatomy, albeit with variable clarity and recognizability: (1) the distal part of the flexor surface of the navicular bone, (2) the distal portion of the deep flexor tendon, (3) the distal sesamoidian ligament, and (4) the soft tissue attachments (enthesis) of P3.

Angiography. Coffman and co-workers described the angiographic appearance of the laminitic horse.[4] Later, Ackerman and co-workers described the angiographic appearance of both the normal and the foundered foot.[5] Bordalai and Nigam described the angiographic appearance of the normal foot in the donkey.[6]

Radionuclide Imaging (Nuclear Medicine, Nuclear Imaging, Nuclear Scintigraphy). Nuclear scintigraphy, also known as *nuclear medicine,* provides another alternate, but a relatively expensive, means of imaging foot diseases in horses. As with CR, the use of nuclear imaging is not confined to the distal extremities, but it can be used anywhere in the skeletal system.[7]

Riddolls and co-workers described how a gamma camera intended for use in people may be modified for use in horses.[8] Neuwirth and Romine addressed the issue of radiation hazards during equine lower-limb scintigraphy, emphasizing the importance of protective shielding for handlers.[9]

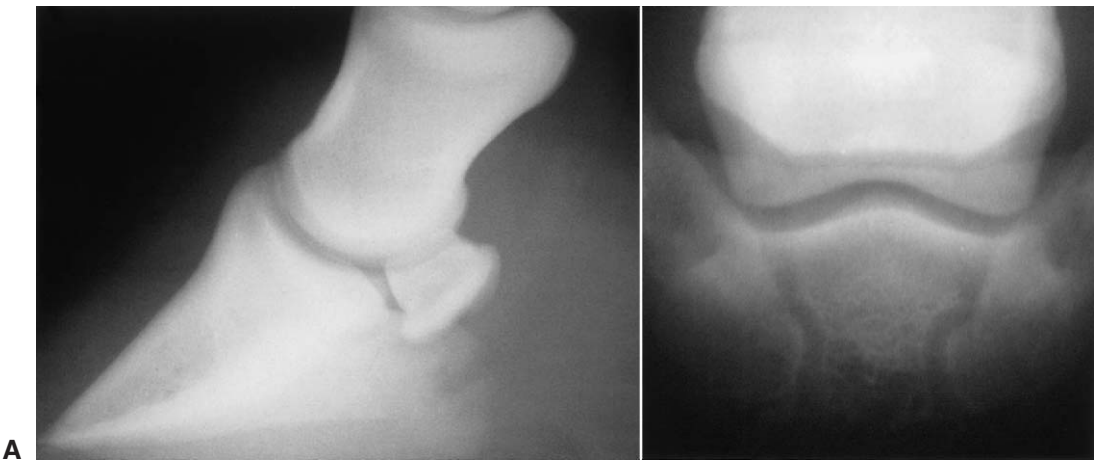


Figure 3-1 • Lateral **(A)** and 65-degree dorsopalmar **(B)** views of the foot.



Figure 3-2 • Bones of an equine forefoot (within the hoof) corresponding to the lateral **(A)** and 65-degree dorsopalmar **(B)** radiographs shown in Figure 3-1.

▮▮▮ RADIOPHARMACEUTICAL UPTAKE PATTERNS

The accumulation of a particular radiopharmaceutical within a specific part of a horse's body is referred to as an *uptake pattern* and is influenced by a number of factors, including (1) age, (2) breed, and (3) use.[10]

Uptake Related to Age

Growth plates (physes), especially in young foals, appear quite intense until they eventually disappear or close once the animal matures. Disappearance of growth plate radiopharmaceutical activity precedes radiographic closure in the distal extremity of foals, as demonstrated by Metcalf and co-workers. Conversely, the distal physeal scars of the radius and tibia may remain scintigraphically visible for years, a phenomenon attributed to a relatively greater amount of regional bone crystal. Scintigraphic activity ceases in the distal femoral physis of a horse by 2.5 years of age, coinciding with radiographic closure.[11]

At about 3 years of age, bone activity begins to resemble more closely that of the surrounding muscle as the result of a reduction in bone turnover and a corresponding decrease in crystalline binding sites.

Uptake Related to Breed and Usage

In general, *jumping horses* show a greater amount of radiopharmaceutical uptake, in a greater number of bones, than Standardbreds or Thoroughbreds.[12]

Uptake Related to Earlier Nerve Block (Regional Perineural Anesthesia)

Trout and co-workers demonstrated that soft-tissue-phase scintigrams can be influenced by certain regional nerve blocks.[13] Specifically, palmar digital and abaxial sesamoid nerve blocks led to a mild short-lived increase in regional activity. High and low palmar blocks caused an even greater increase in uptake. Measured activity was greatest 24 hours after the block and persisted up to 17 days later. Bone-phase scintigrams were unaffected.

Increased Radiopharmaceutical Uptake and Abnormal Radiographic Findings

Roub and co-workers were one of the first groups to point out the important clinical relationship between pain and lameness, bone stress, and abnormal radiographs and nuclear uptake patterns.[14] Specifically, human athletes with shin pain, but normal radiographs, showed vague areas of increased radiopharmaceutical uptake (increased activity). Only later did radiographic changes develop, in the form of focal areas of cortical bone loss.

Subsequently, Twardock asserted that a similar relationship existed in some athletic horses, citing the findings of Morris and Seeherman, who contended that this type of abnormal uptake pattern was not merely *adaptive stress remodeling*, but rather it was a reliable scintigraphic indicator of clinical disease.[15]

Box 3-1
Specific Advantages of Computed Radiography (CR) for Equine Diagnostic Imaging

CR provides greater bone detail, for example, small chip fractures or detached osteochondral fragments.
It optimizes *both* hard- and soft-tissue detail, eliminating the need for separate radiographic exposures.
It allows for viewing of all areas of a specific image, including those typically overexposed or underexposed in a conventional radiograph.
It allows for the adjustment of both brightness and contrast after the initial radiographic exposure has been made, a process referred to as *postprocessing*.
It eliminates or reduces need for repeat exposures.
It eliminates need for multiple film-screen combinations.

Table 3–1 • POTENTIAL DISTAL PHALANGEAL PATHOLOGY ACCORDING TO ANATOMIC REGION AS VIEWED LATERALLY

Anatomic Region of P3	Potential Pathology
Alignment with P2	Traumatic dislocation, lameness accommodation, flexural deformity
Width of distal interphalangeal joint	Infection, reduced use
Position relative to hoof wall	Past or present laminitis
Size and shape of extensor process	Fracture, extensor tendon tear
Dorsal surface	Previous laminitis
Tip	Fracture related to previous laminitis
Solar surface	Osteomyelitis
Wing regions	Fracture
Subsolar region	Abscess

▮▮▮ INDICATIONS FOR NUCLEAR MEDICINE STUDIES OF THE FOOT

Generally, nuclear medicine studies of the foot are reserved for situations in which radiography (and sometimes computed tomography [CT]) fail to reveal the source of the horse's pain and lameness. Diseases that often fall into this category are listed in Box 3-2.

Thermography of the Distal Limb

Thermography has been used on a limited basis to diagnose a variety of equine foot diseases, including (1) laminitis, (2) navicular disease (caudal or palmar heel pain syndrome), (3) solar abscess, and (4) corns. Proponents claim that, like nuclear imaging, thermography's greatest strength lies in its ability to detect otherwise occult soft-tissue disease.[23]

Stromberg is one of the few veterinarians to report thermographic abnormalities obtained from a medium-sized group of horses (116).[24] The following were his findings:

1. ***Joints***: Acute sprains (as indicated by mild swelling) showed an elevated temperature compared with the opposite control leg, even though radiographs appeared normal. As the swelling subsided, the temperature gradually returned to normal. Previously injured joints often became

Box 3-2
Some Lesions Demonstrable With Nuclear Medicine But Not With Radiology

Decreased blood flow (oligemia) secondary to vascular injury or thrombosis[16]
Increased blood flow (hyperemia) secondary to infection, inflammation, or tissue repair[17]
Nondisplaced fracture, especially of P3[18]
Some types of osteomyelitis[19]
Some stages of navicular disease[20]
Some types of suspensory or check ligament inflammation (usually chronic overuse injury)[21]
Some types of flexor tendon inflammation (usually chronic overuse injury)[22]

hotter after a race or training gallop. Reinjury was typically marked by a rise in temperature, as were hairline articular fractures, the latter often being quite localized to a specific area of the joint compared with sprains. Also, as might be expected, infectious arthritis caused an increase in joint temperature before radiographic alterations became evident.

2. ***Long Bones***: Recent periosteal new bone deposits appeared as "hot spots" on thermograms, as did splints in the active phase of development. Mature splints were undetectable thermographically, even though they could readily be seen on radiographs. Shin splints and nondisplaced metacarpal/metatarsal stress fractures were predictably marked by a localized increase in emitted heat.
3. ***Foot***: The coronary band and sole were both amenable to thermographic interrogation; the hoof was not. The coronet temperature was elevated with a variety of ailments but with none specifically. Solar emissions also rose with a variety of disorders, including the following: (1) subsolar abscess, (2) subsolar hemorrhage, and (3) nonspecific solar bruising.
4. ***Tendons, Ligaments, and Muscles***: All these tissues emit heat when injured: the more severe the injury, the greater the amount of heat given off.

Computed Tomography

CT provides superior cross-sectional digital images of complex extremital fractures, but the equipment is expensive to acquire, modify (for horses), and maintain. Control over slice thickness effectively eliminates superimposition by other nearby bones. Once acquired, individual images can be optimized for bone or soft-tissue viewing, termed *bone* or *soft-tissue windows*. Images may also be viewed three-dimensionally provided the slices are thin enough (2 millimeters or smaller) and the necessary software is available, a process known as *three-dimensional (3D) reconstruction*, which greatly enhances the understanding of spatial relationships, especially in planning fracture repair or tumor removal.

Barbee reported that CT in horses is expensive, with respect to both equipment acquisition/modification/installation and later maintenance.[25] The veterinary literature remains relatively sparse with respect to both specific case reports and case series, the latter being especially important in providing data for outcome-based decision making, Diagnostic claims made in review articles on equine CT continue to be based largely on limited case material and, at least in small part, pet and human clinical data.[26] Using dismembered limbs, Widmer compared the diagnostic capabilities of radiography, tomography, and magnetography and, not surprisingly, deemed the latter two methods superior.[27]

Diagnostic competence requires familiarity with the normal cross-sectional anatomy of the head, neck, and limbs of horses; experience with various equine diseases and injuries as they appear in CT images; and a clear understanding of the physical principles that underlie the creation and appearance of CT images.

I must hasten to add at this point that in my experience, getting the affected part of the horse satisfactorily positioned in the bore of the gantry (and keeping it that way during the examination) remains as, or even more, challenging than the diagnostic part of the examination. Likewise, getting the horse from where it is anesthetized to the CT machine, and later back to the recovery stall, can be particularly onerous depending on the physical layout of the facility.

Magnetic Resonance Imaging (Magnetography)

Magnetic resonance imaging (MRI) provides superior multiplanar soft-tissue imagery, but it has comparatively slow image acquisition and is very expensive compared with other kinds of medical imaging. Using a low-field-strength permanent magnet, we are able to do no more than two cases per day. CT is much faster.

Cadaver Feet. Park and co-workers have reported the MR appearance of the foot and fetlock in a dismembered forelimb taken from 6-year-old female Quarter Horse that was euthanized for an unrelated disease. This article is of special value because of the excellent quality of the explanatory line drawings accompanying the included MR images—indispensable normal references for those undertaking such examinations.[28]

Later Denoix and co-workers reported the use of MRI (T1-weighted images) on the disarticulated lower forelimbs of three horses that had previously been diagnosed with digital disease (laminitis, navicular disease, and ringbone).[29] The authors concluded, that at least in frozen, disarticulated horse limbs, it was possible to visualize most of the soft tissues of the foot and to detect a variety of abnormalities not visible in radiographs. For example, altered signal intensity was found in articular cartilage, joint capsule, ligaments, tendons, navicular bursa, and collateral cartilages. Lesions were also detected in the subchondral bone of the phalanges and the navicular bone. Kleitter and co-workers, also working with cadaveric material, drew attention to the fact that some signal intensities emanating from dead tissue varied from those obtained from living animals. For example, a T1-weighted image of a dismembered equine digit portrays synovial fluid as a bright, high-intensity signal but in a living horse as a dark, low-intensity signal.[30] Thus teaching and learning from extirpated equine digits can be misleading.

Busoni and Snaps, also using isolated equine feet, determined that a specimen angle of 55 degrees (relative to the primary magnetic field) produced the optimal imagery for the distal part of the deep flexor tendon as it passed over the navicular bone and beyond. Somewhat theatrically, the authors termed their finding the *magic-angle effect*.[31]

Live Horses. Dyson and co-workers performed medical magnetography on 15 live sore-footed horses, concluding that MRI was capable of detecting navicular lesions impossible to identify by any other means.[32] Abnormalities identified with MRI involved the following: articular cartilage, subchondrium and interior of the navicular bone, distal phalanx, distal sesamoidian ligament, navicular bursa, and deep digital flexor tendon. Most lesions were of the *degenerative type*, as indicated by abnormal tissue water content. However, it was conceded that CT would likely provide a more detailed view of cortical bone surfaces.

In conclusion, the authors emphasized that MRI examination of horse feet was costly and time consuming, and it requires a great deal of procedural and diagnostic experience. Magnetogaphy, in the author's opinion, was best suited to lesion confirmation (or denial), rather than preliminary screening.

▮▮▮ SOME USEFUL FOOT FACTS

As they have with other anatomic regions of the horse, Quick and Rendano produced a list of diagnostically valuable facts about the foot, which are listed below,[33] along with a few of my own:

- P3 has three designated surfaces: (1) articular, (2) parietal (also termed the *face*), and (3) solar (also known as the *bearing surface*).
- The parietal sulcus—appearing in the dorsopalmar view as bilateral notches in the lateral borders of P3 immediately distal to the lateral cartilages—harbors the dorsal artery of the foot.
- The solar canal appears as a pair of small radiolucent ovals in the middle third of the distal phalanx.
- The solar margin is normally highly variable, and it must not be mistaken for disease.
- The size, shape, and number of vascular channels in P3 are also highly variable.
- The density of P3 is normally quite variable and can change with age and activity levels.
- The width of the distal interphalangeal joint often appears uneven as a result of the horse shifting its weight (leaning off) when the opposite foot is lifted.
- Many but not all horses have a notched toe, termed a *crena*, which must not be mistaken for focal osteomyelitis.
- If the solar surface of the hoof is not cleaned and packed before being radiographed, a characteristic V-shaped gas shadow may appear in the high coronary view, the result of gas in the sulci.

Normal Anatomic Variations of P3

Foals Versus Adults. The distal phalanx is relatively smaller and narrower in foals compared with juveniles and adults. Likewise, the solar margin of a young foal is considerably smoother and more conical than it is in adults. Kaneps and co-workers cautioned against mistaking the short, curvilinear, marginal lucency, normally found between the proximal and distal angles of the palmar processes of foals up to 3 months of age, for a fracture.[34]

Unique Vascularity of P3. Before considering the many normal variations found in the distal phalanx, I would like first to draw attention to one of its most unique features: its lavish blood supply. Obviously, individual blood vessels are not visible in a plain radiograph, but the canals through which they pass, termed *vascular channels*, are easily seen. Defleshed bone specimens—some with overlying vascular corrosion casts—readily reveal the sheer magnitude of this phenomenon. Also noteworthy is the extremely roughened surface of P3, which becomes quite pronounced distally, especially along its caudolateral wall (Figure 3-3).

Frontal Profile. The fore and hind distal phalanges exhibit subtle but consistent differences in frontal, 65-degree projections, with the solar margin of the rear phalanx appearing relatively more conical in shape, a difference that can sometimes be used to differentiate one from the other in the case of failed marking or mismarking.

Lateral Profile. The dorsal margin of P3 usually appears relatively straight when viewed laterally, but occasionally it appears gently convex (*Roman-nosed*) or, alternatively, concave (*shovel-shaped*). It most instances these are normal anatomic variants, but if there is doubt, the opposite side can be radiographed for comparison. If both appear similar, they are probably normal; if not, there may be some cause for concern.



Figure 3-3 • Corrosion cast demonstrates the rich distal phalangeal and periphalangeal blood supplies and the myriad of bony channels through which the individual vessels pass, accounting for the porous appearance of this region of the bone.

Cortical Thickness and Degree of Arch. The width or thickness of the dorsal cortex of P3 is reported to be thicker in racehorses than in nonracing animals, a finding that I have not observed consistently.[35] The arch of P3 is also quite variable, an observation readily confirmed by viewing the distal phalanx head-on.

Normal Divergence and Convergence ("Rotation"). Linford and co-workers reported that the dorsal surface of P3 may *diverge* from the corresponding surface of the hoof (palmar/plantar "rotation") by as much as 4 degrees in normal Thoroughbreds. Normal *convergence* (pivoting of P3 forward, toward the hoof wall) has also been described (dorsal "rotation"). An overgrown toe often creates the illusion of divergence, whereas excessive trimming has the opposite effect.

Solar Margin. The outer edge of the distal phalanx, the solar margin, is highly variable, ranging from ragged to smooth and regularly interrupted by vascular channels. Many horses feature a thumbprint-like impression centrally, termed a *crena* (Figure 3-4). As already suggested, where doubt exists about the normalcy of such a finding, the opposite limb can be imaged for comparison.[36]

Vascular Channels. The vascular channels or canals of the distal phalanx differ in size, number, and location. Additionally, channel patterns may differ from side to side and from front to rear (see Figure 3-4).

Trabeculation. As with vascular channels, the trabecular pattern of P3 may differ considerably from horse to horse. In some animals the trabeculae appear quite large and distinct, a pattern sometimes referred to as *coarse,* whereas other horses have very thin, barely perceptible trabeculae, termed *fine* (Figure 3-5).

Side Bones (Ossified Collateral Cartilages). Calcified lateral cartilages, or *side bones* as they are commonly termed, can range from nonexistent to enormous, sometimes reaching the pastern joint and beyond. Most are unevenly marginated and irregularly opacified, with the lateral side bone typically larger than its medial counterpart. Often one or both side bones are divided into two and occasionally three pieces as a result of separate ossification centers, with the topmost piece often being canted to one side or the other, resembling a displaced facture (Figure 3-6).

As far as I can determine, there is no evidence that ossification of one or both lateral cartilages causes lameness in horses, although there is published opinion to this effect.

Ruohoniemi and co-workers described the considerable CT and MRI variability seen in the ossified collateral cartilages of Finnhorse cadaver limbs.[37] In a follow-up communication, Ruohoniemi examined the relationship between side bones, navicular disease, and osteoarthritis of the coffin joint in Finnhorse cadaver forefeet. Ossification of the collateral cartilages was found in 36 of 100 feet; however, no demonstrable link was found between the existence of side bones and the presence of either navicular disease or osteoarthritis of the distal interphalangeal joint. Neither was there any evidence that side bones produced pain or lameness in their own right.[38]

Extensor Process. The appearance of the extensor process of the distal phalanx, as seen in lateral profile, varies from rounded to conical. In some horses and ponies, the extensor process appears disproportionately large compared with the remainder of P3. Other horses have a deep indentation in the periarticular portion of the extensor process, an appearance described as "double pointed."

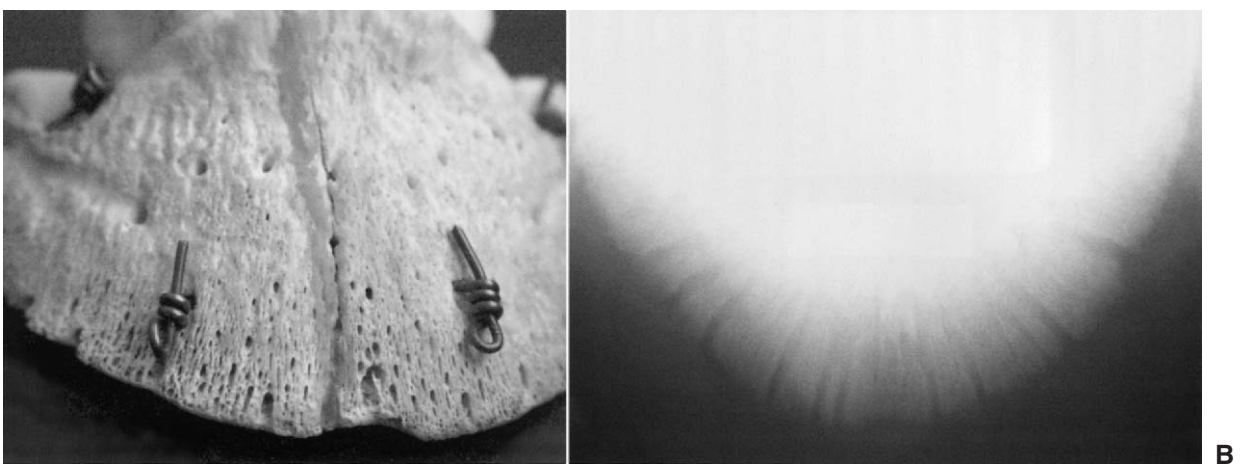


Figure 3-4 • A, Distal phalangeal close-up, frontal perspective, shows a distinctive crena, a shallow concavity located at the center of the solar margin, which is a normal anatomic variation in horses. **B,** A deliberately underpenetrated 65-degree dorsopalmar view of the distal phalanx in a normal horse shows a shallow crena at the center of the solar margin.

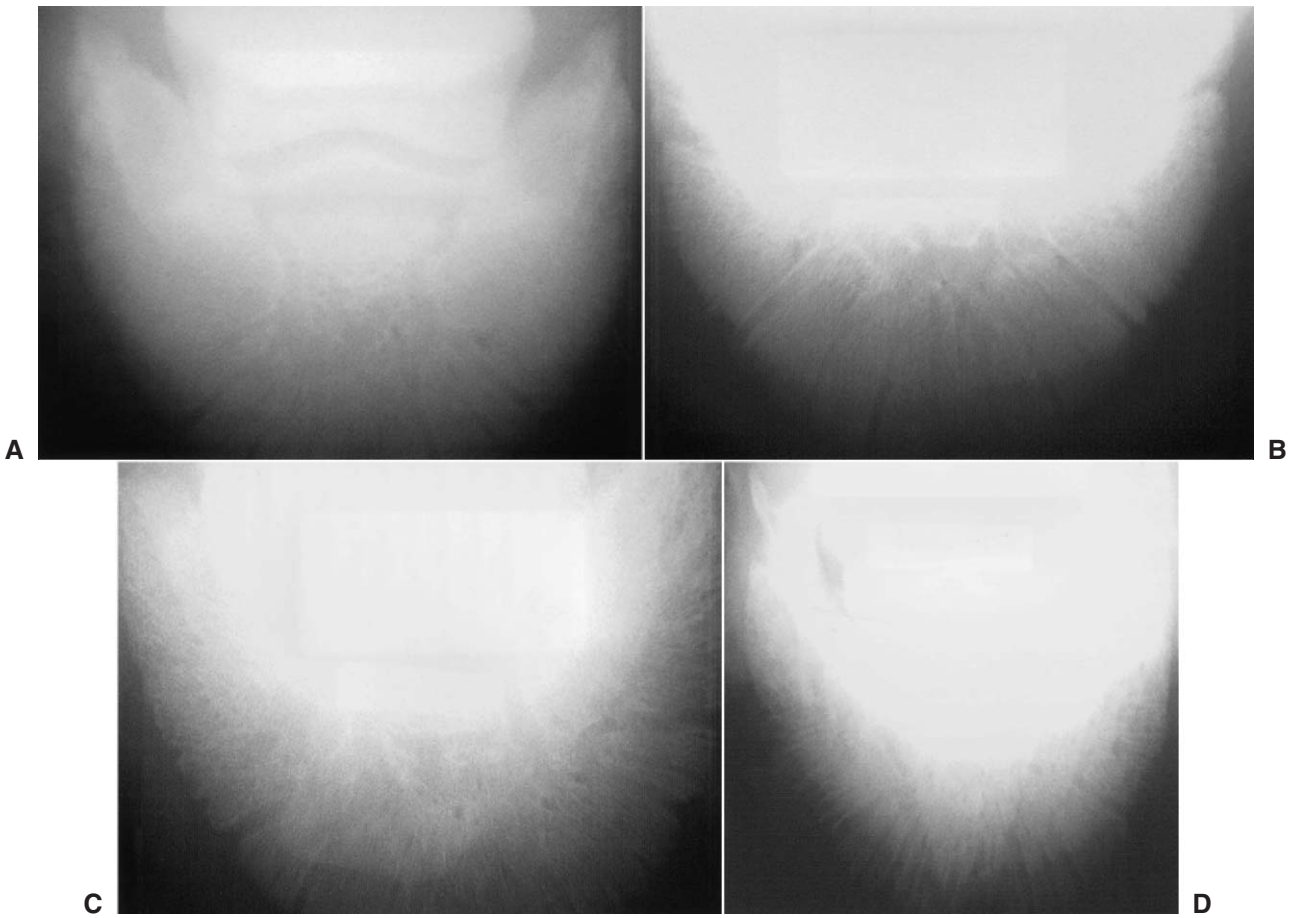


Figure 3-5 • High coronary close-up views of the distal phalanges of four normal horses show variation in normal trabeculation ranging from fine **(A, B)** to coarse **(C, D)**.

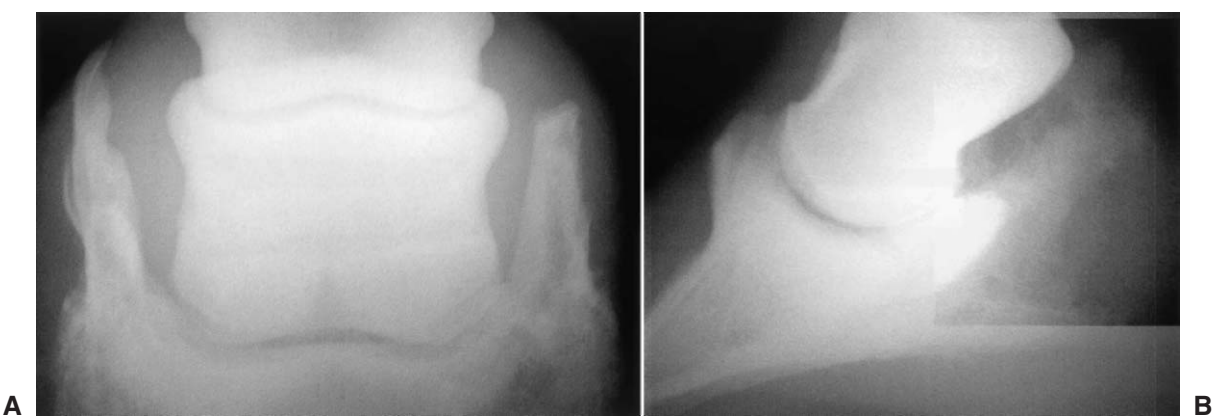


Figure 3-6 • Close-up 45-degree dorsopalmar **(A)** and lateral **(B)** views of a sound horse with large side bone (ossified collateral cartilages).

In newborn foals, the extensor process has been reported as being incompletely mineralized, and thus may be mistaken for osteochondritis or osteomyelitis. The uppermost aspect of the extensor process contains a small curl that functionally behaves as a kind of retainer during flexion.

Figure 3-7 shows a defleshed distal phalanx (emphasis on the extensor process) from four different perspectives.

Simulated Lesions. In 45-degree dorsopalmar dorsoplantar and dorsopalmar oblique views, the dorsal

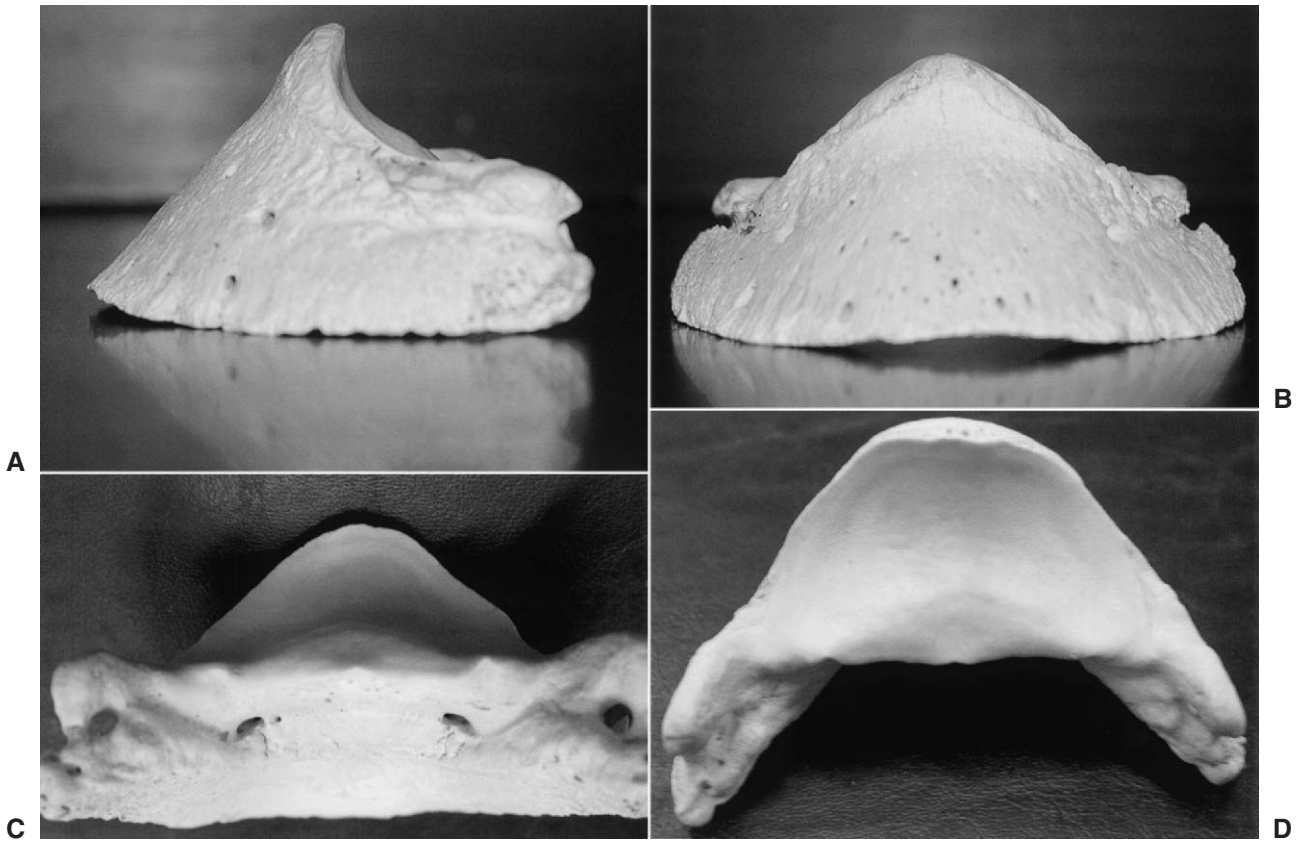


Figure 3-7 • Extensor process of the distal phalanx seen from four different perspectives: side **(A),** front **(B),** rear **(C),** and above **(D).**



Figure 3-8 • A, Proximolateral view of a defleshed distal phalanx shows a distinctive channel running along the caudolateral aspect of the bone, the dorsal groove. **B,** A corrosion cast shows the associated vasculature.

grooves and collateral depressions, situated on either side of P3, can mimic localized bone loss, especially in oblique projections in which symmetry (indicating the unlikelihood of a lesion) is not readily apparent (Figure 3-8).

In lateral views, the solar canal is typically projected end-on, resembling a small bone cyst or focal area of bone loss in the center of P3 (Figure 3-9). See also Pedal Osteitis to follow.

▮▮▮ RADIOGRAPHIC PREPARATION OF THE FOOT

In preparation for radiography and to avoid confusing artifacts, the shoe should be removed and the foot thoroughly cleaned and packed (Figure 3-10). Packing should be done with care, being sure to apply the filler evenly and leaving no misleading gas pockets that might simulate fracture lines or localized infection.



Figure 3-9 • Close-up caudolateral view of a defleshed distal phalanx shows dorsal groove flanked by vascular foramina. The latter may be mistaken for a bone cyst or localized infection.

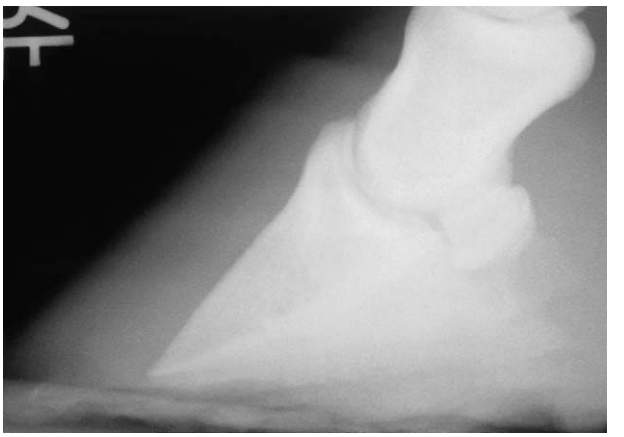


Figure 3-11 • Lateral view of the foot (deliberately underexposed) of a recently foundered horse shows mild distal phalangeal rotation and a faint laminitic lucency. The toe is dangerously close to the sole as a result of the distal phalangeal displacement ("sinking").



Figure 3-10 • Sole of an adult horse seen from below, showing a toothbrush being used to remove soil from the sulci of the frog.

Unevenly applied packing material may cause focal differences in bone density, depending on whether it is relatively thicker or thinner than the surrounding packing. Starrak reported how such differences may be mistaken for disease.[39]

▮▮▮ PEDAL OSTEITIS: ON MYTH AND REALITY

Pedal osteitis is an archaic term that refers to nonspecific inflammation of the distal phalanx. Proponents have traditionally used four radiographic features to render such a diagnosis: (1) decreased bone density; (2) coarse trabeculation; (3) marginal irregularity; and (4) increased size, shape, and number of vascular channels.[40]

Unfortunately, these *supposed* radiographic disease indicators are often found in normal horses. This lack of diagnostic specificity has not only rendered such "signs" unreliable, but worse has led to false-positive diagnosis. Accordingly, I strongly recommend that this diagnosis be used with considerable caution or, better, avoided altogether.

▮▮▮ LAMINITIS (FOUNDER)

The Standard Laminitis Series

A single relatively light, lateral view of the foot is sufficient to confirm distal phalangeal rotation or displacement in most instances (Figure 3-11). Because the coronet is radiographically visible, and thus can be used as a reference point in progress films, metallic marking of the dorsal surface of the hoof—wire, lead shot, and the like—is superfluous, although the practice still exists on a limited basis.

Small fractures from the dorsal edge of the solar margin are often visible as subtle, forward deflections of the tip of P3 as seen in lateral projections. Where uncertainty exists, a 65-degree dorsopalmar view made with a grid may reveal a minimally displaced fragment. Even when shod, it is still possible to assess the central part of the solar margin for such fractures (Figure 3-12).

▮▮▮ PHALANGEAL ROTATION AND RELATED RADIOMETRICS

When the dorsal surface of the distal phalanx pulls away from the inner surface of the hoof wall, it is referred to as *rotation.* Actually, it is the distal two thirds of P3 that rotates away from the hoof, leaving

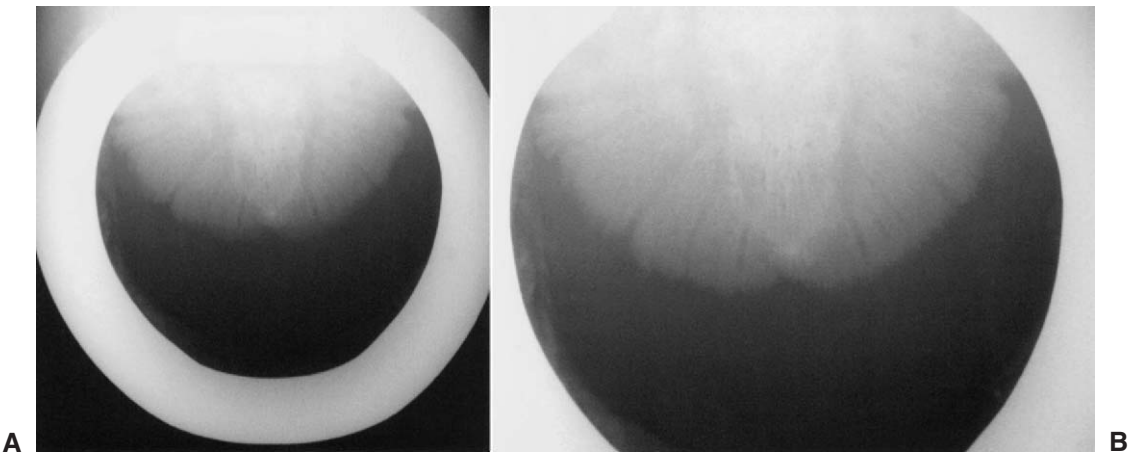


Figure 3-12 • High coronary **(A)** and high coronary close-up **(B)** views of the distal phalanx of a laminitic horse made with the shoes on. The focal concavity in the central solar margin is the crena, a normal variant in horses. The relatively roughened lateral solar margin (best seen in the close-up) is also a normal variant.

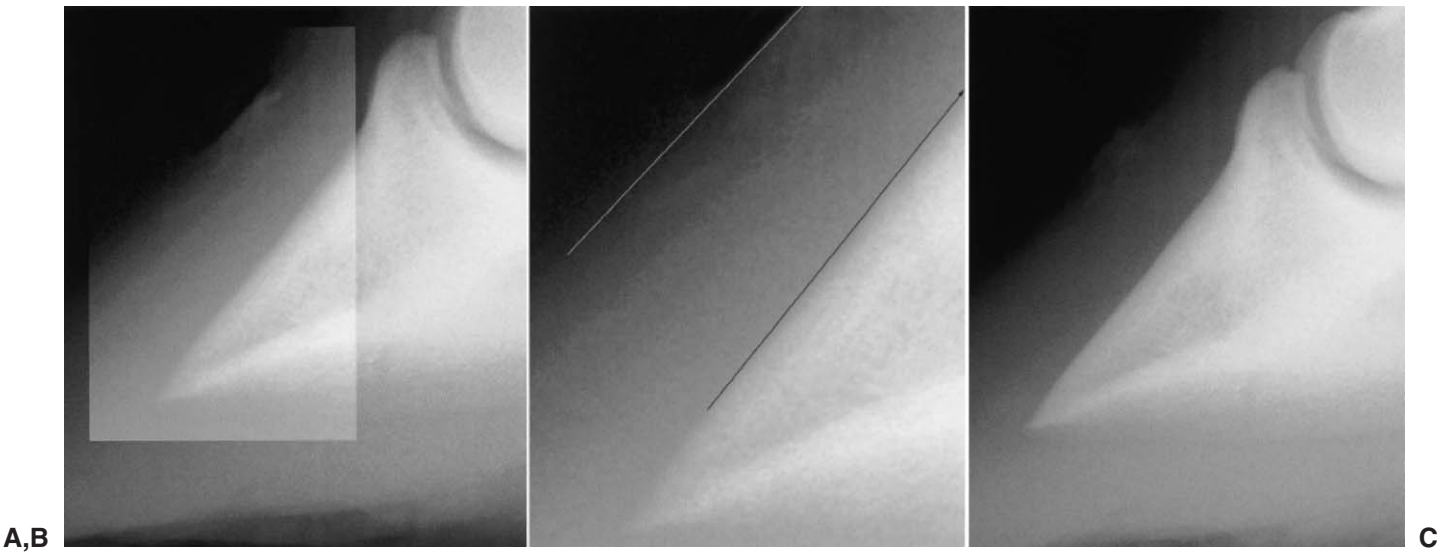


Figure 3-13 • Distal phalangeal radiometrics. **A,** Close-up lateral view of the distal phalanx of a foundered horse (soft tissues emphasized). **B,** Lines drawn along the dorsal surfaces of the hoof wall and as corresponding surface of P3 diverge, consistent with mild rotation. **C,** A lateral radiograph of a healthy horse is provided for comparison.

the extensor process in a comparatively normal location, but the major observation remains the same: P3 is obliquely positioned relative to the outer surface of the hoof.

In a lateral radiograph, the presence and severity of distal phalangeal rotation are judged by the spatial relationship between P3 and the hoof wall, specifically, the *loss of a parallel alignment*. As the laminitic foot degenerates and the distal phalanx detaches, the normal parallel relationship between the two is lost. Imaginary lines drawn along the surfaces of the hoof and P3 will now appear divergent, rather than parallel, as they do in a normal horse (Figure 3-13).[41]

There can be a problem, however: The distal aspect of the hoof may be elongated because of a lack of recent trimming. Thus an imaginary line extended along the leading edge of the hoof will diverge from a corresponding line drawn along the front surface of P3.

An additional, but less significant, problem is the anatomic variation in the lateral profile of P3, which can appear straight, convex, or concave. In the latter instances, and depending on how the line is drawn, false divergence may result. Finally, and as reported by Koblik and co-workers, if something less than a true lateral projection of the distal phalanx is obtained, otherwise parallel lines can appear divergent.[42]

Using Estimation Lines

The aforementioned problems can be largely overcome by being *selective* when placing estimation lines along the dorsal surfaces of the hoof and P3:

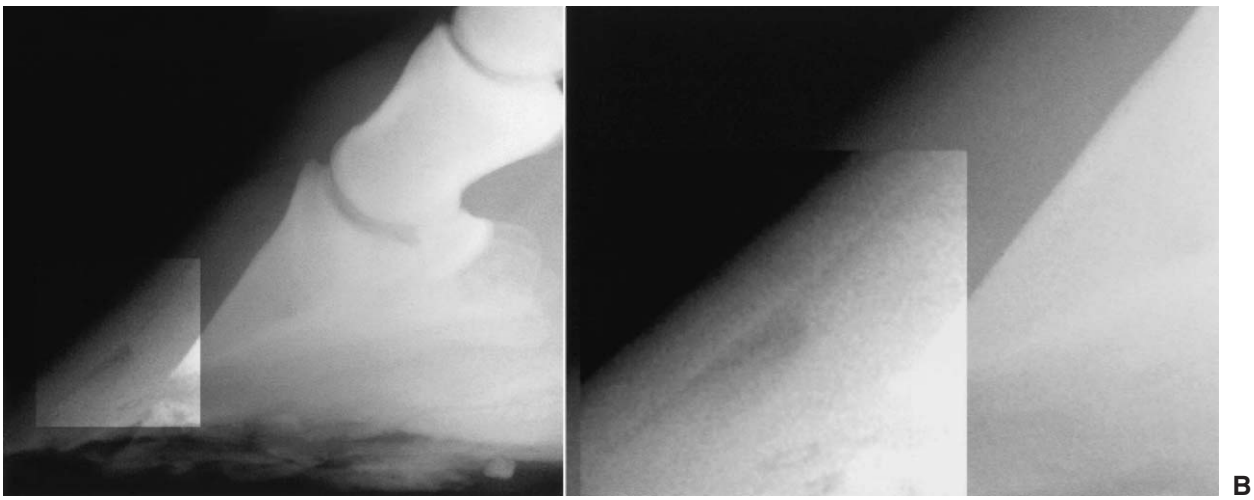


Figure 3-14 • Lateral **(A)** and lateral close-up **(B)** views of distal phalanx show moderate distal phalangeal rotation with a triangular gas pocket underlying the distal hoof *(emphasis zone).*

- In the case of the hoof, begin the line just below the coronet, and extend it distally until reaching the flair of the toe and then stop.
- Begin the line along the front surface of P3 just below the extensor process, and continue to the tip of P3. If the dorsal surface is convex, draw a line of best fit. Do the same if the surface is concave.
- Then compare the lines to see whether they are parallel.

For more practical information on the balancing of horses' feet (with or without laminitis), I strongly recommend the review by Balch and colleagues.[43]

Distal Phalangeal Displacement (Phalangeal "Sinking")

As mentioned earlier, a single lateral image of the distal phalanx is usually sufficient to detect distal displacement of P3 within the hoof, provided the degree of displacement is marked. Otherwise, an earlier or later comparison view is necessary. Metallic markers imbedded in, taped on, or glued to the dorsal surface of the hoof can be used as radiographic reference points for those producing high-contrast, short-scale films, which often fail to portray the hoof wall adequately.[44]

Sinking can also be assessed radiometrically using the *Linford method*, in which the width of the soft tissue overlying the dorsal surface of P3 is computed as a percentage of the length of P3 (as determined from a lateral radiograph).[45]

Gas

Gas lying along the inner surface of the hoof wall constitutes strong presumptive evidence of founder, the result of either atmospheric contamination through a penetrated sole or coronary drainage. Gas may also be released from hemoglobin secondary to disintegrating red blood cells[46] (Figure 3-14).

New Bone and Distal Phalangeal Fractures

With the exception of the extensor process, new bone is not readily formed on the surface of the distal phalanx. This is due in large part to its single layer of fibrous periosteum, which coats all but the extensor process. The carpal and tarsal bones have a similar primitive covering, which responds much more slowly to physical or chemical injury than other portions of the skeleton.

Accordingly, acute and subacute laminitis produces no structural changes in the distal phalanx. The exception to this rule is when there is severe rotation that eventually leads to penetration of the sole, fracture of the tip of P3, and secondary osteomyelitis. Horses that recover from these additional injuries are typically left with a small, deformed foot or, in the severe instance, little more than a digital stump.

Hoof Wall

Laminitis often leaves the hoof wall with a distinctive wrinkled appearance, secondary to the related vascular injury. There may also be large hoof defects, the result of therapeutic trimming.

The Previously Foundered Foot: Radiologic Clues

Horses that have foundered previously, but currently show no evidence of rotation, may provide indirect evidence of their orthopedic past in the form of one or more of the following distal phalangeal alterations, as seen in lateral projection:

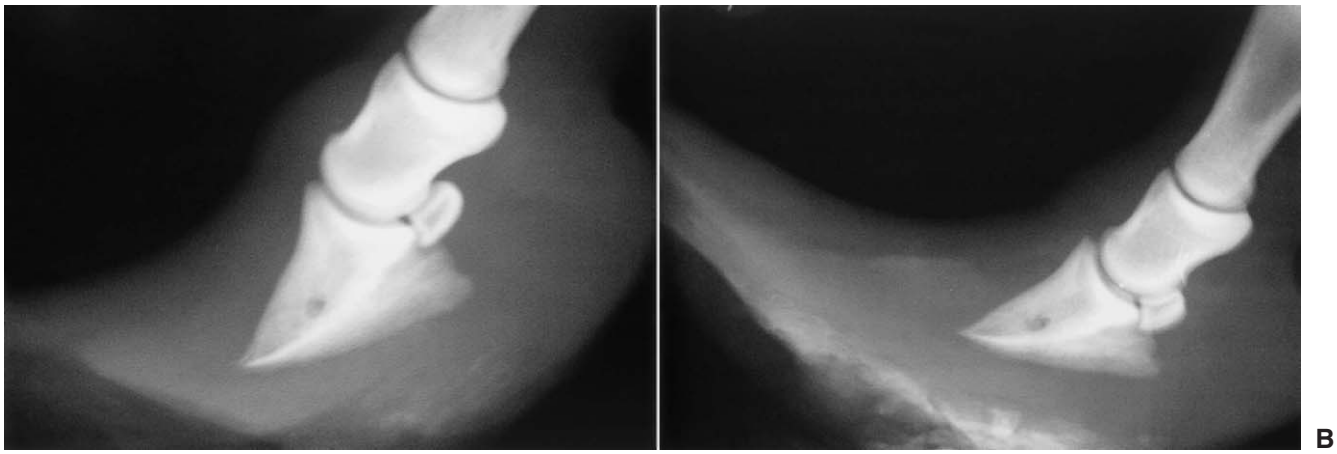


Figure 3-15 • A, Lateral view of laminitic front foot of a 2-year-old pony shows (1) distal phalangeal rotation, (2) secondary fracture of the tip of P3, (3) pronounced rocker sole, and (4) a badly overgrown toe. **B,** The opposite front foot is also badly deformed, but as yet it is not fractured.

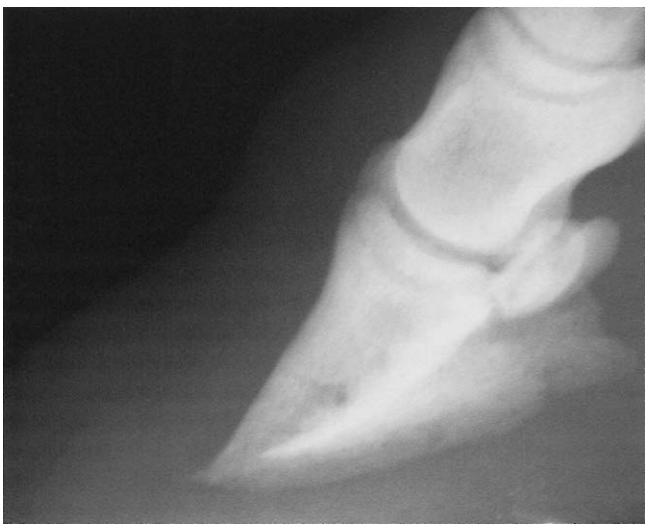


Figure 3-16 • Lateral view of the foot of a foundered pony shows moderate rotation with a secondary fracture of the tip of P3.

- A wrinkled or deformed hoof wall
- A mildly convex, variably laminated dorsal surface
- A triangular, variably sized distal spur
- Reduced bone density at the tip of P3
- Abbreviated size
- Abnormal shape

Various combinations of the foregoing radiographic disease indicators are shown in Figures 3-15 to 3-20.

Radiographic Prognosis in Chronic Laminitis

Generally speaking, the combination of rotation, distal displacement, and laminar gas does not bode well for functional recovery. Solar penetration, with or without fracture or infection, is usually profoundly debilitating and often leads to eventual euthanasia.[47] Even if a foundered animal recovers physically, it may have to contend with a lifetime of chronic foot pain.[48]

Box 3-3
Radiographic Observations in Horses That Develop Laminitis in One Foot and Subsequently in Another

Distal displacement (sinking) occurred before rotation.
A radiometric value of greater than 28.1% (dorsal soft-tissue thickness as a percent of distal phalangeal length) indicates distal phalangeal displacement indicative of laminitis.
Only 25% of the animals studied had radiographic evidence of cavitation of the coronary band.

Development of Laminitis in the Opposite, Initially Normal Foot

Peloso and co-workers published their observations in 20 foundered horses that initially developed laminitis in a single front foot and later in the other.[49] The *duration of lameness* was deemed to be the single greatest risk factor for the eventual development of laminitis in the opposite foot. Surprisingly, and contrary to the prevailing belief at the time, being overweight was not a factor.

The authors made the following radiographic observations regarding the potential development of laminitis in the opposite limb (Box 3-3).

Use of Radiographs as an Aid to Corrective Shoeing and Trimming in Horses With Chronic Laminitis

Readers are advised to consult one or more of the many excellent textbooks and journal articles written

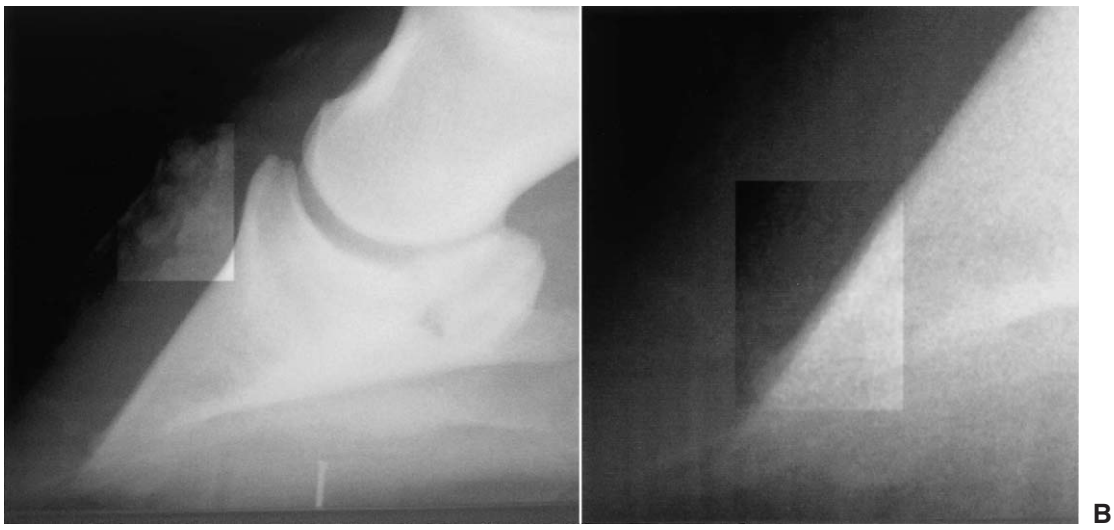


Figure 3-17 • Lateral **(A)** and lateral close-up **(B)** views of a front foot in a foundered mare show: (1) distal phalangeal displaced, without rotation; and (2) a characteristic bone deposit just proximal to the tip of P3 *(emphasis zone).* Mud on the upper part of the hoof *(emphasis zone)* mimics deformity often associated with chronicity.

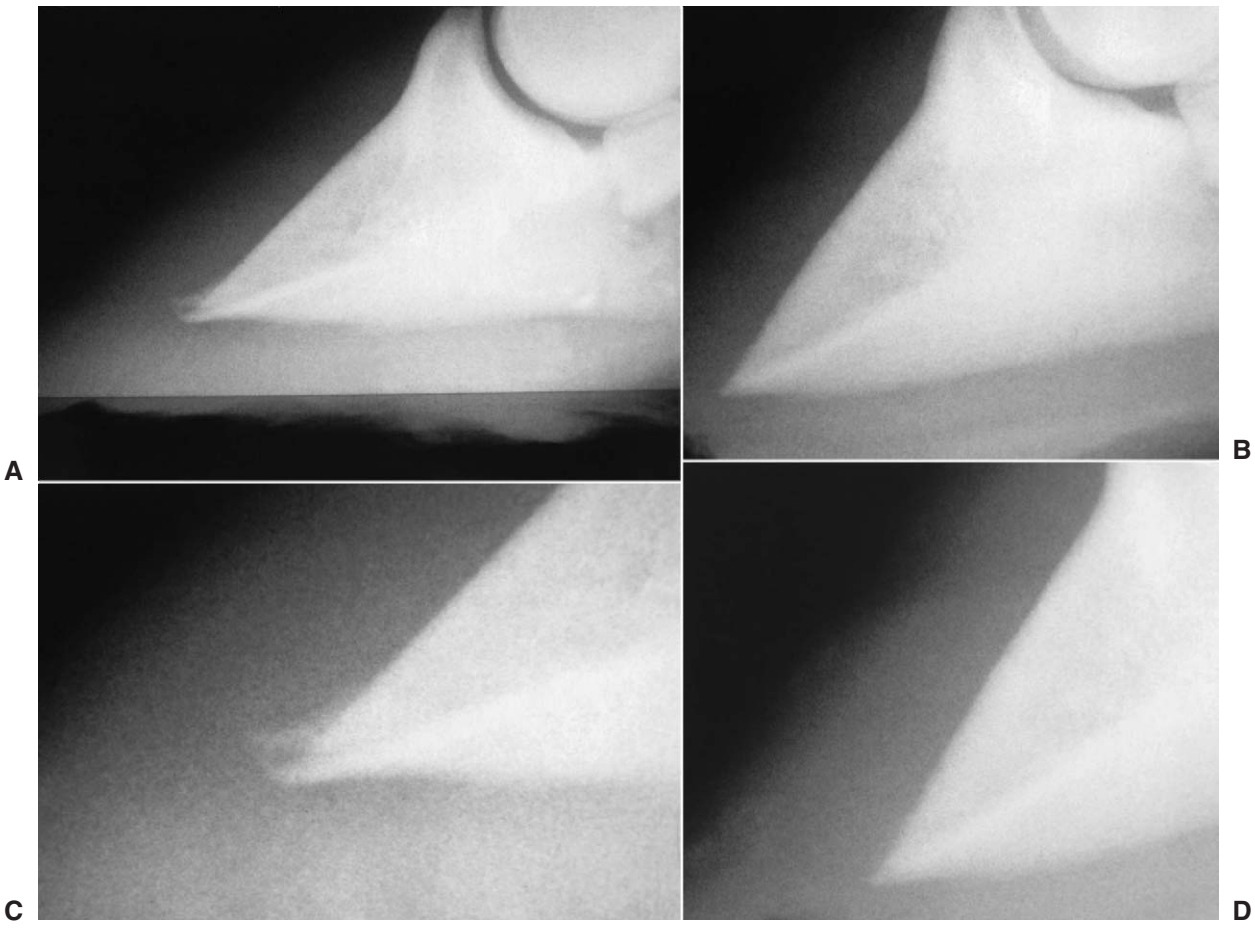


Figure 3-18 • Lateral close-up **(A)** and ultra-close-up **(B)** views of a pathologic distal phalangeal fracture in a foundered horse. Lateral close-up **(C)** and ultra-close-up **(D)** views of the opposite front foot are provided for normal comparison.

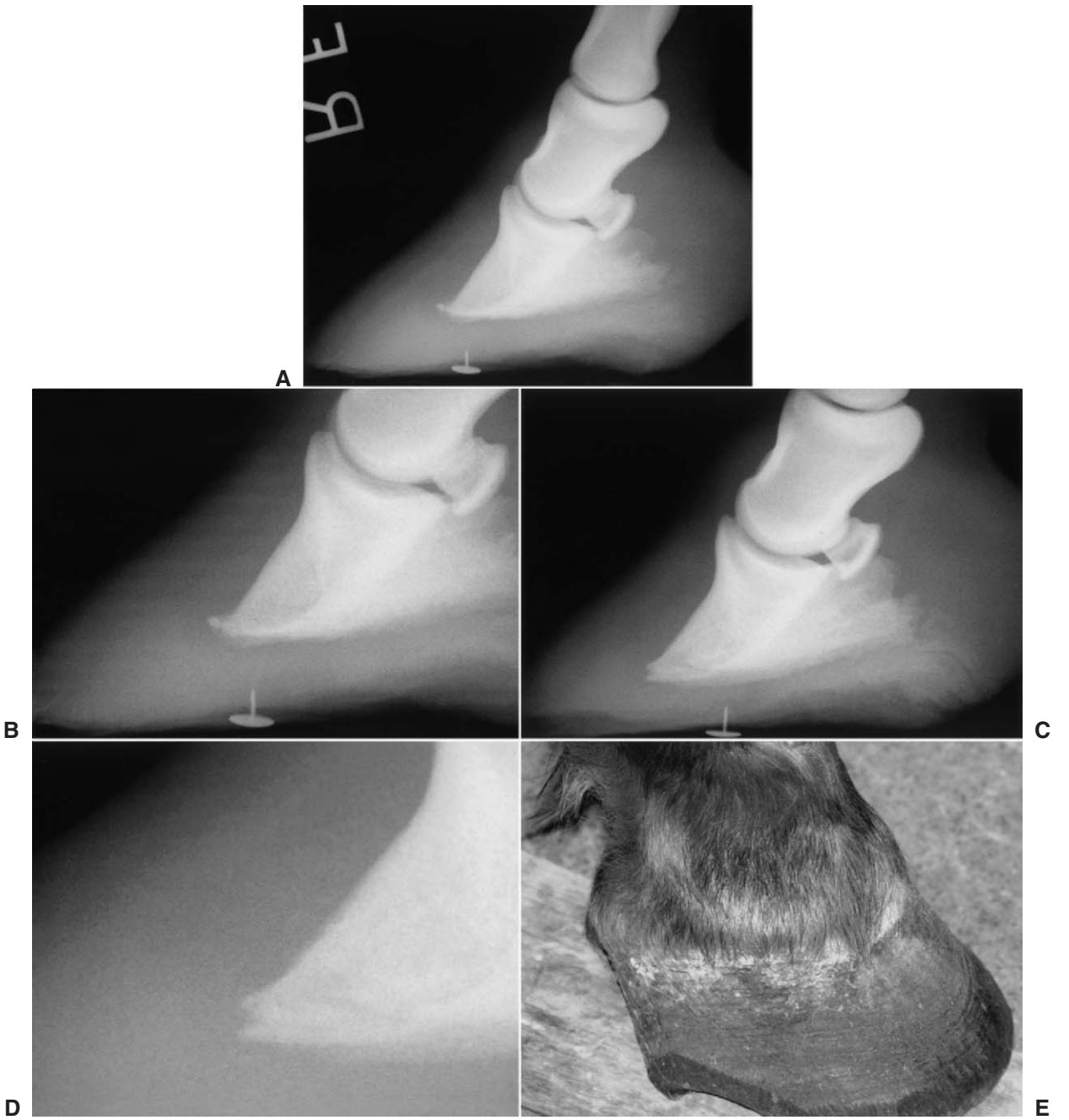


Figure 3-19 • Right **(A, B)** and left **(C, D)** lateral and lateral close-up views of a pony with laminitis show rotation and tip-fractures bilaterally (tack marker was by special request). The animal's recently trimmed and rasped left forefoot is also included **(E).**

by both farriers and veterinarians on the use of radiographs as a guide for shoeing the laminitic horse.[50]

Advanced Age, Pituitary Disease, and Laminitis

Studying nearly 500 older horses and ponies, a third of which had a history of laminitis, Brosnahan and Paradis found pituitary disease prevalent in those 30 years of age and older, suggesting a possible causal relationship.[51]

Blood Supply in Experimental Laminitis

Guffy and co-workers reported that experimentally created laminitis in adult horses caused a *decrease* in the arterial blood supply through the terminal arch and, in some instances, completely destroyed it.[52] Later, Ackerman compared the angiographic appearance of normal and laminitic feet (Table 3-2).[53]

Garner and co-workers created acute laminitis in otherwise healthy horses by overfeeding carbohydrates, determining that even though peripheral

appendicular circulation was decreased, cardiac output was increased.[54]

▮▮▮ MIDDLE PHALANGEAL FRACTURES

Fractures of P2, particularly avulsion fractures of the palmaromedial eminence, are most common in cutting, reining, and barrel racing horses, presumably the result of the tremendous force exerted on this part of the bone when making abrupt turns or stops.[55] The resultant damage to the bearing surface of P2 is often quite severe, featuring large, uneven crevices and numerous small bone and cartilage fragments. Displaced fractures of both the lateral and medial eminences are usually accompanied by additional breaks that may extend distally into the coffin joint.

Table 3–2 • ANGIOGRAPHIC APPEARANCE OF NORMAL VERSUS LAMINITIC FOOT

Normal Foot	Laminitic Foot
Complete filling of terminal arch	Poor filling of terminal arch
Eight to 10 primary arterial branches between 0.1 and 0.2 cm in diameter	Larger but fewer arterial branches
Symmetric vascular network in the corium of the hoof	Corial vasculature less dense and disorganized
Numerous fine vessels in the corium of the coronary band	Irregular vasculature in the corium of the coronary band
Fully vascularized hoof corium	Areas of avascular hoof corium
Regular, smooth corial vessels	Irregular, tortuous vessels in corium of coronary band

Comminuted middle phalangeal fractures can be difficult to assess radiographically, especially with respect to the size and number of fragments and whether or not they enter the proximal or distal interphalangeal joints. The problem is made even greater when pain prevents the fractured leg from being positioned in the standard manner. In such circumstances, CT will often prove indispensable, provided the animal can be put under general anesthesia and, equally important, recovered.[56]

Some comminuted fractures of the short pastern can be reduced and maintained only by plating the damaged phalanx to the adjacent, uninjured, proximal phalanx, a technique described by Crabill and co-workers.[57] Additional examples of middle phalangeal fractures can be seen in Chapter 4.

▮▮▮ DISTAL PHALANGEAL FRACTURES

Distal phalangeal fractures most commonly occur in Thoroughbreds, Standardbreds, and working Quarter Horses, but they can occur in any breed under the right, or perhaps more accurately, the wrong circumstances. Predisposing factors include (1) racing on excessively hard surfaces; (2) blunt trauma, such as kicking a stall door or stock rail; (3) falling or colliding with another horse during a race; and (3) preexisting bone or foot disease, such as laminitis, nonspecific P3 changes (pedal osteitis), and osteomyelitis, the latter being a form of insufficiency fracture. Less certain biomechanical influences include upright conformation, improper hoof trim, or unbalanced shoeing. A hind distal phalangeal fracture was reported in a 7-year-old Tennessee Walker after it fell on pavement.[58]

Scott and co-workers reported that most distal phalangeal fractures were articular and involved the forelimbs. The great majority of breaks were either through the left lateral or right medial surface of the bone, reflecting the uneven weight distribution that occurs when racing counterclockwise.[59]

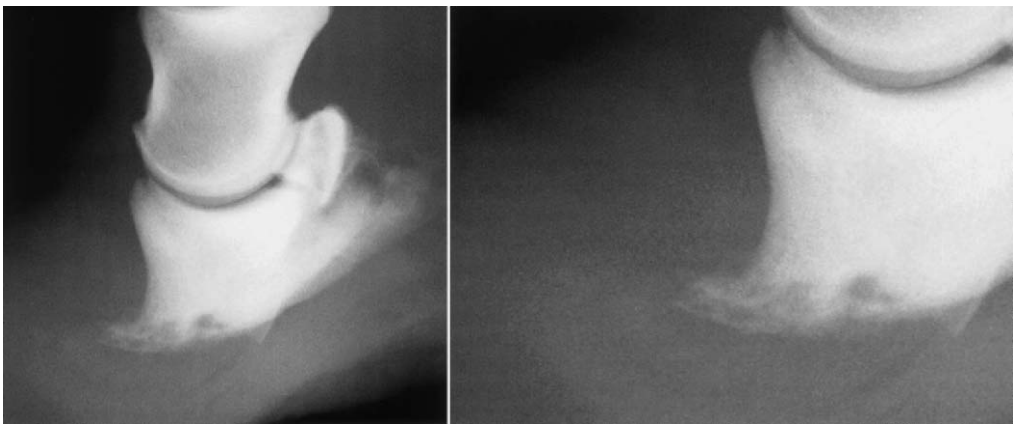


Figure 3-20 • Lateral **(A)** and lateral close-up **(B)** views of the right front foot of a chronically foundered Arabian gelding show a severely deformed distal phalanx, the combined result of rotation, distal displacement, multiple toe fractures, and a failed attempt at repair.

Clinically, horses with acute P3 fractures typically show one or more of the following abnormalities: (1) lameness; (2) regional hyperemia, as indicated by a stronger than normal digital pulse and excessive heat at the coronary band; and (3) withdrawal of the foot when compression is applied with hoof testers. Generally, signs are less pronounced in chronic injuries, especially if they are nonarticular.

Differential diagnosis for P3 fractures is listed in Box 3-4.

The Standard P3 Fracture Series

A standard P3 fracture series consists of four views: a high coronary (70-degree DP), right and left frontal obliques (same projection angle as in standard DP), and a true lateral. The oblique projections are a hedge against missing a minimally displaced articular fracture located in the outside third of the body of P3 or a caudally located wing fracture.[60]

Box 3-4
Differential Diagnosis of Distal Phalangeal Fractures

Sole bruise (severe)
Sole abscess
Foreign body
Osteomyelitis
Navicular disease
Navicular fracture
Navicular infection
Osteochondritis of subchondral bone of P3
Osteochondritis of extensor process
Laminitis

Caution: *Gas or dirt trapped in the sulci of the frog can be mistaken for a fracture, especially in the high coronary view (Figure 3-21).*

Classification of Distal Phalangeal Fractures

Scott and co-workers have numerically classified P3 fractures,[61] although a simple anatomic description is quite acceptable and is my personal preference. As a related aside, I have found that most veterinary students and many of their teachers tend to confuse the numeric designations of these fractures unless they have recently reviewed the literature, lending further currency to the view that in most instances a simple anatomic description is superior to a formal numeric classification (Table 3-3).

Distal Phalangeal Fracture Types

Complete (Articular) Fracture. Most P3 fractures are complete, extending fully through the bone in the sagittal or parasagittal plane. Because these fractures enter the coffin joint proximally, they are also articular in nature. In my experience, fractures breaking into the central third of the coffin joint are generally more painful, cause greater articular disruption, and are slower to heal than outer third fractures.

Solar Margin Fracture (Marginal Fracture)

Toe Fractures. Small elliptical fractures from the dorsal-most aspect of the solar border of P3 (as viewed laterally) are known as *toe fractures.* Most toe fractures are the indirect result of distal phalangeal rotation subsequent to laminitis and, as such, can be considered

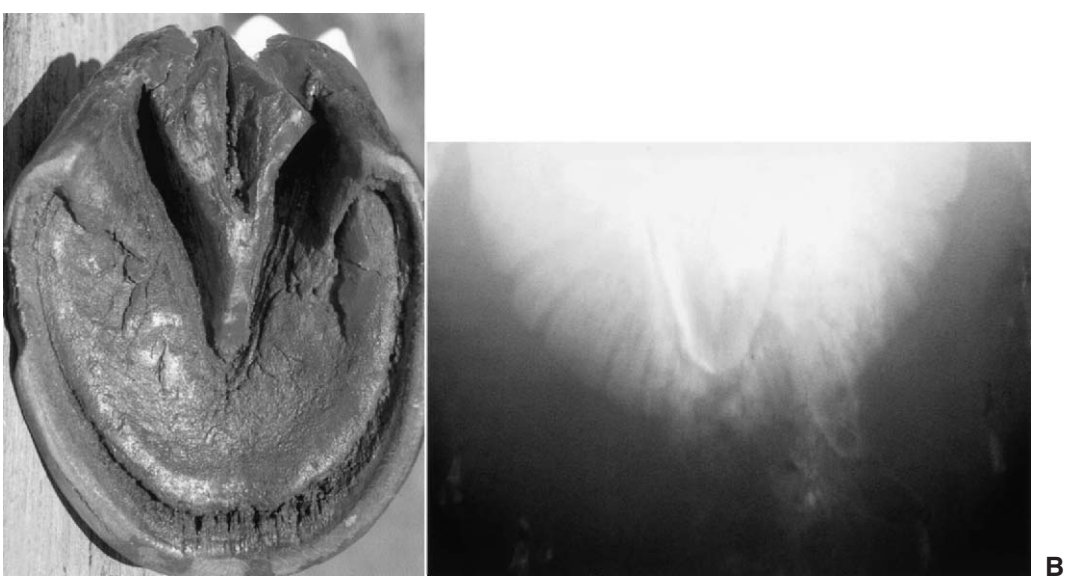


Figure 3-21 • Sole of an adult horse viewed from below **(A)** shows deep, V-shaped crevices: the sulci flanking the caudally situated frog. These channels should be cleaned and packed with radiotransparent material before radiography to avoid diagnostically confusing V-shaped artifacts exemplified in the accompanying radiograph **(B).**

insufficiency fractures. When P3 penetrates the sole, becomes infected, and is structurally degraded, it usually is subject to a similar fate.

Marginal Sequestrum

Osteomyelitis of P3 secondary to a sole abscess or direct inoculation from a penetrating wound can lead to the death and detachment of small pieces of the solar margin, so-called *saucer fractures* or *sequestra.*

Table 3–3 • A NUMERIC CLASSIFICATION FOR P3 FRACTURES

Type 1	Nonarticular fracture of the palmar or plantar process (nonarticular wing fracture)
Type 2	Articular wing fracture
Type 3	Midsagittal articular fracture
Type 4	Extensor process fracture (presumed avulsive in nature)
Type 5	Comminuted fracture
Type 6	Solar margin fracture

From Scott EA, McDole M, Shires MH: A review of third phalanx fractures in the horse, *J Am Vet Med Assoc* 174:1337, 1979.

Medial and Lateral Palmar Process Fracture ("Wing" Fracture)

Complete fractures of the palmar (plantar) process often spare the coffin joint, making them less painful than articular P3 fractures. Because these fractures typically break through the wing transversely, they can be difficult or impossible to visualize in standard frontal or lateral projections, especially if they are fresh. For this reason, right and left frontal obliques should be included when fracture is suspected.

In instances in which the initial radiographic examination appears normal as a result of insufficient fragment displacement, a follow-up examination made 2 to 4 weeks later will usually reveal the break. Alternatively, nuclear medicine can be used,[62] although it is anatomically much less precise and sometimes ambiguous. CT is usually definitive provided that the slices are no more than 2 millimeters thick with a corresponding gap between slices.

Martens and co-workers reported the CT appearance of an incomplete lateral wing fracture in a 2-year-old Standardbred filly, a fracture not identified in two earlier radiographic examinations made 1 and 6 days after the onset of a sudden, non–weight-bearing lameness.[63]

Figures 3-22 to 3-28 illustrate a variety of distal phalangeal fractures described in this section.

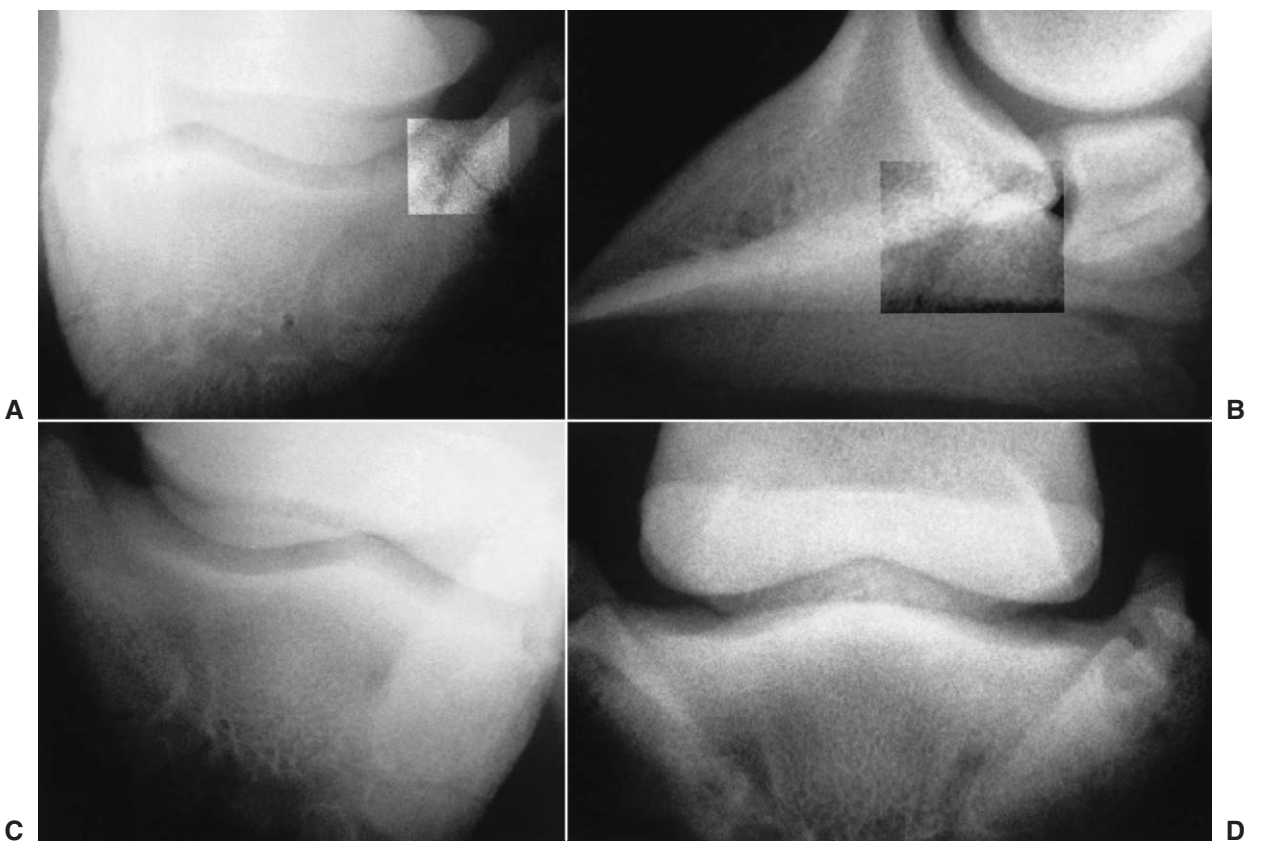


Figure 3-22 • Sixty-five-degree dorsopalmar (DP) oblique **(A)** and true lateral **(B)** views of the distal phalanx show a nonarticular, hairline fracture of the lateral wing. An oblique view of the opposite wing **(C)** and 45-degree DP view **(D)** fail to identify the break.

Extensor Process Fracture

Fragmentation of the extensor process has been attributed to at least five causes: (1) traumatic avulsion by the common digital extensor tendon, (2) blunt-force injury, (3) osteochondritis, (4) pathologic fracture through a subchondral bone cyst,[64] and (5) nonunion of an accessory growth center, a so-called congenital fracture.[65] In the case of the last two possibilities, bilateral involvement should be anticipated, which if absent should cast serious doubt on the diagnosis.

Pathologic Fracture

Verschooten and DeMoor reported the radiographic appearance of what was presumed to be a pathologic fracture of P3, through a bone cyst located just beneath the extensor process. As with most fractures of this type, the extensor process remained in a relatively normal position, whereas the rest of P3 and the navicular bone appeared detached and displaced in a caudoproximal direction.[66]

Healing of Distal Phalangeal Fractures

Radiographic Assessment. Honnas and co-workers evaluated the healing of 36 distal phalangeal fractures using serial radiography.[67] Included among the described injuries were both articular and nonarticular fractures involving the extensor process, sagittal and parasagittal portions of the body, wing, and solar margin. As recognized previously, fracture lines widened during the first few weeks after the initial injury, achieving a maximum width at between 4 and 6 weeks.

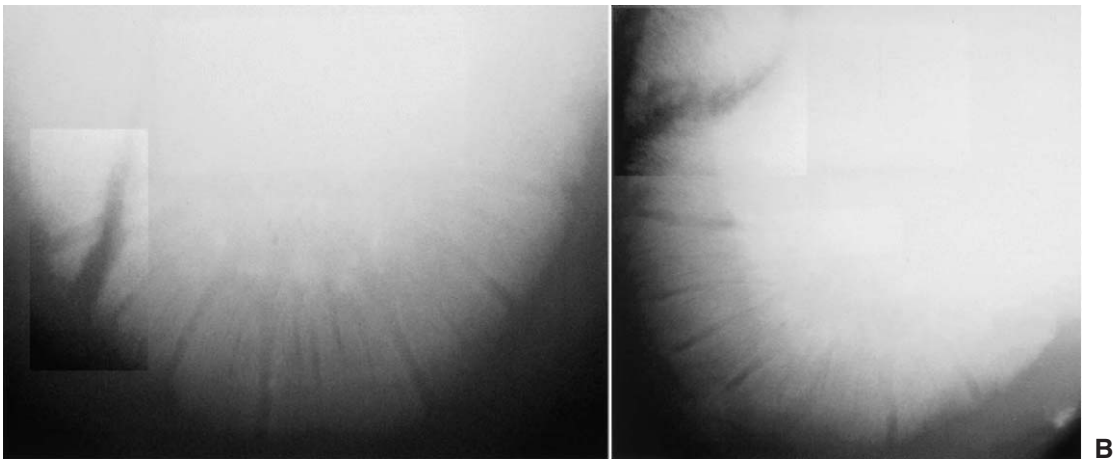


Figure 3-23 • The clarity of distal phalangeal wing fractures, and thus their identification, changes with the projection angle, as illustrated in this pair of films made directly from in front of the foot **(A)** and at a 30-degree angle **(B).**



Figure 3-24 • Sixty-five-degree dorsoplantar oblique view of the distal phalanx shows an articular wing fracture not visible in the nonobliqued projection.



Figure 3-25 • Displaced, parasagittal, articular fracture of the distal phalanx.

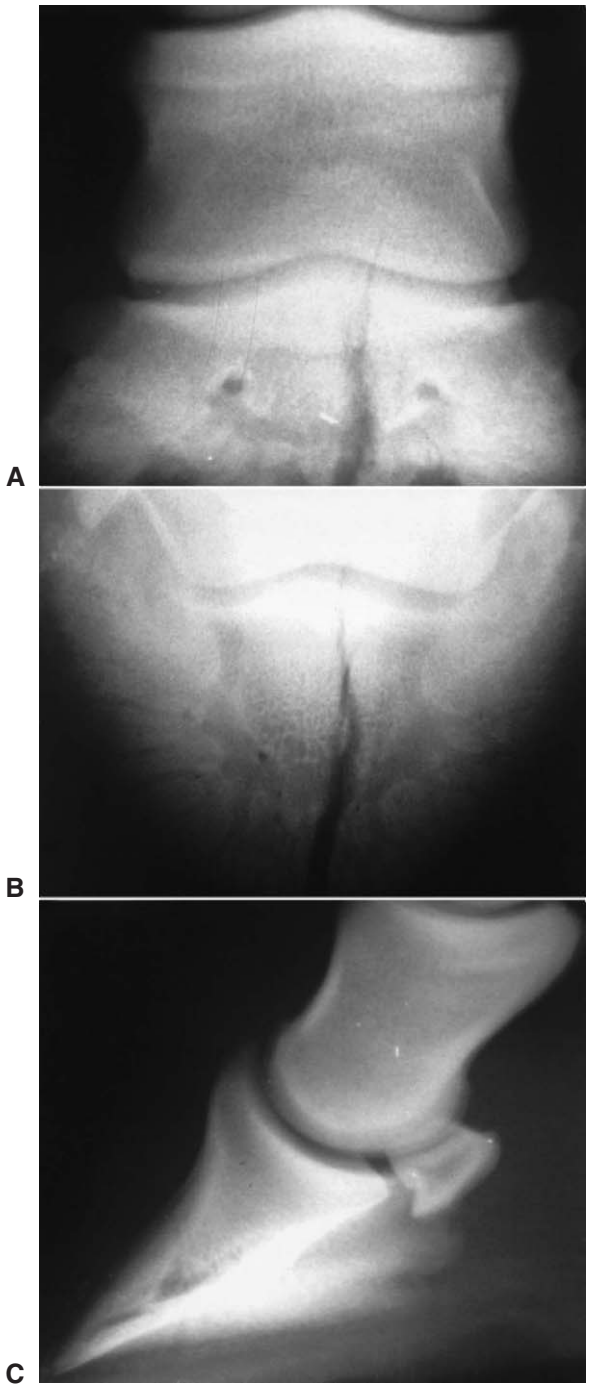


Figure 3-26 • Close-up, 45-degree dorsopalmar (DP) view **(A)** shows a displaced midsagittal, articular fracture of the distal phalanx extending well into (and probably through) the extensor process, a fact not appreciable in the 65-degree DP **(B)** and lateral **(C)** views.

Sixty percent of the fractures healed completely after a mean of 11 months. In eight horses with complete parasagittal fractures, all but the articular portion of the fracture line disappeared at a mean of 11 months. All the fractures that eventually healed showed some signs of healing by 6 months. Nonarticular fractures were more likely to heal completely than those that entered the coffin joint. Only about half the horses with P3 fractures, whether articular or nonarticular, fully healed or not, eventually become sound.

Scintigraphic Assessment. Keegan and co-workers described the scintigraphic appearance of 27 distal phalangeal fractures finding, not unexpectedly, that the fresher the fracture, the greater the isotopic uptake. Compared with radiographs showing the fracture, the palmar scintigraphic projection proved the most accurate in depicting the break.[68]

▮▮▮ DISTAL PHALANGEAL DISLOCATION (SUBLUXATION)

Barber described distal phalangeal subluxation in the horse resulting from a variety of causes, including (1) congenital rupture of common digital extensor tendons, (2) coffin joint infection leading to vascular thrombosis and necrosis of the joint capsule, (3) torn joint capsule, and (4) nonspecific sprain.[69] Working on many of these same cases, I have found that in some instances distal phalangeal subluxation can be demonstrated only using stress radiography; either the passive type—placing the foot on an upwardly inclined plane—or actively stressing P3 by pushing its cranioventral aspect proximally. These stress maneuvers can be painful and sometimes cause the horse to stumble or fall. Analgesia and increased caution during the procedure are advisable. Examples of coffin joint dislocation are shown in Figures 3-29 and 3-30.

▮▮▮ P3 INFECTION

Description: A Function of Depth (Periostitis, Osteitis, Osteomyelitis)

Normally bone infection is described according to depth. For example, surface infection presumed to involve only the periosteum is termed *periostitis,* subsurface or cortical infection is termed *osteitis,* and deep infection involving both the medullary cavity and the cortex is termed *osteomyelitis.*

Periosteal Difference

The value of the foregoing classification is somewhat limited in the case of P3 infection because all but the extensor process is covered by a primitive type of fibrous periosteum that is far less reactive than the double-layer periosteum that coats the long bones. This means that, unlike infected long bones, which usually show new bone deposition within a week or so of becoming infected, most distal phalangeal infections do not become apparent for a month or longer. The carpal and tarsal bones are also covered by a single-layer, fibrous periosteum and typically do not show postinfectious new bone for at least a month.



Figure 3-27 • Sixty-five-degree, mild oblique **(A),** 65-degree, moderate oblique **(B),** and 45-degree dorsopalmar **(C)** views of the distal phalanx show a displaced parasagittal articular fracture, the clarity of which is highly dependent on projection angle.



Figure 3-28 • Forty-five-degree dorsopalmar (DP) **(A)** and 45-degree DP close-up **(B)** views show disruption of the articular surface of P3, the result of a parasagittal fracture.

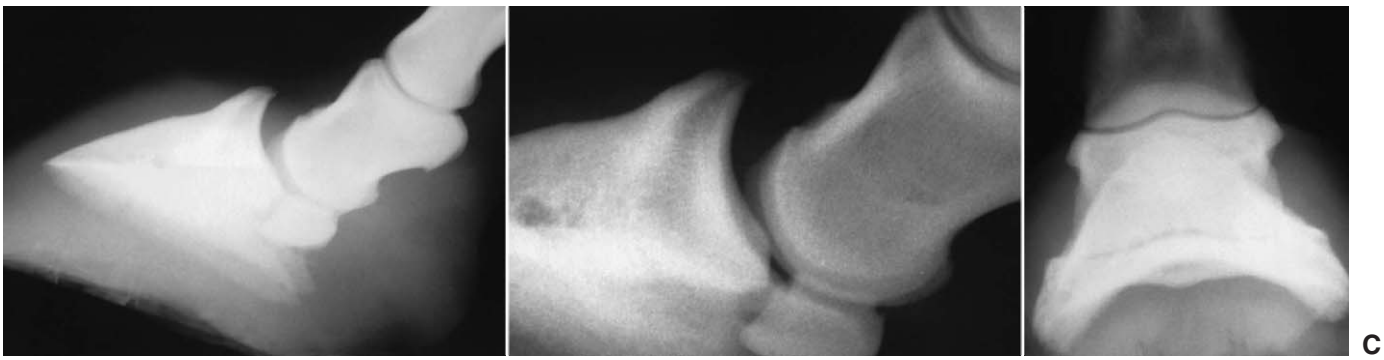


Figure 3-29 • Lateral **(A),** lateral close-up **(B),** and 65-degree dorsopalmar views of a cranially dislocated P3 secondary to ruptured flexor tendons.



Figure 3-30 • Non–weight-bearing, lateral close-up **(A)** view of caudally dislocated P3, secondary to septic arthritis. Normal opposite coffin joint is provided for comparison **(B).**

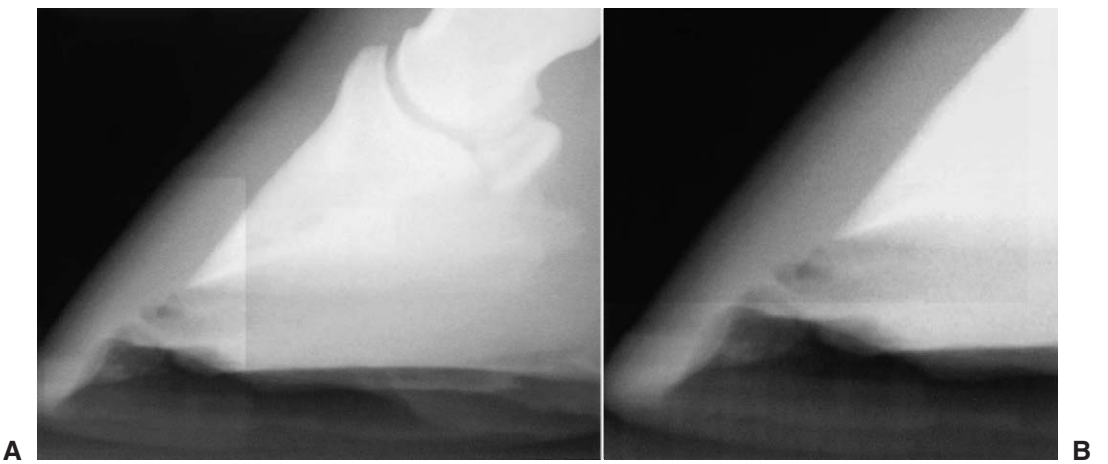


Figure 3-31 • Lateral close-up **(A)** and ultra-close-up **(B)** views of the hoof and distal phalanx (deliberately underexposed to emphasize soft tissues) show large gas-filled defect, accompanied by numerous small gas pockets situated between the solar defect and the tip of P3 *(emphasis zone).*

It is therefore my opinion that the term *infection* is both the simplest and most direct radiographic means of describing sepsis of the distal phalanx.

Points of Attack

Most P3 infections develop secondary to a sole abscess. Deep puncture wounds to the caudal part of the foot, especially those that penetrate the navicular bursa or coffin joint, can result in septic arthritis, which then may spread to the adjacent phalanges.

Direct and Indirect Radiographic Indicators of P3 Infection

Gas. A band of gas located beneath P3 (as seen in lateral projection) is a reliable indicator of sepsis. Such a finding further suggests an existing or future spread of the infection to the nearby bone. Likewise, discrete gas pockets, especially when situated along the outer surface of P3, are strongly indicative of infection, even in the absence of bony abnormality (Figures 3-31 to 3-33).

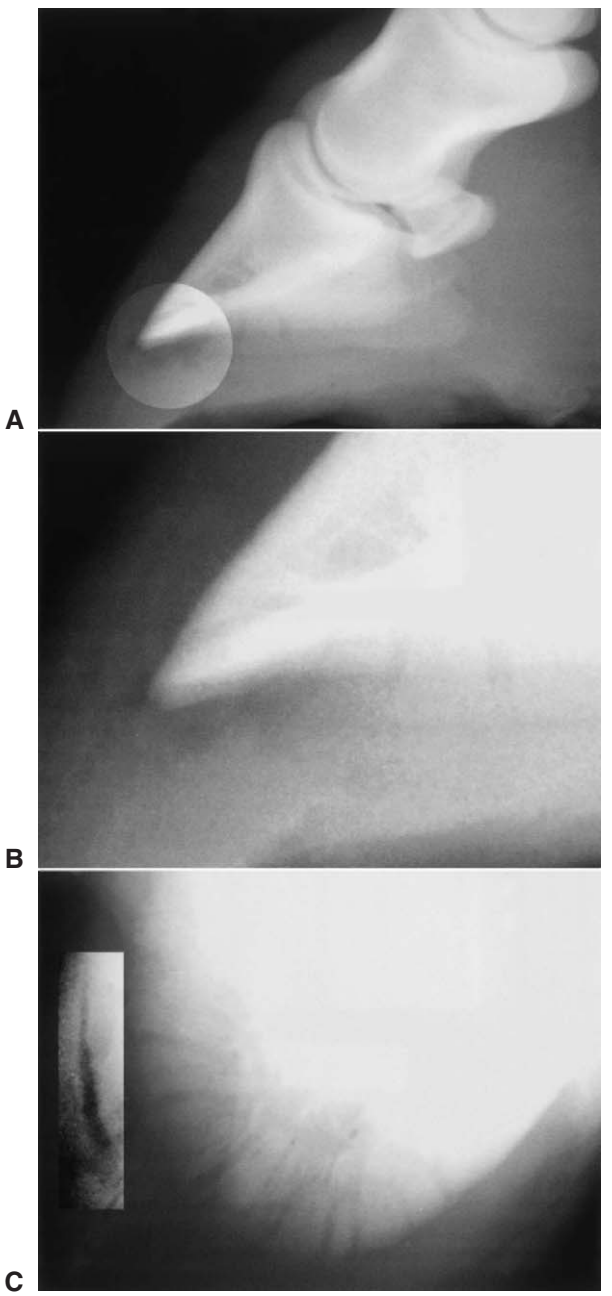


Figure 3-32 • Lateral **(A),** lateral close-up **(B),** and 65-degree dosopalmar oblique **(C)** views show gas pockets surrounding the tip of P3 and extending along the lateral solar margin *(emphasis zone).*

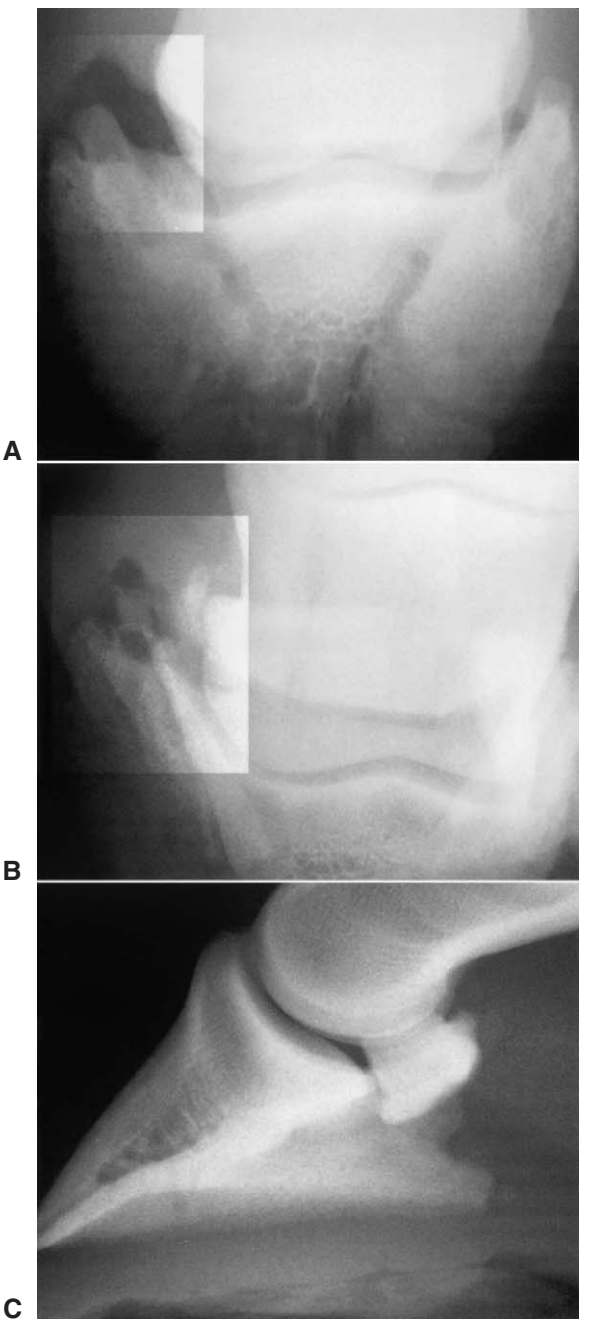


Figure 3-33 • Sixty-five-degree **(A),** 65-degree oblique **(B),** and true lateral **(C)** views of the foot of 10-year-old Thoroughbred gelding with a draining sinus in the medial sulcus show a large gas pocket beneath the medial wing of P3 *(emphasis zone).*

Drainage, Sinography, and Marking Studies

Drainage from one or more sinuses (abnormal openings) in the foot usually heralds abscessation. The depth, extent, and intercommunication of related sinus tracts and cavities can be established only using sinography.[70] Marking studies made with a metallic probe are capable of demonstrating bone contact, but they rarely reveal joint, bursal, or tendon sheath involvement. Probe marking (as opposed to sinography) nearly always underestimates the full extent of a particular lesion (Figures 3-34 and 3-35).

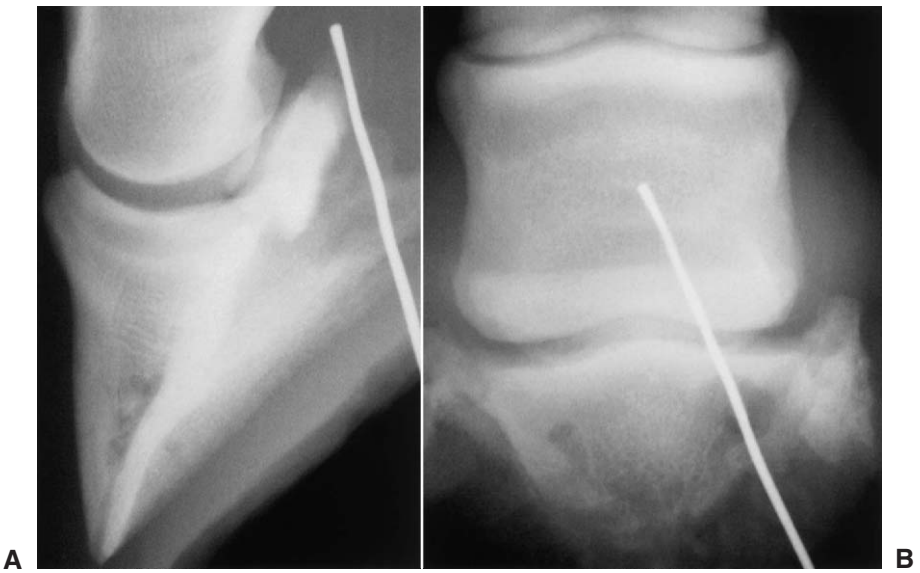


Figure 3-34 • Lateral **(A)** and 45-degree **(B)** marking studies of the horse in Figure 3-33 show that a metallic probe can be extended from the drainage site to a point immediately caudal and proximal to the proximal border of the navicular bone. Currently there is no evidence of osteomyelitis.

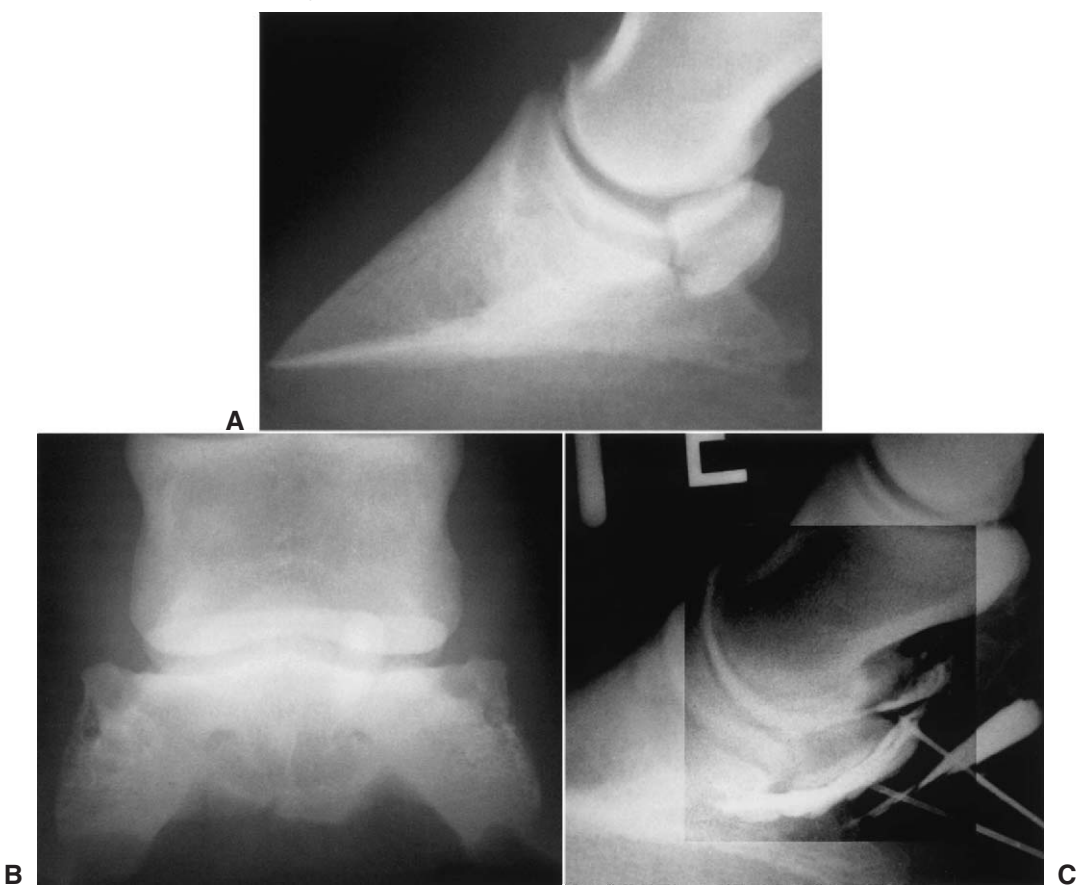


Figure 3-35 • Lateral **(A)** and 45-degree dorsopalmar **(B)** views of the forefoot of a severely lame horse show asymmetric narrowing of the coffin joint, without concomitant signs of arthritis, strongly suggesting septic arthritis. A lateral bursagram **(C)** confirms the suspicion of infection, with contrast solution present in both the coffin joint and distended navicular bursa.

Soft-Tissue Defects

Defects in the sole, especially when associated with past or present drainage, are typical of infection/abscessation and force consideration of infectious extension to the adjacent phalangeal surface (Figure 3-36).

Foreign Bodies

Foreign bodies located in the foot usually, but not invariably, drain from either the sole or coronet. Metallic foreign bodies, such as wires, show clearly, but wooden splinters are radiographically invisible (Figure 3-37).

Focal Marginal Bone Loss

Localized bone loss from the solar margin of P3, as seen in frontal projection, is a convincing sign of infection. However, because of a marked individual variability in the normal radiographic appearance of the solar margin, it can be difficult to distinguish disease from normal variation.

The best solution to this problem is *radiographic comparison,* for example, comparison of a suspected area of bone loss in the right half of the solar margin with a comparable area in the left half of the same bone or comparison of a suspicious area in the right front phalanx with a comparable region in the left front phalanx. Figures 3-38 to 3-41 show four examples of marginal bone loss due to infection.

Infectious Sequestration

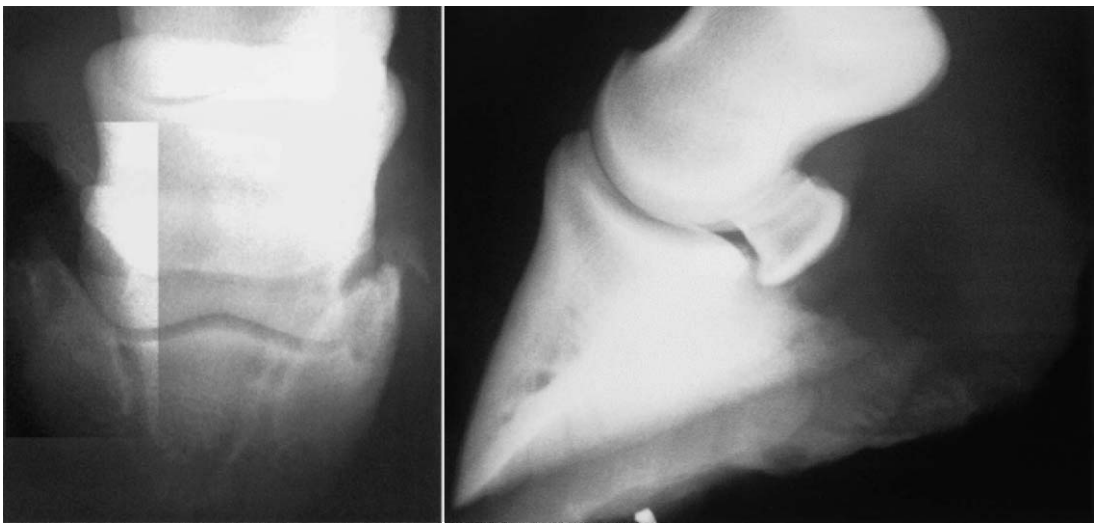
Infectious sequestration from the solar margin of P3 is rare in horses, occurring more commonly in cattle. When it does develop, the fragment of dead bone usually takes the form of a shallow half-circle, resembling the so-called saucer fracture commonly seen in the cannon bone of horses following a deep wire cut. Associated drainage is typically via the heel bulb or coronary band. Baird pointed out the strong resemblance of solar margin sequestra to type VI distal phalangeal fractures.[71,72] With laminitic penetration of the sole, large chunks of the distal phalanx may become devascularized and detach, producing enormous sequestra (Figures 3-42 and 3-43).

Septic Arthritis, Osteomyelitis, and Dislocation of the Coffin Joint

One of the first radiographic indicators of a coffin joint infection is narrowing of the cartilage space. However, it is important not to mistake postural-related joint narrowing (usually asymmetric) for disease (Figure 3-44).

In foals, distal interphalangeal joint infections show sooner and spread faster than in adults, principally because of their vascularized articular cartilage. Once a full-blown osteomyelitis is under way, the subchondral bone begins to disintegrate and the cartilage space widens and often subluxates. Swelling is typically confined to the soft tissues proximal to the coronary band as the result of the confining quality of the hoof wall. When sequestration occurs, it is most likely to affect the extensor process. New bone deposition is also more likely to develop on the extensor process than anywhere else on P3 because of its more reactive periosteum (Figure 3-45).

In adult horses, coffin joint infections normally take a month or more to reveal their presence, usually in the form of a narrowed cartilage space. The delayed



A **B**

Figure 3-36 • Large lucency superimposed on the lateral wing of the distal phalanx *(emphasis zone)* in the 65-degree dorsopalmar view **(A)** and a generalized decrease in caudoventral density in the lateral view **(B)** are the result of partial removal of the lateral aspect of the hoof.



Figure 3-37 • Foreign bodies. Case 1: Forefoot of a lame horse with drainage from the dorsolateral aspect of the coronet **(A).** Close-up lateral **(B),** ultra-close-up lateral **(C),** and 45-degree dorsopalmar **(D)** views show a small gas pocket in contact with the base of the extensor process.

onset of radiographic indicators in adults is due largely to the loss of blood supply in the articular cartilage as the skeleton matures. Eventually, intraarticular bacteria enter the synovial capillaries, and from there they move into the capsular tissues. Thrombosis, necrosis, disintegration, and eventually dislocation can occur thereafter. In such circumstances, gas often accumulates in what was formerly called the cartilage space, the result of atmospheric contamination secondary to drainage (Figure 3-46).

Phalangeal Bone Cysts (Osteochondritis)

The specific cause (or causes) of phalangeal bone cysts is uncertain. Verschooten contends that subchondral bone cysts are caused by subchondral bone necrosis resulting from joint injury.[73] Others believe that bone cysts are a form of osteochondritis. Although infection is usually included in the differential diagnosis of such lesions, this is rarely the case.

Most phalangeal cysts are located along the midsagittal plane and are seen best in frontal projection. In the case of P1, most cysts are usually situated proximally, just below or to one side of the overlying sagittal ridge, which may also appear defective. The radiographic presence of a similar defect in the opposite foot should raise some question as to the clinical importance of either lesion.

Berry described a squamous cell carcinoma in the right hind distal phalanx of a 15-year-old Thoroughbred stallion that resembled a huge, eccentrically positioned bone cyst.[74]

Absence of P3

Taylor reported the congenital absence (agenesis) of a rear distal phalanx in a 2-week-old mule with an angular limb deformity.[75] The foal had a fully developed, asymmetric hoof, but it appeared to move about normally. A vestigial P3 was found on the opposite side.

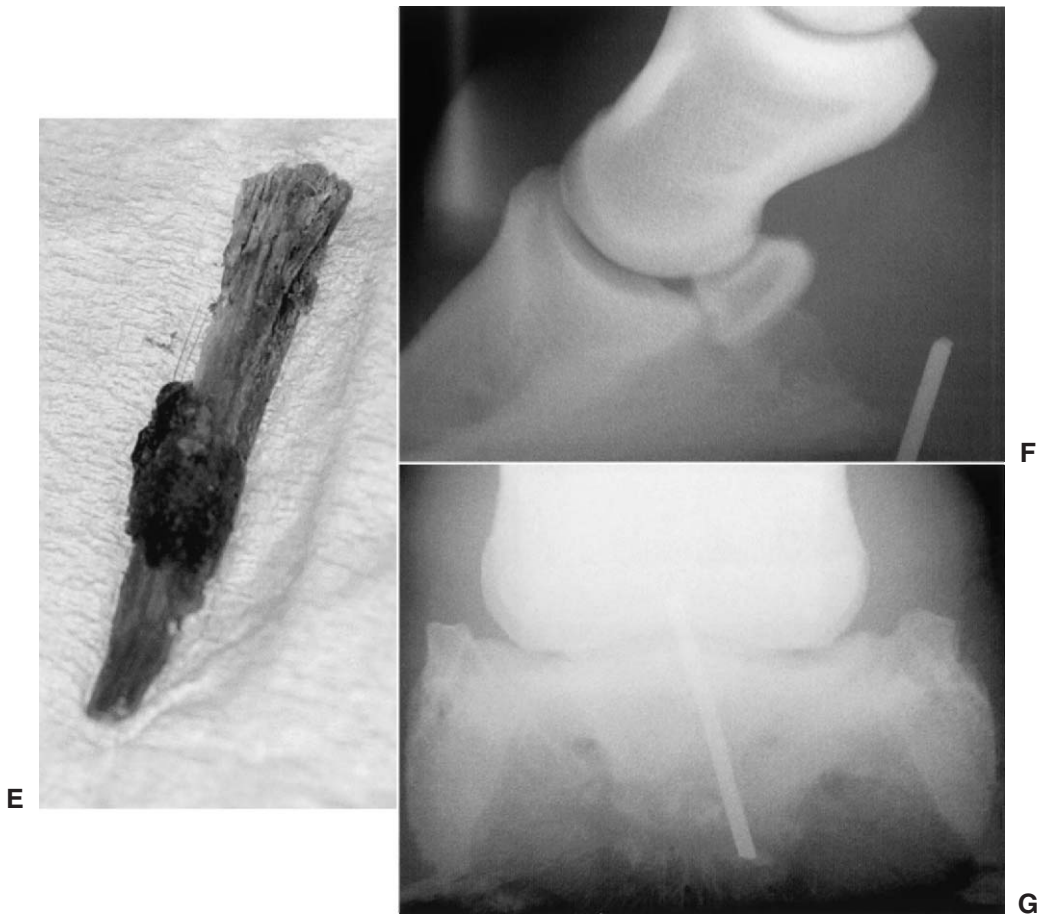


Figure 3-37, cont'd • Surgical exploration revealed an abscess containing a small wooden splinter **(E).** Case 2: Lateral **(F)** and forty-five-degree dorsopalmar **(G)** views show a metal rod fragment imbedded in the heel of a horse.

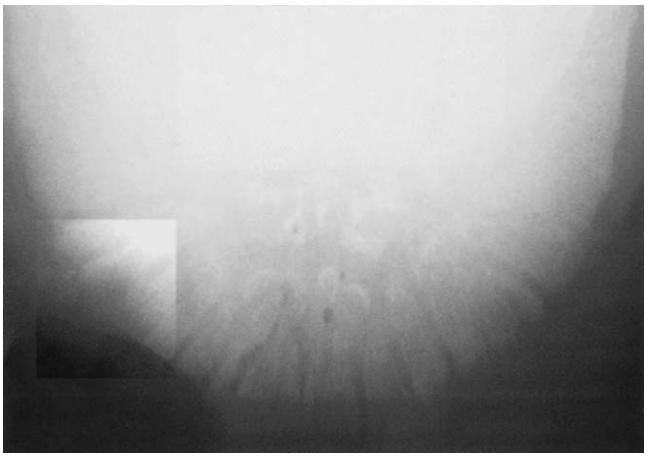


Figure 3-38 • Sixty-five-degree dorsopalmar (light) view shows localized loss of dorsolateral aspect of solar margin consistent with osteomyelitis *(emphasis zone).*

Hypoplasia of P3. Bertone and Aanes described the radiographic appearance of congenital phalangeal hypoplasia of P3 in a mule and two foals. Deficiencies ranged from the majority of P3, to the distal third of P3, to a combined deficiency involving the distal half of P2, the proximal half of P3, and the entire navicular bone. All were unilateral.[76]

▮▮▮ ARTHROGRAPHY AND BURSOGRAPHY

Occasionally there are radiographic situations that call for arthrography of the distal interphalangeal joint, for example, whether or not a bone cyst found in the subchondral bone of P3 communicates with the coffin joint.[77] At least three different approaches to the coffin joint have been described: dorsal, dorsolateral, and lateral. Lateral arthrocentesis has been associated with contrast spillage or diffusion of contrast solution into the navicular bursa and digital synovial sheath in about a third of cases, whereas a dorsal approach usually results in no such problems.[78]

Diagnostic opacification of the navicular bursa is usually achieved with a lateral or lateropalmar approach and, like arthrography, may result in inadvertent opacification of the distal interphalangeal joint.[79]

▮▮▮ TUMOR AND TUMORLIKE LESIONS OF THE CORONARY REGION

Seahorn reported the sonographic diagnosis of a keratoma situated just beneath the coronary band of

Text continued on p. 58.

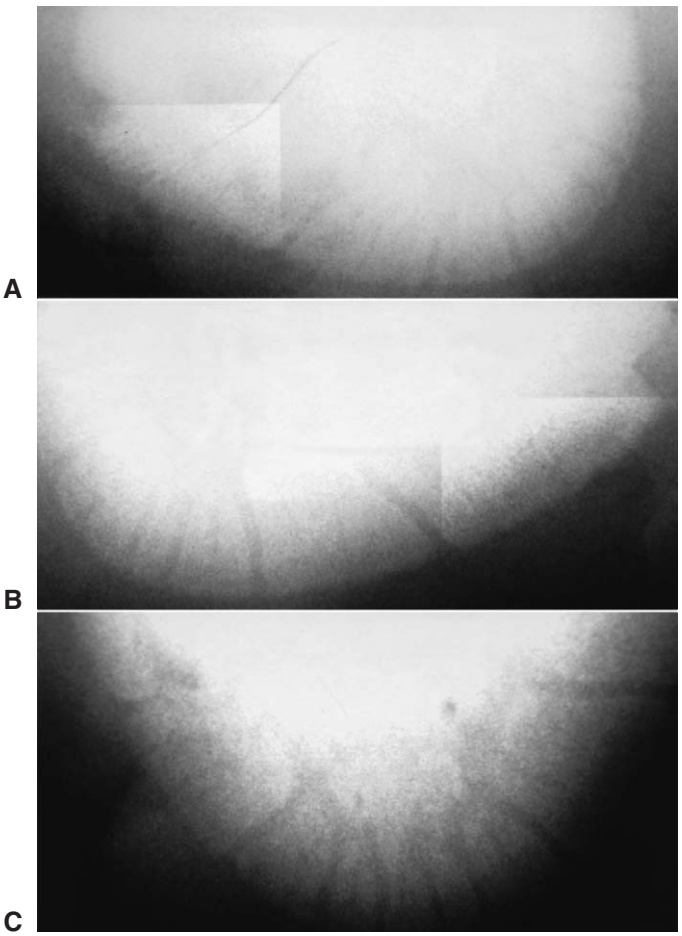


Figure 3-39 • Sixty-five-degree dorsopalmar (DP) oblique (deliberately underexposed) shows subtle bone loss along the caudal aspect of the lateral solar margin **(A),** destruction not appreciable in either the opposite oblique **(B)** or true DP projections **(C).**

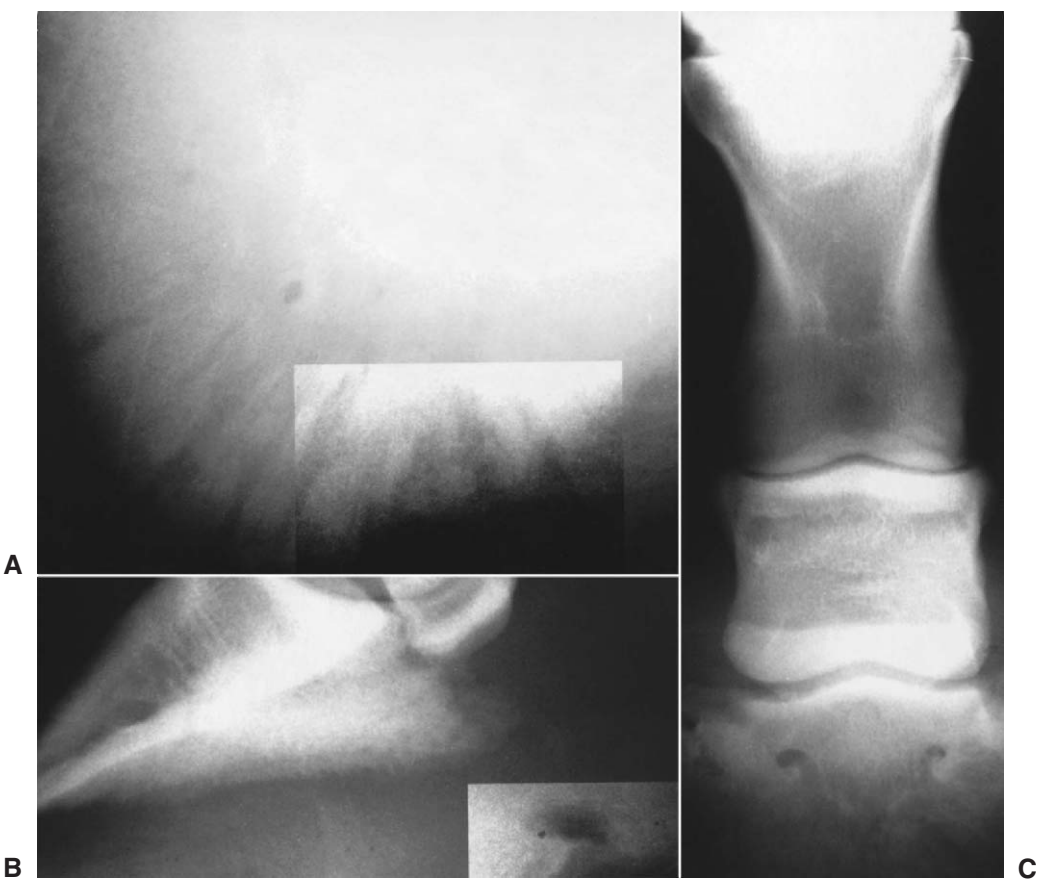


Figure 3-40 • A, Sixty-five-degree dorsopalmar (DP) oblique view of the right front distal phalanx shows bone destruction along the dorsolateral aspect of the solar margin. **B,** Lateral close-up view shows a gas pocket in the caudoventral aspect of the heel *(emphasis zone).* **C,** Forty-five-degree DP view shows narrowing of the medial aspect of the coffin joint, the result of a compensatory weight shift.

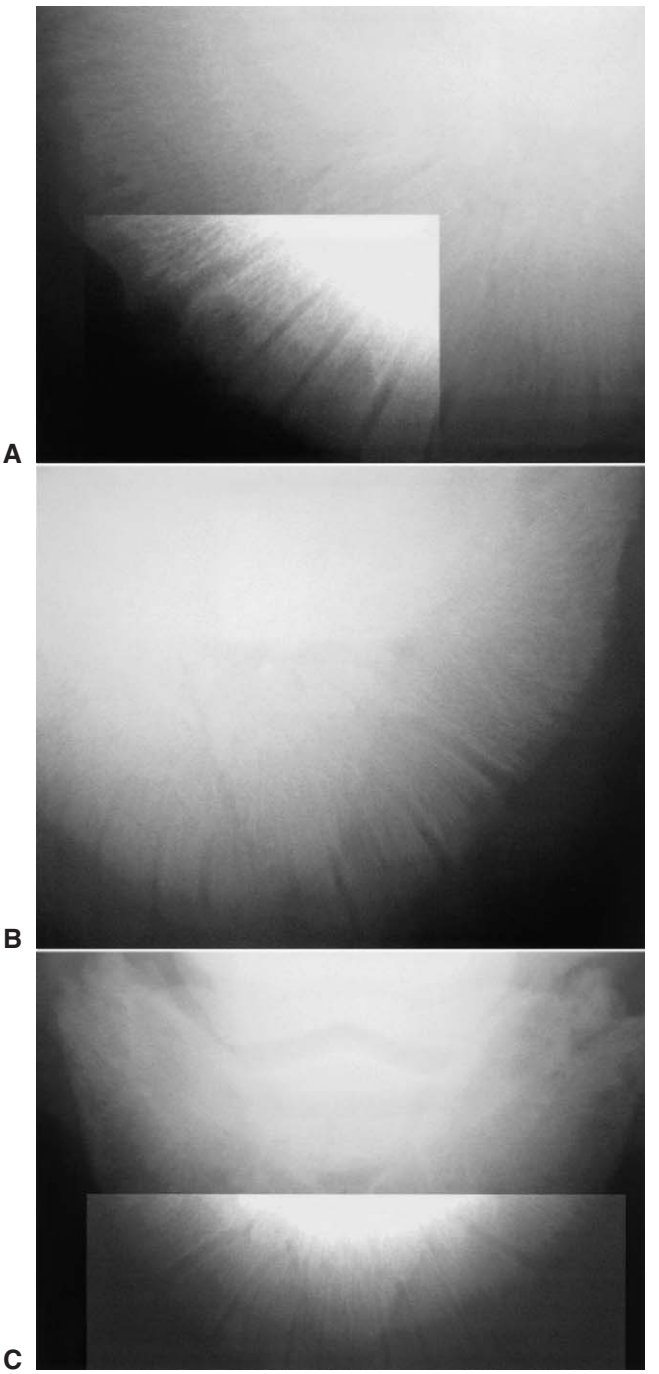


Figure 3-41 • Sixty-five-degree dorsopalmar (DP) oblique view shows localized bone destruction *(emphasis zone)* along the dorsolateral border of P3 **(A).** The opposite oblique **(B)** appears normal, as does the straight 65-degree DP **(C).**

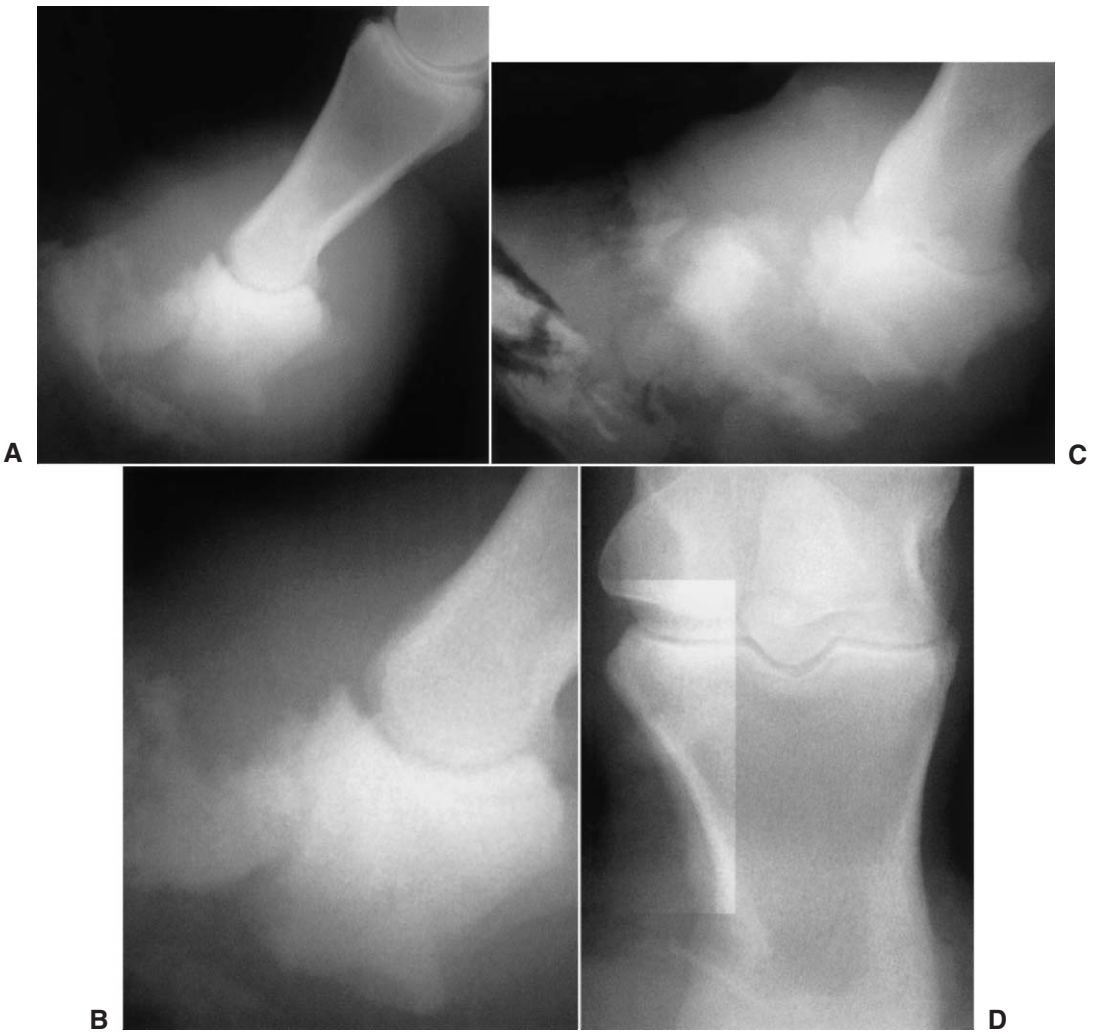


Figure 3-42 • Lateral **(A),** lateral close-up **(B),** and dorsopalmar (DP) oblique **(C)** views of what remains of the left front forefoot of a horse with severe laminitis. The hoof and distal phalanx have been lost to a combination of events, including (1) distal phalangeal rotation, (2) distal displacement, (3) solar penetration, (4) osteomyelitis, (5) insufficiency fracture, and (6) massive vascular thrombosis. A close-up DP view **(D)** of proximal P1 and the fetlock joint show intermediate-duration new bone just below the lateral palmar protuberance, indication the infection has nearly reached the fetlock.

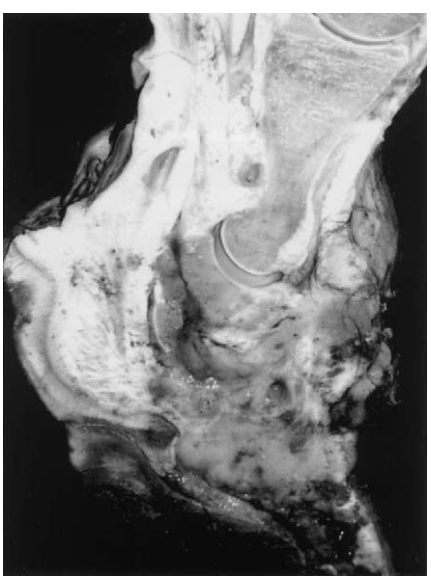
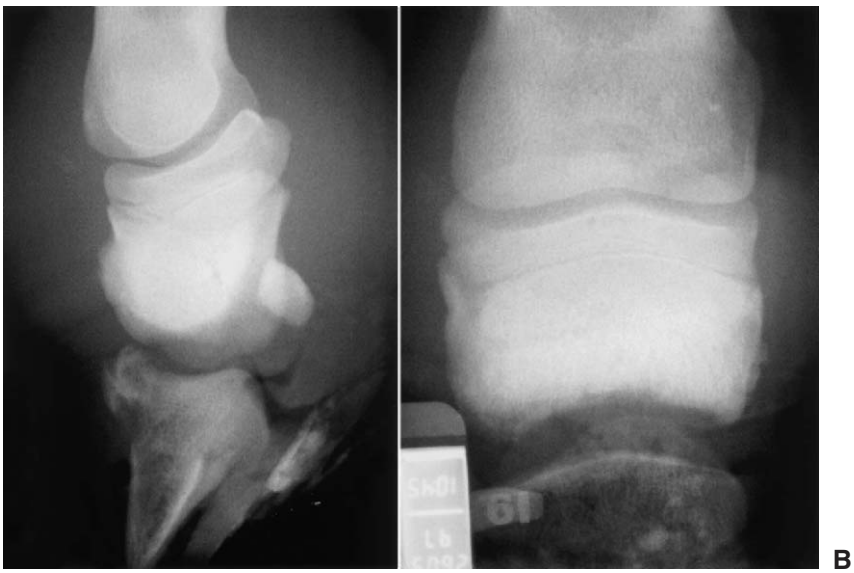


Figure 3-43 • Pathology specimen (sagittal section viewed laterally) of the horse's foot shown in Figure 3-42 shows little recognizable tissue below the pastern.



Figure 3-44 • Dorsopalmar view of the foot of a normal horse shows narrowing of the lateral half of the coffin joint, the result of a compensatory weight-shift caused by lifting the opposite foot, This phenomenon is known as *leaning off* and must be distinguished from permanent narrowing resulting from disease.



A **B**

Figure 3-45 • Lateral **(A)** and dorsopalmar **(B)** views of an infected coffin joint show (1) partial dislocation, (2) extensive subchondral bone destruction, (3) new bone deposition over much of the exterior of P2, (4) insufficiency fracture of the extensor process, and (5) massive proximal swelling to the level of the coronet.

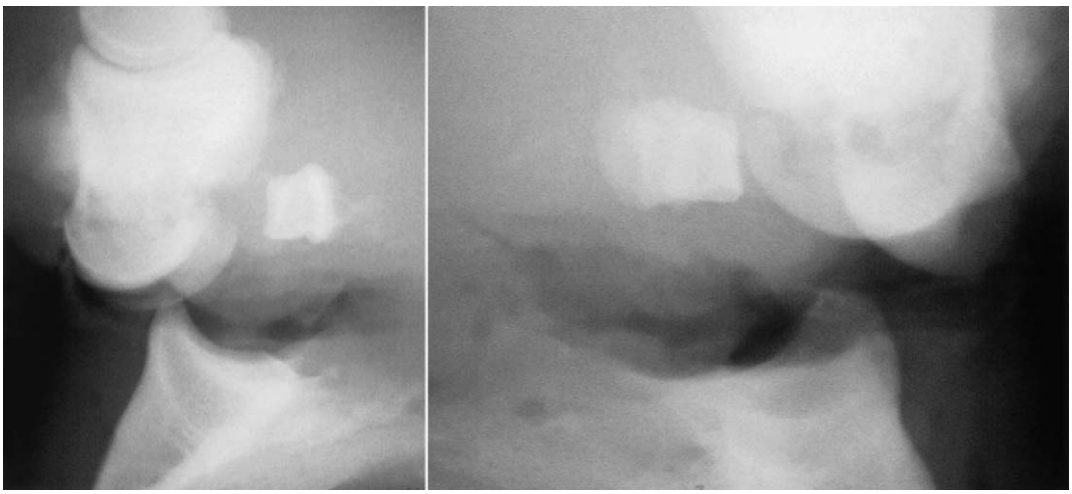


Figure 3-46 • Lateral **(A)** and dorsopalmar oblique **(B)** views of the foot of a 7-year-old American Saddle Horse that caught its foot in a barbed wire fence 6 weeks ago, cutting it deeply and subsequently developing an infection. Radiographs show the following: (1) complete dislocation of the coffin joint, including the navicular bone; (2) gas in the coffin joint (atmospheric contamination of a draining wound); (3) a cloud of new bone enveloping the middle phalanx; and (4) severe regional soft-tissue swelling.

the left front foot.[80] In my experience keratomas most often involve the mid or distal aspect of the dorsal surface of P3. Most resemble either infection or tumor, although the distinction is often unclear. Deep bony cavitation with associated cortical thinning and expansion resembling a bone cyst are often present (Figure 3-47).

Some keratomas are associated with drainage from the coronet or sole, forcing consideration of a foreign body. Most keratomas are painful, but because of their slow growth, typically lead to a gradually developing lameness, unlike infections or tumors in which the onset of lameness may be abrupt. Keratomas involving the solar margin are often mistaken for osteomyelitis, or localized bone reabsorption secondary to a chronic sole abscess.

Monticello and co-workers described a malignant melanoma in an 18-year-old American Paint. In addition to localized destruction of the coronary band laterally, combined bone destruction/production was present in the underlying portions of the second and third phalanges.[81]

Attenburrow reported a nonossifying fibroma in the proximal phalanx of an 8-month-old Thoroughbred colt. Radiographically the lesion resembled a bone cyst, being lytic, expansive, and involving the entire distal half of the bone.[82]

▮▮▮ CLUBFOOT

The presence of a clubfoot neither predicts nor excludes serious underlying disease (Figures 3-47 and 3-48). When associated or concomitant bone or joint disease is present, it can range from fracture to osteoarthritis to osteochondritis.

▮▮▮ NAVICULAR DISEASE

The Standard Navicular Series

In most practices, a standard navicular series consists of four views: a true lateral, two dorsopalmars (45 and 70 degrees), and a skyline, each designed to evaluate a particular part of the navicular bone (Figure 3-49). A fifth view is occasionally added, a penetrated high coronary, to evaluate P3. A standard navicular series and the purpose of each view are as follows (Table 3-4).

Normal Anatomic Variations That May Mimic Navicular Disease

Kaser-Hotz and Ueltschi reviewed the navicular bones of 523 sound horses and frequently found variations in shape and interior appearance (Figures 3-50 to 3-53).[83] Some of their more important observations are listed below (Box 3-5).

- Some normal navicular bones have a focal concavity in the center of the midsagittal ridge as seen in lateral projection. Unfortunately, a similar finding may also be found in horses with navicular disease. A way to try to resolve this sort of diagnostic ambiguity is to make a lateral view of the opposite foot. If the two bones are similar, the probability is that the described indentations are normal variations; if not, navicular disease is more likely.
- Gas in the sulci of the frog, typically appearing as V-shaped lines or bands over the edges of the central third of the navicular bone (as seen in the high coronary projection), can mimic fractures.

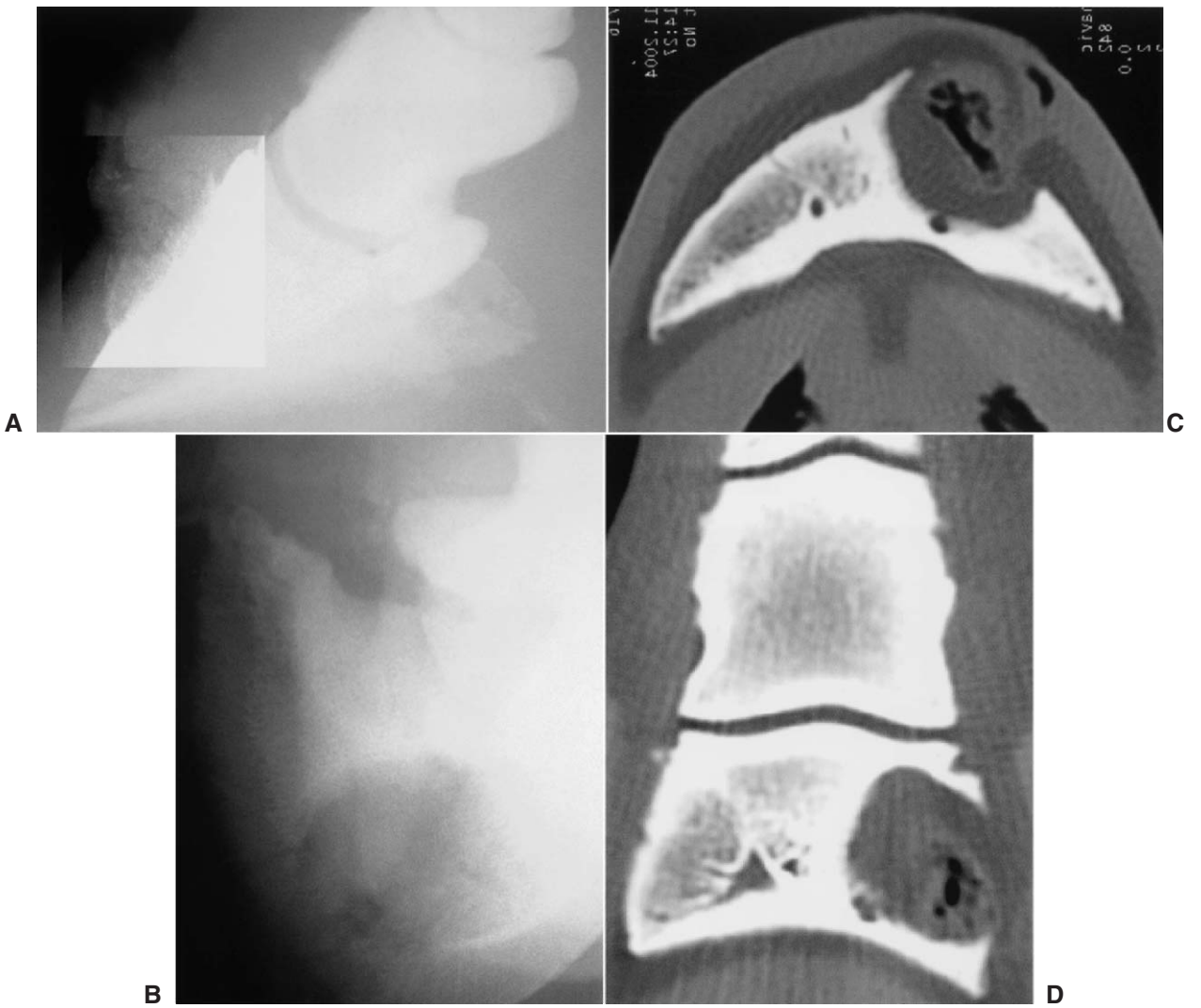


Figure 3-47 • Lateral **(A)** and sixty-five degree DP oblique **(B)** radiographs of the distal phalanx of a horse with a large keratoma show extensive, deep bone destruction accompanied by an ineffective reparative effort. The new bone deposits on the dorsal surface of P2 are unrelated. Axial **(C)** and coronal **(D)** computed tomograms show the true extent of the tumor, which has destroyed much of the interior of the affected bone.

Table 3–4 • THE STANDARD NAVICULAR SERIES

View	Evaluative Purpose
Lateral	Evaluates the flexor and articular cortices of the navicular bone and the presence or absence of corticomedullary distinction (Figure 3-50)
Frontal 1: low coronary (45-degree DP)	Evaluates the proximal border of the navicular bone (Figure 3-51)
Frontal 2: high coronary (65-degree DP)	Evaluates the distal border of the navicular bone (Figure 3-52)
Skyline (special)	Evaluates the flexor border of the navicular bone and corticomedullary distinction (Figure 3-53)

DP, Dorsopalmar.

Box 3-5
Presumed Normal Variations Found in the Navicular Bones of 523 Sound Horses

Proportionately enlarged vascular channels
Enlarged, distorted vascular channels
Calcification of the impar ligament (as seen in lateral projection)
Conical osteophyte present on the proximal articular margin (as seen in lateral projection)
Exceptionally thick flexor cortex (as seen in lateral projection)
Medium-sized, circular lucency in the central body (as seen in high coronary projection)
Oval-shaped lucency in the midflexor cortex (as seen in skyline projection)
Lateral or proximolateral tapering of the lateral corner of the proximal border (as seen in high and low coronary projections)
Elongation of the distal aspect of the flexor margin (as seen in lateral projection)
Flattened sagittal ridge (as seen in skyline projection)



Figure 3-48 • Lateral view of a lame horse with a clubfoot shows a distal phalanx with a Roman-nose profile and a moderate downward inclination **(A).** A second horse, radiographed because of its clubbed foot **(B),** was found to have osteochondritis (fragmenting form) of the extensor process **(C, D).** Subsequent screening of the presumably normal opposite foot reveled it too had a detached extensor process **(E, F),** although lameness was not observed when the horse was examined earlier.

- Poorly defined, localized gas pockets trapped beneath the sole can mimic navicular cysts.

Projectional Variations That May Mimic Navicular Disease

Nearly all the serious projectional problems associated with navicular radiography involve the skyline view, which is by far the most difficult to produce consistently. This is true of both normal and abnormal animals, especially horses with navicular disease, in which positioning the affected foot caudally appears to be quite painful and often results in an unwillingness to maintain the foot in the desired position.

Specifically, the skyline view of the navicular requires that the x-ray beam pass through the center of the bone, as parallel as possible to its cortical surfaces. To do otherwise is to invite obliquity and projections that closely simulate corticomedullary indistinctness and medullary sclerosis (opacification) as seen with some forms of navicular disease. Unrecognized obliquity in the lateral projection may also lead to the false conclusion that there is increased medullary density and thus disease (Figure 3-54).

Underexposed, decentered, and obliqued lateral projections of the navicular bone can also mimic reduced corticomedullary definition and, accordingly, suggest disease (Figures 3-55 to 3-56). Superimposition of the proximal third of the extensor process on the proximal border of the navicular bone can mimic a bone deposit secondary to a sprain or avulsion fracture.

Poulos and Brown described a normal variation in the central ridge of the flexor cortex of the navicular bone as seen in the skyline projection.[84] The described variant, a radiolucent crescent, was most evident with a projection angle of 45 degrees, but it was also visible with greater or lesser projection angles (50 and 40 degrees). The apparent defect was attributed to a normal focal concavity in the center ridge, not to navicular disease as previously assumed.

Ruohoniemi and Tervahartiala reported that many supposed radiographic abnormalities identified along both the proximal and distal navicular margins of fresh Finnhorse forefeet could not be corroborated in follow-up CT examinations.[85] Accordingly, in horses suspected of having navicular disease, the following radiographic findings should be used with caution: (1)



Figure 3-49 • Standard navicular series (12-year-old Quarter Horse mare): Lateral **(A),** 45-degree dorsopalmar **(B),** 65-degree dorsopalmar **(C),** and skyline **(D)** views.

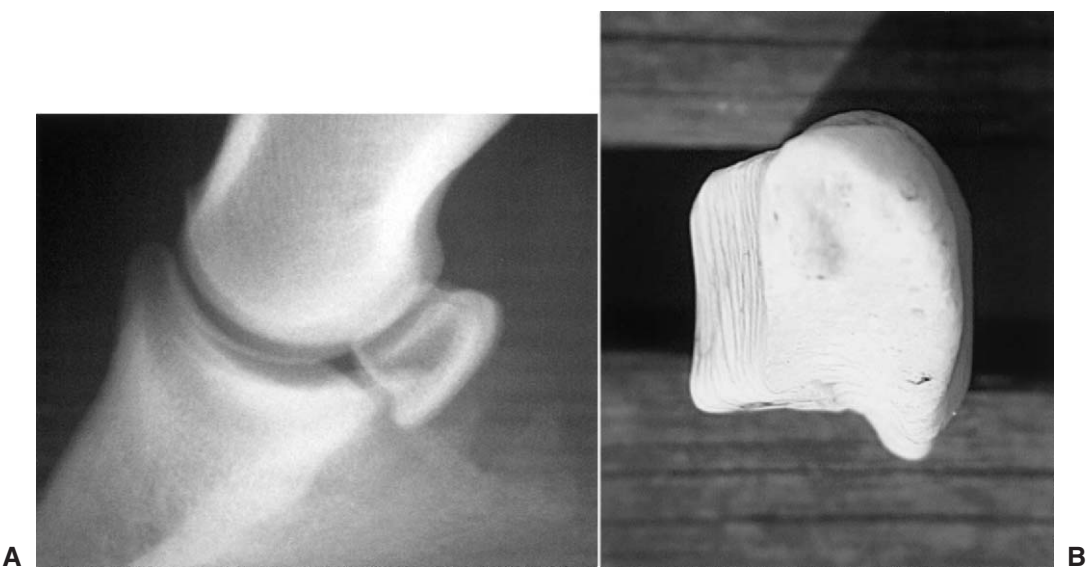


Figure 3-50 • **A,** Lateral close-up view of a normal navicular bone in a 6-year-old Quarter Horse gelding shows the clear distinction between the high-density cortical bone of the flexor cortex and low-density bone of the medulla. **B,** A defleshed navicular bone is provided for comparison.

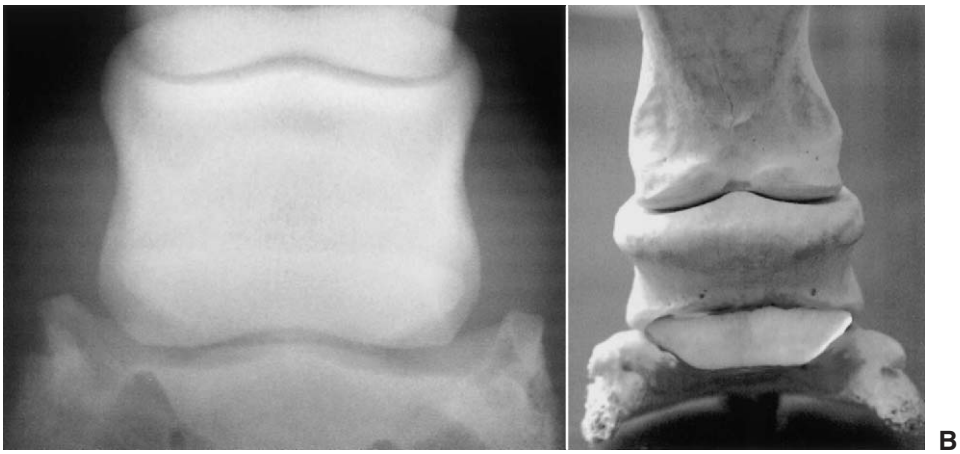


Figure 3-51 • A, Forty-five-degree, close-up dorsopalmar view (low coronary) of a normal navicular bone of the horse described in Figure 3-50. **B,** A caudal view of a defleshed navicular bone (and associated phalanges) is provided for comparison.

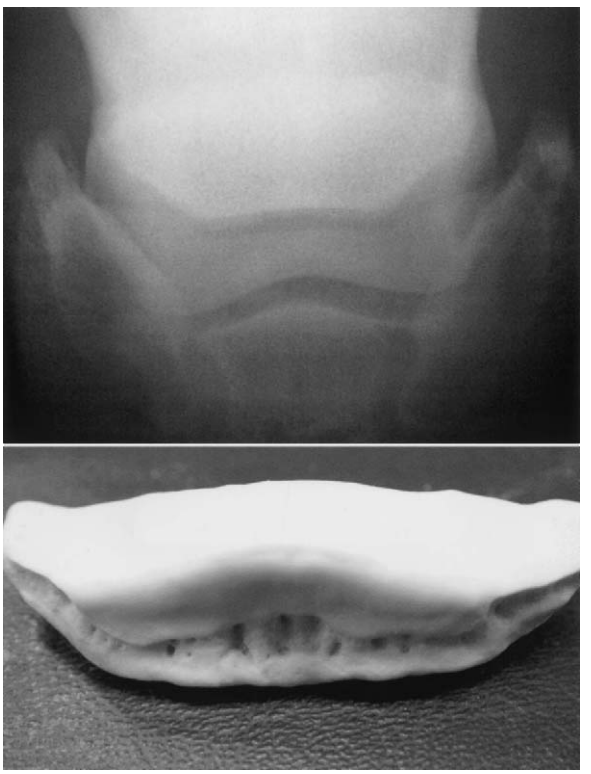


Figure 3-52 • Sixty-five-degree close-up dorsopalmar view (high coronary) of the navicular bone of the horse described in Figure 3-50. A comparable view of a navicular bone is provided for comparison.

decreased corticomedullary distinction, especially in the skyline projection; (2) uneven flexor cortical thickness; and (3) irregular proximal border margination.

Which Navicular Projection Is Best?

Using isolated normal and abnormal navicular bones, DeClerco and co-workers compared lateral, high coronary, and skyline projections. They concluded that, contrary to some previously published reports, the skyline view was instrumental in making a diagnosis in only 10% of the specimens, and in no instance was it indispensable. These findings suggest that some previous claims made for this view have been exaggerated.[86] In my experience the high coronary view—provided it is made with a grid—is diagnostic in more than 90% of cases.

Caudal Heel Pain Syndrome: Is Less More?

More than any other common skeletal disorder of the horse, with perhaps the exception of osteochondritis, navicular disease has been the recipient of numerous recent "makeovers" in terminology: *navicular syndrome* and *caudal heel pain syndrome,* to name but two, neither of which appears to have shed any further etiologic light on the actual cause (or causes) of the disease.

The latest appellation, *caudal heel pain syndrome,* is especially troubling because at best it suggests that many regional disorders are capable of producing a similar clinical profile and, at worst, exonerates the navicular bone altogether, depending on one's personal interpretation of the expression and, in particular, the meaning of the word *syndrome*.[2] For the purpose of radiographic description, however, the choice of diagnostic terminology seems clear: *navicular disease* is currently the least ambiguous and perhaps the least medically pretentious term available.

Gross View

In 1885 Smith, a British military veterinarian noted for his meticulous dissections of horses with navicular disease, described the principal lesion as being located, in nearly every case, over the central ridge or slightly to one side.[87] The disease appeared initially as a brown stain in the fibrocartilage of the flexor surface interspersed with minute calcium deposits. Later the cartilage thinned, ulcerated, and was eventually lost,

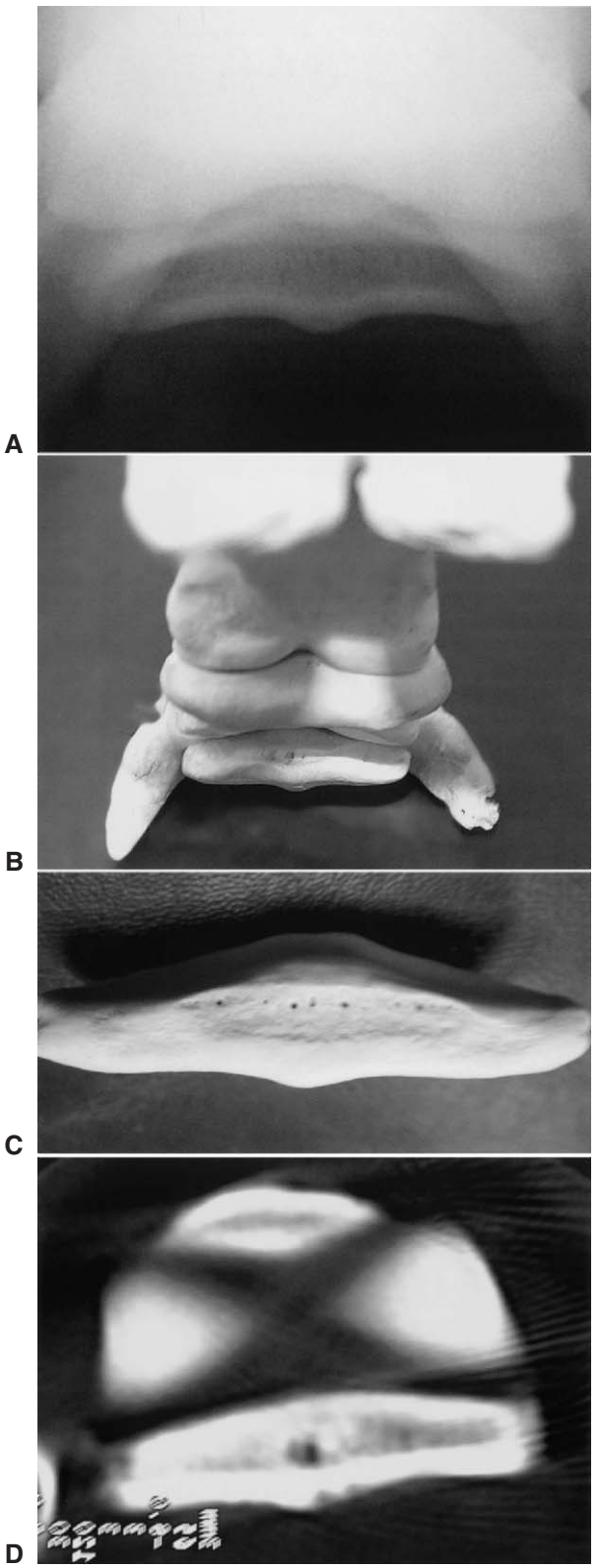


Figure 3-53 • Skyline view **(A)** of the navicular bone of the horse described in Figure 3-50. Comparable contextual **(B)** and isolated rear **(C)** views of a defleshed navicular bone are provided for comparison. Accurate positioning of the foot for computed tomography (CT) is equally important, especially when it comes to differentiating projectional variation from pathology, as seen in the transverse plane **(D)** of a horse with suspected navicular disease but normal radiographs.

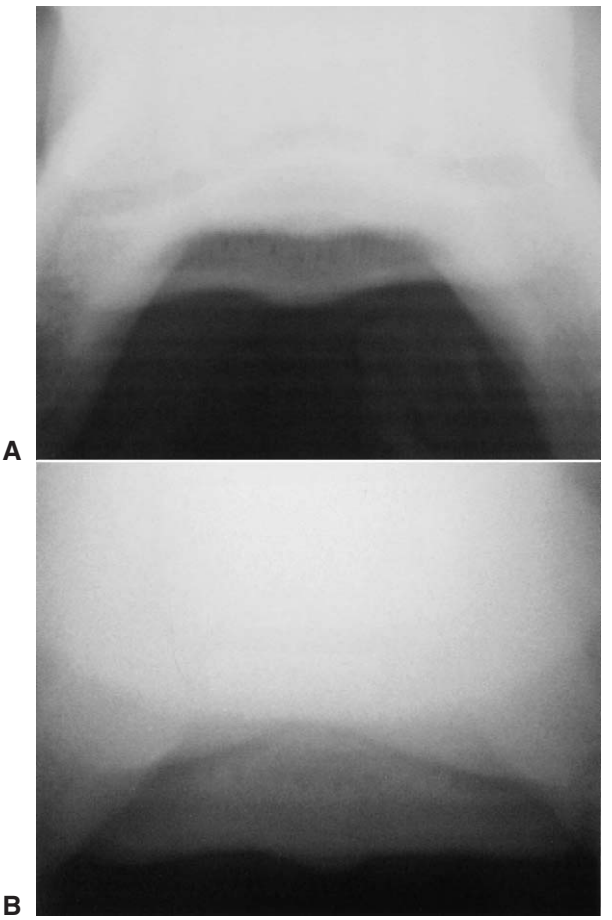


Figure 3-54 • **A,** Incorrect skyline views: In the first instance, the angle of the x-ray beam was too shallow. **B,** In the second, the horse's leg was not drawn back far enough. In both cases, the result is the same: poor corticomedullary definition mimicking disease.

leaving a shallow depression in the underlying cortex (Figure 3-57). The associated vasculature appeared hyperemic. Initially the deep flexor tendon also stained brown where it contacted the central ridge of the navicular bone. As the disease worsened, part of the adjacent peritendineum disappeared and small tears appeared in the tendon, sometimes accompanied by adhesions. This description is consistent with my own necropsy observations.

Radiographic Indicators of Navicular Disease

Table 3-5 contains the radiographic signs of navicular disease, ordered, in my opinion, according to probable diagnostic importance. The reader is encouraged to read other reports on the radiology of navicular disease, such as that by Wright, to further broaden their diagnostic perspective.[88]

Case Examples: One Severe, One Mild. More often than not, navicular disease involves both front feet, but for the sake of comparison let me begin the

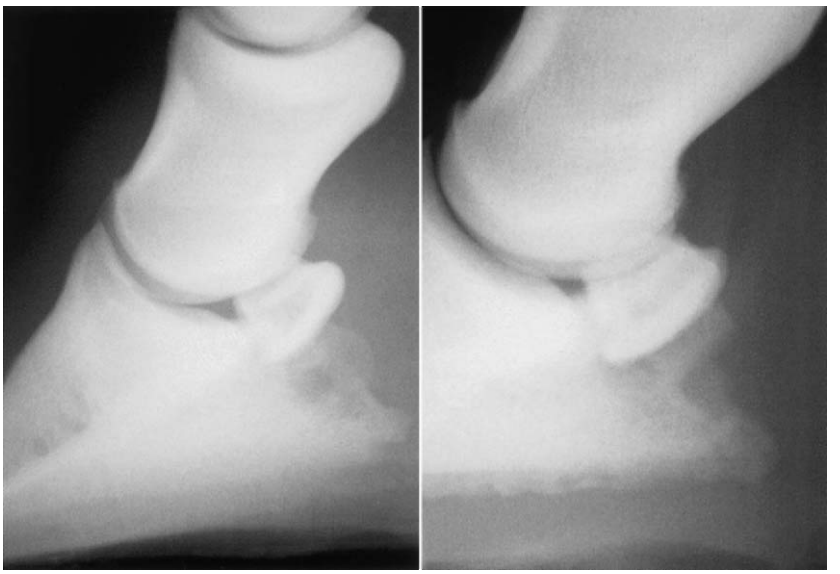


Figure 3-55 • Lateral **(A)** and lateral close-up **(B)** views of the navicular bone show what at first glance appears to be poor corticomedullary definition, sometimes termed *medullary sclerosis*. On closer inspection, the navicular bone is underexposed, accounting for the illusion of increased medullary opacification.

Table 3–5 • RADIOGRAPHIC INDICATORS OF NAVICULAR DISEASE IN DECREASING ORDER OF RELATIVE IMPORTANCE

Order of Probable Importance	Radiographic Disease Indicator (RDI)	Comment
1	Complete body fracture	In my experience (but not everyone's), full-body fractures are usually pathologic in nature, breaking through areas of the navicular bone previously weakened by bone cysts or consolidated vascular channels. In some horses the navicular bone develops from 2 or 3 separate centers of ossification, a condition termed *bipartite* or *tripartite* navicular bone, depending on the number of pieces. As far as I know, this is a congenital condition that is almost always bilateral.
2	Demineralized navicular interior, either in the form of discrete bone cysts, or consolidated vascular channels, or vaguely outlined areas of bone loss	Debate continues as to whether or not true bone cysts exist in navicular disease. Anecdotal reports suggest bone cysts are more painful than other navicular lesions.[89]
3	Multiple enlarged, distorted vascular channels	
4	Single large, distorted vascular channel	
5	Loss of corticomedullary definition as seen in both a true lateral and skyline projections	Oblique views of either the lateral or skyline view will project a portion of the navicular cortex on the medulla, decreasing corticomedullary definition and mimicking medullary sclerosis.
6	Abnormally ragged distal navicular margin as seen in high view	Grid.
7	Spurs on proximal border	
8	Medullary sclerosis	This observation is only reliable if made from near perfect lateral and skyline views.

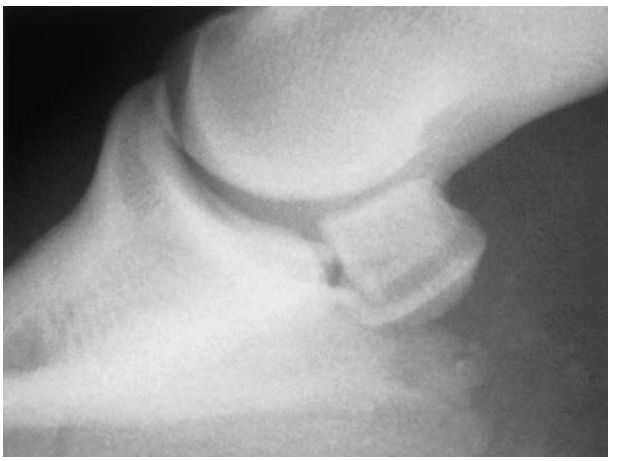


Figure 3-56 • Inadvertently obliqued lateral view of the navicular bone of a normal horse creates the misimpression of subchondral bone loss and flexor surface disintegration, abnormalities that may accompany a puncture-related bursal infection.



Figure 3-57 • Diseased *(top)* and healthy *(bottom)* navicular bones viewed from the flexor surface show (1) a small cluster of regular transverse grooves in the center of the sagittal ridge; (2) irregularly arranged, longitudinal grooves immediately proximal to the distal margin; and (3) small, uneven bone deposits along the lower edge, especially laterally.

radiographic description of this important disease by first showing a severe case of unilateral disease using the opposite normal foot for comparison (Figure 3-58), followed by a mild case (Figure 3-59).

In the high coronary view, the affected navicular bone shows abnormal, plume-like lucencies in the distal half of the bone that appear to communicate with the nearby vascular channels. By comparison, the opposite navicular bone appears homogeneous except for the vascular channels situated along the distal margin.

The lateral projection of the diseased navicular bone shows a distinctive pit in the flexor surface ventrally; the normal navicular bone appears intact. The skyline view of the abnormal navicular bone appears indistinct, with portions of the medulla and corticomedullary junction obscured from view.

Navicular Disease: The Radiographic Particulars

High Coronary View (70-Degree Dorsopalmar). The most common manifestation of navicular disease is enlargement or deformity of the vascular channels, an observation most reliably made in the high coronary projection. When a series of vascular channels become enlarged, especially along the distal border of the bone, the edge, which is normally smooth, appears serrated (Figure 3-60). In some instances, two or more adjacent vascular channels can combine to create the appearance of a bone cyst (Figure 3-61).

Lateral View (True Lateral View). If made properly, the lateral view is the best means of assessing the relationship between the compact bone of the articular and flexor margins and the cancellous bone of the navicular interior. It is the best means of establishing whether there is medullary sclerosis (Figure 3-62). A correct lateral projection of the navicular bone is one in which the horse's foot is placed on a wooden block, and the x-ray beam is centered as nearly as possible on the navicular bone. Centering higher to include the fetlock is false economy, and it typically results in compromised images of both areas. Care must be taken to avoid obliquity because the resultant images can mimic navicular disease.

Skyline View (Special View). O'Brien and co-workers were first to describe what they termed the *special* (or *skyline*) view of the navicular bone,[90] a projection that, when made properly, is a valuable part of the standard navicular series, but when it is made incorrectly, it can lead to misdiagnosis. To quote a line from a familiar nursery rhyme, "When she was good she was very, very good, and when she was bad she was horrid!" Now read the line again, but this time substitute the words *the skyline view* for the word *she.*

First, there is no standard projection angle that will consistently produce a good skyline projection. Why not? Horses with navicular disease are usually very uncomfortable when made to stand with their foot back in maximum extension, even when the heel region has been anesthetized (posterior digital [PD] block). The result is that the horse will predictably move its foot forward into a more comfortable position. This requires both patience and compromise on the part of the radiographer, who must then adjust the beam angle to coincide with whatever degree of caudal foot placement the horse will tolerate (Figure 3-63).

However the foot and x-ray beam are situated, the relationship must be a *parallel* one to produce a diagnostic image. If it is not possible to obtain standard navicular projections, usually because the horse is unwilling to keep its foot positioned caudally,

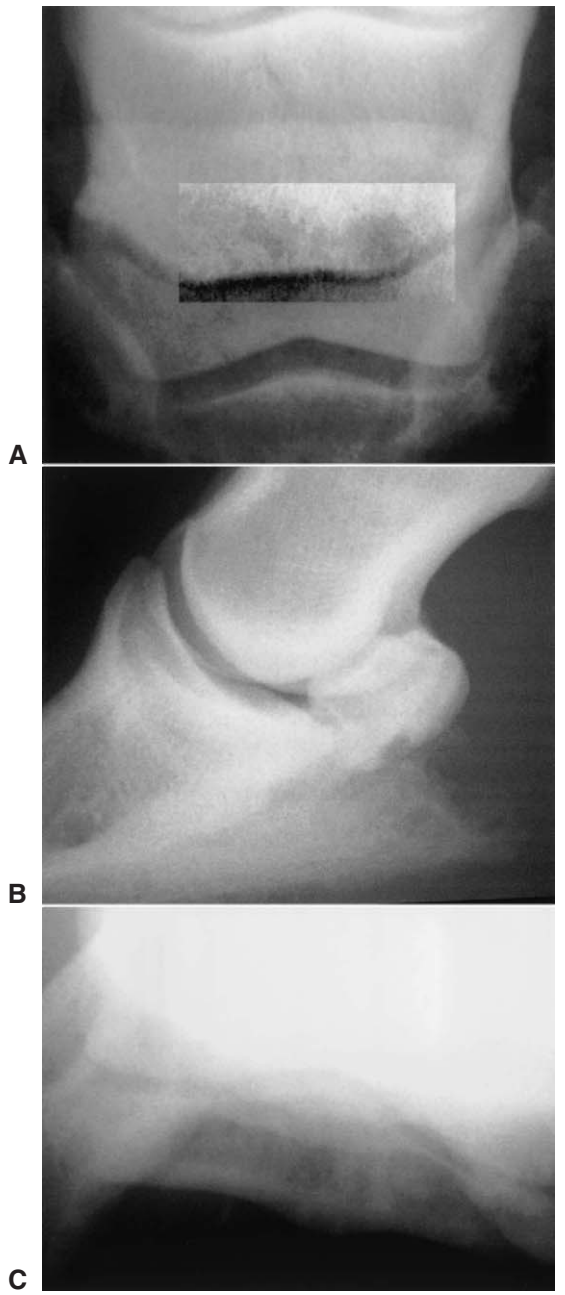


Figure 3-58 • Case 1: Ten-year-old Quarter Horse gelding with severe, unilateral navicular disease. **A,** High coronary view shows multiple, enlarged, distorted vascular channels, some of which have coalesced, resembling bone cysts. **B,** Close-up lateral view, deliberately obliqued, shows a large pit-type defect in the lower half of the sagittal ridge and uneven medullary density, even for an obliged lateral view. **C,** Close-up skyline projection shows poor corticomedullary definition and multiple, vaguely outlined cyst-like lucencies.

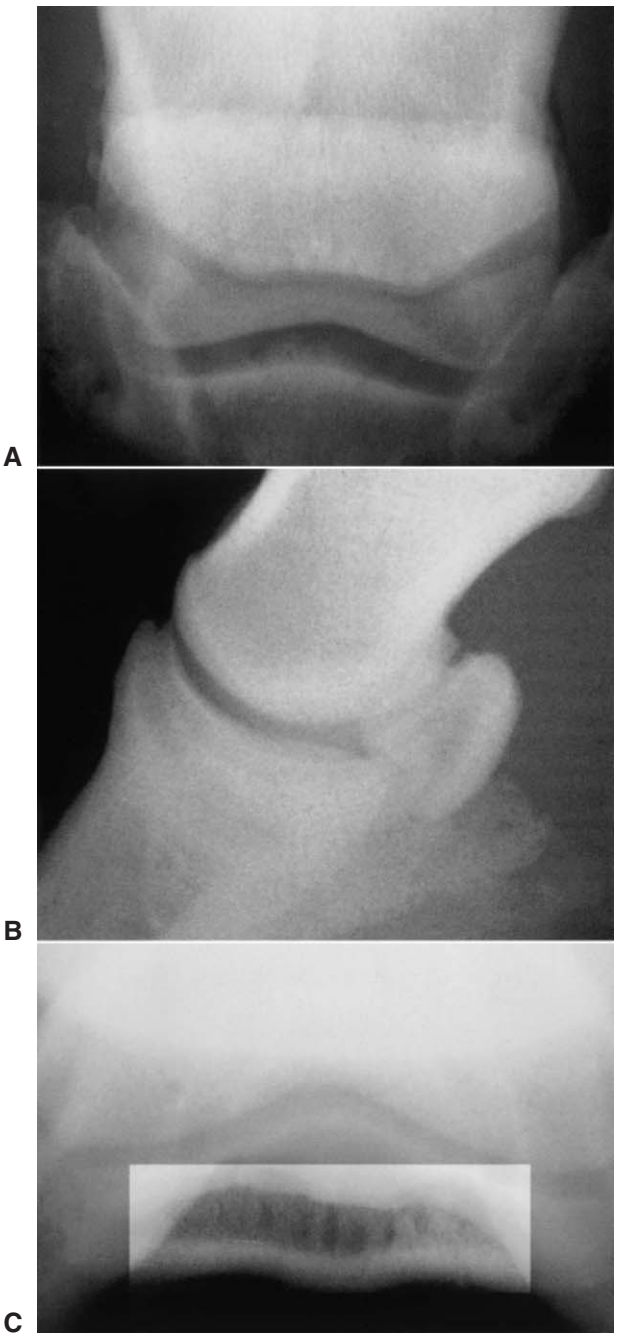


Figure 3-59 • Case 2: Six-year-old Thoroughbred gelding with mild, unilateral navicular disease. **A,** High coronary view shows a mild increase in the size and shape of vascular channels. **B,** Close-up lateral view shows poor corticomedullary definition that is likely due to unintended underexposure and not medullary bone deposition. **C,** Skyline view shows increased size and variability of vascular channels.

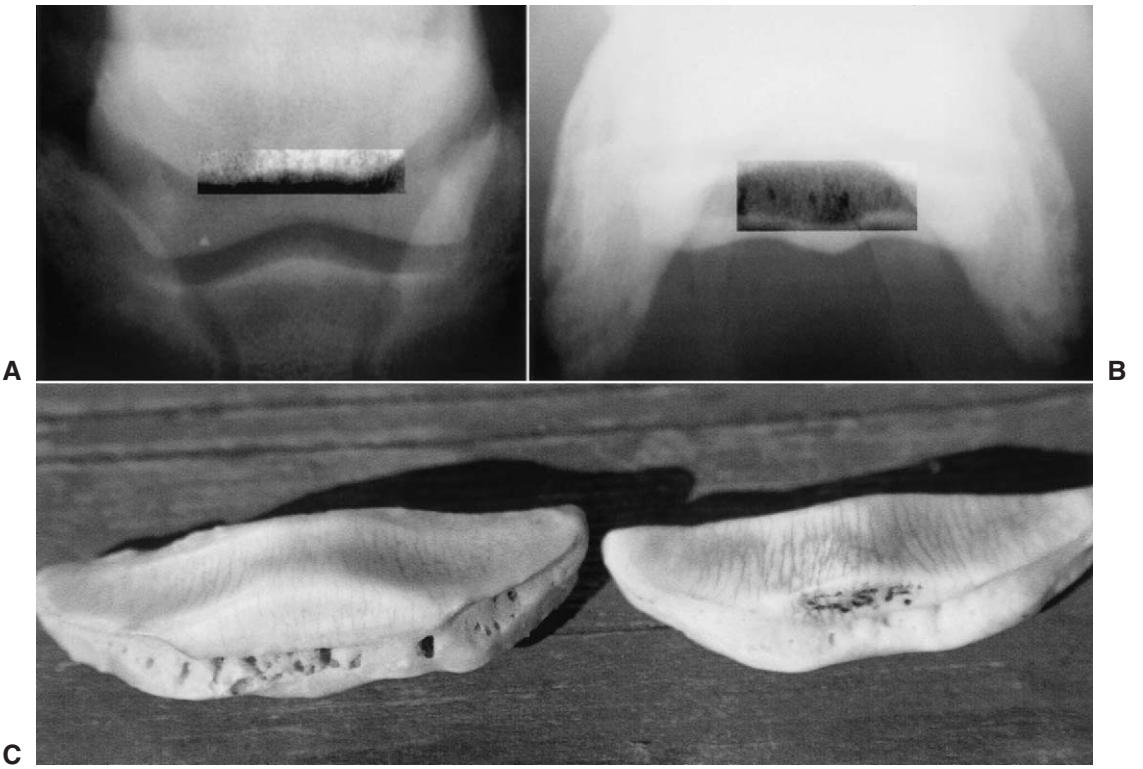


Figure 3-60 • Navicular disease in a 6-year-old Quarter Horse. **A,** High coronary view shows a serrated distal margin. **B,** Skyline projection shows vascular channel prominence but no overt structural abnormalities. **C,** A pair of defleshed navicular bones, diseased on the left and healthy on the right, are provided for comparison.

comparison with the opposite side can be helpful, assuming it is normal (Figure 3-64).

In some middle-aged, older horses with chronic navicular disease, multiple, relatively discrete areas of decreased bone density develop in the flexor cortex, an abnormality that is often appreciable in no other view (Figure 3-65).

Low Coronary View (45-Degree Dorsopalmar). The low coronary view usually contributes little to the diagnosis of navicular disease because there are few important abnormalities that are visible along the proximal border of the bone.

Vascular Channel Redux

The appearance of the vascular channels (vascular foramina) of the navicular bone, currently termed by some as *synovial invaginations,* has been and remains the primary diagnostic focus in navicular disease. Enlargement, distortion, deformity, coalescence, or increases in number have all, in one way or another, been incriminated. Most authorities contend that these abnormalities are caused by inflammatory hyperemia, which leads to bone pain and lameness, prompting the research interest in navicular angiography.

Of late, and coinciding with a movement away from the term *navicular disease,* some veterinarians have vigorously promoted the idea that navicular radiography is an insensitive and nonspecific means of diagnosis, citing normal radiographic examinations in horses that clinically appeared diseased. Armed with this clinical-radiographic contradiction, the diagnostically disenchanted were quick to embrace the expression *caudal heel pain syndrome,* which critics were equally quick to dismiss as "decidedly noncommittal." In this context I offer the following personal viewpoints in a question and answer format.

Questions and Answers About the Diagnostic Utility of Vascular Channels

How Reliable, Diagnostically Speaking, Are Vascular Channel Abnormalities? My own view is that structural changes to the vascular channels, of whatever nature, are a reliable radiographic indicator of navicular disease and one that generally correlates well with both severity and duration.

Does the Absence of Vascular Channel Abnormality Obviate the Possibility of Navicular Disease? Of course not; everything (including navicular disease) must begin somewhere, often without any visible trace. Alternatively, as suggested by some researchers, navicular disease is not a primary bone disorder but rather an overuse injury involving the deep flexor tendon, navicular bursa, and fibrocartilaginous surface of the navicular bone, in which case the vascular channels may never appear abnormal.

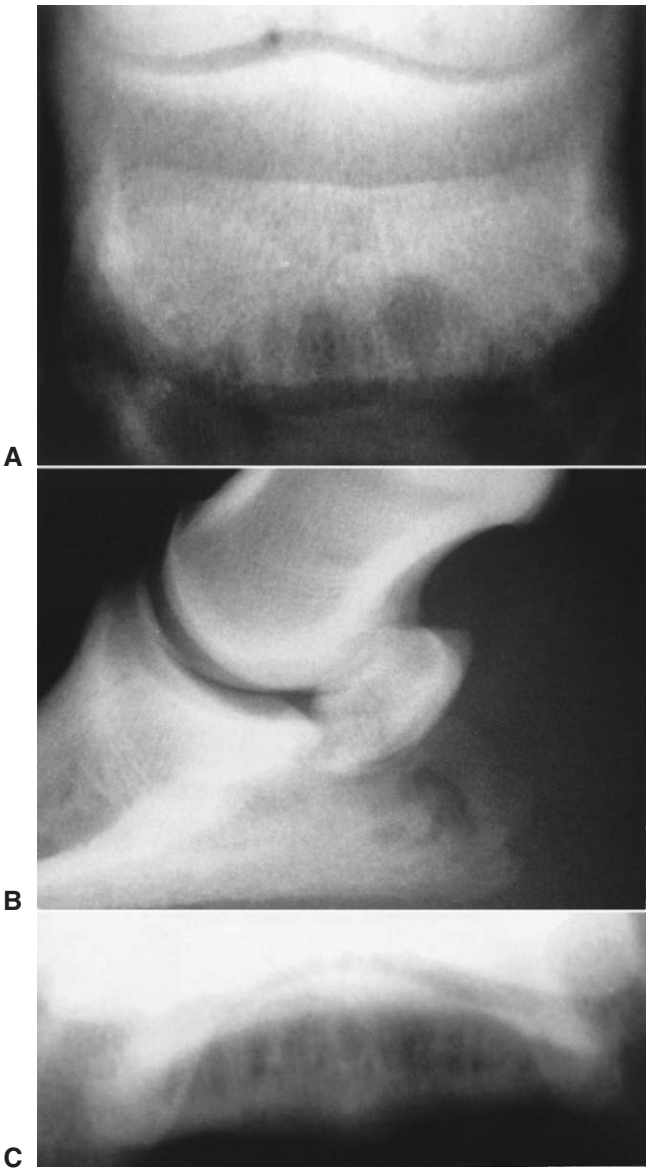


Figure 3-61 • Navicular disease in a 8-year-old Quarter Horse. **A,** High coronary view of navicular bone shows coalescence of enlarged, deformed vascular channels, creating the illusion of multiple bone cysts. **B,** Lateral view shows increased medullary density, making it difficult to distinguish the flexor cortex from the adjacent medulla. **C,** Skyline view features a smudged-appearing bone heavily laced with enlarged, dilated vascular channels.

Do the Vascular Channels Become Abnormal With Age? Although I was taught this as a student more than three decades ago, I have yet to see any substantive proof that this is indeed the case. Thus I do not believe that vascular channels become abnormal merely as a function of advancing age.

Is it Possible to Discriminate Radiographically Between Vascular Channel Enlargement Caused by Hyperemia and That Which Has Been Overgrown by Exuberant Synovium? In my opinion, it is not possible to determine the etiology (or etiologies) of vascular channel enlargement in horses with navicular disease.

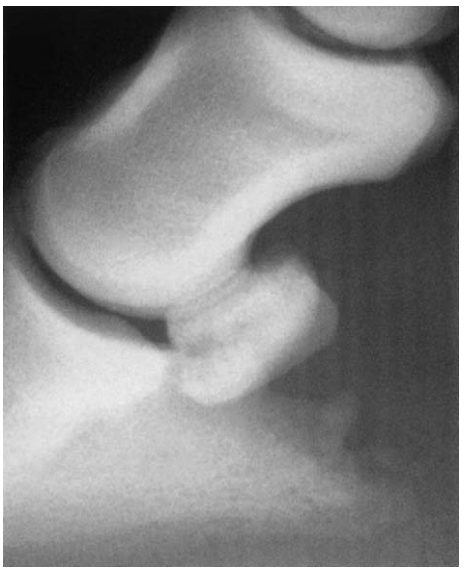


Figure 3-62 • Close-up lateral view of the navicular bone (mildly obliqued) shows increased medullary density, the result of navicular disease.

Scintigraphic Diagnosis of Navicular Disease

Trout and co-workers reported the scintigraphic appearance of navicular disease in 35 proven or suspected cases, concluding that although nuclear imaging appeared to be more sensitive than radiography, combining the two imaging methods proved best (*complementary imaging*). The authors further indicated that scintigraphy might detect navicular abnormalities not visible in radiographs.[91]

Soft-Tissue-Phase Scintigram. Abnormal soft-tissue activity included increased uptake of ^{99m}Tc-MDP in the region of the navicular bone, navicular bursa, and adjacent deep flexor tendon. A highly characteristic lesion (in the opinion of the authors) was seen in some horses consisting of a sharply demarcated *heel void*, a relative loss in activity caused by increased uptake along the *bursal-flexor axis*.

Bone-Phase Scintigram. Abnormal bone activity included increased uptake of ^{99m}Tc-MDP in the region of the navicular bone. Uptake by the collateral cartilages occurred in 15% of the horses examined, making lateral imaging of the navicular field problematic, necessitating greater reliance on the palmar view.

Force-Plate Analysis in Horses With Navicular Disease. Using force-plate analysis, Wilson and co-workers showed, not surprisingly, that horses with navicular disease do their utmost to avoid unnecessary weight bearing over the heel of the foot when trotting.[92] This is accomplished by contracting the deep digital flexor muscle as soon as possible after landing,

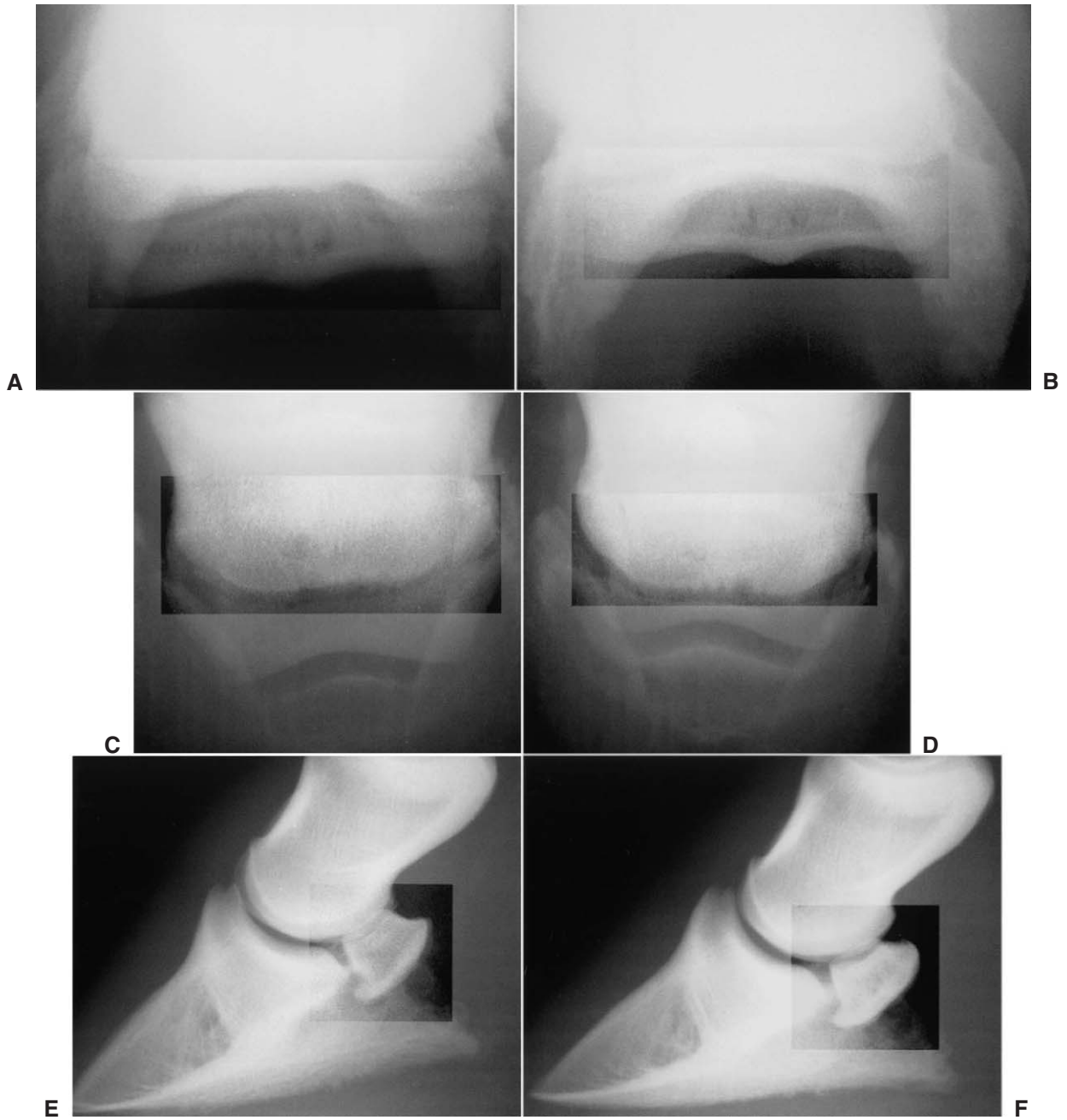


Figure 3-63 • Eleven-year-old Hunter Jumper gelding with unilateral navicular disease. Close-up skyline view **(A)** is imperfect but reveals a genuine increase in medullary density compared with opposite foot **(B).** Close-up high coronary projection **(C)** shows serration of the distal margin and a medium-sized marginal defect compared with opposite foot **(D).** Close-up lateral view **(E)** shows similar corticomedullary opacity compared with opposite foot **(F).**

a kind of quickstep, resulting in minimal load times. These findings appear to validate the time-honored method of symptomatically treating navicular disease by "raising the heel and rolling the toe."

Navicular Infection ("Street Nail")

Deep, penetrating heel wounds can result in bacterial inoculation of the flexor tendon, navicular bursa, or navicular bone, with subsequent osteomyelitis—the so-called *street nail* lesion. Because the flexor margin of the navicular bone is coated by fibrocartilage, evidence of infection may take a month or longer to become radiographically apparent. When it eventually develops, a typical lesion first appears as a shallow concave defect or defects in the central part of the flexor margin (Figure 3-65). Later a shaggy new bone deposit, often resembling a goatee, begins to overlay the original area of bone loss, a characteristic lesion best seen in the skyline projection (Figure 3-66).

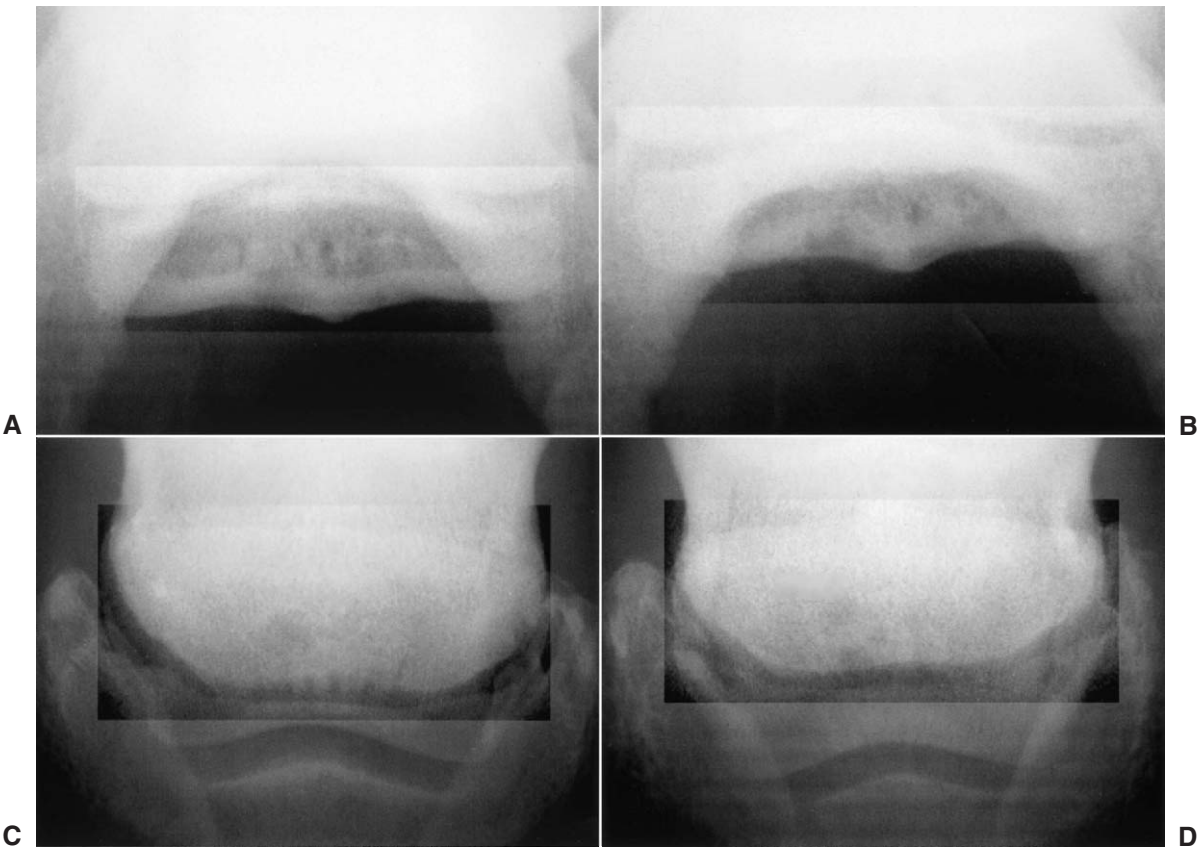


Figure 3-64 • Fifteen-year-old American Saddle Horse with bilateral navicular disease: Right **(A)** and left **(B)** skyline views show extensive bone loss in the central third of the flexor cortex; right **(C)** and left **(D)** high coronary projections reveal multiple enlarged vascular channels, some of which have coalesced.

When a draining sinus is present, sinography will often reveal communication with the navicular bursa or deep flexor tendon, strong presumptive evidence of infection (Figure 3-67).

Richardson and O'Brien reported a medium-sized series of horses (n = 32) that sustained puncture wounds to the navicular bursa, 11 of which developed osteomyelitis within 2 months, the majority of which were eventually destroyed.[93] Steckel and co-workers reported that infections of the navicular bursa, deep flexor tendon, and navicular bone caused by deep puncture wounds of the foot were the most frequent reasons for euthanasia.[94]

Radiographic abnormalities, seen best in the lateral and skyline projections, included (1) flexor cortical irregularity, (2) flexor cortical destruction, (3) pathologic navicular fracture, (4) subluxation of the coffin joint, and (5) osteoarthritis.

Primary and Secondary Navicular Fractures

Insufficiency Fractures (Pathologic Fractures). As mentioned previously, most of the navicular fractures I see are of the insufficiency type, caused by structural weakening to the body of the bone secondary to chronic navicular disease, similar to the reported experience of others.[95] Typically, such fractures occur through large cysts or cystlike areas resulting from the coalescence of two or more adjacent vascular channels (Figure 3-68). Pathologic fractures usually occur at the boundaries between the central and outer thirds of the bone and are visibly, but not greatly, displaced (Figure 3-69). The degree of lameness depends on the duration of the fracture and on whether or not the horse has been nerved.

Primary Body Fractures

Primary fractures of the navicular bone are rare in my experience. Most are complete body fractures located just to one side or the other of the sagittal ridge in healthy-appearing bone. Affected horses are usually acutely and profoundly lame. The opposite navicular bone typically appears normal. So-called wing fractures involving the outer quarters of the bone are even more unusual.[96]

In a small series of horses with acute navicular fractures, Lillich reported the 60-degree DP and skyline views to be most sensitive in identifying complete parasagittal fractures.[97] Progress examinations per-

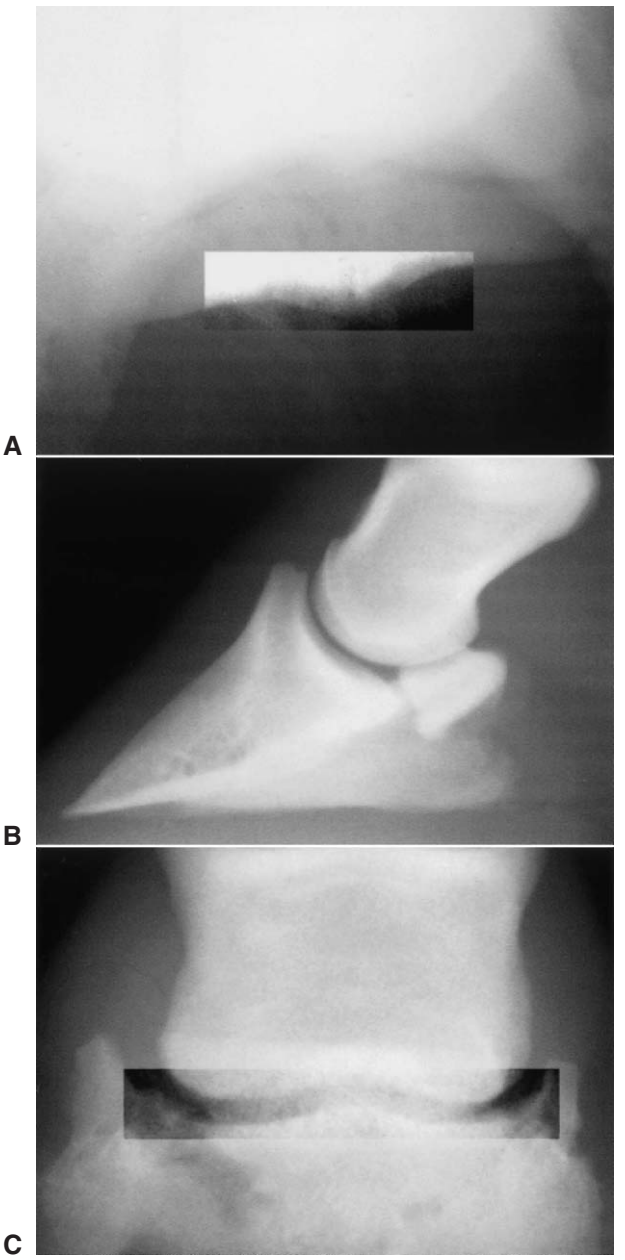


Figure 3-65 • Nine-year-old Appaloosa mare with navicular infection: close-up skyline projection **(A)** shows uneven bone loss along the central part of the distal margin of the navicular bone, lateral view **(B)** shows erosion along the central third of flexor cortex, and close-up 45-degree dorsopalmar projection **(C)** reveals narrowing of the coffin joint.

formed up to 4 months later showed an increase in the width of the fracture line compared with initial images.

Avulsion Fractures. Van De Watering and Morgan were among the first to identify what they termed *chip fractures* along the prominent edge of the distal border of the navicular bone as seen in the high coronary projection (65-degree DP). Based on the presence of other signs of navicular disease in the same specimens, the authors speculated that these fractures might be further evidence of disease.[98]

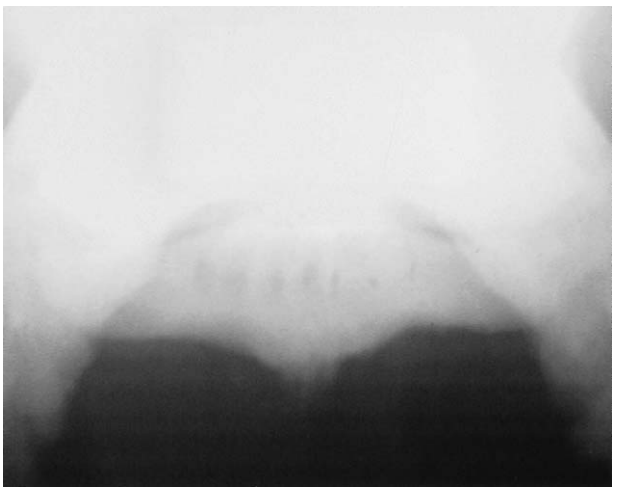


Figure 3-66 • Close-up skyline projection shows a new bone "goatee," often seen in association with street nail navicular infections.

Box 3-6
Possible Radiographic Explanations for One or More Bonelike Objects Seen Along the Distal Border of the Navicular Bone in the High Coronary Projection

Sprain-avulsion fracture of the attachment of the impar ligament
Sprain of the origin of the impar ligament with subsequent dystrophic calcification
Sprain of the origin of the impar ligament with subsequent osseous metaplasia
Microsequestrum
Synovial osteoma
Accessory ossification center
Artifact from underlying sole contaminant (e.g., a pebble)

Modified from Poulos PW, Brown A: On navicular disease in the horse: a roentgenological and patho-anatomic study. part I: evaluation of the flexor central eminence, *Vet Radiol* 30:50, 1989.

Kaser-Hotz and co-workers reported the radiographic and scintigraphic appearance of nonpathologic, avulsion-type fractures from both the proximal and distal navicular borders, the former theorized to be the result of a crush injury stemming from a momentary dislocation of the coffin joint, the latter attributed to a partial tearing of the impar ligament.[99]

Poulos and co-workers, on the other hand, hold the opinion that because there are at least three other possible explanations for discrete, bone-like densities lying along the distal border of the navicular bone (other than fracture), such findings are an unreliable indication of navicular disease (Box 3-6).[100]

Frecklington and Rose reported a confirmed case of sprain-avulsion fracture of the hind navicular bone in a 2-year-old Standardbred colt in which the proximolateral corner of the navicular bone was torn free. As a result, the navicular bone was displaced proximally

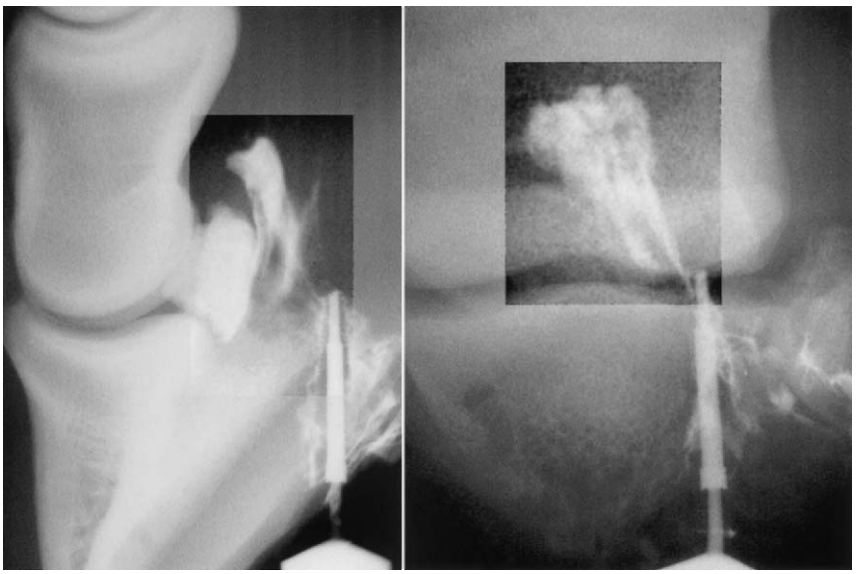


Figure 3-67 • Close-up lateral **(A)** and 45-degree dorsopalmar **(B)** views of a 7-year-old Thoroughbred stallion with navicular infection show contrast solution (within a catheter) outlining a large infectious tract in the heel and entering the navicular bursa and associated deep flexor tendon.

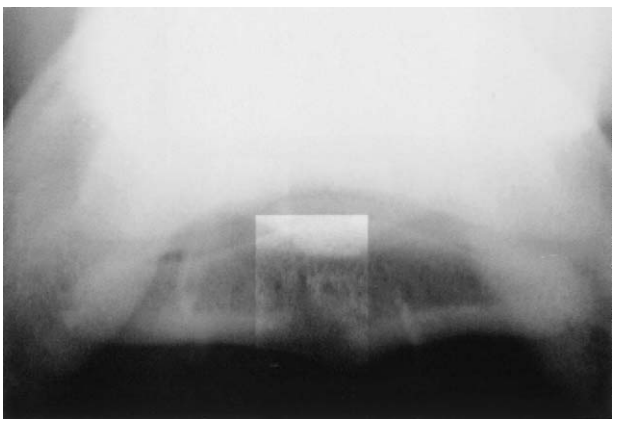


Figure 3-68 • Close-up skyline view of an insufficiency fracture in a horse with advanced navicular disease.

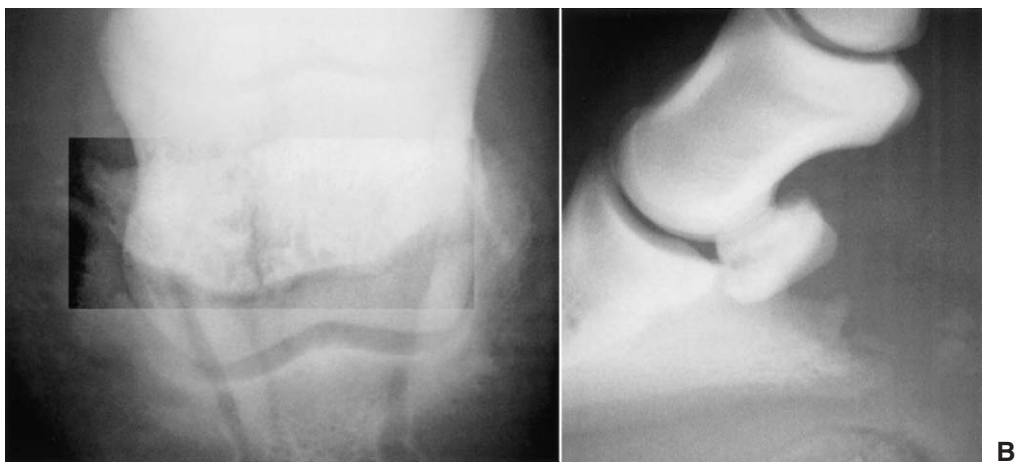


Figure 3-69 • A, Close-up high coronary view of an insufficiency fracture through a demineralized region of the navicular bone, the result of navicular disease. **B,** Predictably, a lateral view provides no indication of the fracture.

and the avulsed fragment remained distally, still attached to the distal phalanx by the impar ligament.[101]

Baird and co-workers reported a fracture-dislocation of the coffin joint as a result of a third-degree sprain of the insertion of the impar ligament.[102]

Congenital Multipiece Navicular Bones (Bipartite, Tripartite Navicular Bones)

Congenital two- or three-piece navicular bones, also termed *bipartite and tripartite deformities*, differ from true fractures insofar as they usually (1) have rounded borders, (2) have larger gaps between fragments, (3) are present bilaterally, and (4) are not painful. Occasionally a long-standing navicular nonunion may resemble a bipartite anomaly, but it will not have a counterpart in the opposite foot.

Multipiece navicular bones are nearly always present bilaterally, but they may not be identical in appearance; for example, one foot may contain a bipartite and the other a tripartite navicular bone as reported by Feeney.[103] Nonunion navicular fractures treated by neurectomy may resemble congenital, multipiece navicular bones, but they are usually only found unilaterally.

Occasionally bipartite or tripartite navicular bones are found in the context of severe navicular disease, with or without previous therapeutic neurectomy (Figure 3-70). In such circumstances, it is difficult to know which came first, the "fracture" or the structural weakening caused by navicular disease.

Associated Soft-Tissue Mineralization

Causes. Soft-tissue mineralization adjacent to the navicular bone may have many causes:



Figure 3-70 • Close-up high coronary view of right front navicular bone in a minimally lame horse shows three-piece navicular bone and severe navicular disease. Radiographic examination of the opposite front foot revealed similar findings. Given the rarity of a multiple navicular bone fracture and the even greater improbability of bilateral, multiple fractures, these were believed to be congenital tripartite navicular bones with concomitant, but unrelated, navicular disease.

- *Dystrophic Calcification:* Dystrophic calcification of the deep digital flexor tendon or distal sesamoidian ligament may result from a severe strain or sprain, chronic tendonitis, or desmitis and occasionally after a regional infection or hemorrhage. Dystrophic calcification as a result of navicular disease has also been reported but without more than radiologic confirmation.[104] The precise cause or causes of dystrophic calcification is not known, as indicated by the many unsuccessful efforts to reproduce it experimentally.
- *Prior Neurectomy*: Palmar digital neurectomy has also been suggested as a possible cause of dystrophic calcification in the navicular region because of its potential to cause necrosis, as shown by Taylor and Vaughan.[105]
- *Prior Bone Graft*: The presence of residual mineralization left over from a previous autogenous cancellous bone graft used to treat a septic navicular bursa or navicular bone may be radiographically detectable up to 450 days following surgery.[106]
- *Bony Metaplasia*: Like dystrophic calcification, the cause or causes of localized soft tissue metaplasia is not known, although I've observed it bilaterally in a sound horse. Vertically oriented bands of disorganized bony tissue occasionally form in and around the surface of the deep digital flexor tendon adjacent to the navicular bone that radiographically resemble one form of *myositis ossificans*. Palmar digital neurectomy has also been suggested as a possible cause.

Radiology. Abnormal calcification (mineralization) on and around the navicular bone is usually linear or band-like in appearance and oriented vertically along the flexor margin of the navicular bone.[107]

The Coffin Joint

Altered States: How Weight-Bearing Affects the Coffin Joint. As emphasized repeatedly, when a horse shifts its weight, especially to compensate for its leg being raised when its opposite foot is being radiographed, its weight-bearing coffin joint often narrows asymmetrically. This normal variant must not be mistaken for disease. One additional clue to the postural, rather than pathologic, nature of such a finding is a similar narrowing that occurs in the associated pastern, and sometimes the fetlock joint as well.

Relationship of the Navicular Bursa to the Distal Interphalangeal Joint

Gibon and co-workers have described the physical relationship between the coffin joint and the navicular bursa using radiographic contrast studies in both living horses and dismembered forelimbs.[108] They concluded that the distal interphalangeal joint and navicular bursa do not normally communicate either in living horses or in cadaveric limbs.

However, the authors did observe contrast solution in the digital flexor tendon sheath of one 11-year-old horse after a navicular bursa injection, prompting speculation that this may be a normal occurrence in "a small percentage of normal horses."

The authors further speculated that the long-held belief that a puncture wound to the navicular bursa causing infection (a so-called *street nail*) would lead eventually to involvement of the coffin joint by direct extension probably is not true. Furthermore, this work appears to cast additional doubt on the validity of the term *caudal heel pain syndrome*, other than as a possible point of diagnostic departure for those with limited clinical experience.

Distal Phalangeal Hyperflexion (Clubfoot). Flexural deformity of the distal interphalangeal joint is a disease of unknown etiology that typically occurs in young foals. With this disorder, the foal maintains its foot in a partially flexed position, although full extension is usually possible. Some authorities speculate that the disease is caused by rapid growth, an unfortunate, catchall diagnosis that unfortunately does little or nothing to elucidate the actual cause or causes of the condition.[109]

Congenital and Acquired Hyperflexion. Kidd and Barr divided flexural deformities in foals into two categories: congenital and acquired.[110] In the former category, they included flexural deformities of the front fetlock and carpus, and in the latter category, hyperflexion of the distal interphalangeal and metacarpophalangeal joints. They further subdivided the condition according to age of onset: foals (6 weeks to 6 months old), yearlings (9 to 18 months old), and fully grown, adult horses.

Theoretical explanations for the congenital form of the disease include abnormal intrauterine positioning, prenatal intoxication, genetic mutation, goiter, neuromuscular disease, and influenza virus. Two possible explanations for acquired hyperflexion include (1) uncoordinated or disparate growth between bones and related muscle-tendon units and (2) pain-related muscle contraction. As far as I am aware, neither of these hypotheses enjoys widespread acceptance.

Acquired flexural deformity of the distal interphalangeal joint usually occurs bilaterally in the front feet of young foals when they are between 1 and 6 months of age. Typically the face of the hoof assumes a near-vertical position, and the heal leaves the ground. The associated deep flexor tendon is often quite taut. If accessory ligament desmotomy is performed,[111] I strongly recommend making preoperative radiographs as a means of showing postoperative improvement.

References

1. Roberts GD, Graham JP: Computed radiography, *Vet Clin N Am (Equine Pract)* 17:47, 2001.
2. Smallwood JE, Holladay SD: Xeroradiographic anatomy of the equine digit and metacarpophalangeal region, *Vet Radiol* 28:166, 1987.
3. Busoni V, Denoix J-M: Ultrasonography of the podotrochlear apparatus in the horse using a transcuneal approach: technique and reference images, *Vet Radiol Ultrasound* 42:534, 2001.
4. Coffman JR, Jonson JH, et al: Hoof circulation in equine laminitis. *J Am Vet Med Assoc* 156:76, 1970.
5. Ackerman N, Garner E, et al: Angiographic appearance of the normal equine foot and alterations in chronic laminitis, *J Am Vet Med Assoc* 166:58, 1975.
6. Bordalai CC, Nigam JM: Angiographic studies of the donkey foot (normal and abnormal), *Vet Radiol* 18:90, 1977.
7. Hoskinson JJ: Equine nuclear scintigraphy: indications, uses, techniques, *Vet Clin N Am (Equine Pract)* 17:63, 2001.
8. Riddolls LJ, Willoughby RA, Dobson H: A method of mounting a gamma detector and yoke assembly for equine nuclear imaging, *Vet Radiol* 32:78, 1991.
9. Neuwirth L, Romine C: Ancillary equipment to increase quality and reduce radiation exposure in the equine nuclear medicine laboratory, *Vet Radiol Ultrasound* 41:470, 2000.
10. Twardock AR: Equine bone scitigraphic uptake patterns related to age, breed, and occupation, *Vet Clin N Am (Equine Pract)* 17:75, 2001.
11. Metcalf MR, Sellet LC, et al: Scintigraphic characterization of the equine foredigit and metacarpophalangeal region from birth to six months of age, *Vet Radiol Ultrasound* 30:111, 1989.
12. Arthur RM, Constantinide D: Results of 428 nuclear scintigraphic examinations of the musculoskeletal system at a Thoroughbred racetrack. In *Proc Am Assoc Equine Practitioners,* 41st Annual Meeting, Lexington, 1995, p 84.
13. Trout DR, Hornof WJ, et al: The effects of regional perineural anesthesia on soft tissue and bone phase scintigraphy in the horse, *Vet Radiol Ultrasound* 32:140,1991.
14. Roub LW, Gumerman LW, et al: Bone stress: a radionuclide imaging perspective, *Radiology* 132:431, 1979.
15. Morris EA, Seeherman HJ: Clinical evaluation of poor performance in the racehorse: the results of 275 evaluations, *Equine Vet J* 23:169, 1991.
16. Lamb CR, Koblik PD: Scintigraphic evaluation of skeletal disease and its application to the horse, *Vet Radiol* 29:16, 1988.
17. Goggin JM, Hoskinson JJ, et al: Scintigraphic assessment of distal extremity perfusion: 17 cases, *Vet Radiol Ultrasound* 38:211, 1997.
18. Keegan KG, Twardock AR, et al: Scintigraphic evaluation of fractures of the distal phalanx in horses: 27 cases (1979-1988), *J Am Vet Med Assoc* 202:1993, 1993.
19. Long CD, Galluppo LD, et al: Scintigraphic detection of equine orthopedic infection using TcHMPOA labeled leukocytes in 14 horses, *Vet Radiol Ultrasound* 41:354, 2000.
20. Trout DR, Hornof WJ, O'Brien TR: Soft tissue and bone phase scintigraphy for diagnosis of navicular disease in horses, *J Am Vet Med Assoc* 198:73, 1991.
21. Ehrlich PJ, Dohoo JR, O'Callaghan MW: Results of bone scintigraphy in racing Standardbred horses: 64 cases (1992-1994), *J Am Vet Med Assoc* 215:982, 1999.
22. Ehrlich PJ, Seeherman HJ, et al: Results of bone injury in horses used for show jumping, hunting, or eventing: 141 cases (1988-1994), *J Am Vet Med Assoc* 213:1460, 1998.
23. Turner TA: Diagnostic thermography, *Vet Clin N Am (Equine Pract)* 17:95, 2001.

24. Stromberg B: The use of thermography in equine orthopedics, *Vet Radiol* 15:94, 1974.
25. Barbee DD, Allen JR, Gavin PR: Computed tomography in horses, *Vet Radiol* 28:144, 1987.
26. Tucker RL, Sande RD: Computed tomography and magnetic resonance imaging in equine musculoskeletal conditions, *Vet Clin N Am (Equine Pract)* 17:145, 2001.
27. Widmer WR, Buckwalter KA, et al: Use of radiography, computed tomography and magnetic resonance imaging for evaluation of navicular syndrome in the horse, *Vet Radiol Ultrasound* 41:108, 2000.
28. Park RD, Nelson TR, Hoopes PJ: Magnetic resonance imaging of the normal equine digit and metacarpophalangeal joint, *Vet Radiol* 28:105, 1987.
29. Denoix J-M, Crevier N, et al: Magnetic resonance imaging of the equine foot, *Vet Radiol Ultrasound* 34:405, 1993.
30. Kleiter M, Kneissi S, et al: Evaluation of magnetic resonance imaging techniques in the equine digit, *Vet Radiol Ultrasound* 40:15, 1999.
31. Busoni V, Snaps F: Effect of deep digital flexor tendon orientation on magnetic resonance imaging signal intensity in isolated equine limbs—the magic angle effect, *Vet Radiol* 43:428, 2002.
32. Dyson S, Murray R, et al: Magnetic resonance imaging of the equine foot: 15 horses, *Equine Vet J* 35:18, 2003.
33. Quick CB, Rendana VT: Equine radiology—the pastern and foot, *Mod Vet Pract* 58:1022, 1977.
34. Kaneps AJ, Stover S, et al: Radiographic characteristics of the forelimb distal phalanx and microscopic morphology of the lateral palmar process in foals 3-32 weeks old, *Vet Radiol Ultrasound* 36:179, 1995.
35. Becht JL, Park RD, et al: Radiographic interpretation of normal skeletal variations and pseudolesions in the equine foot, *Vet Clin N Am (Equine Pract)* 17:1, 2001.
36. Rendano VT, Grant B: The equine third phalanx: its radiographic appearance, *Vet Radiol* 19:125, 1978.
37. Ruohoniemi M, Karkkainen M, Tervartiala T: Evaluation of the variably ossified collateral cartilages of the distal phalanx and adjacent anatomic structures in the Finnhorse with computed tomography and magnetic resonance imaging, *Vet Radiol Ultrasound* 38:344, 1997.
38. Ruohoniemi M, Ryhanen V, Tulamo R-M: Radiographic appearance of the navicular bone and distal interphalangeal joint and their relationship with ossification of the collateral cartilages of the distal phalanx in Finnhorse cadaver forefeet, *Vet Radiol Ultrasound* 39:125, 1998.
39. Starrack GS: Equine foot radiography—hoof preparation, *Vet Radiol Ultrasound* 37:116, 1996.
40. Watters JW, Lebel JL, Park RD: Morphometric analysis of radiographic changes in the distal phalanges of Quarter Horses with lower-leg lameness, *Vet Radiol* 19:60, 1978.
41. Stick JA, Jann HW, et al: Pedal bone rotation as a prognostic sign in laminitis of horses, *J Am Vet Med Assoc* 180:251, 1982.
42. Koblik PD, O'Brien TR, Coyne CP: Effect of dorsopalmar projection obliquity on radiographic measurement of distal phalangeal rotation angle in horses with laminitis, *J Am Vet Med Assoc* 192:346, 1988.
43. Balch O, White K, Butler D: Factors involved in the balancing of equine hooves, *J Am Vet Med Assoc* 198:1980, 1991.
44. Redden RF: Radiographic imaging of the equine foot, *Vet Clin N Am* 19:379, 2003.
45. Linford RL, O'Brien TR, Trout DR: Qualitative and morphometric radiographic findings in the distal phalanx and digital soft tissues of sound Thoroughbred racehorses, *Am J Vet Res* 54:38, 1993.
46. Arnbjerg J: What is your diagnosis? *J Am Vet Med Assoc* 174:291, 1979.
47. Herthel D, Hood DM: Clinical presentation, diagnosis, and prognosis of chronic laminitis, *Vet Clin N Am (Equine Pract)* 15:375, 1999.
48. Morgan SJ, Grosenbaugh DA: The pathophysiology of chronic laminitis: pain and anatomic pathology, *Vet Clin N Am (Equine Pract)* 15:395, 1999.
49. Peloso JG, Cohen ND, et al: Case-controlled study of risk factors for the development of laminitis in the contralateral limb in Equidae with unilateral lameness, *J Am Vet Med Assoc* 209:1746, 1996.
50. Curtis S, Ferguson D: Trimming and shoeing the chronically affected horse, *Vet Clin N Am* (*Equine Pract*) 15:463, 1999.
51. Brosnahan MM, Paradis MR: Demographic and clinical characteristics of geriatric horses: 467 cases (1989-1999), *J Am Vet Med Assoc* 223:93, 2003.
52. Coffman JR, Johnson G, et al: Hoof circulation in equine laminitis, *J Am Vet Med Assoc* 156:76, 1970.
53. Ackerman N, Garner HE, et al: Angiographic appearance of the normal equine foot and alterations in chronic laminitis, *J Am Vet Med Assoc* 166:58, 1975.
54. Garner HE, Hahn C, et al: Cardiac output, left ventricular ejection rate, plasma volume, and heart rate changes in equine laminitis-hypertension, *Am J Vet Res* 38:725, 1977.
55. Turner AS, Gabel AA: Lag screw fixation of avulsion fractures of the second phalanx in the horse, *J Am Vet Med Assoc* 167:306, 1975.
56. Rose PL, Seeherman H, O'Callaghan M: Computed tomographic evaluation of comminuted middle phalangeal fractures in the horse, *Vet Radiol Ultrasound* 38:424, 1997.
57. Crabill MR, Watkins JP, et al: Double-plate fixation of comminuted fractures of the second phalanx in horses: 10 cases (1985-1993), *J Am Vet Med Assoc* 207:1458, 1995.
58. Hathcock JT: What is your diagnosis? *J Am Vet Med Assoc* 181:721, 1982.
59. Scott EA, McDole M, Shires MH: A review of third phalanx fractures in the horse, *J Am Vet Med Assoc* 174:1337, 1979.
60. Sedrish SA, Valdez-Vazquez MA, Pechman R: What is your diagnosis? *J Am Vet Med Assoc* 209:729, 1996.
61. Scott EA, McDole M, Shires GMH: A review of third phalanx fractures in horses: 64 cases, *J Am Vet Med Assoc* 174:1337, 1979.
62. Wan PY, Tucker RL, Latimer FG: Scintigraphic diagnosis. *Vet Radiol* 33:247, 1992.
63. Martens P, Ihler CF, Renneslund J: Detection of a radiographically occult fracture of the lateral palmar process of the distal phalanx in a horse using computed tomography, *Vet Radiol Ultrasound* 40:346, 1999.
64. Scott EA, Snyder SP, et al: Subchondral bone cysts with fractures of the extensor processes in a horse, *J Am Vet Med Assoc* 199:595, 1991.
65. Petterson H: Fractures of the pedal bone in the horse, *Equine Vet J* 8:104, 1976.
66. Verschooten F, De Moore A: Subchondral cystic and related lesions affecting the equine pedal bone and stifle, *Equine Vet J* 14:47, 1982.
67. Honnas CM, O'Brien TR, Linford RL: Distal phalangeal fractures in horses, *Vet Radiol* 29:98, 1988.

68. Keegan KG, Twardock AR, et al: Scintigraphic evaluation of fractures of the distal phalanx in horses: 27 cases (1979-1988), *J Am Vet Med Assoc* 202:1993, 1993.
69. Barber SM: Letters, *J Am Vet Med Assoc* 181:1468, 1982.
70. Barber SM: Subluxation and sepsis of the distal interphalangeal joint of a horse, *J Am Vet Med Assoc* 181:491, 1982.
71. Baird AN, Seahorn TL, Morris EL: Equine distal phalangeal sequestration, *Vet Radiol* 31:210, 1990.
72. Honnas CM, O'Brien TR, Linford RL: Distal phalangeal fractures in horses: a survey of 274 horses with radiographic assessment of healing in 36 horses, *Vet Radiol* 29:98, 1988.
73. Verschooten F: Post-traumatic subchondral bone cysts and subchondral bone necrosis in the horse, *Vlaams Diergeneeskundig Tijdschrift* 49:237, 1980.
74. Berry CR, O'Brien TR, Pool RR: Squamous cell carcinoma of the hoof wall in a stallion, *J Am Vet Med Assoc* 199:90, 1991.
75. Taylor TS, Morris EL: Agenesis of the distal phalanx in a mule, *Vet Radiol* 24:63, 1983.
76. Bertone AL, Aanes WA: Congenital phalangeal hypoplasia in Equidae, *J Am Vet Med Assoc* 185:554, 1984.
77. Verschooten F, De Moore A: Subchondral cystic and related lesions affecting the equine pedal bone and stifle, *Equine Vet J* 14:47, 1982.
78. Vasquez de Mercado R, Stover SM, et al: Lateral approach for arthrocentesis of the distal interphalangeal joint in horses, *J Am Vet Med Assoc* 212:1413, 1998.
79. Turner J: Diagnosis and treatment of navicular syndrome in horses, *Vet Clin N Am* (*Equine Pract*) 1989:5, 131.
80. Seahorn TL, Sams AE, et al: Ultrasonic imaging of a keratoma in a horse, *J Am Vet Med Assoc* 200:1973, 1992.
81. Monticello TM, Jakob TP, Crane S: Malignant melanoma of the coronary band in a horse, *J Am Vet Med Assoc* 188:297, 1986.
82. Attenburrow DP, Heyse-Moore GH: Non-ossifying fibroma in phalanx of a Thoroughbred yearling, *Equine Vet J* 14:59, 1982.
83. Kaser-Hotz B, Ueltschi G: Radiographic appearance of the navicular bone in sound horses, *Vet Radiol Ultrasound* 33:9, 1992.
84. Poulos PW, Brown A: On navicular disease in the horse: a roentgenological and patho-anatomic study. Part I: evaluation of the flexor central eminence, *Vet Radiol* 30:50, 1989.
85. Ruohoniemi M, Tervahartiala P: Computed tomographic evaluation of Finnhorse cadaver forefeet with radiographically problematic findings on the flexor aspect of the navicular bone, *Vet Radiol Ultrasound* 40:275, 1999.
86. DeClerco T, Verschooten F, Ysebaert M: A comparison of the palmaroproximal-palmarodistal view of the isolated navicular bone to other views, *Vet Radiol Ultrasound* 41:525, 2000.
87. Smith F: The pathology of navicular disease, *Vet J* 23:73, 1885.
88. Wright JM: A study of 118 cases of navicular disease: radiological features, *Equine Vet J* 25:493, 1993.
89. Merriam JG, Johnson JH: Subchondral cysts of the navicular bone as a cause of equine lameness. *Vet Med Small Anim Clin* 69:873, 1974.
90. O'Brien TR, Millman TM, et al: Navicular disease in the Thoroughbred horse: a morphologic investigation relative to a new radiographic projection, *Vet Radiol* 16:39, 1975.
91. Trout DR, Hornof WJ, O'Brien TR: Soft tissue and bone-phase scintigraphy for diagnosis of navicular disease in horses, *J Am Vet Med Assoc* 198:73, 1991.
92. Wilson AM, McGuigan MP, et al: The force and contact stress on the navicular bone during trot locomotion in sound horses and horses with navicular disease, *Equine Vet J* 33:159, 2001.
93. Richardson GL, O'Brien TR: Puncture wounds into the navicular bursa of the horse, *Vet Radiol* 26:203, 1985.
94. Steckel RR, Fessler JF, Huston LC: Deep puncture wounds of the equine hoof: a review of 50 cases, in Proceedings, *Am Assoc Equine Pract* 35:167, 1980.
95. Baxter GM, Ingle JE, Trotter GW: Complete navicular bone fractures in horses, in Proceedings, *Am Assoc Equine Pract* 41:243, 1995.
96. Waldridge BM, Ward TA: What is your diagnosis? *J Am Vet Med Assoc* 216:1393, 2000.
97. Lillich JD, Ruggles AJ, et al: Fracture of the distal sesamoid bone in horses: 17 cases (1982-1992), *J Am Vet Med Assoc* 207:924, 1995.
98. Van De Watering CC, Morgan JP: Chip fractures as a radiographic finding in navicular disease of the horse, *Vet Radiol* 16:206, 1975.
99. Kaser-Hotz B, Ueltschi G: Navicular bone fracture in the pelvic limb in two horses, *Vet Radiol Ultrasound* 32:283, 1991.
100. Poulos PW, Brown A: On navicular disease in the horse: a roentgenological and patho-anatomic study. Part II: osseous bodies associated with the impar ligament, *Vet Radiol* 30:54, 1989.
101. Frecklington PJ, Rose RJ: An unusual case of fracture of the navicular bone in the hindlimb of a horse, *Aust Vet Pract* 11:57, 1981.
102. Baird AN, Behrens E, et al: What is your diagnosis? *J Am Vet Med Assoc* 196:1147, 1990.
103. Feeney DA, Booth LC, Johnston GR: What is your diagnosis? *J Am Vet Med Assoc* 177:644, 1980.
104. Turner TA: Dystrophic calcification of the deep digital flexor tendons resulting from navicular disease, *Vet Med Small Anim Clin* 77:571, 1982.
105. Taylor TS, Vaughan JT: Effects of denervation of the digit of the horse, *J Am Vet Med Assoc* 177:1033, 1980.
106. Honnas CM, Crabell MR, et al: Use of autogenous cancellous bone grafting in the treatment of septic navicular bursitis and distal sesamoid osteomyelitis in horses, *J Am Vet Med Assoc* 206:1191, 1995.
107. Blaik MA, Hanson RR: What is your diagnosis? *J Am Vet Med Assoc* 214:482, 1999.
108. Gibson KT, McIlwraith, Park RD: A radiographic study of the distal interphalangeal joint and navicular bursa of the horse, *Vet Radiol Ultrasound* 31:22, 1990.
109. Fackelman GE, Auer JA, et al: Surgical treatment of severe flexural deformity of the distal interphalangeal joint in young horses, *J Am Vet Med Assoc* 182:949, 1983.
110. Kidd JA, Barr RS: Flexural deformities in foals, *Equine Vet Educ* 14:311, 2002.
111. Stick JA, Nickels FA, Williams MA: Long-term effects of desmotomy of the accessory ligament of the deep digital flexor muscle in Standardbreds: 23 cases (1979-1989), *J Am Vet Med Assoc* 200:1131, 1992.

Chapter 4

The Pastern Joint

THE STANDARD PASTERN SERIES

A standard pastern series includes four full-length views of both the long and short pastern bones (P1 and P2), in addition to the fetlock, pastern, and coffin joints (Table 4-1).

The radiographs from two normal pastern joints, a foal and an adult, are shown in Figures 4-1 and 4-2.

Caution: The highly variable bony ridges located on both the front and back surfaces of the first and second phalanges can be mistaken for osteophytes or enthesiophytes. See the section on ringbone in this chapter for further details.

THE NORMAL PASTERN JOINT

The pastern joint, which is also termed the *proximal interphalangeal joint*, is normally wider than the fetlock joint but narrower than the coffin joint. As with the fetlock and coffin joints, the pastern joint is subject to transient, asymmetric narrowing related to natural and induced weight shifting (also termed *leaning off*).

ABNORMAL WIDTH OF THE PASTERN JOINT

Narrowing

As mentioned previously, narrowing of the pastern is usually temporary. The second most common cause of a temporarily narrowed pastern joint is reduced use related to a more distally located lameness, such as navicular disease or a sole abscess. Under such circumstances, the fetlock and coffin joints are typically narrowed as well (Figure 4-3). Once the lameness has resolved, the cartilage spaces quickly return to their original widths, usually within a month or so.

Ringbone is often associated with a narrowed cartilage space, although it is not always clear whether the joint is actually narrowed or just obscured from view. Septic arthritis secondary to bacterial inoculation from a penetrating wound usually results in initial narrowing but later leads to widening. Regional wounds usually produce sufficient lameness to result in reduced use and resultant secondary narrowing.

Widening

The joints of immature horses, especially young foals, are relatively wider than those of adult animals. This is because the cartilage covering the bone ends must serve a dual function: to act as articular cartilage and to serve as a precursor for epiphyseal bone growth (see Figure 4-1). Non–weight bearing, especially in the distal extremital joints, usually results in some measure of observable widening, depending on how the horse is positioned and the specific radiographic projection (Figure 4-4).

Partial dislocation of the pastern joint, as seen in severe sprains and congenital or developmental tendon disease, is also associated with a widened pastern joint (Figure 4-5). Advanced septic arthritis, usually the result of a hematogenous infection such as navel ill, is also capable of increasing joint width, especially in young foals. In most such cases, more than one limb is involved but not always to the same extent.

ADDITIONAL PASTERN FACTS

Quick and Rendano published a series of illustrated reviews on equine anatomy, including the pastern. Although their remarks are intended to describe the front pastern, they apply equally well to the hind pastern.[1]

- P1 is about twice as long as P2.
- The *common* and *lateral digital extensor tendons* attach to the extensor processes (dorsal eminences, "anterior lips") located on the dorsoproximal aspect of P1.



Figure 4-1 • A, Lateral view of the pastern joint of 2-week-old foal (including fetlock) shows a relatively widened pastern joint compared with that of an adult horse. **B,** Dorsopalmar view of fetlock and proximal pastern shows normal growth plates in both the distal third metacarpal bone and proximal phalanx.

Table 4–1 • EVALUATIVE PURPOSE OF THE STANDARD PASTERN SERIES

View	Evaluative purpose
Frontal (dorsopalmar)	Cartilage space width and osteoarthritis.
Lateral (lateromedial)	Cartilage space width and osteoarthritis.
Right lateral oblique	New bone deposition, some longitudinal or long spiral fractures (especially if articular), and proximal eminence lesions such as fractures and the fragmenting form of osteochondritis.
Left lateral oblique	New bone deposition, some longitudinal or long spiral fractures (especially if articular), and proximal eminence lesions such as fractures and the fragmenting form of osteochondritis.

- The proximal articular surface of P1 is composed of two shallow cups flanking a deep sagittal trough, contoured to accommodate the third metacarpal condyle and its prominent central ridge.
- Tubercles situated on the lateral aspects of the caudal eminences moor the distal aspects of the collateral ligaments.
- A pair of long diagonal ridges forms a V on the back posterior surface of P1 where the sesamoidian ligaments attach.
- A vague, radiolucent circle in the distal third of P1 as seen in the dorsopalmar projection is normal and is not a bone cyst or localized bone loss caused by an infection.
- Paired palmar eminences (tubercles) located on the palmarolateral and palmaromedial aspects of P2 account for the relative difference in width when viewed radiographically.
- The palmar eminences moor the distal aspects of the collateral ligaments of the pastern joint, in addition to securing the superficial digital flexor tendon.
- Paired, irregular, semicircular ridges on the dorsal surface of the distal aspect of P2, attachments for the collateral ligaments of the coffin joint and branches of the superficial digital flexor tendon, can be mistaken for ringbone, especially in oblique projections.

▮▮▮ RINGBONE

Ringbone Defined

What sets ringbone apart from most other kinds of osteoarthritis is its initial location relative to the nearby cartilage space. Unlike most types of osteoarthritis, which are typified by *periarticular* osteophytes, ringbone is characterized by *extraarticular* bone deposits, although eventually there may be periarticular osteophytes as well (Figure 4-6). In this latter regard, considerable care must be taken not to mistake the normal (but highly variable) distal lateral ridges of the long and short pasterns for ringbone, especially as viewed obliquely (Figure 4-7).

The predominantly extraarticular nature of ringbone also explains why true, naturally occurring arthrodesis rarely occurs, contrary to popular opinion. Although serial radiographic examinations often create the illusion of gradual fusion, the more likely explanations are that the nearby joint is being partially concealed by the growing mass of extraarticular (and eventually periarticular) new bone, and the articular cartilage is undergoing a lameness-related volume reduction.



Figure 4-2 • Lateral **(A),** dorsopalmar **(B),** lateral **(C),** and medial oblique **(D)** views of normal adult front pastern (P1).



Figure 4-3 • Two radiographic examples of narrowed pastern joints. **A,** Lateral view showing transient narrowing of the fetlock and pastern joints resulting from an unrelated lameness. **B,** Close-up, lateral oblique view showing permanent narrowing of the pastern joint resulting from septic arthritis and periostitis (extraarticular bone on the surface of P2 highlighted).



Figure 4-4 • Lateral, non–weight-bearing view of septic coffin joint in a young foal also shows widening of the pastern joint, which is not infected.



Figure 4-5 • Lateral, weight-bearing view of young foal with early developmental hyperextension shows subluxation and widening of its pastern joint.



A **B**

Figure 4-6 • Lateral **(A)** and lateral oblique **(B)** close-up views of defleshed bone specimen show predominantly extraarticular bone deposits on either side of the pastern joint, colloquially termed *high ringbone*.

Further supporting the mistaken belief that such joints are fusing is the reduced range of joint motion that can often be demonstrated with stress radiography. In my experience, this decreased range of motion is genuine, but it is not caused by arthrodesis. Instead, it is the result of the interfacing extraarticular osteophytes above and below the affected joint, which act as a series of plugs and sockets that mechanically impede normal movement. This distinctive architecture is readily demonstrated with a defleshed ringbone specimen.

Types of Ringbone

In my judgment there are at least two kinds of ringbone, or at least two ways in which the word ringbone may be used: primary and secondary.

Primary Ringbone. Primary ringbone is usually bilateral, often occurring in horses with no history of prior injury (Figure 4-8). The presence of this latter form of ringbone in related individuals suggests heritability, although as far as I am aware, this has not been proven.

Secondary Ringbone. Secondary ringbone is a form of posttraumatic osteoarthritis that typically affects one or both interphalangeal joints. The presence (often preponderance) of extraarticular new bone in such instances strongly suggests that a serious sprain caused these changes and distinguishes them from more typical arthritic patterns (Figure 4-9). In my opinion, the term *ringbone* is not a justifiable synonym for osteoarthritis of either the proximal or the distal interphalangeal joints.

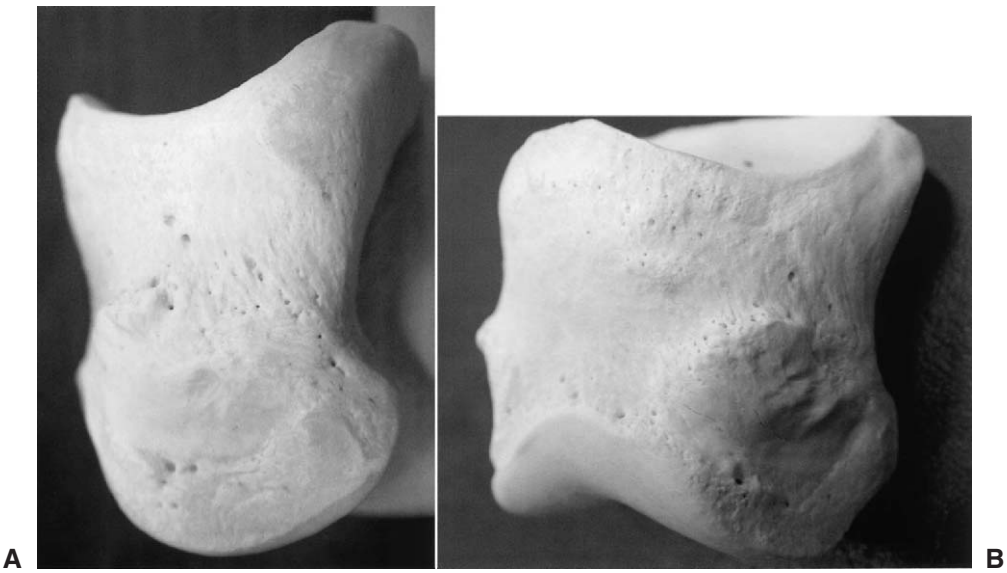


Figure 4-7 • Lateral **(A)** and lateral oblique **(B)** close-up views of the middle phalanx of an adult horse show *normal* laterodistal ridges that must not be mistaken for ringbone.



Figure 4-8 • Orientation **(A)** and close-up dorsopalmar **(B)** views of the front pastern joint of a horse with primary ringbone show near-complete collapse of the cartilage space, enveloped proximally by a combination of extraarticular and periarticular new bone. The opposite fetlock (not shown) was affected to a similar degree.

High or Low Ringbone. Ringbone can further be characterized as being either *high or low*, depending on whether it affects the proximal or distal interphalangeal joint. In some animals, both interphalangeal joints are affected, in which case the animal has both high *and* low ringbone.

Radiographic Evaluation of Attempted Surgical Fusion for Ringbone

Uncomplicated Healing. It is generally accepted by equine surgeons and others that surgical fusion of the pastern joint will eliminate joint pain believed to be caused by ringbone—and thus any related lameness.[2] The procedure typically involves removing as much of the articular cartilage as possible from the opposing bone ends of the first and second phalanges and then transfixing the pastern joint with multiple screws. If this procedure is completely successful, the long and short pasterns will unite, forming a single composite phalanx.

Radiographically, the desired surgical outcome (fusion or arthrodesis) is marked by two key features: (1) the eventual disappearance of the cartilage space and (2) its replacement by new bone. Not all such



Figure 4-9 • Lateral oblique **(A),** close-up lateral oblique **(B),** dorsopalmar **(C),** and close-up dorsopalmar **(D)** views of the proximal phalanx and pastern joint show posttraumatic osteoarthritis (secondary ringbone).

surgeries are successful, however, at least as judged by these criteria. For example, some operated-on joints initially narrow and become indistinct but never fully disappear, implying incomplete fusion, perhaps caused by remaining cartilage. Others clearly fuse in the center but remain open on the perimeter. Of the two surgical methods commonly used to fuse the pastern joint, two crossing or three parallel transarticular screws, the latter technique is reported to heal faster (Figure 4-10).[3]

As might be imagined, the surgical amalgamation of the first and second phalanges alters the alignment of the horse's affected foot at rest and when it moves, although in the latter instance slow-motion video analysis is often necessary to appreciate the nuances of these altered mechanics. Likewise, the normal angulation (and action) of both the fetlock and coffin joints change (adaptive modification), as can readily be appreciated in progress films.

Postoperative Infection, Implant Dislocation, and Breakage. The two most serious postoperative problems are (1) screw breakage and (2) infection, the latter often leading to the dislocation of one or more of the implants.

Screw breakage may occur in either the short or long term, and it may or may not be preceded by bending. Occasionally one or more screws may pull out during a violent recovery. Later a screw may withdraw for a short distance or bend slightly but then remain unchanged indefinitely. Most screws will eventually be overgrown by new bone.

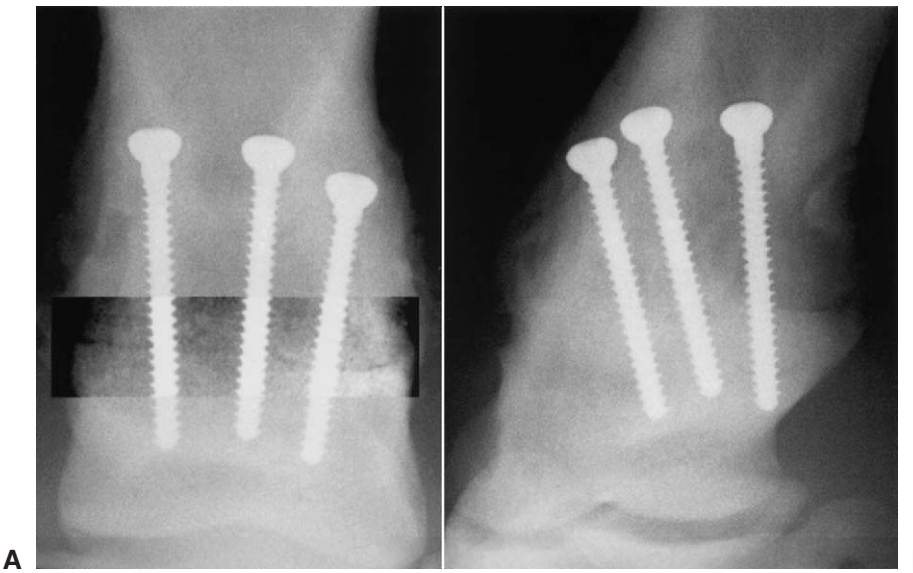


Figure 4-10 • Close-up dorsopalmar **(A)** and dorsopalmar oblique **(B)** views of the pastern joint, which has undergone arthrodesis to relieve chronic pain, show three near-parallel screws crossing the joint space, which is now nearly invisible *(emphasis zone)*. Note the bony encasement of the screws.

Infections can be very difficult to distinguish from the productive effects of the disease combined with the destructive effects of the surgery. Nonpurposeful, peripheral new bone, especially when situated away from the immediate vicinity of the joint, is highly suspicious for an infection. Likewise, interior bone destruction can signal possible sepsis. *Persistence and worsening* of such findings in progress films increase the probability of infection, as does the development of a draining sinus. Postoperative infections of this type are typically very painful and cause severe lameness.

Ringbone Mimics

Phalangeal Lateral Ridges. As mentioned, the most common radiographic misdiagnosis involving the pastern joint is early ringbone—an assessment falsely based on a normal but prominent-appearing lateral ridge, as seen in one or more oblique projections.

Sprains. Severe phalangeal sprains are potentially capable of causing rough bone deposits along the lateral ridges of P1 and P2, which can be difficult to distinguish from normal variations. In such situations, the best strategy is to compare the suspect lesion site to the same point on the opposite limb. Because normal variations are usually similar to one another, and genuine lesions are not (with some exceptions), it is usually possible to confirm or deny a tentative diagnosis (Figures 4-11 and 4-12.)

Deep Punctures and Lacerations. Deep punctures or lacerations may carry to the underlying bone surface, eventually causing bone deposition by wounding, infection, or both. Such injuries differ from ringbone by being decidedly asymmetric, an uncharacteristic appearance for ringbone.



Figure 4-11 • Lateral oblique view of proximal P1 shows a low, broad-based mound of new bone believed to be the result of a sprained fetlock 6 weeks earlier.

▮▮▮ P1 AND P2 FRACTURES

Growth Plate Fractures

Normal Physeal Closure Time. Open growth plates must be distinguished from fractures. Smallwood and colleagues reported that the proximal physis of the middle phalanx closes between 18 and 30 weeks, with a mean of 26 weeks.[4] In my experience the growth plate in both limbs usually close at or around the same time.

Typical Fracture Configuration. Acute proximal phalangeal growth plate fractures, especially when displaced, usually cause profound lameness. Chronic, untreated physeal fractures, on the other hand, may be considerably less painful, resulting in comparatively mild disability. In the latter context, such injuries may be clinically misdiagnosed as a severe bruise, sprain, or in very young animals a blood-borne infection.

Nondisplaced growth plate fractures of the long pastern can be difficult to appreciate, especially in a limited, one- or two-view screening examination. A full study that comprises lateral, frontal, and paired oblique projections, especially when combined with comparison views of the opposite normal leg, is far more likely to reveal the subtle displacement that so often characterizes injuries of this type.



Figure 4-12 • Lateral oblique view of the dorsal surface of P2 shows a chronic-appearing new bone deposit believed to be the result of a previous sprain.

Most displaced P1 growth plate fractures cause a characteristic disfigurement: The proximal epiphysis—along with a variably sized, caudal metaphyseal fragment (Salter-Harris type II growth plate fracture)—remains attached to the fetlock joint; the body of the long pastern is displaced forward, producing a large, distinctive, interfragmentary gap. The associated metaphyseal fragment, which is also termed a *corner sign* in radiology, can vary considerably in appearance, ranging in size from a small equilateral triangle to a large spikelike object. The apex of the metaphyseal fragment is often broken away, particularly on the long, slender fragments (Figures 4-13 and 4-14.)

Occasionally a displaced P1 or P2 growth plate fracture is only clearly seen in a single projection, vaguely visible in another, and invisible in the rest.

Atypical Fracture Configuration

Occasionally the epiphysis of P1 will be split in two, often with varying degrees of fragment displacement and rotation. In extreme instances, one of the fragments may be entirely hidden from view (depending on the projection) resembling congenital epiphyseal hypoplasia (Figure 4-15).

Fracture Healing and Nonhealing

Most nondisplaced phalangeal growth plate fractures heal satisfactorily with a cast. Displaced P1 and P2 physeal fractures are also amenable to casting, provided they are first adequately set. In my experience, such fractures usually radiographically appear healed in 5 or 6 weeks (Figure 4-16).

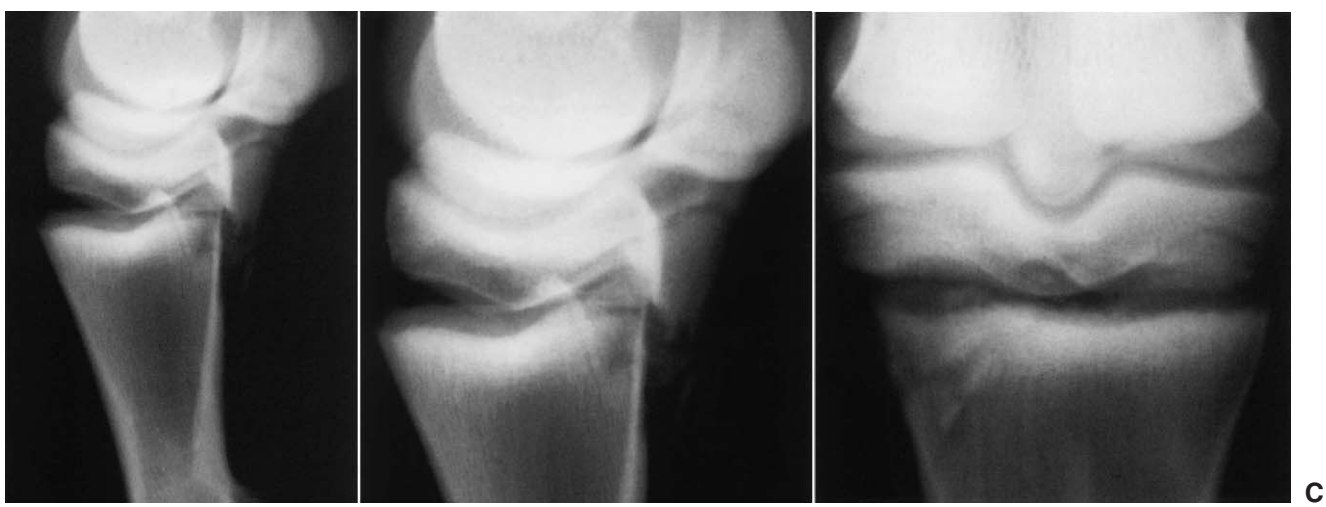


Figure 4-13 • Lateral **(A),** close-up lateral **(B),** and close-up dorsopalmar **(C)** views of a Salter-Harris (type II) growth plate fracture in a foal.

Untreated proximal P1 fractures may or may not heal. As a rule, the greater the number of fragments and the farther the fragments are displaced from one another, the greater the prospects of pain and disability. In the event of malunion, a secondary mechanical lameness may ensue, which is usually the result of the abnormal tension (read stimulation of pain receptors) on one or more tendons or ligaments of the fetlock.

Caudal Eminence Fractures

Fractures to one or both caudal eminences usually produce a characteristic radiographic appearance, especially in lateral projection: the subchondral surface of P1 or P2 becomes decidedly lengthened, as a result of being split, with much of the bearing surface of the fractured phalanx being shifted forward, so that it articulates almost exclusively with the dorsal half of the third metacarpal condyle (Figure 4-17).

This displacement leads in turn to a pronounced angular realignment of the phalanges. In the case of subacute or chronic injury to the proximal interphalangeal joint, new bone deposition is often evident on the dorsal surfaces of the involved phalanges, most likely indicating areas where connective tissue has been partially or fully torn free of the bone.

Frontal and frontal oblique projections often reveal an incongruent joint as evidenced by variable degrees of articular overhang.

Healing and Nonhealing. Unrepaired fractures of this type nearly always lead to severe osteoarthritis. Successful surgical repair is predicated on the anatomic restoration (and thus the congruence) of the fractured joint. Failed surgeries, on the other hand, are characterized by implant and fragment dislocation (often self-inflicted) and later by the development of debilitating osteoarthritis.



Figure 4-14 • Close-up lateral **(A),** lateral oblique **(B),** dorsoplantar **(C),** and medial oblique **(D)** views of the right hind proximal phalanx of foal injured 24 hours earlier while being halter broken.

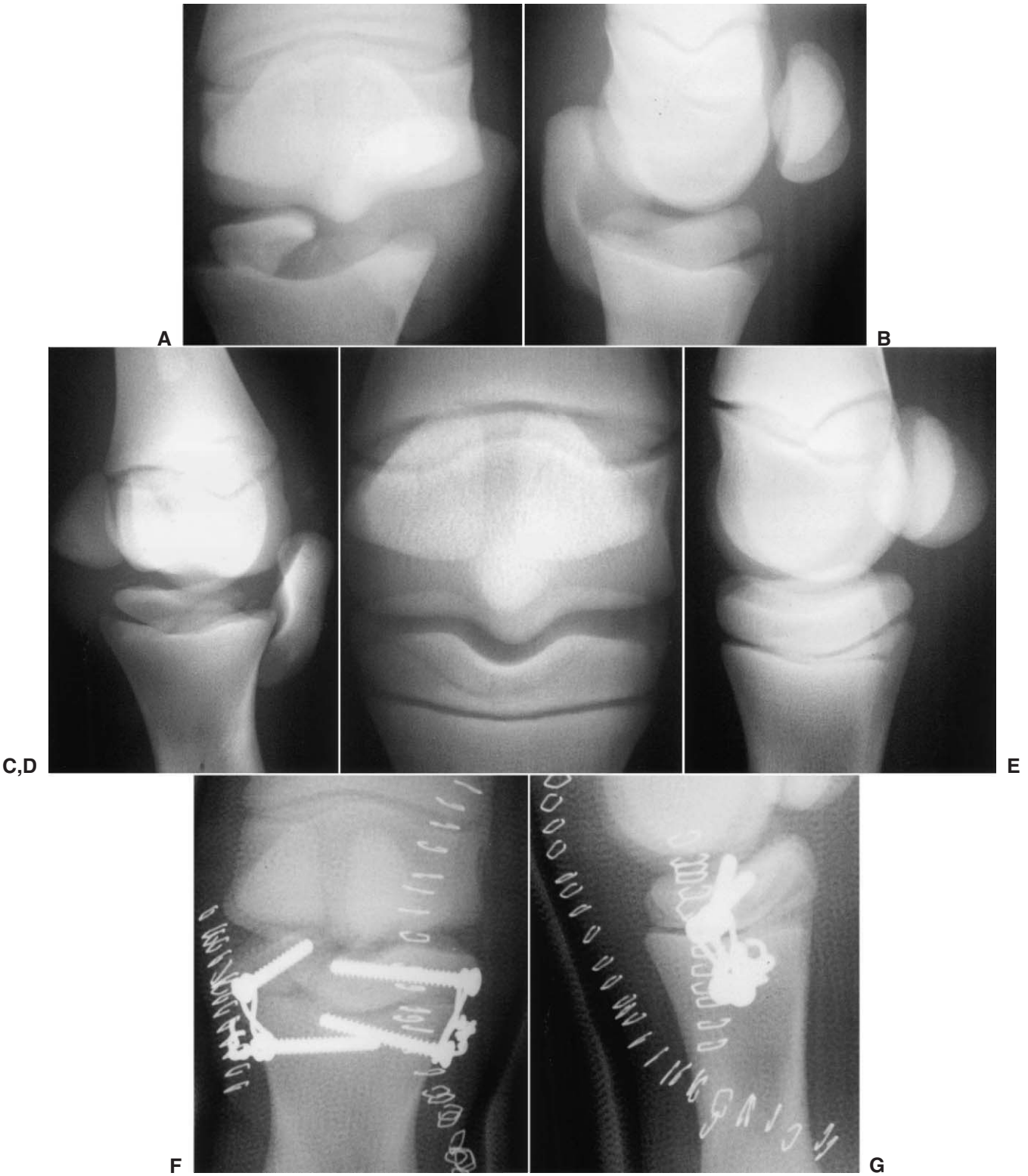


Figure 4-15 • Dorsopalmar **(A),** lateral **(B),** and lateral oblique **(C)** views of the left front fetlock of a 6-day-old Clydesdale filly presented for an acute, non–weight-bearing lameness show what is presumed to be a displaced, vertically split, proximal phalangeal, epiphyseal fracture. Dorsopalmar **(D)** and lateral **(E)** views of the normal opposite front fetlock are provided for comparison. Dorsopalmar **(F)** and lateral **(G)** immediate postoperative views show near-anatomic reduction of the fracture.

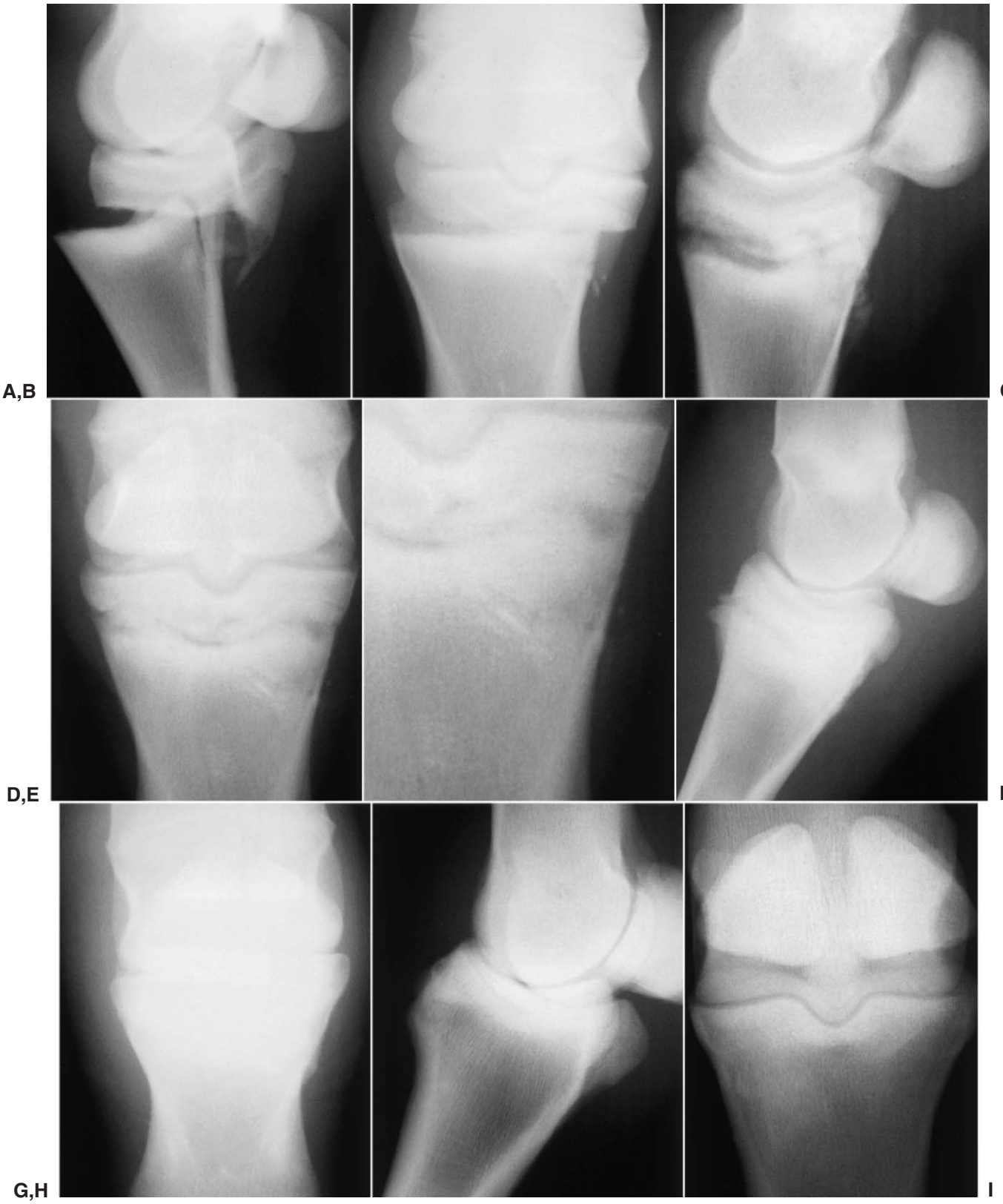


Figure 4-16 • Normal healing sequence: Lateral and dorsopalmar views of a displaced Salter-Harris (type II) proximal phalangeal growth plate fracture in a 6-month-old Hanoverian colt made immediately after the injury **(A, B),** and subsequently at 2 **(C-E),** 5 **(F, G),** and 8 weeks **(H, I)** later.

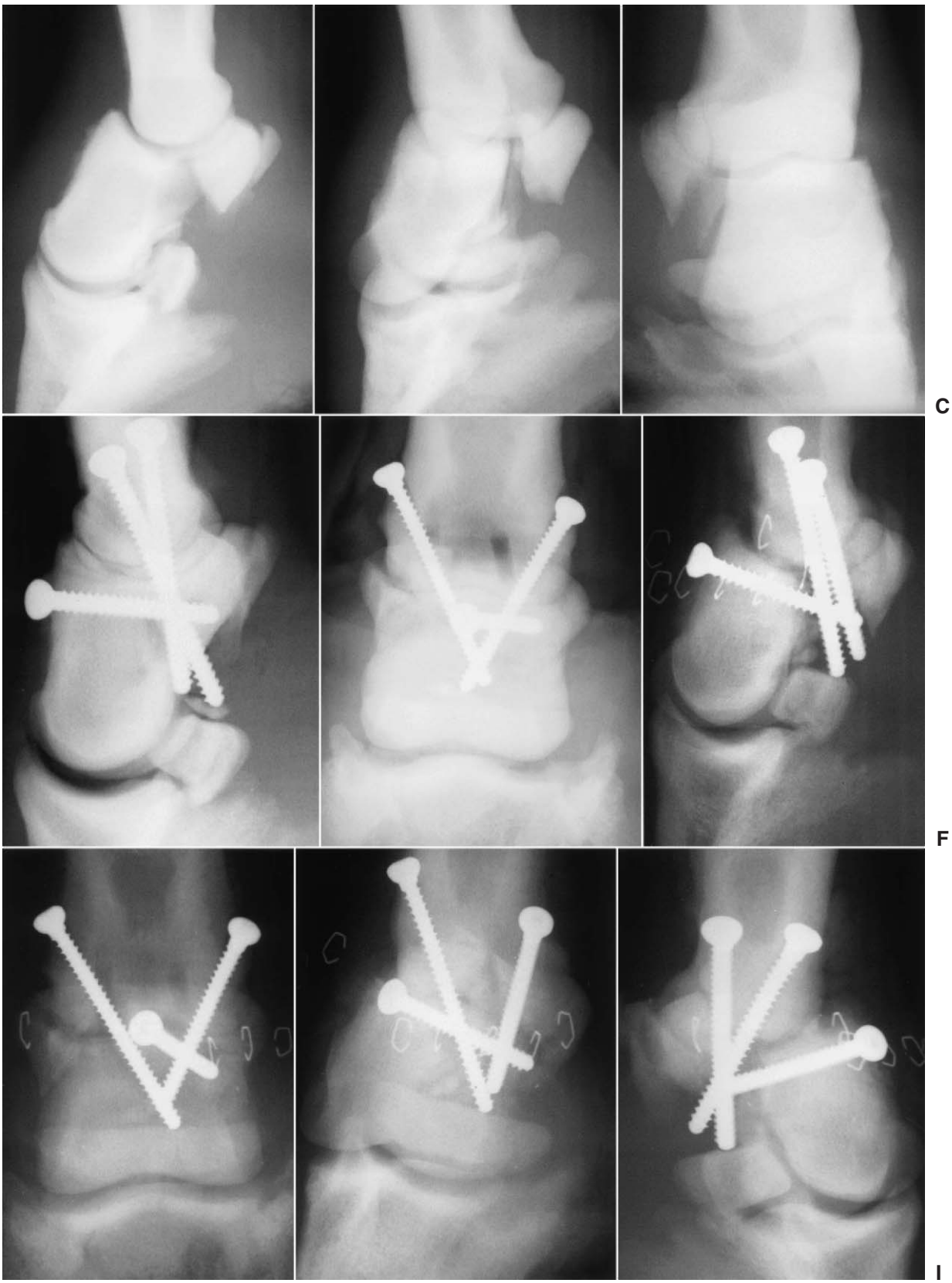


Figure 4-17 • Implant dislocation and reoperation sequence: Lateral **(A),** lateral oblique **(B),** and medial oblique **(C)** views of a severely comminuted fracture of the proximal phalanx show detachment and displacement of both caudal eminences with secondary transport fractures (additional fractures were sustained by the horse when it was shipped to the college for surgery). Immediate postoperative examination: The fracture has for the most part been reduced with bone screws, including restoration of the proximal articular surface of P1 **(D, E).** The joint surfaces were also curetted, and cancellous bone was placed in the former cartilage space. Initial progress examination: dorsopalmar **(F),** lateral **(G),** lateral oblique **(H),** and medial oblique **(I)** views show extensive surgical breakdown with scattering of the major fragments.



Figure 4-17, cont'd • Second progress examination: The original implants have been removed and replaced with a transarticular bone plate, as seen in lateral intraoperative **(J)** and side-by-side, postoperative dorsopalmar/lateral views **(K).** Third progress examination: Although a clear gap exists between the plate and underlying bone, the fetlock joint appears to be ankylosing, albeit in a hyperextended position. The caudal eminences have been partially incorporated into the large proximal callus, as seen in lateral **(L)** and dorsopalmar **(M)** views. Fourth progress examination: Eighteen months after the original injury, lateral **(N)** and dorsopalmar **(O)** views of the pastern joint reveal an angular malunion. This in turn has led to a permanently but not severely flexed distal phalanx.

Transpastern arthrodesis may be used as a primary surgical treatment in cases in which it is impossible to reattach the caudal eminences or as a form of surgical revision (reoperation) where breakdown has occurred.

Biarticular P1 and P2 Fractures

Biarticular phalangeal fractures are those that enter both ends of the bone. Because of the resulting structural weakness, the injured bone is incapable of maintaining its normal form and often undergoes further disintegration as a result. In some two- and three-piece fractures, it may be possible to reduce the fragments with multiple bone screws. More extensive injuries, however, may not contain a sufficient number of large fragments capable of holding implants and maintaining at least a modicum of surgical stability. Under such restrictions, it may be necessary to bypass the facture and instead temporarily stabilize the adjacent bones and joints. Biarticular fractures have a worse prognosis than those that enter only a single joint, irrespective of how they are treated[5] (Figures 4-18 and 4-19).

Nonfracturing Proximal Phalangeal Trauma

Metcalf and co-workers described the scintigraphic abnormalities found in the forelimbs of a series of medium-sized horses with nondisruptive P1 injuries.[6] Evidence of what was described as "exercise-induced



Figure 4-18 • Close-up photograph **(A)** of the left forelimb and hindlimb of a horse assuming the partially flexed, non–weight-bearing posture often seen with distal extremital fractures, in this instance, the middle hind phalanx. Dorsoplantar **(B),** lateral **(C),** 15-degree lateral oblique **(D),** 35-degree lateral oblique **(E),** and 35-degree medial oblique **(F)** views show a middle phalanx that has been broken into five major and an undetermined number of minor fragments. The body of the bone has been split vertically and both caudal eminences detached and displaced. As a result, there are two large crevices in the proximal surface of the bone and a somewhat narrower fissure distally. Note how the degree of apparent fragment displacement changes with the projection angle, especially proximally.

bone injury" was detected in one third of the animals studied (23 of 69 lame horses) with *jumping* considered the primary cause. Age, breed, sex, and duration of lameness did not appear to influence test results.

Two principal patterns of abnormal radioisotopic uptake were observed, both within the dorsal aspect of P1:

1. Focal, well-defined, fusiform or oval-shaped uptake pattern, extending about a third of the length, and half of the width of P1 as seen in lateral perspective.
2. Regional, ill-defined, linear uptake, involving one third to one half of the length, and less than half of the width of P1 as seen in lateral perspective.

Additionally, some of the affected horses also had abnormal uptake in the palmar cortex, usually of the regional, ill-defined, linear variety. Radiographic-scintigraphic correlation is as yet unreported.

▮▮▮ CUTS, PUNCTURES, AND INFECTION

Serious pastern wounds often produce skin flaps, soft tissue defects of varying size and shape, and an equally diverse variety of gas pockets, most of which are discernible radiographically, especially when using a "hot lamp." Deep wounds that expose the bone are usually associated with atmospheric



Figure 4-19 • Indirect fracture stabilization and healing sequence: Dorsopalmar **(A)** and lateral **(B)** views of a severely comminuted, biarticular fracture of the proximal phalanx of an adult horse. Immediate postoperative examination: The fracture has been stabilized *indirectly* with a combination of metacarpal pins **(C),** external support bars (not shown), and a cast **(D).** Initial progress examination: Four weeks later, close-up dorsopalmar oblique **(E)** and lateral **(F)** views show the first indication of *interior callus formation*. External support bars partially obscure the fracture in the lateral projection. Second progress examination: Eleven weeks after the injury, a lateral oblique view **(G)** shows further development of the interior callus. Third progress examination: Twenty-two weeks after the initial injury, dorsopalmar **(H)** and lateral **(I)** views show that the fracture is healed. The bone has not been fully restored and probably will not be. The fetlock joint is arthritic, a predictable, accommodative consequence of this type of displaced articular fracture. The pastern joint is narrowed, with extraarticular bone deposition, again a predictable change given the location and extent of the articular fracture.



Figure 4-20 • Wire cut: The inside surface of the badly swollen pastern is partially denuded of hair and is weeping pus through a small sinus as a result of a wire cut 6 weeks earlier **(A).** Dorsopalmar close-up **(B),** dorsopalmar ultra-close-up **(C),** lateral **(D),** lateral ultra-close-up **(E),** lateral oblique **(F),** and lateral oblique ultra-close-up **(G)** views of the proximal aspect of P1 show irregular, chronic-appearing new bone deposition on the dorsal, dorsolateral, and lateral surfaces with no sequestra. The fetlock joint is temporarily narrowed as a result of the lameness. New bone of this nature is not usually the result of osteomyelitis but rather stems from vascular injury related to nearly soft tissue infection.

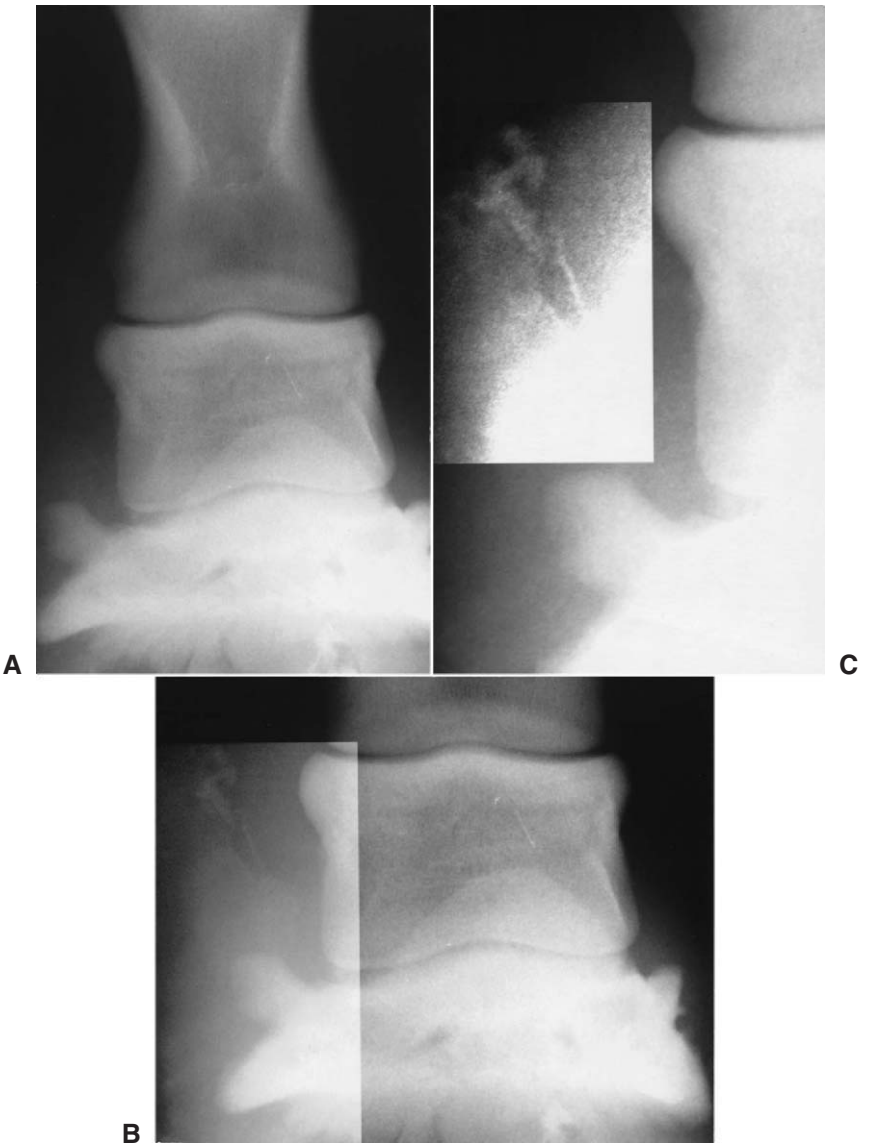


Figure 4-21 • Dorsopalmar **(A),** close-up dorsopalmar **(B),** and ultra-close-up dorsopalmar **(C)** views of a chronically lame horse show presumed dystrophic calcification *(emphasis zone)*, regional soft tissue swelling, and narrowing of the coffin joint as a result of a deep cut received 2 months earlier.

contamination, which enhances bony contrast by creating a distinctive air-bone interface.

Partial or complete severence of the joint capsule, ligaments, or nearby tendons may cause subluxation, but the regional musculature usually prevents complete dislocation. Hyperflexion may be related to associated soft tissue injury, but is more likely to reflect pain and a commensurate unwillingness to fully bear weight. Hyperextension, on the other hand, is usually the harbinger of soft tissue disruption.

Because the joint surfaces are covered by avascular cartilage, primary and secondary infections are slow to dissolve subchondral bone. Thus most such infections—even those sustained at the time of the original injury—will not become apparent radiographically for a month or more (on average).

Cartilage spaces narrow initially—for the most part because of reduced use and a commensurate reduction in volume—but later may widen, but not by a great deal (on average about 30%). If subchondral bone destruction occurs later, it may initially create the illusion of a widened joint space, an impression that should be dispelled on closed inspection. Many of these radiographic disease indicators are illustrated in Figures 4-20 to 4-23.

Osteochondritis

Pettersson and Reiland studied phalangeal bone cysts in Swedish horses, concluding the following[7]:

- Most phalangeal subchondral bone cysts occur in young horses.
- Most have a similar radiographic appearance.
- Most have a similar microscopic appearance.
- Many disappear spontaneously within 1.5 to 2.5 years.
- In most cases, the prognosis is good.

Trotter and co-workers described what they termed "degenerative joint disease with osteochondritis" in the hind pastern joints of six young horses; radiographically, spavin-like, subchondral cysts characterized the principal lesion.[8] Schneider and co-workers reported the radiographic appearance of what they believed was another form of osteochondritis involving the pastern joints of a Thoroughbred and two Standardbred horses.[9] The described bone fragments were small, smooth, and round and accordingly difficult to see in all but the oblique views. The fragments appeared to originate from the dorsal eminence of P2. No accompanying subchondral lesions were present.



Figure 4-22 • Slightly obliqued lateral close-up view of the pastern joint shows multiple contiguous gas pockets caudally, the result of a deep puncture wound.

Tumor and Tumorlike Lesions

Seahorn and colleagues reported the sonographic diagnosis of a keratoma situated just beneath the coronary band of the left front foot.[10]

Monticelio and co-workers described a malignant melanoma in an 18-year-old American Paint. In addition to localized destruction of the coronary band laterally, combined bone destruction and bone deposition were present in the underlying portions of the second and third phalanges.[11]

Attenburrow and Heyse-Moore reported a nonossifying fibroma in the proximal phalanx of an 8-month-old Thoroughbred colt. Radiographically, the lesion resembled a bone cyst, being lytic, expansive, and involving the entire distal half of the bone.[12]

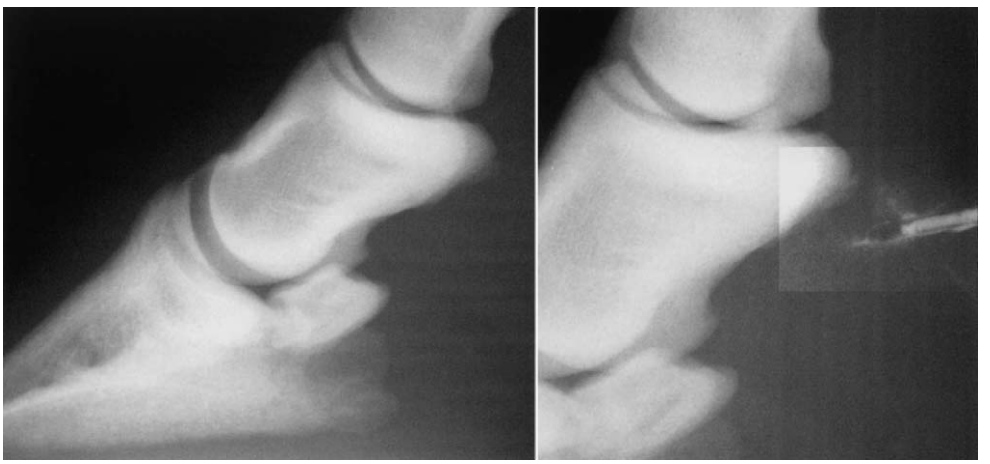
Pastern Arthrodesis

Martin and co-workers reported the radiographic appearance of implant breakage and dislocation related to attempted fusion of the pastern joint.[13]

Schaer and co-workers reported using a combination of three cortical lag screws and a three- or four-hole dorsal compression plate to fuse 22 fractured, dislocated, or chronically arthritic pastern joints. The authors contend that by virtue of the additional support and stability afforded by the bone plate, healing occurred more rapidly.[14]

Desmitis of the Straight Sesamoidian Ligament

Schneider and co-workers reported the sonographic appearance of sprained straight sesamoidian ligament in horses with acute lameness in the distal fore or hind limb, but no visible swelling or radiographic abnormalities.[15] Localized swelling and an irregular decrease in echogenicity of the straight sesamoidian ligament proximal to its insertion on the middle



A **B**

Figure 4-23 • Survey lateral **(A)** and close-up lateral sinogram **(B)** of a horse with a draining sinus related to a deep puncture wound. The survey film shows a faint new bone deposit on the palmar surface of one of the caudal eminences; the sinogram reveals an oval-shaped filling defect *(emphasis zone)* in the same location, the result of an abscess.

phalanx characterized the illustrated lesions. The authors also described a small, circular hypoechogenicity found in the distal sesamoidian ligament of normal horses, in the same area as the described lesion. Unfortunately, its source could not be determined.

▮▮▮ DIGITAL FLEXOR TENDON SHEATH SONOGRAPHY

Using contrast and cadavers, Redding described the normal sonographic appearance of the equine digital flexor tendon sheath and its resident tissues.[16]

References

1. Quick CB, Rendano VT: Equine radiology—the pastern and foot, *Mod Vet Pract* 72:1022, 1977.
2. Schneider JE, Carnine BL, Guffy M: Arthrodesis of the proximal interphalangeal joint in the horse: a surgical treatment for high ringbone, *J Am Vet Med Assoc* 173:1364, 1978.
3. Genetsky RM, Schneider EJ, et al: Comparison of two surgical procedures for arthrodesis of the proximal interphalangeal joint in horses, *J Am Vet Med Assoc* 179:464, 1981.
4. Smallwood JE, Albright SM, et al: A xeroradiographic study of the developing Quarter Horse foredigit and metacarpophalangeal region from six to twelve months of age, *Vet Radiol* 31:254, 1990.
5. Colahan PT, Wheat JD, Meagher DM: Treatment of middle phalangeal fractures in the horse, *J Am Vet Med Assoc* 178:1182, 1981.
6. Metcalf MR, Forrest LJ, Sellett LC: Scintigraphic pattern of 99mTc-MDP uptake in exercise induced proximal phalangeal trauma in horses, *Vet Radiol Ultrasound* 31:17, 1990.
7. Pettersson H, Reiland S: Periarticular subchondral "bone cysts" in horses, *Clin Orthop Relat Res* 62:95, 1969.
8. Trotter GW, McIlwraith CW, et al: Degenerative joint disease with osteochondrosis of the proximal interphalangeal joint in young horses, *J Am Vet Med Assoc* 180:1312, 1982.
9. Schneider RK, Ragle CA, et al: Arthrographic removal of osteochondral fragments from the proximal interphalangeal joint of the pelvic limbs in three horses, *J Am Vet Med Assoc* 205:79, 1994.
10. Seahorn TL, Sams AE, et al: Ultrasonic imaging of a keratoma in a horse, *J Am Vet Med Assoc* 200:1973, 1992.
11. Monticello TM, Jakob TP, Crane S: Malignant melanoma of the coronary band in a horse, *J Am Vet Med Assoc* 188:297, 1986.
12. Attenburrow DP, Heyse-Moore GH: Non-ossifying fibroma in phalanx of a Thoroughbred yearling, *Equine Vet J* 14:59, 1982.
13. Martin GS, McIlwraith CW, et al: Long term results and complications of proximal interphalangeal arthrodesis in horses, *J Am Vet Med Assoc* 184:1136, 1984.
14. Schaer TP, Bramlage LR, et al: Proximal interphalangeal arthrodesis in 22 horses, *Equine Vet J* 33:360, 2001.
15. Schneider RK, Tucker RL, et al: Desmitis of the straight sesamoidian ligament in horses: 9 cases (1995-1997), *J Am Vet Med Assoc* 222:973, 2003.
16. Redding WR: Evaluation of the equine digital flexor tendon sheath using diagnostic ultrasound and contrast radiography, *Vet Radiol Ultrasound* 35:42, 1994.

Chapter 5

The Fetlock Joint

THE STANDARD FETLOCK SERIES

A standard fetlock examination includes four or five radiographic perspectives or views: a frontal (dorsopalmar), true lateral, lateral and medial obliques, and an optional flexed lateral (Table 5-1).

The radiographs from three normal fetlocks are shown in Figures 5-1, 5-2, and 5-3 to illustrate the anatomic and projectional variations commonly associated with this examination. Comparable anatomic specimens follow (Figures 5-4 through 5-7).

SOME USEFUL FETLOCK FACTS

In a radiologic review of equine fetlock diseases, Rendano included a number of useful anatomic facts that can be used to try to determine orientation in instances in which markers have accidentally fallen off the cassette[1]:

- Forelimb proximal sesamoids are larger and more triangular than those of the hindlimb.
- Lateral proximal sesamoids are more conical than medial sesamoids.
- The button of the medial splint (MC2/MT2) is larger than that of the lateral splint (MC4/MT4).
- In some horses the MT4 button is absent.

NORMAL ANATOMIC VARIANTS THAT MAY BE MISTAKEN FOR DISEASE

Variable Locations of Nutrient Foramina in P1

Losonsky and Kneller reported nine separate variations in the radiographic appearance or location of the nutrient foramen in the proximal phalanges of the forelimbs of 100 Standardbred horses.[2] The nutrient foramen was most obvious when projected laterally in either the dorsal or palmar cortex but often differed from the right to left leg. Thus opposite limb comparisons, in the case of a suspected fracture, will often prove futile. Adding to the confusion are the facts that some horses have a visible foramen in one leg but not the other and that 13% of the horses studied had no foramina at all!

MAGNETIC RESONANCE IMAGING OF THE FETLOCK

Martinelli and co-workers reported the three-dimensionally reconstructed, magnetic resonance appearance of a dismembered equine fetlock.[3] Currently clinical studies of this sort remain rare compared with radiography and computed tomography (CT).

PARTS OF A WHOLE: AN INTEGRATED DIAGNOSTIC APPROACH

The fetlock joint of a horse comprises multiple hard and soft tissues. Specific bones include the following: (1) the distal metacarpus, (2) the proximal phalanx, and (3) a pair of proximal sesamoids. Soft tissues include (1) collateral and suspensory ligaments, (2) deep and superficial flexor tendons, and (3) extensor tendons; the joint proper includes the (1) capsule, (2) synovium, (3) synovial fluid, and (4) articular cartilages.

Injury to any of these components usually has some effect on the others, although the exact magnitude of the effect can be hard to quantify. For example, most apical sesamoid fractures are avulsive in nature and thus are usually associated with some degree of suspensory sprain. Likewise, sesamoidian body fractures are often accompanied by flexor tendon strain as well as suspensory sprain. Acute basilar fractures may be associated with ligament injury and hemarthrosis. In

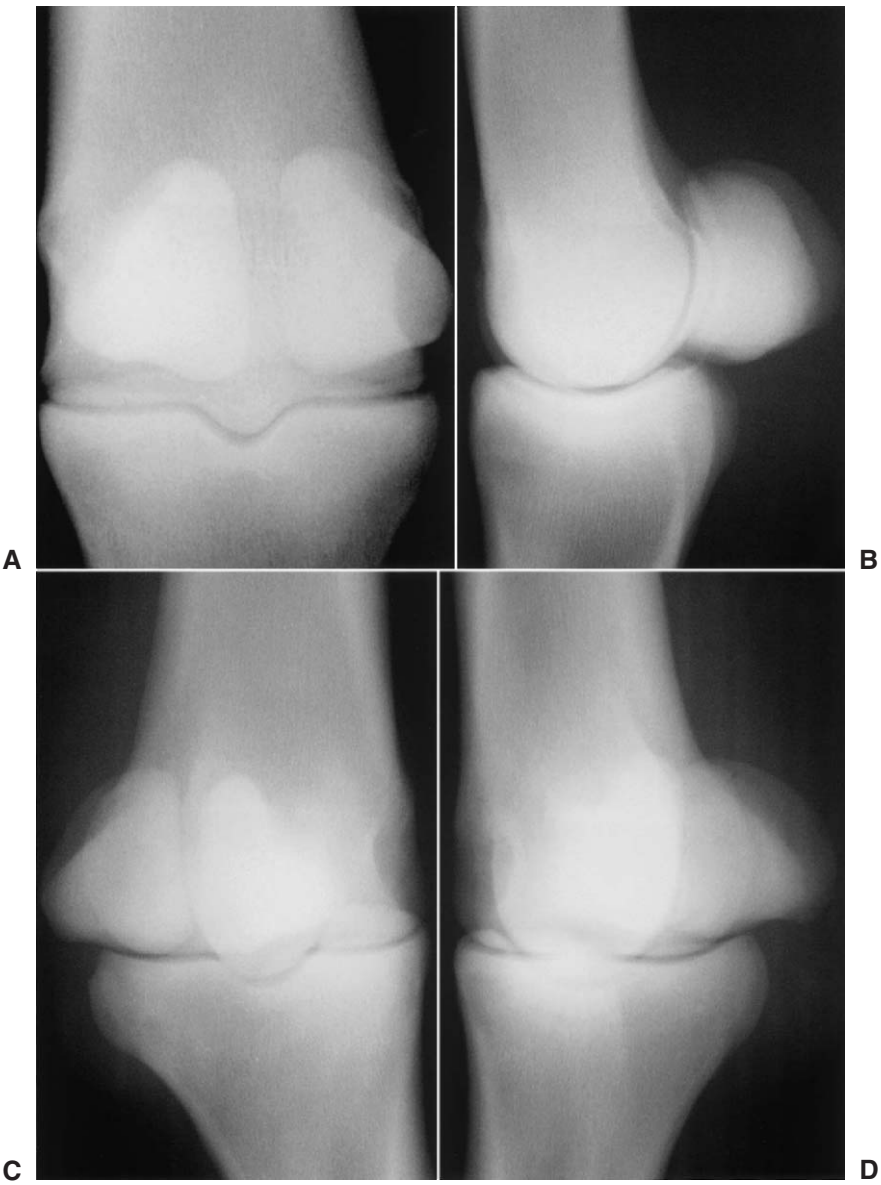


Figure 5-1 • Normal study: Mildly obliqued dorsopalmar **(A),** lateral **(B),** lateral oblique **(C),** and medial oblique **(D)** views of the left front fetlock of a 12-year-old Quarter Horse gelding.

the short term, fractures and dislocations often modify the actions of surrounding tendons and ligaments, especially the directions in which they pull. Under such conditions, the sensory input to these structures is altered, resulting in regional nonspecific pain that may extend to the surrounding musculature.

Given this sort of structural intimacy in the fetlock region, it is often advisable to assess the injured fetlock with both radiology and ultrasound, to include periodic reassessments. CT is also very helpful when planning surgery, especially when enhanced by three-dimensional reconstruction.[4]

▮▮▮ FRACTURES AND DISLOCATIONS OF THE FETLOCK REGION

Serious fracture-dislocations of the fetlock joint or disruption of the associated suspensory apparatus are the leading causes of racetrack euthanasia and as such are often termed *catastrophic injuries* (Figure 5-8).[5,6]

Proximal Phalanx (P1)

Yovich and McIlwraith support the generally held belief that most proximal phalangeal fractures are likely the result of compression of the dorsoproximal aspect of P1 by the overlying third metacarpal condyle during extreme extension of the fetlock joint while racing or fast training.[7] Arthroscopic removal of dorsal lip fractures has a much better prognosis than surgical extraction.[8]

Dorsal Eminence Fracture (Dorsal Lip Fracture, Dorsoproximal Margin Fracture)

Most small, chiptype P1 fractures occur to the bony lip located along its upper front edge, with medial



Figure 5-2 • Normal study: Dorsopalmar **(A),** lateral **(B),** lateral oblique, **(C)** close-up lateral oblique **(D),** and flexed lateral **(E)** views of the right front fetlock of a 6-year-old Thoroughbred filly.

Table 5–1 • EVALUATIVE PURPOSE OF THE STANDARD FETLOCK EXAMINATION

View	Evaluative Purpose
Frontal	Evaluates distal 3rd metacarpal bone, proximal P1, medial and lateral sesamoids, fetlock joint, and periarticular tissues
Lateral	Provides excellent view
Flexed lateral	Provides clear view of basilar regions of sesamoids and surrounding suspensory and flexor fields
	Provides optimal views of dorsolateral and dorsomedial aspects of proximal P1 areas commonly fractured in race horses
Oblique views of the sesamoids	Profiles the flexor margin of the lateral and medial sesamoid bones free of superimposition by the cannon bone

injury being most common (Figure 5-9). The considerably larger bony outcroppings situated at the rear of P1, the palmarolateral/plantarolateral eminences,* are less commonly fractured, although the functional consequences of such an injury are far more serious. The caudal eminences may also become detached as a result of the fragmenting form of osteochondritis, an appearance that closely resembles an old fracture.

*The bony protrusions located on the upper portion of the proximal phalanx—commonly referred to as the palmar/plantar eminences, or simply the caudal eminences—are actually situated laterally. Thus they are more accurately termed the *palmarolateral/plantarolateral eminences* or *caudolateral eminences*. These bony projections serve to moor the collateral ligaments of the metacarpophalangeal joint to the proximal aspect of P1.



Figure 5-3 • Normal study: Dorsopalmar **(A),** lateral **(B),** lateral oblique **(C),** and medial oblique **(D)** views of the left front fetlock of 3-year-old Arabian filly.

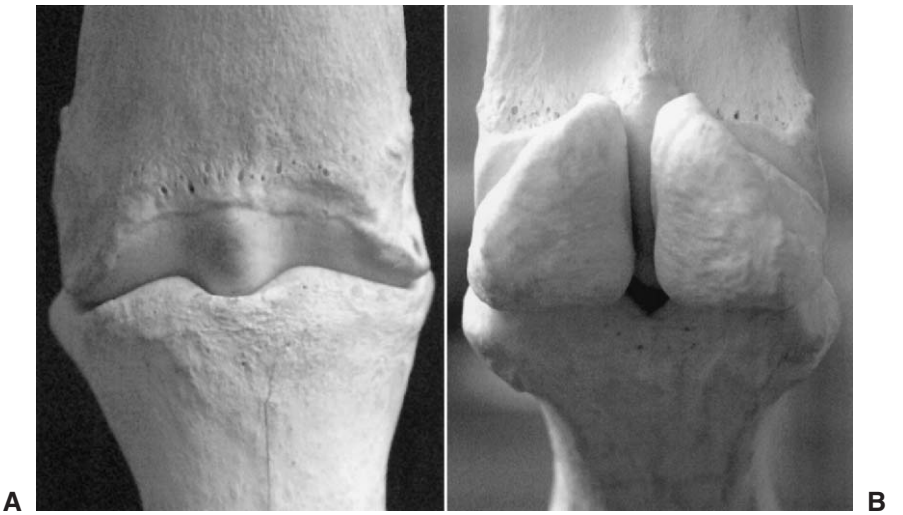


Figure 5-4 • Bones of the equine fetlock: dorsal **(A)** and palmar **(B)** perspectives. Note the highly irregular periarticular lip that must not be mistaken for osteoarthritis.



Figure 5-5 • Bones of the equine fetlock, pastern, and foot: long lateral perspective.

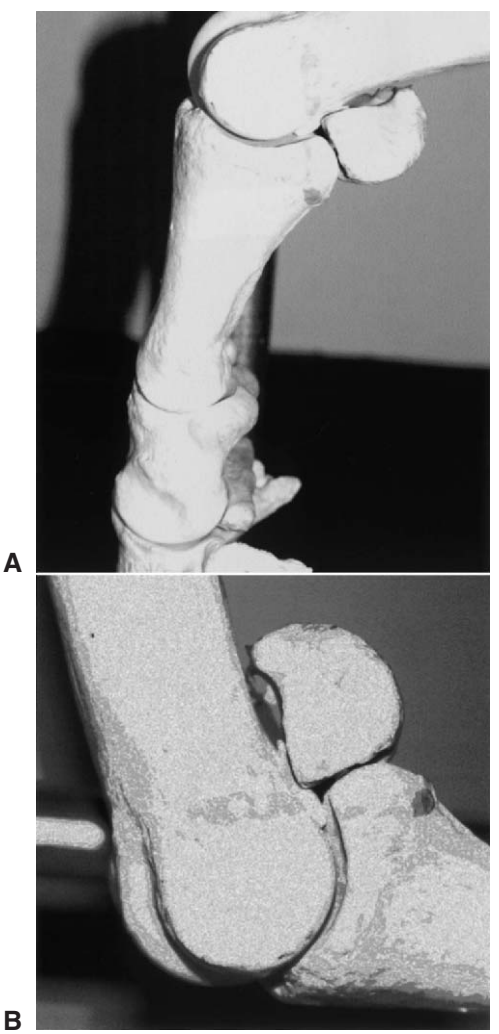


Figure 5-6 • Bones of the equine fetlock: long **(A)** and short **(B)** flexed lateral perspectives.

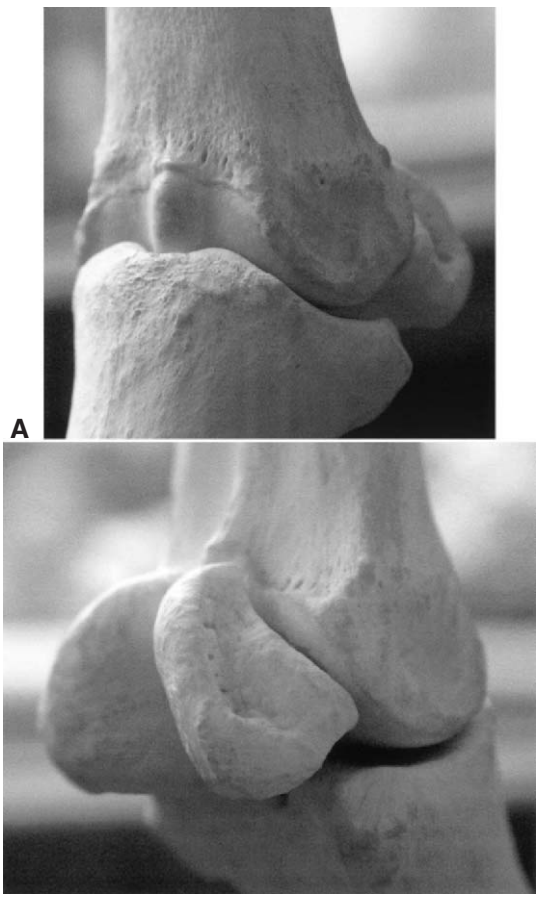


Figure 5-7 • Bones of the equine fetlock: dorsolateral **(A)** and palmaromedial **(B)** perspectives.

Dorsal lip fractures can usually be seen in both the lateral and the medial or lateral oblique views of the fetlock, depending on how far dorsally the fracture fragment is situated. Small, sliver-like fragments can easily be overlooked, especially in dark films. It is also possible to identify such fractures in frontal projections, but only if the films are of high quality and the x-ray beam is angled downward so that the proximal sesamoids are projected well above the metacarpophalangeal joint to avoid confusing superimposition.

Most dorsal lip fractures are unilateral, but fresh bilateral injuries occur occasionally. An alternative explanation for bilateral fractures is that one is recent, whereas the other is old. This is especially true of middle-aged racehorses that have changed hands repeatedly. According to one authority, 90 percent of displaced cranial eminence fractures are firmly attached to the parent bone by fibrous tissue. Nonarthroscopic removal of the fragment often results in calcification and adhesions in the adjacent joint capsule, increasing pain and disability.[9] Figures 5-10 to 5-13 illustrate the various radiographic appearances of dorsal lip fractures.

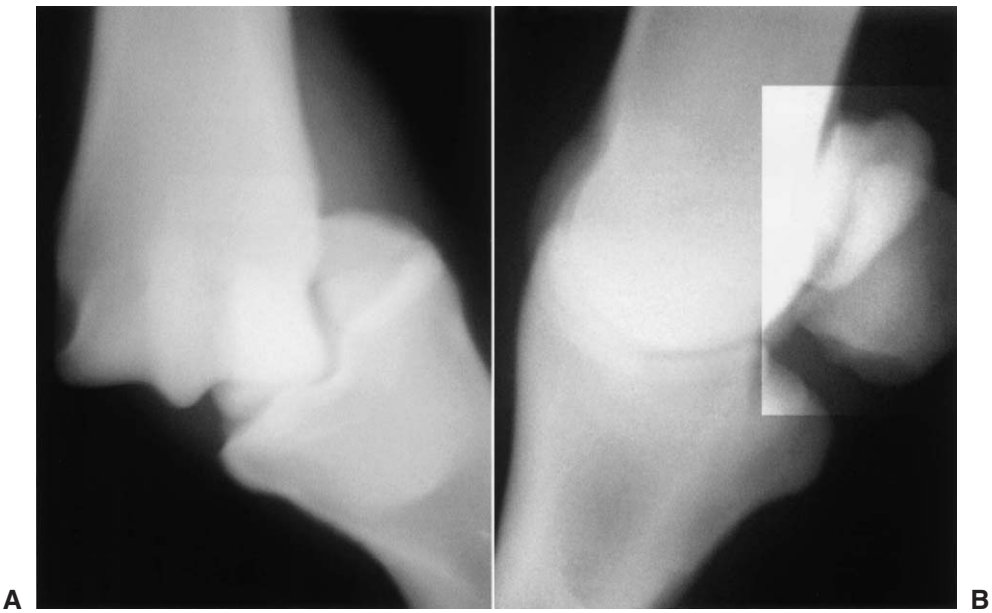


Figure 5-8 • Dorsopalmar **(A)** and lateral oblique **(B)** views of a dislocated fetlock joint.

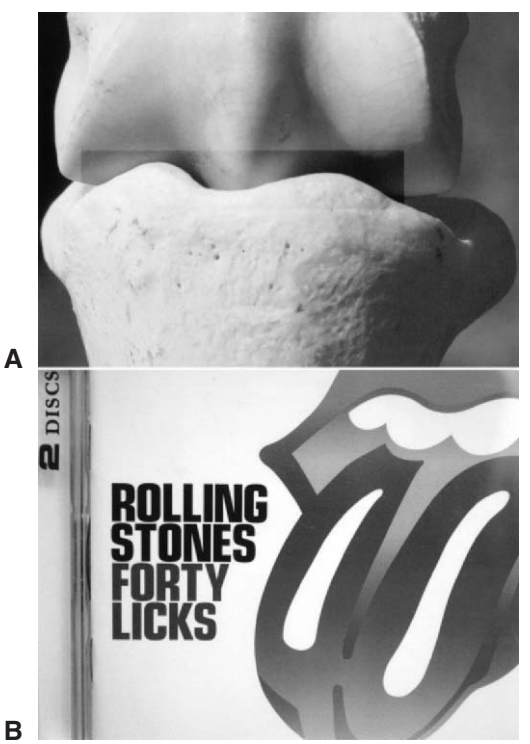


Figure 5-9 • Bones of the equine fetlock. **A,** Close-up frontal view of the fetlock shows a prominent dorsal lip featuring paired cranial eminences, the most commonly injured area of P1 *(emphasis zone)*. **B,** This profile bears a striking resemblance to the upper lip shown on the cover of the Rolling Stones' release, *Forty Licks*.

Occasionally dorsal lip fractures extend deeply into the body of the proximal phalanx after first passing through the medial or lateral dorsal eminence, resulting in a large triangular fragment (Figure 5-14). Because this type of injury usually occurs in young racehorses, overuse and stress mechanisms have been postulated. The following case is of interest because it shows, at least in the case of this individual animal, that surgery or rest can achieve comparable outcomes in comparable injuries incurred a year apart.

Fragmented Caudal Eminence: Fracture or Osteochondritis?

The caudal eminences or protuberances (palmar/plantar tuberosities) of the proximal phalanx are somewhat of a misnomer insofar as they actually wrap well around the caudolateral and caudomedial aspects of P1 before extending farther rearward (Figure 5-15).

The etiologic uncertainty surrounding this disorder is reflected in the great variety of names used to describe it: caudal eminence fracture, axial osteochondral fragments, caudolateral tuberosity fragmentation, nonunited proximoplantar tuberosity, fragmented palmar/plantar protuberance, detached caudolateral tuberosity, and osteochondritis dissecans (OCD).

The cause or causes of fragmented caudal eminence (FCA) of the proximal phalanx in horses is not known. The two most common hypotheses are (1) fracture and

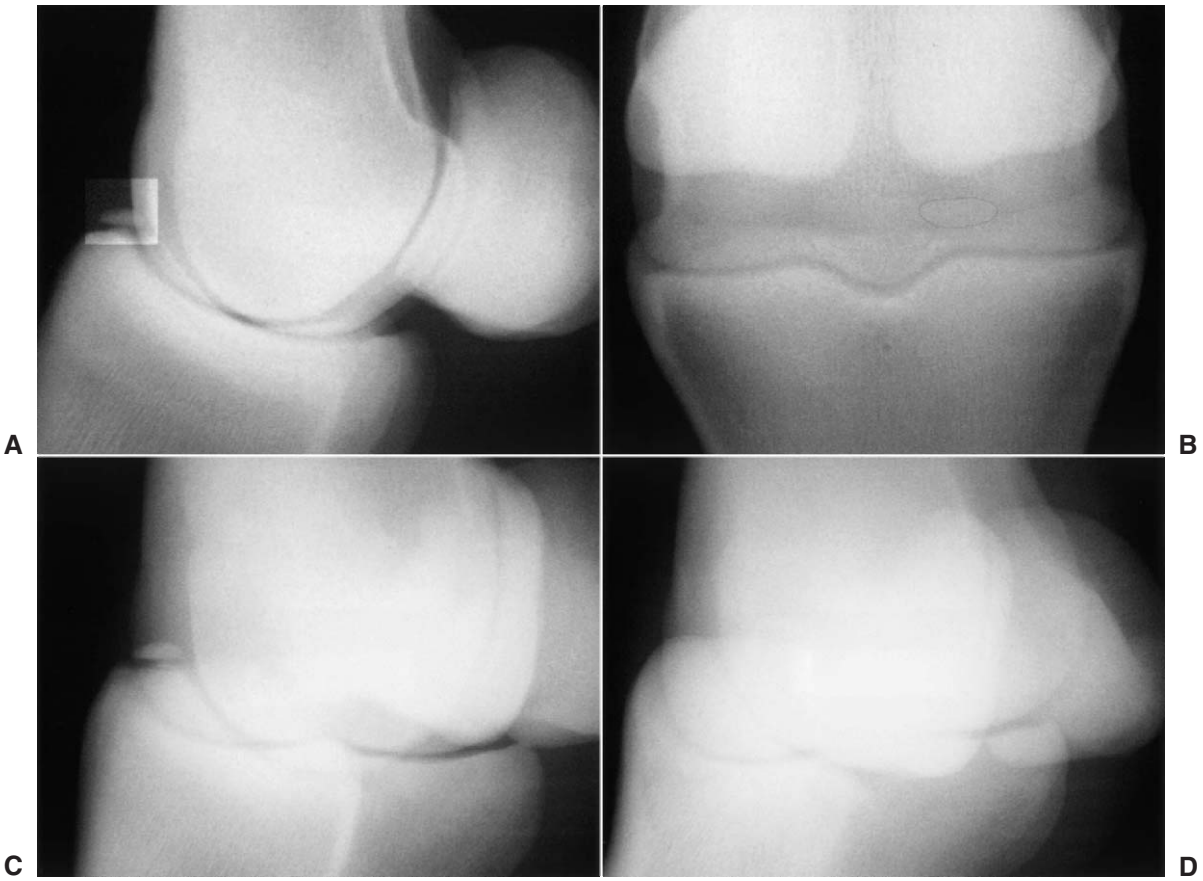


Figure 5-10 • Close-up lateral **(A),** dorsopalmar **(B),** dorsomedial **(C),** and dorsolateral **(D)** views of a fresh proximal phalangeal lip fracture. Typically this type of fracture is best seen in the appropriate oblique view, in this case the dorsomedial projection.

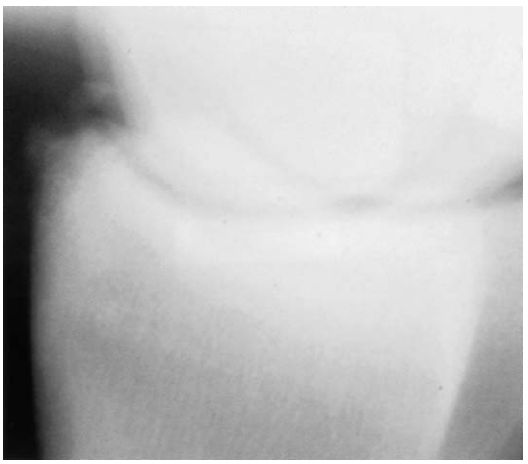


Figure 5-11 • Close-up dorsomedial view of an intermediate duration proximal phalangeal lip fracture shows new bone arrayed over the surface of a rough, demineralized fracture bed just below the displaced fragment.

(2) fragmenting osteochondritis (OCD). A third theory, nonunion of an accessory growth center, has also been proposed but has few vigorous advocates. Although heritability has been suggested, it too remains unproven. Detached fragments can vary in both size and number, but single, medium-to-large, triangular, or crescent-shaped fragments are most common. Bilateral lesions are the rule.

The Case for Fracture. Nixon and Pool reviewed the gross and histologic appearance of 43 osteochondral fragments, arthroscopically removed from the fetlocks of 30 horses, most of which were racing Standardbreds. They concluded that the fragments were most likely fractures (Figure 5-16).[10] The attachments of the obliquely oriented metacarpophalangeal ligaments to the caudolateral aspects of proximal P1 are consistent with this view (Figure 5-17).

Spontaneous Fragment Reattachment. Grondahl described 18 cases of occult fragmented proximoplantar tuberosity discovered in a series of 753 Norwegian

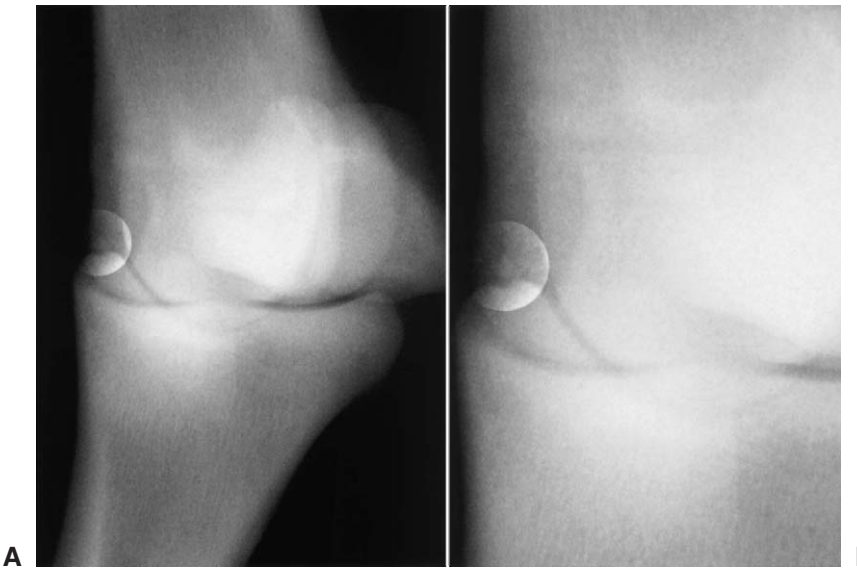


Figure 5-12 • Orientation **(A)** and close-up dorsomedial **(B)** views of a 2-month-old proximal phalangeal lip fracture in a 2-year-old Standardbred filly.



Figure 5-13 • Lateral view of the fetlock shows a pair of chronic appearing chip fractures lying one atop the other, immediately proximal to irregular phalangeal eminences. Without oblique views, it is difficult or impossible to precisely locate the fractures. In this instance they were bilateral. New bone deposition along the dorsal surface of the cannon bone probably reflects combined capsular-periosteal tearing related to the original injury.

yearlings.[11] Sixteen of the affected horses had fragmented lateral tuberosities, one had a medial detachment, and one horse had lateral and medial lesions. It is important to note that the detached fragments in 11 horses appeared radiographically reattached 6 to 12 months after being identified. Four horses showed increased fragment displacement, further fragmentation, calcification, or new bone. One was unchanged, and two were lost to follow-up.

Plantar "Fragments": Virtues of a Generic Description

Later, Fortier and co-workers reported the arthroscopic removal of what they termed *axial osteochondral fragments*, taken from 119 young Standardbreds, most of which were less than 3 years of age.[12] Clinical abnormalities associated with this disorder were decreased performance and subtle lameness running at top speed or when cornering. Most of the fragments were removed from the medial aspect of the left hindleg. Bilateral fragments were present in 21 of the horses (Figure 5-18). Osteochondritis of the sagittal ridge, in addition to P1 fragments, was present in 15 horses. Thirty horses with P1 fragments also had osteoarthritis of the distal intertarsal and tarsometatarsal joints.

Classification of Plantar "Fragments." On a personal note, I often advise my students and graduate trainees, "If you don't know what causes a particular disease, you can always classify it (tongue-in-cheek)." Such is the case with plantar fragments, where three forms (types) of the disorder have been proposed according to the origin of the fragment.[13] All the plantar fragments removed by Fortier and colleagues were of the type I variety:

1. Fragments that originate from the caudal aspect of the glenoid on either side of the sagittal groove
2. Fragments detached from the caudal eminences
3. Fragments from the base of the proximal sesamoids

Growth Plate Fractures

Open physes must be distinguished from growth plate fractures. Smallwood and co-workers reported that the proximal phalangeal physis closes between 22 and 38

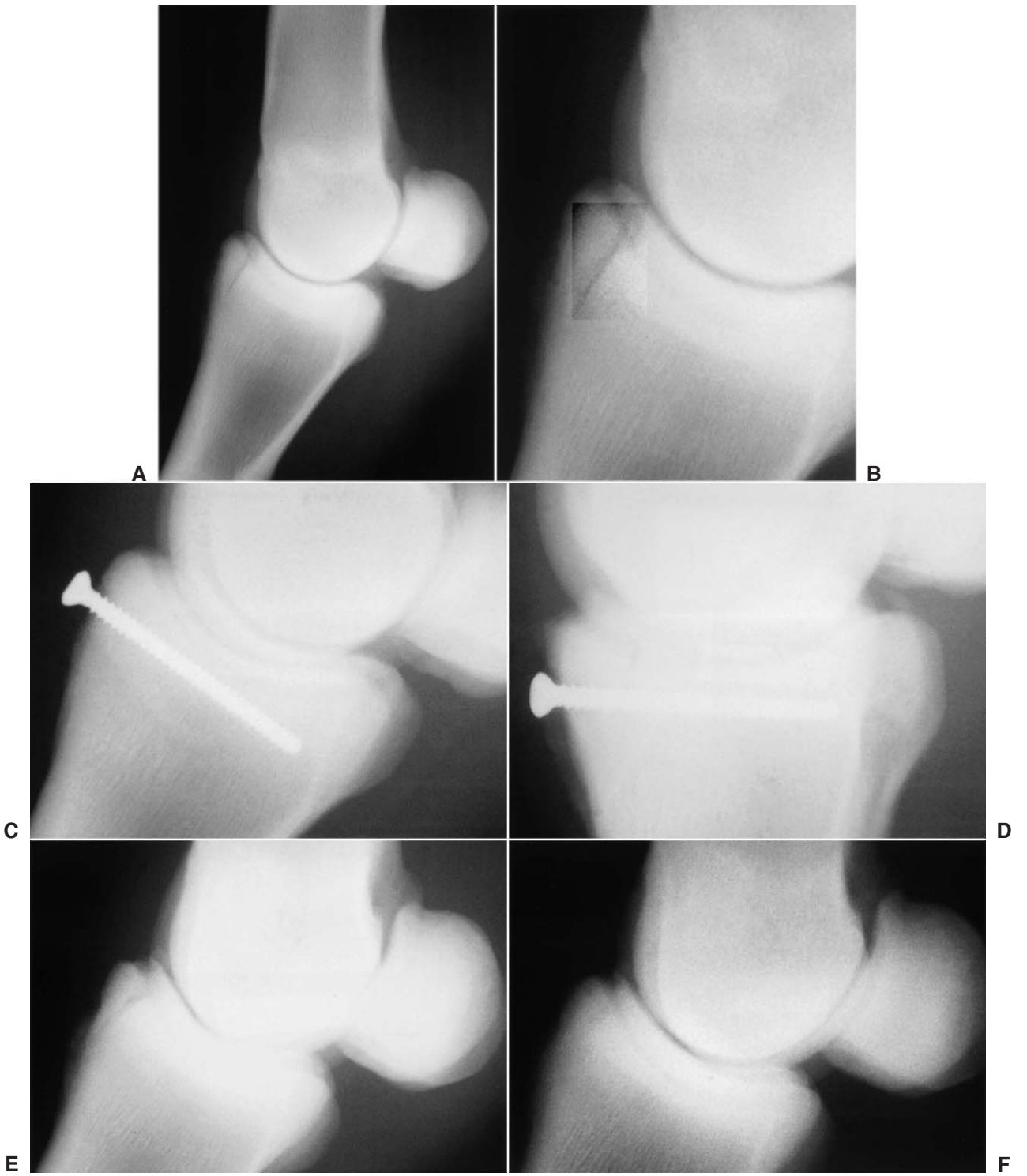


Figure 5-14 • Lateral **(A)** and lateral close-up **(B)** views of the fetlock show a deep dorsal lip fracture, which was subsequently reduced with a bone screw **(C).** Two months later, the fracture is healed, and the screw is partially overgrown with callus **(D).** The next season, the horse sustained a similar fracture of its opposite fetlock **(E)** that was treated conservatively. Two months later the bone appeared fully restored **(F).**

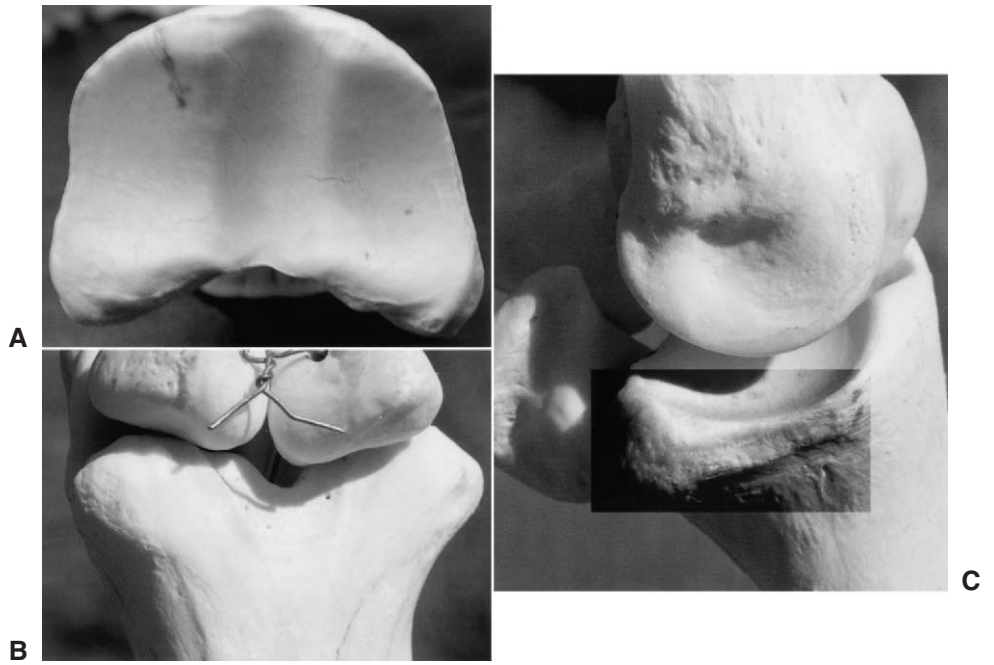


Figure 5-15 • Bones of the equine fetlock emphasizing the palmar protuberances of the proximal phalanx: top **(A),** rear **(B),** and side **(C)** views.

weeks of age (mean, 30 weeks).[14] They also reported that the distal physis of the third metacarpal bone closes between 18 and 38 weeks of age (mean, 29 weeks). An anatomic specimen (Figure 5-19) and radiograph (Figure 5-20) show these accessory growth centers.

Proximal phalangeal growth plate fractures usually involve the physis and a corner of the adjacent metaphysis (Salter-Harris type II injury) with variable degrees of fragment displacement (Figure 5-21). Please refer to Chapter 4 for further examples of proximal phalangeal growth plate fractures.

Congenital deformity of the proximal phalangeal epiphysis and undiscovered neonatal fractures can be difficult or impossible to distinguish from one another, although in my experience the latter are usually unilateral and associated with lameness, and the former are usually bilateral and nonpainful (Figure 5-22).

Longitudinal Fractures (Midsagittal Fractures)

Ellis and co-workers classified complete or incomplete longitudinal P1 fractures into four groups: types 1 through 4.[15]

1. Short or long, complete or incomplete central body fractures originating proximally in the lateral aspect of the sagittal groove. A variant of this type is the proximal longitudinal fracture that breaks through the cortex laterally before reaching the pastern joint, thus creating a separate fragment.
2. Short or long, curved or straight, complete or incomplete, central body fractures originating distally and entering the pastern joint.
3. Long lateral body fractures.
4. Full-length, biarticular sagittal fractures that also break through the lateral cortex in one or more places.

Tetans and co-workers reported that Standardbreds with incomplete midsagittal fractures of P1 are likely to return to racing, but will not perform as well as they did before their injuries.[16] Examples of P1 longitudinal fractures appear in Chapter 4.

Distal Metacarpal/Metatarsal Fractures

Kaweak and co-workers reported the diagnosis and treatment of incomplete fractures of the palmar aspect of the third metacarpal bone in five horses.[17] Radiographically the fracture was often difficult to see in all but the partially flexed frontal view, often appearing as no more than a faint hairline in the medial aspect of the third metacarpal condyle. In some horses, no fracture was detected, forcing the authors instead to rely on circumstantial evidence obtained by scintigraphy. This sort of fracture seems ideally suited to CT detection.

Metacarpophalangeal/Metatarsophalangeal Dislocation

Hubert and co-workers described the radiographic appearance of a metatarsophalangeal dislocation in

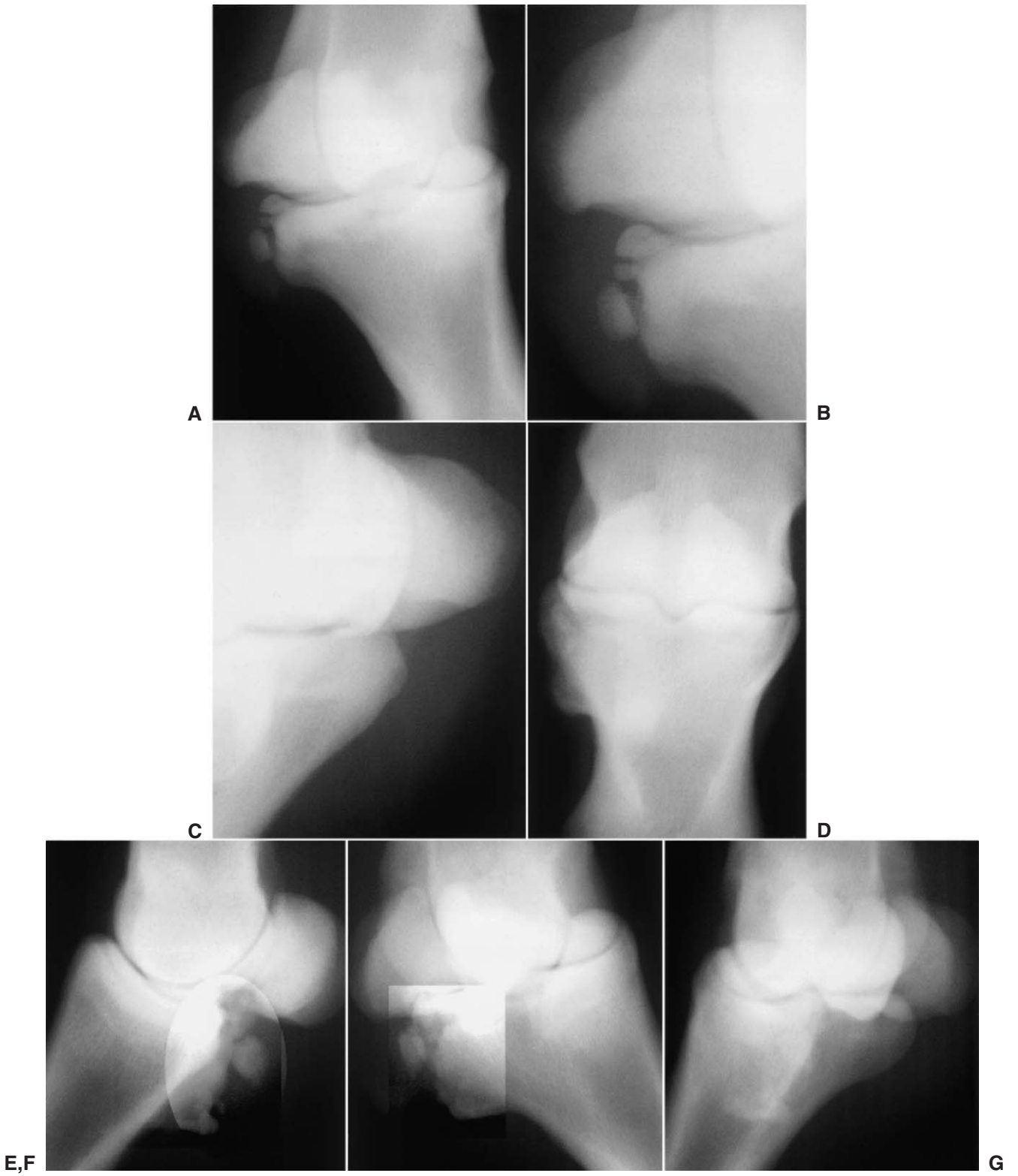


Figure 5-16 • Fragmented caudal eminence: Two cases. Case 1: Caudomedial oblique **(A)** and close-up **(B)** views of a subacute, displaced, comminuted fracture of the medial palmar protuberance. The normal lateral palmar protuberance is included for comparison **(C).** Case 2: Dorsopalmar **(D),** lateral **(E),** lateral oblique **(F),** and medial oblique **(G)** views show a chronic, severely fragmented, partially calloused fracture of the medial palmar protuberance.



Figure 5-17 • Lateral view of an air-dried fetlock specimen (including regional tendons and ligaments) shows insertion of collateral metacarpophalangeal ligament on the caudolateral ridge of the palmar protuberance.

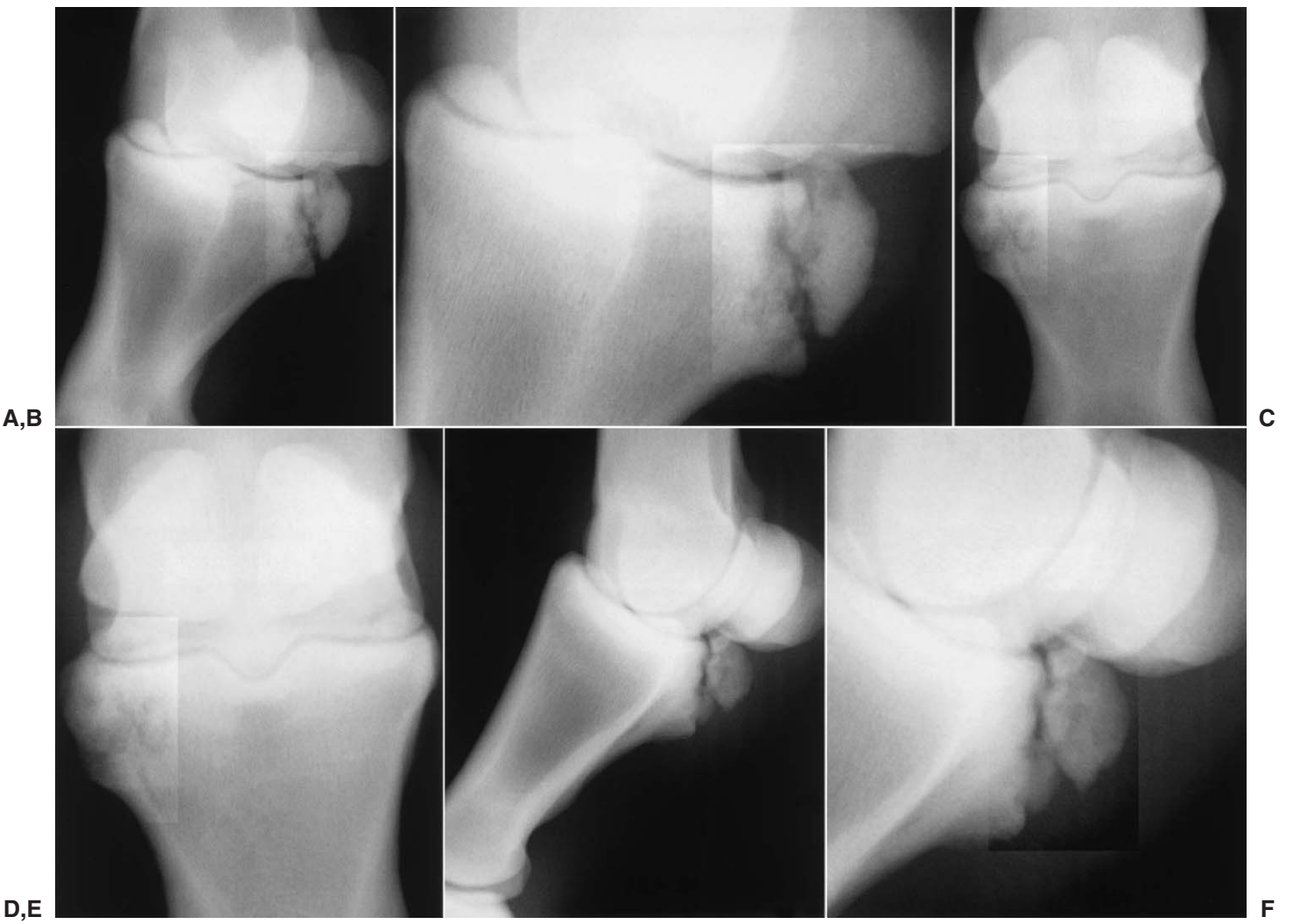


Figure 5-18 • Bilateral plantar fragments: Bilateral osteochondritis (fragmenting form) of the plantar protuberance of the proximal phalanx: right planteromedial oblique **(A),** planteromedial oblique close-up **(B),** dorsoplantar **(C),** and dorsoplantar close-up **(D)** views show a large planteromedial fragment with a ragged fracture line. The opposite hind fetlock shows a similar-appearing lesion as seen in left planteromedial oblique **(E)** and planteromedial oblique close-up **(F)** views.

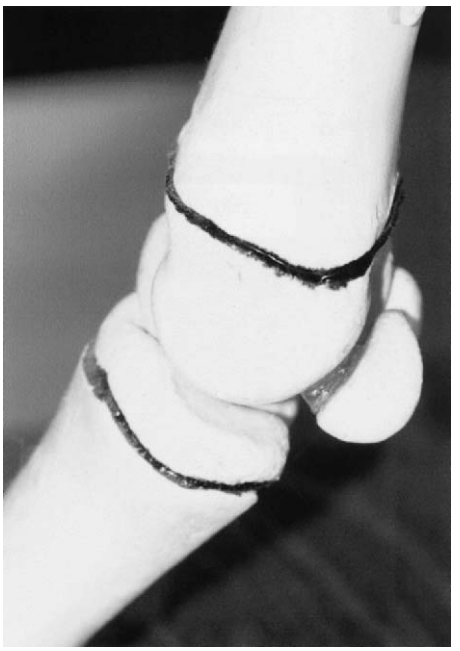


Figure 5-19 • Bones of a foal showing separate ossification centers for distal MC3 (mean closure time, 29 weeks) and proximal P1 (mean closure time, 30 weeks).

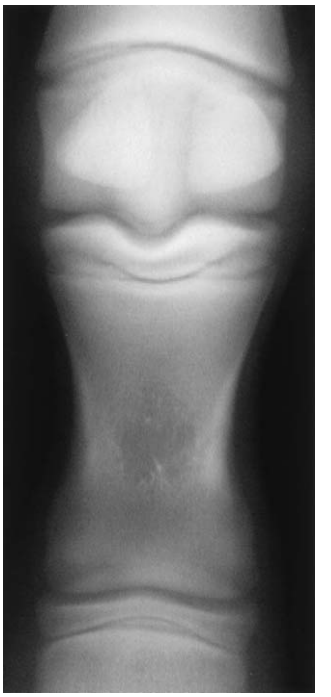


Figure 5-20 • Dorsopalmar view of the fetlock of a 2-week-old foal shows fully open growth plates in the distal metacarpus, proximal, and middle phalanges. The vague lucency in the center of P1 is normal.



Figure 5-21 • Dorsopalmar **(A),** slightly obliqued lateral **(B),** and lateral oblique **(C)** views of the right fetlock show Salter-Harris type II, proximal phalangeal growth plate fractures laterally, with associated apical sesamoid fracture medially. One month later dorsopalmar **(D)** and lateral **(E)** views show that the fracture is well but incompletely calloused.

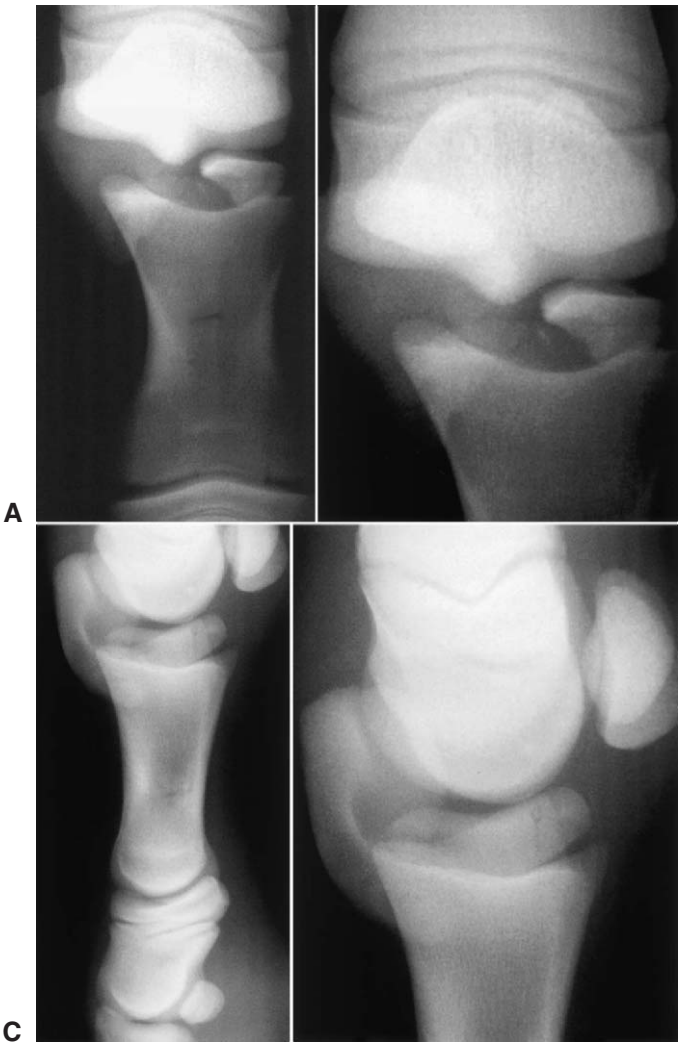


Figure 5-22 • Dorsopalmar **(A),** dorsopalmar close-up **(B),** lateral **(C),** and lateral close-up **(D)** views of the left front fetlock of a young foal with either (1) a neonatal, proximal phalangeal growth plate-epiphyseal fracture or, less likely, (2) a congenitally separated proximal phalanx with dual displaced ossification centers, a fascinating case in either event.

a 3-year-old Thoroughbred gelding.[18] A large bone fragment lateral to the proximal aspect of the medial collateral fossa of MT3, and roughening of the medial plantar eminence of P1 characterized the injury.

A stress radiograph showed dislocation of the fetlock joint believed to be the result of a sprain-avulsion-fracture of the medial collateral ligament. The collateral ligament is composed of superficial and deep elements, which attach proximally to the collateral fossa of MC/MT3 and distally on the caudolateral eminence of P1.

▮▮▮ PROXIMAL SESAMOIDS

The proximal sesamoid bones are part of the suspensory apparatus. Their anatomy is deceptively complex, featuring a uniquely angled articular surface, a distinctly curled proximal flexor margin, and near-complete envelopment by surrounding connective tissues (Figure 5-23).

Primary Injury Mechanisms

Rooney hypothesized that most sesamoidian body fractures occur during fatigue-related hyperflexion of the fetlock, joint, during which there is an anatomic mismatch between the articular surfaces of the sesamoids and the opposing surface of the cannon bone. I share this opinion.

Fractures of the flexor surface of the sesamoid bone are typically *avulsive* in nature. As such they are often characterized by their flakelike appearance, low density, and minimal displacement. A week or two after the initial injury, the immediately surrounding bone begins to lose density, in many instances appearing distinctly porotic. Adjacent vascular channels may appear to enlarge or to become more distinct, the latter probably attributable to a generalized osteopenia. In some instances, one or more vascular channels can become grossly enlarged, called *traumatic dilation.*

Sesamoidian Fractures

In my experience, more than 90 percent of horses with fresh sesamoidian fractures also have sonographically demonstrable soft tissue injuries. I therefore recommend that the associated flexor tendons and suspensory ligaments have ultrasound performed, especially the suspensory branch attached to the fractured sesamoid, whether are not there is visible swelling.

Classification. The proximal sesamoid bones are subject to a wide variety of fractures, some obvious, others not. Probably the simplest way to classify these injuries is to combine classic anatomic and etiologic descriptions as follows:

Apical Fractures. Like many basilar fractures, ease of identification depends largely on the size of the fracture fragment and its degree of displacement. Lindsay and co-workers described the use of a steep (near-vertical) lateral oblique view of the fetlock to identify minimally displaced, interior apical fractures.[19]

Woodie and co-workers reported apical sesamoid fractures in 43 Standardbreds.[20] They found that neither the size of the apical fragment nor the presence of related suspensory branch injury affected a horse's ability to race after surgical removal of the fragment.

Occasionally apical sesamoid fractures must be differentiated from secondary ossification centers, which have also been termed *bipartite proximal sesamoid bones*, as described by Ellis and by Thompson and Rooney.[21,22] In my experience, this relatively rare form of accessory growth center is usually triangular, possesses a broad congruent base, is closely approximated to the adjacent sesamoid, and nearly always is present bilaterally.



Figure 5-23 • A normal front proximal sesamoid bone. Five views of a surprisingly complex bone: articular surface **(A),** abaxial surface **(B),** flexor surface **(C),** apical surface **(D),** and basilar surface **(E).**



Figure 5-24 • Close-up right **(A)** and left **(B)** lateral views of the front fetlocks of a young foal show bilateral apical sesamoid fragments, presumed to be traumatic (as opposed to osteochondritis or accessory ossification centers).

The classification of apical fractures (grades 1-3) according to length, measured from a dorsopalmar or dorsoplantar radiograph, is an exercise in redundancy.[23] If it is important to measure the exact length of the fragment, other than to characterize it as small, medium, or large, then simply record the value in the radiographic report (without grade) for future radiographic reference. Figures 5-24 and 5-25 provide examples of apical sesamoid fractures.

Body Fractures

Sesamoidian body fractures are typically transverse, often with a substantial gap between fragments.[24] The injury is believed to result from fatigue-related hyperextension during strenuous training or racing, which results in temporary incongruency between the articular surfaces of the sesamoidian body and the overlying condylar apex, leading to structural failure.[25]

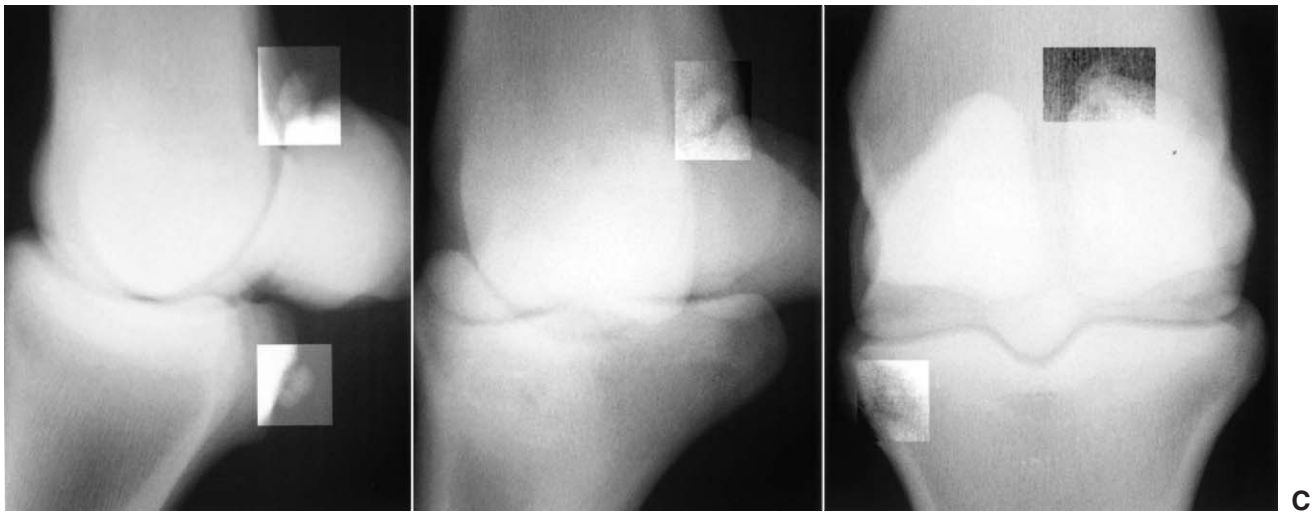


Figure 5-25 • Slight lateral oblique **(A),** full lateral oblique **(B),** and dorsopalmar **(C)** views of the fetlock show small displaced fractures of the apex of the medial proximal sesamoid, and lateral palmar eminence of P1.

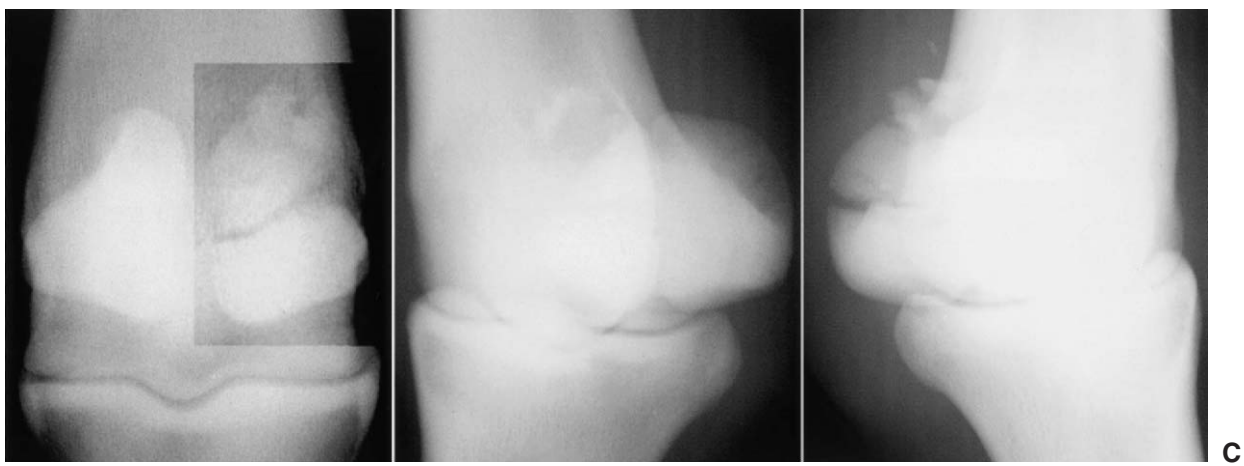


Figure 5-26 • Close-up dorsopalmar **(A),** lateral oblique **(B),** and medial oblique **(C)** views of a 7-year-old Thoroughbred filly with multiple lateral sesamoid fractures involving the apex and body of the bone. There were also second-degree sprains of the lateral branch and distal body of the suspensory ligament (not shown).

In Standardbreds, body fractures occur most often in either the lateral or medial sesamoid bones of the left hind fetlock or the medial sesamoid in the right front. Thoroughbreds usually fracture their right front medial sesamoids.[26] Symmetric body fractures of both medial and lateral proximal sesamoids have also been reported.[27] Because these fractures are articular, it is imperative that they be reduced and stabilized as soon as possible to avoid posttraumatic osteoarthritis. Repair is usually with cortical lag screws combined with a cancellous bone graft.[28] Figure 5-26 shows a distracted midbody fracture.

Basilar Fractures

Basilar sesamoid fractures can assume a variety of shapes and degrees of displacement. When located near the midline (axial), basilar fractures are often round, with very little displacement, making certain diagnosis difficult. Oblique views are often of little help in such situations. Full-width fractures, on the other hand, are more readily diagnosed unless there is inadequate penetration.

Pool and Meagher reported that the *distal sesamoid ligaments* most often tear or rupture at their origins or insertions; in the former instance, often avulsing the base of one or both proximal sesamoids in the process.[29] In an experimental cadaveric study of trained versus rested horses, Burkowiecki and coworkers found that under extreme mechanical stress, the sesamoids of the trained horses broke before the distal sesamoidian ligaments, whereas in the rested animals, the opposite was true.[30]

Southwood and McIlwraith concluded that arthroscopic removal of basilar fracture fragments offered no better than a fair prognosis.[31] By way of a cautionary

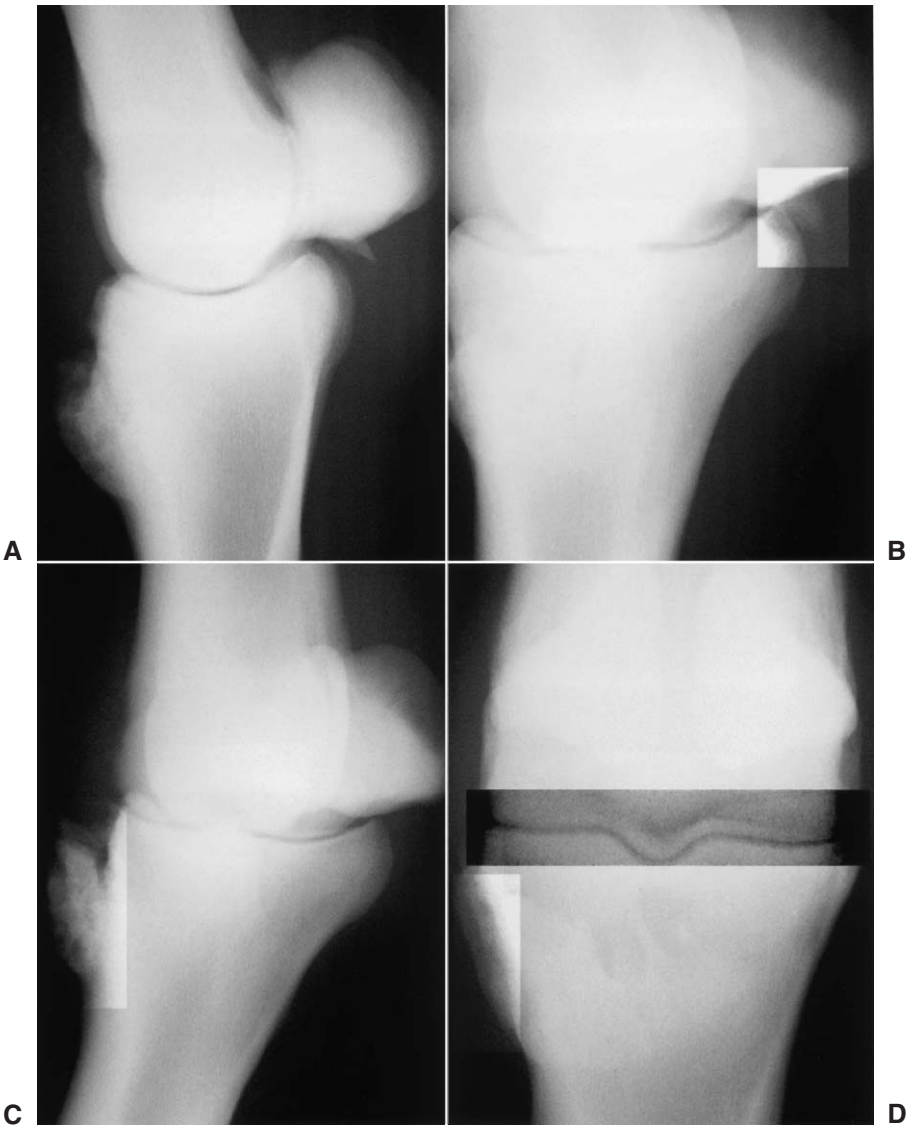


Figure 5-27 • New and old: Close-up lateral **(A),** lateral oblique **(B),** medial oblique **(C),** and dorsopalmar **(D)** views of a racing Thoroughbred with a chronically swollen left front fetlock show a relatively fresh basilar fracture of the left proximal sesamoid; a large, chronic-appearing exostosis on the proximal dorsomedial surface of the cannon bone; and a narrowed (but not arthritic) fetlock joint.

note, osteochondritis of the proximal surface of one or both caudolateral eminences of P1 may produce flakelike bone fragments that can be mistaken for basilar sesamoid fractures. Figures 5-27 to 5-29 illustrate a variety of basilar sesamoidian fractures.

Sesamoidian Avulsion Fractures

Fractures of the flexor surface of the sesamoid bone are typically *avulsive* in nature. As such, they are often characterized by their flakelike appearance, low density, and minimal displacement. As mentioned previously, sesamoidian avulsion fractures undergo a predictable series of changes beginning a week or two after the initial injury. The immediately surrounding bone begins to lose density, in many instances appearing distinctly porotic. Adjacent vascular channels may appear to enlarge or become more distinct, the latter probably being attributable to a generalized osteopenia or, alternatively, traumatic dilation.

Failure to rest such injuries may lead to aggravation, which is often depicted as a further loss in bone density. This type of reinjury may be what some have termed *steroid arthropathy* because many of these animals have had multiple intraarticular steroid injections between the time of the original injury and subsequent recheck.

Sesamoidian Fractures in Foals. Ellis described the radiographic appearance of proximal sesamoid fractures in a series of 18 foals, presumably caused by fatigue-related hyperextension while they attempted to keep up with their mothers.[32] Most of the injuries were simple body fractures, but a small number of chip, avulsion, incomplete, and comminuted fractures were also reported.

Differences in Healing Between Injured Sesamoid and Long Bones. Medina and Morgan drew attention to the differences in how sesamoid bones heal com-

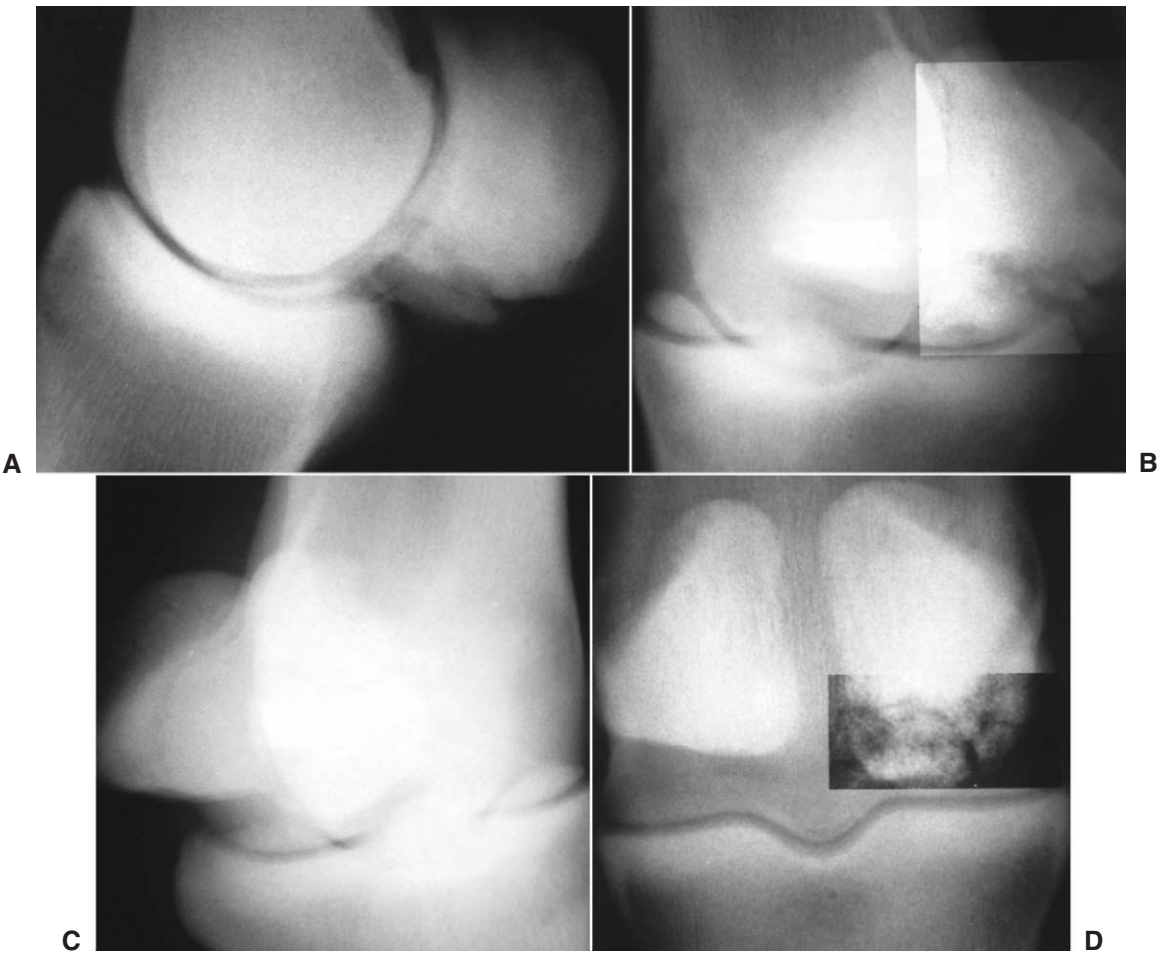


Figure 5-28• Close-up lateral **(A),** medial oblique **(B),** lateral oblique **(C),** and dorsopalmar **(D)** views of a racing Quarter Horse show a chronic-appearing basilar fracture of the medial, right front proximal sesamoid, featuring extensive secondary fragmentation and a partial callus. The fetlock joint is narrowed but not yet arthritic.

pared with long bones, especially the fact that experimentally created basilar sesamoid fractures often showed little or no callus radiographically, even though they had healed clinically.[33] Those who radiographically interpret sesamoid fractures were advised to keep the following considerations in mind:

- The absence of an external bridging callus does not indicate lack of healing and can result in underestimation of healing.
- The presence of periosteal bone is probably stimulated by trauma or fragment motion and does not represent early callus, resulting in overestimation of healing.
- Widening of a fracture line is expected as early osteoclastic activity occurs.
- Use of flexed lateral projections accurately indicates fragment motion, indicating delayed union or nonunion.
- Bridging callus is not as dense as surrounding bone and may escape radiographic detection.
- Oblique projections may obscure the fracture line, falsely suggesting callus and healing.

Diagnostic Oversimplification (Just a Fracture . . .)

As mentioned earlier, serious soft-tissue injury often accompanies fetlock fractures, but not until the advent of ultrasound could such injuries be detected with any degree of certainty. Now that it is possible to evaluate sonographically the flexor tendons, suspensory ligaments, fetlock joint, and periarticular tissues, strong consideration should be given to doing so, especially when substantial regional swelling or excessive disability is present.

Distal Metacarpal Stress Fractures

Stover and co-workers reviewed the radiographic features of bucked shins and metacarpal stress fractures in Thoroughbred racehorses.[34] Using postmortem specimens, Tapprest and co-workers described the

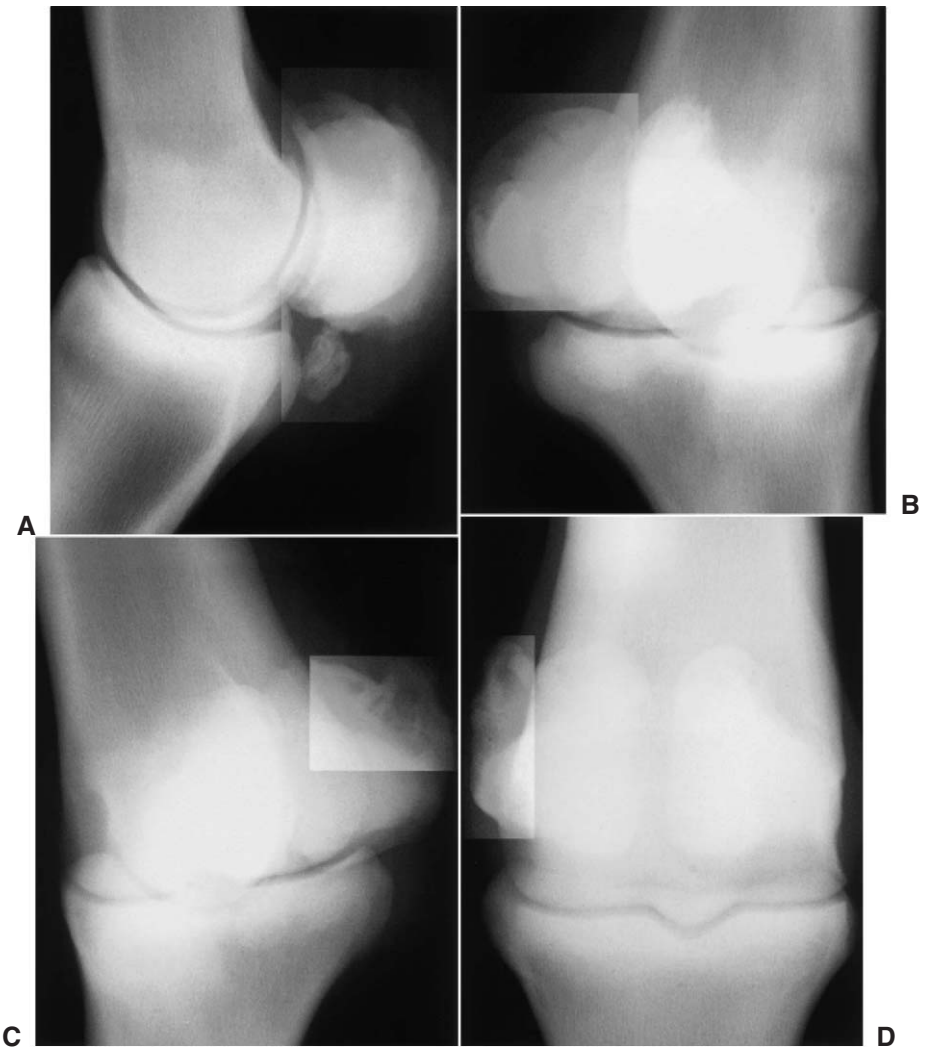


Figure 5-29 • Two serious basilar fractures illustrating how radiographic appearances can be prognostically deceptive. Case 1: Close-up lateral **(A),** lateral oblique **(B),** medial oblique **(C),** and dorsopalmar **(D)** views of left front fetlock of a sound 6-year-old Thoroughbred gelding that first injured its leg as a 2-year-old. Although the term *sesamoiditis* is too often used loosely, it appears justified in this instance, as indicated by the following: (1) a severely displaced basilar fracture of the medial proximal sesamoid; (2) new bone deposition along the abaxial margin of the medial sesamoid; and (3) traumatic, deforming cyst formation in the flexor surface of the lateral sesamoid.

radiographic and magnetographic appearance of bilateral distal metacarpal stress fractures in a 5-year-old French trotter.[35]

In my experience fresh stress fractures may or may not be displaced sufficiently to detect radiographically. When visible, such fractures often appear as a faint half-crescent breaking through the dorsal cortex of the cannon bone distally. These fractures rarely show in clearly in more than one of the four standard views. In older fractures (a month or more) the fracture line is usually replaced by a callus, appearing in lateral projection as a low, broad-based mound of smooth bone, or in the oblique views as a faint oval-shaped medullary opacity.

▮▮▮ OSTEOARTHRITIS OF THE FETLOCK JOINT

O'Brien's "Five-Region" Strategy: A Diagnostic Approach to the Arthritic Fetlock

T. R. O'Brien (one of my more memorable and respected teachers at Davis) performed a radiologic-pathologic correlation on the arthritic fetlocks of 43 Thoroughbreds, concluding that there were five critical regions within the fetlock joint, which, if carefully inspected, would likely yield a radiographic diagnosis in a majority of instances.[36] The

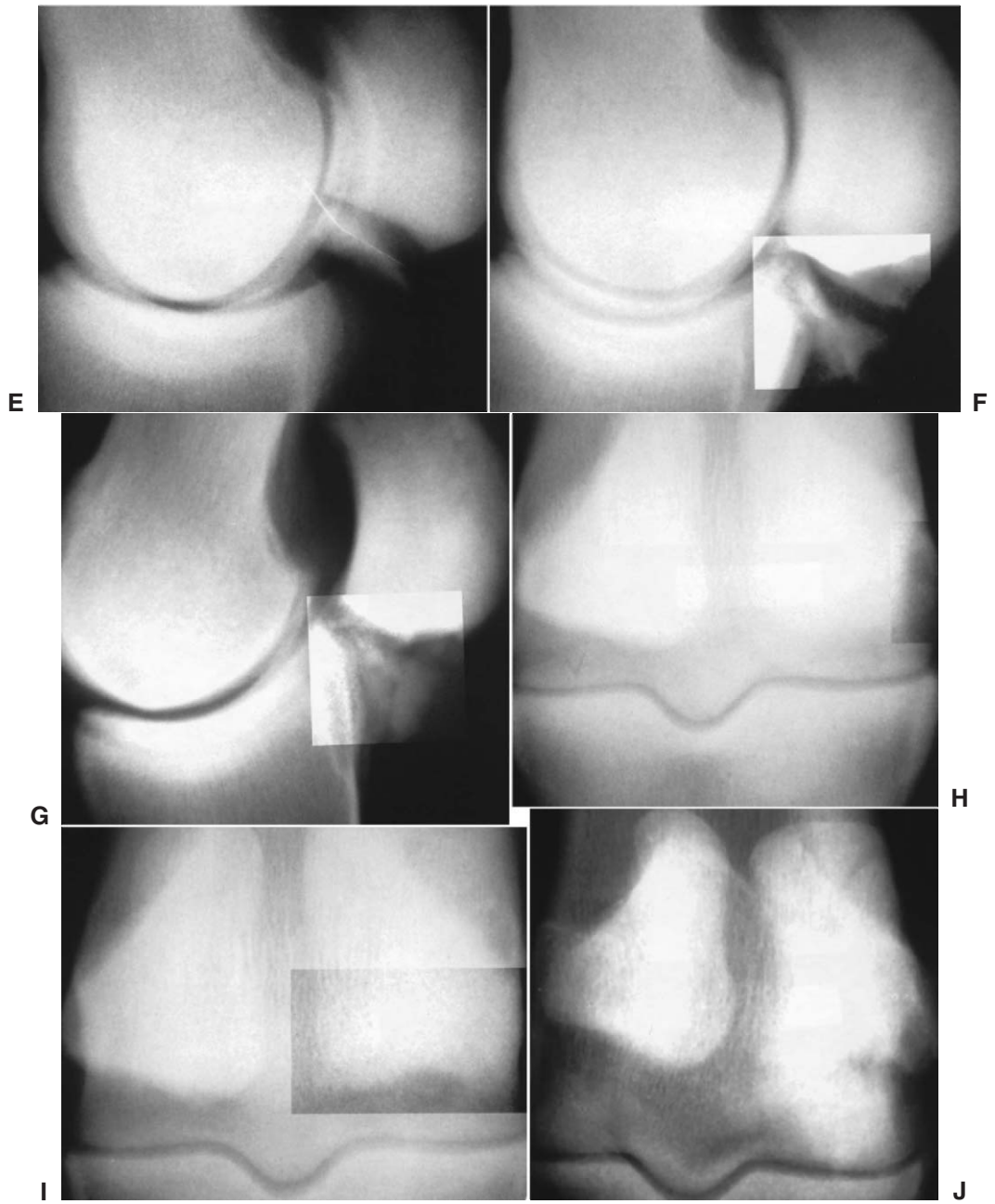


Figure 5-29, cont'd • Case 2: Three lateral **(E-G)** and three dorsopalmar **(H-J)** views of the fetlock of a badly crippled Thoroughbred racehorse. The initial images **(E, H)** show a large triangular fragment detached from the base of the medial proximal sesamoid. Fifteen months later **(F, I),** the fragment is still displaced, with a rudimentary callus. Twenty months later **(G, J),** fragment displacement is relatively unchanged, but the callus has nearly filled the fracture gap, increasing the height of the medial sesamoid by nearly a third and, more important, severely limiting the flexibility of the fetlock.

five regions, from proximal to distal, include the following:

1. The joint capsule
2. The cranial aspect of the distal metacarpus or metatarsus
3. The palmar aspect of the distal metacarpus (plantar aspect of the distal metatarsus)
4. The proximal and distal periarticular aspects of the sesamoid bones
5. The dorsal aspect of the proximal first phalanx

Capsular Region

Joint swelling characterized most fetlock joints with grossly visible disease and was best recognized in the lateral view. Intracapsular swelling typically appeared as a combination of increased soft-tissue density and an area cranial to the fetlock joint and was caused by a combination of capsular or synovial hyperemia and hyperplasia. In no cases were intracapsular bone fragments observed (joint bodies, joint mice).

Cranial Aspect, Distal Metacarpus/Metatarsus

Radiographic findings, best seen in lateral and flexed lateral projections and for the most part confined to the proximal aspect of the condyle and sagittal ridge, included the following: (1) variably shaped osteophytes, (2) focal surface defects or deformities, (3) periosteal new bone, and (4) soft-tissue swelling. Although useful diagnostically, the observed radiographic abnormalities were not as informative as the gross specimens.

Palmar/Plantar Aspect, Distal Metacarpus/Metatarsus

Flattening, abnormal subchondral density, and defects were the major radiographic observations in this region. These findings corresponded to damaged and defective articular cartilage accompanied by commensurate degree of bone loss. As with the cranial aspect of the cannon bone, lateral and flexed lateral projections were the views of choice.

Proximal and Distal Articular Surfaces of Sesamoid Bones

Radiographically, diseased sesamoid bones were characterized by conical rather than rounded corners. This corresponded to periarticular bone deposition and, in some instances, synovial overgrowth and pannus, as seen grossly.

Proximal Phalanx. The optimal projections for evaluating the proximal phalanx proved to be the extended lateral and medial oblique views, which best profiled the paired lateral and medial cranial eminences and caudal protuberances. As elsewhere, the most telling abnormalities were localized bone deposits that produced *peaking* on normally rounded corners and small displaced fractures. In general, the larger the P1 osteophytes, the more extensive the cartilage damage as determined by direct inspection of gross specimens.

▮▮▮ OSTEOCHONDRITIS OF THE FETLOCK

Osteochondritis, with and without fragmentation (osteochondritis dissecans), has been reported in various forms and locations within the fetlock. Some lesions heal spontaneously by 1 year of age, but others do not. Some horses with radiographic evidence of osteochondritis of the fetlock appear sound.[37]

P1

Schoenborn and Hornof described the radiographic, scintigraphic, and CT appearance of a fragmenting form of osteochondritis in the proximal phalanx of a moderately lame 6-year-old Thoroughbred (Table 5-2).[38]

Table 5–2 • LOCATION AND FORM OF RADIOGRAPHICALLY VISIBLE OSTEOCHONDRAL LESIONS OF THE FETLOCK

Location	Form
MC3 epiphysis: usually midway between sagittal ridge and collateral fossa	Lesions range from subtle flattening of subchondral bone to focal concavities, to cystlike lesions (best seen in frontal projection)
MC3 sagittal ridge	When located in the front proximal part of the sagittal ridge, the lesion often appears as a small, smooth oval bone fragment (as seen in lateral projection). Alternatively the midsagittal ridge may appear blunted or detached (as seen in frontal projection)
P1 epiphysis	Lesions are similar to those seen in MC3 epiphysis
P1 palmar (plantar) eminence	Hindlimb, often bilateral lesions are most common. Caudal tuberosity detachment is typical, with long-standing lesions often featuring one or more secondary fragments, surrounded by new bone
Proximal sesamoid bones	There is no typical appearance: sesamoids often appear fractured, with or without displacement, sometimes comminuted, but without the usual amount of associated pain and lameness. Depending on the age of the animal and assuming that most such lesions are present from an early age, extensive remodeling and new bone may be present. These latter lesions can be very hard to distinguish from former injuries

MC/MT III

Hornof and co-workers described the radiographic and histologic appearance of osteochondritis dissecans in the articular surface of the distal metacarpus of racing Thoroughbreds.[39] Viewed from the distal, end-on perspective, the lesions appeared grossly as deep, winglike defects in the articular cartilage. In a related report, O'Brien described six radiographic variations of the aforementioned MC3 lesion, ranging from flattening of the palmar surface to large subchondral cysts[40] (Figure 5-30).

Previously, Hornof and O'Brien described the advantages of moderately flexing the fetlock during frontal radiography by placing the extended foot on a block to profile the central and caudal thirds of the metacarpal condyle, where many osteochondral lesions are situated.[41] The authors described their modified dorsoplantar view as follows: non–weight-bearing, 125-degree, dorsopalmar metacarpal, skyline projection (125 DPMS). Incidentally, I first learned of this view from another of my instructors, Joe Morgan, in the early 1970s and have found it a useful supplementary projection in some instances. Two examples of fragmenting osteochondritis are shown in Figures 5-31 and 5-32.



Figure 5-30 • Young colt with osteochondritis of the left front fetlock **(A).** Close-up dorsopalmar **(B),** ultra-close-up dorsopalmar **(C),** close-up medial oblique **(D),** and ultra-close-up medial oblique—slightly different angle **(E)** views of the left fetlock of a lame horse show a large, oval, subchondral cyst in the distal 3rd metacarpal epiphysis. The underlying cartilage space appears normal. A close-up dorsopalmar view **(F)** of the opposite fetlock is provided for normal comparison.

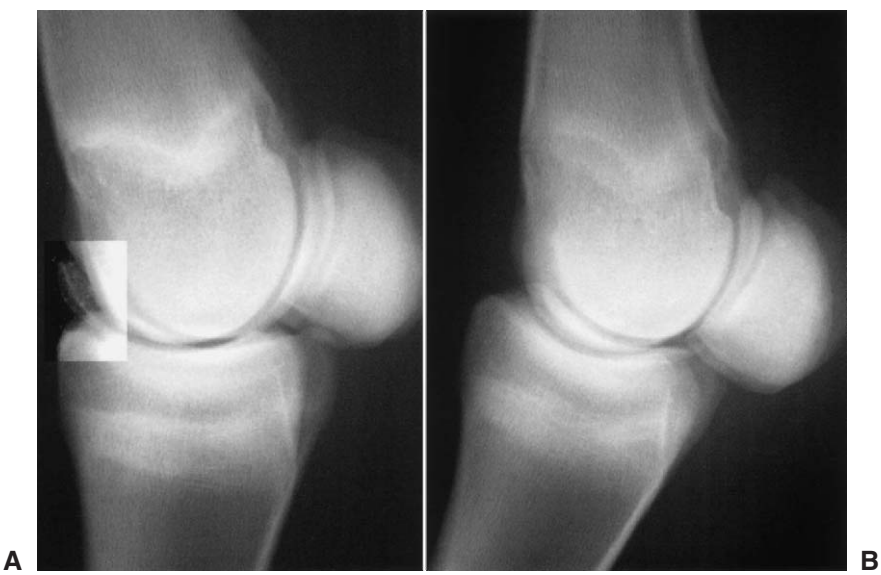


Figure 5-31 • Close-up lateral view **(A)** of the fetlock of a young Standardbred filly shows detachment of the leading edge of the sagittal ridge, a consequence of the fragmenting form of osteochondritis. A close-up lateral view **(B)** of the normal opposite fetlock is provided for comparison.

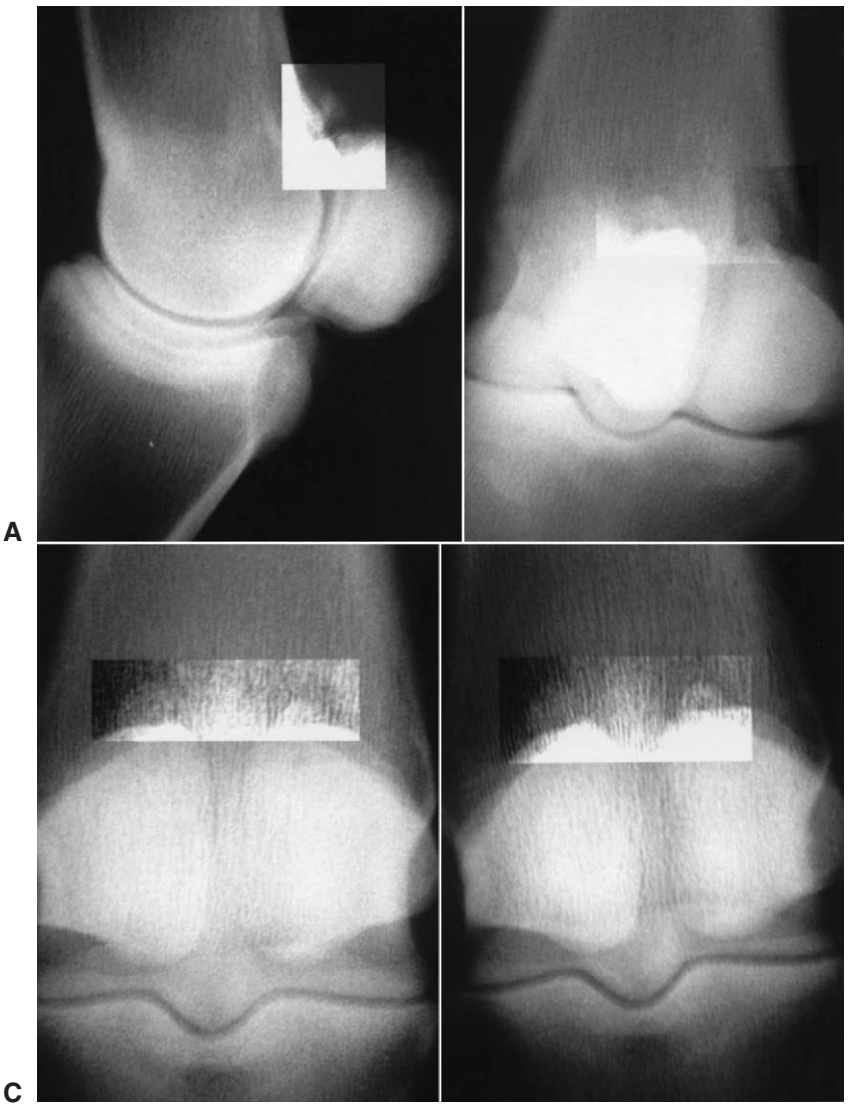


Figure 5-32 • Close-up lateral **(A),** lateral oblique **(B),** and dorsopalmar **(C)** views of the right fetlock front of a young colt show bilateral bone fragments at the apices of the sesamoids. Because of an absence of known injury, minimal lameness, and the presence of similar fragments in the opposite fetlock **(D),** the lesions were believed to be the result of fragmenting osteochondritis, although there is some support for trauma.

▮▮▮ SESAMOIDITIS: A DIAGNOSIS IN DOUBT

O'Brien and Morgan described the radiographic appearance of sesamoiditis in young racing Thoroughbreds, emphasizing—among other things—the importance of evaluating the size, shape, and number of vascular channels, much as with navicular disease.[42]

Later Poulos compared the radiographic and histologic changes found in the proximal sesamoids of young working horses, challenging the idea that these linear lucencies were the result of inflammation and impaired blood supply, or sesamoiditis. He argued instead that such changes developed secondary to a primary suspensory injury or, alternatively, to chronic overuse.[43]

Hardy and co-workers investigated the clinical relevance of radial lucencies and other radiographic findings seen in the proximal sesamoids of 2-year-old Standardbreds at the beginning and conclusion of their first year of race training.[44] They concluded that the larger, more ill-defined and numerous the "linear defects" seen in the flexor surface of the proximal sesamoid bones, the more likely they were to be associated with lameness and poor performance. Like Poulos, they also believed that such changes were indicative of primary suspensory rather than sesamoidian disease (sesamoiditis).

Conversely, horses with proximal sesamoids containing only a few small, well-defined lucencies remained sound and performed well over the season. Also of note was the fact that in no instance of sesamoidian fracture was the injury preceded by an abnormal-appearing sesamoid bone, bringing into to question the long-held belief that enlarged channels structurally weaken the sesamoid bone, causing it eventually to fracture if the animal is not rested.

Examples of sesamoiditis, as defined by enlargement of one or more vascular channels or localized



Figure 5-33 • Close-up lateral **(A),** ultra-close-up medial oblique **(B),** and ultra-close-up lateral oblique **(C)** views of the right front fetlock of a chuck wagon pony with a history of repeated ankle sprain show dilated vascular channels and a central marginal defect consistent with sesamoiditis.

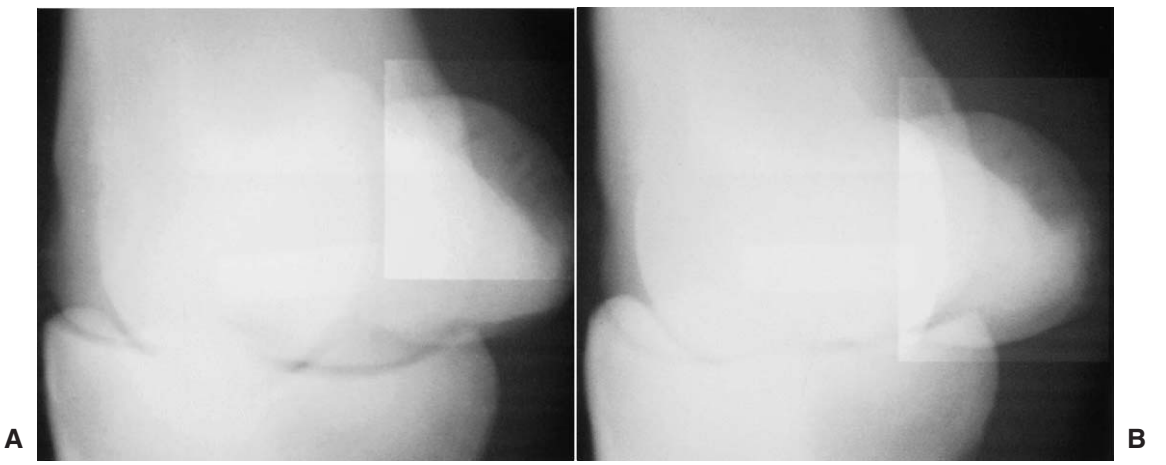


Figure 5-34 • Close-up right **(A)** and left medial oblique **(B)** views of the front fetlocks of a sound middle-aged Thoroughbred show enlarged vascular channels. Although such radiographic findings have traditionally been considered the hallmark of sesamoiditis, such a diagnosis is difficult to justify in this instance.

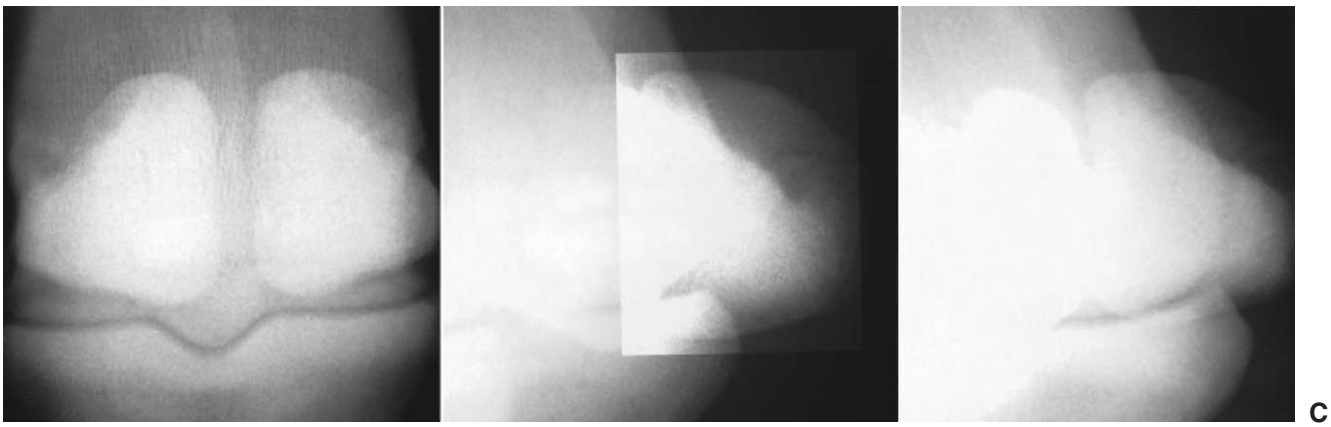


Figure 5-35 • Close-up dorsopalmar **(A),** medial oblique **(B),** and lateral oblique **(C)** views of the right fetlock show defects in the central third of the flexor margin of the medial proximal sesamoid bone consistent with sesamoiditis.

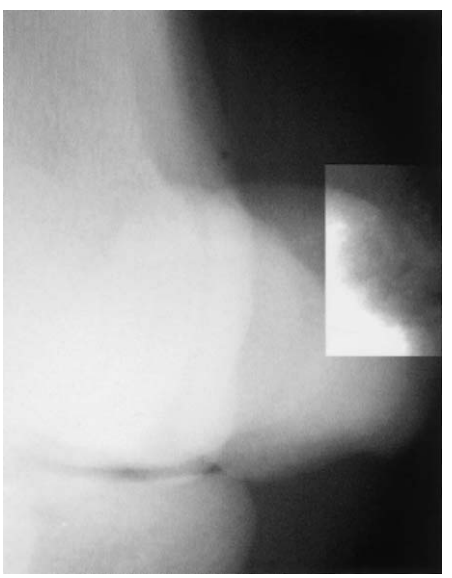


Figure 5-36 • Close-up medial oblique view of the left front fetlock shows a large circular area of bone loss in the central third of the flexor surface of the medial proximal sesamoid consistent with sesamoiditis.

flexor margin defect, are shown in Figures 5-33 to 5-36. Sesamoiditis, as defined by more extensive bony alterations (fragments, osteophytes), is illustrated in Figures 5-37 and 5-38. Sesamoiditis, inferred from nearby dystrophic calcification or small flakes of bone, is shown in Figures 5-39 and 5-40.

Caution: In assessing oblique views of the proximal sesamoids, take care not to mistake the edge enhancement seen in the nonprofiled sesamoid for a fracture (Figure 5-41).

▮▮▮ FETLOCK SPRAINS AND SPRAIN-AVULSION-FRACTURES

Acute fetlock sprains are usually associated with heat, swelling, pain, and accordingly lameness. Diagnosis is most readily, quickly, and inexpensively made with ultrasound, although magnetic resonance imaging (MRI) is capable of producing some superb images, albeit at a premium price. Sprains are characterized according to the degree and extent of ligament injury, as detailed elsewhere in this book. Fetlock swelling associated with an acute second-degree sprain is shown in Figure 5-42; examples of acute and chronic sprain-avulsion-fractures are shown in Figures 5-43 and 5-44.

▮▮▮ OSTEOARTHRITIS

Normal Cartilage Space

The articular cartilage comprises only a relatively small percentage of the curvilinear lucent band observed radiographically between the third metacarpal bone and proximal phalanx. In fact, the so-called joint space is for the most part composed of cartilage (Figure 5-45). Accordingly, this region has been termed the *cartilage space*, a designation I wholeheartedly endorse.

Osteophytes

Osteophytes, or bone spurs as they are termed commonly, are the hallmark of osteoarthritis. Osteophytes typically form on the *periarticular* margins of joints, but they may also be situated just off the joint margins, in which case they are termed *extraarticular* osteophytes. A bone specimen and radiograph showing periarticular osteophytes along the medial cranial lip of the proximal phalanx are shown in Figures 5-46 and 5-47.

▮▮▮ SYNOVIOMA (VILLONODULAR SYNOVITIS)

Nickels and co-workers were among the first to describe equine villonodular synovitis.[45] The disease is



Figure 5-37 • Close-up lateral **(A),** lateral oblique **(B),** medial oblique **(C),** and dorsoplantar view of left hind fetlock show the following: (1) a large defect in the flexor margin of the lateral sesamoid, (2) two nearby fracture fragments, (3) cystic enlargement of the vascular channels, and (4) generalized demineralization. These findings are consistent with posttraumatic sesamoiditis.



Figure 5-38 • Close-up **(A)** and ultra-close-up **(B)** views of the medial proximal sesamoid show the following: (1) a pair of chronic-appearing fracture fragments ventrally, (2) enlarged, mildly cystic vascular channels, and (3) mid and distal flexor surface demineralization consistent with posttraumatic sesamoiditis. An ultra-close-up view **(C)** of the underlying phalangeal shaft shows intermediate-duration new bone characteristic of soft-tissue tearing. A dorsopalmar view **(D)** reveals marked deformity of the medial sesamoid combined with patchy bone loss along the outer perimeter. An oblique view **(E)** of the opposite, unaffected sesamoid (printed in a similar orientation) is provided for comparison.

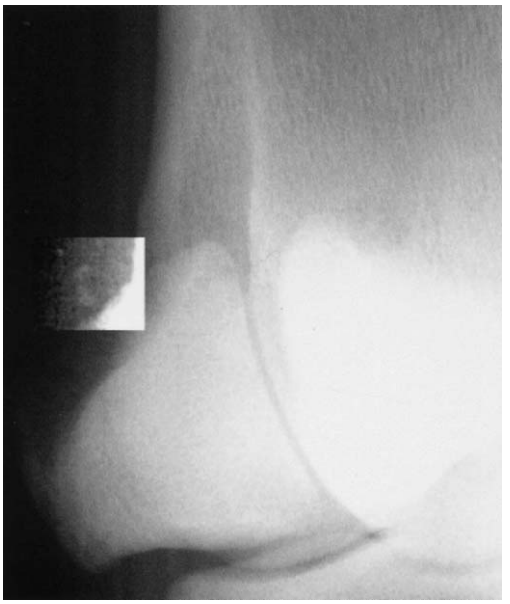


Figure 5-39 • Ultra-close-up medial oblique view of proximal sesamoid bone with nearby dystrophic calcification *(emphasis zone)* presumed to be in or around the medial branch of the suspensory ligament or flexor tendon. Ultrasound indicated that the calcification was in the soft tissue immediately adjacent to the ligament.

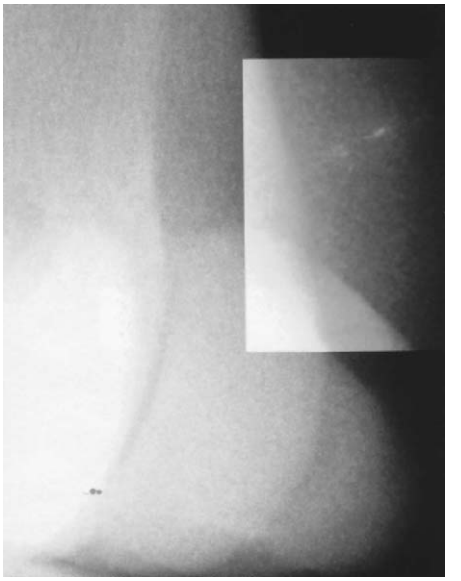


Figure 5-40 • Ultra-close-up lateral oblique view of the fetlock shows presumed dystrophic calcification related to a previous severe sprain of the lateral branch of the suspensory ligament.

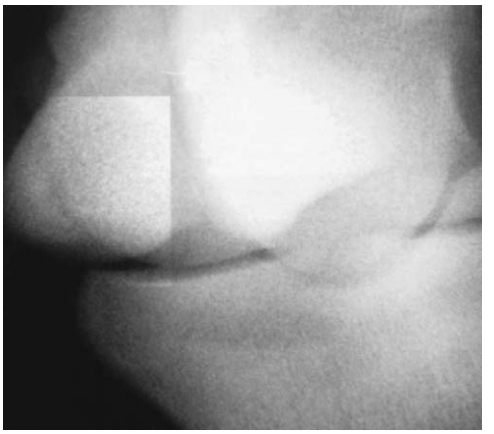


Figure 5-41 • Ultra-close-up lateral oblique view of the fetlock shows false sesamoid fracture caused by the overlap of the lateral proximal sesamoid bone on the outer edge of the underlying metacarpal condyle.



A,B **C**

Figure 5-42 • Close-up dorsopalmar **(A),** lateral **(B),** and medial oblique **(C)** views of the fetlock (deliberately underpenetrated to emphasize soft tissues) show diffuse swelling characteristic of a severe sprain (second or third degree).

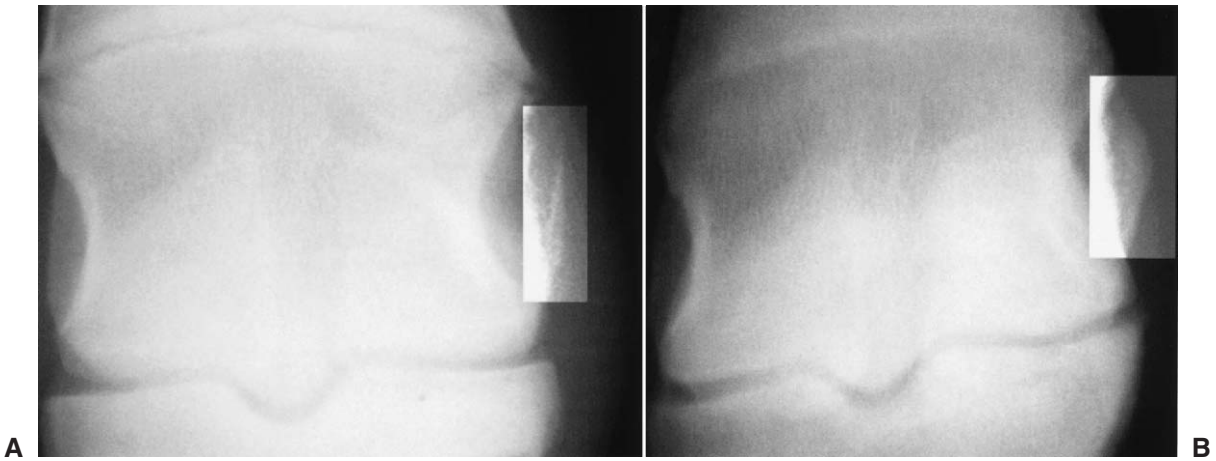


Figure 5-43 • Ultra-close-up dorsopalmar view **(A)** of an acute sprain-fracture of the medial collateral ligament shows a displaced, slender, biconvex fracture fragment lying just off the surface of the medial collateral fossa of the distal third metacarpal bone *(emphasis zone).* Six months later **(B),** a progress film reveals a completely healed fracture *(emphasis zone).*



Figure 5-44 • Close-up dorsopalmar view of the front fetlock, deliberately underexposed to emphasize soft tissues, shows two large bone fragments representing displaced avulsion fractures from the origin and insertion of the medial collateral ligament.

characterized by a discrete mass of synovial tissue located cranially, just beneath the attachment of the joint capsule proximally.

Imaging

Radiographically, there may or may not be bony change. The most characteristic abnormality is a shallow metaphyseal concavity located immediately proximal to the third metacarpal condyle, which is best seen in the lateral projection. This defect may be accompanied by a single large overhanging, or so-called *melting osteophyte*, or alternatively by less organized regional bone deposition (Figures 5-48 and 5-49).

Sonographically, the lesion appears as a medium-sized, circular, oval, or teardrop-shaped mass in the cranioproxial part of the metacarpophalangeal joint, often associated with a thickened joint capsule. Where ultrasound is not available, arthrography (as described later in this chapter) can be used to identify the suspected synovial mass, which typically appears as a radiolucent filling defect in the contrast pool.

▮▮▮ FETLOCK INFECTION

Distal Metacarpal/Metatarsal Growth Plate

Rook and Stickle reported the radiographic appearance of osteomyelitis in the physeal and periphyseal regions of the distal metatarsus of a 3-month-old Holsteiner foal.[46] Two radiographic examinations were performed: one at 3 months, the other at 5 months. Initially the growth plate appeared eccentrically destroyed, creating the illusion of widening. Two months later it was clear that antibiotic treatment had failed, as indicated by a spread of the infection into the metaphysis and distal body, where it had caused further bone destruction, including frank cavitation.

Sesamoids

Puncture wounds are the most common source of fetlock infection. The first radiographic indictor of sepsas is regional soft-tissue swelling that often becomes visible within a day or two after the injury. By comparison, new bone deposition takes far longer to become apparent, often as much as a month. The most common form of sesamoidian involvement is the development of a fringe-like new bone deposit along the flexor margin of one or both sesamoids that may or may not be accompanied by focal or regional osteopenia.

Sedrish and colleagues reported an unusual-appearing sesamoidian infection involving most of the

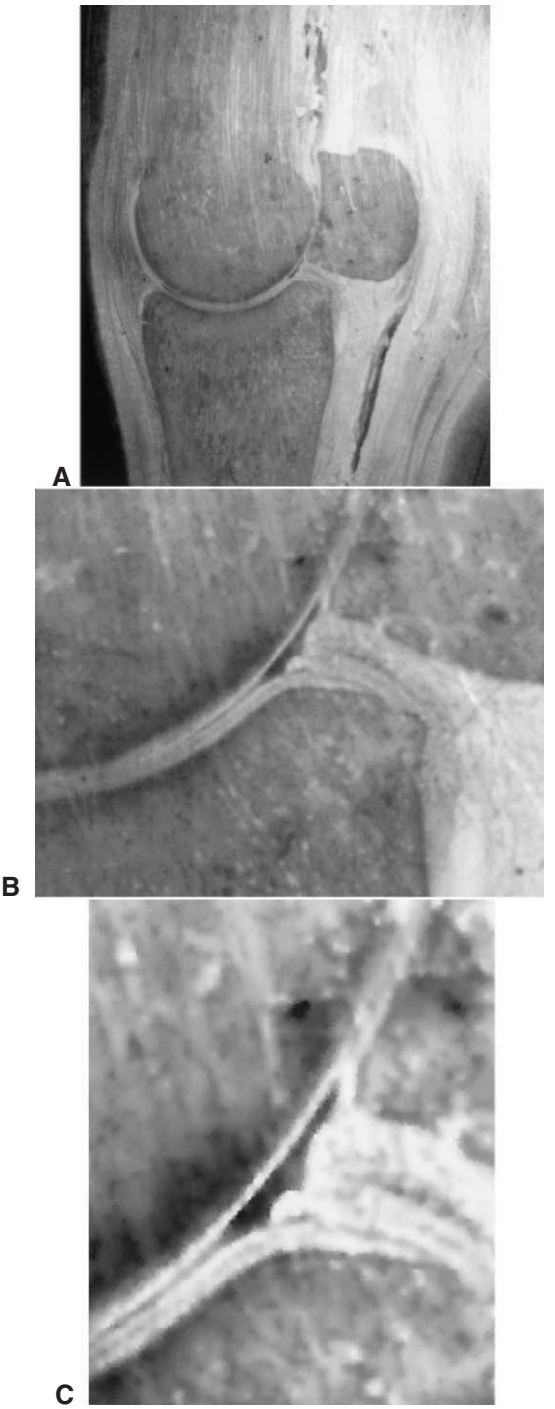


Figure 5-45 • Orientation **(A),** close-up **(B),** and ultra-close-up **(C)** views of an adult equine fetlock (sectioned through the midsagittal plane) show that the so-called joint space is in reality mostly articular cartilage. Accordingly, I prefer to call this area the *cartilage space.*



Figure 5-46 • Proximal phalangeal bone specimen shows loss of medial lip, which has been replaced by three small periarticular osteophytes as a result of a previous racing injury. The bone cracks are the result of postmortem processing.



Figure 5-47 • Radiograph of periarticular osteophyte cranial P1.



Figure 5-48 • Medial oblique **(A)** and close-up medial oblique **(B)** views of the fetlock show chronic-appearing bone deposit on the dorsal surface of the cannon bone just above the condyle *(emphasis zone),* a finding often associated with a long-standing synovioma.

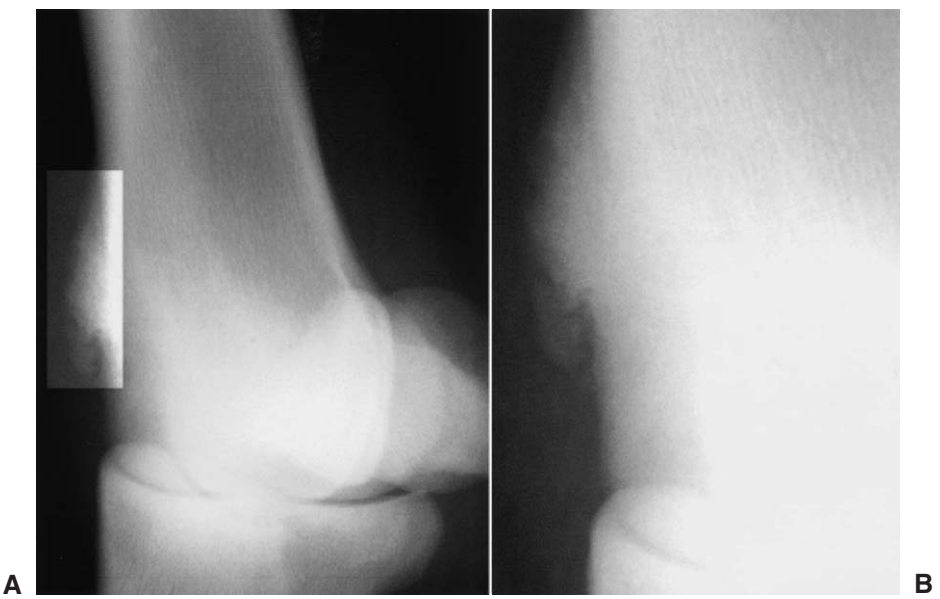
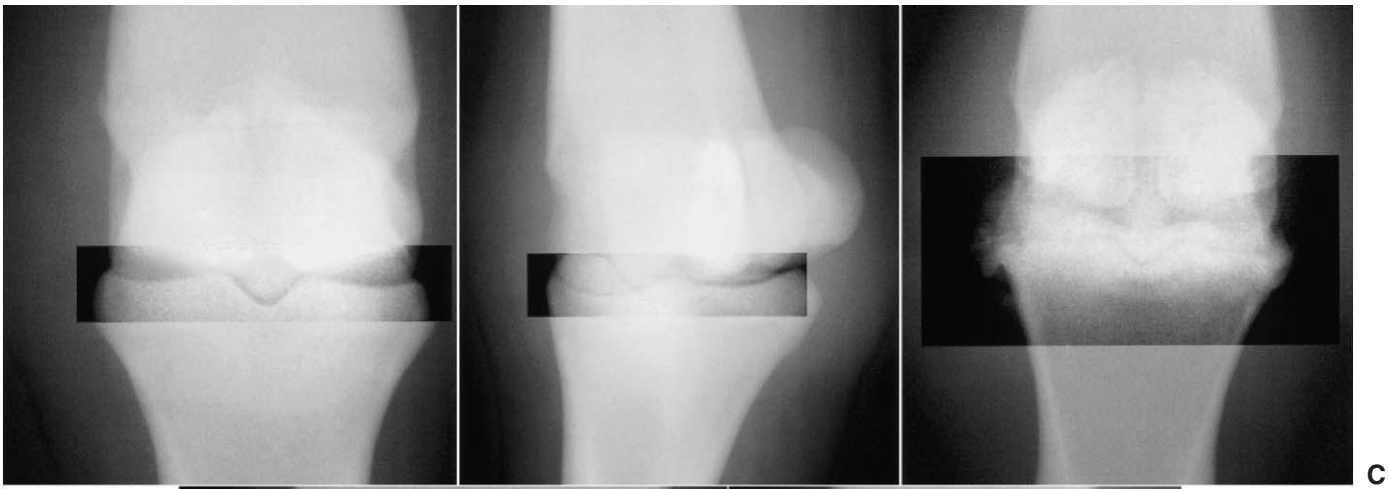


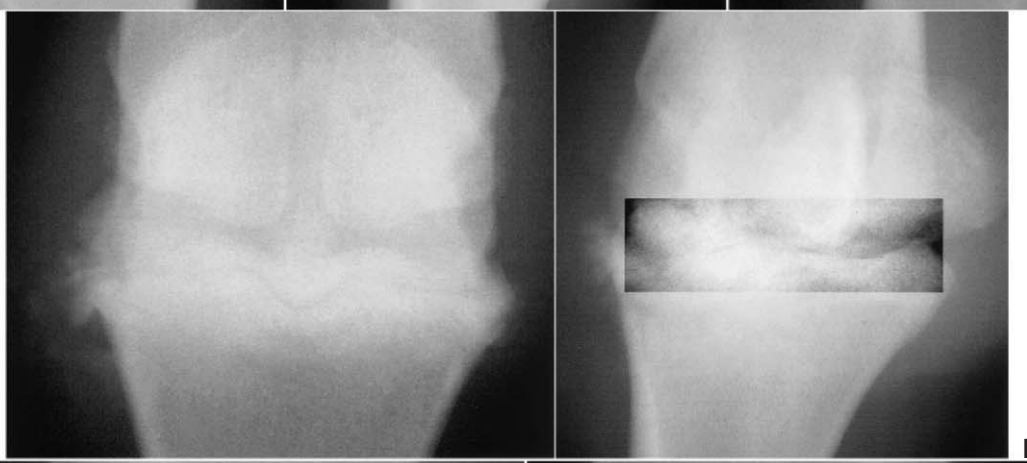
Figure 5-49 • Medial oblique **(A)** and close-up medial oblique **(B)** views of the fetlock show a melting-type new bone deposit on the dorsomedial surface of the third metacarpal bone immediately proximal to the condyle *(emphasis zone),* suggesting a synovioma.

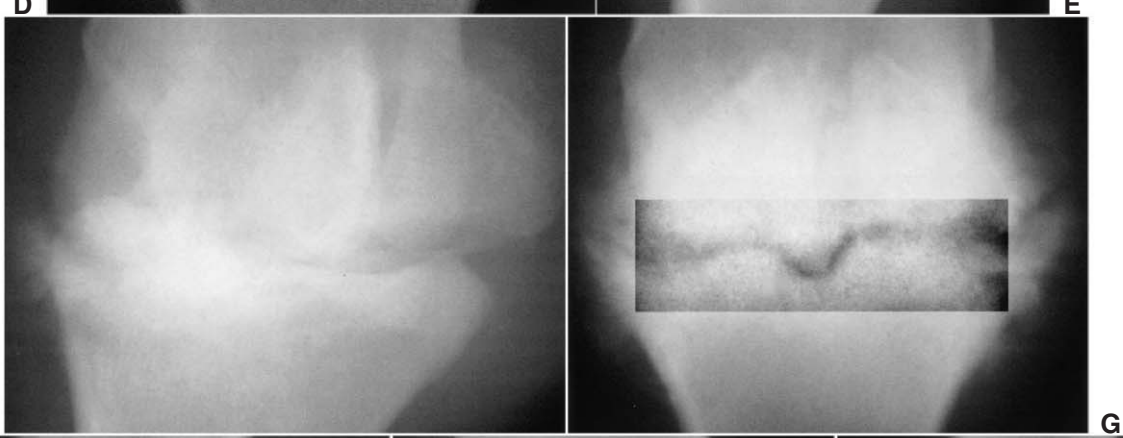
axial surfaces of the proximal sesamoids. Specifically, there was bilateral, axial margin destruction that more closely resembled a tumor than osteomyelitis. Infection of the bone and flexor tendon sheath was presumed, even though fluid from the associated flexor tendon sheath tested negative for bacterial growth; treatment proved ineffective.[47]

P1

The proximal phalanx is, in my experience, usually the first bone in the fetlock to show signs of infection, usually in the form of immature new bone and secondary narrowing of the fetlock joint, sometimes accompanied by narrowing of the pastern and coffin joints (Figures 5-50 and 5-51).


A,B
C


D
E


F
G

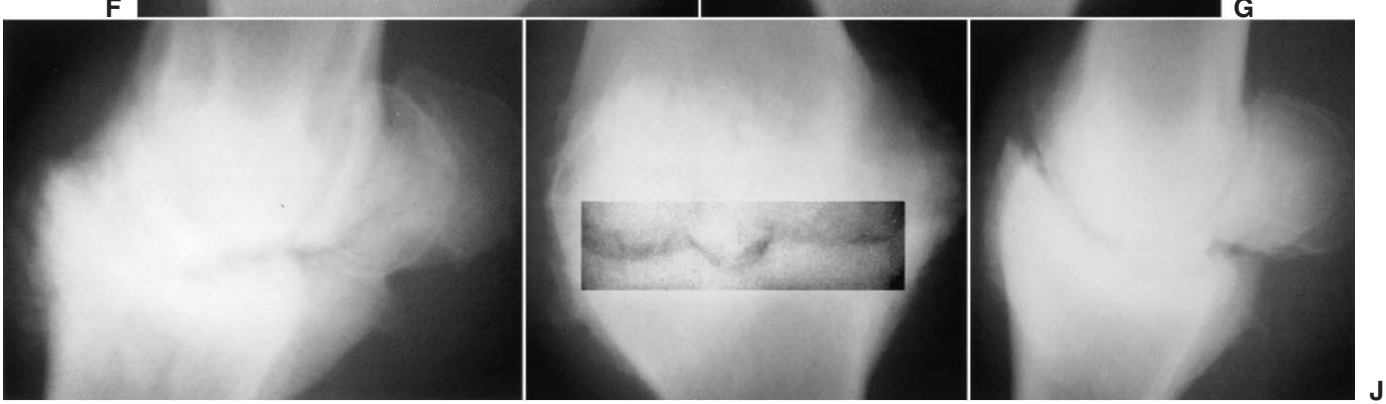

H,I
J



Figure 5-51 • Dorsopalmar oblique **(A),** close-up dorsopalmar oblique, lateral **(C),** and close-up lateral **(D)** views of the fetlock 3 weeks after a deep cut show numerous signs of infection, including the following: (1) immature new bone along much of the lateral and caudal surfaces of P1, (2) recently formed new bone along the lateral and ventral surfaces of the lateral sesamoid, (3) massive regional soft-tissue swelling, and (4) generalized osteopenia.

Figure 5-50 • Chronic fetlock infection. Initial examination: Close-up dorsopalmar **(A)** and medial oblique **(B)** views of the front fetlock of a horse 2 weeks after a deep puncture wound show uniform narrowing of the cartilage space and severe soft-tissue swelling. First progress examination: Two months after the injury, dorsopalmar **(C),** close-up dorsopalmar **(D),** medial oblique **(E),** and close-up medial oblique **(F)** views show the infection taking hold as evidenced by further narrowing of the cartilage space and combined periarticular/extraarticular new bone on either side of the joint. Second progress examination: Six months after the injury, ultra-close-up dorsopalmar **(G)** and medial oblique **(H)** views now show widening of the cartilage space associated with extensive subchondral bone destruction. The previously identified new bone has increased in both amount and coverage. Third progress examination: A year after the injury, the joint surfaces—or what remains of them—appear badly damaged, best appreciated in the ultra-close-up dorsopalmar view **(I).** Continued bone deposition along the joint perimeter gives the fetlock a distinctly bulbous appearance, especially in the lateral projection **(J).**

▮▮▮ ARTHROGRAPHY OF THE FETLOCK JOINT

Swanstrom and Lewis were among the first to describe positive-contrast arthrography of the equine fetlock.[48] Their technique was as follows:

- Three milliliters of diagnostic organic iodine solution was injected into the proximal palmar or plantar sac of the fetlock joint after confirming correct needle placement by aspirating synovial fluid. (I recommend using a nonionic rather than an ionic contrast medium, which will draw less fluid and thus retain its opacity longer.)
- Repeatedly flex and extend the fetlock 15 times. (I gently flex and extend the fetlock about a dozen times over about a minute.)
- Make standard, four-view fetlock series: frontal, lateral, paired obliques, plus supplementary flexed lateral view.

▮▮▮ SWELLING OF THE DIGITAL SHEATH

The front and hind digital flexor tendons are covered by a sheath that extends from the proximal fetlock region to the middle of P2. When the sheath swells, it is usually due to excessive synovial fluid, suggesting tendon injury. Alternatively, swelling combined with a fresh cut or puncture suggests infection.[49] Localized, nonpainful swellings of the digital sheath caused by excessive synovial fluid are called *"wind puffs,"* or *idiopathic tenosynovitis*.[50]

References

1. Rendano VT: Equine radiology—the fetlock, *Mod Vet Pract* 72:871, 1977.
2. Losonsky JM, Kneller SK: Variable locations of nutrient foramina of the proximal phalanx in forelimbs of Standardbreds, *J Am Vet Med Assoc* 193:671, 1988.
3. Martinelli MJ, Kuriashkin IV, et al: Magnetic resonance imaging of the equine fetlock joint: three dimensional reconstruction and anatomic analysis, *Vet Radiol Ultrasound* 38:193, 1997.
4. Cheung TK, Thompson KN: Development of a three-dimensional electronic solids model of the lower forelimb of the horse, *Vet Radiol Ultrasound* 34:331, 1993.
5. Estberg L, Stover SM, et al: Fatal musculoskeletal injuries incurred during racing and training thoroughbreds, *J Am Vet Med Assoc* 208:92, 1996.
6. Estberg L, Stover SM, et al: Relationship between race start characteristics and risk of catastrophic injury in Thoroughbreds: 78 cases (1992), *J Am Vet Med Assoc* 212:544, 1998.
7. Yovich JV, McIlwraith CW: Arthroscopic surgery for osteochondral fractures of the proximal phalanx of the metacarpophalangeal and metatarsophalangeal (fetlock) joints in horses, *J Am Vet Med Assoc* 188:273, 1986.
8. Colon JL, Bramlage LR, et al: Qualitative and quantitative documentation of the racing performance of 461 Thoroughbred racehorses after arthroscopic removal of dorsoproximal first phalanx osteochondral fractures (1986-1995), *Equine Vet J* 32:475, 2000.
9. Raker CW: Calcification of the equine metacarpophalangeal joint following removal of chip fractures, *Vet Surg* 7:66, 1978.
10. Nixon AJ, Pool RR: Histologic appearance of axial osteochondral fragments from the proximoplantar/proximopalmar aspect of the proximal phalanx in horses, *J Am Vet Med Assoc* 207:1076, 1995.
11. Grondahl AM: Incidence and development of united proximoplantar tuberosity of the proximal phalanx in Standardbred trotters, *Vet Radiol Ultrasound* 33:18, 1992.
12. Fortier LA, Foerner JJ, Nixon AJ: Arthroscopic removal of axial osteochondral fragments of the plantar/palmar proximal aspect of the proximal phalanx in horses: 119 cases (1988-1992), *J Am Vet Med Assoc* 206:71, 1995.
13. Foemer JJ, Barclay WP, et al: Osteochondral fragments of the palmar/plantar aspects of the fetlock joint, In *Proc 33rd Am Assoc Equine Pract* 117, 1987.
14. Smallwood JE, Albright SM, et al: A xeroradiographic study of the developing quarterhorse foredigit and metacarpophalangeal region from six to twelve months of age. *Vet Radiol* 31:254, 1990.
15. Ellis DR, Greenwood RES, Crowhurst JS: Observations and management of fractures of the proximal phalanx in young Thoroughbreds, *Equine Vet J* 19:43, 1987.
16. Tetans J, Ross MW, Lloyd JW: Comparison of racing performance before and after treatment of incomplete, midsagittal fractures of the proximal phalanx in Standardbreds: 49 cases (1986-1992), *J Am Vet Med Assoc* 210:82, 1997.
17. Kawcak CE, Bramlage LR, Embertson DE: Diagnosis and management of incomplete fracture of the distal palmar aspect of the third metacarpal bone in five horses, *J Am Vet Med Assoc* 206:335, 1995.
18. Hubert J, Williams J, Moore RM: What is your diagnosis? *J Am Vet Med Assoc* 213:203, 1999.
19. Lindsay WA, Taylor SD, Root CR: What is your diagnosis? *J Am Vet Med Assoc* 178:1090, 1981.
20. Woodie JB, Ruggles AJ, et al: Apical fracture of the proximal sesamoid bone in Standardbred horses: 43 cases (1990-1996), *J Am Vet Med Assoc* 214:1653, 1999.
21. Ellis DR: Fractures of the proximal sesamoid bones in Thoroughbred foals, *Equine Vet J* 11:48, 1979.
22. Thompson KN, Rooney JR: Bipartite proximal sesamoid bones in young Thoroughbred horses, *Vet Radiol Ultrasound* 35:368, 1994.
23. Southwind LL, Trotter GW, McIlwraith CW: Arthroscopic removal of abaxial fracture fragments of the proximal sesamoid bones in horses: 47 cases (1989-1997), *J Am Vet Med Assoc* 213:1016, 1998.
24. Churchill EA. Sesamoid fractures, in *Proc 8th Ann Meeting Am Assoc Equine Pract* 191, 1962.
25. Rooney JR: *Biomechanics of lameness*. Baltimore, 1969, Williams & Wilkins.
26. Fretz PB, Barber SM, et al: Management of proximal sesamoid bone fractures in the horse, *J Am Vet Med Assoc* 185:282, 1984.
27. Hathcock JT: What is your diagnosis? *J Am Vet Med Assoc* 181:1543, 1982.
28. Henninger RW, Bramlage LR, et al: Lag screw and cancellous bone graft fixation of transverse proximal sesamoid bone fractures in horses: 25 cases (1983-1989), *J Am Vet Med Assoc* 199:606, 1991.
29. Pool RR, Meagher DM: Pathologic findings and patho-

genesis of racehorse injuries, *Vet Clin N Am Equine Pract* 6:1, 1990.
30. Burkowieki CF, Bramlage LR, Gabel AA: In vitro strength of the suspensory apparatus in training and resting horses, *Vet Surg* 16:126, 1987.
31. Southwood LL, McIlwraith CW: Arthroscopic removal of fracture fragments involving a portion of the base of the proximal sesamoid bone in horses: 26 cases (1984-1997), *J Am Vet Med Assoc* 217:236, 2000.
32. Ellis DR: Fractures of the proximal sesamoid bones in Thoroughbred foals, *Equine Vet J* 11:48, 1979.
33. Medina L, Morgan JP: Nongrafted and grafted osteotomies of proximal sesamoid bones in the horse, *Vet Radiol* 25:78, 1984.
34. Stover SM, Pool RR, et al: A review of bucked shins and metacarpal stress fractures in Thoroughbred racehorses, In *Proc 34th Annu Am Assoc Equine Pract* 349, 1988.
35. Tapprest J, Audigie F, et al: Magnetic resonance imaging for the diagnosis of stress fractures in a horse, *Vet Radiol Ultra*sound 44:438, 2003.
36. O'Brien TR: Disease of the Thoroughbred fetlock joint—a comparison of radiographic signs with gross pathologic lesions. *Proc Ann Meeting Am Assoc Equine Pract* 369, 1976.
37. Smallwood JE, Kelly EJ: A xeroradiographic study of osteochondrosis in the metacarpophalangeal region of two foals. *Vet Radiol* 27:101, 1986.
38. Schoenborn WC, Hornof WJ: Computed tomographic appearance of osteochondritis dissecans-like lesions of the proximal articular surface of the proximal phalanx in a horse, *Vet Radiol Ultrasound* 43:541, 2002.
39. Hornof WJ, O'Brien TR, Pool RR: Osteochondritis dissecans of the distal metacarpus in the racing Thoroughbred horse, *Vet Radiol* 22:98, 1981.
40. O'Brien TR, Hornof WJ, Meagher DM: Radiographic detection and characterization of palmar lesions in the equine fetlock joint, *J Am Vet Med Assoc* 178:231, 1981.
41. Hornof WJ, O'Brien TR: Radiographic evaluation of the palmar aspect of the equine metacarpal condyles: a new projection, *Vet Radiol* 21:161, 1980.
42. O'Brien TR, Morgan JP, et al: Sesamoiditis in the Thoroughbred: a radiographic study, *Vet Radiol* 12:75, 1971.
43. Poulos P: Radiographic and histologic assessment of proximal sesamoid bone changes in young and working horses, In *Proc Annu Meet Am Assoc Equine Pract* 360, 1988.
44. Hardy J, Marcoux M, Breton L: Clinical relevance of radiographic findings in proximal sesamoid bones of two-year-old Standardbreds in their first year of race training, *J Am Vet Med Assoc* 198:2089, 1991.
45. Nickels FA, Grant BD, Lincoln SD: Villonodular synovitis of the equine metacarpophalangeal joint, *Proc Am Assoc of Equine Pract* 75, 1975.
46. Rook JS, Stickle RL: What is your diagnosis? *J Am Vet Med Assoc* 204:721, 1994.
47. Sedrish S, Burba D, Williams J: Axial sesamoid osteomyelitis in a horse, *Vet Radiol Ultrasound* 37:417, 1996.
48. Swanstrom OG, Lewis RE: Arthrography of the equine fetlock, *Proc Am Assoc Equine Pract* 221, 1969.
49. Honnas CM, Schumacher J, et al: Septic tenosynovitis in horses: 25 cases (1983-1989) *J Am Vet Med Assoc* 199:1616, 1991.
50. Redding R: Ultrasonic imaging of the structures of the digital flexor tendon sheath, *Comp Cont Educ* 13:1824, 1991.

Chapter 6

Metacarpus

THE STANDARD METACARPAL SERIES

A standard metacarpal series consists of four views: a frontal (dorsopalmar), a true lateral, and a pair of obliques (lateral and medial), optimized to profile the lateral and medial splint bones away from the shaft of the cannon bone. It is useful to include portions of the overlying carpus and underlying fetlock for orientation. Combined carpometacarpal or metacarpophalangeal examinations generally produce inferior images because of geometric distortion caused by decentering. The evaluative purpose of each view in the standard metacarpal series is described in Table 6-1. Anatomic specimens are provided for radiographic correlation (Figure 6-1).

CANNON AND SPLINT BONES: AN INTEGRAL UNIT

The central third of the dorsal cortex of the third metacarpal bone is normally twice as thick as that of the palmar cortex (Figure 6-2, *A*). The dorsal cortex also extends farther distally than the palmar cortex (Figure 6-2, *B*). The splint bones, metacarpals 2 and 4, are intimately associated with the cannon bone (third metacarpal bone) in both an anatomic and functional sense. The same might be said of the suspensory ligament and flexor tendons, although to a somewhat lesser extent. Perhaps the most dramatic example of this relationship is the so-called splint, a large callus-like bone deposit, typically situated over the body of the medial splint bone that also incorporates a portion of the adjacent third metacarpal bone and intervening interosseous space (Figure 6-3).

Splint Bone Fractures

Second and fourth metacarpal fractures usually occur in the distal third of the shaft and are typically displaced to some degree. Care must be taken not to mistake the nutrient foramen of the third metacarpal bone for a fractured splint when the two are superimposed in oblique projections (Figure 6-4).

Medial splint (MC2) fractures are most common, but lateral and biaxial injuries (combined medial and lateral splint bone fractures) are reported.[1] Forelimb injuries are more common than those of the hindlimb. Bowman and co-workers reported that 81 percent of Standardbred and 67 percent of Thoroughbred racehorses with distal splint bone fractures also had suspensory desmitis.[2,3] It is uncertain whether the presence of concurrent suspensory disease is causative or coincidental.[4] A variety of splint bone injuries are illustrated in Figures 6-5 to 6-11.

Active Versus Inactive Splint Bone Lesion

Short of showing increased activity in a bone scan, I know of no way to establish with any degree of certainty that a particular lesion is active (as opposed to inactive), although magnetic resonance imaging (MRI) appears promising.[5] It is possible, however, to *infer* from a radiograph that a particular portion of the bone is currently undergoing change. This judgment is based on the appearance of the lesion, in particular its estimated age. This method, which I have described previously, works as follows:

New bone growth (deposition, formation, proliferation), especially that arising from just beneath the periosteum, has a fairly distinctive appearance when viewed in profile, depending on when it was formed or, more simply, its age.

Bone created in the past week or two resembles a freshly sprouted lawn viewed at a ground-level profile: many similar vertically oriented lines separated by small gaps. New bone of intermediate duration, that is, one or two months, has a denser, more filled-in appearance. Mature new bone is much denser, smoother, and more rounded. Hypermature new bone appears very dense with smooth surfaces and may contain one or more defects, usually representing vascular channels.

Table 6–1 • EVALUATIVE PURPOSE OF STANDARD METACARPAL SERIES

View	Evaluative Purpose
Frontal (dorsopalmar)	Good orientation view.
Lateral	Often the best view in which to see a dorsal surface sequestrum, or a palmar surface suspensory avulsion. A callus from a stress fracture is most apt to be detected in this projection.
Medial oblique	• Profiles the medial splint bone (MC II) away from the adjacent cannon bone (MC III). • Best view for seeing medial splint fractures and splint-cannon fusion.
Lateral oblique	• Profiles the lateral splint bone (MC IV) away from the adjacent cannon bone (MC III). • Best view for seeing lateral splint fractures and splint-cannon fusion.

Radiographic Evaluation of Irradiated Splints

Little has been written about the *proven efficacy* of ionizing radiation for the treatment of equine bone disease, such as second and fourth metacarpal or metatarsal fractures.[6] As a result, review articles[7] often cite dated literature, much of which is anecdotal.[8]

Radiographic examples of successful treatment—in the form of preirradiation and postirradiation images—are exceedingly rare, suggesting that radiographic follow-up is unusual. Thus much of the benefit claimed for radiation therapy remains unsubstantiated.

As a trainee, my experience with radiation therapy in horses was largely confined to the postoperative treatment of small metacarpal-metatarsal fractures with cesium-137. Few of these horses were radiographed again after treatment, and accordingly I am unable to say what effect, if any, such treatment may have had on the radiographic appearance of the irradiated bone.

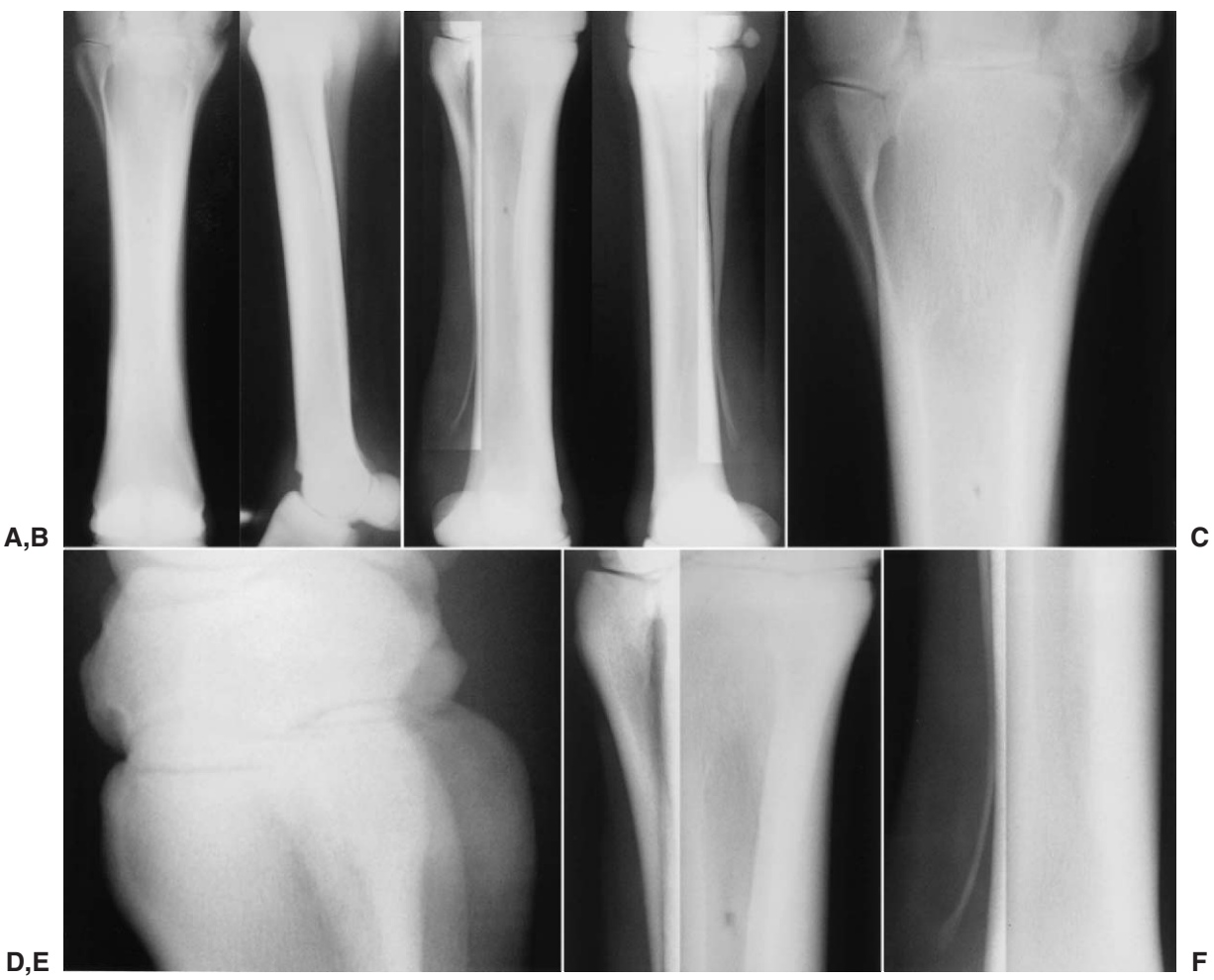


Figure 6-1 • A standard metacarpal series is composed of four views: dorsopalmar and true lateral **(A),** and lateral and medial obliques **(B).** Close-up views including dorsopalmar **(C),** lateral **(D),** proximal and distal fourth metacarpal **(E, F)** are provided for additional detail.

Continued.



Figure 6-1, cont'd • Proximal and distal second metacarpal **(G, H)** are also provided for additional detail. Defleshed metacarpus as seen in dorsal **(I),** palmar **(J),** dorsomedial **(K),** palmarolateral **(L),** and dorsolateral **(M)** views. A close-up view of isolated lateral (left) and medial (right) splint heads is provided to better appreciate differences in size and shape **(N).**



Figure 6-2 • Third metacarpal bone sectioned longitudinally through the midsagittal plane shows that centrally, the thickness of the dorsal cortex is approximately twice that of the palmar cortex **(A).** The dorsal cortex also extends further distally than its palmar counterpart **(B).**

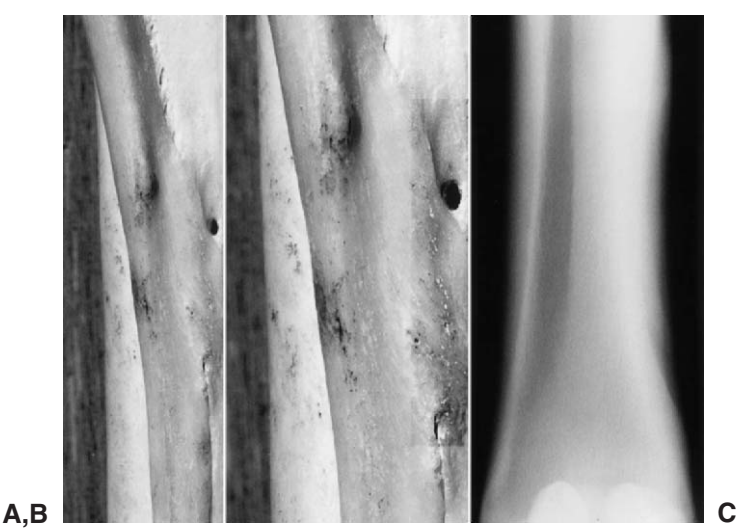


Figure 6-3 • Close-up **(A)** and ultra-close-up **(B)** views of a defleshed metacarpus show fusion of the central portion of the second metacarpal bone to the adjacent surface of the third. Dorsopalmar radiograph **(C)** shows an old medial splint appearing as a focal convexity located on the upper medial surface of the cannon bone *(top right).*



Figure 6-4 • Central metacarpal region seen in the medial oblique projection shows an *apparent fracture* of the interior splint bone, which in reality is the superimposed nutrient foramen of the cannon bone.



Figure 6-6 • A lateral oblique view of a large, irregular callus enveloping a proximally situated body fracture of the fourth metacarpal bone. The injury is about two months old, a fact reflected in the mature appearance of the fracture callus.



Figure 6-5 • Medial oblique view of the carpus and proximal metacarpus of a horse with an unusual, conical bone deposit just below the head of its medial splint bone. The outer edge of the overlying cartilage space is abnormally flared, suggesting bone loss. To the best of my knowledge, the precise cause or causes of this splint-like lesion isn't known, but the prevailing belief is that it is probably the result of injury. A colleague refers to this appearance as *carpometacarpal "spavin."*

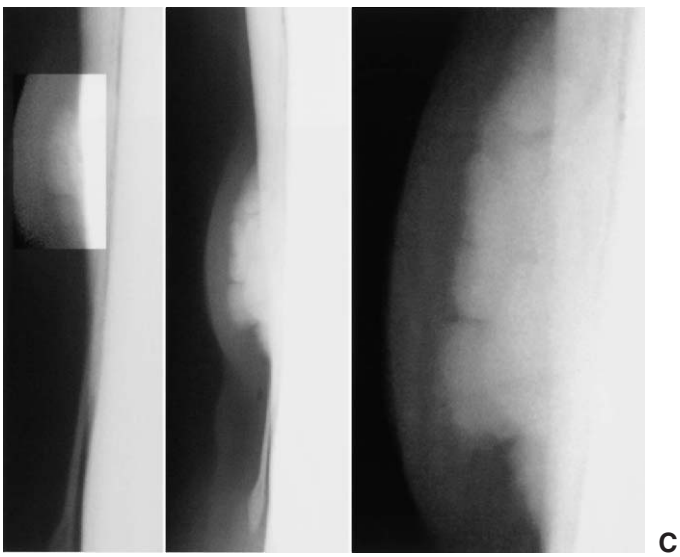


Figure 6-7 • Close-up medial oblique views of two non-displaced splint fractures: the first **(A)** is estimated to be about 10 days old, the second **(B, C)** is about five weeks old. The horizontal gaps in the callus of the older injury are for blood vessels.

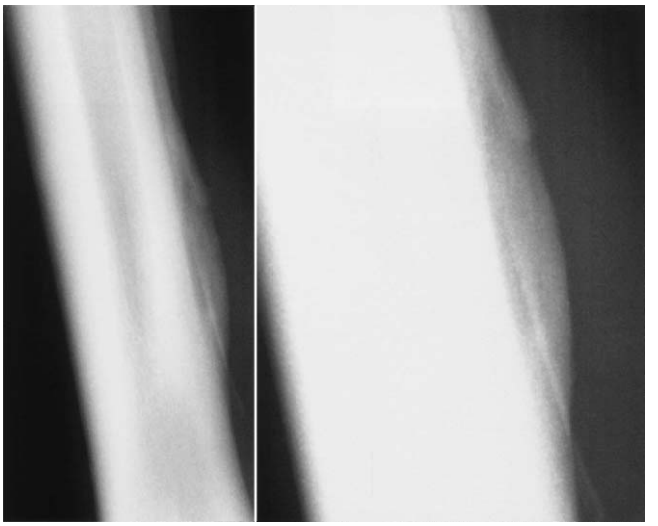


Figure 6-8 • Close-up **(A)** and ultra-close-up **(B)** views of a three-month-old displaced medial splint fracture show that the fragment ends have been fixed and enveloped by a mature callus, but not joined.

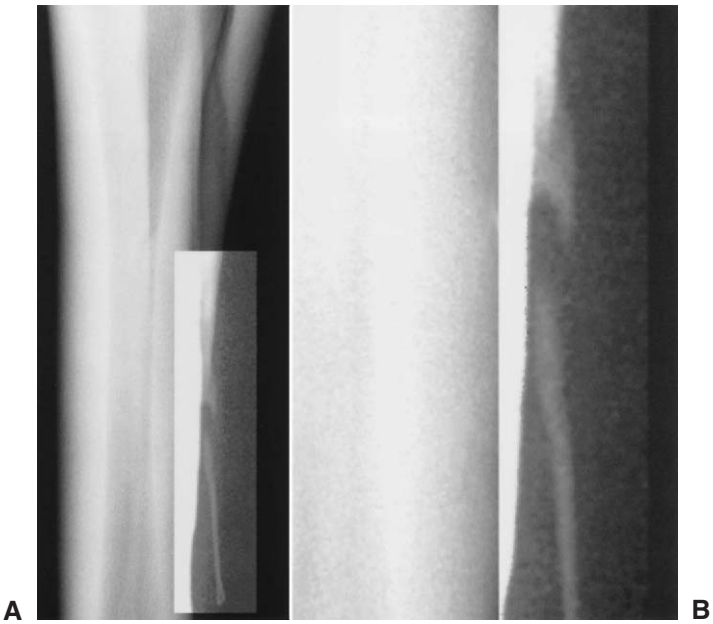


Figure 6-10 • Medial oblique **(A)** and close-up **(B)** views of a two-month-old delayed union involving the midbody of the medial splint. The flared, conforming appearance of the proximal fragment, combined with a large fracture gap, suggests the injury may go on to become a nonunion.



Figure 6-9 • Close-up view of a malunion fracture of the medial "button."

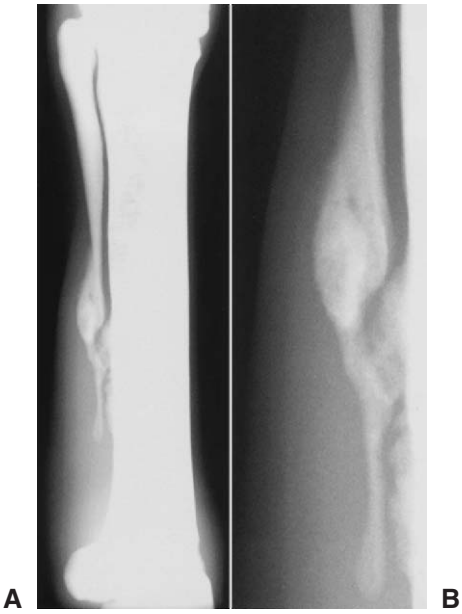


Figure 6-11 • Orientation lateral oblique **(A)** and close-up **(B)** views of the lateral splint bone show an old malunion fracture.

▮▮▮ CANNON BONE (THIRD METACARPAL) FRACTURES

Growth Plate Fractures

Foals often fracture their third metacarpal bones through the distal growth plate, breaking away the epiphysis along with a corner of the metaphysis (Salter-Harris type II fracture). Similar injuries occur to the distal metatarsal physis.

Proximal Palmar Stress Fracture and Proximal Palmar "Stress Reaction"

Pleasant and co-workers reported using a combination of radiography and scintigraphy to diagnose proximal metacarpal injuries in 58 horses (mostly Standardbreds) exhibiting subtle forelimb lameness.[9] In some instances a hairline fracture was detected in the proximal metacarpus, whereas in others a localized new bone deposit was identified. The authors termed the

latter a *stress reaction*, presumably because it resembled bucked shins.

Ross and Martin described the xeroradiographic appearance of proximal articular fractures in the head of the cannon bone in seven Standardbred racehorses.[10] The minimally displaced fractures were located in the dorsomedial aspect of the proximal part of the third metacarpal bone where they entered the carpometacarpal joint. Nearby bone deposition indicated that the fractures were at least a few days old. As might be expected, the fracture was best seen in the medial oblique projection.

Incomplete Dorsal Metacarpal Stress Fracture and Bucked Shins (Dorsal Metacarpal Disease, Complex, or Syndrome)

Incomplete dorsal metacarpal stress fractures, common in 3-year-old Thoroughbred and Standardbred racehorses, are generally believed to be the result of overuse, the legacy of running too hard, too fast, and too often as 2-year olds.[11,12] A less serious but often sufficiently debilitating injury that it significantly interferes with training and racing is a localized new bone deposit on the mid or distal face of the front cannon bone, referred to as *bucked shins.* This is a ubiquitous problem in the United States, estimated to affect up to 70% of 2-year-old racing Thoroughbreds.

Both bucked shins and their more severe counterpart, metacarpal stress fracture, presumably have the same cause: repetitive stress or overuse. The prevailing hypothesis holds that bucked shins are the periosteal expression of many small injuries to the underlying third metacarpal bone (termed *microfractures*, a term of some considerable explanatory convenience), which may eventually culminate in an overt fracture.[13]

▮▮▮ IMAGING FINDINGS

In a medium-sized series of lame horses in which both radiography and bone scintigraphy were performed, radiography proved as good or better than scintigraphy in identifying incomplete dorsal metacarpal fractures. However, the opposite was true in the case of bucked shins.[14]

Fresh metacarpal stress fractures typically appear as partial-thickness "cuts" in the central third of the dorsal cortex (Figure 6-12). As time passes, the fracture line disappears and is replaced by a small callus.

Complete Metacarpal Fracture Masquerading as Stress Fracture

Full-length, spiral metacarpal fractures initially can appear as faint longitudinal lucencies confined to the central part of the proximal diaphysis, resembling a stress fracture. A 2-week progress film typically shows the fracture more clearing, eliminating any doubt as to the source of the horse's lameness. Later radiographic examination, especially if lameness is persistent, may reveal a full-length spiral fracture (Figure 6-12).

Complete Third Metacarpal Fractures

A variety of complete third metacarpal fractures have been reported: transverse, short and long oblique, comminuted, and spiral. A high percentage of the latter are open and thus potentially infected with *Escherichia coli, Pseudomonas, Proteus, Enterobacter, Streptococcus,* hemolytic *Staphylococcus, Actinomyces pyogenes,* and others.[15]

Severely comminuted fractures of the third metacarpal and metatarsal bones are usually repaired with two long bone plates positioned at 90 degrees to one another. Where fractures extend well into the proximal shaft, the plates may be secured in part to the distal portion of the carpus or tarsus. The use of paired plates allows each to protect the other in the bending mode. Associated defects are partially filled with cancellous bone grafts to encourage vascularity.[16]

Associated Arterial Injury and Collateral Circulation

Scott and co-workers reported that otherwise healthy horses that had their medial palmar and medial palmar digital arteries ligated were able to recruit a sufficient number of collateral vessels that circulation to the distal part of the limb was maintained.[17] In this same regard, it is worthwhile determining whether a metacarpal fracture passes through the nutrient foramen, for if it does the injury is likely to heal more slowly.

Metacarpal Fracture Healing

Like most fractures involving the larger long bones of a horse, healing is most dependent on the severity and location of the injury, associated soft-tissue damage, particularly its blood supply, and the skill of the operator (assuming surgery is performed). Once completed, the surgical outcome depends primarily on the maintenance of stability and the prevention of infection. Figures 6-13 to 6-15 illustrate a variety of metacarpal fractures and the manner in which they heal.

▮▮▮ TRAUMATIC METACARPAL EXOSTOSIS

Deep wounds to the dorsal metacarpus often extend to the surface of the underlying cannon bone leaving a *bone scar* or traumatic exostosis, which may become quite large, leaving a plainly visible blemish (Figures 6-16 and 6-17). Potentially, surface deformities of this sort may directly or indirectly affect the overlying tendons. For example, an exostosis may abrade the surface of an adjacent tendon or its sheath, leading to localized hyperemia, filling, or adhesion. A large bone deposit usually results in some degree of

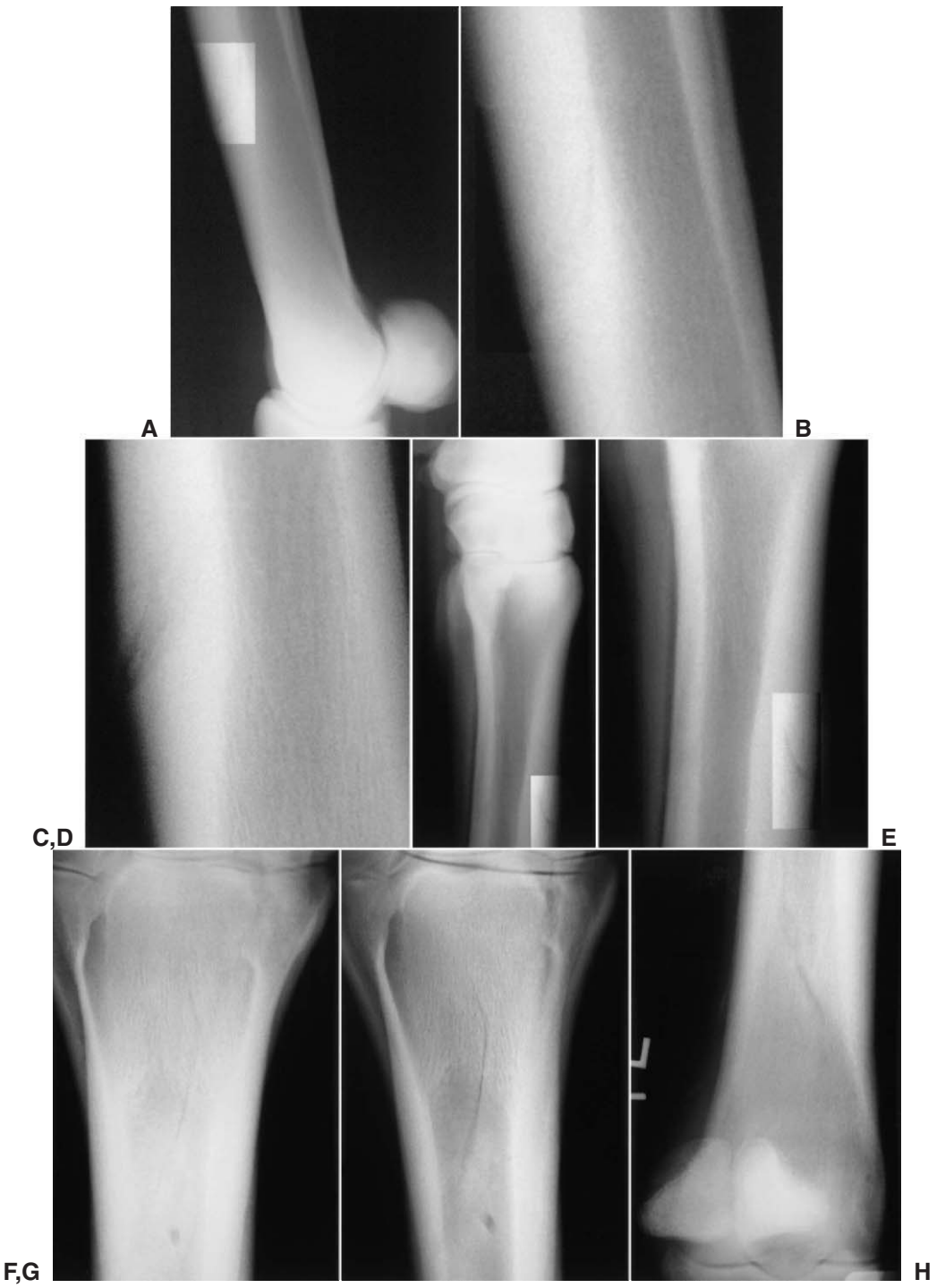


Figure 6-12 • Lateral **(A),** ultra-close-up lateral **(B),** and ultra-close-up medial oblique **(C)** views of a fresh third metacarpal stress fracture appearing here as a cut-type break in the central third of the dorsal cortex. Lateral **(D)** and close-up lateral **(E)** views of the central metacarpus in a second horse show a similar stress-type fracture. Close-up dorsopalmar view **(F)** of an acutely lame Thoroughbred shows a vague, vertically oriented lucency in the center of the proximal metacarpal body initially diagnosed as an incomplete stress fracture. Two weeks later the break has become more visible due to removal of necrotic bone along the fracture edges **(G).** One month following the original injury, progress films show that the fracture actually extends distally, all the way to the fetlock joint **(H).**



Figure 6-13 • Dorsopalmar **(A)** and close-up lateral **(B)** views of a compound, severely comminuted proximal metacarpal fracture involving all of the metacarpal bones. Similar views **(C, D)** made eight weeks later, following external stabilization, reveal incomplete healing. Four months later, although the proximal metatarsus remains badly disfigured **(E, F),** there is now sufficient callus to begin more vigorous rehabilitation. Emphasis zones are to better see peripheral, and thus overexposed, areas of the films.



Figure 6-14 • Two badly fractured legs: Dorsopalmar **(A)** and dorsopalmar close-up **(B)** views of a badly fractured metacarpus (within a cast) show severe comminution and displacement of the central portions of all metacarpal bones. A large fissure extends deeply into the distal fragment, exiting the medial cortex just above the growth plate. Medial oblique **(C)** and close-up medial oblique **(D)** views of a second severely comminuted metacarpal fracture show extreme angular displacement centrally, and a spoon-shaped fissure line proximally that extends into the carpometacarpal joint.

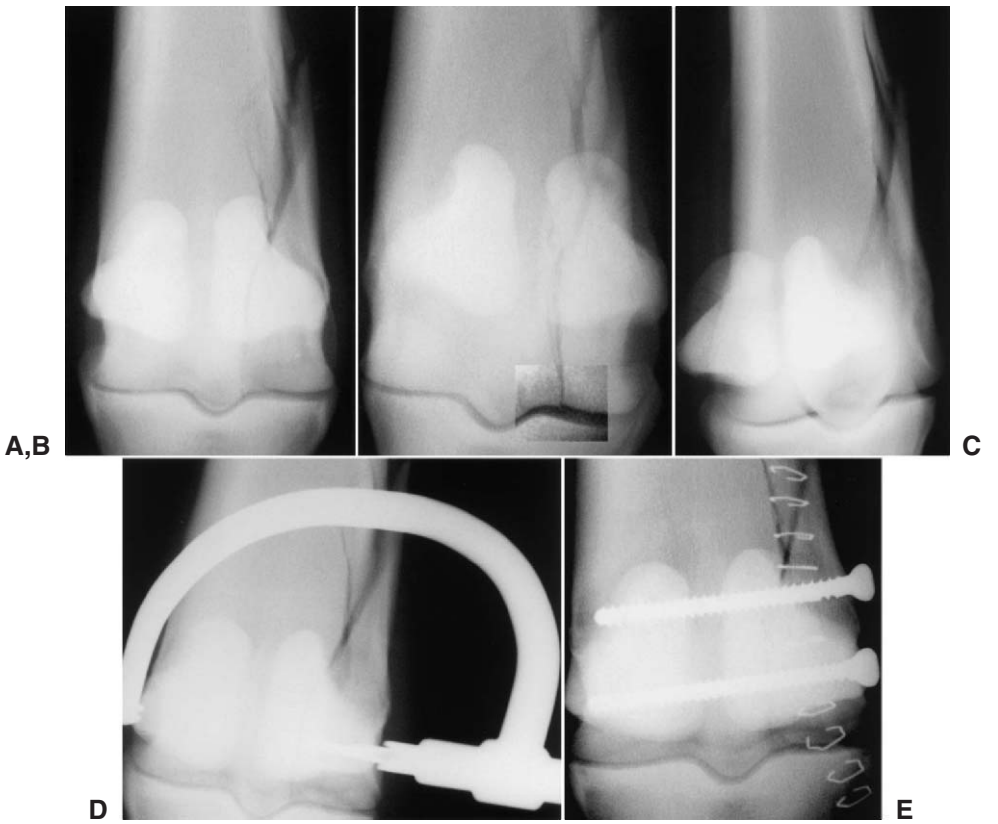


Figure 6-15 • Dorsopalmar **(A),** 15-degree lateral oblique **(B),** and 30-degree medial oblique **(C)** projections of a displaced, long parasagittal articular fracture of the distal third metacarpal bone. Each view reveals something about the fracture not appreciable in the other. For example, only the 15-degree lateral oblique shows unequivocally that the fracture enters the fetlock joint *(emphasis zone)*. For this reason, I often customize the radiographic examination of distal metacarpal fractures, depending on what the initial image shows, and what it is that I suspect. An intraoperative dorsopalmar view **(D)** shows the fracture being clamped just above the fetlock joint, while an immediate postoperative view made in the same plane shows full restoration of the distal articular surface of MC3 **(E).**

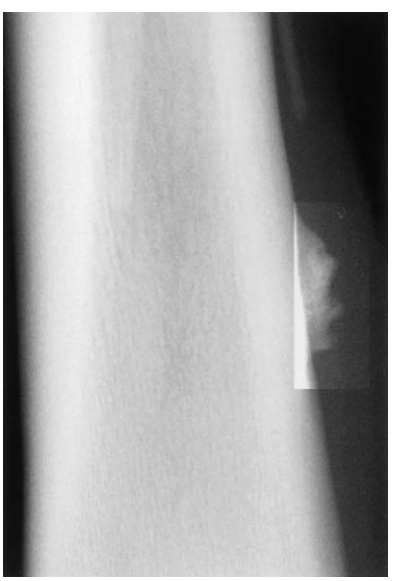


Figure 6-16 • Close-up lateral oblique view of the cannon bone immediately distal to the button of the lateral splint shows a medium-sized bone deposit *(emphasis zone)*, the result of a wire cut sustained a year earlier. Prior to being radiographed, the horse was diagnosed as having a "splint," with elimination of lameness following local anesthesia. Ultrasound (not shown) revealed severe fibrotic thickening of the lateral branch of the suspensory ligament with extensive adhesions.

displacement, which, if pronounced, causes tendon malalignment, stretching, and pain, at least until the tendon and associated muscle can adapt.

▮▮▮ METACARPAL WOUNDS

Swelling and Tissue Defects

Metacarpal wounds are typically associated with swelling that can usually be appreciated radiographically. Deep or lengthy wounds usually result in visible soft-tissue defects that are occasionally accompanied by gas pockets.

Gas Pockets

Gas pockets herald infection, in most instances the result of atmospheric contamination rather than the metabolic by-product of bacteria. Deep punctures seal almost immediately, leaving skin bacteria in their wake. Without drainage, and in the absence of effective medical treatment, such inoculants usually cause abscess to form.

Radiographically, abscesses cannot be differentiated from severe bruising, hematoma, edema, or cellulitis. The presence of one or more fluid levels, as illustrated

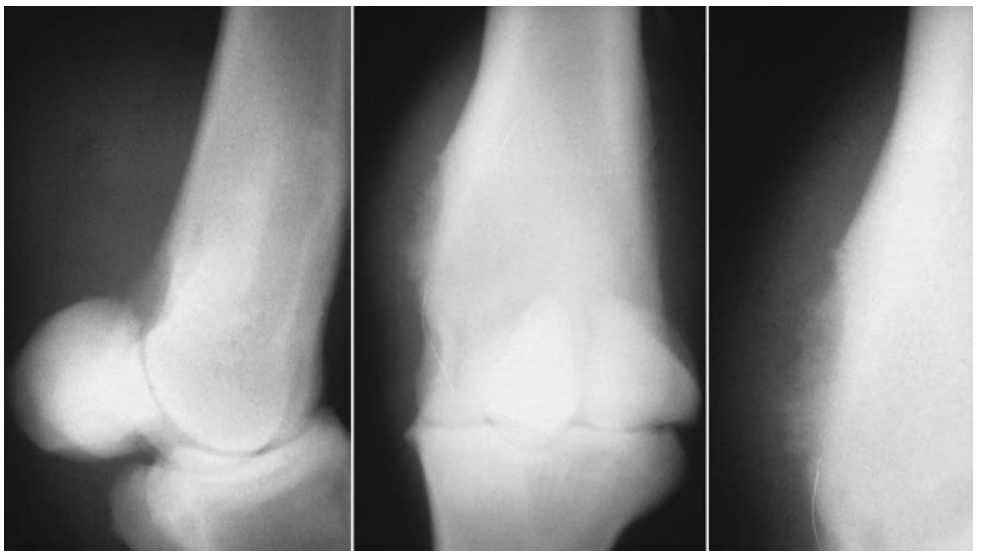


Figure 6-17 • Lateral **(A),** lateral oblique **(B),** and close-up lateral oblique **(C)** views of the distal metacarpus show a large ragged exostosis just above the collateral fossa of the cannon bone, the result of an infected wire cut sustained six months earlier. However, the associated soft tissue swelling, not the bone deposit, proved to be the source of the pain and resultant lameness.

in Figure 6-18, is strongly suggestive of infection, however, and warrants sonographic investigation.

Periosteal New Bone

Periosteal new bone associated with metacarpal wounds usually forms for one or more of the following reasons: (1) direct periosteal injury or its blood supply, (2) compressive obstruction of the periosteal blood supply by adjacent soft tissue related to injury or inflammation, and (3) vascular thrombosis. In a word, the trigger to the formation of new bone is primary or secondary *devascularization*.

Also of vital radiographic importance is the question of when to expect the appearance of new bone after a metacarpal injury. In this regard the following generalizations can be made:

- Periosteal new bone formation will usually become apparent within 2 weeks after an injury.
- Foals and yearlings will reveal new bone formation before adults do, sometimes within a week or less.
- Because of its coating by articular cartilage, the metacarpal condyle may not show new bone for a month or longer, although the collateral fossa and flexor surface of the nearby proximal sesamoids may show new bone much sooner, depending on the nature and extent of the stimulus.

Wound Drainage

New bone deposition underlying a recent metacarpal wound is usually the result of injury, infection, or both. When a continuously or intermittently draining sinus is also present, infection, sequestration, or foreign body is usually responsible.

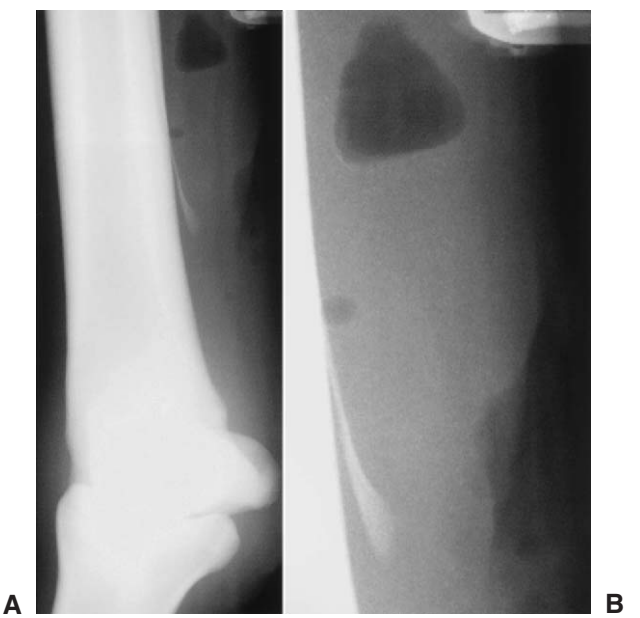


Figure 6-18 • Medial oblique **(A)** and close-up medial oblique **(B)** views of the metacarpus show proximal swelling, containing a large triangular gas pocket and fluid level. A smaller gas pocket is located distally, adjacent to the surface of MC3.

Both sinography and sonography are logical next steps in the diagnostic pursuit of a drainage source; however, there is no consensus as to which procedure is best. I prefer sinography, provided the desired field can be adequately imaged in at least one plane, and preferably two. My reasons for preferring sinography to ultrasound are that sinograms usually provide a more complete view of the drainage source—foreign body, sequestrum, or infective new bone—in addition

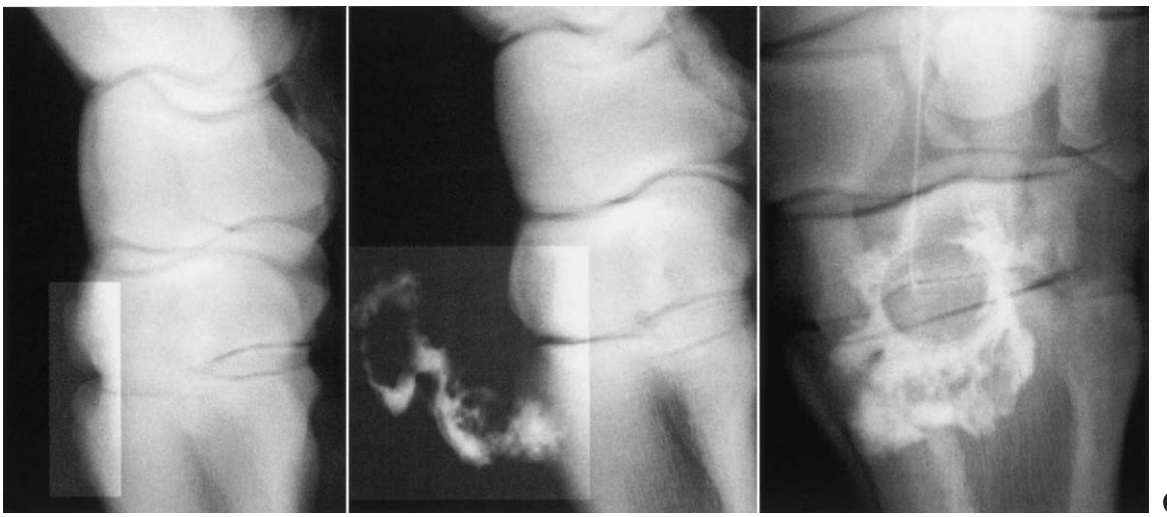


Figure 6-19 • Close-up medial oblique view **(A)** of the carpometacarpal joint shows an immature new bone deposit, the result of a deep puncture wound incurred two months earlier *(emphasis zone).* Close-up medial oblique sinogram **(B)** shows contrast solution initially outlining a large filling defect—a pocket of pus—and continuing into the deeper tissue, eventually entering a small infective alcove on the surface of the adjacent third metacarpal bone *(emphasis zone).* A dorsopalmar oblique sinogram **(C)** shows the inflated catheter cuff (large circular lucency) superimposed on the underlying contrast solution, which in turn is superimposed on the carpometacarpal joint *(emphasis zone).*

to a clearer picture of the associated drainage channels, which in some instances may be quite complex (Figure 6-19).

▮▮▮ DISTINGUISHING OSTEOMYELITIS FROM PERIOSTITIS SECONDARY TO SOFT-TISSUE INFECTION

Chronic cellulitis may give rise to periostitis resembling osteomyelitis.[18] The periosteal reaction secondary to local soft-tissue hyperemia, infection, or edema tends to be of varying thickness, irregular in outline, patchily distributed, and frequently discontinuous. Perhaps most important is that there is no evidence of associated bone destruction.

Physeal Infection

Distal metacarpal growth plate infection is usually caused by septicemia, frequently the result of an earlier umbilical infection. Radiographically, and as exemplified in Figures 6-20 and 6-21, the following are characteristics of a distal metacarpal physeal infection:

- Patchy metaphyseal bone loss, which early on, can be quite subtle
- Follow-on bone destruction along the epiphyseal side of the growth plate
- Progressive, illusionary widening of the physis, which actually represents further paraphyseal bone destruction
- Peripheral or centrally located metaphyseal sequestra, the latter often having a distinctive cone shape
- Circumferential new bone deposition, sometimes appearing to incorporate previously identified sequestra

▮▮▮ SEQUESTRATION

Most MC3 sequestra involve the outer third of the cortex and are associated with a deep overlying wound; some have classic involucra, but most do not.[19] Guffy characterized the radiologic development of metacarpal/metatarsal sequestra as follows:[20]

- Infection introduced through skin wound
- Soft-tissue swelling
- Periosteal reaction
- Bone necrosis (secondary to devascularization)
- Fragment of dead bone that detaches from parent bone, creating sequestrum

Most metacarpal and metatarsal sequestra result from wounds, with the cannon bone being affected more often than either splint bone. The earliest radiographic indicator of pending sequestration is a subtle loss in subperiosteal bone density, which in many instances is appreciable only by comparing the suspect bone with its counterpart in the opposite limb (Figure 6-22). Some sequestra are almost completely cocooned by new bone, whereas others remain fully exposed (Figures 6-23 and 6-24). Although single sequestra are generally the rule, multiple sequestra also occur (Figure 6-25).

The single most important consideration in the radiographic detection of sequestra is beam angle. A

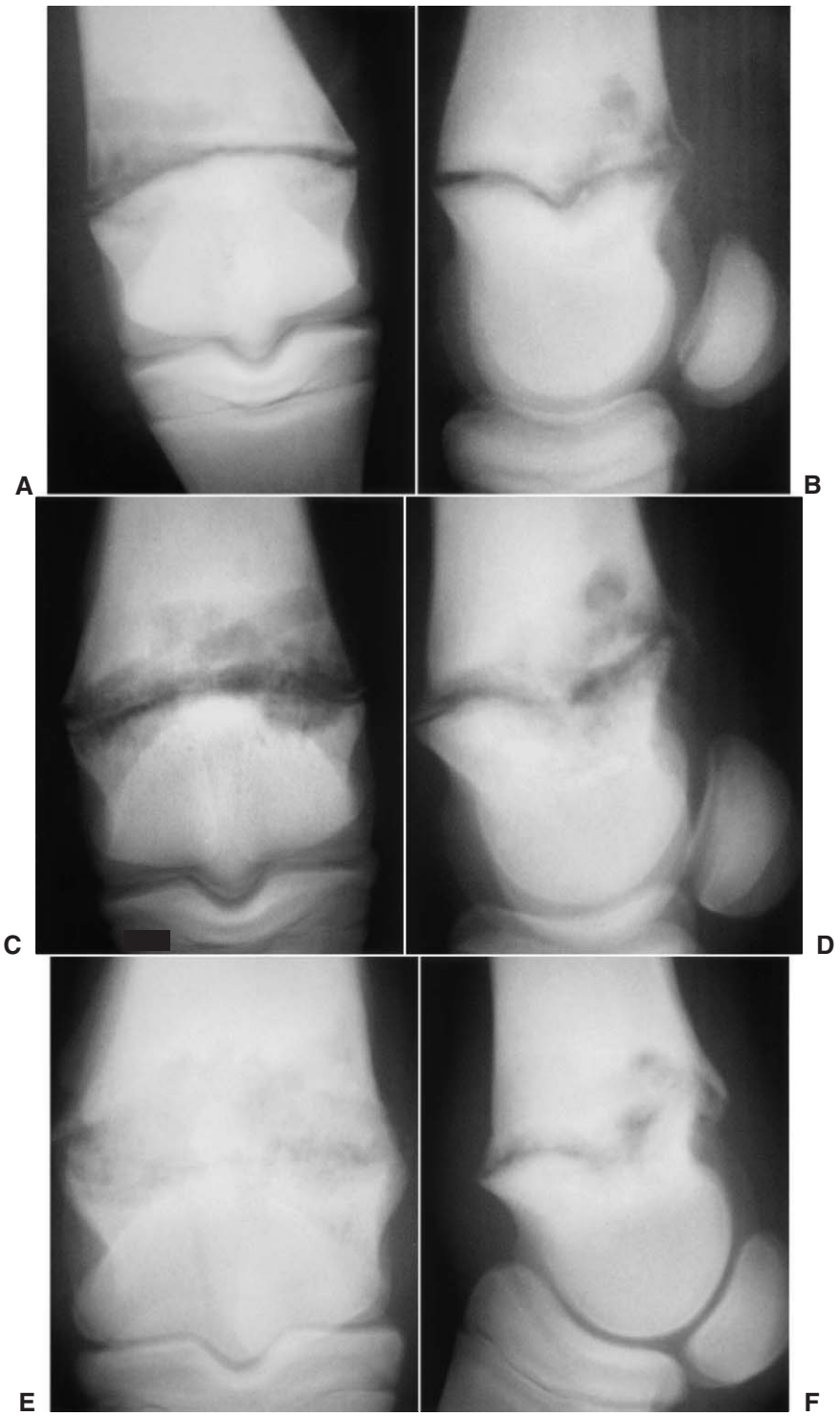


Figure 6-20 • Close-up dorsopalmar **(A)** and lateral **(B)** views of an infected distal third metacarpal bone in a foal, the result of an earlier umbilical infection. Typical of this sort of osteomyelitis, the metaphyseal side of the growth plate is beginning to disintegrate, in the process creating the illusion of a widened growth plate. Small linear sequestra are beginning to appear laterally and caudally. Progress views **(C, D)** made two weeks later after treating with antibiotics show much more extensive bone damage, involving both the metaphysis and epiphysis. Two-month progress check **(E, F)** following a change in antibiotics shows evidence of healing (albeit with considerable deformity), in the form of callus-like new bone and partial disappearance of the growth plate.

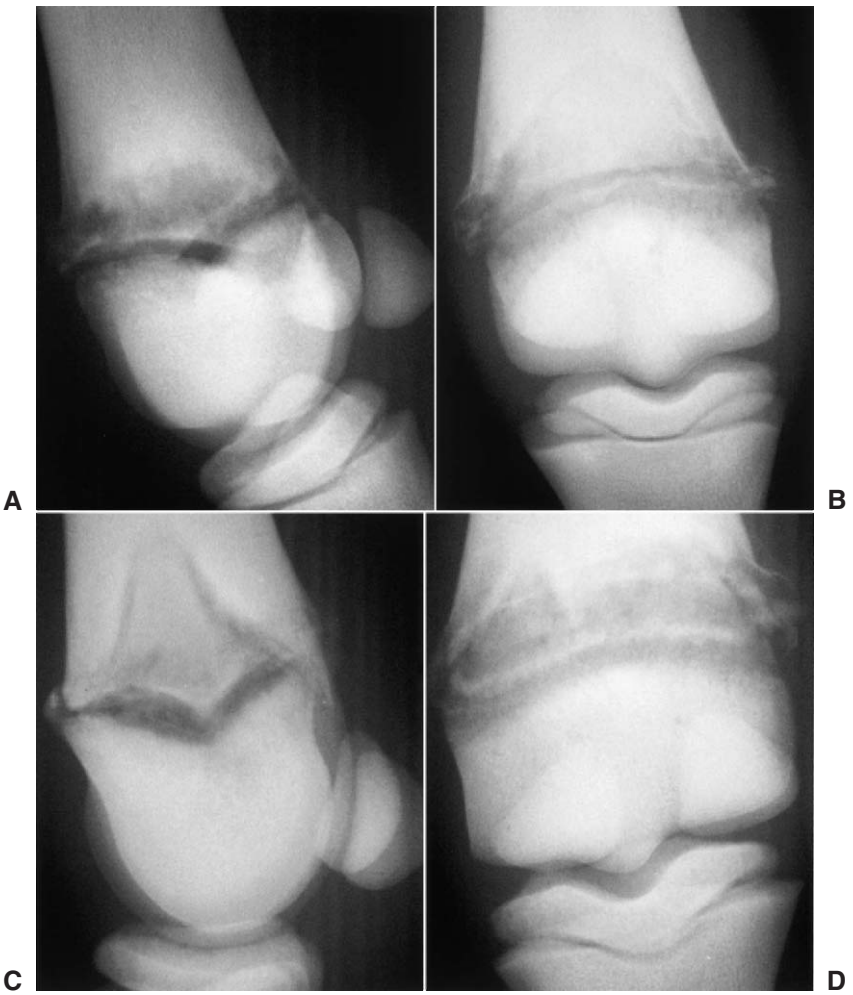


Figure 6-21 • Close-up lateral **(A)** and dorsopalmar **(B)** views of an infected distal third metacarpal bone show transphyseal bone destruction accompanied by numerous small, peripheral sequestra. A one-month progress examination **(C, D)** shows a newly developed, very large cone-shaped sequestrum in the central metaphysis.



Figure 6-22 • Side-by-side comparison: Sequestration of the outer third of the dorsal aspect of the third metacarpal bone is typically preceded by a distinctive density loss *(right, emphasis zone)*, compared with the same area in the opposite MC3 *(left)*.

sequestrum projected from side to side, where it is usually thickest, is most likely to be radiographically visible, whereas those projected head-on or at an angle are not. The visibility of sequestra is also dependent on a number of other factors, including size, shape, and location (Figure 6-26). The degree of fragment separation and the presence of a large involucrum also influence the detectability of sequestra. Involucra are not always evenly marginated, sometimes to the extent that a relatively high edge mimics a sequestrum in one particular view, even though there is none (Figure 6-27).

▮▮▮ CARPAL SPAVIN

The cause of "carpal spavin," a severely debilitating disease of the head of the medial splint, overlying second carpal bone, and associated carpometacarpal joint, is not known. The name *carpal spavin* is derived from its radiographic resemblance to a similarly appearing disease affecting the hocks of horses.

Radiographically, three distinctive features characterize the disease: (1) an elaborate feathered or

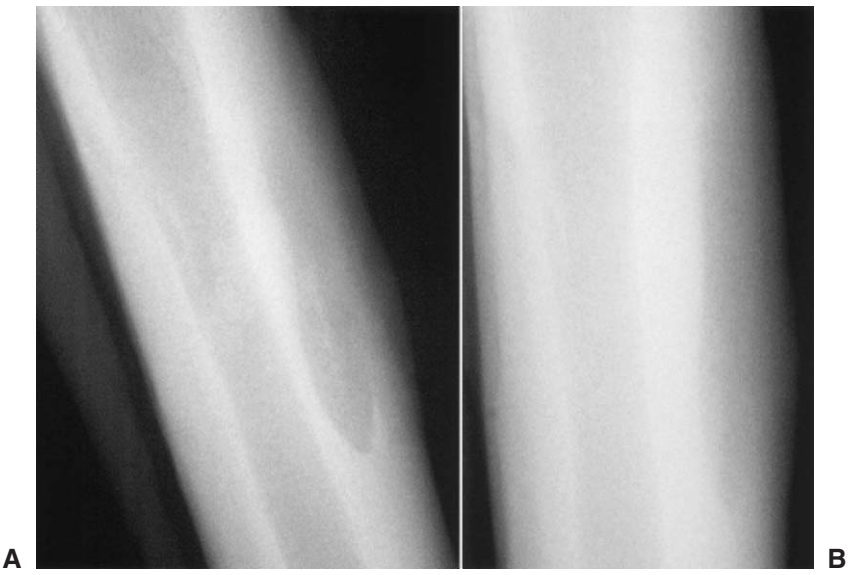


Figure 6-23 • Close-up view of the midbody of MC3 **(A)** shows a well-defined bony cavity containing a faint linear sequestrum, the result of a deep cut received eight weeks earlier. An eight-week progress examination **(B)** shows that the involucrum is fainter, and the associated new bone is being incorporated into adjacent cortex.

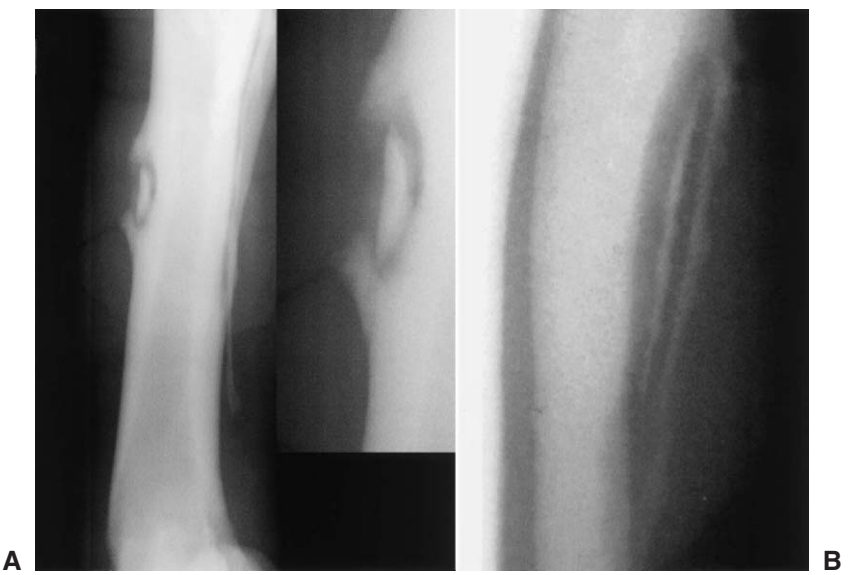


Figure 6-24 • Lateral oblique view of the third metacarpal bone with a detailed insert **(A)** shows a classic sequestrum featuring a discrete involucrum and cloaca. A close-up profile view **(B)** of the medial splint on the same side shows two additional sequestra proximally.



Figure 6-25 • Close-up medial oblique view **(A)** of the proximal half of the second metacarpal bone show complete detachment of its outer third caused by a deep devascularizing wound received nine weeks earlier. Oblique view **(B)** of the lateral splint of a second horse with a chronically infected metacarpal wound shows multiple sequestra and a nonunion.

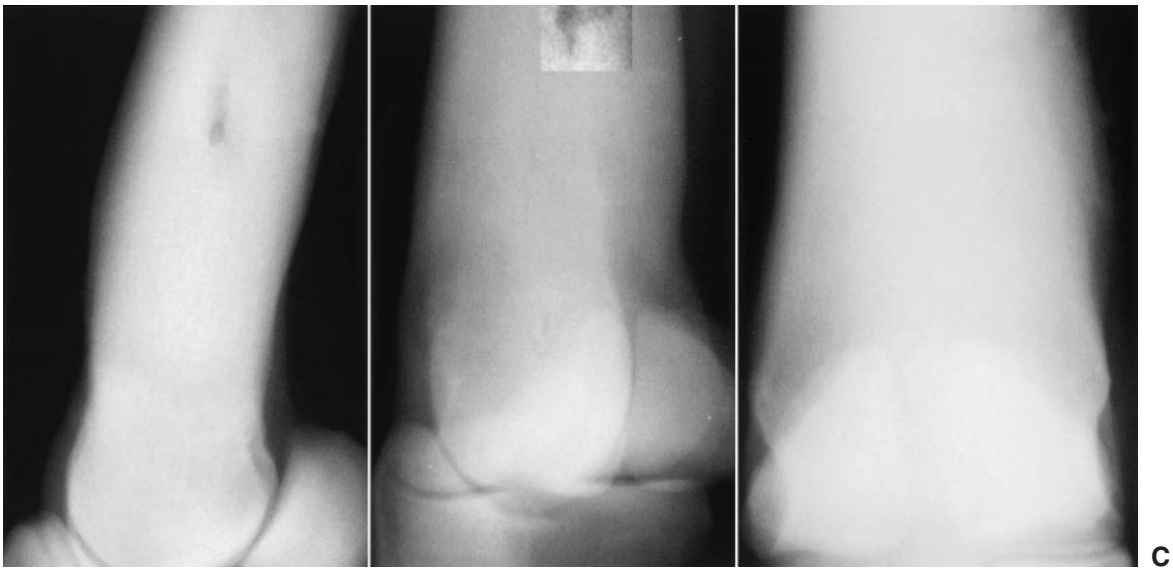


Figure 6-26 • Close-up lateral **(A),** lateral oblique **(B),** and dorsopalmar **(C)** views of the distal third of MC3 show uncertain but suggestive signs of sequestration: (1) regional thickening of the dorsal and lateral cortices as a result of chronic new bone deposition, (2) a vague, centrally located lucency, and (3) a possible bone fragment seen along the surface of the medial cortex of MC3 near the tip of the splint bone.

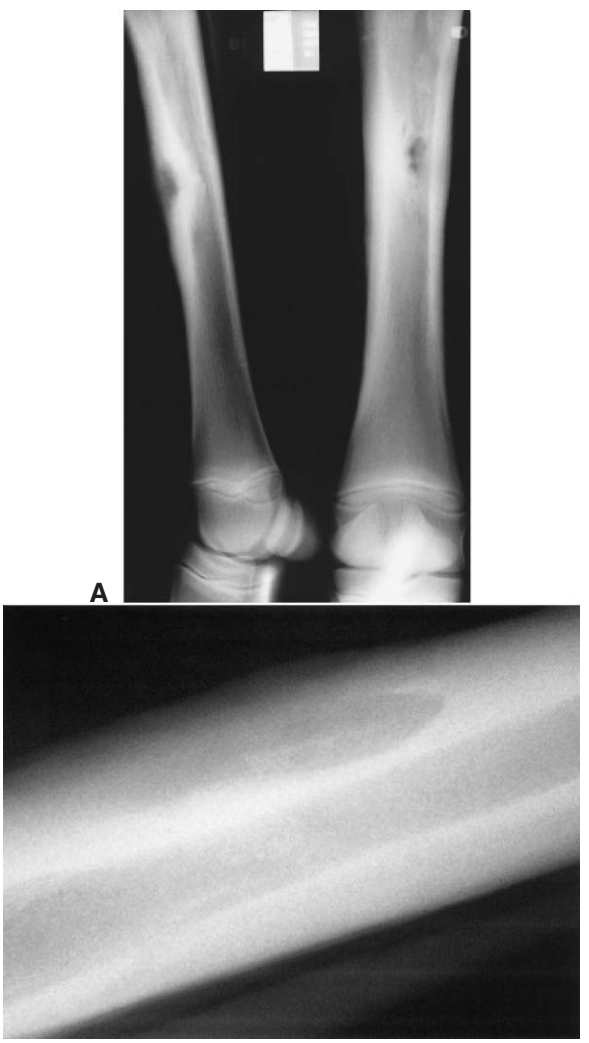


Figure 6-27 • Side-by-side lateral and dorsopalmar orientation views **(A)** of the third metacarpal bone show a chronic but poorly defined involucrum that extends through the entire thickness of the dorsal cortex, and beyond into the adjacent medulla. No sequestrum is visible, although there is a vague suggestion of such a fragment in some of the close-up views **(B):** lateral, dorsopalmar, lateral oblique, and medial oblique. The diseased bone was curetted, but no sequestrum was found.

palisade-like new bone deposit on the proximal aspect of the second metacarpal bone, (2) loss of subchondral bone density in both the second metacarpal and overlying second carpal bones, and (3) collapse of the intervening portion of the carpometacarpal joint (Figure 6-28).



Figure 6-28 • Close-up dorsopalmar view of the medial aspect of the carpometacarpal joint shows a lesion similar to that seen in Figure 6-29, but in this example the collapse of the medial aspect of the carpometacarpal joint is clearly evident, as is the bone loss in the overlying second metacarpal bone. As in the previous case, a large metacarpal bone deposit is affixed to the underlying splint head and adjacent cannon bone. Numerous vascular channels, and the immature appearance of its surface, strongly suggest an active lesion.

As the disease progresses, the new bone formed on the exterior surface of the medial splint reaches the level of the carpometacarpal joint, thus becoming periarticular as well as extraarticular (Figure 6-29). Eventually a large, ragged gap develops in place of the former cartilage space, much as it does with tarsal spavin (Figure 6-30). In some respects, "carpal spavin" resembles the appearance of a chronic articular fracture involving the head and proximal body of the second metacarpal bone; in others it does not (see Figure 6-30).

▮▮▮ SURGICAL INFECTIONS

Plated metacarpal fractures as well as incomplete stress fractures reduced with bone screws occasionally become infected. The first radiographic indicator of orthopedic infection is usually lucency immediately adjacent to the surface of one or more plates or screws. Implant or fragment dislocation usually follows shortly thereafter. When drainage is present, sinography often shows contrast solution contacting or undermining an associated bone plate or screw head. New bone deposits away from the fracture are strongly suggestive of infection, but only in the worst instances is overt bone destruction apparent.

Surgically infected third metacarpal fractures can heal, provided they remain stable and an adequate regional blood supply is maintained.[21] Radiographically, the smoothing and incorporation of infective bone deposits, and an absence of any further deposition characterize elimination of infection.

Although not widely publicized, periosteal stripping is also susceptible to infection, as exemplified in Figure 6-31. Localized new bone deposits that become apparent 1 to 2 weeks after surgery characterize most surgically infected periosteal stripping (Figure 6-31). There may also be accompanying wound drainage.



Figure 6-29 • Medial oblique **(A)** and dorsopalmar oblique **(B)** views of the proximal metacarpus show a large, ragged new bone deposit on the dorsomedial surface of MC2 and the adjacent surfaces of MC3. Although only vaguely seen, the lesion appears to extend proximally to the carpometacarpal joint and the adjacent second metacarpal bone. The cause of this lesion is not known although it severely crippled this horse.



Figure 6-30 • Close-up dorsopalmar **(A)** and medial oblique **(B)** views of an advanced case of "carpal spavin" seen in Figures 6-28 and 6-29 show massive carpometacarpal joint destruction strongly reminiscent of bone spavin or a severe intraarticular infection. Close-up view **(C)** of the medial splint of a second horse shows a subacute, steep oblique, articular fracture of the medial splint head and adjacent body, which bears some resemblance to "carpal spavin."



Figure 6-31 • Close-up medial oblique view of the distal metacarpus of a foal with a valgus deformity attributed to disturbed radial growth shows an amorphous bone deposit along the palmar surface of the bone, the result of an infected periosteal stripping operation.

▮▮▮ OSSELETS

Radiographically visible osselets are typically mineralized; otherwise they are invisible. Because the inflamed synovial tissue is often curved over the surface of the condyle proximally, its appearance may vary with projection angle. Osselets have been misdiagnosed as avulsion fractures because of their being offset from the proximal aspect of the metacarpal condyle (Figure 6-32). In some instances, combined periosteal and capsular tearing produces a large mounded bone deposit on the dorsal surface of the distal metacarpal metaphysis resembling a cross between an osselet and bucked shins (Figure 6-33).

▮▮▮ METACARPAL CURVATURE IN ADULT HORSES

Metacarpal curvature, often without clinical signs, in most instances is probably due to an earlier epiphysitis (Figure 6-34). I must stress, however, that this is an

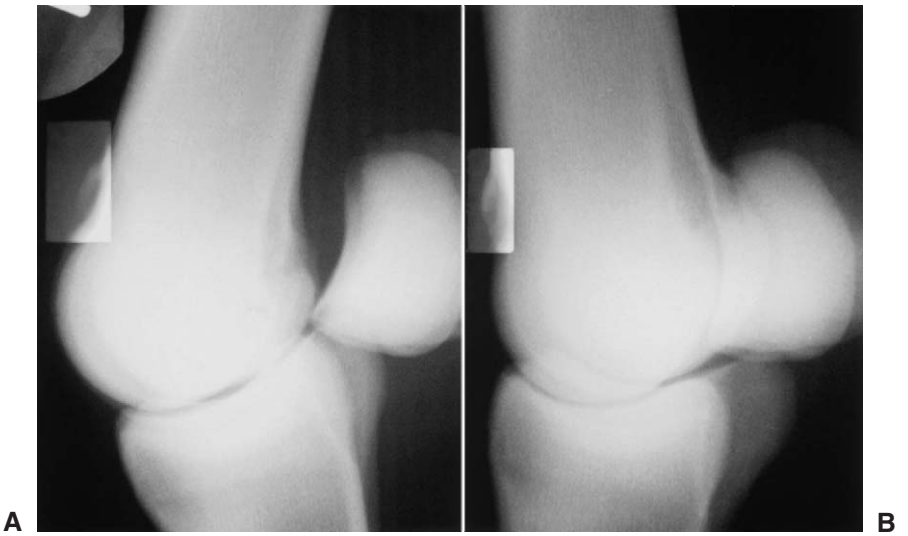


Figure 6-32 • Close-up flexed **(A)** and extended **(B)** views of the fetlock joint show an immature osselet on the dorsal surface of the third metacarpal bone just above the condyle *(emphasis zones)*, mistakenly diagnosed as an avulsion fracture.



Figure 6-33 • Close-up medial oblique view of a severe, subacute periosteal-capsular tear recently aggravated in a race, and initially causing non–weight-bearing lameness.



Figure 6-34 • Full-length dorsopalmar view of the metacarpus of an adult horse showing a mild medial curvature, presumed to be the aftermath of an earlier epiphysitis.

inferential diagnosis. Only when previous radiographs are available for comparison can this diagnosis be made with any degree of certainty.

References

1. Bowman KF, Evans LH, Herring ME: What is your diagnosis? *J Am Vet Med Assoc* 207:562, 1995.
2. Bowman KE, Evans LH, Herring ME: Evaluation of surgical removal of fractured distal splint bones in the horse, *Vet Surg* 11:116, 1982.
3. Verschooten F, Gasthuys F, et al: Distal splint bone fractures in the horse: an experimental and clinical study, *Equine Vet J* 16:532, 1984.
4. Jones R, Fessler J: Observations on small metacarpal and metatarsal fractures with or without associated suspensory desmitis in Standardbred horses, *Can Vet J* 18:29, 1977.
5. Zubrod CJ, Schneider RK, Tucker RL: Use of magnetic resonance imaging to identify suspensory desmitis and adhesions between exostoses of the second metacarpal bone and the suspensory ligament in four horses, *J Am Vet Med Assoc* 224:1815, 2004.

6. Reid CF: *A guide to veterinary radiation therapy*, 1st ed. Kennett Square, Pennsylvania, 1975, KNF Press.
7. Auer JA, Fackleman GE: Treatment of degenerative joint disease of the horse: a review and commentary, *Vet Surg* 10:80, 1981.
8. Dixon RT: Radiation therapy in horses, *Aust Vet J* 43:508, 1967.
9. Pleasant RS, Baker GJ, et al: Stress reactions and stress fractures of the proximal palmar aspect of the third metacarpal bone in horses: 58 cases (1980–1990), *J Am Vet Med Assoc* 201:1918, 1992.
10. Ross MW, Martin BB: Dorsomedial articular fracture of the proximal aspect of the third metacarpal bone in Standardbred racehorses: seven cases (1978-1990). *J Am Vet Med Assoc* 201:332, 1992.
11. Nunamaker DM: The bucked shin complex, *Proc Am Assoc Equine Pract* 133, 1987.
12. Cervantes C, Madison JB, et al: Surgical treatment of dorsal cortical fractures of the third metacarpal bone in Thoroughbred racehorses: 53 cases (1985-1989), *J Am Vet Med Assoc* 200:1997, 1992.
13. Stover SM, Pool RR, et al. A review of bucked shins and metacarpal stress fractures in the Thoroughbred racehorse. *Proc Am Assoc Equine Pract* 349, 1988.
14. Lamb CR, Koblik PD, et al: Comparison of bone scintigraphy and radiography in the evaluation of equine lameness: retrospective analysis of 275 cases. *Proc Am Assoc Equine Pract* 90, 1988.
15. McClure SR, Watkins JP, et al: Complete fractures of the third metacarpal or metatarsal bone in horses: 25 cases (1980–1996), *J Am Vet Med Assoc* 213:847, 1998.
16. Orsini JA, Nunamaker DN: Management of a severely comminuted fracture of the third metacarpal bone in a horse, *J Am Vet Med Assoc* 191:683, 1988.
17. Scott EA, Thrall DE, Sandler GA: Angiography of equine metacarpus and phalanges: alterations with medial palmar artery and medial palmar digital artery ligation, *Am J Vet Res* 37:869, 1976.
18. Butt WP: The radiology of infection. *Clin Orthop Relat Res* 96:20, 1973.
19. Hathcock JT: What is your diagnosis? *J Am Vet Med Assoc* 181:935, 1982.
20. Guffy MM: Bone sequestrums and nonhealing wounds in horses, *J Am Vet Med Assoc* 152:1638, 1968.
21. Kay BA, Ferguson JG, et al: Treatment of chronic osteomyelitis and delayed union in the metacarpus of a horse, *Can Vet J* 17:82, 1976.

Chapter 7

Carpus

THE STANDARD CARPAL SERIES

Strategic carpal radiography has been described by a number a radiologists, including myself.[1,2] Generally the standard carpal series consists of four views: (1) dorsopalmar, (2) lateral, (3) medial oblique, and (4) lateral oblique (Figure 7-1). Figure 7-2 illustrates the appearance of the carpal bones as seen from the described radiographic perspectives.

A fifth view, the flexed lateral, may be added to the standard four-view series to obtain partial separation between the radial and intermediate carpal bones, potentially improving fracture detection in these locations (Figure 7-3).[3] A bone specimen configured in the flexed lateral position is provided for comparison (Figure 7-4).

The evaluative purpose of each of the four standard carpal views, plus the flexed lateral projection, is as follows (Table 7-1).

SUPPLEMENTARY SKYLINE PROJECTIONS

Depending on what standard views show, supplementary skyline projections may reveal otherwise invisible fractures situated along the upper front edges of the distal radius and carpal bones.[4] Skyline views are demanding of both the radiographer and the horse, requiring skill on the part of the former and cooperation by the latter. Acute fractures or sprains are often accompanied by pain and swelling, making the required full flexion difficult or impossible.

Supplementary skyline projections of the carpus (Figure 7-5) include the cranial edge of the distal radius (Figure 7-5, *A*), the dorsal edges of the proximal carpal row (Figure 7-5, *B*), and the dorsal edges of the distal carpal row (Figure 7-5, *C*). Figure 7-6 illustrates the corresponding surfaces of the distal radius, proximal, and distal carpal rows as seen from the perspective of the distally directed x-ray beam used to make the described radiographs.

Uhlhorn and co-workers reported that the skyline view of the distal carpal row in the horse is a reliable means of assessing bone density, including disease-related sclerosis, especially of the third carpal bone.[5] Uhlhorn and Ekman reported how different beam angles (and associated geometric distortion) changed the radiographic appearance of the dorsal margins of the bones of the distal carpal row as seen in the skyline view (dorsoproximal-dorsodistal projection).[6]

Specifically, they concluded that beam-cassette angles of 25 to 40 degrees produced acceptable images and did not unduly influence the assessment of sclerosis. The steeper the beam-cassette angle (up to 40 degrees), the better the visibility of proximal C3 and thus the greater potential for identifying deep, proximal border fractures.

CUSTOMIZED VIEWS

When standard carpal projections or common supplementary views fail to reveal what is strongly suspected to be a carpal fracture, customized images are advisable.[7] Typically such views are predicated on physical features of the suspected injury, such as localized swelling or palpable pain. In such instances, a lead marker is placed on the skin overlying the area of interest, and a tangential film is made of the suspicious location. If it is imaged accurately, the lead marker on the radiograph should appear edge-on.

CUBOIDAL BONES: A MISLEADING AND DIAGNOSTICALLY DANGEROUS OVERSIMPLIFICATION

With closer diagnostic attention being paid to dysplastic carpal bones, the term *cuboidal bone* has increasingly gained favor. Although there is nothing

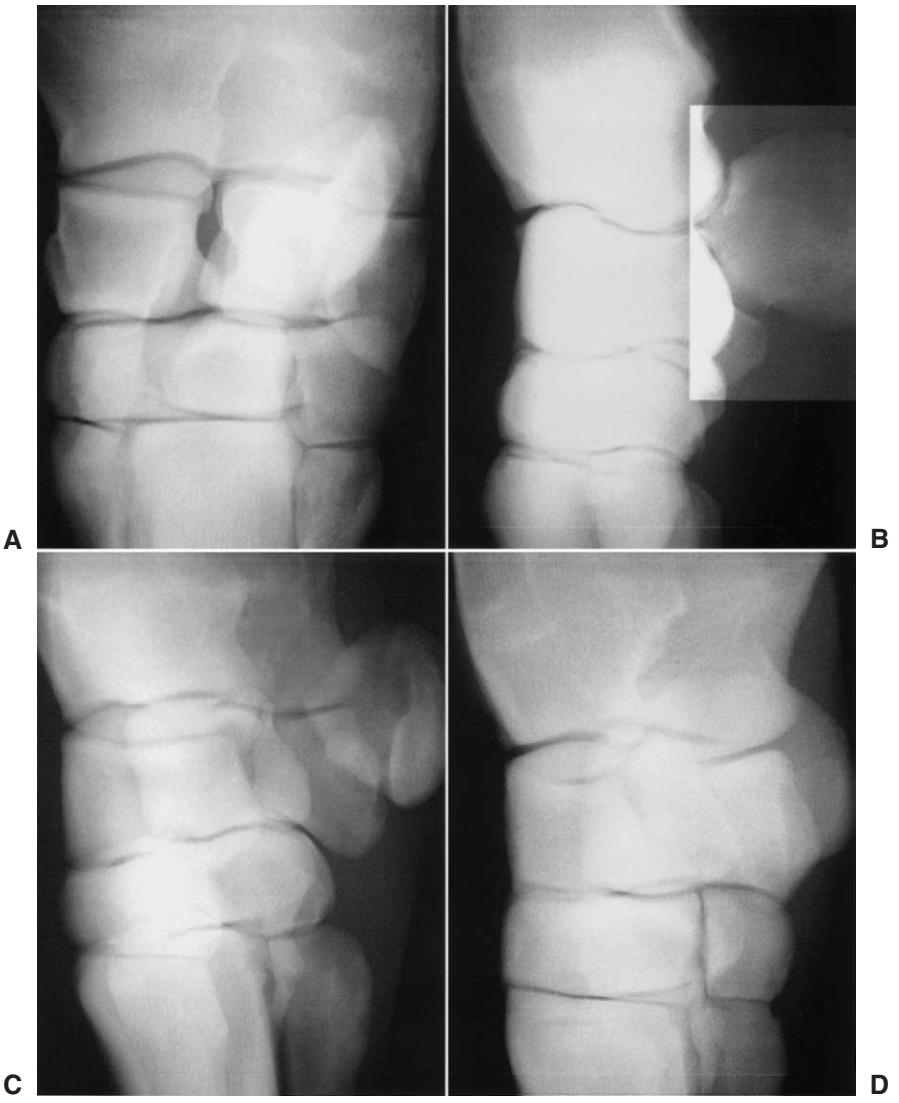


Figure 7-1 • Normal carpus (ideal positioning): dorsopalmar **(A),** lateral **(B),** medial oblique **(C),** and lateral oblique **(D)** views.

inherently wrong with such a notion, it can limit diagnostic perspective, sometimes dangerously so. One need only glance casually at the palmar aspect of a horse's carpus (see Figure 7-2, *D*) to appreciate immediately that most visible surfaces are distinctly convex with rounded outlines, hardly the cubes we all learned to recognize in geometry class.

In point of fact, not one of the seven carpal bones even vaguely resembles a cube. Rather, each is a uniquely crafted, structural entity, so complex that multiple views are typically required to render a diagnosis of fracture.

▮▮▮ INDIVIDUAL CARPAL BONES AND THE CONCEPT OF CARPAL ROWS

There are normally seven carpal bones, each with a unique shape, arranged in two comparably sized rows, one above the other. The upper or proximal row comprises the radial, intermediate, and ulnar carpal bones. The lower or distal row is composed of the second, third, and fourth carpal bones. The accessory carpal bone stands alone, situated immediately behind the ulnar carpal bone.

It is particularly useful to know (or know where to look up) the normal appearance of the individual carpal bones as well as their normal spatial relationships to one another because such observations are the basis for the diagnosis of carpal fracture and dislocation. Figure 7-7 shows the proximal and distal rows of carpal bones from the front, separated from one another for increased visibility. Note the unique shape of each carpal bone, in particular the upper and lower front corners of the radial, intermediate, and third carpals, where fractures commonly occur. Note how different the upper and lower articular surfaces of the second, third, and fourth carpal bones appear, differences that reflect both the uniqueness and the com-

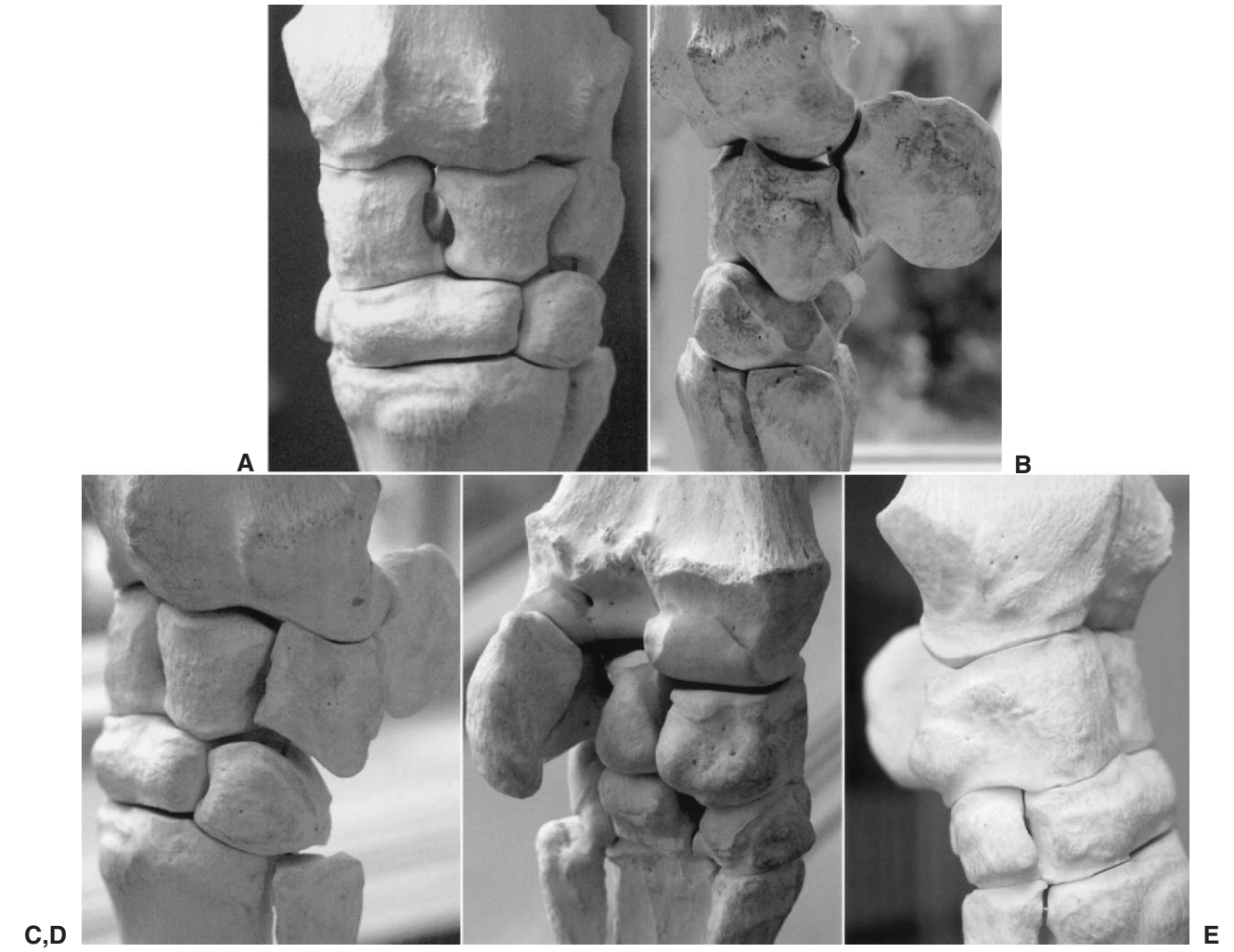


Figure 7-2 • Defleshed carpal bones corresponding to the previous radiographic projections: dorsopalmar **(A),** lateral **(B),** medial oblique from a dorsolateral perspective **(C),** medial oblique from a palmaromedial perspective **(D),** and lateral oblique from a dorsomedial perspective **(E).** Note the comparative complexity of the palmar surfaces of the carpus compared with the dorsal surfaces, seen in D.



Figure 7-3 • Normal flexed lateral view. Note how the radial and intermediate carpal bones separate (the radiocarpal is lowermost), exposing their corners, which are most likely to contain fractures.

plexity of the distal intercarpal and carpometacarpal joints (Figure 7-8).

As further examples of anatomic complexity, observe how the accessory carpal bone articulates equally with both the distal radius and the ulnar carpal bone (Figure 7-9) and how the fourth carpal bone has a shared V-shaped articulation with the lateral aspect of the cannon bone *and* the adjacent splint head (Figure 7-10). Differences such as these are not mere trivia, but rather they are important anatomic waypoints that enable one to determine what is disease and what is simply different.

Vestigial Carpal Bones (Accessory Carpal Bones)

Losonsky and co-workers reported the incidence of *unilateral* first carpal bones in a group of 300 Standardbred horses as being about 11 percent and the *bilateral* incidence about 23 percent.[8] These findings are



Figure 7-4 • Defleshed, flexed carpal bones seen from lateral **(A),** lateral oblique **(B),** and medial **(C)** perspectives.

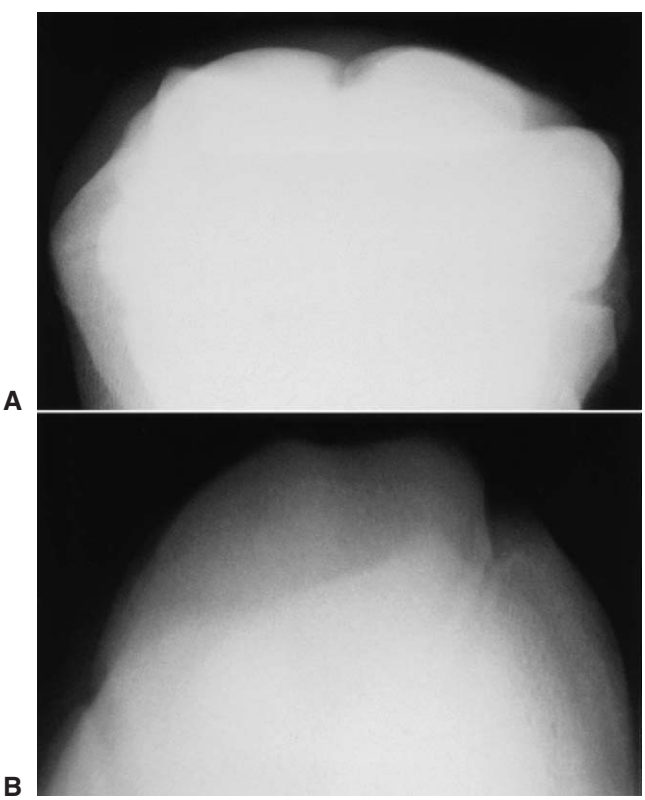


Figure 7-5 • Skyline views of the proximal **(A)** and distal **(B)** carpal rows (medial is to the reader's left).

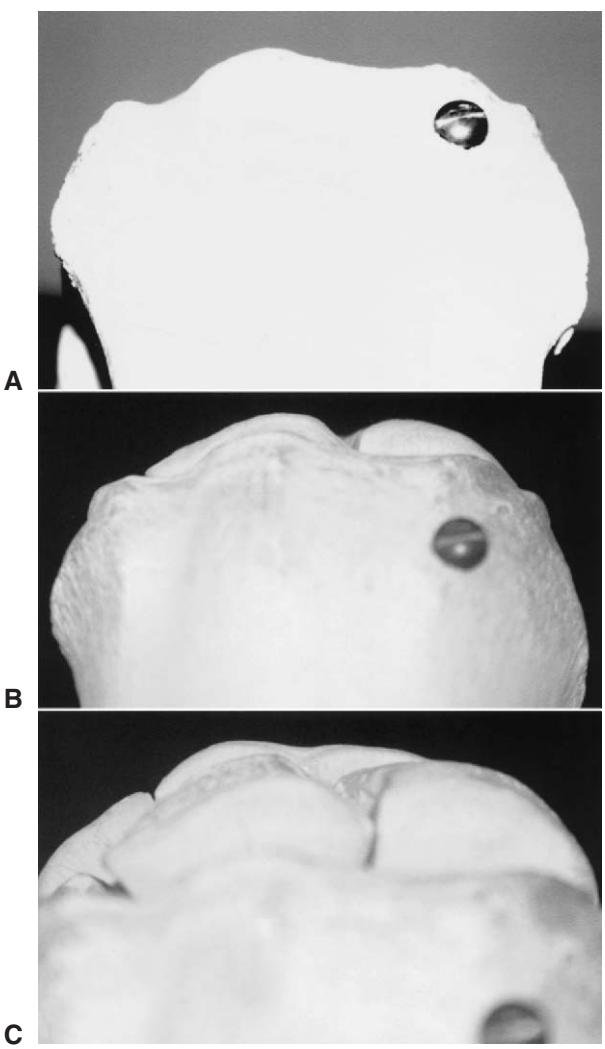


Figure 7-6 • Defleshed carpal bones corresponding to the following skyline projections: distal radial **(A),** proximal carpal **(B),** and distal carpal **(C)** rows. The medial surface of the horse's carpus is to the reader's right.

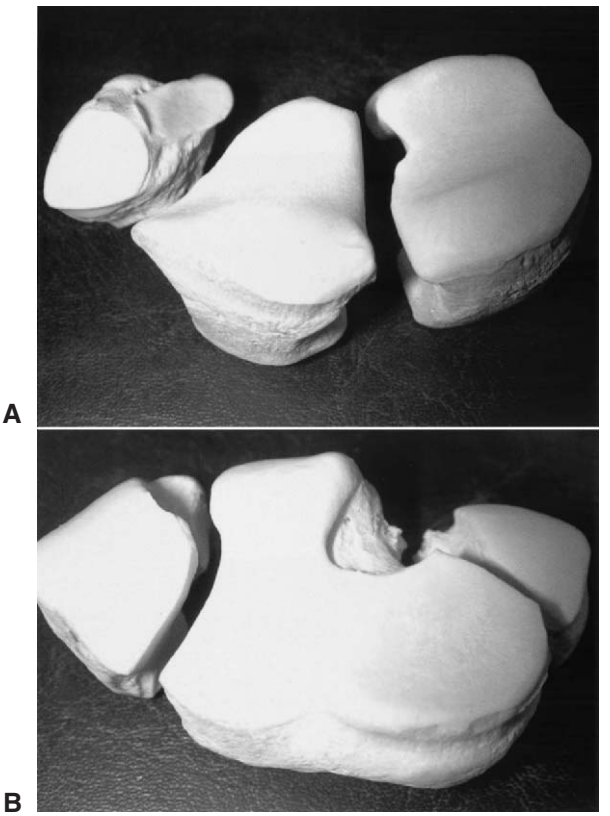


Figure 7-7 • Exploded view of defleshed carpal bones (accessory carpal bone excluded): Proximal row **(A)** from right to left: radial, intermediate, and ulnar. Distral row **(B)** from right to left: second, third, and fourth. Medial is to the reader's right.

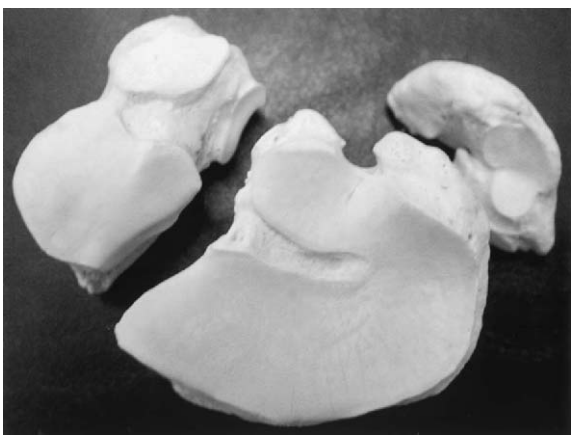


Figure 7-8 • Exploded view of the undersides of the bones of the distal carpal row show an elaborate system of articular facets, not readily appreciable in radiographs. Medial is to the reader's right.

in contrast to my own observations made in our general hospital population, consisting for the most part of Thoroughbreds, Standardbreds, and Quarter Horses, where about 90 to 95 percent of horses with vestigial first carpal bones have them bilaterally.

The diagnostic importance of recognizing vestigial carpal bones for what they are—anatomic variants—is

Table 7–1 • STANDARD CARPAL VIEWS AND THEIR EVALUATIVE PURPOSES

View	Evaluative Purpose
Dorsopalmar	Provides the best view in which to judge the width of the cartilage spaces and an excellent opportunity to evaluate the joints for signs of osteoarthritis Best view for assessing distal radial growth plate for closure Best view for evaluating immature, dysmature, or lax carpal bones
Lateral	Best view for judging major fracture dislocation and conformational abnormalities
Lateral oblique	Profiles the dorsolateral aspect of the carpus; specifically the lateral edges of the distal radius, intermediate and third carpal bones, and proximal 3rd metacarpal bone.
Medial oblique	Profiles the dorsomedial aspect of the carpus; specifically the medial edges of the distal radius, radial and third carpal bones, and proximal third metacarpal bone. Best view for detecting slab fractures of palmar aspect of intermediate and ulnar carpal bones*
Flexed lateral	Separates the lower halves of the radial and intermediate carpal bones, projecting them free of superimposition by one another, making it easier to detect distal corner fractures.

*Dabareiner RM, Sullins KE, Beadley W: Removal of a fracture fragment from the palmar aspect of the intermediate carpal bone in a horse, *J Am Vet Med Assoc* 203:553, 1993.



Figure 7-9 • Lateral close-up view of a defleshed accessory carpal bone shows its unique articular relationship with the adjacent radius and ulnar carpal bone.

to avoid mistaking them for fractures, sequestra, or bone fragments resulting from osteochondritis. Of equal importance is recognizing the structural and density variations that commonly occur in the adjacent surface of the second carpal bone, variants that also may be mistaken for disease (Figure 7-11).

Palmar Carpal Ossicle

Martens identified a previously undescribed bone (or ossicle) usually situated on the palmar aspect of the



Figure 7-10 • Close-up views of the lateral and medial splint heads showing pronounced articular differences: The medial splint head **(A)** articulates almost entirely with the overlying second carpal bone; only a third of the lateral splint head **(B)** contacts the adjacent fourth carpal bone (the rest articulating with the adjacent third metacarpal bone).

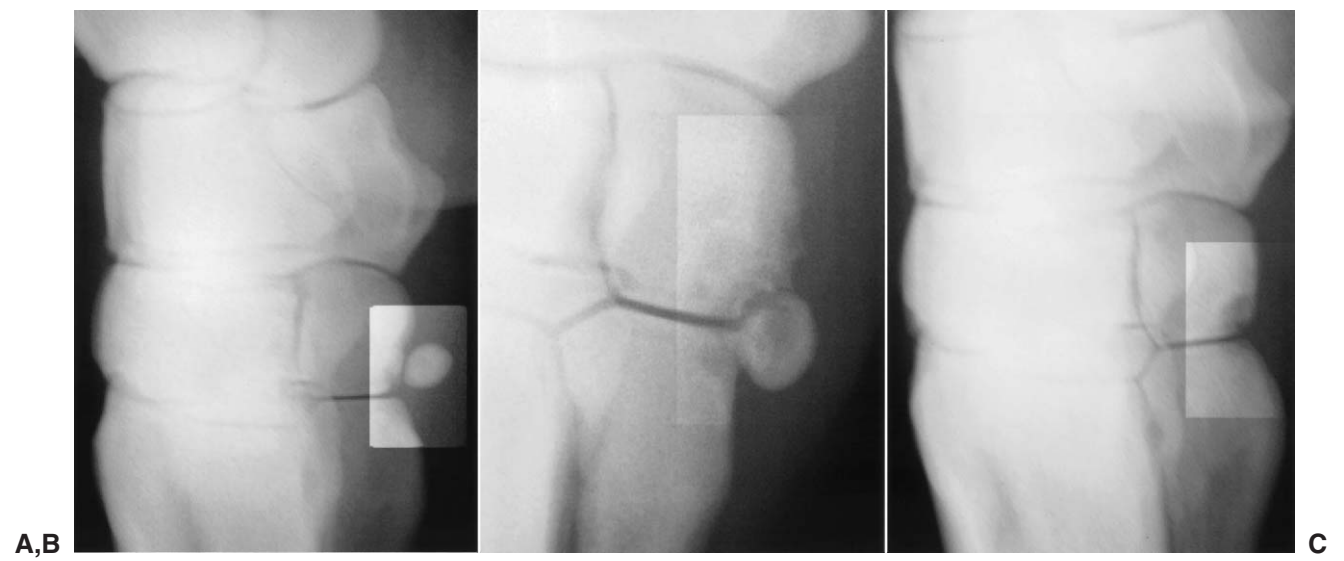


Figure 7-11 • Three variations of a vestigial first carpal bone as seen in lateral oblique projections of the carpi of normal horses: (1) a circular, uniformly dense bone lying just off the surface of a normal-appearing second carpal bone (*emphasis zone*, **A**); (2) an oval, unevenly dense bone situated alongside defective-appearing second carpal and second metacarpal bones (*emphasis zone*, **B**); (3) a small, barely perceptible bone-like density located within a cystic-appearing area in the adjacent second carpal bone (*emphasis zone*, **C**). This later variant may or may not be associated with a visible ossicle. See emphasis zones.

fourth carpal bone at the level of the intercarpal joint. In one instance, the ossicle was found on the palmar aspect of the ulnar carpal bone. Different standard views showed the ossicle with different degrees of clarity, and in three of four horses the ossicle was found bilaterally. It was believed that the ossicle posed no clinical problem, nor was it related to past or present injury.[9]

Radiocarpal Joint Fat Deposits

Dietze and Rendano reported the presence of triangular fat deposits in the cranial aspect of the radiocarpal joint that resembled small gas pockets, as sometimes seen after intraarticular anesthesia.[10] Xerographic-anatomic correlation showed the objects to be composed of intracapsular fat situated in either the synovial membrane of the extensor carpi radialis tendon sheath or the synovial membrane of the antebrachiocarpal joint (Figure 7-12).

▮▮▮ NORMAL RADIOGRAPHIC VARIATION AS A FUNCTION OF BEAM ANGLE

It is not unusual to note small variations in the appearance of individual carpal bones found in a standard carpal series, a consequence of small differences in pro-



Figure 7-12 • Ultra-close-up lateral view of the carpus shows a pair of fat deposits cranial and ventral to distal radius: one appearing as a discontinuous, vertically oriented, radiolucent band, the other as an amorphous gas-like shadow.

jection angle related to one or more of the following factors: (1) pain and disability resulting from injury or infection, (2) a nervous horse, (3) an impatient radiographer, and (4) changes in limb angle caused by a weight shift. Most of these variations are small and do not require repeats. It is important, however, to familiarize oneself with common projectional variations so as not to mistake them for disease. Appreciation of how normal carpal anatomy changes with small differences in projection angle enables one to recognize a nonstandard view and to make the necessary corrective changes required to obtain the desired image (Figures 7-13 and 7-14).

▮▮▮ CARPAL FRACTURES

Carpal fractures in horses, most of which are sustained while racing or during race-related workouts, typically cause visible lameness, swelling, excessive heat, and pain on forceful palpation and manipulation. The degree of lameness *usually* reflects both the severity and duration of lameness.[11]

Fresh Versus Old Chip Fractures

Fresh (Acute) Injury. Fresh first-time carpal chip fractures, in addition to being associated with sudden pain and lameness, are usually characterized by most or all of the following radiographic features: (1) sharp fragment margination; (2) a visible *fracture bed,* which is a comparably sized defect in the adjacent bone; (3) normal surrounding bone density; (4) an absence of osteoarthritis; and (5) localized, hot, indurated, painful joint swelling. Figure 7-15 shows an example of a fresh, minimally displaced distal radial chip fracture.

Table 7–2 • COMPARATIVE RADIOGRAPHIC FEATURES OF RECENT AND CHRONIC CARPAL CHIP FRACTURES

Comparative Features	Fresh Carpal Chips	Old Carpal Chips
Fragment margination	Sharp	Vague
Fracture bed	Usually visible	Occasionally visible
Adjacent bone density	Normal	Decreased
Osteoarthritis	Absent (unless previously injured)	Present
Swelling type	Hot, relatively soft and painful at touch	Normal or cool, firm or hard, non painful to touch

Intermediate (Subacute) Injury. Subacute carpal fractures are often characterized by fuzzy margins, a combination of reabsorption of dead bone from the fragment edges and fracture bed and the initiation of a callus. If the horse is transported for treatment, the original fracture itself may fracture, producing additional fragments—a so-called *transport fracture* (Figure 7-16).

Old (Chronic) Injury. Old chip fractures, especially if multiple or comminuted, usually feature (1) relatively indistinct fragment margination; (2) a vague or absent fracture bed; (3) decreased contiguous bone density; (4) osteoarthritis of the affected joint; and (5) localized, cool, firm-to-hard, nonpainful joint swelling. If a horse reinjures itself, the magnitude of the described abnormalities is typically greater, as it *may* also be with repeated intraarticular steroid injections. In some instances, large fracture fragments, especially corner fractures, disintegrate as a result of reinjury, often leaving behind a large bony defect; numerous small, ill-defined bone fragments; and a cloud of new bone (Figure 7-17).

Table 7-2 summarizes the comparative radiographic features of recent and chronic carpal chip fractures.

▮▮▮ CARPAL FRACTURE TYPES

The three principal types of carpal fracture are the (1) *chip*, (2) *corner*, and (3) *slab* or *biarticular.* Most are detected in lateral, flexed lateral, and lateral or medial oblique projections.

Chip Fracture

Chip fractures, as the name implies, are small flakes or chunks of bone that are sheared off the upper or lower corners of carpal bones, typically while a horse is racing. Some authorities describe these injuries as

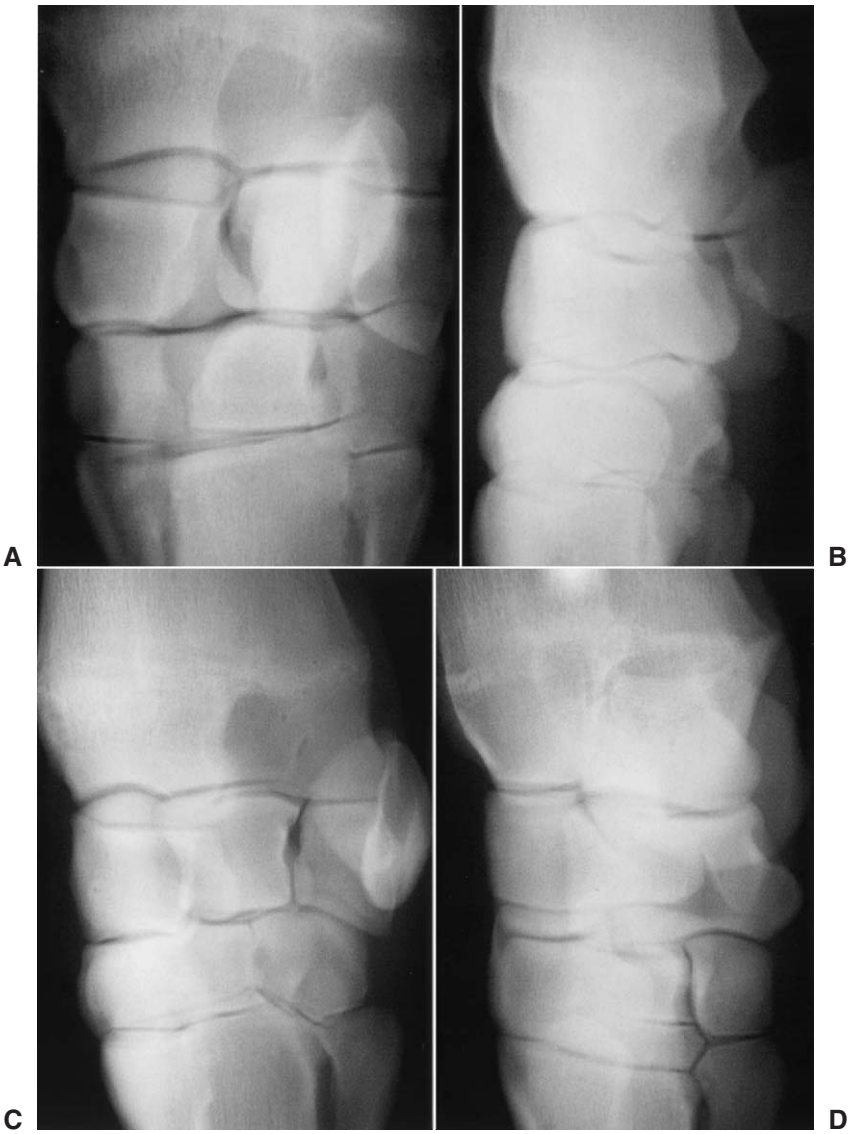


Figure 7-13 • Normal carpus in a 2-year-old Thoroughbred filly consisting of four standard views, including dorsopalmar **(A),** lateral **(B),** medial **(C),** and lateral **(D)** obliques. The projection angles in this examination differ slightly from the ideal shown in Figure 7-1.

osteochondral chip fractures, a somewhat presumptuous description given the fact that cartilage is all but invisible radiographically. The radial and intermediate carpal bones are most often "chipped," often in conjunction with a similar type fracture to the overlying distal radius. An example of a distal radial chip is shown in Figure 7-18.

Corner Fracture

A corner fracture, like a chip fracture, usually originates from either the upper or the lower front corner of a carpal bone (Figure 7-19). Corner fractures are not only larger than chip fractures, but they are more serious as well, creating more bone, cartilage, and capsular damage; a larger volume of intraarticular hemorrhage; and a greater amount of pain and disability. In my experience, corner fractures most often occur in the distal radius, in the proximal or distal corners of the radial carpal bone, and in the proximal aspect of the third carpal bone.

Some fresh corner fractures can be detected only in supplementary tangential views of the affected bone (skyline view), although not all horses with such fractures will tolerate the necessary limb flexion and related pain associated with these projections.

Slab or Biarticular Fracture

Carpal fractures that enter two adjacent joints, typically, but not exclusively, one above and one below, are termed *slab* or *biarticular fractures.* They are the most destabilizing, and thus most serious, of all carpal fractures. In racing Thoroughbreds, slab fractures occur most often to the third carpal bone (Figure 7-20).[12] Even after successful surgical reduction, horses with biarticular fractures of the third carpal bone tend not to perform as well as they before their injuries. Slab

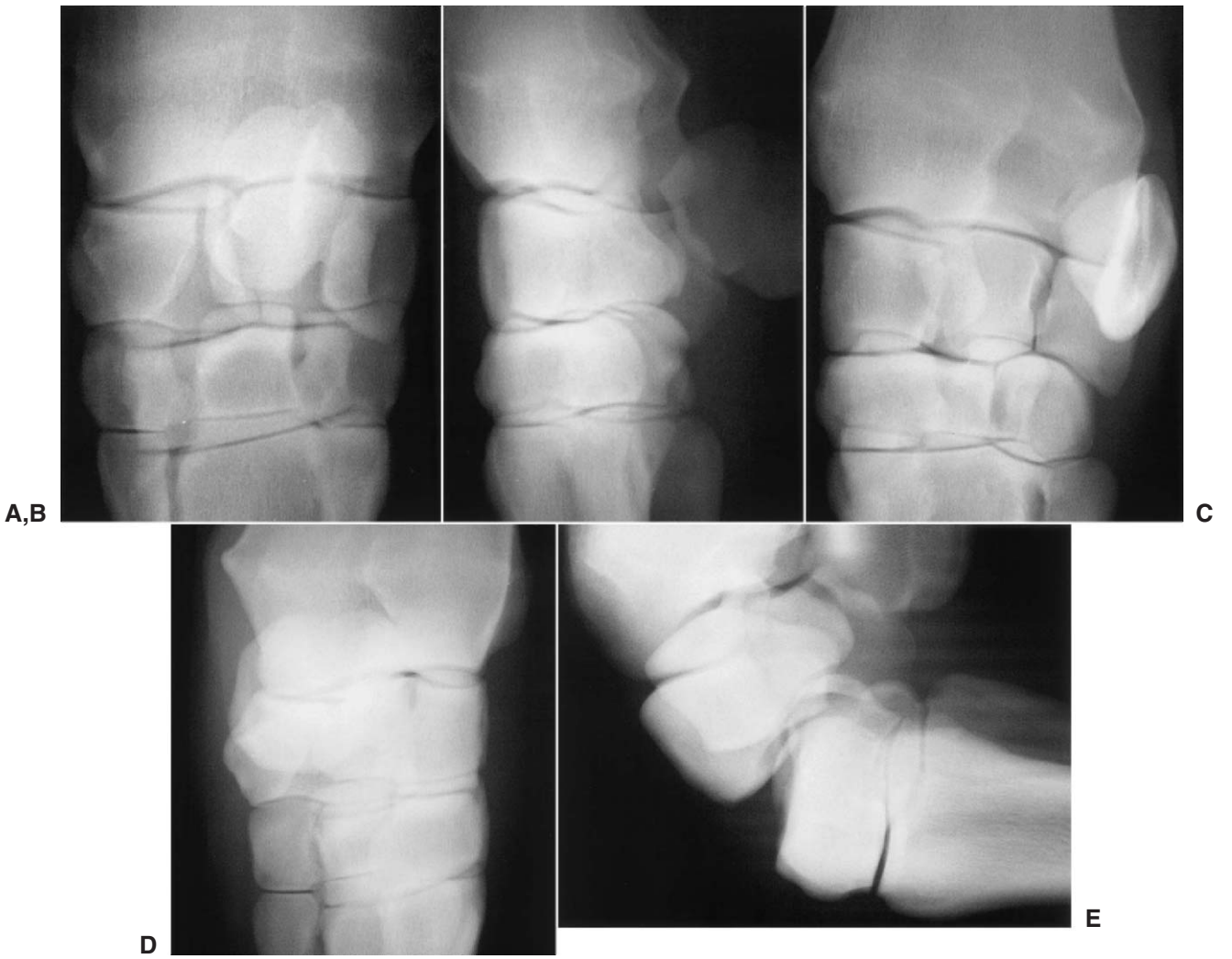


Figure 7-14 • Normal carpus in a 4-year-old Standardbred stallion consisting of four standard views and one supplementary view: dorsopalmar **(A),** lateral **(B),** medial and lateral **(C, D)** obliques, and flexed lateral **(E).** The projection angles of the four standard views in this examination differ slightly from the ideal shown in Figures 7-1 and 7-3.

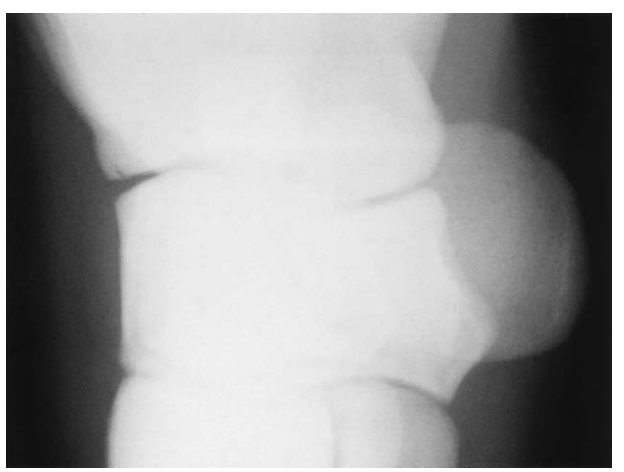


Figure 7-15 • Close-up lateral oblique view of a fresh (24-hour), minimally displaced, distal radial chip fracture.

fractures occur in other carpal bones but not as commonly. Multiple slab fractures in the same animal have occasionally been reported.[13]

DeHaan and co-workers identified the radial fossa as the most common site of third carpal injury and furthermore found that sclerosis in this location often predated subsequent injury.[14] Most fractures appeared comminuted in the standard projections, a feature that often required a skyline projection to confirm.

Sourcing Fracture Fragments

Some chip or corner fractures are clearly associated with a particular bone, the distal radius or radial carpal, for example, based on (1) fragment proximity or (2) the presence of an adjacent fracture bed. Others cannot easily be linked to a particular bone using these criteria because they are situated equidistantly from a pair of nearby bones or there is no discernible fracture



Figure 7-16 • Lateral oblique **(A)** and ultra-close-up **(B)** views (customized angle) of a subacute (10-day-old) distal radial chip fracture. In addition to the original fragment seen shortly after the injury, two smaller chips are now visible in the enlargement, most likely secondary fractures related to long-distance transport for treatment.



Figure 7-17 • Medial oblique **(A)** and ultra-close-up **(B)** views of old nonunion fractures of the radial and third carpal bones. The radial fracture bed has filled with fibrous tissue rather than bone. The exostosis on the face of the radial carpal bone is due to tearing of the intercarpal ligament (sprain). Dorsopalmar **(C)** and dorsopalmar close-up **(D)** views show primary narrowing of the medial half of the proximal intercarpal joints and secondary narrowing of the radiocarpal joints.

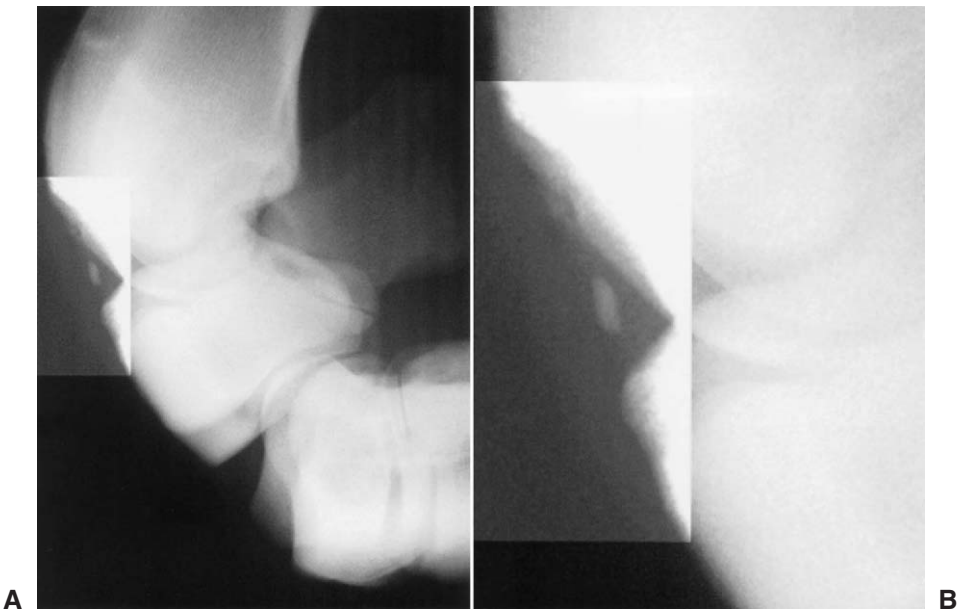


Figure 7-18 • Flexed lateral **(A)** and ultra-close-up, flexed lateral **(B)** views of the carpus show a relatively fresh (1-week-old) chip fracture of the distal radius *(emphasis zone).* Flexion of the carpus not only increases the amount of fragment displacement, making it more visible, but also reveals an otherwise obscure fracture bed containing two smaller fragments in the overlying radius.

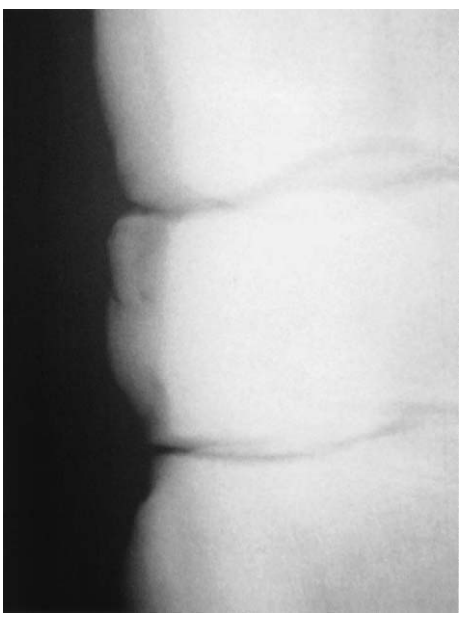


Figure 7-19 • Close-up medial oblique view (customized angle) made to profile a subacute proximal corner fracture of the third carpal bone, which was not clearly seen with the four standard projection angles.

Table 7–3 • INCIDENCE OF CARPAL BONE FRACTURES IN THE HORSE

Bone	No. of Fractures	Total Fractures (%)
Radial carpal bone	69	46.4
Third carpal bone	29	19.4
Intermediate carpal bone	23	15.4
Distal radius	22	14.8
Other carpal bones	6	4.0

From Park RD, Morgan JP, O'Brien T: Chip fractures in the carpus of the horses: a radiographic study of their incidence and location, *J Am Vet Med Assoc* 157:1305, 1970.

bed. In such instances, a flexed lateral or flexed lateral oblique can often identify the true location of the injury (Figure 7-21).

Carpal Fracture: Incidence and Location

Park and co-workers reported that the radial carpal bone was fractured in 50 percent of horses radiographed for suspected carpal injury. The right radial carpal bone was fractured more often than the left.[15] Most fractures occurred on the dorsal surface of the carpus and distal radius. The incidence of proximal versus distal corner fractures was similar. Twenty percent of the radiographed horses had bilaterally symmetric fractures, most often involving the radial carpal bone.

Radiographically the flexed lateral view identified the greatest number of fractures compared with the other standard projections. The frontal view proved the least revealing. Comparing extended and flexed lateral radiographs best assessed fragment mobility. Further incidence data are shown in Table 7-3.

Thrall and co-workers reported that in both Thoroughbred and Standardbred horses, the radial carpal bone was injured twice as often as all other carpal bones combined.[16] Furthermore, the relative incidence of new bone deposition—radial carpal,



Figure 7-20 • Close-up medial oblique **(A)** and ultra-close-up **(B)** views of a nonunion slab fracture of the third carpal bone, appearing as a vague, vertically oriented, radiolucent band in the dorsal quarter of the distal carpal row.

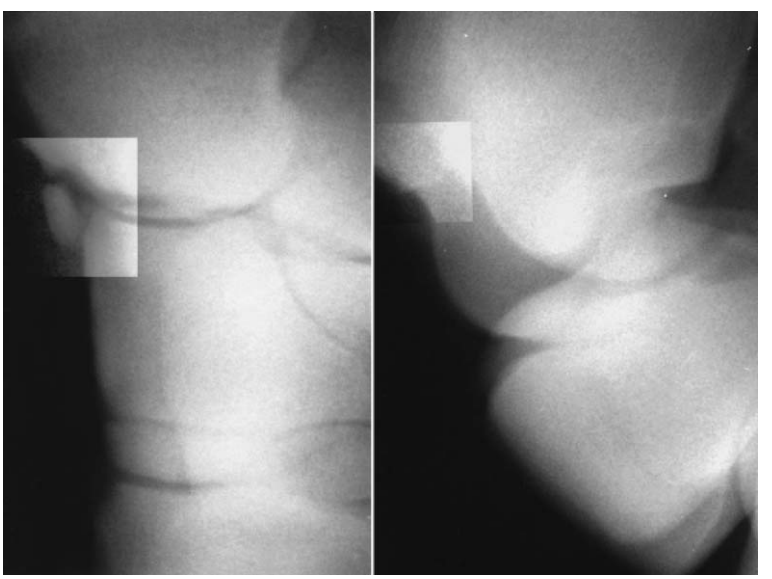


Figure 7-21 • Close-up medial oblique **(A)** view of the dorsal surface of the radiocarpal joint shows a medium sized fracture fragment situated equidistantly from the distal radius (showing a probable fracture bed) and proximal aspect of the radial carpal bone. An ultra-close-up, flexed lateral view **(B)** shows that the fracture has predictably returned to its point of origin in the distal radius, making it much harder to locate *(emphasis zone)*.

distal radius, third carpal, and intermediate carpal—followed the same general pattern as chip fractures.

The vast majority of carpal fractures break from the upper or lower front corners of the bones, most medially. Only rarely do fractures occur on the back surfaces of the carpus, with most reported fractures originating from the proximal row.[17]

In contrast to the American reports described above, Dixon reported that in Australian racehorses, fractures of the intermediate carpal bone were most common.[18] Later Wyburn and Goulden, reporting on a series of New Zealand racehorses, indicated that the third carpal bone was most vulnerable to fracture,[19] a conclusion also reached by Lindsay and Horney in their study of the incidence of carpal fracture in a group of 89 Louisiana racehorses.[11]

A variety of single and multiple distal radial and carpal bone fractures are shown in Figures 7-22 to 7-35.

Accessory Carpal Bone Fracture

Accessory carpal bone fractures are most common in Thoroughbred hunter-jumpers and cross-country

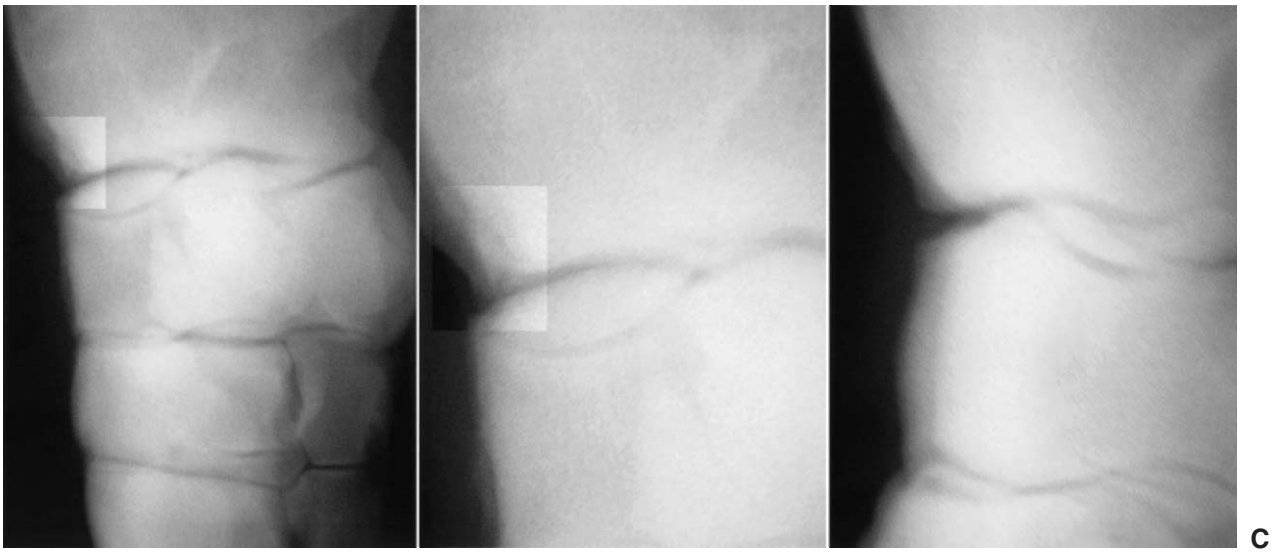


Figure 7-22 • Close-up lateral oblique **(A),** and ultra-close-up **(B)** views of the radiocarpal joint show a triangular, minimally displaced distal radial chip fracture *(emphasis zone).* The craniomedial surface of the bone appears uninjured **(C).**

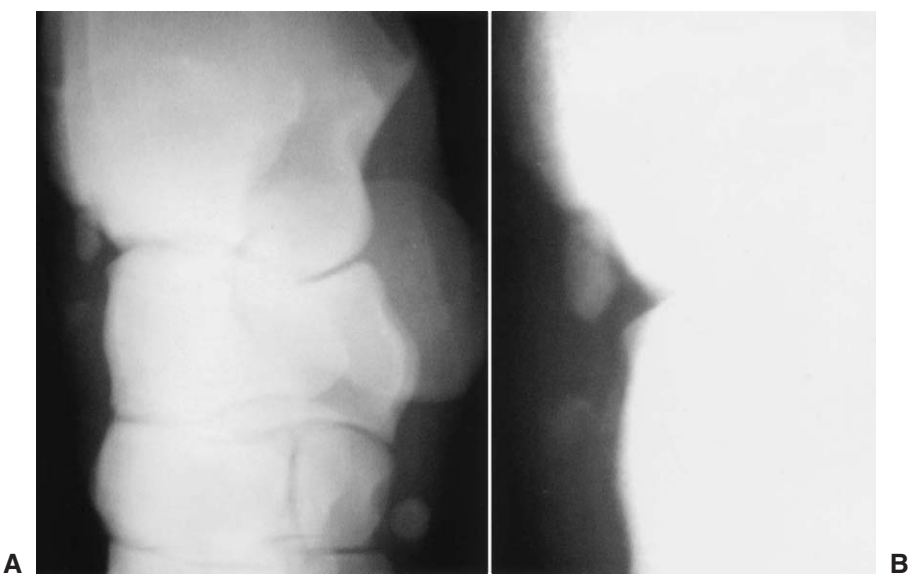


Figure 7-23 • Close-up lateral oblique **(A)** and ultra-close-up **(B)** views of a chronic displaced radial chip fracture also show a faint layer of new bone on the dorsal surface of the intermediate carpal bone and an adjacent area of capsular mineralization.

steeplechasers. Most accessory carpal fractures are vertically oriented, breaking through the lateral groove, which accommodates the long tendon of the ulnaris lateralis. Untreated accessory carpal bone fractures often fail to heal normally, as characterized by varying degrees of fragment displacement and fibrocartilaginous versus bony union.[20] Where doubt exists regarding the unity of an accessory carpal bone fracture, comparison of lateral and flexed lateral views can often resolve the question: the fracture gap increases in the flexed lateral view compared with that in the nonflexed projection.[21]

Transverse fractures of the accessory carpal are less common than vertical ones. The typical break transects the bone proximally, resulting in varying degrees of fragment distraction. Surprisingly, few nonunions occur, although healing is usually protracted (Figure 7-36).

Radiographically Predicting Fracture: Is It Possible?

It has long been theorized that decreased bone density in young racehorses may herald impending fracture. Young and co-workers, using a combination of radiographic, microradiographic, and histologic data obtained from 46 third carpal bones removed from 23 young racehorses, theorized that there *might be* a connection between exercise-induced increased bone density in the region of the radial fossa, bone strength, and fracture.[22]

"Kissing" Lesions

Opposing articular surfaces need one another, anatomically and physiologically speaking. When, for example, there is an untreated proximal corner fracture of the radiocarpal bone, a secondary lesion usually develops in the opposing surface of the radius; likewise, an untreated fracture of the distal corner of the radial carpal bone usually results in a secondary lesion in the underlying third carpal bone. These so-called kissing lesions are primarily the result of mechanical abrasion, first to the articular cartilage and subsequently to the underlying bone, aided and abetted by the infiltration of synovial fluid laden with inflammatory residue from the damaged tissues.



Figure 7-24 • Ultra-close-up, flexed lateral view of the radial and intermediate carpal bones show a very small displaced chip fracture on the proximodorsal aspect of the former *(emphasis zone).*

▮▮▮ CARPAL STRAINS, SPRAINS, AND DISLOCATIONS

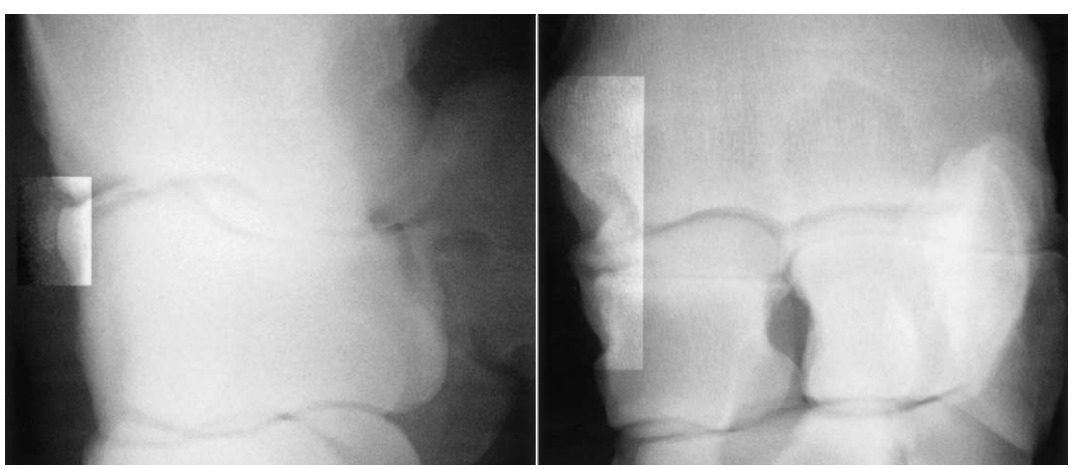
Extracarpal Strains

Extracarpal strains are those that involve the tendons surrounding the carpus, for example, the tendon of the extensor carpi radialis. In some instances, it is the tendon sheath rather than the tendon itself that becomes diseased. Such a case was described by Newell and co-workers in which a 5-year-old Arabian mare with a chronically swollen carpus was found to have numerous faint bonelike densities arrayed over the cranial aspect of its distal radius and proximal carpus.[23] Although the diagnosis was never proven, the authors attributed the abnormal densities to *synovial osteochondromatosis,* a rare disease of tendon sheaths and joints that is occasionally seen in horses and other mammals. In my experience, these densities are often incidental findings.

Intercarpal Sprains

The most common type of intercarpal sprain I have seen occurs between the central third of the carpal bones where they are joined by the intercarpal ligaments. The radiographic evidence of such injuries consists of new bone deposits projecting outward from the carpal face. Generally these osteophytes do not become evident for at least a month after injury because of the relatively unresponsive nature of the carpal periosteum. Before this time, the injured bone surface gradually loses density, providing the initial radiographic clue as to the nature of the injury (Figures 7-37 to 7-39).

A severe intercarpal sprain (grade III) can closely mimic angular deformity in a foal. The potential for misdiagnosis becomes even greater if no telltale avul-



A **B**

Figure 7-25 • Close-up medial oblique **(A)** and dorsopalmar **(B)** views of an osteoarthritic radiocarpal joint *(emphasis zone)* show a deformed proximal radial carpal bone with a *conforming* bone fragment laterally *(emphasis zone).* This appearance is often seen with an old radial chip fracture in which the displaced fragment attaches to the adjacent synovium, becomes vascularized, and grows, eventually conforming to the nearby surface of the damaged carpal bone, promoting a localized hyperostosis.

sion fragment is present. Sanders-Shamis and Gabel described a day-old Appaloosa foal with a unilateral carpal valgus, eventually attributed to a ruptured medial collateral ligament torn from its insertion on the proximomedial aspect of the metacarpus.[24]

Carpal Subluxation

Baily and co-workers reported the radiographic appearance of various dislocations of the equine carpus, including the radiocarpal, intercarpal, and carpometacarpal joints. The carpometacarpal joint was dislocated most often, usually with one or more avulsion fractures of the flanking carpal or splint bones, the latter strongly suggesting sprained collateral ligaments (which insert on the proximal aspects of the second and fourth metacarpal bones).[25] In my experience, third-degree sprains of either collateral ligament resulting in dislocation are invariably attended by damage to one or more intercarpal ligaments (see Figure 7-39, second case).

▮▮▮ CARPAL ARTHRITIS: FACT AND FALLACY

Early Radiographic Detection of Osteoarthritis

Larsen and Dixon described a series of events, which if unchecked would eventually lead to an arthritic carpus, a process they termed the *carpitis syndrome.* Unfortunately, the first of these stages, *serous arthritis,* cannot be recognized radiographically because there are no visible bony abnormalities.[26] Thus, by the time osteoarthritis is detected radiographically, it may be too late to treat other than palliatively. This finding also raises further concern about what can be concluded from the radiographic information used in prepurchase evaluations.

Benefits of Postoperative Irradiation. Grant demonstrated that carpal irradiation following surgical removal of chip fractures had little or no effect on an

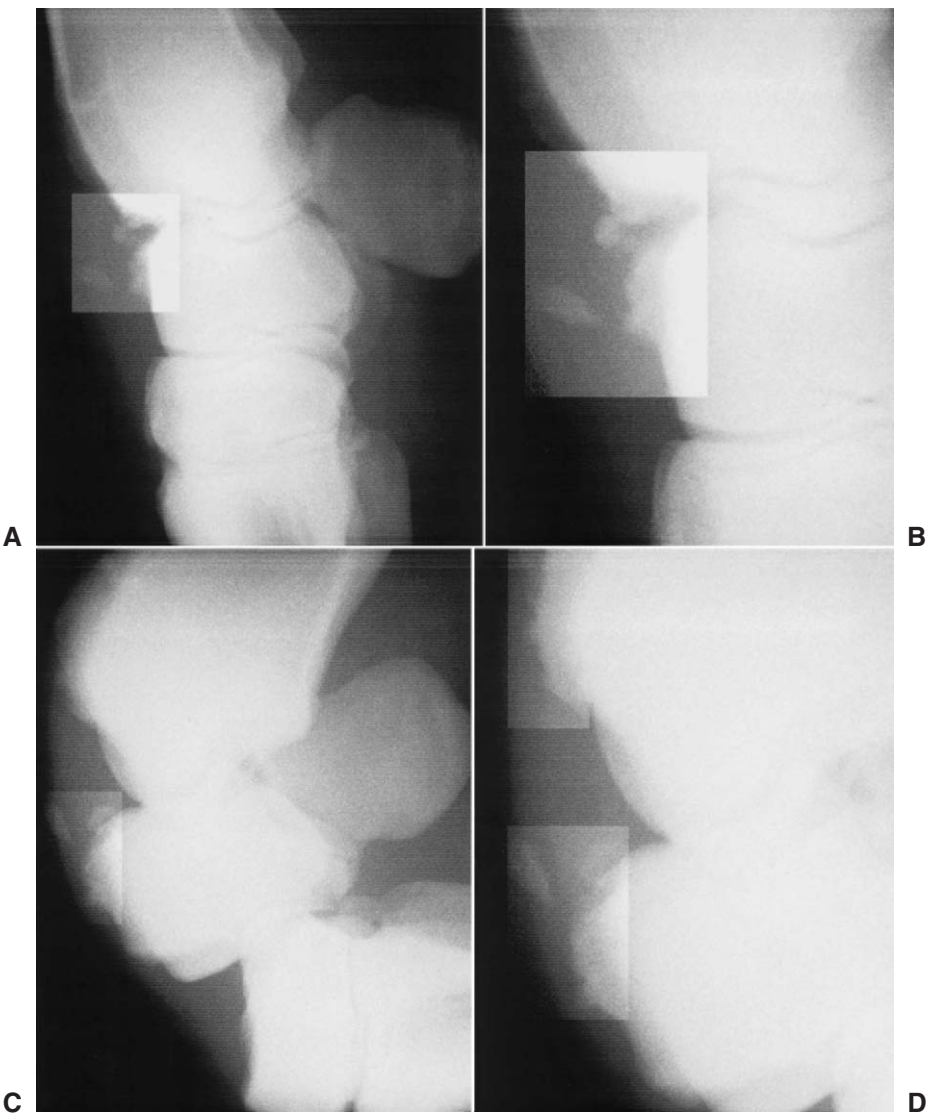


Figure 7-26 • Chronic radiocarpal injury: Distal radial and proximal radial and intermediate carpal bone fractures involving much of the dorsal half of the proximal carpus have led to severe osteoarthritis as seen in lateral **(A),** lateral close-up **(B),** flexed lateral **(C),** and flexed lateral close-up **(D).**

Continued.

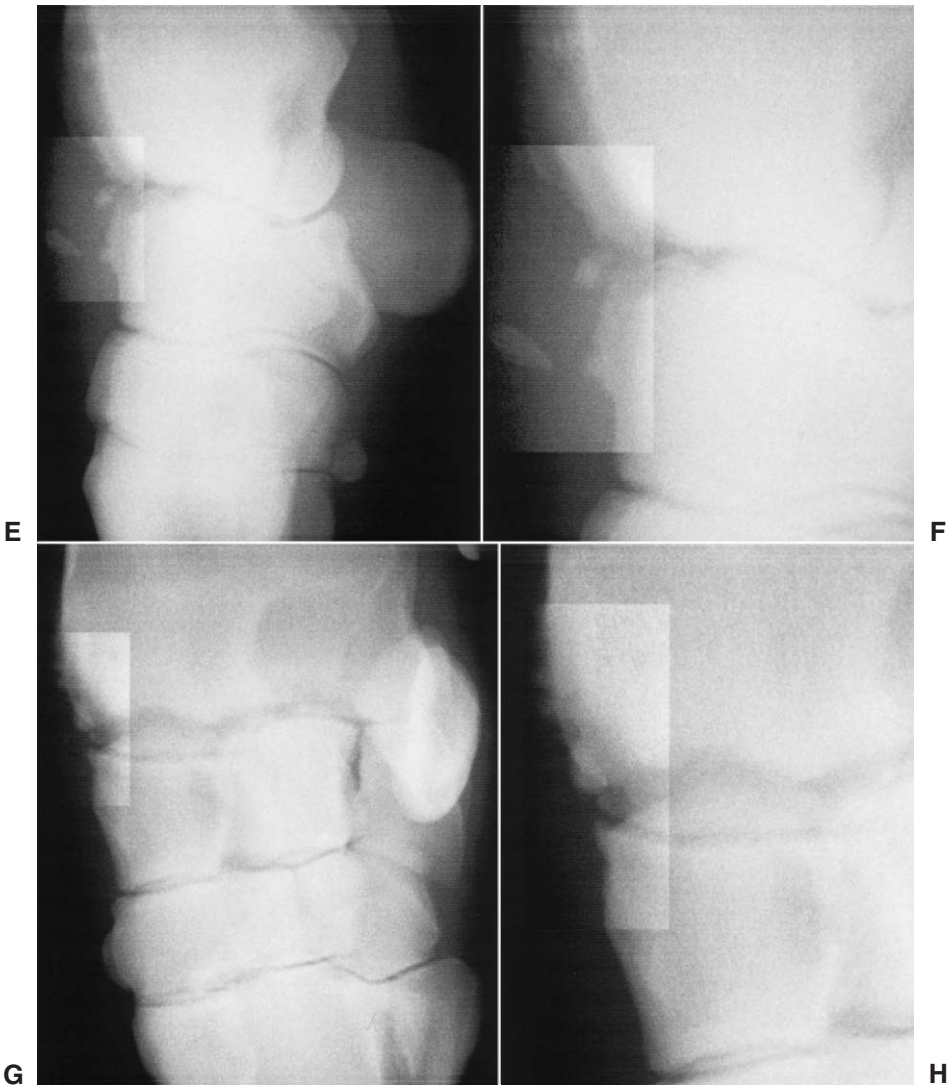


Figure 7-26, cont'd • Other views include lateral oblique **(E),** lateral oblique close-up **(F),** medial oblique **(G),** and medial oblique close-up **(H)** views. See emphasis zones.

individual horse's ability to return to racing.[27] Very little radiographic information on this important subject is available, for example, radiographs of similar carpal fractures showing that irradiated fracture beds fill in more rapidly than nonirradiated beds or that postoperative irradiation reduces adjacent bone deposition compared with nonirradiated injuries. Likewise few controlled studies have been reported showing that postsurgical irradiation prevents or reduces subsequent osteoarthritis.

Experimental Osteoarthritis

Chemically induced osteoarthritis in otherwise healthy horses or ponies is a far cry from the naturally occurring disease that often follows fracture.[28] Although such experimentation allows the investigator to isolate a single variable, cartilage damage, for example, it typically excludes many of the ancillary factors, which also contribute significantly to the end result. Another problem unique to chemically induced injuries is that they are, more often than not, incapable of rendering a realistic injury.

Carpal Canal Syndrome

Although carpal canal syndrome in horses has been compared with that in humans, the comparison is a loose one at best.[29] Typically carpal canal syndrome in people is due to overuse, most often related to word processing, and is a form of repetitive strain injury. In horses, dogs, and other animals, the problem is usually due to posttraumatic deformity of the carpal canal and the resultant effect on adjacent blood vessels and nerves. While repetitive strain injury leading to carpal canal syndrome in horses seems plausible, it remains unsubstantiated as far as I'm aware.

▮▮▮ STEROID ARTHROPATHY: DOES IT EXIST AS A RECOGNIZABLE RADIOGRAPHIC ENTITY?

In my opinion, intraarticular steroids do not cause a *specific*, *radiographically discernible* disease. Rather, steroids regularly administered in this fashion allevi-



Figure 7-27 • Dorsopalmar **(A),** lateral **(B),** medial oblique **(C),** lateral oblique **(D),** and proximal row skyline **(E)** views show the aftereffects of training and racing on an injured carpus: (1) collapse and osteoarthritis of the antebrachial carpal joint, (2) disintegration and dispersal of distal radial and proximal radial carpal bone fractures, (3) extensive soft-tissue calcification, and (4) new bone deposition on the dorsal surface of the radial carpal bone as a result of sprain of the radiointermediate ligament. The horse is chronically lame and no longer capable of racing effectively.



Figure 7-28 • Flexed lateral view of a chronic carpal injury shows a nonunion corner fracture of the distal radius and a large blocklike bone deposit on the dorsal surface of the intermediate carpal bone, effaced by dystrophic calcification. The horse currently trains and races and shows only mild, intermittent lameness.

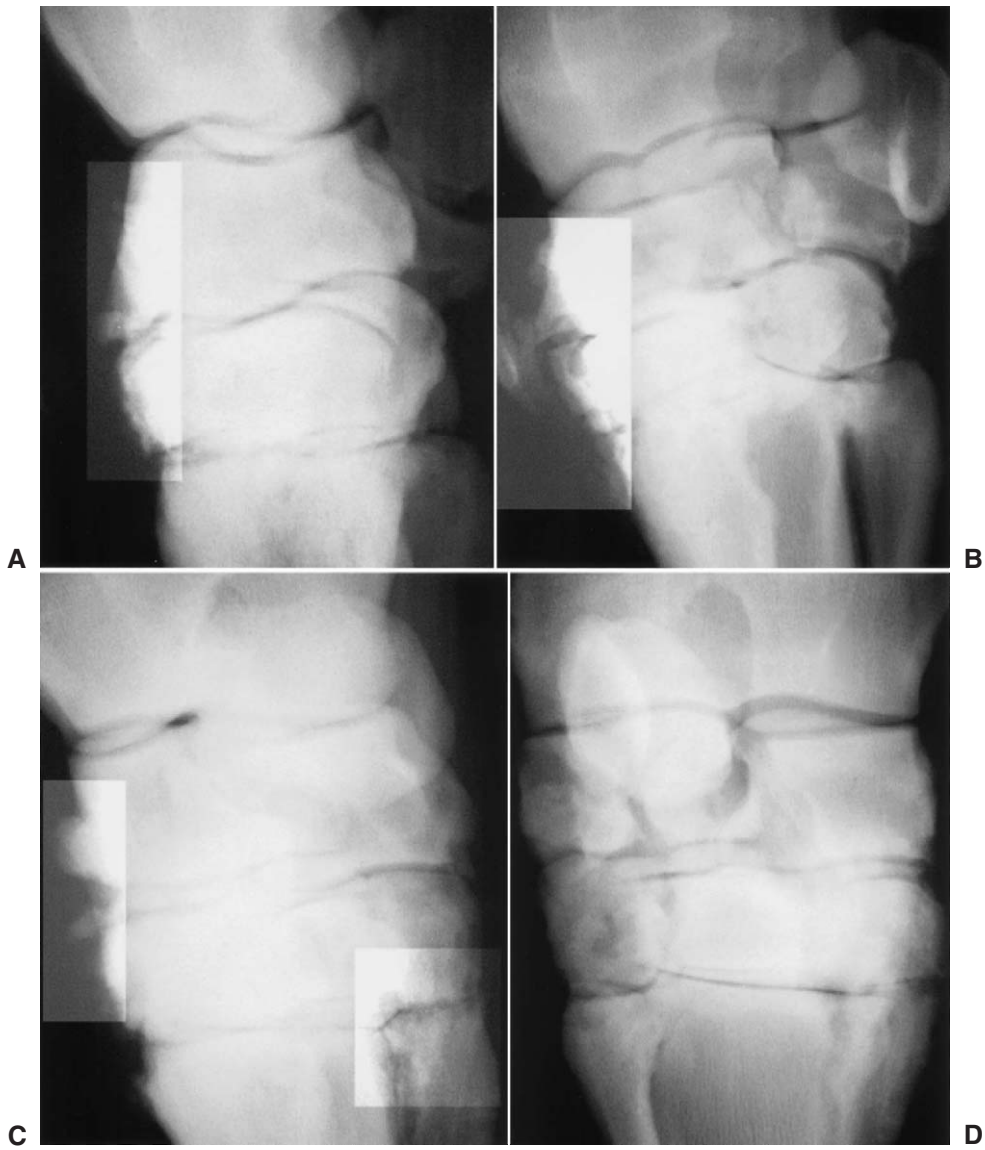


Figure 7-29 • Close-up lateral **(A),** medial oblique **(B),** lateral oblique **(C),** and dorsopalmar **(D)** views of a racing Quarter Horse whose carpus was repeatedly injured over a 14-year period show (1) severely deformed radial and intermediate carpal bones, (2) extraarticular bone fragments, (3) capsular calcification, and (4) osteoarthritis of the intercarpal and carpometacarpal joints. As a general rule, carpal deformities of this magnitude, especially involving the articular corners, are nearly always the result of previous fractures. See emphasis zones.

ate much of the inflammation associated with carpal fractures, allowing the horse to be trained and raced and, in so doing, potentially to aggravate its original injury. This repeated disturbance of damaged hard and soft joint tissues can greatly prolong the healing process or even prevent it altogether.

Injured racehorses treated in this fashion often display a dramatic loss of bone density in and around a fracture site that some attribute to intraarticular steroids, a so-called steroid arthropathy. However (and this is critical), injured carpal bones that have not been treated in such a manner may also develop a similar osteopenic appearance.

Theoretically, and depending on dosage and frequency of administration, intraarticular steroids can adversely affect cartilage metabolism, particularly the processes of repair and rejuvenation. In this respect, intraarticular steroids probably accelerate the development of osteoarthritis after one or more carpal chips, especially when combined with an inadequate postinjury recuperation period.[30]

Radiographs of *experimentally created* radiocarpal chip fractures treated postoperatively with high doses of intraarticular methylprednisolone show increased fragment and fracture-bed lucency compared with nontreated control fractures.

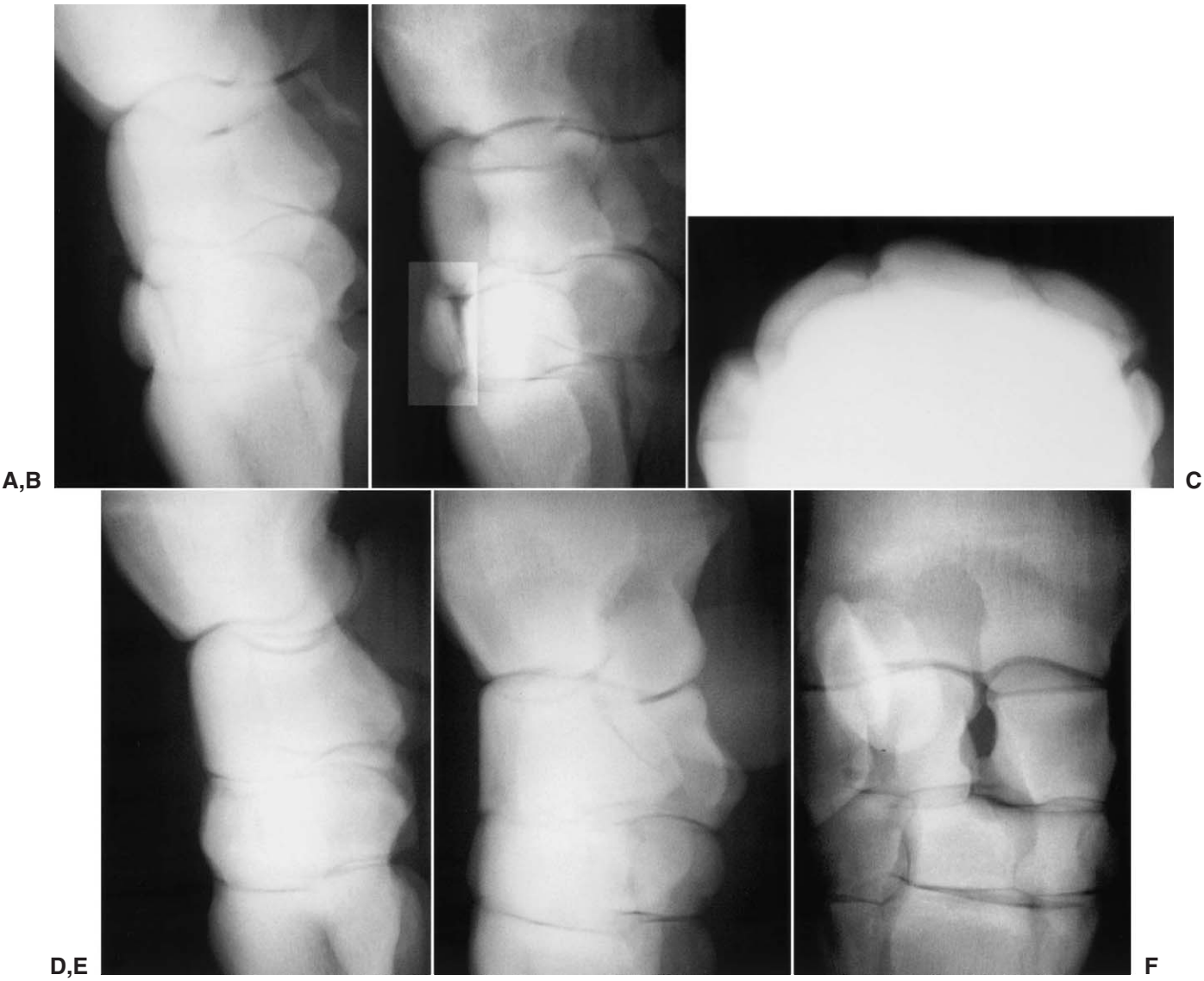


Figure 7-30 • Close-up medial oblique **(A),** medial oblique, customized angle **(B),** and distal row skyline—medial surface is to the right—**(C)** views show slab fracture of the medial aspect of the third carpal bone. Predictably, lateral **(D),** lateral oblique **(E),** and dorsopalmar **(F)** views fail to show the fracture.

▮▮▮ CARPAL DEFORMITY (ANGULAR DEFORMITY IN FOALS)

As mentioned in the opening chapter, most carpal deformities are due either to soft-tissue laxity or uneven distal radial growth, with deformed carpal bones accounting for comparatively few cases, contrary to some reports.[31] Radiographically establishing the location of abnormal angulation (distal radius or carpus) is easily achieved by visual inspection alone and in my experience does not require radiometrics (intersecting line analysis), as described by Fretz and co-workers.[32]

Carpal Bone Deformity Associated With Valgus or Varus Angulation

McLaughlin and co-workers reported the radiographic appearance of the carpi of six newborn foals born with crooked legs attributed to abnormal carpal bones. The bones in question appeared abnormally small (hypoplastic) and in some cases misshapen. Varying degrees of subluxation were present, presumably as the result of incongruity of the abnormal carpal bones. Among the individual carpal bones, the third carpal was affected most frequently. The authors characterized the carpal lesions as consistent with osteochondritis.[33]

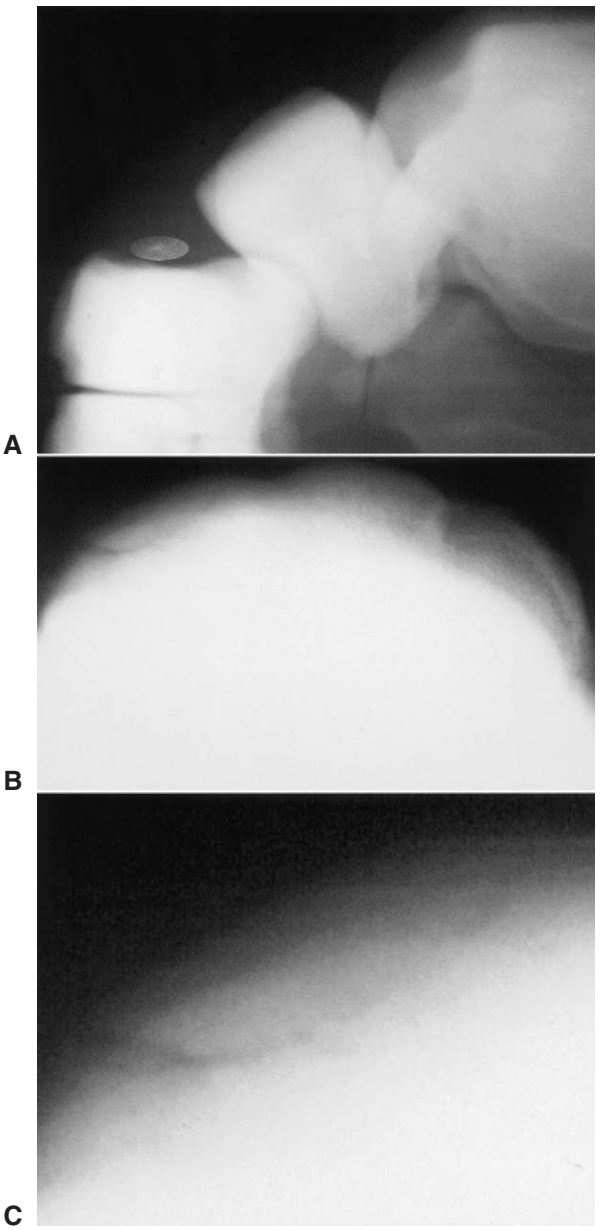


Figure 7-31 • Four standard views showed swelling over the dorsal surface of the distal intercarpal joint, but no fracture. However, a flexed lateral view of the injured carpus reveals mild subluxation and a small chip fracture (*emphasis zone*, **A**), presumably from the third or fourth carpal bone. Because of localized swelling over the face of the third carpal bone and profound lameness, a distal row skyline view was made that showed a large slab fracture **(B, C),** appreciable in no other projection.

Osteochondritis of the Carpus

Osteochondritis of the carpus can take a variety of forms, leading to both interior and exterior defects. In the fragmenting form of the disease, chunks of articular and nonarticular bone may break away, causing both mechanical and biochemical injury as well as incongruity and, later, osteoarthritis. In some instances entire carpal bones can disintegrate, as exemplified by the third carpal bone in Figure 7-40.

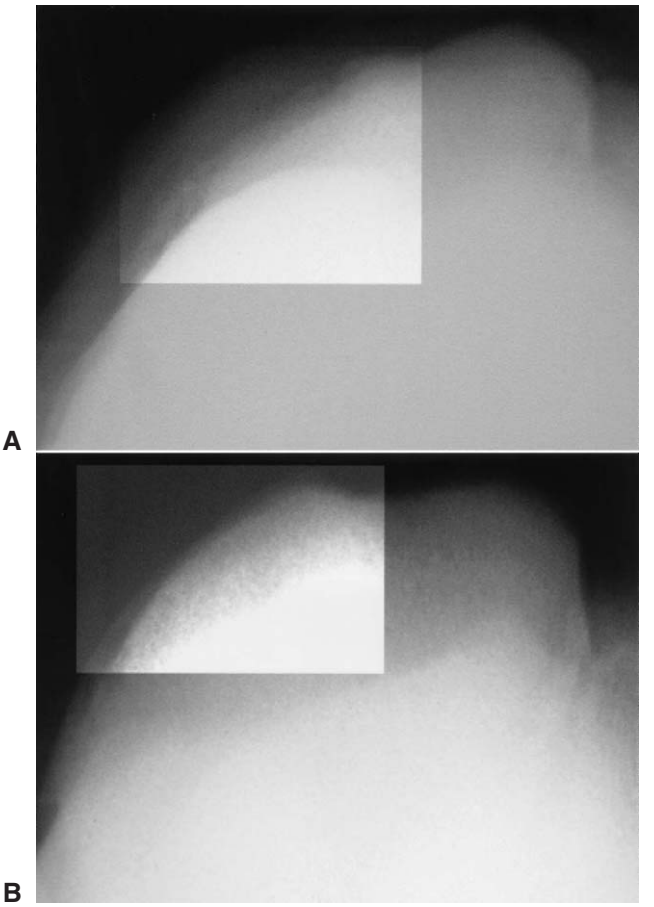


Figure 7-32 • Ultra-close-up skyline view **(A)** of the third carpal bone shows an old disintegrating slab fracture, intermingled with a faint callus. A normal third carpal skyline view is provided for comparison **(B).**

Blood-Borne Infection

The diagnosis of infectious arthritis (with or without associated osteomyelitis) is like so many other things radiographic, a contextual process involving clinicoradiographic disease patterns. For example, a foal with a painfully swollen carpal joint may have an injury or an infection. If more than one joint is swollen, the probability of infection is increased even before a radiograph is made. The same is true if the foal has a history of an umbilical infection. If radiographs show either intracapsular or extracapsular swelling, both differentials remain viable. However, if bone destruction is evident, infection becomes the more likely diagnosis (Figure 7-41).

▮▮▮ INJURIES AND OTHER SOFT-TISSUE DISORDERS OF THE CARPUS

Blunt Trauma, Cuts, and Punctures

Bruise. Extensive bruising can be surprisingly uncomfortable and, in the case of the lung (pulmonary contusion), even fatal. I have seen foals with such

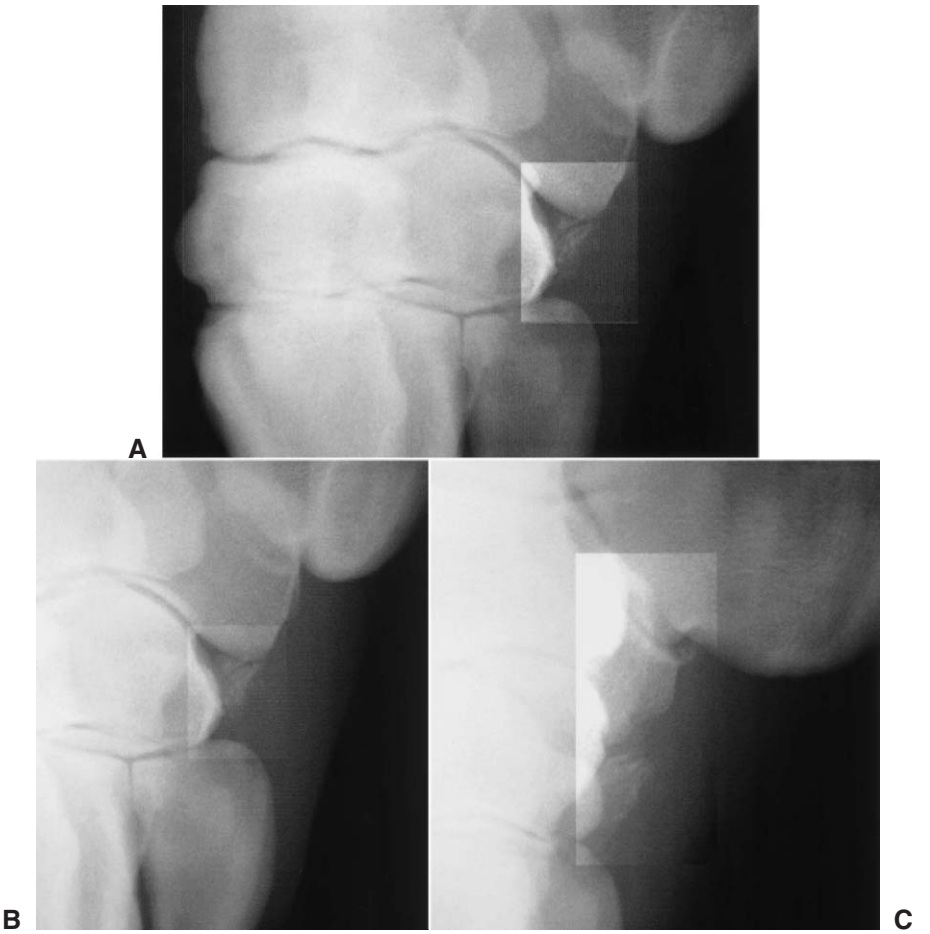


Figure 7-33 • Close-up **(A)** and ultra-close-up **(B)** medial oblique views show a tight cluster of bone chips midway between the ventral aspect of the ulnar carpal bone and palmar aspect of the fourth carpal bone, the result of a recent hyperextension injury. Another medial oblique close-up view **(C)** made from a slightly different angle shows a second group of fragments adjacent to the palmar aspect of the accessory ulnar joint.

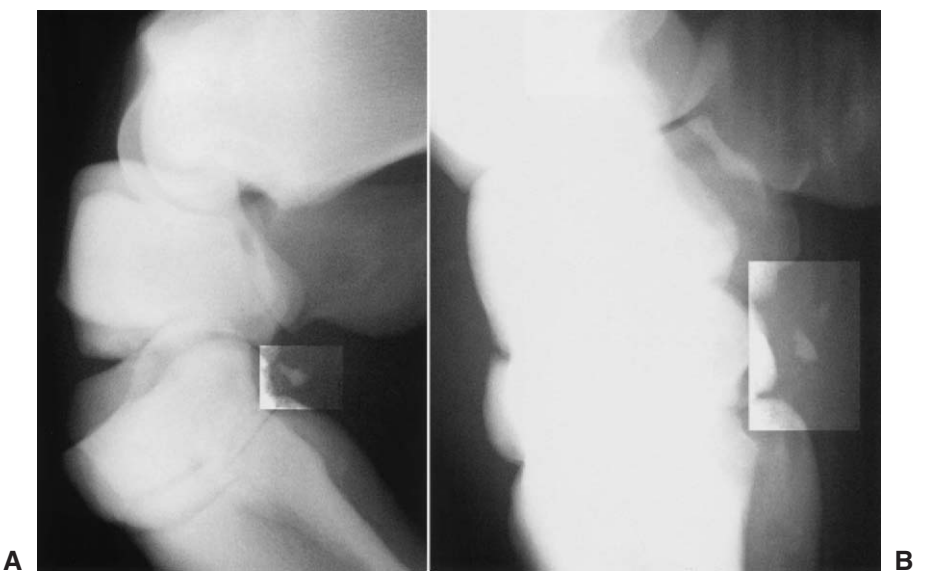


Figure 7-34 • Flexed lateral **(A)** and close-up medial oblique **(B)** views show a pair of fracture fragments believed to have originated from the palmar surface of the fourth carpal bone *(emphasis zone)*.

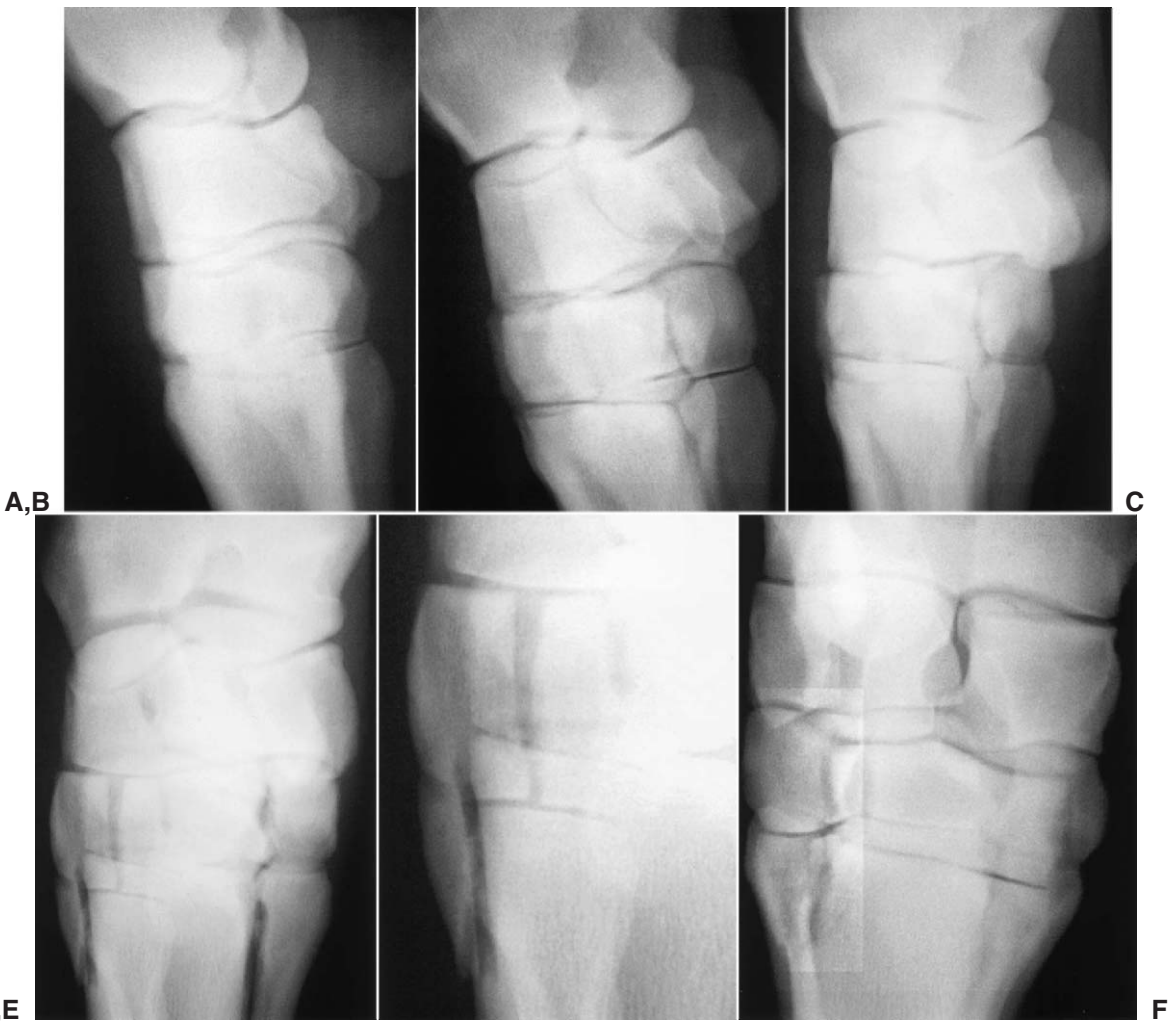


Figure 7-35 • Five different views of adjacent fourth carpal and metacarpal fractures, beginning with a standard lateral oblique projection **(A)** and gradually moving caudally **(B-E)** until a palmarodorsal view is obtained **(F).** Only the steep oblique, customized view **(D, E)** clearly shows the injury.



Figure 7-36 • Close-up dorsopalmar view of a displaced subacute fracture of the proximal aspect of the accessory carpal bone superimposed on the distal radius *(top right).*



Figure 7-37 • Close-up flexed lateral view shows a faint layer of new bone underlain by a band of reabsorption along the distal half of the dorsal edge of the radial carpal bone *(emphasis zone).* This appearance is characteristic of a subacute intercarpal sprain.

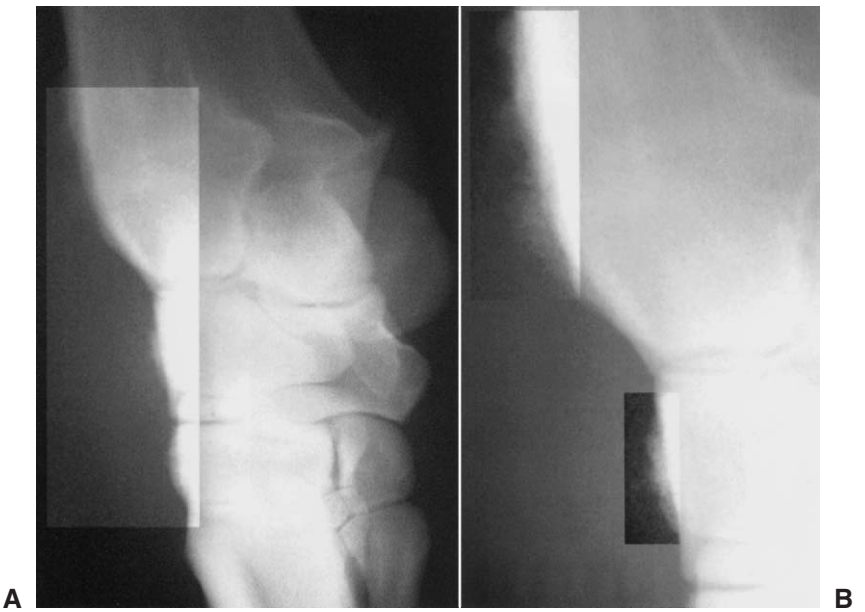


Figure 7-38 • Lateral oblique **(A)** and lateral oblique close-up **(B)** views show a mature bone deposit on the central face of the intermediate carpal bone, the result of an intercarpal sprain. A second, more recently formed bone deposit is located along the leading edge of the distal radius, caused by a partially torn joint capsule.



Figure 7-39 • Lateral oblique **(A)** and lateral oblique close-up **(B)** views show an uneven loss of bone density along the dorsal surfaces of the distal radius and intermediate carpal bone, the result of a recent sprain. Second case: Dorsopalmar **(C),** close-up dorsopalmar **(D),** lateral **(E),** and close-up lateral **(F)** views of a foal with a fresh sprain-fracture-dislocation of the intercarpal joint (medial is to the left). The dorsopalmar view shows a sprain-fracture-dislocation of the C3-4 joint resulting in medial subluxation of most of the distal carpal row and adjoining metacarpus. The lateral projection reveals further dislocation as indicated by a protruding third carpal bone and a third metacarpal corner fracture laterally.

extensive lower-limb bruising that I initially believed they had an infection. Severe bruises to the dorsal part of the carpus can also bruise the underlying tendons, causing pain and discomfort that can persist even after the swelling has subsided. The investigation of this sort of injury is best pursued with ultrasound once it has been established that there is no fracture or dislocation.

Hematoma. According to Larsen and Dixon, carpal hematomas usually result from ruptured branches of the *accessory cephalic vein* overlying the medial aspects of the distal radius and proximal carpus.[26] Such hematomas often occur in Standardbreds, the result of forelimb interference. Large hematomas may in turn lead to further interference injury because the swollen area extends even farther dorsally (Figure 7-42).

Hygroma. Hygromas occasionally develop on the dorsal surface of the carpus and are typically preceded by a blunt injury. Diagnosis is usually made on the basis of a nonpainful fluctuant swelling that sonographically appears as a large fluid-filled sac. If ultrasound is not available, cavography can also be used to confirm the diagnosis (Figures 7-43 and 7-44).

Deep Cuts, Puncture Wounds, and Draining Sinuses. Carpal lacerations can lead to septic tenosynovitis, arthritis, or osteomyelitis, depending on the depth and location of the wound. Honnas and co-workers described septic tenosynovitis in 25 horses, including involvement of the tendon sheaths of the extensor carpi radialis, long digital, and common digital extensors (Figures 7-45 through 7-47).[34] Deep punctures can cause all these problems as well as infective sequestra (Figure 7-48).



Figure 7-40 • Close-up lateral **(A),** dorsopalmar **(B),** and dorsopalmar close-up **(C)** views of the carpus of an immature foal with a minimally displaced fracture of the third carpal bone, believed to be due to osteochondritis.

Radiographically Visible Soft-Tissue Landmarks (Skin Markers)

When radiographing the carpus to see whether a soft-tissue wound or draining sinus has also affected the underlying bone or joint, it is useful to place a small metallic object on the skin (Figure 7-49) to locate the area of interest precisely, bearing in mind that all lesions do not necessarily develop directly beneath the surface of a wound. A hot lamp is indispensable in identifying soft-tissue defects that may not be visible with high- contrast images (Figure 7-50). In my experience, carpal sinography is unsurpassed in establishing the origin of draining carpal sinuses. For examples of sinographic diagnosis, see the following section on carpal contrast studies.

Carpal Tendonitis

Mason described chronic tenosynovitis involving two of the three principal extensor tendons/tendon sheaths of the equine carpus: the extensor carpi radialis and lateral digital extensor. Involvement of the common digital extensor was not encountered. As might be expected, no relevant radiographic abnormalities were found.[35]

In most operated cases, a discrete tendon lesion was discovered, including (1) a torn tendon sheath, (2) adhesions between the extensor tendon and its sheath, (3) villonodular synovitis, (4) multiple rafts of free-floating granulation tissue within the tendon sheath, and (5) a single mass of granulation tissue adhered to the inner surface of the tendon sheath. The author theorized that the presence of specific lesions in these cases likely explained why earlier symptomatic treatment (drainage and corticosteroid installation) failed to provide more than temporary relief.

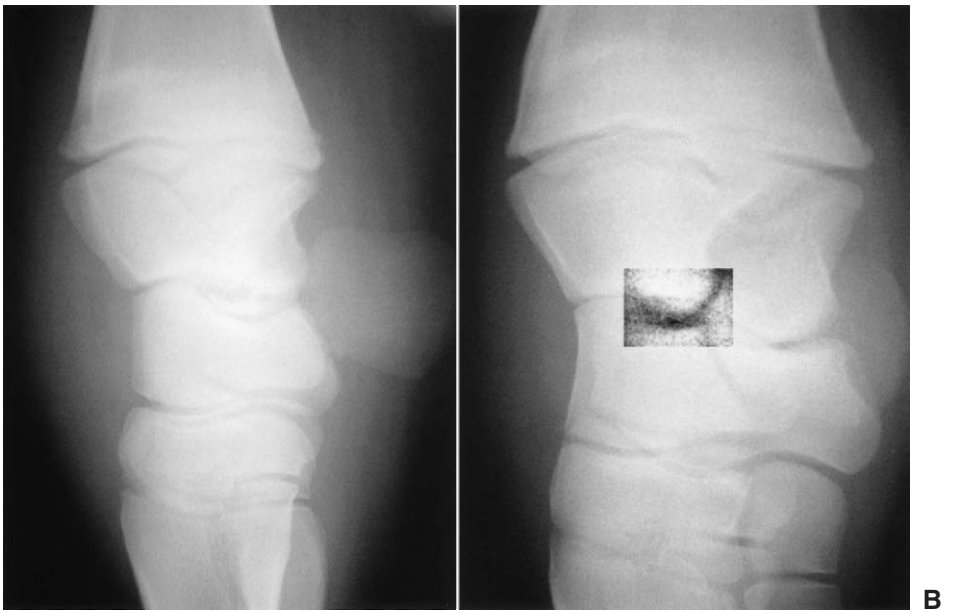


Figure 7-41 • Lateral view **(A)** of a massively swollen carpus, the result of an earlier umbilical infection. A lateral oblique projection **(B)** shows localized bone loss *(emphasis zone)* in the central portion of the radiocarpal joint.



Figure 7-42 • Lateral view of a large hematoma centered over the distal carpal row, which developed while attempting to drain fluid percutaneously from a swollen tendon sheath.



Figure 7-43 • Medial oblique view of a hygroma centered over the proximal carpal row.

▮▮▮ MISCELLANEOUS HARD- AND SOFT-TISSUE DISEASES

Carpal "Spavin"

Carpal "spavin," as a colleague first termed it, is a painful, often debilitating disease of the medial carpometacarpus that begins in the medial splint and gradually progresses proximally, eventually involving the carpometacarpal joint and overlying second carpal bone. Most of the horses I have seen with this disease are mature animals with a history of an acute lameness. Many, but not all, are Arabians. Most appear to recover only to become lame again after a few months.

Three distinctive radiographic features are associated with this disease, shared only by tarsal bone spavin (Figures 7-51 and 7-52):

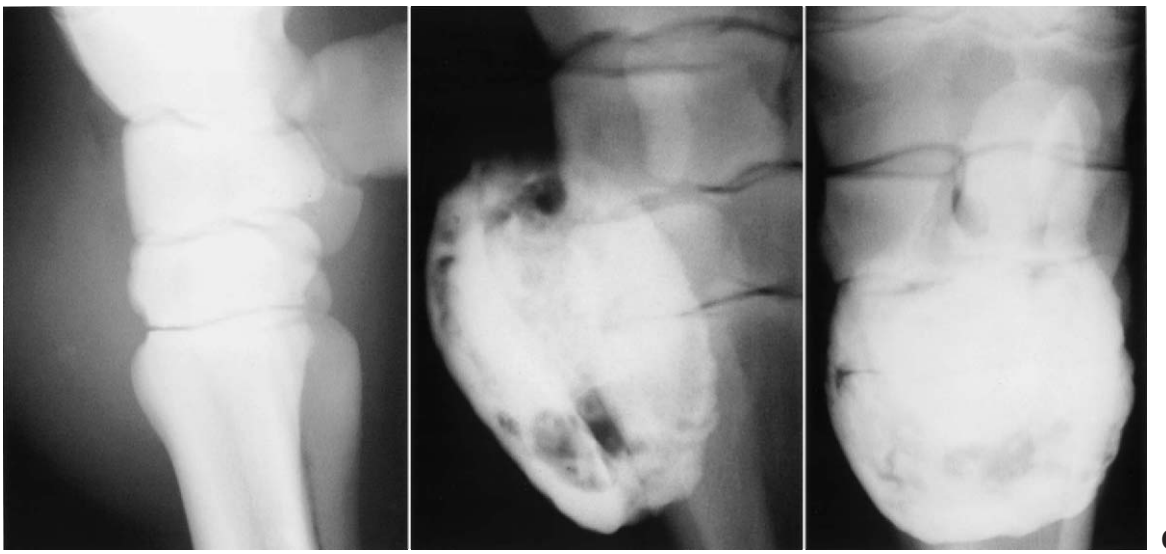


Figure 7-44 • Close-up lateral view **(A)** of a large carpal hygroma, the result of striking a rail a month earlier. Medial oblique **(B)** and dorsopalmar **(C)** cavograms show a large contrast-filled cavity containing numerous filling defects representing peripheral blood clots and a centrally located tendon.



Figure 7-45 • Customized medial oblique sinogram shows opacification of the extensor tendon sheath after injection of a diagnostic iodine solution into a draining sinus on the cranial surface of the radial midbody. The sheath is ruptured distally and is being distorted by a large communicating abscess.

1. A distinctive, feathered new bone deposit on the proximolateral aspect of the second metacarpal bone (medial splint bone)
2. Collapse of the medial edge of the carpometacarpal joint
3. Focal subchondral bone loss on either side of the involved portion of the carpometacarpal joint, which in the case of the second carpal bone may extend quite deeply.

Malone and colleagues theorized that the disease might be caused by a congenital absence of a palmar articulation between the second and third metacarpal bones, predisposing the horse to sprain or entrapment of the medial palmar ligament.[36] This hypothesis remains unproven.

Synovioma

True synoviomas—masses of inflamed, hypertrophic synovial tissue, also termed villonodular synovitis—are typically found in the dorsal aspect of the fetlock joint but only occasionally in the carpus. Sonography is the optimal means of diagnosis, although arthrography can also be used if ultrasound is not available. A triangular bone deposit on the dorsal surface of the distal radius, level with the growth scar, constitutes circumstantial evidence for a synovioma but does not confirm it.

Bursitis

Swelling localized to the medial aspect of the carpus often signals inflammation of the bursa of the extensor carpi obliquis (abductor pollicis longus).[37] Although theoretically possible using sonography, this is a difficult diagnosis to make consistently.

Foreign Body

Burba reported a tooth fragment imbedded in the soft tissue of the proximomedial aspect of the metacarpus associated with a draining wound, but no lameness was noted. Radiographically the foreign body

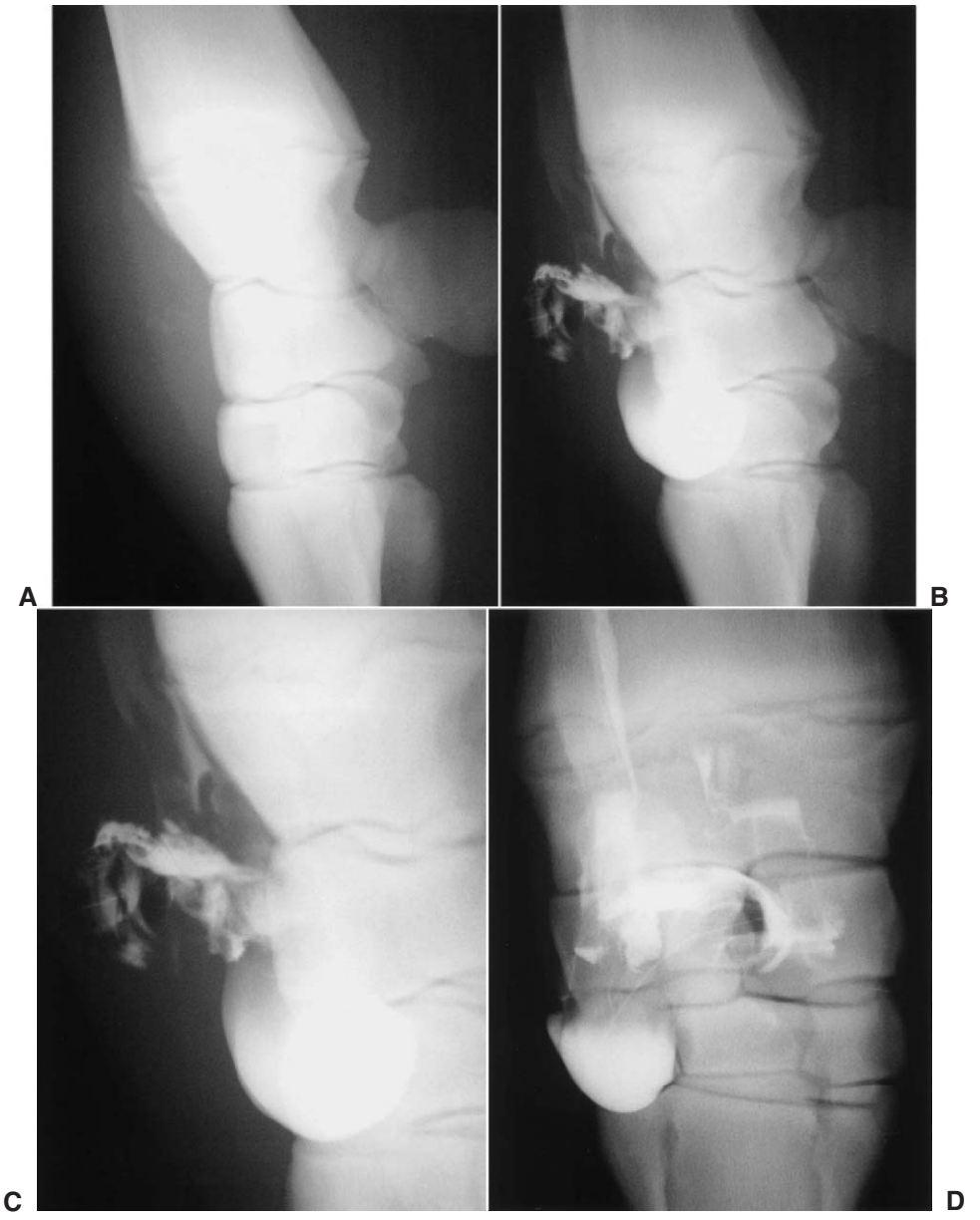


Figure 7-46 • Plain film **(A)** and multiple sinograms: lateral **(B),** close-up lateral **(C),** and dorsopalmar **(D)** views of a badly infected carpus caused by a deep stake wound a month earlier. Contrast solution passed from the surface sinus through a thick irregular channel to the face of the intermediate carpal bone. Contrast has also entered the nearby extensor sheath, extending proximally and distally and, in the latter instance, forming a large hernia-like pouch. No contrast has entered the interior of the carpus.

appeared as a conical density partially superimposed on the outer cortex of the bone and at first glance resembled an osteophyte.[38]

▮▮▮ CARPAL CONTRAST STUDIES: ARTHROGRAPHY, CAVOGRAPHY, AND SINOGRAPHY

Carpal Arthrography

Dik reported the use of three different types of arthrography (negative, positive, and double contrast) in a variety of equine joints, including the carpus.[39]

Negative- and positive-contrast arthrography proved feasible in standing horses, but double contrast required that the horse be anesthetized. Single-contrast examinations were suited to both large and small joints, but double-contrast studies proved to be only diagnostic in large-volume joints where there was sufficient capacity to accommodate an even distribution of both air and iodine (an uneven distribution of contrast agents, as encountered in smaller joints, was often interpreted as filling defects, resulting in misdiagnosis (false-positive and false-negative).

In general, air studies were of little value but were capable of distinguishing between intraarticular and extraarticular bone fragments as well as low-density

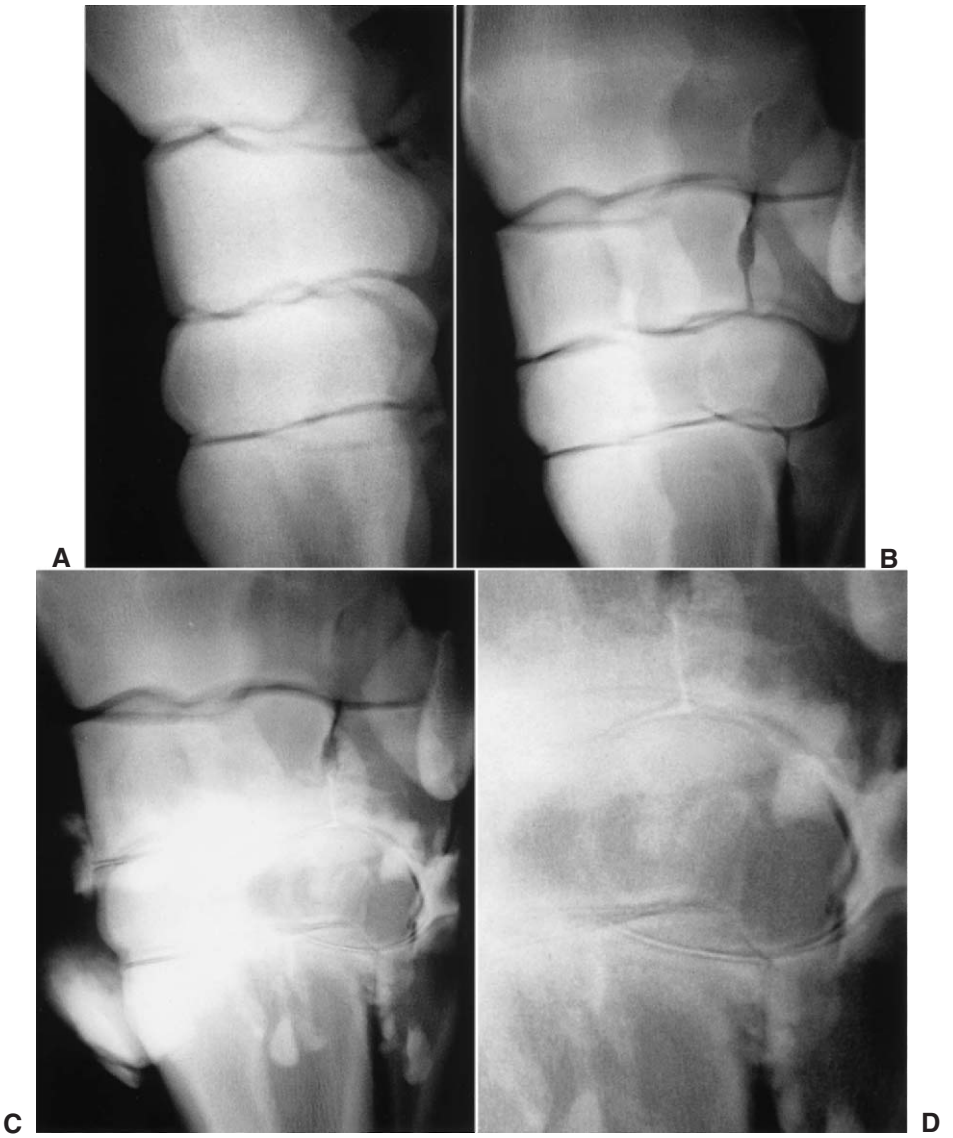


Figure 7-47 • Close-up lateral **(A)** and medial oblique **(B)** plain films of a badly lacerated carpus currently draining bloody synovial fluid. Medial oblique **(C)** and close-up medial oblique **(D)** sinograms shows contrast solution entering both the intercarpal and carpometacarpal joints and, in the process, outlining the fourth carpal bone.



Figure 7-48 • Medial oblique view of a horse that recently received a deep puncture wound to the caudolateral aspect of its carpus, which is now infected as indicated by a small sequestrum within a large communicating involucrum. The arthritic radiocarpal joint is the result of a previous racing injury.



Figure 7-49 • Medial oblique view of the carpus of a horse that recently sustained a deep puncture wound that is now draining. The lead marker identifies the site of the draining sinus, allowing a more focused examination of the directly underlying bone.

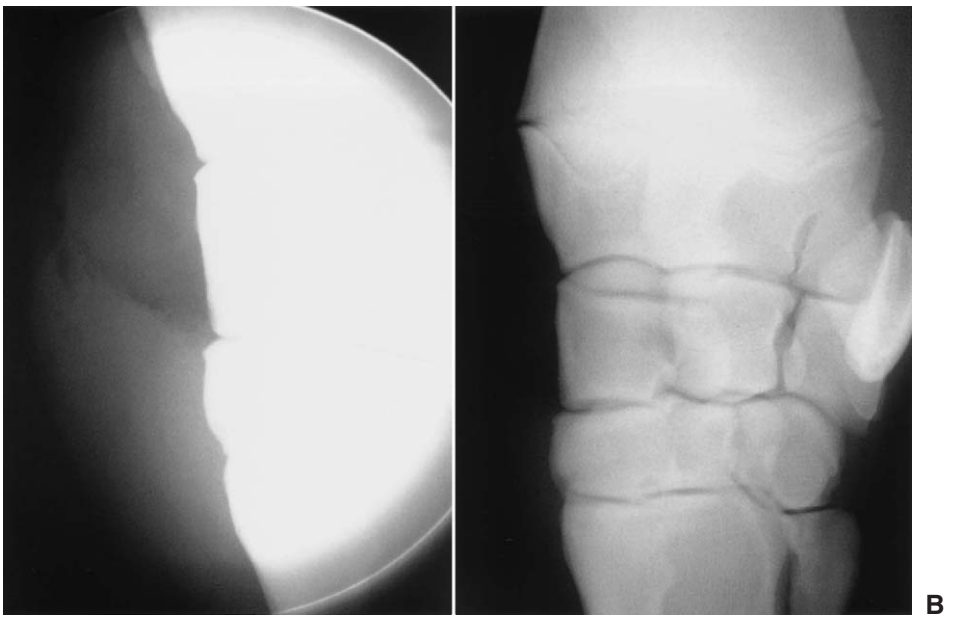


Figure 7-50 • Medial oblique view of the carpus of a horse draining bloody synovial fluid, with **(A)** and without **(B)** high-intensity illumination, shows an irregular soft-tissue band caused by a deep cut extending into the intercarpal joint but not as yet producing any changes on the surface of the underlying bone.

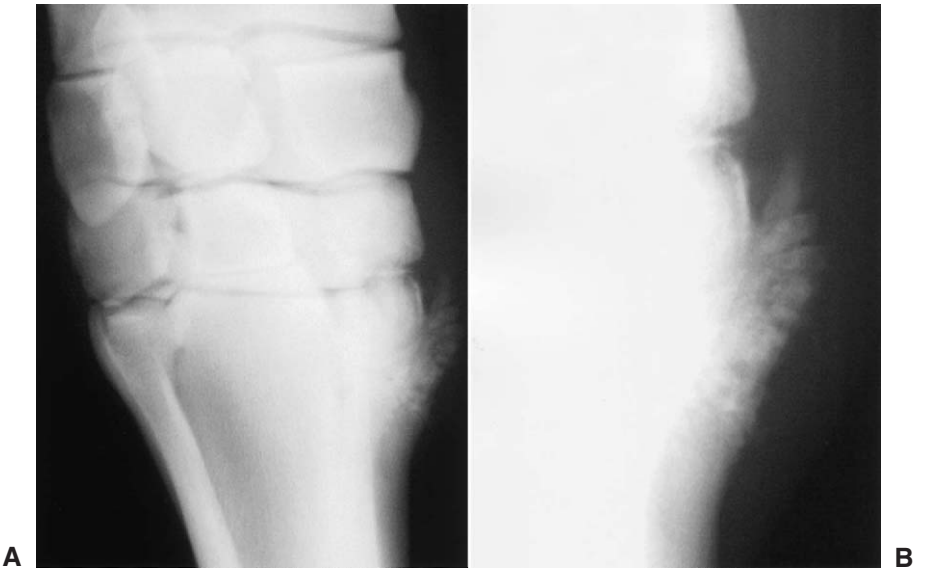


Figure 7-51 • Early carpal spavin. Mildly oblique dorsopalmar **(A)** and close-up dorsopalmar **(B)** views of the distinctive feathered lesion that characterizes this unique disorder.

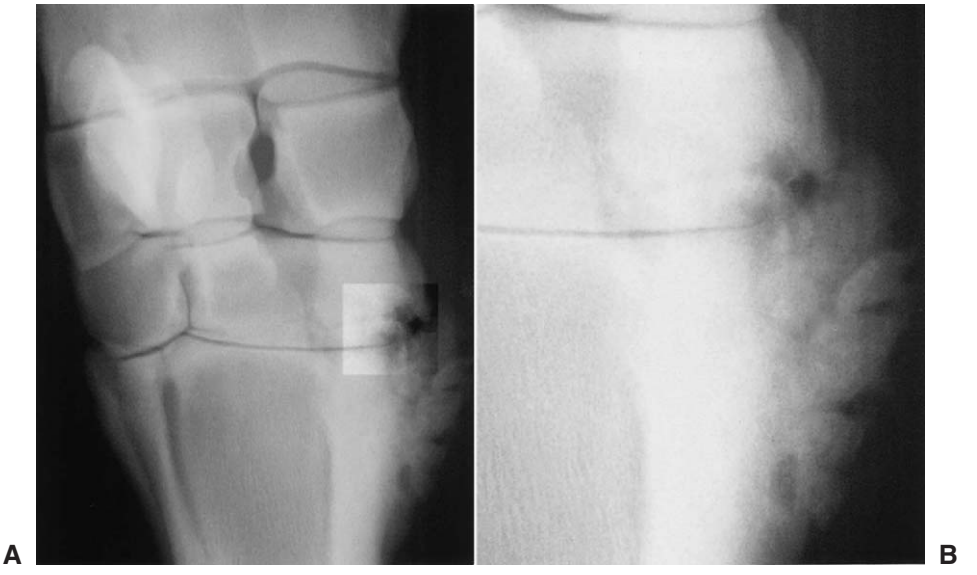


Figure 7-52 • Advanced carpal spavin. Slightly oblique dorsopalmar **(A)** and close-up dorsopalmar oblique **(B)** views show the three classic features of this unique disease: (1) a distinctive feathered lesion on the proximolateral aspect of the medial splint bone, (2) collapse of the medial side of the carpometacarpal joint, and (3) localized bone loss in the overlying second carpal bone.

joint "mice." Using intraarticular opaques, it was possible to identify the following abnormalities: (1) villonodular synovitis, (2) a ruptured or herniated joint capsule, (3) communication between a joint and an adjacent bone cyst (indicating a loss of integrity in the overlying articular cartilage), and (4) cystic periarticular soft-tissue masses.

Double-contrast arthrography provided more detailed information about the articular cartilage and synovial lining than single-contrast studies, although they were technically more difficult to perform.

Carpal Cavography

Carpal cavography, previously illustrated in Figure 7-44, is the simplest of carpal contrast studies. Its primary purpose is to define the limits of a fluid-filled cavity and to establish whether any local communications are present, for example, with a nearby tendon sheath or joint. Generally ultrasound will do a superior job in establishing the interior anatomy of the cavity and the composition of its content, whereas a cavogram will provide a better overall perspective on the lesion. Thus I employ both procedures because of their complementary nature.

Carpal Sinography

Sinography is similar to cavography inasmuch as both employ iodinated contrast media to explore the subcutaneous tissues. However, sinography is usually prompted by the presence of a draining sinus rather than by a closed fluctuant swelling. Here again, ultrasound and sinography form the perfect imaging partnership: sinography to map the extent of the lesion, and in particular its drainage system, and ultrasound to reveal its interior detail.

Carpal Sonography

Tinbar and co-workers described the normal sonographic appearance of the horse's carpus.[40] They were easily able to identify the most prominent regional tendons: (1) the extensor carpi radialis and (2) the common digital extensor as well as their associated tendon sheaths. More difficult to identify were the smaller tendons: (1) extensor carpi obliquus, (2) lateral digital extensor, and (3) ulnaris lateralis. Other visible structures included (1) the lateral collateral ligament (2) the carpal joint capsule, and (3) the articular cartilage of the distal radius.

▮▮▮ COMPUTED TOMOGRAPHY AND MAGNETIC RESONANCE OF THE CARPUS

Kaser-Hotz and co-workers reported the computed tomographic (CT) and magnetic resonance imaging (MRI) appearances of a single disarticulated equine carpus (in a 3-year-old Thoroughbred).[41] Others have made passing reference to such examinations in general review articles, but to date the use of CT and MRI on living horses is not widespread, in part because of the logistical problems associated with moving the horse to and from the gantry and the labor-intense nature of anesthetic induction and recovery in horses. It is difficult to draw nontheoretical conclusions about the relative merits of these procedures based on a metanalysis derived from the current literature.

References

1. Dixon RT: Radiography of the equine carpus, *Aust Vet J* 45:171, 1969.
2. O'Brien TR: Radiography in equine carpal lameness, *Cornell Vet* 61:646, 1971.
3. O'Brien TR, Morgan JP, et al: Radiography in equine carpal lameness, *Cornell Vet* 61:666, 1971.
4. O'Brien TR: Radiographic diagnosis of "hidden" lesions of the third carpal bone, *Proc Ann Meeting Am Assoc Equine Pract* 343, 1977.
5. Uhlhorn H Ekman S, et al: The accuracy of the dorsoproximal-dorsodistal projection in assessing third carpal bone sclerosis in Standardbred trotters, *Vet Radiol Ultrasound* 39:412, 1998.
6. Uhlhorn H, Eksell P: The dorsoproximal-dorsodistal projection of the distal carpal bones in horses: an evaluation of different beam-cassette angles, *Vet Radiol Ultrasound* 40:480, 1999.
7. Spectht TE, Nixon AJ: What is your diagnosis? *J Am Vet Med Assoc* 196:1859, 1990.
8. Losonsky JM, Kneller SK, Pijanowski SK: Prevalence and distribution of the first and fifth carpal bones in Standardbred horses as differentiated by radiography, *Vet Radiol Ultrasound* 29:236, 1988.
9. Martens P: Identification of an ossicle associated with the palmar aspect of the carpus in the horse, *Vet Radiol Ultrasound* 40:342, 1999.
10. Dietze AE, Rendano VT: Fat opacities dorsal to the equine antebrachiocarpal joint, *Vet Radiol* 25:205, 1984.
11. Lindsay WA, Horney FD: Equine carpal surgery: a review of 89 cases and evaluation of return to function, *J Am Vet Med Assoc* 179:682, 1981.
12. Palmer SE: Prevalence of carpal bone fractures in Thoroughbred and Standardbred racehorses, *J Am Vet Med Assoc* 188:1171, 1986.
13. Sedrish SA, Martin GS, Pechman RD: What is your diagnosis? *J Am Vet Med Assoc* 209:1237, 1996.
14. DeHaan CE, O'Brien TR, Koblik PD: A radiographic investigation of third carpal bone injury in 42 racing Thoroughbreds, *Vet Radiol* 28:88, 1987.
15. Park RD, Morgan JP, O'Brien T: Chip fractures in the carpus of the horses: a radiographic study of their incidence and location, *J Am Vet Med Assoc* 157:1305, 1970.
16. Thrall DE, Lebel JL, O'Brien TR: A five-year survey of the incidence and location of equine carpal chip fractures, *J Am Vet Med Assoc* 159:1366, 1971.
17. Wilke M, Nixon AJ, et al: Fractures of the palmar aspect of the carpal bones in horses: 10 cases (1984-2000), *J Am Vet Med Assoc* 219:801, 2001.
18. Dixon RT: Radiography of the equine carpus, *Aust Vet J* 45:171, 1969.

19. Wyburn RS, Goulden BE: Fractures of the equine carpus: a report on 57 cases, *N Z Vet J* 22:133, 1974.
20. Easley KJ, Schneider JE: Evaluation of a surgical technique for repair of equine accessory carpal bone fractures, *J Am Vet Med Assoc* 178:219, 1981.
21. Gerros TC: What is your diagnosis? *J Am Vet Med Assoc* 184:996, 1984.
22. Young A, O'Brien TR, Pool RR: Exercise-related sclerosis in the third carpal bone of the racing Thoroughbred, *Proc Ann Meeting Am Assoc Equine Pract* 339, 1988.
23. Newell SM, Robersts RE, Baskett A: Presumptive tenosynovial osteochondromatosis in a horse, *Vet Radiol Ultrasound* 37:112, 1996.
24. Sanders-Shamus M, Gabel AA: Surgical reconstruction of a ruptured medial collateral ligament in a foal, *J Am Vet Med Assoc* 193:80, 1988.
25. Baily JV, Barber SM, et al: Subluxation of the carpus in thirteen horses, *Can Vet J* 25:311, 1984.
26. Larsen LH, Dixon RT: Management of carpal injuries in the fast-gaited horse, *Aust Vet J* 46:33, 1970.
27. Grant B: Repair mechanisms of osteochondral defects in horses: a comparative study of untreated and x-irradiated defects, *Proc Ann Meeting Am Assoc Equine Pract* 95, 1975.
28. McIlwraith CW, Van Sickle RW: Experimentally induced arthritis of the equine carpus: histologic and histochemical changes in articular cartilage, *Am J Vet Res* 42:209, 1981.
29. Mackay-Smith MP, Cushing LS, Leslie JA: Carpal canal syndrome in horses, *J Am Vet Med Assoc* 160:993, 1972.
30. Owan RH, Marsh JA, et al: Intra-articular corticosteroid- and exercise-induced arthropathy in a horse, *J Am Vet Med Assoc* 184:302, 1984.
31. Leitch M: Angular limb deformities arising at the carpal region in foals, *Comp Cont Educ* 11:S39, 1979.
32. Fretz PB, Turner AS, Pharr JW: Retrospective comparison of two surgical techniques for correction of angular deformities in foals, *J Am Vet Med Assoc* 172:281, 1978.
33. McLaughlin BG, Doige CE, et al: Carpal bone lesions associated with angular limb deformities in foals, *J Am Vet Med Assoc* 178:224, 1981.
34. Honnas CM, Schumacher J, et al: Septic tenosynovitis in horses: 25 cases (1983-1989), *J Am Vet Med Assoc* 199:1616, 1991.
35. Mason TA: Chronic tenosynovitis of the extensor tendons and tendon sheaths of the carpal region in the horse, *Equine Vet J* 9:186, 1977.
36. Malone ED, Les CM, Turner TA: Severe carpometacarpal osteoarthritis in older Arabian horses, *Vet Surg* 32:191, 2003.
37. Sack WO: Subtendinous bursa on the medial aspect of the equine carpus, *J Am Vet Med Assoc* 168:315, 1976.
38. Burba DA: What is your diagnosis? *J Am Vet Med Assoc* 204:1926, 1992.
39. Dik KJ: Equine arthrography, *Vet Radiol* 25:93, 1984.
40. Tinbar M, Kaser-Hotz B, Auer JA: Ultrasonography of the dorsal and lateral aspects of the equine carpus: technique and normal appearance, *Vet Radiol Ultrasound* 34:413, 1993.
41. Kaser-Hotz B, Sartoretti-Schefer S, Weiss R: Computed tomography and magnetic resonance imaging of the normal equine carpus, *Vet Radiol Ultrasound* 35:457, 1994.

Chapter 8

Radius and Ulna

THE STANDARD RADIUS/ULNA SERIES

The standard radius and ulna series consists of two views: a craniocaudal and a lateral. If possible, portions of the elbow and carpus should be included for anatomic reference. Proximal swelling may make it impossible to obtain standard full-length views, especially proximally, necessitating some degree of customization.

DISTAL RADIAL GROWTH PLATE CLOSURE

It is generally accepted that racehorses should not engage in hard training or racing until they are skeletally mature, lest they injure their growth cartilages.[1] One measure of such maturation is the distal radial growth plate, which usually closes, as indicated by radiographic disappearance, somewhere between 24 and 30 months of age, depending on breed, and to a lesser extent on gender.

Customarily, a fully open distal radial growth plate is categorized by the capital letter *C*, the partially open plate by the letter *B*, and the completely closed physis by the letter *A* (Figures 8-1 through 8-4). A plus or minus sign can be added in the case of individuals falling in between primary categories, for example, A– or C+ (Figure 8-5).

When grading distal radial growth plate closure in the dorsopalmar projection, it is necessary to take beam centering and projection angle into consideration. Either variable may cause a fully open growth plate to appear partially closed or a partially open physis to appear closed (Figure 8-6).

Growth Plate Closure Times

Radial growth plate closure times have been reported for various breeds of horses, including Brazilian and Australian Thoroughbreds, Arabians, Italian Trotters, and Brazilian Mangalargas (Box 8-1).[2]

NORMAL RADIOGRAPHIC VARIATION OF THE DISTAL ULNA

Morgan wrote the definitive paper on normal anatomic variation in the distal ulna of the horse.[3] The true importance of this article lies in its pointing out the resemblance of many of the described normal variations to common injuries in the horse such as fracture, infection, and muscle tears (Figure 8-7).

RADIAL AND ULNAR FRACTURES

Radial Fracture: Some General Considerations

Radial fractures in adult horses are often severely comminuted, making plating impossible, especially if one or both metaphyses are involved. The most common way of reducing radial body fractures in adult horses is to use paired dynamic compression plates: one on the cranial aspect and the other on the lateral or medial side of the bone, the latter acting as a neutralization plate. A similar fracture in foals usually requires only a single cranial plate. In the event that there is insufficient bone to secure a neutralization plate, a cable cerclage system may be used instead. A *cable cerclage system* is one in which the cerclage wires are wrapped around the fractured bone as well as the attached compression plate. In the case of radial fractures, this may also include the adjacent ulna.[4]

The Role of Nuclear Medicine

In the event of an acute lameness in which fracture is strongly suspected but not seen, nuclear scintigraphy can be used to identify an area of abnormal activity,

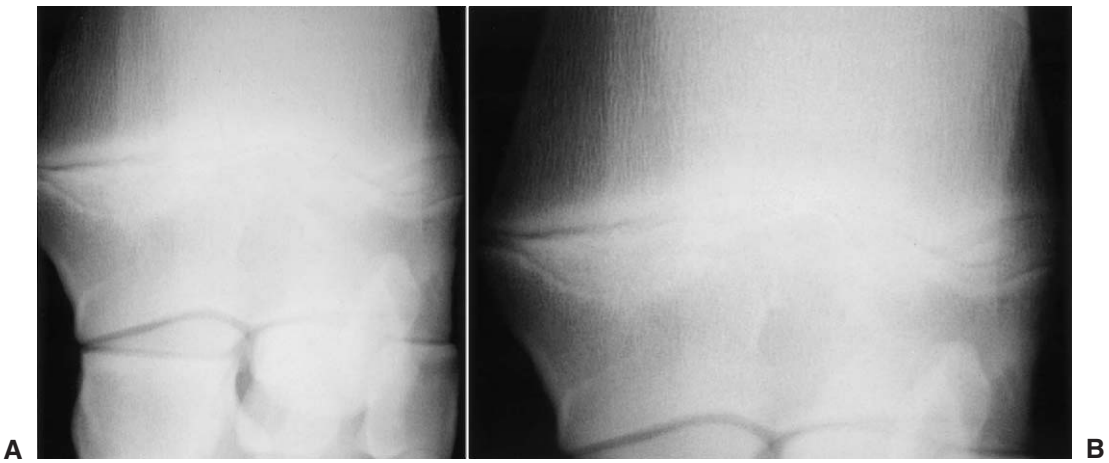


Figure 8-1 • Close-up **(A)** and ultra-close-up **(B)** dorsopalmar views of the distal radius show a fully open distal radial growth plate, *grade C*. Medial is on the left.

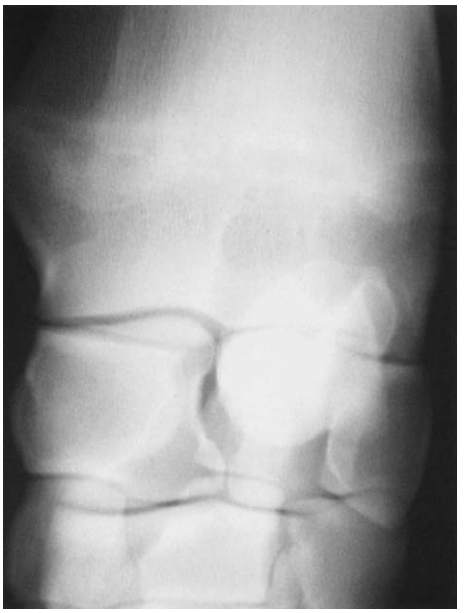


Figure 8-2 • Close-up dorsopalmar view of the distal radius shows a partially open distal radial growth plate, *grade B*. Medial is on the left.

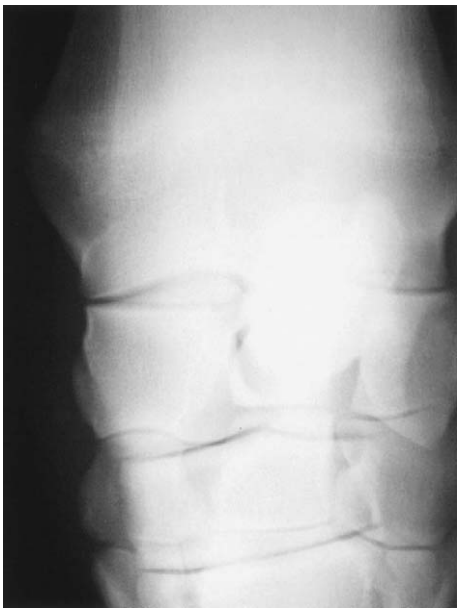


Figure 8-3 • Close-up dorsopalmar view of the distal radius shows a fully closed distal radial growth plate, *grade A*. Medial is on the left.

Box 8-1
Distal Radial Growth Plate Closure Times

BREED	CLOSURE TIMES (DAYS)
Arabian	Female: 708; Male: 724
Australian Thoroughbred	750
Brazilian Mangalarga	750
Brazilian Thoroughbred	Female: 701 (±37); Male: 748 (±55)
Italian Trotter	780-810

possibly related to a fracture. By way of a cautionary note, Allhands and colleagues have warned that nuclear bone scans of the distal radioulnar region may be misinterpreted because of nearby soft-tissue uptake related to an earlier ulnar nerve block.[5]

Radial Stress Fracture

Mackey and co-workers reported the radiographic or scintigraphic appearance of three stress fractures, all located in the radial midshaft.[6] Like their third metacarpal and metatarsal counterparts, radial stress fractures may be diagnosed directly by identifying a partial or, less frequently, a complete break. Stress fractures may also be inferred from a calluslike bone deposit on the dorsal surface of the radial body, especially when it develops within a month or so of an acute lameness.

Radial Body Fractures

Radial fractures are typically accompanied by a similar injury to the adjacent ulna. Although diaphyseal fractures can occur anywhere, most fractures occur in the

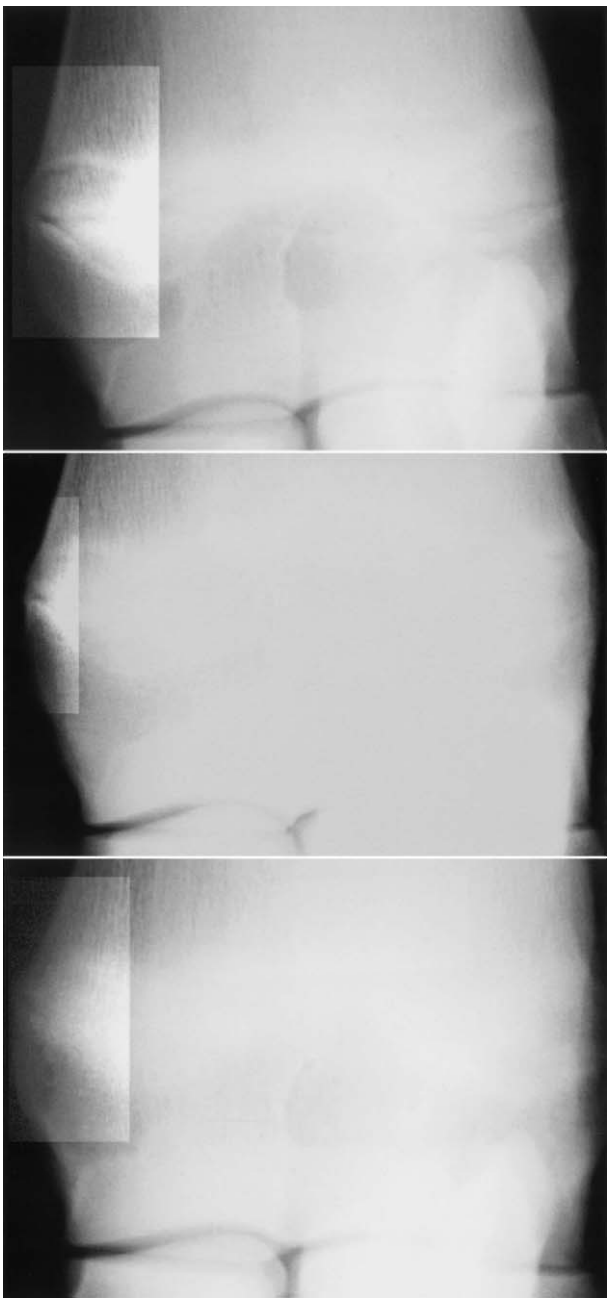


Figure 8-4 • Ultra-close-up dorsopalmar views of the distal radius in a young Arabian horse emphasizing the far medial aspect of the growth plate: fully open **(A),** partially open **(B),** and fully closed **(C).** Note the multiple undulant cartilage bands, which characterize the billowy surface of the metaphyseal side of the physis.

proximal half. All fracture configurations have been described, with transverse and short oblique breaks being among the more common (Figures 8-8 and 8-9). Comminution and fissures occur with about the same frequency as in other long bones.

Distal Radial Pseudofractures

A young adult horse has a single distal radial epiphysis, which fuses with the adjacent radial body at



Figure 8-5 • Close-up dorsopalmar view of the distal radius shows a nearly closed distal radial growth plate, *grade A.* Medial is on the left.

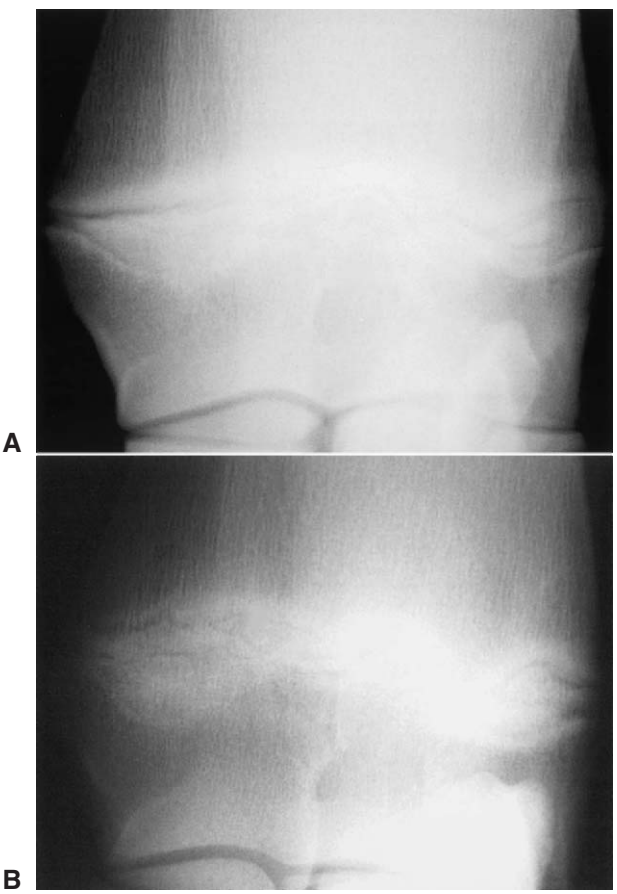


Figure 8-6 • Close-up dorsopalmar views of the distal radial growth plate projected head-on **(A)** and from below **(B).** The decentered projection makes the growth plate appear less distinct (falsely implying closure) and widened overall. This latter appearance may also be mistaken for epiphysitis.

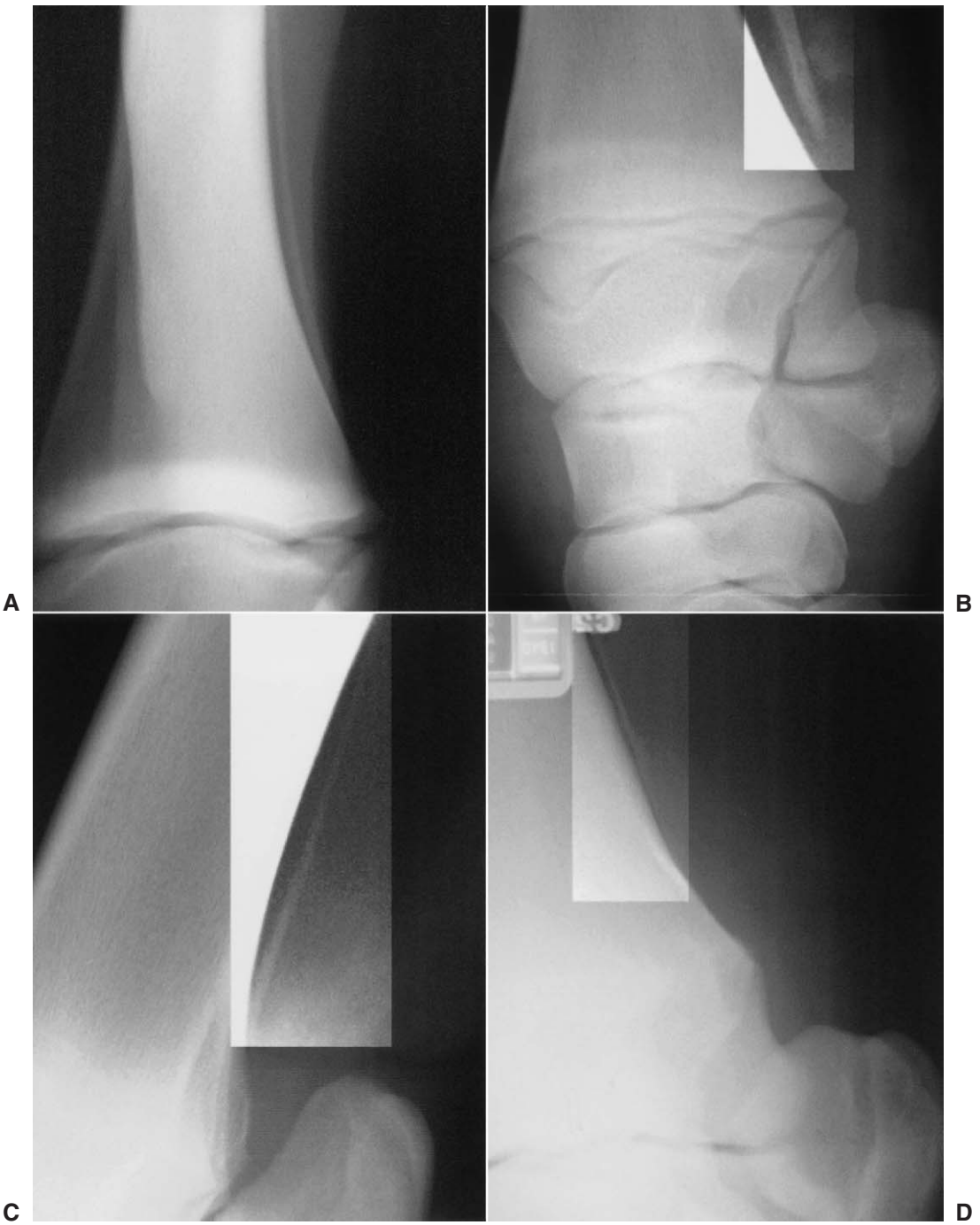


Figure 8-7 • The distal ulna of the horse is highly variable. In foals, it usually extends the length of the radial body along the lateral side **(A)** and appears thicker than in an adult **(B).** In skeletally mature horses the ulna appears abbreviated distally—as seen in the medial oblique projection, often failing to reach the radial metaphysic **(C).** The distal ulna of an adult horse is much smaller than in a foal and consequently appears less distinct **(C, D).**

about *30 months* of age. A foal has two distal "radial epiphyses," one a genuine part of the radius, the other a vestige of the distal ulna, the styloid process. The two become one during the first year of life (Figure 8-10).

Severe angular limb deformities of foals, particularly the valgus variety, can leave a misimpression of a medial metaphyseal fracture. In reality this appearance is due to uneven ossification. Two examples of this phenomenon are shown in Figures 8-11 and 8-12.

Distal Radial Growth Plate Fractures

Occult Growth Plate Injuries. Occasionally newborn foals injure their carpi and appear to recover in a few weeks, only to develop a valgus deformity a month or two later. Radiographs made at the time of injury usually appear normal other than perhaps for some soft-tissue swelling at the level of the radiocarpal joint. About a month or so later, the affected carpus begins to bow medially, seemingly the result of a combination

of factors: uneven distal radial growth and intercarpal laxity. At this point, radiographs become clearly abnormal, featuring (1) an evenly or unevenly widened distal radial growth plate, (2) a distinctive density loss on either side of the radial physis medially that extends well into the overlying radial body, and (3) varying degrees of varus angulation (Figure 8-13).



Figure 8-8 • Full-length medial oblique **(A)** and craniocaudal **(B)** views of a foal with displaced transverse fractures of the proximal bodies of the radius and ulna. The injured leg in wrapped in a Robert-Jones bandage.

Visible Growth Plate Fractures. Most distal radial growth plate fractures are of the Salter-Harris type II variety, with the occasional type III and IV. Sporadically, distal growth plate fractures defy the Salter-Harris classification, in which case it is quite acceptable simply to describe the physical attributes of the injury (Figure 8-14).

Distal Radial Growth Scar

Once axial growth is completed, an irregular radiodense band, the so-called growth scar, replaces the translucent distal growth plate. The distal radial growth scar marks the approximate location of the proximal aspect of the antebrachial carpal joint (radiocarpal joint), and as such, its perimeter is highly irregular, as shown in Figure 8-15.

Proximal Ulnar Fractures

Most proximal ulnar fractures in horses are of the *inverted-L or radiant-T* variety and are almost always articular (Figure 8-16). Many of these fractures are also accompanied by varying degrees of humeroradial dislocation and one or more small avulsion fractures (Figure 8-17).

Untreated, the fractured olecranon typically rocks forward and upward on its humeroulnar pivot point. If the fracture is allowed to heal this way, the horse's ability to extend its injured leg may be reduced, with a commensurate loss of extension. Depending on the degree of dislocation, and thus the size of the fracture gap, healing is often protracted, but there are exceptions. The humeroulnar joint may or may not become arthritic as a result.



Figure 8-9 • Full-length lateral and craniocaudal views **(A)** of a foal with displaced short oblique fracture of the proximal bodies of the radius and ulna. Numerous marginal defects are apparent in the lateral close-up view *(emphasis zone)* **(B),** which are not obvious in the opposite view **(C).**



Figure 8-10 • Ultra-close-up medial oblique view **(A)** of the distal ulna, which in a foal appears as a distinct triangular-shaped bone on the far lateral side of the radius. Once joined to the adjacent radial epiphysis, this initially separate ossification center will become the styloid process. Follow-up medial oblique **(B)** and ultra-close-up medial oblique **(C)** views show partial fusion *(emphasis zone).*

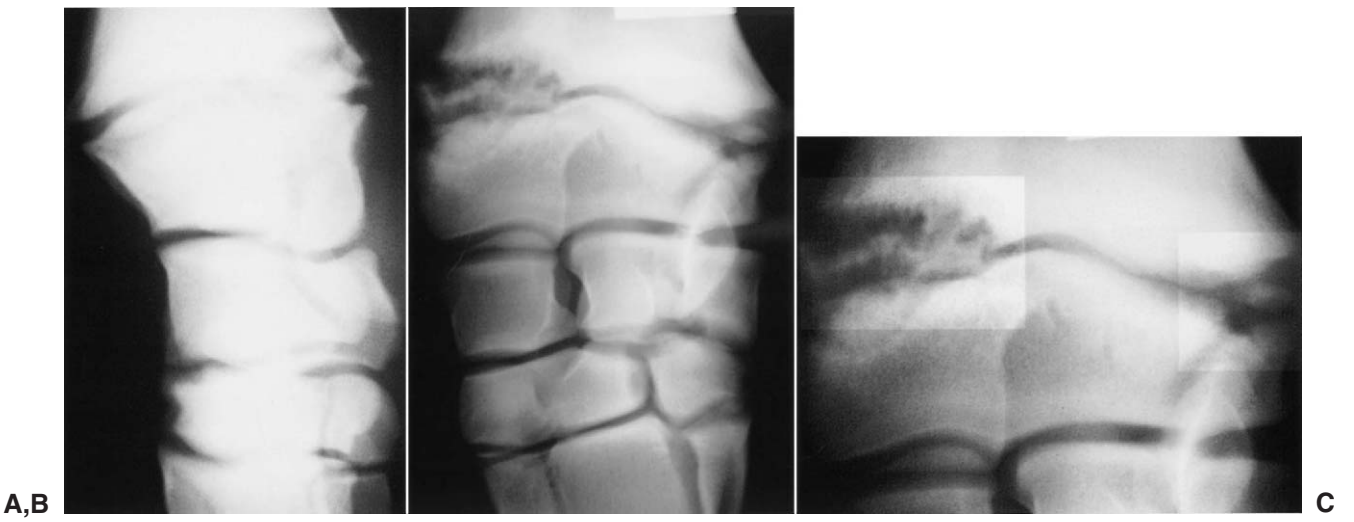


Figure 8-11 • Close-up lateral **(A),** dorsopalmar **(B),** and ultra-close-up dorsopalmar **(C)** views of distal radius show medial and caudomedial pseudofractures secondary to angular limb deformity.

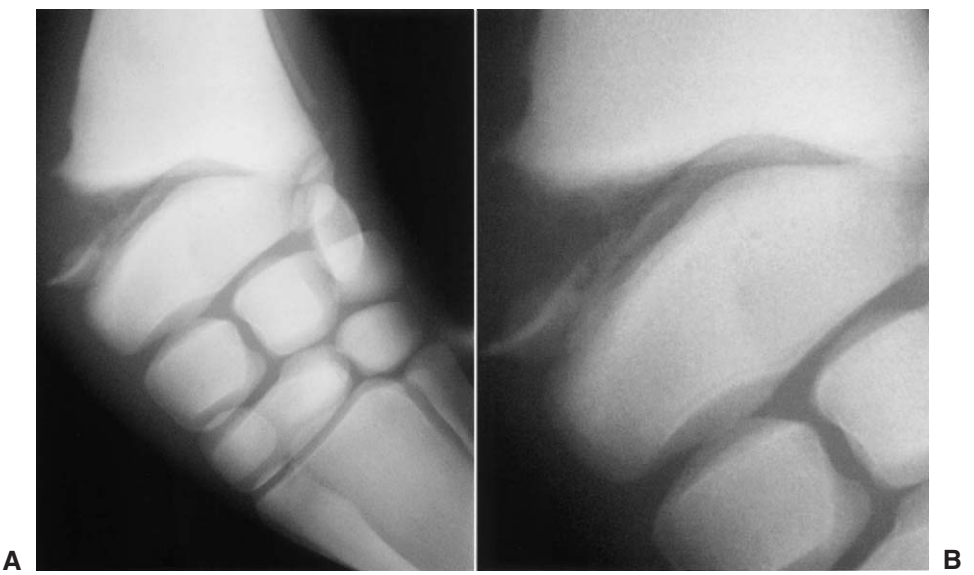


Figure 8-12 • Dorsopalmar **(A)** and ultra-close-up dorsopalmar **(B)** views of the distal radius show a metaphyseal pseudofracture.



Figure 8-13 • Dorsopalmar **(A)** and close-up dorsopalmar (**B)** views of the distal radius of a 2-month-old foal, injured as a newborn, show uneven bone reabsorption on either side of the distal radial growth plate medially, which extends proximally into the radial body *(emphasis zone).*

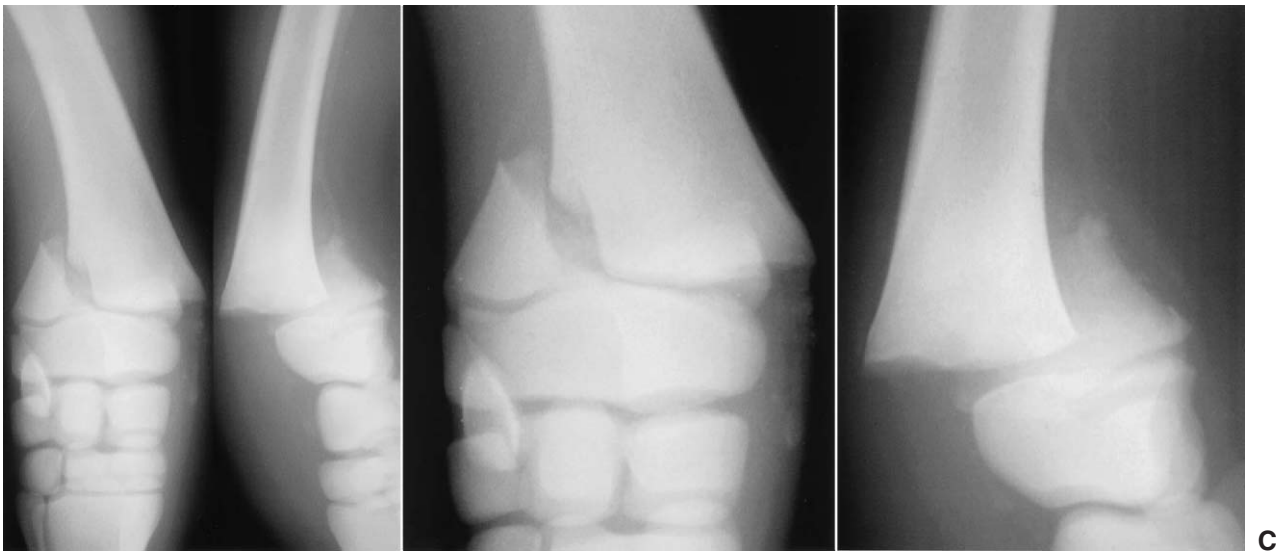


Figure 8-14 • Full-length craniocaudal and lateral views **(A)** of a foal with a badly displaced distal radial growth plate fracture. Close-up craniocaudal **(B)** and lateral **(C)** views reveal that there are two metaphyseal fragments, one on either side of the adjacent radial epiphysis, rather than the usual one.



Figure 8-15 • Defleshed bone specimen shows the highly irregular distal radial growth scar as seen from above and behind. Care must be taken not to mistake this normally roughened area for pathologic osteophytes.

Plating is the most common method of treating ulnar fractures and, as such, it is important to recognize how plated bone heals, compared with a casted fracture, for example. It is also vital to recognize whether a postoperative infection is present and how this differs from simple implant movement. The ulnar repair shown in Figure 8-18 covers a span of 6 months, from injury to recovery, and provides an excellent opportunity to view the full radiographic spectrum of bone healing in this individual.

▮▮▮ PROXIMAL RADIAL DISLOCATIONS

Temporary or permanent proximal radial dislocations (luxations, subluxations) are usually readily identifiable, provided the elbow is not so badly swollen that



Figure 8-16 • Lateral view **(A)** of a fresh inverted-L articular fracture of the olecranon base and proximal ulnar body. The proximal fragment is displaced in a characteristic manner *(emphasis zone).* Three months later, and without any treatment other than rest, lateral close-up **(B),** ultra-close-up lateral **(C),** and craniocaudal **(D)** views reveal a substantial interior callus, which has filled in much of the fracture gap. Six months after the original injury, the fracture is barely discernible and there is no detectable osteoarthritis as determined by ultra-close-up lateral **(E)** and craniocaudal **(F)** views.

the receiver cannot be positioned proximally enough to include the entire radiocarpal joint. Older dislocations, however, are another story. Because most radial head dislocations correct spontaneously, subsequent radiographic diagnosis is usually based on circumstantial evidence such as periarticular new bone (Figure 8-19).

▮▮▮ DISTAL RADIAL GROWTH PLATE INFECTION (SEPTIC PHYSITIS)

Kettner and co-workers recently reported a case of infectious physitis in a 2-week-old foal that included both pretreatment and posttreatment radiographs of the affected bone.[7] Before treatment, the centrally located physeal lesion appeared as a vague circular area of decreased bone density, best seen in the frontal projection. After treatment, the previously affected area of the growth plate appeared denser than the surrounding physis, presumably related to bony repair.

Exactly how and why bacteria colonize certain growth plates of very young foals is not known, although the *slow flow theory* (author's term), as proposed by Trueta,[8] has likely been cited enough that many now think of it as fact, similar to the factual metamorphosis undergone by many long-lived theories.[9,10] Growth plate infections of this sort are often attributed to umbilical infections.

Radial Infections Secondary to Fracture

Swinebroad and co-workers reported five cases of proximal radial osteomyelitis that developed subse-



Figure 8-17 • Close-up lateral **(A)** and craniocaudal **(B)** views of a recently injured elbow show a mild to moderately displaced inverted-L articular fracture of the olecranon base and proximal ulna body. The humerus is partially dislocated, and there is a pair of medium-sized avulsion fragments lying just off the primal corner of the radius (as seen in lateral projection). Lateral **(C)** and craniocaudal **(D)** progress films made 5 weeks later show that the fracture gap has more than doubled as a result of further fragment displacement. Little or no interior callus is evident. The limb can no longer be straightened.

quent to wounds to the elbow region.[11] Stickle and co-workers described an abscess-like, localized form of osteomyelitis in the distal radial metaphysis of a pair of Quarter Horse colts after open radial fracture and surgical reduction.[12]

Radiographically, the lesions were characterized by a thick sclerotic margin, a lytic interior, and what appeared to be a central sequestrum. One of the colts was euthanized after unsuccessful efforts to eliminate the postoperative infection; the other colt recovered uneventfully. The authors speculate that the lesion in the surviving colt may have been a sterile abscess.

Schneider and co-workers described the use of antibiotic-impregnated polymethyl methacrylate for treatment of an open, displaced, distal radial shaft fracture of a horse.[13] The antibiotic beads are radiographically visible, thus allowing for their radiographic surveillance. In some animals, impregnated beads of this sort behave as foreign bodies, impeding healing.

▮▮▮ RADIAL AND ULNAR TUMORS

Radial tumors, like other extremital tumors in horses, are rare. Most lumps are the result of an underlying new bone deposit or scar tissue caused by a previous injury. In this latter regard it is useful to mark the surface of such lumps to verify the accuracy of the radiographic field (Figure 8-20).

Chondroma

Chondromas occur in the flat bones of the head and pelvis, the ribs, the larynx, and the nasal cavity of

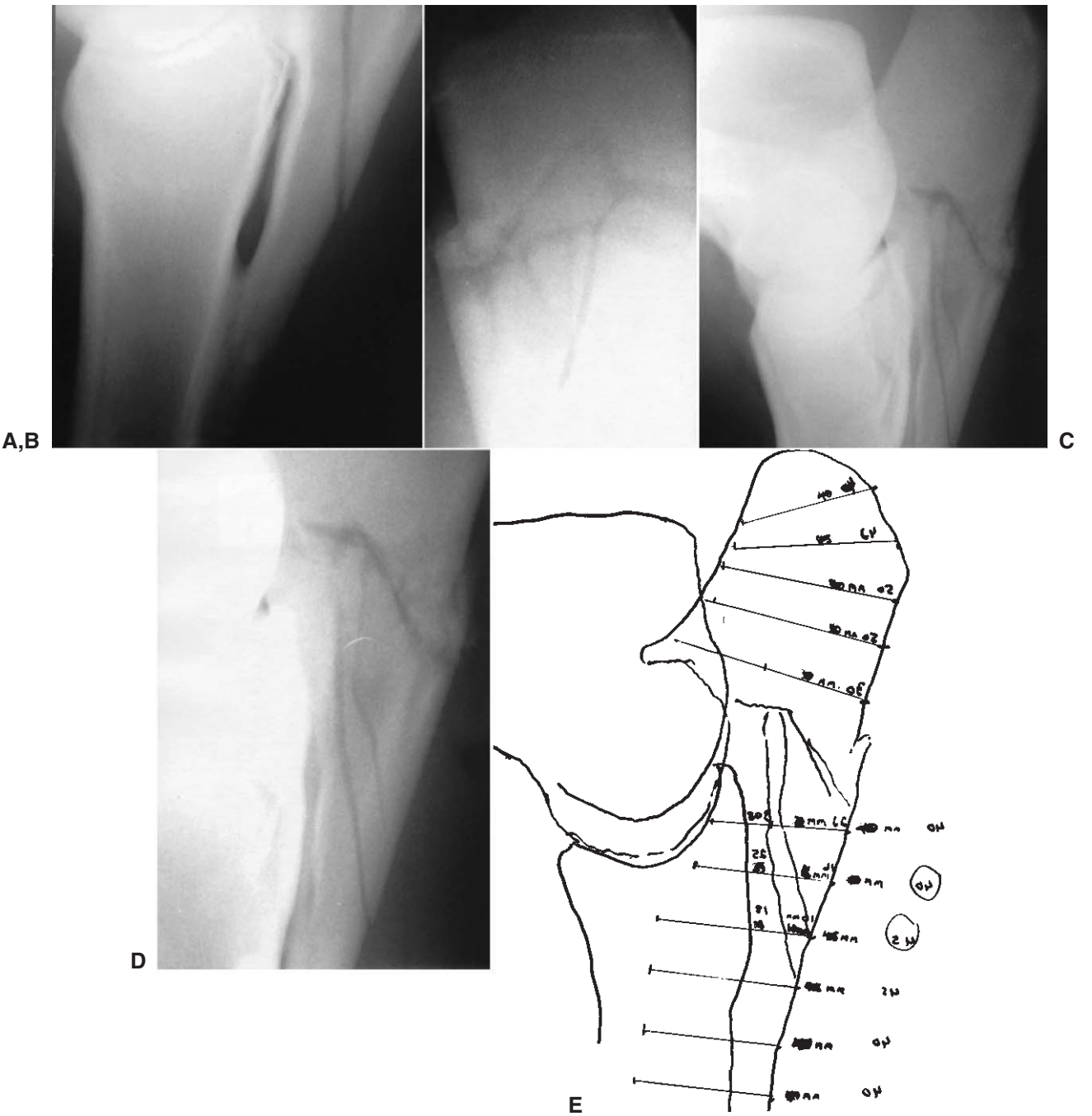


Figure 8-18 • Lateral **(A)** and proximally angled craniocaudal **(B)** views show a displaced, comminuted olecranon fracture. Because of severe swelling and non–weight bearing, it was not possible to place the cassette squarely behind the horse's injured elbow, resulting in incomplete visualization of the proximal part of the fracture. Once the horse was down, it became possible to image the entire fracture: a radiant T variant, as seen in lateral **(C)** and ultra-close-up **(D)** views. Before surgery an overlay **(E)** made from the lateral projection was used to determine the appropriate screw lengths for plate attachment.

Continued.



Figure 8-18, cont'd • An immediate postoperative lateral view shows near-anatomical fracture reduction **(F).** Lateral **(G)** and close-up lateral **(H)** views made 1 month later (projected at a somewhat different angle) continue to show visible fracture lines but no evidence of fragment or implant dislocation. Lateral **(I)** and close-up lateral **(J)** views made 2 months after injury show partial disappearance of the fracture lines and stable implants. Five months after injury, lateral **(K)** and close-up lateral **(L)** views show further development of the interior callus, as evidenced by increasingly vague fracture lines. Proximally the plate is beginning to loosen, as indicated by bone loss around the bases of the first and second screws. Six months after the injury, lateral **(M)** and lateral close-up **(N)** views show that the fracture has healed with only a trace of the original break remaining visible.

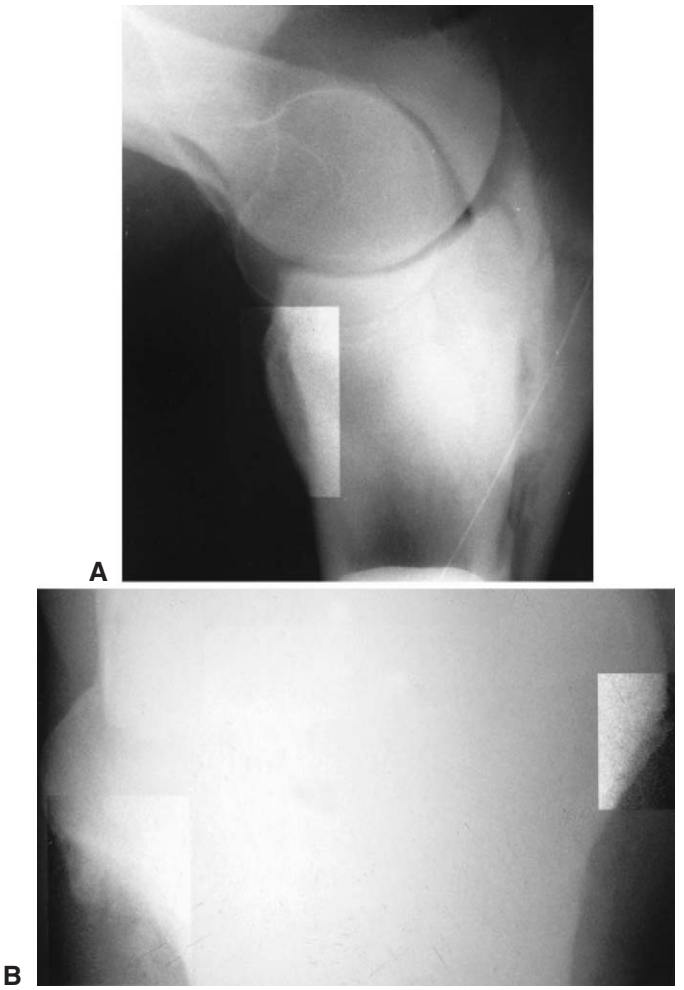


Figure 8-19 • Close-up lateral **(A)** and craniocaudal oblique **(B)** views of the elbow 6 months after a second-degree sprain-avulsion-fracture of the humeroradial joint show chronic-appearing periarticular and extraarticular new bone deposition resulting in an overall increase in regional bone density.

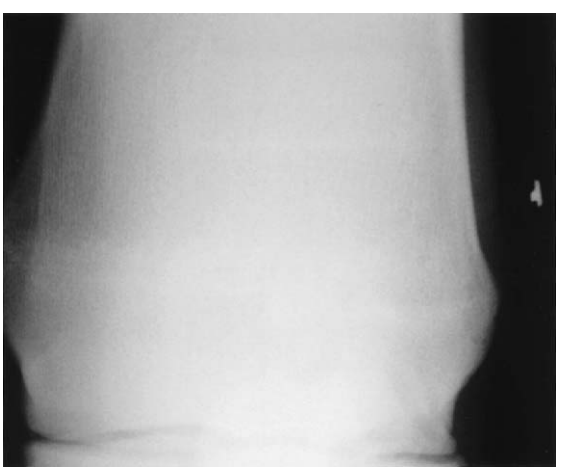


Figure 8-20 • Close-up dorsopalmar projection of the distal radius shows an edge-on view of a metallic marker placed over the apex of a palpable lump on the medial side of the leg.

horses. *Synovial chondromatosis* has also been reported in the horses.[14] Occasionally a benign cartilage tumor becomes cancerous, a process known as *malignant transformation*.

Chondrosarcoma

Turner described the radiographic appearance of a distal radial chondrosarcoma in a 20-year-old Thoroughbred stallion hospitalized for progressive 4-month lameness and swelling of the distal right radius and carpus. Radiographically the tumor appeared predominantly productive, with the exception of the caudal radial shaft and diaphysis, which appeared partially destroyed.

Osteosarcoma

Like other primary bone tumors in horses, osteosarcomas are rare. However, when they occur they are quite varied. Some osteosarcomas are primarily osteoblastic and feature the classic indicators of malignancy: extensive cortical and medullary destruction; poorly demarked transition into adjacent normal bone; production of tumor bone in surrounding soft tissue; and, depending on the rate of tumor growth, elaborate defensive host bone response. Other osteosarcomas are osteoclastic, some intensely so, causing the complete disappearance of a portion of the cancerous bone.

▮▮▮ RADIOULNAR COMPARTMENTAL SYNDROME (ANTEBRACHIAL FLEXOR COMPARTMENT SYNDROME)

Compartment syndrome is a form of regional ischemia, usually caused by a serious muscular injury that results in hemorrhage into a confined space, such as the one that potentially exists between the dorsal surface of the tibia and the adjacent musculature. If the pressure from such a mass effect becomes great enough, the surrounding vasculature is temporarily occluded, leading to regional ischemia; anoxia; and, if not relieved, myonecrosis.

Diagnosis is best confirmed sonographically, with severity being determined using cavitary manometry. I am unaware of the normal values for the horse, but it is often just as well to use the opposite leg as a control. Sullins reported a case of compartment syndrome in a pregnant mare (9 months) attributed to a combination of edema and intramuscular swelling.[15]

Treatment for compartment syndrome is by surgical pressure relief, obtained by splitting the intermuscular fascia and removing the blood clot. An indwelling drain is used to eliminate residual hemorrhage and edema. The fasciotomy is left open, sometimes along with the skin, if the swelling is severe enough. Once the swelling and drainage have sub-



Figure 8-21 • Close-up medial oblique view of the distal radius shows a displaced styloid process *(emphasis zone).* Because the opposite styloid was also displaced and there was minimal lameness but no history of injury, a presumptive diagnosis of osteochondritis was made.

sided (usually with 2 or 3 days), the skin, but not the fascia, can be closed.

Because of the fasciotomy, the operated leg may appear thicker following recovery than the normal leg. I am unaware of any studies indicating that relieving fasciotomies adversely affects the subsequent performance of racehorses, although it may affect the power or mechanics of jumpers.

▮▮▮ OSTEOCHONDRITIS OF THE RADIUS AND ULNA

In my experience, subchondral bone cysts are the most common form of osteochondritis affecting the distal radius; however, they have a much lower incidence than femoral bone cysts. Fragmentation and nonunion of the styloid process occur occasionally and are probably a form of osteochondritis, especially if present bilaterally and if there is no history of trauma (Figure 8-21).

References

1. Speer DP, Braun JK: The biomechanical basis of growth plate injuries, *Physician & Sports Med* 13:72, 1985.
2. Volcano LC, Mamprim MJ, et al: Radiographic study of distal radial physeal closure in Thoroughbred horses, *Vet Radiol Ultrasound* 38:352, 1997.
3. Morgan JP: Radiographic study of the distal ulna of the horse, *Vet Radiol* 11:78, 1965.
4. Bolt DM, Burba DJ: Use of a dynamic compression plate and a cable cerclage system for repair of a fracture of the radius in a horse, *J Am Vet Med Assoc* 223:89, 2003.
5. Allhands RV, Twardock AR, Boero MJ: Uptake of 99mTcMDP in muscle associated with peripheral nerve block, *Vet Radiol* 28:181, 1987.
6. Mackey VS, Trout DR, et al: Stress fractures of the humerus, radius, and tibia in horses, *Vet Radiol* 28:26, 1987.
7. Kettner N-U, Parker JE, Watrous BJ: Intraosseous regional perfusion for treatment of septic physitis in a two-week-old foal, *J Am Vet Med Assoc* 222:3456, 2003.
8. Trueta J: The three types of acute hematogenous osteomyelitis, *J Bone Joint Surg* 41:671, 1959.
9. Firth E: Specific orthopedic infections. In Auer J, editor: *Equine surgery,* Philadelphia, 1992, WB Saunders, pp 932-940.
10. Hance RH: Hematogenous infections in the musculoskeletal system in foals, In *Proceedings 44th Annual Convention of the American Association of Equine Practitioners,* 1998, pp 159-166.
11. Swinebroad EL, Dabareiner RM, et al: Osteomyelitis secondary to trauma involving the proximal end of the radius in horses: five cases (1987-2001), *J Am Vet Med Assoc* 223:486, 2003.
12. Stickle RL, Cantwell, et al: Focal metaphyseal osteomyelitis following open fracture in three horses, *J Am Vet Med Assoc* 183:797, 1983.
13. Schneider RK, Andrea R, Barnes HG: Use of antibiotic-impregnated polymethyl methacrylate for treatment of an open radial fracture in a horse, *J Am Vet Med Assoc* 207:1454, 1995.
14. Von Schmidt E, Schneider J: Synovial chondromatosis in a horse, *Vet Med* 37:509, 1982.
15. Sullins KE, Heath RB, et al: Compartment syndrome in a mare, *Equine Vet J* 19:147, 1987.

Chapter 9

Elbow

THE STANDARD ELBOW SERIES

The standard elbow series consists of a lateral and a craniocaudal view (Figure 9-1). Severe swelling, which often accompanies a fresh fracture, for example, frequently makes it difficult or impossible to place the receiver high enough in the horse's axilla to image the proximal part of the olecranon (Figure 9-2). Extending the injured leg may help but is painful and can cause the horse to stumble or fall, injuring itself further. Accompanying swelling causes a great deal of scatter radiation that reduces image contrast, resulting in a distinctly gray film. Lateral and frontal views of a normal adult elbow are provided for radiographic-anatomic correlation (Figure 9-3).

The foal's elbow appears less angular than that of the adult horse because of its prominent humeral and ulnar accessory growth centers. Numerous growth plates, many of which are superimposed on one another, can be a source of diagnostic uncertainty when assessing the elbow for fracture (Figure 9-4).

SUPPLEMENTARY VIEWS

The most common supplementary view of the elbow is the extended-flexed lateral (Figure 9-5). In the case of fractured olecranon, most horses will hold their injured leg in a partially flexed position, in an effort to minimize weight bearing. When flexed, the radial head rotates, displaying its highly irregular extraarticular surface, which can be mistaken for new bone (Figure 9-6). Lateral and medial oblique projections are usually employed on a case-by-case basis.

NORMAL ANATOMIC VARIATION

There are few diagnostically significant normal variations in the radiographic appearance of the adult elbow. The exception is the immature animal, in whom Brown and MacCallum reported the *inconsistent* presence of a separate center of ossification of the anconeal process in 14 of 23 foals from 52 to 104 days of age.[1]

OLECRANON HYGROMA

An *olecranon hygroma* is a large fluctuant swelling over the point of the elbow. Strictly speaking, a hygroma is not a true bursitis, although it is occasionally characterized as such. Diagnosis is usually made on the basis of location, appearance, and consistency. In the case of doubt, ultrasound can be used to confirm the cystic nature of the swelling, or if sonography is not available, cavography and aspiration can establish the nature of the swelling. Honnas and co-workers provided an excellent discussion of olecranon hygroma in their report of 12 cases.[2]

FRACTURE

Olecranon Fractures

Most olecranon fractures in the horse enter the humeroulnar joint, on occasion in more than one location, and usually result in moderate fragment displacement. Many are comminuted and typically conform to one of two common fracture patterns described previously (Figure 9-7).

Although articular fractures of the proximal ulna can be displaced badly (Figure 9-8), surprisingly many are not (Figure 9-9). This can be explained partially by the "locking effect" of the anconeal process deep within the humeral recess, which limits the further displacement of the fractured olecranon. Although the described displacement of the anconeal process is beneficial insofar as it limits further fragment distraction, it also places enormous stress on the anconeus and may lead to a secondary stress fracture.

Anconeal fractures can lead to instability and, in turn, osteoarthritis of the elbow joint, as shown

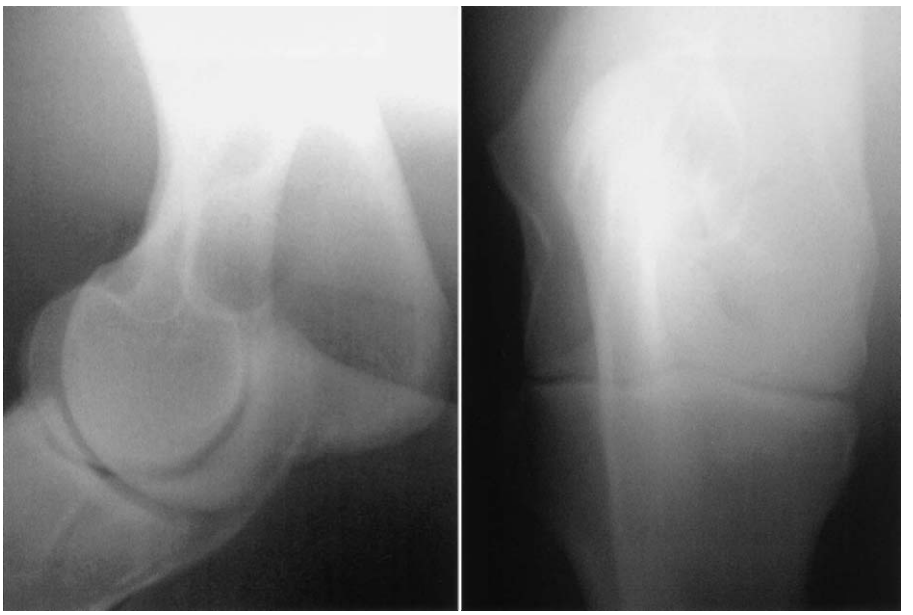


Figure 9-1 • Lateral **(A)** and craniocaudal **(B)** views of the elbow of a normal adult horse.

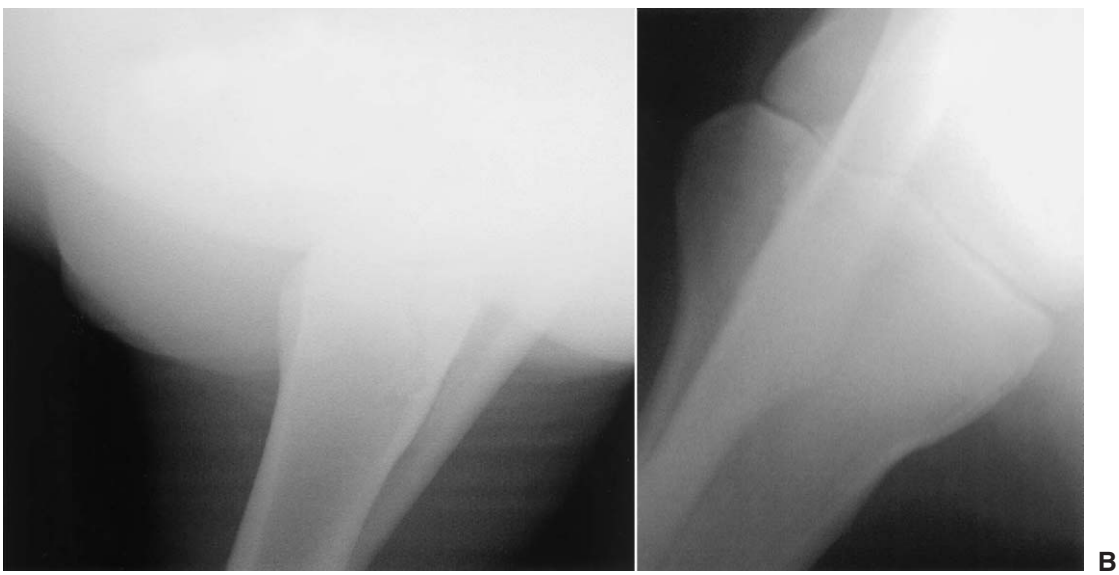


Figure 9-2 • Lateral **(A)** and craniocaudal **(B)** views of the right elbow of a horse suspected of having a fracture. Because of severe swelling, neither view was able to include the most likely injury site, the olecranon.



Figure 9-3 • Defleshed equine elbow corresponding to lateral **(A)** and craniocaudal **(B)** views.



Figure 9-4 • Lateral view of the elbow of a normal foal featuring multiple open growth plates and unfused secondary ossification centers.

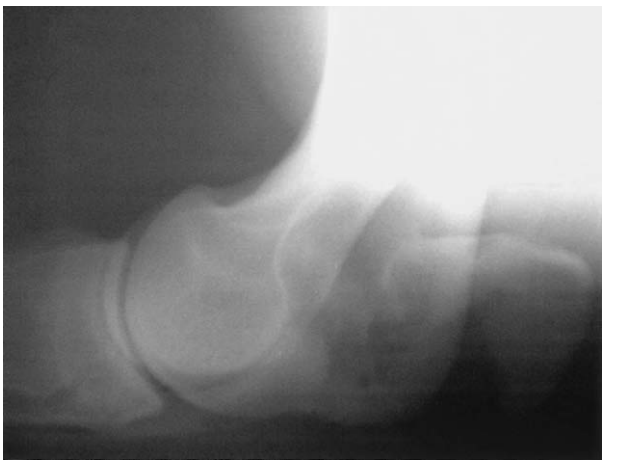
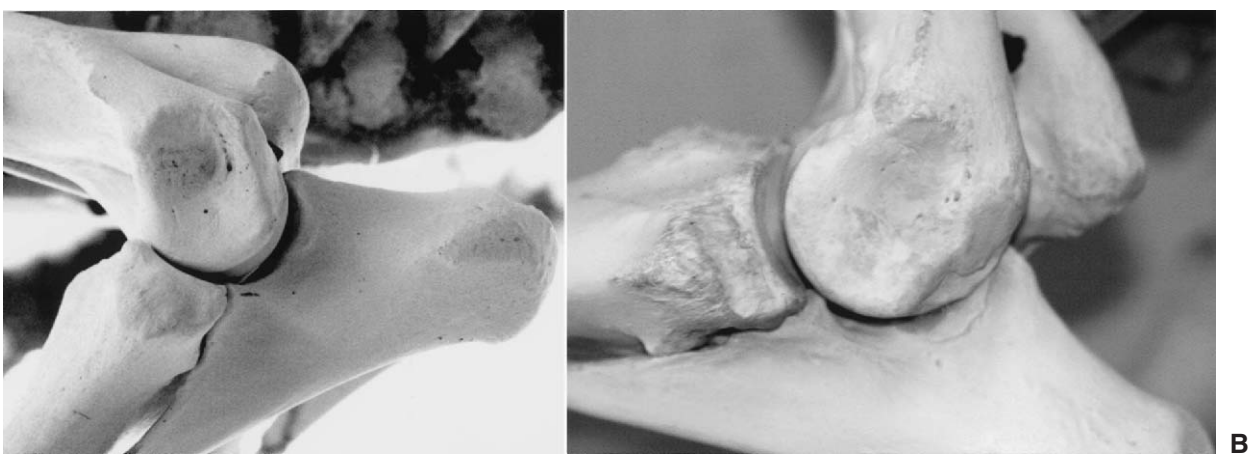


Figure 9-5 • Flexed lateral view of a normal elbow in an adult horse.



A **B**

Figure 9-6 • Defleshed equine elbow corresponding to flexed lateral view **(A).** Close-up view **(B)** of the flexed elbow shows the normally rough perimeter of the proximal radius, which can be mistaken for injury-related new bone.

previously. Even a relatively small callus on the anconeal process, termed an *impingement exostosis*, can interfere with ulnar movement because humeroulnar tolerances are so close.

Malunion, which results from a displaced proximal ulna fracture, prevents a horse from fully extending its cubital joint, which, along with associated pain, leads to muscle atrophy in the upper part of the limb. The resultant lameness may be mechanical, compensatory, or a combination of the two.[3] Fibrous union can resemble nonunion, as evidenced by persistent fracture lines and interfragment widths. Unlike a nonunion, however, a fibrous union will not displace when stressed (Figure 9-10).

Physeal Fractures

Proximal ulnar growth plate fractures typically occur in colts and fillies under a year of age, but they may occur in older animals as long as the physis remains open (up to 36 months in some breeds). Horses with such fractures typically exhibit a dropped elbow.[4] Although the physis is a potential weak spot in the olecranon, it does not follow that it is always the first to break in the event of trauma, as evidenced by numerous reports of comminuted ulnar fractures, most of which were articular, in which the growth plate was not involved.[5]

Although given comparatively little attention in the literature, the immature proximal ulna is susceptible to an unusually type of growth plate fracture in which a small piece of bone breaks free of the cranial edge of the metaphyseal side of the growth plate, with or without apophyseal displacement.

Sprain-Avulsion-Fracture

In the elbow, the collateral ligaments are sprained most often, and the most severe injuries are frequently accompanied by one or more avulsion fractures, a so-

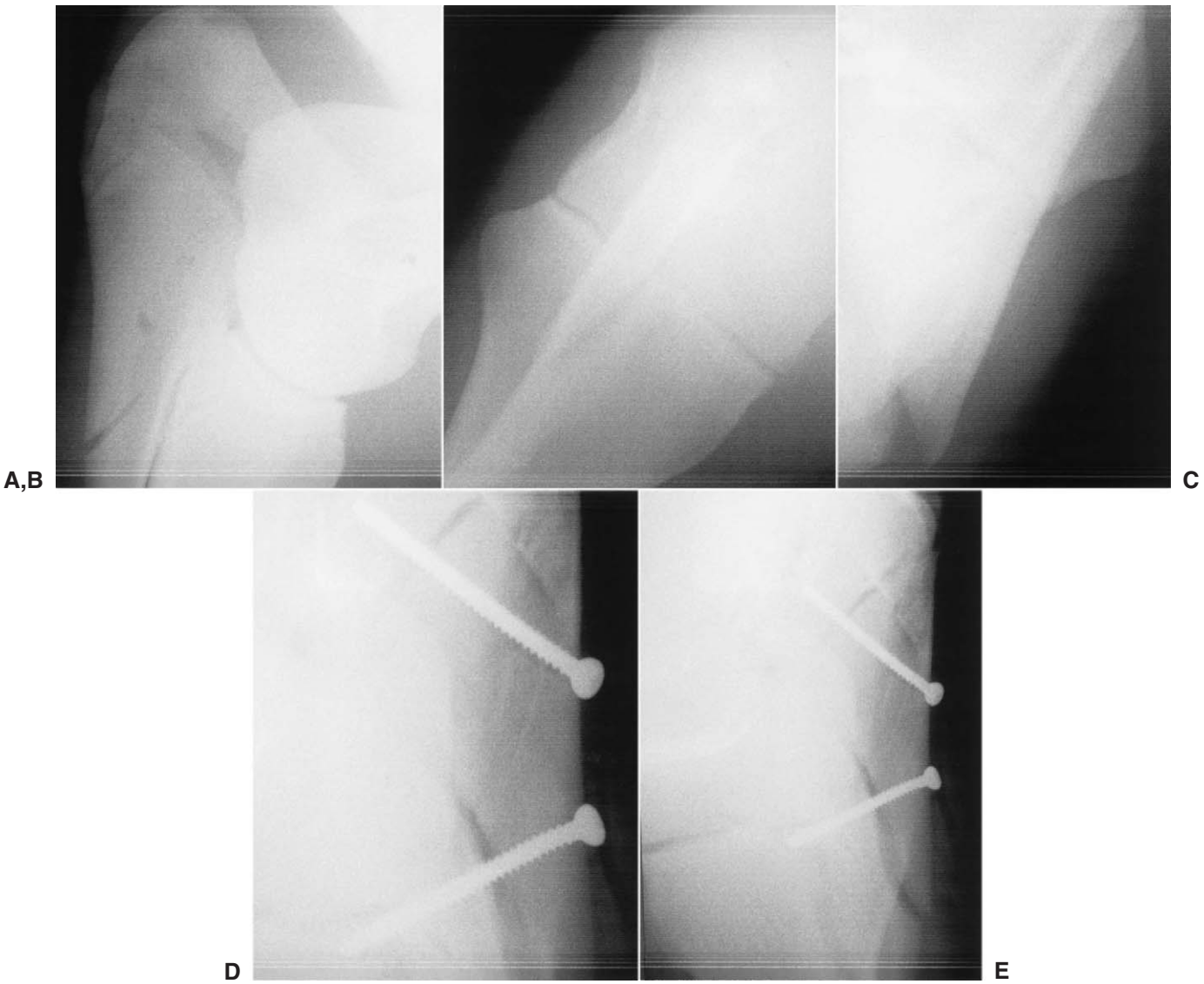


Figure 9-7 • Close-up lateral **(A),** craniocaudal **(B),** and craniocaudal oblique **(C)** views of a severely comminuted olecranon fracture featuring major and minor butterfly fragments. Close-up **(D)** and ultra-close-up craniocaudal **(E)** postrecovery views reveal minor fragment displacement distally and slight bending of the proximal parts of both screws.

called third-degree sprain-avulsion-fracture. Although obvious dislocation may not be evident radiographically, posttraumatic osteoarthritis may develop a few months later (Figure 9-11).

Chopin reported a sprain-avulsion-fracture of the lateral collateral ligament in the elbow of a horse.[6] Radiographically the injury was characterized by multiple avulsive-type bone fragments arrayed along the edge of the collateral fossa, as seen in frontal projection. Sonographically the damaged ligament appeared swollen and hypoechoic compared with a normal control ligament. The injury was confirmed at postmortem. Additional unsuspected cartilage damage was noted in the form of abraded humeral and radial articular surfaces. Small bone shards were also found in the joint cavity.

Growth plate fractures of the medial epicondyle occur occasionally, sometimes with only slight displacement of the growth center, necessitating an opposite side comparison. In some instances, a previous epicondylar fracture can be diagnosed presumptively based on the presence of an abnormal appearing growth plate (Figure 9-12).

▮▮▮ INFECTION

Communicating Bursal Infection

Dunkerly and co-workers reported the *cavographic* appearance of a communicating infection between the ulnaris lateralis bursa and the humeroradial joint.[7]



Figure 9-8 • Lateral view of the elbow of a colt with a history of a nonspecific forelimb injury 3 months earlier shows a badly displaced olecranon fracture with a large articular defect, although the fragment containing the anconeal process remains in place.



Figure 9-9 • Lateral view of the elbow shows a subacute olecranon fracture about 2 inches below the olecranon growth plate.

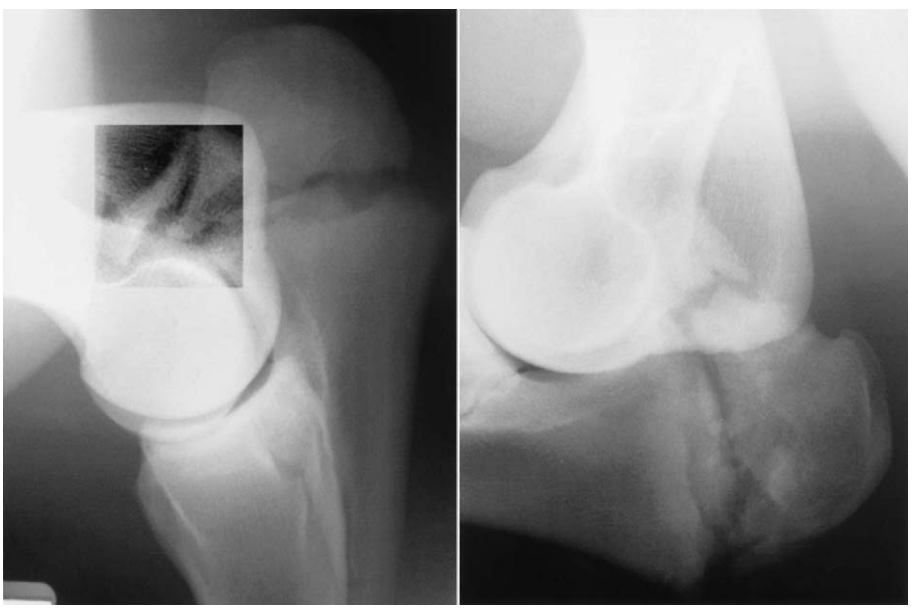


Figure 9-10 • **A,** Lateral view of the elbow at the time of initial injury shows an unusual transverse fracture of olecranon with a presumed secondary stress fracture of the anconeal process *(emphasis zone).* **B,** Six months later a hyperflexed lateral stress view shows that the fracture fragments remain largely unchanged but notably do not displace when the elbow is flexed, consistent with a fibrous union.

Diagnostic iodine solution was injected into a painful fluctuant swelling located on the caudolateral aspect of the elbow, the site of a closed wound received a month earlier. The resultant *cavogram* showed contrast solution in the both the distended bursa of the ulnaris lateralis muscle and the humeroradial joint. The authors noted that in some horses, especially Quarter Horses, there is a natural communication between these two adjacent cavities. In this instance, however, the communication was considered abnormal, and the horse was treated presumptively for infection.

Deep-Muscle Abscess

Deep-muscle abscesses can be quite difficult to diagnose because they rarely produce detectable swelling. Related pain is often quite intense, especially when the affected muscle contracts. One particular form of intra-

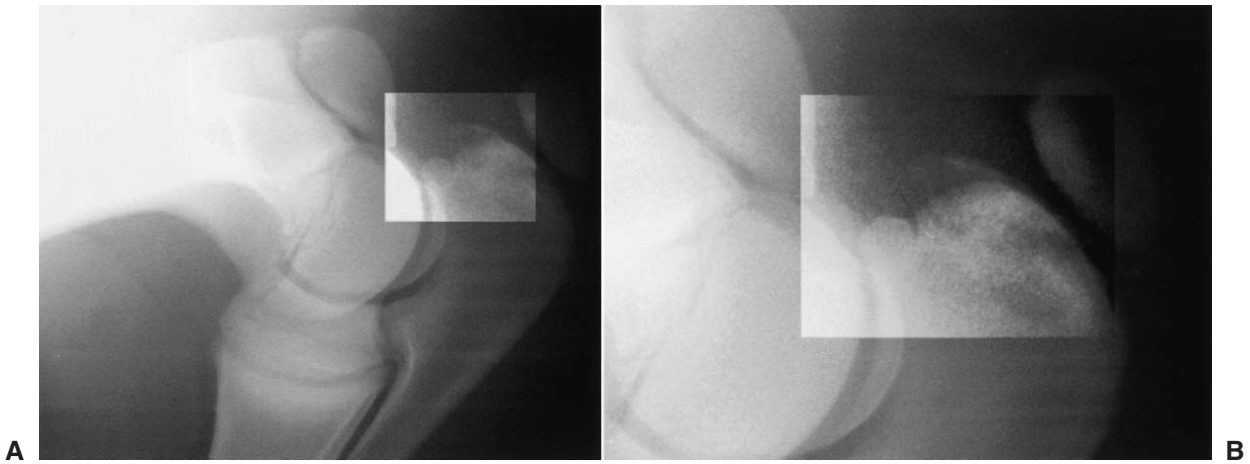


Figure 9-11 • Flexed lateral **(A)** and ultra-close-up flexed lateral **(B)** views of a fresh proximal ulnar sprain. The ultra-close-up view reveals an avulsion-type fracture with a hint of surrounding mineralization *(emphasis zone).*



Figure 9-12 • **A,** Lateral view of the elbow of a foal 7 weeks after severely spraining its leg shows a gaping wedge in the caudal physis of the medial humeral epicondyle *(emphasis zone),* presumably due to a previous avulsion. **B,** An ultra-close-up lateral view of the radiocarpal joint shows a lengthy immature new bone deposit extending from the periarticular area of the radius distally to a point just below the growth plate *(emphasis zone).* **C,** Close-up and ultra-close-up craniocaudal **(D)** views centered on the radiocarpal joint again reveal periarticular and extraarticular new bone on both sides of the radius, including the physis, and partial collapse of the growth plate, findings consistent with a third-degree sprain leading to posttraumatic osteoarthritis.

muscular abscessation in horses is known as *Wyoming strangles* and is caused by *Corynebacterium pseudotuberculosis.* Sonographically the lesion appears as a well-circumscribed hypoechoic mass, somewhat resembling a hematoma, for which it may be mistaken.[8] In addition to the limbs, *Corynebacterium* abscesses can affect the pectoral muscles and those of the ventral abdomen.[9]

Ultrasound is not only very useful in identifying deep-muscle abscesses, but it is also indispensable as a means to guide percutaneous drainage and later to assess healing. Sonographic guidance is especially important when abscesses are internally compartmentalized (loculated), in which case free-hand drainage is often incomplete.

Postoperative Infection

Trostle and co-workers described the appearance of postoperative osteomyelitis after attempted repair of a severe fracture-dislocation of the proximal ulna (also known as a *Monteggia fracture*) in a horse.[10] The authors described the infection as being characterized by "osteolysis at the fracture gap and around 1 bone screw."

Epicondylar Abscess

Huber and Grisel reported an epicondylar bone abscess in an 18-month-old Holsteiner stallion.[11] Radiographically the lesion appeared as a circular lucency in the center of the lateral epicondyle of left humerus, best seen in lateral projection. Scintigraphically the affected area in the distal aspect of the left humerus accumulated more technetium than the same region in the opposite leg.

References

1. Brown MP, MacCallum F: Anconeal process of ulna: separate center of ossification in the horse, *Br Vet J* 130:434, 1974.
2. Honnas CM, Schumaker J, et al: Treatment of olecranon bursitis in horses: 10 cases (1986-1993), *J Am Vet Med Assoc* 206:1022, 1995.
3. Farrow CS: Equine osteology, *Can Vet J* 39:309, 1998.
4. Monin T: Repair of physeal fractures of the tuber olercanon in the horse using a tension band method, *J Am Vet Med Assoc* 172:287, 1978.
5. Scott EA, Mattoon JS, et al: Surgical repair of bilateral comminuted articular ulnar fractures in a seven month-old horse, *J Am Vet Med Assoc* 212:1380, 1998.
6. Chopin JB, Wright JD, et al: Lateral collateral ligament avulsion of the humeromedial joint in a horse, *Vet Radiol* 38:50, 1997.
7. Dunkerley SC, Schumacher J, Marshall AE: Sepsis of the ulnaris lateralis bursa and elbow joint in a horse, *J Am Vet Med Assoc* 208:1238, 1996.
8. Chaffin MK, McMullan WC, Schmitz DG: What is your diagnosis? *J Am Vet Med Assoc* 200:378, 1992.
9. Miers KC, Ley WB: *Corynebacterium pseudotuberculosis* infection in the horse: study of 117 clinical cases and consideration of etiopathogenesis, *J Am Vet Med Assoc* 177:250, 1980.
10. Trostle SS, Peavy CL, et al: Treatment of methicillin-resistant *Staphylococcus epidermidis* infection following repair of an ulnar fracture and humeroradial joint luxation in a horse, *J Am Vet Med Assoc* 218:554, 2001.
11. Huber MJ, Grisel GR: Abscess on the lateral epicondyle of the humerus as a cause of lameness in a horse, *J Am Vet Med Assoc* 211:1558, 1997.

Chapter 10

The Shoulder Region

THE STANDARD SHOULDER REGION EXAMINATION

Radiographic Strategy

Practically speaking, there is no *standard* shoulder examination, at least in the usual sense of the term. We attempt most shoulder examinations with the horse standing, typically screening with a lateral view (Figure 10-1).[1]* An anatomic specimen of an adult shoulder, seen from various perspectives, is provided for radiographic-anatomic comparison (Figure 10-2).

Most of these animals have fractures or fracture-dislocations. Once the location and extent of the injury are established, any additional films are made in conjunction with surgery to avoid any unnecessary anesthesia and associated recovery risks. Sometimes, because of severe pain and disability, it is not possible to extend a horse's injured limb to make the mediolateral view. In this circumstance we usually make a lateral view of the shoulder region using a technique similar to what we use for the craniodorsal view of the thorax. In the case of very young foals, we usually take a portable machine into the trailer after unloading the mare.

As a general rule, I prefer to have in-house films (as well as referral images) of all horses transported to our hospital for fracture repair. This is because some injuries may be aggravated in the course of loading at the point of origin or during a lengthy transport. Obviously such information is of greatest value before surgery.

* Ackerman and co-workers showed that radiation exposure to personnel is greatest during shoulder radiography, especially to the person holding the halter (average 2.9 mrad), and the individual extending the forelimb (average 3.4 mrad). Consequently, all shoulder examinations performed *in their* university-based practice are currently performed with the individual only under general anesthesia.[1]

Radiographic Appearance of the Normal Foal Shoulder

Ossification Centers. Multiple ossification centers are apparent in a lateral radiograph of a young foal's shoulder. These include the supraglenoid tubercle, cranial glenoid, greater tubercle, and humeral head (Figure 10-3). As the foal matures, all the growth centers will fuse with the parent bone, but not simultaneously.

Scapular Pitfall

The appearance of the growth plate separating the supraglenoid tubercle and the adjacent scapular neck can vary greatly with both the projection angle and the horse's stance, especially the degree of weight bearing. Normally the growth plate appears as a thick, irregular band that becomes indistinct distally (Figure 10-4). Some oblique views can resemble a comminuted fracture, which looks somewhat like a lightning bolt (Figure 10-5).

SHOULDER REGION FACTS

- The shoulder or humeral joint is of the ball and socket type.
- The cuplike, articular surface of the scapula is termed the *glenoid* or *glenoid cavity.*
- The craniomedial margin of the glenoid contains a normal defect: the *glenoid notch.*
- There is a normal bony outcrop just proximal to the cranial glenoid termed the *supraglenoid tuberosity,* the attachment for the *biceps brachii muscle.*
- The articular surface of the humeral head is disproportionately large compared with the glenoid.
- The *greater tubercle,* featuring three adjacent vertical elements and two crevices, is situated cranial and lateral to the humeral head.

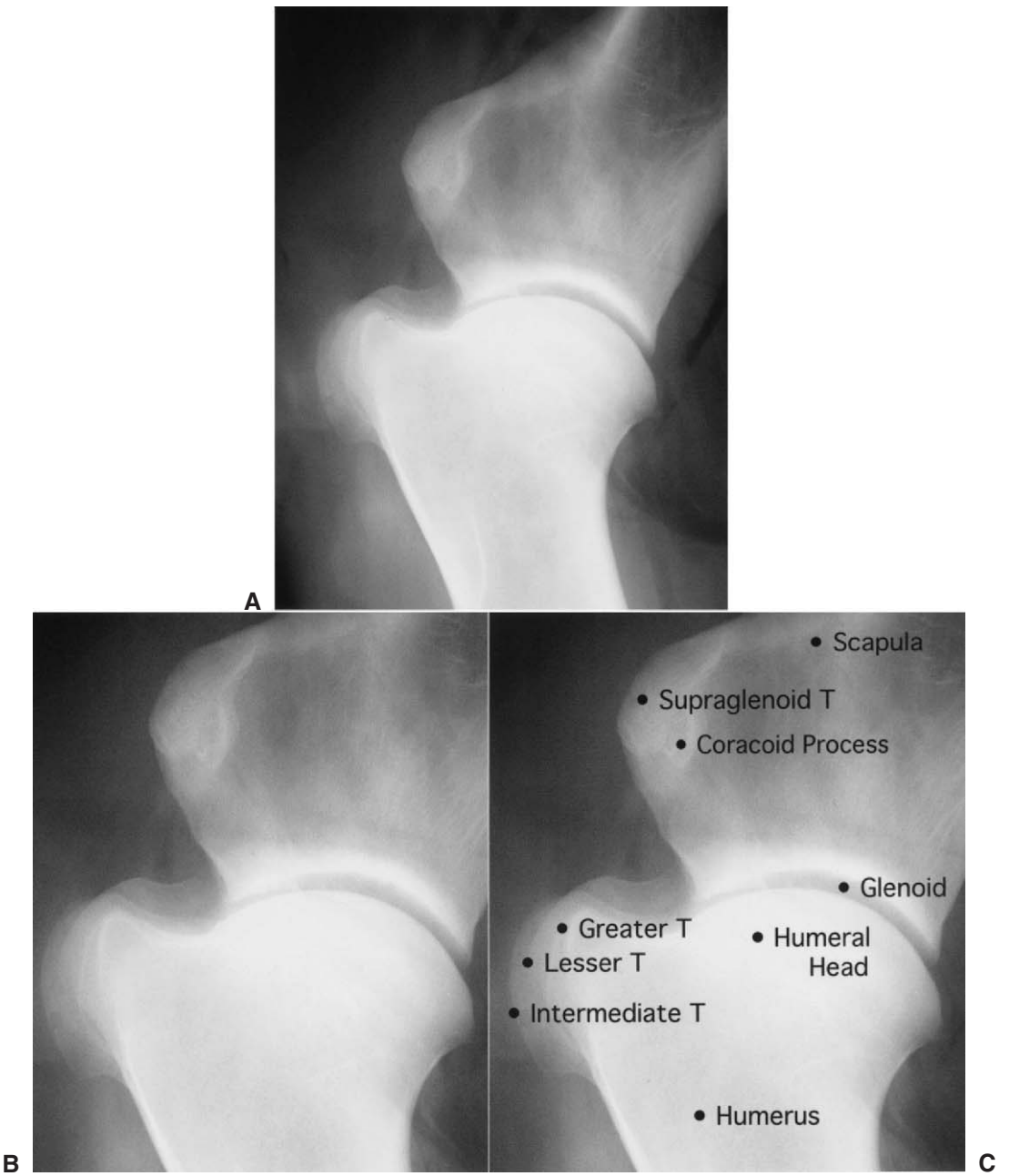


Figure 10-1 • Lateral **(A),** lateral close-up, unlabeled **(B),** and labeled lateral close-up **(C)** views of the humeral joint of an adult horse. *T* stands for tubercle. A disarticulated forelimb was used to improve structural definition, especially of the humeral tubercles, which can be difficult to define clearly in a horse with a fresh injury.

▮▮▮ NORMAL SONOGRAPHIC APPEARANCE OF THE SHOULDER

Pugh and co-workers reported the sonographic appearance of the normal mature and immature equine bicipital regions, including a displaced fracture of the medial tubercle that appeared as a discontinuity in the subchondral contour.[2]

Tnibar and co-workers reported the normal sonographic appearance of the shoulder in both living and dead horses.[3] Using a combination of sonographic and magnetic resonance images correlated with frozen anatomic specimens, it was determined that the following structures could be completely and reliably imaged:

- Biceps brachii tendon and bursa
- Infraspinatous tendon and bursa
- Supraspinatous muscle and tendons
- Superficial shoulder muscles and underlying humerus and scapula

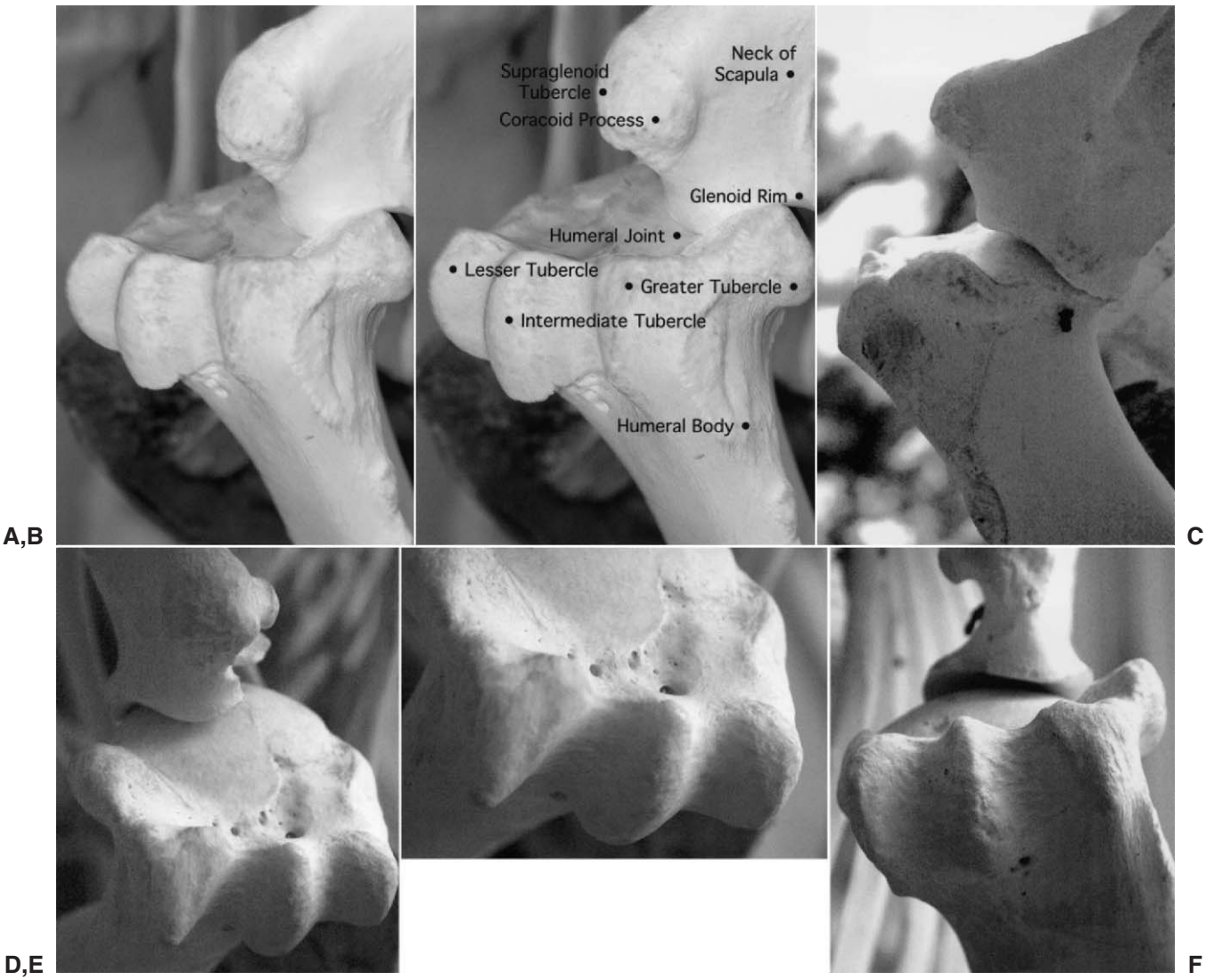


Figure 10-2 • Defleshed humeral joint seen from unlabeled lateral **(A),** labeled lateral **(B),** medial **(C),** upper front lateral **(D),** upper front lateral close-up **(E),** and head-on **(F)** perspectives.

Conversely, only the lateral and part of the caudal humeral head could be visualized, often with some difficulty.

▮▮▮ SCAPULAR FRACTURE

Minimally displaced scapular fractures are often very difficult to identify because of extensive superimposition by adjacent tissue and the limitations associated with having only a lateral view. Even moderately displaced fractures are hard to diagnose because of swelling. If the adjacent suprascapular nerve has been lacerated, crushed, or stretched, the infraspinatous and supraspinatous muscles are usually atrophied and the shoulder joint is unstable.

Scapular Blade Fractures

Scapular blade fractures can be diagnosed readily in young foals but not in adult horses. A comparison view of the normal opposite scapula is helpful when confronted with subtle injuries (Figure 10-6).

Supraglenoid Tubercle Fractures

Watrous and Ackerman described the radiographic appearance of supraglenoid tuberosity fractures in young horses, pointing out that this is the most vulnerable part of the shoulder in immature animals because it is formed from a separate ossification center, which may be avulsed in association with severe strain of the biceps brachii (Figure 10-7).[4]

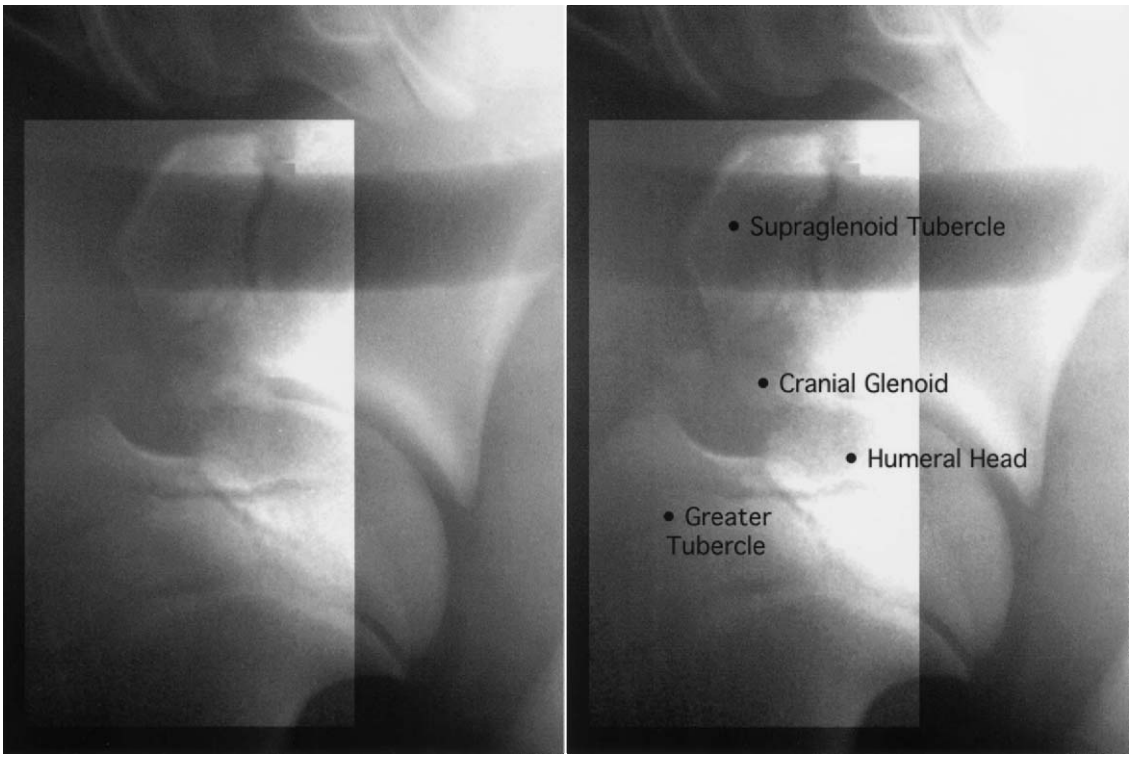


Figure 10-3 • Lateral views of unlabeled **(A)** and labeled **(B)** normal shoulder joint in a young foal.



Figure 10-4 • Close-up lateral view of a normal supraglenoid tuberosity and its growth plate *(emphasis zone)* in a young foal.



Figure 10-5 • Close-up lateral oblique view of a normal supraglenoid tuberosity and its growth plate *(emphasis zone)* resembling a comminuted fracture.

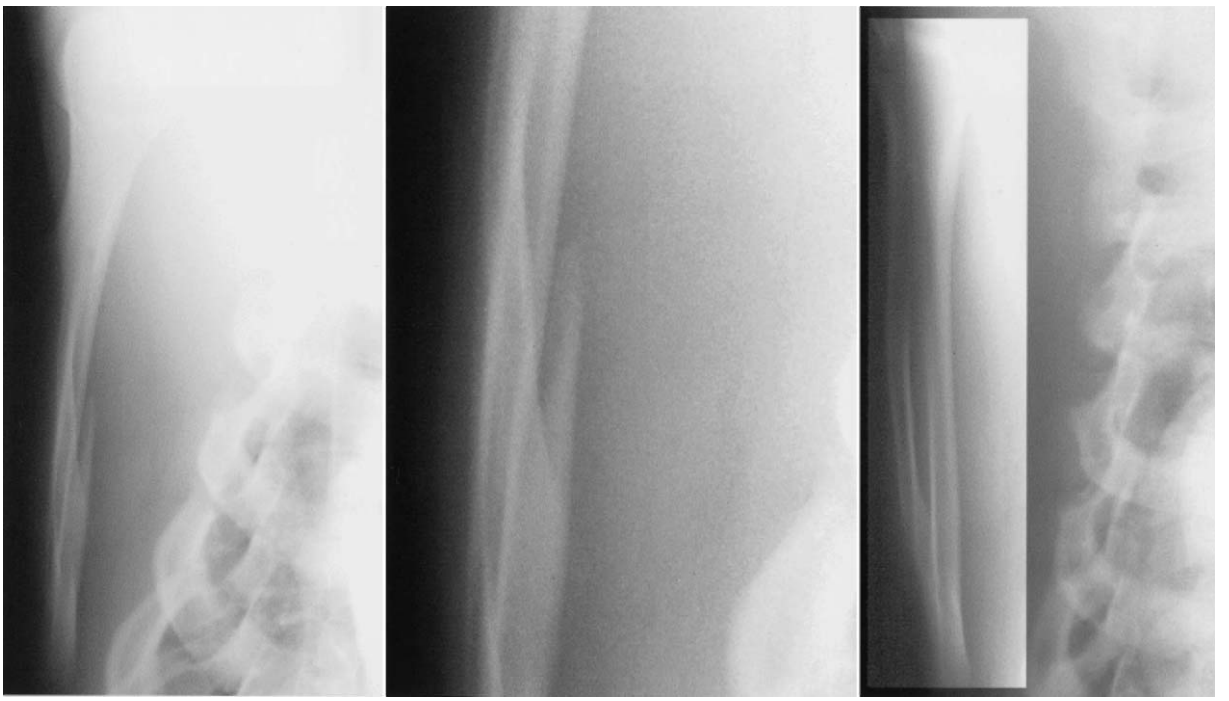


Figure 10-6 • Ventrodorsal **(A)** and close-up ventrodorsal **(B)** views of the scapula show a moderately displaced fracture of the central scapular body. A ventrodorsal view of the normal opposite scapula is provided for comparison **(C).**

Glenoid Fractures

Glenoid fractures run the gamut from invisible, to vague, to obvious. Small cranial corner fractures are the most difficult to diagnose because of their small size and minimal displacement (Figure 10-8). Superimposition of one shoulder on another or the presence of overlapping cervical vertebrae or ribs can make what should be obvious large articular fractures extremely confusing. Conversely, a normal humeral joint may appear fractured for the same reasons (Figure 10-9).

Scapular Tumors

Scapular tumors are rare. Zaruby and co-workers reported the radiographic appearance of a scapular *periosteal osteosarcoma* of an 8-year-old Arabian gelding showing lameness and atrophy of the left forelimb.[5] The tumor appeared predominantly destructive, consuming much of the distal third of the bone. Uncharacteristically, the proximal third of the associated humerus was covered in new bone, causing it to appear abnormally opaque. Necropsy confirmed that the tumor had crossed the shoulder joint to involve the proximal humerus.

Caution: *Although it is generally accepted that primary bone tumors do not cross open growth plates or joint spaces, there are occasional exceptions, as exemplified by the preceding case.*



Figure 10-7 • Ultra-close-up lateral view of a subacute, displaced, multipiece fracture of the supraglenoid tuberosity featuring one large and half a dozen smaller fragments *(emphasis zone).*

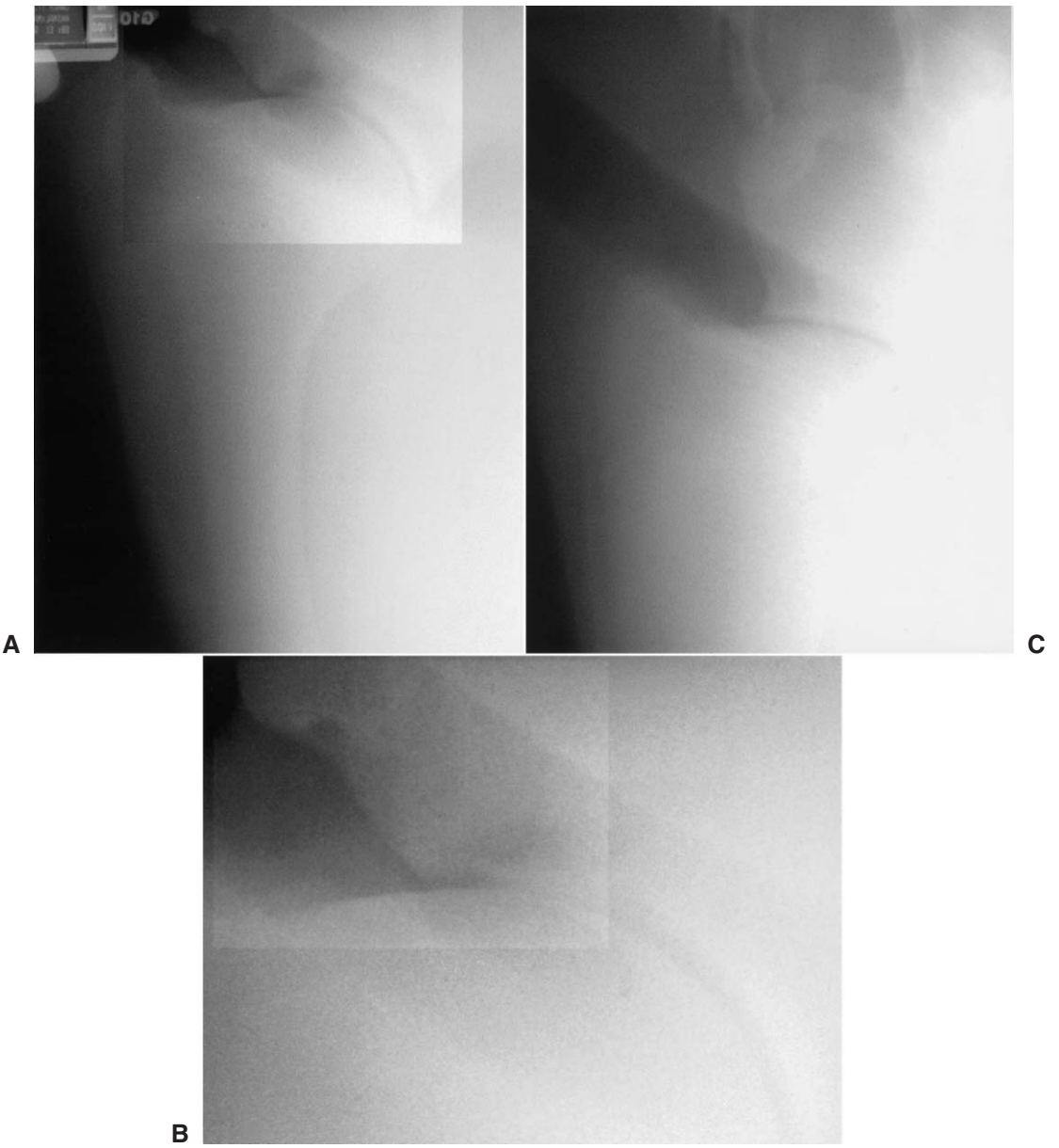


Figure 10-8 • Lateral **(A)** and close-up lateral **(B)** views of the humeral joint and the proximal half of the humerus show a vague lucency and subtle marginal discontinuity along the cranial margin of the glenoid, the result of a minimally displaced articular fracture. A normal humeral joint is provided for comparison **(C).**

▮▮▮ SINOGRAPHIC AND SONOGRAPHC ASSESSMENT OF FOREIGN BODIES, SEQUESTRA, AND RELATED SINUS TRACTS OF THE SHOULDER REGION

Sinography

Sinography has been used to disclose a wide variety of wooden foreign bodies embedded in the muscle of the shoulder and pectoral regions (Figure 10-10). Sinography is also indispensable in establishing the extent to which the bicipital tendon may be involved in diffuse shoulder infections (Figure 10-11). Sinography has also been used to show bursal involvement in the case of a chronically draining shoulder wound.[6] Metal probes can sometimes establish the depth of a tract[7] but cannot be relied on to reveal the complexity of a specific lesion.

Sonography

Cartee and Rumph wrote an excellent pictorial essay on the sonographic appearance of bone, wood, and tendon fragments experimentally embedded in muscle.[8] As might be expected, bone produced the strongest acoustic shadow, followed by wood and tendon. Three naturally occurring cases were also

reported: one with a scapular blade sequestrum and the others with chronic draining tracts. In the case of the latter, ultrasound was instrumental in establishing the full extent of the sinus network.

Mueller and co-workers described the sonographic appearance of a large wooden splinter imbedded deep within the supraspinatous muscle of a horse.[9] Abscessation in the shoulder region, provided its depth does not exceed the capability of the ultrasound probe, is usually straightforward (Figure 10-12).



Figure 10-9 • A lateral view of the humeral joint shows a severe fracture-dislocation in which the glenoid has been split in two; the supraglenoid tuberosity and cranial half of the glenoid are being displaced proximally and the humerus cranially.

▮▮▮ SHOULDER ARTHROGRAPHY

Nixon and Spencer described positive and double-contrast arthrography of the equine shoulder joint.[10] As might be expected, the extended mediolateral view proved most informative (the horse was anesthetized). Also as might be anticipated, arthrography better delineated cartilage flaps in horses with osteochondritis than plain films. Arthrography was also able to establish the presence of an abnormal communication between a subchondral bone cyst and the humeral joint. Iohexol resulted in less synovial inflammation than metrizamide.

Technique

The humeral joint was punctured at a point 1 cm cranial to the infraspinatous tendon of insertion and 1 cm proximal to the greater tubercle of the humerus. One or two milliliters of joint fluid was removed for laboratory analysis, and about 10 ml of nonionic contrast medium was injected. The leg was then flexed and extended several times to distribute the diagnostic iodine solution throughout the shoulder joint, repositioned, and radiographed. If double contrast was desired, the humeral joint was repunctured, and 35 ml of room air was injected. Again the leg was manipulated to distribute the contrast, repositioned, and radiographed.

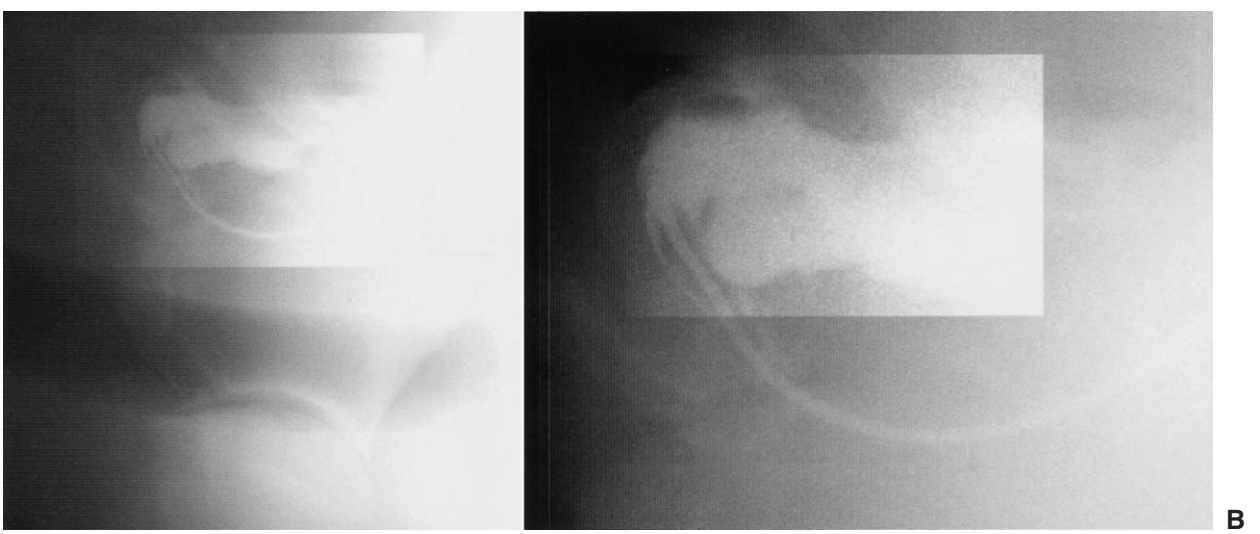


Figure 10-10 • Lateral oblique **(A)** and close-up lateral oblique **(B)** sinograms obtained from the upper shoulder region, proximal to the supraglenoid tuberosity, shows a medium-sized, oblong pool of contrast solution containing a vaguely outlined filling defect, which eventually proved to be a 3-inch wooden splinter *(emphasis zones).*

Femoral Head Fracture

Growth plate fractures of the humeral head typically result in cranial displacement of the associated humeral shaft, causing the bone fragments to overlap in a distinctive manner (Figure 10-13). Proximal humeral fractures often lead to severe distal extremital edema, especially of the elbow region, in some instances so severe that it mimics the swelling seen with a fractured olecranon. Others are accompanied by such severe swelling that it is not possible to image the humeral joint fully, having to rely instead on the abnormal appearance of the proximal humeral shaft to infer a more proximal injury (Figure 10-14).



Figure 10-11 • Close-up lateral sinogram shows filling of the distended bicipital sheath, which traces the enclosed bicipital tendon as it tracks along the cranial surface of the humeral tubercle.

Fracture of the Greater Tubercle

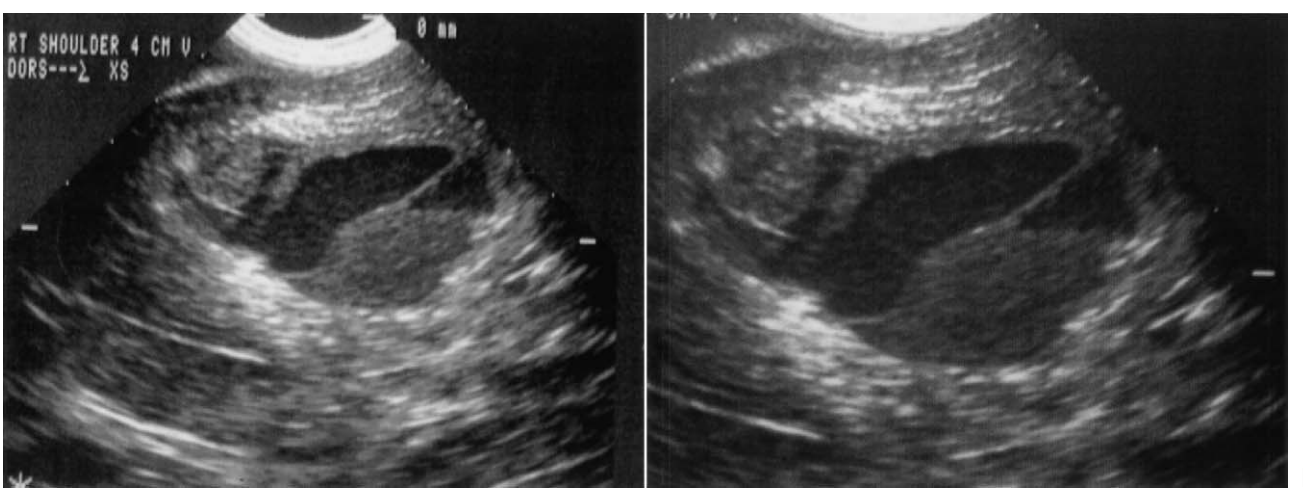
The greater humeral tubercle is divided into cranial and caudal parts, which moor the proximal portions of the supraspinatous and infraspinatous muscles. Tudor and co-workers described a fracture of the caudal aspect of the greater tubercle that was clearly visible only in the caudolateral-craniomedial oblique projection of the humeral joint.[11]

▮▮▮ SHOULDER DISLOCATION

Most horses with acute shoulder dislocations bear little or no weight on the injured leg and may exhibit visible limb shortening. Chronic dislocations have a similar appearance but with the addition of severe atrophy of the shoulder muscles. Fractures may or may not accompany subluxation or luxation.[12]

Radiographically most shoulder dislocations cause overlapping of the glenoid and proximal surface of the humerus, replacing the normally radiolucent shoulder joint with a thick white band, a consequence of lateral dislocation, bony overlap, and increased radiation absorption.[13] Arthrography or, better, magnetic resonance imaging, usually reveals articular cartilage damage, whereas progress radiographs show a gradual loss of regional bone density and eventually osteoarthritis.

Chronic dislocations are usually accompanied by varying degrees of osteoarthritis. However, complete dislocations (luxation) may not appear arthritic but instead show severe osteopenia, reflecting a combination of reduced use and altered muscle pull.



A **B**

Figure 10-12 • Orientation **(A)** and close-up **(B)** sonograms obtained from the craniolateral aspect of the shoulder region show a deep, compartmentalized abscess that is approximately the size of a small lemon.



Figure 10-13 • A, Horse with a displaced proximal femoral growth plate fracture, Salter-Harris type II, accommodates its injury. **B,** Because of severe swelling in the shoulder region, only the caudoventral aspect of the fracture is apparent *(emphasis zone).*

▮▮▮ BICIPITAL TENOSYNOVITIS

Bohn and co-workers reported the sonographic features of bicipital tenosynovitis in a 7-year-old Missouri Fox Trotter mare.[14] These included (1) multiple small hypoechoic foci in the tendon body, interpreted as fiber disruption; (2) increased tendon diameter; and (3) bursal fluid. Earlier radiographs of the humeral joint showed decreased density and abnormal trabeculation in the greater tubercle.

A skyline view of the bicipital groove was also obtained and revealed small osteophytes, which were interpreted as potentially impinging on the bicipital tendon. After surgery the horse eventually recovered, but unfortunately no follow-up images were made to determine whether any of the previously identified radiographic and sonographic abnormalities had resolved.

▮▮▮ OSTEOCHONDRITIS OF THE SHOULDER

Nyack and co-workers reported the radiographic features of osteochondritis of the humeral joint in 38 horses.[15] Radiographic findings included various combinations of the following abnormalities, depending on the severity of the disease:

- Abnormally contoured glenoid and humeral head
- Periarticular osteophytes
- Abnormally dense subchondral bone
- Subchondral cysts

Forty-three percent of the animals had bilateral shoulder lesions; generally, the worse the lesion, the worse the prognosis as determined by an outcome assessment involving 17 horses in this study. Grossly and histologically, osteochondritis of the equine shoulder joint was similar to that described in the dog, bull, pig, turkey, and broiler chicken. There were no specific clinical signs to differentiate osteochondritis from other sources of shoulder pain and related lameness in horses.

Mason and Maclean reported humeral osteochondritis in a 5-month-old Arabian and 4-month-old Standardbred filly. In the case of the latter, the diseased humeral head showed signs of disintegration 7 weeks after the initial radiographic examination, documenting the rapidity with which some lesions of this type can deteriorate (Figure 10-15).[16]

Osteochondritis of the humeral tubercles is usually fragmenting, and as such it resembles a fracture. The most reliable means of distinguishing osteochondritis from a nonunion fracture is the presence of bilateral lesions (Figure 10-16).

▮▮▮ HUMERAL STRESS FRACTURES

Mackey and co-workers reported the radiographic or scintigraphic appearance of 13 humeral stress fractures: 10 involving the proximal and caudolateral cortex and 3 in the distal, craniomedial cortex.[17]



Figure 10-14 • Horse with a humeral head fracture has positioned itself to take as much weight off the broken leg as possible **(A).** After failing to image the right shoulder directly, a lateral cranioventral view of the thorax was made that showed the normal and injured shoulders side-by-side. This radiograph, shown as a series of nonannotated **(B),** annotated **(C),** and close-up views **(D),** revealed a displaced, overlapped fracture of the right humeral head.

▮▮▮ DISTAL HUMERAL FRACTURE

Medial Epicondylar Fracture

Sudden, forceful contraction of the forelimb of a foal can result in an avulsion fracture of the medial epicondyle of the distal humerus, typically in a caudomedial or caudodistal direction. Fractures of this kind are usually of the Salter-Harris II variety and are associated with moderate to severe lameness, depending on duration. One report describes *bilateral* humeral epicondylar fractures in a 3-month-old Thoroughbred foal.[18]

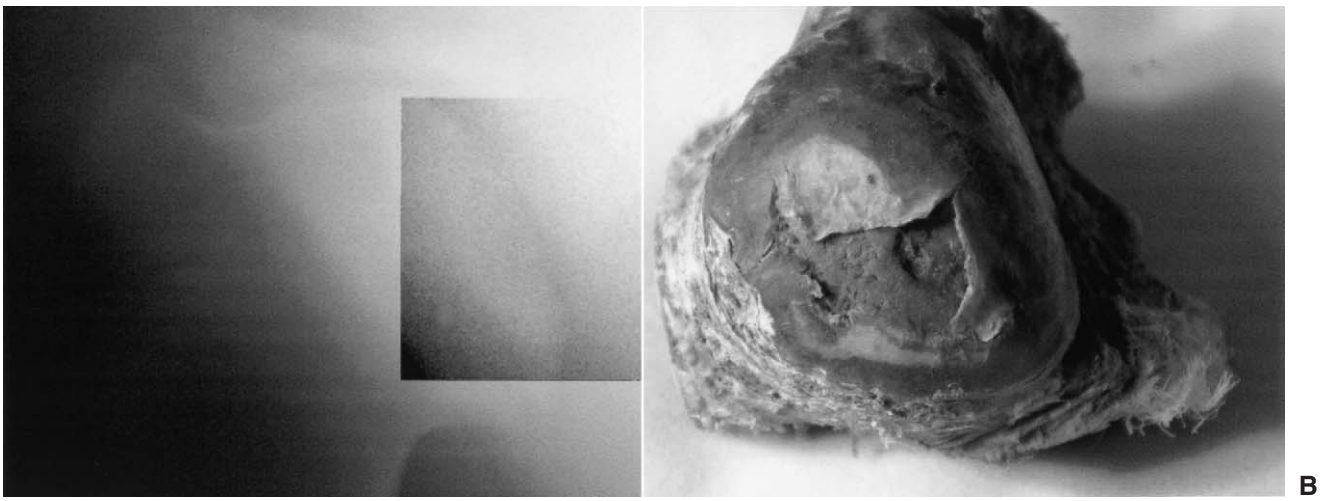


Figure 10-15 • A, Close-up lateral view of a flattened femoral head, the result of disintegration resulting from osteochondritis *(emphasis zone).* **B,** Grossly the femoral head shows severe regional cartilage and bone damage.



Figure 10-16 • Close-up lateral view of the proximal humerus shows detachment of the intermediate tubercle. Because a similar lesion was present on the opposite side of this Arabian, a diagnosis of fragmenting osteochondritis was made.

References

1. Pugh CR, Johnson PJ, et al: Ultrasonography of the equine bicipital tendon region: a case history report and review of anatomy, *Vet Radiol Ultrasound* 35:183, 1994.
2. Tnibar MA, Auer JA, Bakkall S: Ultrasonography of the equine shoulder: technique and normal appearance, *Vet Radiol Ultrasound* 40:44, 1996.
3. Watrous BJ, Ackerman N: The equine shoulder: a radiographic review, *Calif Vet* Feb:7, 1978.
4. Zaruby JF, Williams JW, Lovering SL: Periosteal osteosarcoma of the scapula in a horse, *Can Vet J* 34:742, 1993.
5. Mirza MH, Martin GS, Williams J: What is your diagnosis? *J Am Vet Med Assoc* 212:349, 1998.
6. Peloso JG, Nickels FA, Stickle RL: What is your diagnosis? *J Am Vet Med Assoc* 199:923, 1991.
7. Cartee RE, Rumph PF: Ultrasonographic detection of fistulous tracts and foreign objects in muscles of horses, *J Am Vet Med Assoc* 184:1127, 1984.
8. Mueller E, Watson E, Allen D: What is your diagnosis? *J Am Vet Med Assoc* 203:1402, 1993.
9. Nixon AJ, Spencer CP: Arthrography of the equine shoulder joint, *Equine Vet J* 22:107, 1990.
10. Tudor R, Crosier M, et al: Radiographic diagnosis: fracture of the caudal aspect of the greater tubercle of the humerus in a horse, *Vet Radiol Ultrasound* 42:244, 2001.
11. Semvolos SA, Nixon AJ, et al: Shoulder joint luxation in large animals: 14 cases (1976-1997), *J Am Vet Med Assoc* 213:1608, 1998.
12. Rodgerson DH, Hansen RR: What is your diagnosis? *J Am Vet Med Assoc* 211:701, 1997.
13. Bohn A, Papageorges M, Grant BD: Ultrasonic evaluation and surgical treatment of humeral osteitis and bicipital tenosynovitis in a horse, *J Am Vet Med Assoc* 201:305, 1992.
14. Nyack B, Morgan JP, et al: Osteochondrosis of the shoulder joint of the horse. *Cornell Vet* 71:149, 1981.
15. Mason TA, Maclean AA: Osteochondrosis dissecans of the head of the humerus in two foals, *Equine Vet J* 9:189, 1977.
16. Mackey VS, Trout DR, et al: Stress fractures of the humerus, radius, and tibia in horses. *Vet Radiol* 28:26, 1987.
17. Pooley Al, Slone DE: What is your diagnosis? *J Am Vet Med A*ssoc 200:1139, 1992.

Chapter 11

Pelvis, Sacrum, and Sacroiliac Joint

THE STANDARD PELVIC SERIES

The standard pelvis series consists of a flexed or extended ventrodorsal view, and paired right and left flexed or extended ventrodorsal obliques (Figure 11-1). In adult horses, the flexed ventrodorsal position is easiest; however, in young foals, either position can be used. Various views of the pelvic region of an adult skeleton are provided for reference (Figure 11-2).

The Caudal Lumbosacral Spinal Unit and Sacroiliac Joint

Jeffcott described a technique for radiographing the caudal lumbar and lumbosacral spinal regions in the horse.[1] He also reported the use of linear tomography in the diagnosis of equine lumbosacral disease.[2,3]

Rooney attributed sacroiliac arthritis in racing Standardbreds (so-called hitching or hiking of the hindquarters) to tracks with cambered surfaces and unbanked or underbanked turns—lameness, he said, that was often falsely attributed to stifle pain.[4] Orientation and close-up views or the sacrum are provided for reference (Figure 11-3).

Nuclear Imaging

Erichsen and co-workers described the normal scintigraphic anatomy of the equine sacroiliac joint, finding it consistently positioned between the tuber sacrale and the craniolateral margin of the tuber coxa.[5] Dysen and co-workers determined that a difference in radiopharmaceutical uptake between the right and left sacroiliac joints is a high-probability indicator of disease, especially when found clearly to differ from similar studies performed in age-matched controls.[6,7]

PELVIC FRACTURE

Heinze and Lewis were among the first to describe pelvic radiography in the horse.[8] In a separate communication, the same authors reported their radiographic findings obtained from 126 radiographic examinations performed on clinical cases.[9] Interestingly, nearly half of their studies proved normal. However, many of the examinations were diagnostic, identifying a wide variety of lesions, including displaced fractures of the ileum, acetabulum, pubis, and ischium, and growth plate fractures of the proximal femur and greater trochanter. They were also able to identify septic arthritis and chronic dislocation of the hip.

A subsequent study of 100 equine pelvic fractures by Rutkowski and Richardson indicated that most horses with pelvic fractures improved, *with or without* treatment, even those with acetabular injuries.[10] Clinical indicators of pelvic fracture, including those of the hip, were (1) pelvic asymmetry or *dropped hip*, (2) severe atrophy of many of the hip and thigh muscles, (3) and rectal crepitance. Ilial fractures were most common. As previously reported by Jeffcott, young female horses were at greatest risk.[11]

In my experience, the 30-degree flexed ventrodorsal oblique projection is the best view for identifying minimally displaced central acetabular fractures in horses (Figure 11-4).[12] Care must be taken not to mistake rectal gas bands for a pelvic fracture (Figure 11-5).

PELVIC INFECTION

Clark-Price and co-workers reported osteomyelitis of the pubic symphysis in a 2-year-old Quarter Horse filly caused by *Rhodococcus equi*.[13] Radiographically (ventrodorsal view) the lesion appeared centrally destructive and peripherally productive, characteristic of many bone infections.

Hogan and co-workers reported the radiographic features of ileal osteomyelitis in a 2-week-old Thoroughbred filly hospitalized because of acute hindlimb lameness and fever.[14] Oblique dorsoventral radiographs made with the foal in the standing



Figure 11-1 • Ventrodorsal (VD) and VD obliques.



Figure 11-2 • Left lateral **(A),** caudal **(B),** and right caudolateral oblique **(C)** views of the pelvic region of an adult skeleton are provided for anatomic comparison. Labeled lateral **(D)** and dorsal **(E)** views of a defleshed hemipelvis are also included. Note the callused acetabulum, the result of a partially healed fracture.



Figure 11-3 • Caudoventral **(A)** and caudoventral close-up **(B)** views of the sacrum of an adult horse illustrate the anatomic complexity of the bone and its relatively concealed position within the interior of the pelvis.



Figure 11-4 • Thirty-degree flexed ventrodorsal oblique close-up **(A)** and ultra-close-up **(B)** views of minimally displaced, comminuted pubic and acetabular fractures in a young horse *(emphasis zone).*

position showed partial destruction of the right tuber coxa. Ultrasound revealed a deep fluid pocket adjacent to the damaged ileal surface. These findings strongly suggested osteomyelitis.

Figure 11-6 shows a localized osteomyelitis of the coxal tuberosity, along with a normal control. The margins and surfaces of the pelvic tuberosities (coxal, sacral, and ischial) are normally quite irregular and as such may be mistaken for new bone deposits caused by infection or injury.

▮▮▮ ISCHIAL TUBEROSITY AND THIRD TROCHANTER

Nuclear Imaging

Ischial Tuberosity and Third Trochanter Uptake Ratio. Geissbuhler and co-workers reported the scintigraphic appearance of ischial tuberosity and third trochanter injuries.[15] By determining the relative radiopharmaceutical uptakes of the ischial tuberosity and third trochanter, termed the *uptake ratio,* and comparing them with normal reference values, the authors were able to identify otherwise invisible lesions. Abnormal values were typically two to three times greater than normal.

The authors recommended adding a caudal view to the standard caudolateral oblique scan in instances in which the ischial–third trochanter uptake ratio was increased. This additional view includes both ischial tuberosities in the same image, providing a normal comparison. The latter view also enables the operator to place the calumniator closer to the ischial tuberosities, thus improving image quality.

Abnormal Ischial Tuberosity and Third Trochanter Uptake Patterns. Abnormal uptake patterns associated with ischial tuberosity injuries included (1) deformity, (2) poor margination, (3) increased uptake

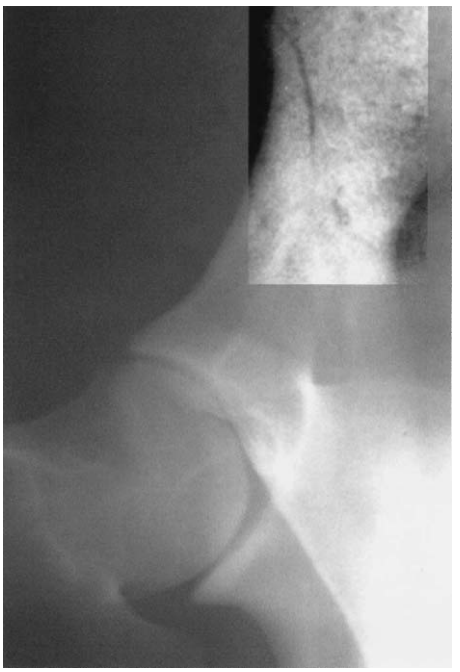


Figure 11-5 • A rectal gas crevice superimposed on the outer neck of the ileum mimics an incomplete fracture *(emphasis zone).*

region, and (4) two separate uptake regions within the tuber ischium.

▮▮▮ GROIN, THIGH, AND GLUTEAL REGIONS

Thigh Strain

A second- or third-degree thigh strain can resemble a hip injury, although to the experienced eye there are differences. Unlike sprains, strains usually heal in a few weeks, provided they are not aggravated by further injury. Like people, animals with strains are often lamest a day or two after the initial injury. By way of example, trail riders often describe a minor slip or stumble, which at the time was thought to be inconsequential, only to be followed the next day by an obvious lameness.

Turner described the thermographic appearance of thigh strain in 29 horses, dividing the injuries into two categories: croup myopathy and caudal thigh myopathy, citing palpation as the principal means of physical diagnosis, and thermography as the method of choice for confirmation.[16] Old muscle injuries, which have led to fibrosis, may leave little or no thermographic evidence of their presence, depending on their size and location. Valentine and co-workers were able to confirm such a case with a combination of electromyography and muscle biopsy.[17]

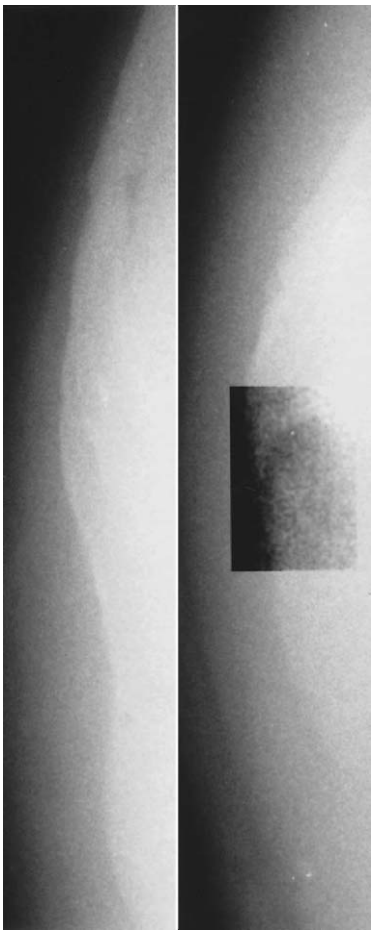


Figure 11-6 • Customized oblique projection (right) of the coxal tuberosity of a horse shows localized bone loss, the result of infection caused by a deep wound *(emphasis zone).* The normal opposite coxal tuberosity is provided for comparison *(left).*

Abscess

Love and Nickels reported the sonographic appearance of a deep gluteal abscess, presumably the result of an earlier intramuscular injection.[18] The abscess initially appeared as a small (2 × 3 cm) circular object featuring a thick, well-marginated, echoic capsule and a hypoechoic, distally enhancing interior. Attempted drainage was unsuccessful, and the horse was treated with injectable antibiotics. The horse was reexamined a month later, still lame and painful. This time the lesion appeared composed of multiple tightly clustered abscesses: one large, two medium, and one small. I have encountered enormous abscesses in and around the large thigh muscles, many of which had elaborate compartmentalization, making complete drainage difficult or impossible (Figure 11-7).

Nerve Injury

Alexander and Dobson reported the normal sonographic appearance of the sciatic, peroneal, and tibial nerves in cadavers and live adult horses.[19]

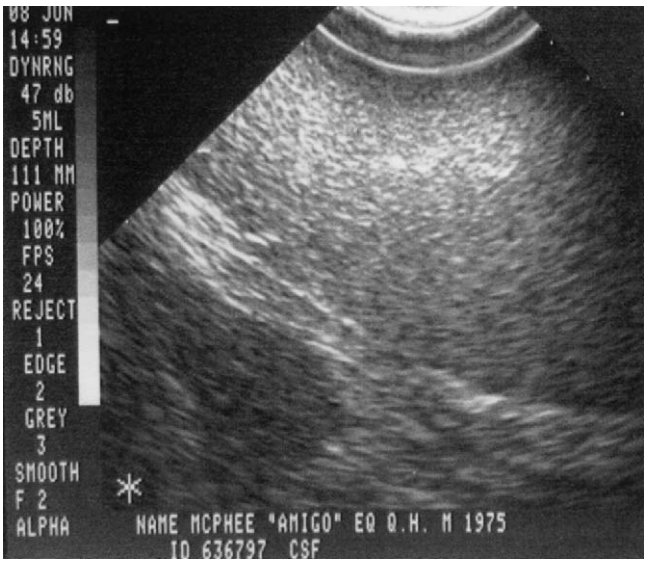


Figure 11-7 • Long section of a very large abscess in the upper rump of an adult horse located immediately caudal to the coxal tuberosity (not shown). The sonogram shows only one of three major and two minor cavities, which communicated through a series of small channels. Numerous small splinters left behind after the removal of a large wooden stake fueled the abscesses.

Vascular Disease

Warmerdam reported the sonographic appearance of femoral arterial thrombosis in three horses as well as the sonographic appearance of the normal equine femoral artery.[20]

Ross and co-workers reported the use of first-pass radionuclide angiography to diagnose an aortoiliac thromboembolism in a 6-year-old Standardbred stallion.[21] The horse became acutely lame in the right rear, featuring swelling of the right gluteal region and an elevated serum creatine kinase. The lameness, first detected during a prerace warm-up, was thought to have occurred in a recent trailer ride.

When examined 4 months later, the horse showed right gluteal atrophy and abnormal right hindlimb mechanics (abnormal circumduction). A nuclear medicine study revealed decreased activity in the right iliac vessels compared with that seen in normal control horses, indicative of reduced blood flow, and consistent with thrombosis.

References

1. Jeffcott LB: Radiographic examination of the equine vertebral column, *Vet Radiol* 20:135, 1979.
2. Jeffcott LB: Technique of linear tomography for the pelvic region of the horse, *Vet Radiol* 24:194, 1983.
3. Jeffcott LB: Radiographic appearance of equine lumbosacral and pelvic abnormalities by linear tomography, *Vet Radiol* 24:201, 1983.
4. Rooney JR: The cause and prevention of sacroiliac arthrosis in the Standardbred horse: a theoretical study, *Can Vet J* 22:356, 1981.
5. Erichsen C, Berger M, Eksell P: The scintigraphic anatomy of the equine sacroiliac joint, *Vet Radiol Ultrasound* 43:287, 2002.
6. Dysen S, Murry R, et al: The sacroiliac joint: evaluation using nuclear scintigraphy. Part 1, *Equine Vet J* 35:226, 2003.
7. Dysen S, Murry R, et al: The sacroiliac joint: evaluation using nuclear scintigraphy. Part 2, *Equine Vet J* 35:233, 2003.
8. Lewis RE, Heinse CD: Radiographic examination of the equine pelvis: technique, *J Am Vet Med Assoc* 159:1388, 1971.
9. Heinze CD, Lewis RE: Radiographic examination of the equine pelvis: case reports, *J Am Vet Med Assoc* 159:1328, 1971.
10. Rutkowski JA, Richardson DW: Pelvic fractures in the horse, *Equine Vet J* 21:256, 1989.
11. Jeffcott LB: Pelvic lameness in the horse, *Equine Pract* 4:21, 1982.
12. Farrow CS: Can Vet Med Assoc Annual Meeting Proceedings, 1999.
13. Clark-Price SC, Rush BR, et al: Osteomyelitis of the pelvis caused by *Rhodococcus equi* in a two-year-old horse, *J Am Vet Med Assoc* 222:969. 2003.
14. Hogan PM, Bernard WV, et al: What is your diagnosis? *J Am Vet Med Assoc* 207:415, 1995.
15. Geissbuhler U, Busato A, Ueltschi G: Abnormal bone scan findings of the equine ischial tuberosity and third trochanter, *Vet Radiol Ultrasound* 39:572, 1998.
16. Turner TA: Hindlimb muscle strain as a cause of lameness in horses, in *Proc Am Assoc Equine Pract* 281, 1989.
17. Valentine BA, Rousselle SD, et al: Denervation atrophy in three horses with fibrotic myopathy, *J Am Vet Med Assoc* 205:332, 1994.
18. Love NE, Nickels F: Ultrasonic diagnosis of a deep muscle abscess in a horse, *Vet Radiol Ultrasound* 34:207, 1993.
19. Alexander K, Dobson H: Ultrasonography of peripheral nerves in the normal adult horse, *Vet Radiol Ultrasound* 44:456, 2003.
20. Warmerdam EPL: Ultrasonography of the femoral artery in six normal horses and three horses with thrombosis, *Vet Radiol Ultrasound* 39:137, 1998.
21. Ross MW, Maxson AD, et al: First-pass radionuclide angiography in the diagnosis of aortoiliac thromboembolism in a horse. *Vet Radiol Ultrasound* 38:226, 1997.

Chapter 12

Hip and Femur

THE STANDARD HIP SERIES

Like the pelvis, the standard coxal joint series consists of three views: a flexed ventrodorsal and a pair of flexed ventrodorsal obliques (Figure 12-1). A lateral view may also be included but frequently is of limited use because of the superimposition of the coxal joints on one another (Figure 12-2). A defleshed hip specimen is provided for radiographic-anatomic comparison (Figure 12-3).

DISLOCATED COXAL JOINT (HIP)

The typical dislocated (luxated) hip, as seen in ventrodorsal or ventrodorsal oblique projection, appears displaced cranially. In lateral view, the same injury usually shows the femoral head positioned well above an empty acetabulum. Surgical repairs as well as surgical salvage procedures have been reported in the horse but only on a limited basis. Most have involved foals or ponies. Reports of intermediate or long-term radiographic follow-up are rare.[1]

FRACTURED FEMORAL HEAD

Acute Proximal Femoral Growth Plate Fracture

In young animals, the proximal femur often breaks cleanly through the growth plate, an injury referred to as a *slipped capital physis* or type I Salter-Harris fracture. According to Embertson and colleagues, type I and type II proximal femoral growth plate fractures are the most common physeal fractures in foals.[2] Bilateral proximal femoral fractures have been reported in a 40-day-old foal after a fall while halter breaking.[3]

Fresh proximal growth plate fractures may be successfully treated with cancellous bone screws, although the surgery is technically demanding with respect to seating at least two screws well into the central two thirds of the femoral head.[4] Although there are published statements to the contrary, not all untreated proximal femoral growth plate fractures result in osteoarthritis of the coxal joint.[5] Multiple pins (stacked pins) have been used with modest success to repair fresh proximal femoral growth plate fractures in foals.[6]

Chronic Proximal Femoral Growth Plate Fracture

Chronic proximal femoral growth plate fractures can be deceptive, often resembling infections . The reason for this appearance is twofold: First, when the capital physis is crushed or fractured (Salter-Harris type I or II injuries), it also loses some or all of its blood supply, a loss that is rarely recouped. Thus devascularized, the femoral head slowly begins to necrose. Concurrently the base of the detached femoral head is being abraded and nonuniformly compressed by the underlying metaphysis as the two incongruent surfaces make contact. The result is collapse and, eventually, overt fragmentation of the femoral head (Figures 12-4 and 12-5).

FRACTURED ACETABULUM

Acetabular fractures are generally diagnosed in one of two ways: (1) directly, by identifying a fracture; and (2) indirectly, by identifying a callus (Figures 12-6 through 12-9). An acetabular fracture can also be inferred from an arthritic hip (Figure 12-10), although there are other causes of coxal arthritis, such as a proximal femoral fracture, chronic dislocation, osteochondritis, and occasionally, hip dysplasia. Fractures of the acetabular lip, even if displaced, are often difficult or impossible to detect radiographically (Figure 12-11).

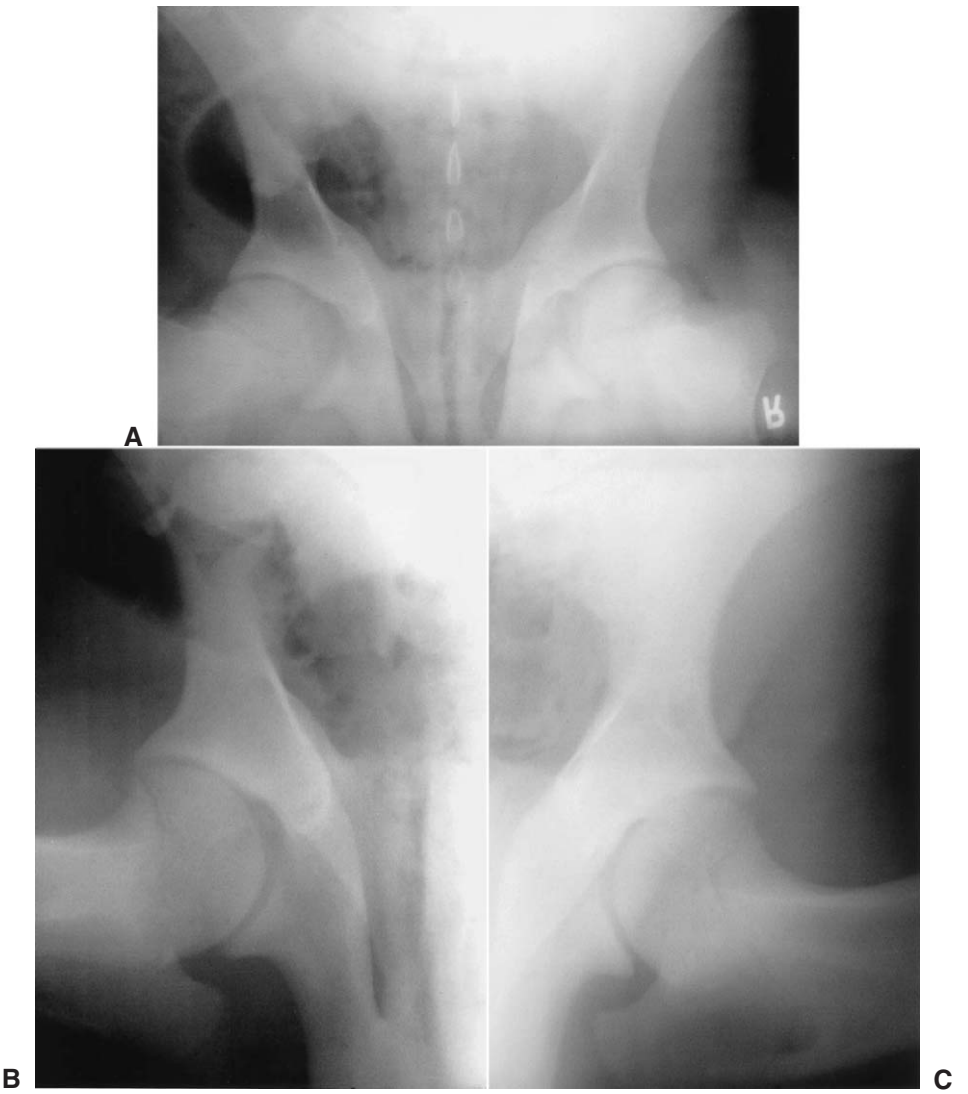


Figure 12-1 • Standard hip series in a horse includes extended ventrodorsal **(A),** right **(B),** and left **(C)** ventrodorsal obliques projections.

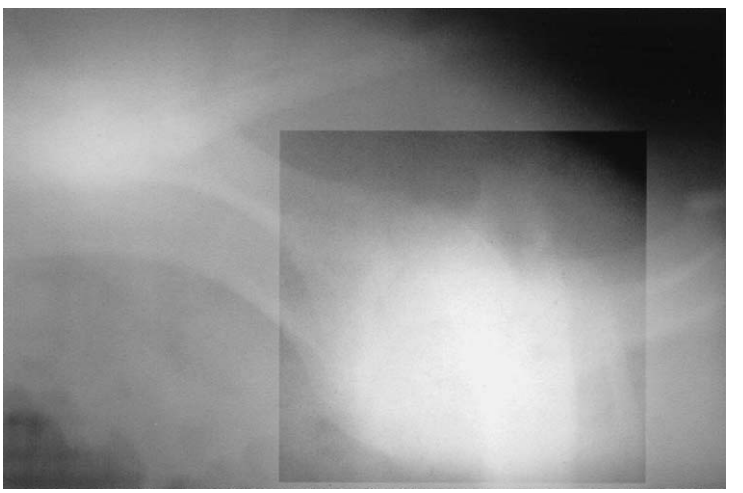


Figure 12-2 • Lateral view of the pelvis of a young foal predictably shows little central detail because of the thickness, density, and superimposition of the hips.

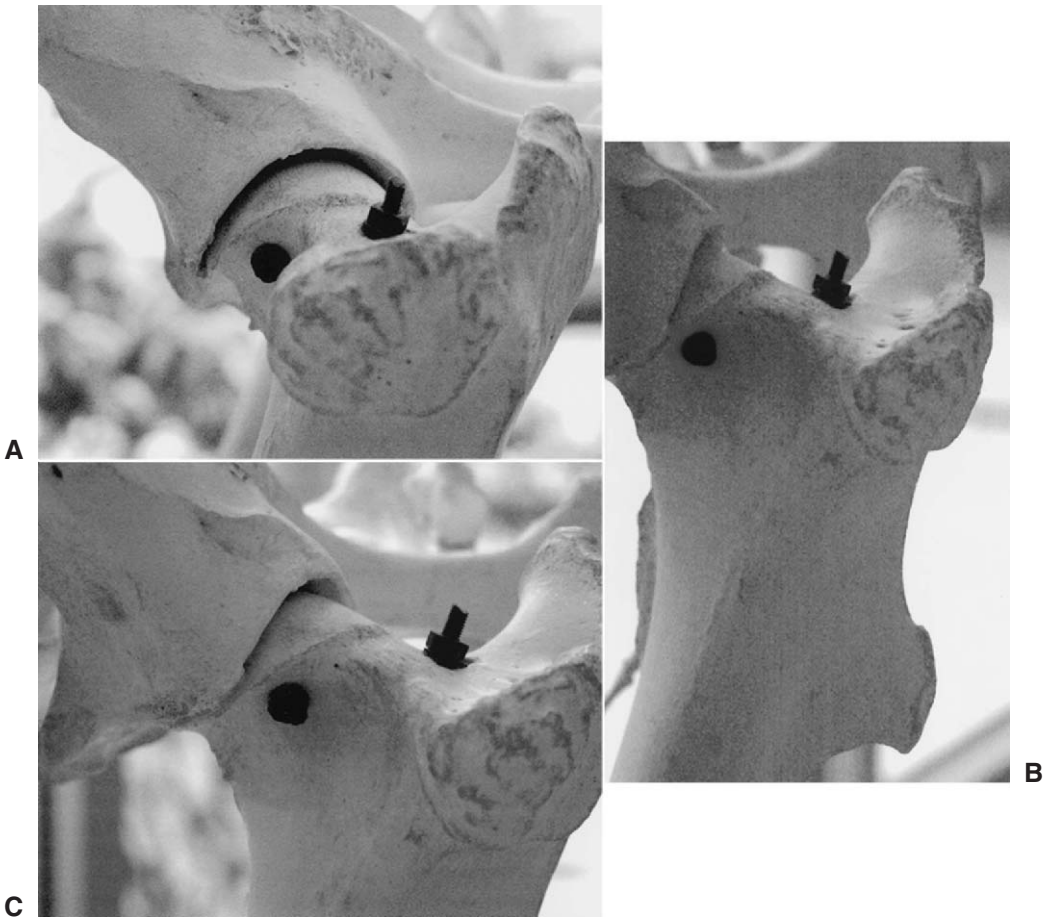


Figure 12-3 • Defleshed bones of a normal adult hip shown from lateral **(A),** cranial **(B),** and cranial close-up **(C)** perspectives.

▮▮▮ INFECTED HIP

In my experience, infectious arthritis/osteomyelitis of the coxal joints of foals and young horses is most likely to be the result of a bacteremia secondary to rhodococcal pneumonia. I and others have reported the radiographic appearance of such infections, which typically feature (1) narrowing and irregularity of the cartilage space; (2) reduced bone density; and (3) increased periarticular soft-tissue density, the latter sometimes indicating a secondary extracapsular abscess. Loesch and co-workers described a case in which a rhodococcal infection of a foal's hip joint infiltrated the joint capsule, tracked through the pelvic canal, and passed ventrally along the lateral body wall, eventually forming an abscess adjacent to the urinary bladder.[7]

I have also encountered septic arthritis-osteomyelitis of the coxal joint secondary to an umbilical infection. This form of infectious arthritis often resembles a chronic slipped capital physis featuring lytic flattening of the femoral head, widening of the cartilage space, metaphyseal new bone, and severe joint swelling (Figure 12-12).

▮▮▮ OSTEOCHONDRITIC HIP (OSTEOCHONDRITIS)

Nixon and co-workers reported bilateral subchondral bone cysts in the femoral heads of a lame 2-year-old male Thoroughbred.[8] Rose and co-workers reported an unconfirmed case of osteochondritis involving the hips of a yearling Thoroughbred colt seen because of a chronic lameness. Specifically the authors identified focal lucencies in the central parts of both acetabula, believed to represent small bone cysts. The changes in the left acetabulum were considered worse than those on the right, theoretically explaining the unilateral lameness.[9]

▮▮▮ THE GREATER, LESSER, AND THIRD TROCHANTERS

There are three femoral trochanters—the greater, lesser, and third—with the first and last of these developing from radiographically distinct, secondary ossifi-

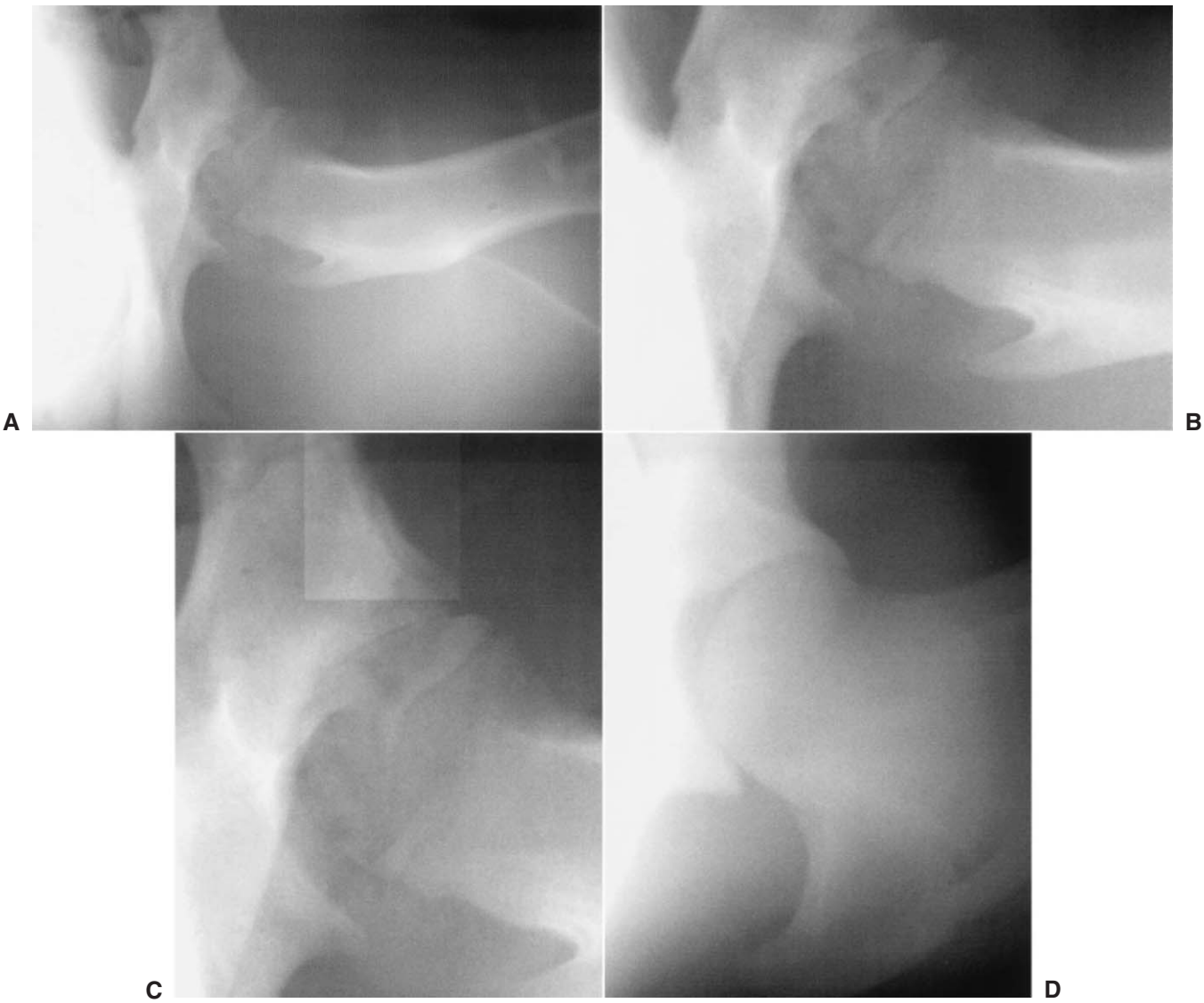


Figure 12-4 • Flexed ventrodorsal **(A),** close-up flexed ventrodorsal **(B),** and ultra-close-up flexed ventrodorsal **(C)** views of a foal's left hip show (1) partial dislocation, (2) collapse of the cartilage space, and (3) evidence of avascular necrosis of the femoral head, believed to have been caused by an earlier fracture-dislocation. The right hip is provided as a normal comparison **(D).**

cation centers. The greater trochanter is the largest of these muscular moorings, being visible from all proximal perspectives. The third trochanter is also quite prominent, appearing as a large, blocky outcropping on the upper lateral margin of the femur. The lesser trochanter is far less distinctive, being little more than a ridge on the medial side of the proximal femur just below the femoral head, somewhat resembling the famous *Hilary Step* just below the summit of Mount Everest.

Depending on its degree of development and angle of projection, the normal third trochanter can appear quite ominous radiographically, ranging in appearance from a fracture, to an infection, to osteochondritis (Figure 12-13). Accordingly great care must be taken not to overdiagnose this structure. The greater trochanter, or more specifically its growth plate, is not nearly as problematic where fractures are concerned. By comparison, the new bone deposition that sometimes accompanies severe hip strains can be quite subtle (Figure 12-14).

▮▮▮ FEMORAL SHAFT FRACTURES

Although femoral fractures are described as being common in foals, their successful surgical repair is not common.[10] Femoral fractures in adult horses are rare,



Figure 12-5 • Flexed ventrodorsal view of the abnormal right hip of a foal shows the aftermath of a presumed fracture-dislocation suffered 3 to 4 months earlier. Abnormalities include (1) a badly fragmented femoral head, (2) caudal dislocation, and (3) a severely deformed acetabulum (shallow, wide, and dense).

in part because of both the size and strength of the bone relative to others in the skeleton.[11]

Proximal shaft fractures can be extremely difficult to image in adult horses because of the great thickness of the upper leg, especially when swollen, combined with the difficulty of positioning a cassette high enough in the groin of a standing horse. We rarely *drop* a horse for the purpose of confirming a femoral shaft fracture radiographically unless we are intending to perform surgery. Generally speaking, displaced femoral fractures are easier to identify than those that are nondisplaced, especially when only one cortex is visible (Figures 12-15 and 12-16).

Because of their relatively small size, surgical reduction of femoral condylar fractures is technically easier and generally more successful in foals than in adult horses, although there are accounts of successful repair in the latter.[12]

▮▮▮ DISTAL FEMORAL GROWTH PLATE AND CONDYLAR FRACTURES

Displaced or fragmented distal femoral growth plate fractures are easier to diagnose radiographically than nondisplaced injuries. In the latter instance, a comparative view of the opposite distal femoral growth plate can prove indispensable in detecting small increases in physeal width or a slight marginal offset.

Text continued on p. 225

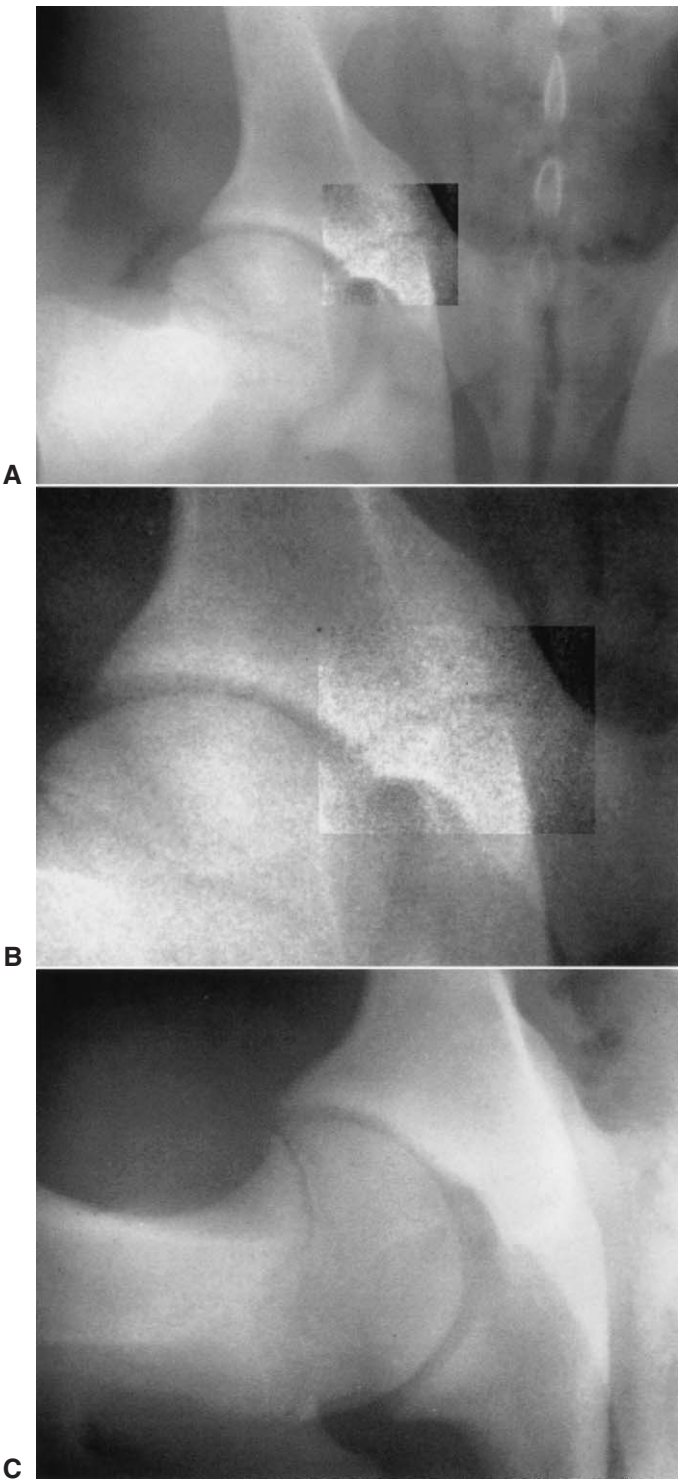


Figure 12-6 • Ventrodorsal **(A)** and close-up ventrodorsal **(B)** views of a fresh, minimally displaced, central acetabular fracture in a foal, a so-called cracked acetabulum. A corresponding view of a normal foal hip is provided for comparison **(C).**



Figure 12-7 • Ventrodorsal **(A)** and close-up ventrodorsal **(B)** views of a mild to moderately displaced, partially healed, central acetabular fracture in a foal *(emphasis zone)*. Close-up ventral **(C)** and dorsal **(D)** views of a defleshed bone specimen from another horse with a similar injury show just how extensive callus formation must become before it is radiographically detectable.



Figure 12-8 • Close-up view of fresh, displaced cranial acetabular fracture in an adult horse.

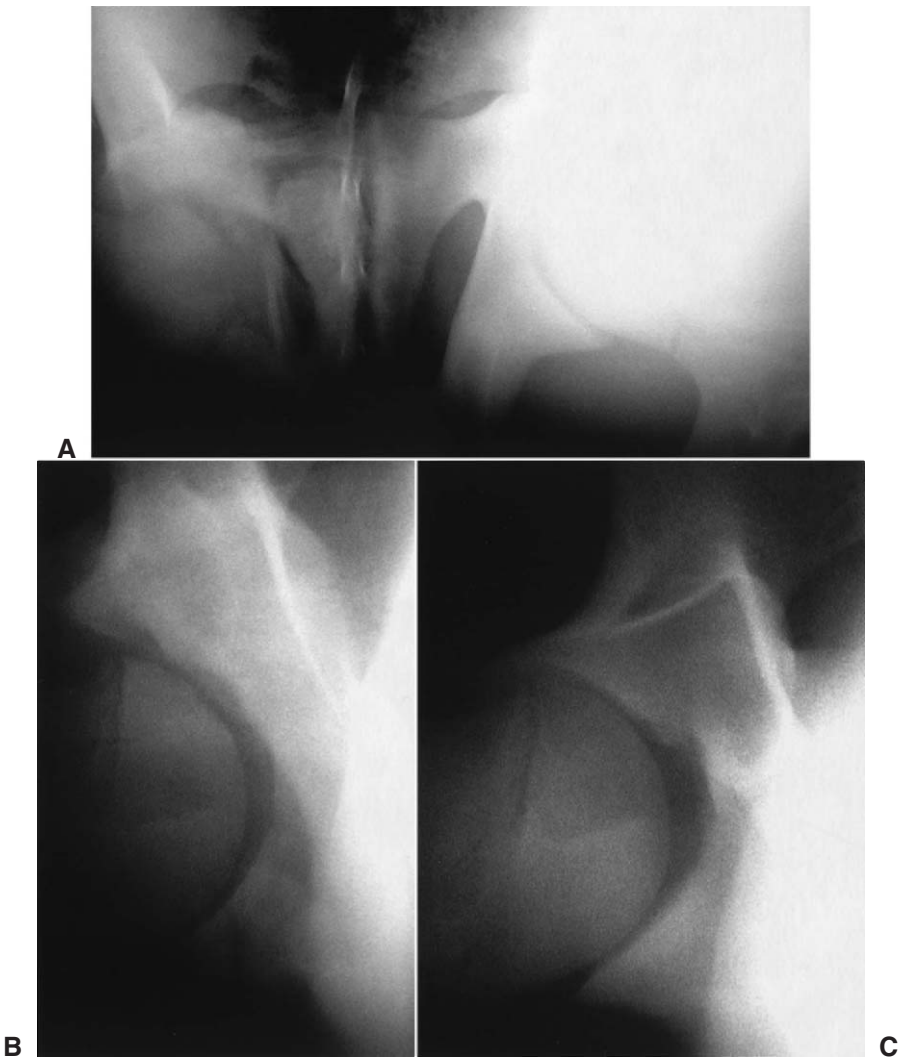


Figure 12-9 • Ventrodorsal oblique **(A)** and close-up ventrodorsal oblique **(B)** views of a fully callused acetabular fracture, estimated to be 2 to 3 months old. In addition to the fracture callus, the margin of the acetabulum is irregular and the cartilage space widened, signs of osteoarthritis. The opposite hip is provided for comparison **(C).**

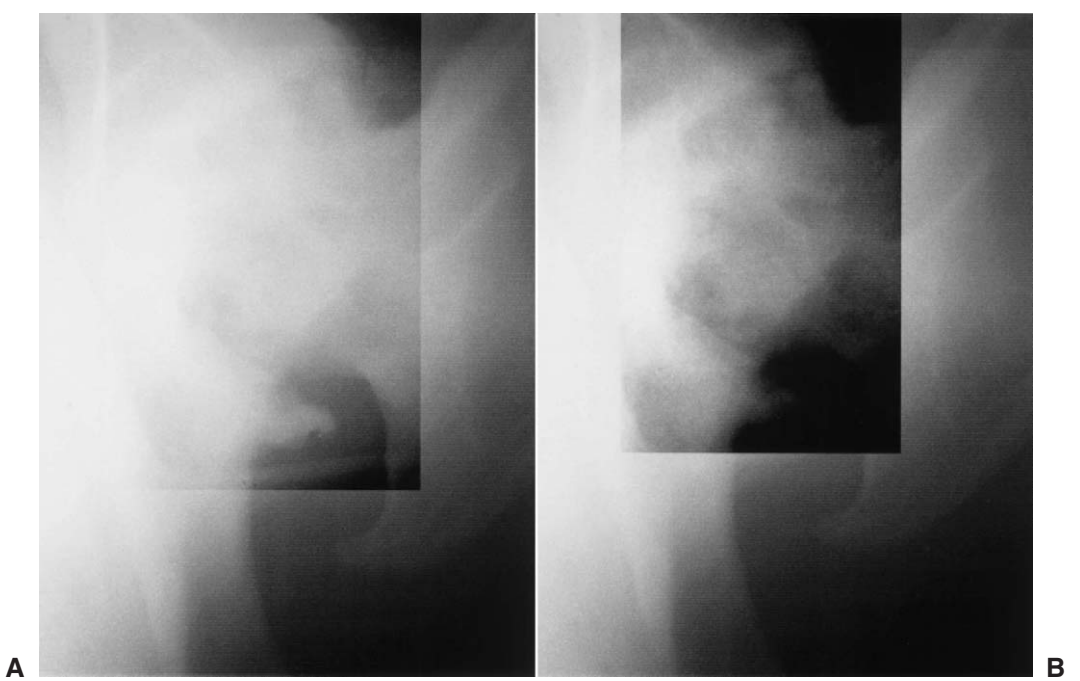


Figure 12-10 • Two close-up flexed ventrodorsal views of a severely arthritic hip in a young adult horse: one deliberately underexposed to emphasize periarticular new bone **(A),** the other overexposed to emphasize interior bone loss **(B).**



Figure 12-11 • Defleshed acetabulum seen from ventral perspective shows a displaced fracture from the caudal lip of the acetabulum, an injury that went undetected in repeated radiographic examinations.



Figure 12-12 • Lateral oblique view of a chronically infected hip that developed after an umbilical infection. The femoral head appears flattened and sclerotic with a markedly widened cartilage space.

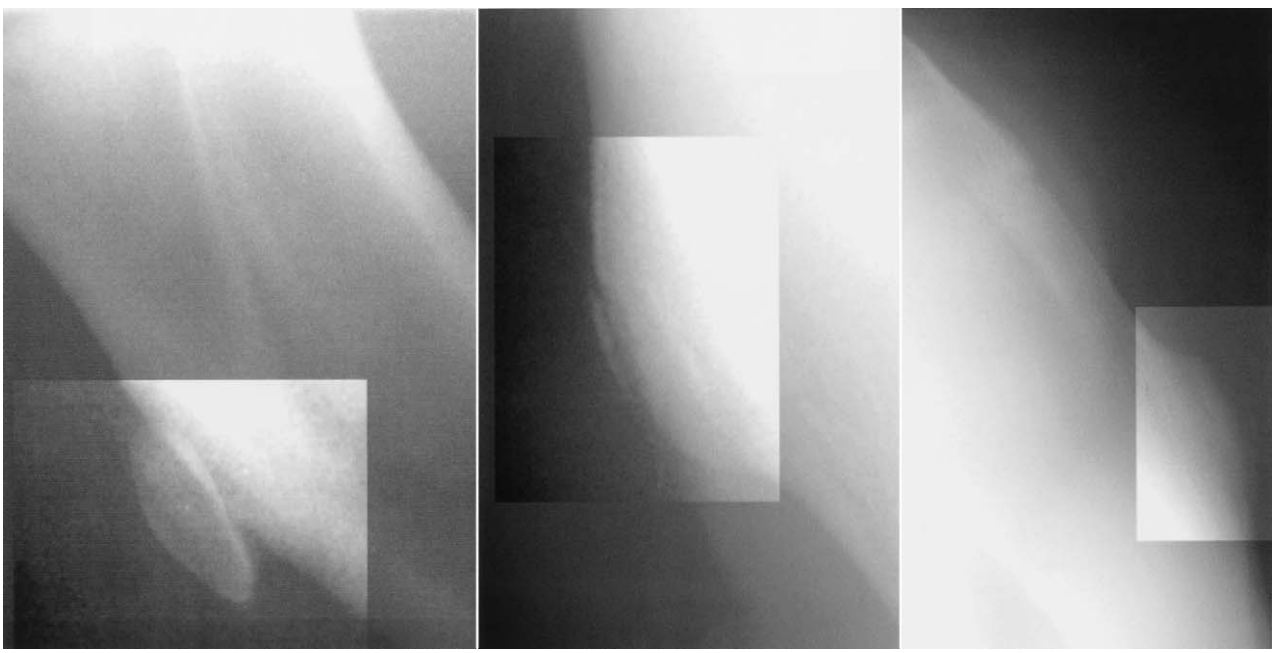


Figure 12-13 • Three normal variations of the third trochanter resembling disease: an avulsion fracture **(A),** a sequestrum **(B),** and an exostosis **(C).** See emphasis zones for details.



Figure 12-14 • Close-up view of greater trochanter shows a recently formed new bone deposit *(emphasis zone)* presumed to be the result of a nonspecific hip injury 2 weeks previously.

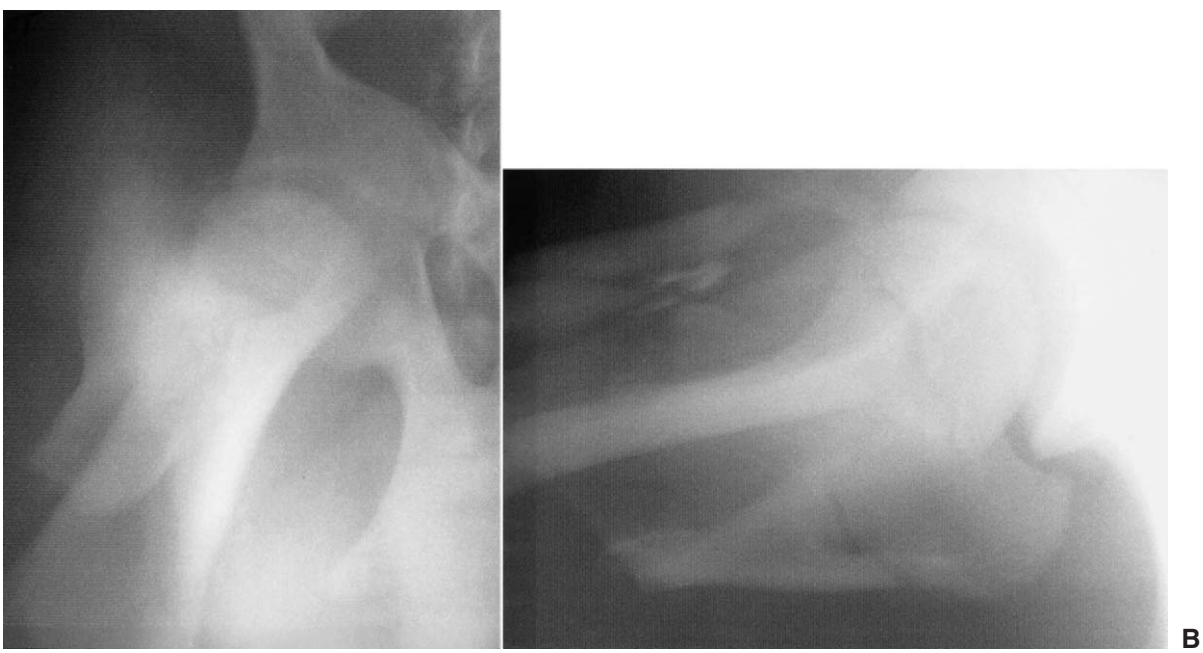
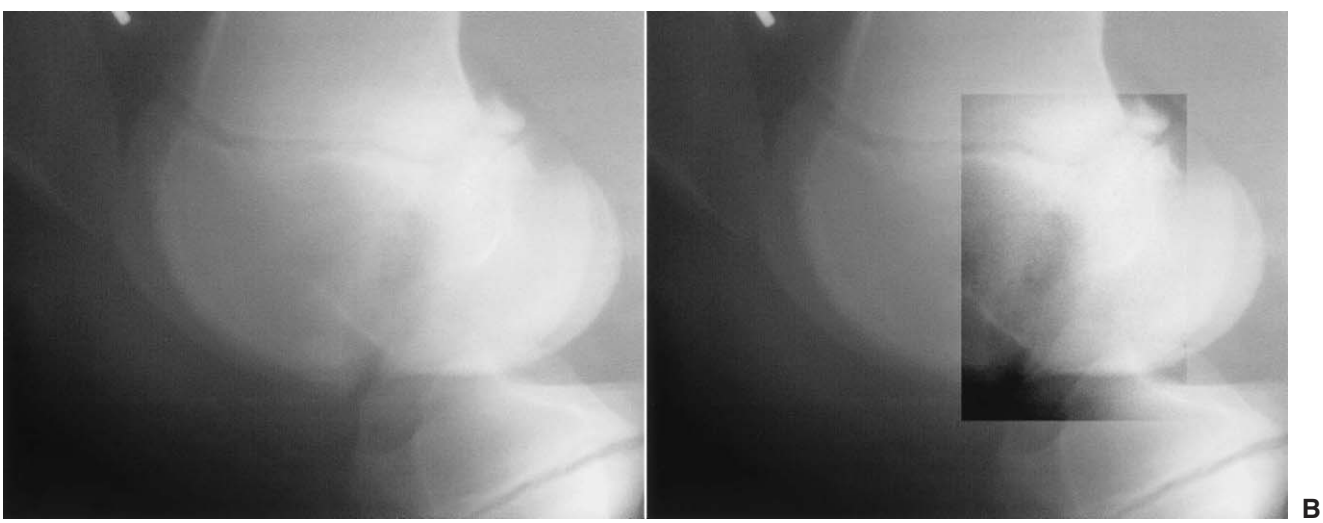


Figure 12-15 • Close-up extended **(A)** and flexed **(B)** ventrodorsal views of a badly displaced proximal femoral shaft fracture in a foal. As usual in such fractures, the coxal joint is widened, a temporary situation that will disappear once the fracture is repaired. Open femoral head and greater trochanteric growth plates are normal.



Figure 12-16 • Close-up lateral view of a severely displaced, badly overridden, distal femoral shaft fracture. Associated hemorrhage and edema are massive, in part because of a lengthy transport before being hospitalized. The open growth plates are normal.



A **B**

Figure 12-17 • Close-up lateral views: plain **(A)** and emphasized **(B)** distal femur of a foal show a displaced condylar fracture.

Likewise, nondisplaced condylar fractures can be difficult to identify, at least with any degree of diagnostic certainty. The presence of a metaphyseal corner fragment seen in a lateral or lateral oblique projection strongly suggests a growth plate fracture or, alternatively, a split distal femoral condyle (Figure 12-17).

▮▮▮ FEMORAL CONDYLAR BONE CYST

Squire and co-workers reported the radiographic and scintigraphic appearance of bilateral femoral bone cysts in a 14-month-old Appaloosa colt. Of greatest interest was that although the cysts appeared to enlarge radiographically after surgery, radiopharmaceutical uptake did not. The horse continued to have pain.[13]

Whereas most authorities believe femoral bone cysts are a manifestation of osteochondrosis, there are other theories. For example, Verschooten contends that subchondral cysts are the aftermath of injury.[14] Numerous radiographic examples of osteochondritis of the distal femur can be found in the following chapter on the stifle.

▮▮▮ PARACOXAL FOREIGN BODY

Paracoxal foreign bodies—for the most part, large wooden stakes and residual splinters—typically

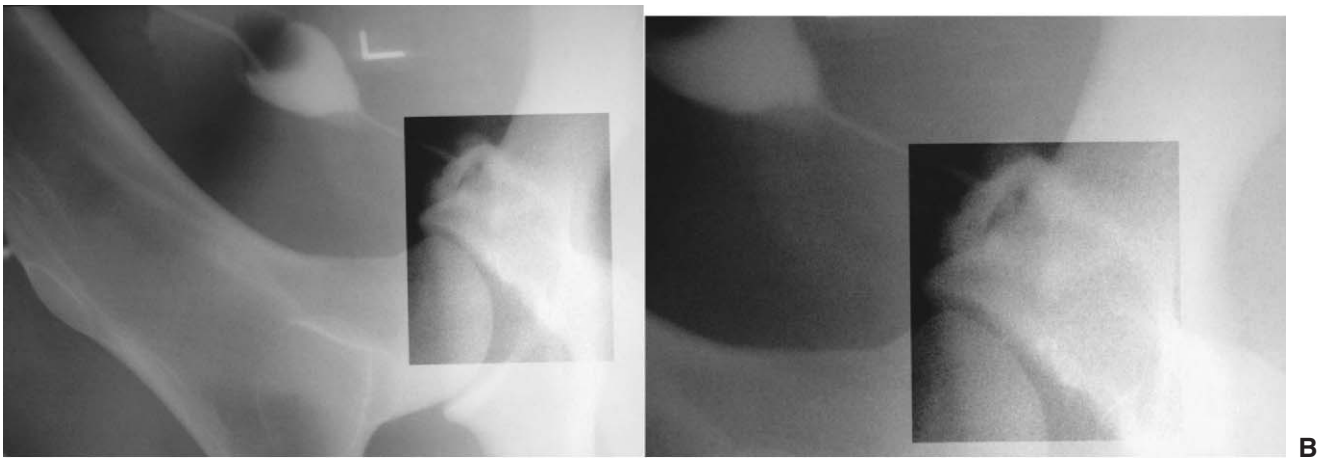


Figure 12-18 • Flexed ventrodorsal **(A)** and close-up flexed ventrodorsal **(B)** sinograms of the shoulder region of an adult horse show a large rectangular cavity superimposed on the cranial aspect of the coxal joint. The vague filling defect *(emphasis zone)* proved to be a large piece of wood.

lead to cellulitis, foreign-body abscessation, sinus development, and intermittent drainage. As mentioned previously, I prefer sinography over sonography for the purpose of identifying deep wooden foreign bodies and their related tissue damage (Figure 12-18).

References

1. Garcia-Lopez JM, Boudrieau RJ, Provost PJ: Surgical repair of coxofemoral luxation in a horse, *J Am Vet Med Assoc* 219:1254, 2001.
2. Embertson RM, Bramlage LR, et al: Physeal fractures in the horse: classification and incidence, *Vet Surg* 15:223, 1986.
3. Blaik MA, Hudson JA: What is your diagnosis? *J Am Vet Med Assoc* 215:933, 1999.
4. Smyth GB, Taylor EG: Stabilization of a proximal femoral physeal fracture in a filly by use of cancellous bone screws, *J Am Vet Med Assoc* 201:895, 1992.
5. Farrow CS: Unpublished observation, 2001.
6. Turner AS, Milne DW, et al: Surgical repair of fractured capital femoral epiphysis in three foals, *J Am Vet Med Assoc* 175:1198, 1979.
7. Loesch DA, Bryant JE, Lopez-Martinez A: Septic coxofemoral arthritis with extension into abdominal cavity of a foal, *Equine Vet Educ* 15:15, 2003.
8. Nixon AJ, Adams RM, Teigland MB: Subchondral cystic lesions (osteochondrosis) of the femoral heads in a horse, *J Am Vet Med Assoc* 192:360, 1988.
9. Rose JA, Rose EM, Smylie DR: Case history: acetabular osteochondrosis in a yearling thoroughbred, *Equine Vet Sci* Sept/Oct:173, 1981.
10. Stick JA, Derkson FJ: Intramedullary pinning of a fractured femur in a foal, *J Am Vet Med Assoc* 175:627, 1980.
11. Schryver HF: Bending properties of cortical bone of the horse, *Am J Vet Res* 39:25, 1978.
12. Byron CR, Stick JA, et al.: Use of condylar screw plate for repair of a Salter-Harris type-III fracture of the femur in a 2-year-old horse, *J Am Vet Med Assoc* 221:1292, 2002.
13. Squire KRE, Fessler JF, et al: Enlarging bilateral femoral condylar bone cysts without scintigraphic uptake in a yearling foal, *Vet Radiol Ultrasound* 33:109, 1992.
14. Verschooten F: Post-traumatic subchondral bone cysts and subchondral bone necrosis in the horse, *Vlaams diergeneeskundig Tijdschrift* 49:237, 1980.

Chapter 13

Stifle

THE STANDARD STIFLE SERIES

The standard stifle examination usually comprises lateral and craniocaudal projections (Figure 13-1). Lateral and medial oblique views are often useful supplements, especially when searching for shallow subchondral defects caused by osteochondritis. Alternatively, a three-view series can be made consisting of (1) lateral oblique, (2) a semiflexed lateral oblique, and (3) a downwardly angled caudocranial view.[1-3] Bones from an adult stifle are provided for the purpose of radiographic comparison (Figure 13-2).

A similar combination of film (Figure 13-3) and bones (Figure 13-4), but of a young foal, illustrates the radiographic prominence of fully open growth plates. A lateral view of a yearling shows a more normal-appearing patella, although the growth plates remain partially open (Figure 13-5).

Author's Note: Obtaining the caudocranial view can be dangerous for the radiographer, even in sedated horses. Caution is recommended.

Emphasizing the Patella

When a patellar lesion is suspected, the standard stifle series is usually adequate. Alternatively the beam center can be moved proximally (about a hand's length) and the patella imaged, as with the stifle (Figure 13-6). For lesions located on the sides of the patella, a skyline view of the patella often reveals otherwise vague or invisible pathology. In general, however, profile views of the patella are more useful than caudocranial projections, which are difficult to read because of femoral superimposition (Figure 13-7).

STIFLE FACTS

Quick and Rendano described a number of useful anatomic features concerning the equine stifle[4]:

- The equine stifle consists of two joints: (1) the femoropatellar and (2) femorotibial.
- The horse lacks gastrocnemius and popliteal sesamoid bones as found in dogs and cats.
- The femoral trochlea contains two large ridges separated by a deep groove. The medial trochlea ridge is larger than the lateral and extends farther forward.
- The patella is a sesamoid bone attached to the quadriceps femoris muscle.
- The position of the patella depends on whether or not the hindleg is extended or flexed: during extension the patella is positioned proximally, whereas during flexion the patella is situated distally.
- The paired menisci are adaptors of a sort, producing congruence between the opposing articular surfaces of the femur and tibia.
- The medial femoral condyle is larger than the lateral.
- The lateral femoral condyle is flattened medially, resembling some forms of osteochondritis.
- The intercondyloid fossa situated between the femoral condyles normally has a dense outer border.
- The tibial intercondylar eminence extends into the intercondyloid fossa.
- The intercondylar eminence comprises two parts or elements: the taller medial element and the shorter lateral element. Both elements are actually upswept extensions of the medial and lateral articular surfaces of the proximal tibia, and not merely a pair of bony peaks situated in the center of the proximal tibia.
- The following *should not be mistaken for lesions*: (1) the ridge of the supracondyloid fossa, (2) the border of the extensor fossa on the lateral surface of the lateral femoral condyle, (3) the caudomedial protuberance of the tibia, and (4) the vascular channel in the proximal tibia.
- The head of the fibula articulates with the lateral surface of the tibia but not with the femur.

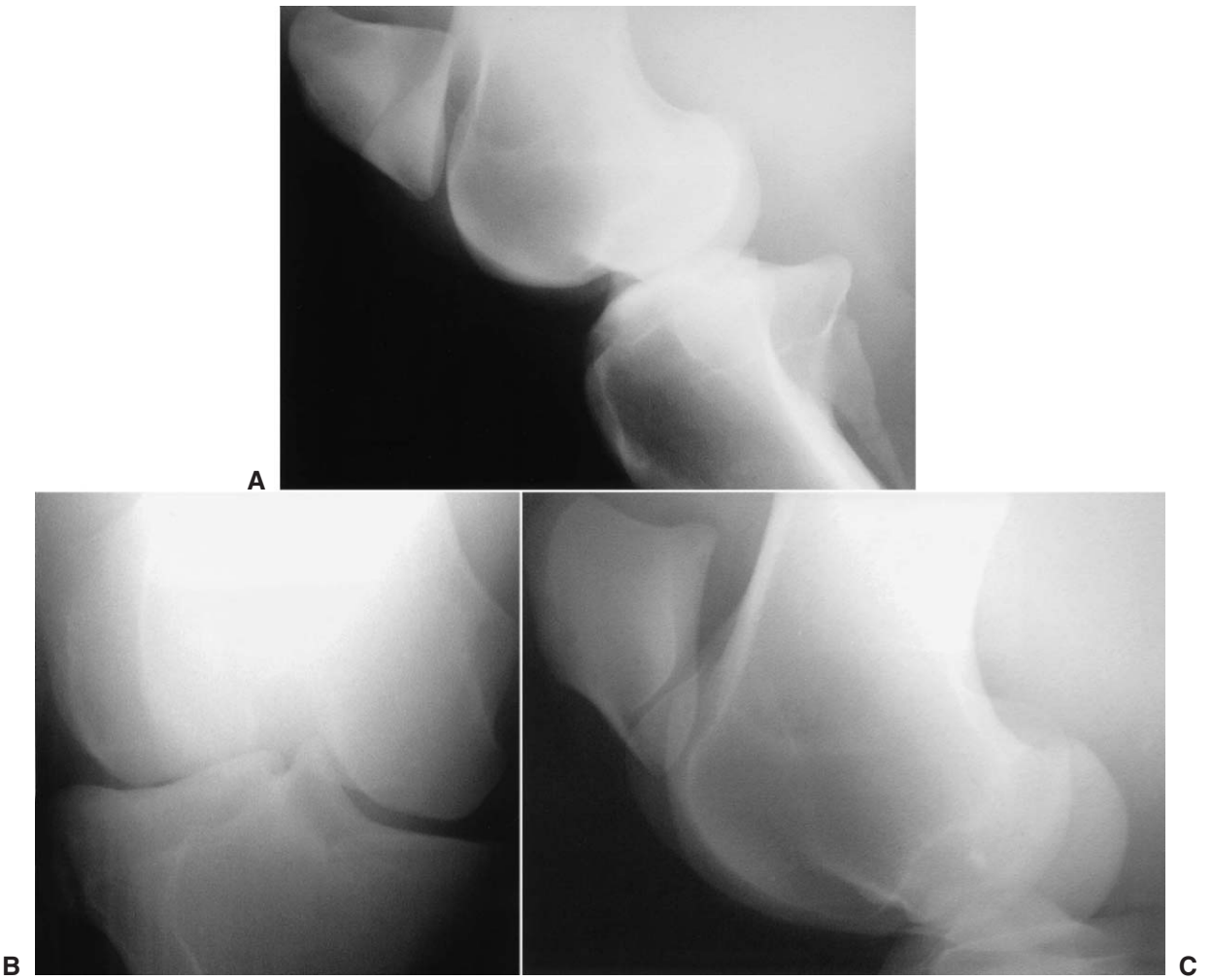


Figure 13-1 • The standard stifle examination consists of lateral **(A)** and caudocranial **(B)** projections, as shown in this adult horse. Note the anatomic foreshortening, especially of the patella, caused by relatively mild projectional obliquity **(C).** In the caudocranial projection medial is to the right.

- The fibula may form from three or more separate ossification centers, which must not be mistaken for fractures.
- The distal femoral growth plate closes between 21 and 42 months of age.
- The proximal tibia contains two growth plates: one for the tibial tuberosity, which closes between 12 and 24 months, and another for the tibial plateau, which closes between 36 and 42 months of age.
- The knee has nine ligaments, five of which are associated with the patella: (1) cranial and caudal cruciate; (2) medial and lateral collateral; (3) medial and lateral femoropatellar; and (4) medial, middle, and lateral patellar.
- A triangular fat pad is located immediately caudal to the quadriceps tendon as seen in the lateral view.
- The stifle joint comprises three cavities: (1) femoropatellar—the largest, (2) lateral femorotibial, and (3) medial femorotibial. The medial femorotibial compartment usually communicates with the femoropatellar sac, but the lateral femorotibial compartment communicates with the femoropatellar cavity only 25 percent of the time.

Interior Anatomy of the Stifle Joint

The stifle or genual joint of horses is divided into two inconsistently communicating cavities. Cranially the *femoropatellar joint* is formed by the patella and femoral trochlea; caudally the *femorotibial joint* is composed of the femoral and tibial condyles (Figure 13-8). The femorotibial joint is further divided into *lateral and medial compartments*, which in turn are subdivided into *cranial and caudal synovial pouches*.

In an estimated 65 percent of horses, the *medial* femorotibial compartment communicates with the femoropatellar joint through an open synovial fold over the distal aspect of the medial trochlear ridge.

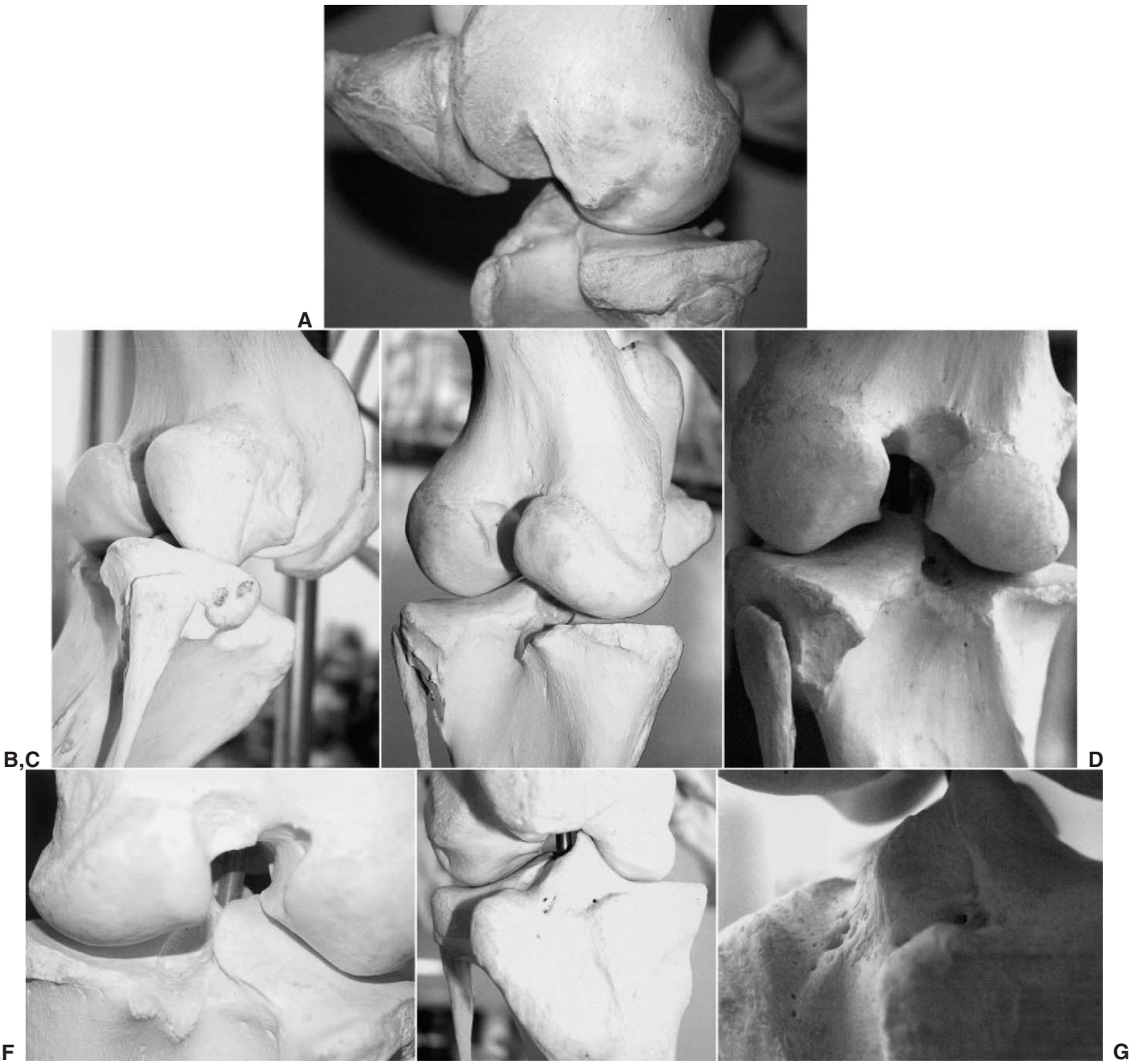


Figure 13-2 • Defleshed bones of an adult stifle shown in lateral **(A),** lateral oblique **(B),** medial oblique **(C),** caudal **(D),** caudal close-up **(E),** and cranial perspectives **(F).** An ultra-close-up cranial view of the stifle **(G)** shows the intercondylar eminence with the taller of its two ridges situated medially. In the cranial and caudal views of the stifle, medial is to the right.

Alternatively, only 3 percent of horses have a communication between the *lateral* femorotibial compartment and femoropatellar joint.[5]

Lateral and medial menisci adapt the articular surfaces of the femur and tibia to one another, whereas the *cranial and caudal cruciate* and the *medial and lateral collateral ligaments* set the limits for stifle motion.

Stifle Arthrography

Nickels and Sande described the normal arthrographic appearance of the adult horse. Because of its large size, arthrography of the equine stifle is simpler and diagnostically more rewarding than it is in the dog.[6]



Figure 13-3 • Lateral **(A)** and close-up lateral **(B)** views of the stifle of a 1-month-old Arabian foal showing three open growth plates, which currently separate the distal femoral trochlea and condyle, proximal tibial epiphysis, and apophysis of the tibial tuberosity from their parent bones. Note the diminutive appearance of the patella *(upper left)* and the fringed appearance of the trochlea ridges, common findings in a foal of this age.



Figure 13-4 • Lateral **(A)** and frontal **(B)** views of the defleshed stifle of a young foal showing a single distal femoral and two proximal tibial growth plates (physes) simulated in the specimen with black plastic.

▮▮▮ RADIOGRAPHIC DETECTION OF STIFLE LESIONS

Numerous authors have indicated a reduced radiographic *detectability* (also termed *radiographic sensitivity*) for certain types of soft-tissue lesions as well as for mild osteoarthritis of the stifle.[7] This is not surprising because it has long been acknowledged that any early bone lesion, by virtue of its resemblance to normal variation, is difficult or impossible to detect radiographically.

Normal Sonographic Anatomy of the Stifle

Using a very high-quality ultrasound machine, Penninck and co-workers described the normal sonographic appearance of the equine genual joint using a combination of living horses and dismembered limbs.[8] They also reported three clinical cases: one each involving the femoral trochlea (osteochondritis), femoral condyle (bone cyst), and tibial crest (fracture).

Although it was possible to visualize both normal and abnormal articular surfaces, the imagery was often mediocre, especially compared with radio-

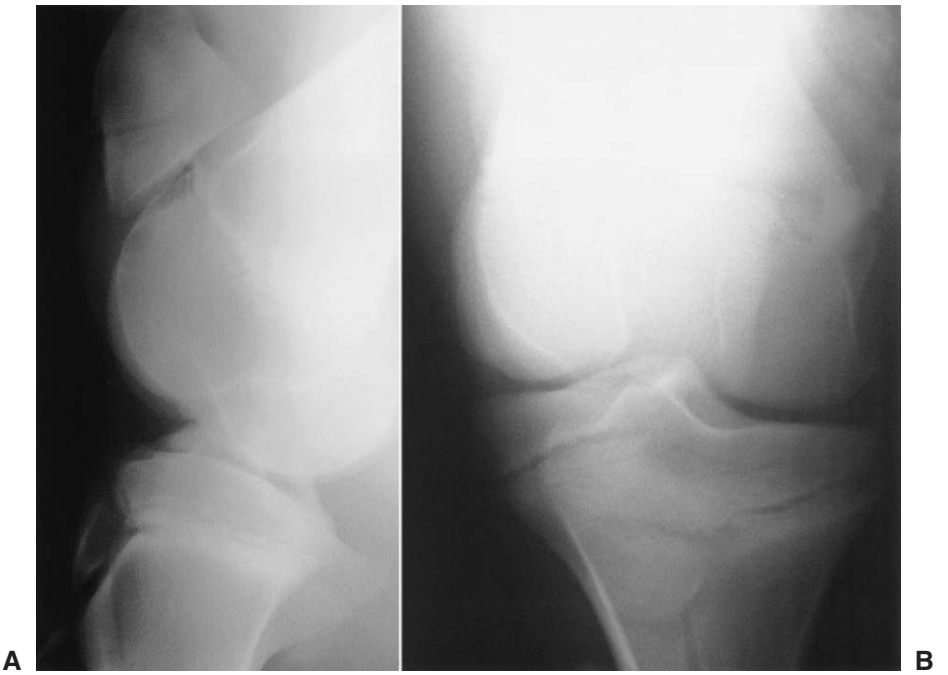


Figure 13-5 • Lateral **(A)** and caudocranial **(B)** views of a normal stifle joint in a yearling filly. Medial is to the right.

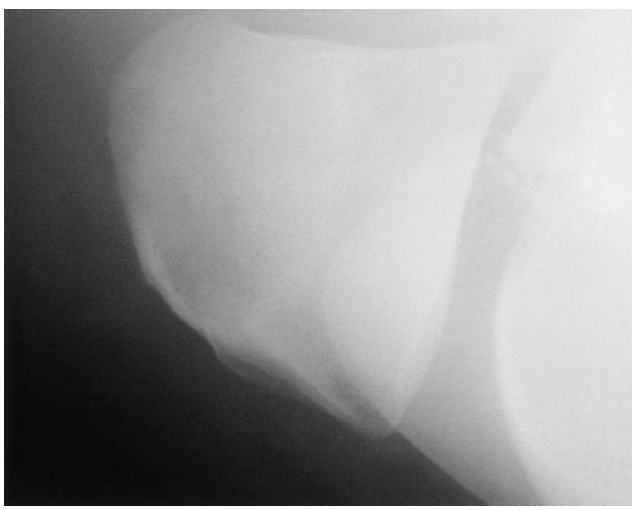


Figure 13-6 • Close-up lateral projection of a normal patella in a 1-year-old Quarter Horse colt.

graphs. On the other hand, the patella and collateral ligaments, menisci, joint capsule, synovium, joint cavity, and its contents were all, for the most part, well or adequately seen.

Although the authors recommend a sonographic as well as a radiographic assessment of horses with stifle disease or injuries, they emphasize that the region is anatomically complex, especially from a sonographic perspective. Therefore quality training and substantial practice are required to attain diagnostic competence.

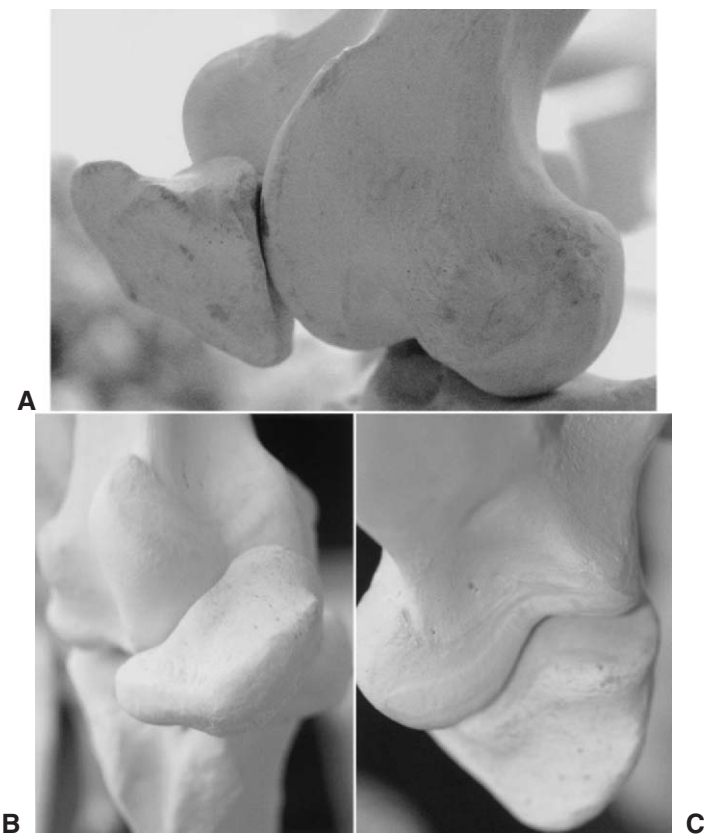


Figure 13-7 • Defleshed stifle joint shown from lateral **(A),** cranial **(B),** and proximal **(C)** perspectives emphasize the extreme variability of the patella, depending on projection angle.

Normal Magnetic Resonance Anatomy of the Stifle

Holcombe and co-workers reported the magnetic resonance (MR) appearance of the normal adult and juvenile equine stifles using disarticulated limbs.[9] To date, however, clinical reports detailing the use of magnetography to diagnose stifle disease or injury in adult horses remain rare.

▮▮▮ PROBABILITY OF SPECIFIC STIFLE LAMENESS AND RECOVERY

Persistent swelling and lameness characterize most serious stifle diseases.[10] Jeffcott and Kold wrote an article on the cause of stifle lameness in a group of 86 referral cases to the Equine Research Center at Newmarket. Their results were interesting and perhaps somewhat surprising (Box 13-1).[11]

Most of the previous animals were treated with rest, followed by gradual rehabilitation. Some were also given a nonsteroidal antiinflammatory drug. Results are as follows:

- Horses with osteoarthritis failed to recover or only improved while being rested.
- Horses with the fragmenting form of osteochondritis failed to recover or only improved while being rested.
- Horses with the cystic form of osteochondritis improved after at least 6 months of rest.
- First- and second-degree sprains improved with rest; third-degree injuries did not.

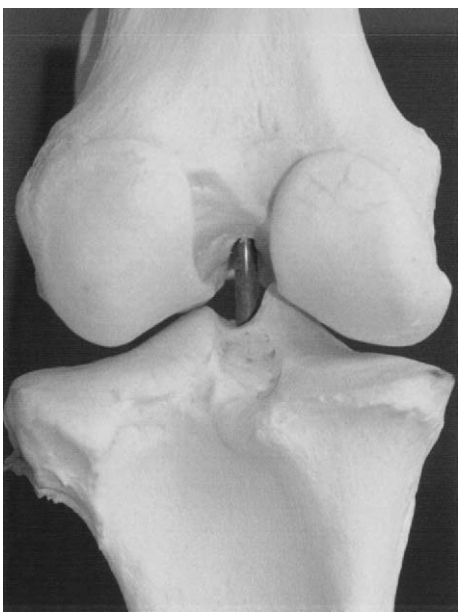


Figure 13-8 • A defleshed specimen (caudal perspective, medial is to the reader's right) shows that the stifle joint contains *four condyles*, not two: two femoral (lateral and medial) and two tibial (lateral and medial).

▮▮▮ FRACTURES OF THE STIFLE

Fractured Patella

Dik and Nemeth and others described patellar fractures in horses.[12] Patellar fractures are generally believed to be the result of a kick or a collision with a stationary object such as a fence post. Described fractures include those of the base, body, and apex. Described fracture configurations include sagittal, transverse, comminuted, and avulsion. The medial patellar fibrocartilage may also be fractured or crushed. Varying degrees of posttraumatic synovitis often accompany such injuries.[13]

Dyson and co-workers describe the radiographic appearance of medial patellar fractures in a small series of horses.[14] The skyline projection (cranioproximal-craniodistal oblique projection) has been reported as necessary to evaluate a fractured patella fully, initially identified in a lateral view.[15] The skyline view is also indispensable for a full assessment of the proximal articular border.[16]

Large fractures can be surgically reduced with screws and tension-band wiring.[17] Regular progress checks are advisable (every 2 to 3 weeks for the first 3 months) because there is a high failure rate. Bony reabsorption around loosened or bent pins is common and must be differentiated from infection, which fortunately is rare.

Patellar Degeneration After Medial Patella Desmotomy. Squire and co-workers reported a single case of distal patellar degeneration after a medial patellar desmotomy performed at the request of the horse's owner but against the advice of the attending veterinarian.[18] Stifle radiographs made immediately before surgery were normal; those made 3 months after the desmotomy were not.

Specifically the postoperative films revealed degenerative changes in the distal articular and periarticular aspects of the patella, which consisted of (1) small bone deposits on the distal surface, presumed to be enthesiophytes; (2) a medium-sized area of demineraliza-

BOX 13-1
Causes of Chronic Stifle Lameness in 86 Referral Cases

BONE LESIONS	PERCENT
Osteochondritis, fragmenting form (osteochondritis dissecans)	13
Osteochondritis, cystic form (bone cyst)	38
Osteoarthritis	3
Fractures	4
Epiphysitis	1
SOFT-TISSUE LESIONS	
Partial upward fixation of the patella	15
Sprained cruciate or collateral ligaments; torn meniscus	12
Nonspecific strains	13
Uncategorized	1

tion located in the articular portion of the distal pole; and (3) a number of small surrounding bone fragments.

The described degenerative-type alterations were attributed to surgical destabilization of the patella, leading to lateral rotation, *stress concentration,* and eventually structural disintegration of portions of the articular cartilage and subchondral bone distally.

The authors counseled caution where medial patella ligament desmotomy is being considered, bringing into question the belief that therapeutic transection of the medial patellar ligament is an innocuous procedure.

Dislocation of the Patella

Medial, lateral, and distal dislocations of the patella have been reported. Proximal dislocation or upward fixation of the patella is not considered a true luxation. Both congenital and acquired causes of patellar displacement have been proposed, with the former usually being attributed to trochlear hypoplasia and the latter to soft-tissue injury such as a ruptured quadriceps.[19] Figures 13-9 and 13-10 show the radiographic and sonographic appearances of a traumatic lateral patellar dislocation in a foal.

Congenital Dislocation of the Patella

Finocchio and Guffy reported congenital patellar ectopia in an 11-day-old Standardbred filly with a distinctive crouching posture. Radiographically both patellas were dislocated caudolaterally.[20] Later Debowes and co-workers described the radiographic appearance of bilateral congenital dislocation of the patella in an 11-day-old Arabian foal.[21] The animal could not stand spontaneously and assumed an exaggerated crouch when partially supported. Caudocranial and lateral radiographs show the patella situated far to the lateral side of the distal femoral condyles.

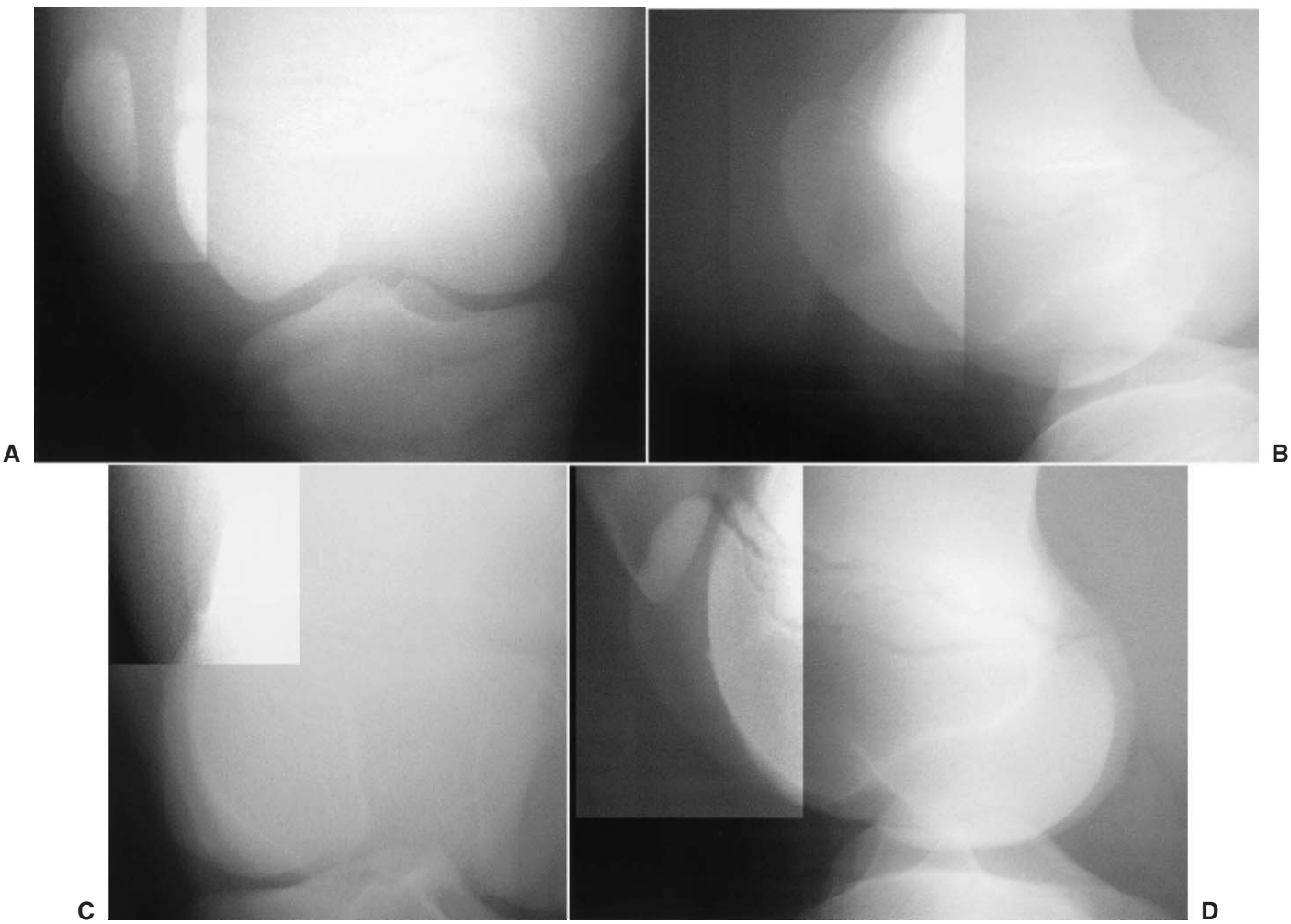


Figure 13-9 • A caudocranial view **(A)** of the stifle of a recently injured foal shows the patella dislocated laterally *(emphasis zone);* predictably, a lateral view **(B)** fails to reveal the patella because of superimposition by the femoral trochlea. Caudocranial **(C)** and lateral **(D)** projections of the normal opposite genual joint are provided for comparison.



Figure 13-10 • A transverse sonogram of the injured knee shown in Figure 13-9 reveals a large subcutaneous seroma containing a partially organized blood clot.

Regarding the consequences of patellar ectopia, one author claimed that degenerative joint disease is the usual sequela to chronic lateral patellar dislocation, but I have been unable to confirm this assertion because there appear to be no case reports featuring before and after radiographs.[22]

▮▮▮ INFECTION OF THE PATELLA

Radiographically visible patellar infections are unusual. Those that are identified are usually chronic and draining when presented for diagnosis. Interior destruction, cavitation, sequestration, and a thick fringe of new bone over all but the articular surface characterize the worst among these infections (Figure 13-11).

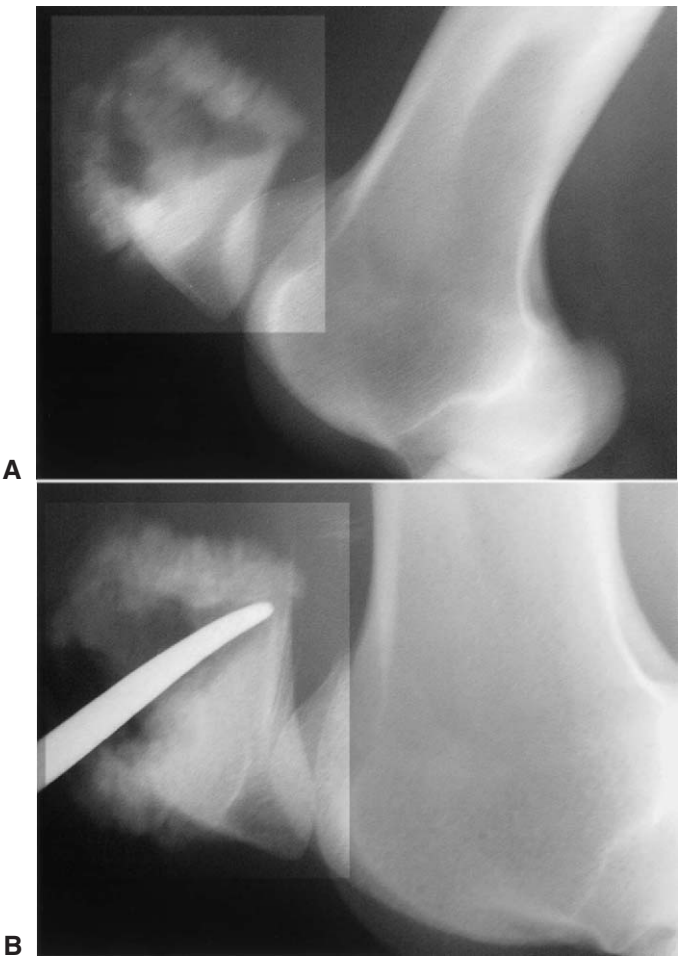


Figure 13-11 • A, Lateral view of infected stifle in a yearling foal shows severe osteomyelitis of the patella featuring interior destruction and cavitation and a thick, irregular layer of new bone over all but the articular surface *(emphasis zone).* **B,** In the second lateral image, a forceps was placed into the draining sinus to confirm that it involved the patella, which it did *(emphasis zone).*

▮▮▮ CONGENITAL ABSENCE OF THE PATELLA

Congenital absence (aplasia) of the patella is rare and in my experience is always bilateral. Premature foals may not have visible patellae because of insufficient ossification.

▮▮▮ SPRAIN-AVULSION-FRACTURES OF THE STIFLE

Cranial Cruciate Ligament

Serious sprains of the cranial cruciate ligament (second- and third-degree) may cause radiographically visible joint swelling and partial dislocation. Occasionally the lateral or medial element of the intercondylar eminence may fracture.

Caudal Cruciate Ligament

Rose and co-workers reported both the radiographic and sonographic appearance of an avulsed caudal cruciate ligament in a 2-year-old Standardbred, the result of a collision with a fence during training.[23]

Radiographically, the injury featured a medium-sized rectangular bone fragment lying just off the caudal aspect of the tibial plateau in the lateral view and superimposed on the medial intercondylar eminence in the frontal (caudocranial) projection. Sonographically the sprained caudal cruciate ligament appeared mildly swollen with an abnormally hypoechoic center accompanied by excessive joint fluid.

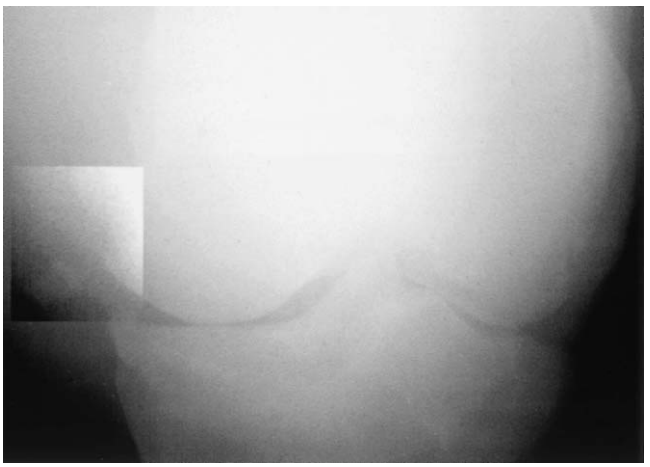


Figure 13-12 • Ultra-close-up caudocranial view of the recently injured stifle of a horse shows a faint bone fragment on the medial side of the joint, the result of a sprain-avulsion-fracture of the medial collateral ligament and medial tibial condyle.

Collateral Ligament

Ruptured collateral ligaments may or may not be associated with avulsion fractures (Figure 13-12).[24] If not, radiographic diagnosis may depend on stress radiography, as I have demonstrated previously.

Patellar Ligament

Unlike pets and people, in whom a severely sprained quadriceps tendon (ligament) is signaled by a proximally displaced patella, horses often show little radiographic evidence of such injuries, largely because of their far more elaborate suspension system (see section on stifle facts earlier).

Long Digital Extensor Tendon

Holcombe and Bertone reported an avulsion fracture of the origin of the extensor digitorum longus muscle in a 9-week-old foal.[25] The fracture was best demonstrated in the craniocaudal and lateral oblique projections as two or three vague bone fragments superimposed on the outer margin of the lateral condyle.

Peroneus Tertius Tendon

Blikslager and Bristol reported the radiographic appearance of an avulsed peroneus tertius tendon in a 3-month-old Quarter Horse filly that caught its leg in a fence.[26] The foal was moderately lame and had a swollen stifle. A lateral oblique radiograph showed a large triangular bone fragment situated in the cranial aspect of the stifle joint, partially superimposed on the proximal tibia, presumably detached from the lateral trochlear ridge.

▮▮▮ OSTEOCHONDRITIS (OSTEOCHONDRITIS DISSECANS, OSTEOCHONDROSIS)

Osteochondritis or Osteochondrosis: What's in a Word?

For the sake of both clarity and simplicity, I prefer the term *osteochondritis* to osteochondrosis in describing developmental skeletal disease in horses. Osteochondritis has the further advantage of also describing the fragmenting form of the disease (rather than having to change suffixes *–osis to -itis*) and adding the word *dissecans*. Likewise, osteochondritis is quite suitable to describe a bone cyst, although arguably less evocative.

Formation of Osteochondral Lesions in the Horse

Stowater and co-workers wrote an exceedingly clear and succinct account of the development of osteochondritis in the horse, which, with the exception of breaking the material into separate paragraphs, is presented verbatim.[27]

"Osteochondrosis (OCD) in the horse, as in other animals, is characterized by a disturbance in the process of osteochondral ossification. Focal persistence of hypertrophied chondrocytes leads to areas of thickened cartilage, the deeper layers of which undergo necrosis. These sites are structurally weak and are susceptible to mechanical injury from weight bearing or pressure exerted by adjacent structures. Fissures develop in the necrotic cartilage, which may extend to the articular surface, resulting in chondral or osteochondral flaps or detached fragments. Once this has occurred, the disease is referred to as *osteochondrosis dissecans*.

Centrally located necrotic foci may not fragment but instead may collapse inward under the stress of weight bearing, creating a cystlike lesion. The initial cause for the disturbance in enchondral ossification is unknown, but numerous factors are considered significant contributors to its occurrence. Controlled studies in swine, poultry, and dogs have demonstrated a higher incidence of OCD when those species were fed a high-energy diet. Clinical impressions in the horse support a similar relationship.

A tendency toward familial occurrence has been noted in humans and animals, and a genetic disposition for rapid growth is believed to be an important etiologic factor. It is generally accepted that in all species the occurrence of OCD is twice as great in males as in females. However, in two retrospective studies, a sexual predilection was not found. The incidence of OCD is greatest in the racing breeds, such as Thoroughbreds and Standardbreds, but other breeds are affected.

As mentioned previously, young foals often have a ragged-appearing lateral trochlear ridge and patella, which are most pronounced between the ages of 3 and

10 weeks.[28] This observation must not be taken as evidence of OCD.

Common anatomic sites in the horse include the stifle, tarsal, shoulder, and metacarpophalangeal joints. In the stifle, the lateral femoral trochlear ridge and medial femoral condyle are the most frequently affected areas. Osteochondral defects with dissecting lesions predominate in the lateral trochlear ridge; cystic-appearing, nondissecting lesions are more common in the medial condyle. In one study, 65 percent of the horses had bilateral lesions.[29] The lateral femoral condyle has been mentioned as an infrequent site of OCD occurrence in the horse by several authors, but few references describe specific cases.

Most horses with osteochondritis of the stifle are young, between 1 and 3 years of age. The stifle may be swollen, but this is not always readily detectable. Affected joints are rarely hot or painful to touch as are infected joints.

Radiologic-Pathologic Correlation

McIlwraith offered his views on the evolution of cystic osteochondritis, supported by gross and subgross specimens.[30] Because the essence of McIlwraith's work is pictorial, it must be seen to be appreciated. I wholeheartedly recommend it.

Comparison of Radiographic and Arthroscopic Findings

Steinheimer and co-workers compared the relative sensitivities of radiographic and arthroscopic examinations of the equine genual joint. Not surprisingly (at least to radiologists and surgeons), they determined that the larger the lesion, the more likely it is to be radiographically detectable and that in general the presence and extent of articular cartilage damage are likely to be underestimated radiographically. Specifically, they concluded the following:

1. Some stifle joints that appear normal radiographically will have arthroscopically detectable cartilage lesions.
2. Radiographically detectable flattening of subchondral bone indicates damaged articular cartilage in a majority of instances.
3. Moderate to severe radiographic abnormalities are reliable predictors of arthroscopically detectable lesions.

In another small study comparing radiography and arthroscopy, Schneider and co-workers found cartilage lesions on the distal aspect of the medial femoral condyle in 11 horses with radiographically normal stifles.[31]

Osteochondritis of the Patella

McIlwraith reported the fragmenting form of osteochondritis in 15 horses: eight Quarter Horses, three Thoroughbreds, two American Saddlebreds, one American Paint, and one Warmblood-Thoroughbred cross.[32] The lesion typically consisted of a small fragment of bone lying just beyond the distal tip of the patella as seen in a lateral radiograph. The adjacent surface of the patella often contained a discrete fracture bed. Another form of this disease typically appears as a vaguely outlined area of decreased bone density in the midcranial aspect of the patella, often accompanied by an irregular margin implying past fragmentation (Figure 13-13). Additional trochlear or condylar lesions may or may not be present.

Femoral Osteochondritis

Osteochondritis of the Lateral Trochlear Ridge. Osteochondritis of the lateral trochlear ridge is highly variable, ranging from a subtle flattening to overt fragmentation. Marginal lesions are generally the easiest to detect, whereas vague areas of reduced interior density are much harder to appreciate. Because bilateral involvement is far more common than unilateral disease, the opposite stifle should always be checked (Figures 13-14 and 3-15).

Postoperative Radiographic Appearance of Osteochondral Lesions of the Lateral Trochlear Ridge. Pascoe and co-workers described the clinical, radiographic, pathologic, and clinical outcomes of 10 horses that were surgically treated (fragment extraction and curettage) for unilateral or bilateral osteochondral lesions involving the lateral trochlear ridge.[33] Their findings were as follows:

- Subcutaneous seroma and partial wound dehiscence occurred in nine animals.
- Operated stifles were pain free 6 to 12 months after surgery.
- The subchondral contour of the operated lateral trochlear ridges was altered in all cases.
- Bone density adjacent to the operative site was increased in all instances.
- Six of 15 animals also had "small focal radiolucent regions within the subchondral bone," which the authors attributed to incomplete removal of the diseased bone.
- Histologic examination of operated lesions in three of the horses showed that healing occurred by a process of *filling in:* granulation tissue from mesenchymal elements in subchondral marrow spaces gradually filled in the defects with fibrocartilage.

Osteochondritis of the Medial Trochlear Ridge. Other than being somewhat more visible, osteochondritis of the medial trochlear ridge differs little from that found in the lateral trochlear ridge (Figure 13-16).

Flattened Condylar Margins and Trough Lesions

Condylar Flattening. Perhaps the most ambiguous of distal femoral lesions is the centrally flattened femoral condyle. This subtle radiographic finding (a *possible*

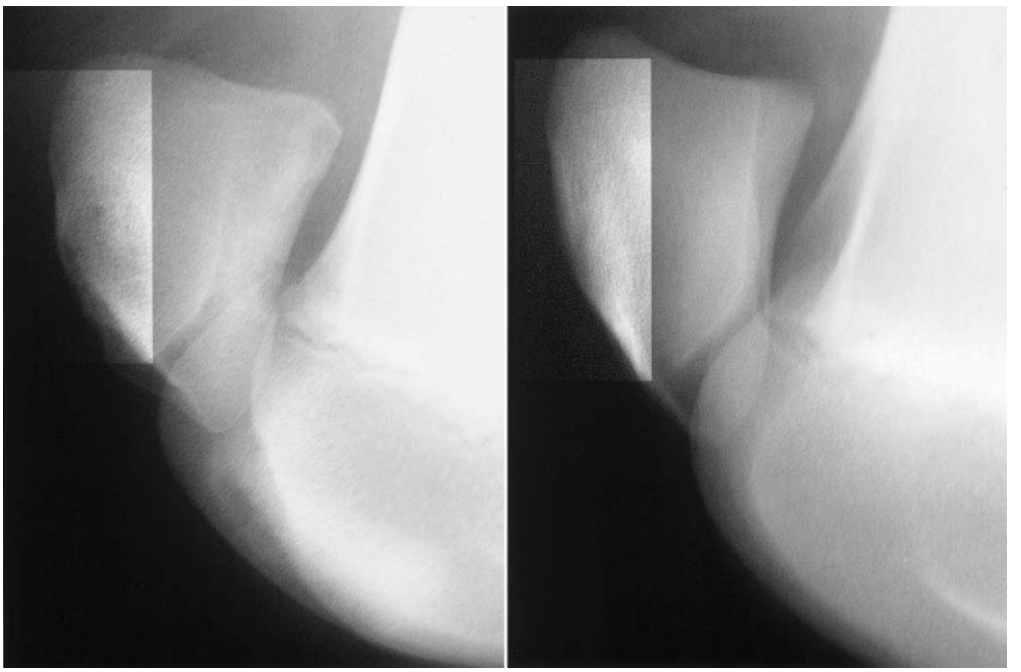


Figure 13-13 • A, Close-up lateral view of the patella of a horse with osteochondritis (OCD), appearing as a vaguely outlined area of decreased bone density *(emphasis zone)*. **B,** A second OCD lesion is present in the medial trochlea. The normal opposite patella is provided for comparison.

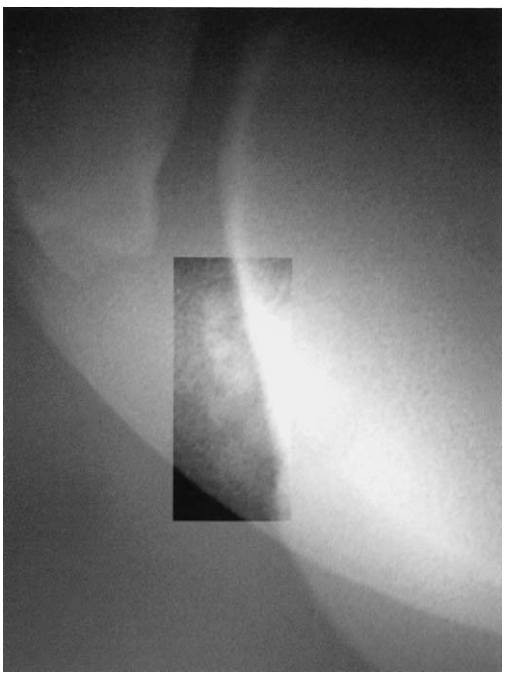


Figure 13-14 • Ultra-close-up view of the lateral trochlear ridge of a young horse with a nonpainful swelling of its stifle shows a centrally located, troughlike defect containing multiple chunks of partially mineralized cartilage. The tip of the patella is also missing, presumably from the same disease.

manifestation of mild osteochondritis) is typically (but not exclusively) found along the central third of the articular margin of the medial femoral condyle and is best seen in the caudocranial projection. Because some normal horses also have a slightly flattened medial femoral condyle, I strongly recommend making a comparison view of the opposite stifle, taking care to project the control joint in a similar manner because projection angle can also influence the degree of apparent condylar arc.

Trough Lesions. Distal femoral trough lesions are the most common form of femoral osteochondritis encountered in our practice. In my opinion, such lesions are most likely a more severe variant of condylar flattening. Some trough lesions can become full-blown condylar cysts over time and in this regard bear watching.

Radiographically, trough lesions are characterized by a shallow trough or concavity in the center of the articular surface of the medial femoral condyle (Figure 13-17) and, rarely, the lateral femoral condyle. Some troughs are shallow, others deep. Occasionally trough lesions are accompanied by fragmentation of the intercondylar eminence. Like condylar flattening, trough lesions are often bilateral, which in my judgment warrants radiographing the opposite stifle, even if it appears physically normal.

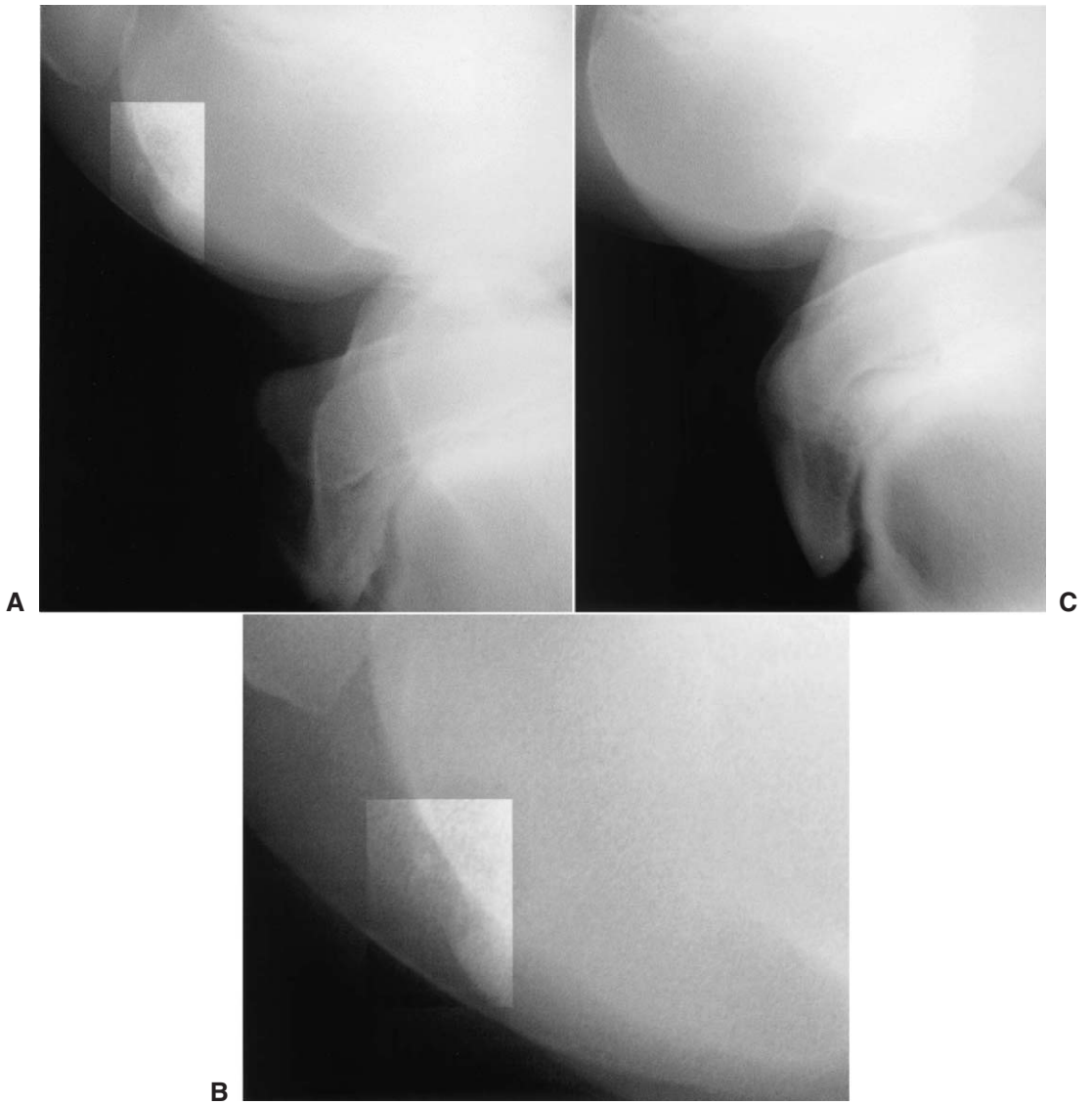


Figure 13-15 • Close-up **(A)** and ultra-close-up lateral **(B)** views of the trochlea of a yearling colt with a fragmenting osteochondritic lesion that has formed a "shelf" in the center of the lateral ridge *(emphasis zone)*. A normal lateral ridge is provided for comparison **(C).**

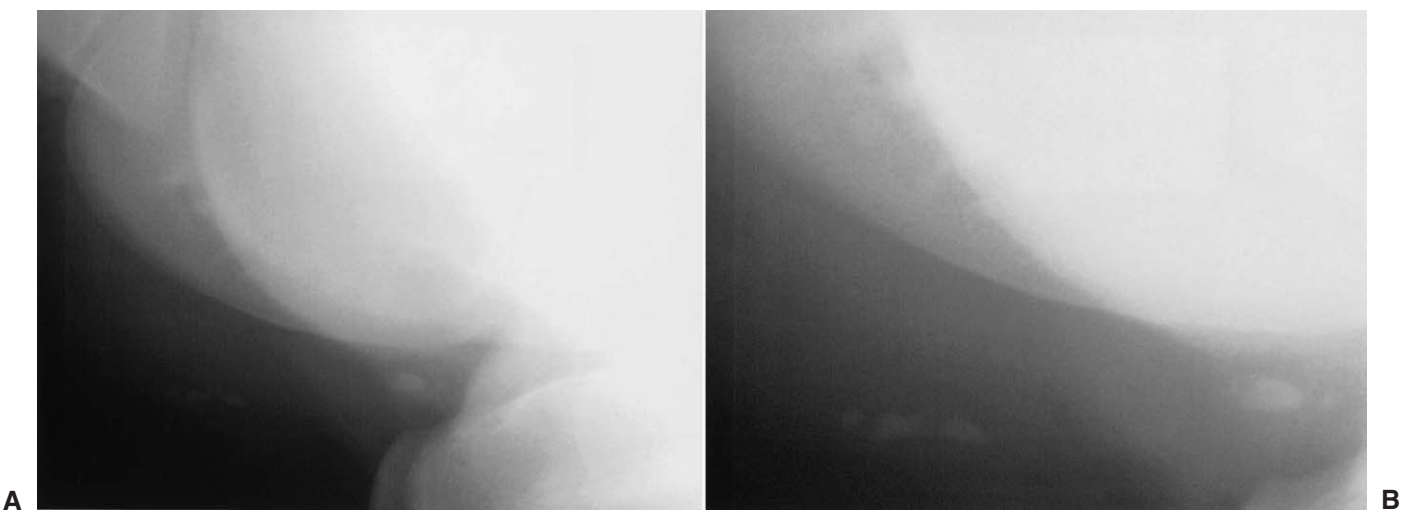


Figure 13-16 • Lateral close-up **(A)** and ultra-close-up lateral **(B)** views of the femoral trochlea of a young horse with a nonpainful swelling of its stifle show one medium and one small bone fragment at the mouth of the femorotibial joint and a series of small fragments at the same level but situated more cranially. Their presumed "fracture beds" are evident in the overlying medial trochlea, just cranial to the lateral ridge.

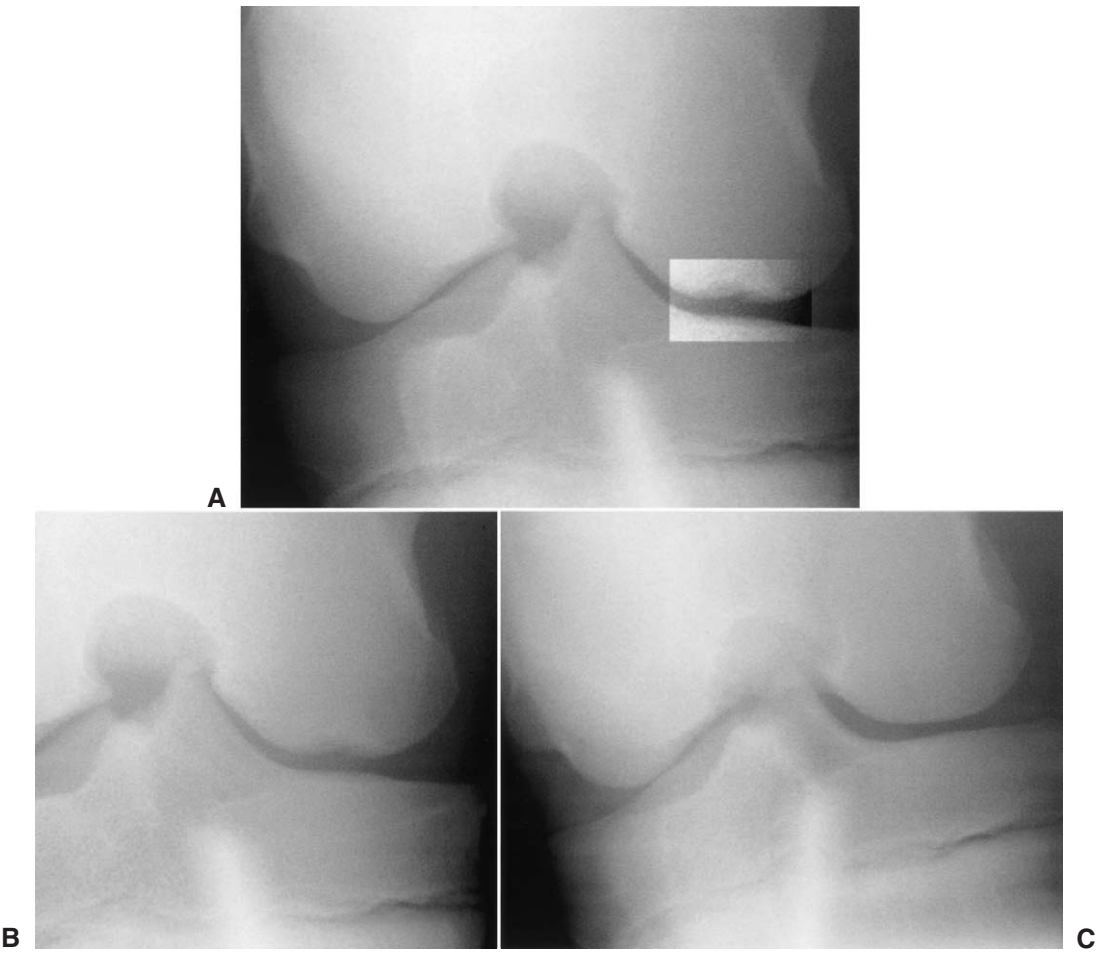


Figure 13-17 • Close-up **(A)** and ultra-close-up **(B)** caudocranial views show a shallow, troughlike osteochondritic lesion along the central edge of the medial femoral condyle. The underlying tibial condyle and meniscal space appear normal *(emphasis zone).* A caudocranial view of the opposite normal stifle is included for comparison **(C).**

Cystic Femoral Osteochondritis (Femoral Bone Cysts)

Jeffcott and Kold described the various disease patterns for subchondral bone cysts of the equine stifle.[34] In a group of 33 young Throughbreds, all but five horses had *unilateral* disease. The authors divided their material into two groups, A and B. In the former category (28 animals), they included large circular or dome-shaped cysts located in the medial femoral condyle with a distinct communication with the femorotibial joint (inferred by an associated marginal defect). Group B (five cases) comprised more variably shaped cysts in a several locations: distal femur adjacent to the intercondyloid fossa or proximal tibia just beneath the tibial spine, for example. No discrete bone fragments were identified.

Most of the described animals were treated with rest exclusively for a period of 6 months. Half the horses in group A recovered fully, but in Group B, only one animal was able to return to full work. Fourteen horses were radiographed a second time 4 to 33 months after the initial radiographic examination. The cysts persisted in all instances, with only a subtle increase in lesion density seen in some animals. In a subsequent publication, Kold and Hickman reported that treating a medial condylar bone cyst with a cancellous bone graft relieved pain and lameness in a majority of cases.[35]

Progression of Femoral Bone Cysts. In my experience, there is no reliable means of predicting whether or not a femoral bone cyst will worsen radiographically. Some do (Figure 13-18), but others do not. Even if a bone cyst appears larger in a progress examination, it does not follow that the horse will necessarily be worse (assuming that it was lame in the first place).

Fragmented Tibial Intercondylar Eminence

Fragmentation of the intercondylar eminence generally occurs for one of three reasons: (1) the fragmenting form of osteochondritis, (2) sprain-avulsion-fracture,

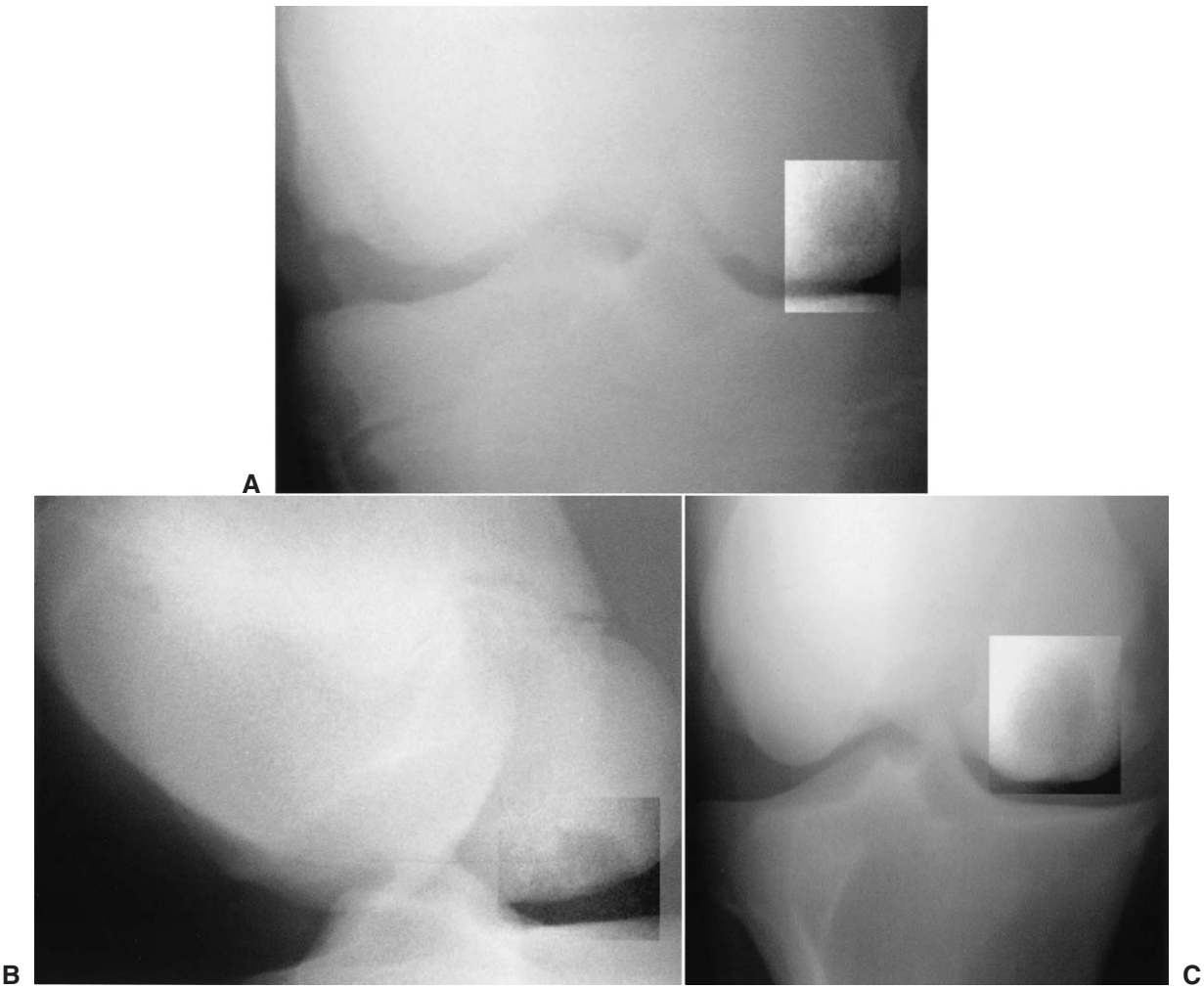


Figure 13-18 • Ultra-close-up caudocranial **(A)** and medial oblique **(B)** views of the stifle of an Arabian yearling show an obvious but poorly marginated osteochondritic bone cyst in the center of the medial condyle; there is no osteoarthritis. Two years later, a progress caudocranial view **(C)** shows that the lesion has become slightly larger and better defined. Even though a small subchondral cone is noted, *seemingly* connecting the cyst with the underlying cartilage space, there is still no evidence of osteoarthritis. However, the horse remains only marginally lame, even after vigorous exercise.

and (3) fracture secondary to traumatic dislocation of the stifle. Radiographically these possibilities can often be separated on the basis of unilateral or bilateral involvement, the latter being characteristic of osteochondritis, the former a consequence of trauma (Figures 13-19 through 13-21).

Fragmented Tibial Tuberosity

A fragmented tibial tuberosity may be the result of an avulsed quadriceps tendon or the fragmenting form of osteochondritis. In the latter instance the lesion is usually, but not invariably, bilateral. In a skeletally immature horse, an open growth plate may resemble a fresh fracture, a radiographic diagnosis that can be quickly confirmed or denied by obtaining a comparison view of the presumably normal opposite stifle.

Synovial Osteochondromatosis

Kirk reported the radiographic and histologic appearance of synovial osteochondromatosis located in the femorotibial bursae of a horse.[36] Radiographically the lesion resembled what have previously been reported as calcified hematomas: a dense, medium-sized, circular or oval mass with a stippled interior and no clear perimeter.

Tumoral Calcinosis

Tumoral calcinosis is a benign, incompletely calcified mass, occasionally seen lateral to the stifle of horses. Some appear superimposed on the head of the fibula, and in this regard have been mistaken for a fracture callus. These lesions also bear some resemblance to calcified hematomas and ossifying fibromas. The cause of tumoral calcinosis is not known.

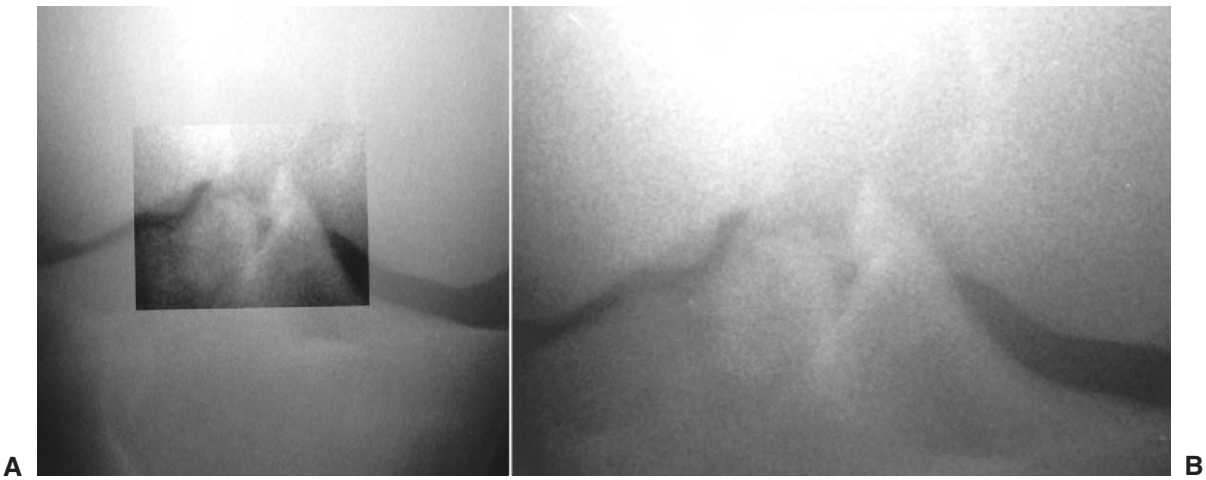


Figure 13-19 • Caudocranial close-up **(A)** and ultra-close-up **(B)** views of the intercondylar eminence *(emphasis zone)* show fragmentation laterally, the result of osteochondritis. The flattened appearance of the medial femoral condyle is also due to osteochondritis.

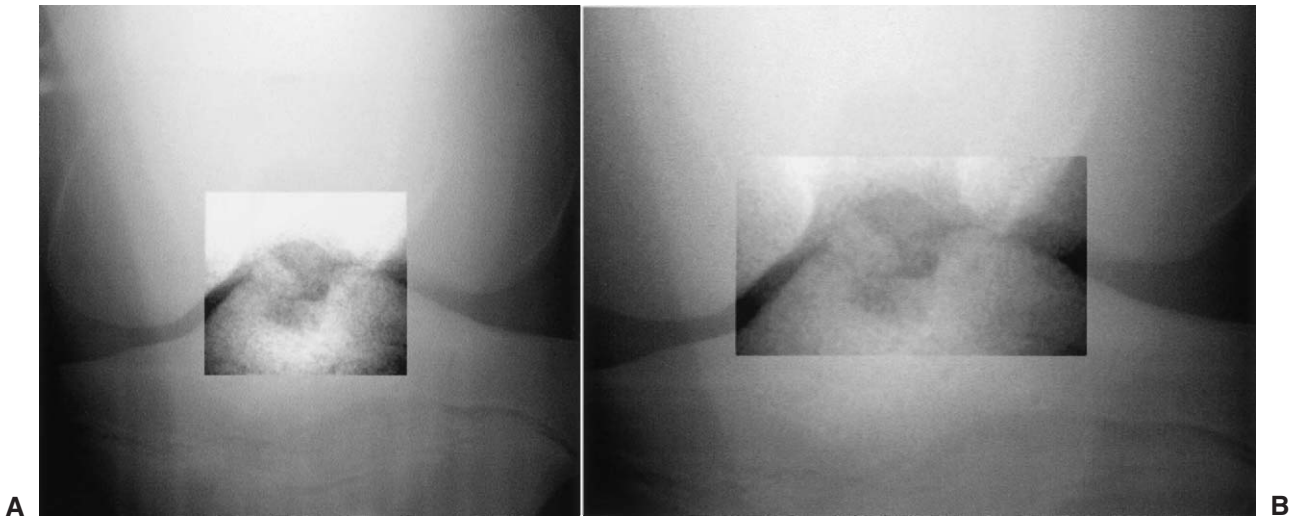


Figure 13-20 • Caudocranial **(A)** and ultra-close-up **(B)** views of a fragmented intercondylar eminence *(emphasis zone)* caused by osteochondritis.

▮▮▮ NONSPECIFIC REGIONAL SWELLING

In young foals, nonspecific, painful regional swelling of the stifle region is most likely to be due to infection, probably septic arthritis. If other joints are swollen, this is a near certainty. As foals age, the probability of infection decreases, and the likelihood of injury increases. Fracture and cellulitis can closely resemble one another, and usually radiography is required to distinguish between the two. If no fracture is found, then ultrasound is the best means to determine whether an abscess is present and then assist in its drainage.

Penetrating wounds can be extremely painful in their own right and can lead to cellulitis, abscessation, and occasionally lymphangitis. *Strongyloides* may enter the muscle of the stifle region through a skin wound, carrying with them highly pathogenic bacteria such as *Rhodococcus*.[37]

▮▮▮ SEPTIC ARTHRITIS AND OSTEOMYELITIS

Steel and co-workers reported septic arthritis and osteomyelitis in 93 foals.[38] The stifle and hock were the most commonly affected joints, presumably the result of septicemia. In our practice the stifle is most often affected.

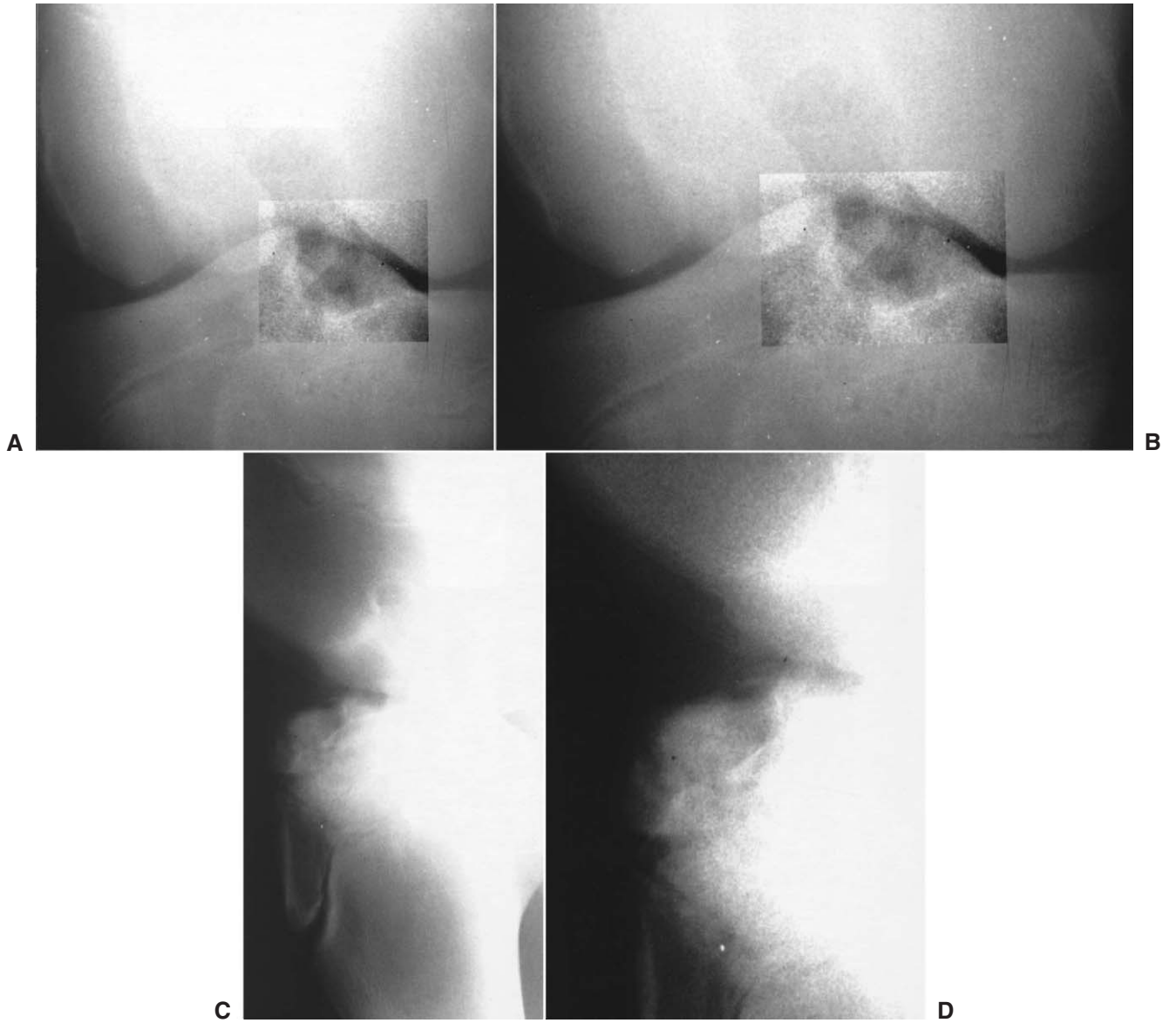


Figure 13-21 • Close-up **(A)** and ultra-close-up **(B)** views of a badly fragmented intercondylar eminence (medial tubercle) caused by osteochondritis. Close-up **(C)** and ultra-close-up **(D)** lateral views of the cranial aspect of the genual joint show a cluster of displaced bone fragments atop the tibial crest.

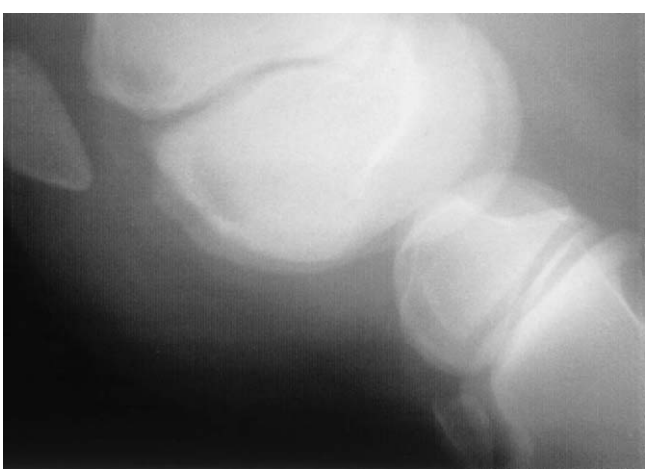


Figure 13-22 • Lateral view of the stifle of a 13-day old Standardbred filly, swollen for the past week, shows radiographic indications of infection: bone loss in the cranial aspects of the distal femoral metaphysis and epiphysis and severe intracapsular swelling.

Radiographically, infection of the immature stifle is frequently characterized by interior bone destruction, appearing as one or more small to medium-sized areas of decreased bone density situated on either side of the physis cranially (Figures 13-22 and 13-23). Some infections selectively affect the caudal aspect of one or both condyles, in severe cases leading to a pathologic fracture.

ARTICULAR FRACTURES

Articular injuries of the stifle are unusual, most occurring in foals in conjunction with growth plate fractures. Many such fractures are not initially apparent because of insufficient fragment displacement or inadequate projection angle (Figure 13-24).



Figure 13-23 • Ultra-close-up lateral view **(A)** of the cranial aspect of an infected stifle in a 1-month-old Appaloosa filly, limping for the past week, shows signs of infection, including focal areas of bone loss *(emphasis zone)* and a severely swollen femoropatellar joint. Fringing along the upper front edges of the patella and femoral metaphysis is normal in a foal of this age, the result of uneven ossification. A caudocranial view **(B)** of the same foal is less revealing, although it does show a faint area of bone loss in the tibial epiphysis medially.

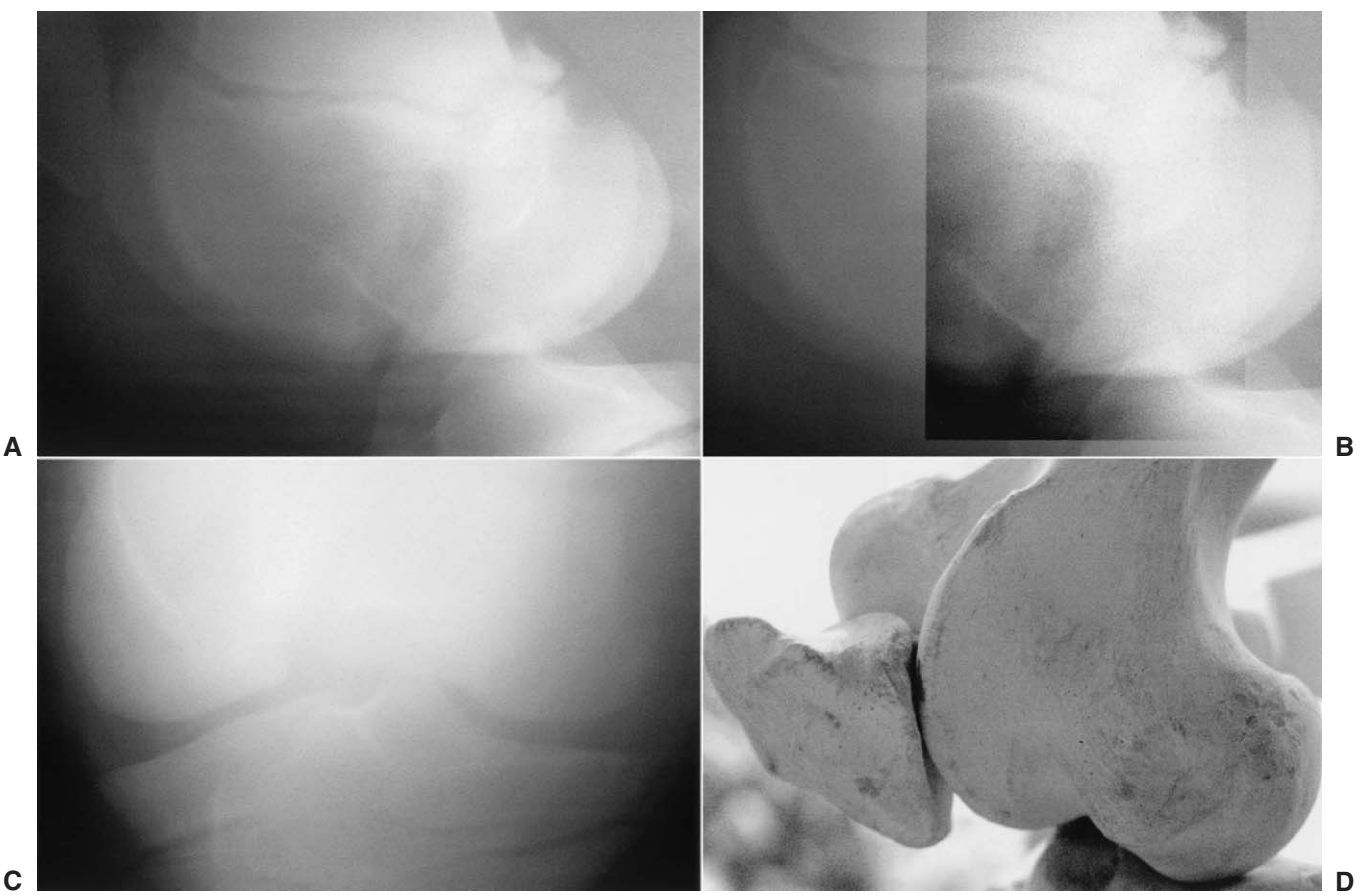


Figure 13-24 • Lateral **(A)** and enhanced lateral **(B)** view of a displaced bilateral condylar fracture (also shown in previous chapter) that breaks through the caudal aspect of the adjacent metaphysis, resulting in a small triangular fragment. A caudocranial view **(C)** fails to show the injury, as might be expected given the near perpendicular angle of the fracture relative to the x-ray beam. A defleshed bone specimen is provided for anatomic comparison **(D).**

References

1. O'Brien TR: Radiology of the equine stifle. *Proceedings of the 19th Annual Convention of the American Association of Equine Practice* p 271, 1973.
2. Adams OR: *Lameness in Horses*, 3rd ed, Philadelphia, 1974, Lea & Febiger.
3. Jeffcott LB, Kold SE: Radiographic examination of the equine stifle, *Equine Vet J* 14:25, 1982.
4. Quick CB, Rendano VT: Equine radiology—the stifle, *Mod Vet Pract* Vol 73:455, 1978.
5. Reeves MJ, Trotter GW, Kainer RA: Anatomical and functional communications between synovial sacs of the equine stifle joint, *Equine Vet Res* 53:1431, 1992.
6. Nickels FA, Sande R: Radiographic and arthroscopic findings in the equine stifle, *J Am Vet Med Assoc* 181:918, 1982.
7. Peroni JE, Stick JA: Evaluation of a cranial arthroscopic approach to the stifle joint for the treatment of femorotibial joint disease in horses: 23 cases (1998-1999), *Am Vet Med Assoc* 220:1048, 2002.
8. Penninck DG, Nyland TG, et al: Ultrasonography of the equine stifle, *Vet Radiol* 31:293, 1990.
9. Holcombe SJ, Bertone AL, et al: Magnetic resonance imaging of the equine stifle joint, *Vet Radiol Ultrasound* 36:119, 1995.
10. Van Pelt RW, Riley WF, Tillotson PJ: Stifle disease (gonitis) in horses: clinicopathologic findings and intra-articular therapy, *J Am Vet Med Assoc* 157:1174, 1970.
11. Jeffcott LB, Kold SE: Stifle lameness in the horse: a survey of 86 referred cases, *Equine Vet J* 14:31, 1982.
12. Dik KJ, Nemeth F: Traumatic patella fractures in the horse, *Equine Vet J* 15:244, 1983.
13. Marble GP, Sullins KE: Arthroscopic removal of patellar fracture fragments in horses: five cases (1989-1998), *J Am Vet Med Assoc* 216:1799, 2000.
14. Dyson S, Wright I, et al: Clinical and radiographic features, treatment and outcome in 15 horses with fracture of the medial aspect of the patella, *Equine Vet J* 24:204, 1992.
15. Anderson BH, Turner TA, Johnson GR: What is your diagnosis? *J Am Vet Med Assoc* 209:1847, 1996.
16. Colbern GT, Moore JN: Surgical management of proximal articular fracture of the patella, *J Am Vet Med Assoc* 185:543, 1984.
17. Hunt RJ, Baxter GM, Zamous DT: Tension-band wiring and lag screw fixation of a transverse, comminuted fracture of a patella in a horse, *J Am Vet Med Assoc* 200:819, 1992.
18. Squire KR, Blevins WE, et al: Radiographic changes in an equine patella following medial patella desmotomy, *Vet Radiol Ultrasound* 31:208, 1990.
19. McIlwraith CW, Warren RC: Distal luxation of the patella in a horse, *J Am Vet Med Assoc* 181:67, 1982.
20. Finocchio EJ, Guffy MM: Congenital patellar ectopia in a foal, *J Am Vet Med Assoc* 156:222, 1970.
21. DeBowes RM, Abrahamsen EJ, Sande RD: What is your diagnosis? *J Am Ved Med Assoc* 183:583, 1983.
22. Leitch M, Kotlikoff M: Surgical repair of congenital lateral luxation of the patella in a foal and a calf, *J Vet Surg* 9:1, 1980.
23. Rose PL, Graham JP, et al: Caudal cruciate ligament avulsion in a horse, *Vet Radiol Ultrasound* 42:414, 2001.
24. Bukowiecki CF, Sanders-Shamis M, Bramlage LR: Treatment of a ruptured medial collateral ligament in a horse, *J Am Vet Med Assoc* 193:687, 1988.
25. Holcombe SJ, Bertone AL: Avulsion fracture of the origin of the extensor digitorum longus muscle in a foal, *J Am Vet Med Assoc* 204:1652, 1994.
26. Blikslager AT, Bristol DG: Avulsion of the origin of the peroneus tertius tendon in a foal, *J Am Vet Med Assoc* 204:1483, 1994.
27. Stowater JL, Kirker-Head CA, et al: Osteochondrosis in the lateral femoral condyles of a horse, *Vet Radiol* 27:115, 1986.
28. Adams WM, Thilstead JP: Radiographic appearance of the equine stifle from birth to 6-months, *Vet Radiol* 26:126, 1985.
29. Howard RD, McIlwraith CW, Trotter GW: Arthroscopic surgery for subchondral cystic lesions of the medial femoral condyle in horses: 41 cases (1988-1991), *J Am Vet Med Assoc* 206:842, 1995.
30. McIlwraith CW: Subchondral cystic lesions (osteochondrosis) in the horse, *Comp Cont Ed* 7:282, 1982.
31. Schneider RK, Jenson P, Moore RM: Evaluation of cartilage lesions on the medial femoral condyle as a cause of lameness in horses: 11 cases (1988-1994), *J Am Vet Med Assoc* 210:1649, 1997.
32. McIlwraith CW: Osteochondral fragmentation of the distal aspect of the patella in horses, *Equine Vet J* 22:157, 1990.
33. Pascoe JR, Pool RR, et al: Osteochondral defects of the lateral trochlear ridge of the distal femur of the horse, *Vet Surg* 13:99, 1984.
34. Jeffcott LB, Kold SE: Clinical and radiological aspects of stifle bone cysts in the horse. *Equine Vet J* 14:40, 1982.
35. Kold SE, Hickman J: Results of treatment of subchondral bone cysts in the medial condyle of the equine femur with an autogenous cancellous bone graft, *Equine Vet J* 16:414, 1984.
36. Kirk MD: Radiographic and histologic appearance of synovial osteochondromatosis of the femorotibial bursae in a horse: a case history report, *Vet Radiol* 23:167, 1982.
37. Etherington WG, Prescott JF: *Corynebacterium equi* cellulitis associated with *Strongyloides* penetration in a foal, *J Am Vet Med Assoc* 177:1025, 1980.
38. Steel CM, Hunt AR, et al: Factors associated with prognosis for survival and athletic use in foals with septic arthritis: 93 cases (1987-1994), *J Am Vet Med Assoc* 215:973, 1999.

Chapter 14

Tibia and Fibula

THE STANDARD TIBIA/FIBULA SERIES

In a foal or young adolescent horse, the tibia can be imaged much like the metatarsus: caudocranial, lateral, and medial and lateral obliques. In an adult it is better to focus on a particular tibial region (upper, mid, or lower shaft); center the x-ray beam appropriately; and make at least two views, depending on the tentative diagnosis. Bear in mind that the tibial body is not a simple cylinder; rather, it is a complex bone, asymmetric proximally and distally, and composed of a variety of triangular, oval, and circular cross-sections, depending on the level of the cut (Figures 14-1 and 14-2).

Potential Misdiagnosis

The proximal fibula is notorious for simulating fracture, depending on projection angle, age of the animal, and clinical context. The adjacent tibial sulcus can also be misleading diagnostically, resembling a localized infection or sequestrum (Figures 14-3 through 14-5).

Another potentially problematic area is the tibial tuberosity, which forms from a separate ossification center and varies greatly with age. As with any accessory growth center, the appearance of the tibial tuberosity varies substantially with different projection angles (Figure 14-6). When the opposite tibial tuberosity is being used as a normal comparison, in the case of a suspected fracture, for example, it is imperative to obtain a similar projection.

PROXIMAL TIBIAL FRACTURE

In young foals, Salter-Harris type II growth plate fractures are most common, typically breaking through the medial side of the growth plate and then passing diagonally through the lateral aspect of the adjacent metaphysis, causing the tibial epiphysis and associated metaphyseal corner fragment to tip precariously in a lateral direction (Figures 14-7 and 14-8). Wagner and co-workers have shown that such fractures can be satisfactorily repaired with cancellous bone screws.[1]

In adult horses, fresh, minimally displaced, proximal tibial fractures can sometimes be hard to diagnose because of the difficulty of placing a cassette behind the swollen stifle. Even with a grid, the obtained images are often murky and feature unfamiliar projection angles.[2] Adding one or two additional oblique views in such instances may confirm an otherwise ambiguous break (Figure 14-9).

PROXIMAL FIBULAR FRACTURE

Distinguishing Proximal Fibular Fractures from Gaps Related to Secondary Ossification Centers

Proximal fibular fractures must be distinguished from normal growth plates, as described previously. Where uncertainty exists, a follow-up radiograph made a month or so later should resolve any question. A fracture will usually appear callused; a growth plate will not (Figure 14-10).

Nondisplaced Tibial Body Fracture (Stress Fracture, Fatigue Fracture)

Mackey and co-workers described the radiographic or scintigraphic appearance of 11 tibial stress fractures in horses. Most fractures (i.e, six) were located in the proximolateral aspect of the tibia; three were in the distal, caudolateral cortex, and three were in the midshaft.[3] Of the fractures depicted in the article, only one showed a clear fracture; the others were diagnosed presumptively based on the presence of an associated new bone deposit, representing an immature callus. The illustrated nuclear medicine scans, on the other hand, appeared conclusive.

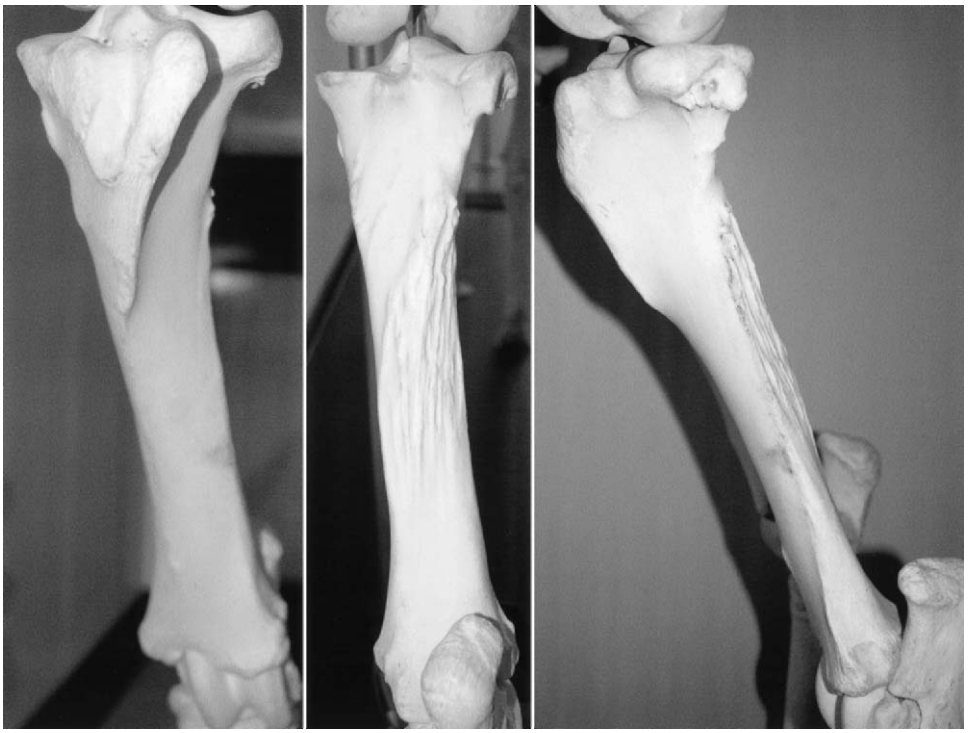


Figure 14-1 • Front **(A),** rear **(B),** and lateral **(C)** views of the defleshed tibia from an adult horse (the fibula has been removed. The parallel ridges located on the caudal and caudolateral surfaces of the tibia (termed simply the *muscular lines*) mark the attachment of the deep digital flexor muscle and must not be mistaken for a so-called bone reaction. The proximal slant of these muscular lines, either right or left, can be used to determine which tibia is being viewed.

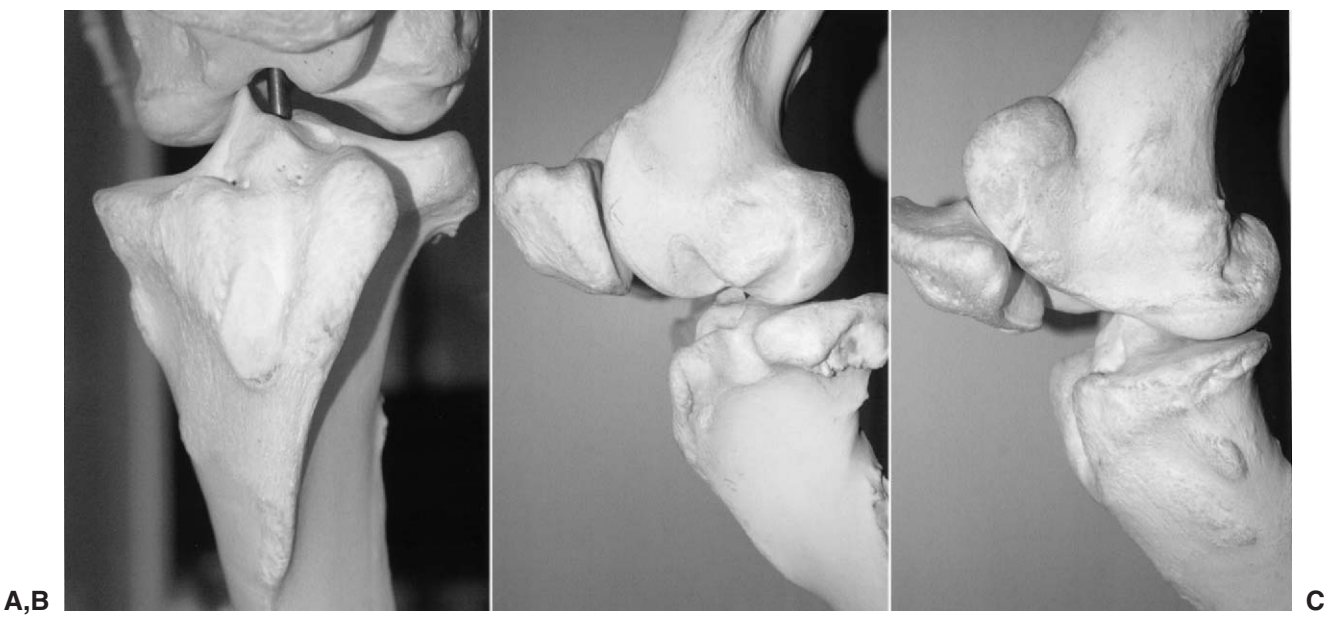


Figure 14-2 • Close-up frontal **(A),** lateral **(B),** and medial **(C)** views of the stifle show the considerable anatomic complexity characteristic of the region. In particular, note the large triangular tibial tuberosity (viewed frontally), which is actually composed of a pair of outcroppings divided by a large groove for the middle patella ligament. The tibial spine (also termed the *intercondylar eminence*) sits above and behind the tibial tuberosity and is flanked by the medial and lateral condyles, the latter creating a prominent overhang in marked contrast to its much smaller medial counterpart.



Figure 14-3 • Ultra-close-up lateral view of the proximal fibula shows a pseudofracture *(emphasis zone),* an anatomic variant, not an injury.



Figure 14-5 • An ultra-close-up caudocranial view of the proximal fibula shows what can variably be interpreted as a sequestrum, actually the fibular head within its tibial fossa or a more distally located fracture, in reality a normal ossification variant.

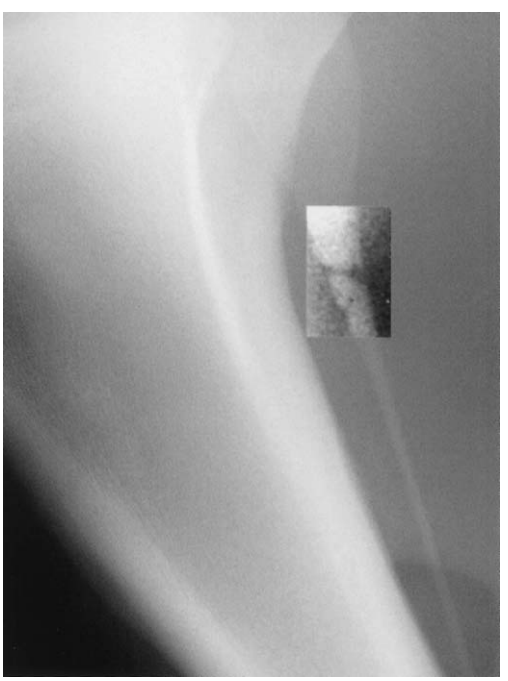


Figure 14-4 • A close-up lateral view of the proximal fibula reveals an apparent comminuted fracture, which in reality is a normal anatomic variant.

Johnson and co-workers also reported the radiographic appearance of incomplete tibial fractures in two horses, describing the fracture as a vertically oriented linear lucency flanked by a pair of radiodense bands.[4] Haynes and co-workers described incomplete tibial fractures in three horses, one of which showed a lengthy, irregular new bone deposit resembling an infection.[5]

Pelaso and co-workers reported an unusual case of bilateral tibial stress fractures in a 2-year-old racing Quarter Horse.[6] Radiographically, the left tibia showed subtle cortical disruption in one oblique projection, but the right tibia revealed only a small, recently formed cortical bone deposit. Both abnormalities were located in the tibial midshaft.

Nuclear scintigraphy showed a focal increase in isotopic uptake in the caudomedial aspect of both tibial diaphyses, consistent with bilateral stress fractures.[6]

Ruggles and co-workers, using a combination of radiology and scintigraphy, diagnosed tibial stress fractures in 13 Standardbreds.[7] Most of these injuries were in 2-year-olds, causing moderate lameness. Eleven of 13 fractures were located in the tibial midshaft, as compared with tibial stress fractures in Thoroughbreds, which typically occur in the proximal diaphysis. Predictably, nuclear imaging revealed a "hot spot" in the tibial body that roughly corresponded to the fracture site, whereas radiography showed an oblique, mid-diaphyseal break in the caudal or caudolateral cortex. The lateral and

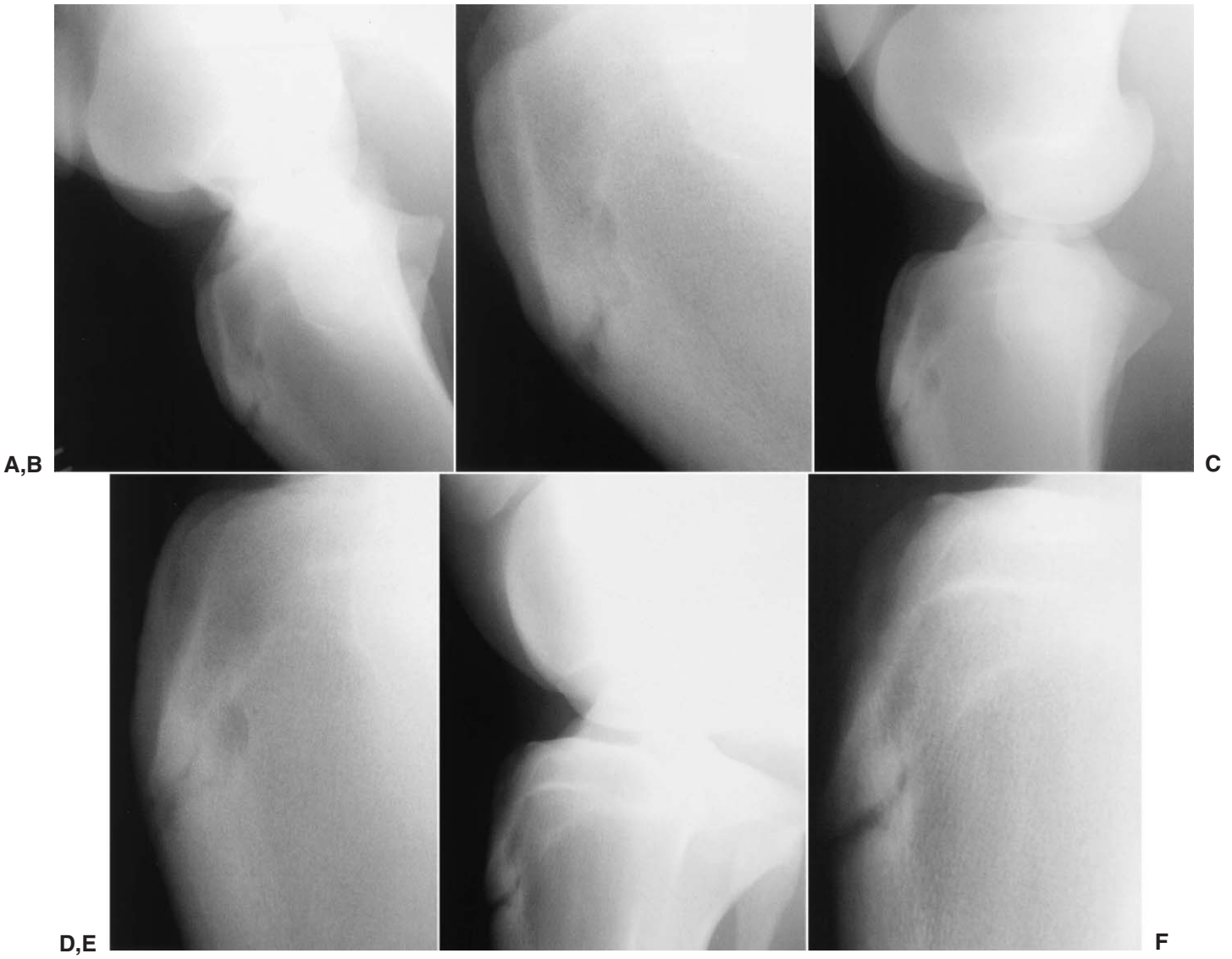


Figure 14-6 • The radiographic appearance of any growth plate, in this instance that of the tibial tuberosity, is greatly dependent on beam angle, as shown in this series of films made of the same animal over a 10-minute period, attempting to obtain a true lateral projection of the stifle, in particular the tibial tuberosity: initial attempt **(A, B),** second attempt **(C, D),** third attempt **(E, F).**

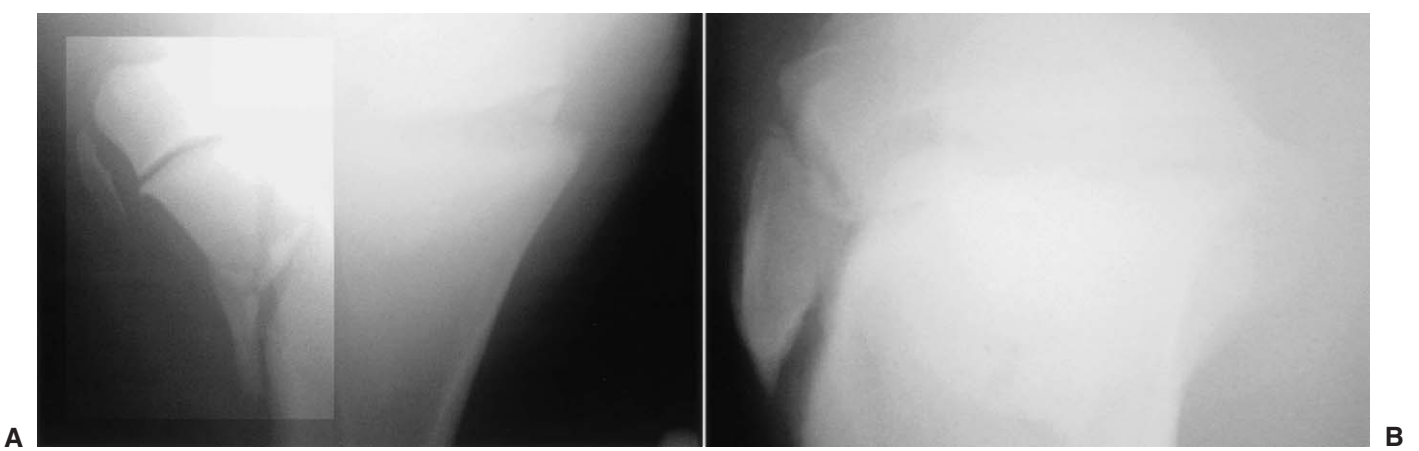
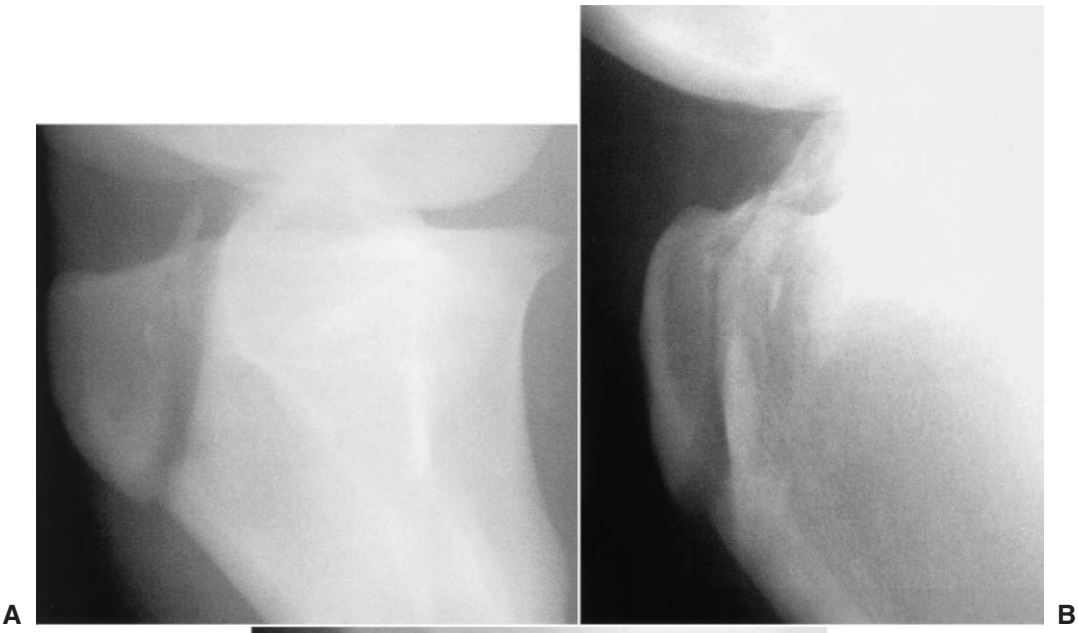


Figure 14-7 • Close-up caudocranial **(A)** and lateral **(B)** views of a displaced proximal tibial growth plate fracture with a comminuted metaphyseal fragment *(emphasis zone).* Although it resembles a fracture, the large triangular bone seen in the lateral view is actually the unfused tibial tuberosity, made even more suspicious looking by the abnormal limb carriage related to the injury and the resultant nonstandard projection angle.



Figure 14-8 • A, Close-up view of a displaced proximal tibial growth plate fracture with a large metaphyseal-diaphyseal fragment laterally and a smaller, detached metaphyseal fragment on the far medial side. **B,** Six weeks later, the fracture is sufficiently healed to allow controlled exercise.



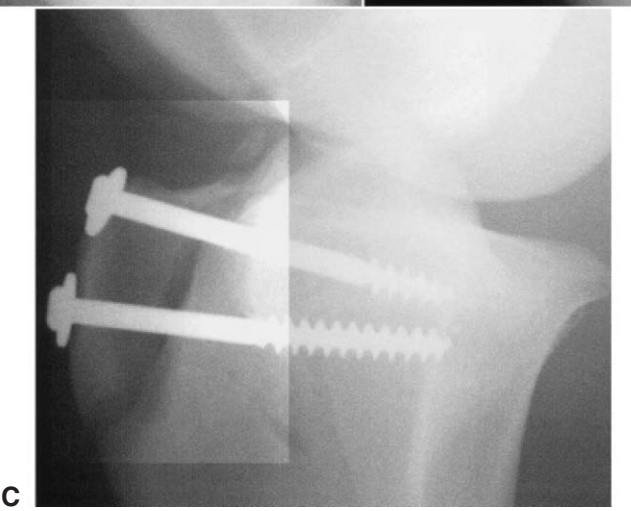
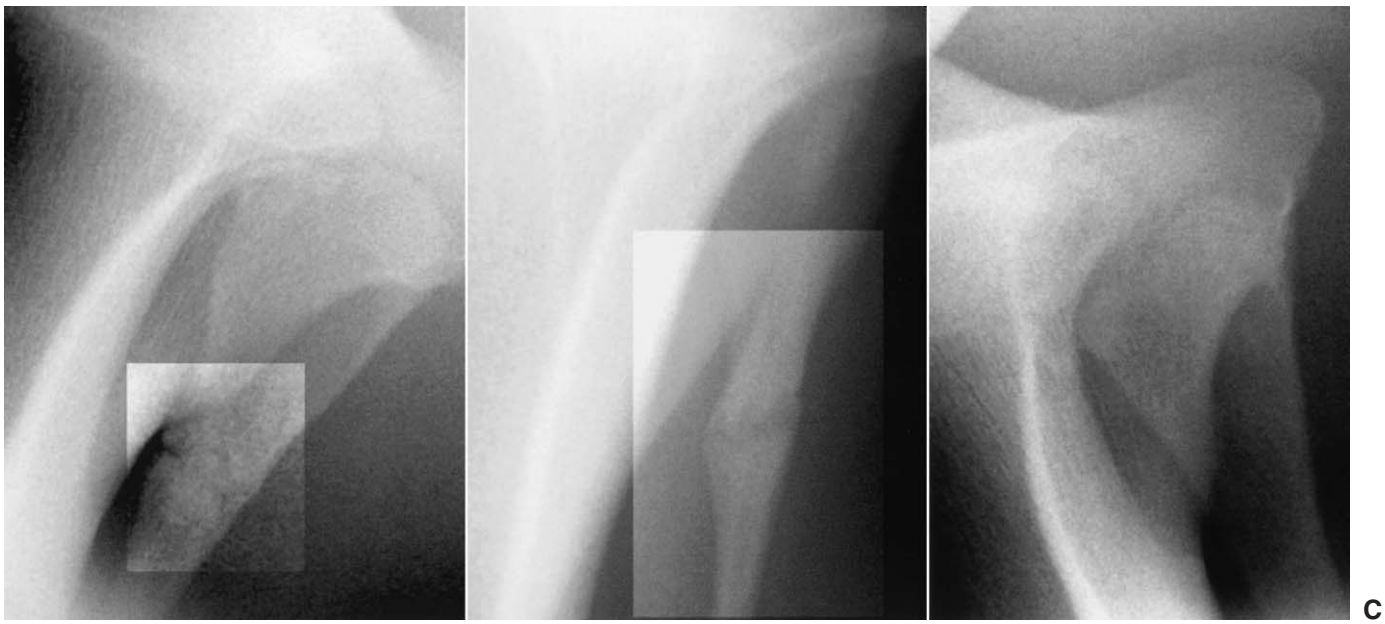
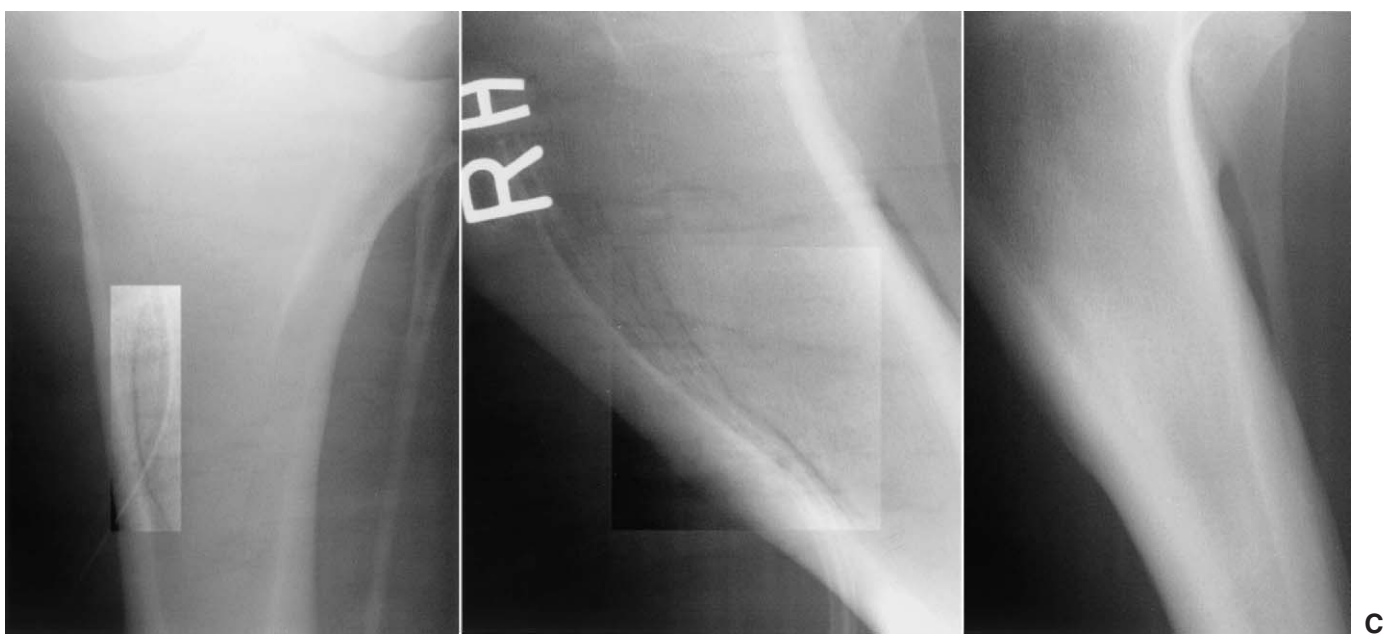


Figure 14-9 • Lateral **(A)** and medial oblique **(B)** views of the stifle of a 10-year-old Arabian mare show a 12-day-old displaced fracture of the tibial tuberosity. The small proximal fragment is from the cranial aspect of the medial intercondylar tubercle. After curing the associated infection, the fracture was subanatomically reduced with a pair of washered cortical bone screws, both of which are slightly bent **(C).**



A,B C

Figure 14-10 • Close-up view **(A)** of the proximal fibula shows a subacute fracture, which appears well callused 10 weeks later **(B).** See emphasis zones. A comparable view of the opposite fibula **(C)** lacked a similar appearance, serving to confirm the fracture.



A,B C

Figure 14-11 • Caudocranial **(A)** and ultra-close-up lateral **(B)** views of a young Quarter Horse with a comminuted hairline fracture of its proximal tibia, by some termed a *stress fracture* (gas along the cranial cortex and the catheter is related to an open wound). A month later, a flourishing callus makes the original injury all but impossible to identify **(C).**

lateral oblique projections showed the fracture best (Figure 14-11).

▮▮▮ DISPLACED TIBIAL BODY FRACTURE

In young foals, untreated displaced tibial body fractures typically heal as a malunion, with most of the callus forming on the concave surfaces of the break. The younger the foal is at the time of injury, the greater the likelihood that the malunion will self-correct by the time it reaches skeletal maturity. In badly displaced fractures, the adjacent fibula is often fractured in two or more places *(multiple fracture),* sometimes assuming a very unusual shape on healing (Figure 14-12).



Figure 14-12 • A, Full-length lateral view of a young foal with what appears to be only a mildly displaced, minimally comminuted fracture of the proximal tibial body. **B,** A plantarodorsal view reveals otherwise, that the fracture is displaced badly. **C,** A 3-month progress lateral close-up shows a substantial callus, which has predictably formed on the concave side of the break. **D,** The accompanying plantarodorsal close-up view exhibits a similar type of callus formation and an enormously enlarged, nearby fibular fragment.

▮▮▮ DISTAL ARTICULAR TIBIAL FRACTURE

Frauenfelder and Rossdale reported the radiographic appearance of a distal articular tibial fracture and described a special radiographic projection designed to eliminate calcaneal superimposition.[8] The special frontal view is made by flexing and extending the hock about 90 degrees to align the calcaneus parallel to the x-ray beam, well away from the distal tibia. The receiver is positioned in a conventional manner.

Frankeny and co-workers described what they termed *bilateral stress fractures* in the medial aspect of the distal tibial metaphysis in a 7-month-old Appaloosa foal. The short, vertically oriented fracture lines appeared to enter the distal tibial physis, although the epiphysis appeared intact. In addition to the bilateral fractures, the foal was also believed to have physitis, based on distal physeal widening. It was uncertain whether the abnormalities were related.[9]

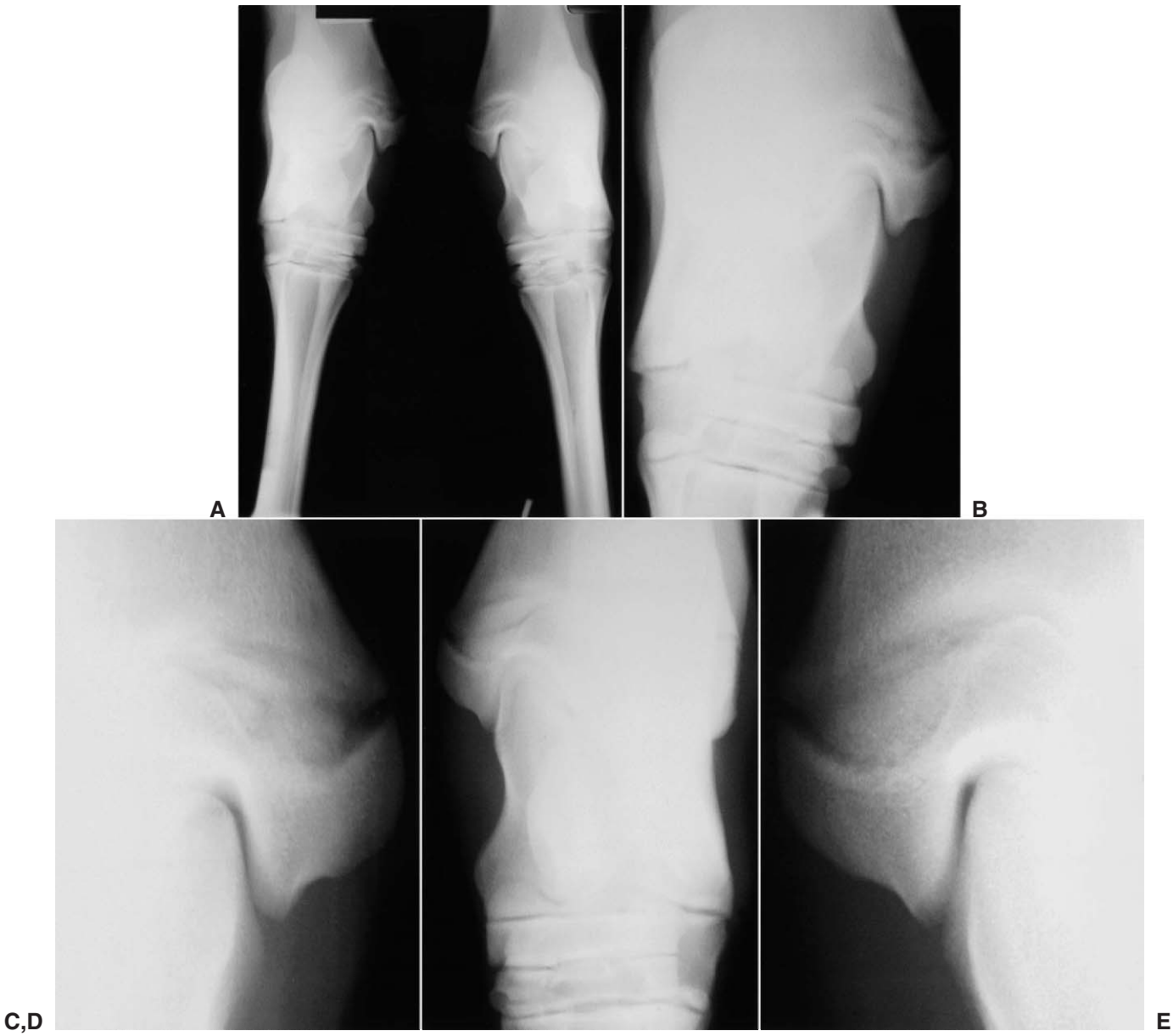


Figure 14-13 • Caudocranial side-by-side view **(A)** of the distal hind extremities shows a mild right-sided valgus (attributed to uneven distal tibial growth) and an overly straight left leg (felt to be compensatory). Close-up **(B)** and ultra-close-up **(C)** views of the right medial malleolus show a relatively subtle peripheral widening of the overlying growth plate compared with similar views **(D, E)** of the medial malleolus on the left. The foal's hind legs eventually straightened of their own accord.

▮▮▮ CHRONIC BONE ABSCESS (BRODIE'S ABSCESS)

Bone abscesses, also known as *Brodie's abscess* in human radiology, are typically considered sterile entities composed of a primary pus-containing cavity, surrounded by scar tissue and a collar of dense bone, the latter often referred to as a *sclerotic rim*. Mature-appearing new bone deposits may or may not be found on the adjacent bone. Sinus formation and drainage are unusual.

Computed tomographic imagery defines bone abscesses with greater precision than radiography, whereas nuclear medicine is more efficient and successful in detecting additional skeletal lesions. In addition to a focal osteomyelitis, bone cysts and primary or secondary bone tumors warrant diagnostic consideration

Young and co-workers have reported a chronic bone abscess in the proximal tibia of an adult horse. Associated radiographic features consisted of (1) a medium-sized, oval-shaped, metaphyseal defect; (2) a

dense but ill-defined perimeter; and (3) a large, ragged, eccentrically positioned bone deposit. Notably, the surface deposit was evident only in the frontal projection, whereas the interior destruction was observed only in the lateral view.[10]

Gustavsson and Stromberg reported a case of osteomyelitis in the medial aspect of the proximal tibia of a horse, which may have led to a pathologic avulsion of the medial collateral ligament. At necropsy, the tibial lesion bore some resemblance to a Brodie's abscess.[11]

▮▮▮ OSTEOCHONDRITIS

Osteochondritis has been described in both the proximal and distal ends of the tibia, usually in the form of a subchondral bone cyst proximally and a fragmented sagittal ridge distally.[12] However, distal epiphyseal bone cysts have been reported.[13]

▮▮▮ UNEVEN PHYSEAL GROWTH AND ABNORMAL LOWER LIMB ANGULATION

A difference in growth rate within the distal tibial physis can result in a deviated lower limb in addition to the obvious curvature; the growth plate overlying the medial malleolus often assumes an abnormally widened appearance, which is characteristic of the disease (Figure 14-13).

▮▮▮ SONOGRAPHY

Normal Sonographic Anatomy of the Tibial Region

Dik described the normal cross-sectional sonographic appearance of the tibial region (crus) using a combination of dismembered and living horses.[14] The utility of ultrasound in the diagnosis of regional muscle and tendon injuries in this area was exemplified with three specific injuries: (1) ruptured peroneus tertius muscle, (2) intramuscular hematoma of the lateral digital extensor muscle, and (3) combined strained Achilles tendon and calcaneal bursitis.

References

1. Wagner PC, DeBowes RM, et al: Cancellous bone screws for repair of proximal growth plate fractures of the tibia in foals, *J Am Vet Med Assoc* 184:688, 1984.
2. Lopez MJ, Pritchard MA, Nicoll RG: What is your diagnosis? *J Am Vet Med Assoc* 210:897, 1997.
3. Mackey VS, Trout DR, et al: Stress fractures of the humerus, radius, and tibia in horses, *Vet Radi*ol 28:26, 1987.
4. Johnson PJ, Allhands RV, et al: Incomplete linear tibia fractures in two horses, *J Am Vet Med Assoc* 192:522, 1988.
5. Haynes PF, Watters JW, et al: Incomplete tibial fractures in three horses, *J Am Vet Med Assoc* 177:1143, 1980.
6. Peloso JG, Watkins JP, et al: Bilateral stress fractures of the tibia in a racing American Quarter Horse, *J Am Vet Med Assoc* 203:801, 1993.
7. Ruggles AJ, Moore RM, et al: Tibial stress fractures in racing Standardbreds: 13 cases (1989-1993), *J Am Vet Med Assoc* 209:634, 1996.
8. Frauenfelder H, Rossdale P: What is your diagnosis? *J Am Vet Med Assoc* 180:1109, 1982.
9. Frankeny RL, Johnson PJ, et al: Bilateral tibial metaphyseal stress fractures associated with physistis in a foal, *J Am Vet Med Assoc* 209:76, 1994.
10. Young, BD, Hendrickson, DA, Park RD: What is your diagnosis? *J Am Vet Med Assoc* 221:1251, 2002.
11. Gustavsson PO, Stromberg B: Osteomyelitis in the tibia of a horse (an unusual case), *Vet Radiol* 12:48, 1966.
12. De Moore A, Verschooten F, et al: Osteochondritis of the tibio-tarsal joint in the horse, *Equine Vet J* 4:139, 1972.
13. Duin YV, Hurtig MB: Subchondral bone cysts in the distal aspect of the tibia of three horses, *Can Vet J* 37:429, 1996.
14. Dik KJ: Ultrasonography of the equine crus, *Vet Radiol Ultrasound* 34:28, 1993.

Chapter 15

Tarsus

THE STANDARD TARSAL SERIES

The tarsus, or *hock,* as it is commonly termed, is usually radiographed in four standard projections: (1) plantarodorsal, (2) lateral, (3) medial oblique, and (4) lateral oblique (Figure 15-1). A second plantarodorsal view may also be added, in which the x-ray beam is centered on the tibiotarsal joint, and the kilovoltage peak (kVp) is increased to penetrate better the thickest part of the hock. This is especially useful when searching for nondisplaced fractures or bone fragments associated with osteochondritis. The corresponding bone anatomy is shown in Figure 15-2.

The Immature Tarsus

The immature tarsus is characterized by smaller, rounder bones with larger cartilage spaces, and growth plates in the adjacent long bones. There is also an open growth plate in the proximal aspect of the calcaneus. Generally, the tarsus of a young foal appears more porous and less dense than that of an adult (Figures 15-3 and 15-4).

Sentinel Tarsal Bones

Like a good golf swing, success in tarsal imaging is based on consistency. Consistency, in turn, is achieved by keying on a specific tarsal bone, or so-called *sentinel bone,* one that has a unique appearance but only in a particular standard view. In this way it becomes relatively easy to assess quickly and accurately each projection for radiographic accuracy. The following images illustrate the use of tarsal sentinel bones:

1. *Lateral View:* The sentinel bone in the lateral view is the calcaneus or, more specifically, the *sustentaculum tali.* Note the thick, distinctive border and the relatively dark interior that characterizes the sustentaculum when imaged laterally (Figure 15-5, *A, B*).
2. *Plantarodorsal View:* The sentinel bone in the plantarodorsal view is the central tarsal bone, which should occupy approximately 80 percent of the width of the tarsus and appear superimposed on the medial half of the fourth tarsal bone. The adjacent proximal and distal intertarsal joints should appear as gently curved, radiolucent bands with varying degrees of clarity depending on beam angle and direction.
3. *Medial Oblique View:* In the medial oblique view (the view that profiles the dorsomedial aspect of the tarsus), the fourth tarsal bone serves as the sentinel. In this projection, the fourth tarsal is the only one of the distal tarsal bones that extends over two rows (Figure 15-5, *C, D*).
4. *Lateral Oblique View:* In the lateral oblique projection (the view that profiles the dorsolateral aspect of the tarsus), the fused first and second tarsal bone has a laterally compressed appearance featuring a dense exterior and a relatively lucent interior.

SUPPLEMENTARY VIEWS

Flexed Lateral

The flexed lateral projection is particularly valuable when trying to clearly see the cochlear process of the calcaneus, which may become detached as a result of a fracture or because of osteochondritis. The cochlear process may also become arthritic following a severe sprain of the talocalcaneal ligament (Figure 15-6).

Skyline Calcaneus

I first reported use of the calcaneal skyline view in 1976, having learned the technique from my teacher, Joe Morgan (Figure 15-7).[1] Others subsequently reported a similar approach to a variety of fractures and infections of the calcaneus that defied detection using the four standard tarsal projections.[2]

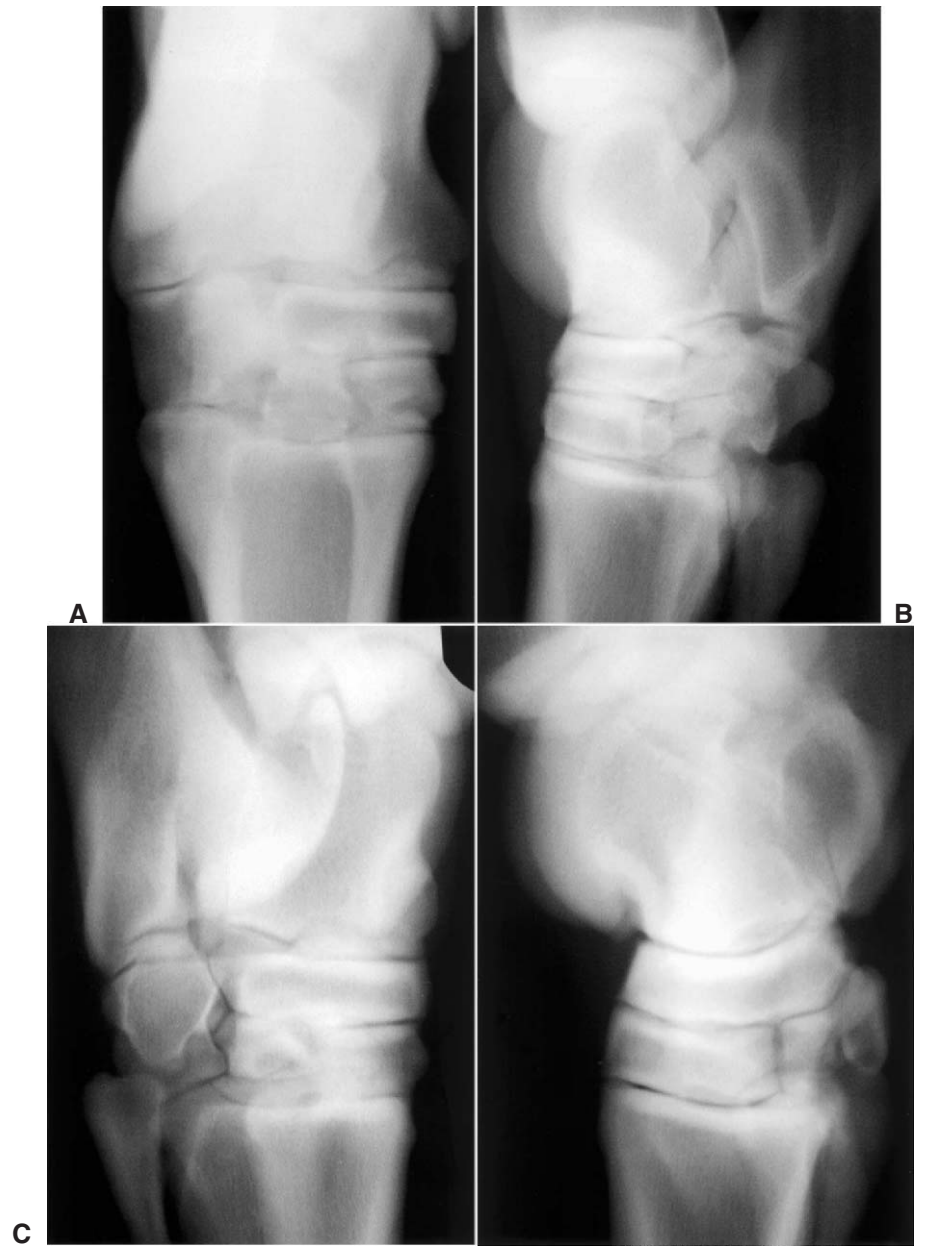


Figure 15-1 • Plantarodorsal **(A),** lateral **(B),** medial oblique **(C),** and lateral oblique **(D)** views of a normal adult tarsus.

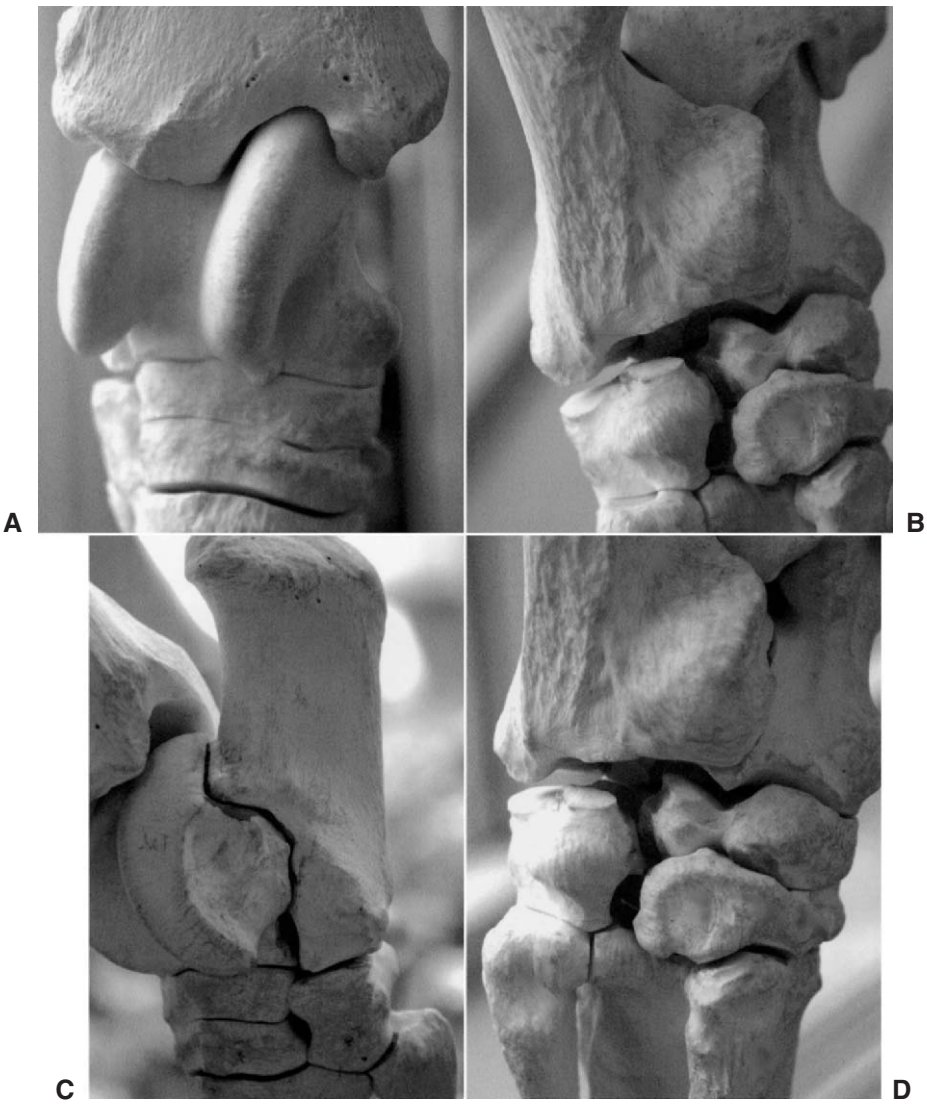


Figure 15-2 • Defleshed tarsal bones shown from front **(A),** rear **(B),** lateral front **(C),** and medial rear **(D).**

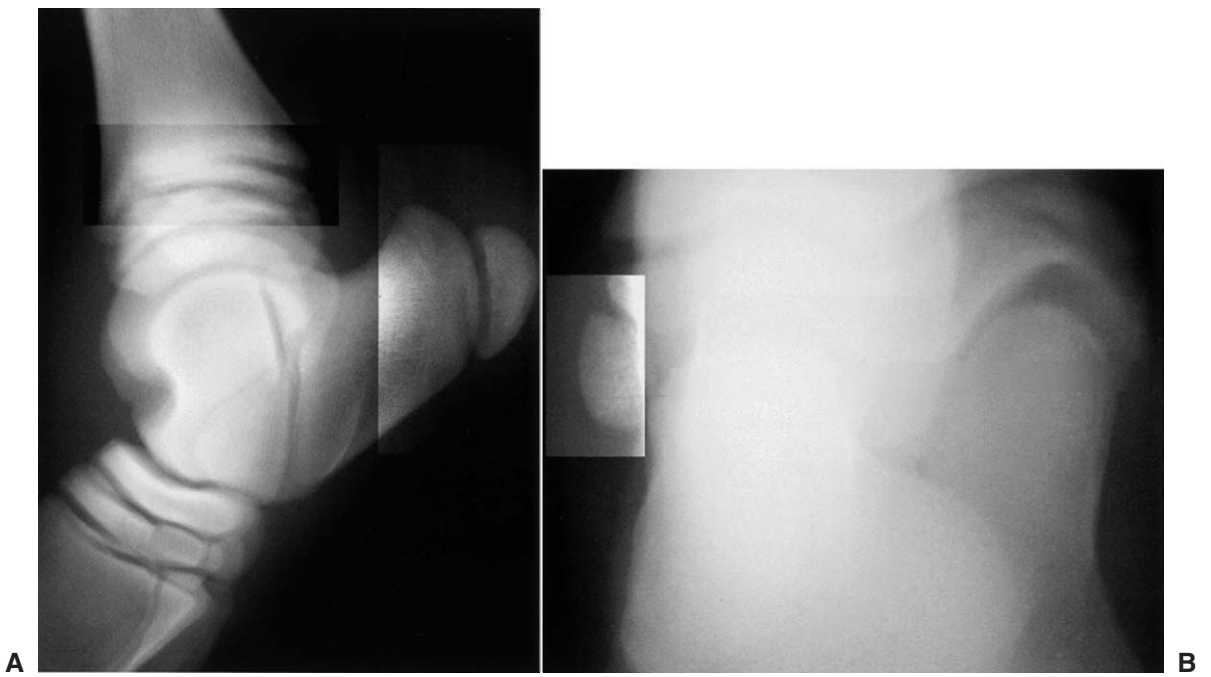


Figure 15-3 • **A,** Lateral view of the tarsus of a 2-week-old foal with distal tibial and calcaneal growth plates highlighted. **B,** Close-up plantarodorsal view of the tarsocrural joint shows secondary ossification center of the distal fibula.

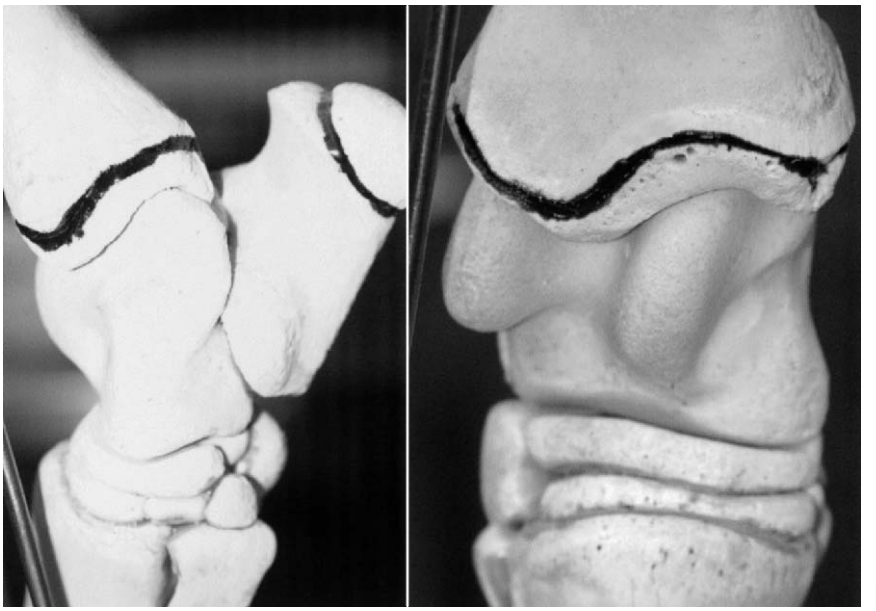


Figure 15-4 • Defleshed lateral **(A)** and plantarodorsal **(B)** views of the tarsus of a skeletally immature foal show the distal tibial and proximal calcaneal growth plates, simulated in black plastic. The distal fibular growth plate is not shown.

ANATOMIC COMPLEXITY OF THE TARSUS

The tarsal bones are even more complex than those of the carpus, a fact that is nowhere more evident than when examining a disarticulated talocalcaneal joint (Figure 15-8). Even more challenging is the radiographic evaluation of the major tarsal joints, which because of their multiplanar surfaces (Figure 15-9) cannot be completely imaged in any single view, irrespective of the projection.

TARSAL FACTS

Rendano and Quick described the following useful anatomic facts about the tarsus (plus a couple of additional pearls)[3]:

- The hock or tarsus comprises six individual bones: (1) talus, (2) calcaneus, (3) central, (4) third, (5) fourth, and (6) fused first and second.
- In skeletally immature horses, there are three separate ossification centers: one each for the head of the calcaneus (an apophysis), the distal tibial epiphysis, and the distal fibular epiphysis.
- The distal tibial epiphysis fuses with the remaining tibia between 18 and 24 months.
- The distal fibula fuses with the distal tibial epiphysis during the first year.
- The calcaneal apophysis fuses with the calcaneal body between 16 and 36 months of age.
- A depression remains on the articular surface of the distal tibia at its junction with the fibula.
- Sometimes a dark band persists where the fibula and tibia join.
- The tarsus comprises four major horizontal joints: (1) tibiotarsal or tarsocrural, (2) proximal intertarsal, (3) distal intertarsal, and (4) tarsometatarsal.
- There are four discrete synovial pouches or sacs: (1) tibiotarsal, (2) proximal intertarsal, (3) distal intertarsal, and (4) tarsometatarsal.[4]
- The tibiotarsal and proximal intertarsal joints communicate dorsally.
- There are usually two synovial fossae: one adjacent to the intermediate ridge of the tibia and the second in the groove between the trochlear ridges of the talus. These normal invaginations of articular cartilage into subchondral bone, which do not appear until 4 or 5 months of age, must not be mistaken for localized cysts of bone destruction.
- The four major ligaments of the tarsus are medial and lateral collaterals, dorsal tarsal, and plantar ligaments.
- The chestnut may be mistaken for a lesion.
- The lateral trochlear ridge can be distinguished from its medial counterpart by a distinctive ventral notch.
- Horses occasionally have congenitally fused central and third tarsal bones, usually bilaterally.[5]

EARLY TARSAL DEVELOPMENT

Smallwood and co-workers chronicled the radiographic-xeroradiographic appearance of tarsal development in six Quarter Horse and three Thoroughbred foals from birth to six months of age.[6] Their findings were as follows:



Figure 15-5 • Sentinel bones as a means of differentiating different standard tarsal views: lateral **(A),** lateral close-up **(B),** plantarodorsal **(C),** close-up plantarodorsal **(D),** medial oblique **(E),** close-up medial oblique **(F),** lateral oblique **(G),** and close-up lateral oblique **(H).**

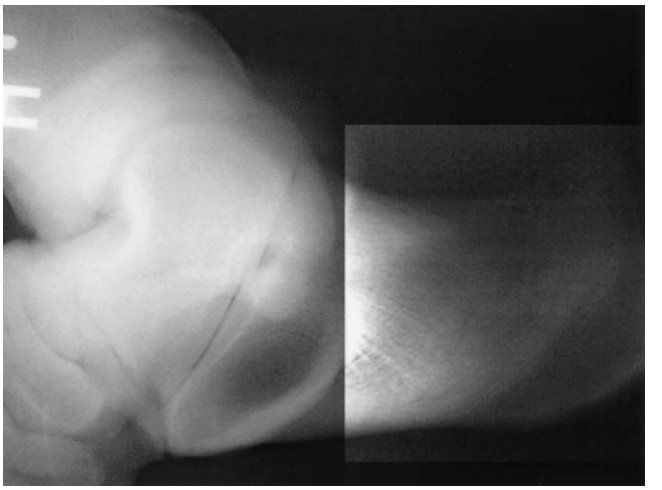


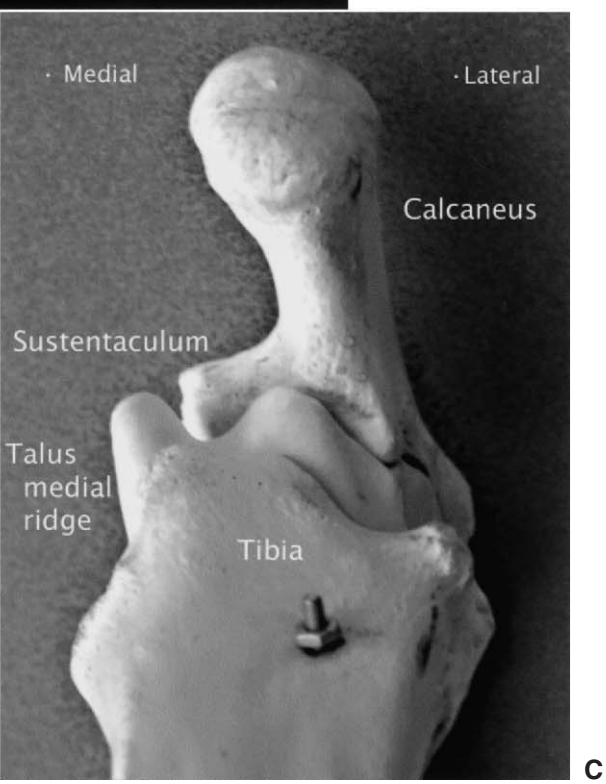
Figure 15-6 • Lateral view of the hock in the flexed position centered over the talocalcaneal joint.



A



B



C

Figure 15-7 • Receiver positioned just beneath the flexed hock of an equine skeleton showing how the skyline view is made **(A)**. Flexed hock and receiver seen from the perspective of the x-ray tube including orientation **(B)** and labeled close-up **(C)** views.

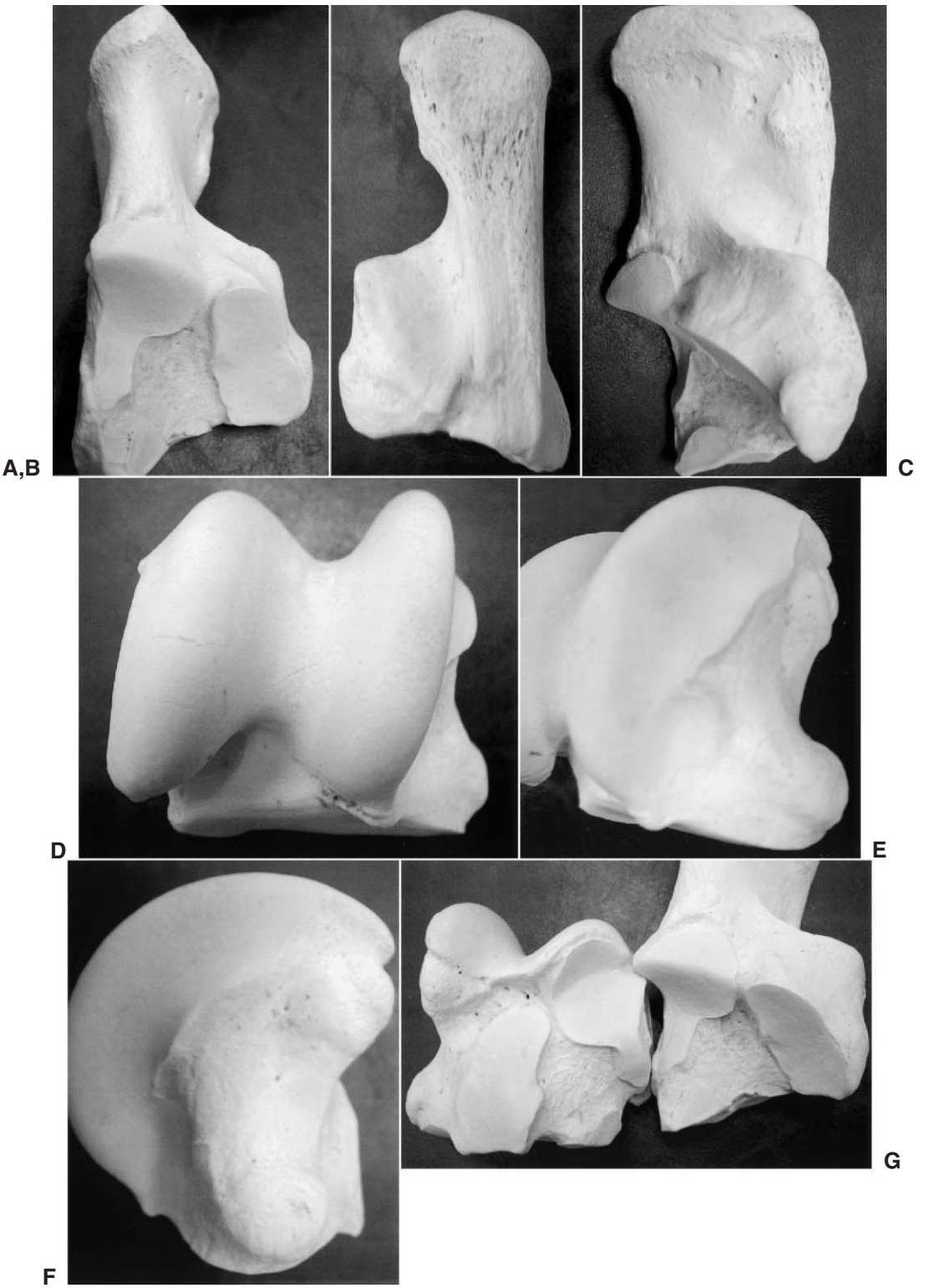


Figure 15-8 • Defleshed calcaneus shown from bottom front **(A),** rear **(B),** and medial **(C)** side; talus from front **(D),** medial **(E),** and lateral **(F)** sides; opened talocalcaneal joint **(G)** from below.

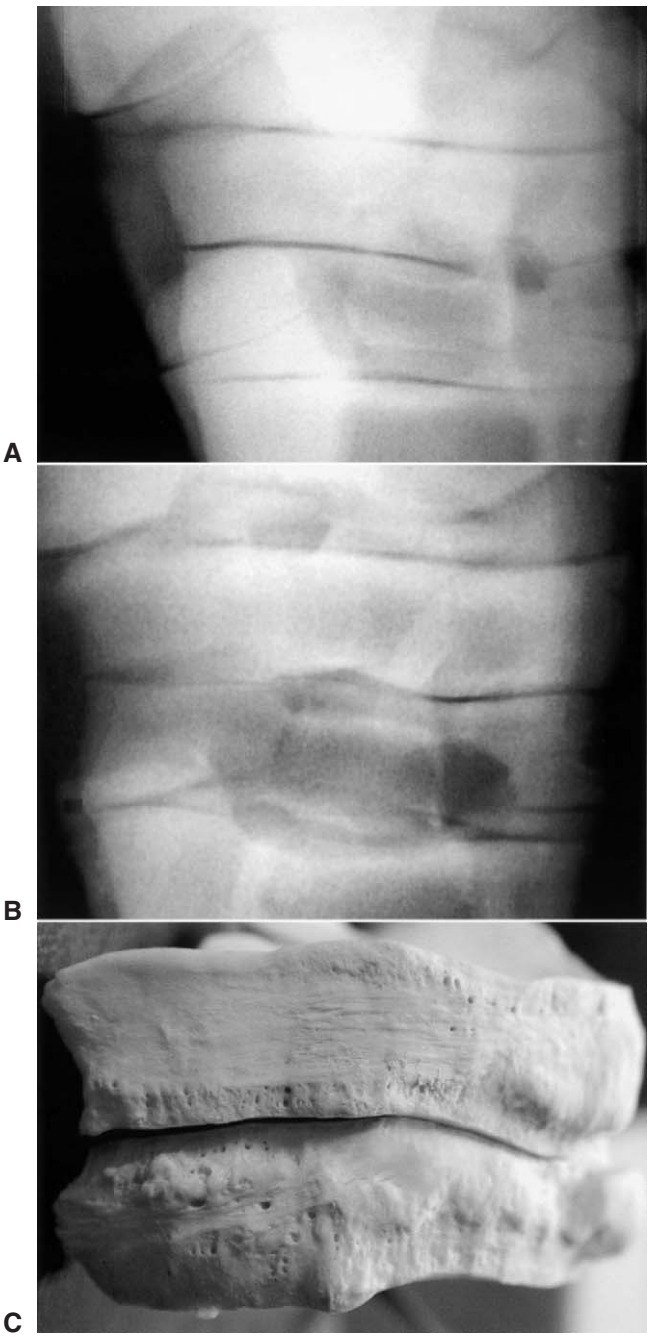


Figure 15-9 • Close-up plantarodorsal radiographs of the central and third tarsal bones and associated cartilage spaces made from slightly different angles. Note that in the first plantarodorsal close-up **(A),** the medial aspects of the cartilage spaces appear clearer than the lateral aspects, whereas in the second plantarodorsal close-up **(B),** the reverse is true. A defleshed bone specimen of the distal tarsal bones is provided for reference **(C).** The *important lesson* to be learned from these images is that *it is impossible* to accurately assess the proximal, distal, or tarsometatarsal joints from a single radiograph, irrespective of beam angle. This knowledge is critically important when it comes to discriminating between the normal variability in joint widths from one side of the hock to the other and the cartilage destruction caused by bone spavin.

Box 15-1
Selected Articular Thicknesses in the Equine Tarsocrural Joint

ANATOMIC LOCATION	MEAN ARTICULAR CARTILAGE THICKNESS (MM)
Medial trochlear ridge (talus)	0.57
Lateral trochlear ridge (talus)	0.58
Distal intermediate ridge (tibia)	0.7

- Right and left calcaneal ossification was similar in individual foals at a given age.
- No correlation was found between gestation length and degree of calcaneal ossification at 1 day of age.
- Some correlation was found between body weight and degree of calcaneal ossification at 98 to 182 days of age.
- Accordingly, ossification of the tuber calcis was deemed a reliable indicator of overall tarsal development in Quarter Horse and Thoroughbred foals.

▮▮▮ NORMAL ULTRASOUND

Tomlinson and co-workers reported the normal sonographic appearance of the clinically relevant articular cartilages of the equine tarsocrural joint, including those covering the lateral and medial trochlear ridges of the talus and the distal intermediate ridge of the tibia (Box 15-1). Sonographic examination of the intertarsal and tarsometatarsal joints proved futile.[7]

▮▮▮ NORMAL COMPUTED TOMOGRAPHY

Using cadaver limbs, Tomlinson and co-workers reported the normal computed tomographic (CT) appearance of the adult equine tarsus, including both soft tissue and bone windows.[8]

▮▮▮ NORMAL MAGNETIC RESONANCE IMAGING

Using detached limbs in a low-field-strength magnet, Blaik and co-workers produced normal reference images of the equine tarsus and correlated them with corresponding tissue slices taken from the imaged parts.[9]

▮▮▮ SOFT-TISSUE INJURY

Bruising and Crushing

Severe bruising or crushing of the hock can produce marked swelling, heat, pain, and lameness, features



Figure 15-10 • Close-up lateral view of a badly bruised hock and metatarsus in a young foal. Initially the injury was misdiagnosed as an infection.

shared by most infections. Generally, a severe contusion can be differentiated from infectious arthritis by the extent of the associated swelling: bruises usually extend well into the metatarsus as blood and edema move distally under the influence of gravity; septic arthritis is usually confined to the infected joint and the immediately surrounding extraarticular tissue (Figure 15-10).

Puncture Wounds

Tarsal puncture wounds are common in horses. Nearly all cause swelling and many lead to infection, especially those that bleed sparsely and close quickly. Initially, associated gas pockets are more likely to be the result of atmospheric contamination than a byproduct of bacterial metabolism. The incidence of associated fracture is extremely low: less than one percent, in my experience.

Deep Lacerations

Deep lacerations usually disrupt soft tissue contours, leave visible defects, and are routinely associated with gas, sometimes within one or more of the tarsal joints. But even if the underlying bone surfaces are abraded, new bone deposition or loss is still weeks away, as far as radiographic detection is concerned.

Strain

Tarsal strains are often diagnosed with a combination of clinical acumen, pain on extension of the damaged tissue, and radiographs that fail to reveal a fracture. In some instances it is not possible to differentiate a possible strain from a sprain (although the healing and recuperation times of these injuries differ substantially).

Ruptured Peroneus Tertius. Although strictly speaking not a part of the tarsus, severe strain or rupture of the peroneus tertius can resemble a hock injury. The peroneus tertius is a muscle that originates in the extensor fossa of the distal femur (along with the long digital extensor), extends down the face of the tibia, and inserts on three different points distally: (1) the dorsal aspect of the third metacarpal proximally, (2) the calcaneus, and (3) the fourth tarsal bone.

In a transverse sonogram, the *normal* peroneus tertius appears as a homogeneous, hyperechoic, oval-shaped object situated between the tibialis cranialis and the long digital extensor. By comparison, a ruptured peroneus tertius is likely to show one or more of the following abnormalities, according to Leveille and co-workers: (1) enlargement, (2) relative hypoechogenicity, and (3) a more uneven echotexture.[10]

Sprain and Sprain-Avulsion Fracture. Radiographically visible sprains most often affect the collateral ligaments and are usually inferred by a combination of swelling in one of the collateral fields and avulsion of a portion of one of the malleoli or talar tuberosities. These avulsion fractures may be obvious, complete with incriminating defects in the adjacent bone (Figure 15-11), or quite small (and thus indistinct), without any nearby bony defects.

Subacute and chronic sprains are usually diagnosed inferentially based on deformity, displacement, and new bone deposition involving one or more ligamentous insertion points. A smoothly surfaced fragment and adjacent fracture bed characterize others. Many chronic collateral sprains feature a very hard lump of scar tissue adjacent to the damaged ligament; this scar tissue can be very difficult to distinguish from bone when palpated (Figure 15-12). Severely destabilizing sprains can lead to osteoarthritis, especially when combined with interior ligament damage (Figure 15-13).

A sprain-avulsion fracture can often be distinguished from the fragmenting form of osteochondritis (the primary differential diagnosis) by its acute onset, hot painful swelling, and normal opposite tarsus. Tarsal osteochondritis, on the other hand, is usually characterized by a gradual onset, cool nonpainful swelling, and bilateral involvement (Figure 15-14).

Stress Radiography of the Hock

Stress radiography of the tarsus is capable of demonstrating excessive or abnormal hock motion, impossible to achieve with conventional radiography. Such findings can then be used to infer a serious sprain injury or sprain-avulsion fracture. Specific stress maneuvers include traction, axial rotation (clockwise and counterclockwise), hyperextension, hyperflexion,

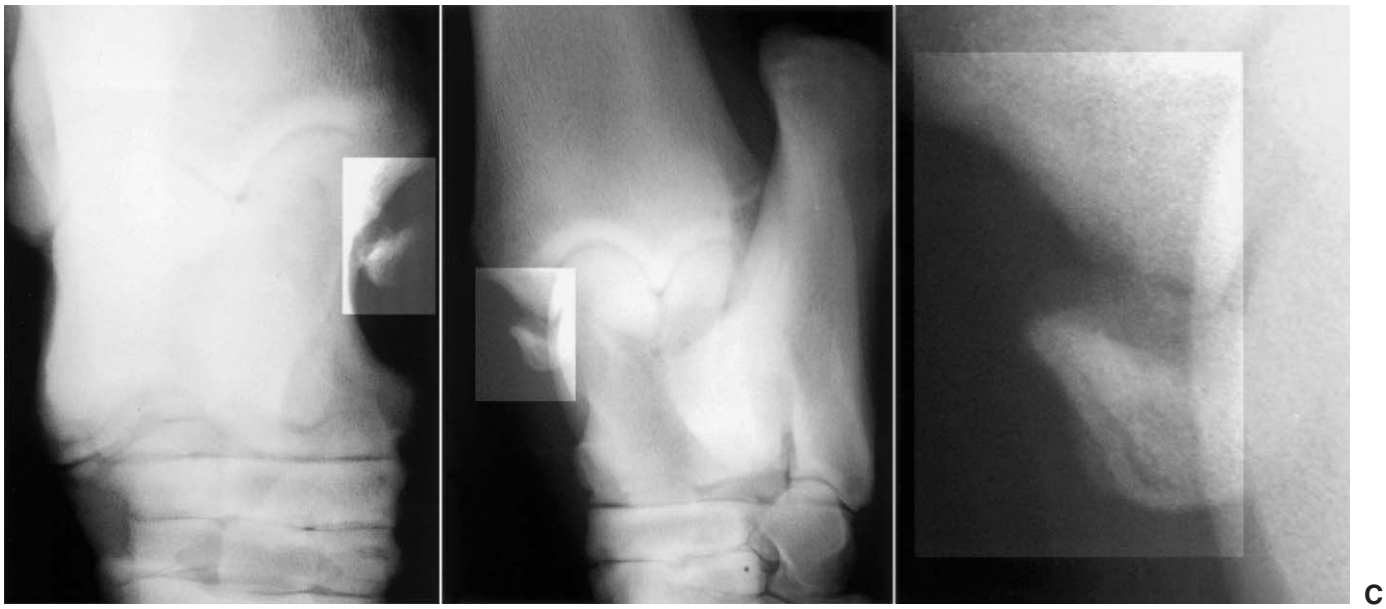


Figure 15-11 • Plantarodorsal **(A),** medial oblique **(B),** and close-up medial oblique **(C)** views of an adult horse with a 2-week-old, eccentrically swollen tarsocrural joint show a moderately displaced avulsion fracture of the distal portion of the medial malleolus, strongly suggesting a sprained medial collateral ligament.

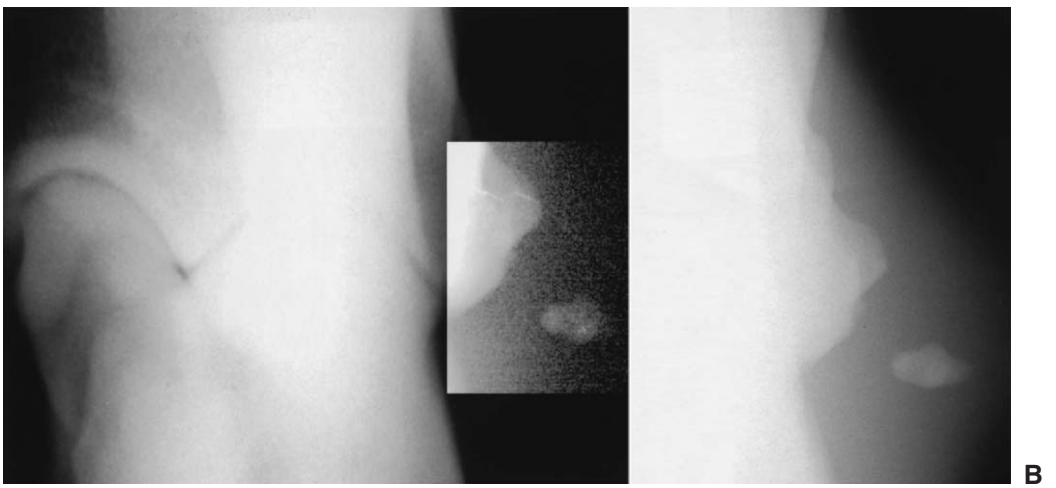


Figure 15-12 • Close-up **(A)** and ultra-close-up **(B)** plantarodorsal views of the tarsocrural joint of an adult horse show an old widely displaced avulsion fracture from the lateral malleolus. In addition to the fragment and malleolar defect *(emphasis zone),* there is also a large lump of scar tissue overlying the damaged bone and collateral ligament.

and fulcrum-assisted medial and lateral flexion; each is designed to expose instability in a particular part of the tarsus and, in the process, to incriminate one or more specific ligaments.

Stress radiography must be performed in a pain-free manner if the horse is to cooperate and the examination performed properly; thus general anesthesia is usually required. Lifting a horse's good leg to stress its abnormal limb is a dangerous practice that can cause the animal to fall, further injuring itself or those around it.

Nuclear Scintigraphy

Boero and co-workers described the clinical, radiographic, and scintigraphic findings of *enthesitis* of the lateral collateral ligament of the tarsocrural joint of the horse.[11] Such findings can indicate an overt sprain or simple desmitis related to chronic overuse.

Capsular Tearing

Although not a true sprain, tearing a portion of the joint capsule from the bone surface can result in a local-

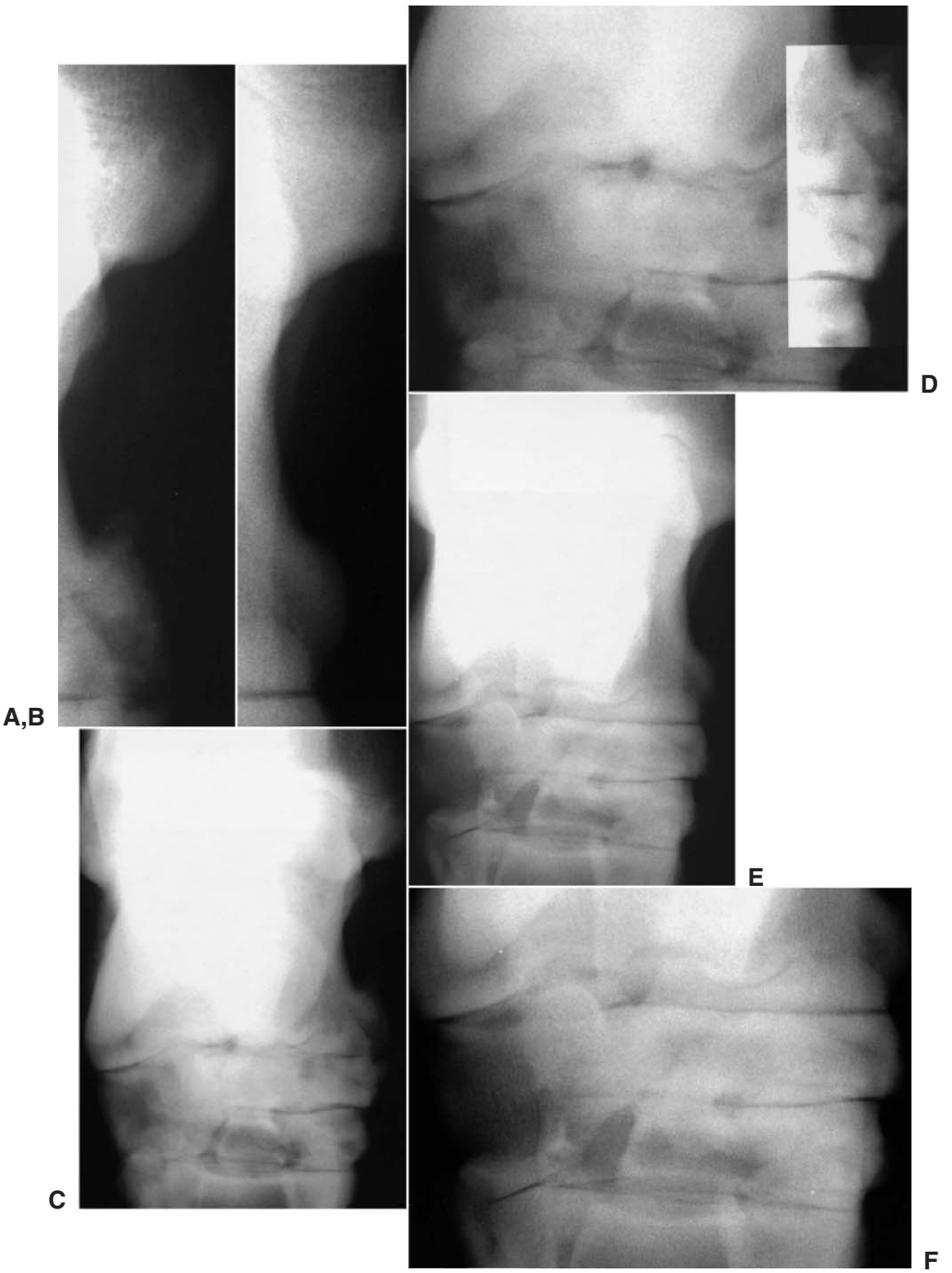


Figure 15-13 • Ultra-close-up plantarodorsal view **(A)** of an old avulsion fracture of the distal talar tuberosity and a normal comparison view of the opposite hock **(B).** Distally centered plantarodorsal **(C)** and close-up plantarodorsal **(D)** views show arthritic proximal and distal intertarsal joints medially *(emphasis zone).* Comparable plantarodorsal **(E)** and close-up plantarodorsal **(F)** views of the opposite tarsus are provided for comparison.

ized bone deposit resembling a sprain. It is also possible to tear both the joint capsule and one or more interior tarsal ligaments, the latter usually requiring CT or magnetic resonance imaging (MRI) to diagnose.

▮▮▮ TARSAL FRACTURES

As described previously, the standard tarsal series consists of four views (plantarodorsal, lateral, lateral and medial obliques); however, not all veterinarians, including a small number of radiologists, routinely include oblique projections.[12] Two-view studies of the tarsi (and some other joints) are becoming increasingly common in screening-type, prepurchase examinations, often with the proviso that if an abnormality is identified, the oblique views should be added. At the risk of appearing self-serving, this seems an inadvisable strategy because the oblique projections generally have a greater sensitivity than the principal orthogonal views.

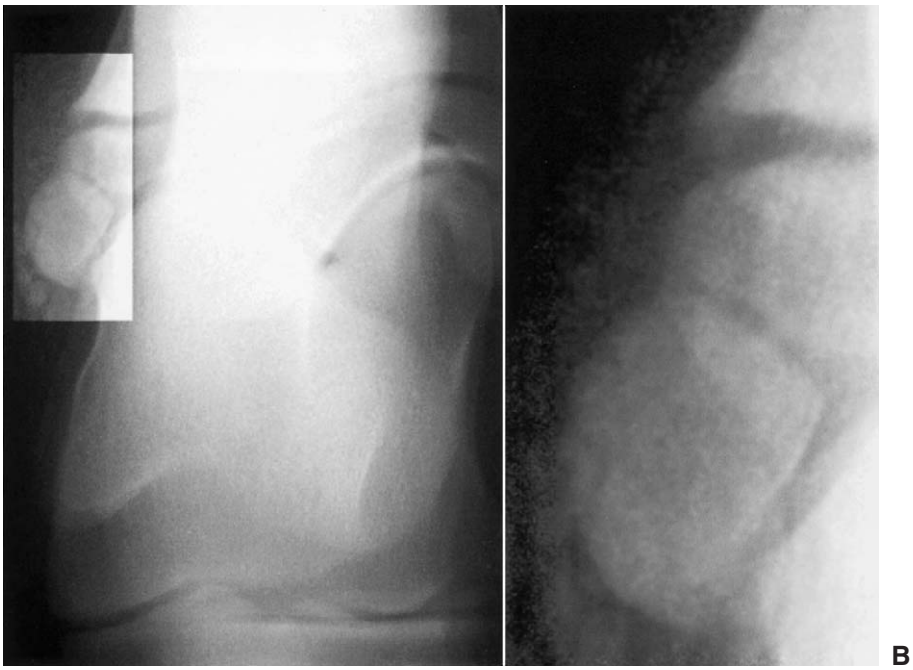


Figure 15-14 • Close-up **(A)** and ultra-close-up **(B)** plantarodorsal oblique views of a fragmented distal fibular epiphysis, presumed to be the result of osteochondritis based on nonpainful swelling of the tarsus, minimal lameness, and similar involvement of the contralateral tarsus.

Commonly fractured equine tarsal or paratarsal bones include the (1) tibial malleolus; (2) calcaneal neck, anconeal process, or sustentaculum; (3) talar ridges; (4) central tarsal bone; and (5) heads of the splint bones. Basilar fractures of the talus and calcaneus are encountered less frequently. Most such injuries are unilateral, but bilateral fractures occur occasionally.[13]

Calcaneal Fracture

Sprain-avulsion fractures involving the lateral collateral ligament and calcaneus are often difficult to detect because of the small size and minimal displacement of the fracture fragment. Often only the frontal view reveals the injury. Goodrich and co-workers showed how nuclear imaging and xeroradiography could be used to confirm (or, more likely, suggest) a suspected calcaneal fracture.[14]

The use of the skyline projection to assess the calcaneus, sustentaculum, and outer talar ridge was first described in 1976.[15] This communication was followed by a retrospective review from the same institution[16] and later by numerous case reports.[17,18]

Basilar calcaneal fractures, assuming some fragment displacement, are usually best seen in the lateral oblique view and less often in the lateral projection. Generally this sort of fracture is invisible in the plantarodorsal view because of an unfavorable projection angle (Figure 15-15).

Talar Fracture

Talar fractures are generally of two types: those that split the condyle, fortunately fairly rare, and those that tear away one or both medial collateral ligaments and, in the process, a portion of the associated tuberosity (sprain-avulsion fractures).

Central Tarsal Bone Fracture. Most central tarsal fractures are complete, breaking into both the proximal and distal intertarsal joints (slab or biarticular fractures). Such fractures can easily be mistaken for vertically oriented joint spaces by those unfamiliar with the radiographic anatomy of the hock. Some authors theorize that such injuries are the result of accumulated bone damage, inflicting so-called microtrauma, which eventually leads to overt structural failure and a radiographically visible break.[19]

Third Tarsal Bone Fracture. Like the central tarsal bone, third tarsal fractures are typically biarticular (slab-type). Radiographically, most fresh third tarsal fractures are characterized by an abnormal vertical band, resembling a normal joint space, and less frequently, by extrusion of the dorsal fragment.[20] Chronic fractures often have vague margination, the result of removal of necrotic bone from the fracture's edges, and in this respect may be mistaken for the irregular interosseous gaps present throughout the normal tarsus. Nuclear imaging can be used to support a diagnosis of tarsal injury, to include fracture, but because of its lack of precision, is better suited to a screening role.[21]

Fourth Tarsal Bone Fracture. The fourth tarsal bone is subject to a wide variety of fractures, in part because of its unique anatomic situation (being a part of both the middle and distal tarsal rows). Small periarticular chips are the most common, followed by intermediate-



Figure 15-15 • Lateral **(A)** and ultra-close-up lateral oblique **(B)** views of the proximal tarsus show a minimally displaced fracture of the medial base of the calcaneus *(emphasis zones)*. A plantarodorsal view **(C)** fails to show the calcaneal injury but does reveal a faint avulsion fracture of the distal talar tuberosity *(emphasis zone)*.

sized corner fragments, vertically oriented slabs, and less frequently, transverse or short oblique fractures—the latter usually accompanied by one or more additional tarsal breaks.

Palmar Process Fractures in Foals. Kaneps and co-workers compared the relative abilities of radiography, CT, and MRI in detecting palmar-process fractures in foals. Somewhat surprisingly, radiography proved as effective as CT or MRI in identifying the fracture, although three-dimensional reconstructions generated from CT and MR slices provided a superior overall perspective.[22]

▮▮▮ PROXIMAL AND DISTAL TARSAL DISLOCATIONS

Dislocations invariably involve ligaments and capsular tissue. Reeves and Trotter reported a fracture-dislocation of the tarsocrural joint of a 14-year-old Quarter Horse–Thoroughbred cross, which had gotten its leg caught in the slats of a stock trailer while being transported.[23] Dislocations of this sort typically involve one or both malleoli.

At the opposite end of the tarsus are the tarsometatarsal fracture-dislocations that may show only minor fragmentation along the margins of the dislocated tarsometatarsal joint. In some instances the degree of dislocation is so slight that only one or two views may show it; in others the dislocation is obvious. Occasionally a deep diagonal metatarsal fracture occurs in which the smaller fragment remains attached to the distal tarsus, resembling a type II growth plate fracture (Figure 15-16).

▮▮▮ OSTEOARTHRITIS

Common causes of osteoarthritis in the hocks of horses include severe sprain, fracture, spavin, and osteochondritis (Figure 15-17). Occasionally hocks become arthritic as a result of growth-related limb deformities and even less often from infections. In principle, anything that disrupts articular congruence, particularly in a high-motion joint, usually leads to some measure of osteoarthritis.

Eksell and co-workers reported that among the standard tarsal projections used in both hocks of 98 Icelandic horses, the *lateral oblique* (plantarolateral-dorsomedial oblique) proved most effective in identifying osteoarthritis, most often found on the dorsolateral aspects of the distal intertarsal (centrodistal) and tarsometatarsal joints.[24] In my experience, the *medial oblique* is the more informative view, an observation that probably reflects the high incidence of bone spavin seen in our practice.

The Solitary Bone Spur

The relevance of a single bone spur, identified radiographically in the tarsus of a horse, is extremely difficult to ascertain, some would say impossible. Although widely acknowledged as the hallmark of osteoarthritis, the isolated periarticular bone spur, identified without companion signs of articular disease, forms the basis of a most tenuous diagnosis. This is particularly true of the solitary osteophyte situated on the dorsal border of the proximal third metatarsal bone, a ubiquitous, often bilateral radiographic finding in the hocks of many sound horses.



Figure 15-16 • Plantarodorsal **(A)** and lateral **(B)** views of a fracture-dislocation of the tarsometatarsal joint. The frontal projection resembles a Salter-Harris type II growth plate fracture.

Swelling of the Tarsal Sheath *(Thoroughpin)* With and Without Associated Sustentacular Osteophytes

Thoroughpin is a classic horseman's term used to describe distension of the tarsal synovial sheath resulting from an excess of synovial fluid. The swelling may arise suddenly and for an obvious reason, following a kick, for example, or it may develop insidiously following a 3-day trail ride. In some instances the swelling is cool, nonpainful, and persistent, whereas in others it is hot, painful, and transient. Chronic swelling of this type may promote adhesions and eventually lead to stenosis of the deep flexor tendon sheath.[25] Radiographs may *infer* tenosynovitis in the form of a series of very small osteophytes situated along the margins of the sustentacular glide path of the deep flexor tendon.

Edwards provided an excellent account of the radiographic changes to the sustentaculum tali found in a group of horses with chronic thoroughpin, specifically the presence of new bone deposition on and around the medial border of the sustentaculum (seen best in an oblique craniomedial projection). Postmortem examination of the deep flexor tendon revealed severe surface fibrillation and adhesions to the sheath, presumed to have resulted from direct abrasion by the new bone.[26]

Welch and co-workers reported the surgical removal of a medium-sized osteophyte from the basilar region of the caudal sustentaculum in a 2-year-old Thoroughbred colt with thoroughpin.[27] At surgery the tendon sheath contained blood-tinged synovial fluid. Portions of the underlying plantar ligament and flexor tendon adjacent to the calcaneus were mineralized. Fibrous adhesions were present between the medial aspect of the calcaneus and the flexor tendon. The authors speculated that the dystrophic calcification might have been caused by a previous corticosteroid injection, citing prior reports of this occurrence.[28,29]

Dik and Merkins reported the tendonographic appearance of a small series of horses with thoroughpin, with and without sustentacular lesions.[30] Later Dik and Keg reported the use of cavography to evaluate thoroughpin-like calcaneal region swelling, terming them *false thoroughpins*.[31]

▮▮▮ TARSAL INFECTION (OSTEOMYELITIS)

Septicemic Joint Infection in Young Foals

Infectious arthritis in young foals is typically heralded by hot, turgid, and painful swelling that is radiographically discernible, provided the radiographic technique allows adequate visualization of soft tissues. In some but not all instances, two or more joints may be similarly affected (Figure 15-18).

When a large compound joint such as the tarsus becomes infected, it usually shows the greatest change in the tarsocrural joint, the synovial compartment with the greatest volume. The resultant swelling typically appears as a large circular density centered over the talocalcaneal joint, a *composite shadow* composed of the joint capsule, synovium, and distended synovial sac and accentuated by extraarticular hyperemia and edema (Figure 15-19).



Figure 15-17 • Close-up plantarodorsal **(A),** lateral **(B),** medial oblique **(C),** and lateral oblique **(D)** views of a foal with an arthritic hock, the result of damage sustained 3 months earlier. The only obvious injury is a displaced fracture of the head of the lateral splint, best seen in the medial oblique projection; but the remodeled third tarsal and underlying third metatarsal bones (lateral and lateral oblique views) suggest that fractures also occurred in these locations as well.

As tarsal infections worsen, subtle areas of bone loss begin to appear in the epiphyses and proximal perimeter of the talus (Figure 15-20).

Inoculation-Type Tarsal Joint Infections in Juvenile and Adult Horses

An inoculation-type infection is one in which bacteria (potentially including skin and hair residents) are carried into the depths of a wound by a sharp object such as a nail or a hypodermic needle. Generally, deep punctures with minimal bleeding are more likely to become infected than shallow wounds with copious hemorrhage. Infection is usually presumed where the bone or joint interior is directly exposed, surrounded by air, or can be shown to communicate with the surface sinographically (Figure 15-21).

The radiographic appearance of an intraarticular infection depends most on its *duration.* Thus, if the tarsus is imaged in the first week or two after bacterial inoculation, the major radiographic observation will probably be a swollen joint.[32] In the following weeks, however, and often by a month, intracapsular new bone deposition appears, shortly followed by varying degrees of subchondral bone destruction.

A reduction in the width of the cartilage spaces frequently accompanies infection of one or more of the tarsal joints, a temporary change probably attributable

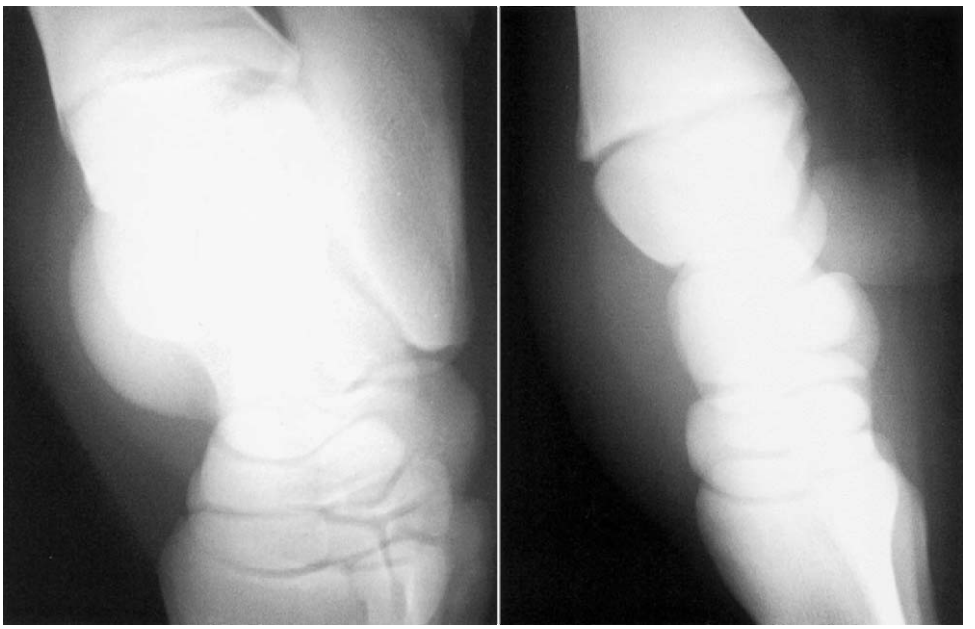


Figure 15-18 • Lateral views of a mild to moderately swollen tarsus **(A)** and severely swollen carpus **(B)** in a foal with infectious arthritis.



Figure 15-19 • Lateral view of a badly infected hock in a neonatal foal.

to limited weight bearing and secondary volume loss rather than cartilage destruction, although that may come later.

In individual horses that are closely and regularly observed, new wounds are usually detected promptly so that the duration of any subsequent infection can be accurately estimated. Not so, however, with large groups of horses, in whom frequent individual inspection is not usually feasible, often making an accurate estimate of infection time impossible.

Septic Arthritis: An Instructive Case Example

Perhaps the best way to begin a radiographic description of infectious joint disease is with an example. In the described animal, the initial injury was a wire-cut to the proximal metatarsus, which later became infected and required surgery. During the course of the operation, the nearby tarsometatarsal joint was inadvertently punctured, presumably allowing bacteria to colonize the cartilage space and later many of the individual tarsal bones.

Over the span of the following 15 months, the infected joint was treated medically and periodically radiographed. Because of the many regular examinations, beginning with initial diagnosis and concluding with cure, this case affords a marvelous opportunity to see and appreciate the *full radiographic spectrum* of septic arthritis (Figures 15-22 through 15-24).

This case is also informative at another level. Because horses, particularly injured ones, frequently change hands, histories related to current lameness are often vague or lacking altogether. Presented with a lame horse and no significant past medical or surgical history, one is often faced with the daunting task of reconstructing probable past events from current radiographs.

Fortunately bones, through radiographs, can inform us, provided we "speak the language." By appreciating the varied appearance of this animal's infected tarsus, from the time of the initial wound to the point where it loosely resembles bone spavin, it becomes possible to backtrack diagnostically and to make an informed guess as to the inciting cause. Obviously case material such as this also improves one's ability to

Text continued on p. 274.

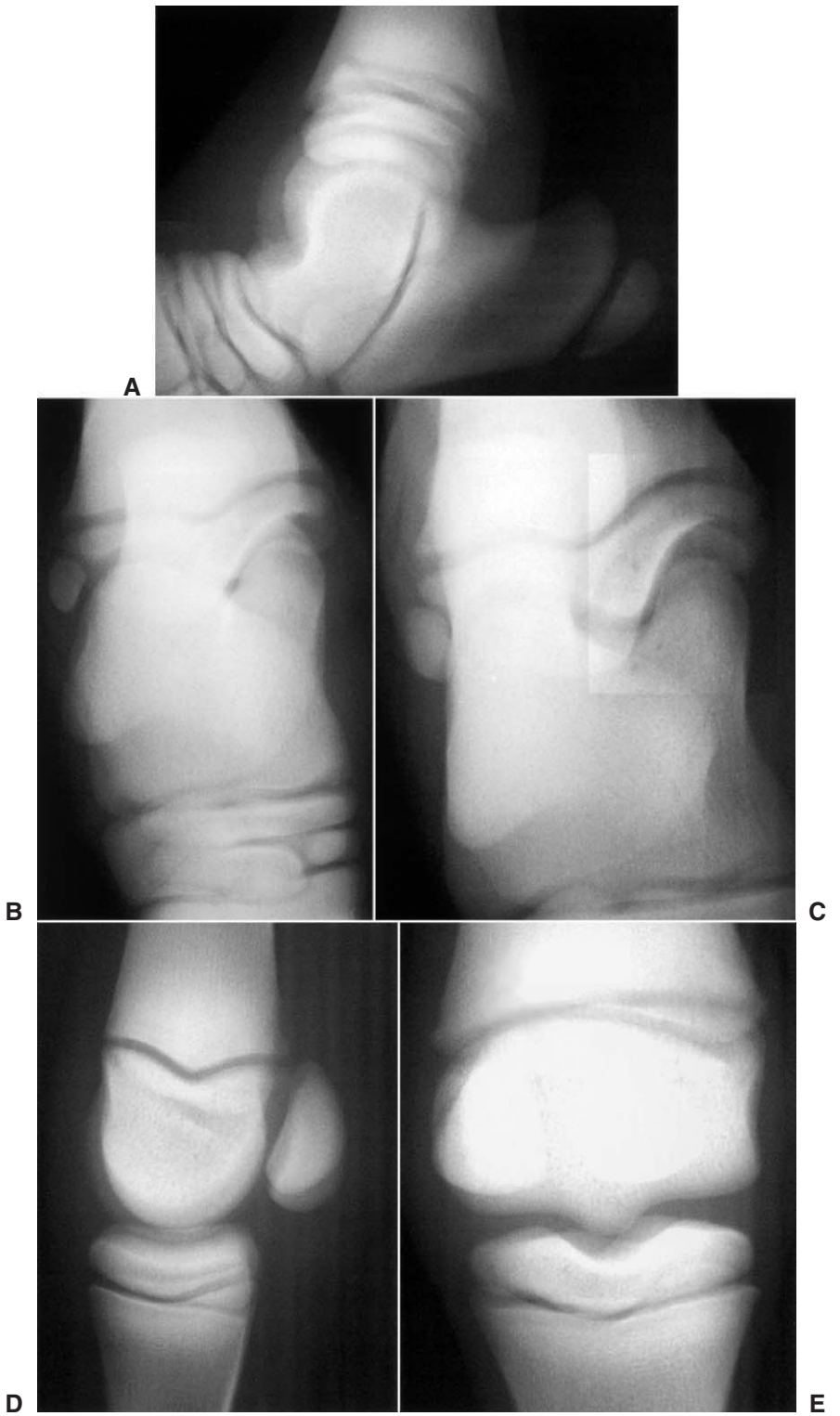


Figure 15-20 • Lateral **(A),** plantarodorsal **(B),** and close-up plantarodorsal **(C)** views of an infected hock in a week-old Quarter Horse filly show characteristic tarsocrural swelling and numerous small areas of bone loss in the distal tibial epiphysis and proximal talus. Lateral **(D)** and close-up dorsopalmar **(E)** views of an infected front fetlock in the same foal show moderate joint swelling and increased epiphyseal porosity.

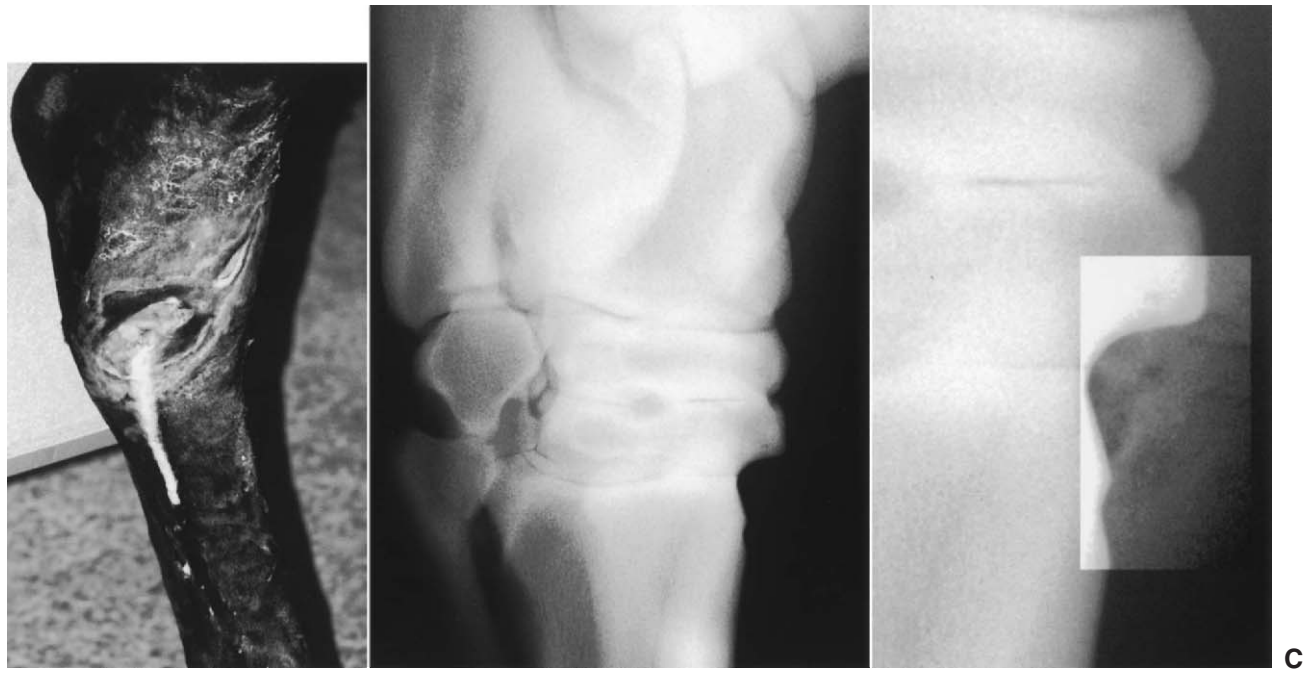


Figure 15-21 • Ten-day-old draining tarsometatarsal wound **(A)** in a young horse: Medial oblique **(B)** and close-up medial oblique **(C)** views show an unusually sharp tarsometatarsal bone surface, the result of enhanced contrast afforded by a contiguous gas pocket *(emphasis zone)*.



Figure 15-22 • Septic arthritis, preoperative assessment: Medial oblique **(A)** and plantarodorsal **(B)** views of a badly infected hock in a young horse show chronic-appearing new bone deposition on the dorsomedial surfaces of the metatarsus reaching the level of the tarsometatarsal joint, and severe swelling that extends beyond the tarsocrural joint proximally. At the time of this examination the horse was moderately lame.

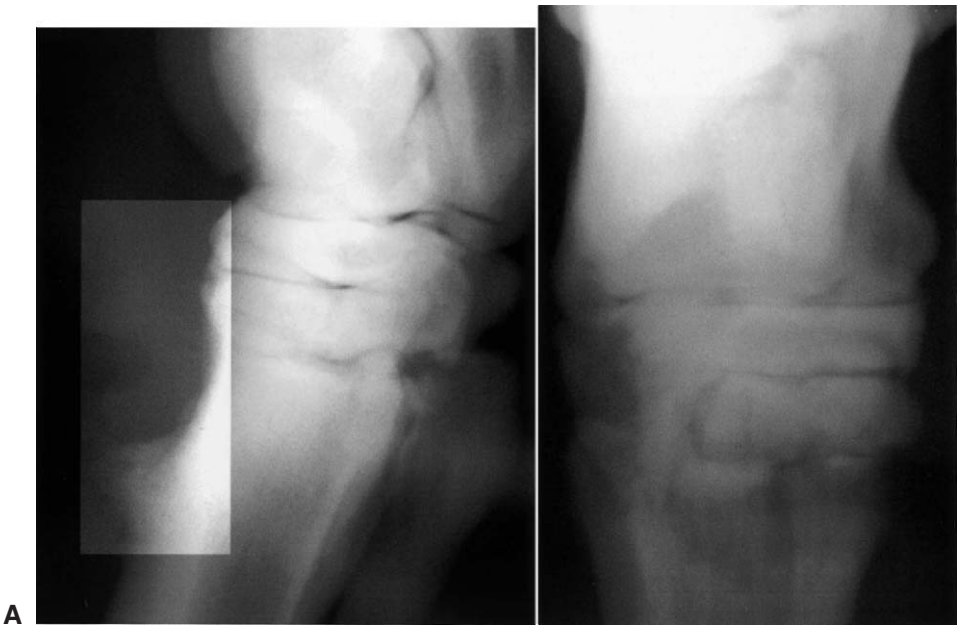


Figure 15-23 • Septic arthritis, immediate postoperative assessment: Medial oblique **(A)** and plantarodorsal **(B)** views show that most of the new bone seen in the preoperative study has been removed.

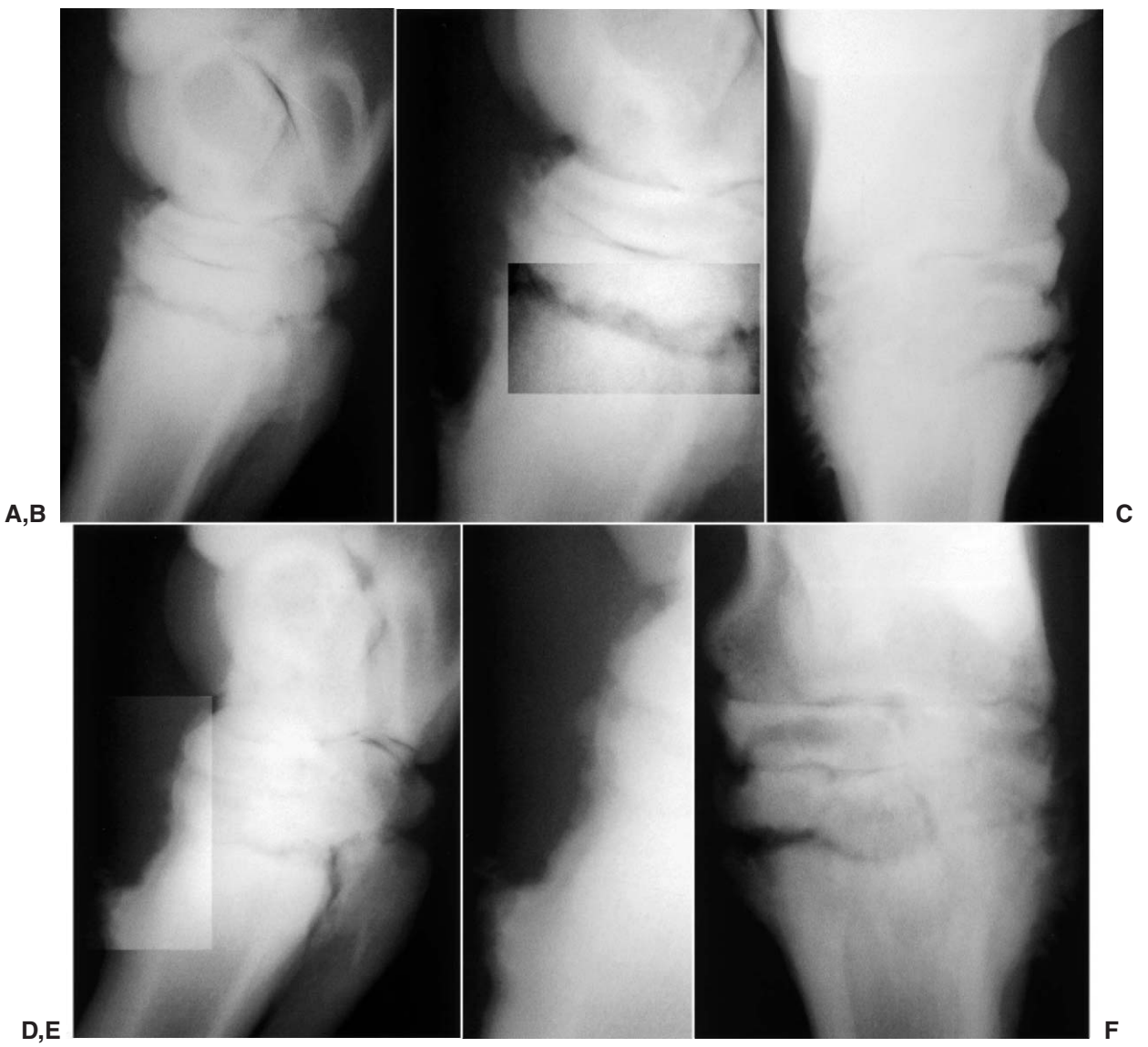


Figure 15-24 • Septic arthritis, progress examinations. *One-month progress examination:* lateral **(A),** close-up lateral **(B),** and plantarodorsal **(C)** views of the tarsus show that the infection has spread extensively, evidenced by new bone over much of the dorsal surface of the tarsus and extensive subchondral destruction of the tarsometatarsal joint. *Two-month progress examination:* close-up medial oblique **(D),** ultra-close-up medial oblique **(E),** and plantarodorsal **(F)** views show further destruction of the tarsometatarsal joint, especially medially, a suggestion that the infection has spread to the distal intertarsal joint, and consolidation of the new bone on the dorsum of the metacarpus.

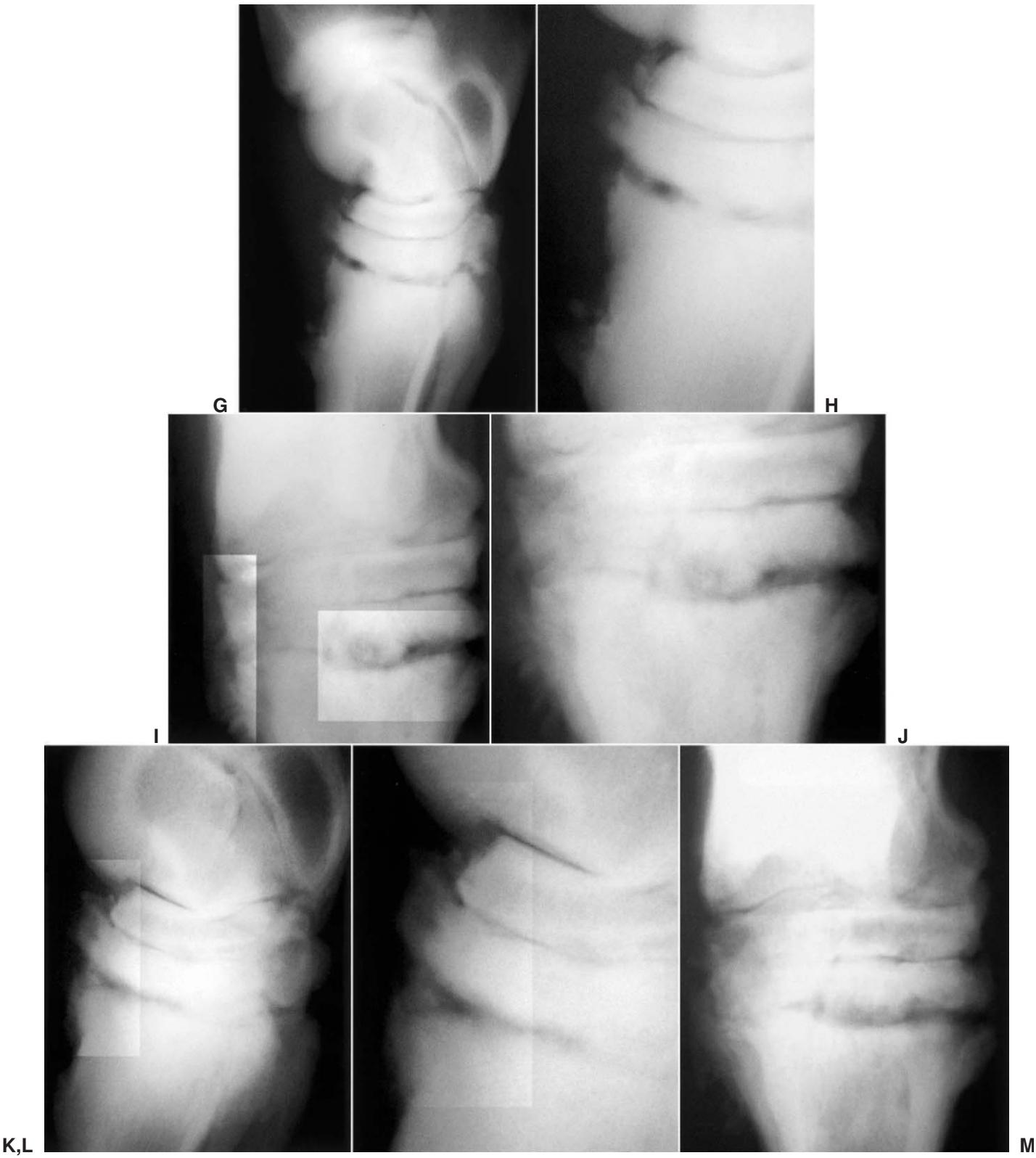


Figure 15-24, cont'd • *Three-month progress examination:* Lateral **(G),** ultra-close-up lateral **(H),** plantarodorsal **(I),** and ultra-close-up plantarodorsal **(J)** views show continued disintegration of the tarsometatarsal joint, which is now accompanied by clear-cut intertarsal destruction. Note the substantial shelves of new bone extending outward from the dorsal surfaces of the central and third tarsal bones and the sunburst bone deposit on the lateral splint head. *Four-month progress examination:* Close-up lateral **(K),** ultra-close-up lateral **(L),** and close-up plantarodorsal **(M)** views show an almost imperceptible smoothing in both the productive and destructive changes occurring in the hock, an indication that the animal may be starting to recover.

Continued.

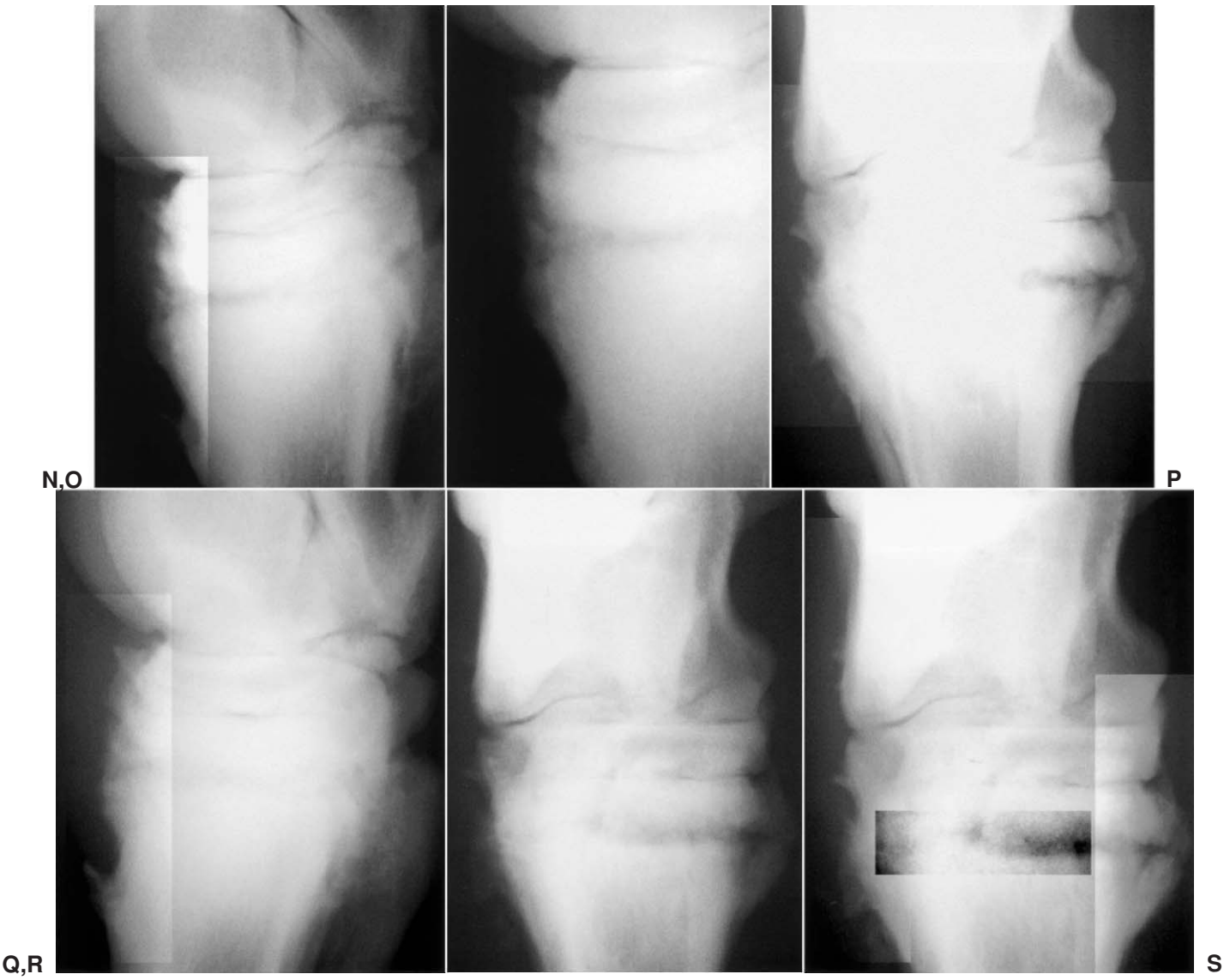


Figure 15-24, cont'd • *Five-month progress examination:* Close-up lateral **(N),** ultra-close-up lateral **(O),** and close-up plantarodorsal **(P)** views continue to leave a visual impression of smoothing, in part an illusion created by joint collapse and the continued deposition of peripheral new bone. *Six-month progress examination:* The process of bony solidification appears to continue as seen in lateral close-up **(Q)** and plantarodorsal **(R)** views; however, a penetrated plantarodorsal **(S)** projection shows clearly that this is not the case, with neither interior or exterior fusion *(emphasis zone).*

predict the future behavior of an infected hock under similar circumstances.

▮▮▮ SUSTENTACULAR AND CALCANEAL INFECTIONS

Infections of the Sustentaculum Tali

The sustentaculum tali, or more simply, the sustentaculum, is a large, blocky outcropping situated on the lower medial side of the calcaneus. Functionally, the sustentaculum serves as a leverage point for the *deep digital flexor tendon* (also referred to as the lateral digital flexor tendon).

Sustentacular infections may spread to the adjacent tendon sheath surrounding the deep digital flexor tendon, causing a secondary tenosynovitis (*tarsal sheath tenosynovitis*).*[1] In a small retrospective study involv-

*The sheath of the deep digital flexor tendon is a regional entity, typical of those found in association with many large tendons as they pass over intraarticular leverage points. The sheath is usually observed during sinography, extending from about a finger's length proximal to the tarsocrural joint to the upper third of the metatarsus. The cavity of the sheath varies with the volume of its content, but it may become wider than the tendon it contains in the case of serious infection.



Figure 15-24, cont'd • *Twelve-month progress examination:* Close-up lateral **(T)** and plantarodorsal **(U)** views shows near-complete solidification of the lower half of the tarsus, making identification of cartilage spaces nearly impossible, especially distally. Lateral **(V)** and plantarodorsal **(W)** views of the normal opposite tarsus are provided for comparison. *Case conclusion:* When examined last, the horse was only mildly lame, usually after prolonged exercise.

ing 10 horses with sustentacular infections, Hand and co-workers found that the presence of a secondary tenosynovitis had little influence on outcome (compared with osteomyelitis alone), provided the infected bone was debrided and the tarsal sheath lavaged.[33]

Although sustentacular infection can be appreciated in the lateral oblique projection, the skyline view often proves to be the most revealing (Figure 15-25). Change in the appearance of the sustentacular glide path (the surface over which the deep digital flexor tendon passes) generally requires a month or longer to develop because of the protective nature of its cartilaginous covering. The surrounding periosteal surfaces are more responsive, however, and should begin to show new bone deposition a week or two after being stimulated, depending on the severity of the infection.

Calcaneal Infection

Like the sustentaculum, calcaneal infections often require a skyline projection to appreciate fully, especially the extent of the lesion.[34] The same can be said of infective sequestra.[35] Such information can be of great importance because it may indicate a need to surgically explore the calcaneal bursa and insertions of the superficial digital flexor and gastrocnemius muscles.

Other calcaneal infections are diagnostically more straightforward, being visible in most standard projections, with the exception of the plantarodorsal view,

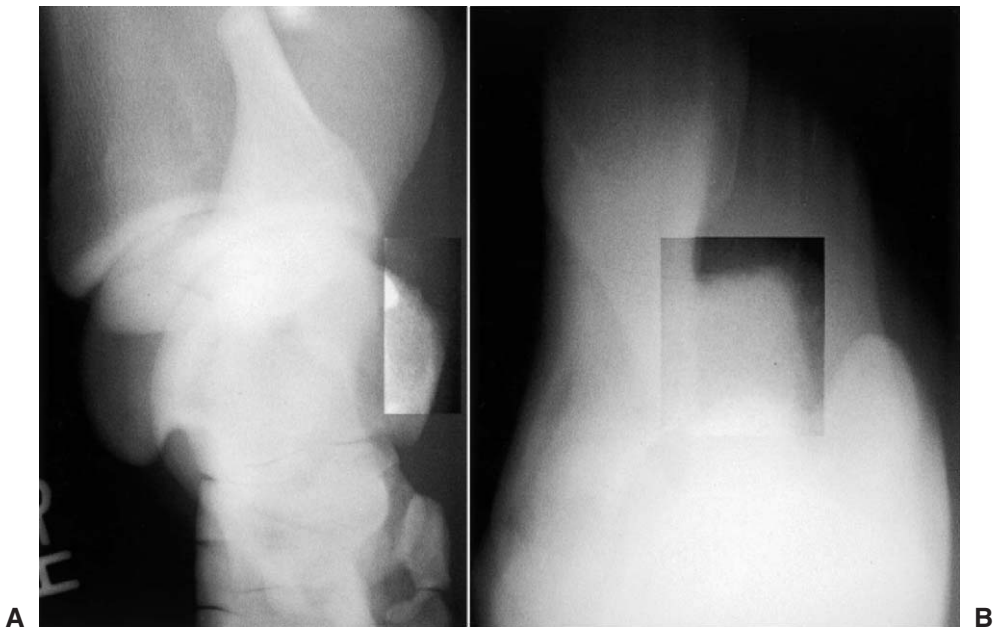


Figure 15-25 • Lateral oblique **(A)** and skyline **(B)** projections of a chronic talar infection show a fringe of new bone along the visible margins of the sustentaculum tali *(emphasis zones).*

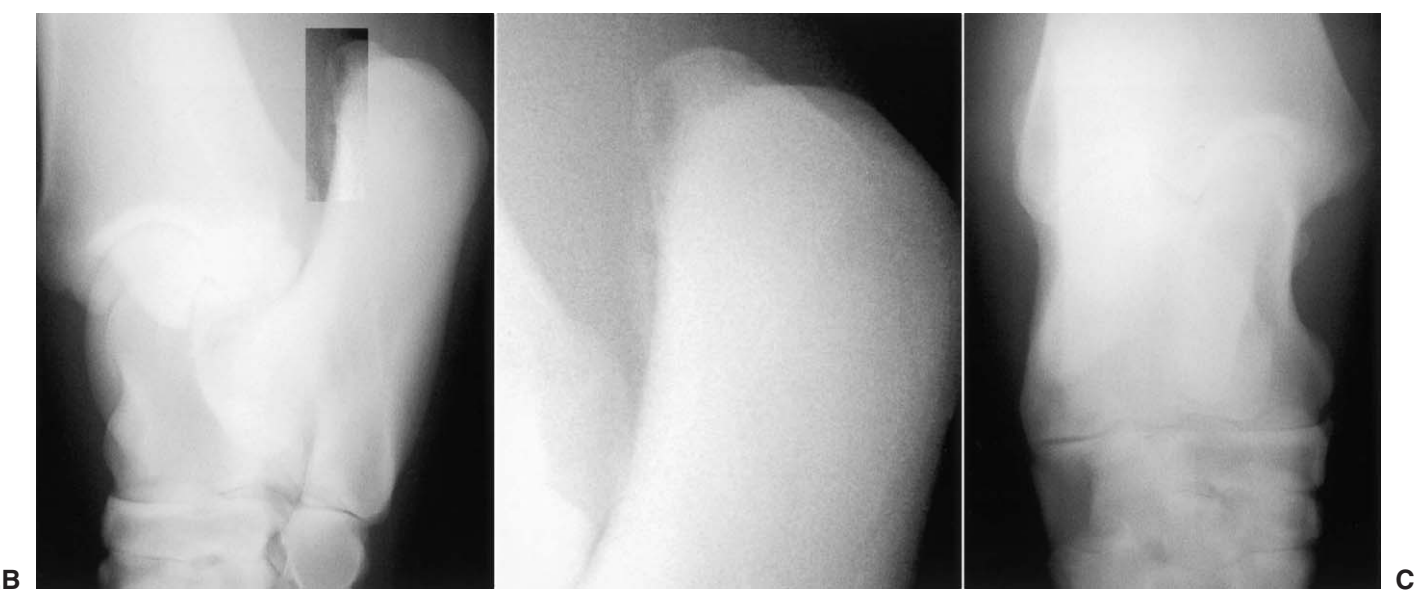


Figure 15-26 • Medial oblique **(A)** and close-up medial oblique **(B)** views of the calcaneal apex show focal bone loss and a small infective sequestrum *(emphasis zone),* the result of a puncture wound received a month earlier. The plantarodorsal view fails to reveal the lesion that resulted from tibial superimposition **(C).**

in which distal tibial superimposition is a consistent problem (Figure 15-26). Blood-borne infection often first appears as a localized density loss on the metaphyseal side of the proximal calcaneal growth plate, which resembles posttraumatic osteoporosis (Figure 15-27).

Wounds to the cap of the hock should be watched closely, especially if they result in one or more deeply situated gas pockets, which indicate atmospheric contamination and potential osteomyelitis. In such instances, I prefer to reradiograph the horse in 2 weeks unless its condition worsens noticeably, in which case I may examine the animal sooner (Figure 15-28).

Calcaneal Sequestra

The absence of a blood supply nearly always guarantees that a sequestrum will be treated as a foreign body, and thus every attempt will be made to isolate it. Such isolation initially takes the form of a fluid bath with a



Figure 15-27 • Medial oblique **(A)** and close-up medial oblique **(B)** views of the proximal calcaneal metaphysis show localized density loss *(emphasis zone),* consistent with a bacteremic osteomyelitis.

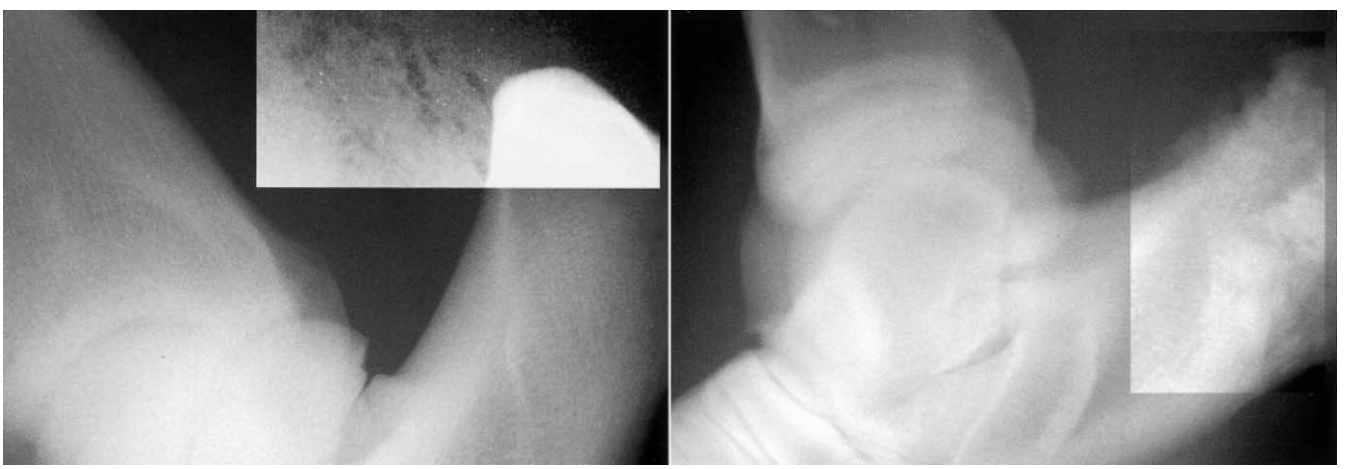


Figure 15-28 • **A,** One week after a deep wound, numerous small gas pockets are seen near the apex of the calcaneus in a close-up lateral view. **B,** Three weeks later, a similar projection shows a cuff of new bone on the surface of the calcaneus signaling the development of osteomyelitis.

soft-tissue retainer and later progresses to a bony trough or full-fledged vault, termed an *involucrum.* At either stage in its development, soft or hard tissue, a sequestrum may be expelled through a pressure-induced opening in the nearby skin, termed a *sinus.* In the case of an infected sequestrum, sinus drainage may or may not persist once the dead bone fragment has been expelled. Sinus drainage often subsides once non-infected sequestra are removed or spontaneously eliminated.

Because calcaneal sequestra remain close to their surface of origin, they can be difficult to differentiate from localized new bone deposits, and accordingly may require customized oblique projections to identify. Once again, skyline projections are especially useful in this regard (Figure 15-29).

Surgical Infection

Long and co-workers reported the use of radioisotope-labeled leukocytes to identify a variety of bone or joint infections in 10 horses, including one with septic arthritis-osteomyelitis of the hock after attempted arthrodesis.[36] With respect to nuclear medicine studies of the equine hock, Eksell and co-workers showed that with digital filtration the quality of a scan could be



Figure 15-29 • Ultra-close-up skyline projection of the proximal calcaneus shows a small infective sequestrum barely detached from the medial surface of the metaphysis, the result of a puncture wound sustained 3 weeks earlier.



Figure 15-30 • Lateral oblique sinogram shows partial filling of an irregularly swollen tendon sheath indicative of septic tenosynovitis.

improved by as much as 200 percent.[37] In my experience the highest incidence of diffuse tarsal infection is associated with the attempted surgical fusion of spavin horses, followed by the drilling or injecting of the distal intertarsal and tarsometatarsal joints for the same purpose.

▮▮▮ SINOGRAPHY AND PROBE-BASED MARKING STUDIES

Sinography

Technical Considerations. I first published a comprehensive guide to equine sinography in the 1986 American Association of Equine Practitioners (AAEP) Proceedings.[38] In this communication, I made the following recommendations, which, if followed, will predictably produce a diagnostic study:

1. Always make survey films first to ensure good film quality and to use as a comparison in instances of sinographic uncertainty.
2. Use a Foley catheter where possible to prevent leakage of contrast solution and associated surface artifacts.
3. Always try to make at least two views at right angles to one another.
4. Do not be hesitant to make custom radiographic projections to see some part of the affected tissue more clearly.
5. Always make a pair of images at least 5 minutes after the initial injection to see whether the contrast pattern has changed (it often does) to estimate lesion vascularity (the more rapid the contrast dilution, the more vascular the surrounding tissue).
6. *Always leave the catheter system in place and the cuff inflated until the examination is complete.*

Diagnostic Capabilities. A correctly performed sinogram is potentially capable of showing the following lesion features:

1. Origin of drainage
2. Bone or implant contact, which implies infection
3. Undermining of a bone fragment indicating sequestration
4. Joint entry implying septic arthritis
5. Tendon sheath entry implying septic tenosynovitis
6. Size and number of tissue channels
7. Size and number of tissue cavities
8. Size, number, and location of intercavitary or interchannel communications
9. Presence of one or more intracavitary or intrachannel filling defects (often geometrically shaped), implying a foreign object, such as a piece of wood
10. Qualitative measure of lesion vascularity based on the rapidity with which the contrast solution is diluted

Three examples of tarsal sinography are provided Figures 15-30 through 15-32. Bear in mind while

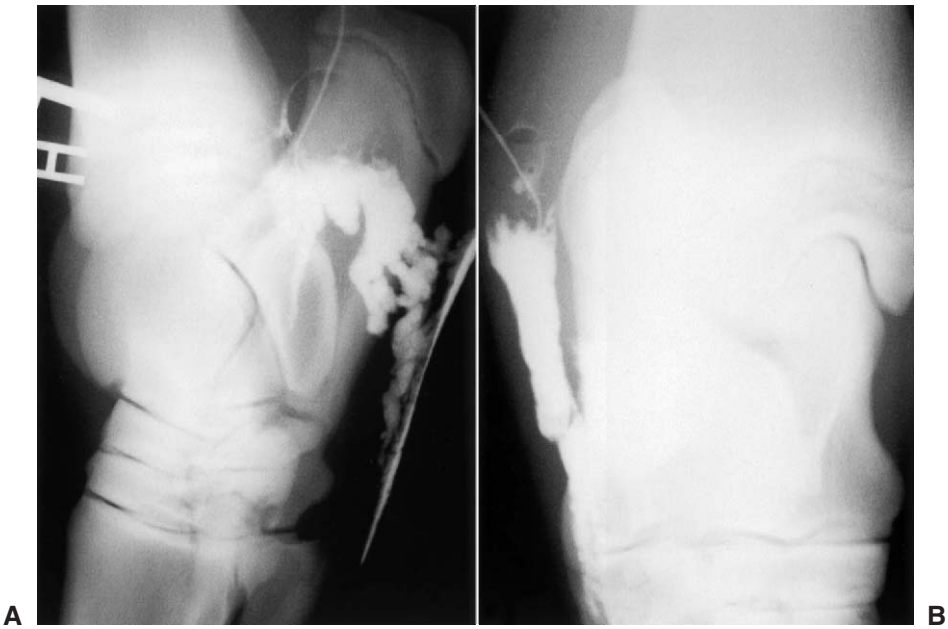


Figure 15-31 • Lateral **(A)** and plantarodorsal **(B)** sinograms show a complex network of irregularly shaped, roughly cylindrical communicating cavities extending from the central calcaneal body to the distal intertarsal joint. Fortunately, most of the cavitation lies in the soft tissue lateral and outside the tarsus proper, a determination that can be made only with orthogonal views. The caudally situated stripe is contrast solution on the skin surface.

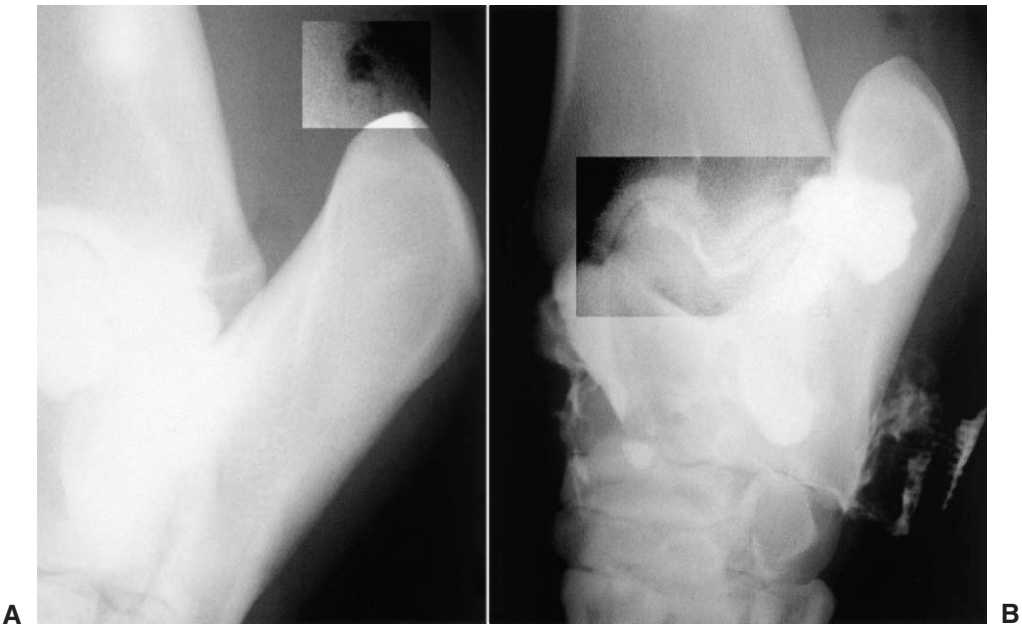


Figure 15-32 • **A,** Medial oblique survey film in a non–weight-bearing horse shows a pair of gas pockets, one of which is situated just above the calcaneus *(emphasis zone)*. **B,** A medial oblique sinogram shows contrast solution in the tarsocrural and proximal intertarsal joints and effacing many of the talocalcaneal surfaces, consistent with septic arthritis-osteomyelitis.

perusing this material that each case is unique and thus is best dealt with on a *patient-tailored basis* (a patient-tailored study is one in which the timing and projection angle of each sinogram are based on what is seen in its immediate predecessor). For example, if one of two views showed possible joint entry, that projection would be repeated immediately to see whether the finding persisted, became more pronounced, or disappeared. This is as opposed to a rigid, protocol-based study, in which films are made at prescribed projection angles and at specified times following contrast administration.

Marking Study (Probe-Based)

A probe-based marking study is used to establish the extent to which a metallic probe can be advanced into a draining sinus (Figure 15-33). It uses no contrast solution and usually provides far less diagnostic information than a sinogram. However, it is comparatively



Figure 15-33 • A, Plantarodorsal view of a horse with a fresh cut on the dorsal surface its distal tarsus appears radiographically normal. **B,** A close-up lateral probe-based marking study is ambiguous because it fails to establish whether the probe is in contact with the bone surface or merely is superimposed on the underlying bone. No other views were made. Exploratory surgery revealed an extraarticular wound.

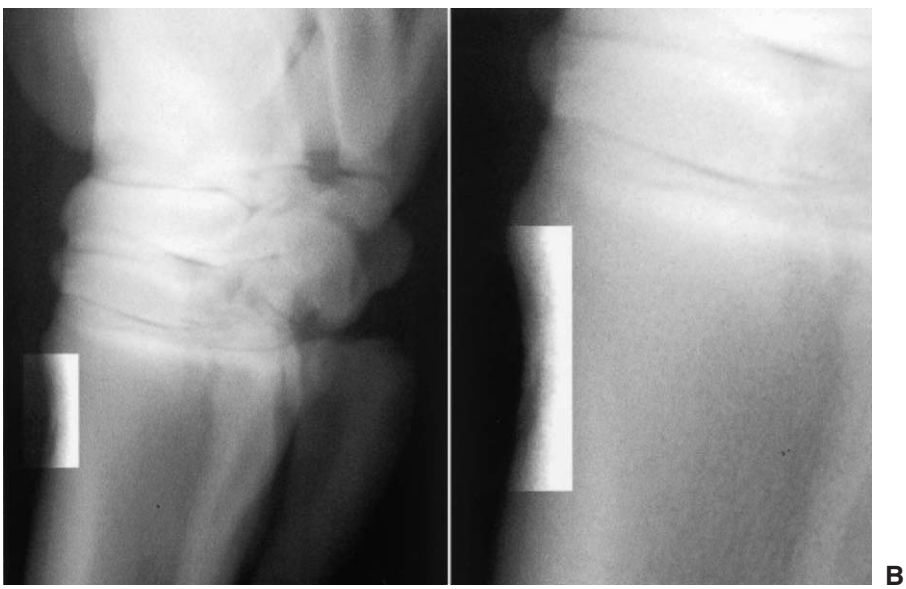


Figure 15-34 • Medial oblique **(A)** and close-up medial oblique **(B)** views of the tarsus show a sliverlike sequestrum just below the dorsal prominence of the third metatarsal bone *(emphasis zone).*

fast, generally less painful than sinography, and requires far less diagnostic skill.

▮▮▮ SEQUESTRATION

Sequestra involving the tarsus proper are rare. However, sequestra that develop on the proximal face of the metatarsal are common and usually produce some degree of accompanying tarsal lameness (Figures 15-34 and 15-35). As with all sequestra, bone death is caused by a devascularizing injury or thrombosis secondary to infection.

▮▮▮ SPAVIN (BONE SPAVIN)

Spavin is a unique form of osteoarthritis seen only in the tarsus of the horse. Typically it first affects the medial aspect of the distal intertarsal joint and then the

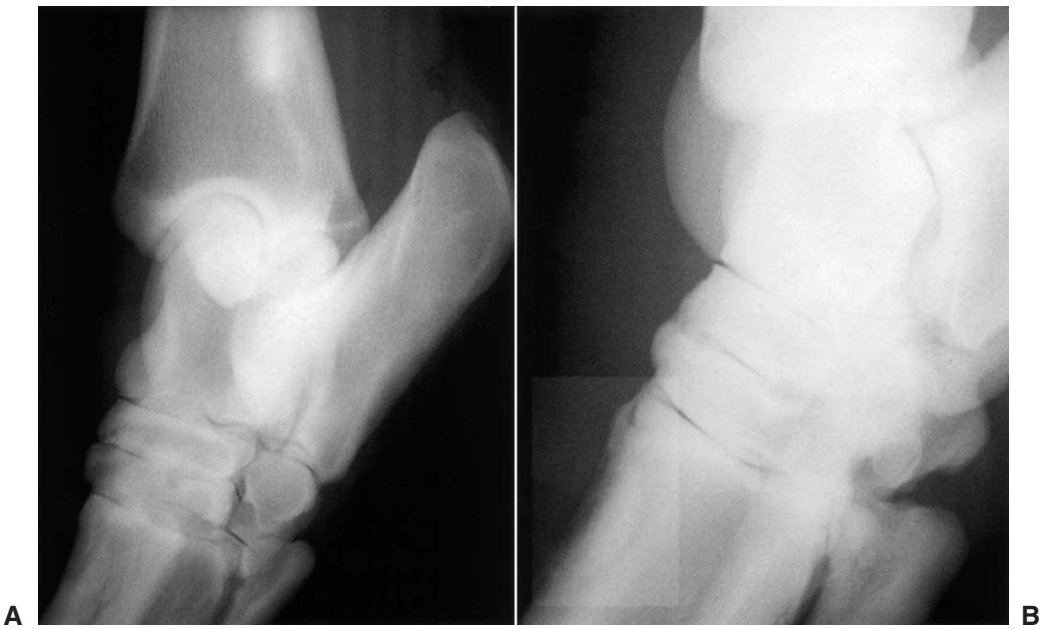


Figure 15-35 • Standard medial oblique **(A)** and customized medial oblique **(B)** views of a pair of partially superimposed sequestra just below the dorsal prominence of the third metatarsal bone.

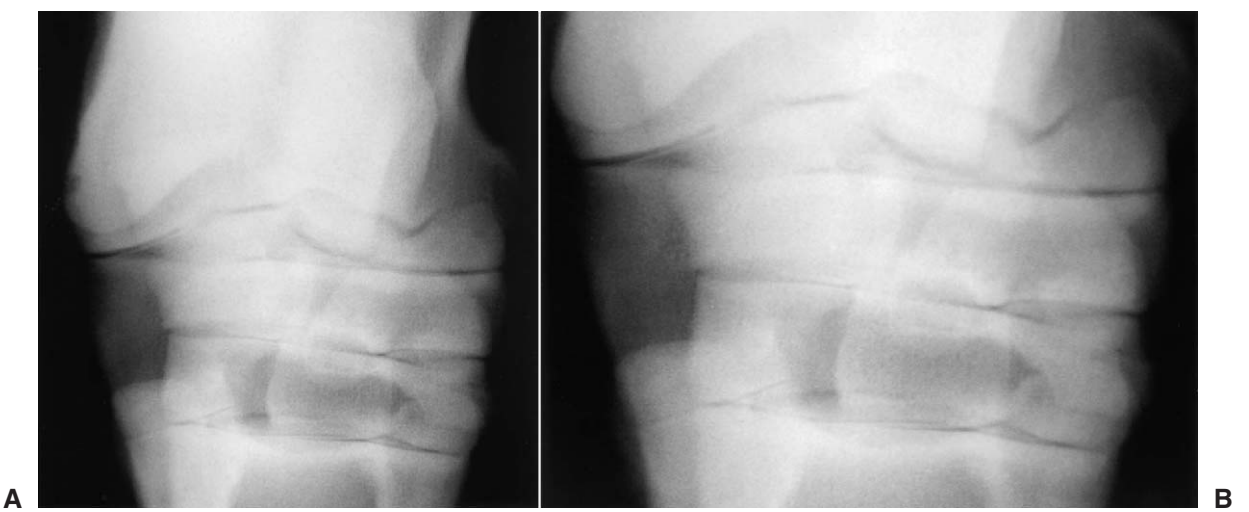


Figure 15-36 • Normal tarsal joints, variant 1: Plantarodorsal **(A)** and plantarodorsal close-up **(B)** views of a normal tarsus show variability in the widths of the distal intertarsal and tarsometatarsal cartilage spaces.

medial aspect of the tarsometatarsal joint, usually bilaterally. In its most severe form, the disease causes extensive cartilage damage and cavitation of subchondral bone. The cause (or causes) of bone spavin is not known.

Hartung and co-workers showed that bilateral bone spavin could occur in young, untrained, but clinically sound trotters. Such a finding casts doubt on the hypothesis that bone spavin is primarily a training or race-related disorder.[39]

The Where and What Principle

Most radiographic diagnoses are made using what I term the *Where and What Principle* (a radiographic diagnosis is fundamentally based on knowing where to look and what to look for). In bone spavin, for example, the *where* is the medial aspect of the distal intertarsal and tarsometatarsal joints, and the *what* is subchondral cavitation with periarticular bone deposition.

When examining the distal intertarsal and tarsometatarsal joints, bear in mind that, because of their multiplanar nature, it is impossible to visualize clearly the entire cartilage space of either joint. Thus portions of each will appear normal, narrow, or wide, depending on the beam angle and limb position (Figures 15-36 and 15-38). These normal radiographic variations constitute a serious potential pitfall for the diagnostically unwary.

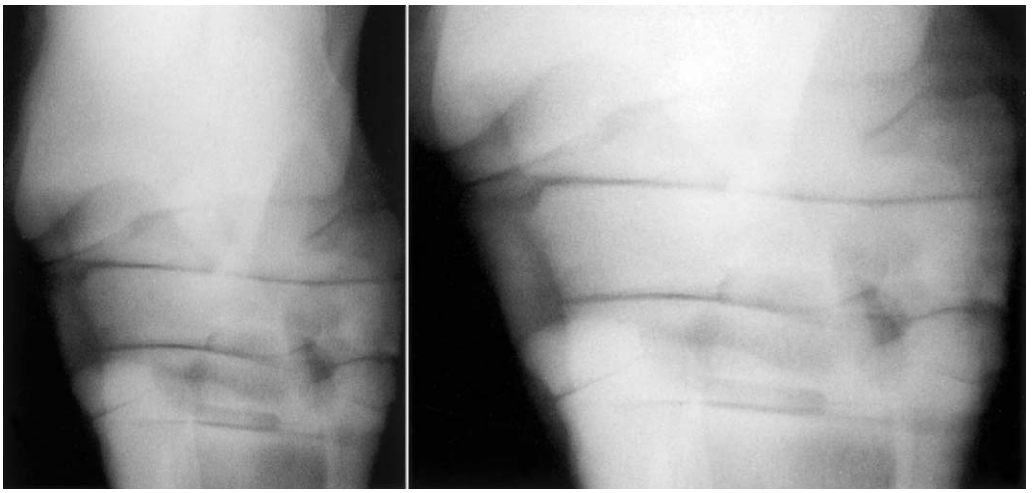


Figure 15-37 • Normal tarsal joints, variant 2: Plantarodorsal **(A)** and close-up plantarodorsal **(B)** views of a normal tarsus show variability in the widths of the distal intertarsal and tarsometatarsal cartilage spaces.

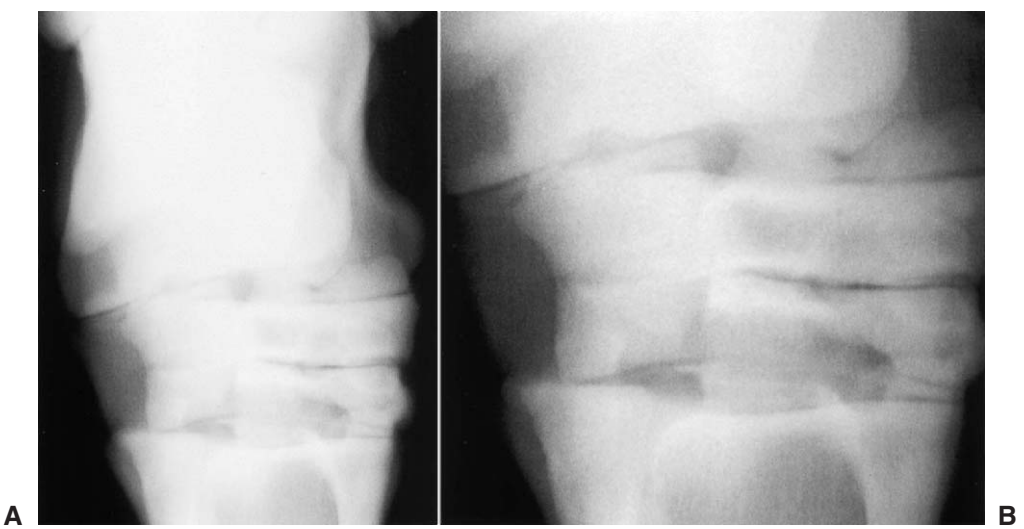


Figure 15-38 • Normal tarsal joints, variant 3: Plantarodorsal **(A)** and close-up plantarodorsal **(B)** views of a normal tarsus show variability in the widths of the distal intertarsal and tarsometatarsal cartilage spaces.

Typical Bone Spavin

The term *bone spavin* can be used in two ways: (1) to indicate a specific form of osteoarthritis unique to the equine tarsus or (2) as a synonym for an arthritic hock in a horse. Used in the former context (my preference), the advanced form of spavin is characterized by subchondral cavitation of the medial aspect of the distal intertarsal joint and subsequently by a similar disintegration in the corresponding part of the tarsometatarsal joint.

The plantarodorsal and medial oblique views best show the highly characteristic distal intertarsal and tarsometatarsal joint lesions (Figure 15-39). Because the disease is usually bilateral, it is advisable to screen the opposite tarsus once the disease is discovered.

Atypical Bone Spavin

A second form of bone spavin (or spavin-like disease) exists in which only the proximal intertarsal joint is involved. Like the typical form of bone spavin, the atypical form of the disease results in extensive subchondral cavitation (Figures 15-40 and 15-41) but, unlike typical bone spavin, usually involves only a single limb.

Radiographic Progression and the Myth of Fusion

I have both heard and read that given time (generally not specified), the intertarsal and tarsometatarsal joints of a horse with spavin will eventually fuse. Based on

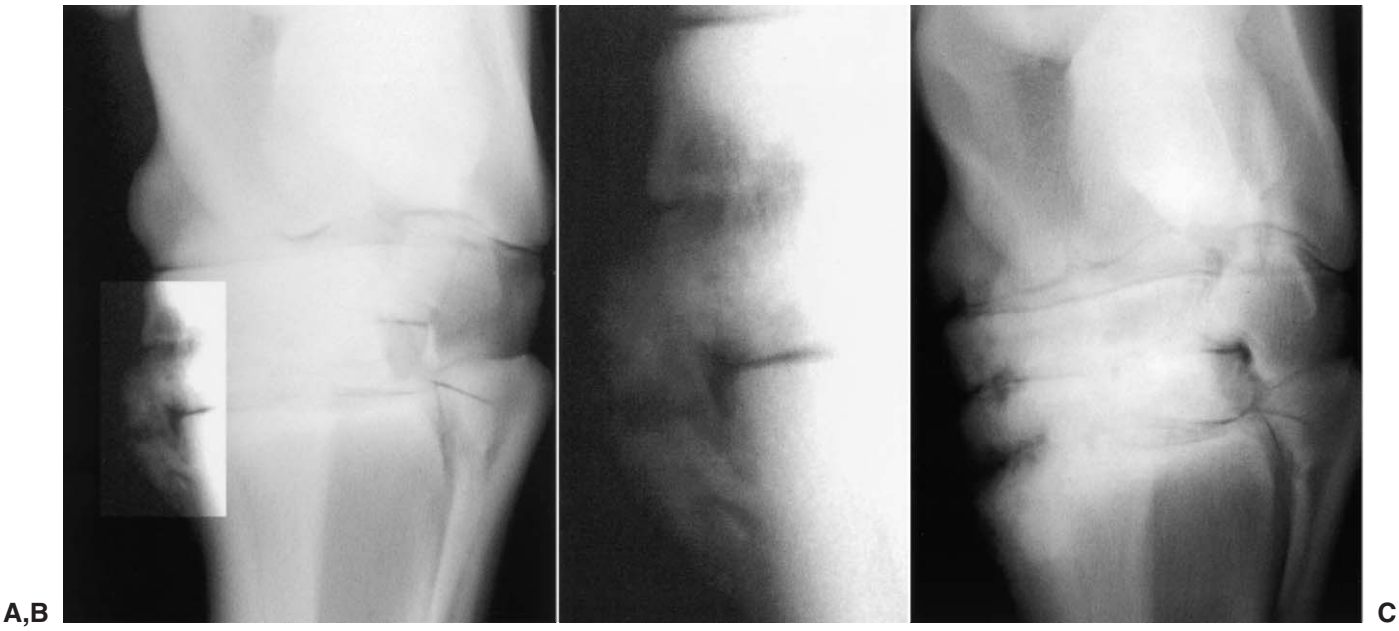


Figure 15-39 • Plantarodorsal **(A),** close-up plantarodorsal **(B),** and medial oblique **(C)** views of a horse with bone spavin show the highly characteristic subchondral cavitation and new bone deposition typically present in the distal intertarsal and tarsometatarsal joints medially.



Figure 15-40 • Plantarodorsal **(A),** close-up plantarodorsal **(B),** lateral **(C),** and close-up lateral **(D)** views of a horse with atypical bone spavin show extensive subchondral cavitation of the proximal intertarsal joint. The large hooklike osteophyte on the proximodorsal surface of the cannon bone is incidental.

numerous radiographic follow-ups and a small number of gross dissections, I can confidently state that solidification of the intertarsal and tarsometatarsal is quite rare, irrespective of disease duration.

I believe the *fusion myth* results from overreliance on the lateral projection, which often gives the impression that the entire dorsal surface of the distal tarsus is encased in new bone, an assessment that a medial oblique view will quickly (and convincingly) refute (Figure 15-42). Underpenetrated and off-angle views can convey a similar misimpression (Figure 15-43).



Figure 15-41 • Close-up medial oblique view of the tarsus of a horse with atypical bone spavin shows deep subchondral cavitation of the *proximal* intertarsal joint with comparatively minor changes in the nearby intertarsal joint.

Differentiating Posttraumatic Osteoarthritis from Bone Spavin

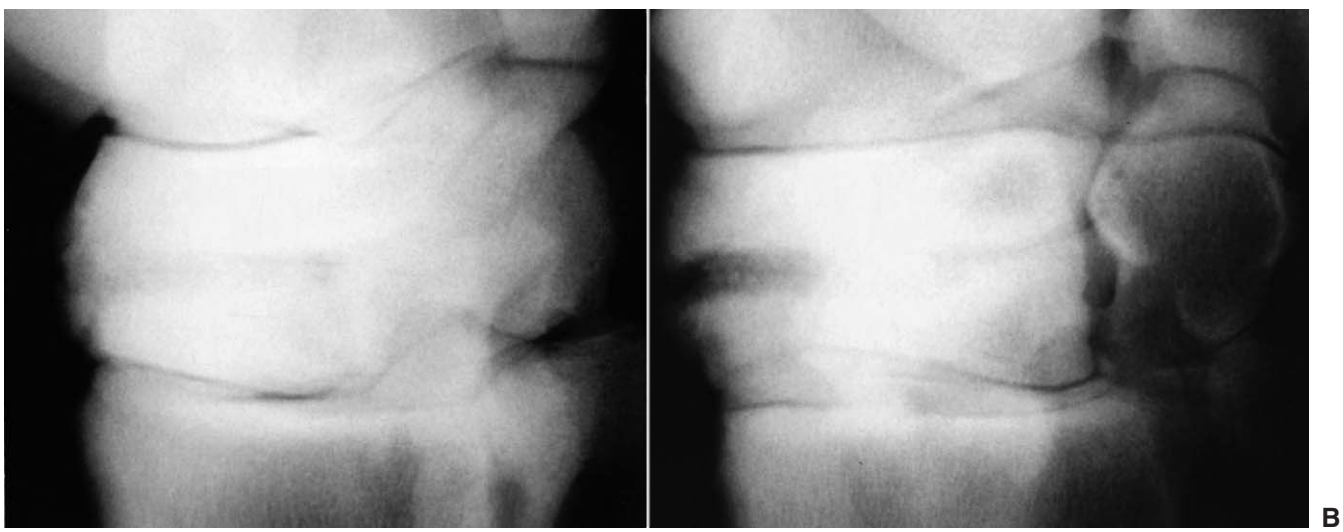
Posttraumatic osteoarthritis can usually be distinguished from bone spavin on the basis of one or more of the following characteristics: (1) no subchondral cavitation, (2) no predictable location, (3) presence of periarticular osteophytes, (4) unilateral involvement, and (5) history of previous injury (Figure 15-44).

However, there are two exceptions, both of which can lead to subchondral cavitation. The first is a displaced articular fracture in which synovial fluid comes into contact with freshly fractured bone, potentially leading to subchondral cavitation that results from encroachment of synovial fluid into the fracture gap. The second is the use of intraarticular steroids on fresh articular fractures, which may also cause subchondral cavitation, a phenomenon some term *steroid arthropathy*.

▮▮▮ TRANSTARSAL DRILLING (INTERTARSAL DRILLING)

Transtarsal drilling, a somewhat dubious therapeutic practice, is claimed to promote intertarsal fusion, decrease intertarsal movement, and eliminate or reduce pain and related lameness, especially in horses with bone spavin. I know of no published reports that unequivocally verify this contention.

Given the multidirectional nature of the intertarsal and tarsometatarsal joints, it is not possible to traverse a specific joint completely, even with the aid of fluo-



A **B**

Figure 15-42 • **A,** Close-up lateral view of a horse diagnosed with bone spavin 1 year previously shows what appears to be an ankylosed distal intertarsal joint. **B,** However, a medial oblique view reveals that the intertarsal joint remains unfused.

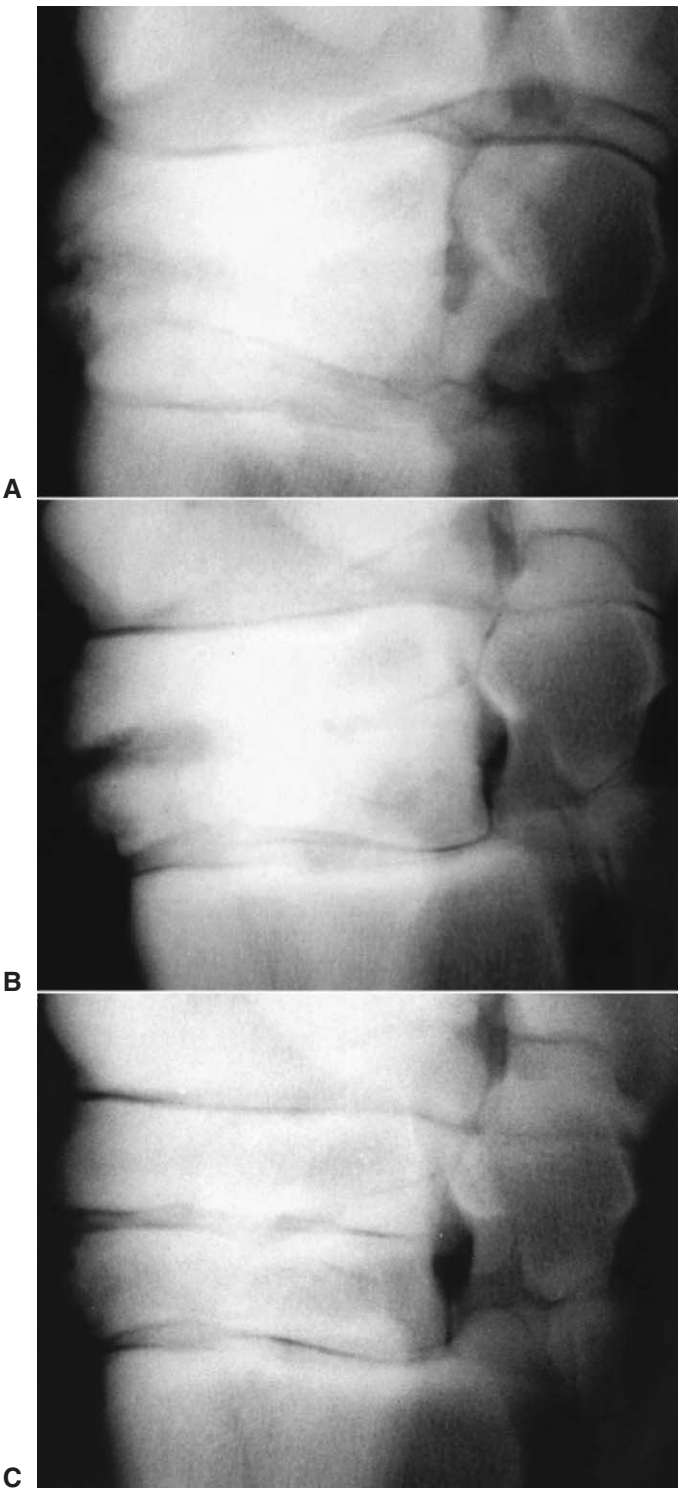


Figure 15-43 • A, Close-up, off-angle medial oblique view appears to show fusion of the distal intertarsal joint in a horse diagnosed with bone spavin 3 years previously. **B,** However, a properly angled medial oblique view refutes this conclusion. **C,** A normal medial oblique view is provided for comparison.

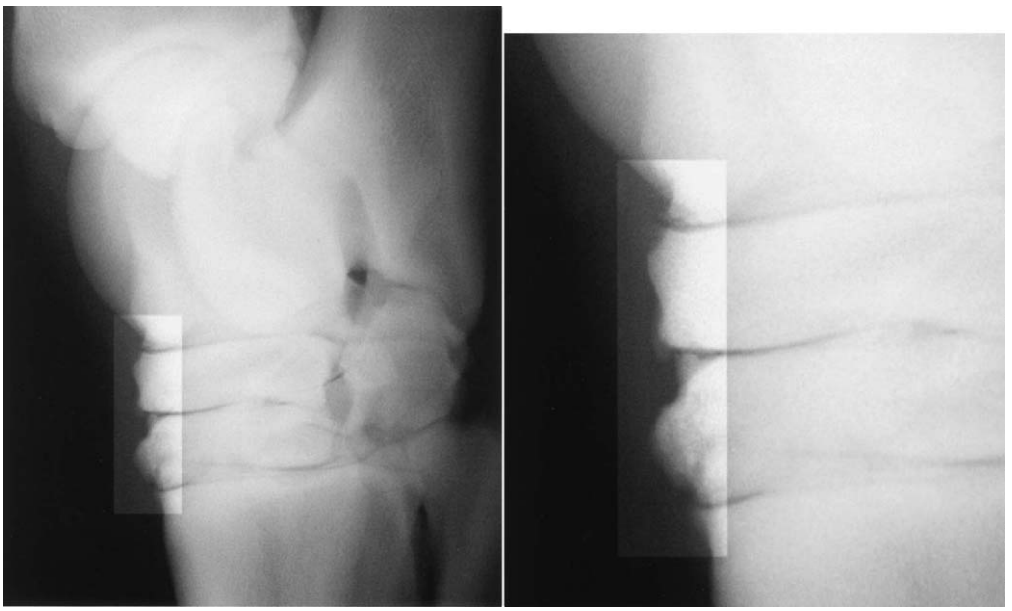


Figure 15-44 • Medial oblique **(A)** and close-up medial oblique **(B)** views of posttraumatic osteoarthritis in the tarsus of a horse injured 2 years previously show numerous bone spurs on the dorsal aspects of the proximal and distal intertarsal joints and tarsometatarsal joints *(emphasis zones)*.



Figure 15-45 • Close-up medial oblique view of a horse diagnosed with bone spavin shows a drill hole in the distal intertarsal joint and flanking central and third tarsal bones and second drill hole in the third tarsal bone just above (but not in) the tarsometatarsal joint.

roscopy. More often than not, it is the bone that is being drilled rather than the adjacent cartilage space.

Radiographically, a drilled tarsus is best characterized by multiple circular lucencies, the clarity of which depends on the angle of projection relative to the long axis of the drill hole (Figure 15-45). In my experience, most of the resultant bone defects disappear within a few weeks of being created. Speaking from very limited experience, most horses I have followed up radiographically for a year or longer after intertarsal drilling do not fuse or at best only partially fuse (Figure 15-46). In general, the greater the number of drill holes, the greater the degree of ankylosis.

Infection is usually characterized by enlargement and deformity of the drill holes, regional swelling, and increasingly severe lameness. Some infections loosely resemble bone spavin, but unlike spavin lesions, they are not typically situated on the medial aspects of the distal intertarsal and tarsometatarsal joints.

▮▮▮ OSTEOCHONDRITIS (OSTEOCHONDROSIS)

Lesions by Location

Distal Tibial Epiphysis. Duin and Hurtig described the radiographic appearance of distal epiphyseal bone cysts in the tibias of three horses.[40] The cysts appeared as circular or oval lucencies, best seen in the plantarodorsal and medial oblique projections. This has been my experience as well, with more than half the affected horses having similar or identical bilateral lesions.

Distal Intermediate Tibial Ridge (Sagittal Ridge). Detached sagittal ridge fragments are seen most clearly in the lateral oblique projection.[41] Most appear as compressed, oval-shaped objects just below the distal margin of the tibia, partially superimposed on the upper portions of the medial and lateral talar ridges (Figure 15-47). Fragmentation of the sagittal

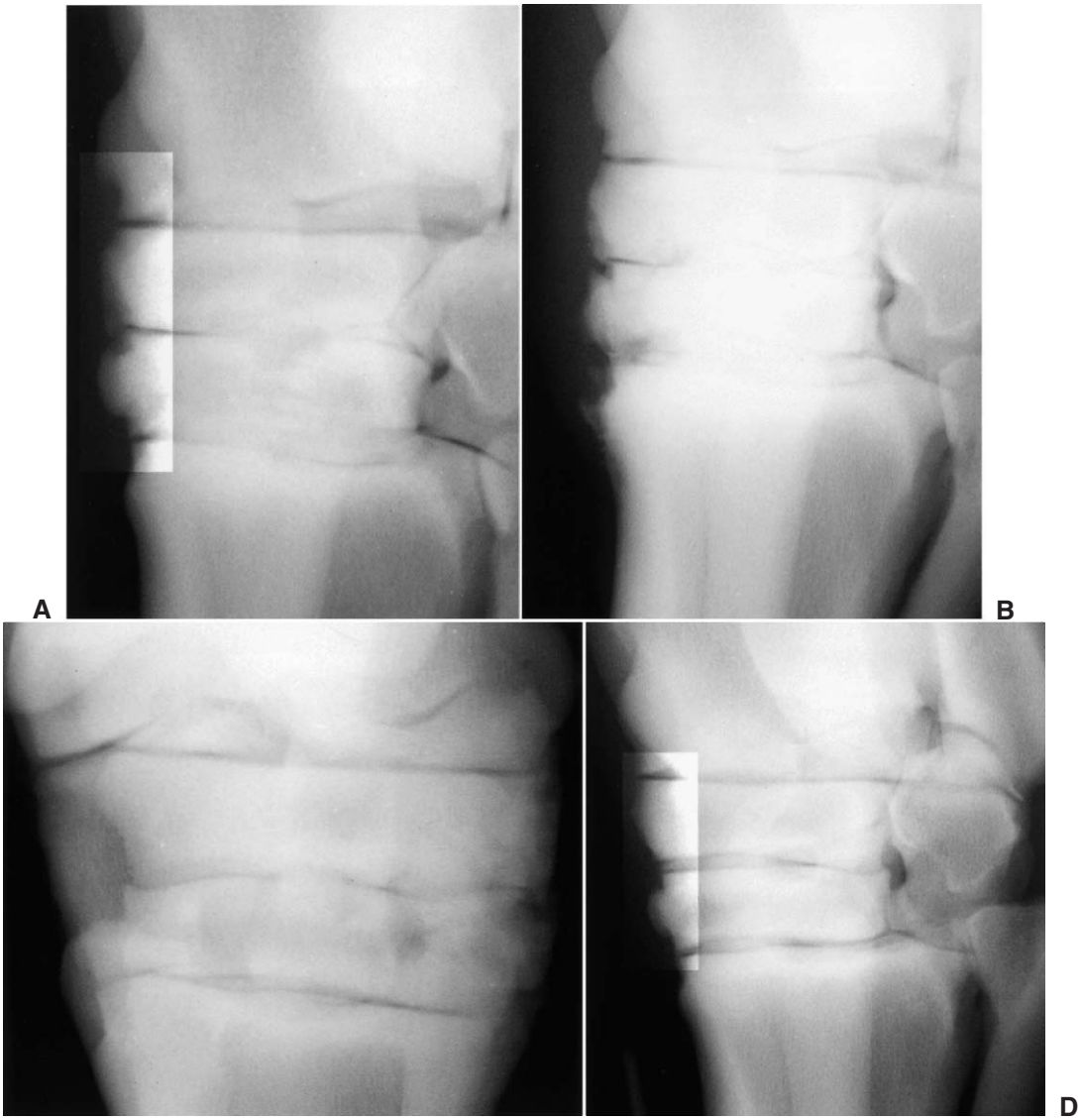


Figure 15-46 • Close-up medial oblique view of a horse with bone spavin immediately before being drilled to accelerate joint fusion **(A).** Three years later, close-up medial oblique **(B)** and plantarodorsal **(C)** views showed that fusion had not occurred, although the arthritis had worsened. A normal medial oblique view **(D)** is provided for comparison.

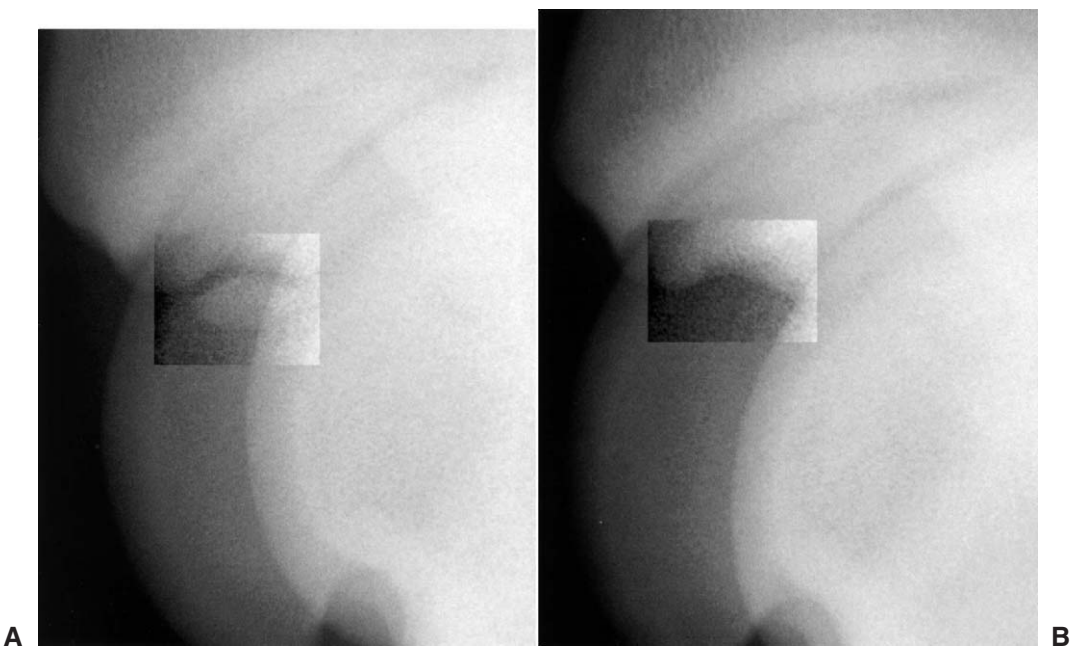


Figure 15-47 • **A,** Ultra-close-up lateral oblique view of the cranial aspect of the tarsocrural joint in a young horse shows a bone fragment detached from the sagittal ridge, the result of osteochondritis. **B,** A telltale articular defect remains postoperatively.

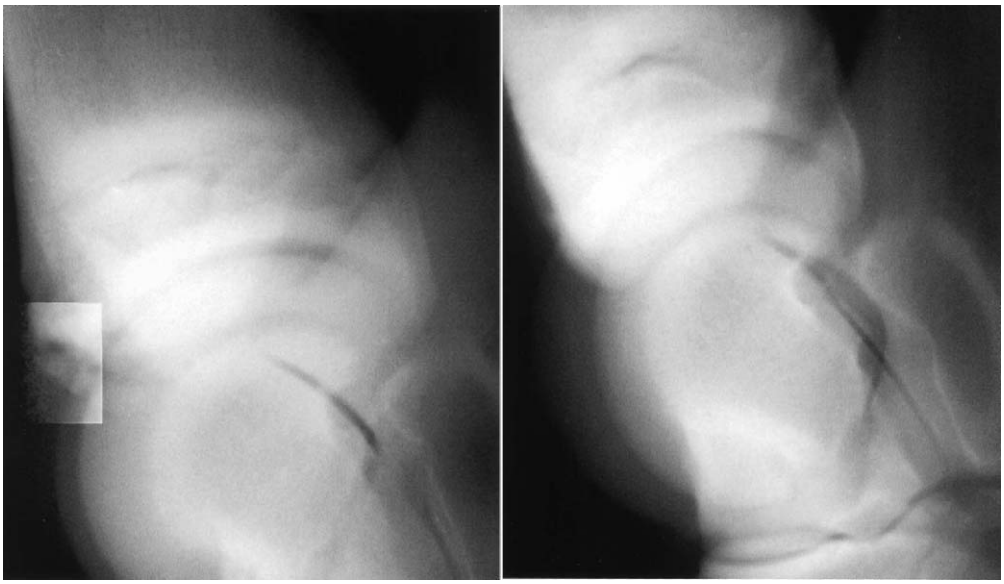


Figure 15-48 • A, Close-up lateral view of the tarsocrural joint shows a poorly defined bone fragment detached from the sagittal ridge. **B,** A normal lateral view is provided for comparison.



Figure 15-49 • Customized tangential view of the tarsocrural joint shows a badly fragmented sagittal ridge *(emphasis zone).* Multiple fragmented osteochondritis lesions were also found in the opposite hock (sagittal ridge, medial malleolus, and distal talar tuberosity), both femoral condyles, and distal radial epiphyses. Surprisingly, although this yearling Arabian colt had had boggy hocks, it was not lame either before or after being trotted.

ridge may also be appreciated from a true lateral perspective, but not as clearly as in the lateral oblique view (Figure 15-48). The medial oblique view is unreliable because it can sometimes project the proximal talar tuberosity as if it were a fragment from the sagittal ridge.

Multiple sagittal ridge fragments are occasionally seen, but only in the most severe cases and frequently in immature horses with multiple lesions (Figure 15-49). In this latter regard, horses treated for multiple osteochondral lesions of the tarsus, particularly those involving larger bones, tend to be less likely to race successfully than horses treated for a single lesion.[42]

Tibial Malleolus. Malleolar fragments resulting from osteochondritis are less common than osteochondral lesions of the tibial or talar ridges.[43] Most appear as minimally displaced, triangular bone fragments located at the distal tip of the medial malleolus (as seen in the oblique dorsomedial projection) and are often bilateral (Figure 15-50). According to McIlwraith, such lesions differ from fractures in that they are notably smaller.[44]

Trochlear Ridges (Talar Ridges). As a general rule, small to medium-sized bone fragments located in or around the dorsal aspect of the tarsocrural joint or ridges of the talus are caused by osteochondritis rather than injury. In some instances, large chunks of one or both ridges may detach, leaving a substantial defect. Focal concavity, regional flattening, or marginal defects in either talar ridge strongly infer osteochondritis, with or without a visible fragment. Figures 15-51 through 15-54 illustrate these various abnormalities.

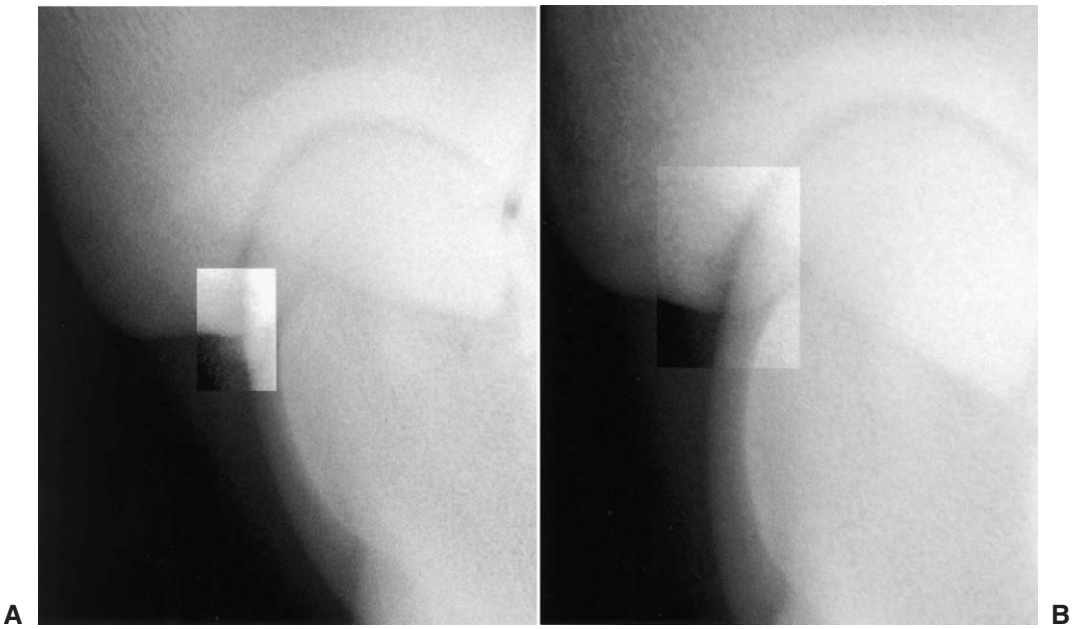


Figure 15-50 • A, Ultra-close-up medial oblique view of the tarsocrural joint shows a small triangular bone fragment lying just beyond the distal edge of the medial malleolus *(emphasis zone).* **B,** The normal opposite side, also with an emphasis zone, is provided for comparison.

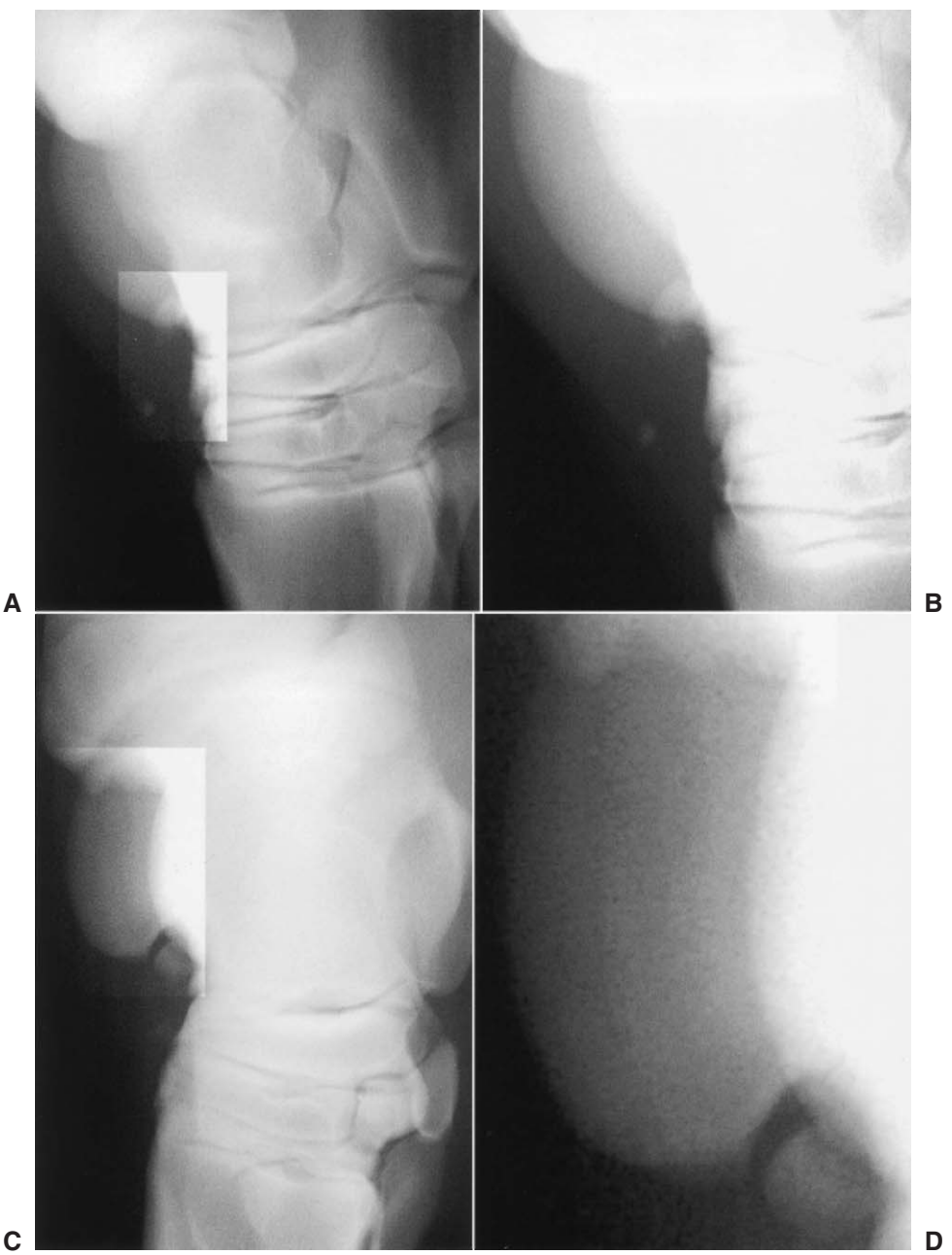


Figure 15-51 • Oblique lateral **(A),** lateral close-up **(B),** medial oblique **(C),** and medial oblique close-up **(D)** views of the tarsus show a cascade of fragments, beginning at the trochlear base and extending distally to the level of the distal intertarsal joint, presumably originating from one or both talar ridges.

Distal Talar Tuberosity

Osteochondritis of the distal talar tuberosity can assume any one of three forms: (1) a defective lateral margin, with or without a visible fragment; (2) a closely approximated detached fragment; and (3) a distant fragment, with or without a comparable defect in the distal tuberosity (Figure 15-55). Stress films typically reveal fragment fixation, further attesting to the rarity of true *joint mice* in horses.



Figure 15-52 • Close-up lateral view of the trochlear base shows a pair of vague fragments superimposed on the lateral notch, presumably detached from an overhanging ridge.

Third Tarsal Bone

Initially reported as *necrosis of the third tarsal bone*, and later theorized to be the result of hyperthyroidism, many now believe that this disease is actually another form of osteochondritis or, alternatively, is multifactorial (Figure 15-56).[45,46] In my experience, foals with this disease may partially recover, and as adults they often appear to have a severe case of bone spavin (both clinically and radiographically).

A variation on this theme is the newborn foal with bilateral disease, featuring one or more tarsal fractures (most often of the third and central tarsal bones); small, incompletely mineralized tarsal bones; and dorsal, stair-step subluxation (Figures 15-57 and 15-58). Some term this combination of abnormalities dysmaturity, but in my view this is little more than a diagnosis of connivance.

▮▮▮ BONE AND SOFT-TISSUE TARSAL TUMORS

Bone tumors are extremely rare in horses. My experience has been limited largely to hereditary osteochondromas and the occasional osteoma. The osteosarcomas I have seen have for the most part been of the osteoblastic variety, in some respects resembling traumatic exostoses. However, once under way, the



A **B**

Figure 15-53 • Lateral oblique **(A)** and close-up lateral oblique **(B)** views of the talus show a large crumbling fragment, all that remains of the distal portion of the lateral ridge.

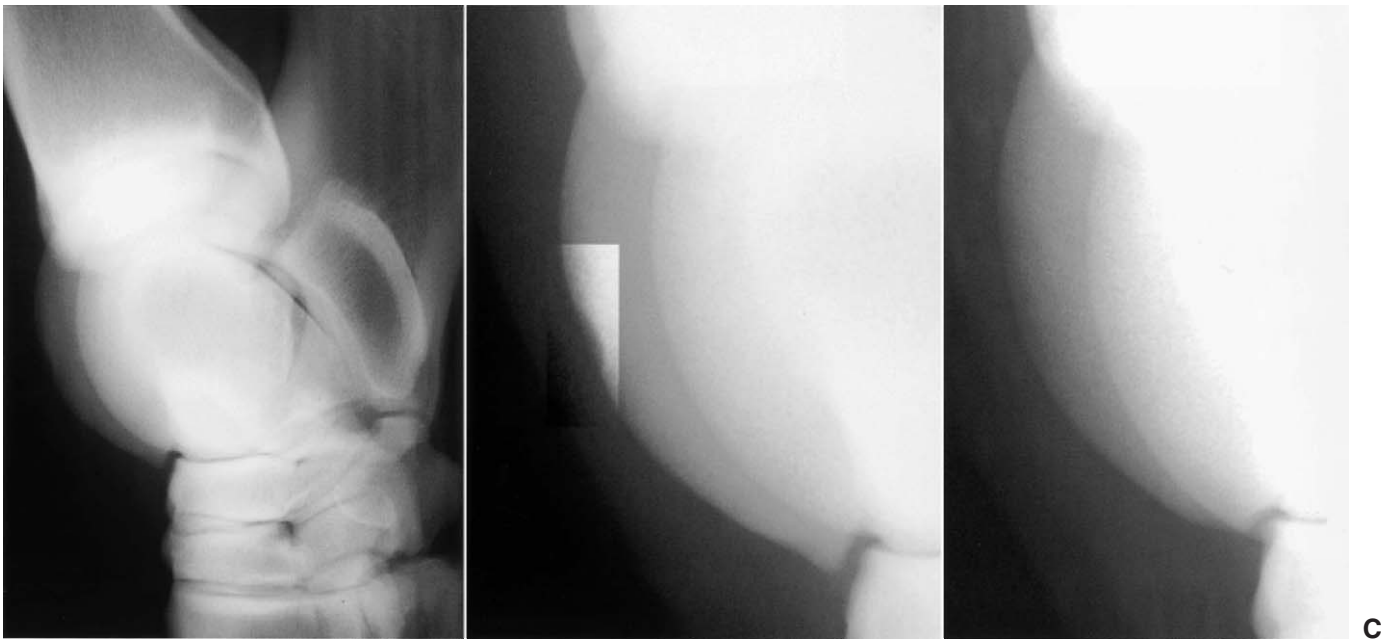


Figure 15-54 • Lateral **(A)** and close-up lateral **(B)** views of the talus show a shallow depression in the central margin of the lateral trochlear ridge *(emphasis zone)* consistent with osteochondritis. A normal talus is provided for comparison **(C).**

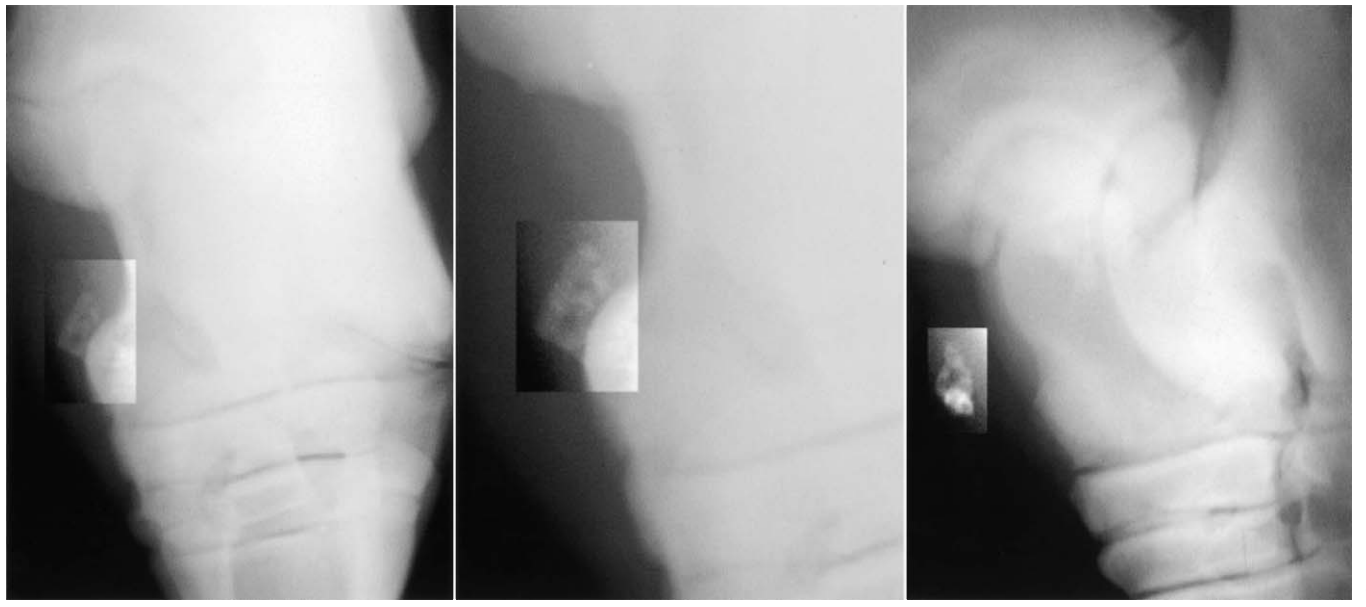


Figure 15-55 • Bilateral osteochondritis: Close-up plantarodorsal **(A)** and ultra-close-up plantarodorsal **(B)** views of the left distal talar tuberosity show a conforming bonelike object lying along the lateral margin *(emphasis zone).* A medial oblique view **(C)** of the opposite tarsus shows a discrete bony object lying in the soft tissue midway between the proximal and distal talar tuberosities. Arthroscopically the object proved to be a detached distal talar fragment attached to synovium.

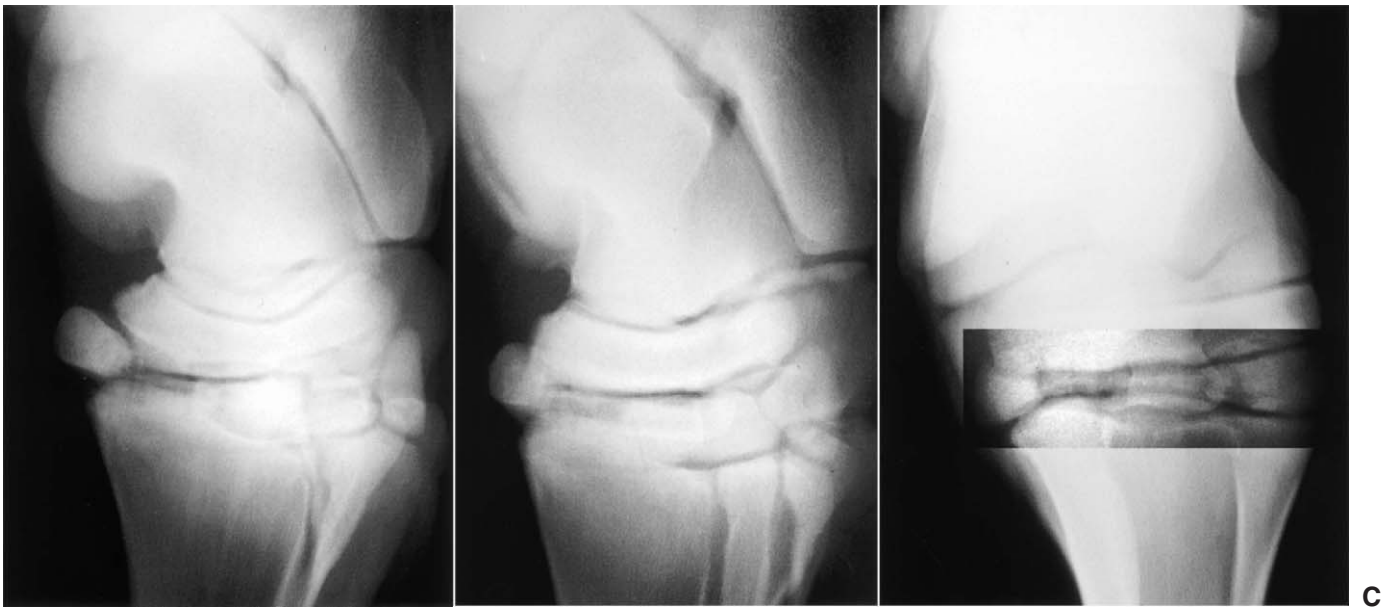


Figure 15-56 • Close-up lateral **(A)** and medial oblique **(B)** views of a fragmented, displaced (also termed *extruded*) third tarsal bone; but only the plantarodorsal projection **(C)** reveals the full extent of the damage and, just as important, the accommodative changes made by the surrounding tarsal bones.

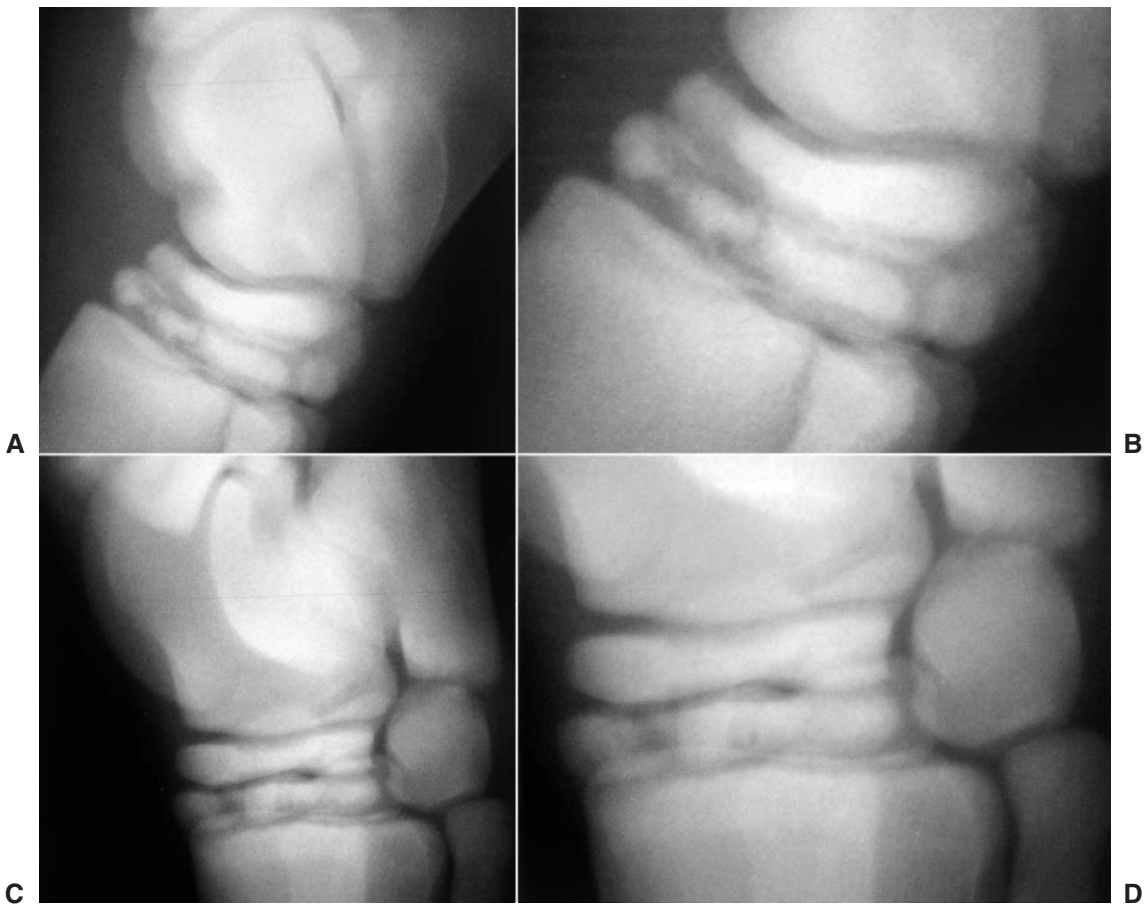


Figure 15-57 • Lateral **(A),** ultra-close-up lateral **(B),** medial oblique **(C),** and ultra-close-up medial oblique **(D)** views of the tarsus of a newborn foal show a fractured third tarsal bone and dorsal subluxation.



Figure 15-58 • Lateral **(A)** and ultra-close-up lateral **(B)** views of the right tarsus of a newborn foal with severe osteochondritis show generalized immaturity, a badly fragmented third tarsal bone, and dorsal stair step subluxation. Lateral **(C)** and ultra-close-up lateral **(D)** views of a normal tarsus are provided for comparison.

highly aggressive appearance of an osteosarcoma soon reveals its malignant nature (Figure 15-59).

Under the heading of *The Strange and Unusual*, Rabuffo and co-workers described an osteoma of the tarsal flexor sheath in a horse, located just beyond the upper lateral edge of the calcaneus. The lesion resembled dystrophic calcification, as osteomas sometimes do.[47]

▮▮▮ MISCELLANEOUS TARSAL DISORDERS AND FINDINGS

Congenital Sustentacular Hypoplasia

Lepage and co-workers reported a single case of unilateral hypoplasia of the sustentaculum tali in an 11-month-old Thoroughbred colt, which presumably caused dislocation of the deep digital flexor tendon.[48]

Radon Seeds

Radon seeds are rarely used any longer, their efficacy in serious doubt. Although short-lived radioactive implants may be found anywhere beneath the skin, they are typically situated near tendons and ligaments, presumably to function as a counterirritant. They have also been used to retard callus formation after splint surgery, a highly speculative claim at best. Radon seeds have been mistaken for sutures from a previous surgery (Figure 15-60).

▮▮▮ TARSAL SONOGRAPHY

Normal Sonographic Anatomy of the Tarsus

Dik described the normal cross-sectional sonographic appearance of the tarsus using a combination of dismembered limbs and living horses.[49] The following

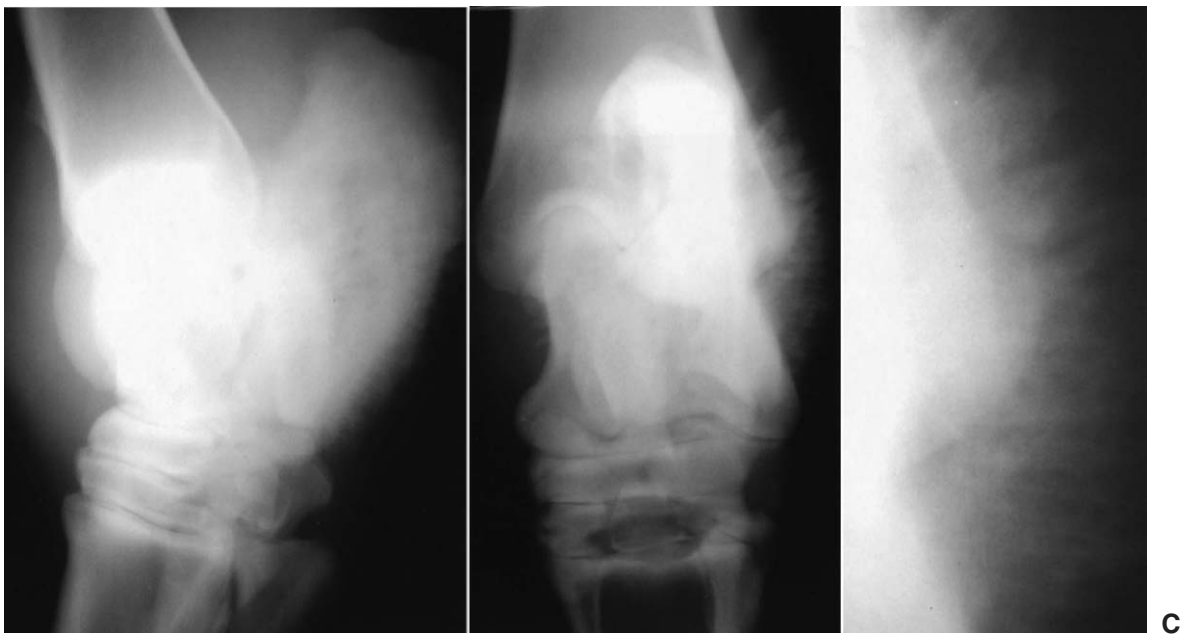


Figure 15-59 • Lateral **(A)** and plantarodorsal **(B)** views of the tarsus and an ultra-close-up plantarodorsal view of the lateral calcaneal margin **(C)** show a classic sunburst reaction, strongly suggesting malignancy.



Figure 15-60 • Lateral view of the tarsus shows an irregular line of exhausted radon seeds in the soft tissue caudal to the tarsometatarsal region.

structures were identified: (1) superficial digital flexor tendon, (2) deep digital flexor tendon, (3) plantar ligament, (4) medial collateral ligament, and (5) dorsomedial aspect of the tibiotarsal joint capsule and attached synovium.

Diagnostic Application

Tarsal sonography proved capable of diagnosing a variety of regional soft-tissue injuries, including (1) strains, (2) sprains, (3) bruises, and (4) hematomas. Additionally, ultrasound was able to detect hypertrophic synovitis, but only if the joint was distended by fluid, allowing for sufficient physical separation (and thus sonographic contrast) between the capsular tissues and underlying bone. Gabel described the clinical features of Cunean tendon bursitis-tarsitis in Standardbred horses, indicating that there are usually no accompanying radiographic changes.[50]

▮▮▮ TARSAL ANGIOGRAPHY

Watrous and co-workers reported using angiography to diagnose a posttraumatic pseudoaneurysm that subsequently disappeared.[51] They hypothesize that the catheterization procedure inadvertently resulted in the subsequent disappearance of the lesion. Proposed mechanisms included (1) catheter-related vasospasm, (2) use of a tourniquet distal to the lesion, and (3) transient retention of contrast solution within the

aneurysm, which according to the authors, may have eventually produced an obliterating thrombosis.

References

1. Farrow CS, McNeal SV, Morgan JP: Visualization of the tuber calcis and sustentaculum in the horse, *Calif Vet* 30:14, 1976.
2. Jones RD: The diagnosis and treatment of avulsion fracture of the sustentaculum tali in a horse, *Can Vet J* 17:287, 1976.
3. Rendano VT, Quick CB: Equine radiology, *Mod Vet Pract* 73:132, 1978.
4. Sack WO, Ferraglio S: Clinically important structures of the equine hock, *J Am Vet Med Assoc* 172:277, 1978.
5. Sack WO, Orsani PG: Distal intertarsal and tarsometatarsal joints in the horse: communication and injection sites, *J Am Vet Med Assoc* 179:355, 1981.
6. Smallwood JE, Auer JA, et al: The developing equine tarsus from birth to six months of age, *Equine Pract* 6:7, 1984.
7. Tomlinson JE, Redding WR, Sage A: Ultrasonographic evaluation of tarsocrural joint cartilage in normal adult horses, *Vet Radiol Ultrasound* 41:457, 2000.
8. Tomlinson JE, Redding WR, et al: Computed tomographic anatomy of the equine tarsus, *Vet Radiol Ultrasound* 44:174, 2003.
9. Blaik MA, Hanson RR, et al: Low-field magnetic resonance imaging of the equine tarsus: normal anatomy, *Vet Radiol Ultrasound* 41:131, 2000.
10. Leveille R, Lindsay WA, Biller DS: Ultrasonographic appearance of ruptured peroneus tertius, *J Am Vet Med Assoc* 202:1981, 1993.
11. Boero MJ, Kneller SK, et al: Clinical, radiographic, and scintigraphic findings associated with enthesitis of the lateral collateral ligaments of the tarsocrural joint in Standardbred racehorses, *Equine Vet J* 6:53, 1988.
12. Jakovljevic S, Gibbs C, Yeats JJ: Traumatic fractures of the equine hock: a report of 13 cases, *Equine Vet J* 14:62, 1982.
13. Markel MD: What is your diagnosis? *J Am Vet Med Assoc* 188:308, 1986.
14. Goodrich LR, Trostle SS, White NA: What is your diagnosis? *J Am Vet Med Assoc* 210:1277, 1997.
15. Farrow CS, McNeel SV, Morgan JP: Visualization of the tuber calcaneus and sustentaculum in the horse, *Calif Vet* 30:14, 1976.
16. Matoon JS, O'Brien TR: Radiographic evaluation of the calcaneus in the horse: a retrospective study, In *Proceedings of the American Association Equine Practitioners* 369, 1988.
17. Specht TE, Moran A: What is your diagnosis? *J Am Vet Med Assoc* 196:1308, 1990.
18. Tulleners EP, Reid CF: An unusual fracture in the tarsus of two horses, *J Am Vet Med Assoc* 178:291, 1981.
19. Sedrish SA, Moore RM, Partington BP: What is your diagnosis? *J Am Vet Med Assoc* 208:1385, 1996.
20. Lindsay WA, McMartin RB, McClure JR: Management of slab fractures of the third tarsal bone in 5 horses, *Equine Vet J* 14:55, 1982.
21. Orsini JA, Bar V: What is your diagnosis? *J Am Vet Med Assoc* 214:1621, 1999.
22. Kaneps AJ, Koblik PD, et al: A comparison of radiography, computed tomography, and magnetic resonance imaging for the diagnosis of palmar process fractures in foals, *Vet Radiol Ultrasound* 36:467, 1995.
23. Reeves MJ, Trotter GW: Tarsocrural joint luxation in a horse, *J Am Vet Med Assoc* 199:1051, 1991.
24. Eksell P, Uhlhorn H, Carlsten J: Evaluation of different projections for radiographic detection of tarsal degenerative joint disease in Icelandic horses, *Vet Radiol* 40:228, 1999.
25. Van Pelt RW, Riley WF, Tillotson RL: Tenosynovitis of the deep flexor tendon sheath in horses, *Can Vet J* 10:235, 1969.
26. Edwards GB: Changes in the sustentaculum tali associated with distension of the tarsal sheath (thoroughpin), *Equine Vet J* 10:97, 1978.
27. Welch RD, Auer JA, et al: Surgical treatment of tarsal sheath effusion associated with an exostosis on the calcaneus of a horse, *J Am Vet Med Assoc* 196:1992, 1990.
28. Pool RR, Wheat JD, Ferraro GL: Corticosteroid therapy in common joint and tendon injuries of the horse. Part II. Effects on tendons, In *Proceedings of the American Association of Equine Practitioners* 407, 1980.
29. Norberg IA: Tendons: surgery and pathology, in *Proceedings of the American Association of Equine Practitioners* 177, 1968.
30. Dik KJ, Merkins HW: Unilateral distension of the tarsal sheath in the horse: a report of 11 cases, *Equine Vet J* 9:307, 1987.
31. Dik KJ, Keg PR: The efficacy of contrast radiography to demonstrate "false thoroughpins" in five horses. *Equine Vet J* 22:223, 1990.
32. Leitch M: Diagnosis and treatment of septic arthritis in the horse, *J Am Vet Med Assoc* 175:701, 1979.
33. Hand DR, Watkins JP, et al: Osteomyelitis of the sustentaculum tali in horses: 10 cases (1992-1998), *J Am Vet Med Assoc* 219:341, 2001.
34. Tulleners EP, Reid CF: Osteomyelitis of the sustentaculum talus in a pony, *J Am Vet Med Assoc* 178:290, 1981.
35. May KA, Moll HD: What is your diagnosis? *J Am Vet Med Assoc* 214:627, 1999.
36. Long CD, Galuppo LD, et al: Scintigraphic detection of equine orthopedic infections using Tc-HMPAO labeled leukocytes in 14 horses, *Vet Radiol Ultrasound* 41:354, 2000.
37. Eksell P, Carlsson S, et al: Effects of digital filters on detectability of a phantom lesion in a scintigram of the equine tarsus, *Vet Radiol Ultrasound* 41:365, 2000.
38. Farrow CS: Sinography in the horse, In *Proceedings of the 32nd Annual Association of Equine Practioners,* Nashville, Tennessee, 1986.
39. Hartung K, Munzer B, Keller H: Radiologic evaluation of spavin in young trotters, *Vet Radiol Ultrasound* 24:153, 1983.
40. Duin YV, Hurtig MB: Subchondral bone cysts in the distal aspect of the tibia of three horses, *Can Vet J* 37:429, 1996.
41. Grondahl AM, Engeland A: Influence of radiographically detectable orthopedic changes on racing performance in Standardbred trotters, *J Am Vet Med Assoc* 206:1013, 1995.
42. Beard WL, Bramlage LR, et al: Postoperative racing performance in Standardbreds and Thoroughbreds with osteochondrosis of the tarsocrural joint: 109 cases (1984-1990), *J Am Vet Med Assoc* 204:1655, 1994.
43. Watson E, Selcer B, Allen D: What is your diagnosis? *J Am Vet Med Assoc* 199:774, 1991.
44. McIlwraith CW: *Diagnostic and surgical arthroscopy in the horse*. Philadelphia, 1990, Lea & Febiger, p. 175.
45. Morgan JP: Necrosis of the third tarsal bone of the horse, *J Am Vet Med Assoc* 151:1334, 1967.

46. O'Brien TR: Radiographic interpretation of the equine tarsus, In *Proceedings of the 33rd American Association of Equine Practitioners,* 1987, 289.
47. Rabuffo TS, Richardson DW, Baird DK: What is your diagnosis? *J Am Vet Med Assoc* 221:635, 2002.
48. Lepage OM, Leveille R, et al: Congenital dislocation of the deep digital flexor tendon associated with hypoplasia of the sustentaculum tali in a Thoroughbred colt, *Vet Radiol Ultrasound* 36:384, 1995.
49. Dik KJ: Ultrasonography of the equine tarsus, *Vet Radiol Ultrasound* 34:36, 1993.
50. Gabel AA: Diagnosis, relative incidence, and probable cause of Cunean tendon bursitis-tarsitis of Standardbred horses, *J Am Vet Med Assoc* 175:1079, 1979.
51. Watrous BJ, Riebold TW, et al: Spontaneous resolution of a pseudoaneurysm in a horse following angiographic diagnosis, *Vet Radiol* 28:49, 1987.

Chapter 16

Metatarsus

THE STANDARD METATARSAL SERIES

A standard metatarsal series consists of four views: a plantarodorsal, lateral, and two obliques, optimized to profile the lateral and medial splint bones away from the shaft of the cannon bone (Figure 16-1). Size allowing, it is useful to include portions of the overlying tarsus or underlying fetlock for orientation; however, combined tarsometatarsal or metatarsophalangeal examinations generally produce inferior images because of geometric distortion caused by decentering. The primary evaluative purpose of each standard view is listed in Box 16-1. Corresponding views of a defleshed metatarsus are provided for radiographic-anatomic comparison (Figure 16-2).

Strategic Metatarsal Facts

- The head of the lateral splint bone (fourth metatarsal) is nearly twice the size of its medial counterpart (second metatarsal), making it easy to tell them apart and thus to determine which is the lateral and which is the medial aspect of the proximal metatarsus (Figure 16-3).
- The lateral splint articulates only partially with the overlying fourth tarsal bone, the rest being nonarticular, another means of differentiating the lateral from the medial aspect of the metatarsus (Figure 16-4).
- The natural curvature of the small metatarsal bones, especially distally, frequently results in their partial concealment by the adjacent cannon bone, simulating a displaced splint fracture (Figure 16-5).
- Immature splint bones contain a separate ossification center distally, termed the *button.* It is separated from the rest of the bone by a growth plate (Figure 16-6). Depending on the projection angle and penetration of the distal splint, this normal physis can resemble a fracture. When in doubt, obtain a comparable image of the opposite distal splint.
- Although used infrequently, the so-called *see-through view* can be very helpful for the questionable splint-bone injury. The see-through view is not really a new or additional view, but rather it is an additional use for the existing lateral and oblique projections. It works this way: The nonprofiled splint bone is often projected on the center of the third metacarpal bone, sometimes more clearly than in any other view, thanks to the high contrast afforded by the medulla (Figure 16-7).
- Variations in the position and attitude of the third metatarsal foramen (foraminal ectopia) can mimic a metatarsal stress fracture.[1]

SOFT-TISSUE FOREIGN BODY

Most soft-tissue foreign bodies do not have sufficient density to be differentiated from their surroundings. Thus most are diagnosed circumstantially on the basis of sinus formation, drainage, pain, and lameness. Occasionally a normally radiotransparent material, such as a hoof-wall fragment, embedded in the leg after a kick will be radiographically visible because of soil contaminants (Figure 16-8).

SPRAIN

Stickle and co-workers described a case of proximal suspensory desmitis in a 9-year-old Quarter Horse in which the initial diagnosis was made radiographically and subsequently supported scintigraphically.[2] Radiographically the lesion appeared as a thickened proximal cortex on the plantar aspect of the MC3, which is best seen in lateral and frontal projections of the affected tarsus. The nuclear medicine study

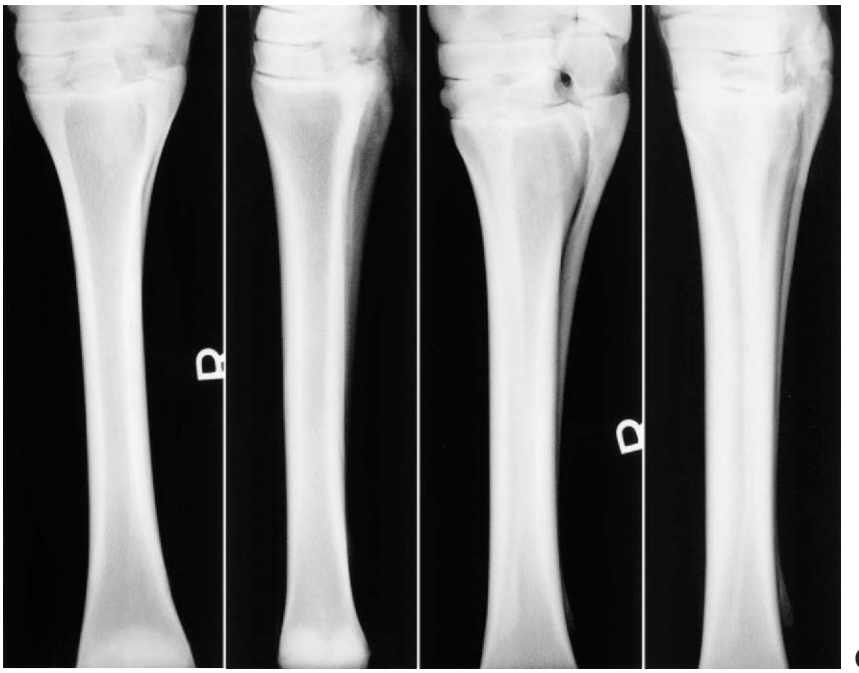
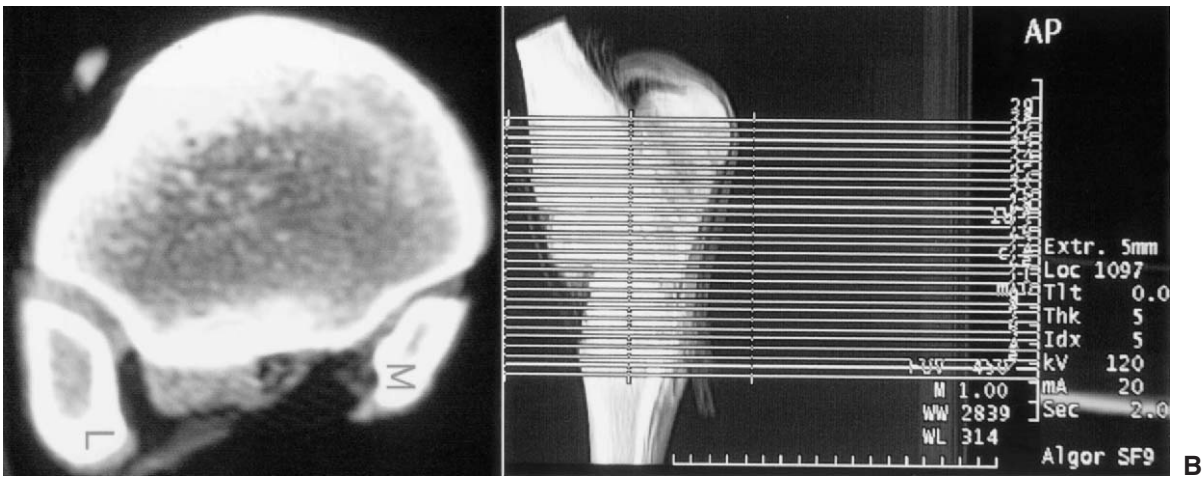


Figure 16-1 • The standard metatarsal series consists of four views: plantarodorsal **(A),** lateral **(B),** and two obliques, optimized to profile the lateral **(C)** and medial **(D)** splint bones away from the shaft of the cannon bone.



Figure 16-2 • Defleshed metatarsus shown from plantar **(A),** medial oblique **(B),** and lateral oblique **(C)** perspectives, corresponding to three of standard radiographic views shown in Figure 16-1.



A B

Figure 16-3 • A, Transverse computed tomograph obtained from the proximal metacarpus. **B,** The distal-most in a series shows the relative size, shape, and positions of the medial *(M)* and lateral *(L)* metatarsal bones.



Figure 16-4 • The articular relationship between the head of the lateral splint bone and the overlying fourth tarsal bone is only a partial one, with better than half of the proximal fourth metatarsal bone being nonarticular, a normal association that must not be mistaken for a dislocation.



Figure 16-5 • As the distal third of either splint, bone dips behind the adjacent surface of the cannon bone, a part of the shaft disappears from view *(emphasis zone)*, making it appear as if the bone has been fractured. Repeating the film, while slightly changing the projection angle and lightening the image, usually confirms, or more often than not denies, the presence of a fracture.

showed increased radioisotopic uptake in the same region of the proximal metatarsus.

▮▮▮ FRACTURE

As previously mentioned, growth plates are structurally weaker than adjacent bone, and thus they are more susceptible to fracture. A case in point is the distal metatarsal physis, which typically fractures diagonally along with the distal third metatarsal metaphysis (Figure 16-9).

Ross and co-workers described an unusual type of proximal corner fracture in five Standardbreds. The fractures, situated at the attachment sites of the peroneus tertius muscles, were displaced cranially and entered the tarsometatarsal joint.[3]

Fresh dorsal cortical stress fractures often have a distinctive scimitar-like appearance (Figure 16-10), similar to stress fractures in the third metacarpal bone. Undiscovered fractures may or may not leave a dis-

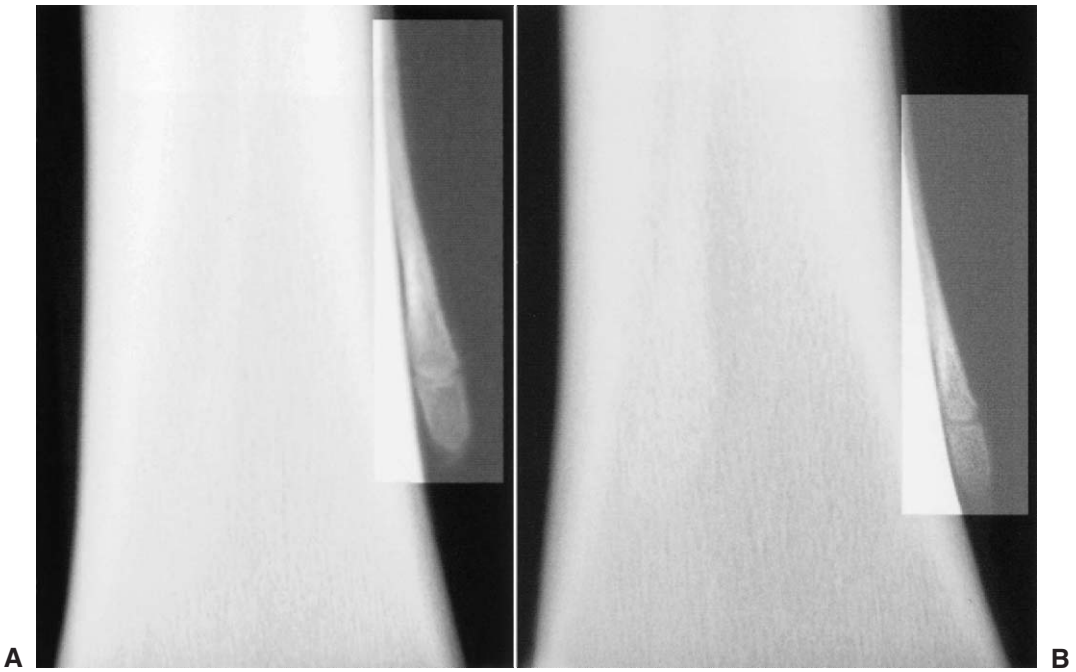


Figure 16-6 • Close-up views of the medial **(A)** and lateral **(B)** splint bones show open growth plates distally.

Box 16-1
Evaluative Purposes of the Four Standard Metatarsal Views

VIEW	EVALUATIVE PURPOSE
Plantarodorsal	One of two best views in which to assess the dorsomedial aspect of the tarsometatarsal joint for signs of bone spavin
Lateral	Often the best view in which to identify a sequestrum or incomplete dorsal cortical fracture
Medial oblique	Profiles the lateral splint bone (MT IV) away from the adjacent cannon bone (MT III). One of two best views in which to assess the dorsomedial aspect of the tarsometatarsal joint for signs of bone spavin
Lateral oblique	Profiles the medial splint bone (MT II) away from the adjacent cannon bone (MT III)

MT, Metatarsal.



Figure 16-7 • "See-through views" of the distal lateral **(A)** and medial **(B)** splint bones.

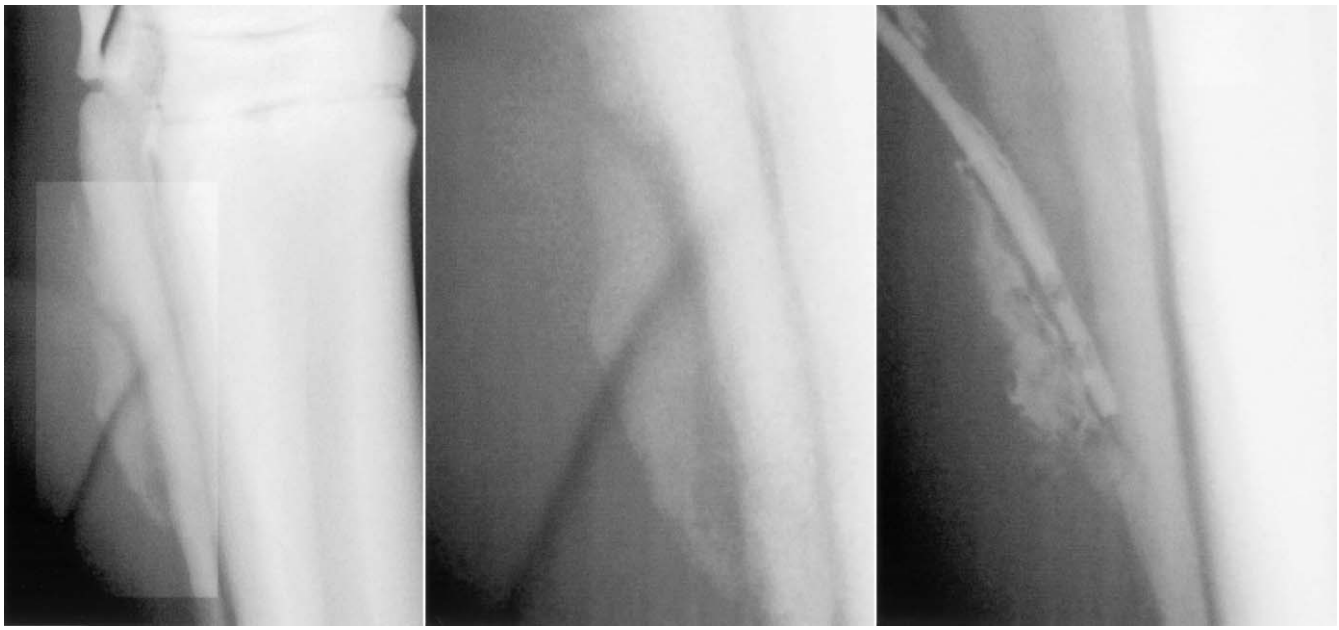


Figure 16-8 • Close-up **(A)** and ultra-close-up lateral oblique **(B)** views of the caudal aspect of the proximal metatarsus show a bonelike object resembling a sequestrum lying just off the surface of the medial splint. Actually the object is a hoof-wall fragment, deeply embedded in the leg as a result of a kick received from another horse. There is a medium-sized new bone deposit on the surface of the second metatarsal bone just above the foreign body and an irregular layer of new bone along the outer surface of the adjacent splint. A sinogram **(C)** reveals a discrete channel extending into the depths of the lesion and contrast solution surrounding the fragment.

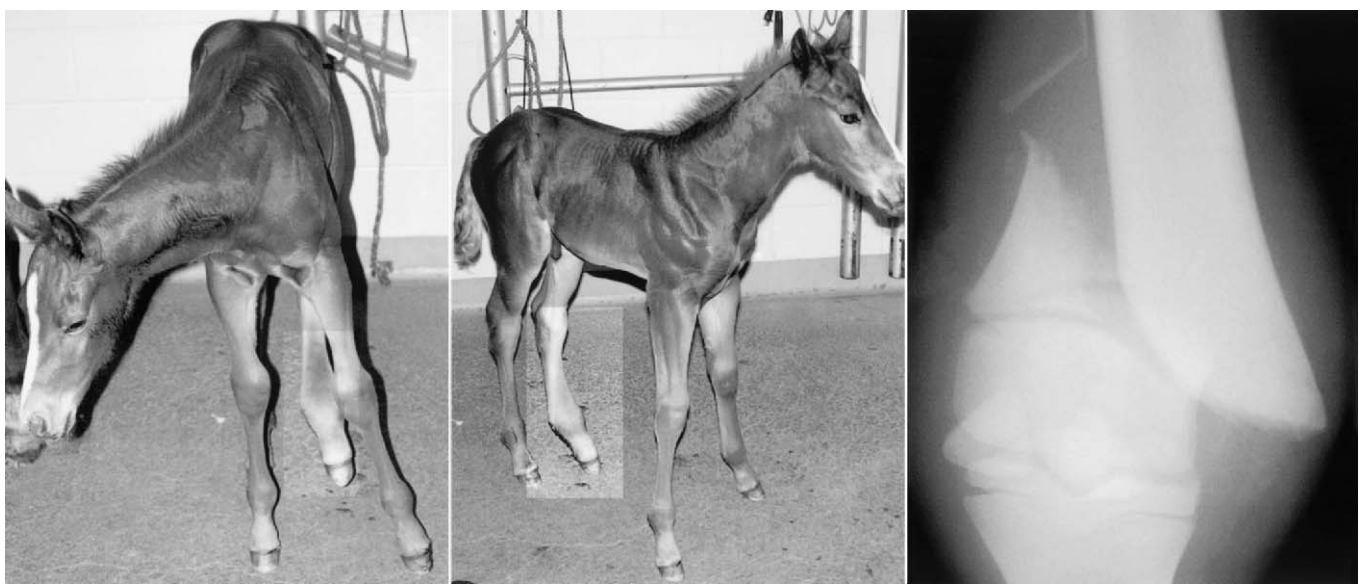


Figure 16-9 • Front **(A)** and right front quarter **(B)** views of a young colt with a left distal metatarsal growth plate fracture show characteristic swelling and minimal weight bearing. Close-up plantarodorsal radiograph **(C)** reveals a badly overridden Salter-Harris type II growth plate fracture along with a multiple fracture of the nearby splint bone and severe swelling.

cernible callus. Disappearance time of the fracture is variable, but as with most fractures, the young heal faster than the old.

The appearance of small metatarsal bone fractures closely resembles that of the small metacarpal bones, ranging from exuberant calluses that encroach on the nearby suspensory ligament to nonunions (Figures 16-11 and 16-12).

▮▮▮ TUMOR

Appendicular bone tumors are extremely rare in horses, although there are sporadic reports, some of which are quite thorough. For example, MacAllister and co-workers reported a case of multiple myeloma in the third metatarsal bone of a 19-month-old Quarter Horse.[4] Radiographically the affected bone possessed

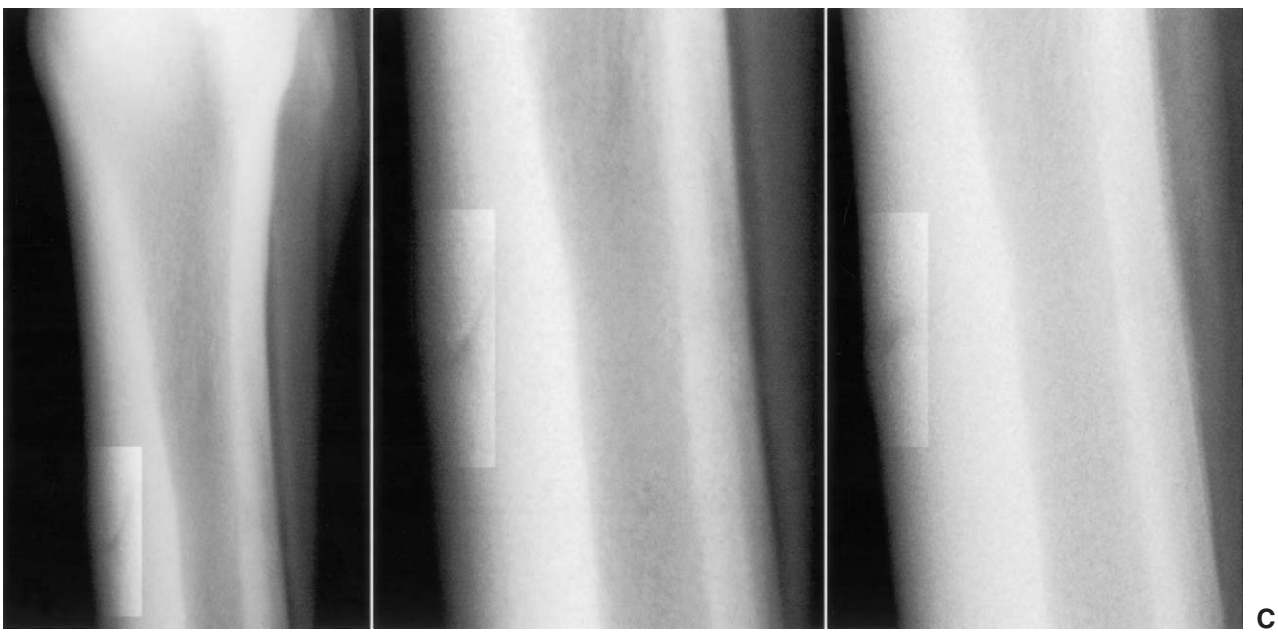


Figure 16-10 • Close-up lateral **(A)** and ultra-close-up lateral **(B)** views of a fresh cortical stress fracture *(emphasis zone)* show characteristic scimitar shape. Three months later, an ultra-close-up lateral view **(C)** shows that the fracture is partially healed.

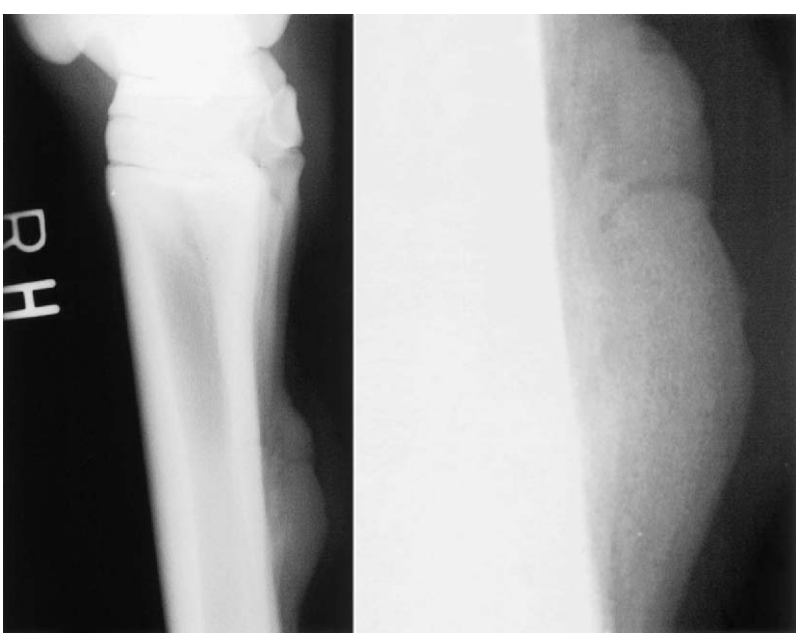


Figure 16-11 • Lateral oblique **(A)** and close-up lateral oblique **(B)** views of the medial splint bone show a large callus distally, the result of a multiple fracture sustained a year earlier. Although the horse appeared to recover fully after a lengthy recuperation, its lameness reappeared once it resumed regular vigorous training, a lameness that was attributed to desmitis secondary to callus impingement.



Figure 16-12 • Medial oblique **(A)** and close-up medial oblique **(B)** "see-through" views show a lengthy, mildly displaced fracture of the second metatarsal bone superimposed on the medulla of the cannon bone.

a nearly opaque midshaft with punctate cortical destruction and periosteal new bone at either end of the diaphysis. Necropsy revealed multiple skeletal lesions in addition to the one described, including the opposite third metacarpal bone, both metatarsal bones, both radii, and the left tibia.

All the bony lesions involved the periosteum and superficial cortex. Even though cancer cells were present in the marrow, they did not produce visible change in the trabeculae. Soft-tissue lesions were found in the kidneys, spleen, lymph nodes, lungs, eyes, and brain. Most multiple myelomas occur in middle-aged and older horses.

In my experience, single and multiple hereditary exostoses are most common, followed by osteoma, chondroma and, less frequently, fibrous dysplasia. Although osteosarcomas are by far the most common primary bone tumor of dogs, they are rare in horses. Deep wounds that abrade the surface of the metatarsus can occasionally produce a monumental exostosis resembling a bone tumor (Figure 16-13).

▮▮▮ METATARSAL LYMPHEDEMA

Fackelman and co-workers described lymphography in the horse, including normal lymphangiograms and three cases of lymphedema.[5] Based on performing lymphangiography in dogs, and in particular the fragility of lymphatics compared with blood vessels, I would strongly recommend practicing the procedure before attempting it in a clinical case. Many excellent references can be found in the German and Austrian literature.

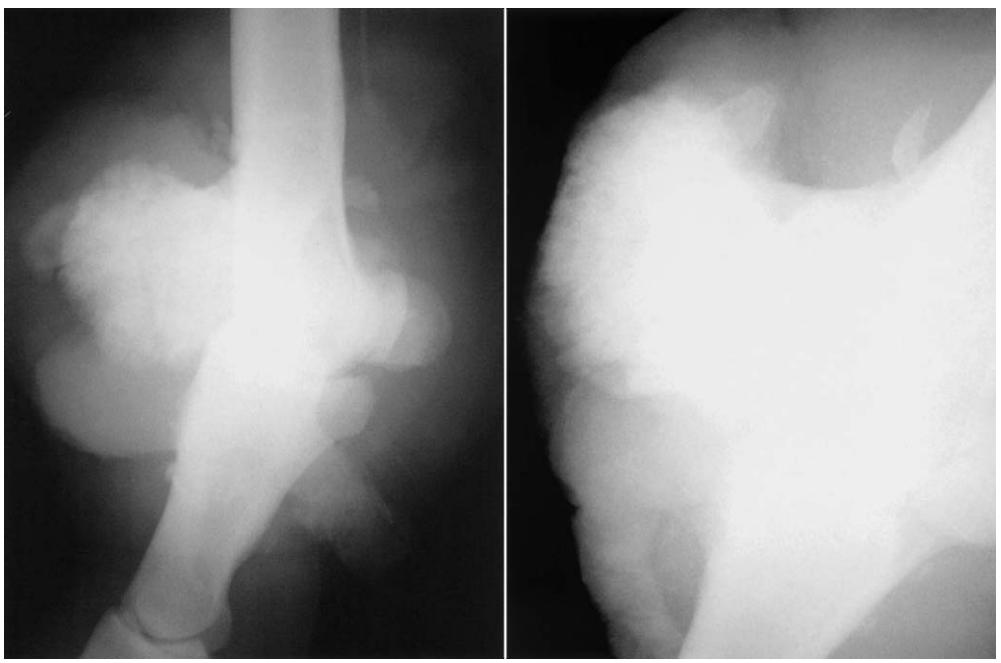


Figure 16-13 • Lateral **(A)** and close-up lateral **(B)** views of the distal metatarsus show an enormous exostosis and granulation tissue caused by a chronically infected wound.

References

1. Godshalk CP, Kneller SK, et al: Anatomic variations in the nutrient foramina of the equine third metatarsal bone in two horses, *Vet Radiol* 26:162, 1985.
2. Stickle R, Tetens J, et al: Proximal suspensory desmitis, *Vet Radiol Ultrasound* 37:105, 1996.
3. Ross MW, Sponseller ML, et al: Articular fracture of the dorsoproximolateral aspect of the third metatarsal bone in five Standardbred racehorses, *J Am Vet Med Assoc* 203:698, 1993.
4. MacAllister C, Qualls C, et al: Multiple myeloma in a horse, *J Am Vet Med Assoc* 191:337, 1987.
5. Fackelman GE, Auer J, Wirth W: Lymphangiography in the horse, *Vet Med Small Anim Clin* May:614, 1974.

Chapter 17

Ligaments and Tendons of the Metacarpal and Metatarsal Regions

NORMAL SONOGRAPHIC APPEARANCE OF THE TENDONS AND LIGAMENTS OF THE METACARPAL AND METATARSAL REGIONS

My preference for sonographically imaging and recording the tendons and ligaments of the metacarpal and metatarsal regions is to divide them into six primary zones. For a more precise identification, decimals may be used, zone 4.5, for example.

Metacarpal Region

Labeled cross-sectional sonographic images of the tendons and ligaments of the metacarpal region of a healthy six-year-old Thoroughbred filly are shown in Figure 17-1. As you study these sonograms keep in mind that their appearance, especially their echogenicity, is strongly influenced by the frequency of the transducer, the machine settings, and the angle of the scanner on the skin surface. Even small departures from a perpendicular scan angle are capable of significantly increasing or decreasing the brightness of the image, possibly mimicking a lesion.

Metatarsal Region

Labeled cross-sectional sonographic images of the tendons and ligaments of the metatarsal region of a healthy eight-year-old Arabian gelding are shown in Figure 17-2. As you study these sonograms keep in mind that their appearance, especially their echogenicity, is strongly influenced by the frequency of the transducer, the machine settings, and the angle of the scanner on the skin surface. Even small departures from a perpendicular scan angle are capable of significantly increasing or decreasing the brightness of the image, possibly mimicking a lesion.

Gross Anatomy of the Digital Flexor Tendons, Inferior Check Ligaments, and Suspensory Ligaments

Numerous authors have described the normal sonographic appearance of the metacarpal/metatarsal tendons and ligaments, some using dismembered cadaver limbs and others using live horses. Among these are works that include companion line drawings or anatomic specimens, both of which enhance understanding of the relevant sonographic anatomy.[1] Air-dried specimens of the flexor tendons, check ligaments, and suspensory ligaments are also extremely useful when interpreting sonograms or explaining sprains and strains to clients (Figures 17-3 through 17-5).

Superficial and Deep Digital Flexor Tendons

Horses have two large overlapping tendons running the length of the backside of the metacarpus and metatarsus, just beneath the skin: the superficial digital flexor tendon and immediately below that the deep digital flexor tendon. As their names indicate, these tendons are responsible for flexing the distal extremity.

Normal Anatomic Variations. The shape and size of the flexor tendons of the metacarpus normally differ from those of the metatarsus. Tendon size and shape also change, depending on the degree of tension or load; the greatest differences occur between full and partial weight bearing.

Check Ligament

The check ligament is an extension of the common palmar ligament of the carpus, which travels distally to the midpoint of the metacarpus before blending imperceptibly with the dorsal surface of the deep digital flexor tendon. At its most visible, the check lig-

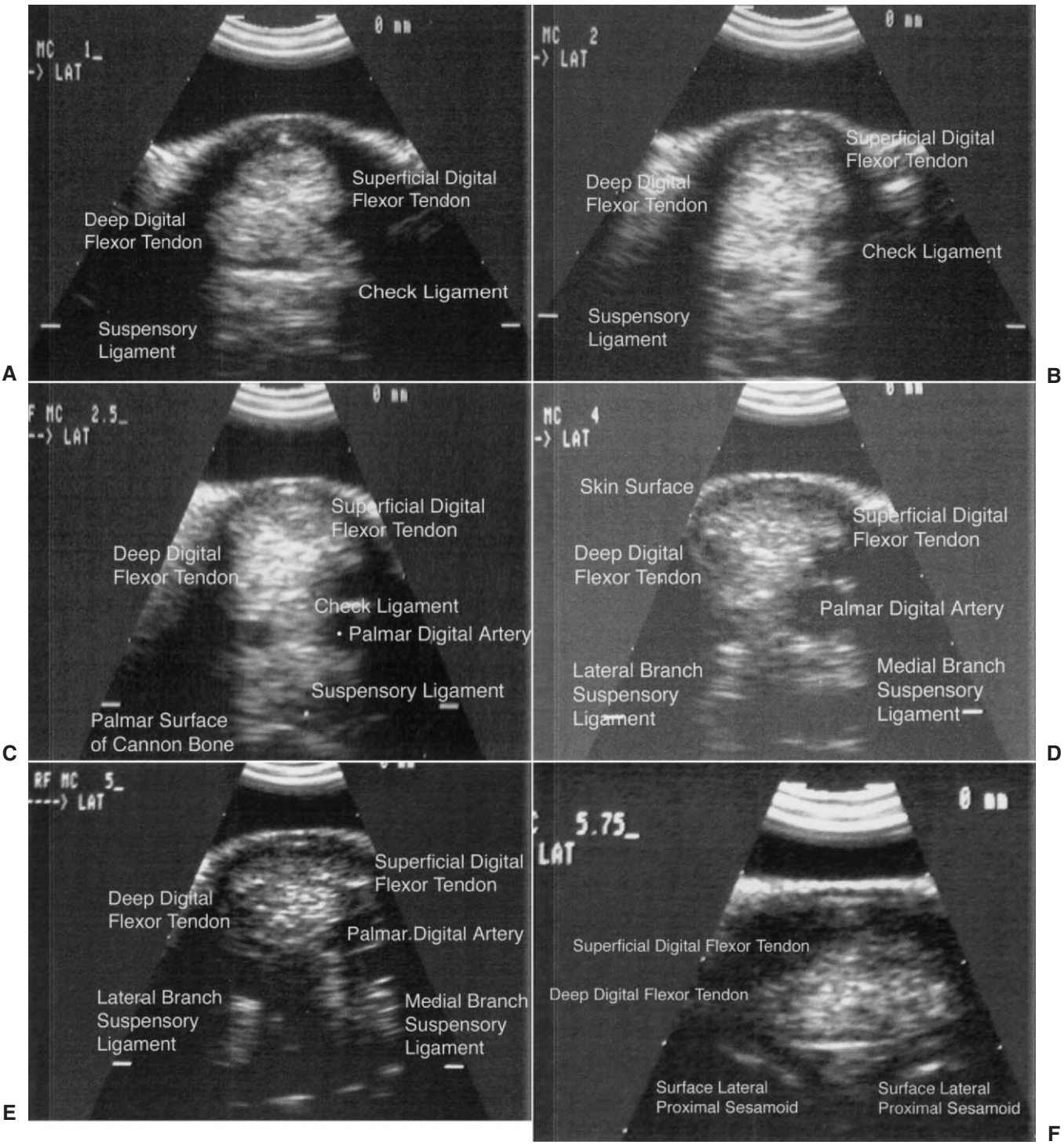


Figure 17-1 • Normal metacarpal tendons and ligaments: **A,** zone 1; **B,** zone 2; **C,** zone 2.5; **D,** zone 4; **E,** zone 5; **F,** zone 5.75.

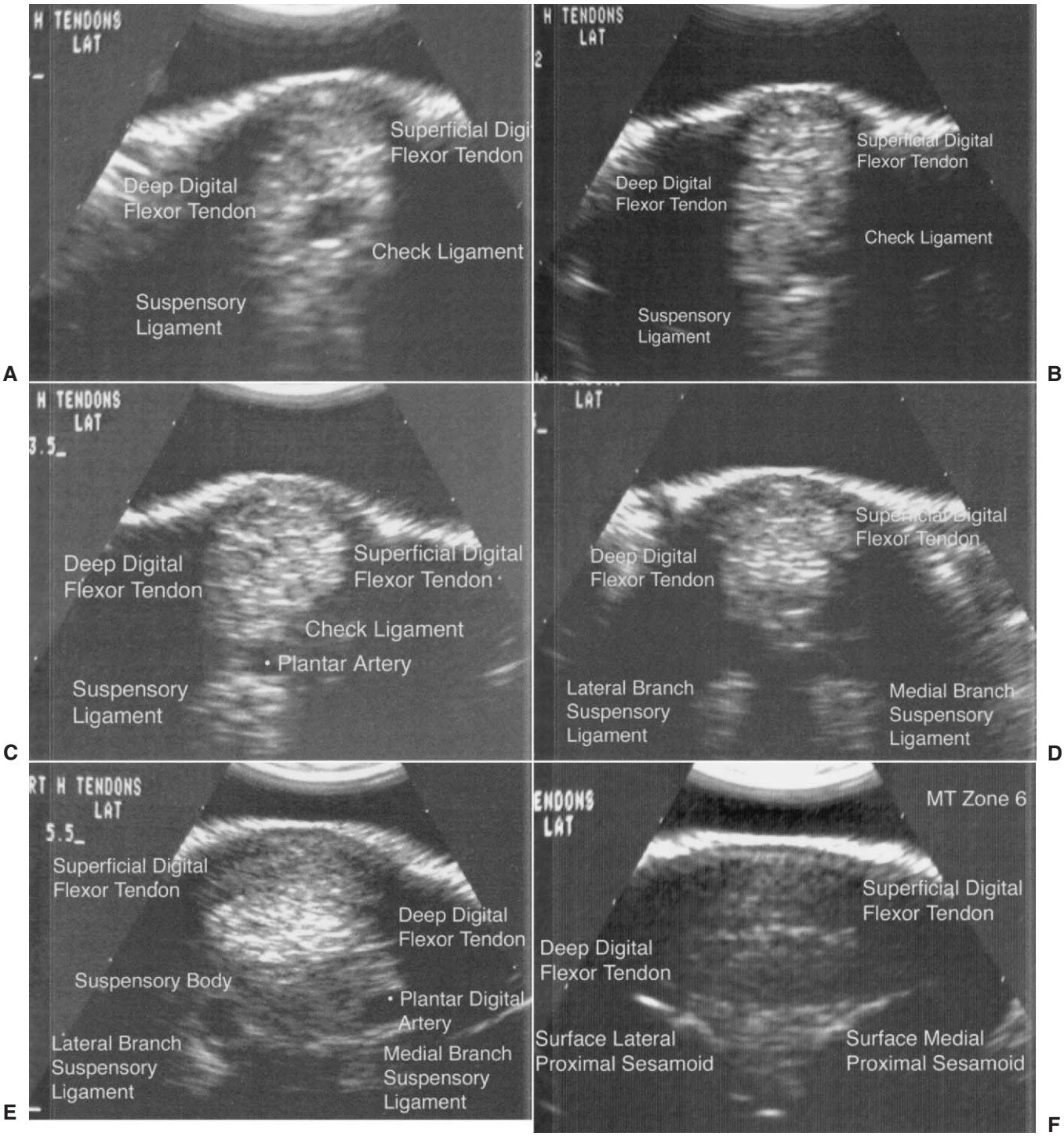


Figure 17-2 • Normal metatarsal tendons and ligaments: **A,** zone 1; **B,** zone 2; **C,** zone 3.5; **D,** zone 4; **E,** zone 5.5; **F,** zone 6.

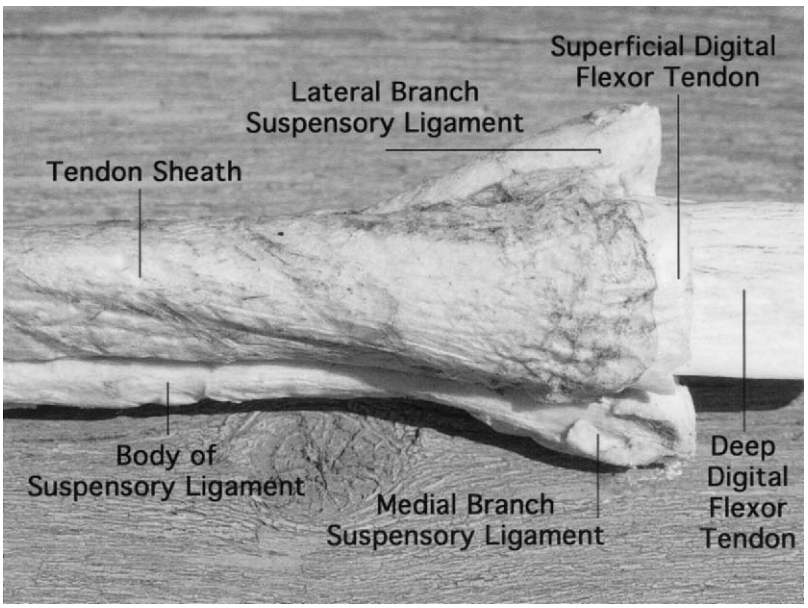


Figure 17-3 • Air-dried specimen shows the majority of the superficial and deep digital flexor tendons, check, and suspensory ligaments removed from the forelimb of an adult Quarter Horse.

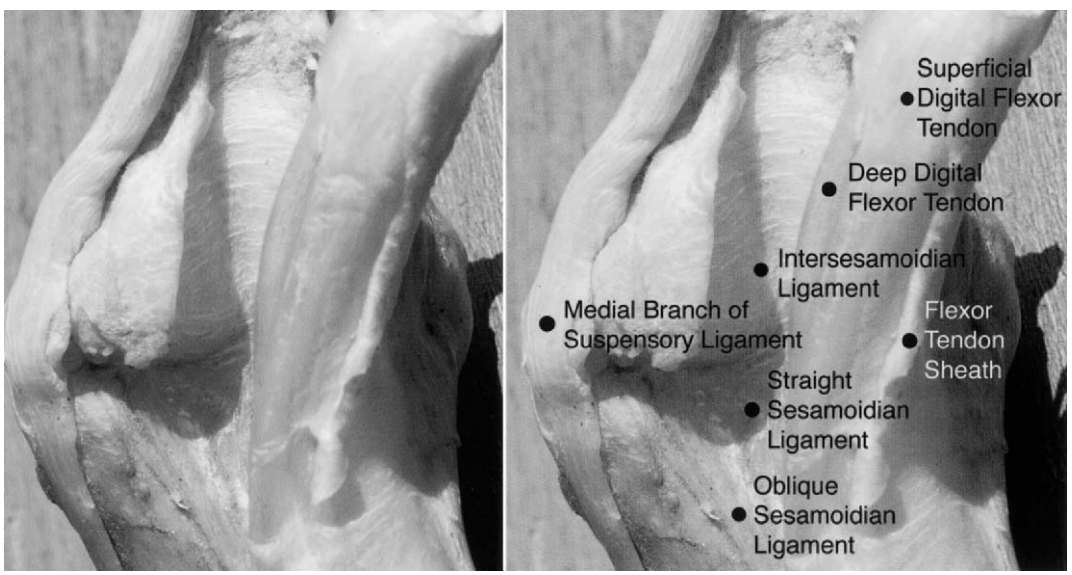


Figure 17-4 • Unlabeled **(A)** and labeled **(B)** air-dried specimen of the palmar aspect of the fetlock region shows flexor tendons (spread apart and partially reflected), suspensory branches, and intersesamoidian, straight, and oblique sesamoidian ligaments.

ament appears brighter (hyperechoic) than the adjacent flexor tendons and suspensory ligament and has a distinctive asymmetric angular appearance in cross-section.

Suspensory Ligament

The suspensory ligament travels most of the length of the palmar surface of the metacarpus and plantar surface of the metatarsus before dividing just above the sesamoids. Unlike the overlying flexor tendons, whose uniform composition results in a strong, even echogenicity, the suspensory ligament appears comparatively dark and mottled because of its complement of striated muscle.

Normal Anatomic Variations. The amount of striated muscle contained in the suspensory ligament varies with (1) breed (Thoroughbred versus Standardbred), (2) type and amount of race training, and (3) gender; it does not vary with age.[2]

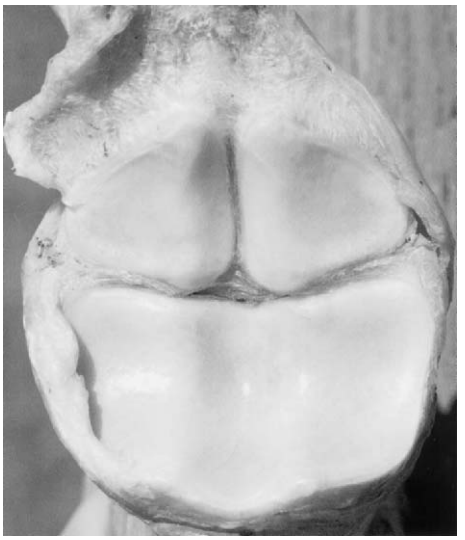


Figure 17-5 • Air-dried specimen of the fetlock (shown from in front and above) with the cannon bone removed to reveal the articular surfaces of the proximal phalanx and sesamoids. Note how the proximal sesamoid bones are inextricably bound to P1 and one another by the distal suspensory branches and to sesamoidian ligaments, explaining why sesamoid fractures are nearly always accompanied by sprain injury.

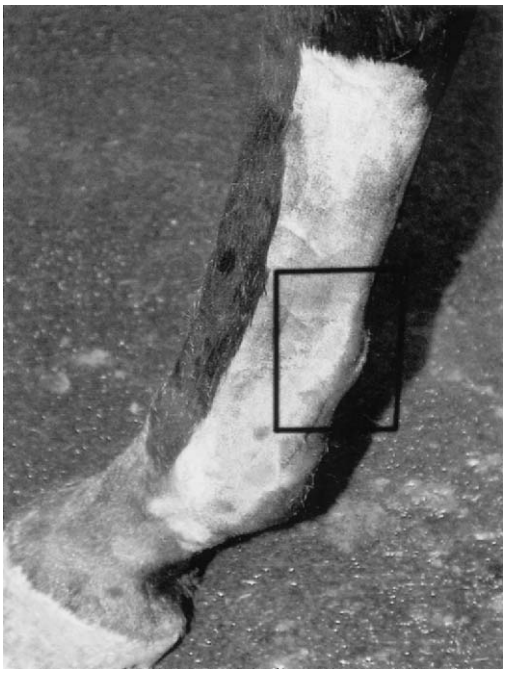


Figure 17-6 • Close-up view of a *low bow* (clipped in preparation for an ultrasound examination).

Table 17–1 • SUBGROSS ANATOMY OF A TENDON

Tendon	0.5-1.1 cm (equine superficial and deep digital flexor tendons*)
Fascicle	50-300 nm
Fibril	50-500 nm
Subfibril	10-20 nm
Microfibril	3.5 nm
Tropocollagen	1.5 nm

*From Craychee TJ: Ultrasonic evaluation of equine musculoskeletal injury. In Nyland TG, Matoon JS, editors, *Veterinary diagnostic ultrasound.* Philadelphia, 1995, WB Saunders.

▮▮▮ MICROSCOPIC ANATOMY OF TENDONS AND LIGAMENTS

Grossly, the flexor tendons, like tendons elsewhere in the body, are composed of longitudinally oriented bundles of *fibrils,* termed *fascicles.* Individual fibrils are in turn subdivided into increasingly smaller elements: *subfibrils*, *microfibrils*, and *tropocollagen* (Table 17-1). The principal subunit, the fascicle, varies in size and shape within a particular tendon and between tendons. The fascicles are separated by loosely and irregularly arranged collagen. Individual fascicles are not straight but are variably wrinkled (also termed *wavy* or *crimped*), an important fact in accounting for the centralized location of many tendon tears, so-called *core lesions.*

▮▮▮ CIRCUMSTANCES ASSOCIATED WITH NONLACERATIVE TENDON AND LIGAMENT INJURY

The fundamental injury in an acute strain is a stretching or tearing of the tendon. The flexor tendons may tear under a variety of circumstances, some of which are listed below (Table 17-2).

▮▮▮ CLINICAL PRESENTATIONS OF HORSES WITH METACARPAL OR METATARSAL REGION STRAINS OR SPRAINS

According to Denoix, horses with tendon or ligament injuries typically present in one of three ways: (1) exhibiting lameness with localizing signs (swelling, heat, pain), (2) exhibiting lameness without localizing signs, and (3) for nonspecific underperformance.[3] However, most serious strains or sprains produce visible swelling within 24 hours and are associated with noticeable lameness. The characteristic swelling that develops in the proximal half of either flexor tendon is known as a *high bow,* and swelling in the lower half is termed a *low bow* (Figure 17-6). A large

Table 17–2 • CIRCUMSTANCES IN WHICH A SERIOUS TENDON INJURY IS MOST LIKELY TO OCCUR

Causes	Comment
Fatigue	Typically occurs near the end of a race or vigorous training session when effort is greatest. The better an animal's conditioning and the more specific its event training, the less likely fatigue injuries are to occur. This axiom applies equally to short sprint-type races as well as longer endurance events.
Excessive effort	*Forced* maximal effort, especially near the end of a race, may cause a racehorse to lose its rhythm and become somewhat uncoordinated. In an athlete, this is known as failing to stay within one's capabilities, where increased effort leads to decreased coordination and thus poor efficiency.
Awkward or misstep, stumble	May occur on a trail ride over rough, slippery terrain while jumping a fence or barrier, or on a racetrack. Sometimes occurs for no known reason, but in each instance leads to some degree of momentary incoordination.
Minor collision	Most often associated with bumping during a race, causing the tendon to be stretched (loaded) in an unusual way.
Major collision	Tendon damaged in a fall or as a result of secondary injury caused by another involved horse.
Aggravation of a preexisting injury	Previously torn tendon has had insufficient time to heal and is thus predisposed to reinjury. Structural weakening caused by prior injury, especially to the superficial digital flexor tendon, greatly increases the odds of reinjury during a race.*
Insufficiency injury	Reinjury to a healed but structurally weakened area of a tendon. May also be termed a *pathologic strain.*
Culmination-type injury	This type of strain usually occurs in an animal that is running or jumping on an already inflamed tendon (running or jumping with tendonitis).
Interval training	A necessary but risky type of training required for the highest levels of performance.
Accelerated training schedule	Tendons and ligaments, like muscles, need time to become accustomed to sustained, forceful exercise such as horse racing. In general, the *gradual introduction* of speed and distance training produces fewer injuries than accelerated programs.

*From Cohen ND, Peloso JG, et al: Racing-related factors and results of prerace physical inspection and their association with musculoskeletal injuries incurred in Thoroughbreds during races, *J Am Vet Med Assoc* 211:452, 1997.

localized hematoma can occasionally mimic a bowed flexor tendon (Figure 17-7).

Microscopic and Biochemical Injury: Some Known and Theoretical Considerations

Goodship and co-workers wrote an excellent account describing how tendons and ligaments are injured and subsequently restored, a reference I wholeheartedly recommend.[4] The frequency of deep interior tears was explained by the fact that centrally located fascicles are less wrinkled or wavy than their peripheral counterparts. Thus, Goodship reasoned, the core fascicles have less reserve length; so when they are overextended, they tear first. Other, less straightforward mechanisms of tendon injury proposed by the authors included (1) exercise-induced hyperthermia, (2) reperfusion injury, (3) ischemia-hypoxia, and (4) subclinical core degeneration.

Exercise-Induced Intratendinous Hyperthermia. During vigorous exercise, body temperature normally rises to include that of flexor tendons, in one recorded instance to as much as 45° C.[5] Goodship and colleagues used the term *heat shock* to describe this phenomenon, theorizing that it may adversely alter the metabolism of tendon fibroblasts, leading to an inferior quality matrix and predisposing to injury. Obviously there are many gaps in the chain of circumstantial evidence.[4]

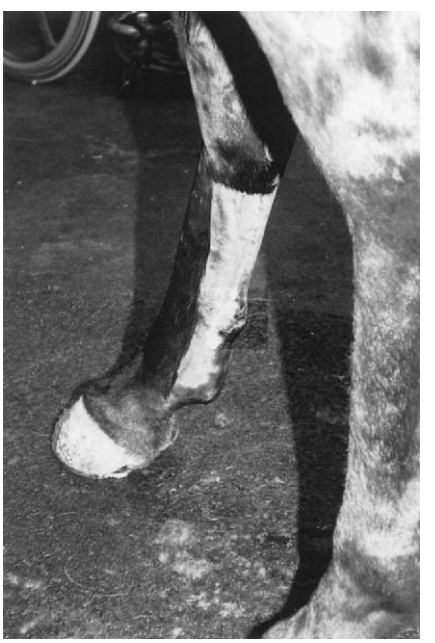


Figure 17-7 • Close-up view of a hematoma resembling a low bow (clipped in preparation for an ultrasound examination).

Reperfusion Injury. Physical changes in tendon diameter and length related to normal limb movements are accelerated during exercise, especially under maximal tensile load. This causes the intratendinous circulation to fluctuate, leading to the formation of potentially harmful *free radicals. Experimentally*, free radicals have been shown to reduce the reproductive capacity of cultured tenocytes taken from the central region of the superficial digital flexor tendon of a horse. Under similar experimental circumstances, the addition of a *free radical scavenger* prevented growth inhibition. To the best of my knowledge, free radial scavengers, such as vitamin E, have not yet proven to be a reliable means of preventing or lessening flexor tendon injuries in horses.[6]

Experimental Ligament Injury

Henry and co-workers described the sonographic appearance of experimental severed check ligaments in previously healthy ponies using the opposite undamaged limb as a control.[7]

Sonographic examinations of the freshly severed check ligaments showed thickening and hypoechogenicity attributed to transection, related hemorrhage, and edema. Predictably the normal linear appearance of the ligament was disrupted or lost altogether, as were its surgically severed margins. In subsequent progress examinations the healing ligament gradually grew brighter (an echogenic recovery attributed to the infiltration of fibrous tissue and collagen deposition). Eventually (about 6 months after being severed), the damaged ligament regained most of its normal linearity, width, and discrete margins.

Experimental Tendon Injury

Spurlock and co-workers reported the sonographic and histologic appearance of experimentally created lesions in the fore and hind superficial digital flexor tendons of seven otherwise healthy Thoroughbred horses.[8] The lesions were induced in three of the four limbs of each horse with various amounts of injectable collagenase, causing localized tendon destruction. The fourth leg was injected with saline, serving as an experimental control.

Predictably, the more collagenase injected, the greater the degree and extent of tendon damage and likewise the more hypoechoic the initial appearance of the lesion. As time passed—10 months in the case of one animal—the lesions gradually became more hyperechoic, attributable to fibrous tissue invasion and collagen deposition.

In my opinion, neither experimentally severing nor chemically destroying part of a tendon or ligament is capable of creating a sonographically realistic lesion. Naturally occurring lesions are far more complex, particularly regarding their effect on contiguous tissue, especially the regional blood supply. One need only observe the hyperemia that typically accompanies a fresh strain or sprain to appreciate this fact.

Magnetic Resonance, Sonographic, and Histologic Correlation of Acute and Subacute Tendon Injuries in Horses

Crass and co-workers, using dismembered equine limbs with previously diagnosed tendon injuries, compared magnetic resonance (MR), sonographic, and histologic appearances.[9] Their findings were as follows:

- All lesions were demonstrable with both ultrasound and magnetography.
- Lesions featuring blood, edema, and cellular accumulation appeared dark on ultrasound and bright on MR.
- As scarring occurred (fibrosis), MR became normal.
- Sonographically, tendons did not appear normal until fibrillar realignment took place.
- Both ultrasound and MR images correlated with observed histologic abnormalities.

▮▮▮ DESCRIPTION AND CLASSIFICATION OF ACUTE TENDON AND LIGAMENT INJURIES

Metacarpal and Metatarsal Zones: Identifying and Recording Lesion Location

Lesion location is usually recorded in one of three ways: (1) three primary and six secondary zones; (2) six primary zones; and (3) fixed, graduated tape measurement.[10] Each method serves not only to locate a lesion but also to relocate it readily in the event of a progress examination.

1. In the first method, the metacarpus or metatarsus is divided into three equal lengths extending from the palmar or plantar surface of the proximal cannon bone (some use the accessory carpal bone) to the proximal sesamoids, numbered one through three. Each of these primary zones is then subdivided into two equal parts, A and B. An individual lesion is identified according to its location, *zone 3B*, for example. Because of its greater length, some prefer adding an additional zone to the metatarsus *(zone 4).*
2. The second scheme (my preference) is quite similar, but instead of dividing the metacarpus or metatarsus into three parts, six are used, which eliminates the need for the A and B subdivisions. As with the first method, individual lesions are identified according to location, *zone 2,* for example. For more precision, decimals can be used, *zone 4.5*, for example.
3. Perhaps the simplest and most accurate method of identifying and recording lesion location is to affix a tape measure to the medial or lateral rear corner of the metacarpus or metatarsus, using the carpometacarpal or tarsometatarsal joint as the *zero point*. A lesion is then designated as being a certain

number of centimeters distal to that point, *27 cm*, for example.

Note: *It should be readily apparent that none of these methods is truly quantitative; that is to say, that even though numeric designations are used, none is capable of consistently reproducing identical results, but that is not their purpose. Rather, these schemes serve to relatively place a lesion within the region of suspected injury and to assist in relocating it in any future examination.*

Sonographic Description of Fresh Strains and Sprains

The following is my personal method of sonographically assessing fresh tendon and ligament injuries, particularly those involving the superficial and deep digital flexor tendons, check ligaments, and suspensory ligaments:

1. Tendon and ligament damage is usually found in one of four locations (as seen in a single cross-sectional image: (1) *central* (or core), (2) *peripheral*, (3) *radial*, and (4) *diffuse.*
2. By stringing together a series of consecutive cross-sectional images covering the full length of the injury, the size, shape, and position of the lesion can be estimated with reasonable accuracy.[11]
3. The foregoing information then allows for a *qualitative* estimate of the injury (e.g., mild, moderate, or severe sprain or strain).

▮▮▮ CLASSIFICATION BASED ON LESION SEVERITY

In 1977 I first proposed a classification for strain and sprain injuries in dogs, which I later modified for use in horses. The scheme, adapted from an existing classification used in human sports medicine, divides injuries into four categories according to severity: mild, moderate, severe, and complete rupture or avulsion. For those preferring a numeric classification, the terms *first, second, third,* and *fourth degree* can be substituted for the previously listed qualitative descriptors.[12]

First-Degree Strain or Sprain

More of a stretch than a tear, a mild strain or sprain features a barely perceptible loss in echogenicity with little or no change in texture.

Second-Degree Strain or Sprain

A moderate tear is characterized by a relatively discrete loss of echogenicity accompanied by abnormal texture.

Third-Degree Strain or Sprain

A severely torn tendon or ligament typically contains a discrete cavity or defect, a so-called *black hole,* with little or no recognizable interior pattern.

Complete Rupture or Avulsion (Fourth-Degree Strain or Sprain)

A complete rupture or avulsion is typically marked by localized or regional discontinuity, nearly always accompanied by a large hematoma.

▮▮▮ CLASSIFICATION BASED ON LESION ECHOGENICITY AND PATTERN (ECHOTEXTURE)

Genovese and Rantanen employ a similar method in which individual tendon lesions are classified or, as the authors term it, *typed* according to echogenicity. A mild tear, represented by a subtle loss in overall echogenicity with little appreciable change in texture, is termed a *type I* lesion. A *type II* lesion features a relatively greater and more obvious loss of echogenicity plus some degree of textural abnormality (usually a loss of definition). *Type III* lesions appear predominantly hypoechoic with fewer visible interior echoes, accompanied by a further loss in pattern detail. *Type IV,* or *"black hole lesions,"* as my students sometimes term them, appear as highly discrete, anechoic cavities with no discernible interior pattern. A normal tendon is termed *type 0*.[13]

▮▮▮ CLASSIFICATION BASED ON LESION LOCATION

Dyson and co-workers proposed a topographic classification scheme for suspensory injuries in which lesions are described according to their relative positions in the suspensory ligament. Categories include (1) proximal, (2) body, and (3) branch lesions.[14]

▮▮▮ OVERUSE INJURIES: TENDONITIS AND DESMITIS

Clarifying Terminology

In my opinion, the terms *tendonitis* and *desmitis* are best reserved for inflamed tendons or ligaments, not for acute overextension injuries or ruptures, which are better termed *strains* and *sprains.*

Causes and Susceptibility

Tendonitis and desmitis in horses typically result from overuse: in racehorses, for example, running *too far, too hard, too fast, too long*, and most importantly *too often.*

Tendonitis and desmitis resulting from overtraining are also quite common in jumping horses. Roping and barrel-racing horses are also susceptible to these sorts of injury because of their repeated abrupt starts, stops, and turns. Event horses are susceptible to overuse injuries because of the difficult terrain they may be required to negotiate, which among other things may be sloped, slippery, irregular, or loose.

Localized Versus Diffuse Disease

Localized Tendonitis or Desmitis. Localized tendonitis or desmitis is often associated with the origin or insertion of a tendon or ligament. Thus in chronic cases there may be bony remodeling or small osteophytes at these attachments. Regional disease appears to be little more than an expansion of what was originally a localized inflammation.

Diffuse Tendonitis or Desmitis. Diffuse tendonitis or desmitis, on the other hand, often seems to start in the central third of the tendon or ligament and subsequently spreads proximally or distally. Bear in mind that these are not highly predictable disease patterns but simply *tendencies*, albeit useful ones.

Imaging the Overuse Injury

Sonology. Many, but not all, overuse injuries are associated with a normal sonographic examination, similar to what has been found in people. Thus a normal sonogram can be compatible with a clinical diagnosis of tendonitis or desmitis but of course will not conclusively confirm it. Likewise, swelling, which often accompanies a serious strain or sprain, is usually absent with generalized desmitis or tendonitis, even when chronic. Some horses with overuse tendonitis or desmitis will have lesions that are so subtle that only an opposite side comparison will divulge their existence.

▮▮▮ SONOGRAPHIC IMAGING OF THE ACUTE FLEXOR TENDON INJURY

Scan Levels, Scan Angles, and Tendon Tension and Relaxation Scan Levels. The sonographic appearance of the superficial and deep flexor tendons, in particular their shape, depends most on the level at which they are examined; the further distally one goes, the more pronounced the difference.

Scan Angles

Note: *The angle at which the probe is held against the skin surface is the principal determinant of tendon echogenicity; a perpendicular relationship is ideal. Oblique probe angles cause one or both flexor tendons to appear overly dark, resembling a lesion. It is critical to bear this in mind during the course of an ultrasound examination, and this is the principal reason why experienced sonographers regularly rock the probe back and forth as they perform the examination, especially when they encounter a possible lesion.*

Tendon Tension and Relaxation. As might be expected, tendons examined while partially flexed (as they might be in a lame horse) differ from those in full extension. Regional buckling, shortening, and thickening resulting from non–weight bearing may substantially change the appearance of the tendons, making it difficult to identify all but the most obvious lesions.

Normal Sonographic Forelimb and Hindlimb Variations That May Mimic Flexor Tendon Injury

Sonographic Disease Indicators. The principal sonographic disease indicators associated with strains are similar to those seen with sprains. These include (1) increased size, (2) abnormal shape, (3) decreased echogenicity, (4) increased echogenicity, (5) nonuniform or otherwise abnormal interior pattern, (6) surrounding hemorrhage or edema, and (7) regional hyperemia.

Size

Increased. It is often prudent to image the opposite, presumably normal limb for comparison because of the wide variation in normal tendon thickness. Initially mild strains or sprains are usually accompanied by edema, whereas moderate or severe injuries are typically associated with overt hemorrhage, accounting for localized or regional swelling. Subsequently, inflammatory cells accumulate within the damaged tissues, adding to or maintaining the swelling. Peripherally situated lesions may imperceptibly merge into surrounding hemorrhage and edema, escaping detection, or, alternatively, make the tendon appear smaller than it actually is.

Decreased. Denoix asserts that tendons and ligaments may undergo disuse atrophy, a claim I have been unable to substantiate other than with nonunion fractures and certain neurologic diseases.[15] Muscle atrophy does cause associated tendons (and joints) to tighten, however, which can affect their sonographic appearance. Anyone who has had a cast removed after several weeks will have experienced this phenomenon firsthand.

Abnormal Shape

Peripheral tendon lesions may change the associated tendon contour, often causing it to bulge slightly. Badly torn tendons sometimes appear to be split in two or to have tissue tags hanging from their injured surfaces. Occasionally tendons are mildly deformed by large

nearby hematomas or, in the case of the flexor tendons, an adjacent lesion. Centrally located lesions (so-called core lesions) usually do not change the shape of the tendon per se but rather uniformly enlarge it.

Echogenicity

Reduced. Decreased echogenicity is the single most defining indicator of tendon or ligament injury (strain or sprain) because of the ease with which it can be sonographically detected. Furthermore, the return of a previously torn tendon to normal echogenicity is a relatively reliable indicator of healing but not of tendon strength or distensibility. As already mentioned, decreased echogenicity is also seen with some nonperpendicular scan angles.

Increased. Mechanical sector scanners often produce a bright, centrally located beam superimposed over an otherwise normal triangular image; this is termed a *bang artifact*. Resolving blood clots may show a gradual increase in echogenicity, as can the formation of scar tissue, dystrophic calcification, and cartilage metaplasia.

Interior Changes

Sometimes referred to as *altered echotexture*, changes in the appearance of a tendon's interior usually accompany serious injury. Excluding reduced echogenicity, the most visible evidence of an overstretched or torn tendon or ligament is a localized or regional loss of a normal interior pattern, often rather imaginatively referred to as a *disrupted*, *misaligned*, or *weak fiber pattern*.[16]

Most serious tendon and ligament injuries are associated with surrounding hemorrhage and edema within 24 to 48 hours of occurrence, depending on how rapidly and effectively the injury is treated.

Associated Hemorrhage and Edema

Hemorrhage and edema associated with an acute tendon strain may develop acutely, or they may be delayed for up to 24 hours. Generally the more rapidly the swelling develops and the greater its magnitude, the more serious the injury.

Regional Hyperemia

Nearly all acute strains are associated with an increased regional blood supply, which usually develops within a few hours of the injury. Hyperemia is what accounts for the increased heat associated with most acute injuries.

Sonographic Examples of Fresh Superficial and Deep Digital Flexor Strains

The following examples of superficial and deep digital flexor tendon injuries illustrate the preceding sonographic disease indicators (Figures 17-8 through 17-16).

Sonographic Appearance and Significance of Flexor Tendon Sheath Effusion

Abnormal filling of the flexor tendon sheath is typically characterized by swelling on the palmar or plantar aspect of the distal metacarpus or metatarsus, which begins just proximal to the sesamoids and extends distally to the middle phalanx. Spaulding published an excellent pictorial essay of this anatomically complex region, which among other things shows how it is possible to distinguish sonographically a swollen joint from a distended digital sheath.[17]

Filling of this sort *may or may not* indicate tendon tearing. Often the *persistence* of such swelling provides insight into its seriousness. For example, flexor tendon sheath swelling that develops after a competitive 3-day trail ride and subsides spontaneously in 24 to 48 hours probably requires little more than icing and compression (Figure 17-17). On the other hand, a similar swelling that persists for 2 or 3 weeks after such an event bears further scrutiny, ideally in the form of an ultrasound examination.

Wilderjans and co-workers recently reported an unusual, difficult-to-diagnose flexor tendon injury causing swelling of the associated tendon sheath and secondary impingement by the annular ligament. Specifically, the authors described an eccentrically located area of decreased echogenicity seen in a cross-sectional view of the deep flexor tendon, which they attributed to a *vertical tear* and later confirmed using tenoscopy.

Additional sonographic abnormalities included (1) irregularity along the lateral margin of the deep flexor tendon, (2) echogenic material lying to either side of the deep digital flexor tendon, and (3) a large volume

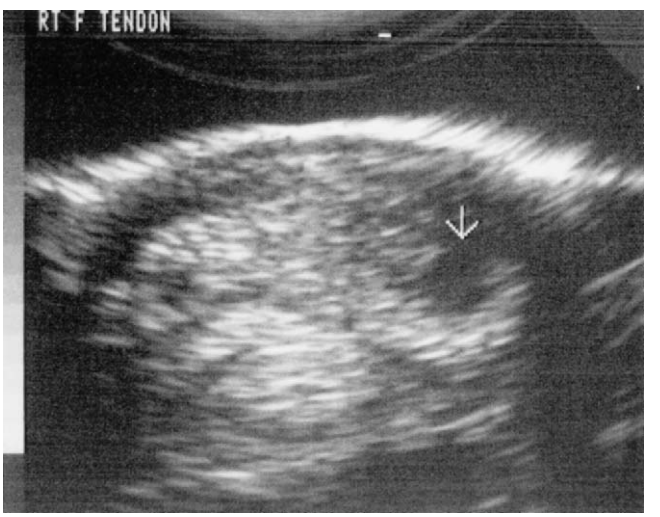


Figure 17-8 • Close-up view of an eccentric tear in the superficial digital flexor tendon *(zone 1)*.

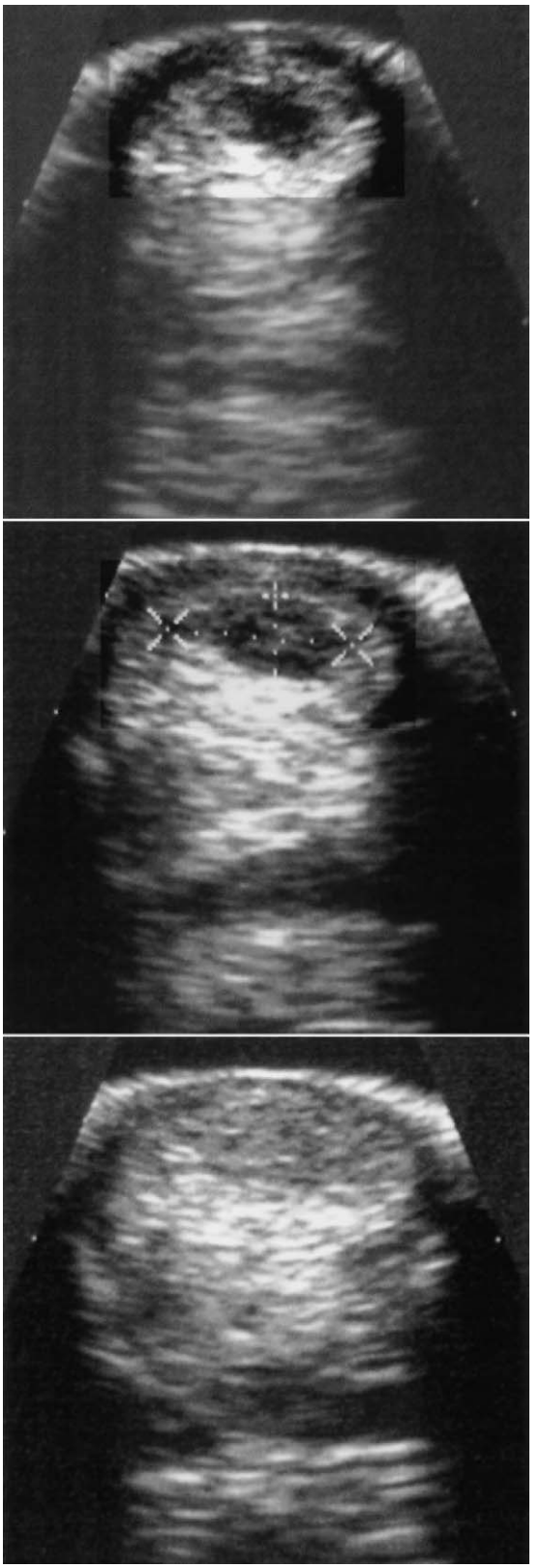


Figure 17-9 • The changing "faces" of a centrally located, three-level tear in the superficial digital flexor tendon involving zone 2 **(A),** zone 3 **(B),** and zone 4 **(C).** A long sectional view of zone 4 **(D)** shows central swelling and decreased echogenicity.



Figure 17-10 • Close-up view of a uniformly swollen deep digital flexor tendon (marked by cursors).



Figure 17-11 • Close-up view of a pair of adjoining peripheral tears in the palmar aspect of the deep digital flexor tendon.



Figure 17-12 • Close-up view of a Z-shaped radial tear in the dorsal half of the deep digital flexor tendon.



Figure 17-13 • Close-up view of an immense tear in the center of the deep digital flexor tendon.

of anechoic fluid in the deep digital flexor tendon sheath (Figure 17-18). Images of 7 of 17 affected horses were described as being normal, a surprising finding because a severely swollen deep digital flexor tendon sheath can usually be inferred from a lateral radiograph.[18]

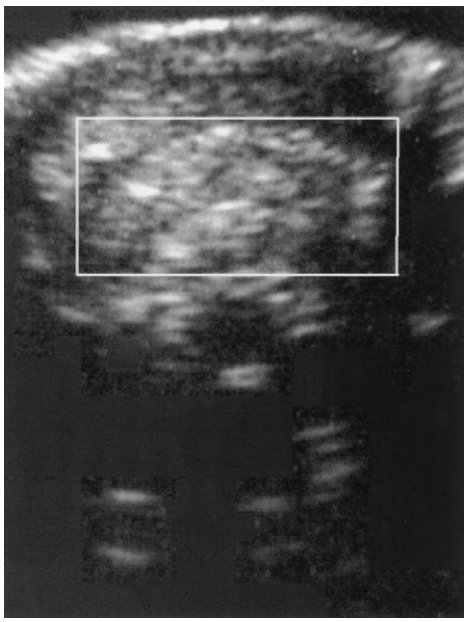


Figure 17-14 • Close-up view of a spiral tear involving most of the deep digital flexor tendon.



Figure 17-15 • Close-up view of a badly damaged deep digital flexor tendon, a portion of which has been torn away (left center) by a ragged piece of sheet metal. Blood surrounds and dissects what remains of the tendon.

▮▮▮ ALTERNATE IMAGING OF THE ACUTE FLEXOR TENDON INJURY

Radiology

Although it is possible to *infer* flexor tendon injury from associated soft-tissue swelling, such injuries are impossible to confirm radiographically. On the other hand, radiographs are indispensable for screening purposes, especially to confirm or deny associated fractures or dislocations.

Tendography (Tendonography)

Verschooten and DeMoor were among the first to describe the clinical use of tendography.[19] Potential

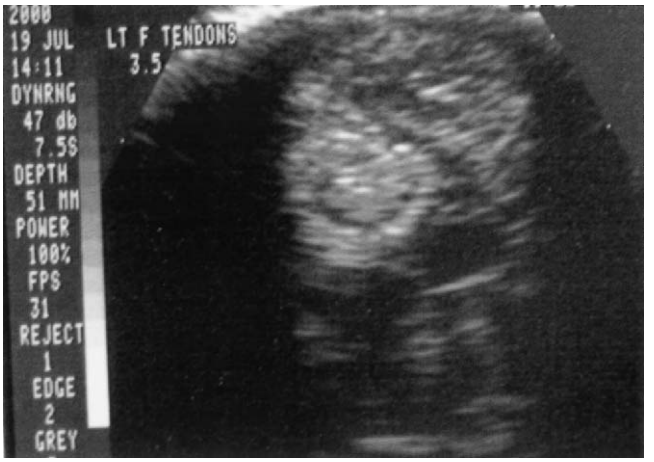


Figure 17-16 • Close-up view of a swollen superficial digital flexor tendon with a peripheral V-shaped tear and a deep digital flexor tendon containing a distinctive ring tear.

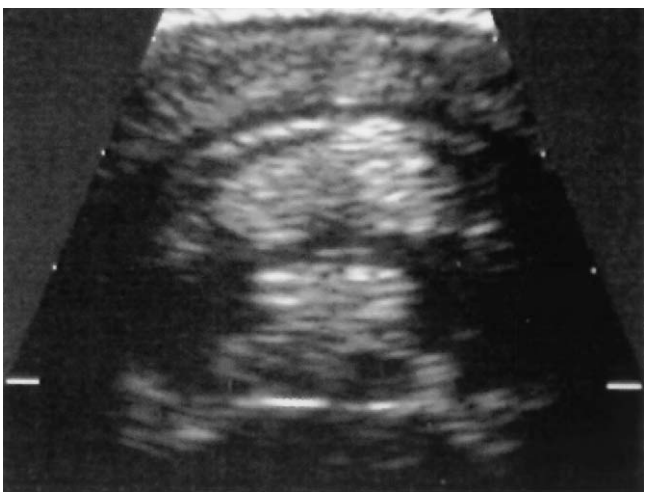


Figure 17-17 • Transient, cool, nonpainful filling of the tarsal sheath (just below the fetlock) without associated tendon injury (the dark circular area in the left center of the uppermost tendon proved to be a scan-angle artifact). The swelling that regularly occurred immediately after a trail ride was not associated with visible lameness and usually dissipated within a week.

diagnostic information obtained by tendonography is detailed below (Box 17-1).

Types of Tendography

Negative-Contrast Tendography (Air Tendography). Air tendography has been used in both clinical and experimental settings to identify injuries and to perform postoperative evaluation of tendon grafts.[20,21] Tendography is capable of identifying various abnormalities in the superficial and deep digital flexor tendons, including (1) tears, (2) discontinuity, (3) avulsion, (4) thickening, and (5) peritendinous adhesions.

Box 17-1
Potential Diagnostic Information Obtained by Single- or Double-Contrast Tendography

Tendon sheath perforation or complete rupture
Tendon sheath thickening
Tendon sheath stenosis
Tendon sheath adhesion
Tendon sheath sinus (communication with, and synovial fluid drainage from, a sinus in the nearby skin)
Tendon-sheath fistula (abnormal communication between tendon sheath cavity and nearby tissue or organ other than the skin)
Intrasynovial tendon sheath masses, mass effects (e.g., hematoma), and foreign bodies
Extrasynovial tendon sheath masses, mass effects, and foreign bodies

Positive-Contrast Tendography. Positive-contrast tendography is performed in a manner similar to that of air tendography, but with a diagnostic iodine solution rather than air. Xeroradiography may be substituted for radiography, with some improvement in tendon detail.[22]

Tendographic Techniques

Air tendography is performed as follows:

- A lateral radiograph of the metacarpal region is made using soft-tissue technique.
- Once the radiographic technique proves satisfactory, a pair of tourniquets is applied—one just above the carpus, the other just below the fetlock—to retain as much of the injected air as possible in the desired location.
- Room air, 30 to 40 ml, is then injected subcutaneously around the superficial digital flexor tendons in the caudal aspect of the midmediocarpal region (sonographic zones 3 and 4).
- A lateral view of the metacarpus is made to determine whether the subcutaneous air is adequately distributed around the flexor tendons. If not, slowly flex the leg three or four times, and repeat the lateral film. If the distribution is still unsatisfactory, add another 20 ml of air, re-flex the leg, and make another test image.
- Once the desired air distribution is obtained, make the following images: (1) full-length lateral (including the carpometacarpal [tarsometatarsal] and fetlock joints), (2) flexed lateral, and (3) frontal views.
- Adjust radiographic technique, and make additional oblique views as needed.

Iodine tendography is performed as follows:

Caution: *The instillation of an ionic diagnostic iodine solution into the tendon sheath cavity can cause varying degrees of inflammation, including a transient increase in fluid*

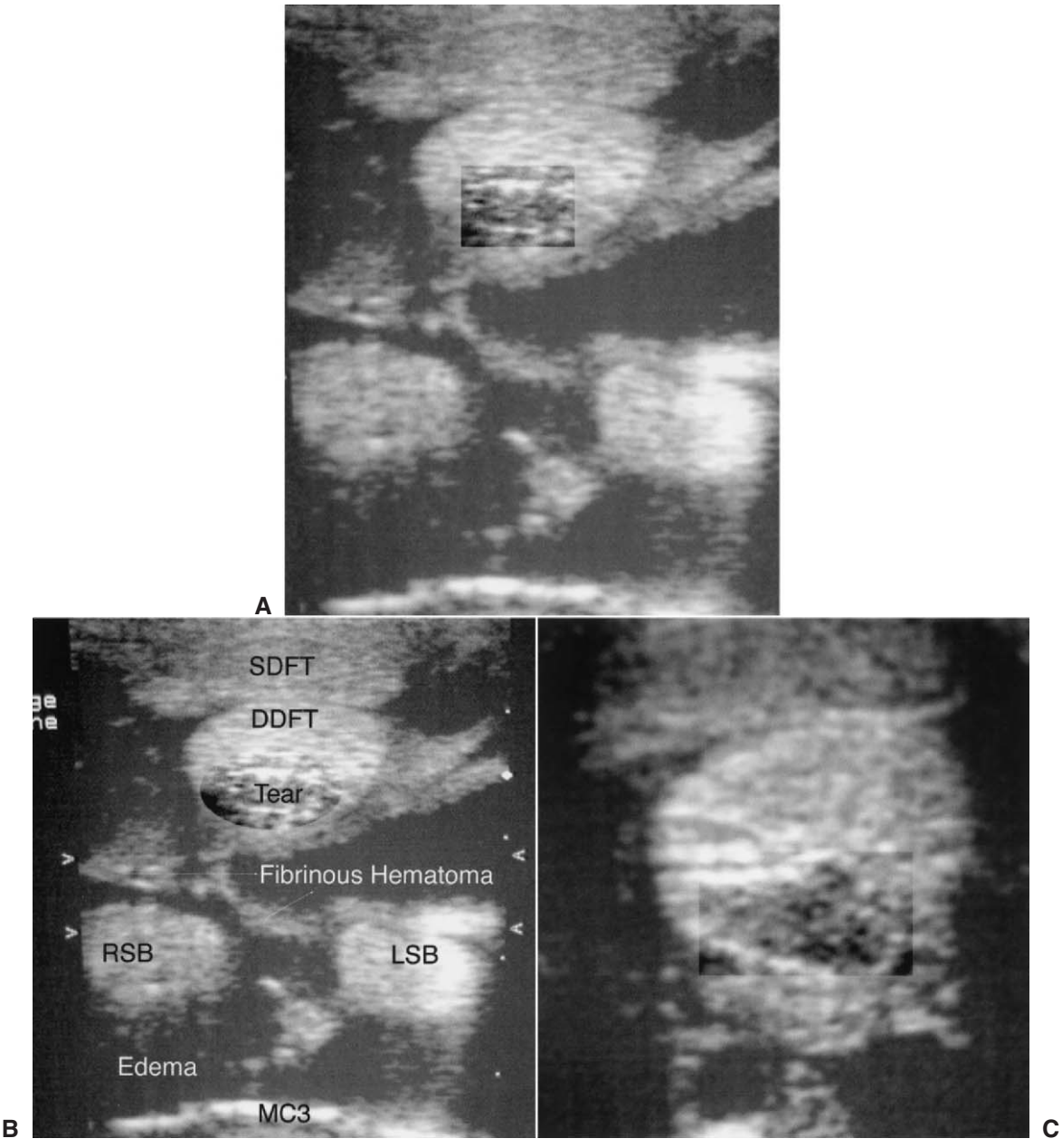


Figure 17-18 • Close-up **(A),** labeled close-up **(B),** and ultra-close-up **(C)** views of a peripheral tear in the palmar aspect of the deep digital flexor tendon causing marginal bleeding, hematoma, and filling of the digital sheath (see *emphasis zones*).

volume. The use of nonionic contrast media can partially overcome these effects.

Double-contrast tendography is performed as follows:

Both air and diagnostic opaque are instilled into the tendon sheath cavity, unlike positive and negative tendography, in which only a single contrast agent is used.

Normal Tendographic Anatomy. Hago and Vaughn, among others, described the normal radiographic anatomy of equine tendon sheaths and bursae.[23]

▮▮▮ NUCLEAR IMAGING AND THERMOGRAPHY

Nuclear Imaging (Nuclear Medicine, Scintigraphy)

Indication. Determining whether a particular tendon abnormality is clinically relevant is not always easy, particularly if the horse in question is not lame or painful to palpation. Findings of this sort are occasionally found when scanning a supposedly normal limb as a control. In such instances, comparative nuclear scintigraphy can often establish whether the discovery represents an actual lesion (increased activ-

ity compared with adjacent tendon) or is merely an incidental finding (i.e., there is no difference between the "lesion" and surrounding tendon). Nuclear medicine may also detect the existence of an unsuspected bone lesion or tendon lesion in a horse that earlier was found to be radiographically and sonographically normal.[24]

Thermography

Turner reviewed the diagnostic applications of thermography in the horse, including strains and sprains of the superficial and deep digital flexor tendons, check ligament, and suspensory ligament.[25] Thermographically, both strains and sprains appear as areas of increased heat emission, termed *thermal patterns, thermal zones,* or *simply hot spots.*

With some minor injuries, thermographic detection may precede physical or sonographic detection by as much as 2 weeks. Debilitating, hard-to-isolate muscle strains that defy other forms of medical imaging may be amenable to thermographic diagnosis, especially those involving the large muscle groups of the upper forelimb, thigh, rump, and back. The same is true of muscles that are difficult or impossible to palpate directly.[26]

▮▮▮ SONOGRAPHY

Sonographic Appearance of Metacarpal Check Ligament Injury

Check ligament injuries are, of course, confined to the upper half of the metacarpus. Unlike suspensory injuries, which can be ambiguous because of hypoechoic muscle tissue, torn check ligaments are usually more straightforward, thanks to their uniform composition and greater echogenicity. Diffuse lesions may be missed because of their resemblance to normal suspensory tissue (Figure 17-19).

Sonographic Imaging of the Acute Suspensory Injury

Normal Sonographic Forelimb and Hindlimb Variations That May Mimic Suspensory Injury. Grossly the normal suspensory ligament is relatively uniform in thickness over most of its length. Likewise its lateral and medial branches are comparable in size and shape. However, this is not the case sonographically, especially in the forelimb, where the suspensory body may vary considerably from level to level in an individual animal and from horse to horse.

Dyson and co-workers studied the sonographic appearance of the front and hind suspensory ligaments in 350 clinically normal horses and ponies and concluded the following (Boxes 17-2 and 17-3).[16]

Potential Sonographic Lesions Found in Injured Suspensory Ligaments. Most suspensory lesions appear as centrally located, relatively discrete areas of reduced echogenicity (Figure 17-20). Some are geometrically shaped: circles, ovals, rectangles, and trapezoids; others resemble fabric tears (Figure 17-21). Lesion length and position within the suspensory ligament are also quite variable, with some lesions situated within a single zone (i.e., zone 1-6), whereas others extend through multiple zones.

Dyson and co-workers described the following sonographic abnormalities associated with suspensory ligament injury (Box 17-4). They advocated scanning

Box 17-2
Sonographic Variations That May Be Seen in the Normal Suspensory Ligament of the Forelimb

Ligament may arise from two distinct heads separated by a less echogenic band.
Dorsal border just below accessory carpal bone appears ill defined or, alternatively, appears relatively hypoechoic (latter observation made in 9% of animals scanned).
Echogenicity is similar bilaterally but often differs between individuals.
A well- or poorly circumscribed area of reduced echogenicity, variable in length, was present in the proximal third of the suspensory ligament in 13% of the animals scanned.
4% of the animals scanned exhibited a patchy rather than usual uniform echogenicity.

Box 17-3
Sonographic Variations That May Be Seen in the Normal Suspensory Ligament of the Hindlimb

Echogenicity is more consistent between horses compared with front suspensory.
Shadowing artifacts and hypoechoic lines on the dorsal aspect of blood vessels interfere with image quality proximally.

Box 17-4
Potential Lesions Associated With Suspensory Injury

Focal or regional swelling.
Ill-defined margination, especially dorsally.
A circular, well-circumscribed area of decreased echogenicity.
A roughly circular, oval, or rectangular-shaped, poorly marginated area of decreased echogenicity.
Multiple small circular or oval-shaped hypoechoic foci, usually found in a cluster.
Vertical, transverse, or diagonal hypoechoic bands or lines (Z tears, V tears).
Star-shaped or stellate hypoechoic area.
Ragged, poorly defined area of decreased echogenicity.

Modified and expanded from Dyson SJ, Arthur RM, et al: Suspensory ligament desmitis, *Vet Clin N Am* 11:177, 1995.

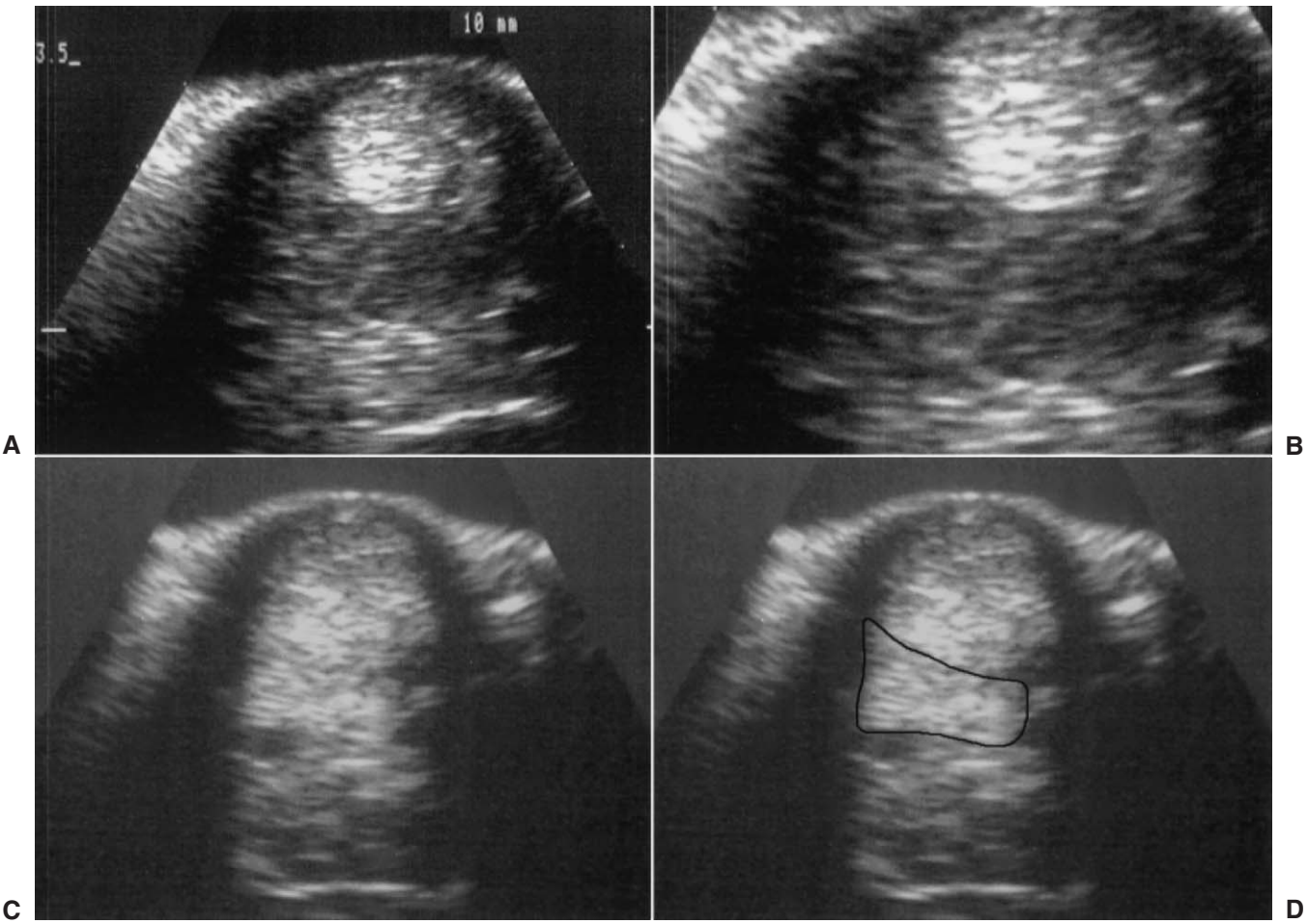


Figure 17-19 • Close-up **(A)** and ultra-close-up **(B)** views of a diffusely torn check ligament. Close-up **(C)** and traced close-up **(D)** views of the normal opposite check ligament are provided for comparison.

the opposite leg as a control because in most horses the suspensory ligaments are sonographically comparable (although there are individual differences). Dyson also warned against using overly high-gain settings that may conceal subtle lesions.

▮▮▮ ALTERNATE IMAGING OF THE ACUTE SUSPENSORY INJURY

Radiology

A variety of bony abnormalities may be found in association with an acute or chronic suspensory injury, but it is often impossible to know whether or not they are *incidental* (Box 17-5).

Stress Radiography

Ligaments and, to a lesser extent, tendons set the *outer limits* to normal joint motion. Thus the demonstration of excessive movement by one or more bones within a particular joint infers a sprain, rupture, or sprain-avulsion fracture. This is the role of stress radiography.

Specific Stress Maneuvers. Stress radiography is ideally performed by an experienced person with a specific objective, for example, establishing that the lateral branch of the suspensory ligament has been ruptured by demonstrating abnormal medial displacement of the fetlock joint. This characteristic displacement of the metacarpophalangeal joint is achieved with what is termed a fulcrum-assisted, medial-flexion maneuver, one of a variety of stress maneuvers designed to show that a particular joint *exceeds its normal range of motion*. Other stress maneuvers are listed in Table 17-3.

Procedural Considerations. For safety reasons, stress radiography is best performed in unconscious horses. Forcing a horse to try to stand on a badly sprained leg by holding up its opposite limb is not only painful but can result in collapse, potentially aggravating the injury and, worse, injuring the radiographer and his or her assistants.

An experienced radiographer, while holding the injured limb off the ground, can perform certain stress maneuvers, but these are painful and require sedation, which increases the animal's instability and the likeli-

Box 17-5
Radiographic Abnormalities Involving the Caudoproximal Aspect of the Third Metacarpal or Metatarsal Bones That May Accompany Suspensory Injury

A displaced, saucer-type cortical fracture, inferring suspensory avulsion*
A dark band or line indicating a fresh but incomplete fracture†
Localized cortical thickening suggesting periosteal injury
Localized cortical thickening and increase in overall bone density suggesting healing stress fracture
A fully mature callous compatible with a healed fracture
Increased medullary density inferring repair of a previous injury
Decreased trabecular detail, inferring the deposition of medullary new bone or the additive effects of one or more superimposed cortices‡

*From Bramlage L: Avulsion fractures of the origin of the suspensory ligament in the horse. In *Proceedings of the 35th Annual Convention of the American Association of Equine Practitioners*, Boston, Mass., 1989, pp 245-247.
†From Lloyd K, Koblik P, et al: Incomplete palmar fractures of the proximal extremity of the third metacarpal bone in horses: ten cases (1981-1986), *J Am Vet Med Assoc* 192:798, 1988.
‡From Dyson S: Some observations on lameness associated with the proximal metacarpal region, *Equine Vet J* 6:43, 1988.

Table 17–3 • SPECIFIC STRESS MANEUVERS AND THEIR PURPOSES*

Fulcrum-assisted hyperextension	Best suited to showing hyperextension of the fetlock joint related to 3rd-degree sprain of the suspensory ligament or 3rd-degree strain of the superficial or deep digital flexor tendons
Fulcrum-assisted hyperflexion	Best suited to showing hyperextension of the fetlock joint related to full-thickness laceration of one or more of the extensor tendons.
Fulcrum-assisted medial flexion	Typically used to show 3rd-degree sprain of the lateral collateral ligament.
Fulcrum-assisted lateral flexion	Typically used to show 3rd-degree sprain of the medial collateral ligament.
Clockwise axial rotation	Best suited to demonstrating 3rd-degree collateral or suspensory sprains not demonstrable with fulcrum-assisted maneuvers.
Counterclockwise axial rotation	Best suited to demonstrating 3rd-degree collateral or suspensory sprains not demonstrable with fulcrum-assisted maneuvers.
Traction stress	May sometimes reveal small periarticular fractures or osteochondritis fragments that cannot be confirmed radiographically.

*For use in unconscious horses only.



Figure 17-20 • A slightly eccentric circular tear is present in the body of the suspensory ligament.

hood of a fall. If a horse is anesthetized to perform stress radiography, the benefits of such an examination must be carefully weighed against the risks of a stormy recovery and the possibility of further injury.

Nuclear Imaging

Edwards and co-workers reported using radiology and scintigraphy to diagnose avulsion fractures of the proximal part of the third metacarpal bone related to third-degree sprain of the suspensory ligament.[27]

With the exception of a discrete fracture fragment—or fracture line (in the case of a nondisplaced fracture)—the radiographic indications of a serious suspensory injury were often vague and nonspecific, frequently requiring opposite-leg comparison. These included (1) localized bone loss, (2) localized bone deposition, and (3) increased bone density or sclerosis.

The prime scintigraphic indication of fracture was increased uptake in the proximal aspect of the third metacarpal bone. Not surprisingly, combined radiographic-scintigraphic imaging proved more diagnostic than either radiography or nuclear medicine alone.

Chronic Desmitis Leading to Acute Tear or Rupture of the Suspensory Ligament

Catastrophic (Irreparable) Injury to the Forelimb Suspensory Apparatus. A catastrophic injury to the forelimb suspensory apparatus is one that causes such severe destabilization of the fetlock joint that the horse must be destroyed. Hill and co-workers believe that minor preexisting suspensory injury may predispose to future failure.[28]

SONOGRAPHIC MONITORING OF TENDON AND LIGAMENT INJURIES

There is value, but not precision, in sonographically monitoring the progress of a sprained or completely ruptured suspensory ligament. Individual lesions, no matter their appearance, size, length, or location, do not in my experience heal consistently. While most suspensory lesions change with time—usually

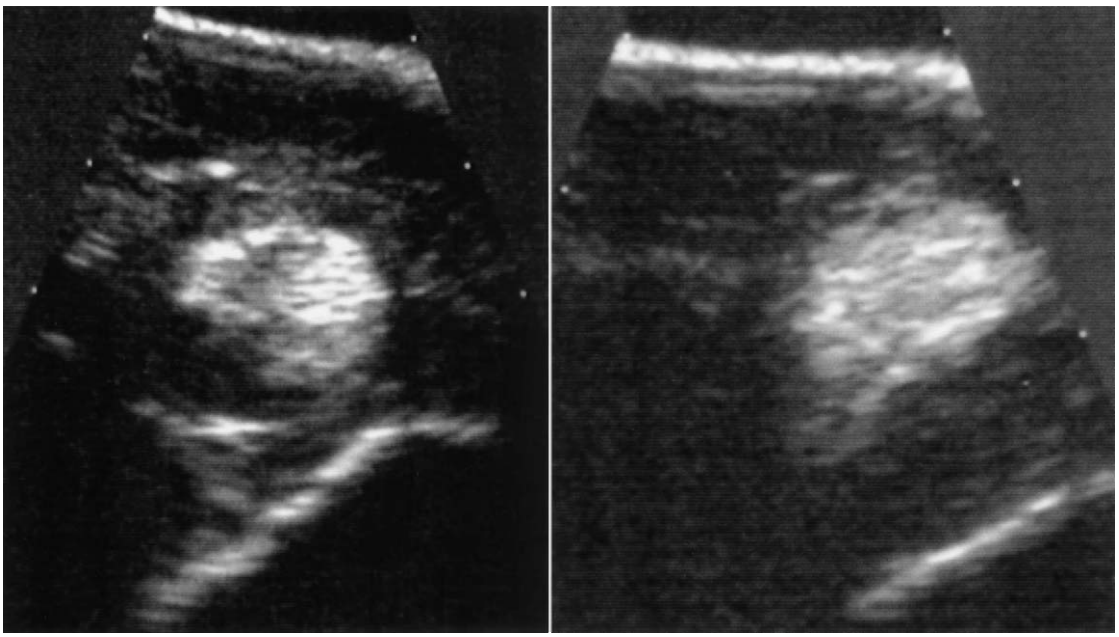


Figure 17-21 • A, A central Z-shaped tear combined with a large margin defect are present in the medial branch of the suspensory ligament. **B,** An image of the normal lateral suspensory branch is provided for comparison.

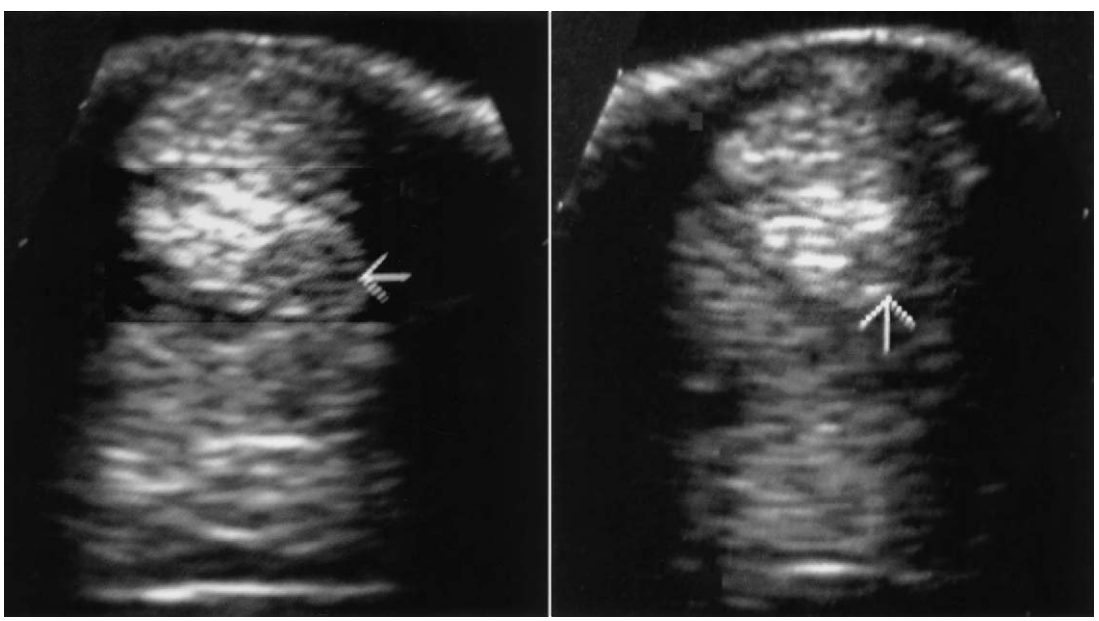


Figure 17-22 • A, Close-up view of a fresh eccentric tear in the deep digital flexor tendon marked with an arrow. **B,** A 1-month progress check shows that the lesion has become smaller and more echogenic. The dark, irregular band running vertically along the right edge of the image is a scan-angle artifact.

becoming smaller and more echogenic (Figure 17-22)—some do the opposite, becoming larger and darker in appearance (at least in the first few weeks after the initial tear. Occasionally, suspensory lesions fail to change, neither increasing nor decreasing in size, or changing echogenicity (Figure 17-23).

Van Schie and co-workers showed that *quantitative* sonographic evaluation of isolated equine superficial flexor tendons, containing both acute and chronic strains, was potentially error prone. Specific sources of examination error included: (1) gain setting, (2) scanner-skin angle, and (3) amount of scanner-skin offset. Even slight variations in any of these variables were capable of having a considerable effect on the gray scale values of the sonographic image.[29]

I performed similar quantitative sonographic evaluations on clinical cases over twenty years ago, but eventually abandoned such measurements as less reliable than an experienced subjective assessment.

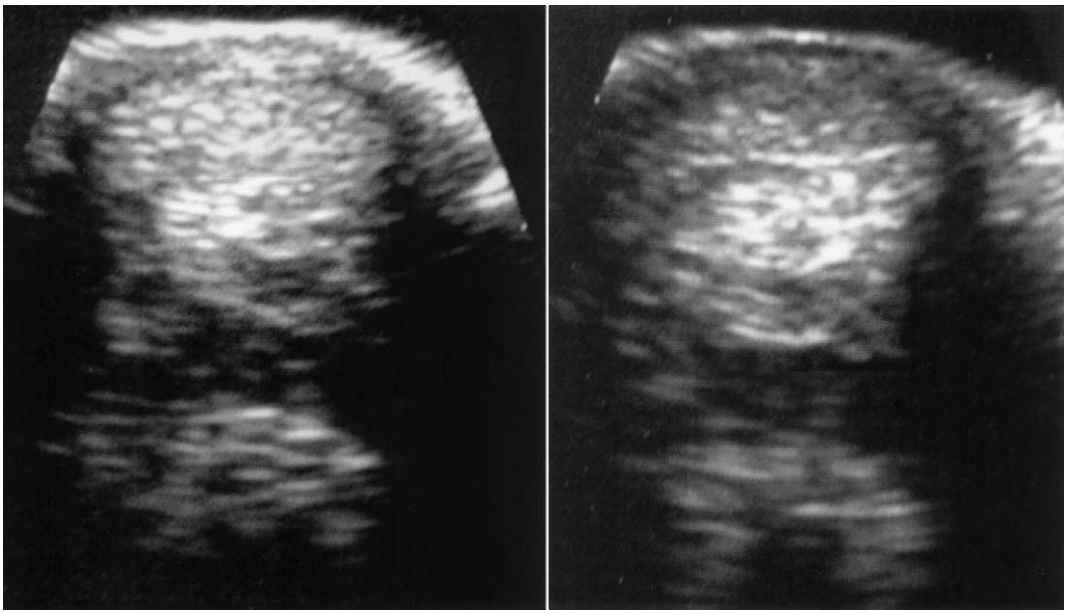


Figure 17-23 • Close-up views of a centrally damaged deep flexor tendon made immediately after **(A)** and 5 weeks after **(B)** a racing injury show very little change, although the related swelling has nearly disappeared and the leg is less painful.

What Can Be Concluded from Sonographic Monitoring?

What, then, may one conclude from sequential sonographic observations made in the weeks and months after a serious suspensory injury (grade II or III)? In my experience, the following generalities appear justified.

1. *Restoration equals healing*, but not necessarily a full return to preinjury flexibility, strength, and, by inference, performance.
2. The more rapidly a torn suspensory ligament heals, the better the prognosis for a full return to function, *provided the horse is gradually reconditioned and does not reinjure itself in the process.*
3. The slower a suspensory tear heals, the more serious the injury, irrespective of initial size and location.
4. The implications of slow or delayed healing are (1) greater tissue damage than originally estimated, especially to blood supply; (2) premature return to training or use; and (3) reinjury.
5. Given what is currently known (and of equal importance, what is not known) about the healing of ligaments in general and the suspensory ligament in particular, prognosis based *solely* on sequential sonographic appearances can be difficult and possibly inaccurate.
6. Sonographic diagnosis and prognosis should always be *contextual,* taking into account both clinical and imaging appearances.
7. Finally, it should be anticipated that the initial *prognosis might require modification* (upgrading or downgrading) according to what sequential sonographic examinations reveal.

Using Sonographic Monitoring to Evaluate Treatment Efficacy of the Superficial Digital Flexor Tendon

Tsukiyama and co-workers described how histographic analysis of standardized progress sonograms could be used to monitor and assess healing in previously injured superficial digital flexor tendons.[30] Reef proposed assessing treatment effectiveness based on five sonographically determined injury features: (1) lesion length, (2) lesion echogenicity, (3) lesion fiber alignment, (4) lesion cross-sectional area, and (5) tendon cross-sectional area. Each individual tendon zone is assessed using the foregoing criteria, and then the results are summed (or scored).[31]

In summary, there are three essential scoring elements:

1. ***Total lesion area*** (area of lesion divided by total tendon area; Table 17-4).
2. ***Estimated lesion echogenicity*** (see echogenicity scoring table; Table 17-5).
3. ***Estimated fiber alignment*** (see fiber alignment scoring table; Table 17-6).

Recommended Sonographic Recheck Schedule

Reef recommends the following sonographic recheck schedule:

- Initial sonographic recheck should be performed 8 weeks after injury or, alternatively, 8 weeks after the start of treatment.
- Subsequent sonographic rechecks should be performed every 8 weeks thereafter or, alternatively, before any increase in the horse's "exercise level."
- Presumably, sonographic rechecks stop once the tendon has healed, although no specifics were provided.

Sonographic Appearance and Tendon Rehabilitation

Reef further attempted to relate rehabilitative exercise with the sonographic postinjury appearance of the superficial digital flexor tendon.[31] Her recommendations are as follows:

- Incremental increases in exercise should be accompanied by sonographic improvement in the appearance of the injured tendon, including: (1) decreased *tendon* cross-sectional area, (2) decreased *lesion* cross-sectional area, (3) increased tendon echogenicity, and (4) improved tendon fiber alignment.
- Exercise level should remain unchanged if the total tendon cross-sectional area is increased by 10 percent compared with the most recent progress examination or, alternatively, if the injury cross-section within a single tendon zone is increased by 20 percent.
- Generalized or localized increases in cross-sectional area as identified in sonographic rechecks may indicate excessive rehabilitation or, worse, reinjury.
- When a sonographic recheck reveals worsening, rehabilitative programs should be cut back until sonographic improvement occurs.
- Horses should not begin galloping or cantering for at least 6 months after treatment or if the injury is likely to be aggravated.
- In the case of severe tendon injuries, galloping or cantering should be postponed for 9 to 12 months.
- Visible improvement in fiber alignment *before the start of galloping or cantering* is a critical factor in determining rehabilitative success.

Table 17–4 • LESION SEVERITY SCORING TABLE FOR SUPERFICIAL DIGITAL FLEXOR TENDON

Percent of Tendon Involved	Lesion Severity
≤15	Mild
16-25	Moderate
>25	Severe

Most normal Thoroughbreds and Standardbreds have a total tendon area between 5 and 6 cm^2 for six tendon zones or divisions, 6 and 7 cm^2 for seven zones, and 7 and 8 cm^2 for eight zones.

Table 17–5 • ECHOGENICITY SCORING TABLE FOR SUPERFICIAL DIGITAL FLEXOR TENDON

Echogenicity	Score
Normal to near-normal echogenicity	0
Mostly echogenic	1
50% echogenic, 50% anechoic	2
Mostly anechoic	3

Table 17–6 • FIBER ALIGNMENT SCORING TABLE FOR SUPERFICIAL DIGITAL FLEXOR TENDON

Fiber Alignment	Score
75% to 100% parallel fiber alignment	0
50% to 75% parallel fiber alignment	1
25% to 50% parallel fiber alignment	2
0% to 25% parallel fiber alignment	3

Postoperative Complications Associated With Repair of Serious Suspensory Injuries

Bowman and co-workers reported various primary and secondary problems associated with fetlock arthrodesis performed as a salvage procedure in horses with badly injured suspensory ligaments. Most of these were radiographic diagnoses, including (1) surgical infection, (2) implant dislocation, (3) implant breakage, and (4) laminitis.[32]

▮▮▮ TENDON LACERATIONS

Tendon Healing

Watkins and co-workers experimentally wounded superficial digital flexor tendons in healthy horses to determine how they healed.[33] Their histologic findings were as follows:

- Cells located outside the lacerated tendon are primarily responsible for its repair.
- This *outside-in type* of repair leads to an overly large scar at the point of separation and to adhesions.
- The scar is composed of both *type 1* and *type 3* collagen fibers, the latter being weaker and less distensible than the former, the primary constituent of normal tendon.
- Thus the scar becomes an area of potential weakness, theoretically subject to future sprain.
- Biomechanically, injuries of this sort are potentially amenable to regular, purposeful physiotherapy.[34]

Strasser and Solamen contend that marginal tears are more likely to be aggravated during controlled, postinjury exercise than lesions located entirely within the tendon interior.[35]

Flexor Tendons

Taylor and co-workers described the surgical treatment and outcome of 50 horses with superficial or deep flexor tendon lacerations.[36] Among their findings were the following:

- The fact that one or both flexor tendons were injured made no difference in outcome.
- The time interval between injury and treatment had no bearing on outcome.
- Wound debridement and infection were inversely related.
- Suturing the lacerated tendon(s) proved no more effective than leaving them unattached.
- Lacerated tendons inside the digital sheath did not heal as well as those located outside the sheath.

Dorsally Situated Metacarpal and Metatarsal Tendon Injuries

Belknap and co-workers reported the clinical aspects of 50 cases of extensor tendon laceration, 89 percent of which involved the hindlimb, specifically, the long digital extensor or lateral digital extensor tendon (Figure 17-24). In the forelimb, the most commonly injured tendons were the common digital extensor and lateral digital extensor. Of the 40 instances in which 1-year progress reports were obtained, three quarters of the animals were described as being "athletically sound," with the others ranging from pasture sound to partially disabled because of severe and persistent lameness. One horse was euthanized because of incurable wound infection.[37]

Localized hematomas may mimic superficial strains. Even more serious is the prospect of a deep dorsal hematoma inducing a compartment syndrome and, subsequently, myonecrosis (Figure 17-25).

Tendon and Tendon Sheath Infections (Infectious Tenosynovitis)

A tendon sheath produces and maintains a small volume of protective synovial fluid around certain critical areas of tendons, which are subject to repetitive pressure and related frictional forces emanating from nearby high-motion joints such as the fetlock, carpus, and proximal tarsus. Thus there are digital sheaths adjacent to the fetlocks and along the flexor and extensor surfaces of the carpus and tarsus.

Most tendon sheaths are infected as a result of an inoculating wound or extension from a nearby cellulitis. Infectious tenosynovitis can usually be differentiated from traumatic synovitis or inadvertent hypodermic injection because of greater degrees of associated heat, pain, and lameness.

Imaging Findings

Radiology. Radiology for the purpose of identifying an associated, presumably precipitating osteomyelitis has been advocated by Bertone, but I have rarely found such examinations informative, other than in very chronic cases.[38]

Ultrasound. Sonographic indicators of tenosynovitis are for the most part nonspecific, the exception being the presence of a large volume of debris-laden fluid in a distended tendon sheath, a finding previously reported in association with infection.[39]

Tenoscopy. Frees and co-workers advocate the use of *tenoscopy* for diagnosis, evaluation, and treatment of infectious tenosynovitis in horses.[40]

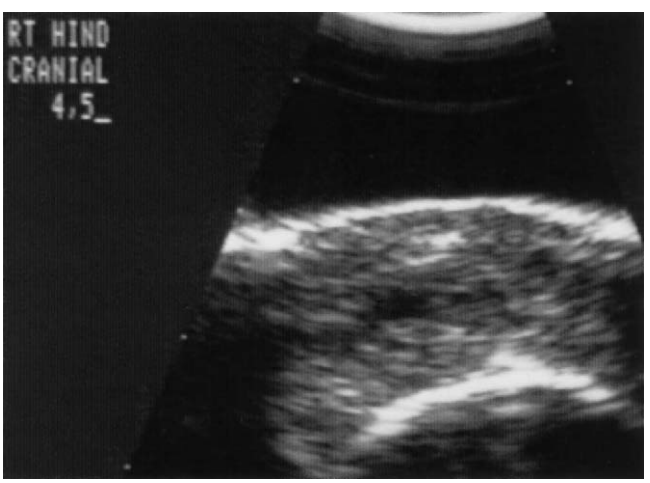


Figure 17-24 • Close-up view of a gently aching tear in the center of the long digital extensor tendon.

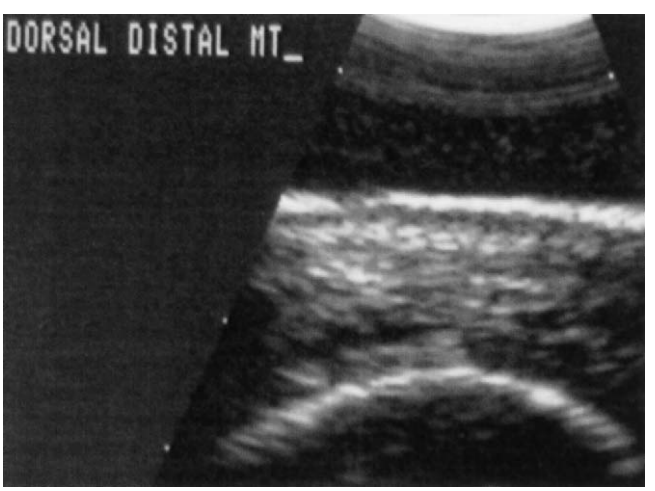


Figure 17-25 • Close-up view of a deep hematoma situated between the dorsal surface of the third metatarsal bone and the overlying muscle.

Surgical Infection

Smith and Ross reported a small series of postoperative *Actinobacillus* infections involving numerous soft tissues, including the check ligament. Their findings, although based on only 10 horses, suggested an emerging pattern of antibiotic resistance.[41] Bertone reported a surgical infection in a forelimb digital sheath after placement of a bone graft in a midbody sesamoid fracture.[38]

Enthesitis and Enthesiophytes. Inflammation at the origin or insertion of a tendon or ligament is termed *enthesitis.* Small bone deposits in similar locations are termed *enthesiophytes.* In general, I have found that these terms are readily used, especially in clinical settings, but rarely confirmed. Thus there are limited reliable clinical data as to either their prevalence or incidence. One authority wrote somewhat obliquely of entheses "that they were of particular interest and require further studies in horses because, at least in human medicine, the *enthesis* is considered to be the weakest point of the bone-tendon or bone-ligament functional unit."[42]

▮▮▮ TENDON SHEATH TUMORS

Lipoma

Hammer and co-workers reported a lipoma in the extensor tendon sheath of a horse that appeared externally as a large oval swelling just below the front of the carpus. This case is a rarity, however, because most equine lipomas typically develop in the mesentery and may, in the case of larger tumors, lead to intestinal strangulation. Other reported locations include the stifle, neck, and chest wall. Lipomas have also been found in the pericardium, myocardium, and meninges.

Fibroma

Adams and co-workers described the radiographic appearance of forelimb and hindlimb fibromas in two horses.[43] In the first case, a sound, 15-month-old Quarter Horse filly was presented for multiple nonpainful, 2- to 4-cm nodules on the dorsomedial aspect of the left hock. Radiographically, only soft-tissue swelling was seen. Surgery determined that the nodules were attached to the tendons of the fibularis tertius and tibialis cranialis muscles. The histologic diagnosis was fibroma.

In the second instance, a sound, 18-month-old Quarter Horse filly was seen for a nonpainful, slowly enlarging swelling located on the craniolateral aspect of the distal radius. Radiographs showed a discrete soft-tissue mass apparently encroaching on the adjacent surface of the radius, as suggested by a shallow cortical concavity. Surgery identified a 6-cm mass attached to the tendons of the extensor carpi radialis and obliquus muscles, which histologically proved to be a fibroma. Because no mention was made of bony invasion by the fibromatous mass, the radial defect was presumed to be benign, pressure-induced remodeling.

▮▮▮ INTERFERENCE OF SONOGRAPHIC EXAMINATION BY REGIONAL NERVE BLOCKS

Zekas and Forrest demonstrated that metacarpal/metatarsal nerve blocks preceding sonographic examination do not significantly interfere with or degrade image quality.[44] This has also been my experience based on similar-appearing preblock and postblock images.

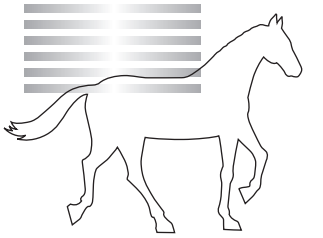
References

1. Pharr JW, Nyland TG: Sonography of the equine palmar metacarpal soft tissues, *Vet Radiol* 25:265, 1984.
2. Dyson SJ, Arthur RM, et al: Suspensory ligament desmitis, *Vet Clin N Am* 11:177, 1995.
3. Denoix J-M: Diagnostic techniques for identification and documentation of tendon and ligament injuries, *Vet Clin N Am* 10:365, 1994.
4. Goodship AE, Birch HL, Wilson AM: The pathobiology and repair of tendon and ligament injury, *Vet Clin N Am* 10:323, 1994.
5. Wilson AM, Goodship AE: Exerercise induced hyperthermia as a possible mechanism for tendon degeneration, *J Biomech* 27:899, 1994.
6. Birch HL: An investigation into the cellular basis of tendon degeneration (PhD thesis) Bristol, England, University of Bristol, 1993.
7. Henry GA, Patton CS, Goble DO: Ultrasonic evaluation of iatrogenic injuries of the equine accessory (carpal check) ligament and superficial digital flexor tendon, *Vet Radiol* 27:132, 1986.
8. Spurlock GH, Spurlock SL, Parker GA: Ultrasonic, gross, and histologic evaluation of a tendonitis disease model in the horse, *Vet Radiol* 30:184, 1989.
9. Crass JR, Genovese RL, et al: Magnetic resonance, ultrasound and histopathologic correlation of acute and healing equine tendon injuries, *Vet Radiol* 33:206, 1992.
10. Pugh CR: A simple method to document the location of ultrasonographically detected equine tendon injuries, *Vet Radiol Ultrasound* 34:211, 1993.
11. Farrow CS: Strains fall mainly on the transverse plane, *Can Vet J* 38:448, 1997.
12. Farrow CS: Carpal sprain injury in the dog, *J Am Vet Med Res* 18:33, 1977.
13. Genovese RL, Rantanen NW: The superficial digital flexor tendon. In Rantanen NW, McKinnon AO, editors, *Equine diagnostic ultrasonography.* Baltimore, 1998, Williams & Wilkins.
14. Dyson SJ, Arthur RM, et al: Suspensory ligament desmitis, *Vet Clin N Am* 11:177, 1995.
15. Denoix J-M: Diagnostic techniques for identification of tendon and ligament injuries, *Vet Clin N Am* 10:365, 1994.
16. Palmar SE, Genovese R, et al: Practical management of superficial digital flexor tendonitis in the performance horse, *Vet Clin N Am* 10:425, 1994.

17. Spaulding K: Ultrasonic anatomy of the tendons and ligaments in the distal metacarpal-metatarsal region of the equine limb, *Vet Radiol* 25:155, 1984.
18. Wilderjans H, Boussauw B, et al: Tenosynovitis of the digital flexor tendon sheath and annular ligament constriction syndrome caused by longitudinal tears in the deep digital flexor tendon: a clinical and surgical report of 17 cases in Warmblood horses, *Equine Vet J* 35:270, 2003.
19. Verschooten F, DeMoor A: Tendinitis in the horse: its radiographic diagnosis with air tendograms, *J Am Vet Radiol Soc* 19:23, 1978.
20. Hago B, Vaughn C: Use of contrast radiography in the investigation of tendon synovitis and bursitis in horses, *Equine Vet J* 18:375, 1986.
21. Saini NS, Mirakhur KK, Sobti VK: Radiographic (air-tendograms and angiographic) observations following homologous tendon grafting in equines, *J Equine Vet Sci* 9:45, 1989.
22. Yovich JV, Livesey MA: An abnormal digital flexor tendon sheath in the metacarpal region in a horse, *Can Vet J* 25:175, 1984.
23. Hago B, Vaughn C: Radiographic anatomy of tendon sheaths and bursae in the horse, *Equine Vet J* 18:102, 1986.
24. Hoskinson JJ: Equine nuclear scintigraphy, *Vet Clin N Am* 17:63, 2001.
25. Turner TA: Diagnostic thermography. *Vet Clin N Am* 17:95, 2001.
26. Turner TA: Hindlimb muscle strain as a cause of lameness in horses, *Proc Am Assoc Equine Pract* 34:281, 1989.
27. Edwards RB, Ducharme NG, et al: Scintigraphy for diagnosis of avulsions of the origin of the suspensory ligament in horses: 51 cases (1980-1993), *J Am Vet Med Assoc* 207:608, 1995.
28. Hill AE, Stover SM, et al: Risk factors for and outcomes of noncatastrophic suspensory apparatus injury in Thoroughbred racehorses, *J Am Vet Med Assoc* 218:1136, 2001.
29. Van Schie JTM, Bakker EM, Van Weeren PR: Ultrasonographic evaluation of equine tendons: a quantitative in vitro study of the effects of amplifier gain level, transducer tilt, and transducer displacement, *Vet Radiol* 40:151, 1999.
30. Tsukiyama K, Acorda JA, Yamada H: Evaluation of superficial digital flexor tendonitis in racing horses through gray scale histogram analysis of tendon ultrasonograms, *Vet Radiol Ultrasound* 37:46, 1996.
31. Reef VB: Superficial digital flexor tendon healing: ultrasonographic evaluation of therapies, *Vet Clin N Am* 17:159, 2001.
32. Bowman KF, Leitch M, et al: Complications during treatment of traumatic disruption of the suspensory apparatus in Thoroughbred horses, *J Am Vet Med Assoc* 184:706, 1984.
33. Watkins JP, Auer JA, et al: Healing of surgically created defects in the equine superficial digital flexor tendon: collagen-type transformation and tissue morphologic reorganization, *Am J Vet Res* 46:2091, 1985.
34. Rooney JR: Passive function of the extensor tendons of the fore and rear limbs of the horse, *J Equine Vet Sci* 7:8, 1987.
35. Strasser S, Solamen B: What is your diagnosis? *J Am Vet Med Assoc* 196:1671, 1990.
36. Taylor DS, Pascoe JR, et al: Digital flexor tendon lacerations in horses: 50 cases (1975-1990), *J Am Vet Med Assoc* 206:342, 1995.
37. Belknap JK, Baxter GM, Nickels FA: Extensor tendon lacerations in horses: 50 cases (1982-1988), *J Am Vet Med Assoc* 199:1616, 1991.
38. Bertone AL: Infectious tenosynovitis, *Vet Clin N Am* 11:163, 1995.
39. Bohn A, Papageorges M, Grant B: Ultrasonographic evaluation and surgical treatment of humeral osteitis and bicipital tenosynovitis in a horse, *J Am Vet Med Assoc* 201:305, 1992.
40. Frees KE, Lillich JD, et al: Tenoscopic-assisted treatment of open distal flexor tendon sheath injuries in horses: 20 cases (1992-2001), *J Am Vet Med Assoc* 220:1823, 2002.
41. Smith MA, Ross MW: Postoperative infection with *Actinobacillus* spp in horses: 10 cases (1995-2000), *J Am Vet Med Assoc* 221:1306, 2002.
42. Denoix J-M: Functional anatomy of tendons and ligaments in the distal limbs (manus and pes), *Vet Clin N Am* 10:273, 1994.
43. Adams SB, Fessler JF, Thacker HL: Tendon fibromas in 2 horses, *Equine Vet J* 14:95, 1982.
44. Zekas LJ, Forrest LJ: Effect of perineural anesthesia on the ultrasonic appearance of equine palmar metacarpal structures, *Vet Radiol Ultrasound* 44:59, 2003.

SECTION II

The Skull: Face, Jaws, and Cranium



Chapter 18

The Equine Skull: Dealing Successfully With Radiographic Complexity

Analysis and interpretation of skull radiographs are difficult tasks at best because of the extreme complexity of the region. Nowhere in the skeleton is there greater structural variability or more superimposition: high-density teeth, low-density conchae, medium-density facial bones—all arrayed against a backdrop of numerous air-filled cavities. Making diagnosis doubly difficult (no pun intended) is the fact that there are two of most things: two sets of teeth on either side of the head, paired facial bones, symmetric turbinates, and twined paranasal sinuses. Usually all this must be interpreted in either lateral or lateral oblique projections—daunting tasks most assuredly, but not impossible.

With an organized and systematic approach, one that is underpinned by a strong knowledge of normal radiographic anatomy, it is possible to diagnose most common disorders of the equine head, including fractures, infections, and sinonasal and dental disease.

STANDARD RADIOGRAPHIC EXAMINATION

Irrespective of the diagnostic objectives, my preference is always to begin with a lateral radiograph that includes as much of the skull as possible, in other words, a survey film. Depending on what is seen in this initial image, a full protocol examination is then performed or the study is customized.

Normal Radiographic Anatomy of the Skull

As with most mammals, the shape as well as the size of a horse's skull change with maturation.[1] For example, the forehead of a newborn foal is far more prominent than that of an adult, whereas the face of an adult appears elongated compared with that of a foal (Figures 18-1 through 18-3).



Figure 18-1 • A miniature mare and her foal demonstrate a normal age-related difference in forehead prominence, a difference that is also appreciable radiographically.

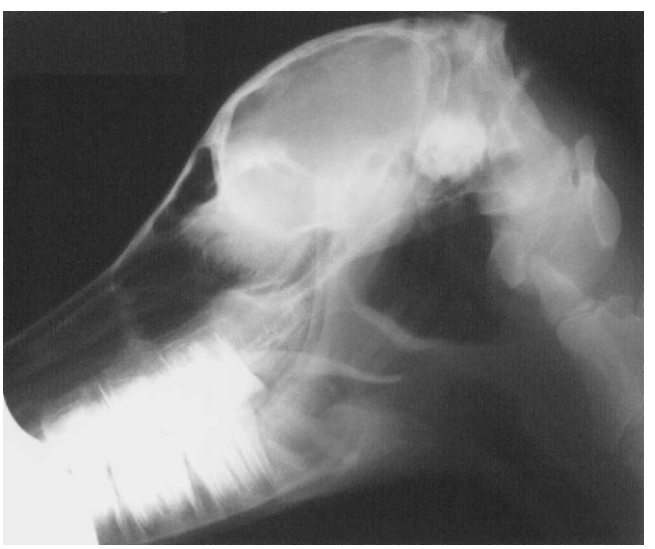


Figure 18-2 • Lateral view of the skull of a 3-day-old foal featuring a characteristically high forehead and short face.



Figure 18-3 • Lateral view of the facial region of an adult horse shows a flattened forehead and an elongated face.

Lateral, lateral oblique, and ventrodorsal views of the skull are provided for reference, along with corresponding radiographs. Selected close-ups are provided to emphasize regions of particular radiographic interest (Figures 18-4 through 18-6).

Normal Computed Tomographic Anatomy of the Skull

Clearly, computed tomography (CT) is the solution to the problem of structural superimposition, a serious limitation that has plagued skull radiography since its inception. With high-resolution CT, it is now possible to see specific interior anatomy, the nasal conchae, for example, with a clarity that was unimaginable as little as a decade ago (Figure 18-7).

Smallwood and co-workers described the CT appearance of the foal skull, supplemented by coinciding anatomic cross-sections, potentially to serve as a normal CT reference.[2] Most images were obtained from the decapitated head of a miniature foal, estimated to be 6 to 8 months old. Morrow and co-workers reported the CT appearance of the adult equine skull using decapitated specimens taken from 4-, 8-, and 11-year-old horses.[3]

Radiotherapy of Sarcoids of the Head

Turrel and co-workers reported a 1-year nonrecurrence rate of 94 percent in 16 horses treated with interstitial

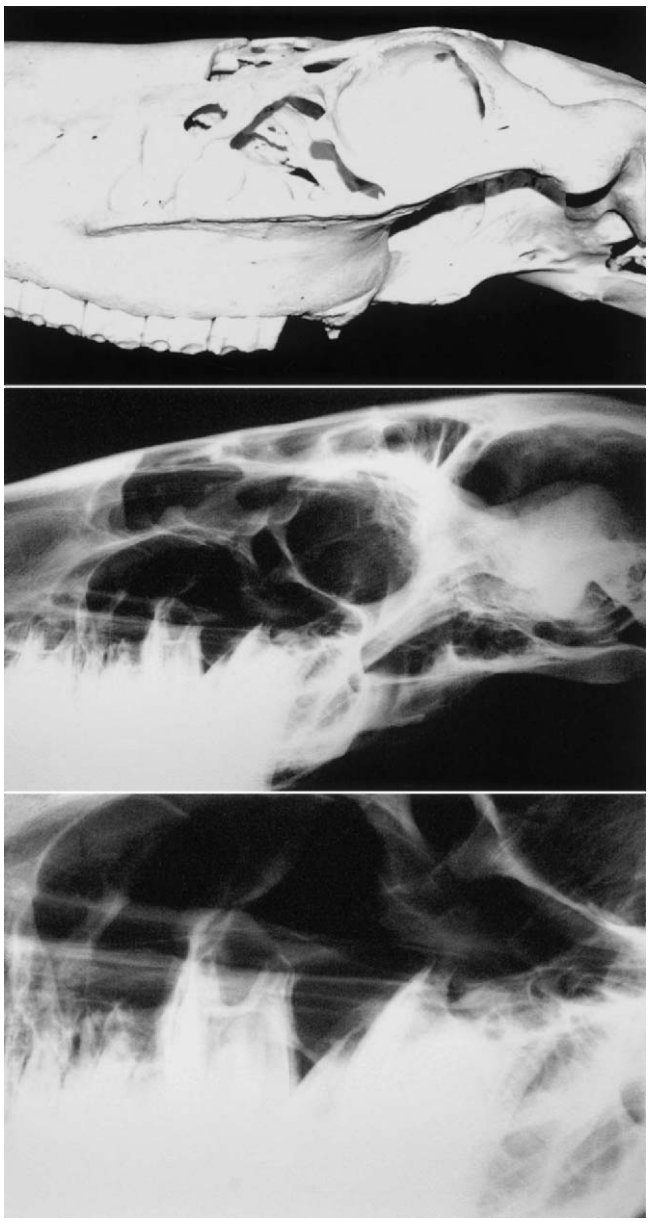


Figure 18-4 • Lateral view **(A)** of the skull of an adult horse with exterior walls of the frontal and maxillary sinuses removed to reveal underlying cavities. Corresponding lateral **(B)** and lateral close-up **(C)** radiographs, the latter showing the close physical relationship between the caudal maxillary cheek teeth and associated maxillary sinus.

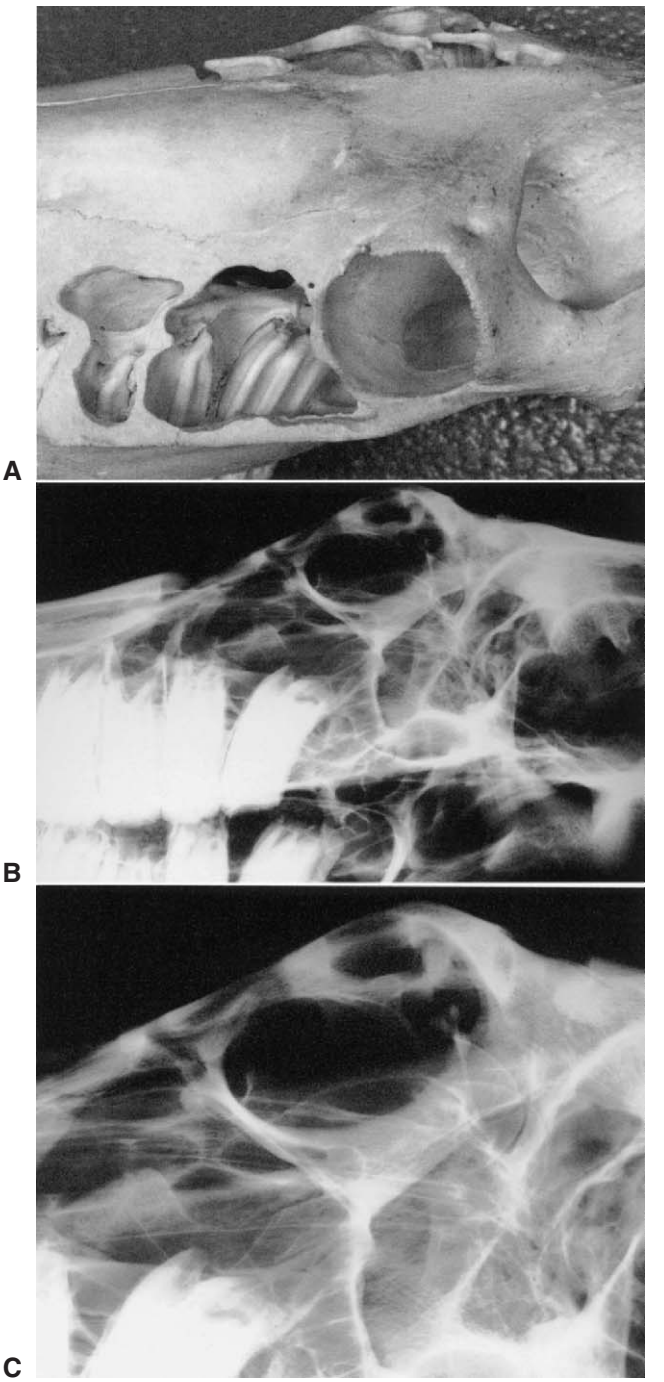


Figure 18-5 • Lateral oblique view of the skull of an adult horse with exterior walls of the frontal and maxillary sinuses removed to reveal underlying cavities **(A).** Corresponding lateral **(B)** and lateral close-up **(C)** radiographs, the latter emphasizing the physical relationship between the caudal maxillary cheek teeth and associated maxillary sinus.

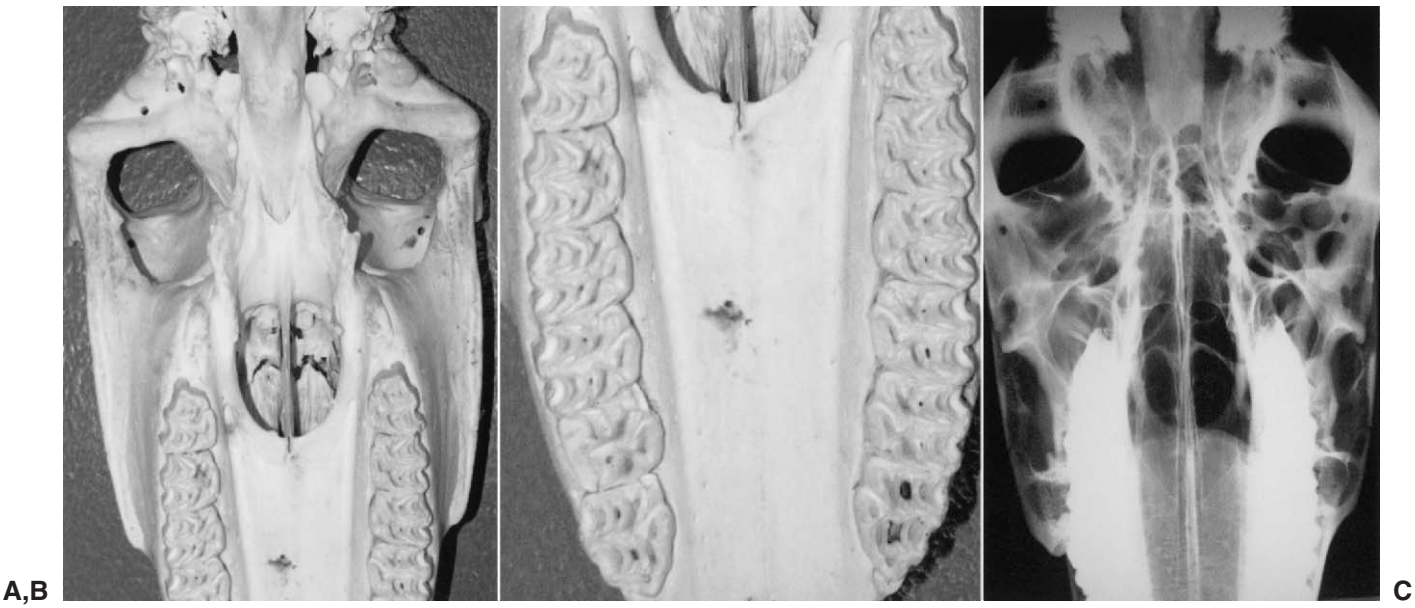


Figure 18-6 • Ventrodorsal view of the skull of an adult horse **(A),** including a ventrodorsal close-up **(B)** view of the maxillary cheek teeth. A corresponding ventrodorsal radiograph **(C)** is included, exposed to emphasize the nasal and paranasal cavities.



Figure 18-7 • Computed tomogram (soft tissue window) obtained from the central nasal cavity of a normal horse shows paired dorsal and ventral chonchae with a clarity that is not possible with conventional radiography.

iridium-192 therapy for sarcoids of the head. Harmful radiation effects, observed in three horses, included radiation necrosis and deep infection.[4]

References

1. Quick CB, Rendano VT: Radiographic interpretation: the equine skull, *Mod Vet Pract* 59:291, 1978.
2. Smallwood JE, Wood BC, et al: Anatomic reference for computed tomography of the head of the foal, *Vet Radiol Ultrasound* 43:99, 1999.
3. Morrow KL, Park RD, et al: Computed tomographic imaging of the equine head, *Vet Radiol Ultrasound* 41:491, 2000.
4. Turrel JM, Stover SM, Gyorgyfalvy J: Iridium-192 interstitial brachytherapy of equine sarcoid, *Vet Radiol* 26:20, 1986.

Chapter 19

Maxillary and Facial Lesions

NASAL BONE FRACTURES

It is difficult to identify clearly fresh nasal bone fractures, even when using a reduced radiographic technique. Most are depression-type fractures, but some are nondisplaced or cracked, the latter often being especially difficult to appreciate unless enhanced by a partial or full callus (Figures 19-1 and 19-2).[1] Customized lateral oblique views often reveal injuries not apparent in conventional projections (Figure 19-3).

Like many facial injuries, nasal bone fractures may be associated with interior soft-tissue disruption, even though the overlying skin is intact. Thus the potential for a related bone infection may go unconsidered. In some instances nasal bone fragments may be driven deeply into the nasal cavity, causing serious obstruction.

COMBINED FACIAL FRACTURES

Nasal bone fractures often occur in conjunction with fractures of the adjacent maxilla and, less frequently, the orbit. To uncover most nasomaxillary and nasoorbital fractures requires multiple lateral and lateral oblique views (Figure 19-4). Many also necessitate one or more customized views. In some instances only a dorsoventral view will reveal the full extent of the injury (Figure 19-5).

ISOLATED MAXILLARY FRACTURES

Isolated maxillary fractures, that is, those confined to a single maxillary bone, are unusual. Most are the result of a sharp, forceful blow to the side of the face, many of which provide little or no external evidence (facial disfigurement) of their presence (Figure 19-6).

FACIAL DEFORMITY RESEMBLING OLD FRACTURES (FACIAL OSTEODYSTROPHIA FIBROSA)

Primary hyperthyroidism may cause osteodystrophia of the facial bones of horses and ponies resembling old fractures. One report describes the radiographic appearance of the head of a 17-year-old pony with osteodystrophia fibrosa caused by excessive parathyroid hormone from primary hyperthyroidism.[2] Radiographically, the pony's head appeared deformed as a result of new bone deposition on the upper and lower jaws. The teeth lacked discrete lamina dura.

PREMAXILLARY INFECTION

Schumacher and co-workers reported a highly destructive fungal osteomyelitis in the premaxilla of a 17-year-old Quarter Horse gelding. Radiographically, the lesion was utterly destructive, closely resembling a malignant tumor.[3]

MAXILLARY INFECTION

Sinonasal disease and dental infection are the primary sources of maxillary infection, followed by open fractures (Figure 19-7). Deep cuts, nail punctures, and gunshot wounds are also capable of causing a maxillary infection and, in the process, secondary sinonasal disease.

PREMAXILLARY TUMORS

Barber and co-workers reported a fibroma and fibrosarcoma in two horses.[4] Both tumors grew rapidly, distorted the face, destroyed portions of the

Text continued on p. 338.

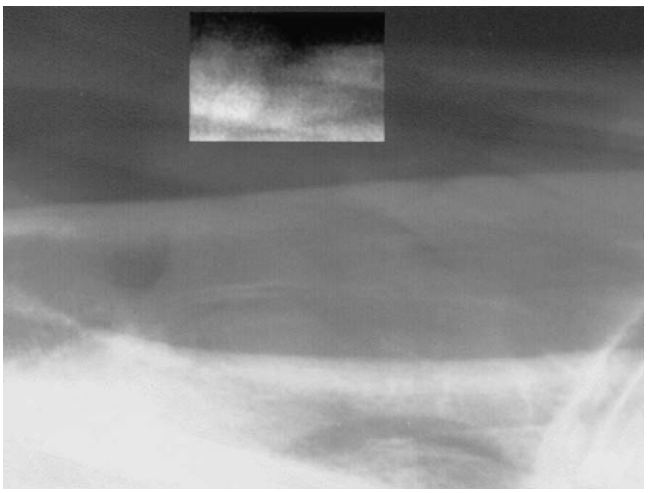


Figure 19-1 • Close-up lateral oblique view of a minimally displaced, calloused nasal bone fracture *(emphasis zone)*.

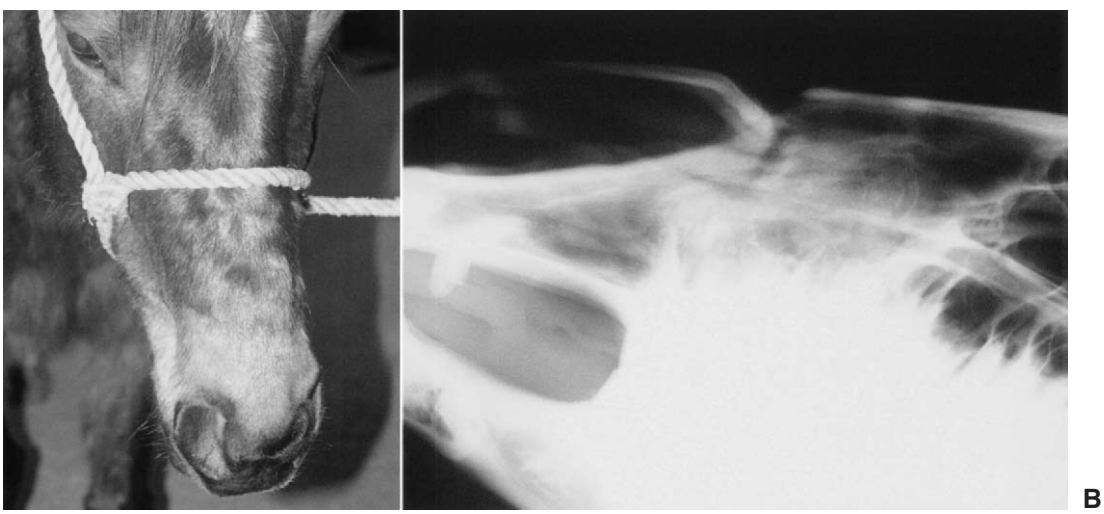


Figure 19-2 • Close-up frontal view **(A)** of the face of a horse with a badly displaced, nonunion fracture of the caudal aspect of the nasal bone, which now blocks the dorsal nasal passage, as seen in a lateral radiograph **(B).**



Figure 19-3 • Ultra-close-up lateral oblique view of a horse with a displaced lateral nasal fracture silhouetted against the maxillary sinus.

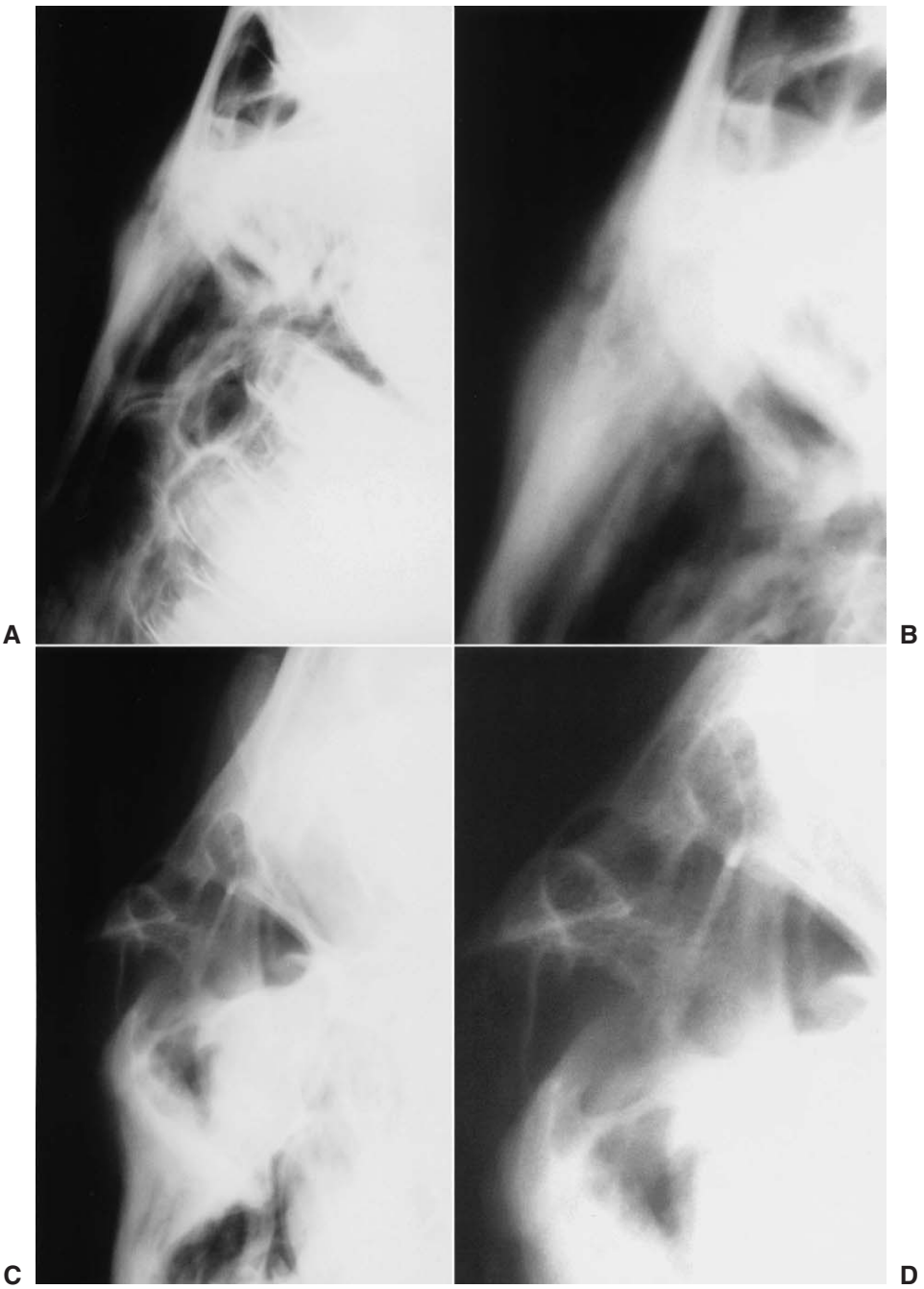


Figure 19-4 • Lateral **(A)** and lateral close-up **(B)** views of a heavily calloused caudal nasal bone fracture, and increased density in the adjacent periorbital region. Close-up **(C)** and ultra-close-up oblique lateral **(D)** views of the orbital region reveal the full extent of the associated callus, including a thin orbital fragment not evident in the true lateral projection.

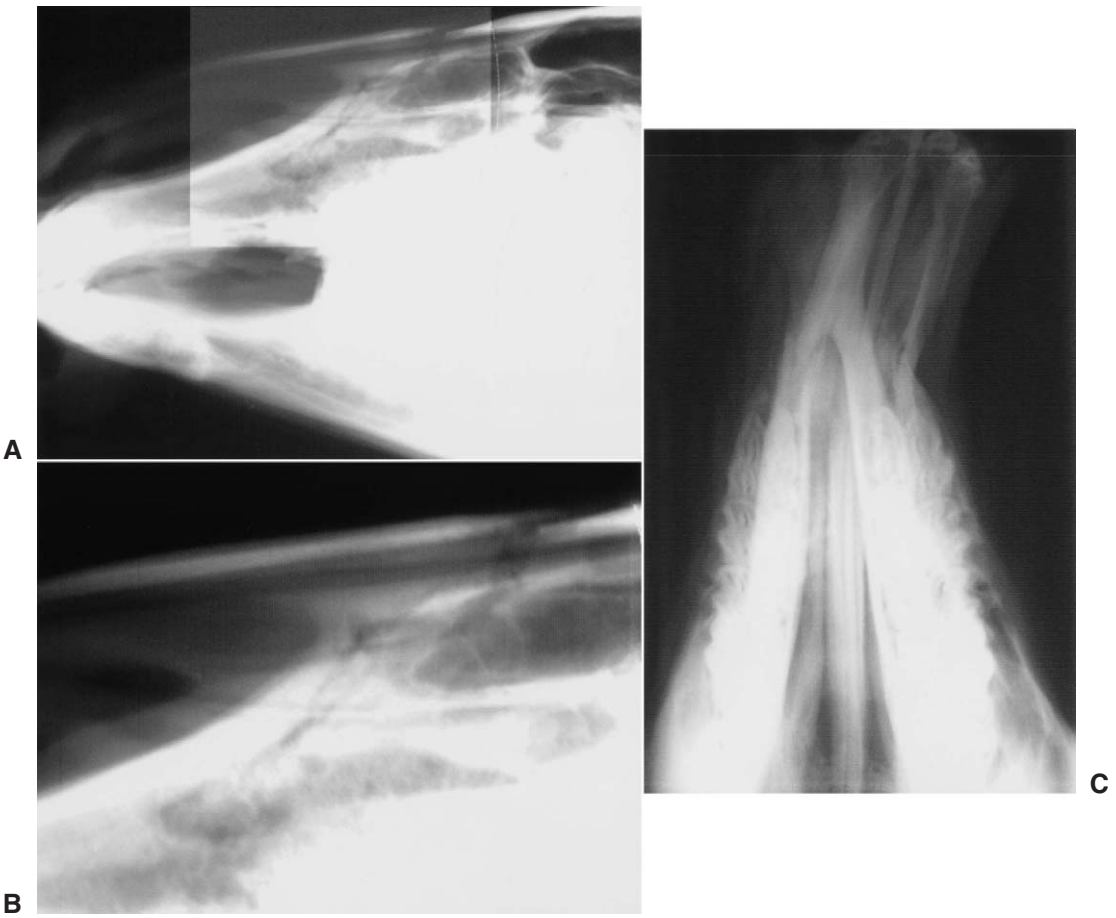


Figure 19-5 • Lateral **(A)** and close-up lateral **(B)** views show a seemingly minimally displaced, comminuted nasolacrimal fracture. Only a dorsoventral projection **(C)** reveals the true extent of the resultant displacement.

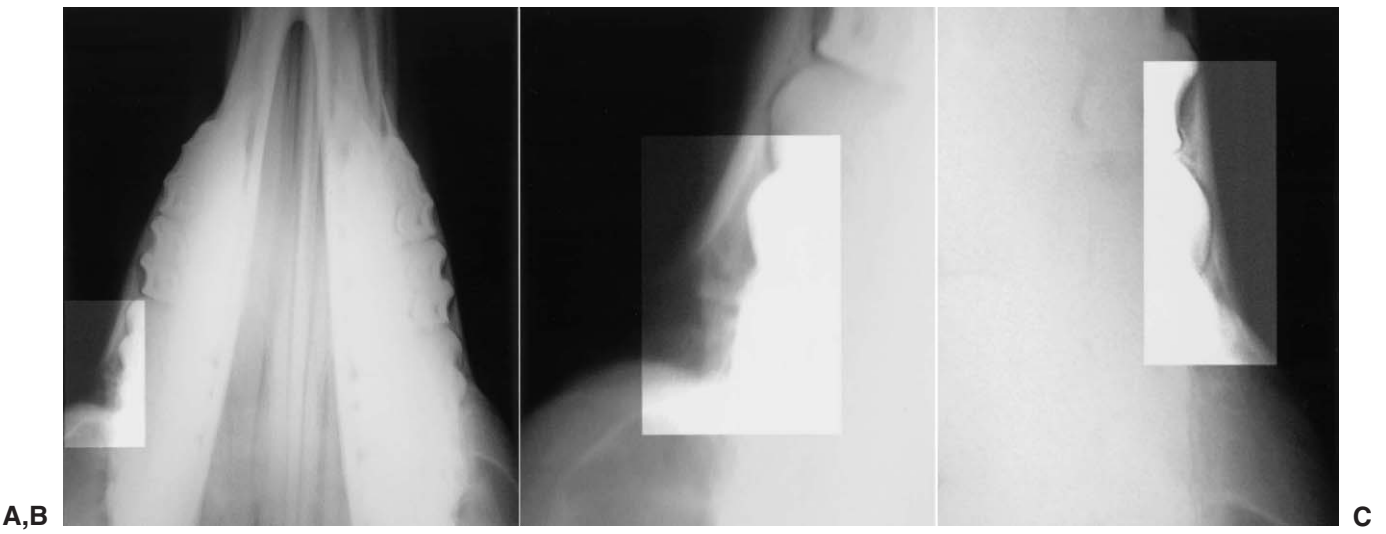


Figure 19-6 • Dorsoventral **(A)** and close-up dorsoventral **(B)** views of the face show a displaced right maxillary fracture overlying the third cheek tooth. The outwardly displaced fracture fragments and fronds on interior new bone also suggest the possibilities of infection and tumor, but the physical and growth attributes of the lesion lend greater support to trauma. A close-up lateral view **(C)** of the opposite facial region is provided for normal comparison.

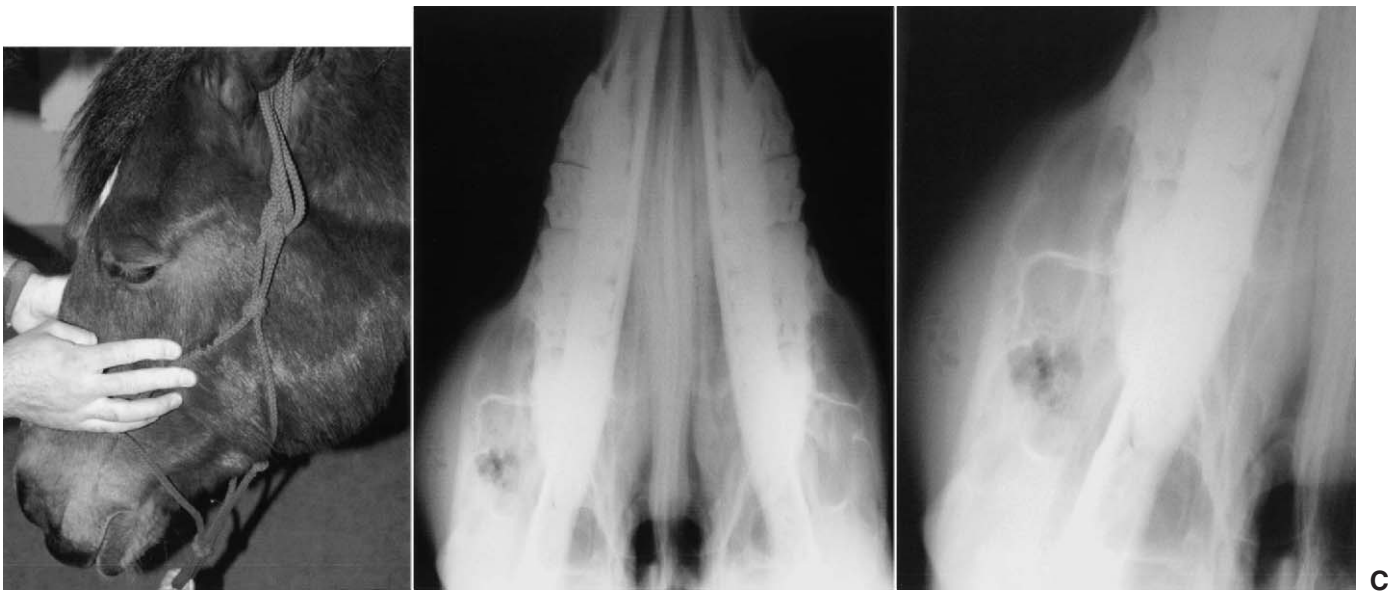


Figure 19-7 • Close-up lateral view of the face shows severe swelling over the caudal jaw **(A).** Dorsoventral **(B)** and close-up dorsoventral **(C)** radiographs show increased density both inside and outside the right maxillary sinus, punctuated by multiple gas pockets, consistent with severe purulent sinusitis and secondary parafacial abscessation.

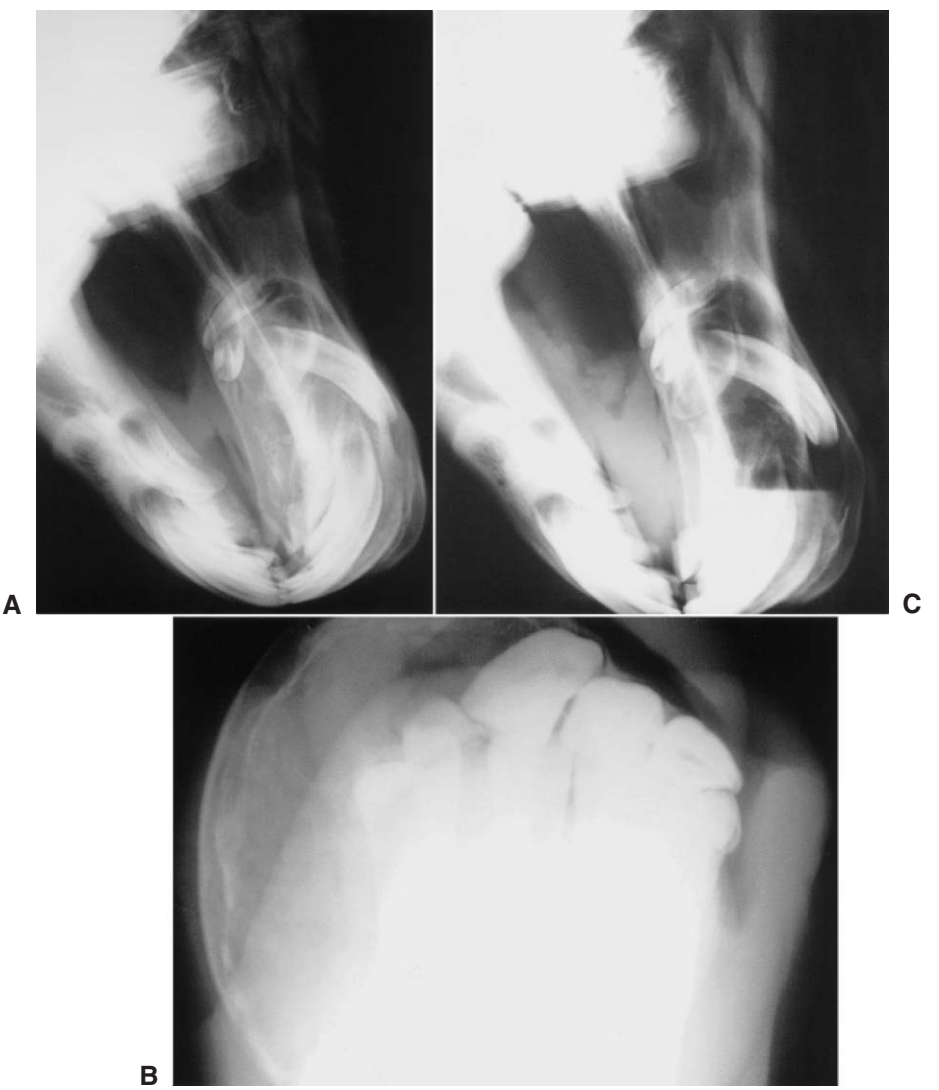


Figure 19-8 • Close-up lateral **(A)** and dorsoventral **(B)** views of the rostral facial region of a horse with a cavitating ameloblastoma show marked facial deformity and displaced incisors characteristic of both dental tumors and oral fibrosarcomas. A second close-up lateral view **(C)** of the rostral facial region made following aspiration of bloody fluid and instillation of an equal volume of air shows a fluid level providing an estimate of the associated cavity.

premaxilla, and displaced teeth. As noted previously in the chapter on dental disease, ameloblastomas have a penchant for hemorrhagic cavitation (Figure 19-8).

References

1. Turner AS: Surgical management of depression fractures of the equine skull, *Vet Surg* 8:29, 1979.
2. Frank N, Hawkins JF, et al: Primary hyperparathyroidism with osteodystrophia fibrosa of the facial bones in a pony, *J Am Vet Med Assoc* 212:84, 1998.
3. Schumacher J, Kemper DL, et al: Removal of the premaxilla and rostral portions of the maxilla of a horse, *J Am Vet Med Assoc* 209:118, 1996.
4. Barber SM, Clark EG, Fretz PB: Fibroblastic tumor of the premaxilla in two horses, *J Am Vet Med Assoc* 182:700, 1983.

Chapter 20

Mandibular and Temporomandibular Joint Fractures, Infections, Tumors, and Tumorlike Lesions

THE STANDARD MANDIBULAR EXAMINATION

Other than a lateral survey film, and perhaps paired lateral oblique projections, there is no standard mandibular series. The reason is twofold: first, the enormous difference in thickness between the rostral and the caudal aspects of the lower jaw, and second, the extensive superimposition on the mandible by the teeth and air-filled parts of the throat such as the pharynx, larynx, and guttural pouches, which can both mimic and conceal fractures. Close-up lateral and lateral oblique views of the caudal mandible illustrate these marked density differences as well as the influence of superimposed air-filled structures on overlying bone (Figure 20-1).

The obvious solution to these problems is to customize the examination from the start, based on observation and examination, or to do so once a fracture is identified in a lateral survey film. My preference is to begin the radiographic investigation of such injuries with a full-length lateral examination of the entire head, getting the lay of the anatomic land as it were, and then customize the rest of the examination, selecting beam angles and setting techniques according to the location and configuration of the fracture.

A full-length lateral view of a defleshed right hemimandible, and close-up views of the ramus, cheek teeth, and rostral body are provided for anatomic-radiographic comparison (Figures 20-2 through 20-5).

MANDIBULAR FRACTURES

The mandible is the most frequently fractured bone in the equine head.[1] Henninger and colleagues reported mandibular and maxillary fractures in 89 horses, most caused by kicks from other horses, falls, or getting the teeth caught in something and violently trying to escape.[2] Minimally displaced fractures were treated conservatively; moderately or severely displaced fractures underwent surgery. Most of the horses recovered eventually, but persistent infection occurred in nearly 20 percent of the animals. Some horses developed sequestra or secondary dental infections. Implant breakage or displacement occurred in a similar number of horses.

Radiographic Detectability of Mandibular Fractures

Rostrally located mandibular fractures, especially those in the interdental space, are in general easier to detect than midbody or ramal fractures. Displaced mandibular interdental fractures often cause malocclusion of the lower incisors or an undershot jaw (Figure 20-6). Clearly imaging ramal fractures often requires some adjustment of the radiographic technique and projection angle, depending primarily on degree of fragment displacement and the amount of air or blood in the guttural pouches (Figure 20-7).

Postoperative Radiographs

An *immediate* postoperative examination is, of course, a necessity, as it is in all fracture repairs (Figure 20-8). This achieves the combined ends of *evaluating and documenting* the surgery, the latter being particularly critical in the event of any future dispute relating to what was or was not done. In this regard, it cannot be overemphasized that the radiographs must be properly identified and dated. Every effort should be made to obtain at least two views.

Mandibular Fracture Healing

Healing of rostral mandibular fractures is often prolonged (delayed union because of the difficulty in

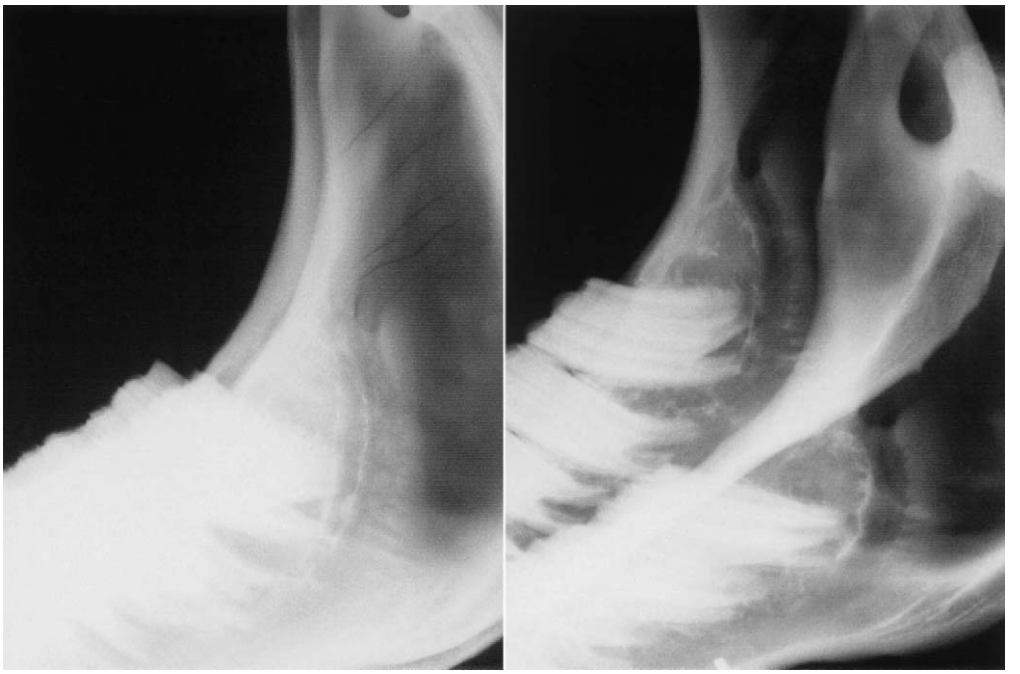


Figure 20-1 • Close-up lateral **(A)** and lateral oblique **(B)** views of the caudal aspect of the lower jaw show the normally lucent appearance of the rami compared with that of the mandibular body. Also note the manner in which the caudal molars angle sharply backwards, assuming a nearly horizontal position, and the distinctive radiolucency of the paired mental foramina.



Figure 20-2 • Full-length view of a hemimandible of a horse.



Figure 20-3 • Close-up views of the mandibular ramus, one directly illuminated **(A),** the other transilluminated **(B),** show the paper-thin central area bounded by comparatively thick peripheral ridges. Also note the irregularity of the caudoventral margin, which can be mistaken for new bone deposition or margin bone loss, depending on the clinical circumstances.



Figure 20-4 • Close-up lateral view of the normal complement of six lower cheek teeth (premolars 2-4 and molars 1-3).

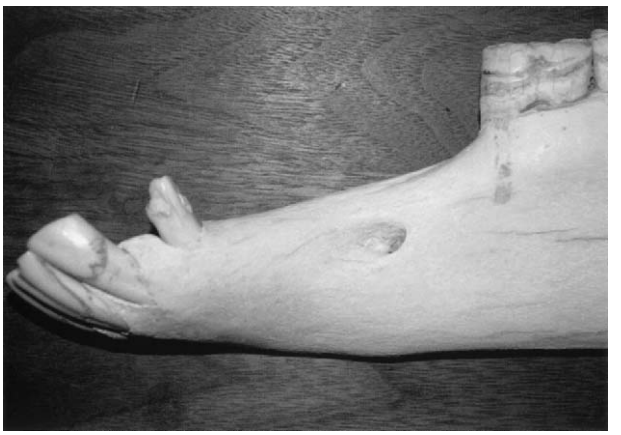


Figure 20-5 • Close-up lateral view of the rostral mandible shows the lower incisors, canine, and second premolar teeth. The gap between the canine and premolar teeth is the interdental space featuring an interalveolar border. The opening in the bone is the mental foramen, the entrance to the mental canal.



Figure 20-6 • Close-up **(A)** and ultra-close-up **(B)** views of a subacute rostral mandibular fracture in a foal show moderate to severe fragment displacement and, as a result, malocclusion of the incisors.

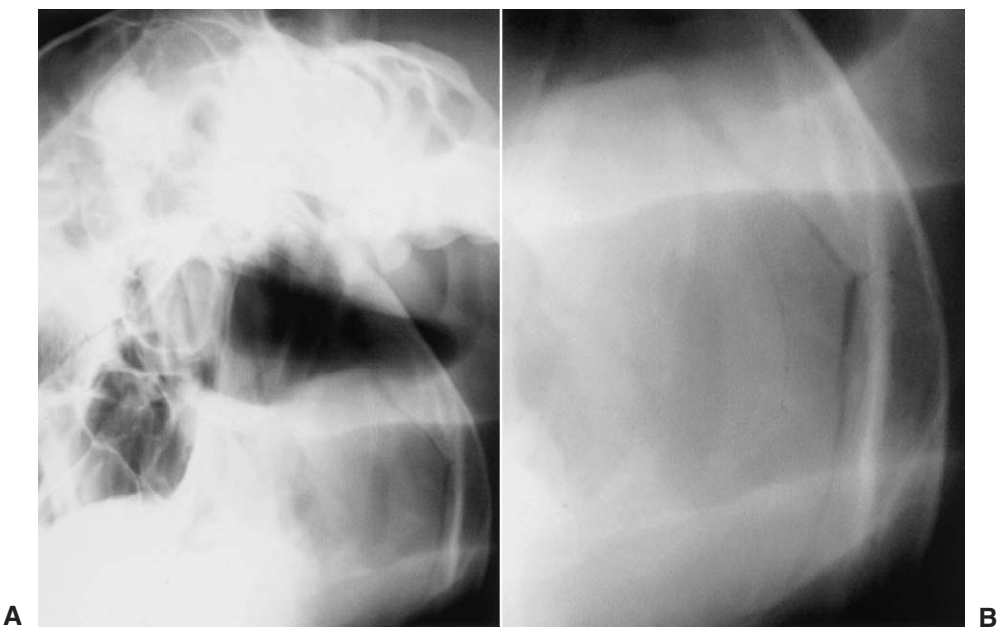


Figure 20-7 • Lateral oblique **(A)** and lateral oblique close-up **(B)** views of an acute, mildly displaced, vertically oriented, comminuted ramal fracture in an adult horse.

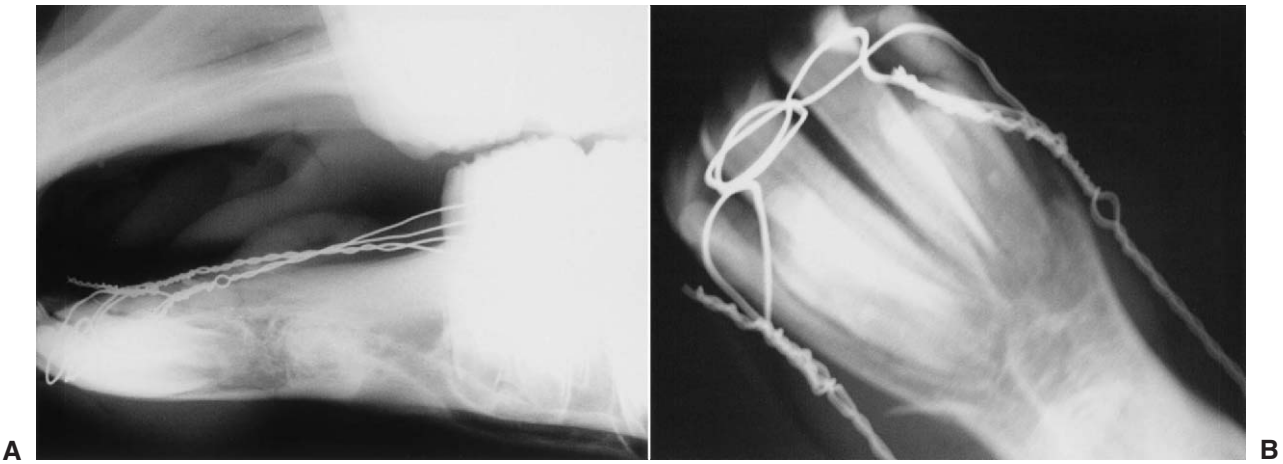


Figure 20-8 • Close-up lateral **(A)** and intraoral **(B)** immediate postoperative views of a complete, transverse, central interdental fracture, which was reduced and stabilized with wires secured to the incisors and first premolars.

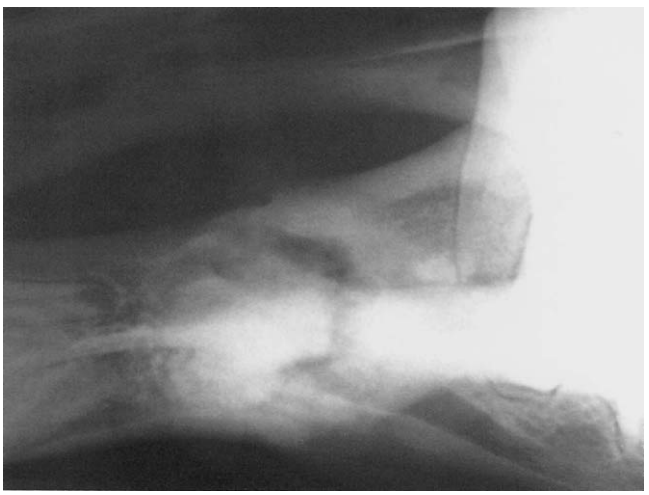


Figure 20-9 • Close-up lateral oblique view of an untreated 3-month-old interdental mandibular fracture shows a mature, moderately sized callus. The apparent "gap" between fracture fragments is actually composed of connective tissue and is caused by repetitive motion. In another month or two the interior callus should be complete, although the fractured jaw is currently nonpainful and quite solid.

stabilizing the fracture fragments) (Figure 20-9) and secondarily because of surgical or postsurgical infection. By comparison, mandibular body fractures tend to heal quite rapidly, provided they do not become infected. Many leave behind large calluses on the medial surface of the fractured hemimandible, which may be mistaken for a calcified nasal mass, especially in the oblique or dorsoventral projections (Figure 20-10).

Posttraumatic Mandibular Sequestration

The surgical repair of mandibular fractures is often hindered by the development of alveolar periostitis and formation of sequestra.[3] The formation of mandibular or related dental sequestra depends on one or more of the following factors: (1) the nature and extent of the original injury, (2) the method of repair of the fracture, (3) the vascularization (or lack thereof) of the mandibular fragments and associated teeth, and (4) the development of a postoperative infection. Mandibular sequestra often accompany infected mandibular fractures, especially those involving one or more adjacent teeth (Figure 20-11).

▮▮▮ MANDIBULAR INFECTION

Mandibular infections are most often associated with infected teeth, dental extraction, poor floating technique, mandibular fractures, and deep penetrating wounds. Most such infections remain localized to the mandible and any associated teeth but occasionally spread to distant organs such as the kidneys, liver, or brain.[4]

Radiographically, mandibular infections are initially characterized by either a faint localized loss of cortical bone density and/or new bone deposition. As infections worsen, overt bone destruction usually becomes more apparent, as does the associated reparative/defensive new bone response. Chronic lower jaw infections can become quite large, assuming the form of hemispherical, often cavitated, bony masses resembling "lumpy jaw" in cattle (Figure 20-12).

Postinfectious Mandibular Sequestration

Specht and Bristal reported the radiographic appearance of a chronic rostral mandibular infection leading

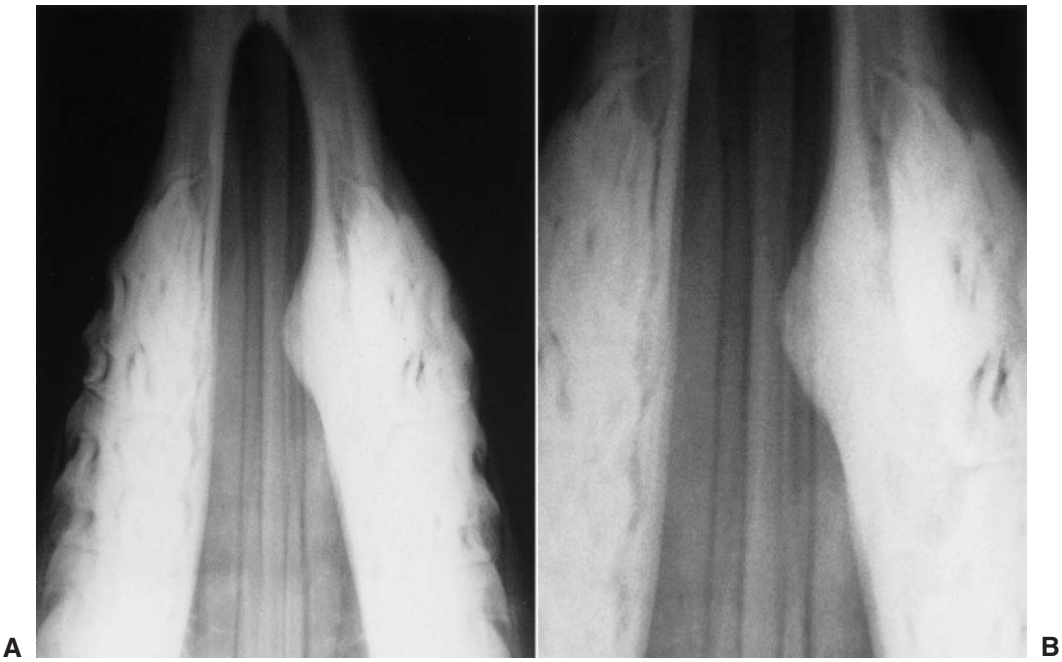


Figure 20-10 • Dorsoventral **(A)** and close-up dorsoventral **(B)** views of a 1-year-old mandibular body fracture show a mature callus on the medial surface of the left hemimandible.

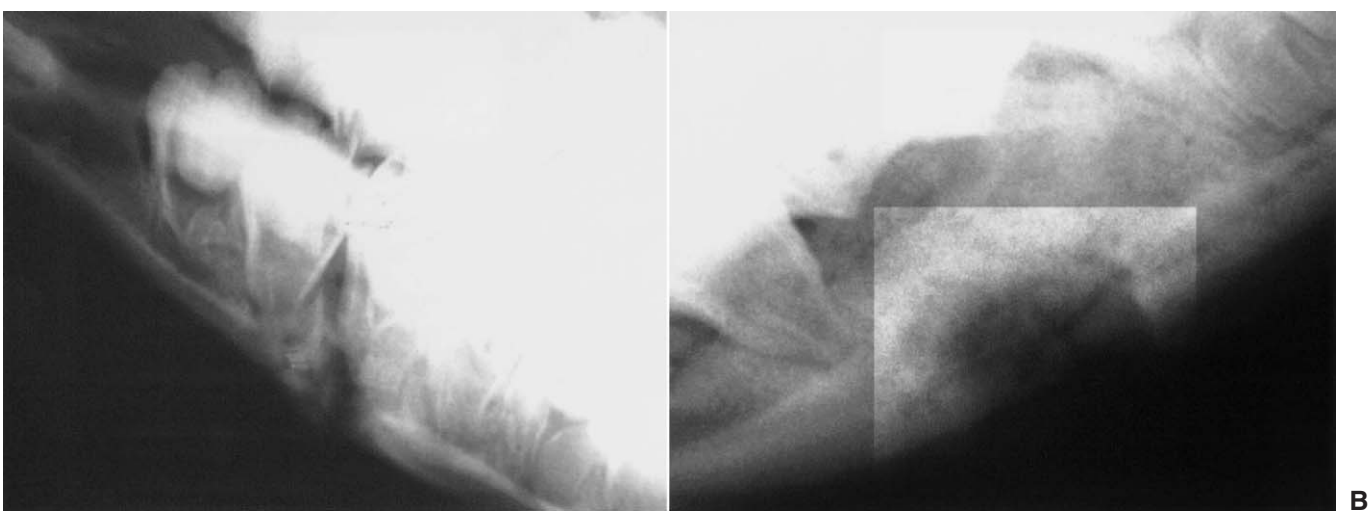


Figure 20-11 • **A,** Close-up lateral oblique view of an infected mandibular body fracture shows a triangular mandibuloalveolar sequestrum situated along the rostral edge of the fracture. **B,** A progress film of the same area made at a different angle shows a large oval-shaped defect in the ventral jaw, the result of infection. The sequestrum is no longer apparent, suggesting that it was discharged through a nearby draining sinus.

to sequestration.[5] In my experience, small sequestra are a common sequela to mandibular osteomyelitis, probably as a function of the relatively fragile blood supply to the region.

Mandibular Foreign Body

Mandibular foreign bodies typically cause sinus formation with intermittent drainage. Some may go undetected for months or even years (Figure 20-13). Associated infection depends on the composition of the foreign body and whether or not it contains bacteria or fungi. Surgical infections may result from prolonged tissue exposure during unsuccessful exploratory surgery.

▮▮▮ MANDIBULAR TUMORS

Osteosarcoma

In horses, osteosarcomas show a predilection for the head, in particular, the lower jaw. Radiographically,

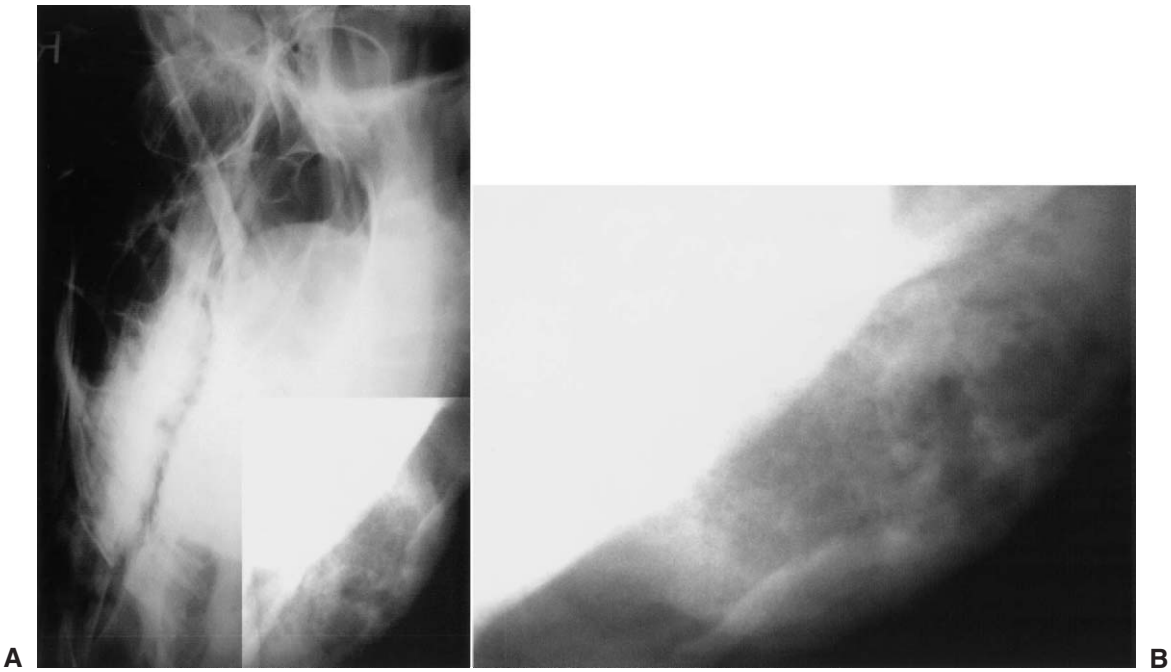


Figure 20-12 • Lateral **(A)** and close-up **(B)** lateral oblique views of the head of a horse with a year-old mandibular infection show a large, predominantly bony mass on the ventral surface of the lower jaw with at least two cavities, believed to be the sources of drainage from a pair of draining sinuses.

most osteosarcomas appear destructive (osteoclastic) and less commonly mixed (osteoclastic-osteoblastic) or productive (osteoblastic). In this latter respect, mixed lesions resemble some dental tumors, particularly adamantinomas. Two varieties of osteosarcoma are shown (Figures 20-14 and 20-15).

Adamantinoma

Mandibular adamantinomas grow from the epithelial remains of tooth germ and have been reported in young, middle-aged, and older horses. Many grow rapidly, become quite large, and in the process deform the face and disrupt the dental arcade. Radiographically, mandibular adamantinomas are reported as being both expansive and lytic.[6] In my experience, most adamantinomas feature bone destruction and production in near equal measure, with most exhibiting some degree of soap bubbling (Figure 20-16).

Ossifying Fibroma

Ossifying fibromas typically involve the rostral portion of the mandible and usually visibly cause swelling and deformity. Radiographically, these tumors appear centrally destructive, often expansile, and often displace adjacent teeth, especially incisors. Histologically, they may be misinterpreted as osteosarcomas of highly reactive, nonneoplastic bone. Although locally invasive, these tumors usually do not metastasize. Richardson and co-workers reported surgical removal of ossifying fibromas (along with the surrounding rostral mandible) in five horses.[7] Occasionally ossifying fibromas occur in the ramal portion of the mandible (Figure 20-17).

Leiomyosarcoma

MacGillvray and co-workers recently reported a most unusual case of multicentric leiomyosarcoma affecting the mandible of a young Thoroughbred. The mandibular lesions appeared as multiple small to medium-sized, circular densities located along the ventral margin of the mandible.

▮▮▮ TUMORLIKE LESIONS

Mandibular Bone Cyst (Aneurysmal Bone Cyst)

Lamb and Schelling reported a large congenital bone cyst in the lower jaw of a full-term fetus, which they believed was responsible for a fatal mechanical dystocia.[8]

Jackman and Baxter described the radiographic appearance of a mandibular bone cyst in a year-old Appaloosa and its appearance 5 and 22 months after surgery.[9] Initially the lesion was very large, expansive, and lytic, as most bone cysts are. Internal septae indicated that the cyst was *multicameral* as opposed to *unicameral*: multiple small compartments versus a single large cavity.

The cyst was surgically opened, drained of serous exudate, curetted, and filled with a combination of cor-

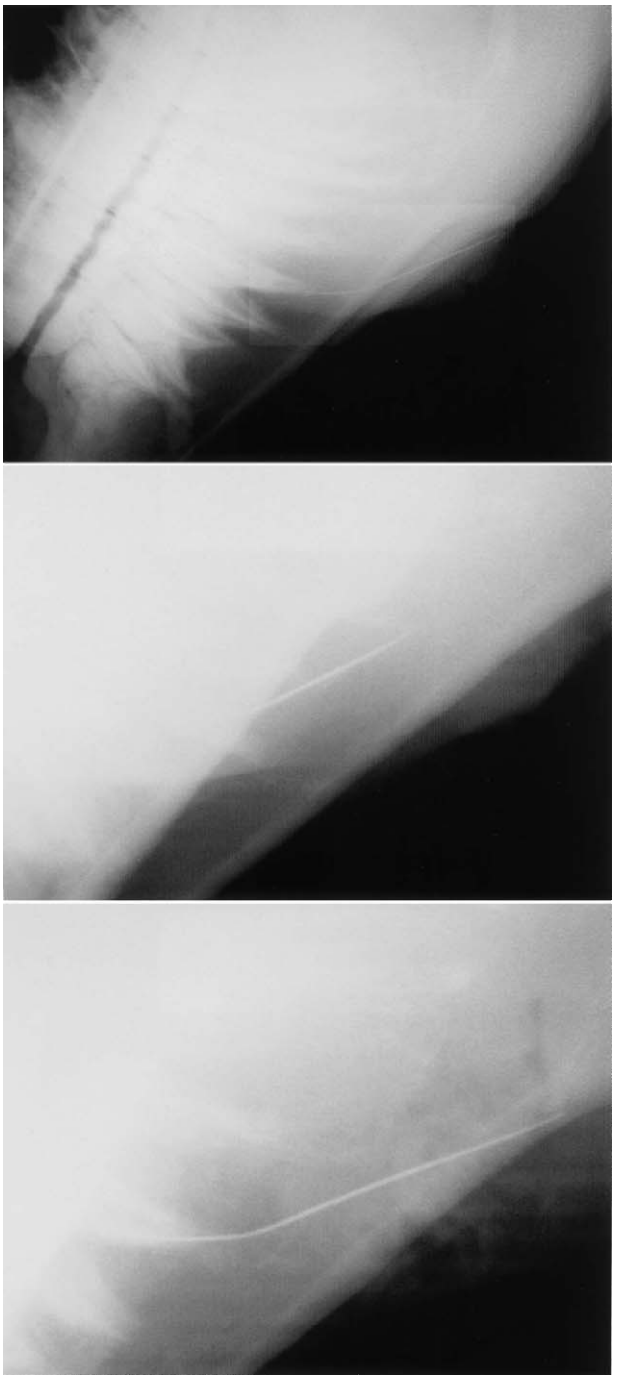


Figure 20-13 • Lateral **(A),** close-up **(B),** and ultra-close-up lateral oblique **(C)** views of the midmandibular body show a large wire embedded in swollen intermandibular soft tissue, which also contains numerous gas pockets. The horse was diagnosed 6 months previously as having an abscessed tooth based on the finding of chronic drainage from the area.

tical and cancellous bone taken from the animal. At 5 months, the lesion appeared smaller and was faintly mineralized. At 22 months the lesion was heavily mineralized, presumably the result of ossification. Although mandibular swelling persisted, it did not seem to interfere with the normal eruption of the permanent lower incisors.

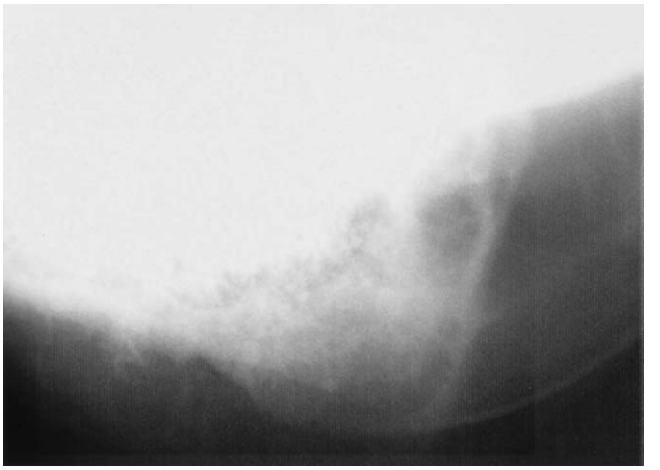


Figure 20-14 • Ultra-close-up lateral oblique view of a productive-destructive osteosarcoma in the angle of the right lower jaw.

Mandibular Intraosseous Epidermoid Cyst

Camus and co-workers described an intraosseous epidermoid cyst in a 21-year-old female American Saddle Horse, hospitalized for a progressive, nonpainful, mandibular enlargement developed over the past 6 months. Radiographically, the diseased mandible appeared lytic, expansive, internally compartmentalized, and vaguely marginated. The lesion appeared to involve the adjacent first mandibular cheek tooth.[10]

▮▮▮ NORMAL TEMPOROMANDIBULAR JOINT SERIES

The normal temporomandibular joint (TMJ) series comprises three projections: a true lateral, a right lateral oblique, and left lateral oblique, all of which are centered on one or both TMJs. An oblique projection of the TMJ is usually more revealing than a true lateral view because there is less overlap by surrounding bone (Figure 20-18). However, nonperpendicular imaging invariably results in some degree of geometric distortion that can be diagnostically confusing. Radiographically assessing the TMJs is a difficult task at the best of times, and as a result most such examinations are associated with a significant degree of diagnostic uncertainty.

Reasons for Poor Radiographic Sensitivity

There are three reasons for this low level of sensitivity: First, the articular surface of the mandibular condyle is markedly billowed, making it impossible to image completely in a single plane. Second, the mandibular condyle sets at a decidedly cocked angle, being tipped medially about 20 to 25 degrees, again making it impossible to view more than a portion of its surface

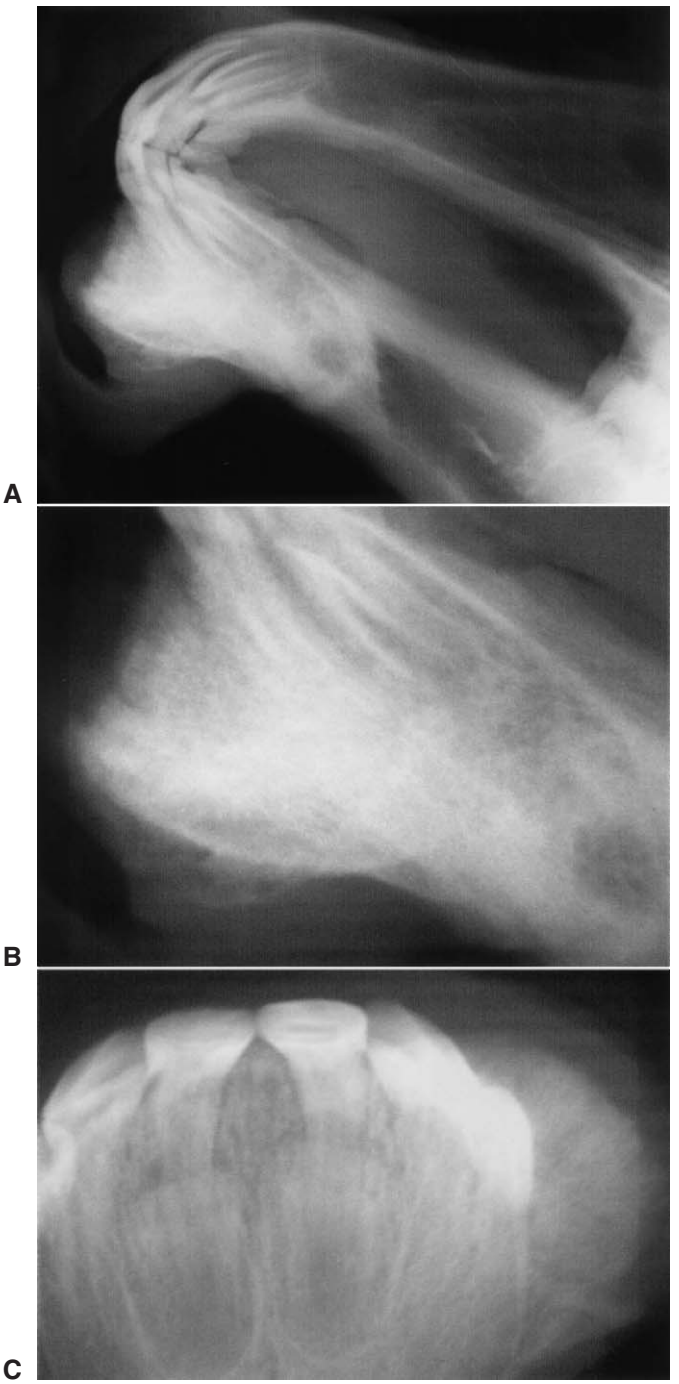


Figure 20-15 • Close-up lateral **(A),** ultra-close-up lateral **(B),** and ultra-close-up ventrodorsal **(C)** views of a productive osteosarcoma.

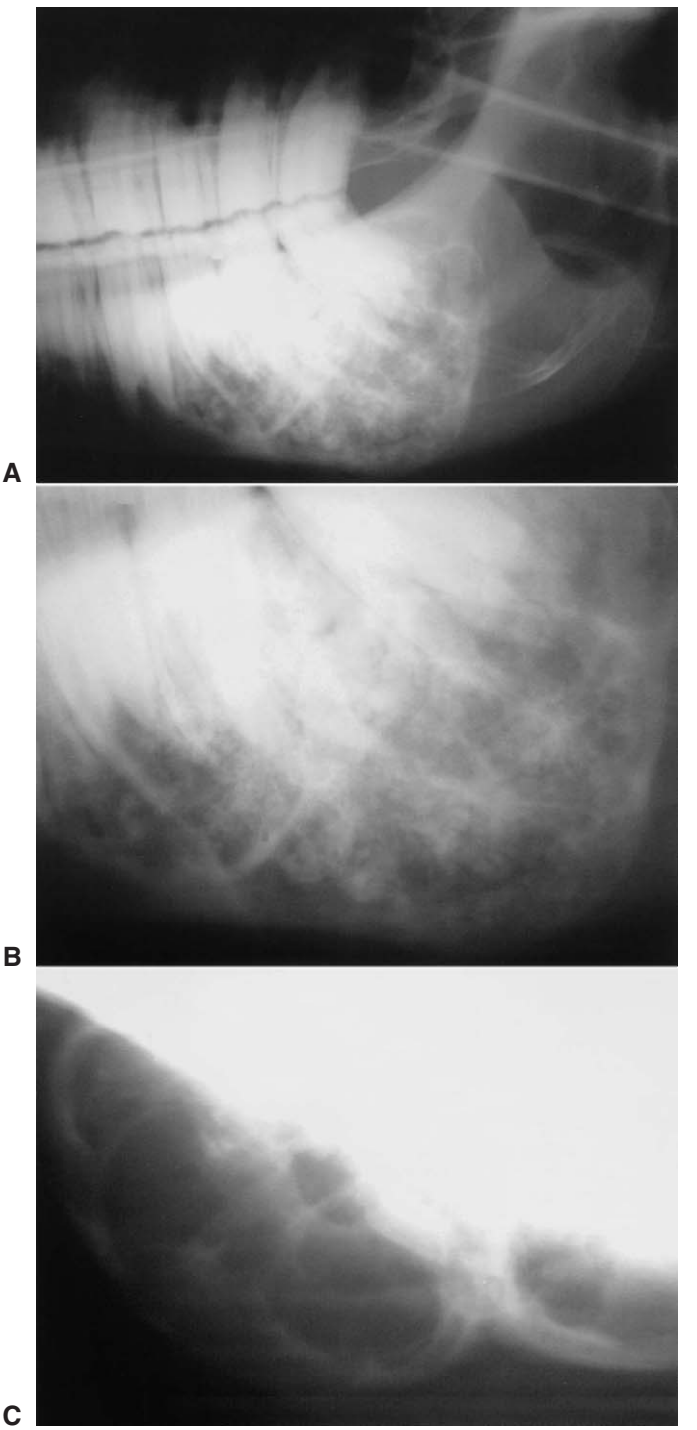


Figure 20-16 • Close-up lateral oblique **(A),** ultra-close-up lateral oblique **(B),** and ultra-close-up ventrodorsal **(C)** views of a mandibular adamantinoma. The ventrodorsal projection shows the soap-bubble appearance often found in such lesions.

with a single projection. Third, the nearby overlapping skull bones eliminate much of the detail and contrast required to see the condyle clearly. Close-up views of a mandibular condylar specimen from an adult horse are provided for radiographic anatomic comparison (Figures 20-19 and 20-20).

Normal Angle-Dependent Variation in the Width of the Temporomandibular Joint

By comparison, the temporomandibular cartilage space shows clearly but is subject to a great deal of geometric distortion, especially when projected at an angle. Depending on the degree of obliquity, the width

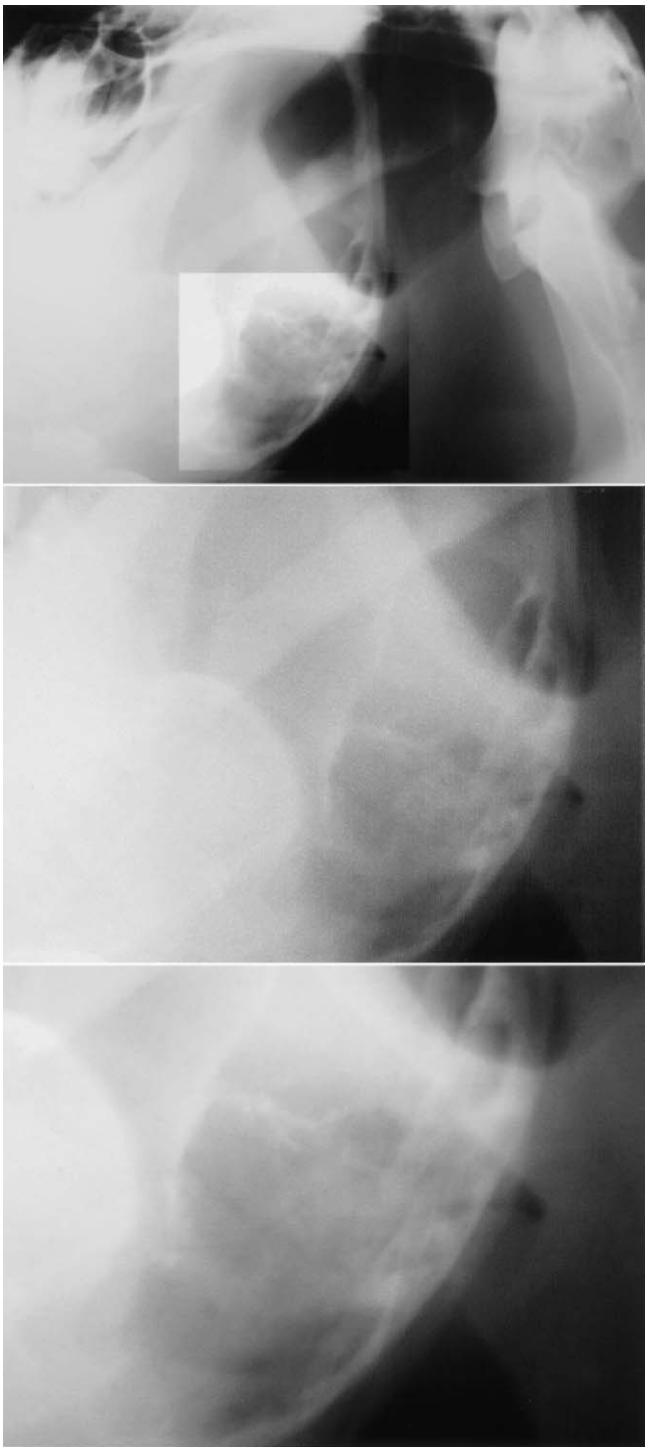


Figure 20-17 • Lateral **(A),** close-up **(B),** and ultra-close-up **(C)** lateral views of an ossifying fibroma in the ventral aspect of the left ramus.

of the temporomandibular cartilage space may increase by as much as 50 percent (or more), often leading to interpretive uncertainty (Figure 20-21).

Customized Views of the Temporomandibular Joint

When conventional views prove unrevealing, further radiographic examination of the TMJ is often abandoned. Alternatively, the study can be customized, specifically by making lesion-specific dorsoventral or dorsoventral oblique views of the TMJ, which eliminate some of the bony overlap that often compromises standard projections; such a case is illustrated in Figure 20-22.



Figure 20-18 • Lateral oblique view of an adult horse shows a normal temporomandibular joint (just to the right of center superimposed on the edge of the guttural pouch).

▮▮▮ TEMPOROMANDIBULAR FRACTURES AND DISLOCATION

Temporomandibular Fracture

Temporomandibular fractures are nearly always associated with some degree of dislocation, especially if the caudal glenoid process is involved. However, varying degrees of condylar displacement may occur as a result of soft-tissue injury without an associated fracture.

Temporomandibular Dislocation

Hardy and Shiroma reported a complete rostral dislocation of the right TMJ in a 20-year-old American Saddlebred gelding, the result of catching its head in a fence.[11] The key radiographic feature in this case was the presence of an empty glenoid, caused by the described luxation of the condylar process.

Complete luxation such as that described by Hardy and Shiroma is relatively easy to diagnose based on the presence of an empty glenoid, but subluxations are far more difficult to detect because of their resemblance to a normal TMJ projected at an oblique angle. A compa-



Figure 20-19 • Defleshed specimen of an adult horse showing side **(A),** rear **(B),** and top **(C)** views of the mandibular condyle. Note its articular curvature and pronounced medial tilt.



Figure 20-20 • Close-up view of a full temporomandibular joint seen from a lower rear perspective illustrates the marked curvature characteristic of this unique articulation, which make effective radiography difficult.

rable oblique projection of the opposite TMJ may help under such circumstances, but bear in mind that both joints can appear abnormal with some injuries or diseases.

Of the various radiographic abnormalities I have encountered with temporomandibular subluxation (not associated with fracture), *condylar-glenoid overlap* has proven most reliable (Figure 20-23). However, if CT is available, then it is by far the best means of diagnosing temporomandibular injury, entirely eliminating the problems of condylar angulation and superimposition (Figures 20-24 and 20-25).

▮▮▮ CONGENITAL MANDIBULAR MALFORMATION AND BRACHYGNATHIA

Congenital Mandibular Malformation Resembling Tumor or Bone Cyst

Tudor and co-workers described the radiographic and computed tomographic appearance of a large deforming cavitated mass in the right mandible of a 1-month-old Arabian colt. Although the lesion strongly resembled a bone cyst or dental tumor, it was considered a probable congenital malformation.[12]

Brachygnathia

Gift and co-workers reported 20 cases of brachygnathia (undershot lower jaw), the majority of which were Quarter Horse colts.[13] The difference in mandibular-maxillary length ranged from 0.75 to 3 cm. Some foals did not develop brachygnathia until they were a month old. Treatment consisted of attempting to retard maxillary growth with wire, which sometimes broke.

▮▮▮ PAROTID DUCT ATRESIA AND OBSTRUCTION

Congenital atresia or acquired obstruction of the parotid salivary duct usually produces a characteristic cylindrical swelling along the lateroventral margin of the lower jaw, representing the distended parotid

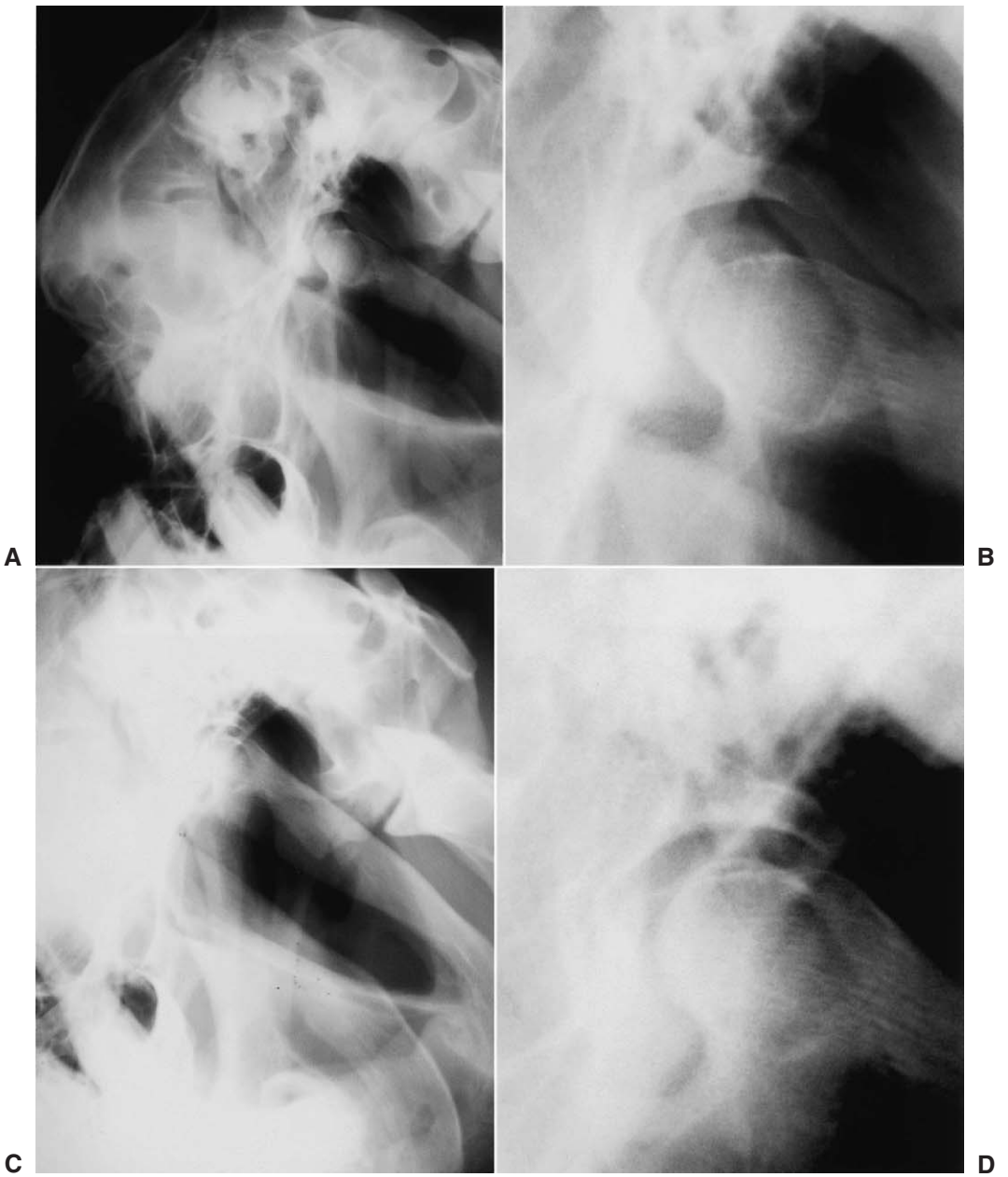


Figure 20-21 • Lateral **(A)** and close-up lateral **(B)** views of a mild to moderately oblique left temporomandibular joint in a normal adult horse. A second pair of lateral **(C)** and lateral close-up **(D)** obliques show a relative narrowing of the cartilage space characteristic of steeper lateral and lateral oblique projection angles.

duct.[14] Aspirating saliva from the swelling confirms the diagnosis. Identification of the blockage site may be by sonography, sialography, or cavography, the last being simplest.

Cavographic Diagnosis

Cavography is performed by percutaneously injecting a nonionic, diagnostic iodine solution into the distended parotid duct. The amount of contrast solution required to opacify the system is highly variable. My preference is to inject 6 ml and then make a lateral radiograph to get an idea of what I am dealing with in each case. Bear in mind that the purpose of salivary cavography is to inject enough contrast solution, which is water soluble, to opacify the saliva. Think of the procedure as opacifying the contents of the cavity—in this instance the saliva—rather than as a mere filling of an empty space.

I cannot emphasize too strongly the importance of using a nonionic contrast solution. Iodinated media are hyperosmolar and, as such, draw water to themselves. Although this may be tolerable in a distended salivary duct, it is potentially very painful when it



Figure 20-22 • Close-up frontal view **(A)** of the orbital and temporomandibular fields of an adult horse show right-sided swelling (viewer's left), resulting in a lack of relative definition in the underlying bone surfaces. A customized dorsoventral oblique projection **(B)** of the temporomandibular joints, including individual right **(C)** and left **(D)** close-up views, shows a difference in the mandibular condyles, which is suggestive (but not diagnostic) of osteoarthritis, the provisional diagnosis in this instance. An additional customized dorsocaudal oblique projection **(E)** with a skin marker over the point of maximal swelling provides unequivocal evidence that the right temporomandibular joint is not arthritic, fractured, or dislocated. Diagnosis: Localized blunt soft-tissue injury.

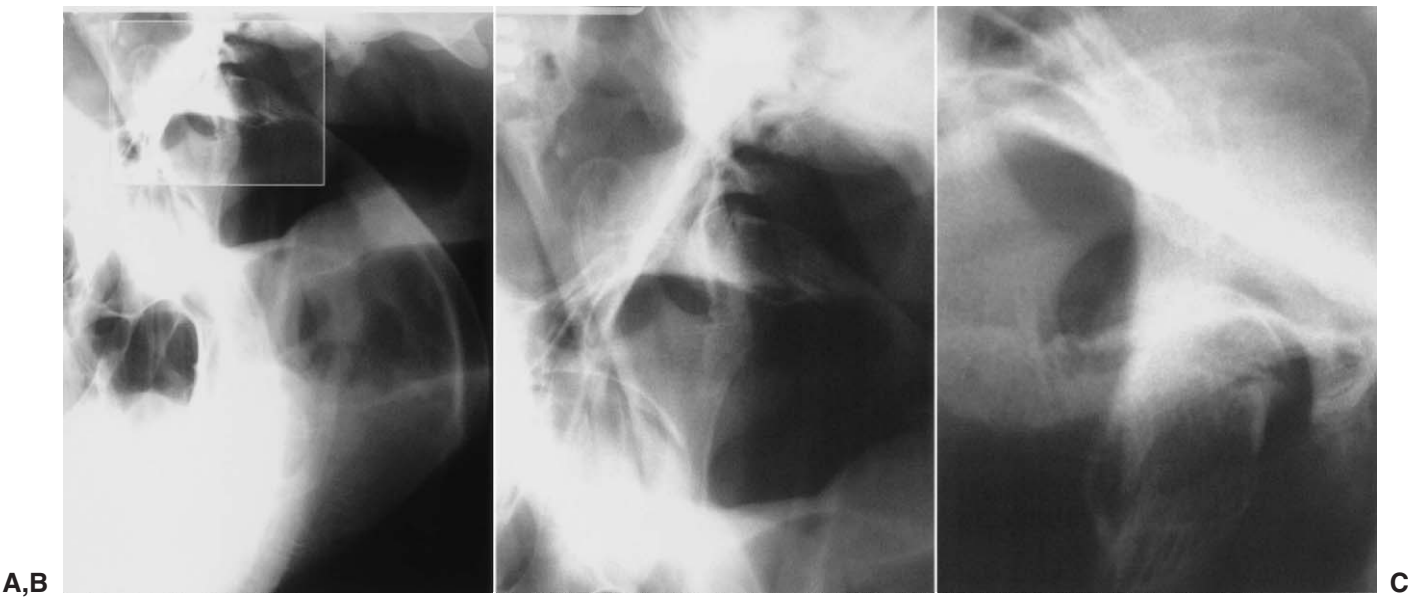


Figure 20-23 • Lateral **(A),** close-up **(B),** and ultra-close-up **(C)** lateral oblique views of a subluxated temporomandibular joint showing ventral overlapping of the mandibular condyle and glenoid margin.

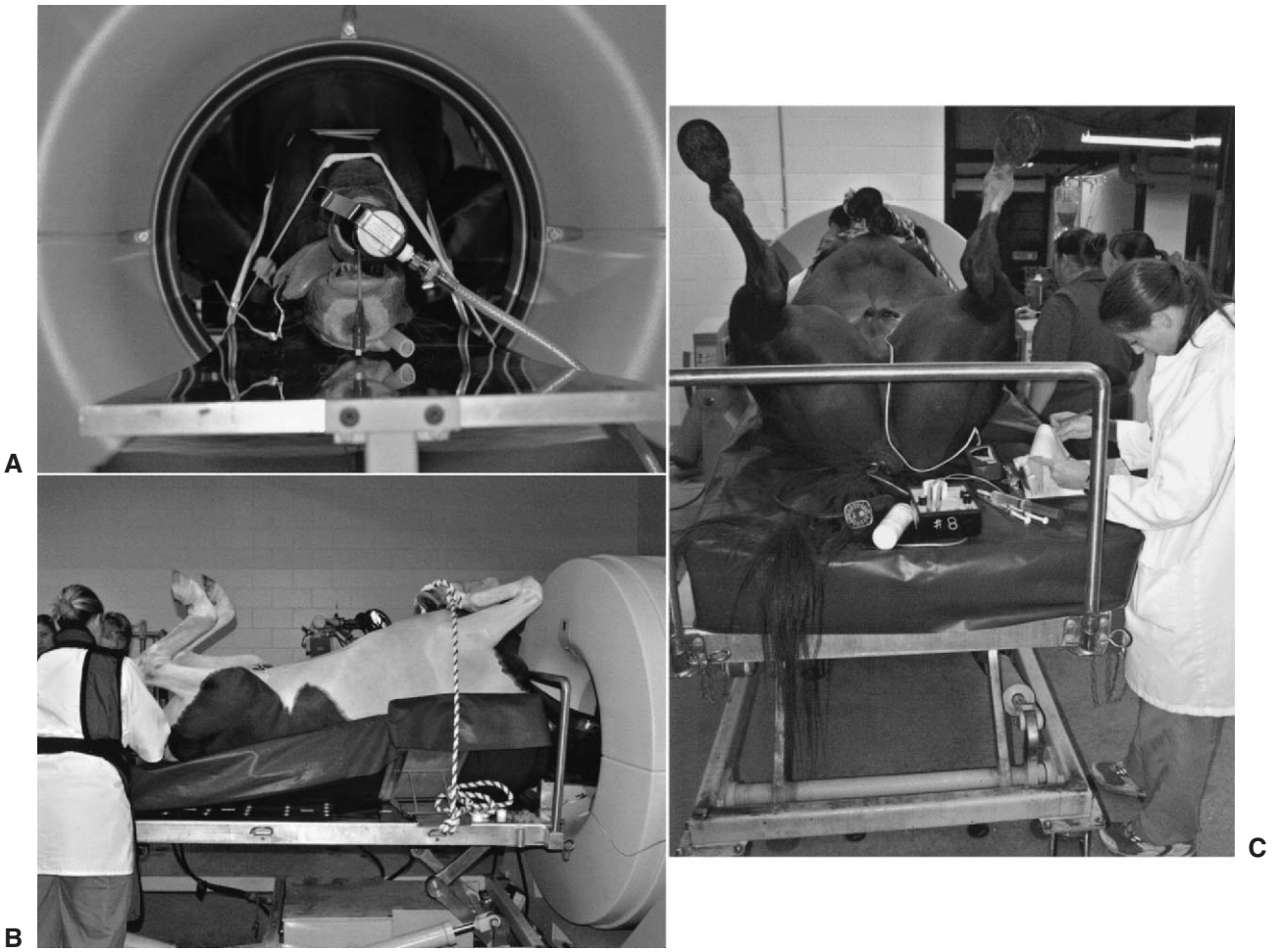


Figure 20-24 • Horse's head positioned in the bore of a CT gantry as seen from front **(A),** side **(B),** and rear **(C).**



Figure 20-25 • Three-millimeter axial tomogram from the center of a normal horse's temporomandibular joints.

occurs in the gland itself, so much so that many animals refuse to eat for 24 to 48 hours, and many even become pyrexic.

References

1. Wheat JD: Fractures of the head and mandible of the horse, *Proc Am Assoc Equine Pract* 21:223, 1975.
2. Henninger RW, Beard WL, et al: Fractures of the rostral portion of the mandible and maxilla in horses: 89 cases (1979–1997), *J Am Vet Med Assoc* 214:1648, 1999.
3. Sullins KE, Turner AS: Management of fractures of the equine mandible and premaxilla, *Compend Contin Educ Pract Vet* 4:480, 1982.
4. Ruggles AJ, Beech J, et al: Disseminated *Halicephalobus deletrix* infection in a horse, *J Am Vet Med Assoc* 203:550, 1993.
5. Specht TE, Bristal DG: Radiographic diagnosis, *Vet Radiol* 31:299, 1990.
6. French DA, Fretz PB: Mandibular adamantinoma in a horse, *Vet Surg* 13:165, 1981.
7. Richardson DW, Evans LH, Tulleners EP: Rostral mandibulectomy in five horses, *J Am Vet Med Assoc* 199:1179, 1991.
8. Lamb CR, Schelling SH: Congenital aneurysmal bone cyst in the mandible of a foal, *Equine Vet J* 21:130, 1989.

9. Jackman BR, Baxter GM: Treatment of a mandibular bone cyst by use of a corticocancellous bone graft in a horse, *J Am Vet Med Assoc* 201:892, 1992.
10. Camus AC, Burba DJ, et al: Intraosseous epidermoid cyst in a horse, *J Am Vet Med Assoc* 209:632, 1996.
11. Hardy J, Shiroma JT: What is your diagnosis? *J Am Vet Med Assoc* 198:1663, 1991.
12. Tudor RA, Ramiriz O, et al: A congenital malformation of the maxilla of a horse, *Vet Radiol Ultrasound* 40:353, 1999.
13. Gift LJ, DeBowes RM, et al: Brachygnathia in horses: 20 cases (1979-1989), *J Am Vet Med Assoc* 200:715, 1992.
14. Tally MR, Modransky PD, et al: Congenital atresia of the parotid salivary duct in a 7-month-old Quarter Horse colt, *J Am Vet Med Assoc* 197:1633, 1990.

Chapter 21

Dental Disease

NORMAL DENTAL ANATOMY AND DEVELOPMENT

Dental Anatomy

The equine tooth is of the *hypsodont type*, having enamel that coats both the crown and root. (Recall that dogs and cats have *brachydont* teeth, which have enamel covering only their crowns.) Horses also differ from dogs and cats in having a deep indentation or *infundibulum* in the occlusal surface of their incisors.

The tooth is secured in its socket or alveolus by the *periodontal membrane,* which appears as a radiolucent line surrounding the perimeter of the unerupted tooth. Just beyond this lies the dense inner surface of the socket or alveolus, termed the *dental lamina dura.*

The outer cementum of the tooth is physically attached to the inner surface of the alveolus by the periodontal membrane and a series of fibrous strands called *Sharpey's fibers.*

Equine Dental Formula

The dental formula of a horse is *3-3, 1-1, 3-3 (or 4-3), 3-3,* times two. This translates into 40 or 42 teeth, depending on whether or not there are any first premolars (wolf teeth).

Eruption Dates

Mechanism. The eruption time of permanent teeth is similar to that of temporary teeth. Adult teeth, through a process of encroachment, devascularization, and root reabsorption, gradually replace the deciduous teeth.

Incisors. Equine incisors erupt at 2.5, 3.5, and 4.5 years. Although initially curved, the incisors gradually straighten with age as the distal portion of the arch is gradually worn away. In another age-related change, the outermost maxillary incisors will have uneven occlusal surfaces between 7 and 20 years of age because of differences in width compared with their mandibular counterparts.

Canine Teeth. In males the maxillary canine tooth is located in the middle of the interdental space, with the mandibular canine tooth situated somewhat more rostrally. Mares usually lack canine teeth or have only a rudimentary, unerupted mandibular canine. The permanent canines arrive at 4 to 5 years of age without interference, there being no deciduous predecessors.

Cheek Teeth. The eruption times for the cheek teeth are listed in Table 21-1. The cheek teeth of the horse continue to grow longitudinally until the sixth year, at which time the basilar pulp divides, narrows, and forms individual radiographically discrete roots or root branches. After the sixth year, the length of the teeth will begin to decrease as the crown surfaces begin to wear because of their quite forceful grinding action.

Numbers of Roots. After an extraction, the removed cheek tooth should be carefully inspected for completeness, especially its roots. The numbers of roots found in cheek teeth are listed in Table 21-2.

Radiolucent Area at Root Apex

The radiolucent area around and between dental roots is not simply an alveolar space but rather a number of extremely important support tissues, including (1) dental germ cells, (2) blood vessels supplying the tooth, and (3) the dental nerve. This is important to bear in mind when creating surgical drainage associated with dental infection, lest important tissue be damaged. Another ramification of these radiographically invisible tissues is that they (or the spaces they reside in) are responsible for the undulant appearance of the ventral mandible found in horses less than 5 years of age.[1]

Table 21–1 • ESTIMATED ERUPTION DATES FOR EQUINE CHEEK TEETH

1st Cheek tooth (2nd premolar)	2.5 yr
2nd Cheek tooth (3rd premolar)	3.0 yr
3rd Cheek tooth (4th premolar)	4.0 yr
4th Cheek tooth (1st molar)	0.75-1.0 yr
5th Cheek tooth (2nd molar)	2.0 yr
6th Cheek tooth (3rd molar)	4.0 yr
A vestigial 1st premolar, termed a *wolf tooth*, may sometimes be present	

Table 21–2 • NUMBERS OF ROOTS FOUND IN MAXILLARY AND MANDIBULAR CHEEK TEETH

Tooth (Teeth)	No. of Roots
First and sixth *maxillary* cheek teeth	3 roots
Second through fifth *maxillary* cheek teeth	Variable: 3 or 4 roots
First through fifth *mandibular* cheek teeth	2 roots
Sixth *mandibular* cheek tooth	3 roots

Box 21-1
Equine Teeth: Some Anatomic and Developmental Facts

Enamel is the densest part of a horse's tooth, being 96%-97% inorganic mineral, and it is the body's most radiodense tissue.
The remaining elements of a tooth, *dentin* and *cement*, are comparable to bone in density.
The *enamel crown* is fully elaborated by the time of eruption.
A *fetal tooth* requires 240 days to complete its development, but its anlage can be seen in jaw specimens as early as 120 days' gestation.
The *anlage of the permanent enamel crown* can be seen in horses up to 4.5 years, when the sixth cheek tooth erupts.
Each crown is formed in sequence: 4, 5, 1, 2, 3, 6; it takes about 360 days to be completed. *Note:* Equine cheek are numbered 1 to 6, from front to back, excluding the wolf tooth (i.e., the 4th cheek tooth = the 1st molar).
Dental *roots are not fully formed* until after eruption.
Eruption is triggered by *increased pulp vascularity*, a condition that is signaled radiographically by a cystlike distension of the lamina dura (a thin white line surrounding the embedded part of a tooth representing the interface of the periodontal ligament and alveolar bone).
Radiographically visible *vertical striations* in the tooth represent the foldings of the enamel crown.
Dentin and enamel are radiographically invisible owing to the greater density of the enamel.
The exposed crowns are in close contact, forming a continuous grinding surface, resulting in the presence of only minimal alveolar bone in the interproximal areas.
During life, the *reserve crown continues to erupt at a rate of 3 mm a year*, making it possible to estimate the age of a horse by measuring the depth of the reserve crown and root definition.
A recent article on the effect of dental floating on rostrocaudal mandibular motion cited dental disease as the third or fourth most common reason that horse owners seek veterinary care.

From Carmalt JL, Townsend HGG, Allen AL: Effect of dental floating on the rostrocaudal mobility of the mandible of horses, *J Am Vet Med Assoc* 223:666, 2003.

▮▮▮ EQUINE DENTAL FACTS

Baker previously described the normal radiographic anatomy of equine teeth and related dental disease. The following *dental facts* are taken from his work (Box 21-1).

The Standard Dental Series

The standard examination for upper or lower cheek teeth consists of a full-length orientation view of the head and a pair of oblique views centered over the region of interest. Where ventrolateral mandibular swelling is present, a spot film using soft-tissue technique is often able to identify recently formed new bone that otherwise would be burned out using conventional bone settings. Normal dental radiographs of the cheek teeth of a foal (Figure 21-1) and an adult horse (Figure 21-2) are provided for comparison with the diseased teeth that will follow.

Supplementary Projections

Barakzai and Dixon recently developed an open-mouth, oblique projection for evaluating the exposed (erupted) portions of the teeth of horses (Figure 21-3).[2] Specifically, the modified oblique view calls for a mouth gag or, more accurately, a mouth wedge, to hold the teeth apart (thus the description "open-mouthed"), a sedative and twitch to restrain the animal while it is being radiographed, and a reduction in beam angle from the usual 30 to 45 degrees to about 10 or 15 degrees (depending on whether the mandibular or maxillary teeth are being imaged). In addition to the mouth being open and a reduction in beam angles, the open-mouth obliques require that standard beam directions be reversed: dorsolateral-lateral for maxillary cheek teeth, and ventrolateral-lateral for mandibular cheek teeth.

The authors contend that by separating the upper and lower teeth during radiography, much of the superimposition typically associated with conventional close-mouthed radiography is eliminated, an assertion strongly supported by the included dental radiographs. Diseases of the dental crown that may be seen better with the lateral open-mouth oblique include (1) interdental crevices or gaps (diastemata), (2) fractures, (3) abnormal wear (transverse ridges,

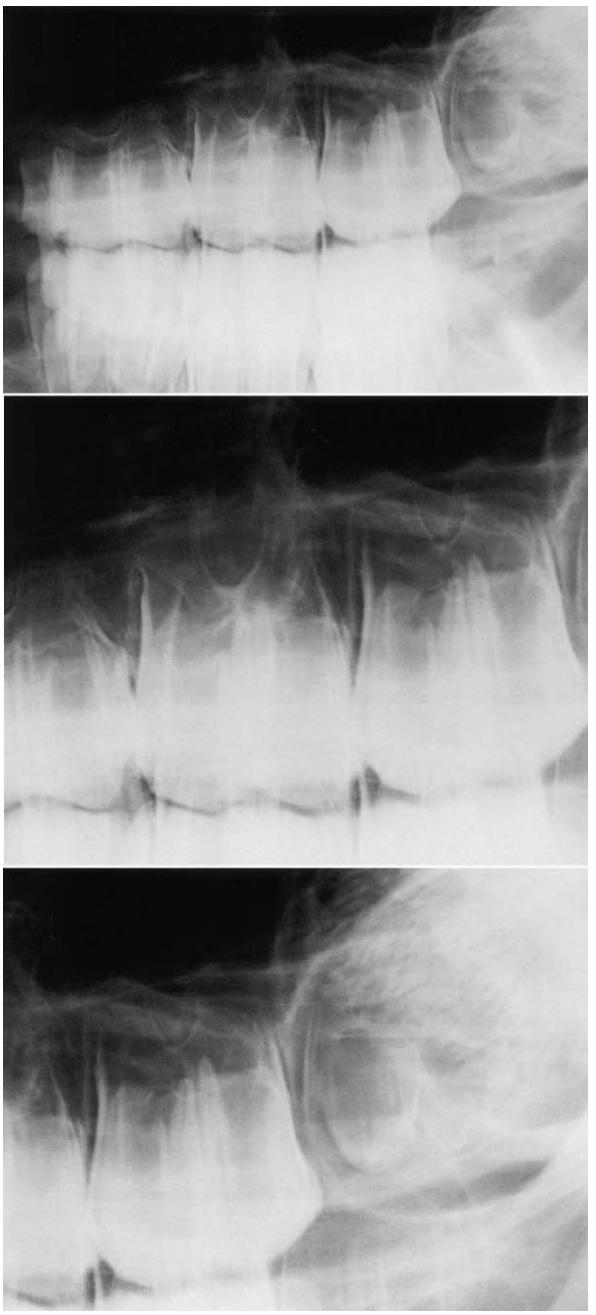


Figure 21-1 • Lateral oblique **(A)** and close-up lateral oblique **(B)** views of the rostral cheek teeth of a foal show the short, blocky morphology typical of an immature tooth. An ultra-close-up view of the caudal aspect of the upper jaw in the same foal shows an unerupted tooth caudally **(C)**.

wave) or stepmouths, (4) polydontia or hypodontia, and (5) retained or impacted deciduous teeth.

The Patient-Tailored Examination

O'Brien reported the use of nonscreen and commercial dental film to selectively examine the maxillary cheek teeth of two horses.[3] Although the method produced superior radiographic images compared with conventional radiography, it did require general anesthesia.

Box 21-2
Possible Adverse Consequences of Supernumerary Cheek Teeth

Feed impaction secondary to a gap or depression in the interdental space resulting from interference with normal eruption by supernumerary tooth.
Secondary malocclusion.
Secondary periodontal disease after gingival irritation and recession.
Premature tooth loss secondary to advanced periodontal disease.
Conchal necrosis (if supernumerary teeth are located in maxillary sinus).
Maxillary sinusitis (if supernumerary teeth are located in maxillary sinus).

Normal Radiographic Anatomy

Radiographically, an adult equine tooth appears as a vertical or variably sloped rectangular object in the jaw, possessing an intensely opaque appearance. The contact surface of the crown is rippled and nearly uniformly wide, whereas the reserve crown and roots appear as a series of closely packed columns, culminating proximally in an irregular and relatively indistinct edge. As the tooth ages, the roots become more distinct.

Various views of a cutaway skull specimen provide further insight into the considerable variation in the size, shape, angle, and root structure of adult cheek teeth and to the intimate relationship between the three caudal cheek teeth and the maxillary sinus (Figure 21-4). An axial tomogram (Figure 21-5) of the teeth through the maxillary sinuses graphically illustrates why so many maxillary dental infections in this region lead to secondary sinonasal disease.

▮▮▮ SUPERNUMERARY CHEEK TEETH

Precisely how and why extra teeth develop in horses is not known, Prevailing theory holds that there is an abnormal division of the permanent tooth germ, creating a pair of teeth where normally only a single tooth should exist. When incisors are involved, there are few if any clinical consequences; however, if cheek teeth are affected, a variety of serious problems may ensue (Box 21-2).

Walesby and Miles reported an unusual case of supernumerary teeth in a 2-year-old Thoroughbred racehorse believed initially to have a fractured tooth.[4] In the described case, a pair of deformed supernumerary maxillary cheek teeth were situated between normal-appearing molars (lateral radiograph); in the

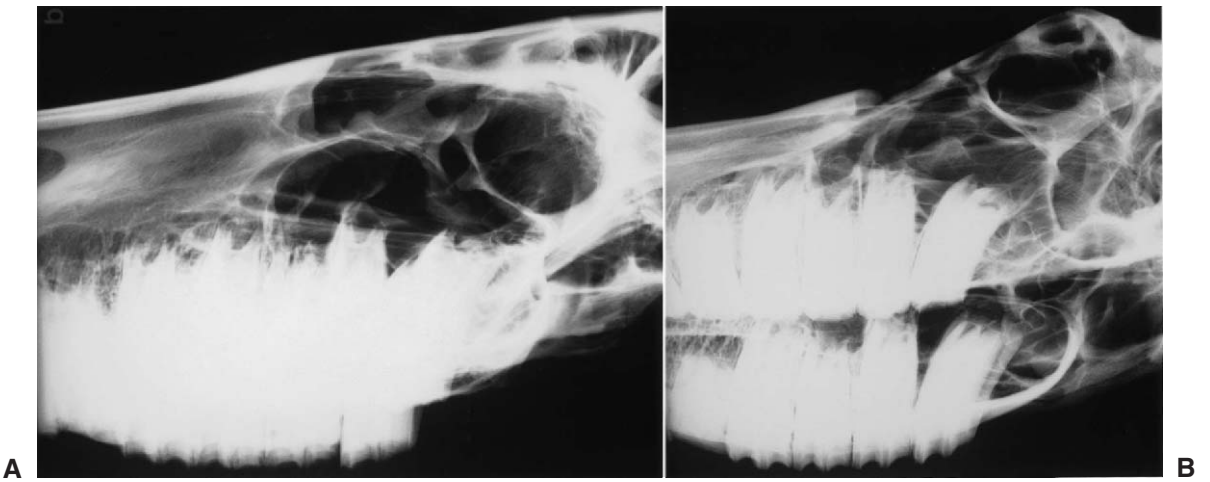


Figure 21-2 • Lateral **(A)** and lateral oblique **(B)** views of the cheek teeth of an adult horse made from a skull specimen to optimize dental detail. Note how in the oblique view much of the confusing dental superimposition is eliminated, but at the cost of some change in the appearance of the teeth (termed *geometric distortion*), especially their roots. A view of the undersurfaces of the maxillary cheek teeth in another specimen that also includes the lower jaw illustrates why oblique teeth appear foreshortened compared with the same teeth projected laterally.

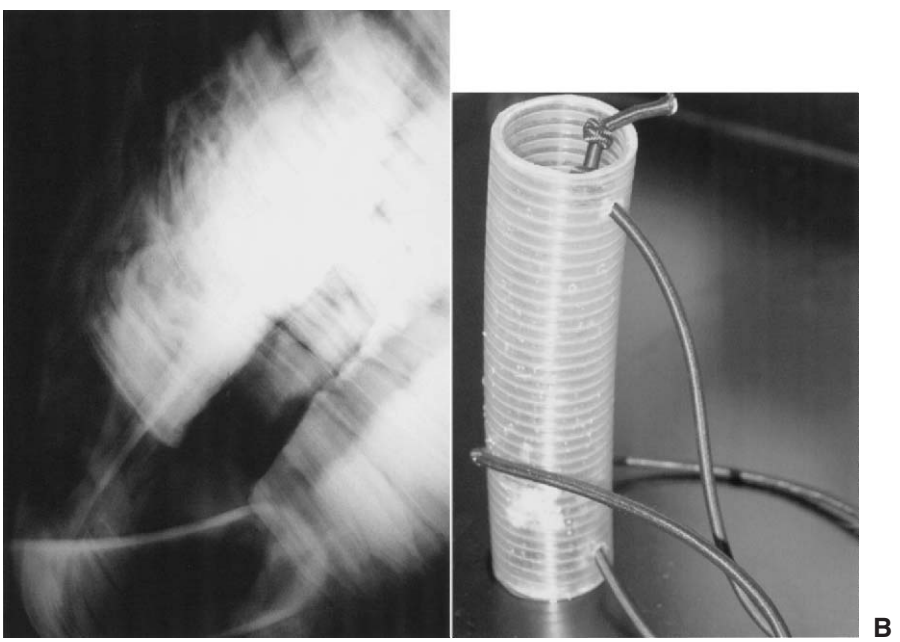


Figure 21-3 • Lateral oblique view **(A)** of the rostral cheek teeth and the wedge **(B)** used to separate them for the open-mouth view.

dorsoventral view, the extra teeth appeared as indistinct opacities within the maxillary sinus.

▮▮▮ MAXILLARY AND MANDIBULAR DENTAL INFECTION

Baker was among the first to publish an illustrated radiographic review of dental infection in the horse in one of the early issues of the *Equine Veterinary Journal*.[5] In this article, he divided diseases into two categories: those that commonly affect the maxilla and those that affect the mandible. This classification is simple and straightforward and is summarized in the following section.

Clinical Presentation

Clinically, pain, swelling, reluctance to eat, and unusual chewing characterize maxillary dental infections. If secondary sinonasal disease develops, there is also a putrid nasal discharge. Mandibular dental infections are frequently associated with a draining sinus ventrally.

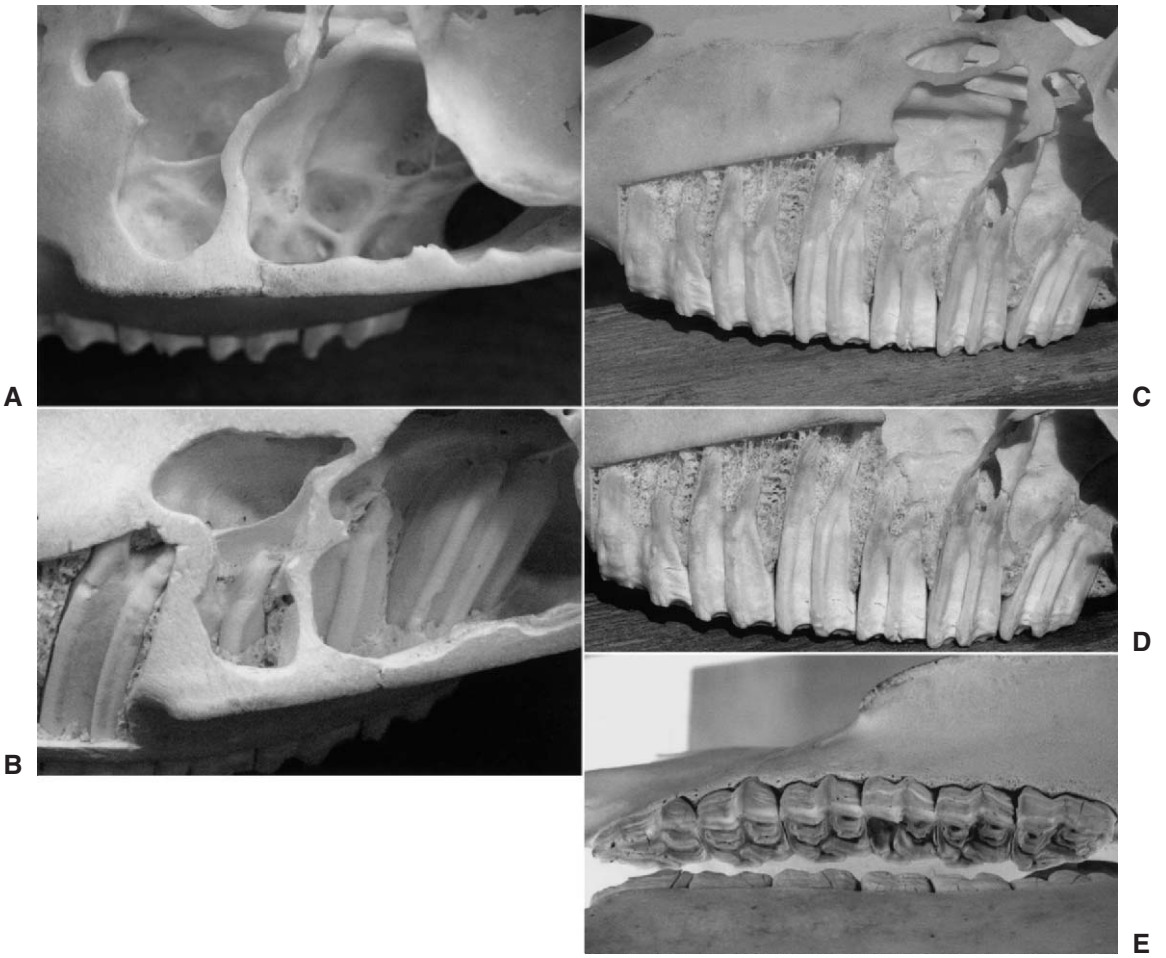


Figure 21-4 • Close-up lateral views of the maxillary region of a pair of adult skulls: one with only the lateral sinus wall burred away **(A)** and the other with *both* the lateral sinus and alveolar walls removed **(B).** Note that when the alveolus is intact, only the profile of the underlying tooth is visible, emphasizing the fact that the last three cheek teeth and their respective alveoli reside together in the maxillary sinus. Lateral **(C)** and close-up lateral **(D)** views of the skull of an adult horse with the lateral facial bones removed revealing the six underlying maxillary cheek teeth. An oblique view of another skull specimen shows the occlusal surfaces of the left maxillary arcade **(E).**

Apical Dental Infections: Cause, Appearance, and Progression

Pulpitis: The Initiating Lesion. According to Baker, pulpitis as a result of infection introduced through an area of cement necrosis or fracture is the most severe form of maxillary dental disease, affecting the tooth, the periodontal membrane, the alveolus, and potentially the surrounding bone or maxillary sinus.

Radiographic Appearance

Maxillary Dental Infection. Radiographically, pulpitis typically features a combination of productive and destructive changes—most visibly the latter—in both the infected tooth and surrounding bone. Apical lesions may be small and confined to a single root or tooth, termed *apical granulomas*, or quite large, sometimes involving a series of two teeth or more, a disease known as *diffuse maxillary alveolar periostitis*. Lesion size depends primarily on which tooth or teeth are involved and for how long. The second, third, and fourth maxillary cheek teeth are most often affected.

Classically, an apical dental infection appears as a roughly circular radiolucency, often accentuated by a sclerotic ring, surrounding the upper part of the infected tooth. Occasionally a fluid level is present, especially if the tooth lies in the maxillary sinus.[6] The involved roots are often rounded and less distinct than the adjacent unaffected roots. New bone may be present on and around the infected tooth (Figures 21-6 and 21-7).

Mandibular Dental Infection. Typically mandibular pulp infections result in mandibular swelling and, if not treated promptly, sinus formation, the latter often resulting in alveolar gas pockets. In such instances, sinography or probe making can be used to identify

the infected tooth or teeth. Although relatively rare, it is possible to have a draining mandibular sinus associated with an infected periodontal membrane and a normal tooth. Occasionally a gas pocket located in the mandibular soft tissue and superimposed on one or more teeth will resemble a dental infection. Figures 21-8 through 21-14 illustrate the foregoing radiographic features.



Figure 21-5 • Ventrodorsal computed tomogram (dental window) through the maxillary sinus shows the normal relationship between the upper and lower cheek teeth.

Progression of Dental Infection

Chronic infections can lead to apical blunting and enlargement, referred to as *clubbing*, or *cementosis*, which is caused by the localized deposition of cement on and within dental roots or root fragments (Figure 21-15). Cementosis may also appear as small spherical densities surrounding but not in direct contact with the apex of an infected tooth (Figure 21-16). Structurally weakened tooth roots may fracture, eventually leading to sequestration (Figure 21-17). Some sequestra may appear relatively larger in progress films, a fact Baker attributes to cement deposition. Parallel mandibular drainage channels may eventually join at either end, sequestering the intervening bone (Figure 21-18).

Infections that extend into the maxillary sinus can cause empyema, pressure-induced enlargement, and overflow into the nasal cavity leading to a nasal discharge (sinonasal disease). Some chronic infections cause a draining sinus *(dental sinus)* to develop on the side of the face, an association that can often be proven with sinography[7-9] or a probe-based marking study. Draining dental sinuses may also be caused by retained root or alveolar fragments after extraction.

Alternate Imaging of Equine Dental Infection

Ultrasound. A standard lateral projection of the mandible, combined with one or more customized tangential views of the area of interest, will usually identify an infected tooth and any associated mandibular infection; but radiology cannot discriminate between

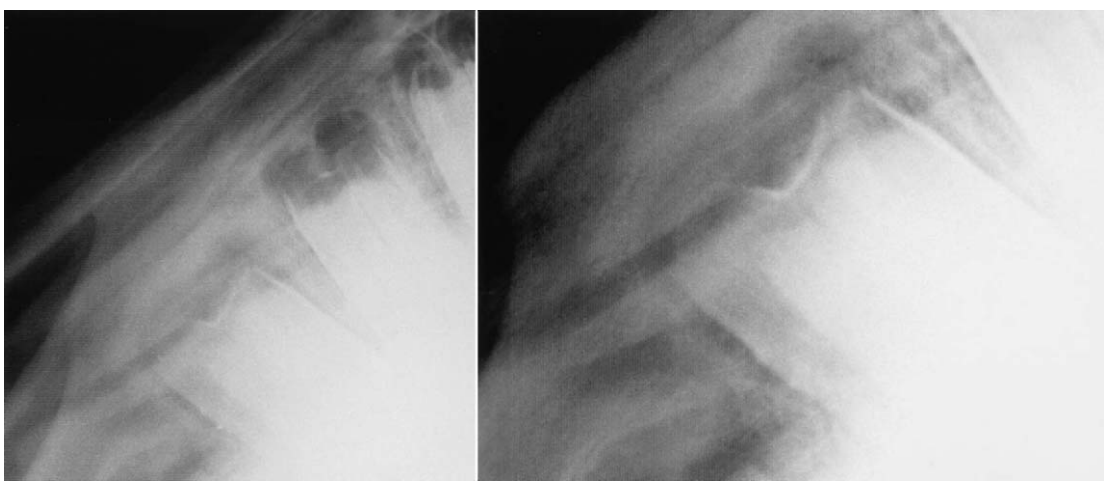


Figure 21-6 • Close-up right lateral oblique **(A)** and ultra-close-up lateral oblique **(B)** views of the second right maxillary cheek tooth show a light gray conforming halo surrounding the apex and upper body of the tooth characteristic of infection. The lucency around the roots of the nearby cheek teeth is normal.

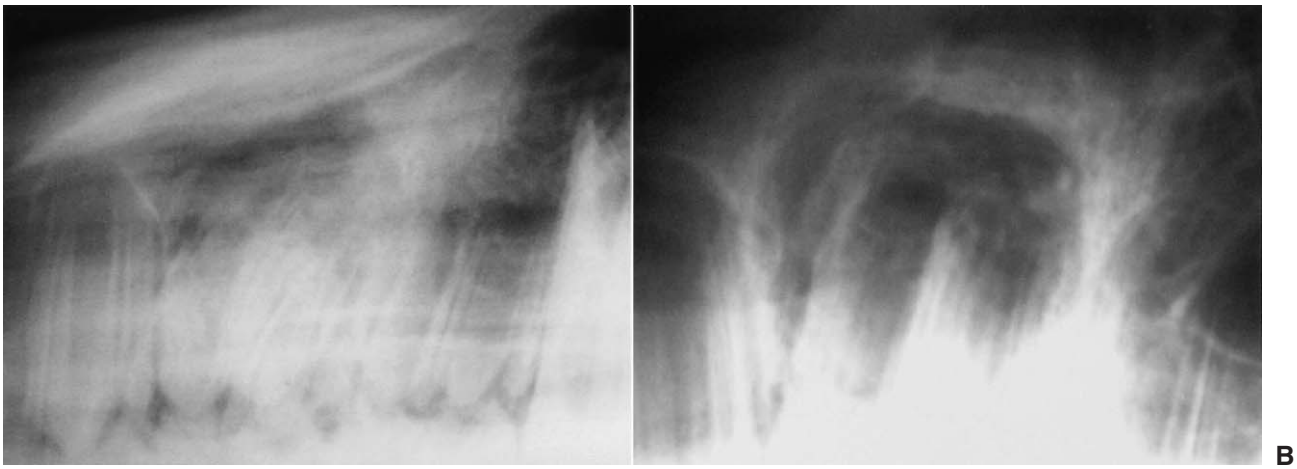


Figure 21-7 • Close-up lateral **(A)** and ultra-close-up lateral oblique **(B)** views of a chronically infected central maxillary cheek tooth showing a mature apical abscess with a well-formed involucrum, extensive root loss, and spread of the infection to the flanking alveoli (diffuse alveolar periostitis).

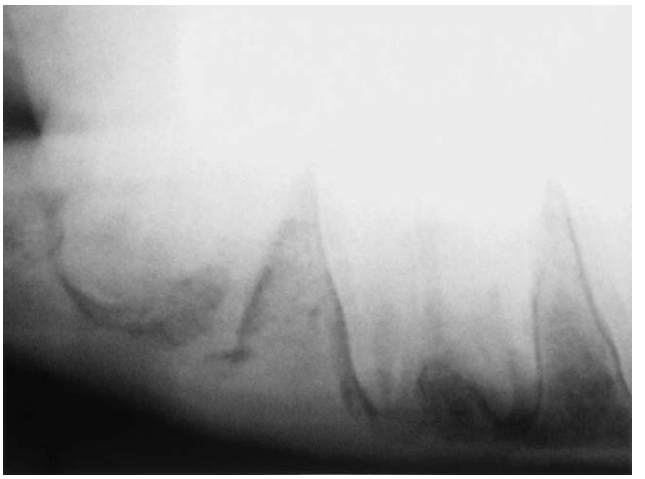


Figure 21-8 • Close-up lateral oblique view of the first and second left mandibular cheek teeth shows alveolar bone loss surrounding both roots indicative of infection.

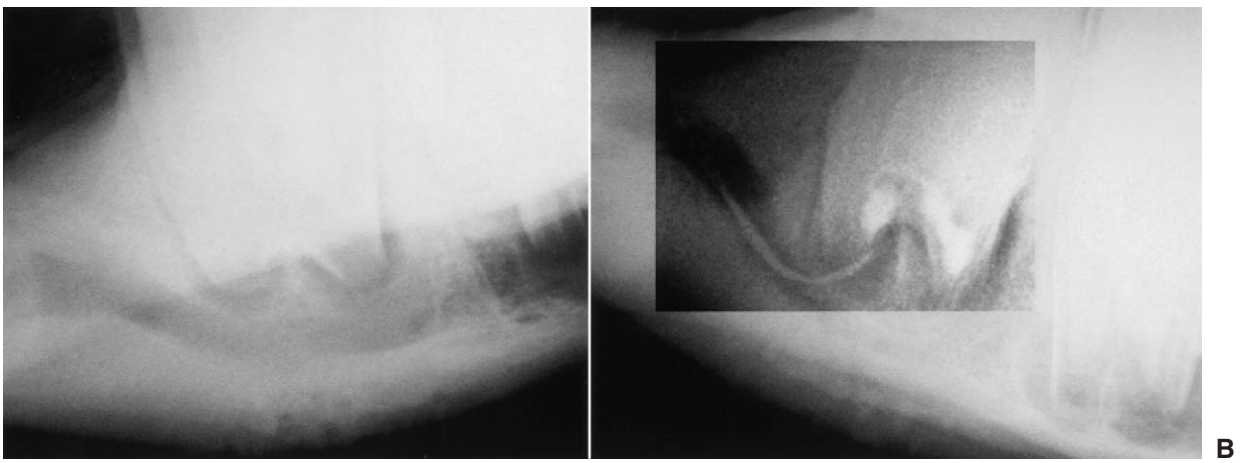


Figure 21-9 • **A,** Ultra-close-up right lateral oblique view of the first mandibular cheek tooth shows abnormal periapical lucency and intermediate duration new bone on the dependent surface of the underlying mandible where there is a draining sinus. **B,** A close-up lateral oblique sinogram shows the catheter tip and contrast solution within the alveolus and in contact with the infected tooth.

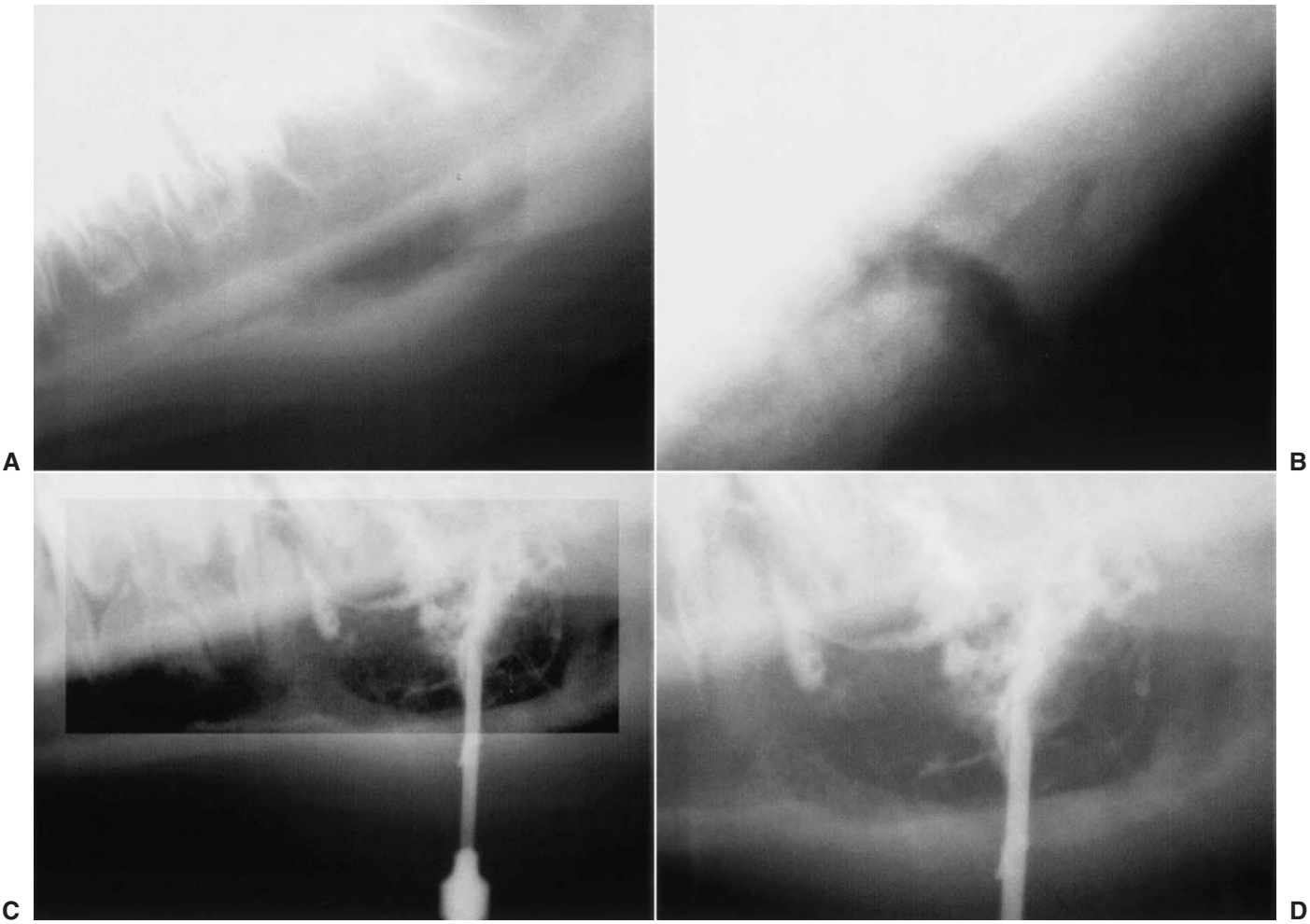


Figure 21-10 • Customized close-up lateral oblique view **(A)** of the caudal portion of the right mandible using soft-tissue technique shows a cavitated mature bone deposit. A second customized lateral oblique projection **(B),** again using soft-tissue technique, shows a distinct drainage channel passing through the center of the new bone. Close-up **(C)** and ultra-close-up **(D)** lateral oblique sinograms made with a teat cannula inserted into the drainage channel show contrast solution within two alveoli consistent with infection.

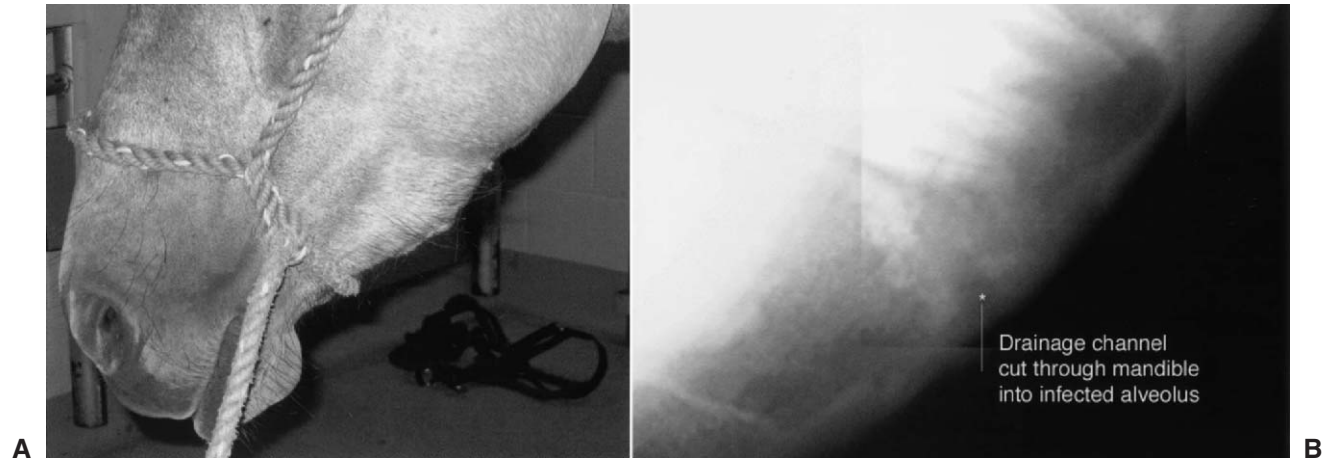


Figure 21-11 • **A,** Close-up view of the swollen left mandible of a horse with an alveolar abscess. **B,** Labeled lateral oblique view of the infected tooth made after drilling a hole into the rostral aspect of the infected alveolus as a means to flush, medicate, and drain the alveolus and hopefully preserve the tooth.

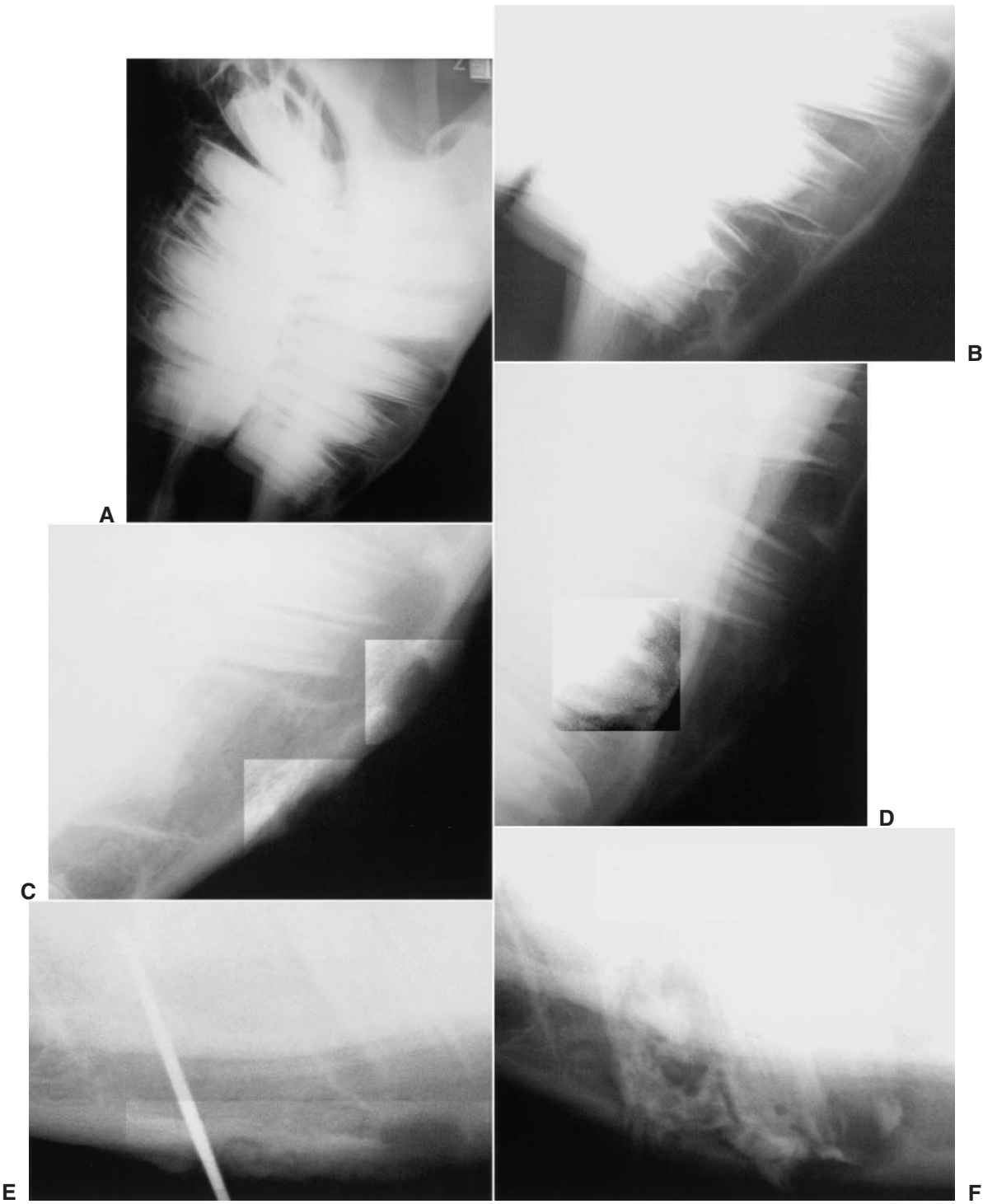


Figure 21-12 • Lateral **(A)** and close-up lateral **(B)** radiographs of the head of a horse with a swollen, painful, draining left lower jaw **(A)** provide some indication as to the source of drainage in the form of overly lucent rostral alveoli. Because of superimposition, it is not possible to implicate a particular tooth. A close-up lateral oblique view **(C)** of the underlying mandible using soft tissue reveals a pair of defects surrounded by new bone consistent with alveolar drainage channels *(emphasis zones)*. A customized rostrocaudal oblique view **(D)** shows root destruction and loss of alveolar integrity involving the second cheek tooth *(emphasis zone)*. A probe placed into the rostral-most mandibular drainage site enters the alveolus of the first cheek tooth **(E),** but a follow-up sinogram **(F)** reveals contrast in both the first and second alveoli, indicating that the infection is more widespread than first suspected.

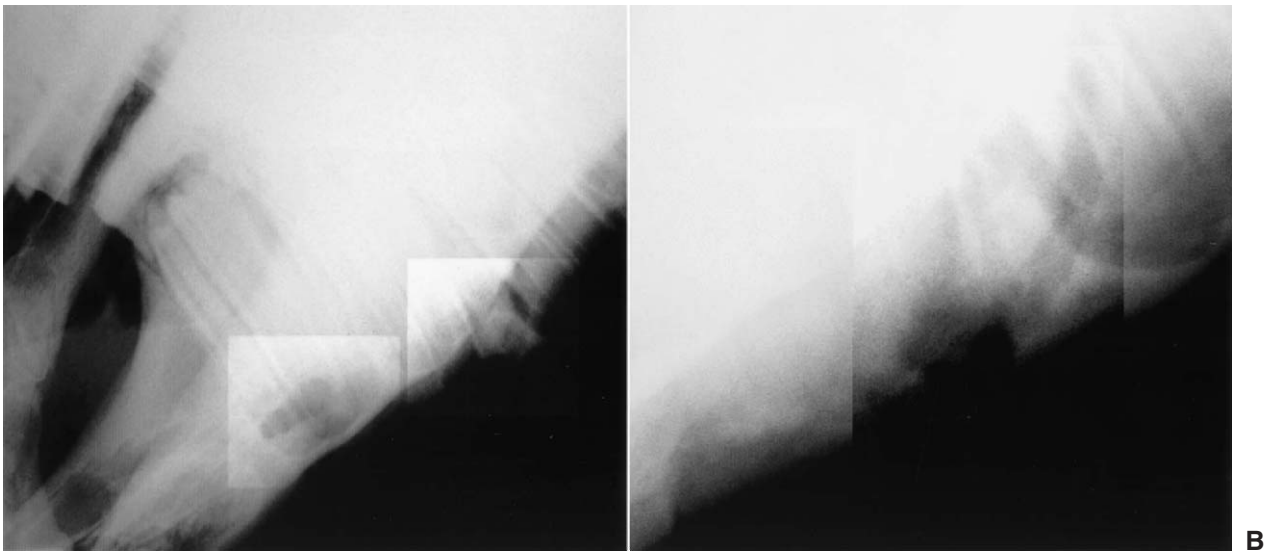


Figure 21-13 • Lateral oblique **(A)** and close-up customized lateral oblique **(B)** views of the left mandible of a horse with multiple draining tracts. Atmospheric contamination has resulted in multiple alveolar gas pockets.

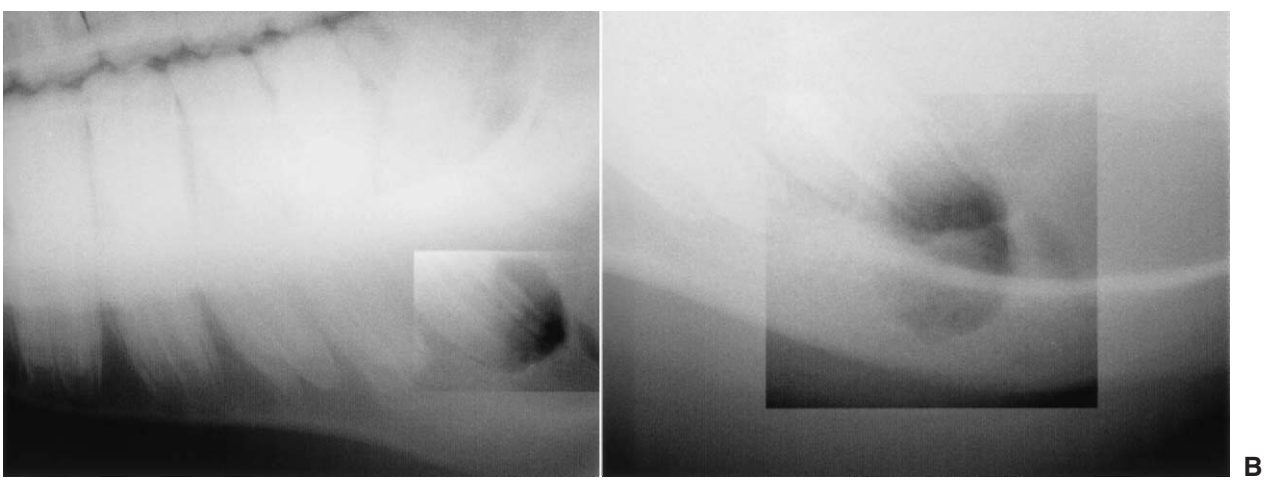


Figure 21-14 • **A,** Lateral oblique view of the right mandible of a horse with mandibular drainage shows what appears to be a caudal alveolar gas pocket. **B,** A second film, however, made at a different projection angle shows that the gas pocket is actually located in the soft tissue adjacent to the tooth, not in the alveolus.

the masseter muscle, edema, and abscessation, although radiology shows gas pockets well. Where questions exist regarding the source of ventral mandibular drainage, in particular its relationship to the adjacent teeth, sinography is the procedure of choice.

Ultrasound, on the other hand, is an elegant means of evaluating the soft-tissue swelling that usually accompanies a badly infected lower cheek tooth and can even be used to suggest a drainage tunnel in the nearby mandible. As shown by Gayle and co-workers, the two essential elements of a probable periapical infection with secondary mandibular osteomyelitis are (1) one or more deep fluid pockets adjacent to the mandible and (2) a focal defect in the underlying reflection from the surface of the mandible.[10]

Computed Tomography. There is no better way to evalauate horses' teeth than with computed tomography (CT). The most difficult and labor intensive part of such an endeavor is getting the horse to and from the CT unit (Figure 21-19).

As for the images themselves, they are unsurpassed by any other means of medical imaging. As an added benefit, CT can provide x-ray transmission values, which are invaluable in differentiating one type of tissue from another, and often characteristic of specific diseases (Figure 21-20).

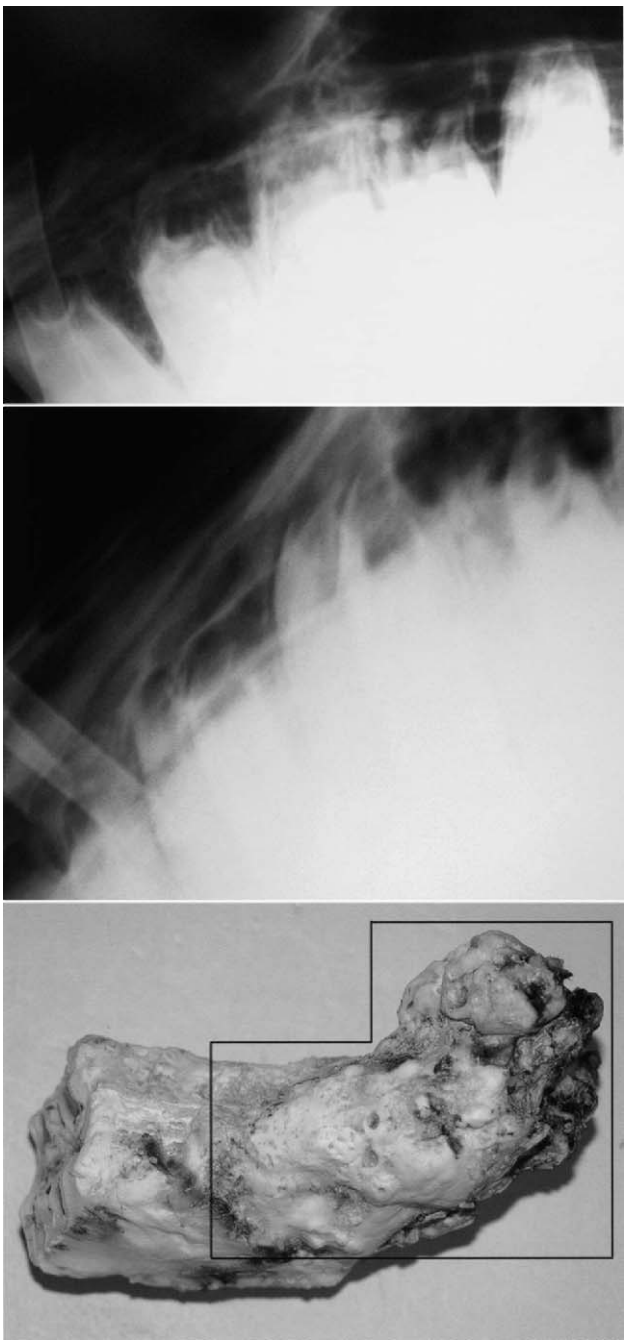


Figure 21-15 • A, Close-up lateral oblique view of a chronically infected third maxillary cheek tooth shows enlargement, deformity, and loss of alveolar integrity consistent with severe cementosis. **B,** A normal oblique view of the central maxillary cheek teeth is provided for comparison. **C,** Photograph of the extracted tooth shows a large mound of disorganized cementum attached to the lateral apical region (polygon). *(Referral radiographs and specimen courtesy Dr. Zygadlo, equine veterinarian, Alberta, Canada.)*

Nuclear Medicine. Metcalf and co-workers reported using nuclear scintigraphy to diagnose radiographically invisible or uncertain dental infections.[11] Gayle has also used nuclear imaging in an effort to identify multiple infected mandibular teeth, but with only modest success.[10] My opinion is that scintigraphy is not particularly well suited to this purpose, especially in situations in which there is concomitant mandibular infection.



Figure 21-16 • Ultra-close-up lateral oblique view of central maxillary region shows multiple spherical cementum deposits superimposed on the roots of the third and fourth cheek teeth consistent with chronic dental infection.

▮▮▮ DENTAL FRACTURES

Most dental fractures occur in conjunction with mandibular fractures and, less often, with facial injuries. Teeth may be chipped or broken into multiple pieces. Displacement is usually inward, either to the nasal cavity or maxillary sinus. Devascularization and denervation are common sequelae under such circumstances, as is foreign-body reaction, especially when a tooth becomes lodged between the conchae. Dislocated rostral cheek teeth usually cause some degree of unilateral nasal cavity obstruction (Figure 21-21).

▮▮▮ DISORDERS OF DENTAL POSITION AND DEVELOPMENT

Dental Malpositioning and Malocclusion

Both O'Brien and Dixon and co-workers have addressed the subject of dental malpositioning.[3,12]

Dental Ectopia (Dentigerous Cyst, "Ear Tooth," Heterotopic Polydontia, Temporal Teratoma)

Ectopia is the term for an abnormally situated tooth or tooth-like object. The most dramatic example is the so-called ear tooth, or dentigerous cyst, typically a medium-sized mass of poorly organized dental tissue

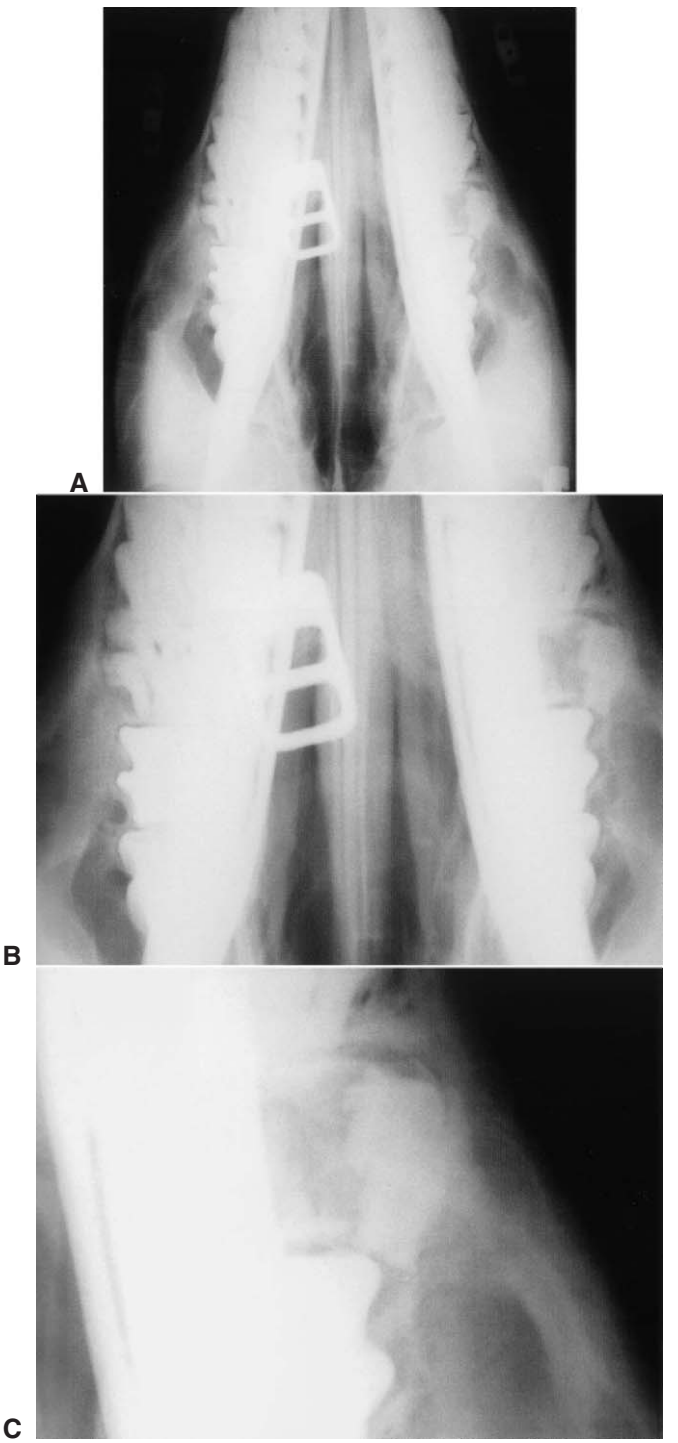


Figure 21-17 • Dorsoventral **(A),** close-up dorsoventral **(B),** and ultra-close-up dorsoventral **(C)** views of the midfacial region of a horse with a large left-sided swelling and copious nasal discharge show a displaced pathologic fracture of the fourth cheek tooth and opacification of the associated left maxillary sinus.



Figure 21-18 • Lateral **(A)** and ultra-close-up lateral **(B)** views of a chronically infected right lower jaw and central cheek teeth show a medium-sized triangular sequestrum situated midway between a pair of large mandibular drainage tracts. Compare these radiographs, and in particular the lesion detail, to a second case of an infected first cheek tooth in which a 3-millimeter axial tomogram **(C)** shows: (1) partial root destruction, (2) near complete alveolar destruction, and (3) infectious relief canalization of the underlying mandible.

found cranial to the ear of foals that often behaves like a foreign body as evidenced by associated drainage. Some ear teeth are contained in small pedunculated sacs that hang from the side of the head; others are intracranial, but most are attached loosely to the outer surface of the temporal bone.[13] Small ectopic teeth lacking any morphologic characteristics of normal teeth are sometimes referred to as *denticles*.

Radiographically an ear tooth typically appears as a medium-sized, circular, bonelike density adjacent to the bullae, which it may strongly resemble (Figure 21-22).

Excessive Angulation

Some degree of inconsequential dental angulation is normally present in horses, especially in the first three lower cheek teeth. However, if the slope of a misdirected tooth becomes too great, it may impact a neighboring tooth, interfering with its normal eruption. The adjacent mandible is particularly prone to expansion under such circumstances, and the involved tooth or teeth may become infected.

Caps and Consequences

Caps is the term given to retained deciduous teeth, which, if persistent, can prevent the underling permanent tooth from erupting, but not from continuing to grow. The result is so-called reverse growth, where, in an effort to find growing room, the blocked tooth pushes ventrally into its alveolus, causing the underlying mandible to undergo a localized, cystic expansion (Figure 21-23). Although quite striking radiographically and painful for the animal, the problem is easily resolved by removing the cap. Occasionally a retained cap causes the following adult tooth to erupt laterally, similar to what happens with some human wisdom teeth. In some instances the resultant

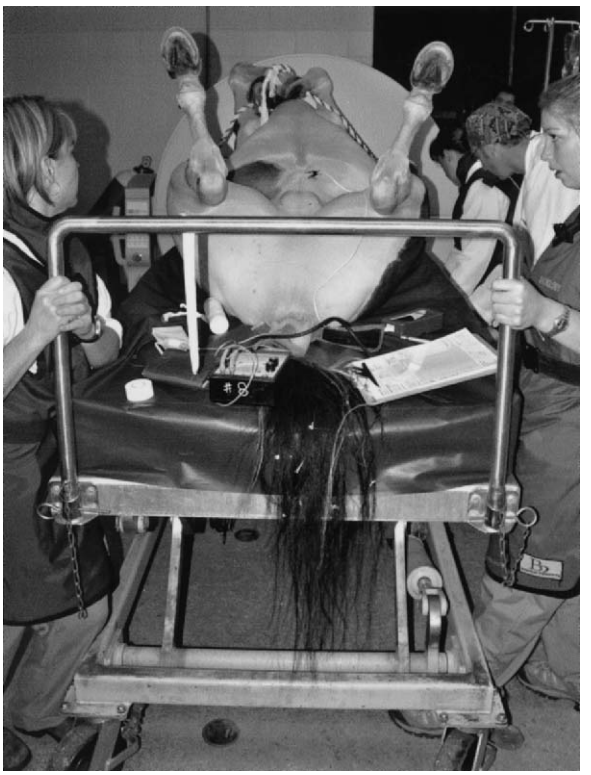


Figure 21-19 • Getting a horse to and from a CT facility in a reasonable period of time can be logistically challenging, requiring a well-trained and coordinated team, as seen in this photograph.

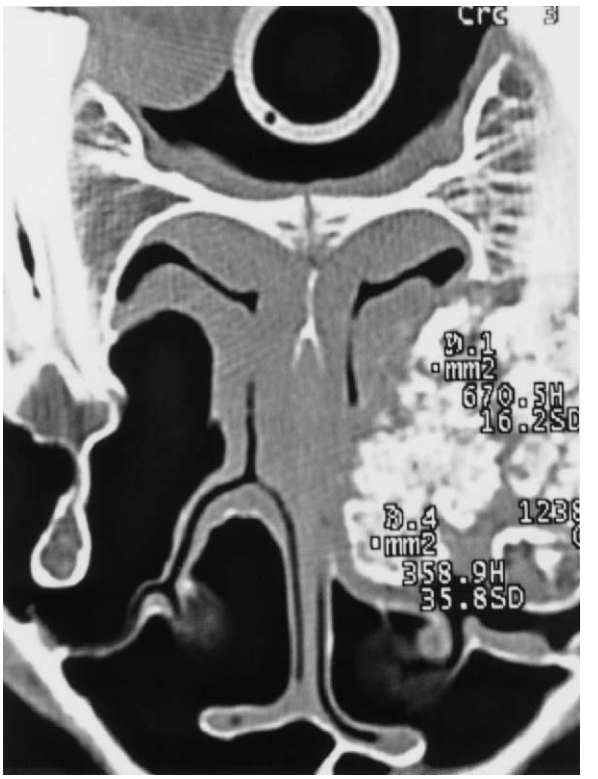


Figure 21-20 • Three-mm axial tomogram through the caudal facial region of a horse shows an expansive cemental overgrowth (cementosis) of the 1st right maxillary molar, which is encroaching on the adjacent paranasal sinuses. Various x-ray transmission values (in Hounsfield units) appear on the associated overlay, indicating the composition of the deformed portion of the diseased tooth.

facial deformity can be quite pronounced (Figure 21-24).

Abnormal Dental Spacing (Diastema)

Congenital or acquired gaps between teeth can lead to uneven wear of both the affected and opposing tooth as well as food trapping. Also termed *diastema* or *diastemata,* these abnormal spaces may develop as a result of a variety of causes.[14]

Malocclusion

Most malocclusion is relatively minor in nature to the extent that can be effectively treated with regular floating (Figure 21-25). Congenital overbites can lead to accommodative structural changes in opposing cheek teeth as well as malocclusion (Figure 21-26), Overgrowth and dental drift usually occur following an extraction (Figure 21-27).

▮▮▮ JUVENILE DENTAL TUMORS

The following tumor and tumorlike lesions tend to grow slowly and are variably invasive.

Ameloblastoma

Although primarily a tumor of enamel, the ameloblastoma is not characteristically dense, as one might expect. Instead, the ameloblastoma is predominantly radiolucent, internally divided, and slowly expansive. Hemorrhage within a developing tooth may result in the formation of *follicular cysts,* a deforming-type dental lesion that closely resembles an ameloblastoma.

Odontoma and Cementoma

Odontoma and cementoma are included together because of their single predominant radiographic feature: their bonelike density. Because of their common quality, these tumors are often misinterpreted as osteomas.

Osteoma

Osteomas are actually bone, not dental tumors, but because they often displace adjacent teeth they are included here. Most of these tumors are extremely

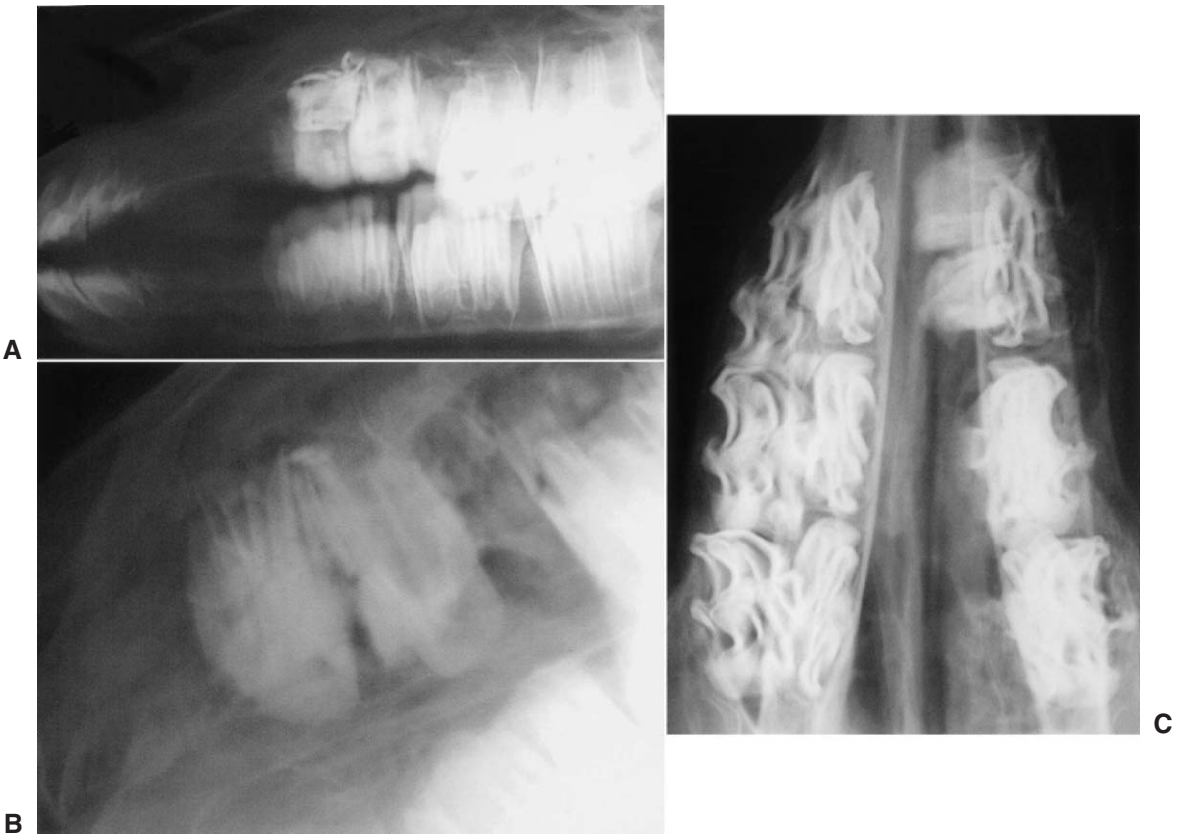


Figure 21-21 • Lateral **(A)** and ultra-close-up lateral oblique **(B)** views of the rostral facial region of a foal show displaced fractures of both the first and second maxillary cheek teeth. A dorsoventral view **(C)** indicates that the broken teeth are on the left side of the face (the reader's right) and that they have displaced into the adjacent nasal cavity.

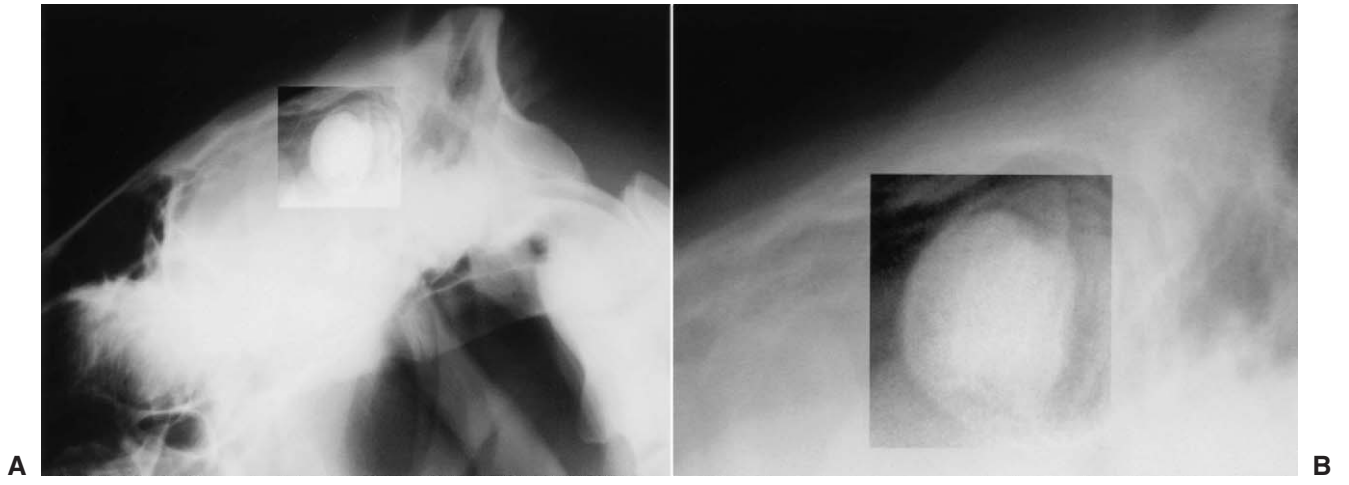


Figure 21-22 • Lateral **(A)** and close-up lateral **(B)** views of the head show a large oval density superimposed on the caudal aspect of the cranium typical of an ectopic tooth.



Figure 21-23 • Close-up dorsoventral **(A)** and ultra-close-up dorsoventral oblique **(B)** views of an impacted first left maxillary cheek tooth show cystic alveolar expansion and thickening of the overlying facial bone. An ultra-close-up view **(C)** of the same area of the maxilla (soft-tissue technique) shows an often-seen distinctive laminated appearance of gradually expanded facial bones.

dense and can become very large, in one instance being reported to resemble a basketball.

Adamantinoma

The adamantinoma is actually a type of gingival tumor that resembles a squamous cell carcinoma. Like the ameloblastoma, the adamantinoma is both radiolucent and expansile. Unlike most other dental tumors, the adamantinoma has been reported in horses as old as 5 years (Figure 21-28).

Ameloblastic Ondontoma

Most of the few reported cases of ameloblastic ondontoma have been in young foals and ponies. The tumor typically involves the maxillary dentition and associated maxillary sinus, obstructing the latter, leading to abnormal fluid accumulation and expansion resembling a maxillary cyst.[15]

▮▮▮ DENTAL ABSCESS

Unlike Baker, O'Brien considers most dental infections to be abscesses rather than apical granulomas. He further cites the additional benefit of radiography in the case of multiple mandibular abscesses, in which the mandible may be so weakened that it fractures during extraction.

▮▮▮ FLUOROSIS

Naturally occurring fluorosis in horses causes dental lesions: discoloration, abrasion, pitting, cavitation, and occlusal irregularity, with the proviso that excessive amounts of fluorine are ingested during the period of dental development. Excessive dietary fluorine can also cause diffuse periosteal new bone deposition,

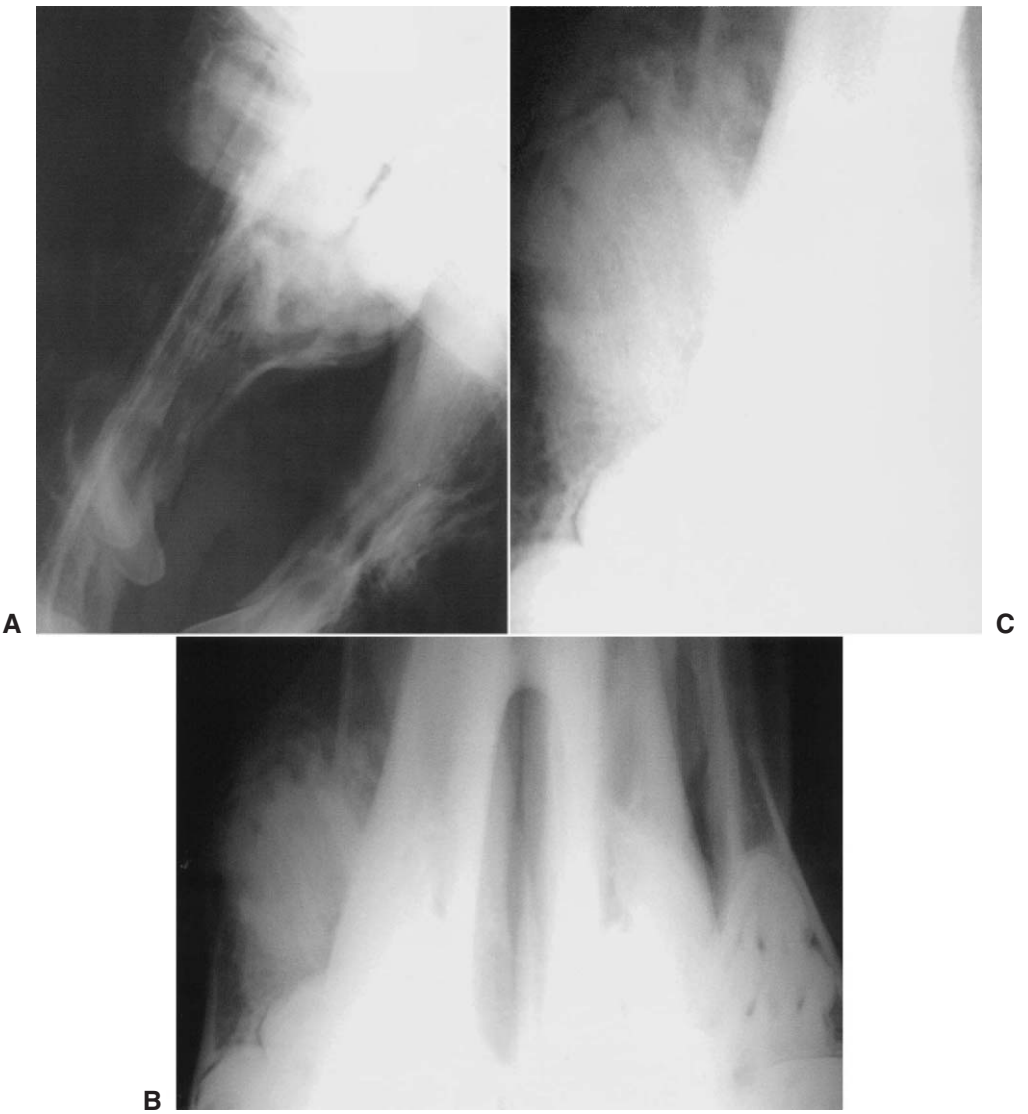


Figure 21-24 • Close-up lateral **(A)** dorsoventral **(B),** and ultra-close-up dorsoventral **(C)** views of the face of a young horse with a large right-sided swelling resulting from a retained cap and the subsequent *lateral* eruption of the adult first maxillary cheek tooth.



Figure 21-25 • Close-up lateral oblique view of a "hook" on the first left maxillary cheek tooth.

giving affected long bones a distinctive shaggy appearance and making the ankles look swollen.[16]

References

1. Quick CB, Rendano VT: Radiographic interpretation: the equine teeth, *Modern Vet Pract* 19:561, 1979
2. Barakzai SZ, Dixon PM: A study of open-mouthed oblique radiographic projections for evaluating lesions of the erupted (clinical) crown, *Equine Vet Educ* 15:143, 2003.
3. O'Brien RT: Intraoral dental radiography: experimental study and clinical use in two horses and a llama, *Vet Radiol Ultrasound* 37:412, 1996.
4. Walesby HA, Miles KG: What is your diagnosis? *J Am Vet Med Assoc* 220:597, 2002.
5. Baker GJ: Some aspects of equine dental radiology, *Equine Vet J* 3:46, 1971.
6. Reeves MJ, Traub-Dargatz J, Park RD: What is your diagnosis? *J Am Vet Med Assoc* 192:239, 1988.

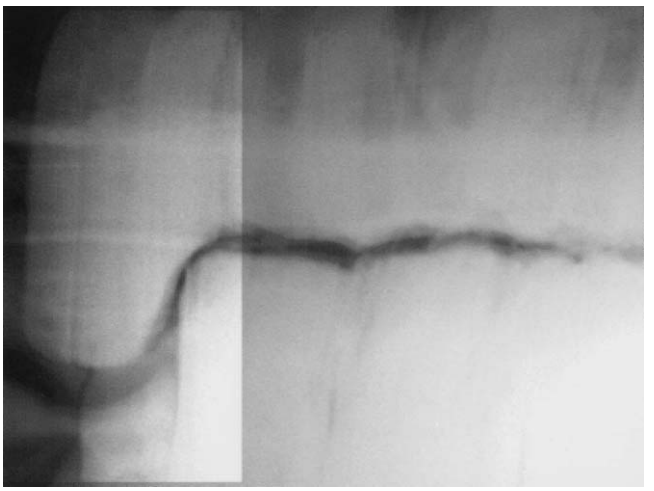


Figure 21-26 • Close-up lateral oblique view of a severe rostral malocclusion features an overriding first maxillary cheek tooth with a corresponding defect in the associated mandibular cheek tooth.

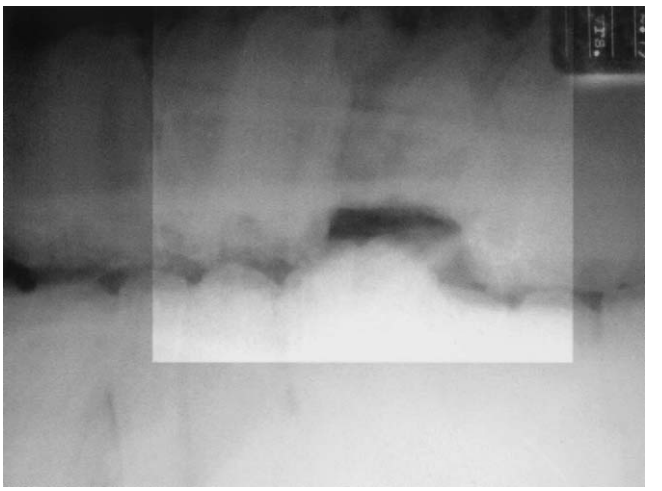
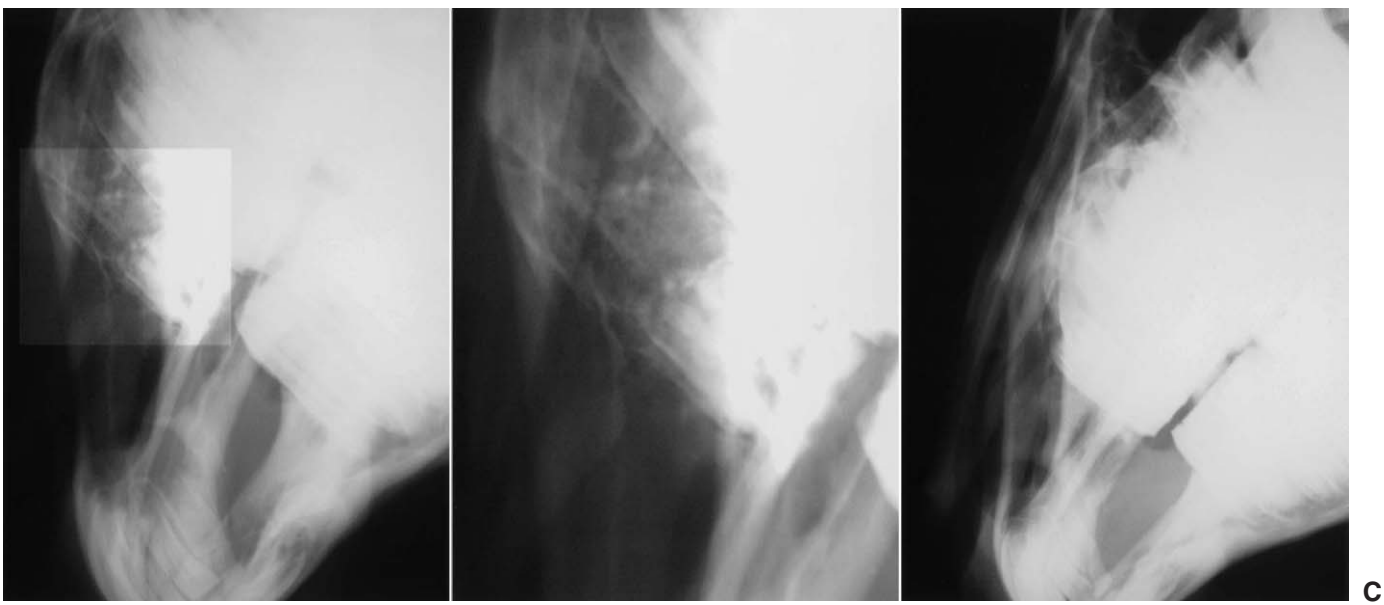


Figure 21-27 • Close-up lateral oblique view of the left central jaw shows an overgrown mandibular cheek tooth caused by the earlier extraction of the opposing maxillary cheek tooth. Predictably, *drifting* (change in direction of one or more teeth following an extraction) has occurred.



A,B **C**

Figure 21-28 • Lateral oblique **(A)** and lateral oblique close-up **(B)** views of an intensely destructive adamantinoma, which has reduced the size of the profiled first cheek tooth by nearly half. A similar view of the opposite maxillary cheek tooth is provided for comparison.

7. Farrow CS: *AAEP*
8. May SA, Wyn-Jones E: Contrast radiography in the investigation of sinus tracts and abscess cavities in the horse, *Equine Vet J* 19:218, 1987.
9. Lundin CS, Bertone AL: Diagnostic fistulography in horses, *Compend Cont Educ Equine* 5:639, 1988.
10. Gayle JM, Redding WR, et al: Diagnosis and surgical treatment of periapical infection of the third mandibular molar in five horses, *J Am Vet Med Assoc* 215:829, 1999.
11. Metcalf MR, Tate LP, Sellett LC: Clinical use of 99m MDP scintigraphy in the equine mandible and maxilla, *Vet Radiol* 30:80, 1989.
12. Dixon PM, Tremaine WH, et al: Equine dental disease. Part 2: a long-term study of 400 cases: disorders of development and eruption and variations in position of the cheek teeth, *Equine Vet J* 31:519, 1999.
13. Fessler JF: Heterotropic polydontia in horses: nine cases (1969-1986), *J Am Vet Med Assoc* 192:535, 1988.
14. Carmalt JL: Understanding the equine diastema, *Equine Vet Educ* 15:34, 2003.
15. Roberts MC, Groenendyk S, Kelly WR: Ameloblastic odontoma in a foal, *Equine Vet J* 10:91, 1978.
16. Shupe JL, Olsen AE: Clinical aspects of fluorosis in horses, *J Am Vet Med Assoc* 158:167, 1971.

Chapter 22

Sinonasal Disease: Conventional Versus Integrated Diagnostic Approaches

A TRADITIONAL APPROACH TO THE FACIAL INTERIOR

The Standard Nasal Series

As mentioned previously, my preference is to begin the radiographic assessment of the nasal cavity with a full-length lateral image of the head, followed by a collimated, lateral view of the facial region, reducing the technique to optimize the appearance of the relatively thin conchae. Beginning the examination with a full-length view of the head not only provides an anatomic context in which to view the less obvious elements of the nasal cavity interior but also affords an opportunity to evaluate the teeth and paranasal sinuses, which may also be diseased.

Supplementary Frontal (Rostrocaudal) View

Depending on how far cranially a particular lesion is situated (and how cooperative the horse is), a frontal (rostrocaudal) projection can be made (Figure 22-1). This view is particularly helpful in establishing the presence of septal deviation and, if so, whether or not it is accompanied by a right- or left-sided nasal mass.

The Standard Sinus Series

As with the standard nasal series, I prefer to begin the examination of the paranasal sinuses with a full-length orientation view of the head. Collimated right and left lateral or rostrocaudal oblique views are then added to assess the maxillary sinuses; if possible, a rostrocaudal projection is included for the reasons mentioned previously (Figure 22-2). Customized views, optimized to profile surface or interior abnormalities, can then made as needed.

Lateral, lateral oblique, and ventrodorsal views of a cutaway skull specimen (Figure 22-3), along with corresponding radiographs (Figure 22-4), are provided for anatomic-radiographic comparison.

AN INTEGRATED APPROACH TO THE FACIAL INTERIOR

The Integrated Sinonasal Series

Instead of dividing the facial interior into the nasal and paranasal regions as described previously (a somewhat arbitrary but nevertheless traditional approach used in equine radiology), one can take a more integrated tack, one in which the nasal and paranasal cavities are viewed as being intimately related rather than separate physical entities. Integrative diagnostic thinking of this sort is not only practical given the comparable imaging of the nasal cavity and paranasal sinuses, but it is consistent with the natural progression of most of the diseases that affect these areas.

Problems and Countermeasures in the Radiographic Diagnosis of Sinonasal Disease

Most of my undergraduate students and many of our clinical trainees find radiographic analysis and interpretation of the horse's skull difficult, in particular the facial region. In large part, this is because of the symmetric nature of the head, the right half mirroring the left, with each structure being superimposed by another of identical shape and size.

Cognitive countermeasures do exist, however. The first is to have at least a rough idea of the appearance and whereabouts of the various objects contained within the facial region. The second is to eliminate superimposition wherever possible with the aid of standardized or customized oblique projections. Finally, the symmetric nature of the skull can become an analytic advantage; for example, a right lateral oblique projection can be compared with a comparable view of the left or, in the case of a dorsoventral view, the right and left sides of the face can be matched against one another.



Figure 22-1 • X-ray tube being moved into position prior to making a rostrocaudal view of the head.



Figure 22-2 • The ideal sinus examination comprises lateral, paired lateral oblique (only one shown), and rostrocaudal views, shown here in a view box.

The Facial Tunnel: Conceptualizing the Sinonasal Interior

Viewed head-on, the facial interior can be conceptualized as a deep, narrow, longitudinally divided cavity, appearing roughly triangular in cross-section. A pair of laterally compressed, irregularly shaped cylinders—the *dorsal nasal concha*—are suspended high on either lateral wall, and a second nearly identical pair—the *ventral nasal concha*—are attached just below (Figure 22-5). At the far mid upper end of the tunnel lies a centrally divided, medium-sized spherical object with a rather distinctive layered appearance: the *ethmoid concha*.

Surrounding the facial tunnel are four anteroom-like chambers, two above the ethmoid conchae (the *frontal sinuses*) and two alongside the last three cheek teeth on either side (the *maxillary sinuses*). Each of the individual sinuses is divided into two subcompartments separated by a communicating partition.

Teaching and Learning the Facial Interior

As mentioned previously, the facial interior is quite complex and difficult to teach to novices because of extensive structural superimposition (Figure 22-6). Boyd and Rantanen demonstrated how this problem could be partially alleviated by selectively coating various interior or exterior surfaces of a skull specimen with a radioopaque material, which would show clearly when radiographed.[1] I use focused transillumination for the same purpose, as demonstrated in Figure 22-3.

Paranasal Sinusography

Behrens and co-workers described the technique of positive-contrast sinusography, exemplifying its clinical utility with five clinical cases.[2,3] Their method consists of hammering a 14-gauge needle, containing a stylet, into the conchofrontal sinus on the affected side, clearing the needle of bone fragments, and then incrementally injecting a diagnostic iodine solution (30, 100, and 70 ml). Dorsoventral and lateral skull radiographs are made immediately after each contrast injection.

A second 14-gauge needle is then placed into the rostral compartment of the maxillary sinus on the same side, and the needle is cleared, followed by incremental contrast injections (20 and 50 ml). Dorsoventral and lateral skull films are made after each injection.

In addition to the technical and restraint considerations of needle placement, great care must be taken to prevent the loss of contrast solution into the nasal passages. Keeping the horse's head and neck extended does this, but the position must be maintained throughout the examination.

Having tried the described technique and found it useful in *selected* cases, I would strongly advise undertaking a thorough radioanatomic review of the region and then practicing the procedure on at least one cadaver skull before attempting it in a clinical case. Allot at least an hour or longer for the examination, and sedate or anesthetize the horse as required.

In my opinion, the study *must be patient-tailored*, with the appearance of each film in the series dictating the timing and projection of the next. Be certain to have a cutaway skull at hand for comparative purposes.

Normal Computed Tomographic Anatomy of the Facial Region

As already pointed out, there is no better way to image the interior of the horse's head than with computed tomography (CT). The clarity of the nasal conchae and their relationship to the frontal and maxillary sinuses can be particularly revealing (Figure 22-7).

Foal. Smallwood and co-workers described the CT appearance of the *foal* skull, supplemented by coincid-

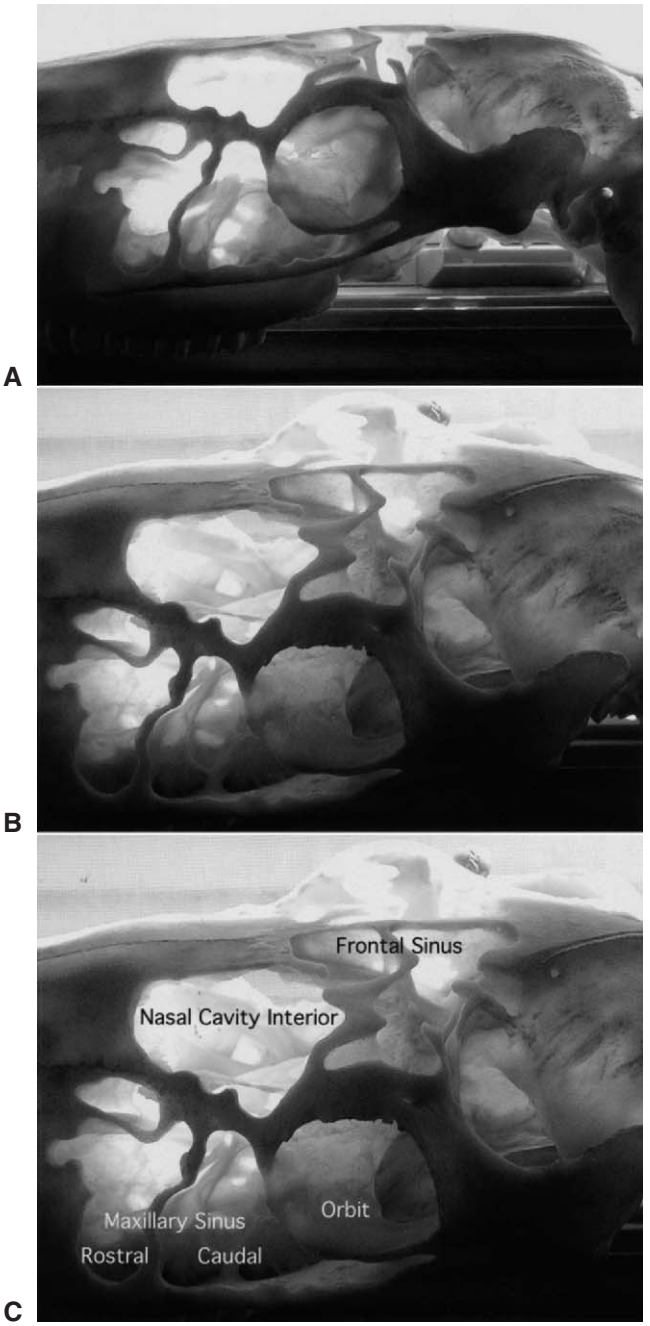


Figure 22-3 • Lateral **(A),** lateral oblique **(B),** and labeled lateral oblique **(C)** views of the backlit skull of an adult horse in which portions of the outer frontal and maxillary sinuses have been removed to allow visualization of the interior. A portion of the dorsolateral wall of the caudal nasal cavity has also been removed for the same purpose.

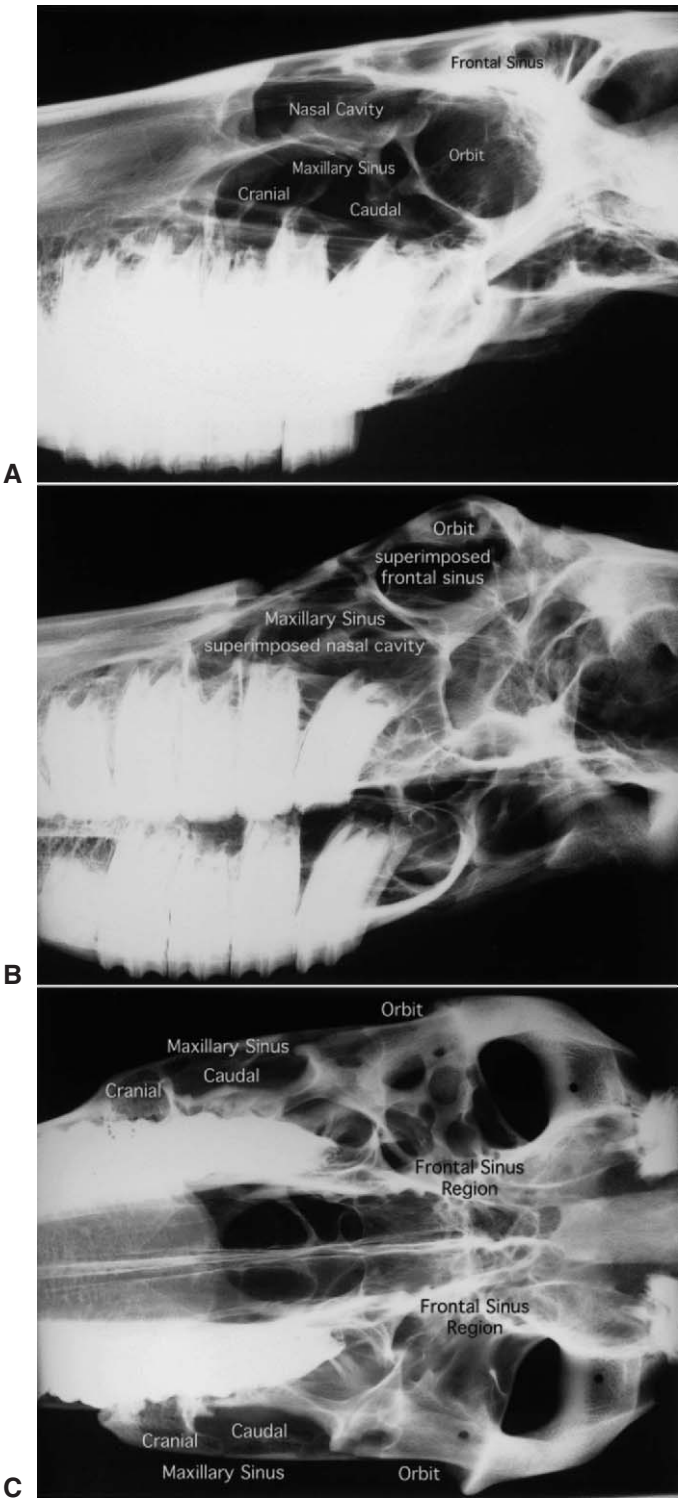


Figure 22-4 • Labeled lateral **(A),** right lateral oblique **(B),** and ventrodorsal **(C)** radiographs made from the skull shown in Figure 22-3. A defleshed specimen rather than a living horse was used to maximize anatomic detail.

ing anatomic cross-sections, to potentially serve as a normal CT reference.[4] Most images were obtained from the decapitated head of a miniature foal, estimated to be 6 to 8 months old. In my experience CT numbers obtained from cadaver skulls are unreliable.

Adult Horse. Morrow and Park reported the CT appearance of the *adult* equine skull. They used decapitated specimens taken from 4-, 8-, and 11-year-old horses.[5] Having performed CT on the sinonasal region of *live horses,* my advice to the novice is to practice the procedure thoroughly before attempting a clinical case, especially positioning the animal's head within



Figure 22-5 • A close-up rostrocaudal oblique view of the nasal cavity shows the wrinkled rostral surfaces of the right dorsal and ventral conchae.



Figure 22-6 • Second-year veterinary students being shown a basilar skull fracture by a senior veterinarian.

the gantry. Do not plan to make reformatted longitudinal (dorsal plane) images unless 1- to 2-mm axial slices are available, and even then the images are coarse and the process very time consuming.

Predicting Therapeutic Outcome Based on Pretreatment Computed Tomographic Examination. As far as I can determine, CT has not been used in horses to predict the success or failure of treatment for sinonasal disease, although this technique has been used in dogs with mixed success and appears to have potential for use in horses with sinonasal disease.[6]

In my estimation the skills of the individuals who analyze and interpret the CT findings and perform the indicated medical or surgical treatment are of much greater relative importance than the theoretical predictive value of a particular type of diagnostic imaging. Obviously, the more severe and extensive any disease, irrespective of how it's established, the worse the prognosis.

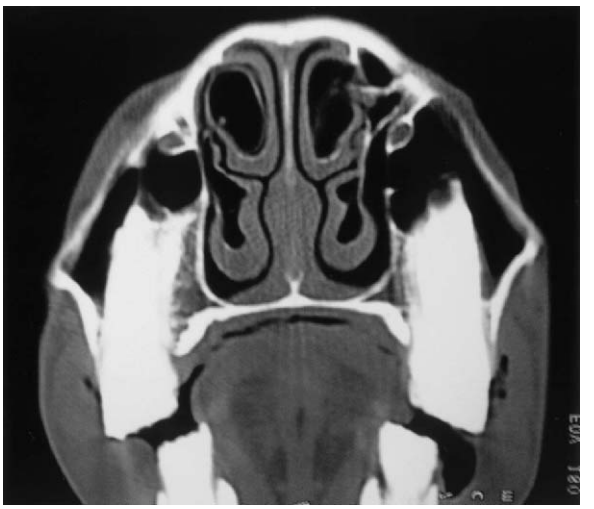


Figure 22-7 • Computed tomogram (soft-tissue window) through the maxillary sinuses clearly shows the intimate relationship between the nasal conchae, nasal passages, paranasal sinuses, and associated teeth.

Magnetic Resonance Imaging of the Adult Facial Region

Arencibia and co-workers described the magnetic resonance imaging (MRI) appearance of the equine facial region using the decapitated heads of adult horses, creating potential normal reference material for clinical MRI.[7] The greatest deterrent to skull magnetography in live horses is the lengthy time required to perform the examination, and the resultant prolonged anesthesia time, especially when compared with CT. The logistics of transporting horses to and from the magnet further add to the time and complexity of such examinations.

▮▮▮ PREVALENCE AND CLINICAL SIGNS OF SINONASAL DISEASE

Boulton challenged the widespread belief that sinonasal disease is a common entity in the horse, estimating its actual incidence to be only about 0.5 percent.[8] On the other hand, Lane and co-workers reported that unilateral nasal discharge was the most common reason given for radiography in a series of 235 horses with suspected sinonasal disease.[9] Other indicators of sinonasal disease are listed in Box 22-1.

Causes of Unilateral Epistaxis in the Horse

Bleeding from a single nostril can be caused by a variety of maladies, including (1) facial trauma causing unilateral sinonasal injury, (2) unilateral sinonasal

Table 22–1 • DIFFERENTIAL RADIOGRAPHIC DIAGNOSIS FOR SINONASAL DISEASE IN THE HORSE

Disease	Radiographic Disease Indicators (RDIs)
Primary sinusitis	Usually normal. Hazy opacification suggests fluid but may also be associated with suboptimal radiographic technique, lack of a grid to reduce scatter, and motion nonsharpness.
Sinusitis secondary to one or more abscessed teeth	Complete or partial opacification of paranasal sinus due to fluid, sometimes with a fluid level. An abnormal tooth is typically seen in, or adjacent to, the diseased sinus.
Injury: facial fracture, dental fracture, infected penetrating wound, foreign body, or gunshot	Facial fracture or callus related to previous facial fracture present, often seen in association with overlying soft-tissue swelling. Fresh fractures are often associated with nasal, paranasal, or guttural pouch bleeding, appearing as increased density in the involved area.
Nasal or paranasal cyst	Regional, often well-demarcated object situated in the nasal cavity that typically shows septal displacement in the dorsoventral view. Cysts in the paranasal sinuses may simply opacify the involved compartment or, in severe instances, deform it.
Tumor	Similar to a cyst but often with a less well-defined margin. Masses vary in density, ranging from soft tissue, to mineralized, to bony. Destruction and deformity of the adjacent conchae and facial bones are also variable, but in general the longer the tumor has been present, the more likely such changes are to be present.
Ethmoid hematoma	Appearance varies with the amount and frequency of bleeding. Some lesions appear as a discrete object superimposed on the ethmoturbinates, others as enlarged ethmoturbinates, but without their usual laminated appearance. Some lesions are undetectable by radiographic means.
Empyema	A pus-filled and therefore radiographically opaque paranasal sinus is usually, but not always, the result of a bad tooth or an earlier nasal infection. Some paranasal cysts and tumors resemble empyema but rarely smell as bad.

Modified and expanded from Beard WL, Hardy J: Diagnosis of conditions of the paranasal sinuses in the horse, *Equine Vet J* 13:265, 2001.

Box 22-1
Indicators of Sinonasal Disease in the Horse*

Unilateral nasal discharge
Facial swelling
Epistaxis
Bilateral nasal discharge
Abnormal behavior
Nasal passage obstruction
Diagnosed dental defects
Draining sinus
Quidding
Epiphora
Neurologic disease
Facial deformity

*In order of decreasing occurrence.

Box 22-2
Causes of Sinonasal Disease in Horses

Atresia of the nasolacrimal duct
Buccomaxillary fistula
Enlarged dental sacs
Ethmoidal abscess
Ethmoidal hematoma
Facial fractures
Fractured teeth
Incomplete eruption or angular deployment of teeth
Maxillary osteoma
Nasal foreign body
Nasal ulceration
Periapical dental infection: PM 2-4 rostral to maxillary sinus; PM 4, M 1-3 within sinus
Rhinitis
Sinonasal carcinoma
Sinus cysts
Sinusitis (bacterial or fungal)
Superficial soft-tissue masses
Suture periostitis

M, Molar; *PM,* premolar.

infection, (3) mycosis or bacterial infection of a guttural pouch, (4) unilateral sinonasal tumor, and, inconsistently, (5) a progressive ethmoidal hematoma. Schumacher and co-workers also reported unilateral epistaxis resulting from an infected nasolacrimal duct (*dacryohemorrhea*).[10]

Differential Radiographic Diagnosis of Sinonasal Disease

The radiographic disease indicators (RDIs) (Table 22-1) of equine sinonasal disease have been reported widely.[11,12] Unfortunately, there is not a great deal of specificity, with many sinonasal disorders sharing two or more radiographic disease indicators; thus radiographic diagnosis is often imprecise.

Diseases Causing Sinonasal Abnormalities

Sinonasal abnormality can be caused by a wide variety of diseases as reported by Gibbs and Lane in a group of 167 horses[13] (Box 22-2).

Congenital/Developmental. Reported congenital and developmental sinonasal diseases in foals include (1)

maxillary sinus follicular cysts, (2) bilateral frontal sinus cysts, (3) facial deformity (e.g., deviated nasal septum or wrynose), and (4) cleft palate.[14,15] Elkins and co-workers reported a congenital ethmoid carcinoma in a foal.[16]

Rhinitis. In my experience, it usually is not possible to diagnose rhinitis radiographically unless it is associated with a visible fluid level. Although one may reasonably expect conchal and conchal sinus detail to be reduced in the case of a moderately severe infection, such subtle departures from normal are often impossible to distinguish from routinely encountered projectional and technical variations. An exception to this rule is when a large or medium-sized mass is present, a granuloma for example, or a large interconchal lymphoma, in which case they may be visible radiographically.[17,18]

Occasionally long-standing, diffuse rhinosinusitis changes the appearance of the nasal interior to the extent that it can be radiographically appreciated, but only by someone who is regularly seeing equine nasal studies. Under such circumstances, the diseased tissue appears increased in density with a corresponding detail loss compared with earlier normal films (Figure 22-8).

Carmalt and co-workers reported severe swelling and deformity of the muzzle of two horses associated

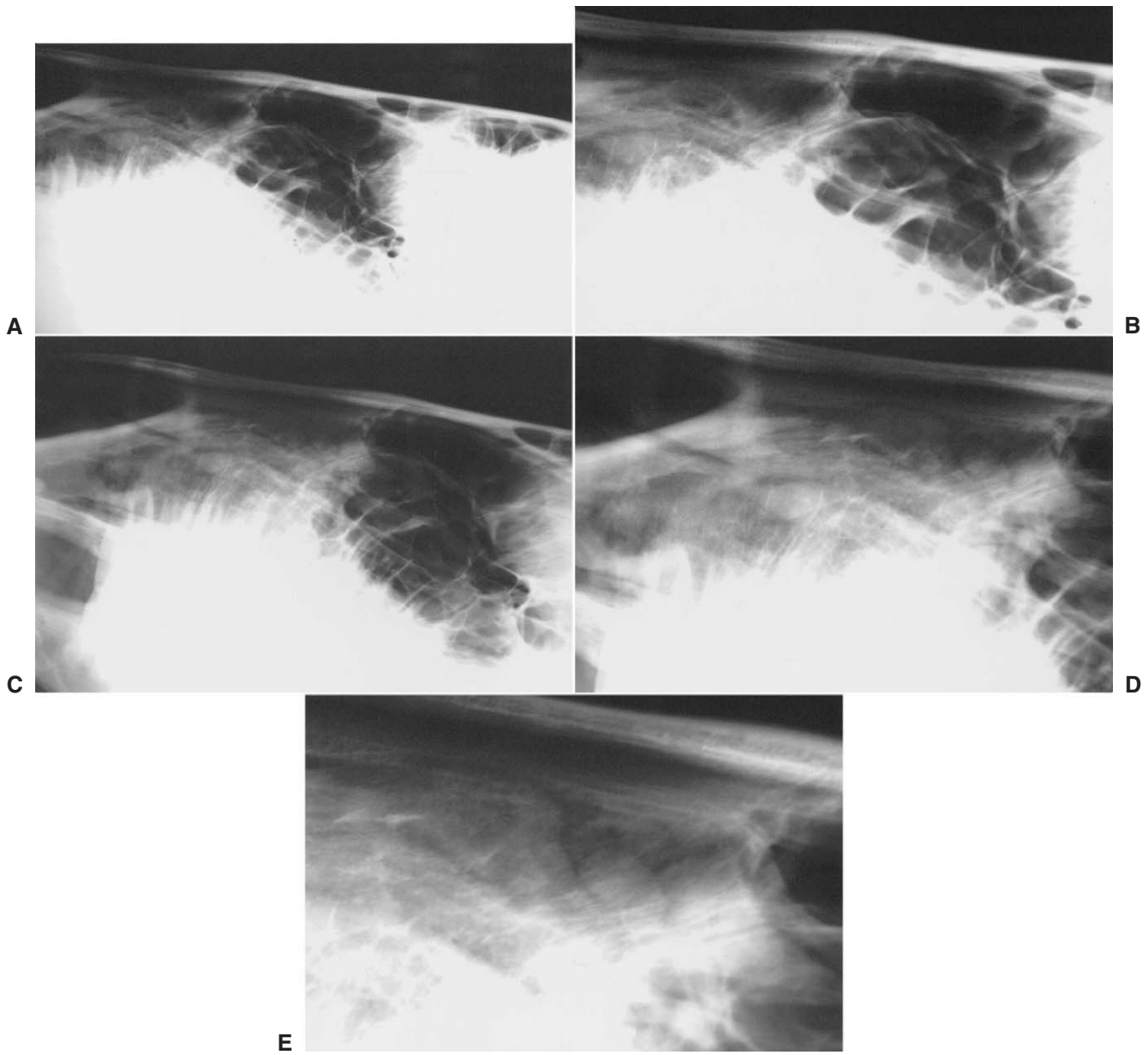


Figure 22-8 • Lateral **(A)** and close-up lateral **(B)** radiographs of a horse with diffuse rhinitis appear normal. Three years later, progress lateral **(C),** close-up lateral **(D),** and ultra-close-up lateral **(E)** films of the central nasal cavity show a loss of conchal detail with a commensurate increase in density, indicating a worsening of the animal's disease.

with nasal obstruction, secondary to *Actinobacillus lignieresii* rhinitis.[19] Depression fractures of the nasal bones are a form of open fracture that can lead to a secondary rhinitis, nasal cavity obstruction, and sequestration.

Rhinosinusitis and Sinusitis

The sinus chambers are most likely to become infected after a nasal infection, resulting in a rhinosinusitis. Although equipped to drain off excessive secretions, the process is relatively slow and inefficient compared with the nasal cavity. Inflammatory by-products, such as pus, are especially slow to drain because of their high viscosity and the limited availability of exits. Once pus becomes congealed, it becomes very difficult to eliminate from the infected sinus. Inspissated pus can also dam the sinus exits, accelerating further desiccation of sinus contents.

Occasionally it is possible to see ill-defined opacification associated with the dorsal or ventral conchal sinus, suggesting the accumulation of inspissated exudate, as reported by Schumacher and co-workers.[20]

Primary Sinusitis

Primary sinusitis is often difficult or impossible to diagnose from radiographs. The associated mucosal swelling and increase in nasal secretions are usually insufficient to increase appreciably the overall density of the sinonasal compartments or to decrease conchal detail. CT and MRI, on the other hand, are capable of showing these sorts of changes; the former is especially effective in revealing otherwise invisible bony abnormalities.

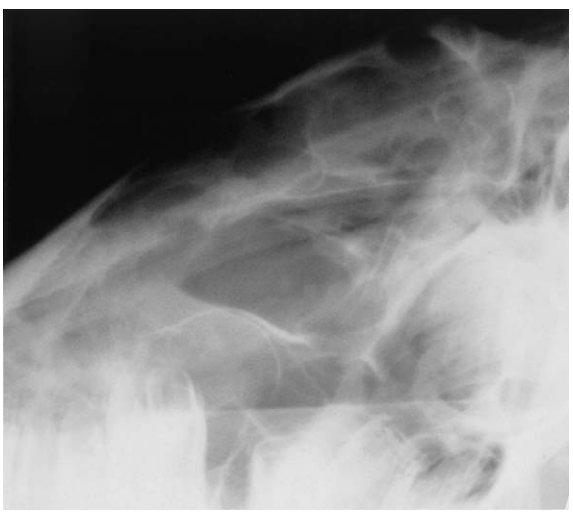


Figure 22-9 • Close-up lateral oblique view of an infected maxillary sinus shows opacification and a faint fluid level ventrally.

Secondary Sinusitis

Infected maxillary teeth often lead to sinonasal disease, typically characterized by a putrid nasal discharge. Under such circumstances, diagnosis requires *integrated radiographic examinations* of the (1) maxillary dentition, (2) nasal cavity, and (3) paranasal sinuses.

Radiographic Findings. The prime radiographic disease indicators (RDIs) of frontal and maxillary disease are (1) sinus opacification (Figure 22-9) and (2) fluid levels (Figure 22-10). Other RDIs include (1) sinus expansion, (2) sinus deformity, (3) sinus destruction, (4) sinus mineralization, and (5) sinus new bone.

Computed Tomographic Findings. Henninger and coworkers described the CT features of sinusitis secondary to dental disease.[21] Common CT features in horses with sinusitis secondary to dental disease included the following.

Teeth

- The *first maxillary molar tooth* was most frequently affected
- Cemental hypoattenuation, enamel destruction, and infundibular gas
- Cavities (caries)
- Periapical gas
- Root fragmentation
- Swelling of sinus lining

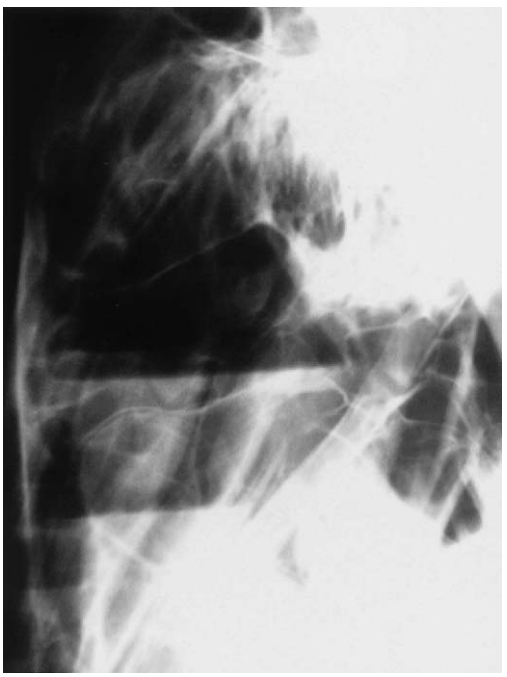


Figure 22-10 • Ultra-close-up rostrocaudal view of an infected, fluid-filled maxillary sinus in a horse with chronic sinonasal disease. The presence of parallel fluid levels indicates involvement of both the rostral and caudal chambers of the maxillary sinus.

Sinuses
- Thickened respiratory epithelium in the rostral maxillary sinus and, less often, the caudal maxillary sinus.
- The infraorbital canal, nasomaxillary duct, and frontomaxillary aperture were usually affected.
- The facial crest is typically affected, showing endosteal sclerosis, thickening, and periosteal new bone.
- Sinus enlargement and distortion causing visible facial swelling.
- Three-dimensional (3D) reconstructions enhanced understanding of the true extent of the disease.

Empyema

Empyema is usually a unilateral disease, but occasionally it occurs bilaterally.[22] It is generally considered the result of an earlier upper respiratory infection or a bad tooth. Affected horses often have a foul-smelling, unilateral nasal discharge, often accompanied by facial swelling. Once a sinus fills with pus, it is very difficult to clear other than by irrigation and surgical drainage. It is very likely that empyema causes severe, unrelenting facial pain in horses, as it does in people. Empyema also probably causes headache, although obviously this is extremely difficult to confirm.

Radiographically, empyema is characterized by a fully or partially opacified maxillary sinus, increased density in the adjacent nasal cavity, in some chronic cases enlargement of the affected sinus cavity, and displacement of the nasal septum away from the infected side of the face (Figure 22-11).

Paranasal Sinus Cysts

Lane and co-workers wrote one of the definitive clinicoradiographic descriptions of equine paranasal cysts (Figure 22-12).[23] RDIs identified with sinus cysts may include the following (Box 22-3).

Sinonasal Tumors, Tumorlike Lesions, Masses, and Mass Effects. Leyland and Baker reported a variety of obstructive sinonasal mass lesions, including (1) osteosarcoma, (2) lymphosarcoma, (3) carcinoma, (4) maxillary cysts, (4) ethmoid hematoma, (5) granulomatous polyp, (6) granuloma, and (7) osteodystrophia fibrosa.[24]

Frankeny reported a medium-sized *epidermal inclusion cyst* (also termed *atheroma*) in the left nasal diverticulum of a horse, causing partial obstruction of the associated nasal cavity.[25]

Box 22-3
Maxillary Cyst Radiographic Disease Indicators*

Increased sinus opacity
Sinus fluid level
Thickened sinus wall
Paranasal sinus enlargement
Mineralization of paranasal sinus interior
One or more displaced teeth
Secondary nasal septal deviation (requires ventrodorsal projection)
Secondary fluid accumulation in the frontal sinus

*As seen in lateral projection.

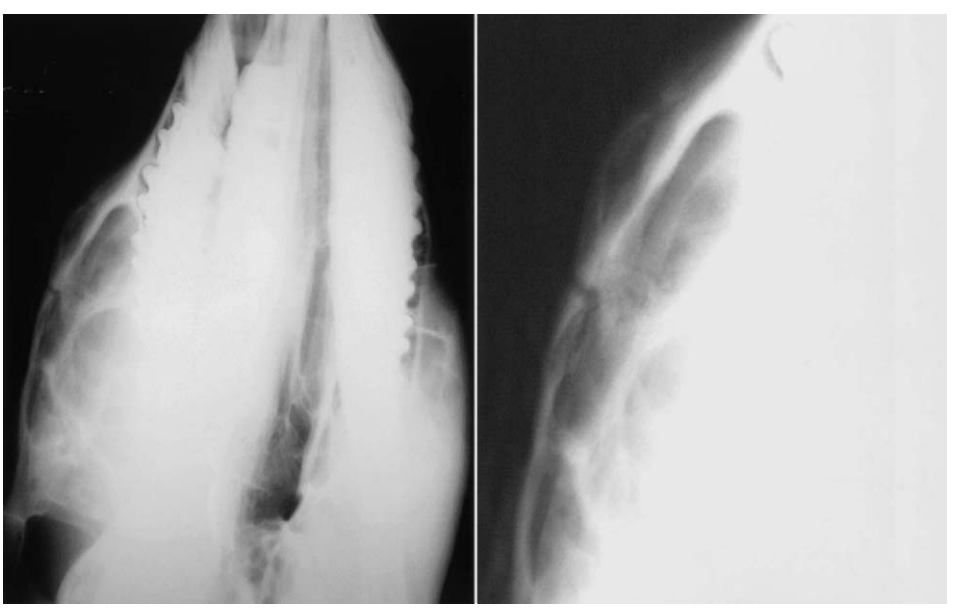


Figure 22-11 • Customized rostrocaudal oblique **(A)** and ultra-close-up rostrocaudal oblique **(B)** views of a severely infected right maxillary sinus and nasal cavity show (1) sinus opacification, (2) expansion, (3) central perforation, and (4) arching new bone deposition.

By one estimate, 68 percent of equine nasal tumors are malignant, with most being squamous cell carcinomas.[26,27] Squamous cell carcinoma is also reported to be the most common tumor of the maxillary sinuses.[28] Reynolds and co-workers reported an adenocarcinoma in the frontal sinus of a horse that had spread to the brain.[29] Other equine nasal tumors include osteoma, osteosarcoma, chondrosarcoma, fibrosarcoma, lymphoma, hemangiosarcoma, mastocytoma, chondroma, fibroma, and myxoma.[30]

Dental tumors such as adamantinoma (ameloblastoma) occasionally affect the caudal cheek teeth, causing secondary sinus expansion and facial asymmetry. Most eventually invade the nearby nasal cavity, destroying and deforming the conchal sinuses. Initially these tumors may resemble an infected tooth but typically lack the characteristic foul-smelling nasal discharge and are far more extensive.

An area of patchy, bonelike density that partially obscures the underlying teeth, especially their roots, often characterizes caudally situated dental tumors, particularly those in the maxillary sinus. In this respect it can be quite difficult to distinguish a chronic dental infection from a facial or dental tumor, although on a probability basis infected teeth are far more common. Less commonly, ossifying fibromas and fibrous dysplasia (rare tumorlike lesions) may also affect the maxillary sinus of horses, but unfortunately neither possesses defining radiographic characteristics.[31]

Both malignant and benign paranasal tumors are capable of destroying intercompartmental partitions, thus filling two adjacent sinus cavities and making it impossible to determine their precise location (Figure 22-13).[32] These malignancies may also destroy a portion of the adjacent maxillary wall and grow into the adjacent nasal cavity. Other than with a dorsoventral view, the full extent of such lesions is difficult or impossible to appreciate radiographically.

The chief clinical indicators of serious sinonasal disease in the horse, including tumors, are (1) mucopurulent or hemorrhagic nasal discharge; (2) expanded, sometimes deformed facial bones; and (3)



Figure 22-12 • Customized lateral oblique **(A),** close-up lateral oblique **(B),** and ventrodorsal **(C)** views show a sharply circumscribed semicircular density in the right maxillary field (appearing on the left in the ventrodorsal projection).

inspiratory dyspnea. In most instances, the onset of these signs is quite subtle, but they of course persist and gradually worsen. Differentiating a tumor from an infection, based on these signs, can be difficult.

Various forms of treatment, or treatment combinations, have been reported: chemotherapy, surgical resection, cryotherapy, and radiotherapy, but none has proven curative. Using cobalt 60, Walker and coworkers reported what they termed the use of "aggressive radiotherapy" (translation: larger fractional and total radiation dosages) in three horses with nasal squamous cell carcinomas; this treatment slowed the growth of the tumors without serious side effects.[33]

Ethmoid Hematoma (Ethmoidal Hematoma)

The cause of spontaneous ethmoidal hemorrhage leading to regional hematoma in horses is not known. Prevailing hypotheses have changed little over the past three decades, with continued focus on the ethmoidal submucosa as the source of the bleeding.[34] Although there is no conclusive evidence that the disease is neoplastic, it does cause localized bone destruction. The mass effect of the resultant ethmoid hematoma may also cause pressure-induced reabsorption and deformity in the surrounding bone.

As the hematoma continues to enlarge, it may extend (1) dorsally into the frontal sinus, (2) ventrally into the sphenopalatine sinus, (3) laterally into the caudal and occasionally the rostral maxillary sinus, and (4) in advanced cases into the caudal part of the nasal cavity. Once in the nasal cavity, the ever-enlarging growth may travel forward between the conchae toward the nostrils or rearward through the choanae into the nasopharynx.[35] In extreme instances,

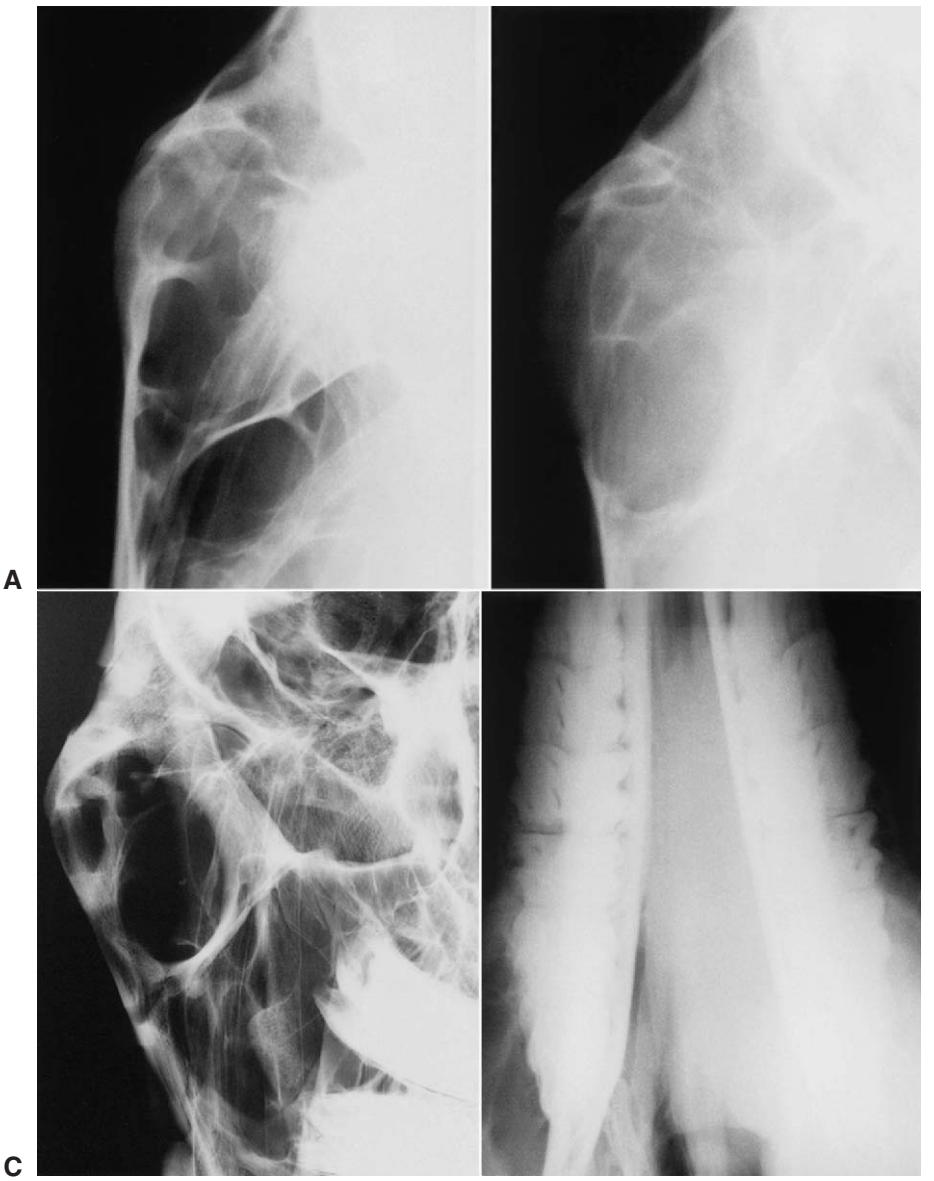


Figure 22-13 • Close-up left lateral oblique **(A),** ultra-close-up lateral oblique **(B),** and normal comparison **(C)** views show diffuse sinus opacification but no fluid lines. A ventrodorsal view **(D)** reveals increased density throughout the left nasal cavity accompanied by right septal displacement, the result of a large sinonasal mass.

ethmoidal hematoma may become large enough to nearly suffocate an animal.[36]

Proposed classifications have focused mainly on the physical rather than the pathologic attributes of the disease. Because the resultant hematoma often gradually enlarges, the disease is sometimes termed *progressive* ethmoid hematoma.

Ethmoid hematomas may be singular or multiple, symmetric or asymmetric, and may involve one or more of the following tissues or cavities, the last one typically by extension: (1) ethmoid turbinate, (2) maxillary sinus, sphenopalatine sinus, and (4) nasal cavity.

Diagnostically, CT[37] and MR are vastly superior to radiography but are currently used on a very limited basis. Radiographically, the disease is most easily diagnosed when the bleeding and resultant hematomas are situated on, or immediately around, the ethmoid turbinate, in which case the bone's normally distinctive laminated appearance is lost and replaced by a homogeneous mass effect (Figure 22-14). Radiologic assessment usually reveals involvement of the frontal or maxillary sinuses, which is not evident endoscopically.[38]

Nasal and Sinus Gunshots

In my experience, most horse owners do not witness their animals being shot; consequently, when the horse is discovered later with blood dripping from its nose, it is often assumed the animal was kicked, ran into a

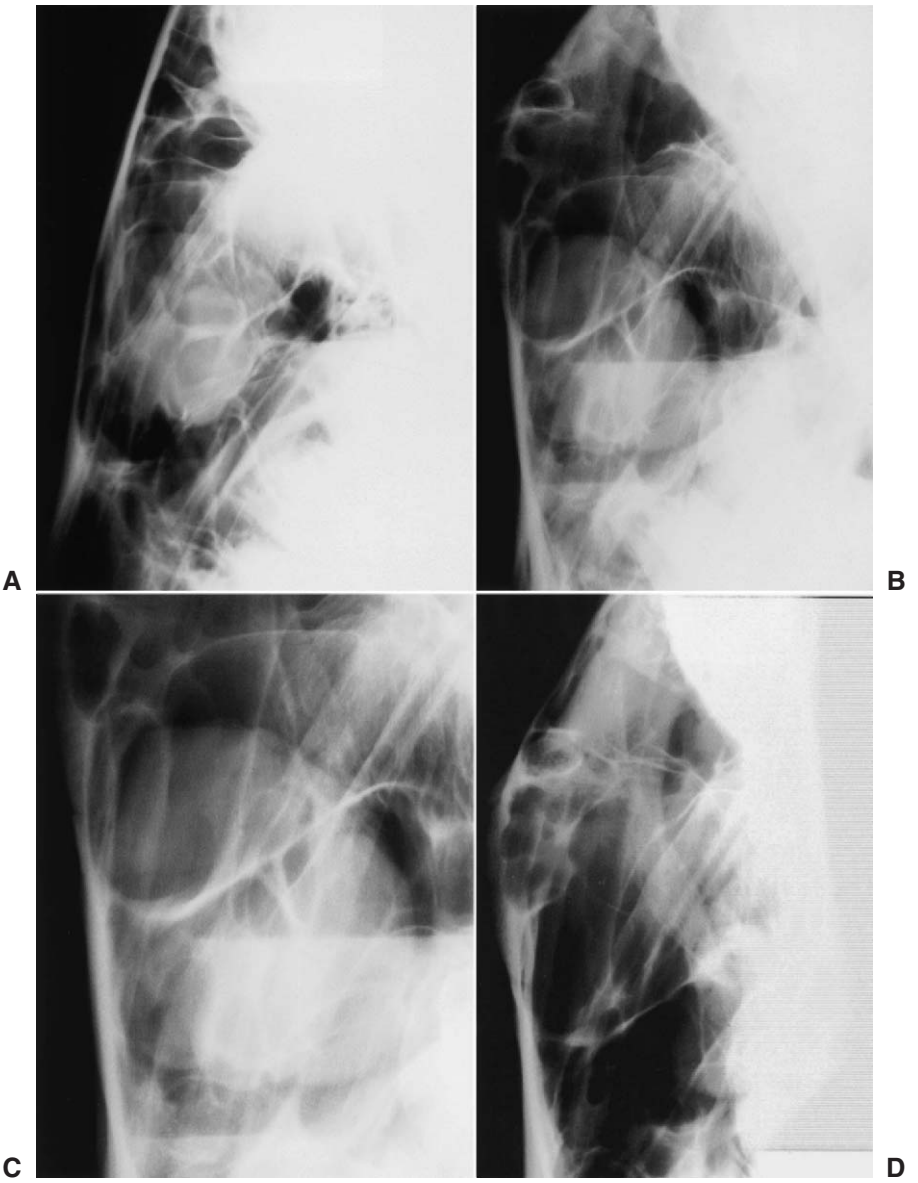


Figure 22-14 • Close-up lateral **(A),** close-up lateral oblique **(B),** and ultra-close-up lateral oblique **(C)** views of an ethmoid hematoma accompanied by paired fluid levels. A normal comparison view **(D)** is provided.

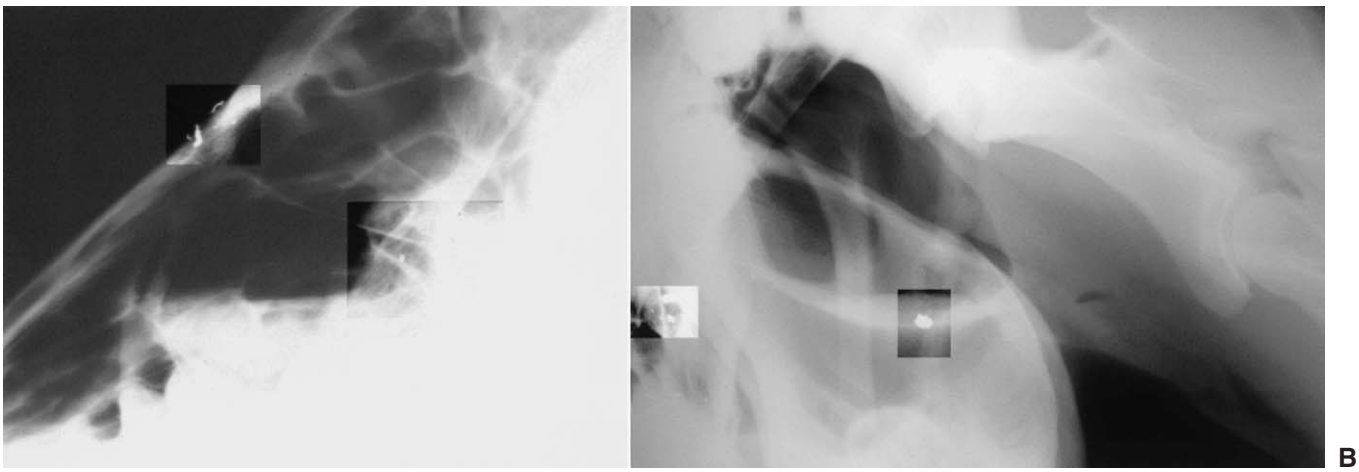


Figure 22-15 • A, Close-up lateral view of the caudal facial region shows lead fragments embedded in the nasal bones above the maxillary fluid level and in the ethmoid turbinates *(emphasis zones).* **B,** A lateral view of the throat shows lead in the ethmoid region and in one of the guttural pouches.

post, or sustained some other sort of blunt trauma. Unless the horse is radiographed, revealing a bullet or suggestive lead fragments (Figure 22-15), a presumptive diagnosis of nonspecific head injury is usually made, and the horse is treated accordingly.

Nasal and Sinus Foreign Bodies

Nasal foreign bodies are unusual. Occasionally nasal depression fractures fail to heal completely, leaving one or two devascularized fragments, which predictably lead to a foreign body reaction. I have also seen a fragment from a maxillary fracture driven into an adjacent concha, where it sequestered. Most recently, I encountered two instances of medicated beads behaving radiographically as foreign bodies (Figure 22-16).

Dentigerous Cyst (Ear Tooth)

McClure and co-workers reported a dentigerous cyst in the ventral conchal sinus of a 14-year-old Quarter Horse presented for a chronic purulent, unilateral nasal discharge.[39] The roughly square, high-density mass was situated dorsal to the infraorbital canal adjacent to the maxillary sinus.

Dentigerous cysts, a form of heterotopic polydontia caused by incomplete closure of the first branchial cleft, are present at birth and most often are located on the surface of one of the temporal bones adjacent to the ear (thus the name ear tooth). Most result in a foreign-body reaction featuring localized swelling and drainage. Nasal cavity involvement and delayed clinical involvement, as found in this animal, are rare.

Septal Deviation

Septal deviation is most often the result of a slowly growing nasal mass or paranasal mass effect. Less often, septal deformity is congenital.[40] Medium-sized and large masses or mass effects located in the nasal cavity of paranasal sinuses often reveal their presence by their influence on adjacent structures, especially the nasal septum. The radiographic demonstration of lateral septal displacement requires a ventrodorsal view, which can be made in a standing horse, provided a ceiling-suspended x-ray tube is available.

Computed Tomography

Axial CT images provide the best all-around means for presurgical assessment of sinonasal lesions, especially tumors or tumor-like lesions. Figures 22-17 and 22-18 illustrate the relative merits of radiography and CT as employed in two tumors, one involving the nasal cavity and the other the maxillary sinus.

▮▮▮ NASOLACRIMAL DUCT OBSTRUCTION SECONDARY TO SINONASAL DISEASE

Gross Ductal Anatomy

The nasolacrimal duct system begins as a series of small openings *(lacrimal punctae)* located along the medial edges of both eyelids that lead to a network of small channels *(lacrimal canaliculi).* These ductules then converge, forming a small cistern *(lacrimal sac),* which continues into the bony infraorbital canal as a single tube *(nasolacrimal duct).* On exiting the infraorbital canal, the lacrimal duct travels along the inner surface of the maxilla in a shallow trough *(lacrimal groove)* covered by mucosa. The duct then passes ventrally, where it enters the basal fold, an extension of the ventral concha, finally emptying its contents onto the floor of the nostril *(nasolacrimal meatus).*

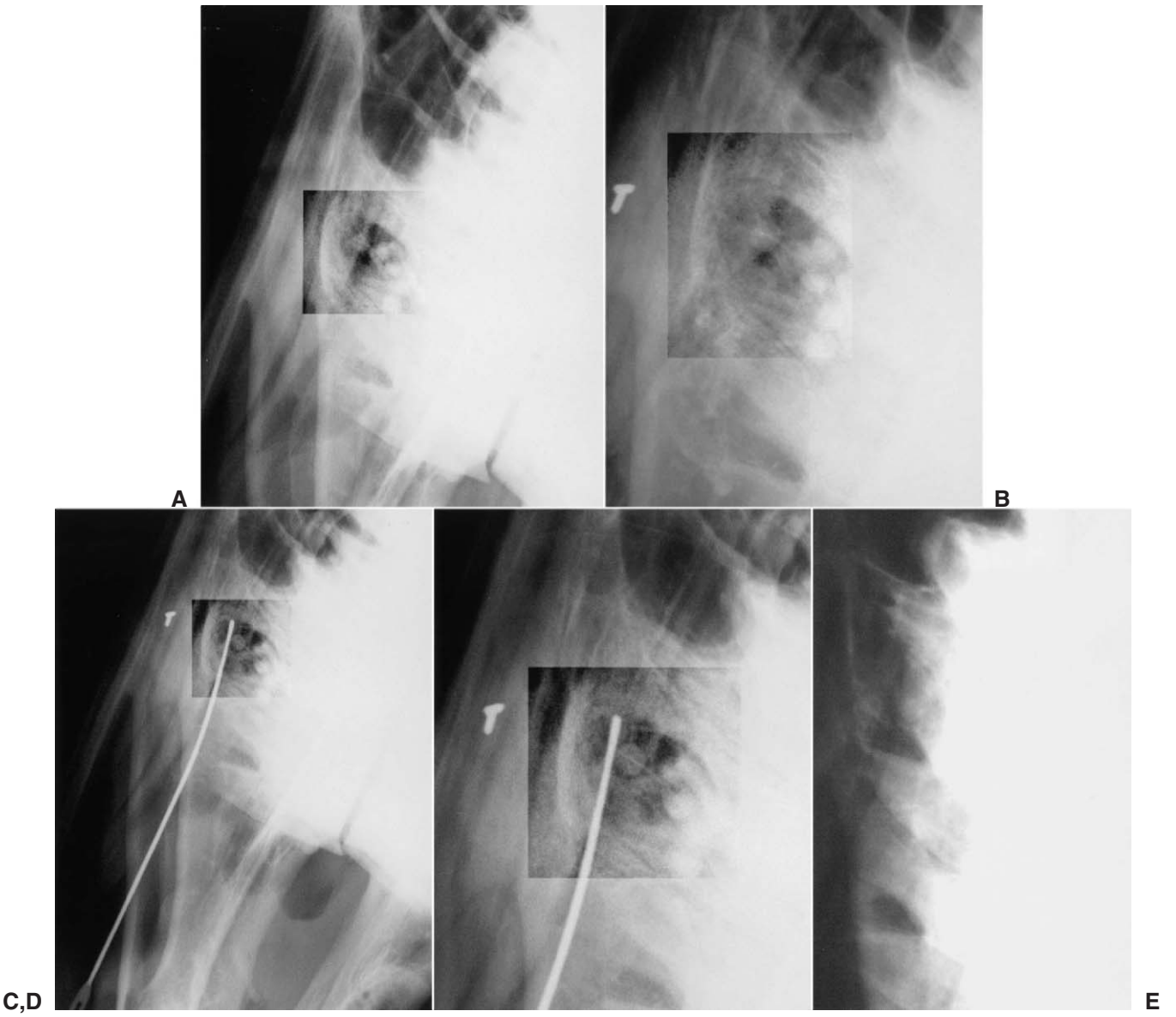


Figure 22-16 • Customized lateral **(A)** and lateral close-up **(B)** views show multiple medicinal beads *(emphasis zone)* placed during a recent dental surgery but now acting as foreign bodies. Lateral **(C)** and close-up lateral **(D)** views of a marking study in which a metallic probe was used to establish communication between the medicinal beads and a nearby draining sinus. Immediate postoperative **(E)** view following surgical removal of medicinal beads.

Dacryocystorhinography and Radiographic Anatomy

Burt and co-workers described the normal radiographic anatomy of the equine nasolacrimal duct.[41]

Ductal Disease

Acquired. Chronic sinonasal disease may secondarily obstruct the nasolacrimal duct, usually as a result of stenosing adhesions or mass blockage. The duct may also become blocked because of interior swelling caused by infectious or noninfectious inflammation *(dacryocystitis)* or by a foreign body.

Congenital. Congenital nasolacrimal disease is most often due to atresia of the nasolacrimal meatus, which typically results in excessive tearing from the affected eye and later a mucopurulent ocular discharge, which may be mistaken for conjunctivitis. Latimer and Wyman have written a highly readable, illustrated account of the more common forms of this disease.[42]

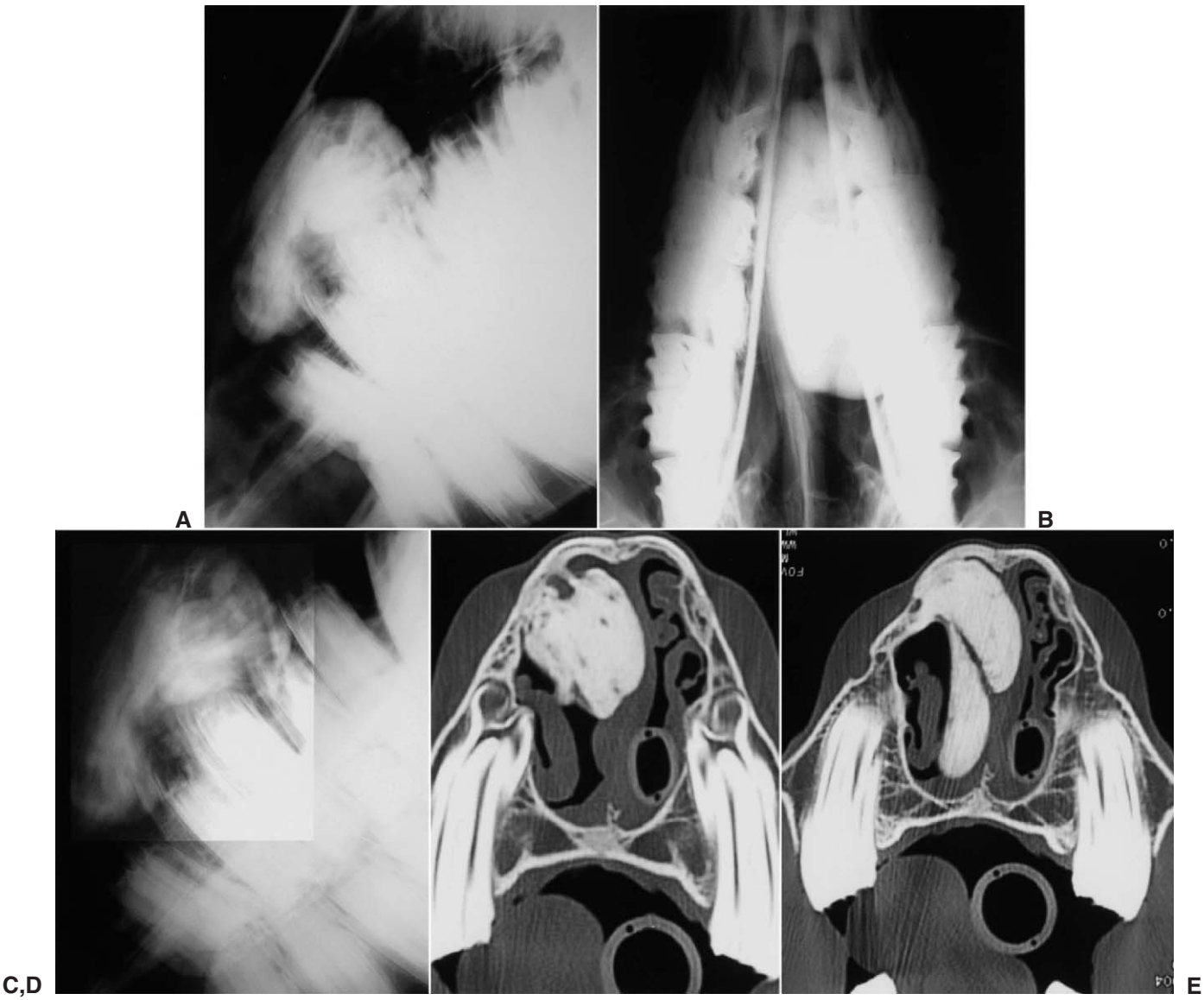


Figure 22-17 • A, Lateral view of the nasal cavity shows a large bony mass centered over the second and third cheek teeth. **B,** A ventrodorsal projection indicates that the object is on the left side and has displaced the nasal septum to the right. **C,** A penetrated lateral view indicates that the mass probably is not originating from a tooth. **D,** A computed tomographic (CT) image through the second maxillary cheek teeth (premolar 3 [PM 3]) shows the mass attached to (and presumably originating from) the lateral aspect of the left nasal bone, in the process deforming and displacing the adjacent dorsal concha and nearby nasal septum. **E,** A second CT image made through the maxillary sinus and fourth cheek tooth (M1) shows the mass has divided, with its medial element reaching nearly to the floor of the left nasal cavity.

Dacryocystorhinography. The size, shape, and direction of the lacrimal duct change considerably over the course of its passage from the eye to the nose, reflecting the varied anatomy of the nasal interior, a fact that must be borne in mind when interpreting *dacryocystorhinograms*.

References

1. Boyd J, Rantanen NW: Silver impregnation in situ, *Vet Radiol* 25:220, 1984.
2. Behrens E, Schumacher J, et al: Equine paranasal sinusography, *Equine Vet J* 32:98, 1991.
3. Behrens E, Schumacher J, et al: Contrast paranasal sinusography for evaluation of disease of the paranasal sinuses of five horses, *Equine Vet J* 32:105, 1991.
4. Smallwood JE, Wood BC, et al: Anatomic reference for computed tomography of the head of the foal, *Vet Radiol Ultrasound* 43:99, 1999.
5. Morrow KL, Park RD, et al: Computed tomographic imaging of the equine head, *Vet Radiol Ultrasound* 41:491, 2000.
6. Saunders JH, Duchateau L, Van Bree H: Use of computed tomography to predict the outcome of a noninvasive

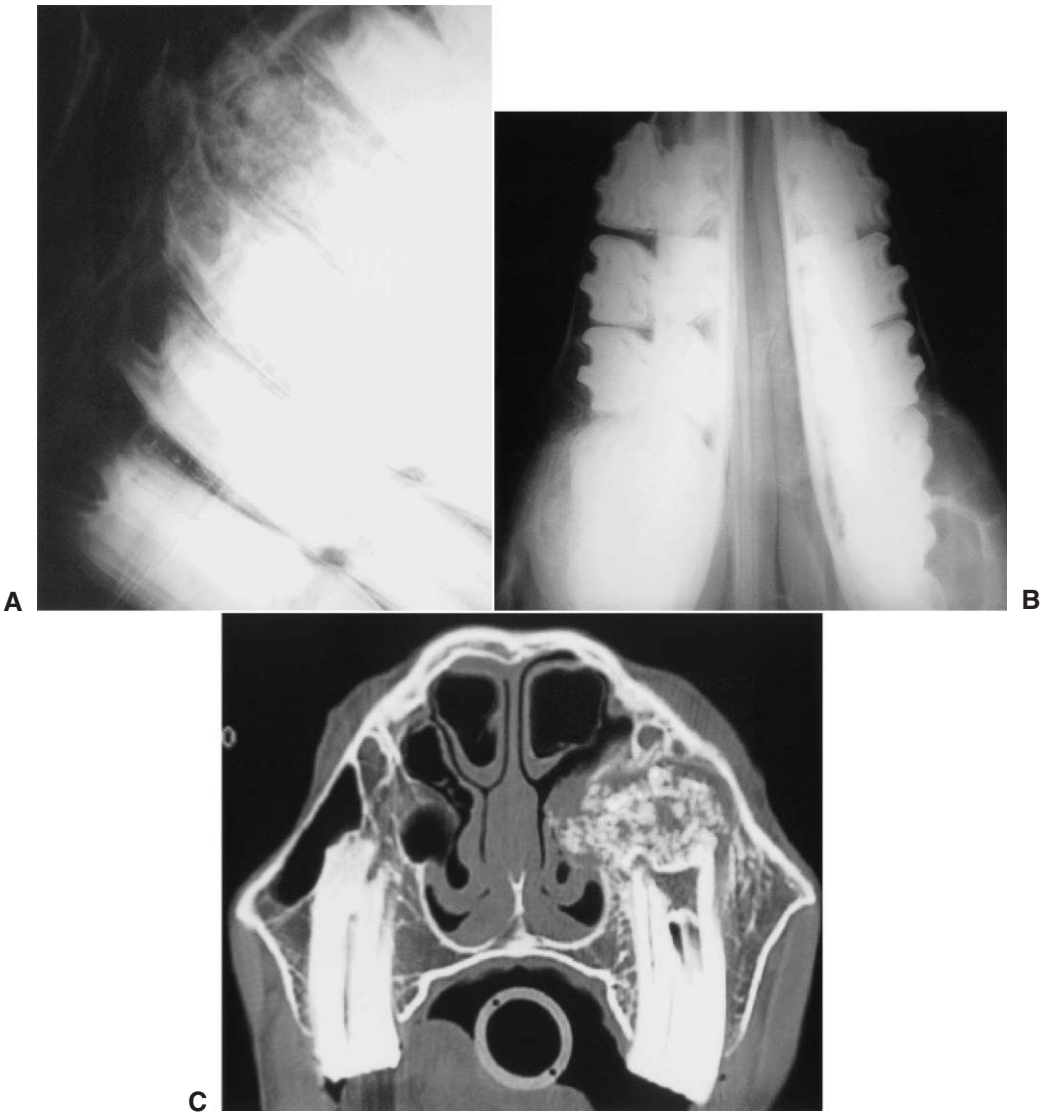


Figure 22-18 • A, Close-up lateral oblique view of the left maxilla shows the roots of the third and fourth cheek teeth overlain by an uneven bony density that extends dorsally over the surface of the adjacent maxilla. **B,** No maxillary fluid level is apparent. A ventrodorsal view shows partial opacification of the left maxillary sinus. **C,** A computed tomographic (CT) image through the maxillary sinus at the level of the fourth cheek tooth shows destruction of the root, alveolus, and nearby interior maxilla. Patchy mineralization or tumor bone fills much of the maxilla and has entered the adjacent nasal cavity and ventral concha. The overlying infraorbital canal is starting to become involved.

intranasal infusion in dogs with nasal aspergillosis, *Can Vet* J 44:305, 2003.
7. Arenchibia A, Vazquez JM, et al: Magnetic resonance imaging and cross sectional anatomy of the normal equine sinuses and nasal passages, *Vet Radiol Ultrasound* 41:313, 2000.
8. Boulton CH: Equine nasal cavity and paranasal sinus disease: a review of 85 cases, *Equine Vet Sci* 5:268, 1980.
9. Lane JG, Gibbs C, et al: Radiographic examination of the facial, nasal and paranasal regions of the horse. I. Indications and procedures in 235 cases, *Equine Vet J* 19:466, 1987.
10. Schumacher J, Dean P, Welsh B: Epistaxis in two horses with dacryohemorrhea, *J Am Vet Med Assoc* 200:366, 1992.
11. Beard WL, Hardy J: Diagnosis of conditions of the paranasal sinuses in the horse, *Equine Vet J* 13:265, 2001.
12. Lane JG, Gibbs C, et al: Radiographic examination of the facial, nasal and paranasal sinus regions of the horse: 1. indications and procedures in 235 cases, *Equine Vet J* 19:466, 1987.
13. Gibbs C, Lane JG: Radiographic examination of the facial, nasal and paranasal sinus regions of the horse. II. Radiological findings, *Equine Vet J* 19:474, 1987.
14. Valdez H, McMullan WC, et al: Surgical correction of deviated nasal septum and premaxilla in a colt, *J Am Vet Med Assoc* 172:1001, 1978.
15. Beard WL, Robertson JT, Leeth B: Bilateral congenital cysts in the frontal sinuses of a horse, *J Am Vet Med Assoc* 196:453, 1990.

16. Elkins S, Lee JW, et al: Congenital ethmoid carcinoma in a foal, *J Am Vet Med Assoc* 184:979, 1984.
17. Hodgin EC, Conaway DH, Ortenburger AI: Recurrence of obstructive nasal coccidioidal granuloma in a horse, *J Am Vet Med Assoc* 184:339, 1984.
18. Meschter CL, Allen D: Lymphoma within the nasal cavities of an 18-month-old filly, *Equine Vet J* 16:475, 1984.
19. Carmalt JL, Baptiste KE, Chirino-Trejo: *Acinobacillus lignieresii* infection in two horses, *J Am Vet Med Assoc* 215:826, 1998.
20. Schumacher J, Honnas C, Smith B: Paranasal sinusitis complicated by inspissated exudate in the ventral conchal sinus, *Vet Surg* 16:373, 1987.
21. Henninger W, Frame EM, et al: CT features of alveolitis and sinusitis in horses, *Vet Radiol* 44:269, 2003.
22. Coumbe KM, Jones RD, Kenwood JH: Bilateral sinus empyema in a six-year-old mare, *Equine Vet J* 19:559, 1987.
23. Lane JG, Longstaff JA, Gibbs C: Equine paranasal sinus cysts: a report of 15 cases, *Equine Vet J* 19:537, 1987.
24. Leyland A, Baker JR: Lesions of the nasal and paranasal sinuses of the horse causing dyspnea, *Br Vet J* 131:339, 1975.
25. Frankeny RL: Intranasal administration of formalin for treatment of epidermal inclusion cysts in five horses, *J Am Vet Med Assoc* 223:221, 2003.
26. Cotchin CH: A general survey of tumors in the horse, *Equine Vet J* 9:16, 1977.
27. Boulton CH: Equine nasal cavity and paranasal cavity disease: a review of 85 cases, *J Equine Vet Sci* 5:268, 1985.
28. Jubb KVF, Kennedy PC: *Pathology of domestic animals*, vol I, ed 2. New York, 1970, Academic Press.
29. Reynolds BL, Stedman MA, et al: Adenocarcinoma of the frontal sinus with extension to the brain in a horse, *J Am Vet Med Assoc* 174:734, 1979.
30. Scarratt WK, Crisman MV: Neoplasia of the respiratory tract, *Vet Clin N Am Equine Pract* 14:100, 1998.
31. Orsini JA, Baird DK, Ruggles AJ: Radiotherapy of a recurrent ossifying fibroma in the paranasal sinuses of a horse, *J Am Vet Med Assoc* 224:1483, 2004.
32. Schumacher J, Smith BL, Morgan SJ: Osteoma of paranasal sinuses of a horse, *J Am Vet Med Assoc* 192:1449, 1988.
33. Walker MA, Schumacher J, et al: Cobalt 60 radiotherapy for treatment of squamous cell carcinoma of the nasal cavity and paranasal sinuses in three horses, *J Am Vet Med Assoc* 212:848, 1998.
34. Cook WR, Littlewort MCG: Progressive hematoma in the ethmoid region of the horse, *Equine Vet J* 6:101, 1974.
35. Ethrington WG, Vasey JR, Horney FD: Ethmoid hematoma of the equine, *Can Vet J* 23:231, 1982.
36. Hanselka DV, Young MF: Ethmoidal hematoma in the horse, *Vet Med Small Anim Clin* 75:1289, 1975.
37. Gasser AM, Love NE, Tate LP: Ethmoid hematoma, *Vet Radiol Ultrasound* 41:247, 2000.
38. Boles C: Abnormalities of the upper respiratory tract. *Vet Clin N Am (Large Anim Pract)* 1:89, 1979.
39. McClure SR, Schumacher J, Morris EL: Dentigerous cyst in the ventral conchal sinus of a horse, *Vet Radiol Ultrasound* 34:334, 1993.
40. Boles C: Abnormalities of the upper respiratory tract, *Vet Clin N Am (Large Anim Pract)* 1:89, 1979.
41. Latimer CA, Wyman CD, et al: Radiographic and gross anatomy of the nasolacrimal duct of the horse, *Am J Vet Res* 46:451, 1984.
42. Latimer CA, Wyman CD: Atresia of the nasolacrimal duct in three horses, *J Am Vet Med Assoc* 184:989, 1984.

Chapter 23

Diseases of the Eye and Orbit

ORBITAL AND OCULAR IMAGING

Radiology

Plain radiography has only a limited role in most orbital and periorbital lesions in the horse; the principal exceptions are periorbital fractures. Another exception is a draining, periorbital sinus, where sinography can prove indispensable in establishing the depth, extent, and origin of the drainage.

Although often ordered for the sake of "completeness" to comply with a mandatory database or to rule out alternative diagnoses, facial radiographs of horses with ocular or perioccular lesions are usually normal. In my experience, unless there is an associated facial deformity, the likelihood of demonstrating bony involvement is less than 1%.[1]

Various radiographic projections of a normal adult orbit, along with corresponding views of a cutaway skull specimen, are provided for anatomic-radiographic comparison (Figure 23-1). An additional view of the normally serrated dorsal orbital rim is also included (Figure 23-2).

Ultrasound

The most common reasons for ocular ultrasound are to "see" beyond an opaque cornea, a hemorrhagic anterior chamber, or a cataract. Sonographic evaluation of the retrobulbar region is usually performed in cases of exophthalmia, typically searching for one of four things:

1. Retrobulbar abscess (with or without an accompanying foreign body)
2. Cellulitis
3. Tumor
4. Hematoma

Although few retrobulbar lesions have a characteristic appearance, most appear relatively *hypoechoic* compared with their immediate surroundings.[2]

Normal Ocular Sonometrics

Rogers and co-workers described the sonographic appearance of 95 normal extirpated equine eyes, including its interior and exterior measurements (Figure 23-3).[3]

EYE INJURIES

Eye injuries are a common occurrence in horses, and they range from minor corneal abrasions, to deep scratches, to perforation. The latter may cause collapse of the anterior chamber, intraocular hemorrhage, tearing, prolapse or adhesion of the iris, lens displacement, and infection.

Displaced orbital fractures may bruise, lacerate, perforate, or crush the globe. The optic nerve may be stretched, bruised, severed, or avulsed. Hematomas may form around the eye, leading to deformity or displacement.

Topical and local anesthesias (auriculopalpebral nerve block) are usually required because of pain associated with the pressure of the scanner on the horse's injured eye. Sedation further minimizes head movement. Sonographic examples of ocular trauma follow (Figures 23-4 through 23-6).

Orbital Fracture

In most instances plain radiographs are sufficient to *screen* the head for orbital injury, but they should be supplemented by computed tomography (CT) whenever possible. Orbital fractures may also involve the frontal sinus, causing air to leak out and accumulate under the skin over the forehead (Figure 23-7).

Orbital and Periorbital Infection

Bacterial. Bacterial infections of the orbit are often impossible to detect radiographically unless they are

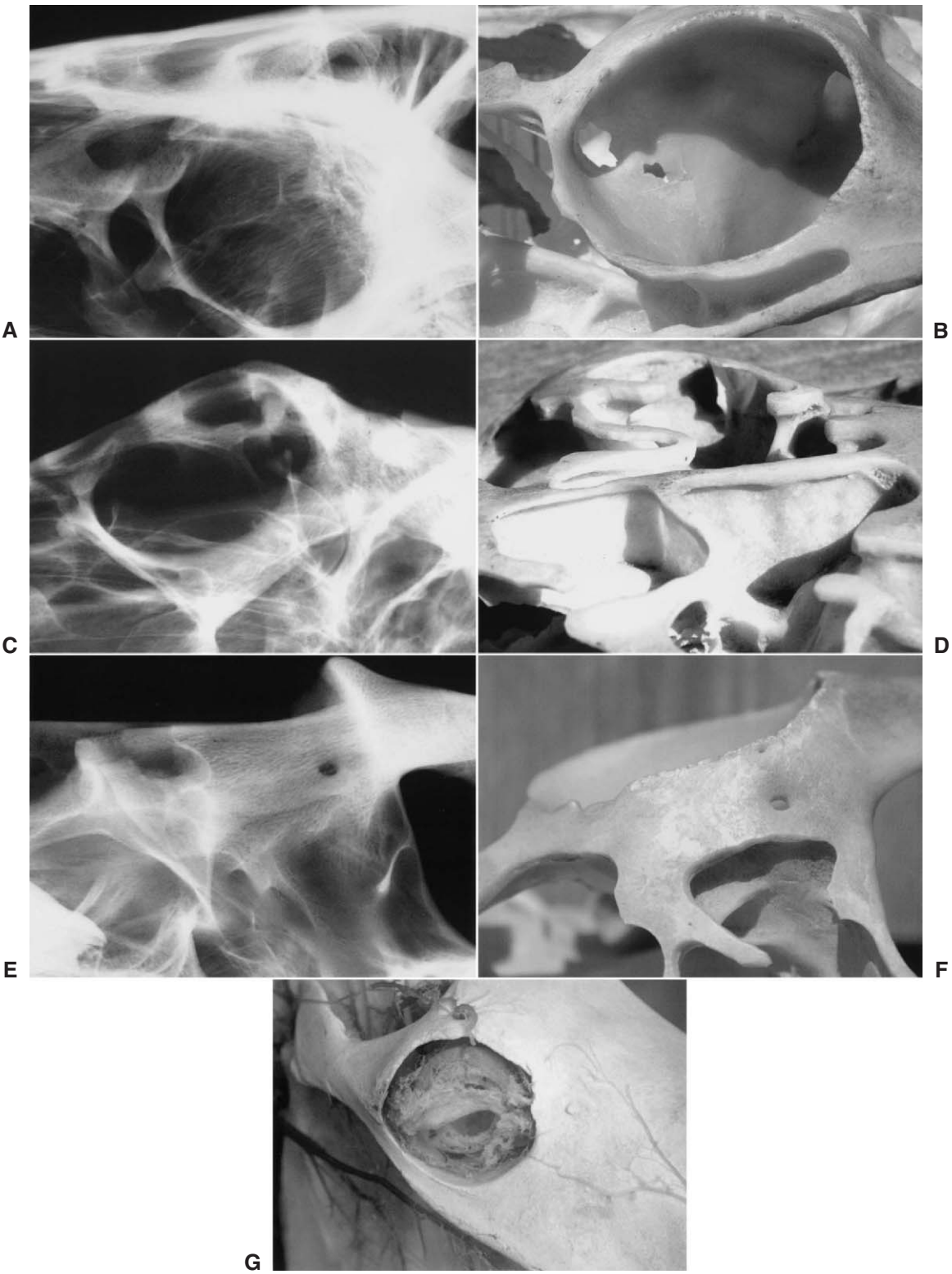


Figure 23-1 • Close-up lateral **(A, B),** lateral oblique **(C, D),** and ventrodorsal **(E, F)** radiographs, with corresponding specimen photographs of the orbital region of an adult horse. A skull specimen containing a preserved eye and surrounding soft tissue provides an understanding of the anatomic relationship between the two **(G).**

accompanied by periorbital drainage or by abscessation or fluid in a nearby sinus (Figure 23-8). Some orbital infections merely cause an increase in regional density (Figure 23-9).

Granulomatous. Pearce and co-workers reported a periorbital granulomatous infection in a horse caused by *Halicephalobus gingivalis*.[4] The infection was somewhat unusual in that it destroyed periorbital bone and caused soft-tissue mineralization (confirmed sonographically), similar to what is found with some tumors. The authors speculated that the infection was probably hematogenous.



Figure 23-2 • Close-up lateral oblique view of the orbit of an adult horse shows the normally serrated dorsal rim, which must not be mistaken for bone destruction.

Retrobulbar Abscessation

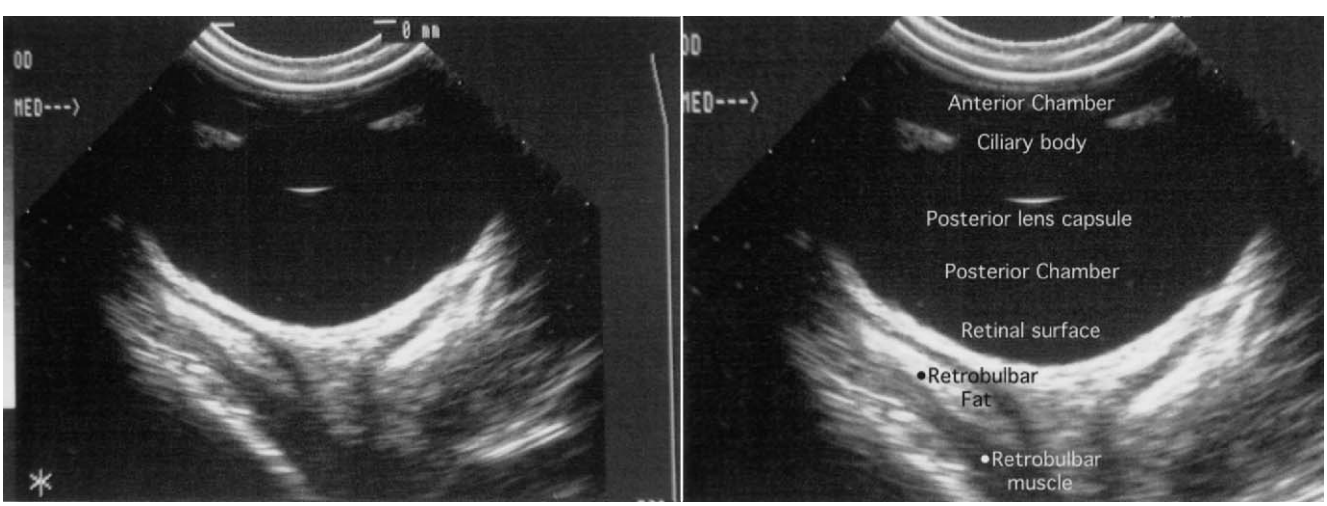
Sonology. Retrobulbar abscesses, as seen sonographically, can be well or poorly marginated and may or may not have a discrete wall. A typical retrobulbar abscess appears as a relatively round, hypoechoic object that sometimes flattens or indents the adjacent surface of the eye.[5] Many retrobulbar abscesses are impossible to distinguish from orbital tumors.

Retrobulbar Hematoma

Boroffka and co-workers reported the CT and sonographic appearance of a retrobulbar hematoma in a horse with moderate dorsal periorbital swelling and mild exophthalmia. The hematoma appeared as a large, retrobulbar, anechoic mass containing what appeared to be a medium-sized blood clot. Ultrasound proved more effective than CT in assessing the full extent of the lesion. Positioning the scanner over the periorbital swelling provided a better image than when it was placed on the cornea.[6]

Orbital Foreign Body

A wide variety of foreign objects may become embedded in and around the orbit of horses; sticks and wooden splinters are the most common. These materials lead to the accumulation of pus and eventual drainage through either an associated wound or a newly created sinus. Small splinters often are often discharged with the pus, but medium-sized and large fragments tend to remain behind, leading to a cycle of sinus drainage-sinus closure-sinus reformation and so forth until the foreign body is removed. Sinography is the most precise means of locating a nonopaque orbital foreign body and determining its size and shape (Figure 23-10).



A B

Figure 23-3 • Normal unlabeled **(A)** and labeled **(B)** sonograms of the normal eye of an adult horse.

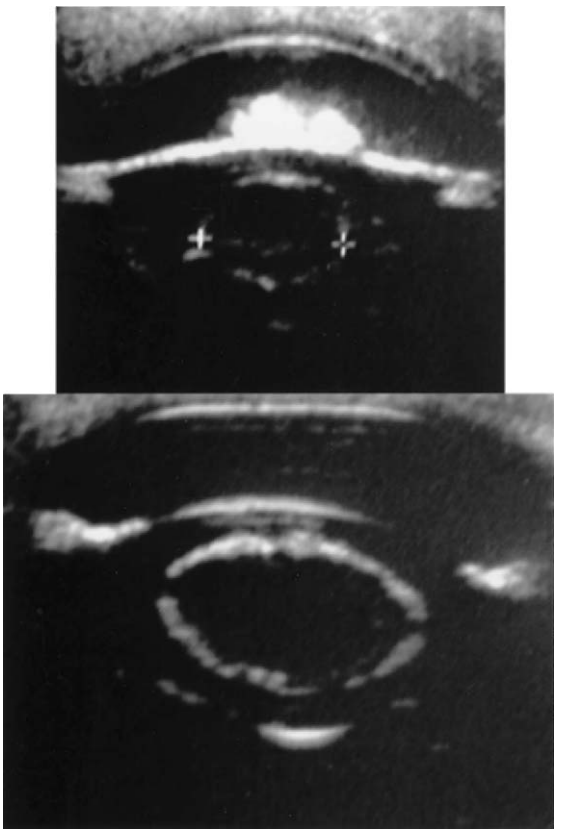


Figure 23-4 • Ocular sonogram shows a medium-sized hematoma centered on the corpora nigra and hemorrhage in the anterior chamber caused by blunt trauma *(top).* The normal opposite eye is included for comparison *(bottom).* Bilateral cataracts are also present.

Table 23–1 • NORMAL OCULAR SONOMETRICS

Structure	Average Size (mm)	Range (mm)
Cornea	2.33	1.5–3.7
Anterior chamber	4.22	1.1–6.6
Lens	2.50	1.4–4.8
Ciliary body	3.99	1.6–7.6
Lens	11.93	9.1–16.0
Vitreous	17.37	14.0–22.8
Retina	2.20	1.2–3.4
Craniocaudal dimension *(Axis bulbi)*	39.4	34.6–45
Dorsoventral dimension	42.5	35.0-55

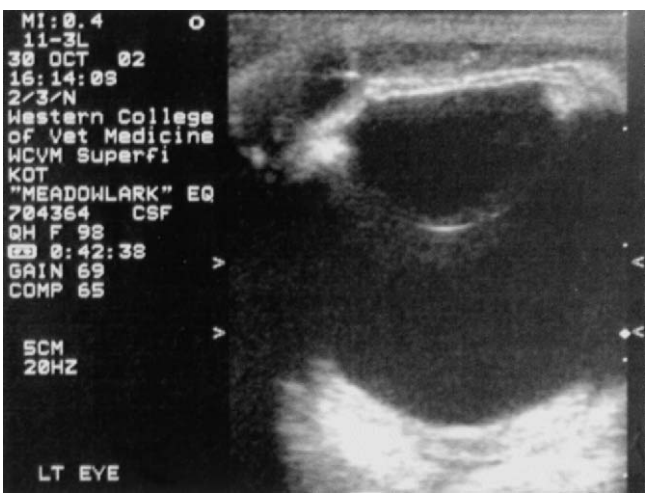
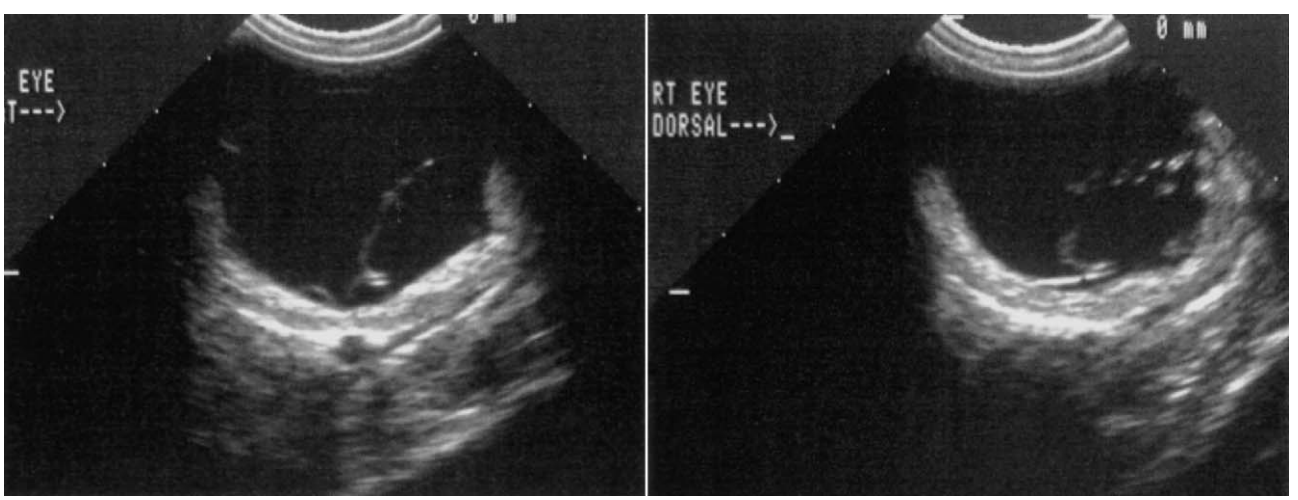


Figure 23-5 • Ocular sonogram shows partial collapse of the anterior chamber, a hemorrhagic aqueous, and iris prolapse.



A B

Figure 23-6 • **A,** Ocular sonogram shows the characteristic tendrils of a retinal detachment and vitreal hemorrhage. **B,** Another view of the same eye shows the considerable effect scan angle can have on the appearance of a detached retina.

Orbital Sequestra

Orbital sequestra, either posttraumatic or infectious, may lead to periorbital drainage, much like foreign bodies. A combination of radiography and sinography (where possible) usually provides the best estimate of the lesion, thereby facilitating surgical treatment. Customized oblique orbital projections (optimized to profile drainage sites), combined with reduced exposure to facilitate thinner surface bone, typically produce the best results. Lead markers taped to the draining sinuses aid in orientation (Figure 23-11).



Figure 23-7 • Close-up view of the lateral forehead region shows subcutaneous emphysema caused by a combined fronto-orbital fracture.

▮▮▮ ORBITAL TUMORS

Primary Orbital Tumors

Basher and co-workers reported neuroendocrine tumors in three older horses (13, 24, and 29 years old), all of which exhibited some degree of exophthalmia. In the horse that had ultrasound examination, the initial transpalpebral examination was negative. Only when a lateral, transcutaneous approach was used could the tumor be seen, appearing as a large lobulated, hypoechoic mass.[7]

In addition to neuroendocrine tumors, other reported types of orbital tumor include adenocarcinoma, lipoma, medulloepithelioma, microglioma, melanoma, multiple osteoma, neuroepithelial carcinoma, and neuroepithelial tumor of the optic nerve.

Secondary Orbital Tumors

Squamous Cell Carcinoma. Walker and co-workers reported the 2-year nonrecurrence rates for equine ocular and periocular squamous cell carcinoma after radiotherapy.[8] Seventeen horses with a total of 18 tumors were evaluated. Two different methods of radiotherapy were used to treat the lesions after removal of as much of the tumor as possible using

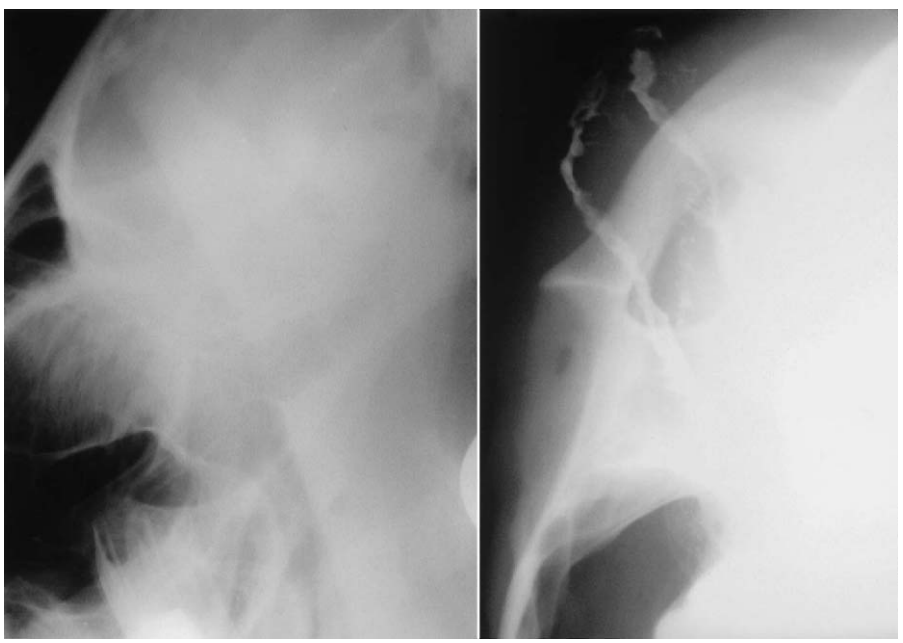


Figure 23-8 • **A,** Close-up lateral view of the orbit appears normal even though there is pus draining from the periorbital region. **B,** A follow-up sinogram shows two large, separate tracts leading to the depths of the orbit, where two large splinters were subsequently removed.

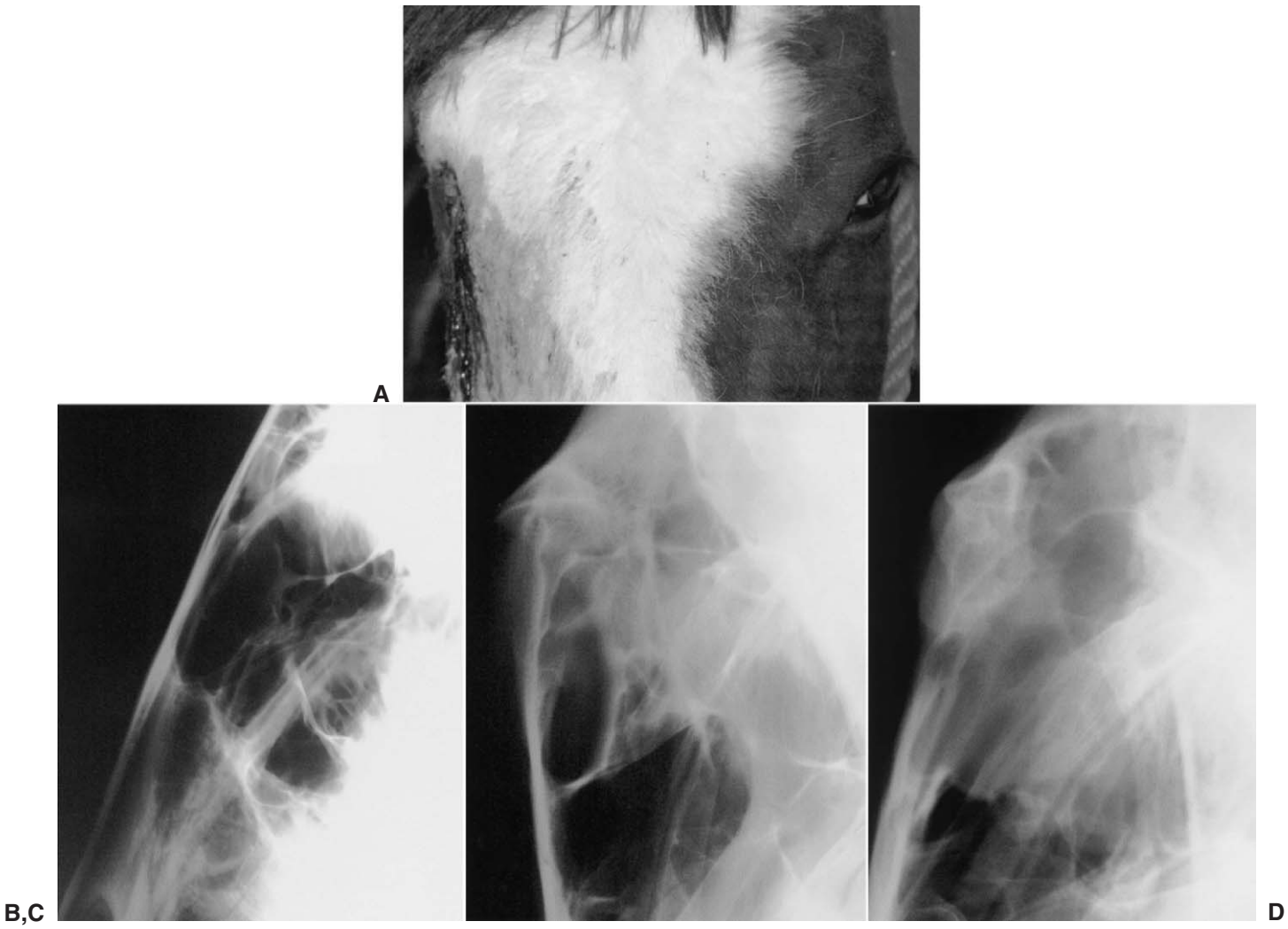


Figure 23-9 • Close-up frontal view **(A)** of a horse with a badly infected right eye and orbit shows copious drainage. Although close-up lateral **(B)** and left lateral oblique **(C)** views appear nearly normal, a right lateral projection **(D)** does not, showing increased density throughout the orbital region, subsequently found to be the result of a cluster of small and medium-sized communicating abscesses.

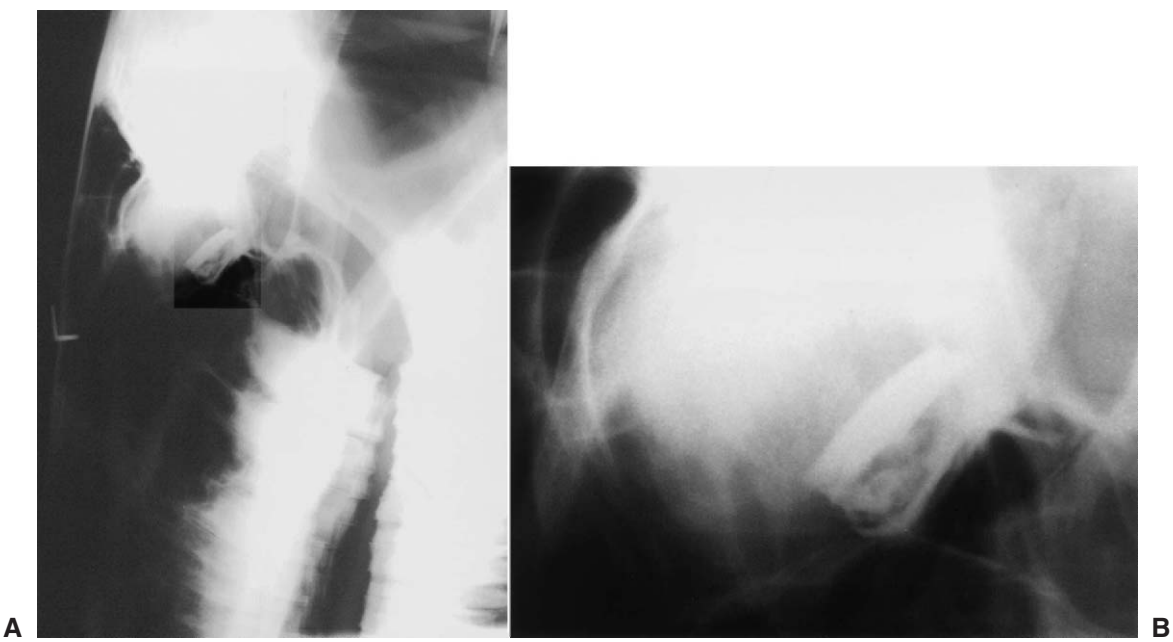


Figure 23-10 • Lateral **(A)** and close-up lateral **(B)** sinograms of the left orbital region show contrast solution surrounding a fragment of wood, appearing here as a rectangular filling defect.

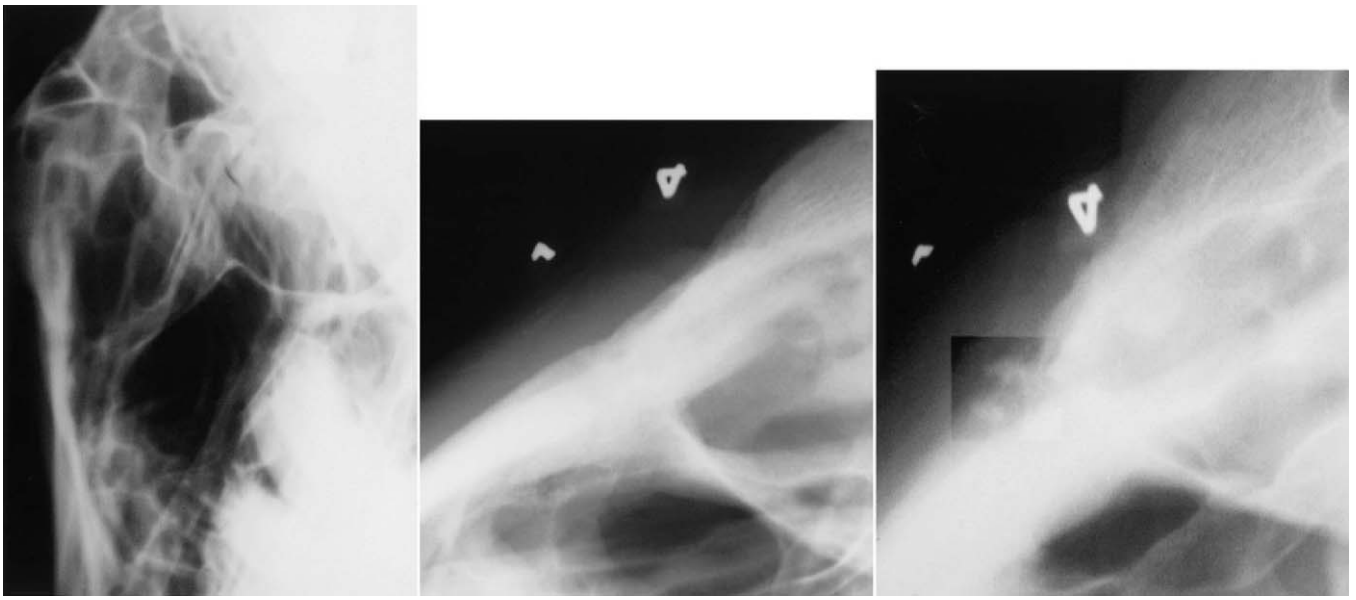


Figure 23-11 • A, Close-up lateral oblique view of a draining right orbital region appears normal. **B,** A customized lateral oblique projection of the same area but with soft-tissue technique shows an irregularly contoured maxilla as a result of recently formed new bone and soft-tissue swelling. The lead markers show the locations of the draining sinuses. **C,** A second customized lateral oblique view shows two small infective sequestra *(emphasis zone)* and a ragged layer of recently formed new bone; again, lead markers identify the drainage sites.

cryosurgery. Of these, radioactive strontium (^{90}Sr) applied at the surface of the tumor proved most effective, resulting in a 2-year nonrecurrence rate of 88 percent (rounded to the nearest whole number). Radiation emitted from implants placed within the tumor: radon-222, iodine-125, and iridium-192 resulted in a corrected 2-year nonrecurrence rate of 70 percent.

▮▮▮ ORBITAL SINOGRAPHY AND CAVOGRAPHY

Sinography

As described previously, sinography is an excellent means of imaging what lies deep to a draining sinus. Sinograms often provide detailed, multidimensional "roadmaps" leading to one or more foreign bodies as well as detailing their principal drainage routes and associated tributaries. Sinography is safe, rapid, and often not much more expensive than a standard radiographic examination; but sinography is often painful and therefore requires analgesia if it is to be done properly.

No sinographic protocols have been established. Each examination is patient tailored. Initial images are based on a combination of the specific objectives of the examination, lesion location, and radiographic intuition. Subsequent images are determined for the most part by what each preceding film in the study reveals.

Cavography

Cavography is a technique reserved for the radiographic investigation of closed fluid accumulations, specifically, their size, shape, and relationship to surrounding tissues. Cavographic technique is illustrated in the following case example (Figure 23-12).

▮▮▮ NASOLACRIMAL DUCT OBSTRUCTION

Anatomy

The nasolacrimal duct conducts tears away from the eye to the nostril. The component parts of the system consist of the (1) lacrimal punctae, (2) canaliculi, (3) lacrimal sac, (4) common lacrimal duct, and (5) nasal orifice. The common duct travels through the lacrimal canal, which is radiographically visible. Obstruction or infection of the nasolacrimal duct typically leads to epiphora.

Causes of Obstruction

Absence of the lacrimal puncta or canaliculi is likely the most common congenital defect found in the nasolacrimal apparatus of the horse. Most acquired nasolacrimal obstructions in the horse are temporary and can usually be alleviated with retrograde flushing.[9]



Figure 23-12 • Cavographic technique illustrated in an adult horse with a suspected tumor, manifested as a fluid-filled conjunctival swelling **(A).** A short 22-gauge needle is gently inserted into the center of the swollen conjunctiva, and 1 or 2 ml of fluid are removed for analysis **(B).** With the needle secured in the thumb and forefinger of the operator (as shown), an assistant attaches an extension tube and syringe *prefilled* with nonionic contrast solution and slowly injects the solution until *mild* distension is achieved **(C).** The needle is removed, and a lead marker is placed just below the swelling to aid radiographic location. Initial lateral **(D),** close-up lateral **(E),** and close-up dorsoventral **(F)** views show the contrast solution confined to the fluid pocket except for a small amount of leakage at the injection site. Close-up lateral **(G)** and ventrodorsal views **(H)** made immediately after a second, top-off injection continue to show the contrast medium confined to the swollen tissue, without evidence of sinus tracts or fistula.

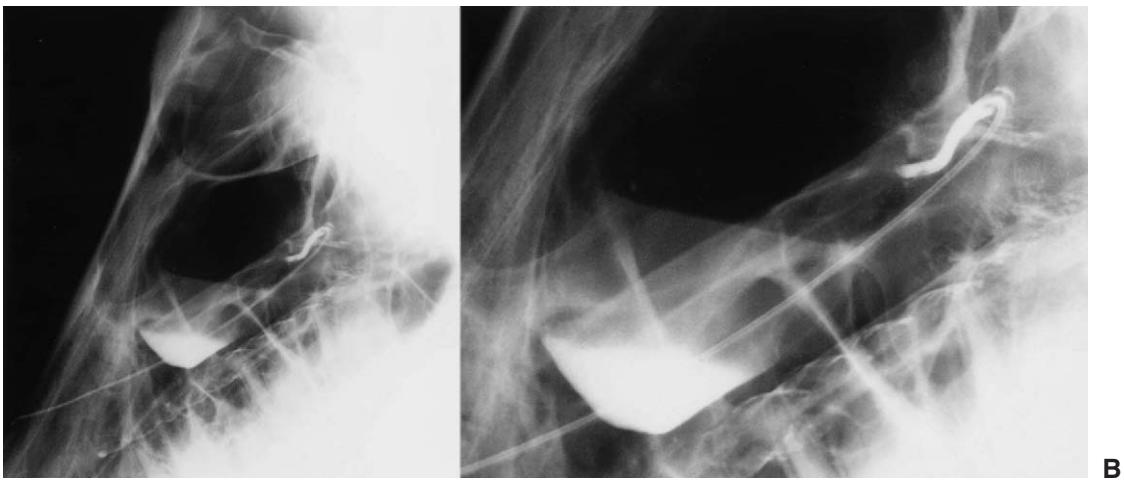


Figure 23-13 • Rostrocaudal oblique **(A)** and close-up rostrocaudal **(B)** views of a contrast study of the nasolacrimal duct show obstruction proximally with spillage into the nearby maxillary sinus.

Acquired blockages are usually of a secondary nature, resulting from the spread of a nearby dental or sinus infection (Figure 23-13). Occasionally depressed nasal or maxillary fractures secondarily damage the nasolacrimal canal and its associated nasolacrimal duct. Large, expansive maxillary or nasal tumors may displace, distort, and eventually compress the nasolacrimal canal. Nykamp and co-workers described the combined use of dacryocystography and CT as a means to evaluate the integrity of the nasolacrimal duct in a horse with multiple facial fractures.[10]

References

1. Farrow CS: Unpublished observations, 1999.
2. Freestone JF, Glazer MB, McClure DE: Ultrasonic identification of an orbital tumor in a horse, *Equine Vet J* 21:135, 1989.
3. Rogers M, Cartee RE, et al: Evaluation of the extirpated equine eye using B-mode ultrasonography, *Vet Radiol* 27:24, 1986.
4. Pearce SG, Boure LP, et al: Treatment of a granuloma caused by *Halicephalobus gingivalis* in a horse, *J Am Vet Med Assoc* 219:1735, 2001.
5. Hubert J, Williams MS, et al: What is your diagnosis? *J Am Vet Med Assoc* 209:1704, 1996.
6. Boroffa S, Antoon JM, Van Belt JM: Retrobulbar hematoma in a horse, *Vet Radiol Ultrasound* 37:441, 1996.
7. Basher AW, Severin GA, et al: Orbital neuroendocrine tumors in three horses, *J Am Vet Med Assoc* 210:668, 1997.
8. Walker MA, Goble D, Geiser D: Two-year non-recurrence rates for equine ocular and periorbital squamous cell carcinoma following radiotherapy, *Vet Radiol* 27:146, 1986.
9. McIlnay TR, Miller SM, Dugan SJ: Use of canaliculorhinostomy for repair of nasolacrimal duct obstruction in a horse, *J Am Vet Med Assoc* 218:1323, 2001.
10. Nykamp SG, Scrivani PV, Pease AP: Computed tomography dacryocystography evaluation of the nasolacrimal apparatus, *Vet Radiol Ultrasound* 45:23, 2004.

Chapter 24

Cranial Fractures and Bulla Disease

THE STANDARD CRANIAL FRACTURE SERIES

In a standing horse with a suspected cranial fracture, I prefer a lateral view. In a recumbent or unconscious animal, I make both lateral and ventrodorsal views, in the latter instance using a horizontal beam to minimize head movement, which could aggravate the injury (Figure 24-1). Customized oblique projections are made as needed.

Cranial fractures can be very difficult to diagnose in horses because of superimposition by the vertical rami, temporomandibular joints, zygomatic arches, and petrous temporal bones. Gibbs favors the ventrodorsal over the lateral projection because it affords a left side–right side comparison (provided there is little or no obliquity).[1]

BASILAR SKULL FRACTURES

Basilar fractures, other than those of the basisphenoid-basioccipital bone, are very difficult or impossible to diagnose radiographically. Many are associated with bruising of the brain and compressive, subdural hemorrhage and, as such, often prove fatal.[2] Basilar fractures are often associated with collateral damage to one or more nearby soft-tissue structures, including the (1) jugular vein; (2) carotid artery; (3) ninth, tenth, and twelfth cranial nerves; (4) cavernous sinus; and (5) basilar artery. One or both guttural pouches are often blood filled.

Ramirez and co-workers reported a series of related radiographic abnormalities, which may be used to *infer* a basilar skull fracture.[3] These include (1) increased guttural pouch density, (2) uneven ventral basioccipital contour, (3) indistinct or invisible nasopharynx, (4) dorsal pharyngeal compression, and (5) one or more small bone fragments in the guttural pouch field.

Ragle and co-workers described the computed tomography (CT) appearance of a basioccipital avulsion fracture in a 3-month-old Arabian foal that fell backwards while having a seizure.[4] If it is available, CT is a more sensitive means of detecting basisphenoid-basioccipital and other skull fractures than radiology is.

Basisphenoid-Basioccipital Bone Fractures

In the immature horse, a radiographically transparent suture separates the basisphenoid and basioccipital bones located at the caudal skull base, which closes once the horse has finished growing (Figures 24-2 and 24-3).

Drawing an imaginary line through the caudal aspect of the ventral basisphenoid tubercle and the rostral edge of the foramen lacerum in either the lateral or ventrodorsal projections approximates the former location of the basisphenoid-basioccipital suture in instances where it has closed (Figures 24-4 and 24-5).

Ackerman and co-workers determined that the *spheno-occipital suture* in the horse closed somewhere between 2 and 3 years of age and that its width could be as much as three times greater ventrally than dorsally. They theorized that spheno-occipital fractures occurred as a result of sudden and forceful contraction of the basilar skull muscles as opposed to a direct blow.[5] By comparison, a more recent equine radiology text reports a closure time of 5 years.[6] I have seen a 6-year-old Arabian stallion with a partially open spheno-occipital suture.

Fractures of the basisphenoid-basioccipital bone are often very difficult to identify because of their minimal displacement and strong resemblance to a preexisting suture. Occasionally spheno-occipital fractures become sufficiently displaced that they are visible in a lateral radiograph, especially if it includes the guttural pouch, which greatly enhances contrast. In one published case report, a basisphenoid-basioccipital fracture appeared as a large rectangular bone fragment superimposed on the guttural pouches



Figure 24-1 • Preparing to make a ventrodorsal view of the cranium in a recumbent but conscious horse suspected of having a recent basilar skull fracture. By moving the x-ray tube and receiver rather than moving the animal to make both the lateral and ventrodorsal views, potentially injurious patient movement can be kept to a minimum.

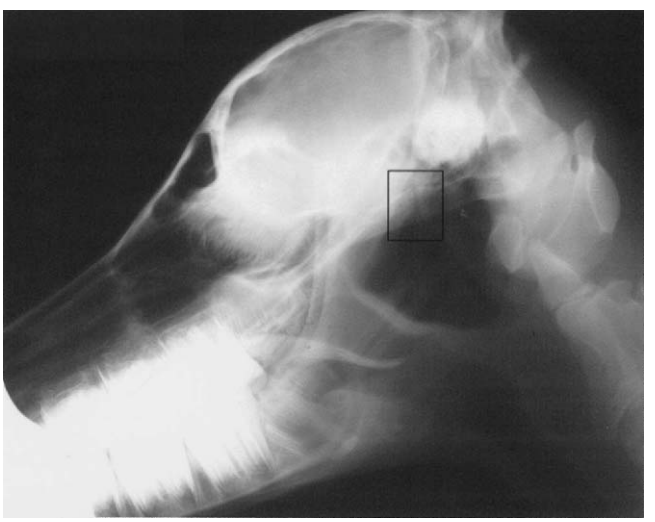


Figure 24-2 • Lateral skull film of a young foal shows the normal gap between the basisphenoid and basioccipital bones *(box)*, representing a fibrous suture that disappears with skeletal maturity.

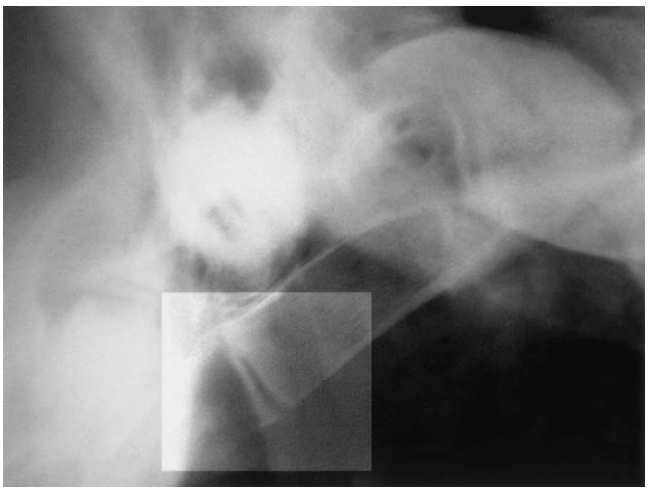


Figure 24-3 • Ultra-close-up lateral view of a normal basisphenoid-basioccipital suture in a 2-year-old filly. *Note:* Conflicting reports exist regarding the precise closure time of this suture, with most sources reporting a 4- or 5-year disappearance time.

just caudal to the upper portions of the large hyoid bones.[7]

Spheno-occipital Fracture Types

In my experience there are at least three types of basisphenoid-basioccipital fracture: (1) splintered, (2) compressed, and (3) offset. In the splintered-type injury, one or more large bone splinters are visible just ventral to the spheno-occipital suture or where the suture was formerly located (Figure 24-6). The compression-type injury resembles a train wreck, where one car piles up on another, crushing and deforming the ends of one another in the process (Figure 24-7). The offset or stepped-type injury is simply a fracture-dislocation in which the normally straight ventral contour of the basisphenoid-basioccipital junction is replaced by a step. The fracture line may or may not be apparent.

There is a fourth type of spheno-occipital fracture, which fortunately is quite rare. In this type of injury, the fracture line is oriented obliquely so that it lies in both the transverse and longitudinal planes, making it difficult or impossible to appreciate from a lateral perspective. This fracture is particularly difficult to diagnose radiographically. If CT is not available, a ventrodorsal view is the next best alternative.

There are accounts of spheno-occipital fractures causing collapse or wedging of the dorsal third of the suture, but regrettably this appearance also closely resembles a common normal spheno-occipital variant as well as a suture in the process of closing. Because of these ambiguities, I consider dorsal wedging to be an unreliable fracture indicator.

Presphenoid Bone Fractures

Taylor and co-workers reported an unusual case of free air in the subarachnoid spaces of the brain and cranial spinal cord of a horse after it fractured its presphenoid bone; leakage of air from the sphenopalatine sinus was also found.[8]

Temporal Bone Fractures

Blythe and co-workers described vestibular syndrome secondary to pathologic fracture of the temporal bone

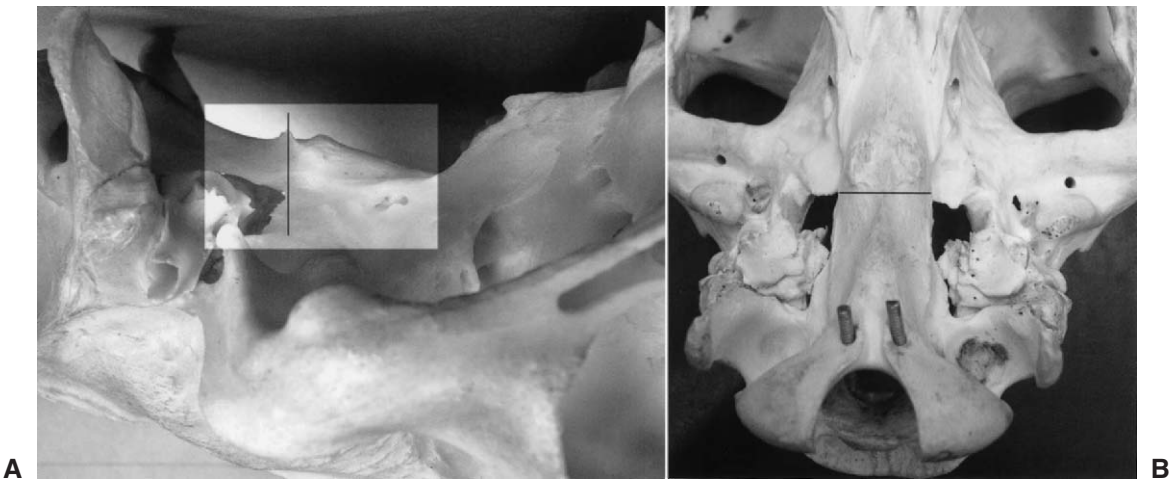


Figure 24-4 • Close-up lateral **(A)** and ventrodorsal **(B)** views of the cranium of an adult horse show the approximate location of the spheno-occipital suture (marked with vertical and horizontal black lines, respectively).



Figure 24-5 • A close-up view of a closed spheno-occipital suture in an adult horse, naturally marked by paired tubercles located on the caudoventral aspect of the basisphenoid bone. This normal finding can be mistaken for a fracture or a new bone deposit, especially in a large horse.

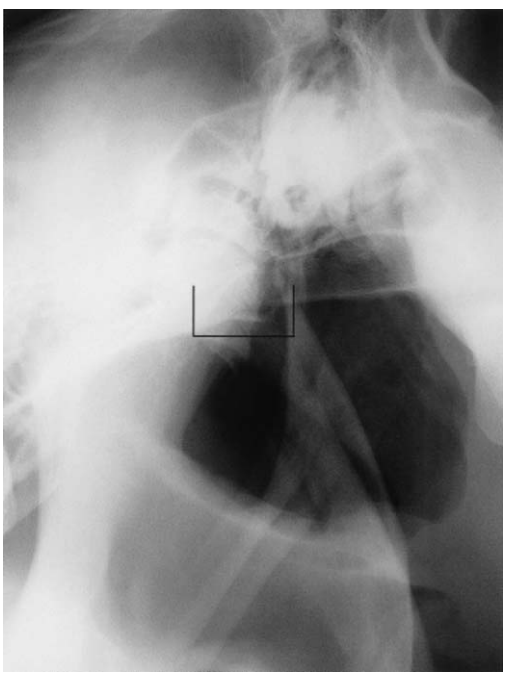


Figure 24-6 • Close-up lateral view of the skull base shows an open but disfigured spheno-occipital suture with a large ventrally situated bone splinter (U-bracket) consistent with fracture.

in three horses. Presumably, a chronic inner ear infection had spread to the adjacent temporohyoid joint, causing ankylosis and eventually fracture.[9]

Occipital Condylar Fractures

Most occipital condylar fractures are difficult to diagnose because of their relative lack of displacement, relatively small size, and curved shape. The normal radiographic variability of the occipital-C1 joint further complicates radiographic diagnosis. Sometimes it is possible to infer an occipital fracture or partial atlanto-occipital dislocation based on a loss of detail or narrowing, bearing in mind, however, that a wryneck or osteoarthritis might cause a similar appearance (Figure 24-8).

▮▮▮ BULLA INFECTION (OTITIS MEDIA)

Inner Ear Infection

Inner ear infection (otitis media) is rare in horses compared with dogs, or at least it is recognized and

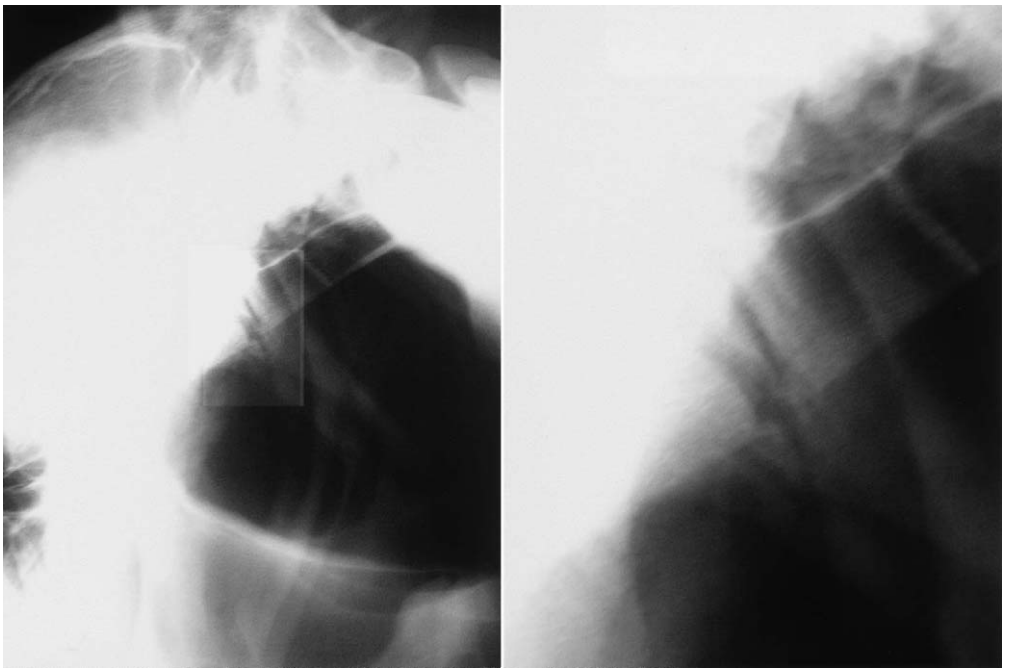


Figure 24-7 • Close-up **(A)** and ultra-close-up **(B)** views of the skull base show a fractured spheno-occipital suture and adjacent basisphenoid and basioccipital bones.

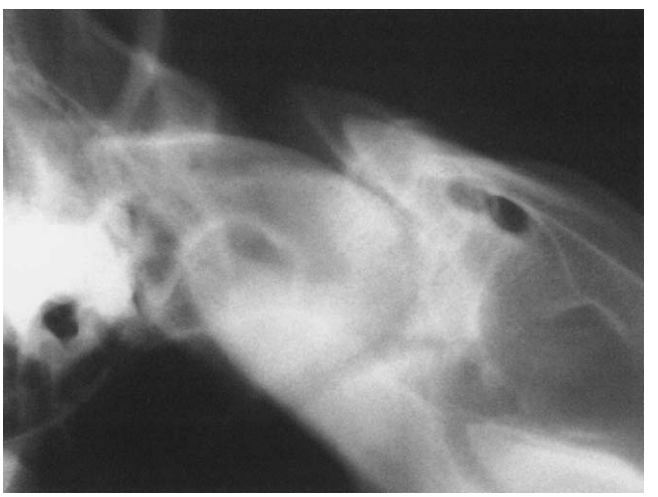


Figure 24-8 • Close-up lateral view of the atlanto-occipital joint in an ataxic horse reveals a clarity loss, the result of bilateral articular fractures of both occipital condyles and associated subluxation.

reported less frequently; however, it produces similar clinical and radiographic signs. Specifically, severe long-standing infection can lead to varying degrees of bulla opacification, which is usually best appreciated in a ventrodorsal projection in which only one bulla is diseased, thus allowing comparison with the normal opposite side (Figure 24-9).

Unfortunately, and as reported previously with pet animals, bulla radiography only detects severe, advanced disease.[10] In other words, many horses with the bulla disease will appear radiographically normal. CT, on the other hand, is highly sensitive, and in my opinion it is the imaging method of first choice.

Temporohyoid Osteoarthropathy (Secondary Thyrohyoid Infection)

Bony fixation and immobilization of the proximal aspect of either thyrohyoid bone are theorized by some to be the result of a chronic inner ear infection. The theory further holds that new bone deposition on the surface of the affected hyoid bone is the result of an extension of the infection.

An alternative (but unsupported) theory holds that temporohyoid osteoarthropathy is actually a form of degenerative joint disease that is unrelated to an inner ear infection.[11] In either instance, the proximal stylo-

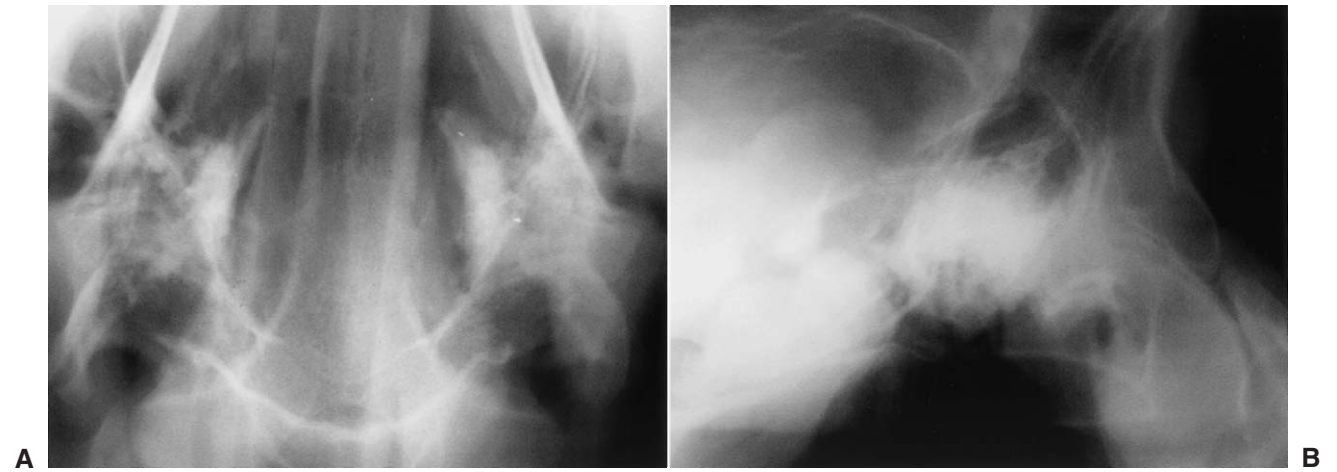


Figure 24-9 • Close-up ventrodorsal **(A)** and lateral **(B)** views of the skull of a horse with left-sided head tilt show near complete opacification of the left bulla (reader's right), consistent with severe otitis media.

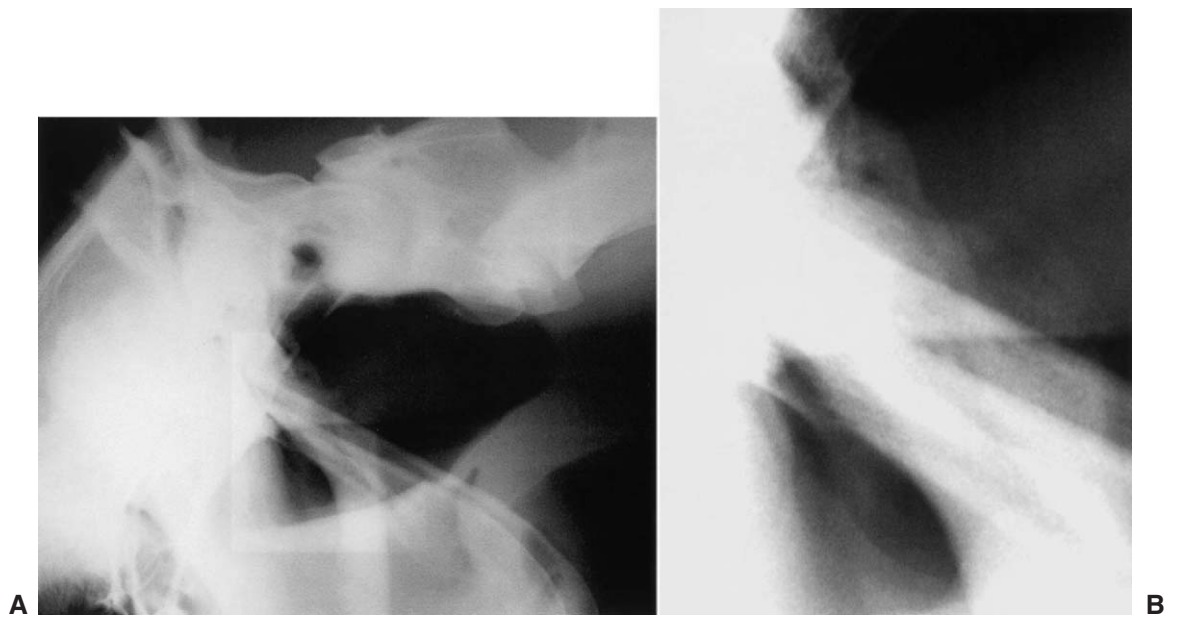


Figure 24-10 • Close-up **(A)** and ultra-close-up **(B)** lateral views of the throat of a pregnant mare with paralysis of the left facial nerve and protrusion of the left side of the tongue show a proximal stylohyoid enveloped (and presumably fixed) by a large, chronic appearing new bone deposit, presumably caused by the spread of an inner ear infection.

hyoid bone or its point of fusion with the petrous temporal bone may fracture, leading to neurologic dysfunction involving the facial and vestibulocochlear nerves or, in severe cases, seizures.

Figures 24-10 and 24-11 show examples of presumed unilateral otitis media leading to secondary thyrohyoid fixation and disfigurement by inflammatory new bone. A normal thyrohyoid bone is provided for radiographic-anatomic comparison (Figure 24-12).

References

1. Gibbs C: The equine skull: its radiological investigation, *Vet Radiol* 15:70, 1974.

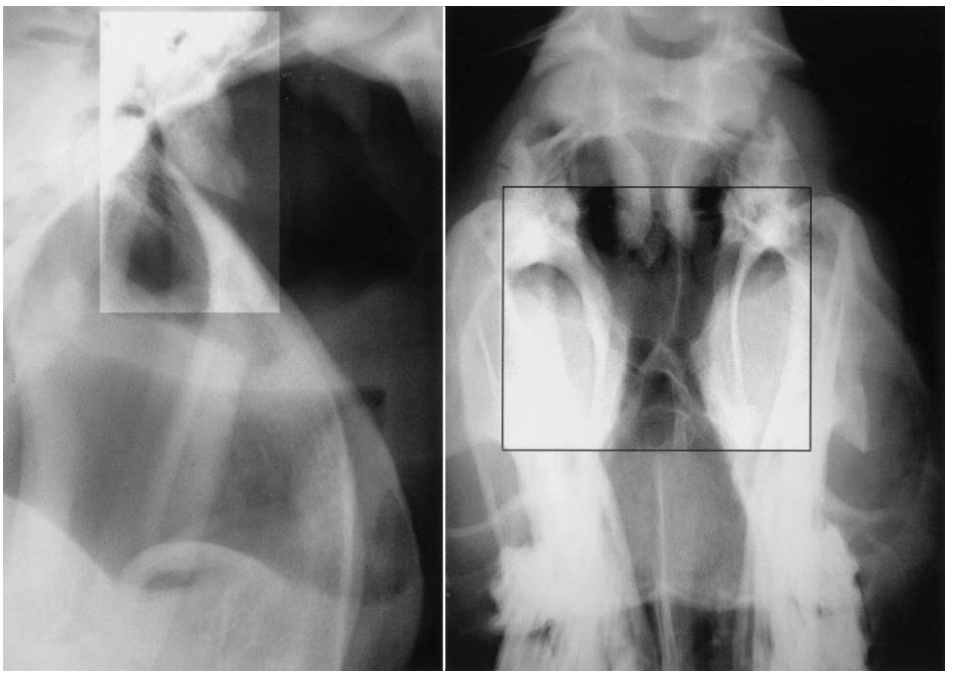


Figure 24-11 • Close-up lateral **(A)** and dorsoventral **(B)** views of the throat show a chronic appearing, high-density bone deposit coating the proximal half of one of the right thyrohyoid bone *(box)*, reader's left.



Figure 24-12 • Close-up view of a normal left thyrohyoid bone *(box)* situated within the lower jaw of an adult horse as seen from a right rear perspective.

2. Stick JA, Wilson T, Kunze D: Basilar skull fractures in three horses, *J Am Vet Med Assoc* 176:228, 1980.
3. Ramirez O, Jorgensen JS, Thrall DE: Imaging basilar skull fractures in the horse: a review, *Vet Radiol Ultrasound* 39:391, 1998.
4. Ragle CA, Koblik PD, et al: Computed tomographic evaluation of head trauma in a foal, *Vet Radiol* 29:206, 1988.
5. Ackerman N, Coffman JR, Corley EA: The sphenooccipital suture of the horse: its normal radiographic appearance, *Vet Radiol* 15:79, 1974.
6. Poulos P: The head, In *Clinical radiology of the horse*, ed 2. Philadelphia, 1993, Blackwell Science.
7. Alexander K, Baird JD, et al: What is your diagnosis? *J Am Vet Med Assoc* 220:297, 2002.
8. Taylor DS, Wisner ER, et al: Gas accumulation in the subarachnoid space resulting from blunt trauma to the occipital region of a horse, *Vet Radiol Ultrasound* 34:191, 1993.
9. Blythe LL, Watrous BJ, et al: Vestibular syndrome associated with temporohyoid joint fusion and temporal bone fracture in three horses. *J Am Vet Med Assoc* 185:775, 1984.
10. Farrow CS: The ear, In *Veterinary medical imaging: the dog & cat*, vol 1. St Louis, 2003, Mosby.
11. Walker AM, Sellon DC, et al: Temporohyoid osteoarthropathy in 33 horses (1993-2000), *J Vet Intern Med* 16:697, 2002.

Chapter 25

Inner Ear Disease, Brain Tumors, Abscesses, and Brain Trauma

STANDARD BRAIN IMAGING

Indisputably, primary brain imaging is the purview of cross-sectional imaging, specifically computed tomography (CT) and magnetography, with no reasonable argument yet to be advanced for the initial use of radiology, even on a screening basis.

MAGNETIC RESONANCE IMAGING OF THE NORMAL BRAIN

Chaffin and co-workers described the magnetic resonance (MR) appearance of normal brain in five live 3- to 6-day-old Quarter Horse foals.[1] Arencibia and co-workers reported the normal MR appearance of the adult equine brain using the decapitated head of an 8-year-old male Thoroughbred.[2]

Ferrell and co-workers described the use of MR to evaluate 11 live horses for suspected neurologic disease of the brain and cranial nerves.[3] The diseases that were diagnosed included *Sarcocystis neurona*, stylohyoid osteoarthropathy, cerebral hematoma, pituitary macroadenoma (presumed), yellow-star thistle poisoning (nigropallidal encephalomalacia), hydrocephalus, and otitis media.

INNER EAR INFECTION

Isolated otitis media can produce a variety of clinical signs, some of which suggest neurologic disease: head tilt, nystagmus, facial paralysis, and forelimb incoordination. Involvement of the adjacent stylohyoid bone can affect swallowing, in particular the action of the tongue. Blythe referred to this disorder as *temporomandibular osteoarthropathy* and theorized as to its pathogenesis.[4] The radiographic features of this condition are described in the previous chapter.

BRAIN TRAUMA

Ragle and co-workers described the computed tomographic appearance of an extradural hematoma in a 3-month-old Arabian foal with a basilar skull fracture.[5] The hematoma appeared on CT as a 2.5 × 4.5-cm hyperdense soft-tissue mass adjacent to the outer margin of the right temporal lobe with a mean attenuation of 78 Hounsfield units (compared with a Hounsfield value of 38 on the normal opposite side of the brain).

BRAIN ABSCESS

Spoormakers and co-workers reported the magnetographic appearance of brain abscesses in four horses. These abscesses developed secondary to strangles (purulent pharyngitis/lymphadenitis caused by *Streptococcus equi*).[6] Later Smith and co-workers described seven horses with bacterial meningitis and brain abscesses secondary to primary sinonasal, periocular, or regional lymph node infections. Unfortunately, medical imaging did not play a significant role in diagnosis.[7]

UREMIC ENCEPHALOPATHY

Frye and co-workers reported five cases of equine uremic encephalopathy identified in a retrospective study spanning 20 years.[8] The neurologic components of this disorder can apparently be triggered by either acute or chronic renal disease. In this latter regard, two of five horses that underwent ultrasound showed poor corticomedullary definition and focal areas of increased echogenicity interpreted as either small calculi or dystrophic calcification. Cerebrospinal fluid (CSF) samples were nonrevealing. Astrocytic swelling

was present in all four horses that were necropsied, a finding that could prove useful in magnetic resonance imaging (MRI).

▮▮▮ YELLOW-STAR THISTLE POISONING (EQUINE NIGROPALLIDAL ENCEPHALOMALACIA)

Saunders and co-workers described the MR appearance of yellow-star thistle poisoning in a single horse.[9] MR abnormalities included (1) bilateral, focal, well-circumscribed, heterogeneous, hyperintense areas in the region of the substantia nigra on proton density; (2) heterogeneous increased signal of the globus pallidus on proton density and T2; (3) bilateral, focal hyperintense signals circling the globus pallidus and substantia nigra on the T1-transverse, preg-adolinium images; (4) normal enhancement of choroid plexus of lateral and third ventricles, vein of the corpus callosum, and dorsal sagittal sinus on T1-weighted post-gadolinium images; but (5) no enhancement of the globus pallidus and substantia nigra. The sagittal post-gadolinium T1 images revealed distinctive, bilateral, hyperintense rings surrounding the globus pallidus.

▮▮▮ COMMON CAROTID BLOOD FLOW IN THE ANESTHETIZED HORSE

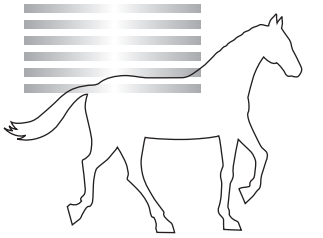
Using Doppler ultrasound, Schmucker and co-workers determined that horses under general anesthesia show an increase in common carotid blood flow attributable to vascular enlargement, increased velocity, and decreased resistance. From this finding, the authors deduced that a commensurate increase in cerebral blood flow was probable.[10]

References

1. Chaffin MK, Walker MA, et al: Magnetic resonance imaging of the brain of normal neonatal foals, *Vet Radiol Ultrasound* 38:102, 1997.
2. Arencibia A, Vasquez JM, et al: Magnetic resonance imaging of the normal equine brain, *Vet Radiol Ultrasound* 42:405, 2001.
3. Ferrell EA, Gavin PR, et al: Magnetic resonance for evaluation of neurologic disease in 12 horses, *Vet Radiol Ultrasound* 43:510, 2003.
4. Blythe LL: Otitis media and internal and temporohyoid osteoarthropathy, *Vet Clin N Am Equine Pract* 13:21, 1997.
5. Ragle CA, Koblik PD, et al: Computed tomographic evaluation of head trauma in a foal, *Vet Radiol* 29:206, 1988.
6. Spoormakers TJR, Ensink JM, et al: Brain abscesses as a metastatic manifestation of strangles: symptomology and the use of magnetic resonance imaging as a diagnostic aid, *Equine Vet J* 35:146, 2003.
7. Smith JJ, Provost PJ, et al: Bacterial meningitis and brain abscesses secondary to infectious disease processes involving the head in horses: seven cases (1980-2001), *J Am Vet Med Assoc* 224:739, 2004.
8. Frye MA, Johnson JS, et al: Putative uremic encephalopathy in horses: five cases (1978- 1998), *J Am Vet Med Assoc* 218:560, 2001.
9. Saunders SG, Tucker RL, et al: Magnetic resonance imaging features of equine negropallidal encephalomalacia, *Vet Radiol Ultrasound* 42:291, 2001.
10. Schmucker N, Budde K, et al: Duplex-ultrasonographic evaluation of the common carotid artery in the resting sedated and anesthetized horse, *Vet Radiol Ultrasound* 41:168, 2000.

SECTION III

The Throat and Neck



Chapter 26

The Throat: Guttural Pouches, Pharynx, and Larynx

STANDARD EXAMINATION

The throat is best examined with a single lateral projection using a vertically oriented, 14- by 17-inch receiver and soft-tissue technique (Figure 26-1).

SALIVARY GLANDS

Congenital Defects

Ductal Atresia. Sadler and co-workers reported congenital parotid ductal atresia in a 19-month-old Quarter Horse with a large left-sided facial swelling. Plain films were unrevealing. *Cavography* was performed by percutaneously injecting nonionic, diagnostic iodine solution directly into the swelling. *Cavograms* revealed a large curvilinear opacity originating in the region of the guttural pouch and extending ventrally along the caudoventral margin of the left mandible, consistent with a distended (and probably obstructed) parotid duct, a diagnosis confirmed in a subsequent surgery.[1] Only two previous reports of parotid duct atresia were found, supporting the rarity of this disease in horses.[2,3]

Salivary Tumors

Salivary tumors rarely occur in horses, although small series and individual cases have been described.[4] For example, Fintel and Dixon described the clinical features of parotid melanoma in three horses and two ponies.[5] Like a number of equine cancers, grays are more vulnerable than other colors. Parotid melanoma may metastasize or encroach on nearby tissues, most notably causing pharyngeal or laryngeal compression leading to airway obstruction and dyspnea. Some parotid melanomas grow quite slowly over a period of years, never spreading; others initially grow slowly, conveying the impression of benignity, only suddenly to turn malignant.

Radiographic Findings. Radiographically, parotid melanomas and most other salivary tumors lack defin-

ing features, although it may be possible to detect secondary pharyngeal compression in the case of larger masses. Ultrasound is useful in distinguishing a solid mass, such as a parotid melanoma, from an abscess, edema, cellulitis, or a distended duct.

▮▮▮ THE GUTTURAL POUCHES

In my estimation, Cook's article on the guttural pouch of the horse remains a classic even though it was written more than three decades ago.[6] For those who have access to *Veterinary Radiology & Ultrasound*, I strongly recommend reading (or rereading) this excellent article. I too have written extensively about the guttural pouches, for the most part describing the radiographic appearance of a variety of diseases.

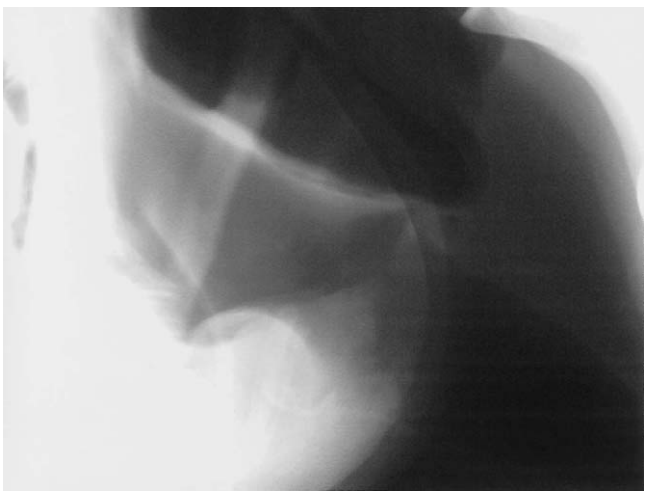


Figure 26-1 • Normal throat: the translucent guttural pouches appear uppermost; the pharynx lies just to the left of center (overlying the epiglottis); the larynx is to the right of that.

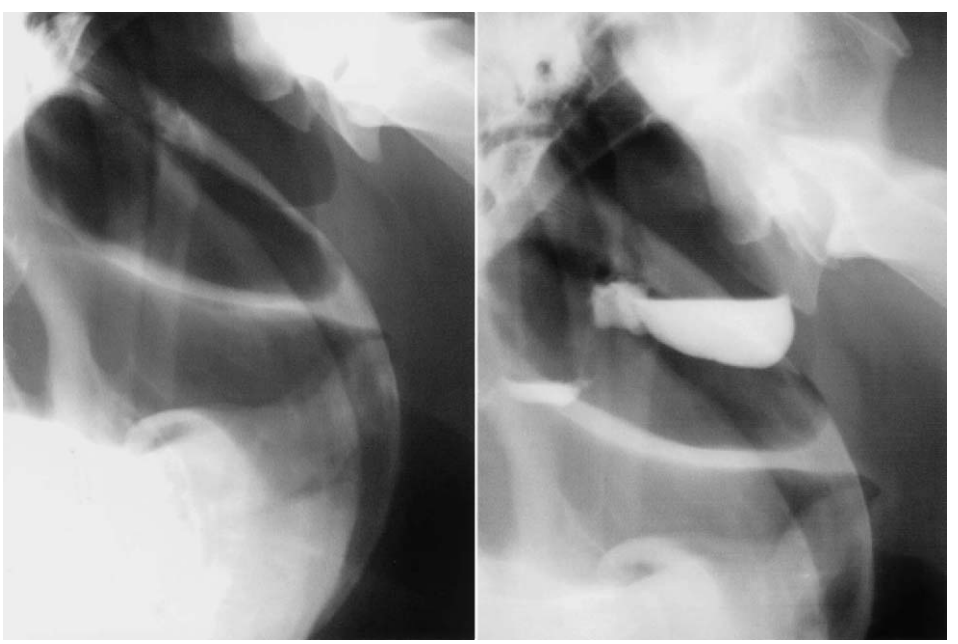
Standard Radiographic Examination

I prefer three views of the guttural pouches: (1) a lateral projection of the head including as much of the face, cranium, and throat as possible; (2) a collimated view of the throat, centered on the guttural pouches; and, where possible, (3) a ventrodorsal view. If it is not possible to make a ventrodorsal projection, right and left lateral oblique views can be substituted, although they are not nearly as revealing.

Normal Radiographic Anatomy of the Guttural Pouches

Viewed from a lateral perspective, the guttural pouches appear as superimposed radiolucent objects, roughly triangular in shape, situated immediately above the common pharynx (as seen in lateral projection). Although each guttural pouch is subdivided into medial and lateral compartments, these divisions are not always readily apparent radiographically (Figure 26-2). Better to use the stylohyoid bones, which can be easily identified in a lateral radiograph, to approximate the line of demarcation between the medial and lateral compartments of the guttural pouches.

Because of their soft, flexible walls, normal head movements—particularly flexion and extension—cause considerable (but predictable) deformation of the guttural pouches. Accordingly, radiographic evaluation of the guttural pouches should always be preceded by noting the position of the head, in particular



A **B**

Figure 26-2 • Close-up lateral view of the guttural pouches **(A)** fails to clearly show their division into medial and lateral compartments, a fact that becomes obvious once the lateral pouch is opacified with a diagnostic opaque **(B)**.

whether or not it is flexed or extended, so as not to mistake these normal variants for compressive disease.

Empyema, Pharyngeal Compression, and the Manta Ray Sign

Infection of one or both guttural pouches resulting in empyema causes varying degrees of pharyngeal and laryngeal compression, in some instances leading to severe dyspnea. Empyema often follows strangles caused by *Streptococcus equi* and may lead to massive distension, occluding both the larynx and esophagus, as reported by Nyack and co-workers.[7] Judy and co-workers, reporting on 91 horses with guttural pouch empyema, determined that horses with chondroids had greater pharyngeal and laryngeal compression than those that did not have chondroids.[8]

Radiographically, empyema is characterized by opacification of the guttural pouch (or pouches), often accompanied by one or two fluid levels, depending on whether or not both compartments are involved and how much air remains (Figure 26-3). As the volume of pus increases, the guttural pouch enlarges gradually, compressing the underlying pharynx and leading to dyspnea.[9] Because the crushed pharynx resembles the silhouette of a manta ray, it is termed the *manta ray sign* (Figure 26-4).

Secondary Extraguttural Disease: Cellulitis, Abscessation, and Fistulation

Transmural spread of a guttural pouch infection into the surrounding tissues can lead to a variety of adverse consequences, including cellulitis, abscessation, and fistulation. Frank rupture of the guttural pouch and its various radiographic appearances are described later.

Cellulitis. The tissues surrounding an infected guttural pouch may become secondarily inflamed or infected, leading to swelling, turgor, and increased sensitivity. Occasionally affected horses become reluctant to eat or appear to eat with some difficulty, resembling a person with a sore throat. In such circumstances, the throat usually appears radiographically normal.

Abscessation. Cellulitis can lead to localized abscessation or to abscessation in a nearby lymph node. In some instances, it is possible to demonstrate a communication between the abscess and the adjacent guttural pouch, indicating its probable origin, but in other instances no such physical relationship exists.

Radiographic abnormalities are most dependent on the size of the abscess, its proximity to the guttural pouch, and thus its potential contrast and the extent to which it displaces surrounding tissues. Rashmir-Raven and co-workers reported a large, highly compressive, dorsopharyngeal abscess in a 3-year-old filly Paint, which communicated with an infected left guttural pouch.[10]

Fistulation. True fistulation (an abnormal communication between two organs) is rare in horses, although it has been reported. For example, Jacobs and Fretz described fistulation between an infected right guttural pouch (bacteria and fungi) and the adjacent dorsal pharyngeal recess. The only radiographic indication of the lesion was a fluid level in the affected pouch.[11]

In my experience there are no reliable plain film indicators of guttural pouch fistulation, although extraguttural gas pockets are suggestive. I have seen one instance of a guttural-pharyngeal fistula, appar-

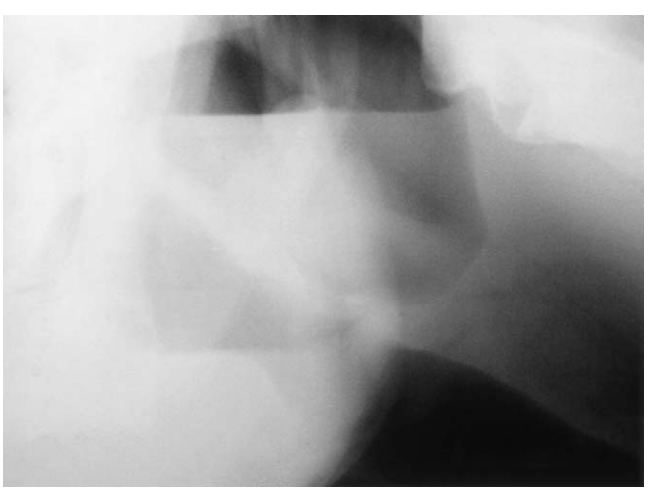


Figure 26-3 • Empyema: Close-up lateral view of the throat shows that one of the guttural pouches is partially fluid filled, which along with the accompanying air produces a distinctive fluid level. As a result, the underlying pharynx is being severely compressed.



Figure 26-4 • When the pharynx is being compressed and deformed by an enlarged guttural pouch or pouches, it often assumes a characteristic shape that resembles the profile of a giant manta ray. This unique appearance, indicative of severe pharyngeal compression, is termed the *manta ray sign*.

ently caused by a chronic guttural pouch infection. One of the most interesting features of the case was the owner's complaint, namely, that his horse would periodically cough violently, sometimes appearing to choke. Apparently when the horse would flex or extend its head, the pus in the infected guttural pouch would be discharged through the fistula into the pharynx, subsequently entering the larynx, causing the coughing and choking.

Guttural Pouch Masses and Mass Effects

Chondroids (formed inspissated pus) are occasionally visible in plain films, as I have reported previously. For this to occur, however, there must be ample luminal gas, ideally surrounding as much of the object or objects as possible, and little or no fluid, which would obscure the chondroids. Large blood clots may also be seen under similar circumstances.

Guttural Pouch Cysts

Guttural pouch cysts are a rarity but have been reported in both immature and mature animals. Hance and co-workers described cysts in the guttural pouch of a 1-month-old Quarter Horse colt and a 3-year-old Standardbred gelding. Although both lesions caused secondary pharyngeal compression, only the adult horse was dyspneic.[12] It was not clear whether these were congenital or acquired lesions. A large accumulation of intramural or extramural gas can sometimes be mistaken for a cyst, although the latter can usually be discounted if on no other basis than probability. Scoping the guttural pouch should resolve any question.

Guttural Pouch Tumors

Horses may develop both primary and secondary tumors of the guttural pouch. Primary squamous cell carcinoma, hemangioma, and fibroma have been described. Baptiste and co-workers reported three cases of presumed metastatic guttural pouch disease: two hemangiosarcomas and a malignant melanoma.[13] Few such reports featured any medical images.

An exception to this generality is the case report by Tyler and Fox describing a large, multilobulated, amelanotic melanoma in a 9-year-old gelding that involved the pharynx and guttural pouch. Radiographically, a portion of the tumor could be seen within one of the guttural pouches, clearly outlined by air. Sonographically, the tumor was visible from both the right and left parotid fields as single or multiple spherical objects, featuring decreased echogenicity but no far-field enhancement, thus indicating their solid nature.[14]

Guttural Pouch Mycosis, Hemorrhage, and Perforation

Mycotic infection of the guttural pouch may erode the wall of a contiguous artery, causing luminal hemorrhage and epistaxis. The most common bleeding sites are the internal carotid and maxillary arteries (Figure 26-5).[15] Interventional radiology, in the form of balloon-tipped arterial occlusion, has been reported as an effective means of secondary hemostasis.[16]

Erosive mycosis can also lead to perforation of the guttural pouch with escape of contents into the surrounding tissues. Extraguttural air accumulations can be quite striking radiographically, appearing in a

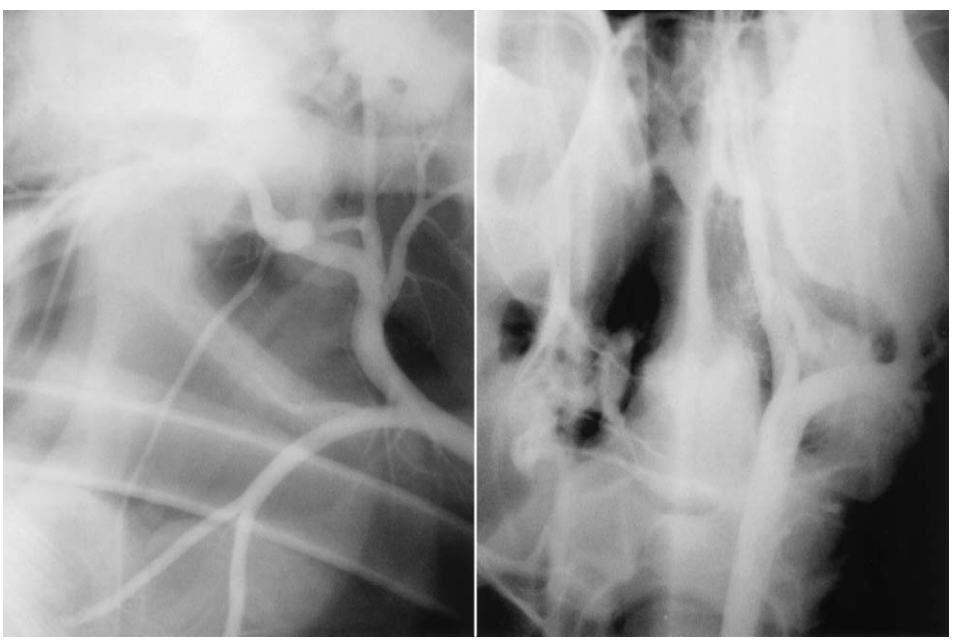


Figure 26-5 • Lateral **(A)** and ventrodorsal **(B)** views of a carotid angiogram in an adult horse show the physical proximity of these arteries to the guttural pouch.

variety of ways, such as single or multiple large gas pockets, clusters of small gas bubbles, deep interfacial gas bands, or any combination of these findings (Figure 26-6).

Occasionally escaped gas remains closely approximated to the outer wall of the damaged pouch at or near the site of perforation. In this circumstance, the escaped gas often appears as if it is located in the interior of the damaged pouch rather than on the outside (Figure 26-7). Because the medical implications of extraluminal gas are extremely serious, it is important to be able to make the distinction radiographically.

Guttural pouch mycosis, with or without hemorrhage or extraguttural disease, may also cause laryngeal paralysis, which may lead to pneumonia.[17]



Figure 26-6 • Lateral view of the throat shows large amounts of extraluminal gas and fluid obscuring much of the guttural pouches after a unilateral perforation.

Guttural Pouch Deformity Secondary to Retropharyngeal Adenopathy

Moderate unilateral or bilateral enlargement of the retropharyngeal lymph nodes causes a characteristic indentation of the ventral margin of one or both guttural pouches (Figures 26-8 and 26-9). The exact point of encroachment (caudal, caudoventral, or ventral), as determined radiographically, is strongly influenced by the position of the head and neck. With the head extended, the affected pouch or pouches are usually indented ventrally, whereas with the head down, there is more of a caudal deformity. A neutral head position usually results in a caudoventral disfiguration. Bear in mind that these are only generalities that are also subject to the anatomic nuances of both the extent of the disease and the various technical considerations related to radiographic imaging, such as beam center, projection angle, and respiratory phase.

Gaseous Distension of the Guttural Pouch (Tympany)

One-way blockage of the pharyngeal openings to one or both guttural pouches can lead to the accumulation of gas, secondary distension, and compressive displacement of the pharynx and larynx. Swallowing may

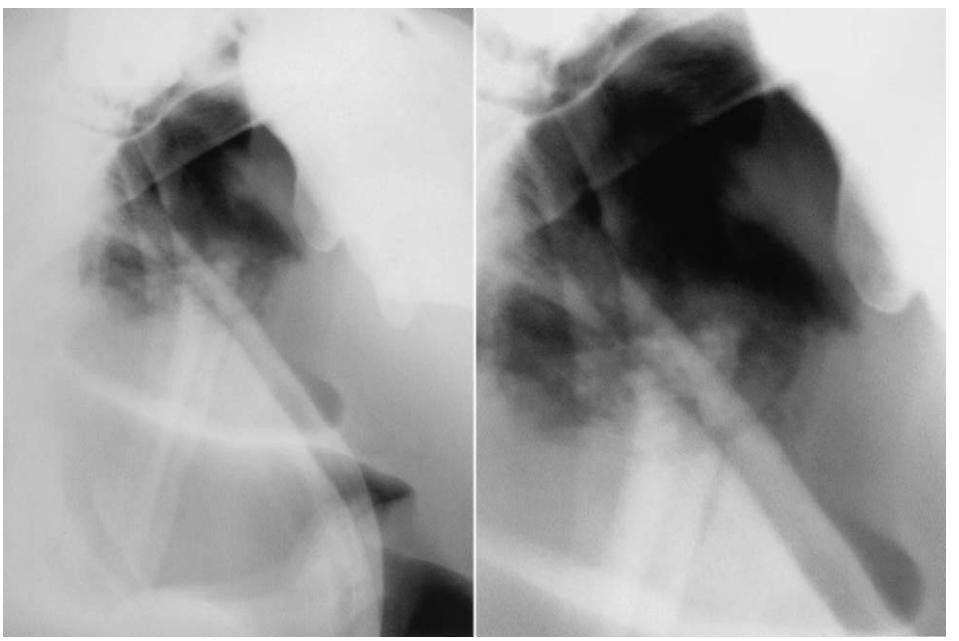


Figure 26-7 • Lateral **(A)** and lateral close-up **(B)** views of a perforated left guttural pouch in which escaped air has accumulated against the exterior surface, giving the false impression that gas bubbles are in the lumen.

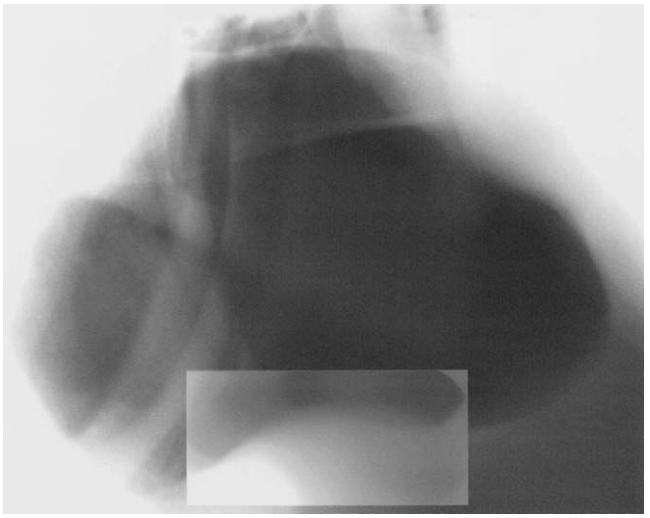


Figure 26-8 • Ultra-close-up lateral view of the guttural pouch of a young horse shows the characteristic ventral indentation caused by retropharyngeal adenopathy *(emphasis zone).*



Figure 26-9 • Lateral close-up view of the throat shows the characteristic caudoventral indentations of the guttural pouches caused by enlarged retropharyngeal lymph nodes secondary to strangles.

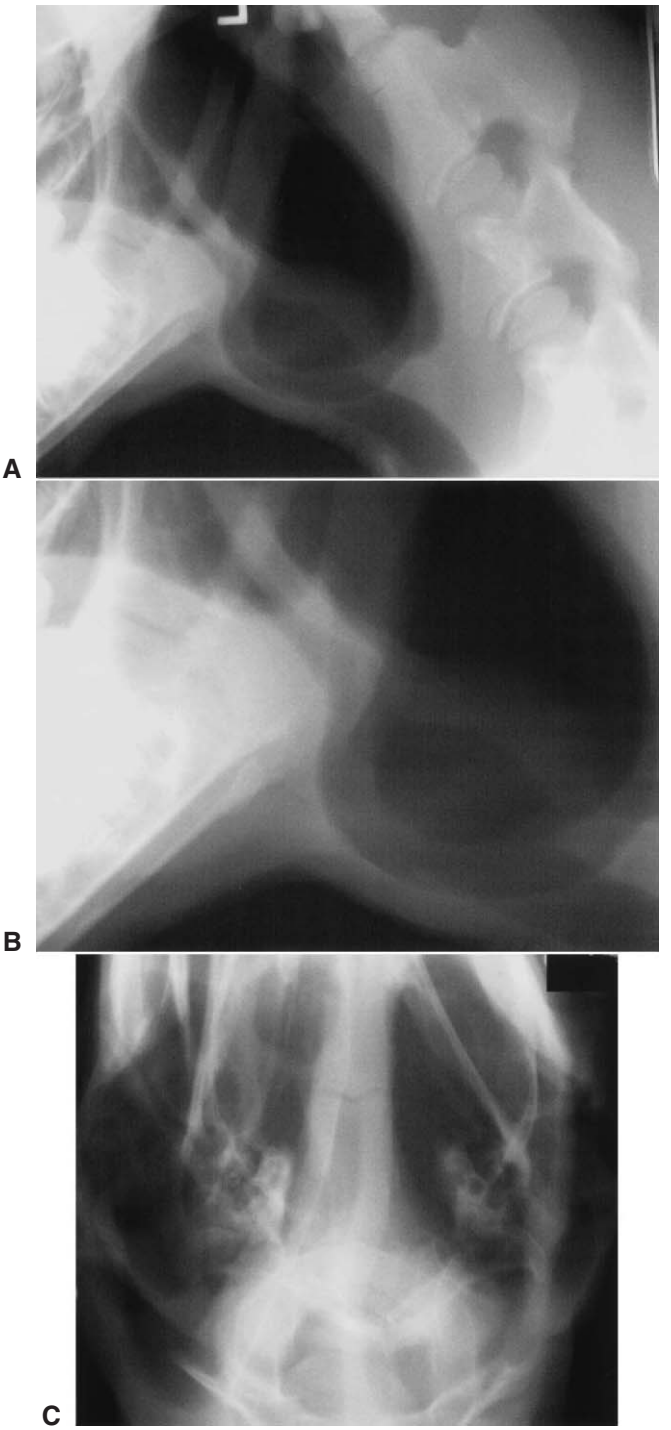


Figure 26-10 • Lateral **(A),** lateral close-up **(B),** and ventrodorsal **(C)** views of the throat of a foal show severe gaseous distension of both guttural pouches, causing severe compression of the pharynx (*manta ray sign*), caudoventral displacement of the larynx and trachea, and potential dysphagia secondary to esophageal mechanical obstruction.

also be impeded, causing dysphagia or simply a reluctance to eat. As the guttural pouches enlarge, they also deform in accordance with their immediate surroundings. In other words, the expanding pouch goes where there is available space. Consequently, the tympanitic pouch can assume a variety of sizes and shapes, depending on its surroundings, as well as the position of the head and neck (Figures 26-10 through 26-13).

Middle Ear Infection: Extension to Nearby Petrous Temporal and Stylohyoid Bones

Spread of inner ear infection to the nearby petrous temporal and stylohyoid bones may lead to osteomyelitis, arthrodesis, and occasionally pathologic fracture, as theorized by Blythe and co-workers.[18] Diagnosis has traditionally been made radiographically, but Hassel and co-workers contend that endoscopy of the guttural pouch is diagnostically



Figure 26-11 • Lateral radiograph of the throat shows massive gaseous distention of both guttural pouches, causing crushing of the pharynx and displacement of the larynx and trachea ventrally. In this instance, the distended pouches have moved to the ventral depths of the throat rather than caudally, resulting in a distorted rectangular-shaped deformation.

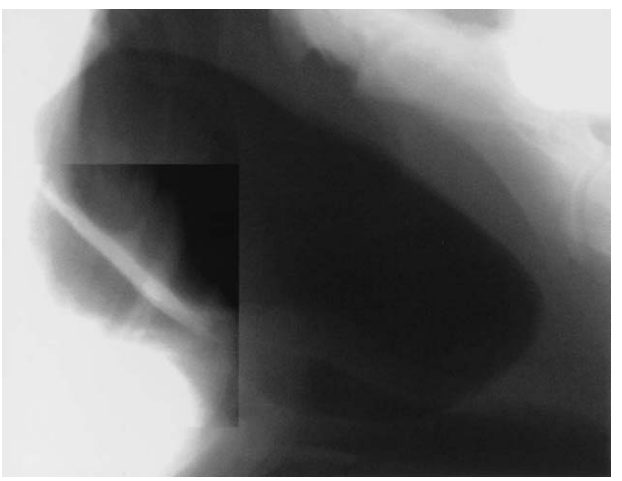


Figure 26-12 • Lateral view of the throat shows unilateral gaseous distension of the right guttural pouch reaching caudally nearly to the third cervical vertebra. The presence of a *manta ray sign* indicates serious pharyngeal compression.

superior.[19] Based on existing publications, it appears fair to say that the cause of this unusual disease remains the subject of speculation.

▮▮▮ THE NORMAL PHARYNX AND PHARYNGEAL VARIATION

The normal pharynx changes measurably with inspiration and expiration as well as with head and neck position; normal variants are exemplified in Figure 26-14. The pharynx is also likely to change during swallowing. Because of these variations, it is important that any suspected pharyngeal abnormality be demonstrated radiographically in at least two comparable films. Such evidence at least establishes the persistence of the finding, if not its validity.



Figure 26-13 • Lateral radiograph of the throat of a severely dyspneic, dysphagic horse, initially diagnosed with strangles and pneumonia, shows marked gaseous distention of the right guttural pouch, which has nearly obliterated the pharynx. The extension of the pouch into the caudal reaches of the neck has displaced the trachea and erased much of its lumen caudally.

Pharyngeal Disease

Palatal Hypoplasia. Palatal hypoplasia may be symmetric or asymmetric, also termed *unilateral* or *bilateral* palatal hypoplasia. This congenital disease may cause secondary aryepiglottic entrapment,[20] a difficult diagnosis to render radiographically, with nearly all conclusions based on circumstantial evidence such as the size, shape, or position of the soft palate. Because of these limitations and the need for a functional assessment, most authorities rely on endoscopy rather than on radiography.

Palatal Displacement (Dorsal Palatal Displacement). Normally the caudal aspect of the soft palate is situated immediately ventral to the cranial portion of the epiglottis, as seen in a lateral radiograph of the throat. Dorsal palatal displacement is not so much a diagnosis as an observation. In other words, a displaced palate is nearly always a secondary sign of a primary disorder elsewhere, not a disease in its own right.

Forward (Rostral) Displacement of the Palatopharyngeal Arch. In my opinion, and contrary to a

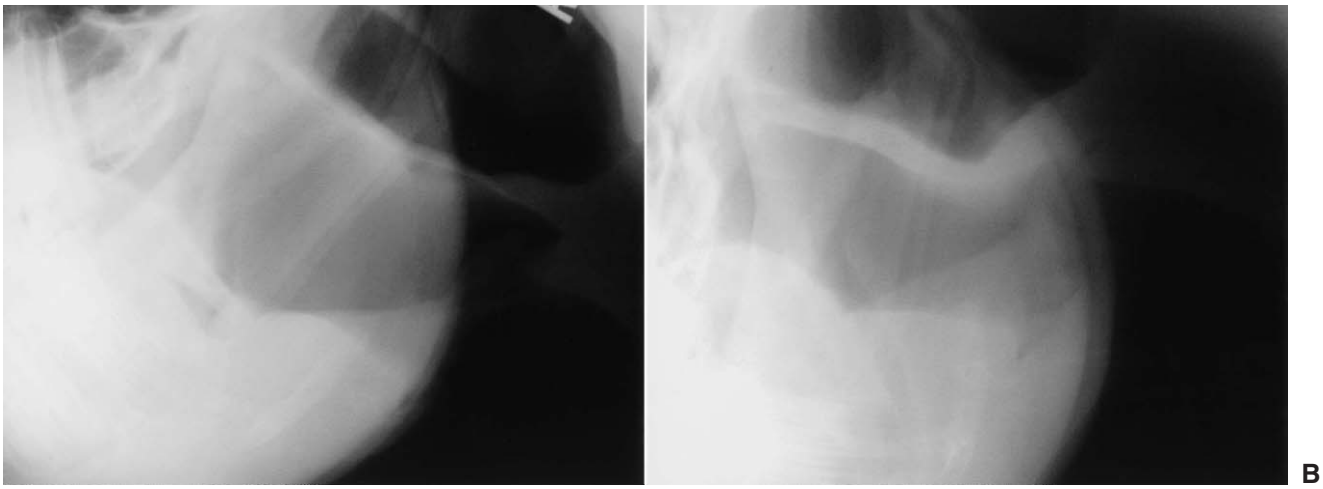


Figure 26-14 • Lateral view of the throat made with the head extended during inspiration **(A)** and expiration **(B).** During inspiration with the head extended, the pharynx appears roughly triangular, with the overlying guttural pouch conforming dorsally. By comparison, during flexed expiration, the pharynx assumes a flattened V-shape or gull-wing appearance, with the floor of the guttural pouch following suit. Likewise, the attitude of the aryepiglottic folds changes from horizontal to gently sloped, whereas the epiglottis tends to "straighten."

previously published report,[21] it is extremely difficult—if not impossible—to diagnose rostral displacement of the palatopharyngeal arches based on pharyngeal deformity, as seen in a flexed lateral view of the throat. The difficulty is that flexion normally results in temporary deformation of the pharynx, just as extension does; thus it is impossible to differentiate normal anatomic variation from disease.

Paralaryngeal Abscessation. Barber and I reported the radiographic features of a communicating paralaryngeal abscess in a 4-year-old Thoroughbred filly.[22] The major radiographic observation in this case was the presence of a pair of medium-sized fluid levels superimposed on the larynx, as seen in a lateral view of the throat.

Medium and large parapharyngeal abscesses nearly always cause pharyngeal compression that can lead to severe dyspnea. Large-volume abscesses can also compress and displace the larynx and trachea, which further exacerbates the breathing problem (Figure 26-15).

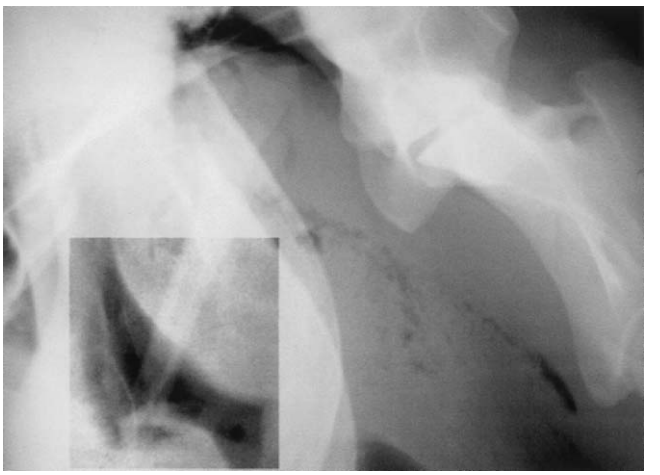


Figure 26-15 • Lateral view of the throat of a young horse with a large parapharyngeal abscess that is crushing the underlying pharynx and overlying guttural pouch. Because of the great length of the lesion, the pharynx and trachea are also being compressed as well as being displaced ventrally *(emphasis zone).*

Pharyngeal Foreign Body

Kiper and co-workers reported the clinical, radiographic, and surgical appearances of metallic foreign bodies in the mouth and throat of seven horses.[23] Most horses in the group had a swollen throat, dyspnea, bad breath, or a purulent nasal discharge for an average of 2 weeks, showing only transient improvement with administration of antibiotics and steroids. The most common foreign body was a wire fragment, presumed to have come from baled hay. The shaft of a broken hypodermic needle was detected in one animal.

Of the various methods used to detect the source of illness (a foreign body, as it turned out), radiographs proved most effective and were of immeasurable help in planning a surgical approach. Associated abscesses were not detected radiographically but presumably could be identified using ultrasound. Specific foreign-body locations included the cricopharyngeus muscle, tongue, soft palate, right guttural pouch, laryngeal wall, and paralaryngeal tissues.

Pharyngeal Lymphoid Hyperplasia

Pharyngeal lymphoid hyperplasia is most prevalent in horses less than 5 years old, with the highest prevalence in 2-year-olds.[24] I and others have described the

radiographic appearance of this disease, pointing out that radiographic diagnosis is usually only possible under the following conditions: (1) the x-ray beam is centered on the throat, (2) a soft-tissue technique is used, and (3) the lesions are large and numerous.

Pharyngeal Cysts (Thyroglossal Duct Cysts)

Pharyngeal cysts are usually situated on the ventral surface of the epiglottis, and in this respect may also be thought of as epiglottic or subepiglottic cysts. Less often, cysts may be found on the dorsal surface of the epiglottis.[25] Cysts in either location can cause (1) epiglottic or palatal displacement, (2) laryngeal obstruction, and (3) laryngeal incompetence.

Palatal Myositis

Blythe and co-workers, working with a medium-sized group of normal and abnormal horses, theorized that observed dorsal displacement was most likely due to one of three causes: (1) fatigue and weakness of the palatal muscles, (2) injury to the soft palate during periods of displacement, or (3) a combination of these two causes.[26]

Pharyngeal Cancer

Adams and co-workers reported the gross and histologic similarities between malignant lymphoma and ulcerative pharyngitis.[27] Although such lesions can be readily seen endoscopically, they are rarely appreciable radiographically unless there is an associated mass. If nervous tissue is involved, there may be palatal displacement or entrapment. Gross palatal deformity can cause similar problems.

Primary Pharyngeal Collapse

Using videoendoscopy and a high-speed treadmill to determine the cause or causes of poor performance in 348 racehorses, Martin and co-workers found previously undiagnosed pharyngeal collapse in 40 horses.[28] This is a difficult or impossible diagnosis to make radiographically other than by inference.

▮▮▮ LARYNGEAL DISEASE

The Normal Epiglottis

The radiographic appearance of the equine epiglottis is variable, being subject to technical, anatomic, and physiologic influences. Like the guttural pouches and pharynx, the larynx is optimally imaged with a lateral projection of the throat using a soft-tissue exposure. A neutrally positioned head ensures a standardized image of the throat. When the head is flexed, the epiglottis often appears tipped downwardly. Conversely, when the head is extended, the epiglottis tends to stand off the soft palate, appearing relatively long and thin.

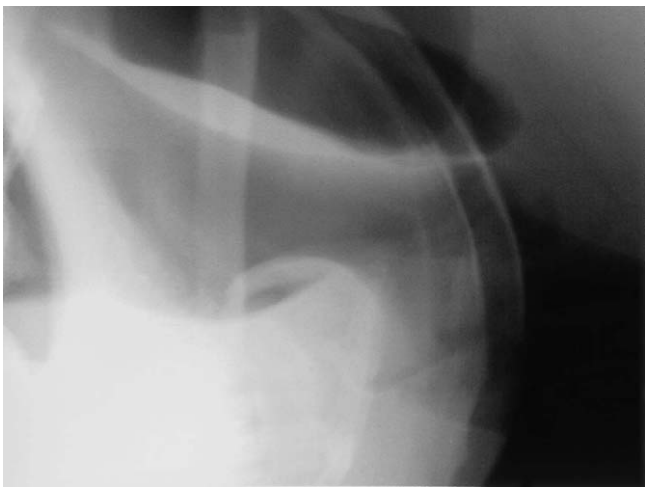


Figure 26-16 • Close-up lateral view of the throat of a horse with the its head in a natural position, neither flexed nor extended, shows a normal-appearing, horizontally oriented epiglottis, underlain by an upwardly arching soft palate. A roughly rectangular larynx provides a high-contrast background against which to view the epiglottis.

The perception of epiglottic morphology is also influenced by the size and, to a lesser extent, the shape of the pharynx. When the epiglottis is compared with a large rectangular pharynx, it is usually judged to be normal (Figure 26-16). When viewed against the backdrop of a small triangular pharynx, however, the epiglottis is more likely to be considered small, thickened, and even hypoplastic, which in most instances is an illusion fostered by an increased epiglottic-pharyngeal ratio related to head and neck position and, to a lesser extent, the phase of respiration (Figure 26-17).

Oblique, decentered projections of the throat, as sometimes made accidentally or with the intent of partially separating the guttural pouches from one another, often change the normal appearance of the epiglottis, sometimes quite dramatically, as illustrated in Figure 26-18. In such circumstances, the epiglottis frequently loses its individual identity and is instead incorporated into the shadows cast by the soft palate and aryepiglottic folds. The resultant appearance may be incorrectly attributed to palatal displacement or, alternatively, a hypoplastic, hypomotile epiglottis rather than a nonstandard projection angle.

Localized Laryngeal Collapse

In their study on underperforming racehorses, Martin and co-workers also found partial laryngeal collapse involving the arytenoid cartilages, aryepiglottic folds, and vocal folds. Additionally they also observed intermittent epiglottic entrapment, epiglottic retroversion, and collapse of either the nostril or alar fold.[28]

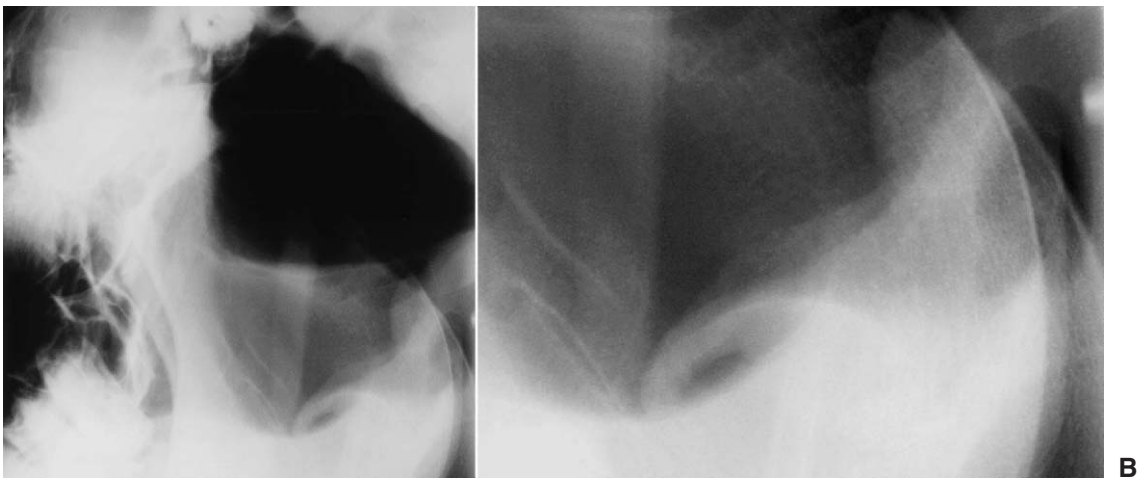


Figure 26-17 • Lateral **(A)** and close-up lateral **(B)** views of the throat of a horse with its head partially flexed show a downwardly tipped epiglottis, partially hidden by the soft palate. The pharynx is small and triangular compared with the horse in Figure 26-16, leading to the false impression that the epiglottis is hypoplastic.

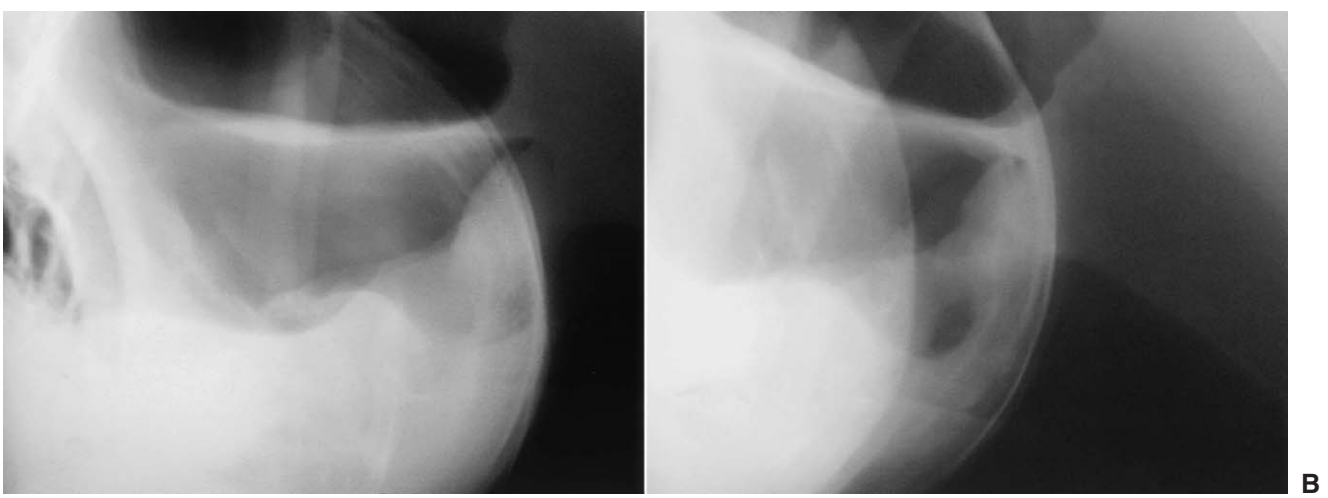


Figure 26-18 • **A,** Lateral close-up view of a normal epiglottis with the x-ray beam centered on the throat. **B,** A second view of the same animal, but with the x-ray beam centered more caudally. In the decentered image, the epiglottis, soft palate, and aryepiglottic folds have formed a composite shadow, making it difficult to assess the true appearance of the epiglottis and falsely suggesting disease.

Congenital Laryngeal Web

We previously reported the radiographic and pathoanatomic appearance of a congenital laryngeal web in a 10-day-old Quarter Horse filly.[29] A lateral radiograph of the throat showed a small, stubby, vertically oriented epiglottis and laryngeal hypoplasia with blunted corniculate processes. Endoscopy revealed fixed, dorsal displacement of the soft palate, epiglottic hypoplasia (about half normal size), and vocal cords joined ventrally by an abnormal web of epithelial tissue.

Arytenoid Chondritis

Haynes and co-workers reported asymmetric, deforming osseous metaplasia in the cricoid cartilage of a horse with chronic chondritis, which caused laryngeal obstruction.[30] Terry and co-workers reported a case of severely obstructive arytenoid chondritis in a horse involving a large mass on the axial margin of the right arytenoids, which caused severe, progressive dyspnea.[31]

The precise cause of arytenoid chondritis is unknown; racehorses are affected more than other breeds. Current hypotheses focus on mucosal injury, for example, by an endotracheal tube, leading to streptococcal infection, cartilage cavitation, granulation, fibrosis, and eventually a well-defined fibrocartilaginous mass that deforms and obstructs the larynx. The combination of obstructive chondritis and corrective surgery may lead to posterior glottic stenosis secondary to the formation of a dorsal laryngeal web.[32]

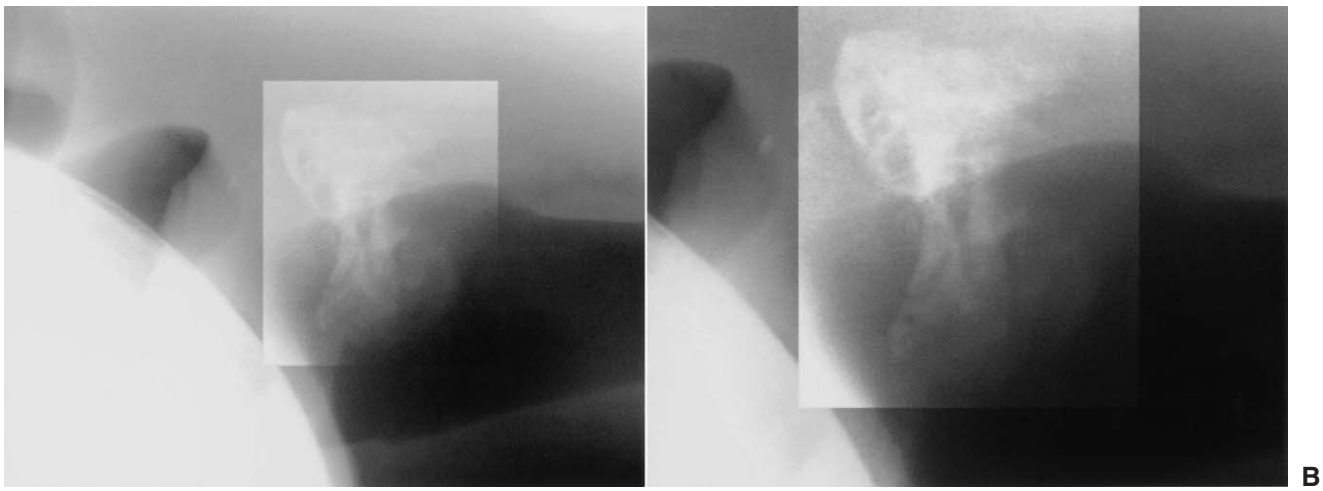


Figure 26-19 • Close-up **(A)** and ultra-close-up **(B)** views of the larynx and cranial portion of the trachea show extensive laryngeal and paralaryngeal calcification, caused by a previous surgery, and presumably dystrophic in nature *(emphasis zone)*.

Laryngeal Calcification

Postsurgical Laryngeal Calcification (Dystrophic Calcification). Calcification of one or more laryngeal cartilages is a common and possibly serious consequence of laryngoplasty, as described by Tulleners and others.[33] Chondral mineralization can cause laryngeal deformity (Figure 26-19) at the expense of cross-sectional area, and it may also hinder normal pharyngeal movement, both of which are critical during vigorous exercise when ventilatory effort is at or near its maximum.

Age-Related Laryngeal Calcification (Laryngeal Mineralization, Laryngeal Metaplasia). Laryngeal mineralization may also be quite innocent, presumably an age-related form of metaplasia, causing neither deformity nor dysfunction (Figure 26-20). Although laryngoscopy is usually capable of identifying suspected laryngeal dysfunction, it can neither implicate nor exonerate the role played by cartilaginous calcification, other than circumstantially.[34]

Contextual Diagnosis. Radiographically the appearance of laryngeal calcification (mineralization/metaplasia) is quite varied; consequently diagnosis is often *contextual*: dystrophic calcification in horses that have undergone previous laryngoplasty and osseous metaplasia in horses that have not. The combination of laryngeal deformity and mineralization strongly suggests previous surgery, even when a corroborating history is lacking.

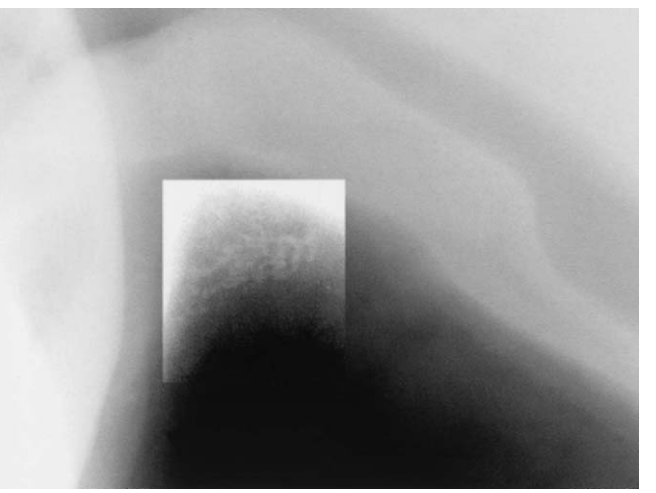


Figure 26-20 • Close-up lateral view of the larynx (soft-tissue technique) shows a banded mineralization pattern *(emphasis zone)* sometimes seen in middle-aged and older horses. The cause (or causes) and consequences of this finding are debatable.

▮▮▮ BRANCHIAL CYSTS

Branchial cysts (also termed *branchial arch cysts*) are cystic aberrations of the branchial arch system or, more specifically, one of its five pouches. Radiographically, branchial cysts have no defining characteristics other than possibly the displacement and deformity of adjacent tissues. Sonographically, branchial cysts are characterized by a well-defined perimeter, discrete wall, and fluid content.[35]

Differential diagnoses of masses or mass effects situated in the throat or cranial neck region are listed in Box 26-1.

▮▮▮ HYOID BONE FRACTURE

Fracture of a single stylohyoid bone has been reported in association with middle and inner ear infections. The proposed mechanism of injury is as follows:

Box 26-1
Possible Causes of Throat and Cranial Cervical Masses and Mass Effects in Horses

Traumatic hematoma
Traumatic seroma
Pus-distended guttural pouch (*empyema*)
Blood-distended guttural pouch
Air-distended guttural pouch (*tympany*)
Abscessed retropharyngeal or cervical lymph node
Salivary mucocele
Esophageal duplication cyst
Tracheal duplication cyst
Solid tumors
Tumors with internal cavitation secondary to liquefactive necrosis
Cranial esophageal foreign body (*choke*)
Paraesophageal abscess secondary to esophageal perforation
Cervical esophageal atony (regional megaesophagus)
Tracheal perforation with secondary deep fascial emphysema (including leaking tracheotomy sites)
Deep penetrating foreign bodies and related abscessation (especially wooden stakes)
Surgical sponge seroma
Surgical suture seroma
Severe hyoid fractures
Severely displaced basilar skull fractures (especially those involving the basisphenoid-basioccipital bone)

Modified and expanded from Slovis NM, Watson JL, et al: Marsupialization and iodine sclerotherapy of a branchial cyst in a horse, *J Am Vet Med Assoc* 219:338, 2001.

1. Infection spreads from the right or left inner ear to the proximal portion of the nearest stylohyoid bone.
2. In so doing, the intervening joint is destroyed and subsequently fused.
3. As a result of a number of factors, but in particular one free and one fixed stylohyoid bone, the normal hyoid mechanism is abolished, making it susceptible to fracture.
4. Alternatively, and as a direct result of structural weakening caused by the infection, the adjacent stylohyoid bone may simply break, either proximally or in midbody, irrespective of any existing hyoid rigidity, an unusual form of *insufficiency or pathologic fracture.*

Of further concern is the potential harm to the nearby facial, vestibulocochlear, glossopharyngeal, and vagal nerves.[36]

▮▮▮ RETROPHARYNGEAL LYMPH NODE ABSCESSATION (STRANGLES)

Streptococcus equi may infect the retropharyngeal lymph nodes of horses, leading to enlargement, secondary compression of the throat, and abscessation. The infection may spread to the guttural pouches, causing empyema; the lung, causing a suppurative bronchopneumonia; or the heart, causing myocarditis.[37]

▮▮▮ EPIGLOTTIC DISEASE

Normal, Age-Related Epiglottic Variations

Much of what is currently known of epiglottic function and dysfunction in the horse is the result of endoscopic observation. Furthermore, endoscopy has revealed significant differences in the normal upper airways of yearlings compared with adult horses, findings that require consideration when interpreting radiographs of the throat. For example, yearlings have more pharyngeal lymphoid tissue than adults. Yearlings also have shorter, narrower, and less rigid (or more flaccid) epiglotti than a mature horse.[38]

Primary Epiglottic Dysfunction

Endoscopic evaluation of the larynx focuses on three areas: (1) movement (or lack of movement) and physical appearance of the arytenoid cartilages, (2) appearance and movement of the epiglottis, and (3) position of the soft palate. Taking direct laryngeal visualization a step further, videoendoscopy allows for laryngeal assessment during strenuous exercise, potentially revealing functional abnormalities not observed at rest or during mild or moderate exercise.[39]

Radiology can sometimes suggest the cause of epiglottic dysfunction, for example, an epiglottic cyst, especially when combined with direct endoscopic observation. A radiograph is in some ways superior to endoscopy in that it provides a natural (no twitch, no scope) view of the throat. In other instances, however, a radiograph may appear normal even though there is severe laryngeal dysfunction (Figure 26-21).

Secondary Epiglottic Dysfunction

Duggan and co-workers theorized that spasm of the muscles innervated by the hypoglossal nerve might cause cranial displacement of the basihyoid bone, traction on the epiglottis, and misalignment of the soft palate, which together partially obstructed the larynx and interfered with normal breathing. They based their hypothesis on the fact that after being tranquilized with xylazine, a horse exhibiting these abnormalities became normal.[40]

Epiglottic Radiometrics

Linford and co-workers proposed a series of laryngopharyngeal measurements that can be obtained from a lateral radiograph of the throat to determine whether or not they are normal, specifically, whether the epiglottis is hypoplastic or entrapped and whether the soft palate is displaced dorsally.[41]

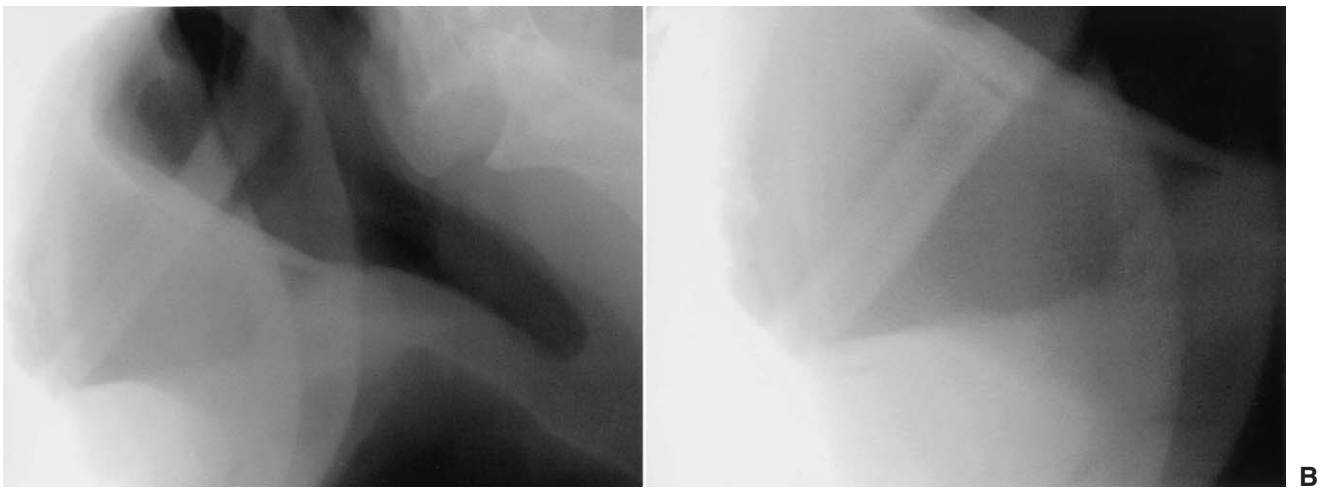


Figure 26-21 • Lateral **(A)** and lateral close-up **(B)** views of a normal-appearing larynx in a horse with severe laryngeal dysfunction as identified using laryngoscopy. The flattened appearance of the epiglottis is attributable to a combination of factors, including (1) a partially extended head, (2) an oblique projection angle, and (3) caudal decentering.

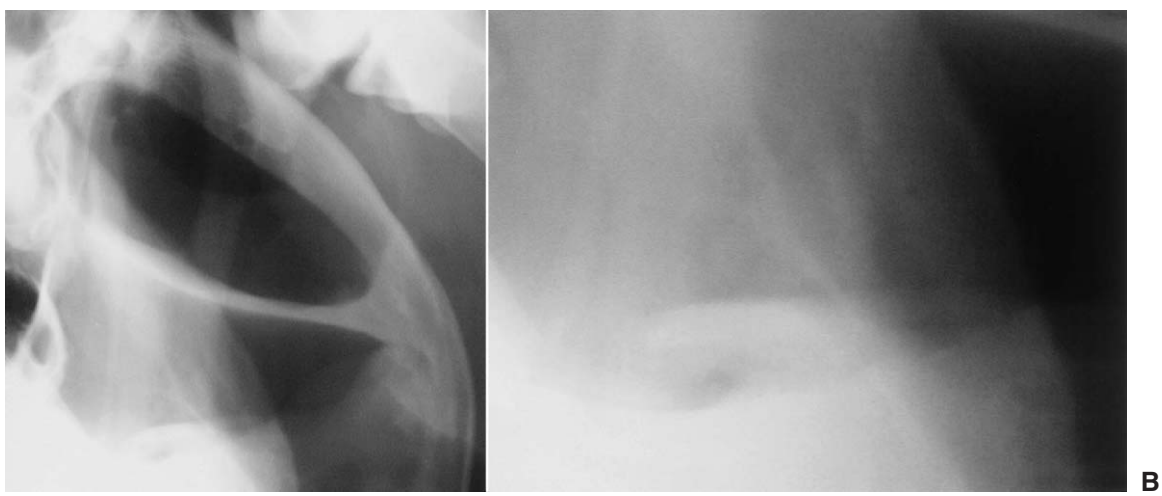


Figure 26-22 • Lateral **(A)** and close-up lateral **(B)** views of a mild to moderately hypoplastic epiglottis, the result of dysplasia.

Measurements of this sort have generally garnered a stronger following among novices than experts, the latter generally preferring the practiced eye over the ruler.

Epiglottic Dysplasia and Hypoplasia

Epiglottic dysplasia is usually associated with some measure of laryngeal dysfunction, which is *inferred* radiographically based on diminished epiglottic size or outright deformity. Of course the only true means of determining laryngeal dysfunction is to observe it directly using laryngoscopy.

Radiographically, epiglottic hypoplasia may exhibit a variety of appearances. The least detectable of these is the proportionately small epiglottis that otherwise appears normal (Figure 26-22). Somewhat easier to appreciate is the small but disproportionately thickened epiglottis, which may be mistaken for epiglossitis or a shallow subepiglottic growth such as a chondroma (Figure 26-23). A variation on this last theme is the small, thickened epiglottis that exhibits a reduced range of motion. Extreme epiglottic deformity, especially when combined with persistent malpositioning, leaves little doubt as to the existence of dysplasia (Figure 26-24). Stickle has described a case of combined epiglottic deformity and hypoplasia, which radiographically resembled an epiglottic mass.[42]

Epiglottic Entrapment

Epiglottic entrapment is caused by the envelopment of the epiglottis by the arytenoepiglottic folds. Advocates of *dynamic laryngeal evaluation* contend that a complete assessment should include treadmill endoscopy, ideally performed during strenuous exercise.[43] Laryngeal radiography is also helpful because it pro-

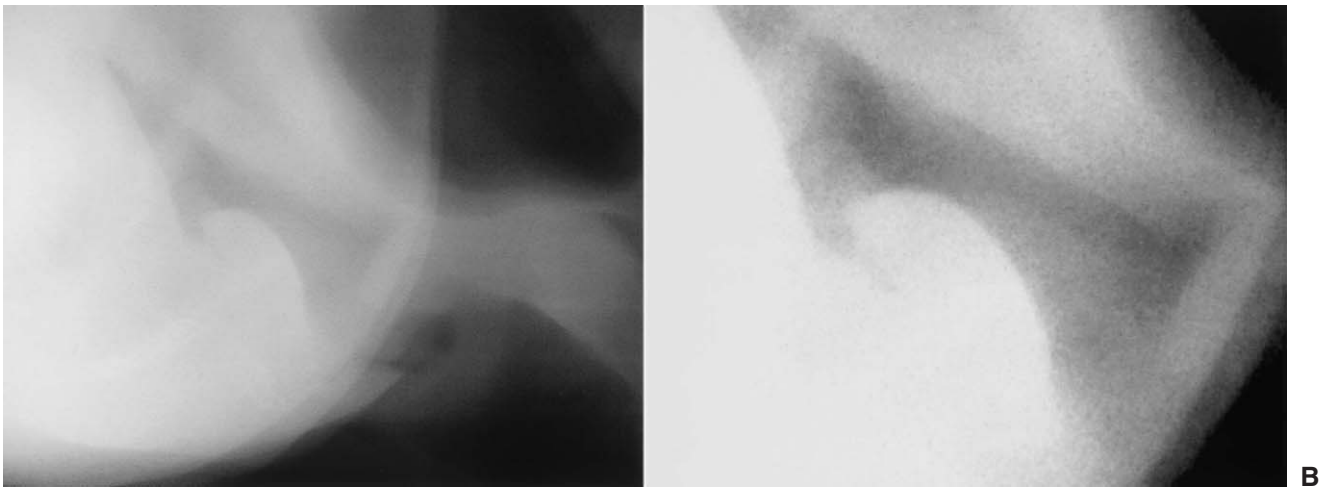


Figure 26-23 • Close-up **(A)** and ultra-close-up **(B)** views of the ventral throat region in a young foal show a small, thickened epiglottis consistent with hypoplasia.

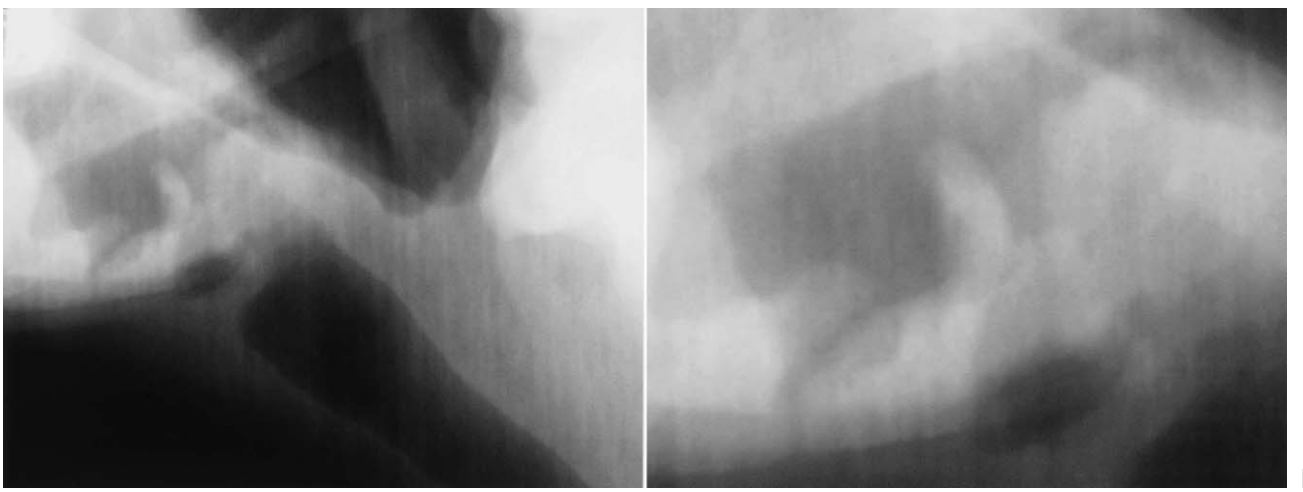


Figure 26-24 • Lateral **(A)** and close-up lateral **(B)** views of the throat of a young foal show severe laryngeal dysplasia indicated by an abbreviated, thickened, persistently erect epiglottis and palatal displacement.

vides a lateral perspective not possible with endoscopy, albeit a static one.

Arytenoid Chondritis

Like many other laryngeal diseases, the radiographic detection of arytenoid chondritis depends on the degree of deformity. In my experience, most such cases cannot be reliably diagnosed radiographically. Figure 26-25 illustrates the diagnostic ambiguity often associated with such cases.

Epiglottic Cysts

Epiglottic cysts may be associated with a variety of functional abnormalities, most of which relate to either obstructed laryngeal airflow or impede laryngeal closure, the latter potentially leading to respiratory infection secondary to the inhalation of feed. I, and others, have described the radiographic appearance of subepiglottic cysts in horses (Figure 26-26), whereas Tulleners has described their endoscopic characteristics.[44]

It is generally believed that epiglottic cysts, like most cysts, result from ductal obstruction. Some believe that ductal obstruction and resultant cyst formation may lead to infection. Both *Staphylococcus aureus* and *Escherichia coli* have been cultured from infected epiglottic cysts. Subepiglottic cysts are attributed to a variety of causes to include the following: (1) remnants of the thyroglossal duct, (2) iatrogenic and noniatrogenic injury, and (3) inflammation or infection.[45]

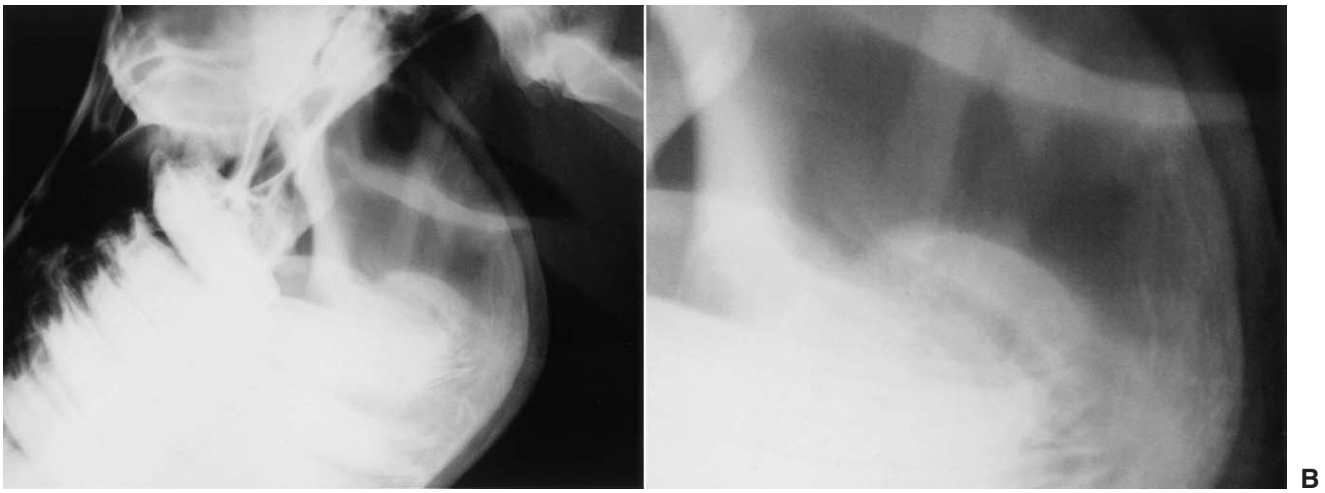


Figure 26-25 • Lateral **(A)** and lateral close-up **(B)** views of a horse with a severe case of arytenoid chondritis show a thickened epiglottis with a reduced range of motion (as determined by laryngoscopy). The animal was referred with a diagnosis of laryngeal hypoplasia.

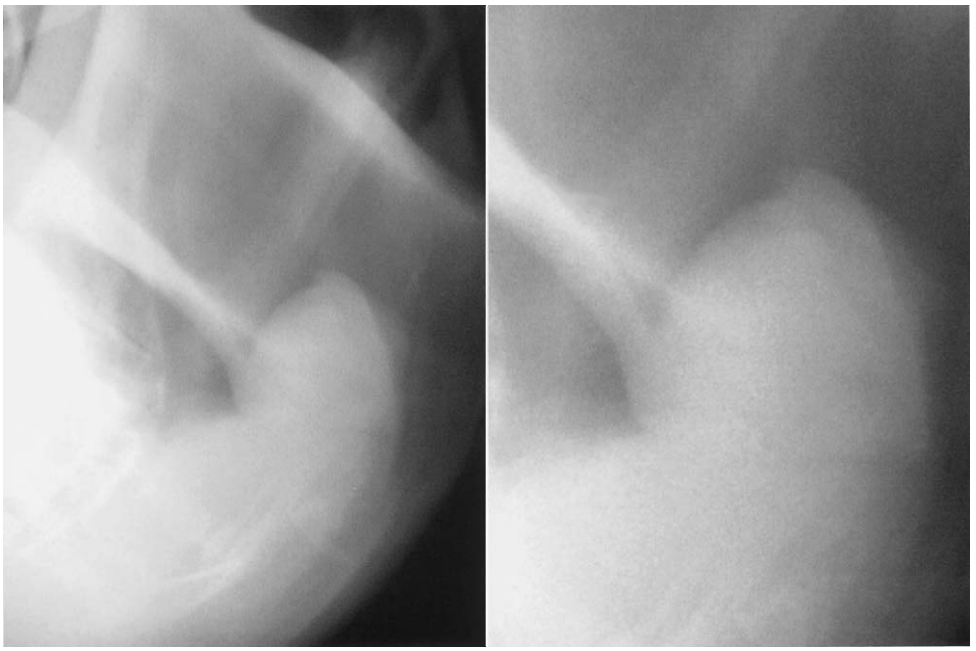


Figure 26-26 • Lateral close-up **(A)** and ultra-close-up **(B)** views of a large subepiglottic cyst causing dyspnea and dysphagia.

Epiglottic Abscess

Abscesses may occur on either the laryngeal or pharyngeal surfaces of the epiglottis, with the former being most common. Most abscesses are diagnosed endoscopically, appearing as symmetric swellings on the laryngeal surface of the epiglottis.[46] The likelihood of radiographic detection depends on the size of the abscess: larger lesions cause circular or semicircular deformity, and smaller lesions are not visible.

Epiglottic and Paraepiglottic Foreign Bodies

An improperly installed or infected laryngeal prosthesis may elicit a foreign-body response, including the accumulation of pus, sinus formation, and drainage (Figure 26-27). Unabsorbed sutures may behave in a similar manner.

Epiglottitis

Hawkins and Tulleners reported the endoscopic findings of epiglottitis in 20 horses.[47] Their findings are shown in Box 26-2. I do not believe epiglottitis can be diagnosed radiographically.

Proximal Esophageal Region

Shiroma and co-workers reported a large paraesophageal cyst in a 2-year-old Morgan gelding located just above and caudal to the larynx.[48] Sonographically

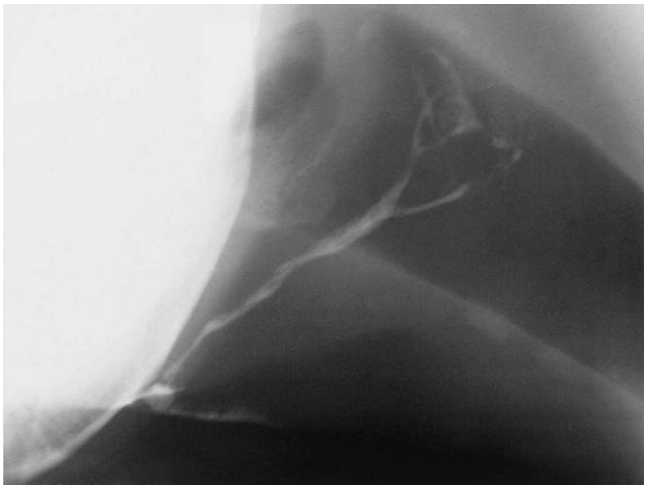


Figure 26-27 • Lateral sinogram of the throat shows a pair of overlapping filling defects superimposed on the cranial aspect of the trachea, surrounded on all sides by secondary tracts. These lead to a major conduit that exits through a draining sinus located on the ventral surface of the neck, appearing as a circular opacity just beyond the edge of the ramus.

Box 26-2
Endoscopic Features of Epiglottitis in the Horse

Reddening of the epiglottis
Epiglottic thickening
Epiglottic edema
Thickening and discoloration of the aryepiglottic folds
Epiglottic ulceration resulting in exposed cartilage
Granulation tissue on the lingual surface of the epiglottis
Upward tipping of the epiglottis

the mass appeared round with a discretely echoic perimeter corresponding to an earlier radiograph that had shown a peripherally mineralized object in a similar location. The interior of the mass appeared solid or semisolid with a uniformly stippled pattern. A later biopsy showed the mass to be hollow, containing a gelatinous material laden with sheets of squamous epithelial cells consistent with an inclusion cyst.

Before biopsy, differentials considered by the authors for nonpainful masses in the throat and proximal neck region included the following:

- Esophageal inclusion cyst
- Branchial cyst
- Thyroid tumor
- Enlarged lymph node (reactive lymph node)
- Abscessed lymph node
- Salivary mucocele
- Abscess
- Esophageal carcinoma

▮▮▮ POSTANESTHESIA DYSPNEA

Inhalation anesthesia in horses may lead to varying degrees of postrecovery breathing difficulties related to prolonged recumbency or intubation-extubation. Lying with its head down, an unconscious horse tends to develop capillary congestion and increased permeability, which can lead to conchal edema. Intubation may also cause regional pharyngeal and laryngeal edema, and extubation may temporarily result in dorsal displacement of the soft palate and, occasionally, paralysis of the arytenoid cartilages.[49]

In my experience, only palatal displacement is radiographically perceptible; conchal edema cannot be detected radiographically, although it can be seen using computed tomography or magnetic resonance imaging. Thoracic radiography is capable of identifying related inhalation pneumonia, provided it is severe enough. However, the abnormal lung opacification caused by inhaling esophageal or stomach contents past a incompetent endotracheal tube is difficult or impossible to distinguish from *postural atelectasis*, a constant feature of inhalation anesthesia, and thus recumbent imaging is of little or no use in such circumstances.

References

1. Sadler VM, Wisner ER, et al: Congenital atresia of the parotid duct in a horse, *Vet Radiol* 40:259, 1999.
2. Talley MR, Modransky PD, et al: *J Am Vet Med Assoc* 197:1633, 1990.
3. Fowler MF: Congenital atresia of the parotid duct in a horse, *J Am Vet Med Assoc* 146:1403, 1965.
4. Scarratt WK, Crisman MV: Neoplasia of the respiratory tract, *Vet Clin N Am Equine Pract* 14:199, 1998.
5. Fintel C, Dixon PM: A review of five cases of parotid melanoma in the horse, *Equine Vet Educ* 13:17, 2001.
6. Cook WR: The auditory tube diverticulum (guttural pouch) in the horse: its radiographic examination, *Vet Radiol* 14:51, 1973.
7. Nyack B, Dennis A, Padmore CL: Empyema of the guttural pouch associated with *Streptococcus equi* and *E. coli* infection in a mare, *Mod Vet Pract* 78:399, 1983.
8. Judy CE, Chaffin MK, Cohen ND: Empyema of the guttural pouch (auditory tube diverticulum) in horses (1977-1997), *J Am Vet Med Assoc* 215:1666, 1999.
9. Baxter GM, Schwensen K: Radiographic diagnosis, *Vet Radiol* 28:23, 1987.
10. Rashmir-Raven AM, DeBowes RM, et al: What is your diagnosis? *J Am Vet Med Assoc* 198:1991, 1992.
11. Jacobs KA, Fretz PB: Fistula between the guttural pouches and the dorsal pharyngeal recess as a sequela to guttural pouch mucosis in a horse, *Can Vet J* 23:117, 1982.
12. Hance SR, Robertson JT, Bukowieki CF: Cystic structures in the guttural pouch of two horses, *J Am Vet Med Assoc* 200:1981, 1992.
13. Baptiste KE, Moll HD, Robertson JL: Three horses with neoplasia including growth in the guttural pouch, *Can Vet J* 37:499, 1996.
14. Tyler RJ, Fox RI: Nasopharyngeal malignant amelanotic melanoma in a gelding age 9 years, *Equine Vet Educ* 15:49, 2003.
15. Smith KM, Barber SM: Guttural pouch hemorrhage associated with lesions of the maxillary artey in two horses, *Can Vet J* 25:239, 1984.
16. Caron JP, Fretz PB, et al: Balloon-tipped catheter arterial occlusion for prevention of hemorrhage caused by gut-

tural pouch mycosis: 13 cases (1982-1985), *J Am Vet Med Assoc* 191:345, 1987.
17. Dixon PM, McGorum BC, et al: Laryngeal paralysis: a study of 375 cases in a mixed-breed population of horses, *Equine Vet J* 33:452, 2001.
18. Blythe LL, Watrous BJ, et al: Vestibular syndrome associated with temporomandibular joint fusion and temporal bone fracture in three horses, *J Am Vet Med Assoc* 185:775, 1984.
19. Hassel DM, Schott HC, et al: Endoscopy of the auditory tube diverticula in four horses with otitis media/interna, *J Am Vet Med Assoc* 207:1081, 1995.
20. Bertone JJ, Traub Dargate JL Trotter GW: Bilateral hypoplasia and aryepiglottic entrapment, *J Am Vet Med Assoc* 188:727, 1986.
21. Crabill M, Schmacher J, Walker M: What is your diagnosis? *J Am Vet Med Assoc* 204:1347, 1994.
22. Farrow CS, Barber SM: What is your diagnosis? *J Am Vet Med Assoc* 179:830, 1981.
23. Kiper ML, Wrigley R, et al: Metallic foreign bodies in the mouth or pharynx of horses: seven cases (1983-1989), *J Am Vet Med Assoc* 200:91, 1992.
24. Raphel CF: Endoscopic findings in the upper respiratory tract of 479 horses, *J Am Vet Med Assoc* 181:470, 1982.
25. Koch DR, Tate LP: Pharyngeal cysts in horses, *J Am Vet Med Assoc* 173:860, 1978.
26. Blythe LL, Cardinet GH, et al: Palatal myositis in horses with dorsal displacement of the soft palate, *J Am Vet Med Assoc* 183:781, 1983.
27. Adams R, Calderwood-Mays MB, Peyton LC: Malignant lymphoma in three horses with ulcerative pharyngitis, *J Am Vet Med Assoc* 193:674, 1988.
28. Martin BB, Reef VB, et al: Causes of poor performance of horses during training, racing, or showing: 348 (1992-1996), *J Am Vet Med Assoc* 216:554, 2000.
29. Lees MJ, Schuh CL, et al: A congenital laryngeal web defect in a Quarterhorse filly, *Equine Vet J* 19:561, 1987.
30. Haynes PF, Snider TG, et al: Chronic chondritis of the equine arytenoid cartilage, *J Am Vet Med Assoc* 177:1135, 1980.
31. Terry C, Shumpert K, et al: An unusual case of upper respiratory obstruction in a horse, *Vet Radiol Ultrasound* 43:43, 2002.
32. Harrison IW, Raker CW: Dorsal glottic stenosis after bilateral arytenoidectomy in two horses, *J Am Vet Med Assoc* 192:202, 1988.
33. Tulleners EP, Harrison IW, Raker CW: Management of arytenoid chondropathy and failed laryngoplasty in horses: 75 cases (1979-1985), *J Am Vet Med Assoc* 192:670, 1988.
34. Lane JG: Larynx (pp. 74-96). In Traub-Dargatz JL, Brown CM, editors: *Equine endoscopy*, ed 2, St Louis, 1997, Mosby.
35. Slovis NM, Watson JL, et al: Marsupialization and iodine sclerotherapy of a branchial cyst in a horse, *J Am Vet Med Assoc* 219:338, 2001.
36. Waldridge RM, Holland M, Taintor J: What is your neurologic diagnosis? *J Am Vet Med Assoc* 222:687, 2003.
37. Sweeney CR, Bensen CE, et al: *Streptococcus equi* infection in horses—part II, *Comp Cont Educ* 9:845, 1987.
38. Stick JA, Peloso JG, et al: Endoscopic assessment of airway function as a predictor of racing performance in Thoroughbred yearlings: 427 cases (1997-2000), *JAMA* 219:962, 2001.
39. Hammer EJ, Tulleners EJ, et al: Videoendoscopic assessment of dynamic laryngeal function during exercise in horses with grade-III left laryngeal hemiparesis at rest: 26 cases (1992-1995), *J Am Vet Med Assoc* 212:399, 1998.
40. Duggan VE, MacAllister CG, Davis MS: Xylazine-induced attenuation of dorsal displacement of the soft palate associated with epiglottic dysfunction in a horse, *J Am Vet Med Assoc* 221:399, 2002.
41. Linford RL, O'Brien TR, et al: Radiographic assessment of epiglottic length and pharyngeal and laryngeal diameters in the Thoroughbred, *Am J Vet Res* 44:1660, 1983.
42. Stickle R: Radiographic diagnosis, *Vet Radiol Ultrasound* 31:207, 1990.
43. Morris EA, Seeherman HJ: Evaluation of upper respiratory tract function during strenuous exercise in racehorses, *J Am Vet Med Assoc* 196:431, 1990.
44. Tulleners EP: Evaluation of peroral transendoscopic contact neodymium:yttrium aluminum garnet laser and snare excision of subepiglottic cysts in horses, *J Am Vet Med Assoc* 198:1631, 1991.
45. Wilson DV, Peroni JE, Nickels FA: Anesthesia case of the month, *J Am Vet Med Assoc* 214:629, 1999.
46. Tulleners EP: Use of transendoscopic contact neodymium:yttrium aluminum garnet laser to drain dorsal epiglottic abscesses in two horses, *J Am Vet Med Assoc* 198:1765, 1991.
47. Hawkins JF, Tulleners EP: Epiglottitis in horses, *J Am Vet Med Assoc* 205:1577, 1994.
48. Shiroma JT, Clark CK, et al: Paraesophageal cyst in a horse, *Vet Radiol Ultrasound* 35:158, 1994.
49. Abrahamsen EJ, Bohanon TC, et al: Bilateral arytenoid cartilage paralysis after inhalation anesthesia in a horse, *J Am Vet Med Assoc* 197:1363, 1990.

Chapter 27

The Neck

THE JUGULAR VEIN

The Normal Jugular: Means of Evaluation

Venography. Blood vessels, including the jugular vein, are radiographically indiscernible from their soft-tissue surroundings. To visualize the jugular, or any other vein or artery for that matter, an appropriate diagnostic opaque must be injected into the vessel so that the blood is opacified, a special procedure termed *angiography,* or more specifically in the case of a vein, *venography.* If an intraluminal obstruction is present, such as a thrombus, a *filling defect* is created, an area within the vessel that fails to opacify (Figure 27-1).

Sonography. If ultrasound is available, the suspect jugular vein can be assessed anatomically and its blood flow evaluated. If necessary, the opposite jugular can be scanned for comparison. Veins, such as the jugular, can be readily differentiated from nearby arteries like the carotid on the basis of their characteristic flow patterns, using spectral Doppler (Figure 27-2).

Jugular Thrombosis and Thrombophlebitis

The most common causes of jugular thrombosis and thrombophlebitis are intravenous injection and catheterization. If infection is present, it may lead to endocarditis, pulmonary embolism, or bacteremia and septicemia.

Clinical indicators of thrombosis and thrombophlebitis in horses are those typical of inflammation: palpable heat, pain, and swelling. In the case of septic thrombophlebitis, there may also be fever and elevated levels of white cells and fibrinogen.

Sonographic Classification of Jugular Thrombi: Cavitating and Noncavitating

Gardner and co-workers reported the sonographic appearance of jugular thrombophlebitis in 46 horses.[1] As with previously published sonographic descriptions in people, the authors divided the lesions into two types: (1) *cavitating* and (2) *noncavitating.*

Cavitating thrombi were defined by their nonuniform echogenicity, featuring anechoic or hypoechoic areas representing fluid or localized necrosis within the thrombus or, alternatively, hyperechoic foci, indicative of gas. Cavitating thrombi were most likely to be infected, according to the authors (Figure 27-3).

Noncavitating lesions were characterized by uniformly low- or medium-strength echoes and were unlikely to be infected.

Catheter-Related Jugular Thrombosis

Warmerdam reported the sonographic appearance of a nonobstructive, cordlike object in the jugular vein of a horse. The structure, which in some respects resembled a thrombus, had apparently formed around the outside of a jugular catheter, placed and removed some 4 years earlier. Presumably, when the catheter was removed from the jugular vein, a sleeve of fibrous tissue remained behind, eventually collapsing and forming the fibrous cord.[2]

Accidental Severance, Dislodgement, and Migration of a Jugular Catheter

If accidentally severed, part of a jugular catheter may become dislodged and travel through the jugular outflow to the heart and, in some instances, to the pulmonary arteries beyond. In one such case reported by Little and co-workers, a 7-inch catheter fragment was removed from the right ventricle and main pulmonary artery of a week-old foal using an improvised intravascular retrieval device.[3]

Severed catheter fragments can migrate deep into the jugular vein, the vena cava, or the azygos vein. Fragments can lodge in the heart or continue into a pulmonary artery until their size, shape, or inflexibility prevents further migration. The catheter fragment may abrade the interior surface of the vessel in which

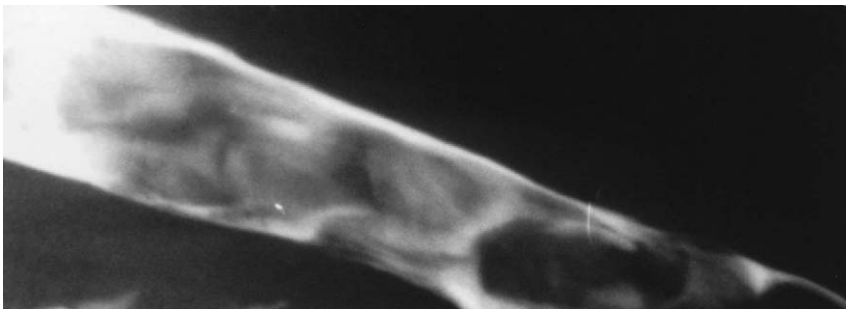
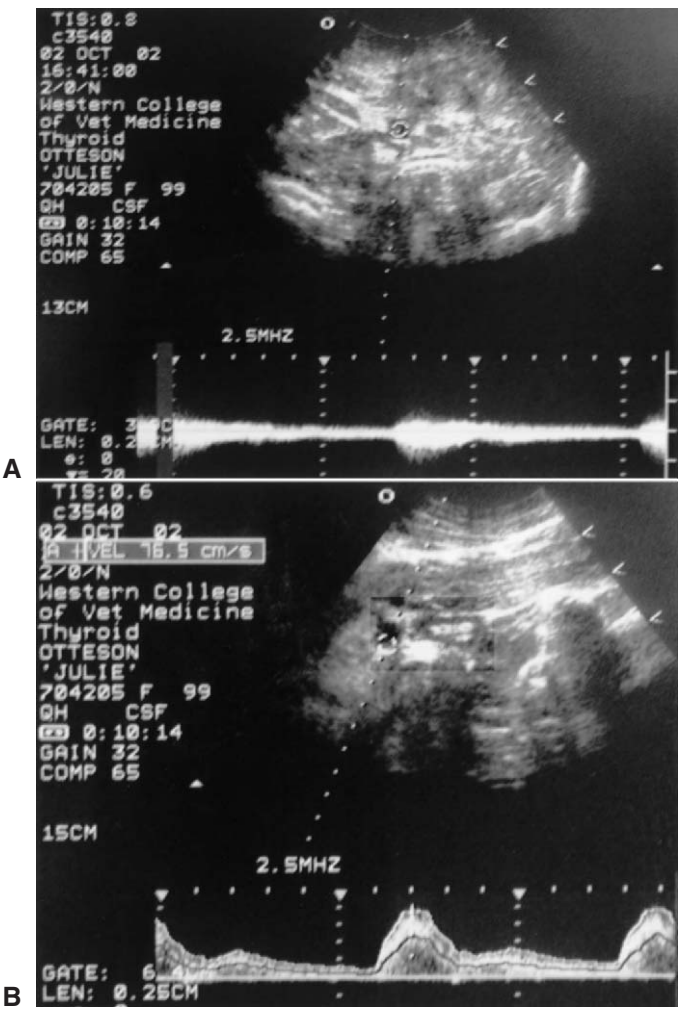


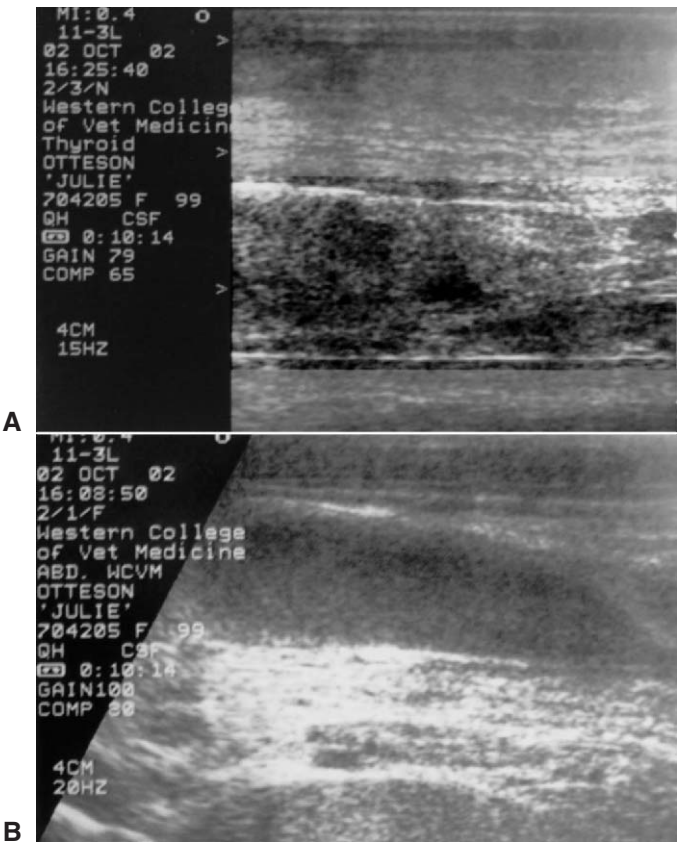
Figure 27-1 • Lateral venogram shows a lengthy, irregularly shaped jugular thrombus in the neck of a Quarter Horse.



A

B

Figure 27-2 • Spectral Doppler tracings of a vein **(A)** and artery **(B)** in the neck of a Quarter Horse show characteristic waveforms.



A

B

Figure 27-3 • **A,** Sonographic long section of a thrombophlebotic jugular vein in a horse shows uneven echogenicity and fluid pockets characteristic of cavitating thrombi. **B,** The normal opposite jugular is provided for comparison.

it is lodged, causing thrombophlebitis, potentially leading to pulmonary embolization and infarction. Potential consequences of catheter fragments on the cardiovascular system are listed in Box 27-1.

Fluoroscopy can be indispensable in determining the location of a lost jugular catheter, as in this case, although it by no means guarantees success. It is important to reiterate that the foal in question was only a week old and probably weighed no more than 100 pounds; but imagine how much more difficult the task would be in an adult horse weighing upwards of 1000 pounds, 10 times the size of the described foal—in most instances, difficult or impossible.

Well-opacified catheter fragments can also be detected radiographically, whereas unmarked catheters may be occasionally detected as a subtle filling defect when angiography is used.

Carotid-Jugular Fistula

Guglielmini and Bernardini reported the sonographic appearance (including Doppler) of a presumed con-

genital jugular-carotid fistula in a 7-month-old Standardbred colt.[4] Physically the foal showed left maxillary, linguofacial, and jugular distension. Jugular blood gases were unbalanced, showing higher oxgenation on the left side. Pulsed and color Doppler of the left jugular showed disturbed bidirectional blood flow, compatible with an arteriovenous fistula.

▮▮▮ THE CAROTID ARTERY

Normal Doppler

Cipone and co-workers described the normal pulsed-wave Doppler appearance of the common carotid artery in the resting Standardbred.[5]

▮▮▮ TRACHEA

The Normal Trachea

A horse's trachea normally appears as a thick, slightly rippled, radiolucent band. Individual tracheal rings appear as faint, closely approximated densities crossing the long axis of the trachea at right angles. Ventrally the tracheal rings appear as rectangular densities, separated from one another by smaller, relatively lucent areas (Figure 27-4).

Tracheal Injury

Caron and Townsend reported widespread subcutaneous emphysema of the head and neck of a horse caused by a penetrating wound in the caudal aspect of the cervical trachea.[6] In addition, the horse also had a large-volume pneumomediastinum.

Radiographically, tracheal perforation is usually heralded by the presence of extraluminal air, arranged in an orderly fashion along the exterior surface (Figure 27-5). It is this ability to identify the normally invisible tracheal wall that signals the possibility of perforation, although a similar appearance may also be seen with a severe pneumomediastinum or pharyngeal perforation.

Occasionally escaped tracheal gas acts uncharacteristically, accumulating in small or medium-sized pockets in and around the site of leakage (Figure 27-6). Unfortunately, from a diagnostic perspective, gas escaped from an esophageal perforation may behave the same way.

Transtracheal Aspiration

Nearly 30 years ago, I reported the high incidence of paracervical emphysema and pneumomediastium caused by diagnostic transtracheal aspiration in horses.[7] Since that time I have seen dozens of additional cases, and in only one instance was there any

Box 27-1
Potential Injury or Harmful Effects of Detached Catheter Fragments Situated in the Jugular Outflow, Pulmonary Arteries, or Heart

Phlebitis
Thrombosis
Thrombophlebitis
Vascular or cardiac perforation
Pulmonary embolism
Pulmonary infarction
Pneumonia
Pulmonary abscessation
Septicemia
Endocarditis
Cardiac arrhythmia
Endocardial abrasion or laceration
Valvular injury or obstruction

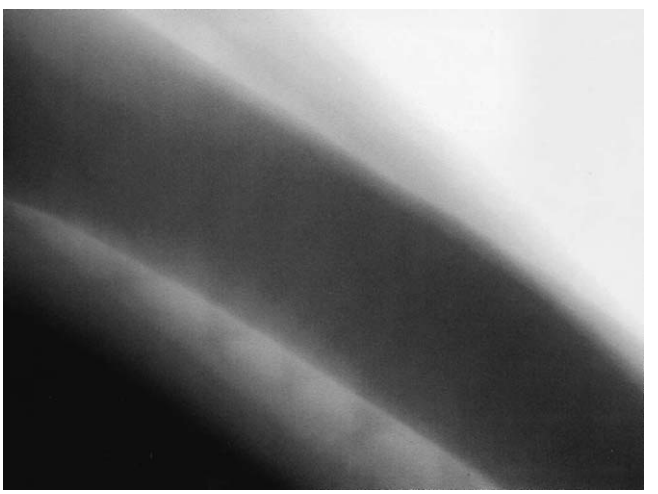


Figure 27-4 • Close-up lateral view of the cranial third of the trachea in a normal adult horse.

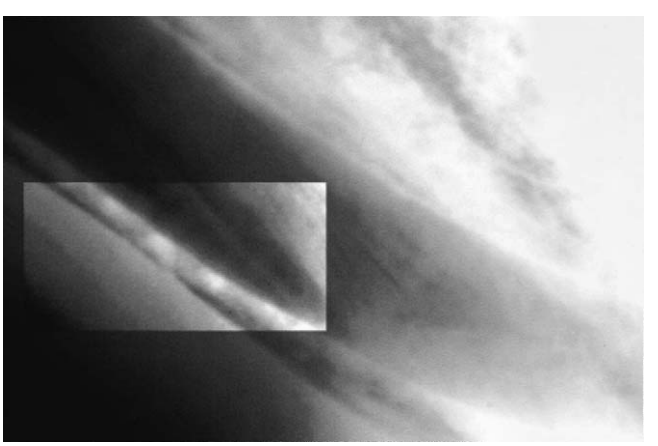


Figure 27-5 • Close-up lateral view of the neck of a horse with a tracheal wound shows escaped gas outlining the exterior surfaces of the trachea, rendering the wall visible *(emphasis zone)*. Luminal leakage is also responsible for the striated appearance of the trachea caudally and for the dorsally situated gas accumulations.

certain evidence of a serious side effect, namely, probable bacterial mediastinitis.

I have also determined beyond any doubt that the magnitude of a pneumomediastinum caused by transtracheal aspiration is primarily a function of the *time* taken to perform the procedure; the longer the needle is in the tracheal lumen, the larger the hole in the tracheal wall. Thus novices, who are often tentative or awaiting further guidance and approval from their instructors, take a great deal longer to perform a transtracheal aspiration than an experienced person and, as such, are much more likely to cause a large-volume pneumomediastinum.

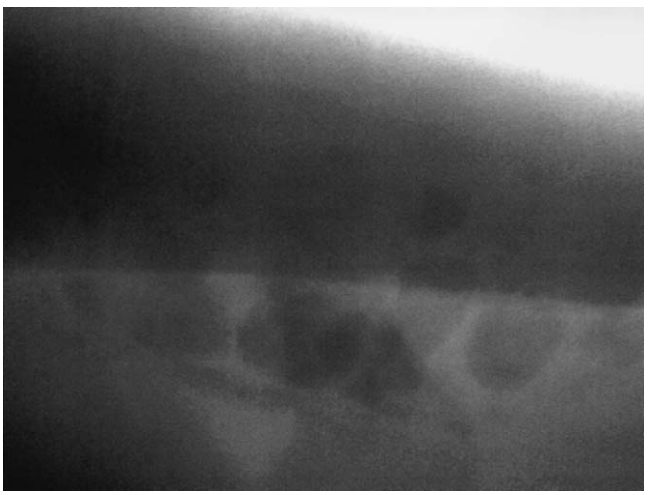


Figure 27-6 • Close-up lateral view of the neck of a horse with a tracheal wound shows a half dozen or so medium-sized gas pockets just outside the ventral tracheal wall. Although the extraluminal gas in this instance has escaped from a tracheal wound, atmospheric contamination from a nonpenetrating injury may have a similar appearance. Thus distinguishing between these two possibilities may prove difficult or impossible.

The obvious lesson here is to practice the procedure on a model (they are easy to build) before performing it on a live animal. If a student has not performed the procedure in some time, it is wise to first do a step-by-step run-through to refamiliarize the student with the procedure, in particular, the order in which things are to be done. It should also prove less uncomfortable for the horse.

Tracheostomy

Tracheostomy devices are prone to leakage, and in general the larger they are, the more they leak. Regular manipulation, particularly that related to nebulization, tends to exacerbate the problem. In severe instances, more air is located outside the trachea than inside (Figure 27-7).

Tracheal Collapse

Using *videoendoscopy*, Tetens and co-workers were able to diagnose tracheal collapse in a 2-year-old Thoroughbred filly, which was not evident using conventional endoscopy. They referred to this type of dorsoventral collapse, which was observed over a 10-cm section of the trachea during inspiration and resulted in a 70 percent reduction in luminal cross-section, as *dynamic tracheal collapse,* presumably to differentiate it from a permanent disfiguration.[8]

Carrig and co-workers reported tracheal collapse in a 15-year-old pony, causing chronic dyspnea.[9] The fact that the pony was as old as it was strongly suggests that the disease was acquired. Yovich and Stashak reported tracheal collapse caused by a lipoma.[10]

Woodford and co-workers reported the xerographic appearance of a severe, lengthy tracheal stenosis, located in the caudal cervical region of a 10-year-old mule. Endoscopy showed that the lesion was 30 cm long and resulted in near-complete obliteration of the tracheal lumen.[11]

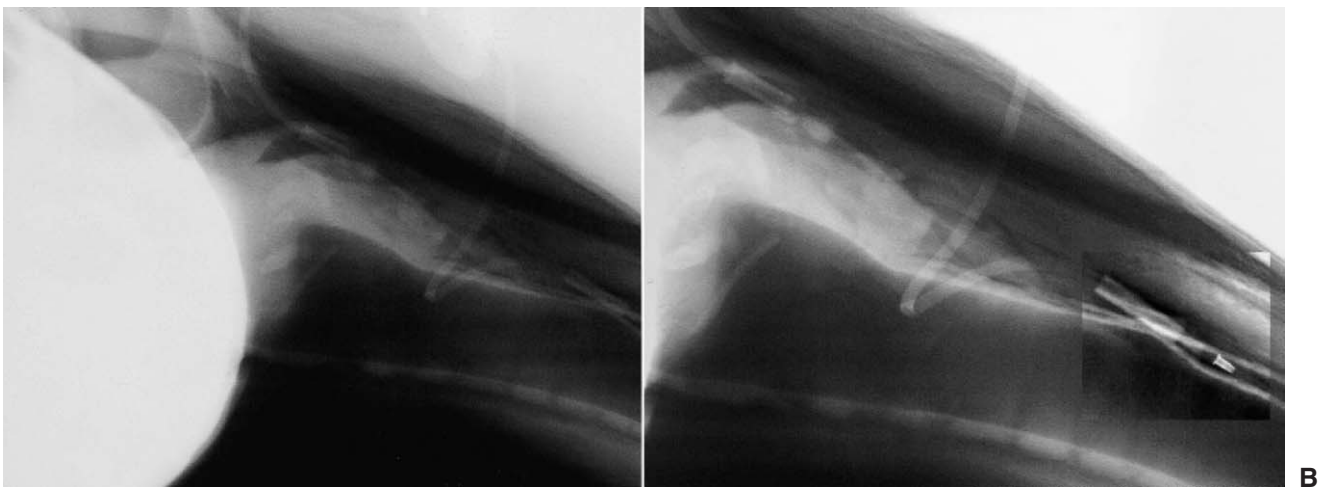


Figure 27-7 • Lateral **(A)** and close-up lateral **(B)** views of the neck of a foal with a badly leaking tracheostomy show a large volume of escaped gas outlining the trachea, esophagus, and ventral neck muscles. Catheter and needle hub are emphasized.

▮▮▮ THE CERVICAL ESOPHAGUS

Normally the esophagus is radiographically invisible. Occasionally small pockets of esophageal gas are present in radiographs of the throat, neck, or thorax but should not persist in subsequent films.

Cervical Radiography

One of the first descriptions of equine esophageal radiography was by Uri Bargai, an Israeli radiologist studying in Sweden.[12] Quick and Rendano also described esophageal radiography in the horse, pointing out the wide variety of diseases that may be diagnosed.[13]

Later Greet, working at the Equine Research Center in Newmarket, further considered the role of radiology, especially esophagography, in the diagnosis of esophageal disease in horses.[14] As might be expected, barium films were far more useful than plain films, although in most instances, a choke could be readily diagnosed from the latter.

On the subject of contrast administration, Greet considers a dose syringe the best way to administer barium, being preferable to the difficulty often associated with giving barium paste by mouth or maneuvering a stomach tube into the optimal position immediately proximal to a lesion site. Oral administration also affords an opportunity to evaluate swallowing and to see the proximal part of the esophagus.

On average, barium required 4 to 10 seconds to pass through the esophagus to the stomach. Most esophageal diseases resulted in prolonged passage times, ranging from a few minutes to a few hours. As previously noted by Bargai, thin lines of residual barium were often observed in the mucosal folds of the esophagus once the bulk of the barium had passed into the stomach (Box 27-2).

For routine esophageal radiography, the authors recommend placing the receiver (cassette with film) on the left side of the horse's neck where the cervical esophagus is normally situated. This should produce a relatively sharper image than if the receiver is placed on the right, where magnification would be greater. A ventrodorsal or dorsoventral view can be useful but will require a powerful x-ray generator.

Depending on contrast volume and radiographic timing, the entire esophagus may be visualized, usually as a gently curving band partially superimposed on the trachea and not exceeding 2 cm in diameter (except for boluses). Occasionally, multiple boluses are present, especially if the contrast has been administered orally. Repeated swallowing of barium, particularly paste, may prolong esophageal opacification and should not be interpreted as prolonged retention due to disease.

Esophagography (Barium Swallow)

Esophagography may be performed with either barium mixed with water, a commercial barium suspension, or a diagnostic iodine solution in the case of suspected perforation.

Quick recommends giving 9 to 12 ounces of barium by stomach tube or dose syringe. In the case of localized lesions, it is best to inject the barium as close as possible to the area of interest. For larger regional abnormalities, the contrast injection can be made in the mouth or in the proximal esophagus, taking care not to choke the horse. For relatively subtle mucosal lesions, high-viscosity barium paste is recommended, which is best squeezed onto the back of the tongue rather than administered by stomach tube.

Esophageal Pressure, Pressure Zones, and Pressure Profiles

Stick and co-workers measured esophageal pressures in five healthy adult horses, and from these measurements they constructed normal esophageal pressure profiles. Based on regional pressure differences, they determined that there were four functionally distinct zones: at the cranial and caudal esophageal sphincters and what the authors termed *fast and slow* esophageal regions. These latter areas—the fast and slow zones—refer to portions of the esophagus situated between the cranial and caudal sphincters that differ in how rapidly they contract during swallowing, similar to what has been described in people.[15]

Box 27-2
Functional, Structural, and Spatial Disorders of the Equine Esophagus

FUNCTIONAL DISORDERS
Enlargement dilation (megaesophagus)
Esophageal atony (often accompanies enlargement)
Abnormal retention of contrast medium (often seen with enlargement and atony)
Delayed transit
Choke (feed impaction)

STRUCTURAL DISORDERS
Persistent right aortic arch
Inflammatory stricture
Fistula (tracheoesophageal is the most common)
Diverticulum
Ulceration
Esophagitis (inferred from mucosal erosion and irregularity)
Diverticulum
Foreign body
Spontaneous rupture or perforation
Traumatic laceration
Tumor
Abscessation
Granuloma

SPATIAL DISORDERS
Dorsal esophageal displacement secondary to a mediastinal mass or cardiomegaly
Ventral displacement of esophagus (hematoma, cellulitis, abscess, tumor)

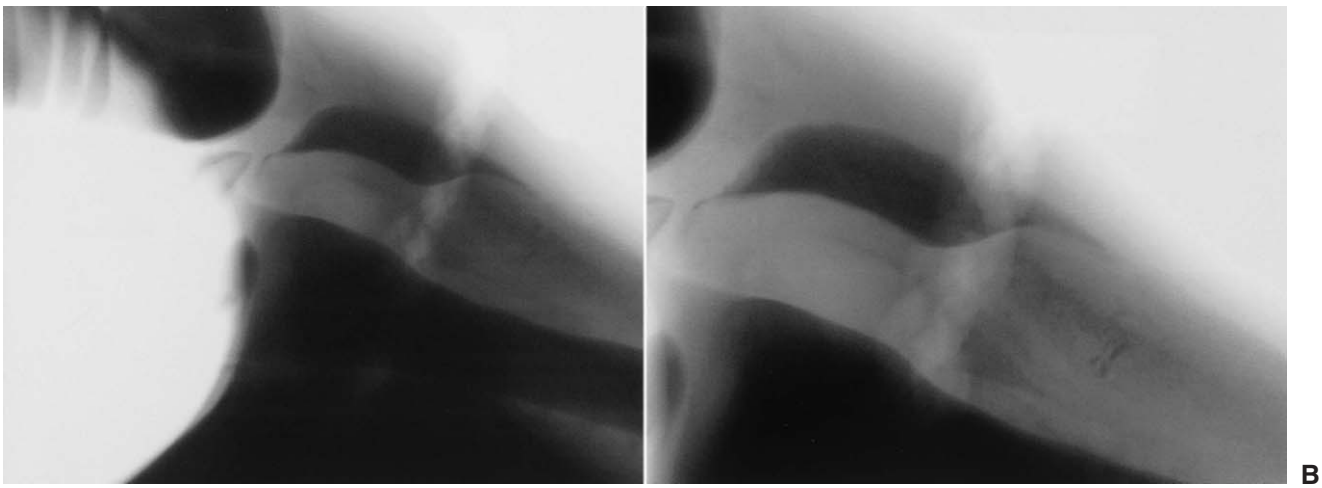


Figure 27-8 • Lateral **(A)** and close-up lateral **(B)** views of the proximal esophagus of a horse with a feed impaction, appearing here as a fine granular mass with a characteristically snouted gas-cap cranially.

Esophageal Obstruction (Choke)

Mechanical Blockage. Blockage of the esophagus, commonly termed *choke,* is generally of a mechanical nature and usually involves high roughage feed or a discrete object such as an apple. Any mass-type lesion, for example, an abscess, granuloma, or tumor, is potentially capable of luminal obstruction, although if it enlarges gradually, an animal can initially adapt to it quite well. Conversely, primary and secondary transport disorders are comparatively rare in horses, especially compared with dogs. The radiographic identification of an enlarged esophagus, sometimes termed *megaesophagus*, is not a diagnosis per se but rather an *indication* of disease.

Although plain films are often capable of showing large-volume, medium- to high-density esophageal impactions (Figure 27-8), barium films are often more convincing, especially in establishing the totality plus or minus the extent of the blockage (Figures 27-9 and 27-10). Barium is also necessary to demonstrate most small objects, especially when they are located in the thoracic portion of the esophagus (Figure 27-11).



Figure 27-9 • Cervical esophagram in a "choked" horse shows from left to right: (1) a characteristically snouted gas cap, (2) fluid level, (3) barium pool, and (4) filling defect representing impacted feed.

Post-Esophagitis Obstruction. The actual incidence and prevalence of esophagitis leading to obstructive stricture is not known but Erkett and co-workers reported the radiographic appearance of a mass of granulation tissue that was partially obstructing the cervical portion of the esophagus in an adult horse (Box 27-3).[16]

Box 27-3
Some Potential Causes of Esophageal Obstruction in the Horse

Feed impaction
Obstruction by a single piece of food, such as an apple
A nonorganic foreign body
Nonspecific postinflammatory stenosis
Posttraumatic formation of a mass of granulation tissue
Esophageal diverticulum
Compression, deformity, or displacement by an adjacent mass
Primary or secondary esophageal cancer
Benign esophageal tumor
Esophageal tone deficit (dilation and paralysis)
Congenital vascular ring
Congenital cyst

Nonobstructive Persistent Esophageal Dilation (Megaesophagus)

An abnormally dilated but nonobstructed esophagus usually contains a combination of air and fluid. Because of the downward inclination of the cervical esophagus (and the influence of gravity), accumulated

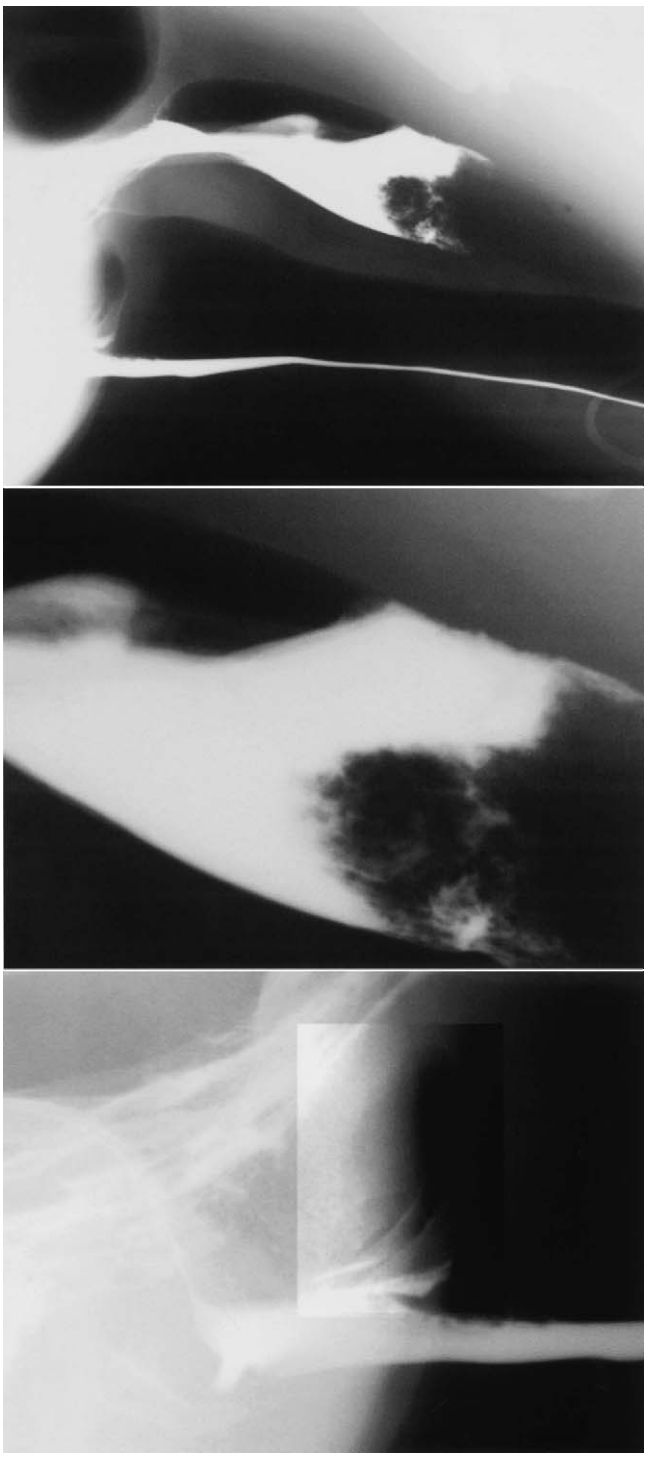


Figure 27-10 • Lateral **(A)** and lateral close-up **(B)** views of the cervical esophagus after administration of barium suspension shows, from left to right: (1) a characteristic gas cap and (2) barium pool and irregular filling defect representing impacted feed. A thin stripe of barium coats the interior surface of the ventral tracheal wall and partially fills the larynx **(C)**.

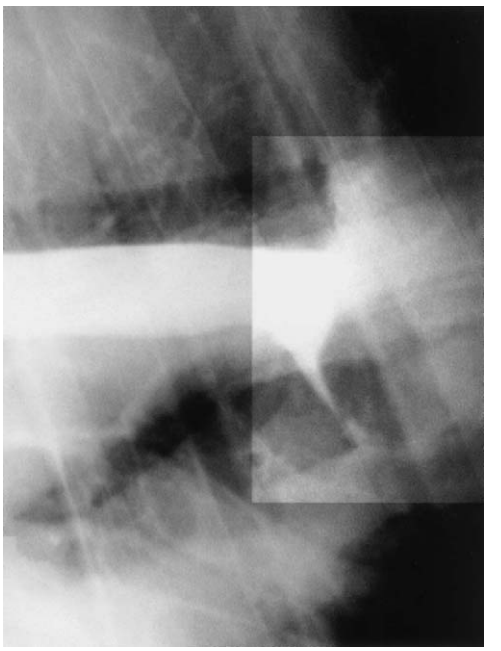


Figure 27-11 • Close-up lateral thoracic esophagram shows a large circular filling defect surrounded by contrast solution, which is partially obstructing the esophagus. The offending object was a medium-sized, partially decomposed apple.

secretions usually pool caudally, typically in and around the thoracic inlet. Thus air distension may be the only indicator of esophageal disease, at least as judged from a cervical radiograph (Figure 27-12).

Bowman and co-workers reported megaesophagus in a 6-month-old Thoroughbred colt that had choked repeatedly over the past 48 hours.[17] Contrast radiography revealed generalized esophageal dilation, atony, and retention of barium. Postmortem examination failed to confirm suspected achalasia, suggesting instead a nonspecific paralysis.

Persistent Right Aortic Arch (Vascular Ring Anomaly)

Barber and co-workers reported proximal esophageal dilation and atony in a sickly 1-month-old Quarterhorse colt.[18] Structurally the esophagus closely resembled what is typically seen with a persistent right aortic arch, but none was found at postmortem examination. The caudal, nondilated portion of the esophagus was hypertrophied, however, a finding reported in humans with a dysfunctional distal esophageal sphincter (cardiospasm, achalasia).

Esophageal Diverticula

Esophageal diverticula (pouches) may follow a choke or, alternatively, develop for no known reason. Presumably diverticula are caused by injury to the esophageal muscle, its blood supply, or its innervation. Many are characterized by a cervical swelling that becomes apparent during or after eating.

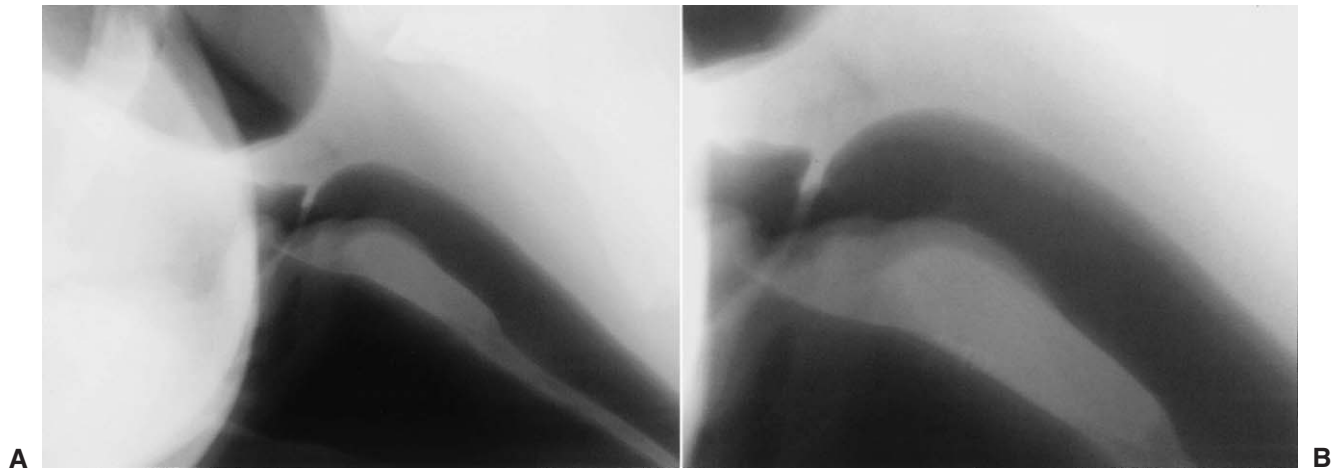


Figure 27-12 • Close-up **(A)** and ultra-close-up **(B)** views of the cranial esophagus of a horse with esophageal atony show moderate air distension but no fluid or feed.

Pulsion Diverticulum. Diverticula are of two types: pulsion or traction.[19] A pulsion diverticulum is a kind of hernia in which the mucosa extends through a rent in the muscularis, being prevented from further displacement only by the serosa.

Traction Diverticulum. A *traction diverticulum* is an outward tenting or mounding of the esophageal wall caused by a localized adhesion, which fixes the esophagus at that point, precluding coordinated movement with the rest of the esophagus. In either case, such cul-de-sacs trap food and lead to intermittent regurgitation. As might be anticipated, diverticula are morphologically quite variable and, as such, are best studied fluoroscopically during a barium swallow.

Esophageal Phytobezoar

MacDonald and co-workers described the radiographic appearance of an esophageal phytobezoar in an emaciated 23-year-old Thoroughbred stallion with a 2-year history of caudal swelling of the neck after eating.[20] Contrast radiography revealed regional dilation of both the caudal cervical and cranial thoracic portions of the esophagus, with only a trail of barium beyond.

At necropsy the esophagus was found to contain a large phytobezoar, just beyond the thoracic inlet, which filled the esophageal lumen. Several large longitudinal tears were present in the muscular layer of the caudal cervical esophagus, one of which contained herniated mucosa, forming a large diverticulum. A healed, nonobstructive tracheal fracture was discovered nearby, suggesting a possible cause for the esophageal disease Additional findings included a multifocal, aspiration-type pneumonia and acute gastric ulceration.

Complications Associated With Cervical Esophagostomy and Feeding Tubes

Stick and co-workers reported harmful effects caused by cervical esophagostomy and feeding tubes in 11 ponies.[21] These included (1) reflux of food around the feeding tube, (2) traction diverticula, (3) feeding-tube obstruction and esophageal injury related to clearance, (4) dislodgement of the feeding tube, leakage of esophageal contents and infection, (5) fistula development, (6) esophageal erosions, and (7) jugular vein thrombosis.

Employing an esophageal tube to clear an obstruction (with or without concurrent irrigation) is also potentially dangerous, sometimes causing mucosal injury, hematoma, and occasionally perforation (Figure 27-13). Erosions may eventually lead to ulceration, scarring, or stenosis.

Esophageal Stricture

Esophageal strictures may be either congenital or acquired, with the latter being more common. Strictures may be associated with a variety of radiographic abnormalities, most of which require barium to demonstrate. Proximal to the stricture there may be (1) dilation, (2) a tapered appearance to the contrast column (also termed *coning*), (3) one or more fluid levels, and (4) a filling defect created by retained food. Barium is often unevenly distributed within the stricture, and the mucosal folds often appear undulant and incomplete. Beyond the lesion the esophagus appears normal.

Esophageal patch grafting can create its own set of postoperative radiographic abnormalities, including (1) localized contrast accumulation related to weak transit, (2) dilation, (3) gas, (4) filling defects, and (5) marginal irregularity.[22]

Esophageal Cysts

Cysts are presumed to be the result of an embryologic accident in which a miniature fluid-filled, esophageal remnant develops within the wall of the esophagus, potentially causing blockage. In one reported case, the cyst could be seen in plain films, contrasted by flanking gas pockets, and displacing the adjacent trachea ventrally. Barium films of the same horse showed the

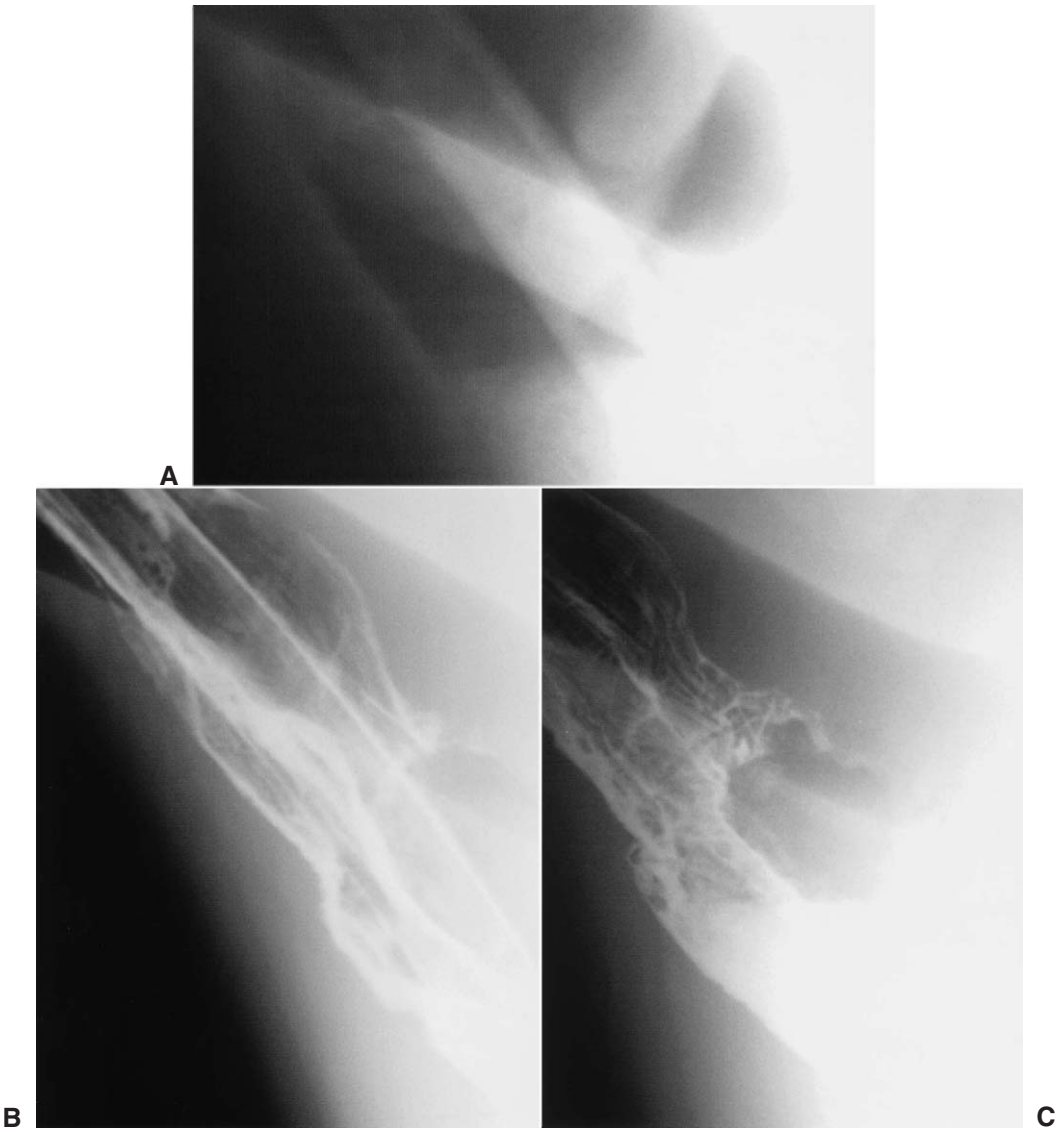


Figure 27-13 • A, Plain film of the caudal cervical esophagus of a "choked" horse shows the trachea diagonally crossing an air-distended esophagus, which contains an irrigation tube and what appears to be a fluid level *(bottom center)*. **B,** After administration of barium and air (the tube remains in place), another radiograph of the same region shows an irregularly distended barium- and air-filled esophagus. **C,** After withdrawing the esophageal tube, a third image reveals persistent distension, the result of prolonged obstruction, and a large, well-marginated filling defect caused by a large iatrogenic hematoma sustained while trying to forcefully relieve the obstruction with the esophageal tube.

cyst as an ill-defined filling defect within a dilated cranial esophagus.[23]

Esophageal Fistula

Vrins and co-workers described an esophageal diverticulum and fistula joining the esophagus and left guttural pouch in an 11-year-old Quarterhorse gelding.[24] When studying fistulas or potential fistulas, it is best to do so using iodinated contrast media.

Esophageal Rupture

Risner and Mair reported an esophageal rupture in a horse, the result of a kick by another animal.[25] The diagnosis was made with contrast esophagography, specifically the leakage of contrast solution into the periesophageal tissues. Other sources of contrast leakage considered by the authors were (1) necrotic ulcer, (2) traumatic nasogastric intubation, (3) retropharyngeal abscessation, (4) ruptured esophageal diverticulum, and (5) rupture secondary to obstruction.

Esophageal Tumors

Squamous cell carcinoma is reported as being the most common type of esophageal tumor in the horse. Other reported cell types are shown in Box 27-4.

Box 27-4
Reported Types of Esophageal Tumors in the Horse

Squamous cell carcinoma
Rhabdomyoma
Rhabdomyosarcoma
Leiomyoma
Leiomyosarcoma

Box 27-5
Causes of Draining Cervical Sinuses in the Horse

Foreign body
Suture
Feeding-tube infection
Abscess
Fungal infection

▮▮▮ DRAINING CERVICAL SINUSES

Sources of cervical sinus drainage are shown in Box 27-5. Dolente and co-workers reported disseminated blastomycosis in a horse causing mediastinitis and shoulder and neck abscesses, the latter resulting in a draining sinus.[26]

▮▮▮ CERVICAL BRONCHUS

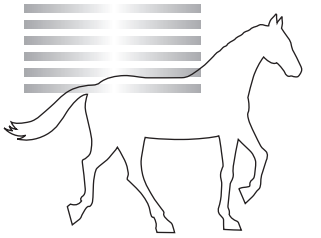
Davis and co-workers reported a cervical bronchus and associated air sac in a 3-day-old Thoroughbred filly.[27] The bellows-like, vestigial lung was nearly as large as the foal's head, extending from the angle of the jaw to the thoracic inlet. Even though cervical radiographs revealed displacement (and presumably some measure of compression) of the throat and esophagus, the foal was apparently able to breathe and suckle normally. The anomalous bronchus and associated air sac were successfully removed surgically.

References

1. Gardner SY, Reef VB, Spencer PA: Ultrasonographic evaluation of horses with thrombophlebitis of the jugular vein: 46 cases (1985-1988), *J Am Vet Med Assoc* 199:370, 1991.
2. Warmerdam EPL: Pseudo-catheter-sleeve sign in the jugular vein of a horse, *Vet Radiol Ultrasound* 39:148, 1998.
3. Little D, Keene BW, et al: Percutaneous retrieval of a jugular catheter fragment from the pulmonary artery of a foal, *J Am Vet Med Assoc* 220:212, 2002.
4. Guglielmini C, Bernardini D: Echo-Doppler findings of a carotid-jugular fistula in a foal, *Vet Radiol Ultrasound* 44:310, 2003.
5. Cipone M, Pietra M, et al: Pulsed wave-Doppler ultrasonographic evaluation of the common carotid artery in the resting horse, *Vet Radiol Ultrasound* 38:200, 1997.
6. Caron JP, Townsend HGG: Tracheal perforation and widespread subcutaneous emphysema in a horse, *Can Vet J* 25:339, 1984.
7. Farrow CS: Pneumomediastinum in the horse: a complication of transtracheal aspiration, *Vet Radiol* 17:192, 1976.
8. Tetens J, Hubert JD, et al: Dynamic tracheal collapse as a cause of exercise intolerance in a Thoroughbred, *J Am Vet Med Assoc* 216:722, 2000.
9. Carrig C, Groenendyk S, Seawright AA: Dorsoventral flattening of the trachea in a horse and its attempted surgical correction: A case report, *Vet Radiol* 14:32, 1973.
10. Yovich J, Stashack T: Surgical repair of a collapsed trachea caused by a lipoma in a horse, *Vet Surg* 13:217, 1984.
11. Woodford AM, Baird DK, Orsini JA: What is your diagnosis? *J Am Vet Med Assoc* 216:488, 2000.
12. Bargai U: The radiological examination of the digestive system of the horse. *Acta Radiol Diagn Stockholm Suppl* 319:59, 1972.
13. Quick CB, Rendano VT: Equine radiology-—the esophagus, *Mod Vet Pract* 73:625, 1978.
14. Greet TRC: Observations on the potential role of oesophageal radiography in the horse, *Equine Vet J* 14:73, 1982.
15. Stick JA, Derkson FJ, et al: Equine esophageal pressure profile, *Am J Vet Res* 44:272, 1983.
16. Erkett RS, MacAllister CG, et al: Use of a neodymium: yttrium-aluminum-garnet laser to remove exuberant granulation tissue from the esophagus of a horse, *J Am Vet Med Assoc* 221:403, 2002.
17. Bowman KF, Vaughn JT, et al: Megaesophagus in a colt, *J Am Vet Med Assoc* 172:334, 1978.
18. Barber SM, McLaughlin BG, Fretz PB: Esophageal ectasia in a Quarterhorse foal, *Can Vet J* 24:46, 1983.
19. Hackett RP, Dyer RM, Hoffer RE: Surgical correction of esophageal diverticulum in a horse, *J Am Vet Med Assoc* 173:998, 1978.
20. MacDonald MH, Richardson DW, Morse CC: Esophageal phytobezoar in a horse, *J Am Vet Med Assoc* 191:1455, 1987.
21. Stick JA, Derkson FJ, Scott EA: Equine cervical esophagostomy: complications associated with duration and location of feeding tubes, *Am J Vet Res* 42:727, 1981.
22. Hoffer RE, Barber SM, et al: Esophageal patch grafting as a treatment for esophageal stricture in a horse, *J Am Vet Med Assoc* 171:350, 1977.
23. Scott EA, Snoy P, et al: Intramural esophageal cyst in a horse, *J Am Vet Med Assoc* 171:652, 1977.
24. Vrins A, O'Brien TR, Carlson G: Diverticulum and fistula of the lower cervical esophagus in a horse, *Can Vet J* 24:385, 1983.
25. Risner I, Mair TS: Traumatic esophageal rupture in a horse complicated by subsequent rupture of the common carotid artery, *Equine Vet Educ* 15:120, 2003.
26. Dolente BA, Habecker P, et al: Disseminated blastomycosis in a miniature horse, *Equine Vet Educ* 15:139, 2003.
27. Davis DM, Honnas CM, et al: Resection of a cervical tracheal bronchus in a foal, *J Am Vet Med Assoc* 198:2097, 1991.

SECTION IV

The Spine



Chapter 28

The Cervical Spinal Region

STANDARD CERVICAL SERIES

The standard cervical examination, as performed in a *standing* foal or adult horse, typically comprises lateral views only. Coverage must extend from the base of the skull to include the entire atlantooccipital joint, to the body of the first thoracic vertebra. The number of 14- by 17-inch films required to complete the examination depends on the size of the animal and the desired degree of field overlap. The radiographic technique must be gradually increased as the neck thickens caudally, in particular, where the shoulders overlap the cervicothoracic junction. A grid is an absolute necessity in this last region.

Two or three evenly distributed lead markers taped to the animal's hair coat will greatly enhance orientation in the event additional images are needed.

Foal

Reduced size and open growth plates are the principal distinguishing features of the immature cervical spinal region (Figure 28-1). The most complex of these is the second cervical vertebra, which is anatomically unique compared with the rest of the spine by virtue of its large rudderlike dorsal spinous process and distinctly snouted dens, the latter containing a pair of vertically oriented growth plates that may be mistaken for fractures (Figure 28-2). Caudally, superimposition of the body of C7 and the growth plate of the supraglenoid tubercle can resemble a fracture (Figure 28-3).

Adult

The appearance of an adult cervical spine is similar to that of the foal, only proportionately larger and with most or all the vertebral growth plates fully closed. The greater structural definition often apparent in the cervical spine of foals is due to a relative decrease in part thickness (compared with an adult), which invariably results in less scatter radiation and, consequently, improved anatomic detail (Figure 28-4). Cervical

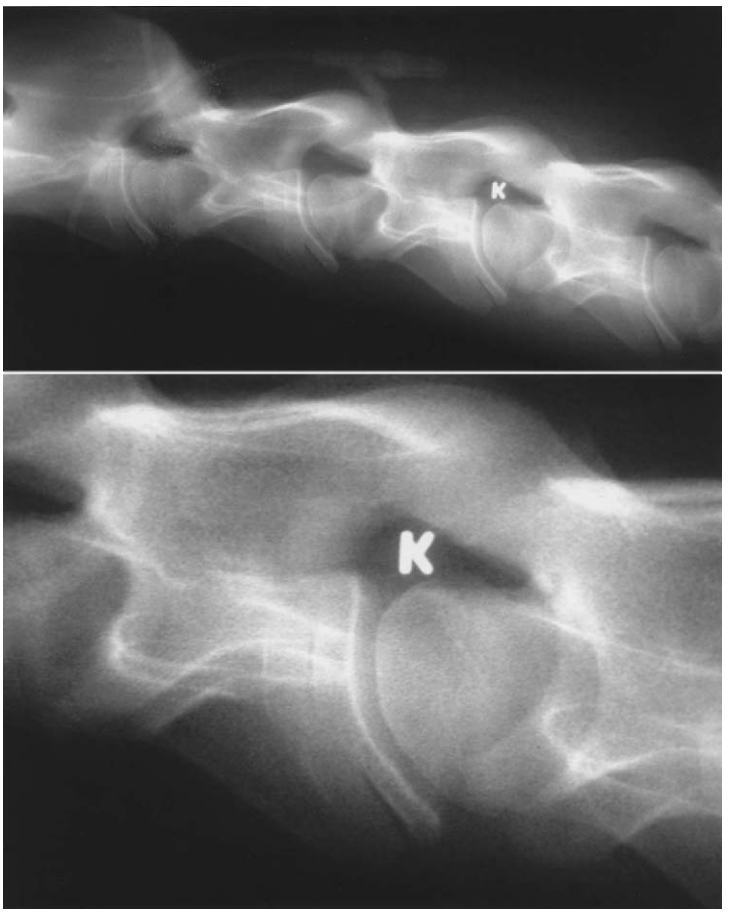


Figure 28-1 • Lateral **(A)** and close-up lateral **(B)** views of the cervical spinal region of a young foal show open cranial and caudal growth plates on each vertebral body, separating accessory from principal growth centers. The letter *K* is a radiographic reference marker.

specimens are provided for radiographic-anatomic comparison (Figure 28-5).

▮▮▮ FRACTURE AND DISLOCATION OF THE CERVICAL SPINAL REGION

Cervical Fracture

Cervical fractures in horses are almost always the result of a frontal collision, serious fall, or direct blow to the head. Occasionally congenital malformation or abnormal angulation related to cervical vertebral instability may be difficult to distinguish from a cervical fracture-dislocation.

Growth Plate Fractures

Whitwell and Dyson report that in their experience cervical growth plate fractures most commonly involve C1.[1] My experience has been similar, although I would hasten to add that most fractures involving the C1-2 spinal unit result in a significant degree of dislocation, which is a greater concern with respect to associated cord injury. Two such examples are provided, one of which contains a rare ventrodorsal view of the injury (Figure 28-6).

Ventral Element Fractures (Body Fractures, Compression Fractures)

Vertebral body fractures are often characterized by subtle shortening or asymmetry, abnormalities most readily detected by comparing the fractured vertebra with those on either side, taking into account any regional differences in vertebral size and shape. Splinterlike fragments are sometimes seen along the ventral margin of a fractured vertebra, but they can easily be confused with a comminuted fracture of the associated rib head.

Dorsal Element Fractures (Arch and Process Fractures)

Fractures of the vertebral arch involving one or both pedicles, lamina, or facets most often involve the caudal portion of the cervical spine, usually C5-6, and less often C6-7. The inciting injury is usually a sudden, forceful blow delivered to the forehead, which drives the head and neck backwards into the rigid thoracic spine, literally exploding the dorsal and ventral elements of C6 or C7. Mechanistically speaking, the fracturing force has been likened to that exerted by a pile driver, thus the expression *pile-driver fracture.*

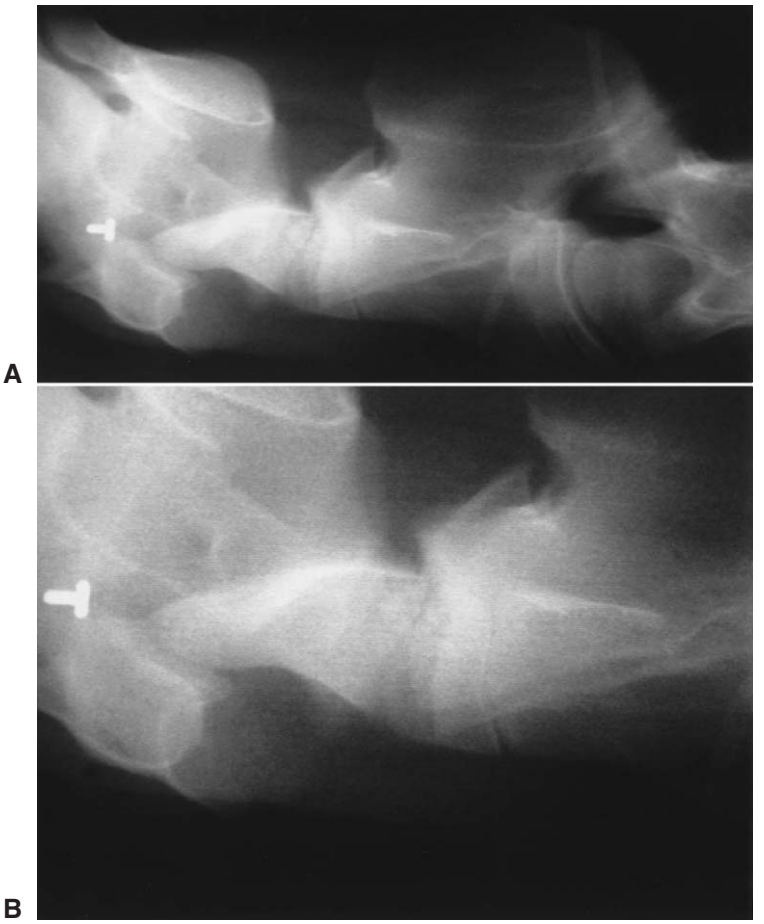


Figure 28-2 • Close-up lateral **(A)** and ultra-close-up lateral **(B)** views of the C1-2 spinal unit show the paired, vertically oriented growth plates and distinctively snouted appearance that characterize the immature dens.

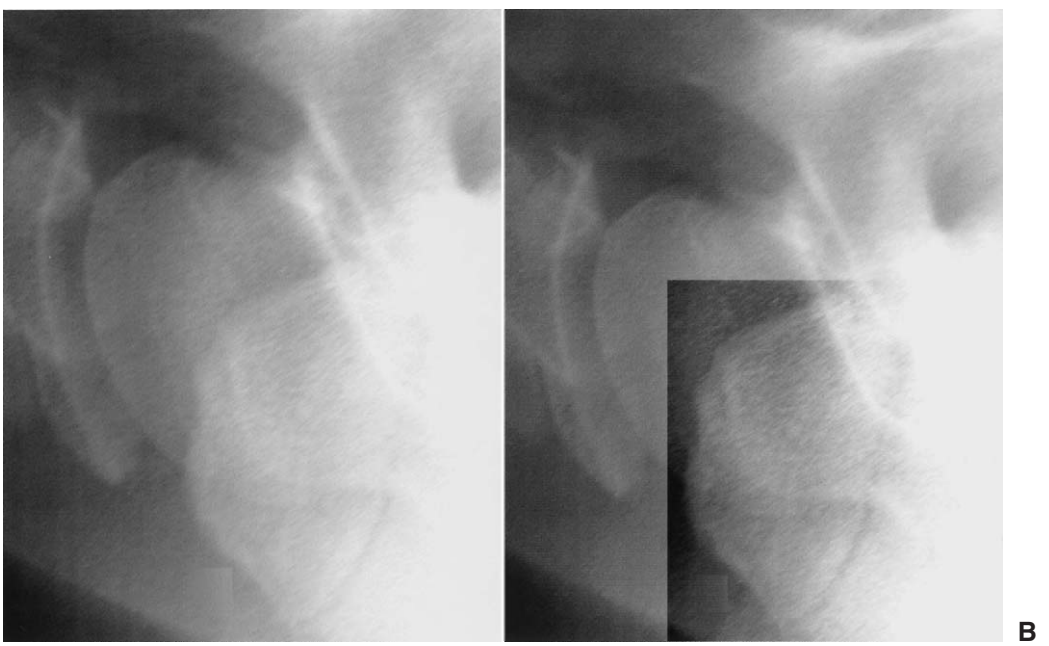


Figure 28-3 • **A,** Ultra-close-up lateral view of the cranial aspect of C7 shows what in some circumstances might be mistaken for a displaced vertebral fracture. **B,** In reality this is a normal finding in skeletally immature horses, representing the growth center and growth plate of the supraglenoid tubercle superimposed on the seventh cervical vertebrae *(emphasized).*



Figure 28-4 • Close-up lateral views of a young adult horse centered over the C1-2 **(A),** C2-3 **(B),** and C4-5 **(C)** spinal units. Remnants of the accessory vertebral body growth plates are still visible. The letter *T* has been taped to the hair coat as a reference marker in the event any additional images are required.

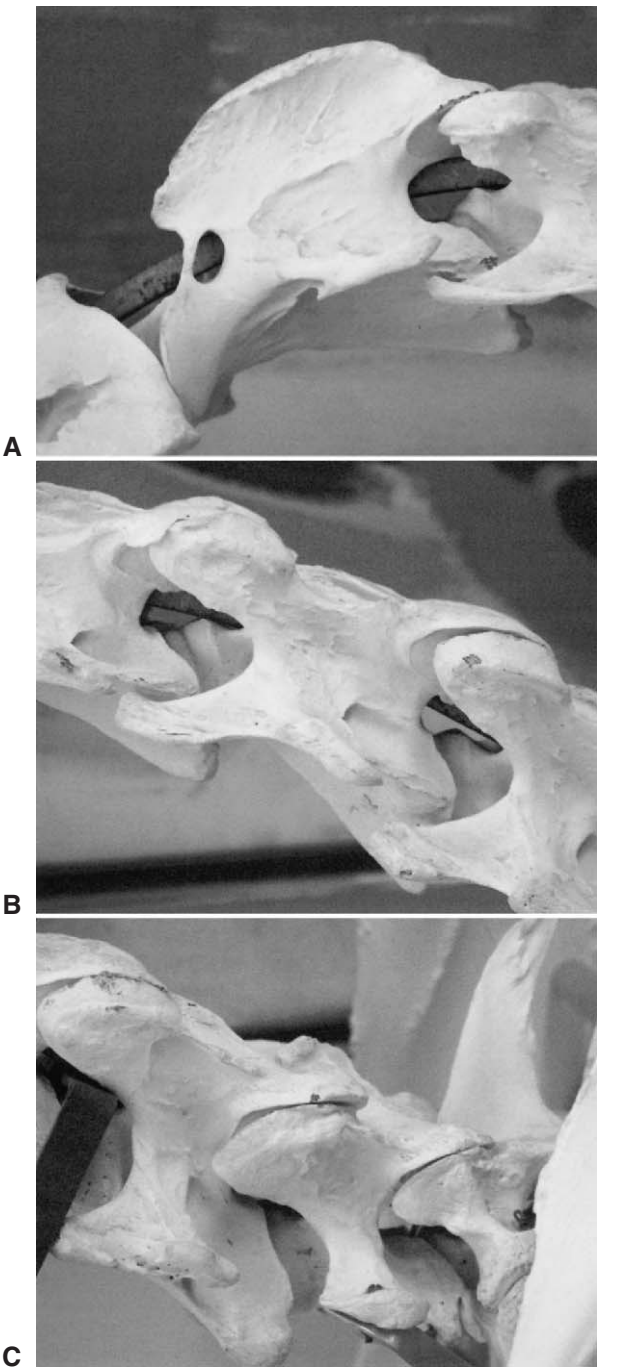


Figure 28-5 • Close-up C1-2 **(A),** C3-4 **(B),** and C6-7 **(C)** views of a defleshed cervical spine provided for radiographic-anatomic comparison.

The degree to which the associated spinal cord can be deformed or compressed can be extraordinary (see Figure 28-9 in the section on myelographic assessment).

Isolated transverse process fractures are rare, and related infections are even more unusual. Sysel and co-workers reported a case of a draining, infected C4 transverse process fracture, presumably caused by an earlier puncture wound.[2]

Cervical Dislocation (Cervical Subluxation, Luxation)

Most cervical dislocations occur in foals and are accompanied by one or more fractures, often involv-

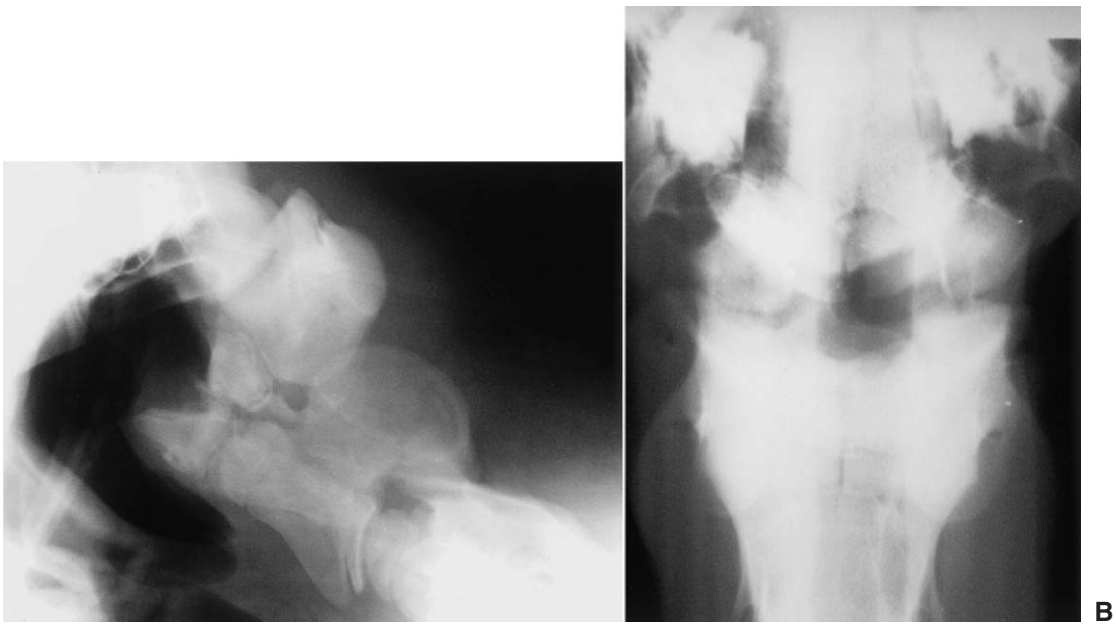


Figure 28-6 • Close-up lateral **(A)** and ventrodorsal **(B)** views of the C1-2 spinal unit in a young foal show a severe fracture-dislocation involving the ventral aspect of the first and the cranial aspect of the second cervical vertebrae; early callus formation is already in evidence. *Note:* A month before these radiographs were made, this foal fell over backwards, was momentarily stunned, but then quickly regained its feet. A week later the foal moved about gingerly, favoring its neck, but showed no overt ataxia. Forced lateral head and neck movements were resisted during physical examination.

ing the growth plate of the dens (Figure 28-7). Some of these injuries are immediately apparent on radiographs, whereas others are quite subtle, with minimal subluxation and only one or two small fracture fragments (Figure 28-8).[3] Most of these animals are ataxic or fully paralyzed immediately after the injury, but some have only a wryneck and a somewhat hesitant step.

Guffy and co-workers reported dislocation of the C1-2 spinal unit, without an associated fracture, in a 10-day-old foal. The authors hypothesized that the atlantoaxial dislocation seen in this case was actually the result of two separate injuries: an initial C1-2 sprain at 3 days of age and reinjury to the same area 6 days later. Their theory was histologically supported in a subsequent necropsy.[4]

Isolated neck sprains usually do not require radiography/myelography, other than to exclude a related fracture in instances of a wryneck or neurologic deficiency. An increase in the distance between C1 and C2 (as seen in a lateral radiograph) may herald such an injury as a result of tearing one or more of the following ligaments: (1) *apical*, a pair of ligaments that attach the apex of the dens to the occipital condyles on the ventral aspect of the foramen magnum; and (2) *longitudinal*, a single ligament that attaches the dens to the ventral arch of the atlas. The horse does not have a *transverse atlantal* ligament.

Myelographic Assessment. The risks of cervical myelography are amplified in the case of recent injury. Specifically, the contrast solution may be absorbed by the injured spinal cord, causing direct cellular damage. Ionic media, if absorbed by the injured cord, will also cause edema, leading to varying degrees of compression and secondary compromise.

Most severely displaced cervical fractures result in predictable injury to the associated portion of the spinal cord, but there are occasional exceptions, one of which is illustrated in Figure 28-9.

Caution: *In my opinion, stress films, particularly traction maneuvers, should be avoided because they may further bruise the spinal cord, especially in the case of fracture-dislocation of the C1-2 spinal unit.*[5]

Acquired Cervical Torticollis

Torticollis (or wryneck) refers to a sustained, abnormal twisting of the neck, typically to one side or the other, caused by asymmetric tension in the cervical musculature. A foal may be born with congenital malformation of the cervical spinal region, causing a torticollis, or it may develop a wryneck from other causes (see following). The optimal way to differentiate between a temporary, adaptive carriage of the head and neck,

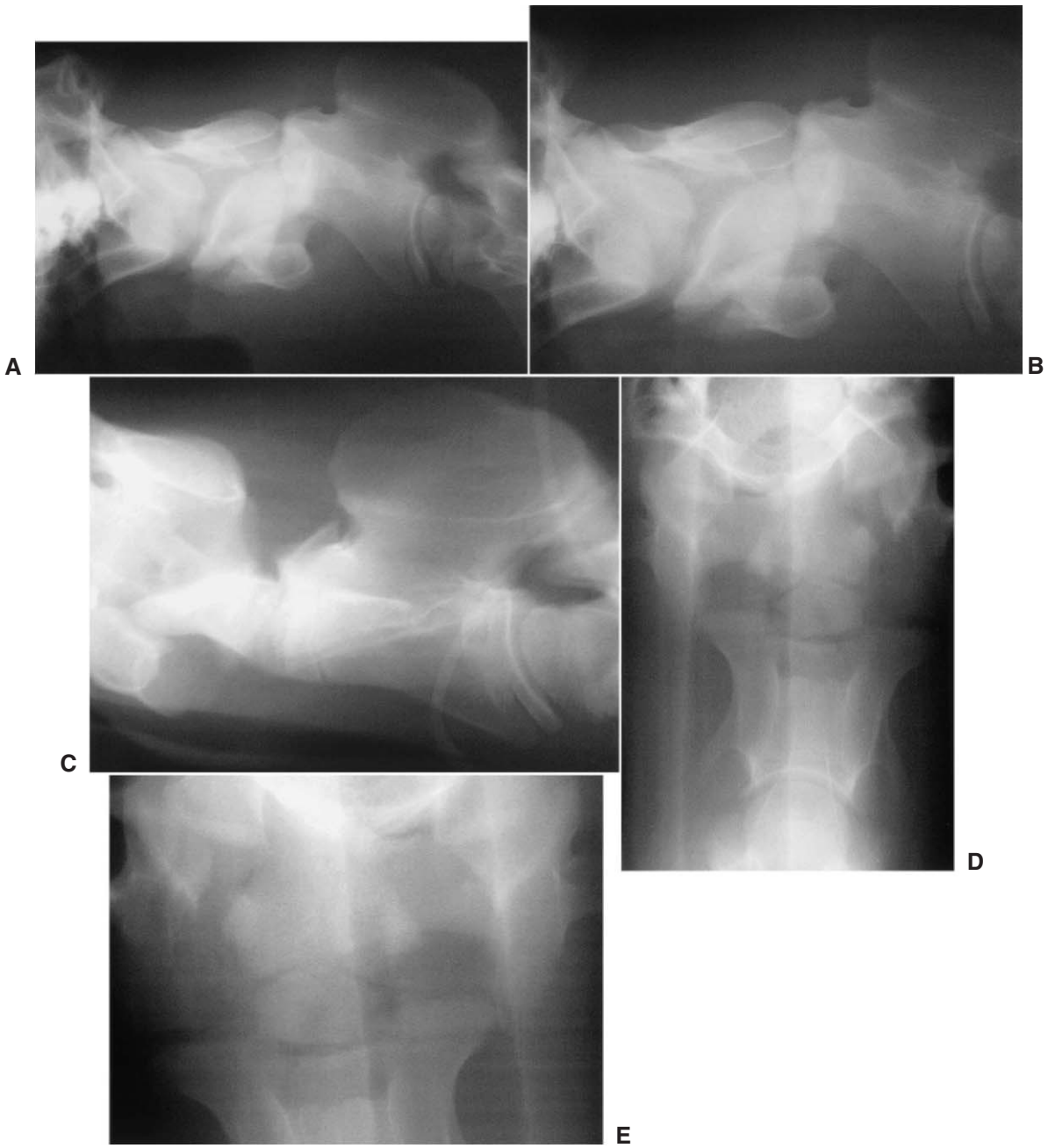


Figure 28-7 • Lateral **(A)** and close-up lateral **(B)** views of a fracture-dislocation of the C1-2 spinal unit in which the dens has been snapped off and the remainder of C-2 arches caudally, obliterating the associated portion of the spinal canal in the process. The cranial cervical spine of a normal foal is provided for comparison **(C).** Because the foal was unconscious, and *its neck safely braced*, ventrodorsal views **(D, E)** were made that show a degree of displacement not fully appreciable in the initial lateral views.

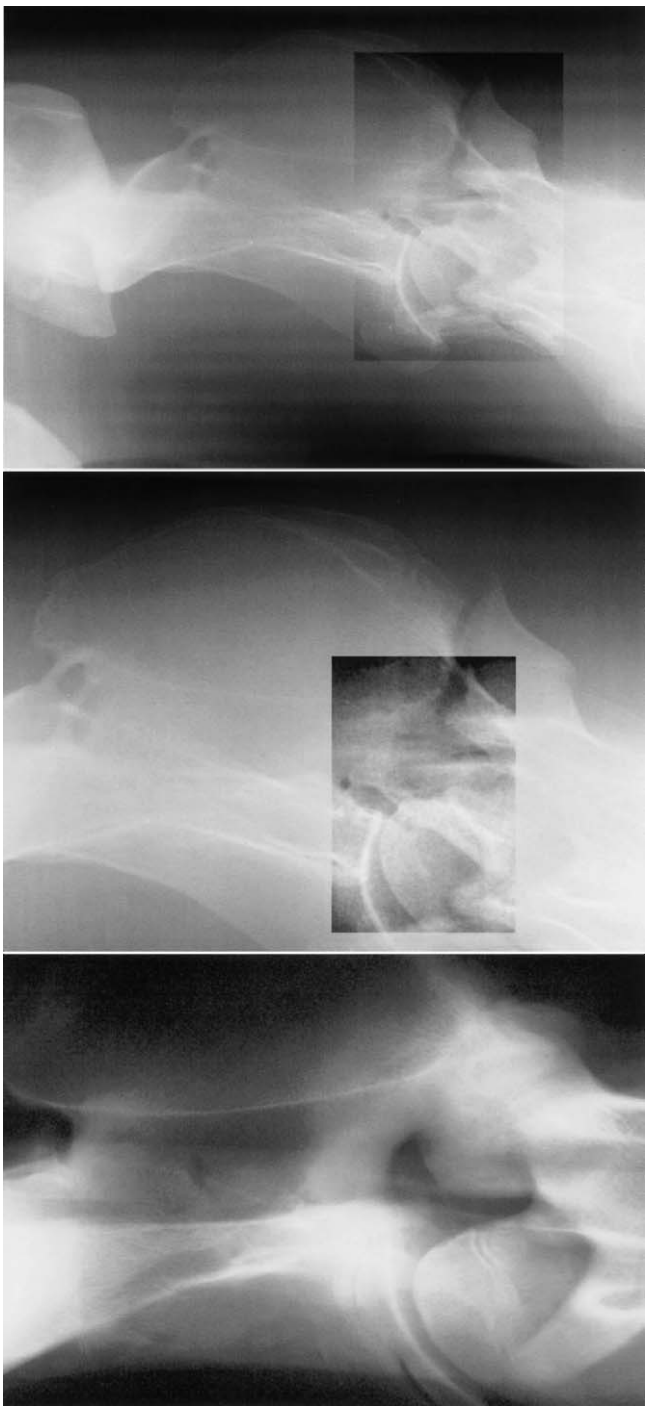


Figure 28-8 • Lateral **(A)** and close-up lateral **(B)** views of the C2-3 spinal unit show mild dorsal dislocation of C-3, with paired facetal fractures and only mild narrowing of the spinal canal *(emphasis zone)*. A normal C2-3 spinal unit is provided for comparison **(C).**

termed a *position of protection,* and an involuntary neck deformity is to anesthetize the horse and see whether or not the torticollis persists.

Dollar[6] was among the first to describe the principal causes of acquired torticollis in the horse, which included the following:

1. Cervical fracture-dislocation
2. Unilateral cervical muscle contracture
3. Unilateral cervical muscle rupture
4. Unilateral cervical muscle paralysis

Sometime later, McKelvey and Owen[7] reported four additional causes of acquired equine torticollis, including the following:

1. Skull fracture
2. Neurogenic, unilateral muscle atrophy
3. Unilateral muscle degeneration (dystrophic myodegeneration)
4. Intervertebral disk rupture

Posttraumatic Cervical Osteoarthritis

Displaced cervical fractures may potentially lead to osteoarthritis, depending on the degree of fragment displacement. Even a small amount of incongruity, especially if it involves a facetal joint, can produce neck pain and accompanying disability; however, such changes are nearly impossible to detect reliably on radiographs, although they may be detectable using computed tomography (CT).

Partial cervical dislocations, or more usually fracture-dislocations, frequently leave a radiographically visible aftermath, typically in the form of one or more deformed, arthritic facetal joints. Chronic subluxations of the occipitocervical joint are particularly susceptible to posttraumatic osteoarthritis.

When foals and juvenile horses sustain serious cranial neck injuries, they are not always paralyzed or even paretic, probably because of the relatively large size of the spinal canal compared with that of the cord. In any event, skeletally immature animals often "cope" under such circumstances by undergoing significant remodeling of the damaged or dislocated vertebral unit. At other times, the injured bone appears to make little or no accommodation to its injury.

Radiographic Findings. Radiographically, posttraumatic cervical osteoarthritis, especially of the occipitoatlantal joint, is usually associated with an alteration in the width of the cartilage space, as seen in lateral projection. As a general rule, assuming there are no images of the original injury, the wider the joint space, the greater the probability of a previous occipitoatlantal dislocation, fracture, or fracture-dislocation (Figure 28-10). Conversely, the narrower the cartilage space, the greater the likelihood of a comparatively minor injury, albeit one that has led to osteoarthritis (Figure 28-11).

Posttraumatic osteoarthritis of the middle and caudal cervical spinal units is difficult to establish radiographically. In most instances, the diagnosis is made *inferentially* on the basis of indistinct facetal joints, marginal bone deposition, or a combination of

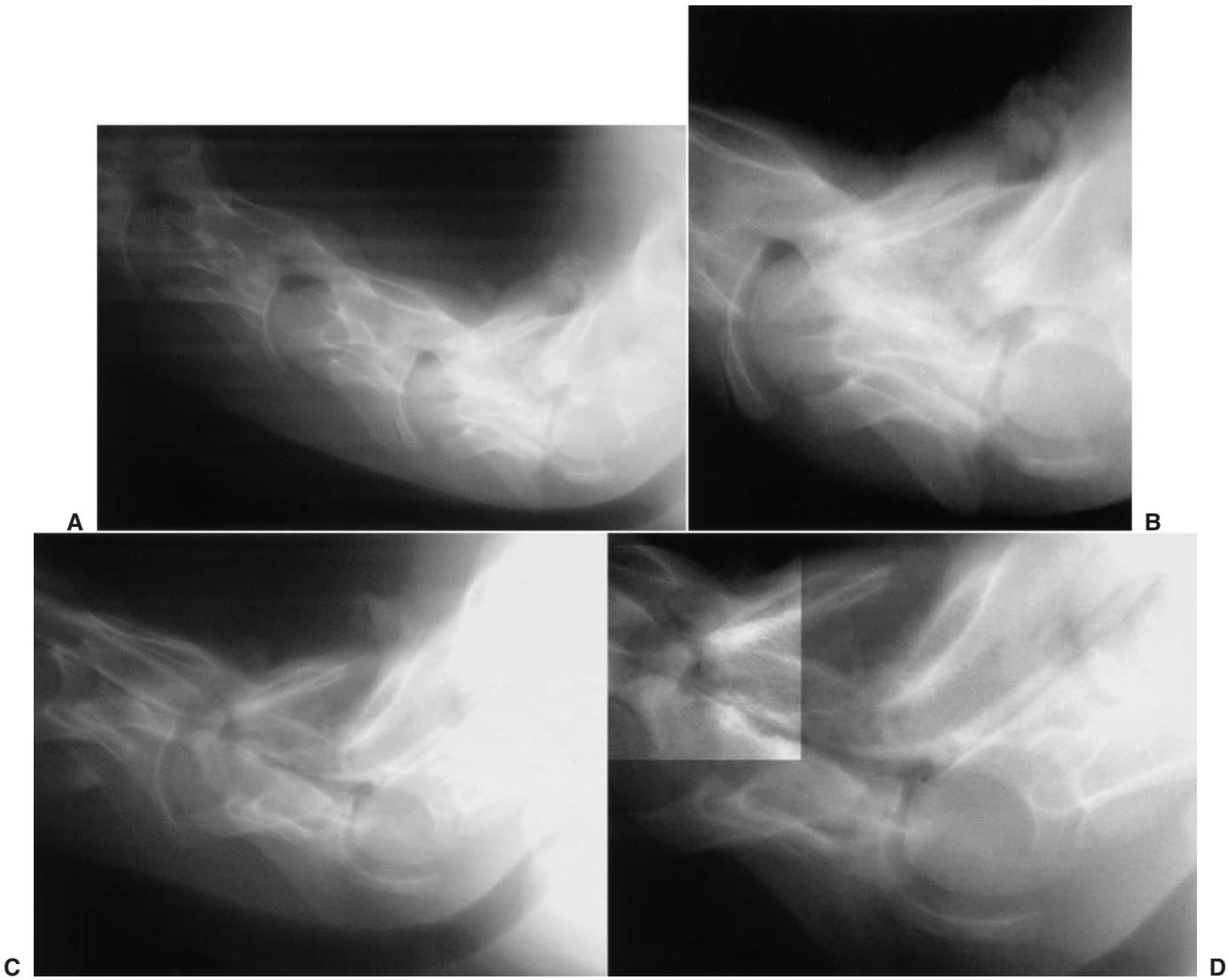


Figure 28-9 • Nonstress lateral **(A)** and close-up lateral **(B)** views of the neck of a foal that recently ran head on into a wall shows a severely displaced, *pile-driver fracture-dislocation* of the C5-6 spinal unit. A lateral myelogram **(C),** including close-up **(D),** was performed at the request of the owners and their insurance company, which showed the most severe cord compression (and presumed injury) at the center of the C4-5 unit, not the C5-6 unit, where it was originally predicted.

the two. The same abnormalities have also been used to *infer* vertebral instability (wobbler) in horses. CT, if available, is the superior method of evaluating known and suspected cranial cervical lesions in the horse.

Primary Osteoarthritis of the Cervical Spinal Region

As far as I am aware, the incidence of primary degenerative osteoarthritis of the cervical spinal region of the horse, in particular the occipitoatlantal joint, is not known. I, and others, have reported cases of idiopathic osteoarthritis of the cervical region of horses, but most such accounts have dealt with young or middle-aged animals, suggesting that trauma continues to be the most likely explanation for such findings.

Cervical Osteoarthritis Secondary to Congenital Facetal Joint Asymmetry (Without Associated Incoordination)

This is a genuine problem area. Some ataxic horses, as well as some normal horses, have multiple bone deposits on the margins of one or more of their cervical facetal joints, especially caudally. As mentioned

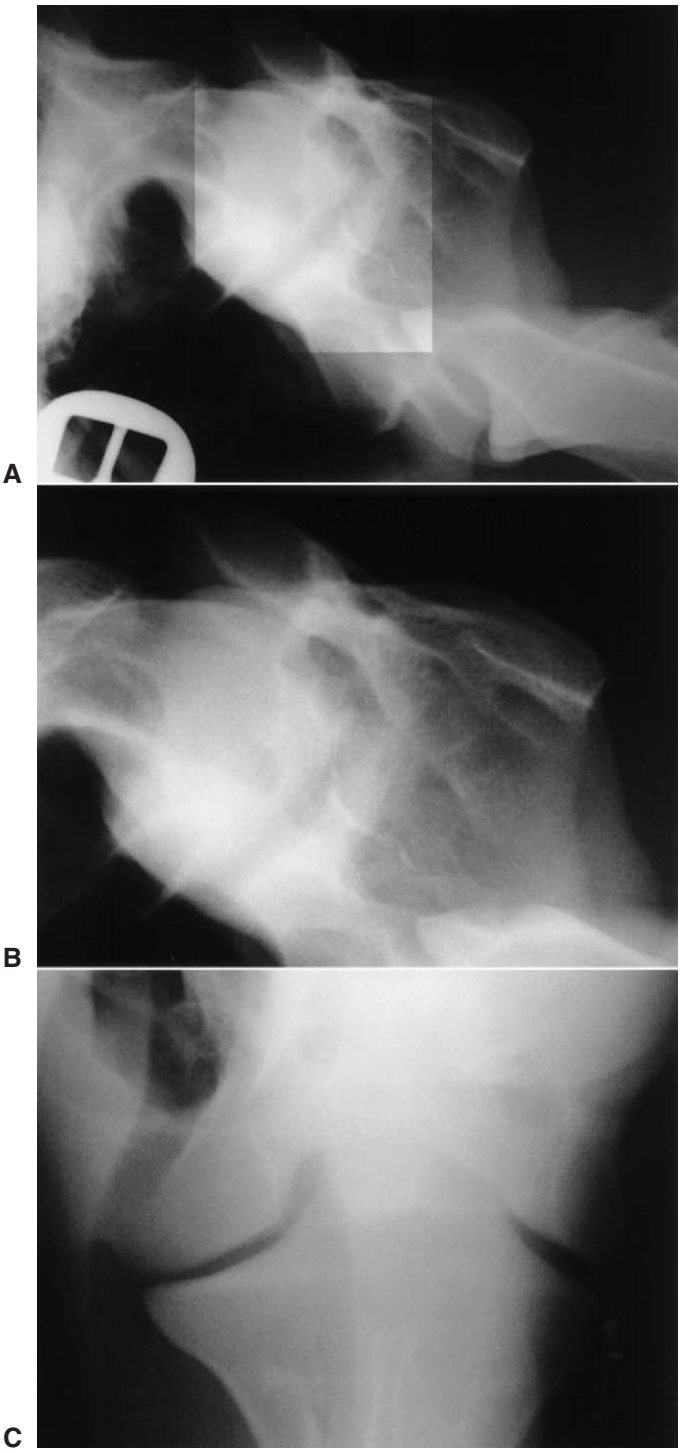


Figure 28-10 • Posttraumatic osteoarthritis: Close-up lateral **(A)** and ultra-close-up lateral **(B)** views of an arthritic occipitoatlantal joint, the result of a previous fracture-dislocation. The C2-3 spinal unit appears uninvolved as seen in a ventrodorsal view **(C).**

earlier, such findings have been offered as inferential evidence in support of secondary osteoarthritis, prompted by a variety of diseases. Depending on the context, this explanation may seem plausible, especially in the ataxic horse or in the horse with pain, but what of the clinically normal animal in which such changes are found? The question remains: incidental finding, source of neck pain, or harbinger of future disability?

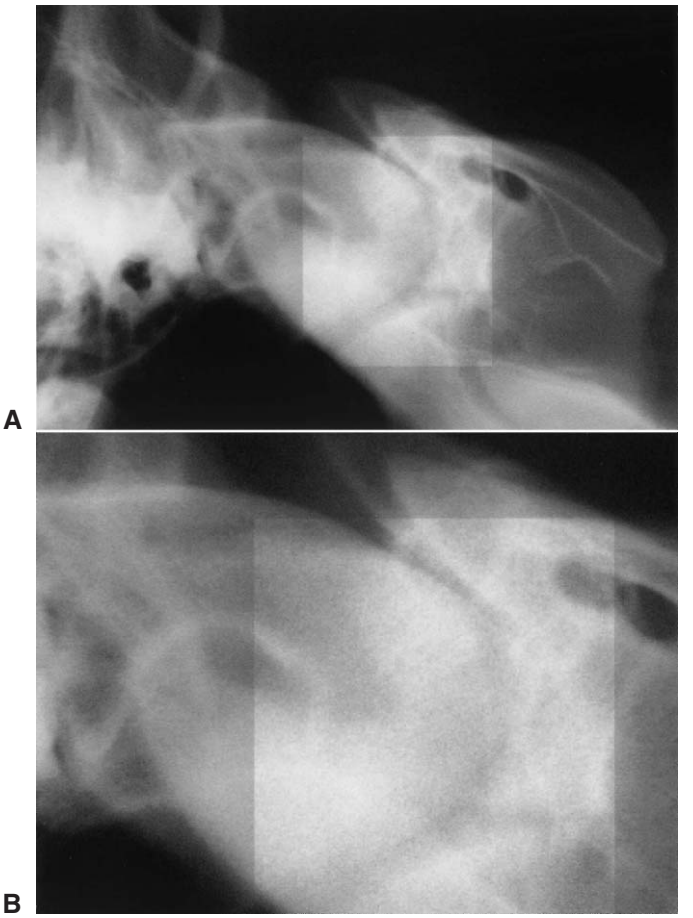


Figure 28-11 • Posttraumatic osteoarthritis: Close-up lateral **(A)** and ultra-close-up lateral **(B)** views of an arthritic occipitoatlantal joint found at necropsy and attributed to a previous nondisplaced fracture.

▮▮▮ CERVICAL VERTEBRAL INSTABILITY (WOBBLER)

What Is Cervical Vertebral Instability?

The precise cause (or causes) of cervical vertebral instability remains in doubt, although there has been, and continues to be, much speculation (Table 28-1).[8,9] In any event there appears to be no lack of names for this unusual disorder: cervical vertebral instability, cervical spondylopathy, cervical vertebral malformation, cervical ataxia, wobbler's, wobbler syndrome). I have chosen to entitle this section Cervical Vertebral Instability (Wobbler) because of personal preference—and for no other reason. I leave it to the reader to select your favorite designation as well, but be prepared to defend your choice because the "proper" naming of this disease can lead to heated debate.

Table 28–1 • PROPOSED CAUSES OF EQUINE WOBBLER DISEASE

Cause	Comment
Spinal injury	Spinal fracture or dislocation, spinal cord contusion, spinal cord laceration
Congenital spinal deformity (also known as cervical vertebral malformations)	Particularly that which narrows or encroaches on the spinal canal or intervertebral foramina Occipitoatlantoaxial malformations are most common
Abnormal, especially asymmetric, facetal joints	Usually congenital but occasionally the result of polyarthritis
Intervertebral disk rupture or bulge	May be secondary to trauma or spontaneous but is usually caused by primary degenerative disease
Encroaching spondylosis	Rare but when it occurs nearly always compresses a nerve root rather than the spinal cord
Spondylitis	A bit of a stretch
Diskospondylitis	Like spondylitis, a bit of a stretch
Encephalomyelitis	Various etiologies
Epidural tumor	Epidural melanoma, plasma cell myeloma, and lymphosarcoma[37]
Granuloma	Affecting brain or spinal cord or both
Abscess	Affecting brain or spinal cord or both
Equine cerebrospinal nematodiasis	Presumed due to *Strongylus vulgaris*[38]
Equine protozoal myeloencephalitis	*Sarcocystis*
Equine degenerative myelopathy	No radiographic changes; requires MR
Fibrocartilaginous embolism	No radiographic changes; requires MR
Equine infectious anemia	No radiographic changes; requires MR
Cerebellar disease	No radiographic changes; requires MR
Congenital venous malformation	No radiographic changes; requires MR

MR, Magnetic resonance.

Radiography

Plain Films. Radiography for the purpose of confirming suspected wobbler's disease is the same as that used for fractures and other cervical disorders, with one exception. Because some forms of cervical vertebral instability become apparent only when the neck is flexed, conventional radiographs may have to be supplemented with stress radiography.

Natural Stress Radiography. In addition to conventional cervical radiographs, I often employ a *feeding stress maneuver,* in which a suspected wobbler is encouraged to flex its neck naturally by placing a feedbag or bucket full of feed on the floor in front of the horse. The exposure is then made while the animal is eating and the neck is maximally flexed.

The feasibility of this procedure in a particular animal can be easily assessed by first offering the horse a small amount of food and observing its reaction, in particular its stability (Figure 28-12). If the animal has difficulty reaching the food or if it staggers, move the food closer to the head. Once the examination parameters are set, bring the x-ray machine over and make the radiographs (Figure 28-13). I always make at least two films (often three) so that I can be confident in the repeatability of my finding. A lateral view of a defleshed skull and cervical spine is provided for anatomic reference.



Figure 28-12 • Photograph of a horse with cervical vertebral instability about to eat a small amount of feed off the floor before natural stress radiography of the cervical spinal region was done.

Plain-Film Assessment

Normal Anatomy. Rendano and Quick published a concise, highly informative review of the cervical spine of the horse, which emphasizes normal radiographic anatomy.[10] The following "cervical facts" are taken from this publication (Box 28-1).

Abnormal Anatomy. Papageorges and co-workers reported that in a series of 306 ataxic horses that underwent both plain-film and myelographic diagnosis, the former proved diagnostically inferior and in many instances resulted in false-positive or false-negative errors.[11] Radiographic criteria for spinal ataxia included the following:

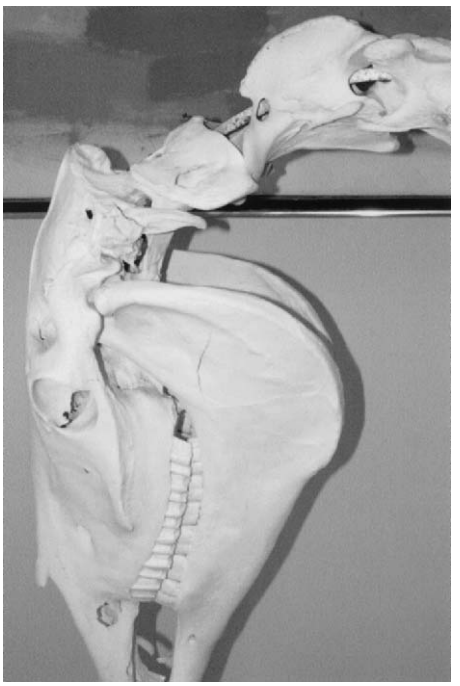


Figure 28-13 • Equine skeleton with the head and neck flexed in a manner similar to that seen when a horse reaches to the floor to eat, the desired posture for a natural stress radiograph in a suspected wobbler.

Box 28-1
Important Anatomic Features of the Cervical Spinal Region of the Horse

There are normally seven cervical vertebrae. If only six are visible, check for congenital fusion (*blocked vertebrae*), or ribs on C7.
The first cervical vertebra (the *atlas*) is roughly shaped like a vertically compressed ring, featuring a pair of stubby wings, each of which is perforated by two small openings: the *alar foramina* cranially and the *transverse foramina* caudally. There are also small *lateral foramina* located in the dorsal arch of C1 adjacent to the alar foramina.
The roof of the spinal canal through C1 appears as a linear density in a lateral radiograph, but the floor of the canal is invisible.
C2, also known as the *axis,* has a very large rudderlike *dorsal spinous process* and a snoutlike, upwardly inclined cranioventral element known as the *dens*.
Paired *lateral foramina* are located along the cranial edges of the vertebral arch of C2, which in most horses is incomplete until about 2 years of age.
The radiographic appearances of C3-5 are similar, with each vertebra sharing of number of common features including (1) vertebral body, (2) ventral crest, (3) cranial and caudal articular facets, and (4) transverse processes.

- Remodeling of the caudal aspect of the floor of the vertebral canal
- Proliferative response (new bone) at the articular process
- Apparent narrowing of the vertebral canal in standard lateral and stress views: ventroflexion and traction

Radiographic Disease Indicator. In my opinion, the premier and most reliable plain-film radiographic disease indicator (RDI) of cervical vertebral instability in horses (and dogs) is *malalignment*. Combined with cervical myelography, one should be able to confirm or deny the presence of related cord compression in most instances. As mentioned previously, CT is even more sensitive; however, it is often impossible to get the caudal cervical region deep enough into the bore so that it can be imaged. In this circumstance, one is then forced to rely on radiography.

Other potential RDIs related to wobblers include facetal arthritis and malformed vertebral bodies, the latter often nonspecifically described as remodeling. Stenosis of the spinal canal potentially can be detected in either plain or contrast films. In this regard it goes without saying that one must be able to distinguish the normal range of cervical flexion, especially as seen during stress radiography. It is also imperative to appreciate that during stress radiography the C4-5 spinal unit is the most flexible point in the neck. Because this is also a likely lesion location, the potential for false-positive diagnosis exists.

Figures 28-14 through 28-17 show a variety of plain-film abnormalities likely to be seen in wobblers when using conventional or stress radiography.

Myelographic Assessment

Metrizamide Myelography in Normal Horses. Nyland and co-workers reported the clinical, radiographic, and pathologic findings in seven normal horses that underwent cervical myelography using a dose of 57 ml of isotonic metrizamide administered via a cervical puncture.[12] Neutral (head in natural position) flexed and extended lateral views were considered to be of excellent quality, but only cranial ventrodorsal projections were of any use diagnostically.

Although no postprocedural seizures occurred, one horse was mildly ataxic on recovery. All the animals were depressed and febrile for at least 5 hours after recovery but fully recovered within 1 to 2 days. Five horses necropsied 48 hours after myelography showed mild, acute suppurative meningitis of the brain and spinal cord, attributed to the contrast medium.

Myelographic Contrast Media, Image Quality, and Procedural Risk

Image Quality. Maclean and co-workers were among the first to declare iohexol to be superior to metrizamide for equine myelography, finding it safer, less expensive, and of superior diagnostic quality.[13] I share this view.

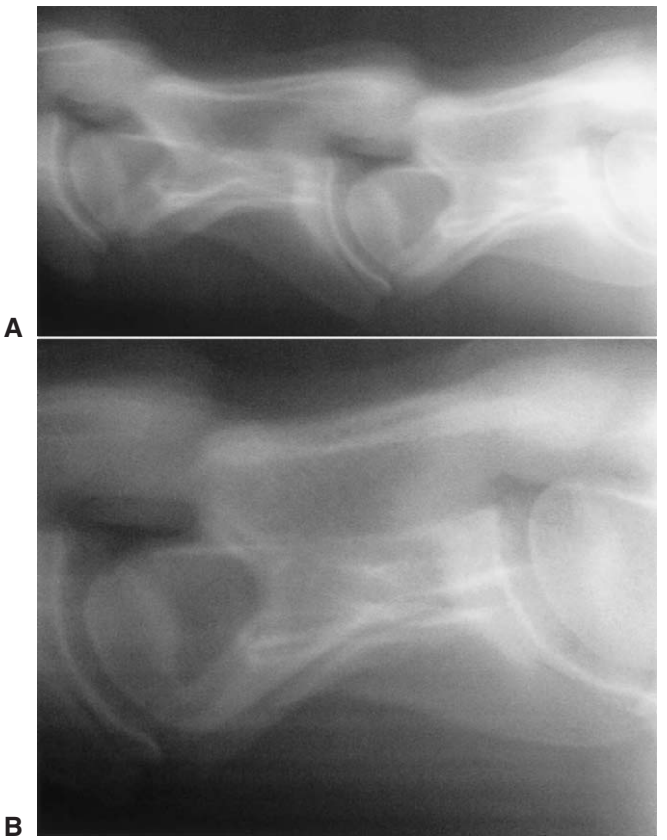


Figure 28-14 • Lateral **(A)** and close-up lateral **(B)** views of the midcervical region of a yearling filly with cervical vertebral instability show malalignment of both the C4-5 and C5-6 spinal units.

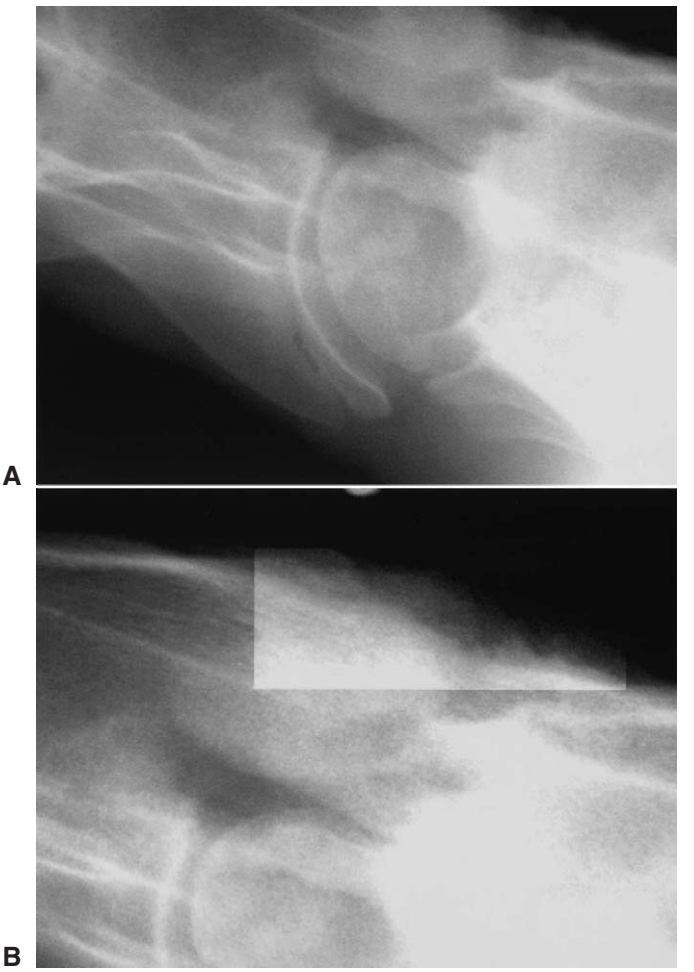


Figure 28-15 • Arabian yearling with ataxia and hindlimb weakness. **A,** Close-up lateral view of the spinal canal centered on the C3-4 unit shows mild subluxation and stenosis of the overlying spinal canal. **B,** An ultra-close-up view of the same unit, but centered on the facetal joints, shows new bone deposition consistent with secondary osteoarthritis.

A decade later, Widmer and co-workers compared the relative merits of metrizamide and iohexol for use in equine cervical myelography, concluding that although there was no significant difference in myelographic quality, iohexol was safer and caused fewer postprocedural seizures.[14]

Procedural Risk. The precise manner in which diagnostic contrast media injure nervous tissue, especially the spinal cord and brain, is not known, although theories abound. Suffice to say that risks exist, although they are not extensively documented. In addition to procedural risks, the associated anesthesia and recovery are also potentially dangerous owing to the marked instability typically exhibited by wobblers, which is exaggerated by sedatives and anesthetic gases (Figure 28-18).

Using metrizamide (35 to 40 ml, 180 mg iodine per milliliter), Hubbell and co-workers reported that the combination of general anesthesia and myelography posed a serious risk to horses, especially those that were moderately ataxic.[15] Many animals were reported to be neurologically worse after recovering from anesthesia.

Using iohexol (20 ml, 300 to 350 mg of iodine/milliliter), Maclean and co-workers reported myelography performed under general anesthesia to have no serious clinical or neurologic side effects.[16]

Lesion Probability. According to Papageorges and co-workers, the C4-5 spinal unit is at greatest risk, followed by C6-7, C5-6, and C4-5. The overall probability of detecting a cervical lesion using myelography was about 60 percent, with about 30 percent of these having multiple lesions.

Employing a much smaller patient group (14 animals), Conrad reported a very different lesion distribution, headed by the C3-4 spinal unit, followed by C2-3 and C4-5.[17]

The Normal Nonstress Myelogram. Figures 28-19 through 28-21 show a normal myelogram in an adult horse, which can be compared with cervical images of horses suspected of having cervical vertebral instability or congenital spinal canal stenosis.

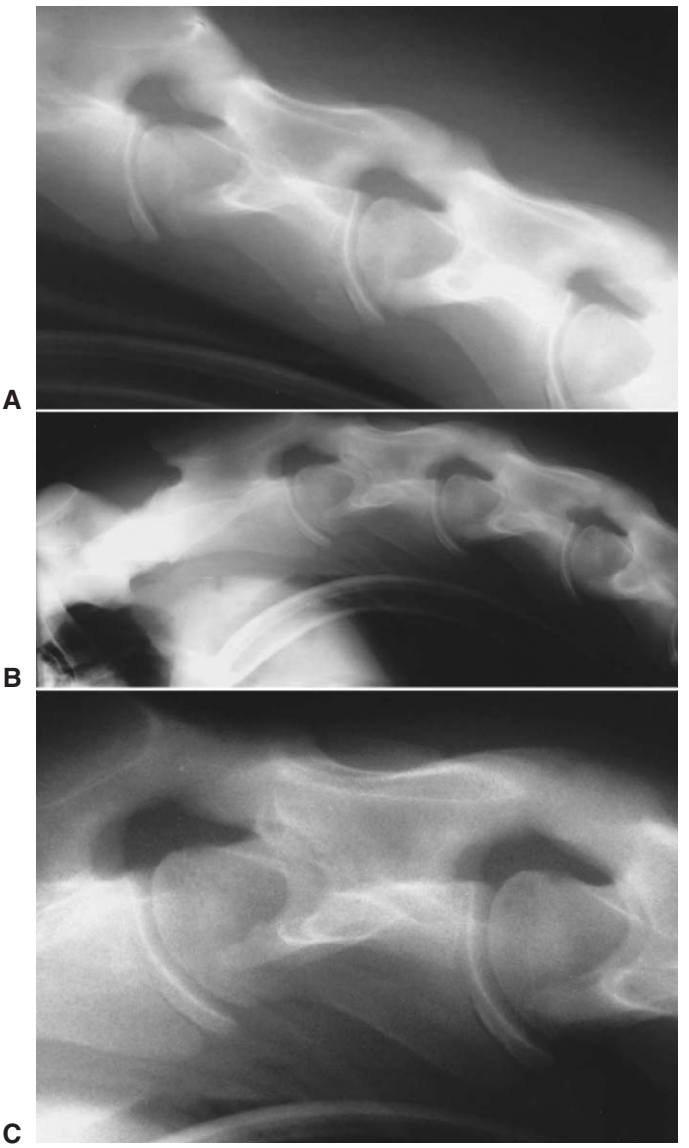


Figure 28-16 • Nonstress lateral radiograph **(A)** of the mid-cervical region of an ataxic foal shows mild subluxation and associated spinal canal stenosis of the C3-4 spinal unit. Flexed lateral **(B)** and close-up flexed lateral **(C)** views of the same region show increased C3-4 dislocation, as well as malalignment of the C4-5 unit (not appreciable in the nonstress view).

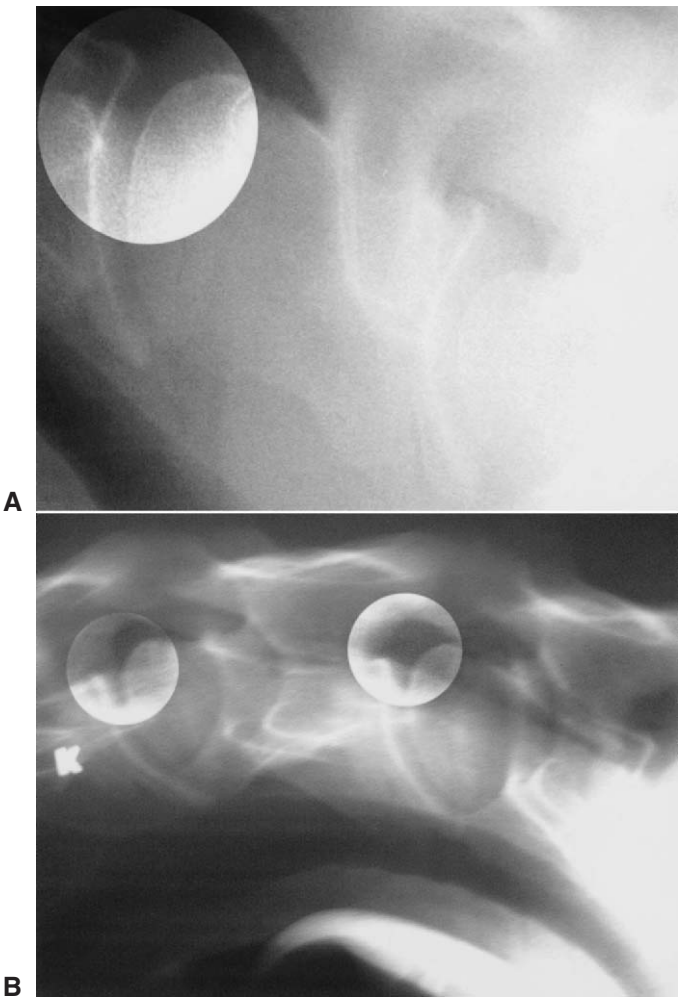


Figure 28-17 • A close-up nonstress lateral view **(A)** of the C5-6 spinal unit appears normal, but a subsequent flexed lateral view **(B)** clearly shows subluxation of the C5-6 and C4-5 units, again attesting to the value of stress radiography.

Fulcrum-Assisted Ventroflexion, Dorsiflexion, and Lateroflexion Stress Radiography. Rantanen and co-workers published an excellent pictorial essay, which includes examples of hyperflexion, hyperextension, and traction stress maneuvers.[18]

A Cautionary Note. Fulcrum-assisted stress radiography should be done only by experienced personnel (preferably large animal radiologists), especially where vertebral malalignment is identified in non-stress plain films because of the potential for further injuring the spinal cord. The ventroflexion stress maneuver *must not be maintained* any longer than absolutely necessary if a nonreinforced endotracheal tube is used (Figure 28-22). Even if a guarded tube is employed, cervical flexion time should be as brief as possible, and never maintained beyond the time required to make the exposure,

Myelographic Diagnosis

Dural Pinching. The principal myelographic indicator of spinal cord compression causing ataxia is dural pinching. According to Papageorges, reduction of the widths of both the dorsal and ventral aspects of the thecal sac by at least 50 percent is diagnostic. My own view in this regard is that, as with any radiometrics, numbers, especially of this sort, should not be used in isolation. Better to integrate the *50 percent rule* with any other radiographic abnormalities, such as diskal indentation, cord lift, or abnormal angulation, as detailed in the following section.

Diskal Indentation. Diskal indentation of the ventral surface of the dural sac, as observed in a flexed lateral



Figure 28-18 • Anesthetist ministers to an unconscious suspected wobbler before cervical myelography. Recovery of a horse with cervical vertebral instability is always potentially dangerous to both the animal and attending personnel alike.

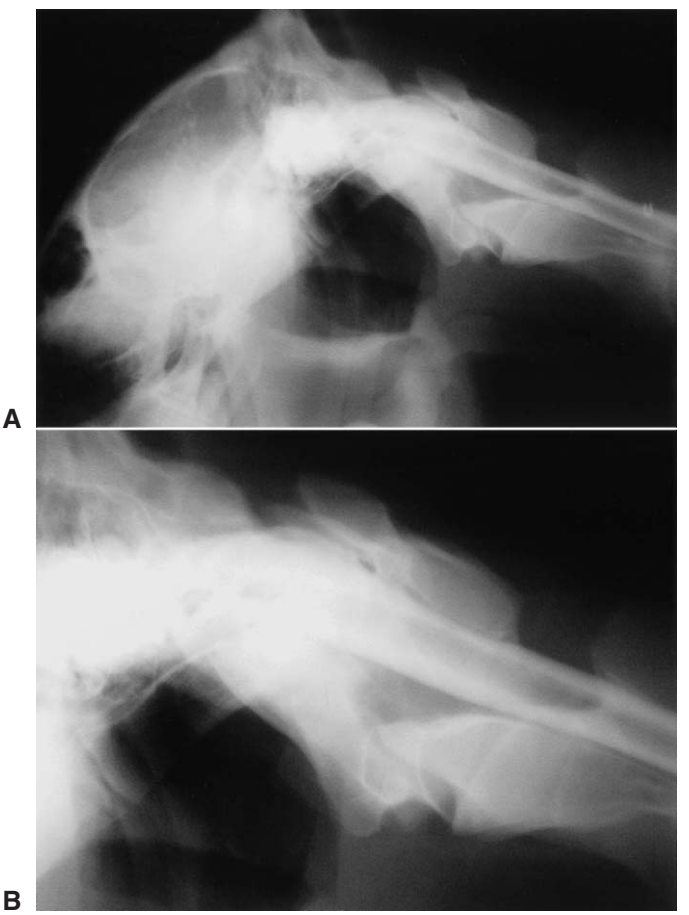


Figure 28-19 • Lateral **(A)** and close-up lateral **(B)** myelograms of the *cranial* portion of the cervical spinal region of an adult horse.

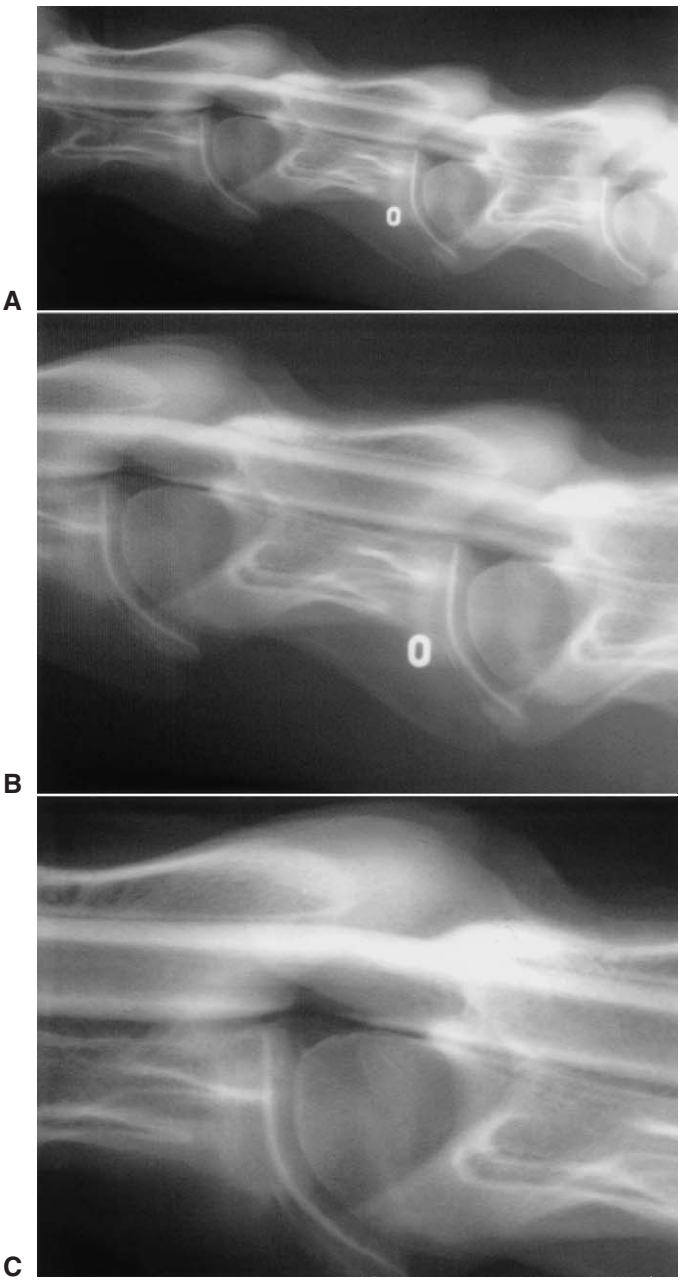


Figure 28-20 • Lateral **(A),** close-up lateral **(B),** and ultra-close-up lateral **(C)** myelograms of the *central* portion of the cervical spinal region of an adult horse.

view of the neck, is a normal radiographic variation, which becomes more pronounced with increased flexion and a caudally positioned fulcrum. Some of these variants are shown in Figure 28-23.

Cord Lift. Cord lift is the dorsal displacement of the dural sac and spinal cord; it typically accompanies moderate to severe vertebral malalignment in horses with cervical vertebral instability (Figure 28-24).

Abnormal Cord Angulation. Vertebral malalignment often leads to an abnormally angular spinal cord and

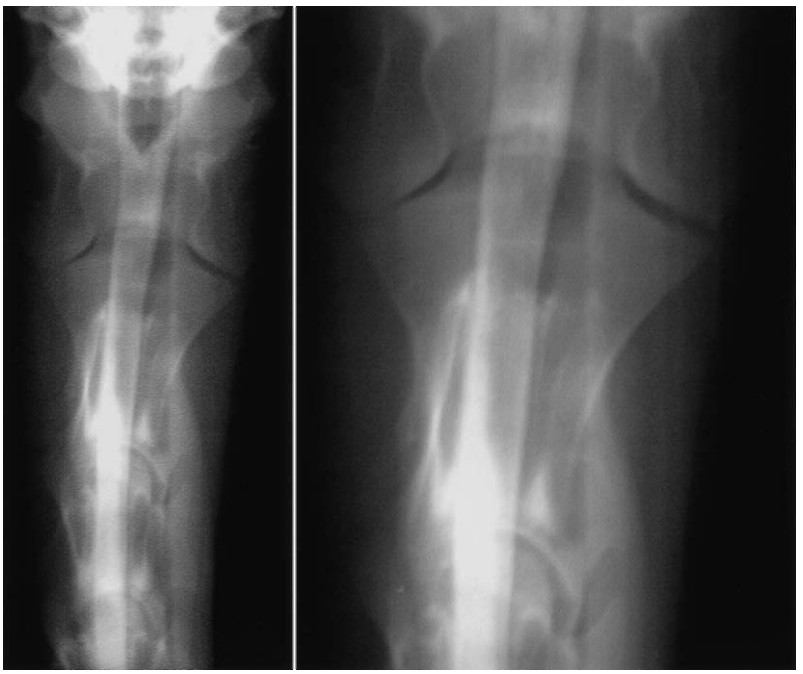


Figure 28-21 • Ventrodorsal **(A)** and close-up ventrodorsal **(B)** myelograms of the cranial portion of the cervical spinal region of an adult horse.



Figure 28-22 • Ventroflexion stress maneuvers may cause nonreinforced endotracheal tubes to kink, causing a reduction or cessation of airflow.

dural sac; these myelographic features are often associated with cervical cerebral instability. An abnormally angled caudal cervical spinal cord is shown in Figure 28-25.

"Dynamic Versus Adynamic Lesions": An Artificial Distinction. It is indisputable that stress views of the cervical spinal region, especially during ventroflexion, are capable of revealing vertebral dislocation that cannot be demonstrated otherwise (Figure 28-26); but describing cervical cord lesions as variable or not (i.e., dynamic/adynamic) based on comparing different stress maneuvers performed in conjunction with myelography has little or no diagnostic value because it rarely serves to do more than state the obvious, or at least what *should be* the obvious. The terms *dynamic* and *adynamic* may sound impressive, but they serve little purpose given the fact that nearly all cervical lesions in the horse change to some degree during stress myelography.

The physical relationship that exists between the supple spinal cord and its protective dural sac and its hard but flexible bony encasement *guarantee* variations in the size, shape, and position of the contrast-filled dural sac when the head and neck are manipulated during myelography.

A More Logical Approach

A more logical and realistic approach to the radiographic-myelographic assessment of cervical spinal disease in horses is whether or not the spinal cord is being compressed when the cervical spine is in a natural or nonstressed position. Using a modification of Breton's classification,[19] compressive spinal cord lesions may be divided as follows:

1. *Static cervical stenosis:* Dislocation or spinal canal stenosis, which is consistently demonstrable during myelography, while the head and neck are in natural, nonstressed positions.
2. *Dynamic cervical stenosis:* Dislocation or spinal canal stenosis, which is consistently demonstrable during myelography, while the head and neck are being stressed with one or more of the following

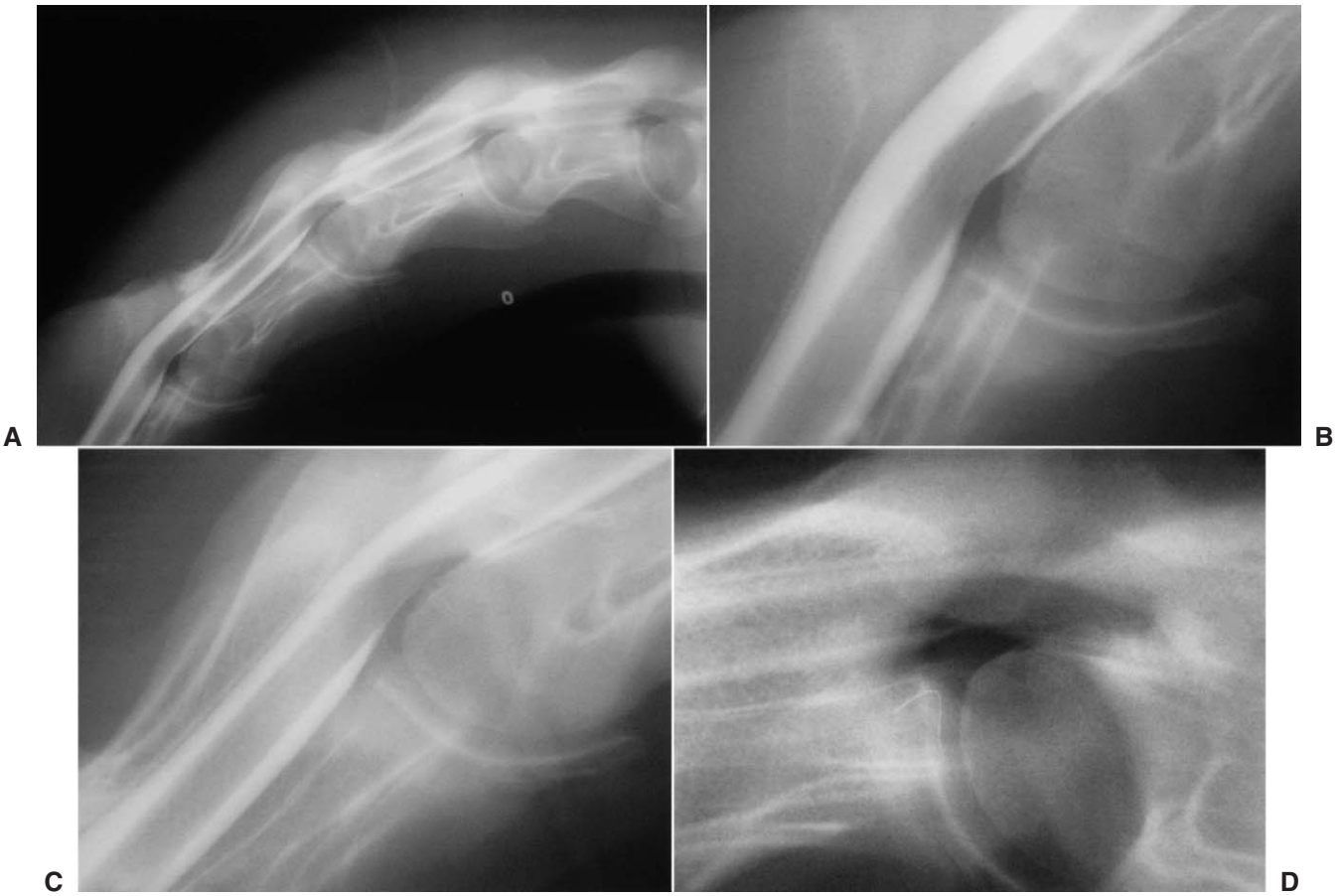


Figure 28-23 • Flexed lateral **(A)** view of the central cervical region shows normal variation in diskal indentation at the level of C2-3 **(B),** C3-4 **(C),** and C4-5 **(D).**

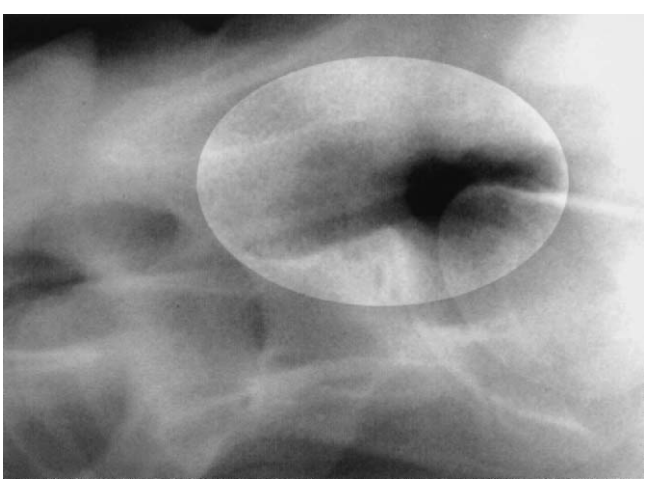


Figure 28-24 • Ultra-close-up, ventroflexed, midcervical myelogram shows partial dislocation of the C3-4 spinal unit associated with pronounced cord-lift.

maneuvers: (1) ventroflexion, (2) dorsiflexion, (3) lateroflexion, or (4) traction.

3. *Combined static-dynamic cervical stenosis:* Stenosis of the cervical portion of the spinal cord, consistently observed during myelography, with and without supplementary stress maneuvers (Figure 28-27).

Myelographic Misdiagnosis

Failure to Flow. Arguably, failure to flow is the most common source of myelographic misdiagnosis. As far as I am aware, the cause or causes of this important phenomenon are not known. Failure of the organic iodine contrast media to go into solution, with cerebrospinal fluid resulting in opacification of the dural sac and outlining of the spinal cord, is usually apparent in the initial images at the level of the C1-2 spinal unit. In most instances, the contrast solution gradually mixes with the cerebrospinal fluid, eventually leading to a diagnostic study. However, the time to complete the process can be quite variable, in some instances, 30 minutes or more. Changing the position of the horse from one side to the other may help. Of course the principal concern when this occurs is how long the horse can remain down, even on a well-padded surface. A failure-to-flow sequence is shown in Figure 28-28.

Factors That May Adversely Affect Myelographic Diagnosis. A variety of factors have been incriminated in equine myelographic misdiagnosis, all of which must be considered in the course of analyzing and interpreting equine myelograms. The most important of these appear in Box 28-2.

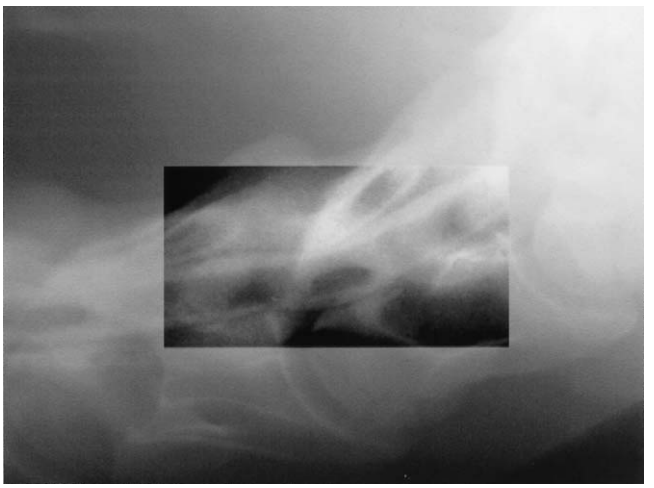


Figure 28-25 • Close-up, dorsoflexed, caudal cervical myelogram shows subluxation of the C6-7 spinal unit, dorsal and ventral pinching of the dural sac, and abnormal cord angulation.

Box 28-2
Factors That May Adversely Influence the Accuracy of Myelographic Diagnosis in the Horse*

- Normal variation in the size of the subarachnoid space (smaller space will be more readily narrowed by stress radiography).
- Normal variation in the size of the spinal canal (smaller canal will more readily deform dural sac during stress radiography).
- Lateral (versus ventral) cord compression (where there are no ventrodorsal views).
- The dynamic nature of most compressive spinal cord lesions.
- Subjective evaluation of the degree of cord compression based on the appearance of the associated opacified dural sac.
- Epidural hemorrhage.
- Decreased dural opacification related to prolonged examination time.

*Other than poor radiographic technique or nonstandard positioning.

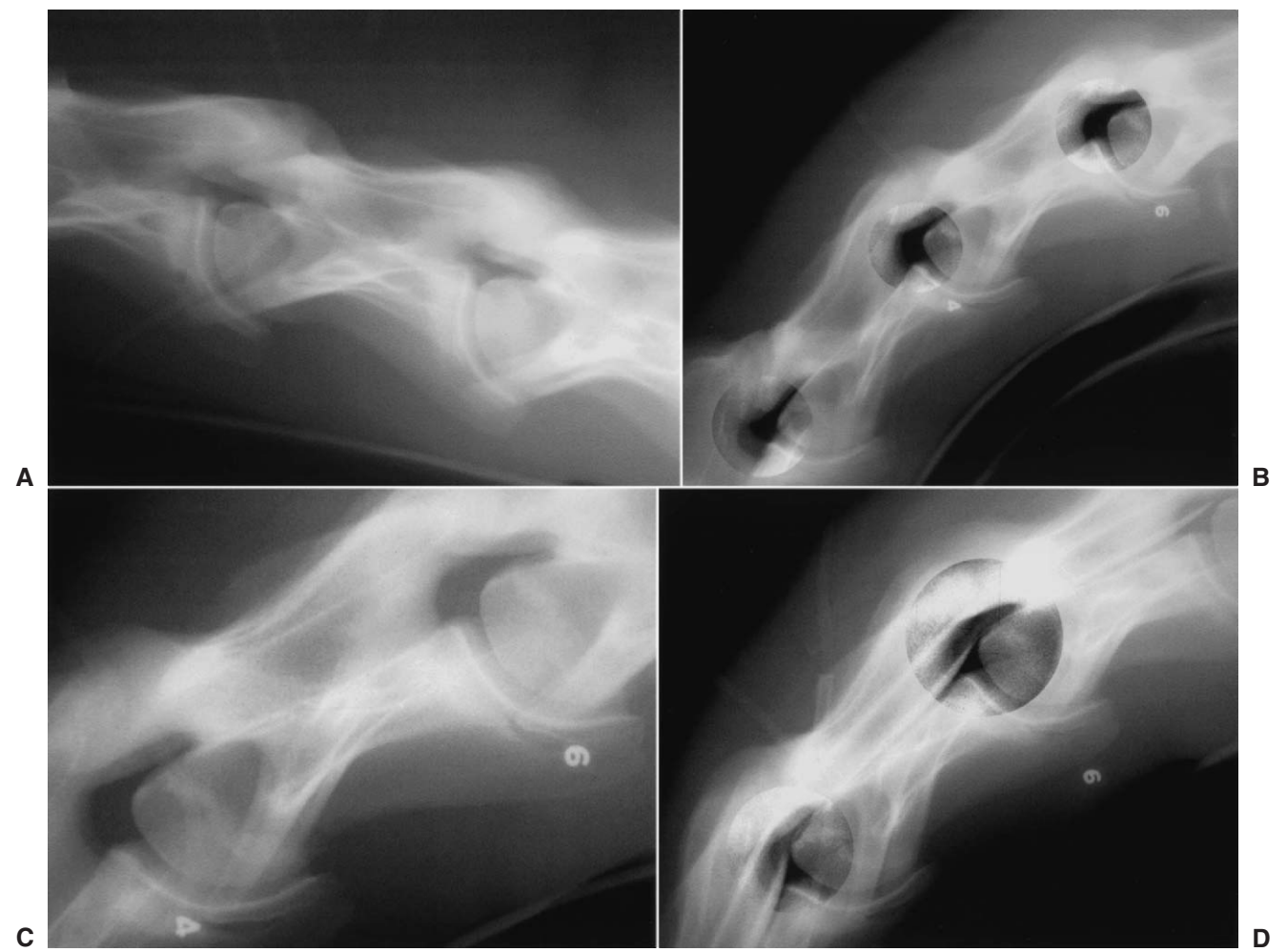


Figure 28-26 • Lateral nonstress view **(A)** of the C3-4 and C4-5 spinal units shows no evidence of vertebral dislocation. However, flexed lateral **(B)** and close-up flexed lateral **(C)** views of the same region show subluxation of both the C3-4 and C4-5 spinal units. Flexed lateral myelogram shows diskal indentation of the ventral aspect of the dural sac but little or no cord-lift **(D).**

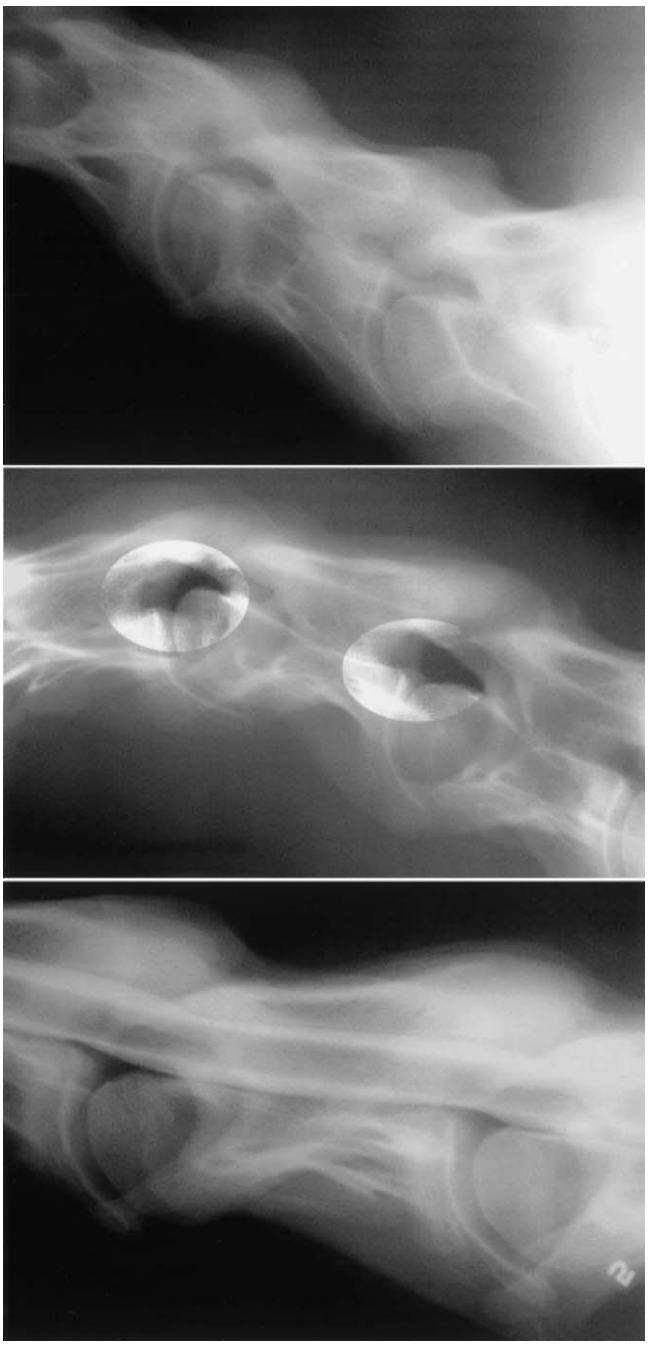


Figure 28-27 • A, Nonstress lateral views of the C4-5 and C5-6 spinal units show mild subluxation of the latter. **B,** A flexed lateral view of the same area shows marked subluxation of the C3-4 spinal unit and stenosis of the cranial vertebral foramen. **C,** A nonstress lateral myelogram of the same region shows an abnormally wavy dural sac and cord, consistent with cervical vertebral instability.

Standing Myelography. Foley and co-workers reported performing myelography in six neurologically normal horses.[20] The quality of the included radiographs was satisfactory, supporting the feasibility of the procedure, although I have not performed standing myelography in a normal or an ataxic horse. While acknowledging the benefits of not having to "drop" and recover an ataxic horse, I have some reservations about the *safety* of the procedure, both from the standpoint of radiation exposure to the radiographers and the possibility that the horse may stumble and fall, injuring itself and others in the process.

▮▮▮ EQUINE PROTOZOAL MYELOENCEPHALITIS IN HORSES

Equine protozoal myeloencephalitis is generally believed to be caused by *Sarcocystis* neuroma; however, recent research suggests there may be an additional or less common cause, *Neospora* spp.[21] Clinically, the disease is difficult to differentiate from wobbler's disease (Figure 28-29).[22]

▮▮▮ CONGENITAL CERVICAL MALFORMATIONS

The Range of Possibilities

Classifying Congenital Cervical Malformations
Cervical Vertebral Instability Versus Cervical Static Stenosis. Powers and co-workers classified congenital cervical malformations in horses as either (1) cervical vertebral instability or (2) cervical static stenosis.[23] In the former instance, typical of midcervical lesions, the vertebrae of one or more individual spinal units move excessively relative to one another, in the process encroaching and eventually damaging nearby nervous tissue.

Static lesions, on the other hand, are more commonly found in the caudal third of the neck and are characterized by permanent stenosis of the spinal canal, frequently initiated by facetal asymmetry and later aggravated by secondary bone and soft-tissue mass effects.

Dynamic Versus Static (Dynamic Versus Adynamic). As mentioned previously, a classification of congenital cervical lesions into two categories—those that change (dynamic) and those that do not change (static, adynamic)—seems both straightforward and intuitive. However, on further consideration, there are problems with such a scheme, particularly with the idea that such a clear-cut distinction is routinely possible using either plain films or myelography.

As Stickle and co-workers showed, so-called static lesions, as seen myelographically, change when subjected to various stress maneuvers, particularly traction and ventroflexion.[24] Thus, I recommend the same diagnostic approach be used with congenital cervical malformations as with cervical vertebral instability (described previously).

Quantifying Congenital Cervical Malformations: Cervical Radiometrics

Mayhew and co-workers published their radiometric approach to quantifying cervical vertebral stenosis in

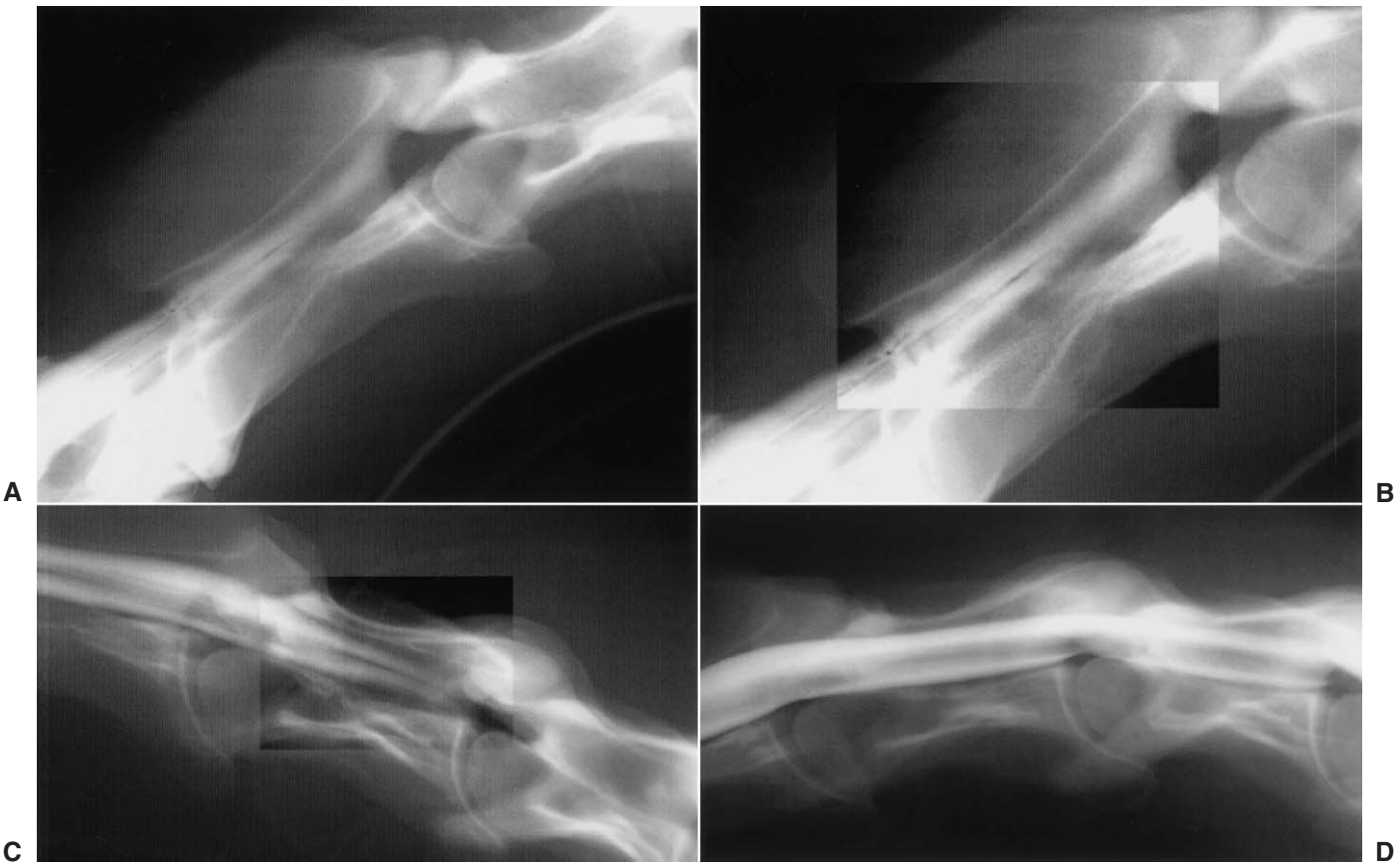


Figure 28-28 • Lateral **(A)** and close-up lateral **(B)** views of a mildly ventroflexed, proximal cervical spine made immediately after administration of diagnostic iodine solution show a gradually elevated, blunted cone of contrast that barely reaches the C2-3 disk, characteristic of failure-to-flow phenomenon. Ten minutes later, the contrast cone has become symmetric and nearly reached the center of the C3-4 unit **(C).** Thirty minutes following injection, the contrast solution has reached the fifth cervical vertebra **(D).**

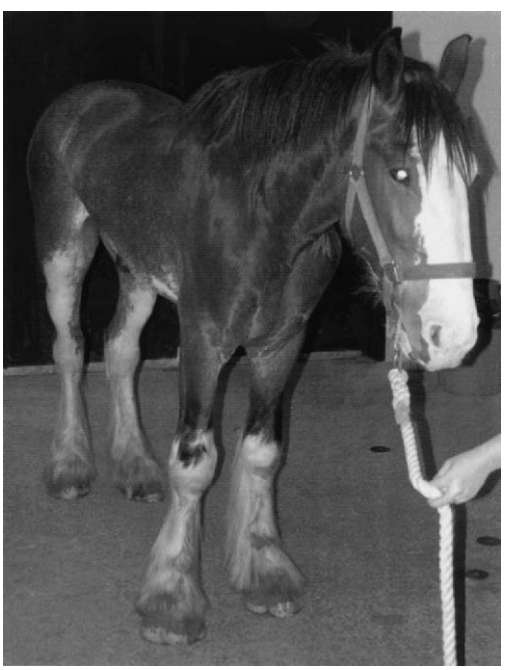


Figure 28-29 • Extremely thin draft horse is reluctant to eat because of associated neck pain attributed to equine protozoal myeloencephalitis.

horses. Specific measurements include (1) minimum sagittal diameter, (2) minimum flexion diameter, and (3) flexion angle, among others.[25] These data are of particular value in insurance cases involving valuable animals.

I do not routinely make such measurements, relying instead on a practiced eye, and often the opinion of my colleagues. As most are aware, experienced equine radiologists report their subjective evaluation of equine cervical myelograms to be as reliable as physical measurement.

Differentiating Congenital Spinal Malformation from Previous Injury

Old Injury. The key to differentiating a congenital cervical malformation from an old injury lies in the appearance of the adjacent vertebrae: Conforming vertebrae usually flank congenitally deformed spinal units, whereas previously injured vertebrae generally enjoy no such relationship.

By *conforming vertebrae*, I am referring to the spatial relationship that exists between two adjacent vertebrae or, more specifically, their fit. A conforming vertebra is characterized by a relatively smooth, even fit, even

though it too may be deformed, the latter reflecting the adaptive capabilities of the developing skeleton as first described by Wolfe.

Vertebrae adjacent to an old fracture may also remodel in an attempt to adjust to their new anatomic circumstances, but not so effectively as with congenitally deformed vertebrae. The end result is a mismatched, somewhat half-hearted accommodation that in most instances is readily apparent for what it is: an old injury.

Unfortunately, associated narrowing of the spinal canal is not a reliable means of discriminating between congenital and traumatic cervical spinal deformities because it may be present in both circumstances. Likewise, both conditions may be associated with a delayed onset of clinical signs.

The availability of a ventrodorsal view usually makes diagnosis easier, especially with occipitoatlantoaxial lesions, where distinguishing a congenital malformation from a remodeled fracture-dislocation can be very difficult.[26]

Recent Injury. Differentiating a recent cervical injury from a preexisting congenital deformity can be difficult or impossible, especially if overt signs of fracture are absent. Isolated dislocation, as observed radiographically, is not usually sufficient to discriminate between injuries to a previously normal cervical spine versus injury to a congenitally deformed spine. Even firsthand accounts of recent injury cannot be relied on completely to resolve the question because preexisting, but clinically silent, congenital deformities may be activated by relatively minor injuries, such as a fall or collision.[27]

Theoretically the awakening of congenitally quiescent cervical lesions by minor injury may be best explained on the basis of a congenitally *narrowed spinal canal*. Narrowing may be due to (1) a series of diminished vertebral foramina in an otherwise normal cervical spine, (2) blocked or hemivertebrae, or (3) malalignment. In each instance, extreme flexion may cause pinching of the spinal cord where the surrounding canal is abnormally narrowed and/or angled. Pinching typically occurs at the level of the facetal joints in the center of one or more vertebral units, where space is at a premium, even in normal horses.

▮▮▮ OCCIPITOATLANTOAXIAL DYSPLASIA

Mayhew classified equine occipitoatlantoaxial dysplasia into three categories[28]:

1. Familial occipitalization of the atlas with atlantalization of the axis in Arabian horses
2. Congenital asymmetric occipitoatlantoaxial malformation
3. Asymmetric atlantooccipital fusion

The greater the intricacy of a particular occipitoatlantoaxial dysplasia, the more difficult it is to diagnose, especially without a ventrodorsal projection. In such circumstances, CT can prove indispensable.[29]

▮▮▮ CERVICAL SPINA BIFIDA AND MENINGOMYELOCELE

Rivas and co-workers reported cervical spina bifida and meningomyelocele in a 1-day-old miniature horse.[30] *Spina bifida* refers to incomplete closure of the spinal canal; *meningomyelocele* denotes a protruding dural sac, which may be associated with drainage of cerebrospinal fluid through a sinus in the skin. Radiographs often show an absence of one or more of the dorsal elements of a spinal unit, such as the facetal joints or the transverse or dorsal spinous processes. Radiographic diagnosis was made by injecting a nonionic contrast solution into a fluctuant swelling overlying the C5-6 spinal unit and finding that it communicated with the subarachnoid space, a procedure termed *cavography.*

▮▮▮ RUPTURED INTERVERTEBRAL DISK (PROLAPSED, PROTRUDED, HERNIATED INTERVERTEBRAL DISK)

Ruptured intervertebral disk is extremely rare in the horse, with only six horses and a pony reported to date.[31] All but the pony involved a single spinal unit. Nixon and co-workers reported an insufficiency fracture of the body and arch of C6 following a ventral slot procedure performed to relieve a ruptured disk in an 18-year-old Quarter Horse.[32]

▮▮▮ CERVICAL TUMORS

Cervical tumors, as with skeletal tumors elsewhere, may be malignant or benign, primary or secondary, and involve bone or soft tissue. Traditionally spinal tumors have been divided into three groups: (1) paraspinal, (2) spinal, and (3) intraspinal.

Dunkerly and co-workers reported a nonpainful, slowly growing lipoma in the dorsal midcervical region of a 9-week-old Appaloosa foal, which radiographically appeared as a relatively dark, soft-tissue mass.[33] MacGillivray and co-workers reported the radiographic and myelographic appearance of a destructive hemangiosarcoma in the C4-5 spinal unit of a 16-year-old miniature donkey.[34]

▮▮▮ CELLULITIS OF THE CERVICAL REGION

Cellulitis in the cervical region of horses is frequently associated with a previous intramuscular injection. Of these, clostridial infection is the worst, often

proving fatal.[35] Sonographically the most valuable clue to the clostridial nature of a cervical cellulitis is the presence of gas pockets. Paraspinal infection always has the potential of reaching the spine, leading to spondylitis or, worse, myelitis. Accordingly all such infections should be promptly dealt with and closely monitored.

Persistent, unexplained cervical drainage should be pursued both sonographically and sinographically to confirm or deny a foreign body, especially large wooden splinters, some of which may lodge against the spine, potentially leading to spondylitis.

▮▮▮ CERVICAL SPONDYLITIS, DISKOSPONDYLITIS, AND SPONDYLOSIS

Cervical spondylitis, diskospondylitis, and spondylosis rarely occur in horses. In most instances, cervical spondylitis is the result of an inoculating wound. Richardson reported spondylitis of the dorsal spinous process of C2 caused by *Eikenella corrodens*. The 7-month-old Standardbred colt exhibited severe neck pain and fever but no neurologic signs.

▮▮▮ POSTOPERATIVE EVALUATION OF ATTEMPTED CERVICAL FUSION

Debowes and co-workers showed that intervertebral autografts, supported by stainless steel baskets, provided a greater degree of intervertebral rigidity ("interbody fusion") than bovine xenografts. This was because the autografts typically led to some degree of bony fusion, whereas the xenografts provided only a relatively flexible fibrous union.[36] Interest in surgically treating horses with cervical spondylopathy currently appears to be at an all-time low, pessimism likely engendered by poor intermediate and long-term outcomes.

References

1. Whitwell KE, Dyson S: Interpreting radiographs 8: equine cervical vertebrae, *Equine Vet J* 19:8, 1987.
2. Systel AM, Moll HD, et al: What is your diagnosis? *J Am Vet Med Assoc* 213:607, 1998.
3. Slone DE, Bergfeld WA, Walker TL: Surgical decompression for traumatic atlantoaxial subluxation in a weanling filly, *J Am Vet Med Assoc* 174:1234, 1979.
4. Guffy MM, Coffman JR, Strafuss AC: Atlantoaxial luxation in a foal, *J Am Vet Med Assoc* 155:754, 1969.
5. Nixon AJ, Stashak T: Laminectomy for relief of atlantoaxial subluxation in four horses, *J Am Vet Med Assoc* 193:677, 1988.
6. Dollar JAW: *Textbook of surgery,* Chicago, 1920, Eger.
7. McKelvey WAC, Owen R: Acquired torticollis in 11 horses, *J Am Vet Med Assoc* 175:295, 1979.
8. Rooney JR: Equine incoordination, *The Cornell Veterinarian* 53:411, 1963.
9. Dahme E, Schebitz H: Spinal ataxia in the horse, *Zentralblatt fur Veterinarmedizin* 17:121, 1970.
10. Rendano VT, Quick CB: Radiographic interpretation: equine radiology—the cervical spine, *Modern Vet Pract* 73:921, 1978.
11. Papageorges M, Gavin PR, et al: Radiographic and myelographic examination of the cervical vertebral column in 306 ataxic horses, *Vet Radiol* 28:53, 1987.
12. Nyland TG, Blythe L, et al: Metrizamide myelography in the normal horse: clinical, radiographic, and pathologic findings, *Vet Radiol* 20:67, 1979.
13. Maclean AA, Jeffcott LB, et al: Use of iohexol for myelography in the horse, *Equine Vet J* 20:286, 1988.
14. Widmer WB, Blevins W, et al: A prospective clinical trial comparing metrizamide and iohexol for equine myelography, *Vet Radiol & Ultrasound* 39:106, 1998.
15. Hubbell JAE, Reed SM, et al: Sequelae of myelography in the horse, *Equine Vet J* 20:438, 1988.
16. Maclean AA, Jeffcott LB, et al: Use of iohexol for myelography in the horse, *Equine Vet J* 20:286, 1988.
17. Conrad RL: Metrizamide myelography of the equine cervical spine, *Vet Radiol* 25:73, 1984.
18. Rantanen NW, Gavin PR, et al: Ataxia and paresis in horses. Part II. Radiographic and myelographic examination of the cervical vertebral column, *Compend Cont Ed* 3:161, 1981.
19. Nappert G, Vrins A, Breton L: A retrospective study of nineteen ataxic horses. *Vet Radiol & Ultrasound* 30:802, 1989.
20. Foley JP, Gatlin SJ, Selcer BA: Standing myelography in six adult horses, *Vet Radiol* 27:54, 1986.
21. Marsh AE, Barr BC, et al: Neosporosis as a cause of equine protozoal myeloencephalitis, *J Am Vet Med Assoc* 209:1907, 1996.
22. Daft BM, Barr BM, et al: Sensitivity and specificity of Western blot testing of cerebrospinal fluid and serum for diagnosis of equine protozoal myeloencephalitis in horses with and without neurologic abnormalities, *J Am Vet Med Assoc* 221:1007, 2002.
23. Powers BE, Stashak TS, Nixon TS: Pathology of the vertebral column of horses with severe cervical static stenosis, *Vet Pathol* 23:392, 1986.
24. Stickle R, Darien B, et al: Radiographic diagnosis, *Vet Radiol* 29:28, 1988.
25. Mayhew IG, deLahunta A, et al: Spinal cord disease in the horse, *Cornell Vet* 68:13 (suppl 6), 1978.
26. Stickle R, Arden W, Shappell K: Radiographic diagnosis, *Vet Radiol* 29:204, 1988.
27. Nelson KM, Scarratt K, et al: What is your diagnosis? *J Am Vet Med Assoc* 204:47, 1994.
28. Mayhew IG, Watson AG, Heissan JA: Congenital occipitoatlantoaxial malformation in the horse, *Equine Vet J* 10:103, 1979.
29. Rosenstein DS, Schott HC, Stickle RL: Occipitoatlantoaxial malformation in a miniature horse foal, *Vet Radiol Ultrasound* 41:218, 2000.
30. Rivas LJ, Hinchcliff KW, et al: Cervical meningomyelocele associated with spina bifida in a hydrocephalic miniature colt, *J Am Vet Med Assoc* 209:950, 1996.
31. Jannson N: What is your diagnosis? *J Am Vet Med Assoc* 219:1682, 2001
32. Nixon AJ, Stashak TB, et al: Cervical intervertebral disk protrusion in a horse, *Vet Surg* 13:154, 1984.
33. Dunkerly SA, Williams AW, Gillis P: Lipoma in a foal, *J Am Vet Med Assoc* 210:332, 1997.

34. MacGillivray KC, Sweeney CR, et al: Vertebral body hemangiosarcoma in a 16-year-old miniature Sicilian donkey, *Vet Radiol Ultrasound* 44:429, 2003.
35. Valberg SJ, McKinnon AO: Clostridial cellulitis in the horse: a report of five cases, *Can Vet J* 25:67, 1984.
36. Debowes RM, Grant BD, et al: Cervical vertebral interbody fusion in the horse: a comparative study of bovine xenografts and autografts supported by stainless steel baskets, *Am J Vet Res* 45:191, 1984.
37. Rousseaux CG, Doige CE, Tuddenham TJ: Epidural lymphosarcoma with myelomalacia in a seven-year-old Arabian gelding, *Can Vet J* 30:751, 1989.
38. Frauenfelder HC, Kazacos KR, Lichtenfels JR: Cerebrospinal nematodiasis caused by a filarid in a horse, *J Am Vet Med Assoc* 177:1521, 1977.

Chapter 29

The Thoracic, Thoracolumbar, Lumbar, and Lumbosacral Spinal Regions

SPINAL RADIOGRAPHY

Jeffcott described a technique for radiographing the thoracolumbar and proximal lumbar spinal regions of the horse in the standing position.[1] Generally we follow this protocol, although we also customize many studies. For the most part, our examinations are either to search for fractures or to confirm or deny fistulous withers.

NORMAL RADIOGRAPHIC ANATOMY OF THE EQUINE THORACOLUMBAR SPINAL REGION

Jeffcott and others also described the normal radiographic anatomy of the equine thoracolumbar spinal region.[2] The most important features to recognize (with respect to avoiding misdiagnosis) are the presence of separate ossification centers in immature horses and the presence of irregular bony ridges on both the leading and trailing surfaces (cranial and caudal edges) of the dorsal spinous processes (Figures 29-1 and 29-2).

ACUTE AND CHRONIC BACK PAIN RELATED TO LIGAMENT INJURY

Acute Back Sprain

Acute sprains are, in my experience, rarely demonstrable by either radiology or ultrasound. The best chance to see such injuries is with ultrasound, provided they are fresh (a week or less), moderately serious, and unilateral, allowing sonographic comparison with the uninjured side of the back.

Overuse Injury

In my experience, chronic overuse injuries are extremely difficult or impossible to *diagnose consistently* by currently available means, with perhaps the exception of magnetic resonance imaging (MRI). Overviews dealing with chronic sprains and overuse injuries of the back, and the means by which they can be imaged, are provided for those desiring specific information on ultrasound,[3] nuclear medicine,[4] and thermography.[5] Reference normals remain scarce, but some are available; for example, Erichsen and co-workers described the scintigraphic variation found in the thoracic spinal region of *normal* riding horses.[6]

ASSORTED BACK INJURIES

Denoix described the use of ultrasound for a variety of back injuries, including sprains of the supraspinal ligament and lumbosacral intervertebral disks.[7] Scattered, largely anecdotal reports have touted ultrasound as a reliable means of diagnosing injuries to spinous and articular processes, a claim I can neither substantiate nor deny because I am rarely called on to perform such examinations.

Fractures of the Thoracic Spinal Region

Vertebral compression fractures are most likely to occur in the cranial and caudal portions of the thoracic spinal region: T1 to T3 and T11 to T13. Most are the result of an injury but can also occur in vertebrae weakened by osteomyelitis or cancer, forms of insufficiency, or pathologic fractures. Thoracic compression fractures have also been reported as a result of a lightning strike secondary to sudden contraction or spasm of the spinal muscles.[8]

DeBowes and co-workers reported a midthoracic vertebral compression fracture in a 3-month old foal after electrocution.[9] Kothstein and co-workers described severe kyphosis in a previously injured 20-month-old horse resulting from multiple thoracic compression fractures sustained as a 1-month-old filly.[10] What was especially interesting about this case

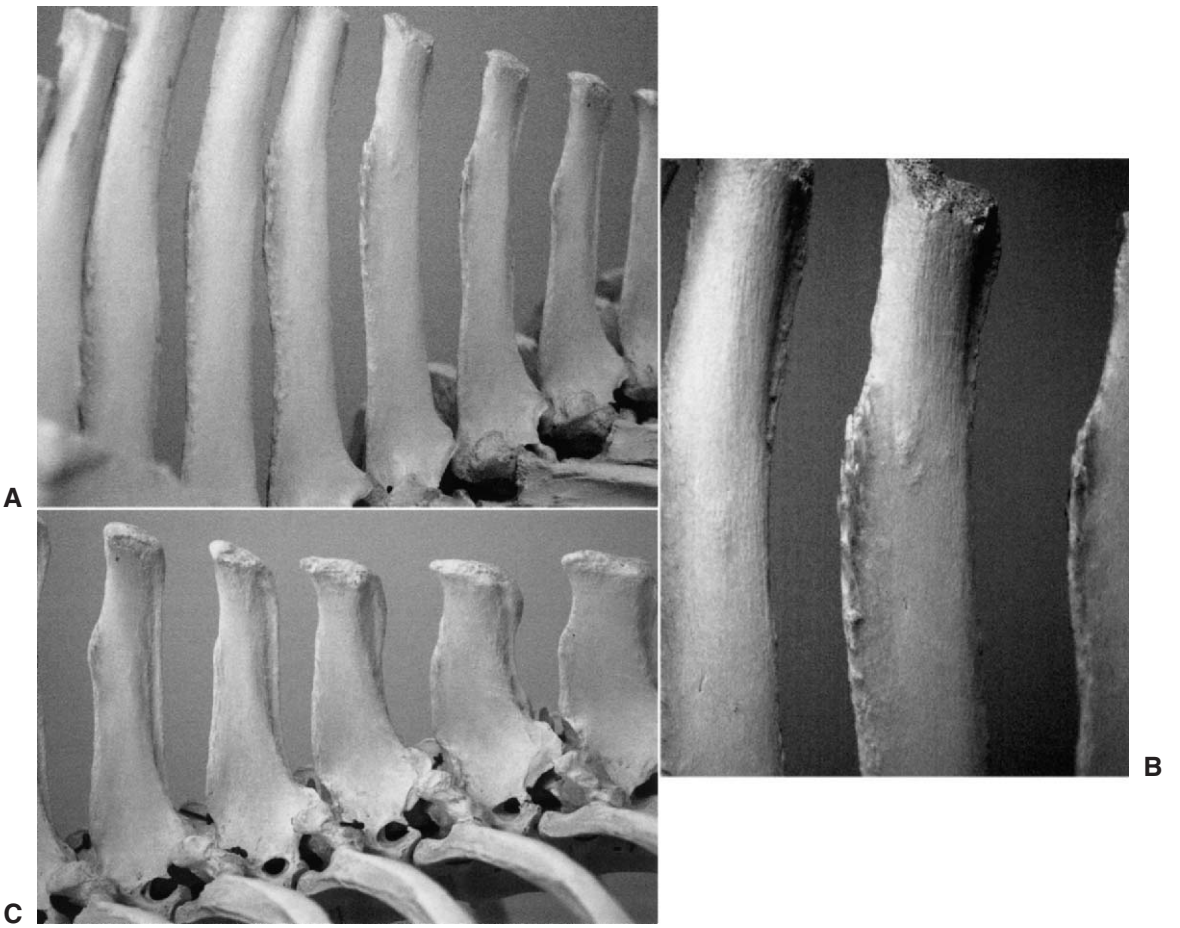


Figure 29-1 • Equine skeleton: Dorsal spinous processes of the withers region seen from the left front **(A),** including close-up **(B).** Adjacent, more caudally situated dorsal spinous processes are shown from the left side **(C).** Lengthy bony ridges are present cranially and caudally. Note that the caudal ridge begins at the very top of the spine while the cranial ridge starts one third to half the way down. The caudal ridge is most likely to be *mistaken* for new bone, implying infection.

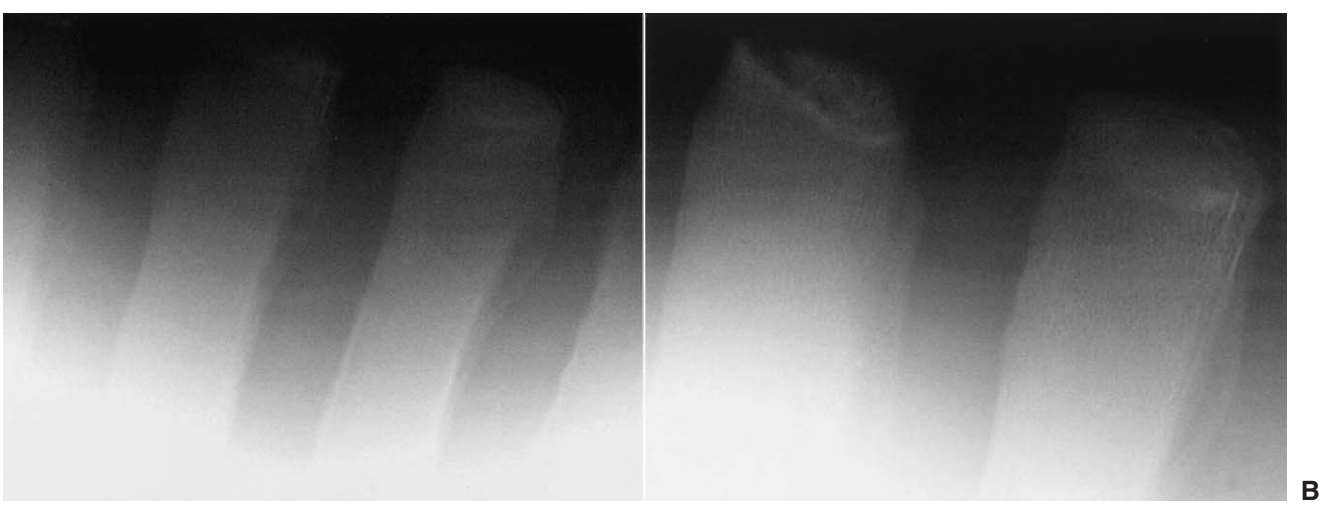


Figure 29-2 • Close up **(A)** and ultra-close-up **(B)** views of the upper surfaces of some of the dorsal spinous processes of the withers region of an adult horse show normally prominent caudal ridges, which simulate chronic new bone deposits.

was the fact that the damaged vertebrae had adapted so well, and although clearly deformed they were in a near-perfect curvilinear alignment, more closely resembling a congenital malformation than an old injury.

Fractures of the Lumbar Spinal Region

Ramey and Selcer reported a displaced L5 fracture in a 7-month-old Quarter Horse colt that injured itself while trying to jump a fence.[11] The resultant fracture narrowed the overlying spinal canal by about 50 percent, but initially it caused only a mild left hind lameness; however, 12 days later the foal could not stand, even with assistance. According to the authors, lumbar fractures are rare in the horse, citing a study of 443 horses referred for suspected lumbar back pain in which only two animals were found to have lumbar fractures.[12]

Theoretically it is the most flexible thoracolumbar spinal units that are susceptible to injury: T1-2, L1-2, T11-12, and T12-13 (the latter being related to the position and weight of the rider). Conversely spinal injury theorists contend that the caudal lumbar region (including L5) is unlikely to be injured owing to its substantial muscular and bony surrounding (obviously not the case in this instance). As might be expected in such cases, prognosis is generally based on the neurologic examination, which along with radiology is used to estimate the degree of spinal cord and nerve root injury.

▮▮▮ SPINAL INFECTION

Spondylitis

Penetrating wooden foreign bodies to the neck and shoulder regions of horses are often associated with residual fragments and splinters, which typically lead to the formation of a draining sinus. Occasionally such foreign bodies lodge in the muscle alongside the spine,

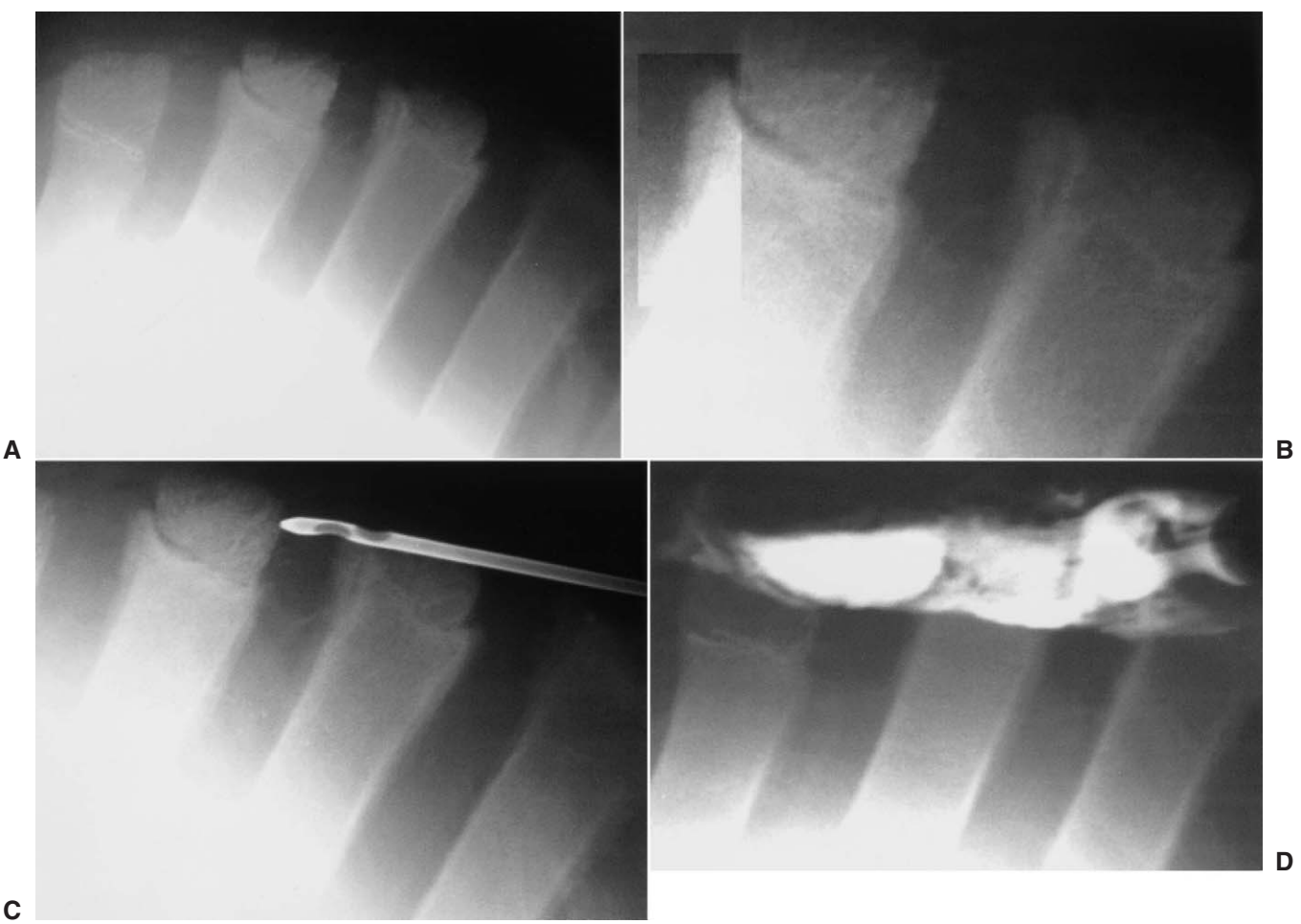


Figure 29-3 • A, Lateral view of the of the central withers region shows new bone deposition along the cranial edges of the dorsal spinous processes of T6, T7, and T8 (T5, far left, is uninvolved). **B,** A close-up lateral view of T6 and T7 shows new bone *(emphasis zone)*, which is of intermediate duration (weeks-months) based on its density and surface contour. **C,** A marking study shows the metallic probe paralleling the tops of the affected dorsal spinous processes. **D,** A sinogram reveals a lengthy, lobulated cavity in the same location.

potentially abscessing or causing spondylitis. Having performed both sonography and sinography in such cases, I have generally found the latter to be the more rewarding, provided the horse is not so large that radiography is impractical.[13]

Hematogenous spondylitis is largely confined to foals. Radiographic detection depends most on lesion size: the larger the area of vertebral production or destruction, the greater the chance it will be identified. Subtle lesions may sometimes be uncovered with nuclear scintigraphy, although it may not be possible to localize the lesion to a specific vertebra.

Diskospondylitis

Chaffin and co-workers described the radiographic appearance of rhodococcal diskospondylitis in a foal,[14] and Furr and co-workers described a nonspecific granulomatous diskospondylitis in an adult horse, the latter combined with a ruptured intervertebral disk.[15]

Fistulous Withers (Supraspinatous Bursitis) and Spondylitis

The supraspinatous bursa is situated beneath the nuchal ligament and dorsal spinous processes of the second through fifth thoracic vertebrae. Infection or inflammation of the supraspinatous bursa is known as *fistulous withers* or *supraspinatous bursitis* and is often associated with draining sinuses.[16]

Hathcock advised caution when radiographically interpreting the dorsal spinous processes of horses with fistulous withers, pointing out the resemblance of incompletely ossified epiphyses to that of osteomyelitis.[17] One discriminating factor that I have used with considerable success is the presence of irregularly marginated new bone along the top leading edges of the affected dorsal spinous processes just below the epiphyses, as seen in a closely calumniated view of the cranial portion of the thoracic spinal region made with a grid. Where drainage is present, metallic probe marking and sinography can be used to identify precisely the areas of involvement (Figure 29-3).

Paraspinal Abscess and Hematoma

Paraspinal Abscess. Rooney reported a paraspinal abscess in a horse presumably secondary to "strangles."[18] If bone deposition occurs on the nearby vertebrae, it may be possible to identify the affected portion of the spine. If not, then ultrasound or computed tomography may be the only way such lesions can be identified.

Paraspinal Hematoma. Paraspinal hematomas may be situated directly atop one or more dorsal spinal processes or alternatively lie alongside the spine. Paraspinal hematomas (or abscesses) are not usually detectable radiographically, but they are relatively easily identified with ultrasound. As with hematomas elsewhere, paraspinal hematomas may be intramuscu-

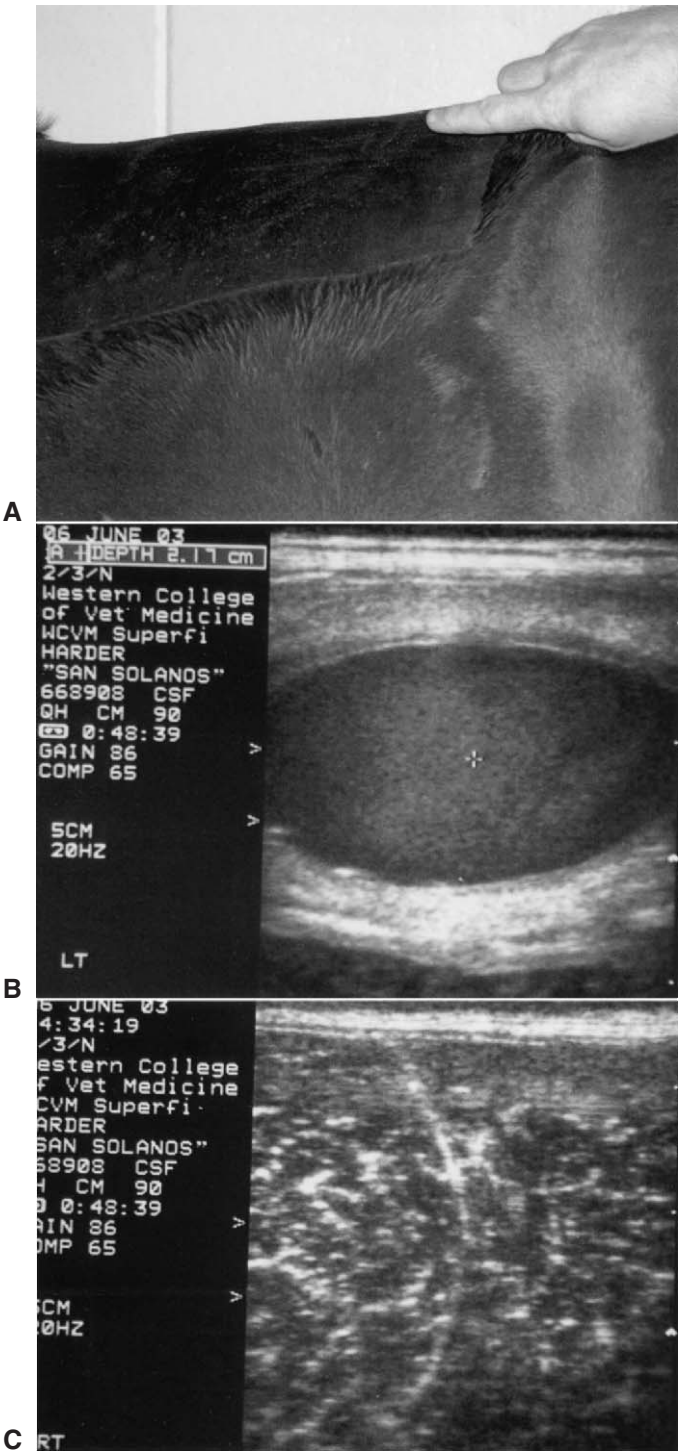


Figure 29-4 • A, Close-up view of a swollen, painful left paralumbar region in a Quarter Horse gelding (clipped). **B,** Left-sided sonogram shows a well-defined, oval-shaped cavity containing semisolid material resembling pus just beneath the fascial surface. An abscess was diagnosed sonographically, but it subsequently proved to be a hematoma. **C,** The normal right paralumbar region is provided for comparison.

lar or extramuscular, the latter being more dangerous, potentially leading to myonecrosis. Sonographically, it is often difficult to distinguish a hematoma from an abscess (Figure 29-4).

▮▮▮ SPINAL TUMORS

Spinal tumors, like appendicular tumors, are rare in horses. Intensely destructive vertebral lesions, even when accompanied by pathologic fracture, are far more likely to be due to infection rather than malignancy.

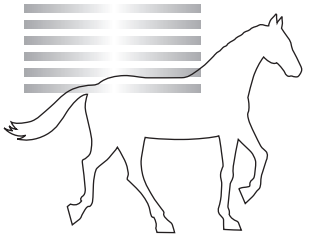
Drew and Greatorex reported multiple myeloma in the spine of a horse, causing posterior paralysis.[19] Schott and co-workers described cervical melanoma in two Arabians exhibiting hindquarter collapse, both of which underwent myelography. In one horse, the myelograms were initially read as normal, but following necropsy they were reevaluated and determined to be abnormal, revealing extradural compression at the level of C7. The second horse showed a dorsal extradural mass above the C7-T1 spinal unit, subsequently proven to be a melanoma.

References

1. Jeffcott LB: Radiographic examination of the equine vertebral column, *Vet Radiol* 20:135, 1979.
2. Jeffcott LB: Radiographic features of the normal equine thoracolumbar spine, *Vet Radiol* 20:140, 1979.
3. Gillis C: Spinal pathology, *Vet Clin N Am Equine Pract* 15:97, 1999.
4. Weaver MP, Jeffcott LB: Radiology and scintigraphy, *Vet Clin N Am Equine Pract* 15:113, 1999.
5. Schweinitz DG: Thermographic diagnostics in equine back pain, *Vet Clin N Am Equine Pract* 15:161, 1999.
6. Erichsen C, Eksell P, et al: Scintigraphic evaluation of the thoracic spine in the asymptomatic riding horse, *Vet Radiol Ultrasound* 44:330, 2003.
7. Denoix JD: Ultrasonographic evaluation of back lesions, *Vet Clin N Am Equine Pract* 15:131, 1999.
8. Rhodes WS, Cox JH: What is your diagnosis? *J Am Vet Med Assoc* 210:755, 1997.
9. DeBowes RM, Wagner PC, et al: Vertebral compression fracture in a foal following electric shock, *J Vet Orthop* 2:14, 1979.
10. Kothstein T, Rshmir-Raven, et al: Thoracic spinal fracture resulting in kyphosis in a horse, *Vet Radiol Ultrasound* 41:44, 2000.
11. Ramey DW, Selcer BA: Radiographic diagnosis, *Vet Radiol* 25:218, 1984.
12. Jeffcott LB: Disorder of the thoracolumbar spine of the horse—a survey of 443 cases, *Equine Vet J* 12:197, 1980.
13. Barber SM: An unusual location of foreign body in the horse, *Can Vet J* 24:63, 1983.
14. Chaffin MK, Honnas CM, et al: Discospondylitis in a foal, *J Am Vet Med Assoc* 206:215, 1995.
15. Furr MO, Anver M, Wise M: Intervertebral disk prolapse and diskospondylitis in a horse, *J Am Vet Med Assoc* 198:2095, 1991.
16. Hawkins JF, Fessler JF: Treatment of supraspinatous bursitis by use of debridement in standing horses: 10 cases (1968-1999), *J Am Vet Med Assoc* 217:74, 2000.
17. Hathcock JT: What is your diagnosis? *J Am Vet Med Assoc* 181:609, 1982.
18. Rooney JR: Sequelae of strangles, *Mod Vet Pract* 60:463, 1979.
19. Drew RA, Greatorex JC: Vertebral plasma cell myeloma causing posterior paralysis in a horse, *Equine Vet J* 6:131, 1974.

SECTION V

The Thorax



Chapter 30

Thoracic Imaging and Diagnostic Strategy

IMAGING

Value of Thoracic Radiography

The value of thoracic radiography in foals and adult horses is well established.[1] Short of pulmonary function testing or nuclear imaging, thoracic radiology is the best *overall* means of evaluating the equine lung, especially its degree of aeration. Of course there are exceptions to this generality. For example, life-threatening hyaline membrane disease in a newborn foal may be associated with a perfectly normal-appearing lung. Likewise, thoracic radiographs of many adult horses with debilitating chronic obstructive pulmonary disease (COPD) often appear entirely normal.

Field Radiography

Although it has its advocates,[2] radiographic field imaging of foals and horses with suspected respiratory disease generally has proven diagnostically inferior to images produced in fixed facilities. The same holds true for sonographic imaging, although the quality gap is not as large.

Alternate-side Radiography

Alternate-side radiography (right and left laterals) occasionally proves useful in decidedly unilateral lung lesions, but it is of no use in the case of mediastinal disease. Inspiratory films are easier to interpret than expiratory images, but they are not always easily obtained. It is often difficult or impossible to establish whether radiographically identified lung disease is unilateral or bilateral using lateral thoracic films.

THE STANDARD THORACIC SERIES

Foals

The thorax of most newborn foals can be imaged on a single 14- by 17-inch film (Figure 30-1). When radiographing foals, bear in mind that their respiratory

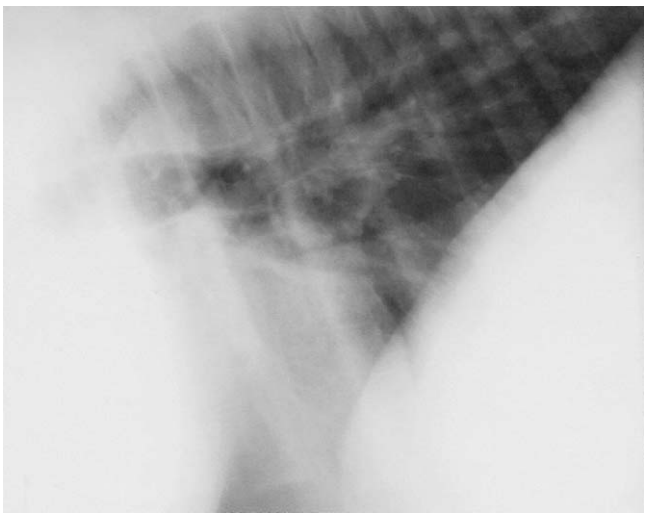


Figure 30-1 • Normal foal thorax. Lateral view of the thorax of a young foal. The shoulder muscles are obscuring the cranioventral aspect of the lung, which is typical of standing images.

pattern differs from that of adult horses, being monophasic rather than biphasic.[3] Because of superimposition of the shoulder muscles, it usually is not possible to view the cranioventral lung field. This problem can sometimes be overcome by drawing either of the forelimbs forward, although some foals will not tolerate this stance for very long.

Adults

Standard Examination. Because of its great size, at least four large films (14 × 17 inch) are required to capture the entire thoracic field in most adult horses. As published previously, a standard film series consists of (1) craniodorsal, (2) cranioventral, (3) caudodorsal, and (4) caudoventral views (Figure 30-2).[4]

Modified Examination: A Fifth View. Since this recommendation was originally published, I have modified it somewhat to include a fifth view. What I now propose is to image the dorsal half of the thorax with three films instead of two, which provides more comprehensive coverage of what is an extremely complex area (Figure 30-3). The ventral portion of the lung field can still adequately be covered with two large films, as previously recommended. Once a lesion (or a suspicious area) is identified, the examination can be customized to optimize the area of concern. A full, five-view thoracic examination is shown in Figure 30-4.

Customizing a Thoracic Examination. Customization typically takes the form of centering and collimating on a particular area of concern (usually a vaguely seen mass or suspicious area of the lung) and increasing or decreasing the kilovoltage. The examination can be further customized by deliberately making an *expiratory* image of the area, which will sometimes cause a small portion of the adjacent lung to collapse temporarily, forming an *atelectatic rim* that will enhance lesion visibility.

▮▮▮ NORMAL ANATOMIC AND PHYSIOLOGIC VARIANTS THAT MAY MIMIC LUNG DISEASE

Foals

At birth, some but not all normal foals show increased lung density, which typically dissipates within a day or two.[5] Weak or sick newborn foals often have abnormally dense lungs as a result of *prolonged recumbency and resultant postural atelectasis*, a conclusion that can readily be confirmed with a ventrodorsal view. These normal variants must be distinguished from bona fide lung diseases that also subtly increase lung density, such as surfactant deficiency (respiratory distress syndrome) and viral pneumonia.

Adults

Superimposed Blood Vessels Mimicking Lung Masses. The greatest limitations to an accurate and complete radiographic assessment of the adult equine thorax are (1) extensive structural superimposition and (2) the absence of a ventrodorsal view. To comprehend the magnitude of the overlap problem, consider the fact that the chests of many horses are about a meter wide, whereas a sheet of x-ray film measures only about a millimeter, a thousand-fold difference. Then imagine how many blood vessels theoretically could be superimposed on one another on a line drawn across the thorax just above the heart or, alternatively, in the caudodorsal lung fields, where the largest-diameter arteries and veins reside. Dozens? Hundreds? Thousands? The exact number of large, overlapping blood vessels is not important; however, the fact that vascular superimposition is inevitable and, more importantly, that it can mimic a pulmonary mass such as an abscess is important. Some common examples of this phenomenon are illustrated (Figures 30-5 through 30-7).

Bronchial Cross-Sections Mimicking Cavitary Lung Lesions

Large and medium-sized bronchial cross-sections can resemble cavitary lung lesions, sometimes quite convincingly, as exemplified in Figure 30-8. This is particularly true of the hilar region of the lung, where large bronchi are numerous and, accordingly, most visible.

Bronchial Thickening: A Dangerous Observation

In my opinion, bronchial thickening cannot be reliably diagnosed from radiographs, although it may be

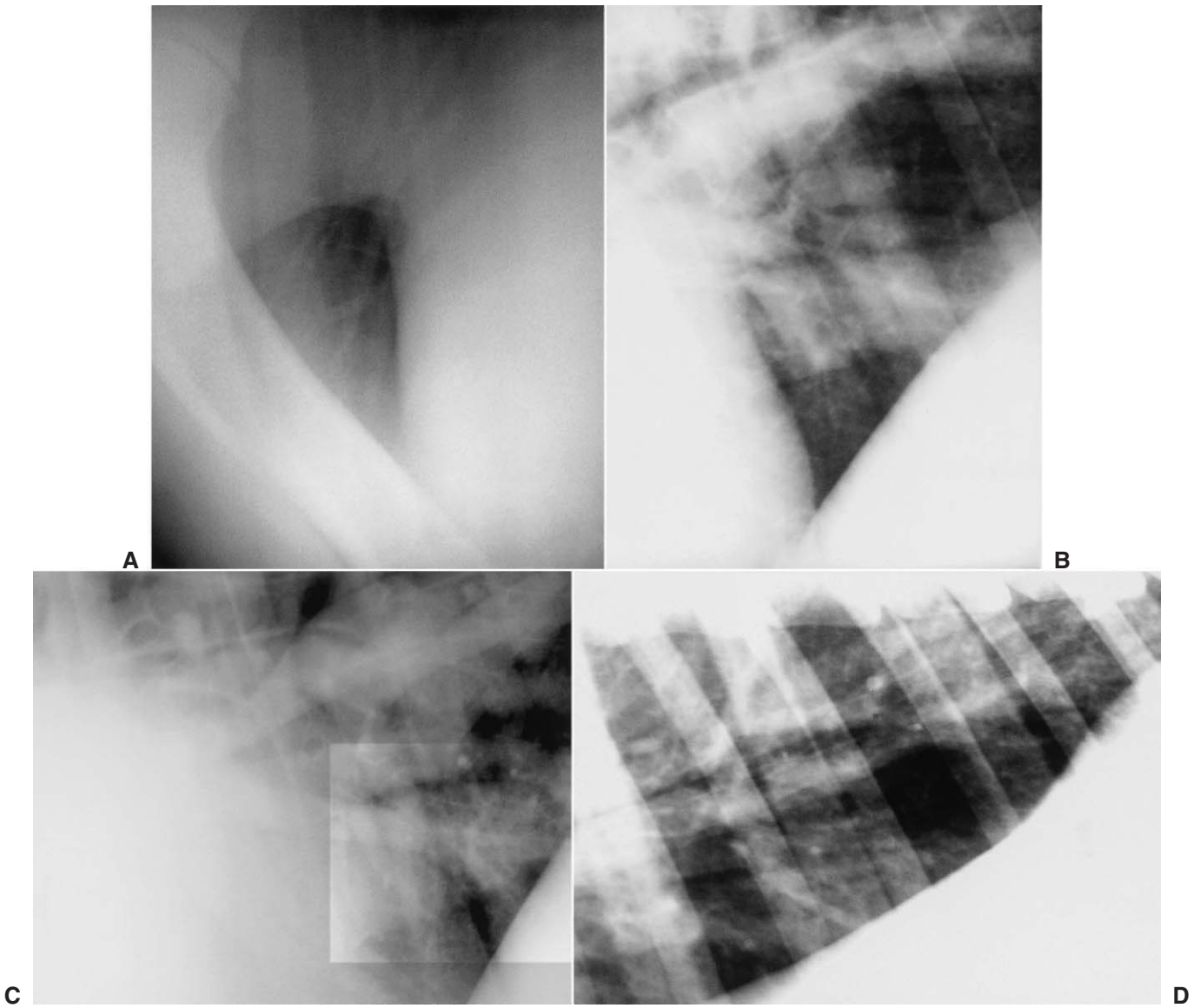


Figure 30-2 • Standard adult thorax examination. Until recently, a standard thoracic examination in an adult horse consisted of four views: cranioventral **(A),** caudoventral **(B),** craniodorsal **(C),** and caudodorsal **(D).**

detected with high-resolution computed tomography (CT), but only if it is severe. In nearly every case of supposed bronchial thickening (sometimes termed a *bronchial pattern*), there is another, more plausible technical explanation. For example, (1) bronchial superimposition, especially in and around the hilus; (2) beam decentering, causing geometric distortion; (3) motion unsharpness resulting from long exposure times, rapid breathing, or a combination of the two; (4) expiratory filming; (5) lack of a grid, resulting in excessive scatter radiation; and (6) disease-related weight loss resulting in a thinner chest wall and improved bronchial detail.

Another common cause of bronchial misdiagnosis is *bias*, the clinician's strongest ally and worst enemy. For example, if one strongly suspects that a horse has emphysema or some other form of COPD, it is not difficult to imagine that some of the bronchi are dilated, especially in the hilar region of the lung, a form of self-fulfilling prophesy. Although we all guard against such tendencies, the temptation to incriminate the bronchi is considerable (Figure 30-9).

▮▮▮ PULMONARY PATTERN RECOGNITION

Some veterinarians, including specialists, appear to have become unduly reliant on the supposed diagnostic and prognostic capabilities of pulmonary pattern recognition. It is difficult to recall another widely held clinical belief, other than perhaps the mistaken notion that bronchitis can be diagnosed radiographically, where an unproven method such as

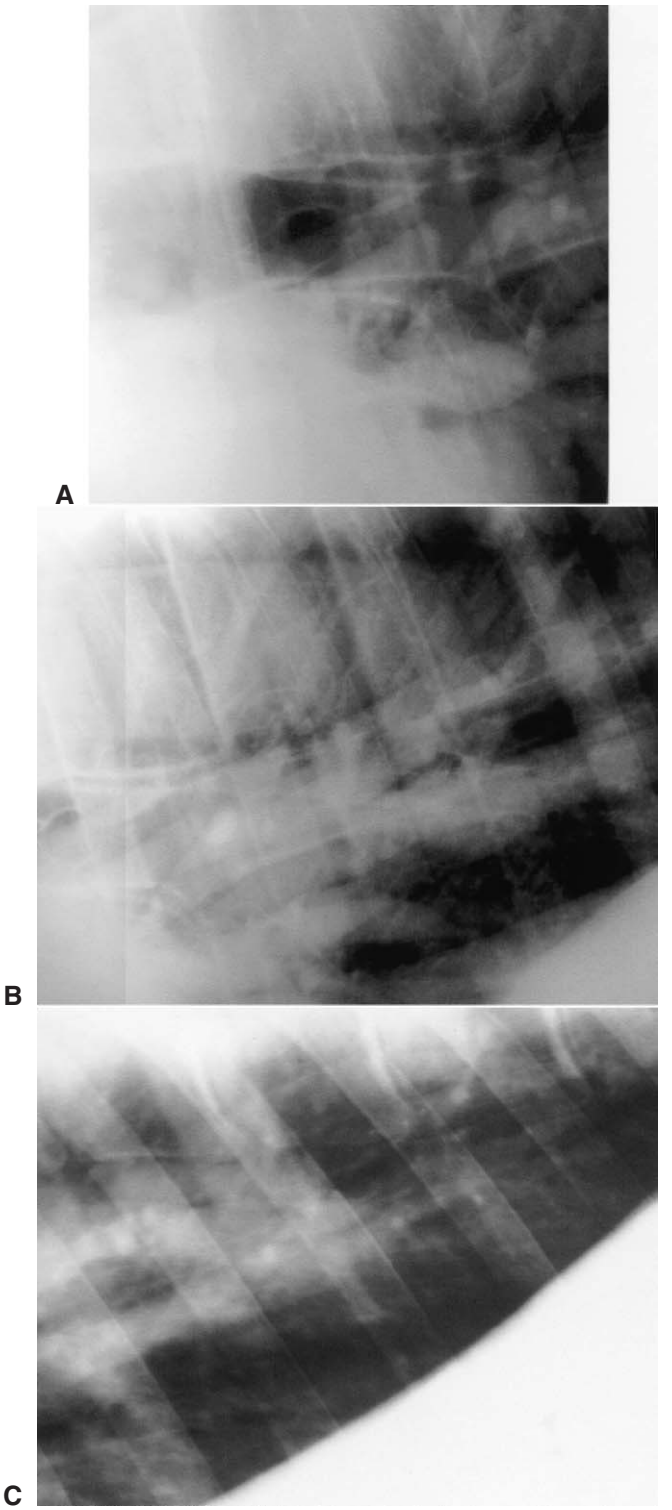


Figure 30-3 • Expanded adult thoracic examination. Based on further study, I now believe that at least five views are necessary to completely image the thorax of larger adult horses, especially those weighing 1200 pounds or more. Accordingly the dorsal half of the thorax is now *optimally imaged with three* 14- by 17-inch films, covering most of the dorsal aspects of the middle **(A),** midcaudal **(B)** and caudal **(C)** lung fields; the cranioventral and caudoventral lung fields can be imaged as before.

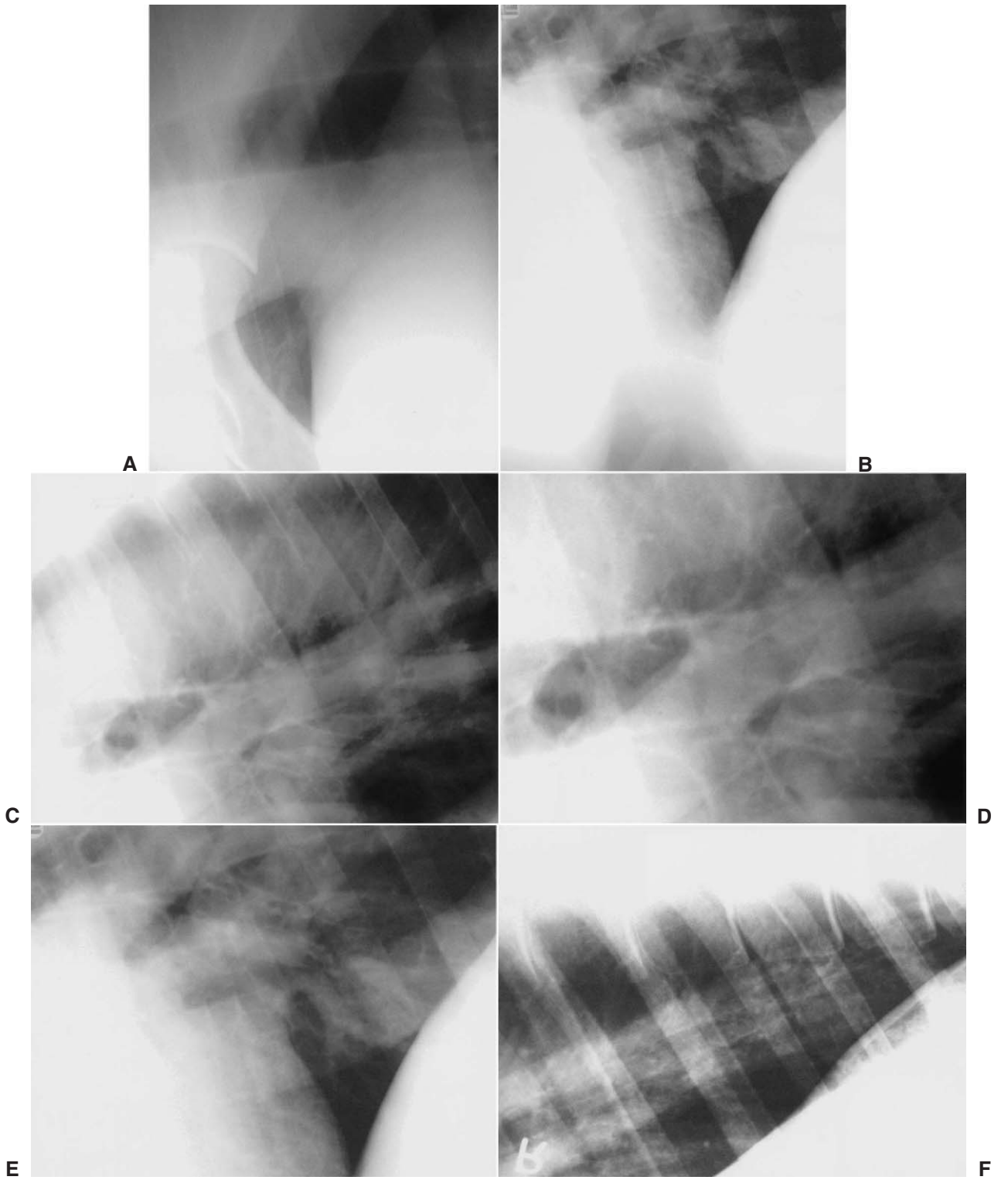


Figure 30-4 • Normal five-view thoracic examination in a large adult horse: cranioventral **(A),** caudoventral **(B),** craniodorsal **(C),** close-up craniodorsal **(D),** mid-dorsal **(E),** and caudodorsal views **(F).**

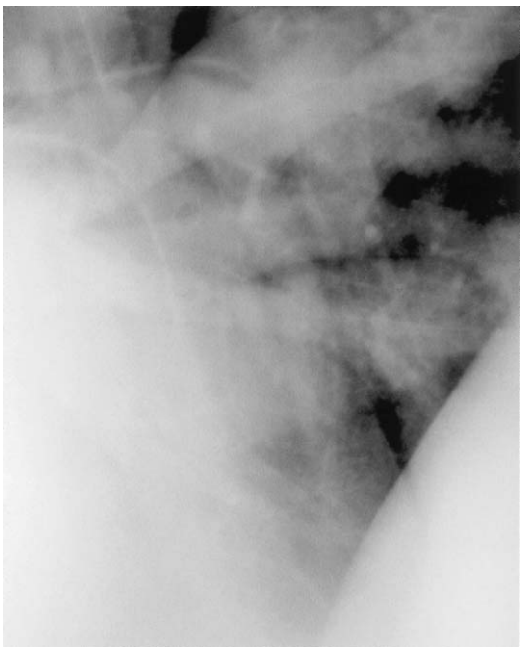


Figure 30-5 • Caudoventral lung field in a normal adult horse shows what appears to be a medium-sized, oval-shaped mass just above the caudal edge of the left atrium, which in reality is no more than normal vascular overlap.

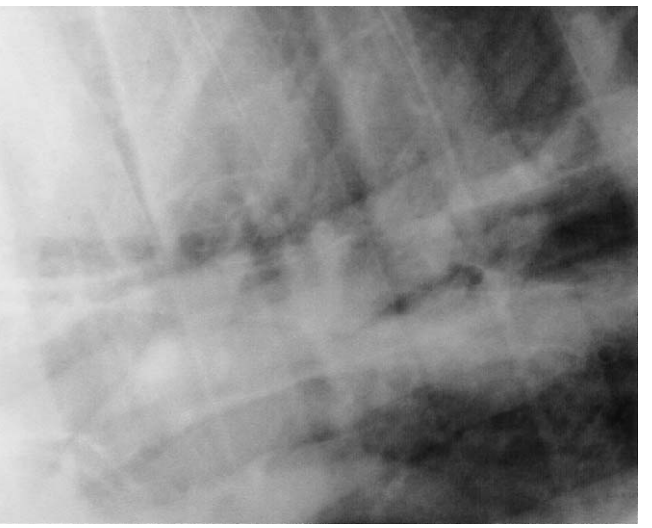


Figure 30-6 • Midcaudal aspect of the dorsal lung field in a normal horse shows an apparent oval-shaped lung mass superimposed on a large blood vessel in the right lower half of the image. This is not a mass, but rather it is three arching blood vessels, configured and aligned in such a way as to create the illusion of a mass.

pattern recognition has been so readily, so completely, and so uncritically embraced.

Perhaps more disappointing is the fact that pulmonary pattern recognition continues to be taught in numerous veterinary curricula, without even a semblance of critical debate. Not surprisingly, then, both scientific articles and textbooks continue to tout its virtues, seemingly oblivious to the fact that pattern recognition remains unvalidated.[6]

Although I am forced to acknowledge that I, too, was once a member of the coalition of the convinced, this is no longer the case. Well over a dozen years ago, after carefully reanalyzing all the data on the subject, little of which was of a truly objective nature, I concluded that pattern recognition remained unproven, even after nearly three decades of widespread use. Moreover, I could find no evidence that the use of pulmonary pattern recognition resulted in either improved diagnostic efficiency or cure rate among horses with significant lung disease, as promised by its supporters.

So the obvious question becomes, Should pattern recognition be abandoned? That, of course, is up to the individual veterinarian; but for my part, I now do the following:

1. First, I have dropped the *bronchial and vascular patterns* altogether. Who really requires categorization for something as simple as too large or too small?
2. Next, I have replaced the *alveolar pattern* with consolidation, atelectasis, or a combination of the two, admitting freely that such distinctions are not always easily made in horses owing to the lack of a ventrodorsal view, which is indispensable in establishing the presence of a pulmonary volume loss, the hallmark of atelectasis.
3. I have retained the *interstitial pattern* but only in instances of truly diffuse disease. Such cases are then divided into two groups: those with one or more, clearly defined, repeating elements (most commonly small nodules) and those without a repeating element. These are termed, respectively, *structured and nonstructured interstitial patterns.*
4. I do not use the expression *mixed pattern* (bronchovascular or brochointerstitial), for example, believing it to be little more than a catch-all or, worse, an expression of indecision, one that in my experience becomes increasingly attractive with time, much like the term *open diagnosis,* something to say or place in the patient record, which does not reflect a great deal of thought.

▮▮▮ RELATIVE DIAGNOSTIC ROLES OF RADIOLOGY AND ULTRASOUND

As recently as 1991, some experts continued to see medical imaging as some sort of rivalry, vigorously (and sometimes stridently) touting the virtues of their particular modality over that of the "competition," and nowhere were the trumpets sounded louder than in the camps of large-animal ultrasound.[7] Now that ultrasound has matured, and rightfully assumed its place alongside radiology as a *complementary* form of medical imaging, its time to retire the "mine is bigger than yours" rhetoric and get on with the business of medical imaging.

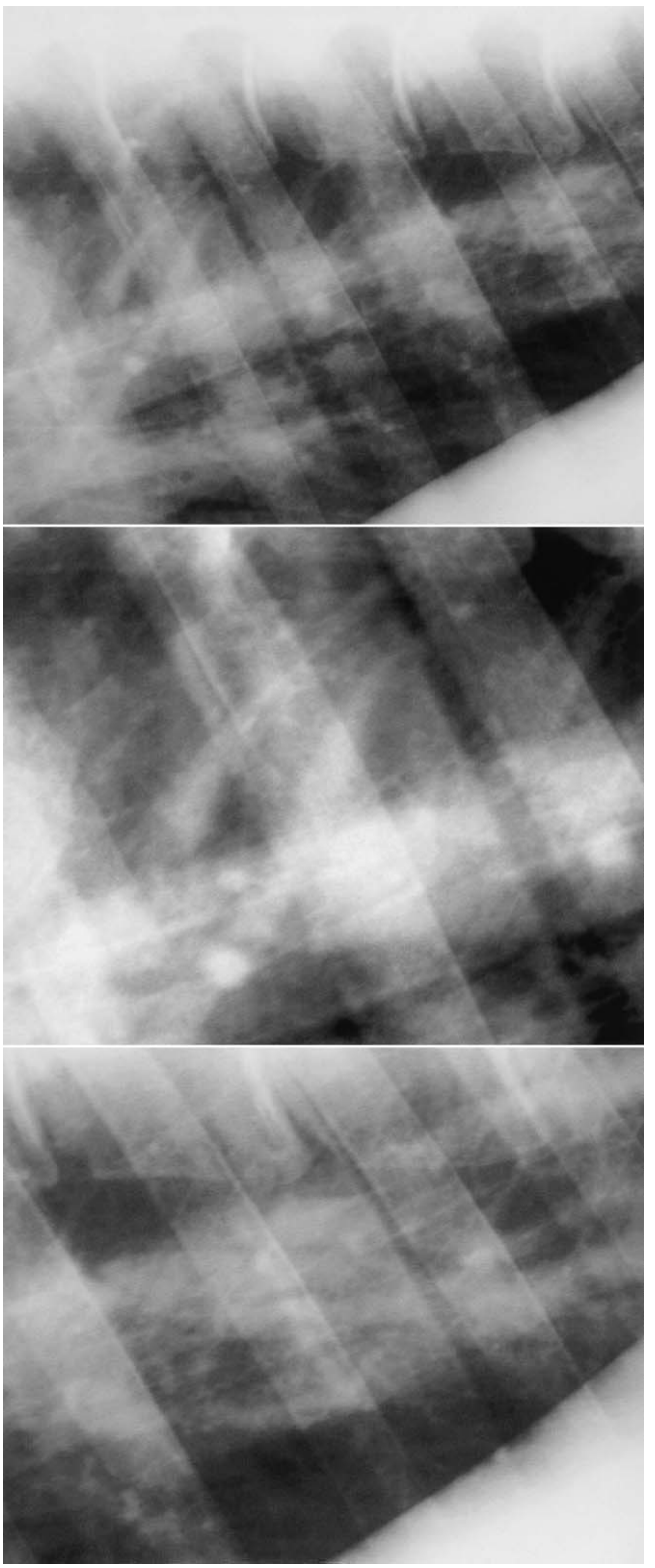


Figure 30-7 • Lateral **(A)** view of the caudodorsal aspect of the lung shows what at first appear to be a pair of vaguely outlined lung masses superimposed on the large pulmonary arteries and veins of the caudal lung lobes, perhaps abscesses, or less likely, secondary tumors. Closer inspection, provided by a pair of adjacent enlargements of the areas in question **(B, C),** instead reveals that these are overlapping blood vessels, not lung masses.

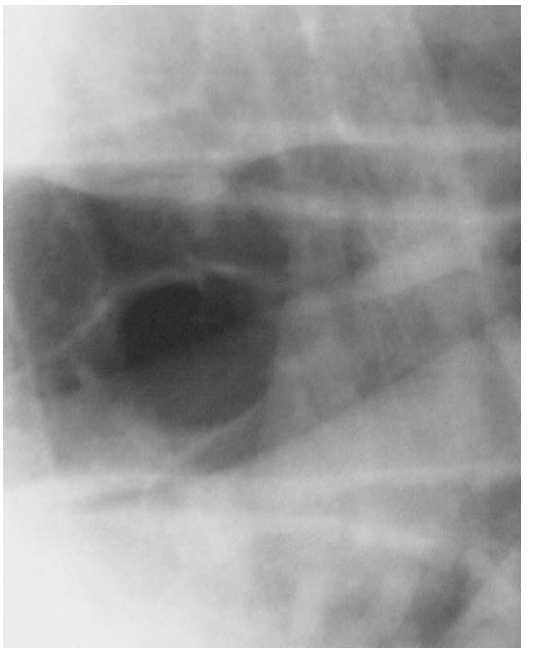


Figure 30-8 • Ultra-close-up lateral view of the distal aspect of the trachea shows a circular object with a lucent interior, representing a bronchial cross-section, not a cavitary lung lesion. The width, margination, and density of the tracheal and bronchial walls are normal, given the beam centering (over the heart base) and exposure factors.

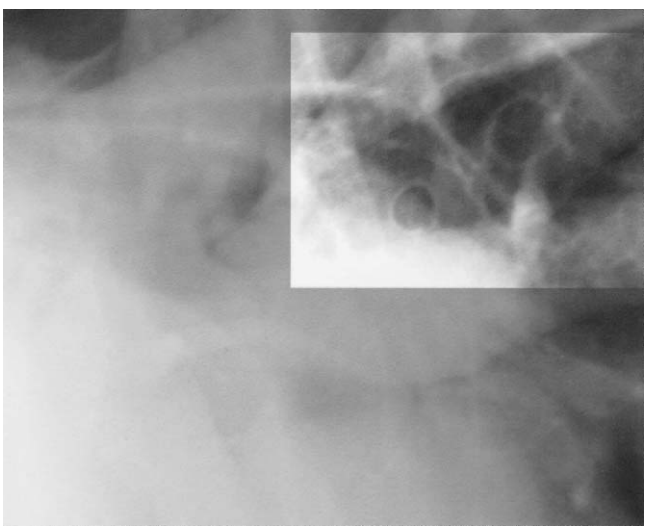


Figure 30-9 • A normal cluster of perihilar bronchial long- and cross-sections made all the more clear by virtue of a thin animal and a high-quality radiograph.

For example, radiology often provides an anatomic overview or diagnostic context that is enormously helpful, irrespective of the disease; ultrasound, on the other hand, can usually reveal the *interior* of a surface lesion with clarity unobtainable by any other means. Radiology defines the exterior surface of the heart, thus providing diagnostic perspective, whereas ultrasound reveals the cardiac interior and that which it entails: chamber size, valvular motion and competency, contractility, and the presence or absence of pericardial fluid.

Quite predictably, many of those performing only radiology or ultrasound expend much of their energy speaking of what the other modality will not do: for example, ultrasound is inable to scan thorough an air-filled lung to reach a lesion situated deep within the parenchyma.

▮▮▮ NUCLEAR MEDICINE (NUCLEAR IMAGING, SCINTIGRAPHY)

Nuclear medicine, like ultrasound, is a complementary form of medical imaging whose principal diagnostic contributions are in the areas of pulmonary ventilation and perfusion. However, the facilities and expertise to carry out such examinations are extremely limited.

▮▮▮ RADIOGRAPHIC DISEASE INDICATORS OF EQUINE LUNG DISEASE

The following radiographic abnormalities are reliable radiographic indicators of lung disease in horses:

- Pleural fluid
- Pleural air
- Mediastinal air
- Cardiac shift
- Pumonary atelectasis
- Hyperinflated lung
- Hyperlucent lung
- Pulmonary consolidation
- Solitary lung nodule
- Multiple lung nodules
- Solitary lung mass
- Multiple lung masses
- Cavitated lung mass
- Mineralized lung mass
- Generalized, nonstructured increase in lung density
- Generalized, structured increase in lung density
- Hilar adenopathy
- Sternal adenopathy
- Generalized bronchial dilation or deformity
- Localized bronchial dilation or deformity

References

1. Beech J: Respiratory problems in foals, *Vet Clin N Am Equine Pract* 1:131, 1985.
2. O'Brien RT, Biller DS: Field imaging of the respiratory tract: radiology and ultrasonography, *Vet Clin N Am Equine Pract* 13:487, 1997.
3. Koterba AM, Wozniak JA, Kosch PC: Changes in breathing pattern in the normal horse at rest up to one year of age, *Equine Vet J* 27:265, 1995.
4. Farrow CS: Radiography of the equine thorax: anatomy and technique, *Vet Radiol* 22:62, 1981.
5. Lamb CR, O'Callaghan MW, Paradis MR: Thoracic radiography in the neonatal foal: a preliminary report, *Vet Radiol Ultrasound*. 31:11, 1990.
6. O'Callaghan MW, Seeherman HJ: New ways of looking at lung diseases in the horse using radiography and scintigraphy. *Proceed 32nd Ann Conv Am Assoc Equine Pract*, Nashville, Tennessee. AAEP 1989.
7. Reef VB, Boy MG, et al: Comparison between diagnostic ultrasonography and radiography in the evaluation of horses and cattle with thoracic disease: 56 cases (1984-1985), *J Am Vet Med Assoc* 198:2112, 1991.

Chapter 31

Pleural Fluid

The hallmark of most forms of pleuritis and pleuropneumonia is pleural fluid. Although it is possible to diagnose large volumes (and sometimes medium volumes) of pleural fluid in foals and adult horses radiographically, identification of small amounts of fluid is very difficult or impossible. Fortunately this is not the case with ultrasound, which is capable of detecting very small pleural effusions, as shown by Rantanen and others.[1]

CAUSES OF PLEURAL FLUID IN HORSES

A number of review papers have been written on causes of pleural fluid in horses (Box 31-1).[2]

THE FUNCTIONAL CONSEQUENCES OF PLEURAL FLUID

Either interior or exterior forces may adversely affect lung compliance. Fibrinous pleuritis is a classic example of a peripherally restrictive disease, where much of the lung exterior is coated by fibrin, preventing full inflation. Extensive parenchymal disease may also prevent normal lung expansion by stiffening the lung; in fact, most pneumonias have this effect, but not to the extent that they are classified as *large R*, restrictive lung disease. In the final analysis, restrictive (or obstructive lung disease, for that matter) is diagnosed on the basis of abnormal blood gases and pulmonary function testing: (1) abnormal dynamic compliance and (2) pulmonary resistance values.[3]

THE RADIOGRAPHIC APPEARANCE OF PLEURAL FLUID

Fluid Level Versus Fluid Zone

Large volumes of pleural fluid are easily detected radiographically, but small volumes are not. As might be imagined, then, medium amounts of pleural fluid may or may not be visible.

The first thing to understand about a large volume of pleural fluid in the chest of a horse, let us say 20 L, is that it *does not result in a fluid level*.

Fluid Level. The creation of a fluid level requires *two* essential ingredients: air and fluid. Furthermore, the air and fluid must reside together in an existing or newly created cavity, and the radiograph must be made in the standing position (or if the animal is recumbent, with a horizontal beam). Under such circumstances, a classic thoracic fluid level appears as a *sharply demarcated* linear interface, black or dark gray dorsally and white or light gray ventrally (Figure 31-1). Fluid levels are most often encountered in the guttural pouches (see Chapter 26 for examples) and occasionally in the lung as erosive abscesses or traumatic bullae (Figure 31-2).

Fluid Zone. Fluid zones, on the other hand, are far more common, nearly always accompanying a large volume of pleural fluid. Unlike a fluid level, a *fluid zone* is indiscrete, poorly demarcated, and nonlinear, more of a vertically oriented step wedge than a discernible line. This perception of change from a relatively dark dorsal to a light ventral lung field is rather complex, but it can be simplified as follows. The pleural fluid superimposed on the lung surfaces, both

Box 31-1
Causes of Pleural Fluid In Horses

Pleuropneumonia
Bacterial, granulomatous, fungal, or viral pneumonia
Lung, pleural, or mediastinal cancer
Congestive heart failure
Chronic liver disease
Hypoproteinemia secondary to severe enteritis
Viral pleuritis
Penetrating chest wounds
Blunt thoracic trauma
Secondary diaphragmatic inflammation
Ruptured thoracic esophagus
Diaphragmatic hernia
Surgically related visceral manipulation
Neonatal septicemia
Equine infectious anemia
Coccidioidomycosis
Pulmonary embolism
Pulmonary infarction
Disseminated intravascular coagulation
Ruptured thoracic duct (chylothorax)
Ruptured lung abscess
Thoracic gunshot

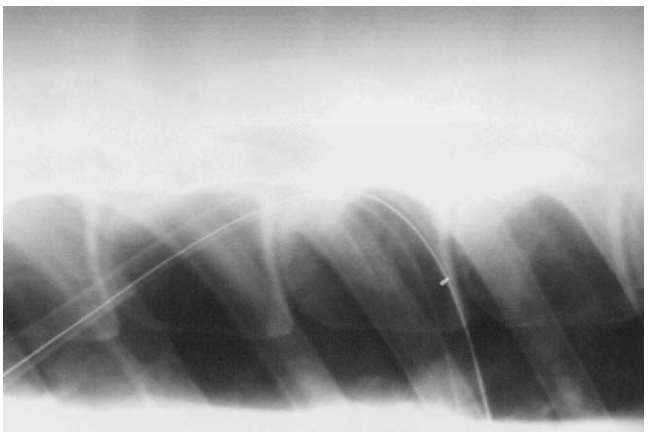
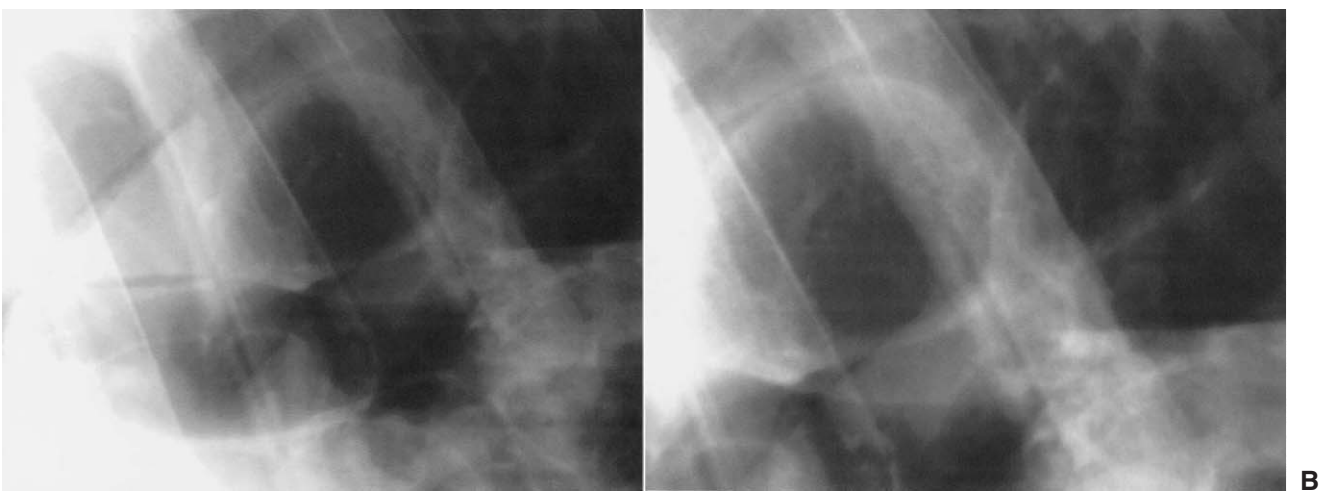


Figure 31-1 • Close-up view of the dorsal aspect of the caudal lung field of an adult horse shows large volumes of *free pleural air and fluid* resulting in a distinctive fluid level. A chest drain is also present.



A **B**

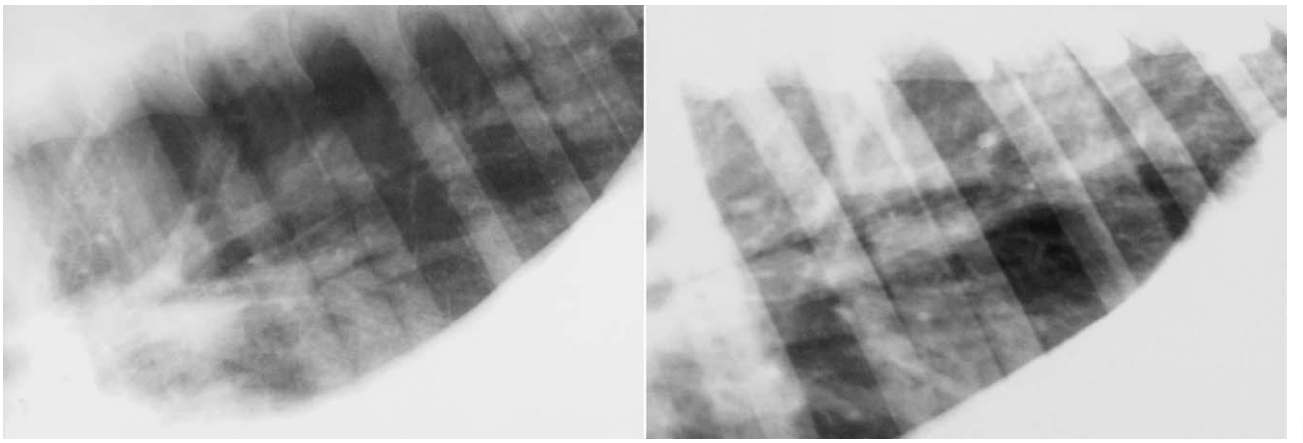
Figure 31-2 • Close **(A)** and ultra-close-up **(B)** views of the mid-dorsal lung field show side-by-side *cavitary lung lesions*, the caudal one of which displays a distinctive fluid level.

medially and laterally, absorbs some of the incoming and outgoing radiation, causing the lung to appear lighter than normal.

The compressive effects of the fluid on the portion of the lung lying beneath the fluid, combined with the compensatory hyperinflation of the lung above the fluid and the flotational tendency of the lung in the fluid bath, are what produce a gradual top-to-bottom, black to gray to white transition that characterizes a fluid zone (Figure 31-3).

Diaphragmatic Slope

When a large volume of fluid is present in the chest of a horse, the dorsal half of the lung above the surface of the fluid hyperinflates, compensating for the atelectasis that exists below the surface of the fluid. This results in increased convexity of the dorsal half of the diaphragm, as seen in a lateral radiograph. The described convexity is visually exaggerated by the pleural fluid, which gradually curves upwardly as it effaces the diaphragm (see Figure 31-1).



A **B**

Figure 31-3 • A, Lateral view of the caudodorsal lung field of an adult horse with a *large volume of thoracic fluid* secondary to pleuropneumonia shows (1) a hyperinflated dorsal lung field, (2) a central fluid zone, and (3) an opaque ventral lung field devoid of interior detail. Additionally, the visible portion of the lung is abnormally grayed associated with vascular crowding in the caudal caval region. Also note the exaggerated curvature the dorsal half of the diaphragm caused by the "roll-up" of pleural fluid. **B,** A comparable view of a normal horse lung is provided for comparison.

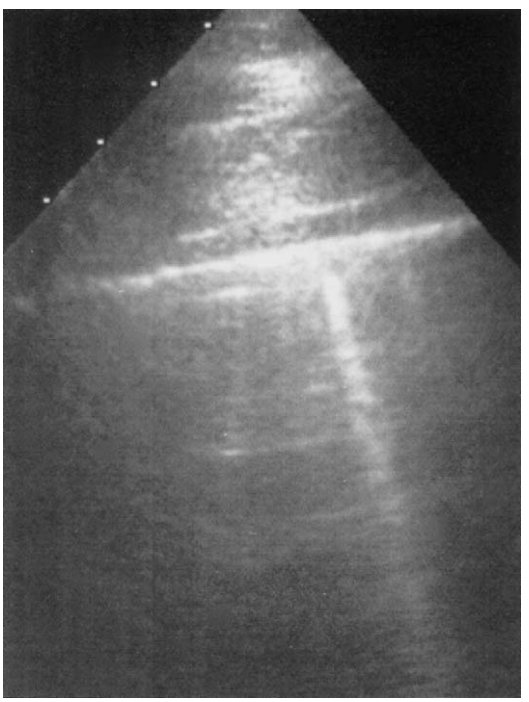


Figure 31-4 • Thoracic sonogram of a normal lung surface in a horse appears as a thick, white horizontal band just below the inner surface of the chest wall (muscle). A single reverberation can be seen radiating into the lung interior, resembling a ray of sunshine breaking through the clouds.

▮▮▮ THE SONOGRAPHIC APPEARANCE OF PLEURITIS AND PLEURAL FLUID

Normal Lung Surface and Ribs

When struck by the ultrasound beam, the surface of a normal air-filled lung produces a characteristic thick, white band or series of bands, which are often accompanied by one or two vertically oriented, central reverberations (Figures 31-4 and 31-5). A thin band of anechoic pleural fluid may also be visible situated between the thoracic muscle and lung surface. The associated rib surfaces are also strongly reflective, creating a series of regularly spaced, thick black columns, or sonographic voids, in the image (Figure 31-6).

Pleuritis

The surface of an inflamed or infected pleura changes from smooth to rough, a transformation aggravated by fibrin accumulation and underlying lung consolidation. Consequently, the white band normally produced at the lung surface becomes thicker, brighter, and more irregular, while the associated reverberations become more numerous and closely spaced (Figure 31-7).

Pleural Fluid

Pleuritis may or may not be accompanied by pleural fluid. The fluid may appear dark or light, depending on its composition. Generally, transudates are uniformly black or anechoic (Figure 31-8), whereas exudates and hemorrhage typically appear uniformly mottled (Figure 31-9). Rafts of fibrin or pus in the pleural space appear hyperechoic and are made all the more so by surrounding pleural fluid (Figure 31-10).

Pleural fluid can be distributed in a variety of ways, for the most part appearing as bands, wedges, and circles (Figures 31-11 and 31-12). The underling lung may be normally aerated, pleuritic, atelectatic, or consolidated. Subsurface lung consolidation can usually

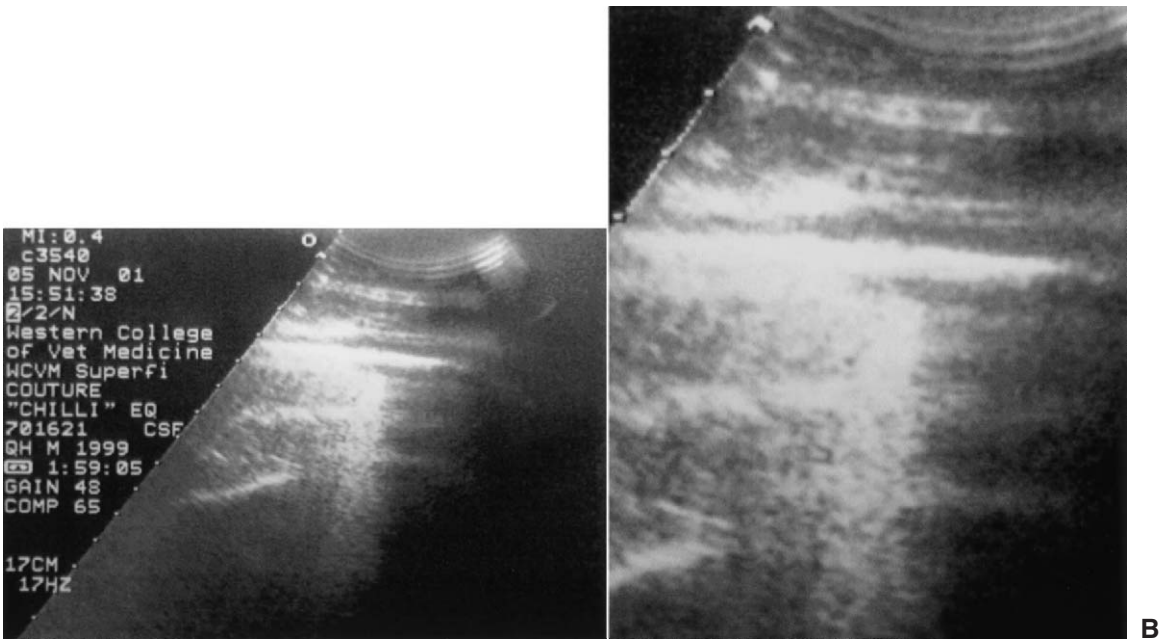


Figure 31-5 • Orientation **(A)** and close-up **(B)** thoracic sonograms of a normal lung surface in a horse, appearing as a thick, hyperechoic band underlain by a series of parallel but less well-defined reverberation artifacts. As in the previous example, there is also a thick, vertically oriented central reverberation.



Figure 31-6 • Close-up thoracic sonogram of the surface of a horse's lung shows a thick, black, vertically oriented band to the left of the image containing a series of shaggy white arcs representing the rib surface and resultant reverberations. The hyperechoic reverberations to the right are from the mildly pleuritic lung surface.

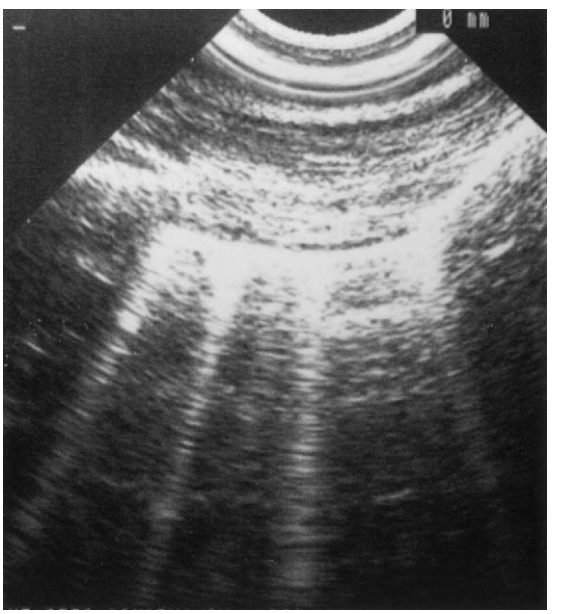


Figure 31-7 • Thoracic sonogram of a horse with mild pleuritis shows an abnormally thick, bright, and irregular lung surface accompanied by excessive reverberation.

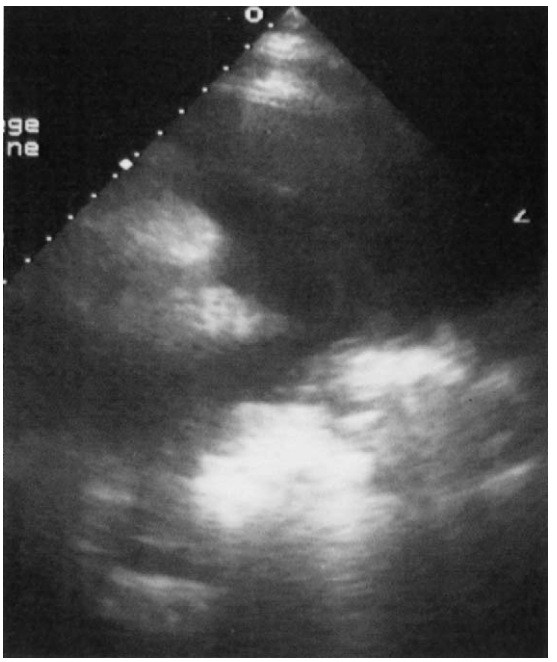


Figure 31-8 • Close-up thoracic sonogram of a large volume of pleural fluid (transudate) surrounded by fluffy, highly echogenic lung surfaces beginning to collapse peripherally.

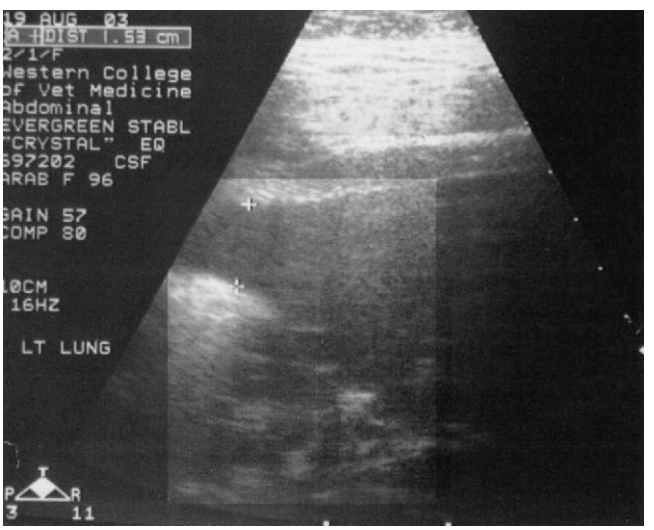


Figure 31-9 • Thoracic sonogram of a horse with severe pleuropneumonia shows a large volume of echogenic pleural fluid with pneumonic lung below.

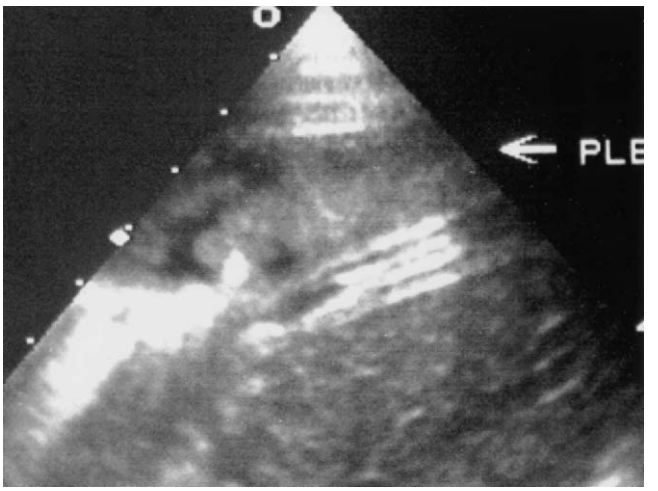


Figure 31-10 • Thoracic sonogram of a horse with chronic pleuritis shows multiple echoic rafts in the pleural cavity surrounded by pleural fluid *(arrow)* caused by freely moving clumps of inspissated pus and fibrin.

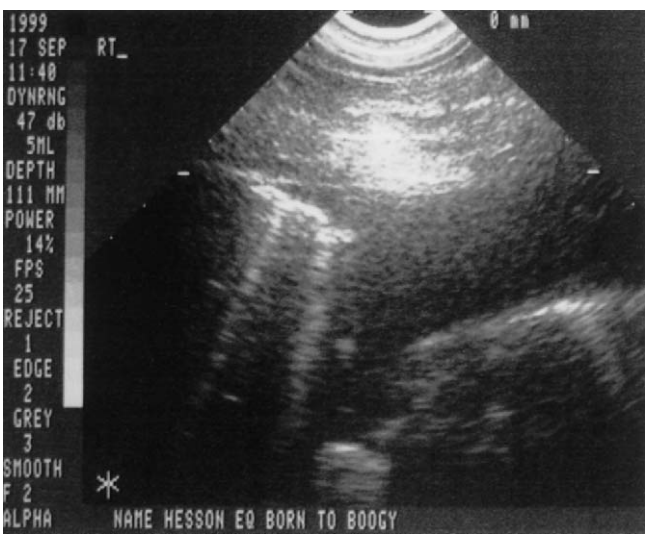


Figure 31-11 • Sonogram of the right midthorax of a horse with pleuropneumonia shows a medium-sized, rectangular fluid pocket situated just beneath the surface of the upper left chest wall. Strong reverberations are emanating characteristically from the normal lung surface to the left of the lesion.

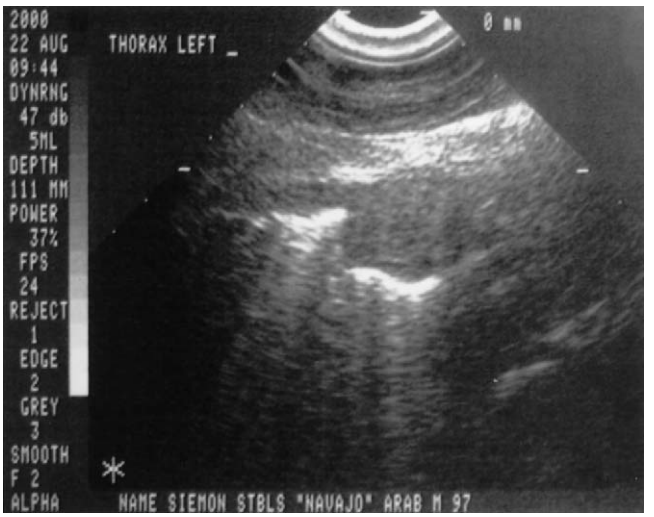


Figure 31-12 • Sonogram of the left ventrolateral thorax of a horse with pleuropneumonia shows a circular pleural fluid pocket associated with a small bandlike tail.

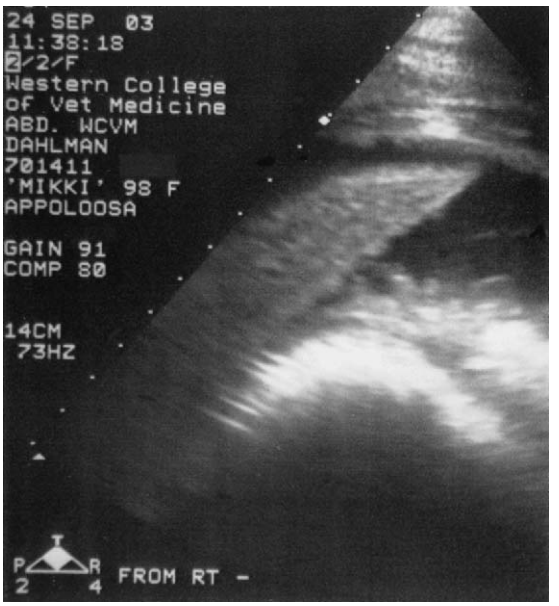


Figure 31-13 • Thoracic sonogram shows a large volume of clear (anechoic) fluid surrounding an atelectatic lung lobe to the left and a pair of pleuritic lung surfaces below.

be differentiated from a fluid pocket by its semistructured interior markings, for example, alveolar air pockets or air- and fluid-filled bronchi. A fluid pocket, on the other hand, appears uniformly anechoic or mottled, surrounded by one or more highly reflective lung surfaces. Atelectatic lung surrounded by pleural fluid typically appears uniformly gray with a well-defined margin and a structured interior (Figure 31-13).

References

1. Rantanen NW, Gage L, Paradis M: Ultrasonography as a diagnostic aid in pleural effusion of horses, *Vet Radiol* 22:211, 1981.
2. Sweeney C: Causes of pleural effusion in the horse, *Equine Vet Educ* 4:15, 1992.
3. Derksen FJ, Slocombe RF, et al: Chronic restrictive pulmonary disease in a horse, *J Am Vet Med Assoc* 180:887, 1982.

Chapter 32

Chest Trauma

CHEST WALL INJURY

Subcutaneous Emphysema and Its Diagnostic Implications

In the horse, subcutaneous emphysema is most often due to (1) transtracheal aspiration; (2) iatrogenic pharyngeal injury; (3) tracheal puncture, fracture, or avulsion; (4) leakage from a pharyngostomy site; and (5) pneumomediastinum. Pneumothorax rarely leads to pneumomediastinum or subcutaneous emphysema, nor does pneumomediastinum or subcutaneous emphysema usually result in pneumothorax,[1] although a few reports have indicated otherwise.[2,3]

As a general rule, when pneumomediastium and pneumothorax are present together, seek at least two different sources for the abnormally situated air.

Rib Fractures

Fresh rib fractures can appear as cracks, marginal steps, or obvious discontinuities, the last often featuring large interfragment gaps (Figure 32-1). Old rib fractures are typically callused even when the original fractures were not displaced (Figure 32-2).

Minor Lung Bruising

Minor lung injury usually takes the form of regional bruising to one side of the lung or the other, which may or may not be radiographically distinguishable from normal lung. When detectable, lung contusions are usually represented by a subtle increase in lung density. The lung typically returns to normal within a week or so.

Major Lung Bruising

Unlike minor lung bruising, major lung injuries are characterized by wider involvement and a greater degree of opacification, the latter often accompanied by obvious bronchograms and alveolagrams, hallmarks of severe consolidation.

Penetrating Chest Wounds

Collins and co-workers reported on 43 horses that had sustained deep thoracic stab wounds and, as a result, developed secondary pleuropneumonia.[4] Rosenstein and Schott reported bilateral pneumothorax in a horse after it sustained a deep cut on the right side of the chest, attributing the left-sided involvement to an incomplete caudal mediastinum.[5]

When wooden stakes are driven deeply into the thorax or when a horse impales itself on a post, hemothorax usually accompanies the pneumothorax. When horses receive deep penetrating wounds to the cranial part of the chest, especially between the pectoral muscles, the offending object may carry far into the lung and beyond into the mediastinum, causing both a pneumothorax and pneumomediastinum.

Pneumothorax (Free Pleural Air)

Beach reported that the most common type of pneumothorax in horses was traumatic.[6] A decade later, Boy and Sweeney, reporting from the same university, found that pleuropneumonia was the leading cause of pneumothorax in a retrospective study involving 40 horses.[7] In the later group, those with free pleural air resulting from pleuropneumonia were less likely to survive than those with pneumothorax from other causes. Furthermore, horses with pleuropneumonia usually had unilateral pneumothorax, whereas horses with pneumothorax from other causes were more likely to have bilateral involvement (Box 32-1 and Table 32-1).

Unilateral Versus Bilateral Pneumothorax

Theoretically, what begins as a unilateral pneumothorax *should progress* to a bilateral one because of a horse's fenestrated caudal mediastinum. Unfor-

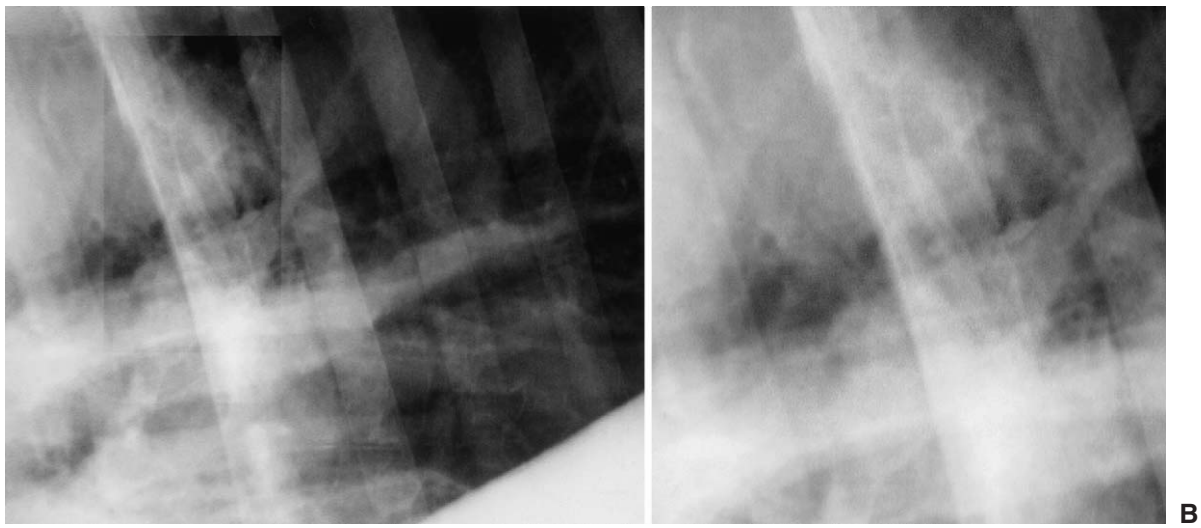


Figure 32-1 • Lateral **(A)** and close-up lateral **(B)** views of a 2-week-old displaced rib fracture, which is just beginning to show a bony callus.

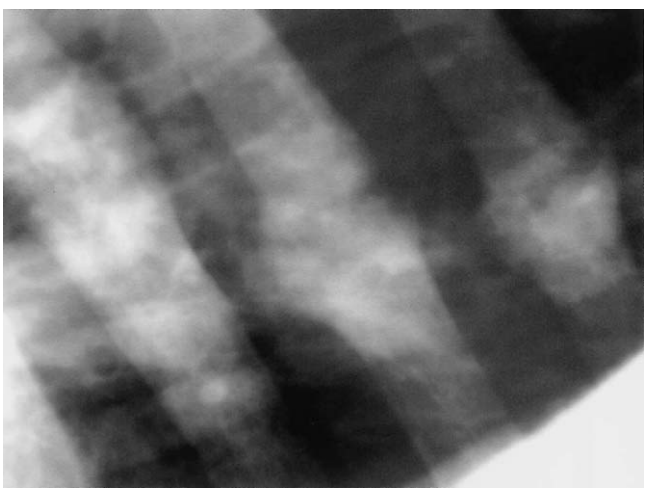


Figure 32-2 • Five-month-old caudal thoracic rib fractures.

Box 32-1
Potential Sources of Pneumothorax in Horses

Pleuropneumonia
Torn interpleural adhesion
Open chest wound
Blunt chest trauma
Thoracic surgery
Ruptured bulla
Ruptured lung abscess
Secondary to drainage of pleural fluid
Secondary to transthoracic fine-needle biopsy (especially if multiple)

Table 32–1 • CLASSIFICATION OF PNEUMOTHORAX

Type of Pneumothorax	Definition
Primary	Pneumothorax originating from within the lung
Secondary	Pneumothorax initiated by extrapulmonary causes
Traumatic	Pneumothorax caused by thoracic injury
Iatrogenic	Pneumothorax caused by veterinarian, usually in the act of providing treatment
Open	Chest cavity is open to the atmosphere, which then becomes the source of the free pleural air
Closed	Chest cavity is closed to the outside with free pleural air originating from the lung
Tension	Definitions vary somewhat, but my preference is as follows: A severely compressive pneumothorax that often becomes worse with time as demonstrated in serial radiographs
Small	Only a small volume of free pleural air is present, and there is minimal lung collapse
Large	A large volume of free pleural air is present, lung collapse is severe, and there is usually a pronounced cardiac shift
Spontaneous (idiopathic)	Cause unknown (a temporary categorization, used until cause is eventually determined), a category of convenience

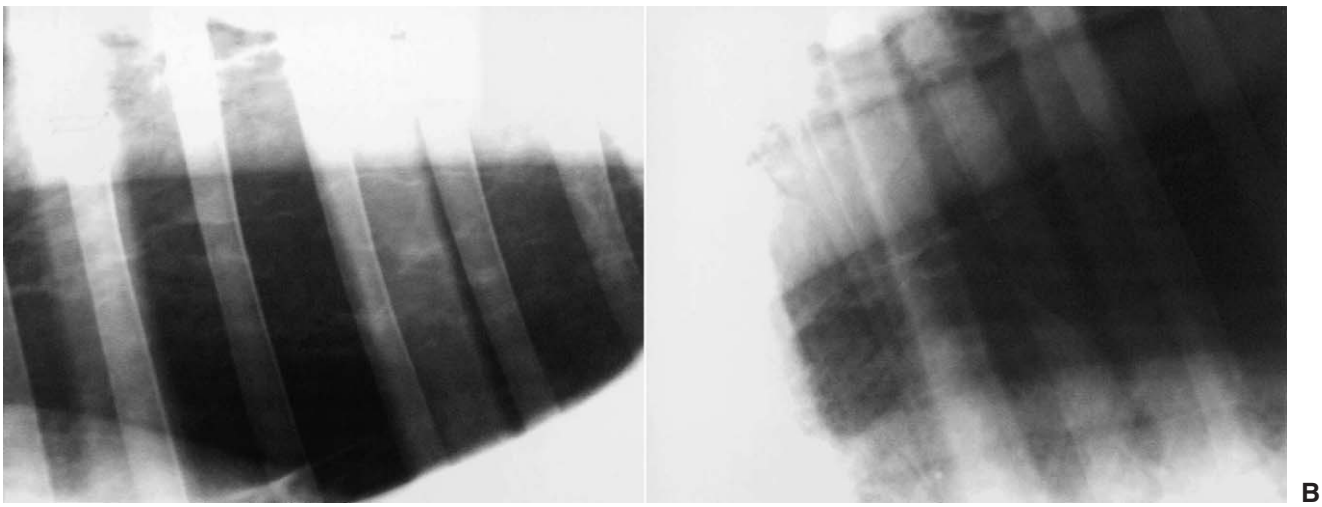


Figure 32-3 • A, Right lateral view of a horse that recently sustained a deep wound to the right axillary region shows a severe pneumothorax as indicated by an abnormally clear ventral aortic margin, pulmonary oligemia, and collapse of the right caudal lung lobe (appearing here as a curved solid object in the left lower corner of the image). **B,** The left lateral view is comparatively less informative.

tunately, this seemingly straightforward thinking is not true in most cases. Why not?

Although it is quite correct that a horse's caudal mediastinum usually contains a vertically oriented slit through which free pleural air may potentially pass, in most instances, the escaped air remains on the side of the chest where it originated.[8] This is because the caudal mediastinum is extremely deformable and, as such, is subject to a variety of compressive forces that routinely accompany pneumothorax: compressive forces that usually so deform the caudal mediastinum that transmediastinal communication is impossible.

In my experience, the more severe the pneumothorax, the more pronounced the cardiac shift, the greater the mediastinal distortion, and the less likely that a unilateral pneumothorax will become bilateral. In horses with pleuropneumonia, or for that matter any kind of chronic fibrin-containing pleural fluid, the caudal mediastinal opening is often permanently sealed shut by fibrin sheets or pleuromediastinal adhesions.

Radiographic Detection of Pneumothorax

The upright or standing position is far superior to the recumbent position for detecting a small- or medium-volume pneumothorax. If a foal or adult horse is unable to stand, a decubital view is far superior to a film made with a vertical x-ray beam. Although there is no diagnostic advantage to making inspiratory versus expiratory images, as far as identifying a pneumothorax is concerned, there are enough other benefits associated with inspiratory filming to warrant its use.[9]

Radiographically, pneumothorax is characterized by seeing that which is normally invisible, for example, the dorsal edge of one or both caudal lung lobes or the aortic margins. Although a horse has a fenestrated caudal mediastinum, as mentioned previously, free pleural air is often confined to one side of the chest. In such situations, alternate-side radiography can be used to determine which side of the thorax is affected (Figures 32-3 and 32-4). In general, the larger the volume of free pleural air, the greater the degree of ventral displacement of one or both caudal lung lobes. Conversely, as a horse recovers, its injured lung gradually reinflates.

▮▮▮ TRAUMATIC BULLA (TRAUMATIC LUNG CAVITIES)

An extremely forceful blow delivered to the chest wall or a severe fall can cause one or more variably sized, temporary lung cavities, termed *traumatic bullae*. Most such cavitary lung lesions resolve in a week or so. Only rarely do bullae rupture, causing a secondary pneumothorax.

Radiographically, traumatic bullae may be sharply or vaguely marginated, depending for the most part on the size of the lesion and the amount of peripheral lung compression, which is often mistakenly referred to as "wall thickness"(Figures 32-5 and 32-6). The location of the bulla also influences its visibility, with dorsal midthoracic and caudal thoracic lesions being the easiest to identify.

▮▮▮ PLEURAL FLUID

Potential causes of pleural fluid are listed in Box 32-2. Of these causes, pleural effusion secondary to pneumonia, also known as *pleuropneumonia,* is most common.[10]

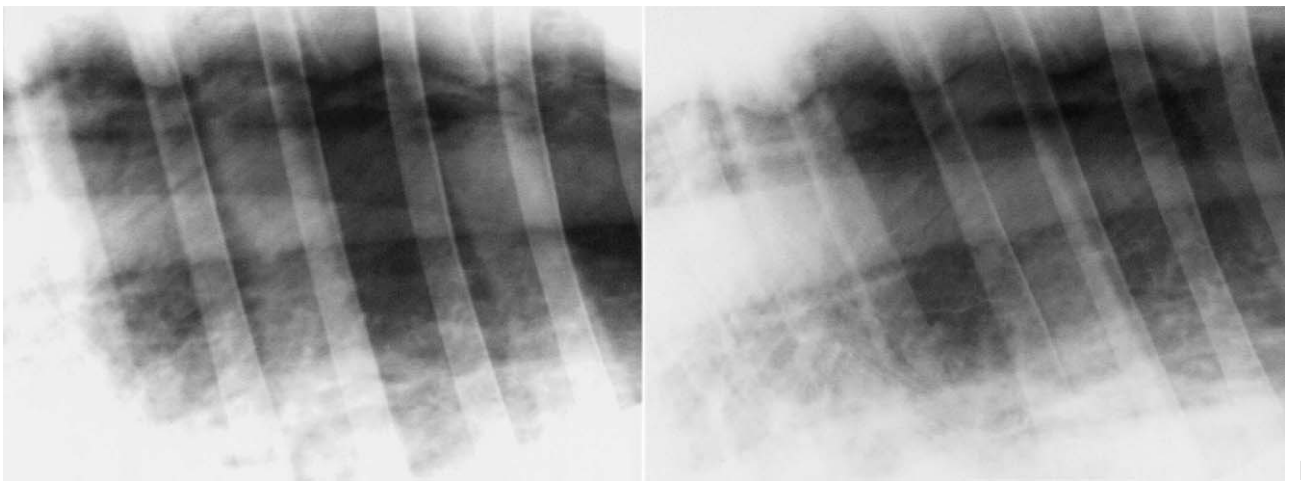


Figure 32-4 • A, Progress right lateral view made 48 hours after the injury shows less free air with improved but as yet incomplete inflation of the right caudal lung lobe (the dorsal edge of which is seen here as a curved line crossing over the left and central thirds of the ventral half of the aorta). **B,** A left lateral view is less revealing.

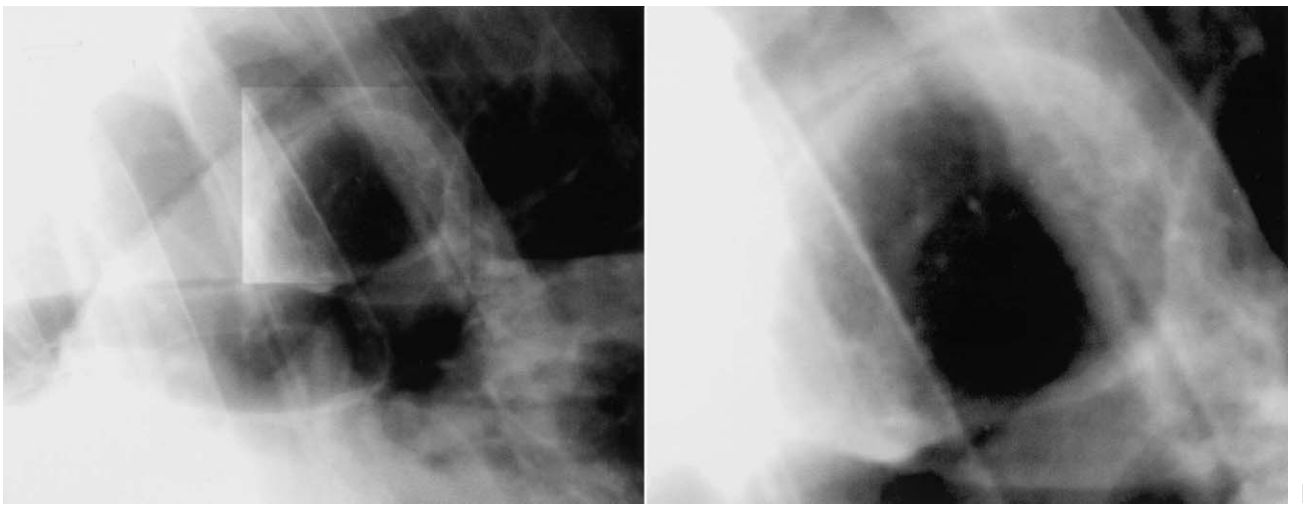


Figure 32-5 • Lateral **(A)** and ultra-close-up lateral **(B)** views of a distinct traumatic bulla *(emphasis zone)* located just above the carina. The dense rim surrounding the cavity is formed by compressed lung tissue and associated hemorrhage and edema.

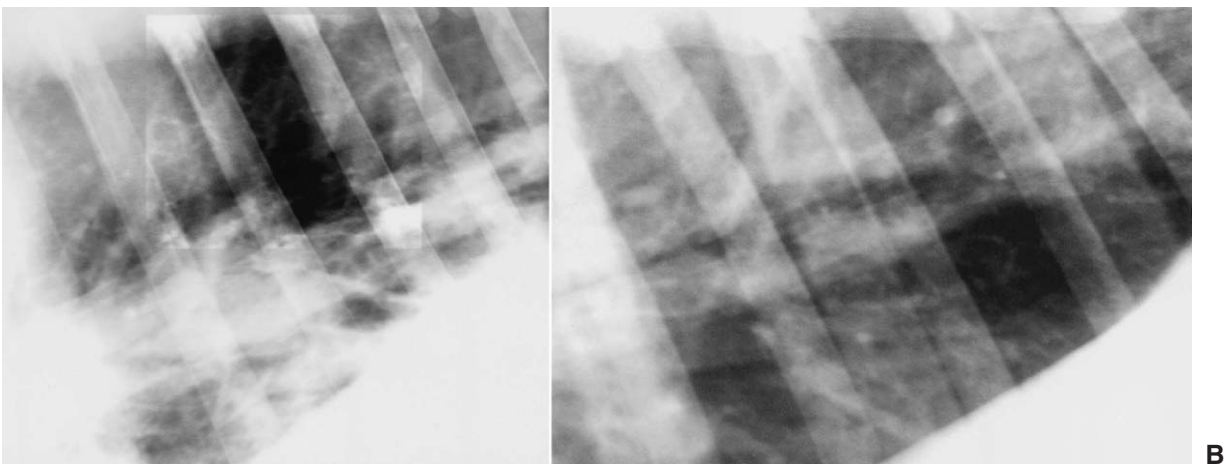


Figure 32-6 • A, Lateral view of the dorsocaudal lung field of an adult horse shows an indistinct traumatic bulla just below the spine centrally *(emphasis zone).* **B,** A normal lung is provided for comparison.

▮▮▮ HYDROPNEUMOTHORAX (PLEURAL FLUID AND PNEUMOTHORAX)

When fluid and air occupy the same confined space, for example, the pleural cavity, the air rises and the fluid falls, creating a distinctive black-white interface, which is termed a *fluid level* (Figure 32-7), provided the horse is radiographed in the standing position.

▮▮▮ PNEUMOMEDIASTINUM

The most common source of mediastinal air in horses is a recent transtracheal aspiration (Figure 32-8).[11] Hance and Robertson reported subcutaneous emphysema, pneumomediastinum, and bilateral pneumothorax in a horse after it incurred a deep axillary wound.[12] Throat wounds and perforation of a guttural pouch can also lead to a pneumomediastinum. It is important to recognize that a pneumomediastinum rarely causes a pneumothorax, and conversely a pneumothorax is very unlikely to result in a pneumomediastinum.

Box 32-2
Potential Sources of Pleural Fluid in Horses

Pleuropneumonia
Pulmonary abscessation
Lung-lobe torsion
Rapid lung reinflation following tension pneumothorax
Diaphragmatic hernia
Metastatic hemangiosarcoma
Congestive heart failure
Obstructive or erosive mediastinal tumor or other mass
Penetrating wounds
Granulomatous lung disease
Coccidioidomycosis
Equine infectious anemia
Nocardiosis
Chylothorax

▮▮▮ DIAPHRAGMATIC HERNIA

Because the diaphragm is radiographically invisible (unless surrounded by air, as in a pneumothorax), of necessity the diagnosis must usually be indirect. Likewise, sonographic diagnosis of diaphragmatic hernia is based primarily on indirect evidence, even though the diaphragm can be visualized sonographically.

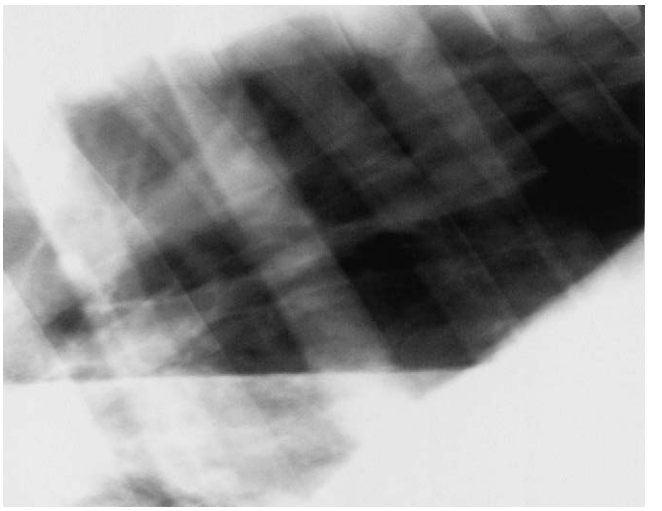
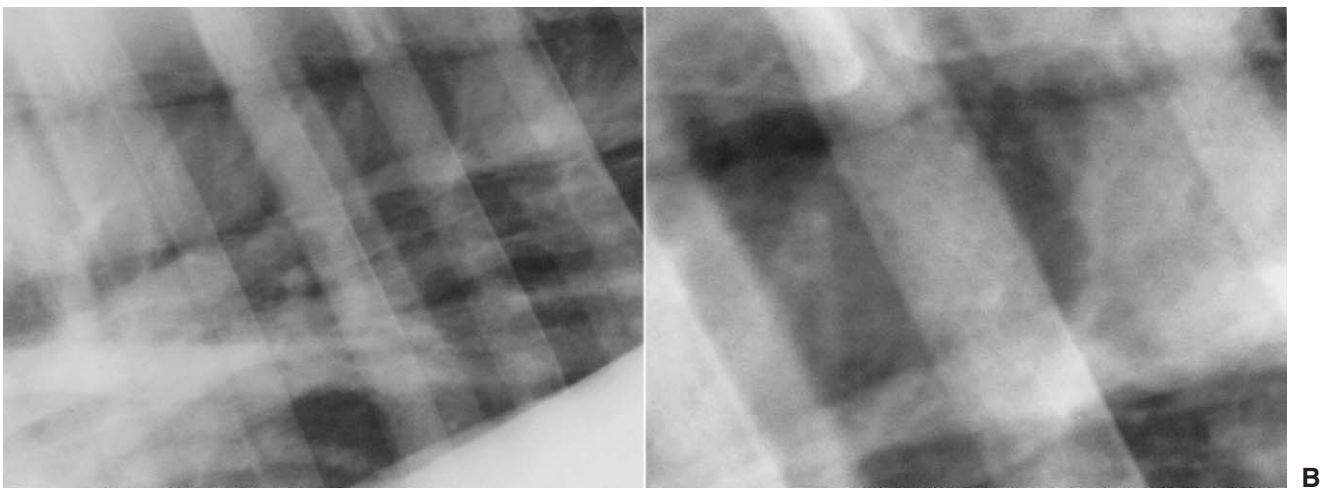


Figure 32-7 • Dorsocaudal lung field of an adult horse that recently suffered a penetrating chest wound. The presence of a distinctive fluid level indicates that there are large volumes of air and fluid in at least one side of the thorax.



A **B**

Figure 32-8 • Close-up **(A)** and ultra-close-up **(B)** views of the dorsocaudal lung field of a horse that recently underwent a transtracheal irrigation-aspiration show an exceptionally clear caudal aorta, the result of an accumulation of mediastinal air secondary to leakage from the tracheal puncture site.

In both types of imaging, diagnosis is typically based on one of two abnormal findings: (1) absent abdominal viscera or (2) inappropriate thoracic viscera. In the latter regard, ultrasound is more informative than radiology because it can show the interior of questionable objects, whereas radiology cannot (excepting air, of course). Thus ultrasound is usually capable of differentiating between a herniated, fluid-filled stomach lying in the caudal thorax and a large, blood-filled cavitary lung lesion.

Radiographically, air-filled bowel is often readily detectable in the chest, provided there is enough of it, and that pulmonary atelectasis, consolidation, and pleural hemorrhage are not excessive. Displaced intestinal segments can be detected sonographically,[13] provided no large pneumothorax is present to prevent access. Verschooten and colleagues reported a diaphragmatic tear in a horse in which the characteristic sacculations of the cecum were observed in the thorax.[14]

Occasionally a small, undiagnosed diaphragmatic hernia may secondarily trap and constrict part of the small intestine, leading to signs of colic, rather than dyspnea.[15]

References

1. Caron JP, Townsend HGG: Tracheal perforation and widespread subcutaneous emphysema in a horse, *Can Vet J* 25:339, 1984.
2. Marble SL, Edens LM, et al: Subcutaneous emphysema in a neonatal foal, *J Am Vet Med Assoc* 208:97, 1996.
3. Hance SR, Robertson JT: Subcutaneous emphysema from an axillary wound that resulted in pneumomediastinum and bilateral pneumothorax in a horse, *J Am Vet Med Assoc* 200:1107, 1992.
4. Collins MB, Hodgson DR, Hutchins DR: Pleural effusion associated with acute and chronic pleuropneumonia and pleuritis secondary to thoracic wounds in horses: 43 cases (1982-1992), *J Am Vet Med Assoc* 205:1753, 1994.
5. Rosenstein DS, Schott HC: What is your diagnosis? *J Am Vet Med Assoc* 214:1323, 1999.
6. Beech J: Pneumothorax. In Smith B, editor: *Large animal internal medicine,* St Louis, 1990, Mosby.
7. Boy MG, Sweeney CR: Pneumothorax in 40 cases (1980-1997), *J Am Vet Med Assoc* 216:1965, 2000.
8. Jorgensen JS: What is your diagnosis? *J Am Vet Med Assoc* 210:1109, 1997.
9. Seow A, Kazerooni EA: Comparison of upright inspiratory and expiratory chest radiographs for detecting pneumothoraces, *Am J Radiat* 166:313, 1996.
10. Raphel CF, Beech J: Pleuritis secondary to pneumonia or lung abscessation in 90 horses, *J Am Vet Med Assoc* 181:808, 1982.
11. Farrow CS: Pneumomediastinum in the horse: A complication of transtracheal aspiration, *Vet Radiol* 17:192, 1976.
12. Hance SR, Robertson IT: Subcutaneous emphysema from an axillary wound that resulted in pneumomediastinum and bilateral pneumothorax in a horse, *J Am Vet Med Assoc* 214:1324, 1999.
13. Bryant JE, Sanchez LC, et al.: What is your diagnosis? *J Am Vet Med Assoc* 220:1461, 2002.
14. Verschooten F, Oyaert W, et al: Diaphragmatic hernia in the horse: four case reports. *Vet Radiol* 18:45, 1977.
15. Ethell MT, Haines G, et al: What is your diagnosis? *J Am Vet Med Assoc* 215:321, 1999.

Chapter 33

Pneumonia, Pleuropneumonia, Lung Abscess, and Pleuritis

RADIOGRAPHIC APPEARANCE OF PNEUMONIA

Kangstrom and I published the radiographic appearance of equine pneumonia.[1,2] Although there are tendencies, for example, caudoventral consolidation, there are few if any reliable disease patterns and no evidence to support the use of pattern recognition (e.g., interstitial pattern, bronchial pattern).

PNEUMONIA

Newborn Foals

Potential Causes of Abnormal Lung Density. Newborn foals (also termed *neonatal foals*) may have abnormally dense lungs for a variety of reasons, the most common of which include (1) pneumonia, (2) an insufficient volume of pulmonary surfactant, (3) postural atelectasis that may or may not be disease related, and (4) the presence of residual lung water and atelectasis, often observed in *normal* foals for a brief period of time shortly after birth.

What Precisely Is a Septicemic Foal, and Are There Any Reliable Radiographic Abnormalities? In my experience, there are no consistently reliable, specific signs of septicemia in newborn foals (see the potential causes of abnormal lung density listed in the preceding section); but not everyone agrees with this viewpoint. Some contend that there are dependable signs of neonatal lung disease that produce characteristic lung patterns.[3]

Bacterial Pneumonia in Foals. Foals do not show etiospecific pulmonary disease patterns (Figure 33-1).

Rhodococcus equi (Formerly *Corynebacterium equi*)

Rhodococcus equi is the most serious form of pneumonia, and it affects foals between the ages of 3 weeks and 5 months. In addition to lung abscesses, the infection can cause (1) ulcerative enterocolitis, (2) colonic or mesenteric lymphadenopathy, (3) immune-mediated synovitis or uveitis, (4) septic arthritis, and (5) osteomyelitis.[4-6] Falcon and co-workers described the clinical and radiographic features of *Corynebacterium* pneumonia in foals, emphasizing the diagnostic value of thoracic radiography in detecting pulmonary abscessation.[7] Ainsworth and co-workers showed that foals that survive *R. equi* pneumonia and go on eventually to race do so as effectively as horses that did not previously have pneumonia.[8]

Radiographically, *R. equi* pneumonia may appear in at least three different ways:

1. Nonspecific lung consolidation over the heart base, often extending as far caudally as the diaphragm
2. Nonspecific lung consolidation over the heart base associated with numerous vague patchy masses greater than 0.5 cm in diameter
3. Multiple, variably sized masses resembling pulmonary metastasis

Interstitial Pneumonia in Foals

The term *interstitial pneumonia* may be used in at least two distinct ways: (1) as a radiographic diagnosis and (2) as a pathologic diagnosis. Used in radiology, it refers to abnormal lung density *perceived* to be in the interstitium, which is then attributed to one cause or another, depending on the clinical context. In *pathology*, interstitial pneumonia generally refers to a specific type of equine lung disease of unknown etiology (Figure 33-2).

According to Buergelt, there are two types of equine interstitial pneumonia: one that occurs in foals, the other in adults.[9] In foals the disease usually occurs between 6 days and 6 months of age and causes severe respiratory distress and elevated heart rate. No effective treatment is known, and the disease is often fatal.

Postmortem findings in the acute form of the disease include (1) grossly moist, rubbery, diffusely

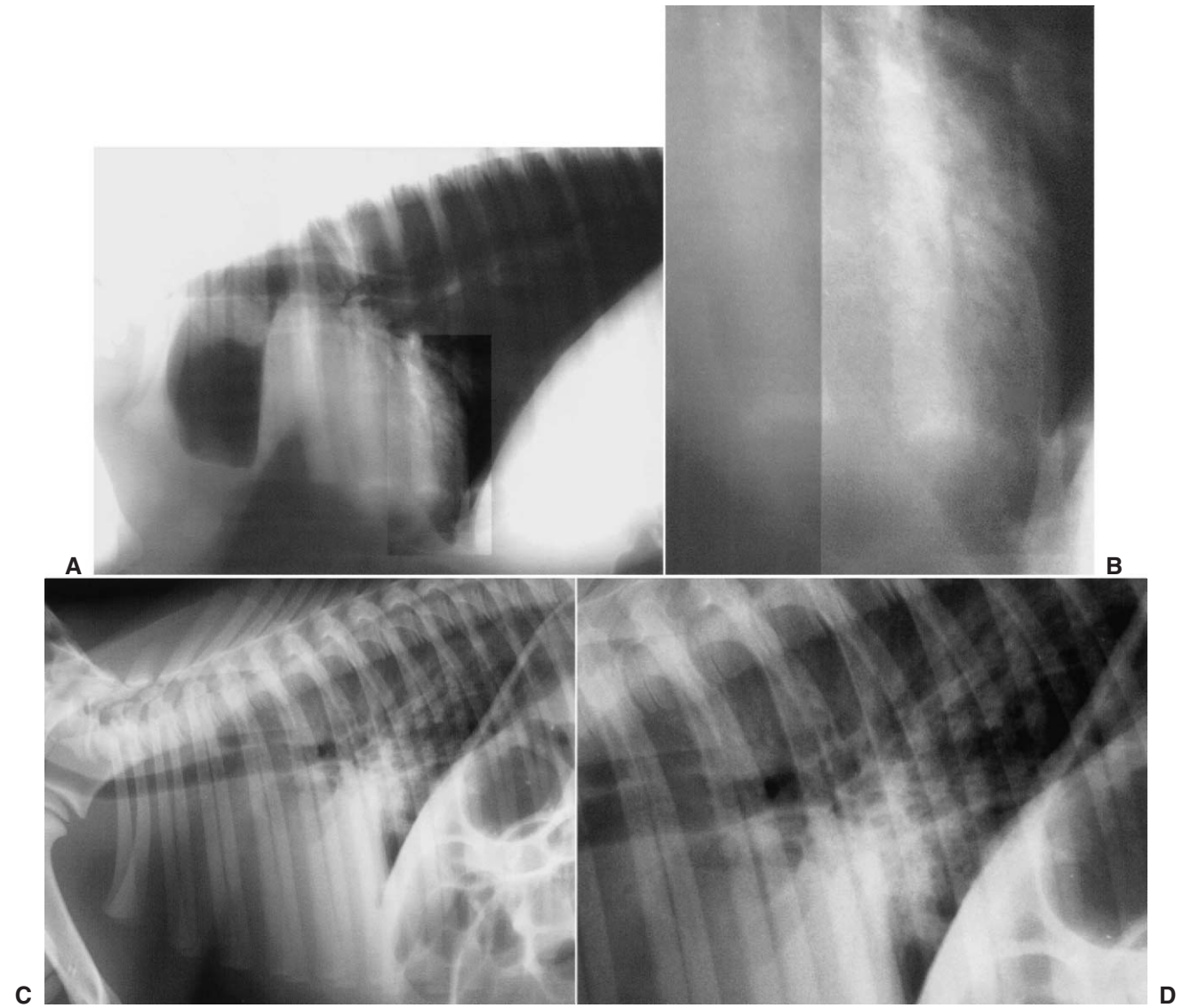


Figure 33-1 • Acute bronchopneumonia in a pair of foals. Foal 1: Lateral **(A)** and ultra-close-up **(B)** views show a faint vertical band of consolidation running along the caudal edge of the heart, consistent with pneumonic consolidation. Foal 2: Lateral **(C)** and lateral close-up **(D)** views show a roughly circular area of consolidation just caudal to the heart base, which then drapes down over the caudal margin of the heart nearly to the sternum. This is the most commonly identified site of pulmonary consolidation in pneumonic foals and adult horses.

mottled lungs; (2) microscopically necrotic alveolar walls; (3) hyaline membranes; (4) alveolar hemorrhage; and (5) fibrinous thrombi in the alveolar capillaries. In effect, the foal suffocates to death.

Combined Immunodeficiency of Arabian Horses. Heritable deficiency of T- and B-lymphocytes leaves Arabian foals vulnerable to a variety of bacterial, viral, and protozoal infections, especially rhodococcal pneumonia.[10] The last of these usually appears as numerous metastatic-like lung lesions.

***Pneumocystis carinii* Pneumonia.** Ewing and coworkers reported the clinicopathologic features of *Pneumocystis carinii* in three Quarter Horse foals between 2 and 3 months of age. Unfortunately there was no characteristic radiographic appearance.[11] In my experience, the radiographic findings associated with a pure *Pneumocystis* pneumonia are often quite subtle and impossible to distinguish from postural atelectasis. As far as I know, *Pneumocystis* pneumonia is the only equine lung disease that begins in the alveoli and thus is capable of producing a pure alveolar pattern on a thoracic radiograph.

Adult Horses

Bacterial Pneumonia and Pleuropneumonia in Adult Horses

Radiology. Bacterial pneumonia in adult horses is characterized by a wide variety of nonspecific radiographic appearances, with many featuring some

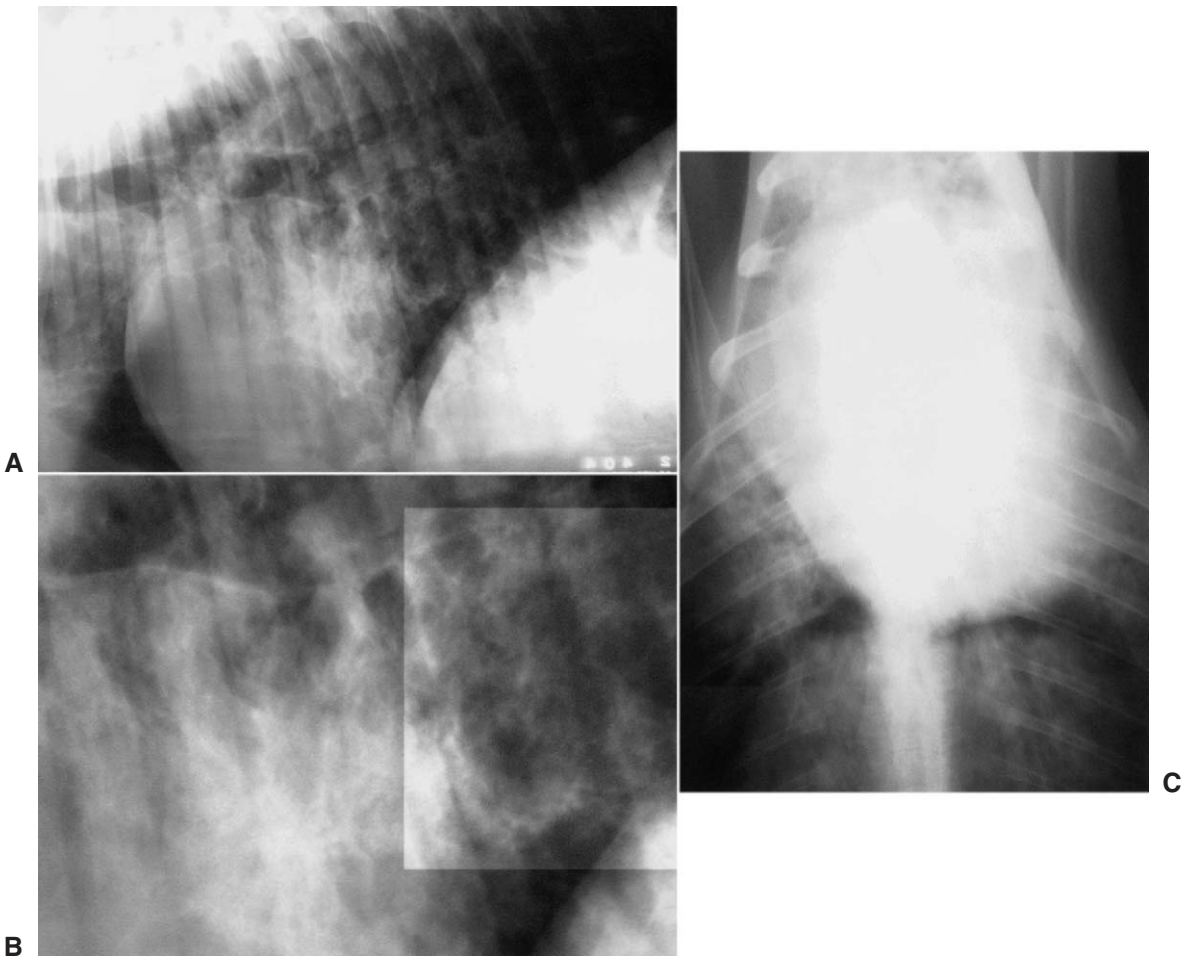


Figure 33-2 • Chronic interstitial pneumonia in a foal. Lateral **(A),** close-up lateral **(B),** and ventrodorsal **(C)** views show severe widespread lung consolidation with secondary bronchial dilation.

degree of lung consolidation, usually situated in the ventral half of the lung. Thus there is no single characteristic lung pattern that signifies bacterial pneumonia in horses, with perhaps the exception of rhodococcal abscesses (Figure 33-3).

Once the infection spreads to the lung surface and into the pleural space, the disease is referred to as *pleuropneumonia.* More often than not, pleuropneumonia is associated with pleural fluid, sometimes in very large quantities. It is quite important to emphasize at this point that even very large volumes of pleural fluid *do not result in a discrete fluid line,* contrary to some reports.[12] Seltzer and Byars estimate that the probability of a full recovery in an active racehorse that develops pleuropneumonia is about 61 percent.[13]

A distinct fluid line or level will form only when free air and fluid are in direct contact with each another within a confined space, such as a traumatic bulla, a lung abscess that communicates with a functional bronchus, or a hydropneumothorax. Intrathoracic fluid levels may also be seen in some diaphragmatic hernias that result in gastrointestinal displacement. Only rarely do gas-forming bacteria result in radiographically visible intrathoracic fluid levels.

With severe pleuritis, pleural adhesions may develop, which in turn may lead to pleural abscessation or, if they tear, pneumothorax. Radiographically, it is difficult or impossible to distinguish pleural from pulmonary abscesses unless they are situated on the foremost portion of the diaphragm, where it may be possible to make such distinctions.[14]

Sonology

Requisites of Pleuropneumonia. Sonographically pleuropneumonia must, at the very least, feature pleuritis and lung consolidation. Usually there is also pleural fluid, although the amount is highly variable. Peripheral atelectasis, often in company with consolidation, is a common sonographic feature of medium and large volumes of pleural fluid (Figure 33-4).

Consolidated Lung. Sonographically, peripheral consolidation can be difficult to distinguish from fluid. The most reliable means of distinguishing between the two



Figure 33-3 • Acute bronchopneumonia in an adult horse. Close-up lateral view of the caudoventral lung field shows a faint triangular density superimposed on the caudoventral aspect of the heart caused by localized lung consolidation. The adjacent large white area is one of the upper forelimbs.

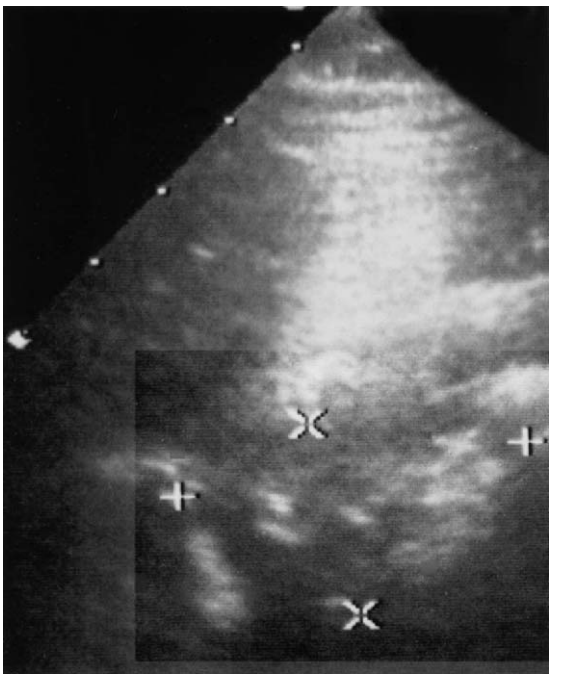


Figure 33-5 • Close-up thoracic sonogram of a horse with pleuropneumonia shows a roughly circular area of consolidation (electronic cursors) featuring a poorly marginated exterior and a nonuniform interior.



Figure 33-4 • Close-up thoracic sonogram of a horse with pleuropneumonia shows a small wedge of mildly echogenic pleural fluid overlying a partially consolidated, partially atelectatic lung lobe.

is *nonuniform interior structure:* air pockets, fluid pockets, and fluid- and air-filled bronchi. Consolidated lung usually has some or all of these features (Figure 33-5), but pleural fluid does not (Figure 33-6). Small amounts of fluid may become trapped between the visceral and parietal pleural surfaces, loosely resembling protective bubble wrap. The underlying lung may be partially consolidated or atelectatic, merging almost imperceptibly with the loculated fluid (Figure 33-7).

Atelectatic Lung. The fully atelectatic lung, surrounded by fluid, is distinguishable from consolidation by the following characteristics: (1) leaflike shape, (2) discrete margin, (3) relatively bright exterior, and (4) uniform interior echo texture.

Interstitial Pneumonia in Adult Horses. A disease of 2-year-olds and beyond, the adult form of interstitial pneumonia (as opposed to that seen in foals) causes alveolar fibrosis, leading to a distinctive radiographic appearance consisting of multiple diffusely distributed, fluffy lung densities, which may be diagnostically mistaken for pulmonary metastasis or mycotic pneumonia, especially in high-contrast films in which the ribs accentuate the abnormally dense lung (Figure 33-8).

Septicemia and Toxemia (Toxic Shock, Toxic Shock Syndrome). Toxic shock has been reported as a consequence of *Staphylococcus aureus* pneumonia in a horse, resulting in vasculitis and intractable fever.[15] Anaerobic bacterial pneumonia *(Bacteroides)* can also lead to septicemia, as described by Carlsen and O'Brien.[16] Radiographically, there does not appear to

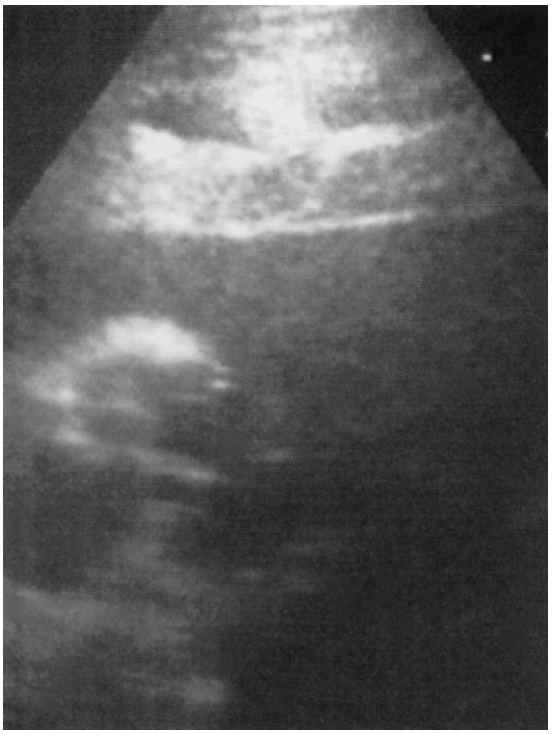


Figure 33-6 • Close-up thoracic sonogram of a horse with pleuropneumonia shows a thick band of uniformly echoic pleural fluid underlain by the tip of a consolidated lung lobe.

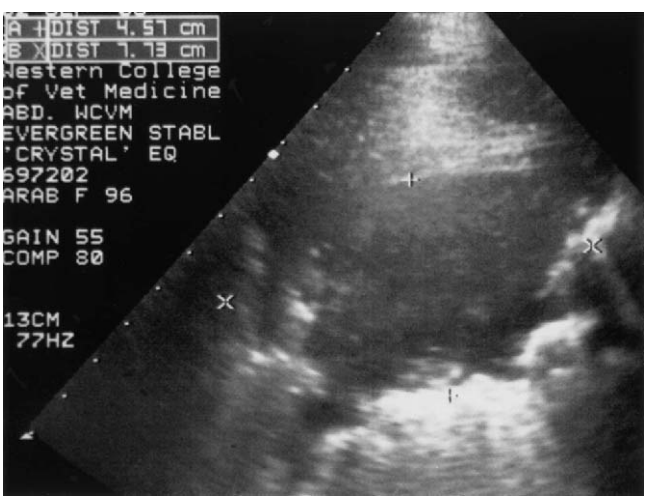


Figure 33-7 • Close-up thoracic sonogram of a horse with pleuropneumonia shows a loculated fluid pocket blending almost imperceptibly with underlying lung consolidation and atelectasis.

be any consistent appearance associated with these diseases.

Fungal Pneumonia (Mycotic Pneumonia). In the United States, fungal pneumonia is most common in the southern region of the country, but in no instance is it the prevalent form of pneumonia in horses.

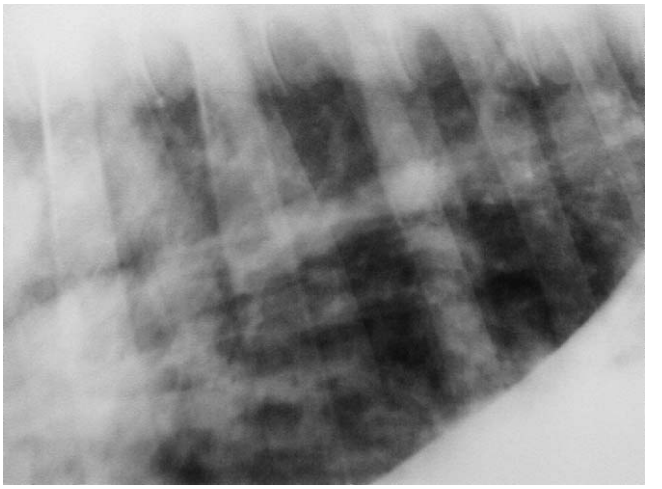


Figure 33-8 • Chronic interstitial pneumonia in an adult horse. Close-up view of the dorsocaudal lung field shows an increase in overall lung density accentuated by rib superimposition, making it falsely appear as if there are multiple lung masses and nodules.

Histoplasma and *Coccidiodes* are the most commonly encountered pathogenic fungi in horses, and *Aspergillus*, *Cryptococcus*, *Pthium*, and *Candida* are the usual opportunists.[17]

Although not widely appreciated, disseminated fungal pneumonia has a rather characteristic appearance comprising large numbers of nodules or small masses.[18] Although pulmonary metastasis may also appear this way, it rarely does so in the horse. Bacterial pneumonia, depending on its form and causative organism, usually results in defined consolidations (typically over the caudal heart base or, alternatively, nonstructured opacification).

▮▮▮ PULMONARY COCCIDIOIDOMYCOSIS

Coccidioidomycosis is a fungal disease of mammals, including people, and is found in Utah, Nevada, California, Arizona, New Mexico, and Texas. Infection is usually by inhalation; chronic weight loss is the most common clinical sign.

Radiographic Findings

According to Ziemer and co-workers, the most common radiographic expression of pulmonary *coccidioidomycosis* in horses appears to be a nonspecific increase in interstitial lung density, with or without associated pleural fluid.[19] Discrete lung masses, as described by Kramme and Ziemer, are less common. Spread of the infection to regional lymph nodes, and eventually the skeleton (distal scapula), has also been described.[20]

▮▮▮ PULMONARY ASPERGILLOSIS (INVASIVE PULMONARY ASPERGILLOSIS)

Pulmonary aspergillosis (also termed *invasive pulmonary aspergillosis*) is uncommon in horses, with most infections involving the guttural pouch or uterus. Immunocompromised horses are more likely to be infected than healthy animals. Concurrent pulmonary and enteric aspergillosis has been reported, suggesting a causal relationship.[21-23]

Pulmonary Blastomycosis

Toribio and co-workers reported a case of thoracic and abdominal *blastomycosis* in a 5-year-old Quarter Horse mare. A lateral thoracic radiograph showed a large, well-marginated object in the caudodorsal part of the lung, initially believed to be an abscess. Thoracic sonography revealed pleural fluid and surface fibrin, and sonographic assessment showed an abdominal abscess situated between the spleen and left kidney.[24]

Mycetoma and Other Cavitating Lung Lesions

Fungal infection of the lung may eventually lead to cavitation, although this is by no means a certain outcome. Alternatively, opportunistic fungi such as *Aspergillus* spp. may colonize a preexisting lung lesion and in so doing cause secondary cavitation.[25]

▮▮▮ VIRAL PNEUMONIA

Equine Viral Arteritis

Equine viral arteritis causes a generalized influenza-like illness in adult horses, abortion in mares, and interstitial pneumonia in foals. After the acute phase of the infection, recovery is usually complete. Foals, mares, and geldings can infect other animals for about 2 weeks after infection; however, stallions may shed the virus in their semen for much longer periods.[26]

Granulomatous Pneumonia

Pearson and co-workers described the radiographic appearance of *cryptococcal* pneumonia in a 3-year-old Quarter Horses mare, hospitalized because of chronic cough and nasal discharge.[27] Radiographically, the lung contained a combination of discrete masses and nondescript consolidation. Fluid levels were mentioned but were not visible in any of the published images.

▮▮▮ INHALATION PNEUMONIA

Acute Versus Chronic Forms

The inhalation of liquid or particulate matter into the tracheobronchial tree is termed *aspiration pneumonia.* There are two forms: acute and chronic. The *acute* form results from the inhalation of foreign material over a short span, causing an acute onset of clinical signs. The aspirate may be in either solid or liquid form. Aspiration of solid particulate matter causes varying degrees of bronchiole obstruction. Aspiration of highly acidic digestive fluids can cause severe illness, including dyspnea, cyanosis, and occasionally shock.

The chronic form of inhalation pneumonia results from repeated aspiration and frequently leads to granulomatous pneumonia. This form of the disease is most common in horses with chronic choke or dysphasia. Inhalation of oil-based medicaments may result in lipoid pneumonia.

Radiographic Findings

There are no defining radiographic findings in inhalation pneumonia. The nature and volume of the aspirate and the position of the animal at the time of occurrence dictate specific disease patterns. The initial radiographic appearance is often quite labile, depending on the type of treatment (if any), the presence of related infection, and the duration of the illness.

On a probability basis, pulmonary consolidation resulting from inhalation will initially develop in the dependent portion of the lung. For example, if an anesthetized horse is lying on its right side when it inhales esophageal contents past its endotracheal tube, consolidation of collapse is most likely to first appear in the right middle or caudal regions of the lung. Horses that inhale low-viscosity liquids while standing may or may not show caudodorsal lung lesions; but if they do, follow-up radiographs will often reveal ventral consolidation, presumably gravitationally induced.

Typically radiographs made within a few hours after inhalation show nothing. Twenty-four-hour progress films often show peribronchial cuffing but rarely any overt lung consolidation. Later films (24 to 72 hours) may show consolidation or collapse, strong presumptive evidence of a secondary pneumonia and bronchial obstruction. Generally the more opaque the lung becomes, the more serious the disease, especially when combined with abnormal blood gases. Abscessation, if it develops, may take weeks to become apparent radiographically.

I have performed bronchography in horses with inhalation pneumonia in an effort to establish the extent of bronchial obstruction (nuclear ventilation assessment is preferable, but was not available at the time). In addition to blockages, I found that many of the conducting bronchi were dilated, presumably an attempt to improve ventilation.[28]

▮▮▮ LUNG ABSCESS

Most but not all lung abscesses are the results of pneumonia. In a retrospective study, Lavoie and co-workers reported lung abscesses in 40 foals and adult horses

(mostly Standardbreds), *unassociated* with pleuropneumonia.[29] Most of the affected animals were 6 months old or younger, typically presenting with fever, elevated heart and respiratory rates, and neutrophilia. The most common bacteria obtained by transtracheal aspiration were *Streptococcus zooepidemicus* and *R. equi.* Most animals—foals and adults alike—had multiple lung abscesses visible on thoracic radiographs.

Spurlock and co-workers described pneumothorax in a 3-year-old Thoroughbred with pneumonia, which, based on radiographic appearances, was most likely due to a ruptured lung abscess.[30] In addition to a pneumothorax, a ruptured lung abscess may also cause pleuritis and or pyothorax.

Ainsworth and co-workers determined that, based on their experience treating 45 Thoroughbred and Standardbred racehorses with primary lung abscesses, long-term performance prospects were unlikely to be seriously affected.[31] Of imaging interest is the fact that two thirds of the abscesses were situated in the caudodorsal lung field, raising question as to a possible relationship to exercise-induced pulmonary hemorrhage.

Radiographically, the visibility of lung abscesses depends mostly on their size: the larger they are, the more likely they are to be detected, all other factors, such as location, being equal. Small abscesses (i.e., 2 to 3 cm in diameter) situated in or around the hilus are difficult to distinguish from normal vascular cross-sections, which are large and numerous in this region of the lung.

The relatively sharp borders of a lung abscess can generally be used to distinguish it from a localized area of consolidation (Figure 33-9). Clusters of large abscesses, for example, those caused by *Rhodococcus*, can mimic a huge solitary lung abscess or a primary lung tumor (Figure 33-10).

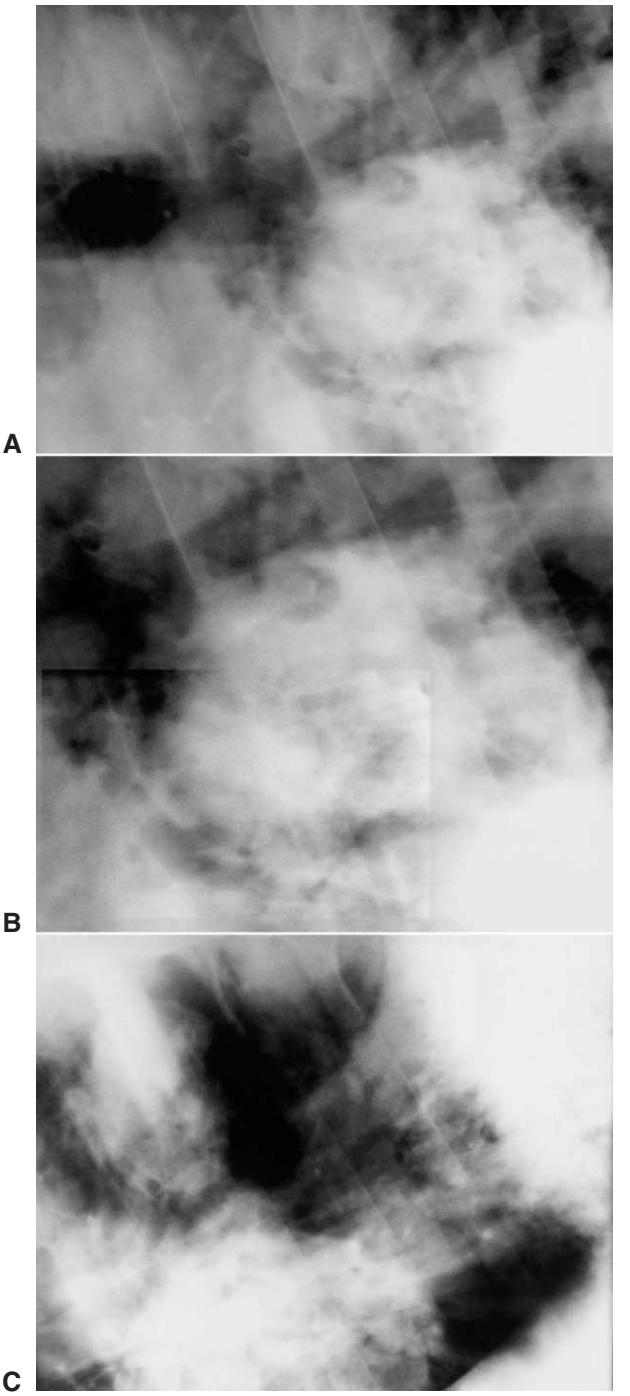


Figure 33-9 • Close-up **(A)** and ultra-close-up **(B)** views of the hilar region of the lung show multiple rhodococcal abscesses featuring a great deal of marginal variability, most of which is attributable to superimposition by adjacent blood vessels and other abscesses. Another close-up **(C)** from the top center of the dorsocaudal lung field shows more abscesses, most of which are superimposed on one another, exaggerating their size, sometimes by as much as 200 or 300 percent.

▮▮▮ PNEUMOCONIOSIS (INDUSTRIAL LUNG DISEASE)

Schwartz and co-workers described a series of California horses suffering chronic silicosis inhalation causing pulmonary fibrosis.[32] Pack animals chronically exposed to coal dust inevitably develop anthracosis, which may then lead to emphysema.

▮▮▮ IMMUNOPNEUMONIA (HYPERSENSITIVITY PNEUMONIA)

Winder and co-workers described the clinicopathologic findings in two horses with immunopneumonia.[33] Diagnostic criteria included (1) a history of dyspnea, cough, and fever when exposed to organic dusts; (2) the presence of antigen-specific antibodies in the blood; and (3) radiographic evidence of diffuse lung disease.

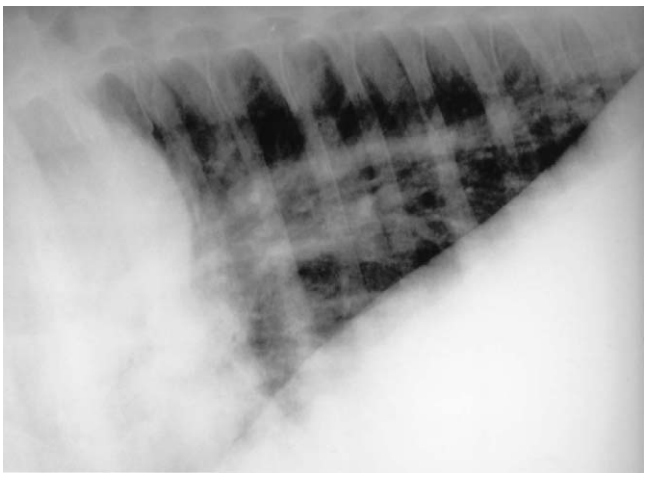


Figure 33-10 • Lateral thoracic radiograph shows multiple large lung abscesses clustered around the heart base of a foal resembling a single lung mass, for example, a juvenile lung tumor.

▮▮▮ PARASITIC PNEUMONIA

Lungworm (*Dicyocaulus arnfieldi*) has been reported in horses kept with donkeys.[34] The larval stages of some intestinal parasites may migrate to the lung, causing pneumonitis, with or without associated hypersensitivity. A full appreciation of the potential threat posed by primary and secondary lung parasites to horses requires some understanding of the associated environmental and host factors coming into play in any type of equine respiratory disease, as aptly provided by Clarke in his excellent review of the subject.[35]

▮▮▮ ADULT RESPIRATORY DISTRESS SYNDROME

In my experience adult respiratory distress syndrome (ARDS) is most likely to develop in horses exposed to large volumes of smoke, in barn fires, for example. *Myocardial depressant factor* resulting from related burns may cause pulmonary edema, which is hard to distinguish from the atelectasis caused by ARDS. Horses suffering from serious smoke inhalation may subsequently develop bacterial pneumonia.

▮▮▮ PULMONARY THROMBOSIS

Not a great deal is known about pulmonary thrombosis in the horse, as evidenced by few publications on the subject. One of the best of these, in terms of high-quality radiographs and substantiating subgross and histologic-bacteriologic evidence, is a case report by Kerr and co-workers, which regrettably was published under the unrevealing title of "Radiographic Diagnosis" and, as such, escaped the attention of many potential readers.[36]

The animal in question, a 21-year-old Arabian/Quarter Horse mare, showed extensive consolidation in one half of the lung but not the other, as revealed by alternate-side radiographs. Postmortem examination revealed a diffusely pneumonic left lung, featuring a large thrombus lodged in the base of the left pulmonary artery that extended into two of its secondary branches. The diseased lung was surrounded by an estimated 1 to 2 L of serosanguineous pleural fluid. The right lung was partially consolidated ventrally. *Escherichia coli* was cultured from both the thrombus and the consolidated portion of the left lung, lending credence to the authors' theory that the thrombus was caused by endothelial inflammation secondary to the pneumonia.

▮▮▮ PULMONARY INFARCTION

Carr and co-workers described the radiographic and sonographic appearance of acute hemorrhagic pulmonary infarction in 21 horses with necrotic pneumonia.[37] Typical presentations included (1) a serosanguineous nasal discharge, (2) increased respiratory rate, (3) increased heart rate, and (4) fever. Many of the horses had a cough and were not eating.

Radiographic Findings

Most of the horses had ventral consolidation and pleural fluid. More than half of the animals had multiple discrete lung masses located in various parts of the lung. The lung abnormalities did not resemble those typically found with exercise-induced pulmonary hemorrhage.

Sonographic Findings

Discrete areas of consolidation, although not unique in any way, corresponded to pulmonary infarcts identified at postmortem examination. Less discrete areas of consolidation correlated with pneumonia. Pleural fluid and fibrin tags were also found.

▮▮▮ PNEUMONIA AND PNEUMOMEDIASTINUM

As mentioned in an earlier chapter, the most common cause of pneumomediastinum in horses is transtracheal irrigation-aspiration.[38] Accordingly, the first question that should be asked once a pneumomediastinum is identified, especially in a pneumonic foal or horse, is whether or not there has been a recent tracheal wash.

References

1. Kangstrom L-E: The radiological diagnosis of equine pneumonia, *Vet Radiol* 9:80, 1969.

2. Farrow CS: Radiographic aspects of inflammatory lung disease in the horse, *Vet Radiol* 22:107, 1981.
3. Lamb CR, O'Callaghan MW, Paradis MR: Thoracic radiography in the neonatal foal: a preliminary report, *Vet Radiol Ultrasound* 31:11, 1990.
4. Huguchi T, Taharaguchi S, et al: Physical and serologic examinations of foals at 30 and 45 days of age for early diagnosis of *Rhodococcus equi* infection on endemically infected farms, *J Am Vet Med Assoc* 212:976, 1998.
5. Giguere S, Gaskin JM, et al.: Evaluation of a commercially available hyperimmune plasma product for prevention of naturally acquired pneumonia caused by *Rhodococcus equi* in foals, *J Am Vet Med Assoc* 220:59, 2002.
6. Clark-Price SC, Rush BR, et al: Osteomyelitis of the pelvis caused by *Rhodococcus equi* in a two-year-old horse, *J Am Vet Med Assoc* 222:969. 2003
7. Falcon J, Smith BP, et al: Clinical and radiographic findings in *Corynebacterium equi* pneumonia in foals, *J Am Vet Med Assoc* 186:593, 1985.
8. Ainsworth DM, Eicker SW, et al: Associations between physical examination, laboratory, and radiographic findings and outcome and subsequent racing performance of foals with *Rhodococcus equi* infection: 115 cases (1984-1992), *J Am Vet Med Assoc* 213:510, 1998.
9. Buergelt CD: Interstitial pneumonia in the horse: a fledging morphological entity with mysterious causes, *Equine Vet J* 27:4, 1995.
10. Perryman LE, Torbeck R: Combined immunodeficiency of Arabian horses: confirmation of autosomal recessive mode of inheritance, *J Am Vet Med Assoc* 176:1250, 1980.
11. Ewing PJ, Cowell RL, et al: *Pneumocystis carinii* pneumonia in foals, *J Am Vet Med Assoc* 204:929, 1994.
12. Smith BP: Diseases of the pleura, *Vet Clin N Am Large Animal Pract* 1:197, 1979.
13. Seltzer KL, Byars TD: Prognosis for return to racing after recovery from infectious pleuropneumonia in Thoroughbred racehorses: 70 cases (1984-1989), *J Am Vet Med Assoc* 208:1300, 1996.
14. Jeffrey SC, Furr MO: What is your diagnosis? *J Am Vet Med Assoc* 206:797, 1995.
15. Holbrook TC, Munday JS, et al.: Toxic shock syndrome in a horse with *Staphylococcus aureus* pneumonia, *J Am Vet Med Assoc* 222:620, 2003.
16. Carlsen GP, O'Brien MA: Anaerobic bacterial pneumonia with septicemia in two racehorses, *J Am Vet Med Assoc* 196:941, 1990.
17. Ruoff WW: Fungal pneumonia in horses. *Am Assoc Equine Pract* 422-425, 1988.
18. Green SL, Hager DA, et al: Acute diffuse mycotic pneumonia in a 7-month-old colt, *Vet Radiol* 28:216, 1987.
19. Ziemer EL, Pappagianis D, et al: Coccidioidomycosis in horses: 15 cases (1975-1984) *J Am Vet Med Assoc* 201:910, 1992.
20. Kramme PM, Ziemer EL: Disseminated coccidioidomycosis in a horse with osteomyelitis, *J Am Vet Med Assoc* 196:106, 1990.
21. Long JR, Mitchell L: Pulmonary aspergillosis in a mare, *Can Vet J* 12:16, 1971.
22. Slocombe RF, Slauson DO: Invasive pulmonary aspergillosis of horses: an association with acute enteritis, *Vet Pathol* 25:277, 1988.
23. Hattel AL, Drake TR: Pulmonary aspergillosis with acute enteritis in a horse, *J Am Vet Med Assoc* 199:589, 1991.
24. Toribio RE, Kohn CW, et al: Thoracic and abdominal blastomycosis in a horse, *J Am Vet Med Assoc* 214:1367, 1999.
25. Green SL, Spencer CP, et al: Radiographic diagnosis, *Vet Radiol* 30:181, 1989.
26. Hullinger PJ, Gardner IA, et al: Seroprevalence of antibodies against equine arteritis virus in horses residing in the United States and imported horses. *J Am Vet Med Assoc* 219:946, 2001.
27. Pearson EG, Watrous BJ, et al: Cryptococcal pneumonia in a horse, *J Am Vet Med Assoc* 183:577, 1983.
28. Farrow CS: Exercise in diagnostic radiology, *Can Vet J* 23:340, 1982.
29. Lavoie JP, Fiset L, Laverty S: Review of 40 cases of lung abscesses in foals and adult horses, *Equine Vet J* 26:348, 1994.
30. Spurlock SL, Spurlock GH, Donaldson LL: Consolidating pneumonia in a horse, *J Am Vet Med Assoc* 192:1081, 1988.
31. Ainsworth DM, Erb HN, et al: Effects of pulmonary abscesses on racing performance of horses treated at referral veterinary medical teaching hospitals: 45 cases (1985-1997). *J Am Vet Med Assoc* 214:750,1999.
32. Schwartz LW, Knight LW, et al: Silicate pneumoconiosis and pulmonary fibrosis in horses from the Monterey-Carmel peninsula, *Chest* 80:82, 1982.
33. Winder C, Ehrensperger F, et al: Interstitial pneumonia in the horse: two unusual cases, *Equine Vet J* 20:298, 1988.
34. Round MC: Lungworm infection of the horse and donkey, *Vet Rec* 99:393, 1976.
35. Clarke AF: A review of environmental and host factors in relation to equine respiratory disease, *Equine Vet J* 19:435, 1987.
36. Kerr LY, Harkema R, O'Brien LY: Radiographic diagnosis, *Vet Radiol* 26:123, 1985.
37. Carr EA, Carlsen GP, et al: Acute hemorrhagic pulmonary infarction and necrotizing pneumonia in horses: 21 cases (1967-1993), *J Am Vet Med Assoc* 210:1774, 1997.
38. Farrow CS: Pneumomediastinum in the horse: a complication of transtracheal aspiration, *Vet Radiol* 17:192, 1976.

Chapter 34

Lung, Pleural, and Mediastinal Cancer

THE RADIOGRAPHIC APPEARANCE OF PRIMARY AND SECONDARY LUNG TUMORS

The appearance of primary and secondary lung tumors is similar in most mammals, including the horse. Primary lung tumors are typically solitary, well-marginated masses, often discovered in the course of searching for some other disease. The most common nonsystemic effect of these masses is tracheal or bronchial compression, which usually causes coughing, especially during vigorous exercise.

Pulmonary metastasis classically appears as numerous, variably sized objects, spread throughout the lung, which may or may not be well marginated. As mentioned previously, superimposition makes it extremely difficult to measure individual lesions accurately. Occasionally metastases can resemble diffuse patchy consolidation and thus be mistaken for pneumonia (Figure 34-1).

Primary Lung Tumors

Most primary lung tumors are carcinomas, although other cell types, such as chondrosarcoma, are occasionally reported.[1] As with metastatic disease, some primary lung tumors are associated with epistaxis, and some are not. Unlike the dog, however, in the horse few are incidental radiographic findings.

Secondary Lung Tumors (Pulmonary Metastases, Metastatic Lung Disease)

Sweeney and Gillette described a variety of metastatic tumors in horses, including (1) adenocarcinoma, (2) squamous cell carcinoma, (3) hemangiosarcoma, and (4) undiffentiated sarcoma.[2] Some specific cell types are discussed in the following sections.

Squamous Cell Carcinoma. Cook and others described the radiographic appearance of metastatic pulmonary carcinoma in horses exhibiting chronic weight loss and inappetence. Typically, and in the relatively advanced stages of the disease, metastatic pulmonary carcinoma appears as multiple lung nodules and masses spread randomly throughout the lung. Rapid respiratory rates, sometimes associated with diffuse metastasis, may result in a blurred image and a mistaken diagnosis of pneumonia.[3]

Hemangiosarcoma

Johnson and co-workers reported a case of disseminated hemangiosarcoma in a 7-year-old Thoroughbred gelding hospitalized because of dyspnea and epistaxis.[4] Initially diagnosed as execise-induced pulmonary hemorrhage, the horse was given supportive therapy over the next 15 days, but to no avail, and was eventually euthanized. Necropsy revealed widely disseminated hemangiosarcoma, principally involving the lung, which contained numerous metastases ranging in size from 2 mm to 5 cm in diameter, surrounded by 2 L of bloody pleural fluid. Other metastases were found throughout the abdomen, in the esophagus, and in multiple areas of the brain.

Jean and co-workers also reported a case of pulmonary metastases, apparently originating from a cutaneous hemangiosarcoma, in which multiple pulmonary nodules and masses were identified on a thoracic radiograph.[5] Other reported primary sites include the eye, paranasal sinus, guttural pouch, synovial sheath, skeletal muscle, pericardium, and vagina.

Fibrosarcoma

Jorgansen and Geoly reported the radiographic appearance of what was presumed to be a metastatic pulmonary fibrosarcoma associated with a medium volume of pleural fluid.[6] A related left humeral lesion was also identified, first as a vague radiolucency in the caudal aspect of the proximal humerus and then as an

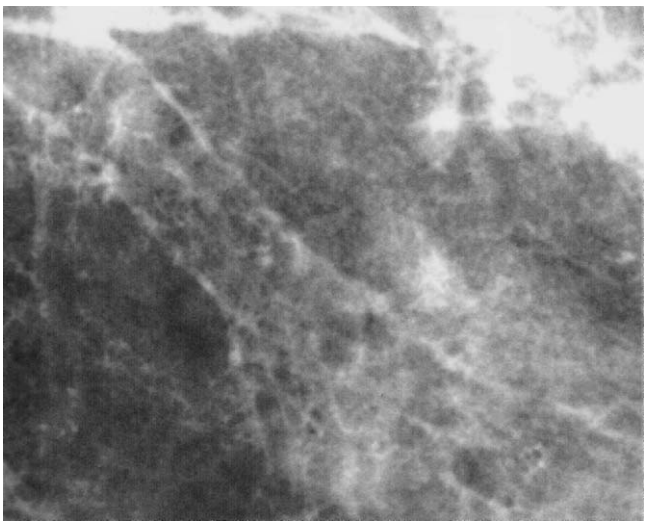


Figure 34-1 • Radiograph of a 1-inch-thick, air-dried slice of a cancerous lung shows numerous metastases (medium-sized fluffy white objects), many of which are superimposed on one another, resembling patchy lung consolidation sometimes seen with pneumonia.

area of increased isotopic uptake in a nuclear medicine scan.

▮▮▮ PLEURAL TUMORS

Malignant Mesothelioma

Mair and co-workers reported a case of mesothelioma in a 13-year-old Welsh Cob gelding, hospitalized because of sternal edema, cough, dyspnea, and intermittent fever.[7] Thoracic radiographs showed a large volume of pleural fluid (estimated at 45 L) obscuring all but the dorsal lung field. Ultrasound confirmed the presence of a large volume of pleural fluid, pleural thickening, and fibrin fronds on the lung surface, which falsely suggested chronic pleuritis. Thoracentesis was blood tinged and contained sheets of malignant-appearing mesothelial cells.

Pleural tumors such as malignant mesothelioma are too small to be seen radiographically and are equally difficult to identify sonographically. However, the presence of pleural fluid, especially in the absence of any constitutional signs of infection, suggests at least the possibility of pleural malignancy.

▮▮▮ MEDIASTINAL TUMORS AND TUMORLIKE LESIONS

Mediastinal Lymphosarcoma

Lymphosarcoma is the most common form of thoracic neoplasm found in horses, often resulting in the formation of a large cranial mediastinal mass and extensive infiltration of regional lymph nodes. Larger mediastinal masses may interfere with the regional circulation, leading to dependent edema. Occasionally cancerous lymphocytes also find their way into the lung.

Clinical Findings. Most horses were presented for one or more of the following abnormalities: dysphagia, dyspnea, or cough. Abnormal physical findings included one or more of the following: (1) ventral pectoral edema, (2) forelimb edema, (3) edema of the head and neck, (4) bilateral jugular distension, (5) muffled heart sounds, and (6) peripheral adenopathy.

Radiographic Findings. I find mediastinal tumors such as lymphosarcoma difficult to diagnose consistently unless accompanied by enlargement or deformity of the mediastinum, usually the cranial portion.

Sonographic Findings. Garber and co-workers reported the sonographic characteristics of mediastinal lymphoma in 13 horses.[8] The observed tumors were often irregularly marginated or overtly lobulated and featured variable interior echogenicity. Most displaced the heart caudally and were accompanied by pleural fluid.

Mediastinal Abscess and Loculated Mediastinal Fluid Secondary to Pleuropneumonia

Byars and co-workers reported the sonographic appearances of cranial mediastinal abscesses and loculated mediastinal fluid secondary to pleuropneumonia.[9] Abscesses were characterized as discrete, thick-walled objects. By comparison, loculations lacked a clear-cut perimeter. Related abnormalities included caudal displacement of the heart observed exclusively from the left side, jugular distension, and jugular thrombosis.

▮▮▮ PLEURAL FLUID AS A CONSEQUENCE OF LUNG CANCER

Mair reported that in England 60 percent of pleural effusions in horses are due to lung or mediastinal cancer. By comparison, approximately two thirds of North American horses with pleural fluid have pneumonia. The reason or reasons for this difference are not known.[10,11]

References

1. Clem MF, O'Brien TD: Pulmonary chondrosarcoma in a horse, *Compend Cont Educ (Equine)* 8:964, 1986.
2. Sweeney CR, Gillette DM: Thoracic neoplasia in equids: 35 cases (1967-1987), *J Am Vet Med Assoc* 195:374, 1989.
3. Cook G, Divers TJ, Rowland PH: Hypercalcemia and erythrocytosis in a mare associated with a metastatic carcinoma, *Equine Vet J* 27:316, 1995.

4. Johnson JE, Beech J, Sail JE: Disseminated hemangiosarcoma in a horse, *J Am Vet Med Assoc* 193:1452, 1988.
5. Jean D, Lavoie J-P, et al: Cutaneous hemangiosarcoma with pulmonary metastasis in a horse, *J Am Vet Med Assoc* 204:776, 1994.
6. Jorgensen JS, Geoly FJ: Lameness and pleural effusion associated with an aggressive fibrosarcoma in a horse, *J Am Vet Med Assoc* 210:1328, 1992.
7. Mair TS, Hillyer MH, Brown PJ: Mesothelioma of the pleural cavity in a horse: diagnostic features, *Equine Vet Educ* 4:59, 1992.
8. Garber JL, Reef VB, Reimer JM: Sonographic findings in horses with mediastinal lymphosarcoma: 13 cases (1985-1992), *J Am Vet Med Assoc* 205:1432, 1994.
9. Byars TD, Dainis CM, et al: Cranial thoracic masses in the horse: a sequel to pleuropneumonia, *Equine Vet J* 23:22. 1991.
10. Mair T: Treatment and complications of pleuropneumonia, *Equine Vet J* 23:5, 1991.
11. Scarratt WK, Crisman MV: Neoplasia of the respiratory tract, *Vet Clin N Am Equine Pract* 14:100 1998.

Chapter 35

Bronchial and Terminal Airspace Disease

BRONCHIAL ANATOMY

From a radiographic perspective, the equine lung can best be conceptualized as having two major and two minor lobes, one on each side of the thorax, with intervening "cutouts" to accommodate the heart. The preponderance of visible bronchi are situated in the right and left major lobes, which have been mapped by Smith and co-workers.[1] Because only the trachea and bronchi are visible radiographically, the designation *tracheal* or *bronchial disease* is preferable to the term *airway disease,* which is ambiguous.

BRONCHITIS: THE INVISIBLE DISEASE

In my judgment, bronchitis cannot be reliably diagnosed radiographically. Thus a normal radiograph is theoretically consistent with bronchitis. However, this is not to say that there are no bronchial disorders that are radiographically detectable. Bronchiectasis, an irreversible bronchial disease that enlarges and deforms the bronchi, can be readily identified, provided the disease is moderately advanced. High-resolution computed tomography may be capable of detecting bronchitis in horses, as it sometimes can in humans.

BRONCHOGRAPHY

Walker and Goble described the use and normal appearance of barium bronchography in horses.[2] Using 100 ml of 100% wt/vol premixed barium sulfate suspension in 1000-lb adult horses, excellent-quality bronchograms were obtained through five to seven bronchial divisions (also termed *generations*) for at least 30 minutes after contrast insufflation. Although much of the barium was still present at 24 hours, most had disappeared by 24 hours. The only observed side effect was a mild, short-lived cough in one animal. Histologic examination of the lungs of two horses 6 weeks after bronchography showed mild inflammation.

Two years later, O'Callaghan and Sanderson reported the use of finely powdered barium and methylcellulose, insufflated through an endotracheal stomach tube in normal standing horses, to evaluate the bronchi. The authors believed that their method, a modification of a technique used in people, was equivalent or superior to previously published methods.[3]

COMPENSATORY BRONCHIAL DILATION (SECONDARY "BRONCHIECTASIS")

Varying degrees of compensatory brochodilation occur with pneumonia, probably as a result of increased airway resistance and bronchiole obstruction. In my opinion the term *secondary bronchiectasis*, which is sometimes used in place of bronchial dilation, is both contradictory and dangerously misleading because, unlike bronchiectasis, which is permanent disease, bronchial dilation is a temporary disorder.

BRONCHIECTASIS

Bronchiectasis is an irreversible disease that enlarges and deforms bronchi. There is no cure. Bronchiectasis and emphysema are the core elements of the broader disease designations: *chronic obstructive lung disease* and *chronic obstructive pulmonary disease (COPD).*

Bronchiectasis has been classified according to the manner in which the bronchi are deformed: tubular, saccular, and varicose. In some individuals all three morphologic types of bronchial deformity are present. Saccular bronchiectasis can sometimes resemble cavi-

tary lung disease, even to the extent of including fluid levels.

Mild, transient bronchial dilation in Thoroughbreds may be caused by furosemide, administered as an aerosol or intravenously, just before a race to prevent or limit exercise-induced pulmonary hemorrhage.[4] Radiographically, visible bronchial dilation may also occur after administration of a bronchodilator.

▮▮▮ OBSTRUCTIVE LUNG DISEASE: WHAT ACTUALLY IS IT?

A recent international workshop on equine chronic airway disease pointed out the similarities between chronic obstructive lung disease in horses and asthma in people.[5] Dixon and co-workers reported that in a series of 300 horses referred for pulmonary disease, 148 had COPD as clinically characterized by coughing and nasal discharge.[6,7]

Hypersensitivity reactions have long been believed to play a role in chronic obstructive lung disease, especially in horses, which also suffer from urticaria or allergic dermatitis.[8] Derksen and Woods describe the potential role of aeroallergens in allergic lung disease of horses.[9] Lamb and co-workers theorized that neonatal pneumonia can lead to heaves in adult horses.[10] On the subject of heaves, I would like to offer the unedited viewpoints of Breeze, which, although published nearly 25 years ago, remain just as timely today as ever.[11]

▮▮▮ HEAVES*

The Problem of Disease Definition

Standard texts in veterinary medicine and pathology contain comfortable descriptions of heaves that give the reader no indication of the antiquity of the sources of many categoric statements or the slender factual basis of the experimental or field studies whose results are cited. Contemporary accounts are usually a mixture of modern research and terminology and interpretations of an older literature that contains many largely anecdotal or dogmatic statements derived from experience of equine practice that is very different from that of today.

The plain fact is that we have little detailed knowledge of the clinical and functional abnormalities, epidemiology, and pathology of heaves as it presently occurs in the United States, principally because all these aspects have never been adequately described in the same series of horses. The drawback in investigating only one aspect of the problem, no matter how thoroughly this is undertaken, lies in satisfactorily defining the population under study so that it can be clearly identified by others, a snag that has been responsible for many unwarranted generalizations and misunderstandings.

The term *heaves* is old fashioned and ambiguous, but this admitted archaism was adopted here because it seemed a good starting point for clarifying the nomenclature of chronic respiratory disease in horses. Heaves and broken wind are colloquial or farriers' names applied to horses with long-standing respiratory disease manifested as double expiratory effort. Both are misleading terms because they imply that this clinical sign is the result of a single disease process, which is not the case.

In the last 25 years, a number of new terms have been introduced in attempts to be more specific, including chronic alveolar emphysema, emphysema, chronic bronchitis, COPD, and chronic asthmoid bronchitis and bronchiolitis. Unfortunately these have made the situation more confusing because such diagnoses have frequently been applied in a manner that defies accepted methods of disease definition and differentiation.

The Clinical Picture

Most practicing veterinarians would agree that heaves is a common problem and would accept that it refers to a complex of clinical signs rather than to a specific disease entity. A diagnosis of heaves usually implies that the horse exhibits a chronic respiratory disorder with some or all of the following features: poor work performance or exercise intolerance, chronic cough, dyspnea, and double expiratory effort with increased or wheezing breathing sounds on auscultation.

Chronic in this context is taken to mean duration of at least 6 months. Dyspnea refers to obvious respiratory distress or labored breathing, irrespective of respiratory rate. Cases of acute heaves are mentioned in the literature in relation to animals with similar but more severe clinical signs of apparently sudden onset and short duration (i.e., 1 or 2 days).

The clinical signs listed in the preceding section are traditionally regarded as characteristic of heaves or broken wind and serve to distinguish this syndrome from such conditions as bacterial pneumonia or viral respiratory infections. However, physical examination alone cannot differentiate the various entities included in the heaves syndrome, and so considerable effort has been expended to develop observer-free physiologic measurements capable of identifying subgroups for further examination, a process responsible for the evolution of the concept of equine COPD.

▮▮▮ CHRONIC OBSTRUCTIVE PULMONARY DISEASE

Chronic obstructive pulmonary disease has become a popular term in equine medicine since its introduction by Sasse, who found that lack of stamina and poor

**Heaves* reprinted with permission from Veterinary Clinics of North America: Large Animal Practice 1:219, 1979.

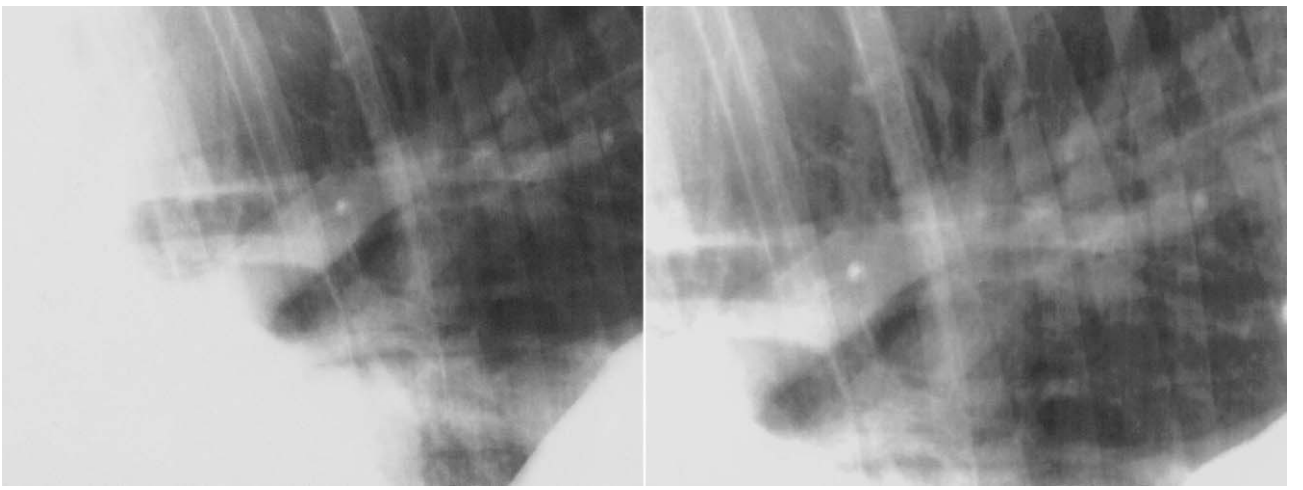


Figure 35-1 • Lateral **(A)** and close-up lateral **(B)** views of the cranial portion of the dorsocaudal lung field of a horse with emphysema show pulmonary hyperinflation and oligemia.

work performance in some horses with respiratory disease were the result of an increase in the work of breathing after obstruction of airflow in the lung. This observation could be used as an aid to differential diagnosis by identifying those animals with "chronic obstructive pulmonary disease."

Although many aspects of lung and airway function were measured, the most important parameters in determining the presence of COPD were the partial pressure of arterial oxygen (Pa_{O_2}) and the maximum change in intrapulmonary pressure during inspiration and expiration (maxΔ Ppl). Using these two measurements, British workers found that horses with COPD were distinguished by having a Pa_{O_2} equal to or less than 82 mm Hg and maxΔ Ppl equal to or greater than 6 mm Hg either on admission or in response to challenge with inhaled antigen. Normal horses had Pa_{O_2} equal to or greater than 83 mm Hg and maxΔ Ppl equal to or less than 5 mm Hg.

Horses with other forms of respiratory disease (including those with clinical signs of heaves otherwise indistinguishable from those with COPD) had intermediate values. Physiologic examination can thus be used to identify horses in which airflow obstruction is believed to be a prominent feature. It is important to realize that variations in the defining characteristics of COPD are to be expected between laboratories and that these measurements are only a crude means of identifying a population for further study. The results of equine function tests should not be overinterpreted.

Pathology of Heaves

Published descriptions of the pulmonary lesions of horses with heaves vary considerably and are fraught with poorly defined descriptive terms that are not applied uniformly.

Imaging of Chronic Obstructive Lung Disease in Horses

Radiology. Radiography may prove inadequate in detecting the minimal anatomic alterations that occur in the lungs of horses with COPD. In other words, the lungs of some horses with COPD may appear radiographically normal. Classically, the emphysematous or chronically obstructive lung features hyperlucency and oligemia, attributable to hyperinflation, air trapping, and a pathophysiologic reduction in pulmonary venous blood flow (Figure 35-1).

Scintigraphic Ventilation Imaging. O'Callaghan and co-workers reported the use of aerosolized technetium as a means to assess airway functionality in horses, particularly with regard to the effects of chronic obstructive lung disease.[12]

References

1. Smith BL, Aguilera-Tejero E, et al: Endoscopic anatomy and map of the equine bronchial tree, *Equine Vet J* 26:283, 1994.
2. Walker M, Goble D: Barium sulfate bronchography in horses, *Vet Radiol* 21:85, 1980.
3. O'Callaghan MW, Sanderson GN: Clinical bronchography in the horse: development of a method using barium sulfate powder, *Equine Vet J* 14:282, 1982.
4. Hinchcliff KW: Effects of furosemide on athletic performance and exercise-induced pulmonary hemorrhage in horses, *J Am Vet Med Assoc* 215:630, 1999.
5. Martin J: International workshop on equine chronic airway disease, *Equine Vet J* 33:5, 2001.
6. Dixon PM, Railton DI, McGorum BC: Equine pulmonary disease: a case control study of 300 referred cases. Part 1: Examination techniques, diagnostic criteria and diagnosis, *Equine Vet J* 27:416, 1995.
7. Dixon PM, Railton DI, McGorum BC: Equine pulmonary disease: a case control study of 300 referred cases. Part 2:

Details of animals and of historical and clinical findings, *Equine Vet J* 27:422, 1995.
8. Jose-Cunilleras E, Kohn CW, et al: Intradermal testing in healthy horses and horses with chronic obstructive pulmonary disease, recurrent urticaria, or allergic dermatitis, *J Am Vet Med Assoc* 219:1115, 2001.
9. Derksen FJ, Woods PSA: Chronic lung disease in the horse: role of aeroallergens and irritants and methods of evaluation, *Equine Pract* 16:11, 1994.
10. Lamb CR, O'Callaghan MW, Paradis MR: Thoracic radiography in the neonatal foal: a preliminary report, *Vet Radiol Ultrasound* 31:11, 1990.
11. Breeze RG: Heaves, *Vet Clin N Am Large Anim Pract* 1:219, 1979.
12. O'Callaghan MW, Hornoff WJ, et al: Ventilation imaging in the horse with technetium radioaerosol, *Equine Vet J* 19:19, 1987.

Chapter 36

Thoracic Esophageal Disease

ESOPHAGEAL DILATION RELATED TO TRANQUILIZATION AND TUBING

King and co-workers reported persistent esophageal enlargement encountered while performing esophagography in a foal. The authors speculated that the observed dilation was due to a combination of factors, especially the use of sedation combined with the repeated placement of a nasogastric tube.[1]

ESOPHAGEAL FOREIGN BODY

Plain-film identification of thoracic esophageal foreign bodies can be extremely difficult, especially over the heart base, where numerous large vascular cross-sections can be easily mistaken for foreign objects (Figure 36-1). Fluid and air distension proximal to the point of esophageal obstruction may or may not be present; its recognition depends on many factors, including (1) foreign-body composition, (2) volume (and thus degree of distension), (3) point of obstruction, and, most important, (4) film quality, particularly the absence of motion "unsharpness."

Low-density foreign materials may be *inferred* by the presence of gas cranial to the point of esophageal obstruction, especially if it is flared caudally (Figure 36-2). Likewise esophageal perforation may be inferred by the presence of a pneumomediastinum or mediastinitis.

CONGENITAL ESOPHAGEAL STENOSIS

Clabough and co-workers reported the radiographic appearance of an intrathoracic esophageal stenosis in a 7-day-old Thoroughbred colt; the stenosis was presumed to be congenital.[2] An initial barium swallow revealed mild dilation and contrast retention of the thoracic esophagus, ending just dorsal to the heart base. A progress double-contrast esophagram obtained 3 days later showed localized dorsal displacement and focal stenosis in the same area. Notably, the appearance of the lesion changed decidedly depending on whether the colt was standing or lying on its side while being imaged.

ACQUIRED ESOPHAGEAL STRICTURE

Nixon and co-workers described the radiographic appearance of a stricture in the intrathoracic portion of the esophagus of a 5-month-old Arabian colt.[3] Survey radiographs showed air in the cranial portion of the thoracic esophagus, and barium films demonstrated a focal esophageal stenosis caudal to the heart base, with backup of contrast cranially. Esophagomyotomy was performed to relieve the stricture.

A 6-week progress esophagram revealed a transient delay in passage of a hay-barium mixture at the surgery site; however, a 1-year follow-up showed normal transit, with only a mild localized dilation to mark the former surgery site. At $2^1/_2$ years of age, the horse appeared normal, and the owner reported only occasional problems when the animal was fed grass hay.

ESOPHAGEAL ATONY

Esophageal atony typically results in dilation and, if severe, an inability to propel food to the stomach. The consequence is an accumulation of fluid, air, and feed (assuming the horse is eating). Esophageal atony can be inferred by an esophageal profile, which fails to change from one film to the next. Another important consequence of atony is regurgitation leading to inhalation and pneumonia. Atony may also sometimes be seen after blunt chest trauma, but fortunately it is usually transient.

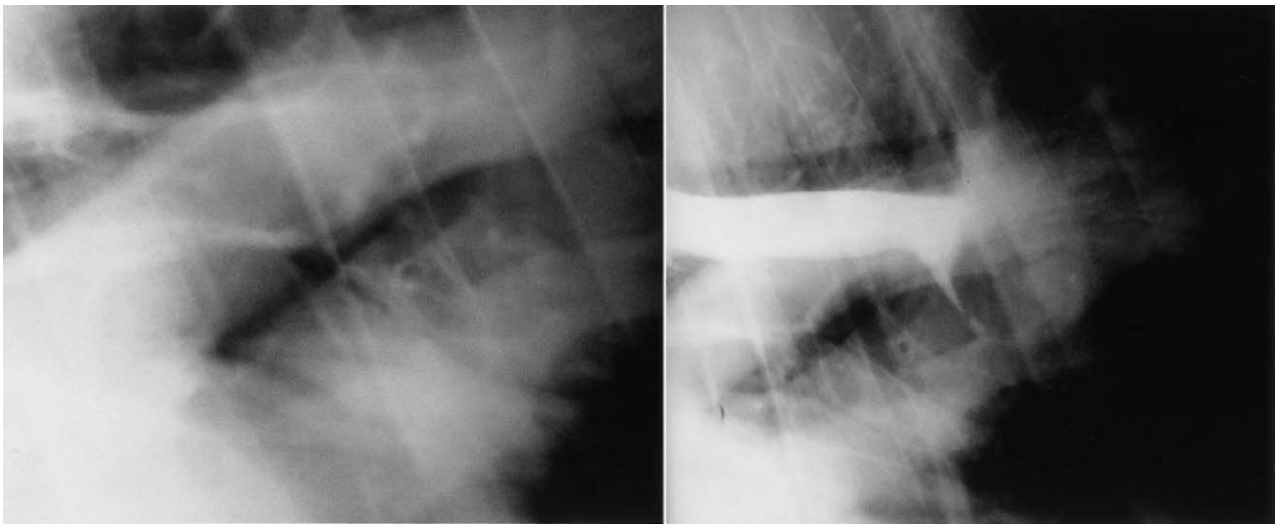


Figure 36-1 • A, Lateral ultra-close-up view of the mid-dorsal thorax of an adult horse shows a variety of variably shaped densities just beyond the caudal heart base, any one of which might represent a foreign body. **B,** Close-up esophagram from the same area shows a circular filling representing a foreign body.

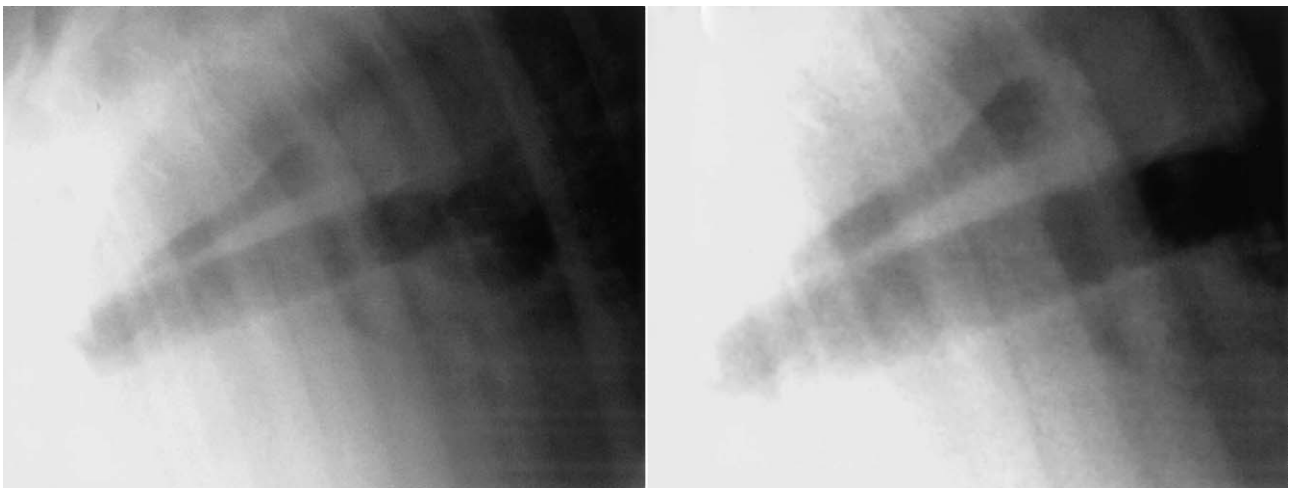


Figure 36-2 • Lateral **(A)** and close-up **(B)** lateral views of the craniodorsal lung field in a foal show a band of esophageal gas just above the trachea, the result of a translucent foreign body. The shape of the gas pocket, in particular its caudal flare, suggests a localized luminal blockage.

References

1. King JN, Davies JV, Gering EL: Contrast radiography of the equine esophagus: effect of spasmolytic agents and passage of a nasogastric tube, *Equine Vet J* 22:133, 1990.
2. Clabough DL, Malcolm MC, Robertson I: Probable congenital esophageal stenosis in a Thoroughbred foal, *J Am Vet Med Assoc* 199:483, 1991.
3. Nixon AJ, Aanes WA, et al: Esophagotomy for relief of an intrathoracic esophageal stricture in a horse, *J Am Vet Med Assoc* 183:794, 1983.

Chapter 37

Miscellaneous Lung Diseases

PERSISTENT FETAL PULMONARY CIRCULATION

Before birth, pulmonary arterial hypertension is the norm, ensuring preferential blood flow away from the lung and into the systemic circulation via the foramen ovale and ductus arteriosus. Drummand as well as Cottrill and O'Conner reported a patent foramen ovale and persistent arterial duct in a 10-hour-old Thoroughbred foal with presumed functional pulmonary hypertension.[1,2]

CONGENITAL BRONCHOPULMONARY DYSPLASIA

Freeman and co-workers described bronchpulmonary dysplasia in a premature Anglo-Trakehner filly foal hospitalized because of profound weakness and respiratory distress.[3] Widespread pulmonary consolidation, noted in films made on admission, was interpreted as consistent with pulmonary atelectasis secondary to surfactant deficiency. Progress films made 2 weeks later showed worsening of the previously identified lung consolidation. The foal was euthanized shortly thereafter.

Necropsy findings were consistent with congenital bronchopulmonary dysplasia, including the following characteristic features:

- Atelectatic lobules
- Diffuse alveolar septal thickening
- Bronchioles and alveoli clogged with eosinophilic material
- Peribronchial infiltrates with secondary luminal narrowing
- Segmental fibrinoid degeneration of arteries and arterioles with medial and adventitial proliferation

EXERCISE-INDUCED PULMONARY HEMORRHAGE

The precise cause or causes of exercise-induced pulmonary hemorrhage in racehorses are not known. Etiologic speculation has long focused on preexisting lung disease, specifically that involving the terminal bronchioles and associated vasculature. However, this theory has not been uniformly accepted, as evidenced by new explanations regularly appearing in the literature. One such example of alternative thinking is the *capillary-failure theory,* which contends that some pulmonary capillaries are simply not strong enough to withstand the extremely high blood pressure that develops during racing, and under such stress, ruptures.[4]

Whatever the cause or causes of exercise-induced pulmonary hemorrhage, in its severest expression the disease can lead to death.[5] Fatal pulmonary hemorrhage, unassociated with racing, was reported in a 3-year-old Thoroughbred filly after a swim.[6] Exercise-induced pulmonary hemorrhage has also been described in polo ponies.[7] Martin and co-workers recommend that tracheal wash, to search for evidence of bleeding, be performed after exercise rather than before.[8]

Radiology

O'Callaghan and Goulden described two distinct radiographic appearances associated with exercise-induced pulmonary hemorrhage in horses, both appearing in the dorsocaudal aspect of the lung as seen in a lateral thoracic radiograph: (1) a small to medium-sized, horizontally oriented, oval-shaped opacity high in the caudal lung field (Figure 37-1) and (2) a vague increase in the density of the dorsocaudal aspect of the lung.[9] Later, as a result of a radiologic-pathologic correlation, O'Callaghan and co-workers noted a significant correlation between (1) *lesion density,* (2) hemosiderin content, and (3) neovascularization of the regional bronchial arteries.[10,11]

▮▮▮ HYALINE MEMBRANE DISEASE (RESPIRATORY DISTRESS SYNDROME)

Hyaline membrane disease is, in nearly all instances, a disease of premature foals that have yet to develop pulmonary surfactant. Without this critical compound, it is impossible to maintain normal lung inflation, which results in hypoxia. The production of surfactant can sometimes be induced in premature foals or, alternatively, a foal can be kept in an oxygen tent. Positive-pressure ventilation is needed in severe cases, but associated intensive care unit costs can be substantial, and there are many potentially fatal complications associated with such therapy. Murry theorized that a lack of surfactant in full-term foals may be due hypothyroidism.[12]

Radiology

Regrettably, some of the published information about the radiology of hyaline membrane disease in foals is either misleading or incorrect. For example, in one review on neonatal intensive care, the authors state that "hyaline membrane disease is *typically represented* (my italics) by a diffuse ground glass appearance with prominent air bronchograms in the human infant: the same appears to be true in the horse."[13] Although this statement may be true sometimes, especially in severe disease, it is by no means typical or even representative. In another report, the authors state that in its *initial* stages respiratory distress syndrome (RDS) is "characterized radiographically by alveolar and granular interstitial patterns," which is not true.[14] RDS nearly always first appears as an extremely subtle, generalized increase in interstitial lung density and only later shows as obvious opacification resulting from atelectasis.

It may also be possible that reports of this nature, especially those reporting regional consolidation in foals,[15] are actually describing a particularly severe form of pneumonia, causing a precipitous and uncontrollable fall in blood oxygen tension resembling that seen with surfactant deficiency.

Based on observing radiologists working in the neonatal intensive care unit at Emory University in Atlanta, Georgia, and performing a dozen or more radiographic examinations on what subsequently proved to be hyaline membrane disease in premature foals, I offer the following personal observations:

- Most premature foals with hyaline membrane disease appear normal, or nearly normal, at the time they are initially radiographed.
- The most frequently observed disease pattern seen with hyaline membrane disease, which is only visible in the highest-quality films, is a subtle, uniform increase in lung density; there is rarely overt consolidation and accordingly no bronchograms.
- Most premature foals suspected of having hyaline membrane disease are radiographed while lying on their sides and often have been recumbent for some time before being imaged. This means that there will almost always be substantial postural atelectasis,[16] which will cause the partially collapsed lung to falsely appear consolidated (opaque), complete with bronchograms.
- If the foal is in respiratory distress, its breathing rate will almost certainly be elevated, increasing the potential for motion unsharpness and creating the illusion of increased interstitial density. Overly light images may create the same effect.
- RDS in septicemic foals can create dramatically abnormal lung that may be mistaken for hyaline membrane disease.

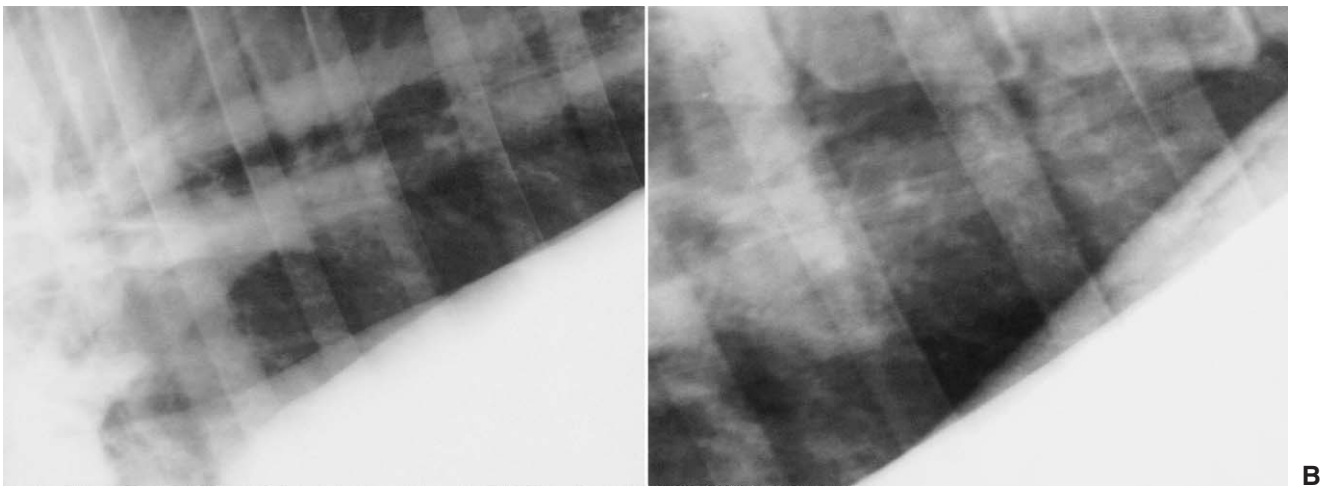


Figure 37-1 • Lateral **(A)** and close-up lateral **(B)** views of the caudodorsal lung field of an adult racehorse with exercise-induced pulmonary hemorrhage show a characteristic narrow, oval-shaped density in the thoracodiaphragmatic angle.

▮▮▮ ADULT RESPIRATORY DISTRESS SYNDROME

In a word, the difference between RDS in premature foals and in adult horses is *surfactant;* the former lack it, and the latter do not. How, then, does surfactant play a role in the adult form of the disease? It is actually quite simple. Certain diseases cause protein, usually fibrin, to leak from the alveolar capillaries into the alveolus. The fibrin eventually coats the alveoli, rendering the pulmonary surfactant ineffective, resulting in uneven lung inflation and hypoxemia. As with premature foals, adult horses can be put on positive pressure ventilators, but unfortunately the delivery and maintenance of positive end-expiratory pressure (PEEP) is not without its own set of serious problems, such as oxygen toxicity and pressure-induced lung injury *(barotrauma).* Most horses that develop adult respiratory disease syndrome (ARDS) eventually die of their illness or are euthanized.

▮▮▮ CHYLOTHORAX

Chylothorax can be caused by a wide variety of diseases (Box 37-1). In the case of diaphragmatic injury, the right crus is most vulnerable because of its association with the thoracic duct as it emerges through the aortic opening in the diaphragm.[17] Shumacher and co-workers reported an idiopathic chylothorax in a 7-month-old Arabian filly.[18]

▮▮▮ NEAR DROWNING

I previously reported the radiographic appearance of near drowning in dogs and horses. Humber also reported a case of near drowning of a horse, in which thoracic radiographs revealed pneumothorax and pneumomediastinum, in addition to increased interstitial density.[19] Nuclear scintigraphy showed a small area of ventilation-perfusion mismatching in one of the caudal lung lobes dorsally.[20]

Box 37-1
Causes of Chylothorax in the Horse as Related to the Integrity and Pressure of the Thoracic Duct

- Traumatic rupture (rib fracture, diaphragmatic hernia, or congenital malformation)
- Neoplastic erosion
- Nonneoplastic, inflammatory erosion, including pneumonia, pleuropneumonia, and pleuritis
- Accidental puncture during catheterization (iatrogenic wounding)
- Right heart failure
- Large cranial mediastinal mass such as lymphoma
- Congenital anomaly, including malformation, atresia, and abnormal drainage
- Undetermined cause (idiopathic)

▮▮▮ DISSEMINATED INTRAVASCULAR COAGULATION

Disseminated intravascular coagulation (DIC) is a mammalian blood disorder that is apparently triggered by a variety of diseases that cause excessive thrombin formation, which in turn activates and then exhausts the proteins responsible for coagulation. The result is fibrinous thrombosis, which may be confined to a single organ or, alternatively, involve the entire body.

Morris and Beech reported DIC in six horses. Unfortunately, not all the horses were radiographed, and those that were showed no consistent pulmonary disease pattern.[21]

Plants from the *Senicio* family occasionally lead to severe respiratory disease in addition to liver failure. The precise cause of the dyspnea is not known, but pharyngeal or laryngeal paralysis is suspected. Thoracic radiographs show increased lung density, which necropsy indicates is the result of lung consolidation caused by pulmonary edema.[22]

▮▮▮ PULMONARY OSTEOPATHY (MARIE'S DISEASE, HYPERTROPHIC PULMONARY OSTEOARTHROPATHY)

Pulmonary osteoarthropathy is a secondary inflammatory bone disease that is usually triggered by a large lung mass, such as an abscess or tumor. Precisely how and why the characteristic bone lesions develop is not known, but removing the inciting lung lesion or cutting the vagus nerve leads to regression. Occasionally pulmonary osteopathy is initiated by mild lung disease, as reported by McClintock and Hutchins.[23] An ovarian dysgerminoma was reported as the cause of pulmonary osteopathy in a mare without lung disease.[24]

Unlike pulmonary osteoarthropathy in dogs, which is associated with distinctive diaphyseal palisades of periosteal new bone, lesions in horses are much less well-defined and generally confined to the metaphyses and adjacent diaphyses.

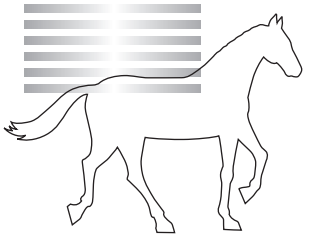
References

1. Drummand WH: Neonatal pulmonary hypertension, *Equine Vet J* 19:169, 1987.
2. Cottrill CM, O'Conner WN: Persistence of fetal circulatory pathways in a newborn foal, *Equine Vet J* 19:252, 1987.
3. Freeman KP, Cline JM, et al: Recognition of bronchopulmonary dysplasia in a newborn foal, *Equine Vet J* 21:292, 1989.
4. West JB, Mathieu-Costello O: Stress failure of pulmonary capillaries as a mechanism for exercise induced

pulmonary hemorrhage in the horse, *Equine Vet J* 26:441, 1994.
5. Gunson DE, Sweeney CR, Soma LR: Sudden death attributable to exercise-induced pulmonary hemorrhage in racehorses: nine cases (1981-1983), *J Am Vet Med Assoc* 193:102, 1988.
6. Qualls CW: Cleft soft palate, nasal septal deviation, and epiglottic entrapment in a Thoroughbred filly, *J Am Vet Med Assoc* 179:910, 1981.
7. Voynick BT, Sweeney CR: Exercise-induced pulmonary hemorrhage in polo and racing horses, *J Am Vet Med Assoc* 188:301, 1986.
8. Martin BB, Beech J, Parente EJ: Cytologic examination of specimens obtained by means of tracheal washes performed before and after high-speed treadmill exercise in horses with a history of poor performance, *J Am Vet Med Assoc* 214:673, 1999.
9. O'Callaghan MW, Goulden BE: Radiographic changes in the lungs of horses with exercise-induced eoistaxis, *N Z Vet J* 30:117, 1982.
10. O'Callaghan MW, Pascoe JR: Exercise-induced pulmonary hemorrhage in the horse: results of a detailed clinical, post mortem and imaging study. VI. Radiological/pathological correlations, *Equine Vet J* 19:419, 1987.
11. O'Callaghan MW, Pascoe JR: Exercise-induced pulmonary hemorrhage in the horse: results of a detailed clinical, post mortem and imaging study. VIII. Radiological/pathological correlations, *Equine Vet J* 19:428, 1987.
12. Murry MJ: Hypothyroidism and respiratory insufficiency in a neonatal foal, *J Am Vet Med Assoc* 197:1635, 1990.
13. Koterba AM, Drummond WH, Kosch P: Intensive care of the neonatal foal, *Vet Clin N Am Equine Pract* 1:1985, 1985.
14. Costa LRR, Mirza MH, Williams J: What is your diagnosis? *J Am Vet Med Assoc* 215:623, 1999.
15. Lloyd KC, Kelly AB, Dunlop CI: Treatment of respiratory distress in a prematurely born foal, *J Am Vet Med Assoc* 193:560, 1988.
16. Clabough DL: Diseases of the equine neonate, *Equine Vet Sci* 9:5, 1988.
17. Mair TS, Pearson H, et al: Chylothorax associated with a congenital diaphragmatic defect in a foal, *Equine Vet J* 20:304, 1988.
18. Schumacher J, Bruise R, Spano J: Chylothorax in an Arabian filly, *Equine Vet J* 21:132, 1989.
19. Humber KA: Near drowning of a gelding, *J Am Vet Med Assoc* 192:377, 1988.
20. Weaver MP: Pulmonary perfusion and ventilation: a mismatch? *Equine Vet J* 27:80, 1995.
21. Morris DD, Beech J: Disseminated intravascular coagulation in six hours, *J Am Vet Med Assoc* 183:1067, 1983.
22. Pearson EG: Liver failure attributable to pyrrolizidine alkaloid toxicosis and associated with inspiratory dyspnea in ponies: three cases (1982-1988), *J Am Vet Med Assoc* 198:1651, 1991.
23. McClintock SA, Hutchins DR: Case report: Hypertrophic osteopathy in a stallion with minimal thoracic pathology, *Aust Vet Pract* 11:115, 1981.
24. McClennan MW, Kelly WR: Hypertrophic osteopathy and dysgerminoma in a mare, *Aust Vet J* 53:144, 1977.

SECTION VI

The Heart



Chapter 38

Radiographic and Sonographic Examination of the Heart

THE STANDARD RADIOGRAPHIC EXAMINATION

Immature Individual

In young foals the standard cardiac examination consists of a single full-length lateral and ventrodorsal view if possible. In older foals, two or more overlapping views are needed to see the entire chest; ventrodorsal views normally are not made.

Mature Individual

A cardiac examination in an adult horse consists of one or two overlapping views of the heart using vertically oriented 14- by 17-inch cassettes and two or three views of the dorsal half of the lung using horizontally oriented cassettes, depending on the size of the horse. The latter are to assess the aorta, the cranial and caudal vena cava, and the larger central pulmonary arteries and veins.

THE STANDARD SONOGRAPHIC EXAMINATION

Sonographic Normals, Sonographic-Anatomic Correlation, and Sonometrics

Carlsten reported the normal sonographic appearance of the equine heart using 10 adult Standardbreds.[1] Sonographic evaluation of the adult equine heart is considered highly reliable, as demonstrated by Voros and co-workers, who compared echocardiographic examinations conducted in 15 adult horses with their gross cardiac anatomy immediately after euthanasia.[2]

The standard sonographic assessment of the heart consists of the following four parts:

1. Careful review of any current *thoracic radiographs*, including any prior films
2. *Systematic anatomic assessment* of the heart, including both the right and left inflow-outflow tracts (sometimes referred to as a two-dimensional or 2D study).

3. *Color Doppler mapping* of the heart valves and adjoining chambers or vessels for turbulent or misdirected blood flow
4. *Spectral Doppler assessment* of transvalvular blood flow with emphasis on velocity, turbulence, and transvalvular pressure gradient.

Radiographic Review

Radiographs provide an overall view of the heart's shape and size not obtainable by other means of medical imaging. Radiographs also indicate whether the lung is overcirculated, undercirculated, or normally circulated; this information is exceedingly valuable in cases of cardiac tamponade, heart failure, or congenital shunts. Likewise, thoracic radiography is capable of detecting pulmonary edema related to heart disease as well as many unrelated thoracic diseases.

Anatomic Assessment

An anatomic assessment can be used to evaluate the following features of the cardiac interior: (1) absolute and relative chamber size; (2) wall thickness; (3) the presence of septal deviation or defect; (4) abnormal chamber partitioning; (5) valve size, shape, position, and movement; (6) papillary muscles and associated cords; (7) pericardial thickness and content; (8) presence of intracardiac or extracardiac masses or mass effects, such as thrombi; and, finally, (9) cardiac contractility coordination.

Color Mapping

Color mapping provides a sensitive and relatively easy means of evaluating the four valvular regions of the heart for disturbed, high-speed, or misdirected blood flow associated with valvular stenosis or regurgitation. Color mapping can also be used to identify transseptal blood flow resulting from structural defects. This form of Doppler is also prognostically useful, for example, in determining what percentage of the left atrium is receiving regurgitant blood flow from the left ventricle because of an incompetent mitral valve.

Spectral Doppler

Pulsed or continuous-wave Doppler traces can be extremely informative, although they are often underutilized. For example, pulsed Doppler can be moved gradually through a valve to determine precisely where a stenosis is situated, and then continuous Doppler is used to calculate the transvalvular pressure gradient. By examining individual Doppler waveforms, one can gain additional insight into the dynamics of valvular disease, particularly the time and speed with which valves open and close. Although at first glance these may seem to be esoteric considerations, in reality they can prove to be quite practical, particularly in concretely documenting the efficacy of medical or surgical treatment.

▮▮▮ STRESS ECHOCARDIOGRAPHY

Stress echocardiography has been advocated for use in poorly performing horses, especially in cases of suspected, but as yet unproven, myocardial disease (also sometimes referred to as *subclinical myocardial disease*).[3]

Standard Stress Echocardiographic Examination

Triphasic Sonographic Examination. The standard echocardiographic examination consists of three separate sonographic assessments made while the horse is (1) resting, (2) making maximal effort, and (3) recovering. Data from the recovery phase are the most important, especially in establishing the presence of what Reef terms *exercise-induced myocardial dysfunction*.[3]

1. Baseline *resting* echocardiographic examination
2. *High-speed* treadmill echocardiographic examination (performed while the horse is at or near maximal effort).
3. *Recovery* echocardiographic examination (performed within 2 minutes after the conclusion of high-speed testing).

Sonographic Views. Four views are obtained in each of the aforementioned sonographic examinations, all from the right parasternal position: (1) long-axis view of the left ventricular outflow tract, (2) long-axis view of the left ventricle, (3) short-axis view of the upper left ventricle just beneath the mitral valve, and (4) short axis view of the mid left ventricle at the level of the papillary muscles.

Comparative Cardiac Assessment

Cardiac performance is assessed with the aid of specialized computer software, which enables the radiologist to view simultaneously the synchronized cardiac cycles of any two examinations, for example, the images taken before and after exercise, and assess them comparatively.

At rest, left ventricular *systolic function* can be assessed by determining (1) whether or not the left ventricle (interventricular septum and left ventricular free wall) is thickened and (2) the value of the *shortening fraction.*

Using dedicated software and electronic cursors, the *percent* shortening fraction is calculated from the described screen images as follows:

1. Subtract the left ventricular internal diameter during *systole*, from the left ventricular internal diameter during *diastole* (cm).
2. Multiply the remainder by 100.
3. Divide the result by the left ventricular internal diameter during *diastole*.

Normal Sonographic Findings During Recovery. During the immediate recovery period after intense exercise and at heart rates of at least 100 beats per minute, the normal left ventricle (including the interventricular septum) undergoes the following systolic changes:

1. Left ventricle (including the interventricular septum) thickens uniformly
2. Fractional shortening increases
3. The diameter of the left ventricular outflow tract decreases during systole as a result of increased cardiac output.

Abnormal Sonographic Findings During Recovery. Myocardial disease often results in regional weakness or in severe disease, in which there is total immobility of a portion of the heart wall or septum. These conditions are termed *hypokinesis* and *akinesis,* respectively. One indication of an underperforming myocardium is a shortening fraction that shows little or no increase immediately after exercise. Another is *asynchrony,* or uncoordinated wall motion. These and other indicators of myocardial dysfunction are listed below:

1. Absence of left ventricular thickening
2. Failure of shortening fraction to increase
3. Area of left ventricular immobility or weak contractility (compared with the rest of the left ventricle)
4. Area of normal but uncoordinated movement (compared with the rest of the left ventricle).

Possible Causes of Exercise-induced myocardial Dysfunction. Assuming that *exercise-induced myocardial dysfunction* is indeed a separate disease entity, not merely a subcategory of cardiomyopathy, the following theoretic explanations may explain its presence (Box 38-1).

▮▮▮ UNKNOTTING INTRAVASCULAR CATHETERS AND INTRACARDIC CATHETER FRAGMENT RETRIEVAL

Cho and co-workers described the technique for unknotting intravascular catheters in people by using fluoroscopic assistance.[4]

Hoskinson and co-workers reported the retrieval of a catheter fragment from the heart of a young foal.[5] Using a purpose-built basket catheter, the fragment was withdrawn according to a technique devised for similar situations in people.[6]

In human radiology the accidental cutting or breakage of the end of an intravascular catheter, and the subsequent loss of the resultant fragment into the central circulation, is referred to (somewhat euphemistically) as *catheter embolization,* a term adopted by some veterinary authors.[7] There are also reports in the human literature of Seldinger spring guidewires suffering the same fate.[8]

Although there is some difference of opinion as to whether or not a catheter fragment should be surgically or nonsurgically removed from the interior of the heart,[9] in most cases an attempt is made to do so based on the fear of one or more of the following possibilities: (1) cardiac arrhythmias, (2) endocardial abrasion, (3) valvular interference, (4) relocation to a potentially more dangerous location such as the lung or a coronary artery, (5) infection, (6) thrombosis, and (7) secondary emboli.

With respect to mechanical interference with a heart valve, Ames and co-workers described the radiographic identification and subsequent retrieval of a jugular catheter fragment in a 2-month-old foal. The object was lodged in the orifice of the tricuspid valve, and it interfered with intracardiac blood flow, as indicated by a load, right-sided heart murmur. The fragment was removed with the foal under general anesthesia using a fluoroscopically guided intravascular snare.[10]

Box 38-1
Possible Causes of Exercise-induced Myocardial Dysfunction

Exercise-induced myocardial ischemia
Exercise-induced myocardial hypoxia
Preexisting myocardial disease
Myocarditis

References

1. Carlsten JC: Two-dimensional, real-time echocardiography in the horse, *Vet Radiol* 28:76, 1987.
2. Voros K, Holmes JR, Gibbs C: Anatomical validation of two-dimensional echocardiography in the horse, *Equine Vet J* 22:392, 1990.
3. Reef VB: Stress echocardiography and its role in performance assessment, *Vet Clin N Am Equine Pract* 17:179, 2001.
4. Cho SR, Tisnado J, et al: Percutaneous unknotting of intravascular catheters and retrieval of catheter fragments, *AJR Am J Roentgenol* 111:467, 1971.
5. Hoskinson JJ, Wooten P, Evans R: Nonsurgical removal of a catheter embolus from the heart of a foal. *J Am Vet Med Assoc* 199:133, 1991.
6. Fischer RG, Ferreyro R: Evaluation of current techniques for nonsurgical removal of intravascular iatrogenic foreign bodies, *AJR Am J Roentgenol* 130:541, 1978.
7. Richardson JD, Grover FL, Trinkle JK: Intravenous catheter emboli: experience with twenty cases and a collective review, *Am J Surg* 128:722, 1974.
8. Cope C: Intravascular breakage of Seldinger spring guide wires. *JAMA* 180:1061, 1962.
9. Decker HR: Foreign bodies in the heart and pericardium—should they be removed? *J Thorac Surg* 9:62, 1940.
10. Ames TR, Hunter DW, Caywood DD: Percutaneous transvenous removal of a broken jugular catheter from the right ventricle of a foal, *Equine Vet J* 23:392, 1991.

Chapter 39

Congenital Heart Disease

ASSESSING HEART SIZE IN NEWBORN FOALS

Judging heart size radiographically in sick foals, especially newborns, is often problematic. This is because sick foals are often quite weak and can stand only briefly, if at all. Accordingly, most such foals are radiographed while lying on their sides.

Lateral recumbency, especially in sick foals with high respiratory rates, often produces an expiratory phase radiograph, along with an artificial increase in the cardiac-thoracic ratio. Postural atelectasis caused by prolonged recumbency can falsely increase the apparent heart size (as seen in a lateral thoracic projection) because of cardiopulmonary superimposition, a radiographic observation known as a *positive silhouette sign.*

Lamb and others have pointed out that transient cardiomegaly observed in newborn foals may in some instances be due to a persistent arterial duct (patent ductus arteriosus, or PDA), which normally closes between 1 and 3 days after birth.[1-3]

VENTRICULAR SEPTAL DEFECT

Ventricular septal defect (VSD) is the most common congenital heart defect found in horses. In general, the longer the defect is present, the more likely the animal will appear ill. A murmur of varying intensity is typically detected.[4]

Radiographically, the heart may or may not appear enlarged. In foals the heart can be imaged on a single 14 by 17 film, right-sided heart enlargement, or emphasis can be readily appreciated; assessment in adults is far more difficult because of the segmented nature of the examination. Increased pulmonary blood flow associated with large defects usually results in pulmonary hyperemia, also termed *pulmonary congestion, overcirculation,* or *hypervascularization.*

Sonographically, a medium or large VSD typically appears as a defect in the uppermost portion of the interventricular septum. Small VSDs are often invisible (Figures 39-1 and 39-2). Depending on the scan angle, the membranous portion of the septum may appear incomplete, mimicking a VSD, a phenomenon commonly referred to as *dropout.*

Lombard and co-workers described cardiac catheterization in six horses with VSD, most of which were foals. The presence of a relative increase in oxygen saturation between the right atrium and ventricle, the latter being the higher—a so-called step-up phenomenon—was considered consistent with a VSD.[5]

Koblik and Hornof described the use of first-pass *nuclear angiocardiography* to diagnose left-to-right cardiac shunting in five horses.[6]

PERSISTENT ARTERIAL DUCT (PATENT DUCTUS ARTERIOSUS)

The arterial duct (ductus arteriosus) *may persist for up to week or longer in newborn foals.* Kienle contends that distinguishing a true PDA from a normally closing duct is difficult in foals less than 2 weeks old, and I would agree.

Radiographically, it is difficult to ascertain whether the heart is enlarged or misshapen, especially if the foal is reluctant or incapable of standing so that only recumbent views are possible. In such circumstances it is often difficult or impossible to distinguish abnormal lung density caused by postural atelectasis from that resulting from pulmonary edema, pneumonia, or hyaline membrane disease. In some animals it may be possible to identify an atrial dome, which is indicative of enlargement; extension of the aortic root into the precardiac mediastinum, also indicative of enlargement; and pulmonary hyperemia reflecting a left to right extracardiac shunt.

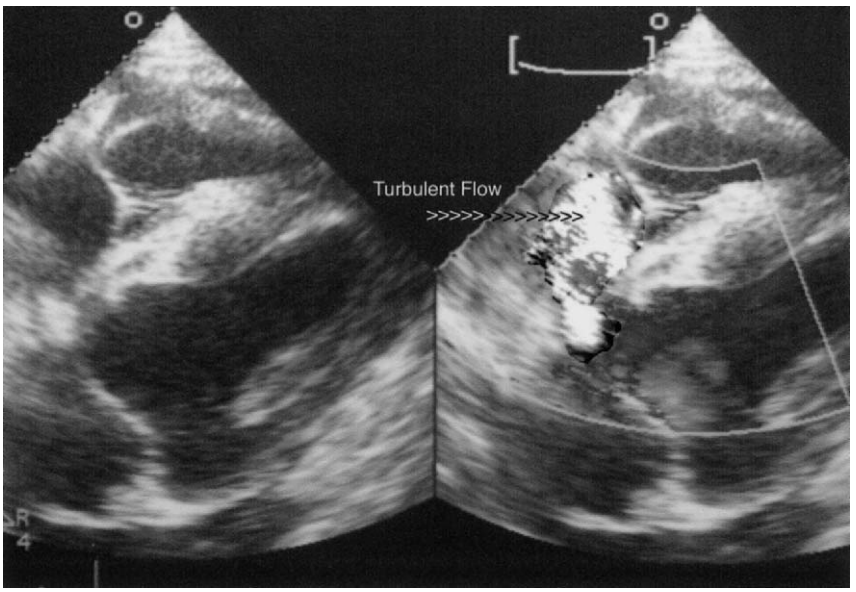


Figure 39-1 • Split-screen, sonographic long section of a ventricular septal defect in a 2-year-old gelding shows a color Doppler image (appearing on the right side in gray scale) featuring a large turbulent jet moving from the left to the right ventricle through a septal defect.

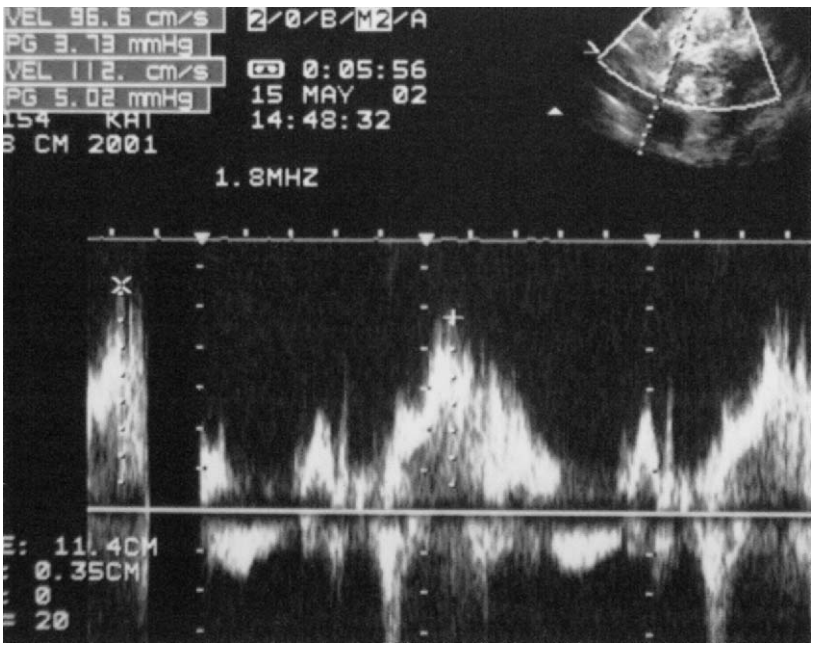


Figure 39-2 • Pulsed-wave spectral Doppler tracing on the right ventricular side of the defect mapped in Figure 39-1 shows turbulent transseptal blood flow.

Sonographically, a PDA is characterized first and foremost by turbulence in the main pulmonary artery (MPA) (Figure 39-3). The arterial duct is usually not identified when the heart is assessed anatomically, but it can occasionally be seen with color mapping. Regardless, the disturbed blood flow in the MPA is a highly reliable disease indicator especially when combined with a continuous machinery murmur.

▮▮▮ CONGENITAL ABSENCE OR CLOSURE OF TRICUSPID VALVE (TRICUSPID ATRESIA)

Complicated Tricuspid Atresia

Button and co-workers described the radiographic and angiographic appearance of tricuspid atresia com-

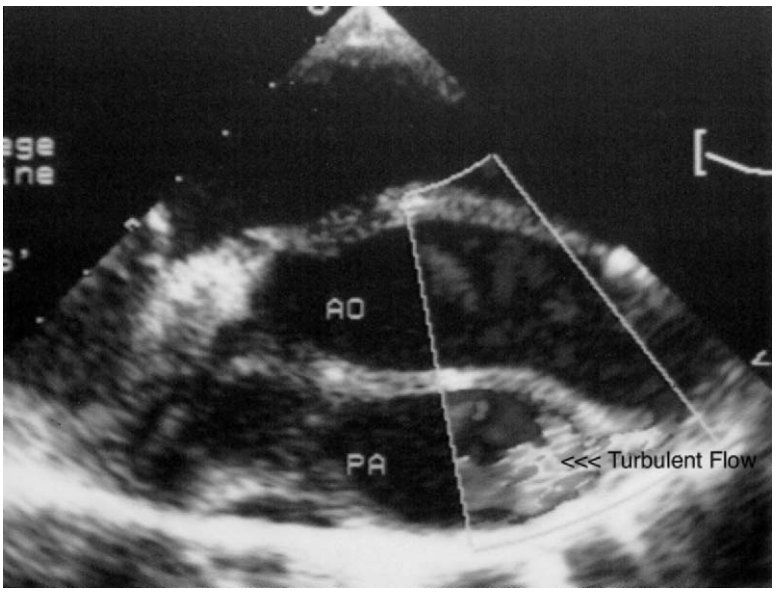


Figure 39-3 • Sonographic image of a foal with suspected congenital heart disease shows color-mapped aortic and pulmonic arterial long sections. Turbulent flow in the main pulmonary artery, along with a continuous machinery murmur, is consistent with a patent ductus arteriosus (PDA).

bined with multiple other cardiac anomalies in a 10-week-old Arabian foal with cyanosis and a load holosystolic murmur.[7] Radiographically, the heart appeared normal and the lungs clear. Initially angiographic findings were ambiguous, but later review revealed right-to-left shunting.

Necropsy revealed absence of the tricuspid valve (tricuspid atresia) and eight additional anomalies: (1) right atrial enlargement, (2) a foramen ovale covered by a fenestrated membrane, (3) a large VSD, (4) eccentric left ventricular hypertrophy, (5) hypoplastic right ventricle, (6) right ventricular hypertrophy, (7) valvular and supravalvular pulmonic stenosis, and (8) a single branching coronary artery.

CARDIAC HYPOPLASIA (HYPOPLASTIC LEFT HEART SYNDROME)

Hypoplasia of the left side of the heart, also known as *hypoplastic left heart syndrome,* features the following anatomic abnormalities: (1) diminished left atrial and ventricular size, (2) left ventricular hypertrophy, (3) mitral or aortic stenosis or both, (4) VSD and atrial septal defects (ASDs), and (5) hypoplasia of the aortic root.

Tadmor and co-workers described such a case in a 2-week-old Arabian filly suffering from severe respiratory distress.[8] The foal had a load machinery murmur and was undersized. Angiocardiography revealed simultaneous opacification of the aorta and main pulmonary artery consistent with a persistent arterial duct. Later, a postmortem examination revealed the presence of atrioventricular hypoplasia and an ASD.

INTERRUPTION OF THE AORTIC ARCH

Scott and co-workers described interruption of the aortic arch and VSD in two young foals.[9] In this unusual anomaly, the aorta is divided into two parts: a cranial component corresponding to the aortic root and a caudal component—actually a continuation of the main pulmonary artery corresponding to the descending aorta.

MULTIPLE, COMBINED CONGENITAL ANOMALIES

Multiple congenital heart anomalies in the same individual are rare compared with single anomalies. Bayly and co-workers have reported combined cardiac anomalies in five Arabian foals, which included: (1) pseudotruncus arteriosus, (2) patent arterial duct, pulmonic stenosis, and tricuspid insufficiency, (3) pentalogy of Fallot, (4) tricuspid atresia, and (5) VSD, plus either a PDA or persistent truncus arteriosus.[10] Diagnosis was based on a combination of radiography, cardiac catheterization (to include pressures), cardiac ultrasound, and blood gas analysis.

PERICARDIOPERITONEAL HERNIA

Orsini and co-workers described a pericardioperitoneal hernia, presumed to be traumatic, in a 3-year-old Standardbred stallion. The pericardioperitoneal hernia was identified during surgery to correct a

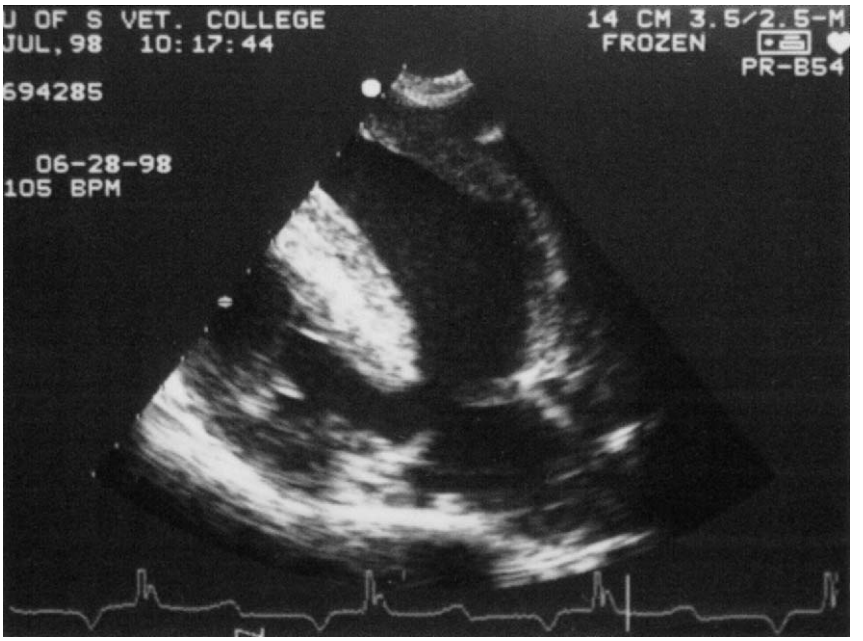


Figure 39-4 • Sonographic long section of the heart of a newborn foal with a truncus arteriosus shows: (1) a large ventricular septal defect, (2) a common outflow tract, (3) an anomalous artery, the truncus arteriosus, and (4) thickened, deformed valves.

diaphragmatic hernia, identified in an earlier radiographic examination.[11]

▮▮▮ CYANOTIC HEART DISEASE

Right-to-Left Shunt

Right-to-left intracardiac shunting typically leads to cyanosis. Extracardiac right-to-left shunting such as a reversed PDA secondary to pulmonary hypertension has a similar effect. Intrapulmonary shunting may also lead to cyanosis but is comparatively rare. Causes of right-to-left shunting in foals are listed in Box 39-1.

Box 39-1
Causes of Right-to-Left Shunting in Foals

Persistent truncus arteriosus
Pseudotruncus arteriosus
Tetralogy of Fallot
Tricuspid atresia
Reversed patent ductus arteriosus secondary to congenital or acquired pulmonary hypertension
Intrapulmonary shunting

Persistent Truncus Arteriosus

Foals are occasionally born with only a single large anomalous artery exiting the heart. The abnormal artery typically sets astride a large VSD, receiving blood from both right and left ventricles. A second anomalous artery branches proximally, equivalent to the pulmonary artery. The prevailing pressure differentials, which regulate intracardiac and extracardiac blood flows, typically misdirect unoxygenated blood to the systemic circulation rather than to the lung, causing cyanosis.

Radiographically, I have not been able to distinguish any defining features of this disease, at least related to the heart, aorta, or pulmonary artery; however, I have been able to consistently detect pulmonary oligemia, which suggests right-to-left shunt, which thus accounts for the cyanosis.

Sonographically, the following disease features characterize a truncus: (1) a shared ventricular outflow tract, (2) a large VSD, and (3) a single anomalous artery instead of a discrete MPA and aortic root. The vessel's valves are often thickened and deformed and may move asynchronously. The right ventricle may be hypertrophied and the associated atrium dilated, resulting in annular distension and high-speed, reversed atrial blood flow (Figures 39-4 through 39-6).

Contrast echocardiography using agitated saline—a so-*called bubble gram*—is capable of demonstrating the presence and direction of abnormal intracardiac blood flow in the case of a suspected shunt. Precisely where to look after an intravenous injection of microbubbles depends on the location of the defect and the nature of any associated pressure gradient.

Tetralogy of Fallot

Intrapulmonary Shunting. Southwood and coworkers reported what they believed was *intrapul-*

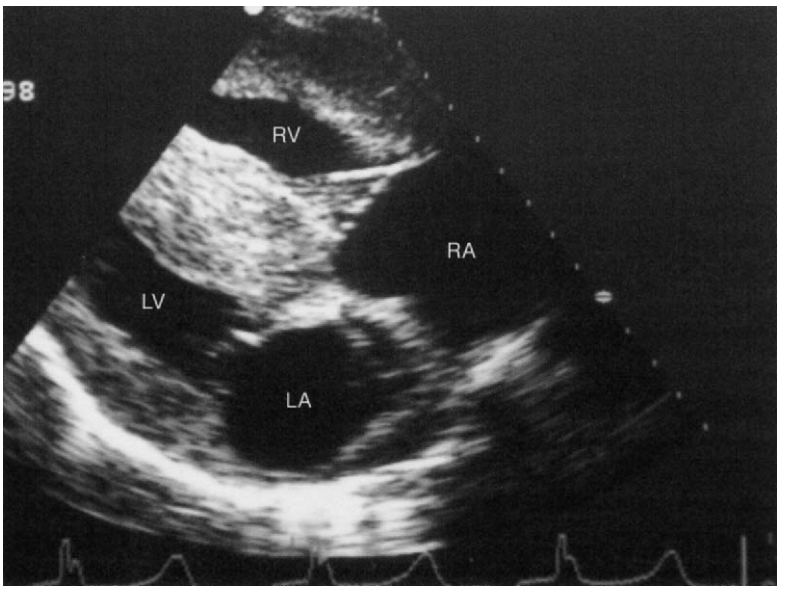


Figure 39-5 • Sonographic long section of the foal shown in Figure 39-4 shows hypertrophy of the right ventricle and dilation of the associated atrium.

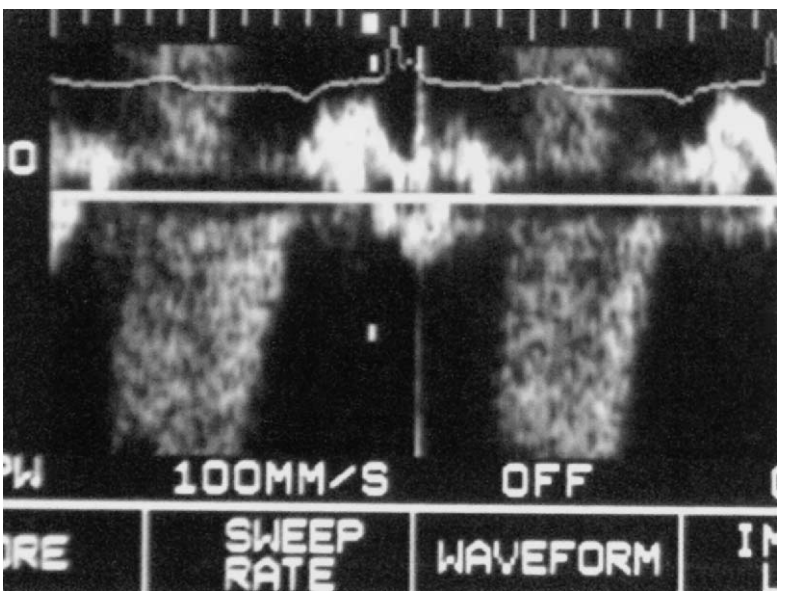


Figure 39-6 • Spectral Doppler tracing of regurgitant right atrial blood flow of the foal shown in Figures 39-4 and 39-5.

monary shunting in a cyanotic newborn with a load murmur.[12] Clinically a right-to-left, intracardiac shunt was suspected but could not be confirmed radiographically or sonographically. However, color-flow mapping revealed reversed systolic blood flow in the pulmonary artery, which, combined with similar oxygen saturations in the front and hindquarters of the animal, supported pulmonary hypertension and the authors' theory of intrapulmonary shunting. The foal's cyanosis resolved after medical treatment (supportive and antimicrobial), and its murmur could not be heard 3 months later.

Note: *A difference in front and hindquarter oxygen saturation of 50 mm of Hg or more is consistent with a reversed PDA (right-to-left shunt) secondary to persistent fetal or acquired pulmonary hypertension.*

References

1. Lamb CR, O'Callaghan MW, Paradis MR: Thoracic radiography in the neonatal foal: a preliminary report, *Vet Radiol Ultrasound* 31:11, 1990.

2. Scott EA, Kneller SK, Witherspoon DM: Closure of the ductus arteriosus determined by cardiac catheterization and angiography in newborn foals, *Am J Vet Res* 36:1021, 1975.
3. Machida N, Yasuda J, et al: A morphological study on the obliteration processes of the ductus arteriosus in the horse, *Equine Vet J* 11:24, 1979.
4. Reef VB: Cardiovascular disease in the equine neonate, *Vet Clin N Am Equine Pract* 1:117, 1985.
5. Lombard CW, Scarratt WK, Buergelt CD: Ventricular septal defect in the horse, *J Am Vet Med Assoc* 183:562, 1983.
6. Koblik PD, Hornof WJ: Use of first-pass nuclear angiography to detect left-to-right shunts in the horse, *Vet Radiol* 28:177, 1987.
7. Button C, Gross DR, et al: Tricuspid atresia in a foal, *J Am Vet Med Assoc* 172:825, 1978.
8. Tadmor A, Fuschel R, Shem Tov A: A condition resembling hypoplasic left heart syndrome in a foal, *Equine Vet J* 15:175, 1983.
9. Scott EA, Chafee A, et al: Interruption of aortic arch in two foals, *J Am Vet Med Assoc* 172:347, 1978.
10. Bayly WM, Reed SM, et al: Multiple congenital heart anomalies in five Arabian foals, *J Am Vet Med Assoc* 181:684, 1982.
11. Orsini JA, Koch C, Stewart B: Peritoneopericardial hernia in a horse, *J Am Vet Med Assoc* 179:907, 1981.
12. Southwood LL, Tobias AH, et al: Cyanosis and intense murmur in a neonatal foal, *J Am Vet Med Assoc* 208:835, 1996.

Chapter 40

Acquired Heart Disease

PREVALENCE AND SIGNIFICANCE OF HEART MURMURS IN RACEHORSES

Kritz and co-workers reported the prevalence and clinical importance of heart murmurs in more than 800 racehorses.[1] Amazingly, murmurs were detected in more than 80 percent of the horses. Most of these were systolic murmurs, heard best over either the pulmonic or aortic valves. Systolic murmurs were also frequently detected over the tricuspid valve but rarely over the mitral valve. Diastolic murmurs were rare by comparison. Most of the murmurs were thought to be clinically insignificant.

ATRIAL FIBRILLATION

Atrial fibrillation is a common arrhythmia of horses. Research performed by the Japan Racing Association suggests that in slower-finishing racehorses (i.e., 4 to 5 seconds behind the winner), atrial fibrillation was more likely to develop in 4-year-olds compared with 2-year-olds and more likely to occur when racing on turf than on dirt.[2] Divers and Byers contend that atrial fibrillation and bacterial endocarditis are the two heart diseases most likely to cause poor performance and weight loss in horses.[3] Atrial fibrillation is an electrocardiographic (ECG) diagnosis.

VENTRICULAR TACHYCARDIA

Ventricular Tachycardia Secondary to Myocardial Disease

Traub-Dargatz and co-workers described the anatomic and M-mode features of ventricular tachycardia secondary to myocardial disease in a 6-year-old Westphalian stallion.[4]

Traumatically Induced Ventricular Tachycardia

In addition to myocardial contusion secondary to blunt chest trauma, some specialists proposed what they believed to be more likely mechanisms, including (1) posttraumatic electrolyte imbalance, (2) autonomic nervous dysfunction, and (3) acid-base disturbance.[5]

BACTERIAL ENDOCARDITIS (VEGETATIVE ENDOCARDITIS)

Bacterial endocarditis can involve any of the heart valves, and it may or may not be associated with thrombus formation.[6] Valvular lesions are sonographically characterized by excessively bright, thickened, and occasionally abscessed cusps, deformities that may in turn lead to stenosis and regurgitation resulting from imperfect coaptation by the damaged leaflets. The lesions are sometimes referred to as *vegetations* (Figure 40-1).

Endocarditis usually involves the mitral or aortic valves, but occasionally it affects the tricuspid valve (in about 10 percent of cases). When present, thrombi are typically situated in the adjacent atrium. Individual thrombi range in size from barely perceptible to those that fill the atrium. Blood cultures from horses with endocarditis are often negative; positive cultures often contain *Streptococcus equi,* believed by many to originate from a previous or concurrent throat infection.

Bonagura and Pipers reported the following sonographic abnormalities associated with endocarditis in dogs, cows, and horses[7]:

- Aortic regurgitation
- Prolapse of the aortic vegetation during diastole
- Left ventricular dilation

- Mitral valve flutter during diastole
- Premature mitral closure

Congestive Heart Failure Secondary to Septic Cordal Rupture

Reef reported mitral insufficiency in three foals with ruptured cords (chordae tendineae).[8] The foals had clinical signs of congestive heart failure believed to be the result of pulmonary hypertension secondary to mitral insufficiency. In at least one of the foals, the parting of the cord was believed to be the result of damage caused by endocarditis (Figures 40-2 and 40-3). Ewart and co-workers also reported a case of mitral endocarditis and ruptured cord in a 2-year-old Arabian stallion caused by *Serratia marcescens*. However, there were no secondary chamber enlargements or valvular prolapse.[9]

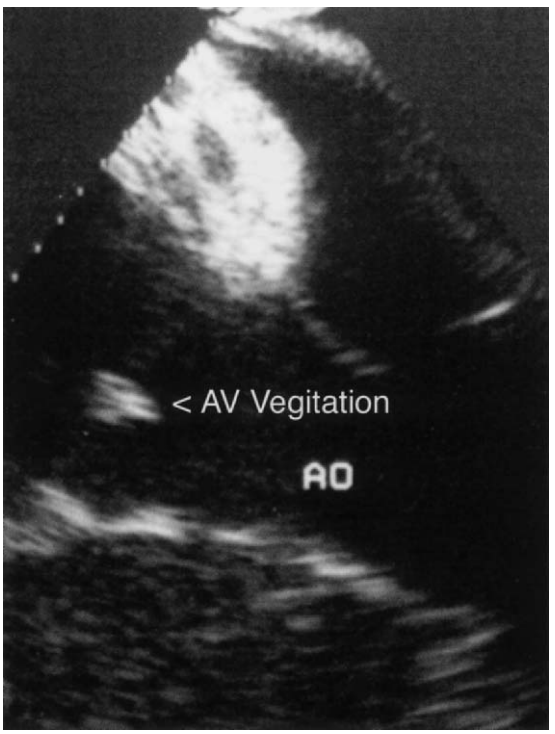


Figure 40-1 • Close-up sonogram of the left ventricular outflow tract (AO) of a horse with endocarditis shows a vegetative lesion on the aortic valve (AV).

▮▮▮ PERICARDITIS

Classification

Worth and Reef divided pericarditis in the horse into three types: (1) that associated with pericardial fluid, or *effusive pericarditis;* (2) that which causes intrapericardial fibrin formation, or *fibrinous pericarditis;* and (3) that which causes fibrosis and, as a result, cardiac constriction, or *constrictive pericarditis*.[10] Whether by compression, constriction, or restriction, all types of pericardial disease are capable of causing right-sided heart failure. The precise cause of pericarditis is not determined in most horses, although cytologic findings may be consistent with infection.

Effusive Pericarditis

Bernard and co-workers reported pericarditis in six horses; their findings emphasized the diagnostic and therapeutic value of cardiac ultrasound. Sonography proved indispensable in the installation of a pericardial catheter used periodically to drain, flush, and

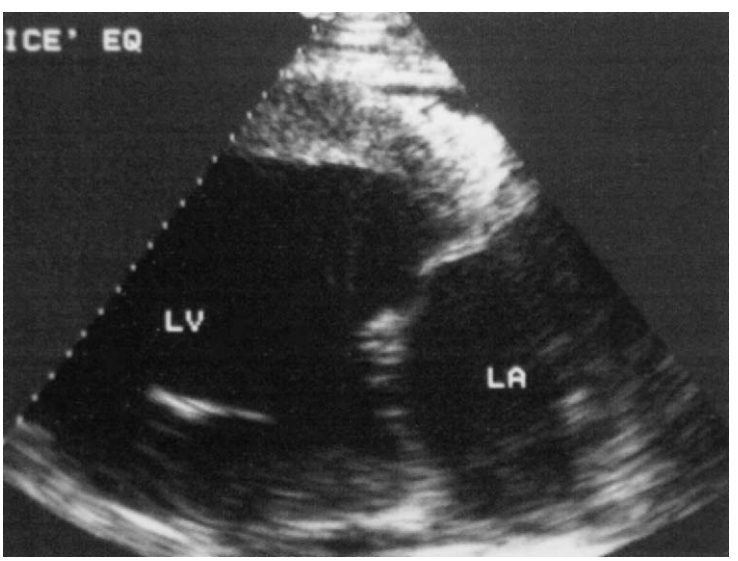


Figure 40-2 • Long-section sonogram of the left ventricular inflow tract of an adult horse shows moderate left ventricular and left atrial dilation. Vegetation on the mitral valve centrally is associated with mild inversion.

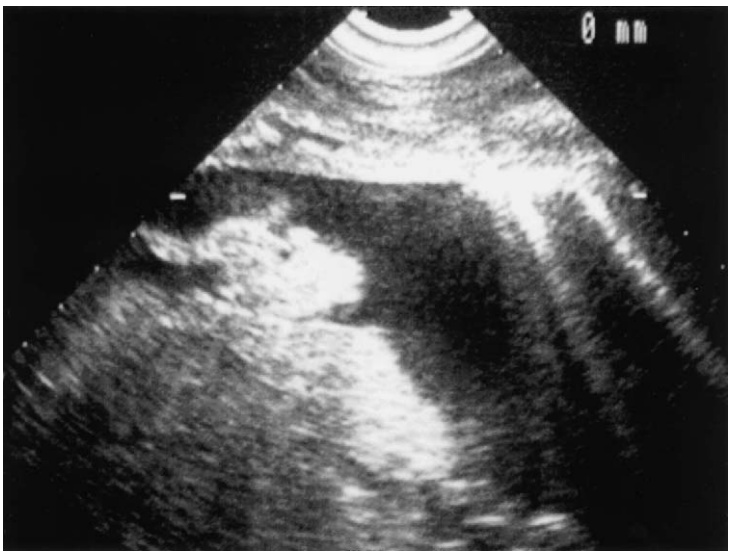


Figure 40-3 • Thoracic sonogram of the horse shown in Figure 40-2 shows a medium volume of pleural fluid causing relaxation atelectasis of the lung.

medicate the pericardial cavity.[11] Voros and co-workers reported using echocardiography in a young Arabian colt to assist in the relief of a cardiac tamponade caused by an infected thoracic stab wound.[12]

Fibrinous Pericarditis

Dill and co-workers reported fibrinous pericarditis causing heart failure in four horses. Radiographs showed an enlarged, rounded heart with relatively small lung vessels, suggesting cardiac tamponade or restrictive pericarditis.[13]

Seahorn and co-workers recently reported that fibrinous pericarditis among central Kentucky horses *may be* associated with *mare reproductive loss syndrome* and that exposure to Eastern tent caterpillars was the greatest risk factor.[14]

Inflammatory Pericardial Disease (Restrictive Pericarditis, Constrictive Pericarditis)

Pericarditis can cause adhesions between the pericardium and epicardium, which if severe can both restrict and modify the motion of the heart. Of critical importance in such instances is whether or not any of the heart chambers are affected, particularly the right atrium, which is particularly susceptible to external compression or restriction. In the event of right atrial compression or restriction, stroke volume and cardiac output are reduced.

Accordingly it is the amount of *right auricular volume loss,* not right ventricular compression, that is the true measure of the adverse effects of inflammatory pericarditis or pericardial fluid. Sonographically, the degree of right atrial compression is estimated as a percentage of the total right atrial volume, a 50 percent volume loss, for example. Progressive pericarditis may lead to chronic cardiac tamponade.

Box 40-1
Causes of Cardiac Tamponade

Idiopathic, aseptic, effusive pericarditis
Fibrinous pericarditis
Constrictive pericarditis
Traumatic hemopericardium
Idiopathic hemopericardium
Pericardial hernia
Pericardial hematoma
Pericardial tumor
Bacterial or fungal pericarditis
Viral pericarditis
Congestive heart failure

▮▮▮ CARDIAC FLUID COMPRESSION (CARDIAC TAMPONADE)

Accumulated fluid between the nondistensible pericardium and the readily deformable heart is a dangerous situation that can lead to sudden or gradual cardiac compression, depending on the rapidity with which the fluid forms. Fibrin encasement can gradually strangle the heart, reducing both its chamber sizes and contractility. A pericardial hernia may cause secondary blockage of one or more descending coronary arteries, leading to myocardial infarction.

Idiopathic, effuse pericarditis is reportedly the most common cause of pericardial fluid in horses. Pericardiocentesis, with or without corticosteroid treatment, is reported to cure or improve 60 percent of

the horses with the disease. This and other causes of cardiac tamponade are listed in Box 40-1.

In a report of 10 horses with cardiac tamponade secondary to effusive pericarditis, Freestone and co-workers reported the following clinical signs: (1) tachycardia, (2) ventral edema, (3) distended jugular veins, and (4) diminished (muffled) heart sounds.[15] ECG abnormalities included reduced voltages and electrical alternans. Six of the horses underwent ultrasound examination and were found to have pericardial fluid. Pericardiocentesis relieved clinical signs in 9 of the 10 animals. Laboratory analyses of the pericardial fluid samples were classified as follows:

- Aseptic serofibrinous (six cases)
- Eosinophilic (three cases)
- Histiocytic (one case)

Radiographic Findings

Moderate to severe heart enlargement combined with distinctive rounding is the cardinal feature of large volumes of pericardial fluid secondary to pericarditis. Under such conditions, cardiac compression, especially to the right side of the heart during diastolic filling, can be anticipated. This is reflected by pulmonary oligemia and pleural fluid with associated pulmonary atelectasis. Peritoneal fluid and hepatic congestion are also usually found under such circumstances but are best diagnosed sonographically.

Sonographic Findings

The pericardium is usually thickened and its inner surface coated by a thickly fringed layer of fibrin. The epicardium has a similar appearance. Chamber sizes typically appear diminished, with the right ventricle often exhibiting a distinctive wavelike motion indicative of its fluid surroundings. Diastolic collapse of the right ventricle and systolic collapse of the right atrium have also been described as consistent M-mode features in horses with tamponade. Generally (and quite reasonably) the greater the degree of chamber collapse, especially on the right side, the greater the probability that the horse is in heart failure.

Pericarditis Causing Hypertrophic Pulmonary Osteoarthropathy

Long and co-workers reported hypertrophic pulmonary osteoarthropathy (HPOA) in a 5-year-old American Saddlebred gelding, apparently triggered by fibrinous pericarditis and epicarditis.[16] Radiographs revealed multiple bony abnormalities, only one of which was included in the described article. The tibial lesion consisted of a broad-based, medium-sized, smoothly elevated bone deposit situated on the caudal aspect of the distal tibial body. Unlike in dogs, there was no characteristic pallisading. Nuclear scintigraphy revealed numerous areas of focally increased radiopharmaceutical uptake (hot spots) corresponding to the radiographic lesions.

▮▮▮ AORTIC ROOT DISEASE

Aortic Root Tearing Leading to Cardiovascular Fistula (Aortocardiac Fistula, Aorticoventricular Fistula). Marr and co-workers reported the sonographic appearance of cardiovascular fistulas in seven adult horses.[17] The typical sonographic lesion appeared as a defect in the wall of the aortic root, with or without an associated dissecting aneurysm.

The affected horses ranged from 6 to 18 years of age and typically presented with acute distress, bounding arterial pulse, a right-sided continuous murmur, or ventricular tachycardia. Fistulous communications were identified between the aorta and the right ventricle in four horses, the aorta and right atrium in two horses, and the aorta and left ventricle in one horse. Survival varied from a single day to 4 years. Stallions were affected most often.

Sleeper and co-workers described the sonographic appearance of aortic root tearing leading to an aorticoventricular fistula.[18] The same authors also reported the sonographic appearance of aortic aneurysm.

▮▮▮ AORTIC ANEURYSM AND RELATED THROMBOSIS

Derkson and co-workers reported right heart failure in a 7-year-old Arabian mare resulting from a communicating aortic aneurysm.[19] The aneurysm, located at the base of the aortic root, communicated with the adjacent pulmonary artery. The horse also had an aneurysmal bicarotid trunk.

In their discussion of equine aortic aneurysms, the authors listed the following causes of weakening of the medial aortic wall (elastic layer), the first step in its dilation and eventual disintegration: (1) blunt trauma, (2) parasitic infiltration, (3) bacterial infection, (4) fungal infection, (5) arteriosclerosis, and (6) medial cystic necrosis.

Lester and co-workers reported the sonographic appearance of a dissecting aortic root aneurysm in a 12-year-old Thoroughbred stallion.[20] The aneurysm appeared as a small, thinly walled outpouching on the surface of the sinus of Valsalva.

True or false aortic aneurysms are rarely identified in horses, especially radiographically. They typically appear as areas of tapered enlargement in the aortic arch or cranial aorta (Figure 40-4). Related thrombi can occasionally be inferred from a diminished downstream circulation, as suggested by regional or generalized oligemia.

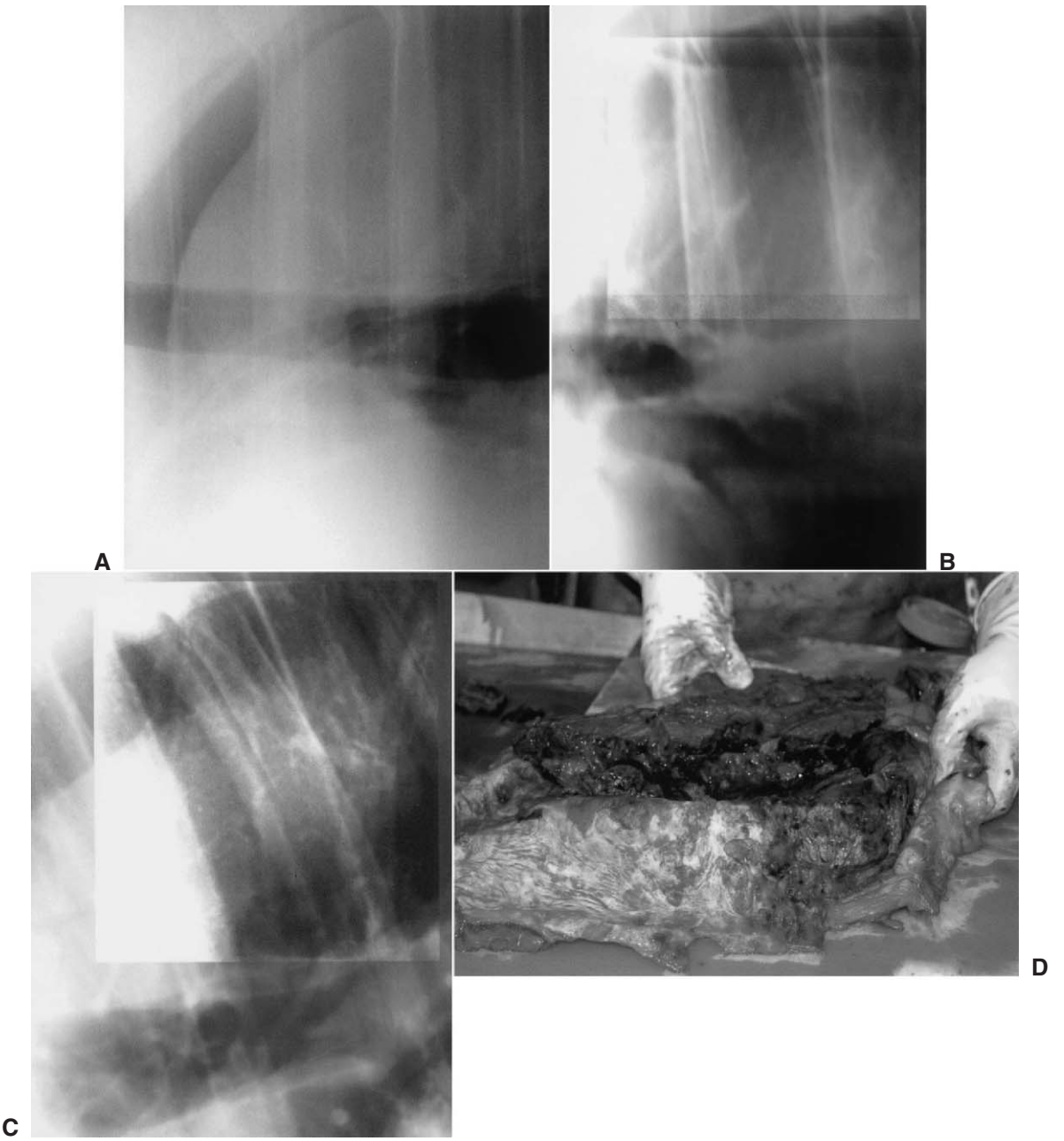


Figure 40-4 • Close-up lateral views of aortic arch **(A)** and cranial aorta enlarged nearly twice normal size **(B).** A normal aortic arch and cranial aorta are provided for comparison **(C).** A necropsy photo shows the dilated portion of the aorta split longitudinally to reveal the large, knobby thrombus **(D).**

▮▮▮ VALVULAR INSUFFICIENCY (VALVULAR REGURGITATION, DEGENERATIVE VALVULAR DISEASE)

The precise cause or causes of degenerative valve disease causing valvular insufficiency are not known, but it is generally considered a form of acquired heart disease. A recent review article on equine degenerative valvular disease suggests that such disorders are age related, but the article fails to specify the specific nature of the relationship.[21]

Inflow Insufficiency

Mitral Insufficiency (Mitral Regurgitation, Mitral Endocardiosis). Pulmonary hypertension secondary to mitral insufficiency is the leading cause of heart failure in horses. Varying degrees of underperformance in the horse are also commonly associated with mitral insufficiency.

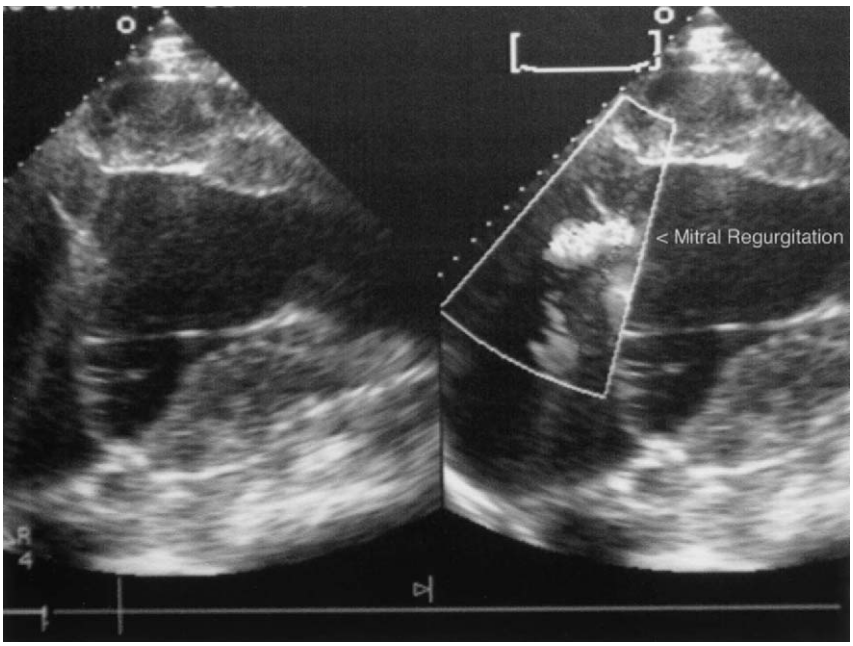


Figure 40-5 • Close-up, split-screen sonograms of the left inflow tract emphasizing the mitral valve, which has been color mapped on the right, show mild to moderate regurgitation estimated to involve approximately 10 percent of the left atrial cross-section.

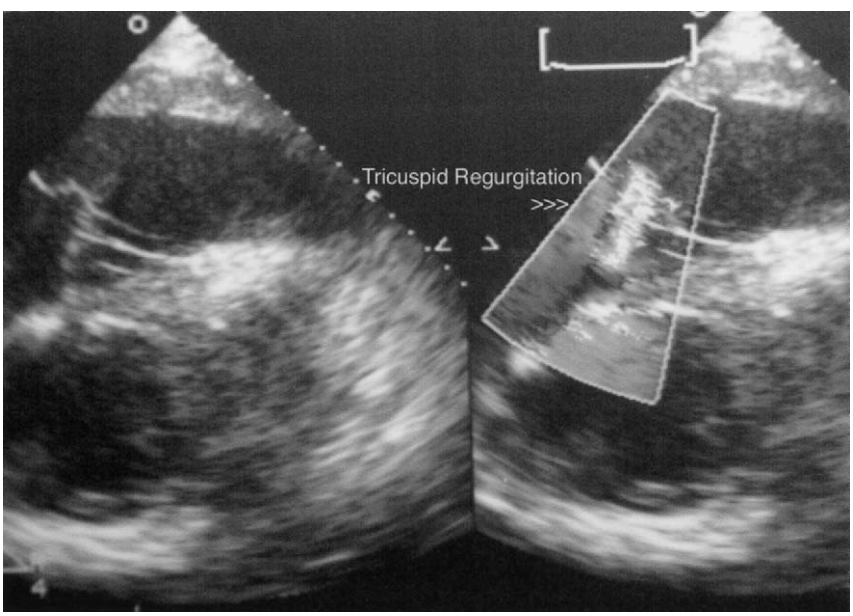


Figure 40-6 • Close-up, split-screen sonograms of the right inflow tract emphasizing the tricuspid valve, which has been color mapped on the right, show mild to moderate regurgitation estimated to involve approximately 30 percent of the right atrial cross-section (only partially shown).

Sonographically, a leaky mitral valve may appear entirely normal, including its range of motion. Alternatively, an incompetent valve may appear uniformly thickened, irregular, or abnormally bright. Its leaflets may move asynchronously or prolapse into the left atrium. Torn cords still attached to the papillary muscles may undulate in the left ventricle, and cord fragments still attached to the valve cusps may whip back and forth into and out of the atrium.

The appearances of the diseased mitral valve and its abnormal motion notwithstanding, most mitral insufficiencies are detected and quantitatively evaluated through color mapping or, alternatively, spectral Doppler (Figure 40-5). The degree of involvement can

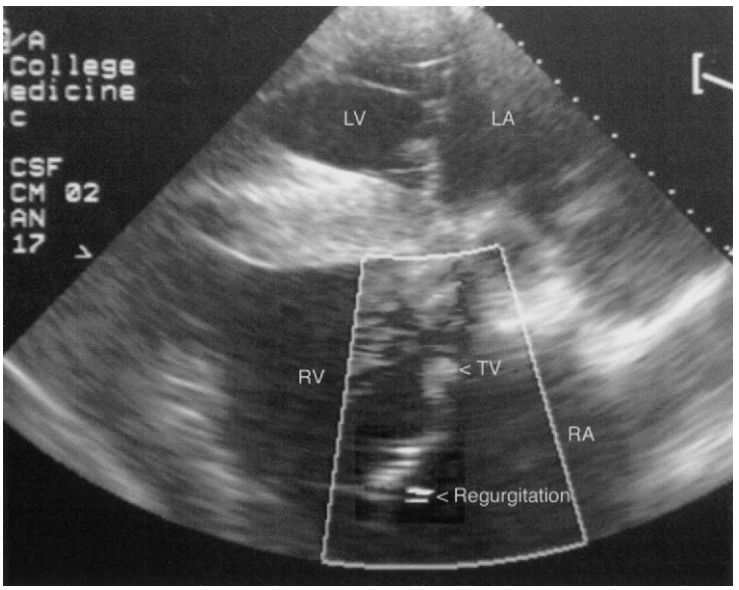


Figure 40-7 • Long-section, four-chamber cardiac sonogram emphasizing the tricuspid valve shows a very small regurgitant jet that, by virtue of its minute size, is often referred to as trivial.

be *estimated* using color Doppler and expressing the regurgitant flows as a percentage of the total atrial area.

Tricuspid Insufficiency (Tricuspid Regurgitation, Tricuspid Endocardiosis). Although relatively common compared with other sources of valvular leakage in horses, tricuspid insufficiency is usually of no clinical consequence. Accordingly, the murmurs caused by tricuspid insufficiency are often referred to as *innocent* (i.e., innocent of causing illness).

Sonographically, tricuspid insufficiency shares many disease characteristics with mitral insufficiency: excessive echogenicity, deformity, abnormal cusp motion, and right atrial prolapse (Figure 40-6). Very small regurgitant jets are often referred to as *trivial* (Figure 40-7).

Outflow Insufficiency

Aortic Insufficiency (Aortic Regurgitation, Aortic Endocardiosis). Aortic valvular insufficiency in horses is likely a true *geriatric disease,* which comes about as a result of advancing age. If the disease is infectious, no single cause has yet been identified. Nodular, noninfectious endocardiosis can grossly resemble the vegetative lesions of endocarditis.

It is unclear whether small defects in the edges of the aortic valve cusps or cordal tears are related to endocardiosis, although clearly they are capable of causing valve leakage. Deformed valve leaflets invariably lose some of their hydrodynamic properties. For example, a medium- or large-sized nodule increases drag on the valve cusp as it attempts to close, behaving like a biomechanical sea anchor. The result is delayed closure and leakage. Once in contact with the other cusps, the nodular leaflet fails to fit snugly with its companions, causing further leakage.

A variety of other terms have been used to describe diseased aortic valves: *degenerative valvular disease, valvulitis,* and *valvulosis,* each with its own shortcomings. For example, deformed valves, particularly those with nodules, are more generative than degenerative in quality. The suffixes *-itis* and *–osis* appear unjustified based on a lack of characteristic sonographic features that warrant such distinctions.

In my opinion, it is not radiographically possible to consistently distinguish aortic insufficiency from other forms of valvular disease that commonly affect horses. On the other hand, sonography is quite capable of making such distinctions, especially when color enabled.

Compared with a healthy aortic valve, a noninfected aortic valve often appears thicker than normal in both cross-sections and long sections (Figure 40-8). Bear in mind, however, that a normal-appearing aortic valve may prove dysfunctional once it is color mapped or examined with spectral Doppler (Figure 40-9). As with other incompetent heart valves, the volume of regurgitant blood may be large or small, the former a reliable risk factor for future heart failure (Figures 40-10 and 40-11). As might be anticipated, associated chamber enlargement usually accompanies serious or long-standing valvular incompetence (Figure 40-12).

Pulmonic Insufficiency (Pulmonic Endocardiosis). Primary pulmonic insufficiency is exceedingly rare in horses. Secondary insufficiency may accompany pul-

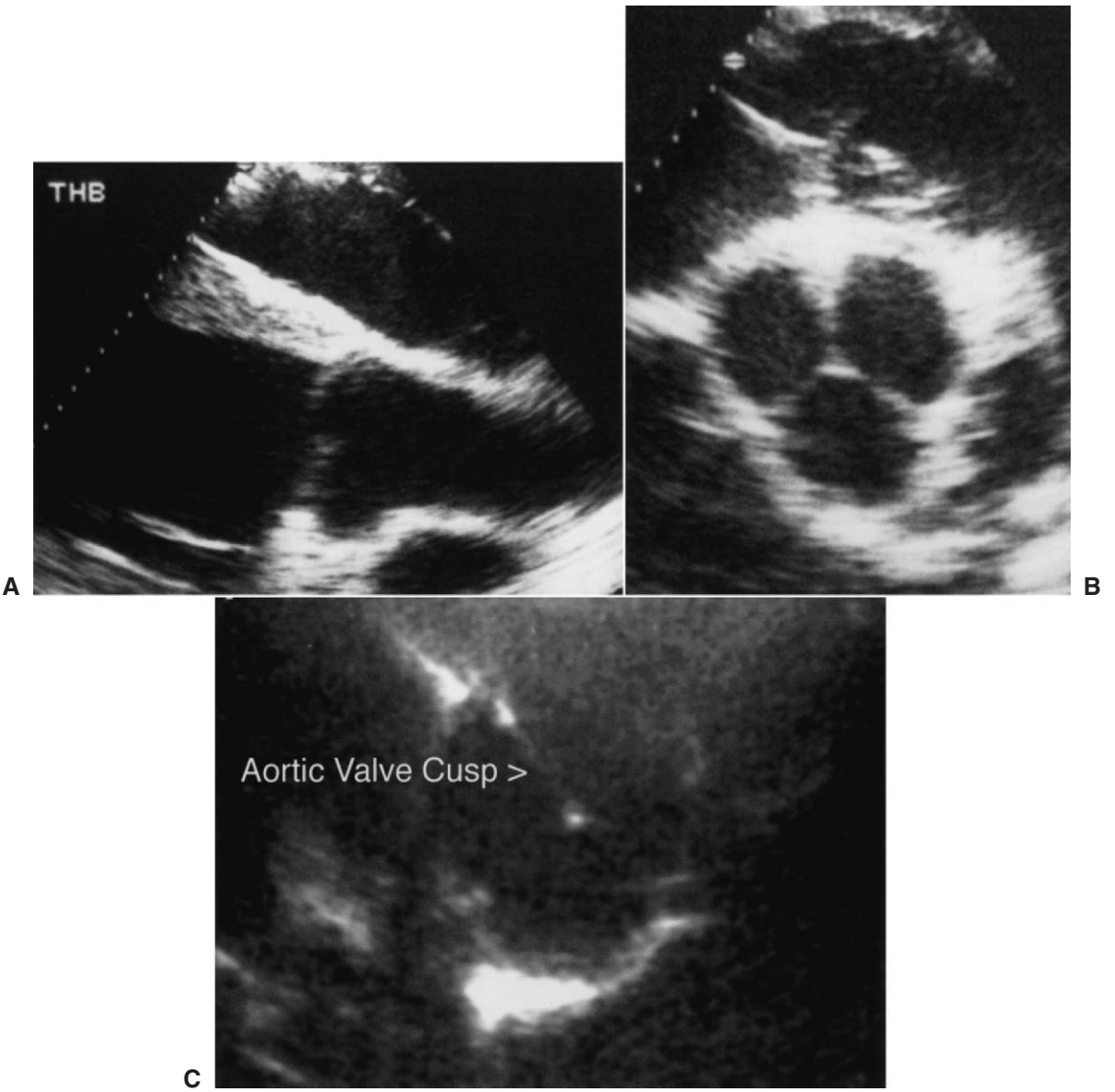


Figure 40-8 • Close-up long- **(A)** and cross-section **(B)** views of the aortic outflow tract show a thickened mitral valve, which proved to be incompetent when subsequently color mapped. A normal aortic valve is provided for sonographic comparison **(C)**.

monary hypertension and, less often, congestive heart failure.

▮▮▮ COR PULMONALE

A priori, one might expect a high incidence of cor pulmonale in horses with chronic obstructive lung disease; however, this does not appear to be the case. Actually cor pulmonale is quite rare compared with most other acquired heart diseases in this species. According to Dixon and co-workers, based on their study of the hearts of horses with chronic obstructive pulmonary disease (COPD), the low incidence of cor pulmonale can be explained by the reversibility of the pulmonary hypertension that initially accompanies COPD.[22]

Radiographically, cor pulmonale is suggested by cardiomegaly with right-sided emphasis when found in conjunction with chronic severe lung disease, including pulmonary hypertension. Sonographically, pulmonary hypertension can lead to dilation of the right atrium and ventricle as well as ventricular hypertrophy (Figure 40-13). Depending on the magnitude of

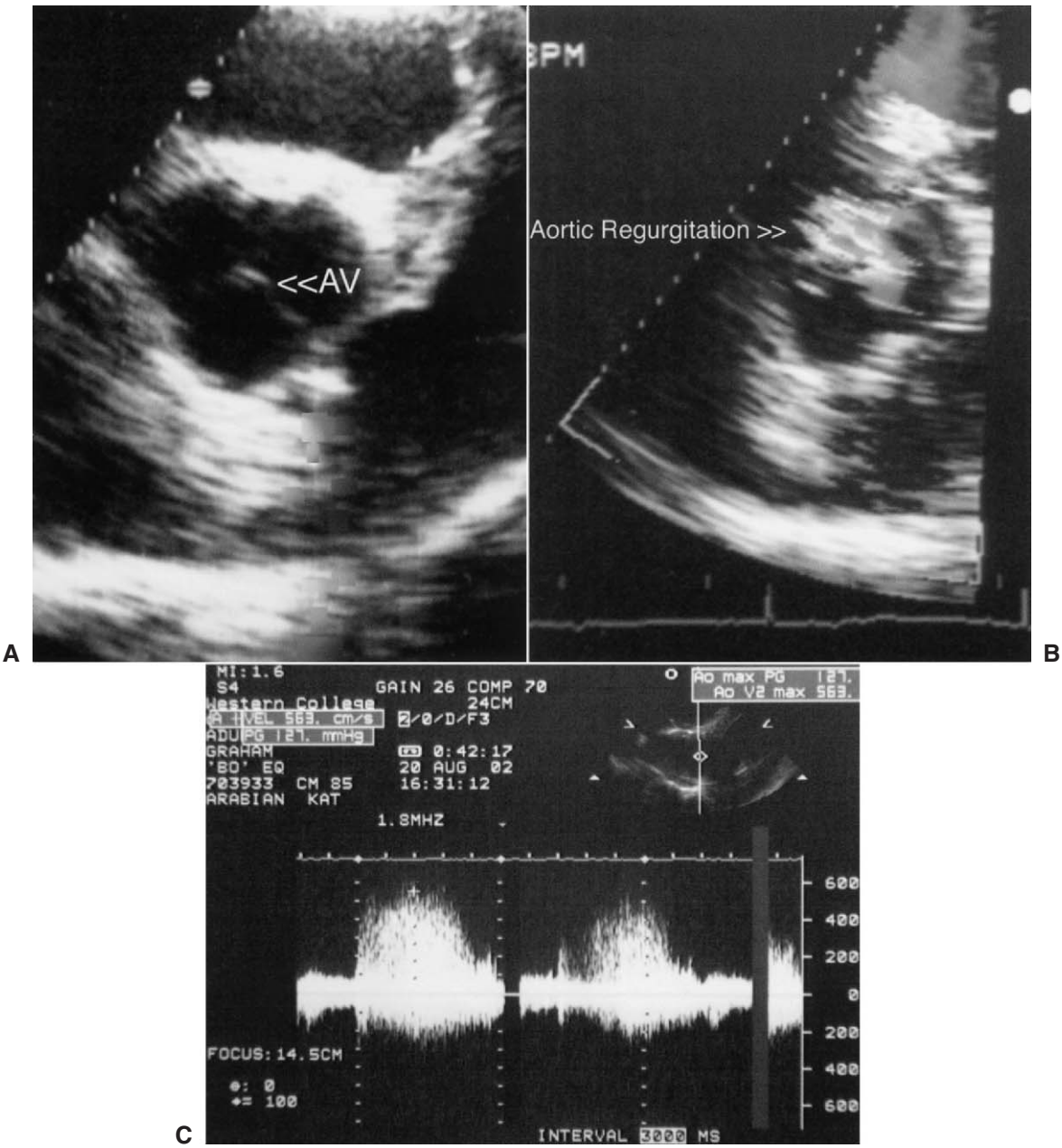


Figure 40-9 • An anatomically normal-looking aortic valve **(A)** appears incompetent when it is color mapped **(B)** and examined with spectral Doppler **(C),** illustrating that an anatomic assessment alone is not capable of determining whether or not a valve is competent.

these changes, both the pulmonic and tricuspid valves may leak.

▮▮▮ CONGESTIVE HEART FAILURE

Congestive heart failure in the horse may or may not be age related. If it is, the disease can justifiably be termed *geriatric* and considered under the purview of *gerontology.* It is arguable, however, whether *geriatric* is an appropriate synonym for *aged,* although some authors have used the word in this way, perhaps in an effort to appear more erudite.[23] In my opinion, geriatric should be restricted to the description of specific *age-related diseases,* not merely as a synonym for *old.* For example, an old healthy horse is just that, an old healthy horse, not a geriatric horse; but an old horse with an *age-related heart problem* is an old horse with *geriatric* heart disease.

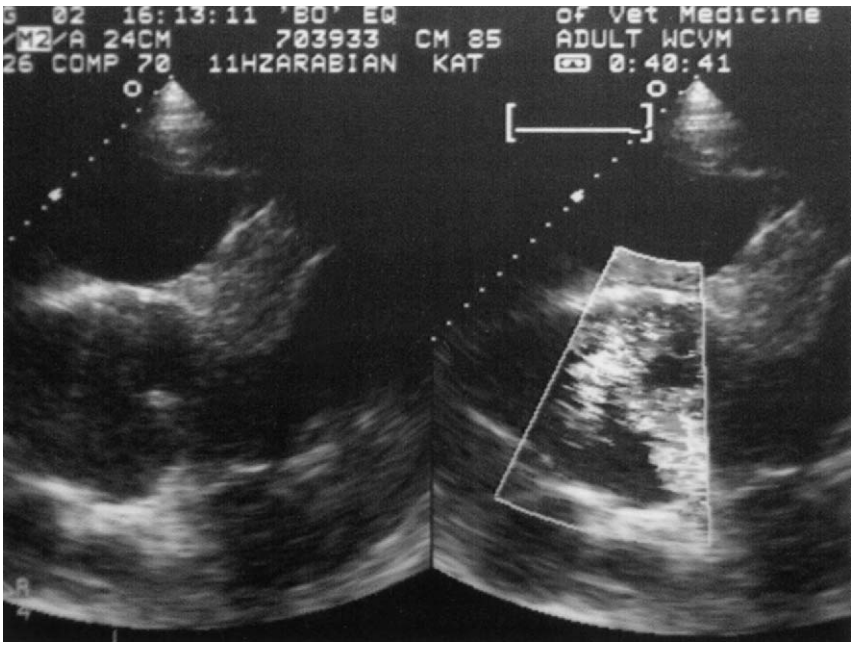


Figure 40-10 • Close-up, split-screen sonograms of the left outflow tract centered on the aortic valve and color mapped on the right show a moderate to severe regurgitant plume, indicating valvular incompetency.

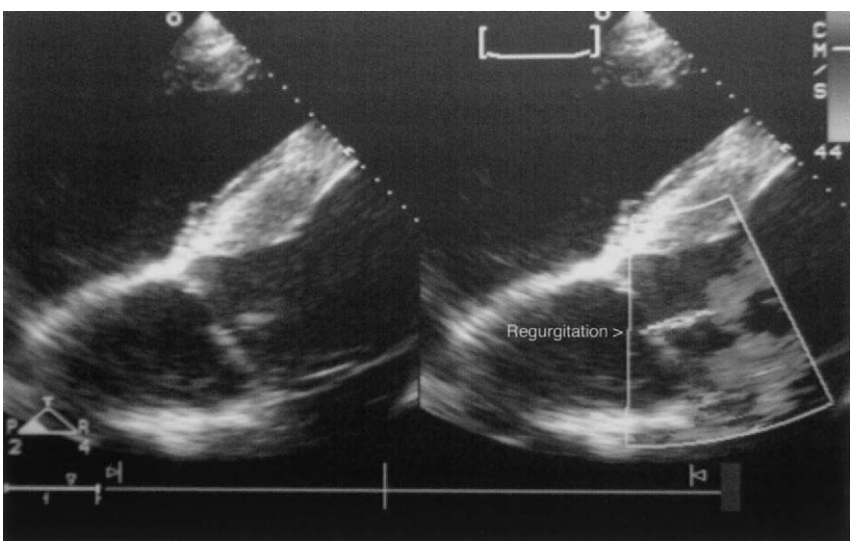


Figure 40-11 • Close-up, split-screen sonograms of the left outflow tract emphasizing the aortic valve, which is thickened, show a small but lengthy regurgitant jet passing through the center of the aortic valve.

Imaging Findings

Answering the Critical Radiographic Question: Is the Horse in Failure? A radiographic diagnosis of *left-sided heart failure* requires three essential radiographic disease indicators (RDIs): (1) cardiomegaly with left-sided emphasis or, less often, generalized cardiomegaly; (2) pulmonary hyperemia; and (3) pulmonary edema.

A radiographic diagnosis of *right-sided heart failure* also features three essential RDIs: (1) cardiomegaly with right-sided emphasis or, in the case of a large volume of pericardial fluid, generalized enlargement; (2) normal or oligemic lung vasculature; and (3) peritoneal fluid. Sonology is not capable of diagnosing heart failure, although it may suggest it.

References

1. Kriz NG, Hodgson DR, Rose RJ: Prevalence and clinical importance of heart murmurs in racehorses, *J Am Vet Med Assoc* 216:1441, 2000.

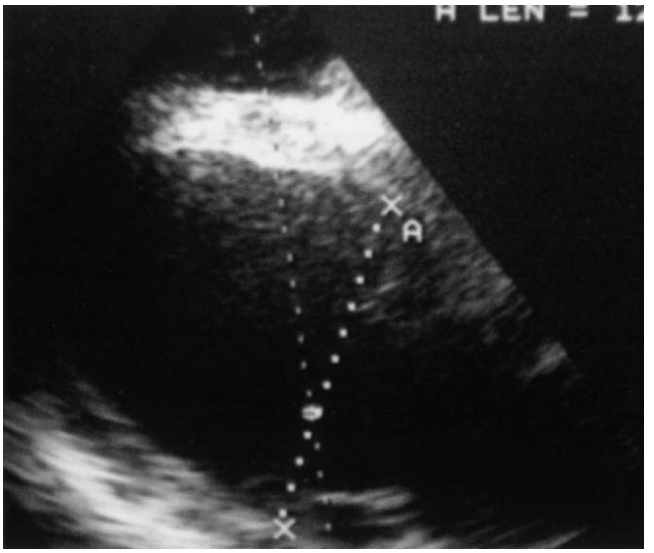


Figure 40-12 • Sonographic long-section view of the left ventricle shows mild dilation secondary to aortic insufficiency.

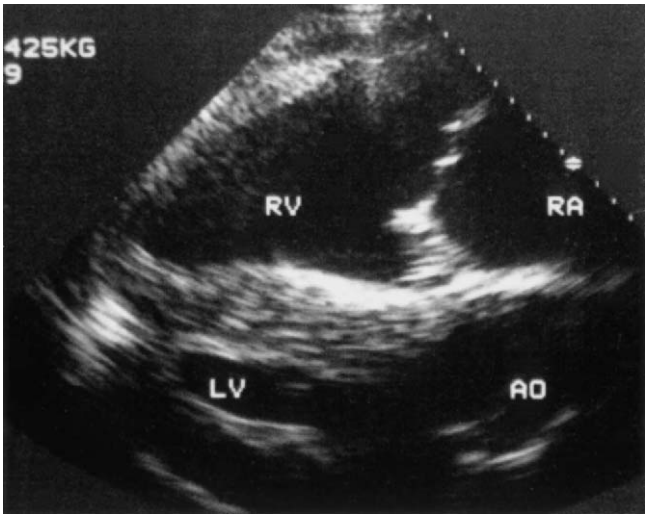
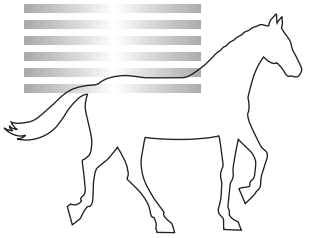


Figure 40-13 • Four-chamber view of the heart shows hypertrophy and dilation of the right ventricle and associated atrial dilation secondary to pulmonary hypertension.

2. Ohmura H, Hiraga A, et al: Risk factors for atrial fibrillation during racing in slow-finishing horses, *J Am Vet Med Assoc* 223:84, 2003.
3. Divers TJ, Byers DT: Equine cardiac disease, *Georgia Vet* 30:16, 1978.
4. Traub-Dargatz JL, Schlipf JW, et al: Ventricular tachycardia and myocardial dysfunction in a horse, *J Am Vet Med Assoc* 205:1569, 1994.
5. Sponseller BT, Ware WA: ECG of the month, *J Am Vet Med Assoc* 221:196, 2002.
6. Hines MT, Heidel JR, Barbee DD: Bacterial endocarditis with thrombus formation and abscessation in a horse, *Vet Radiol Ultrasound* 34:47, 1993.
7. Bonagura JD, Pipers FS: Echocardiographic features of aortic valve endocarditis in a dog, a cow, and a horse, *J Am Vet Med Assoc* 182:595, 1983.
8. Reef VB: Mitral valvular insufficiency associated with ruptured chordae tendineae in three foals, *J Am Vet Med Assoc* 191:329, 1987.
9. Ewart S, Brown C, et al: *Serratia marcescens* endocarditis in a horse, *J Am Vet Med Assoc* 200:961, 1992.
10. Worth LT, Reef VB: Pericarditis in horses: 18 cases (1986-1995), *J Am Vet Med Assoc* 212:248, 1998.
11. Bernard W, Reef VB, et al: Pericarditis in horses: six cases (1982-1986), *J Am Vet Med Assoc* 196:468, 1990.
12. Voros K, Felkai C, et al: Two-dimensional echocardiographically guided pericardiocentesis in a horse with traumatic pericarditis, *J Am Vet Med Assoc* 198:1953, 1991.
13. Dill SG, Simoncini DC, et al: Fibrinous pericarditis in the horse. *J Am Vet Med Assoc* 180:266, 1982.
14. Seahorn JL, Slovis NM, et al: Case-control study of factors associated with fibrinous pericarditis among horses in central Kentucky during spring 2001, *J Am Vet Med Assoc* 223:832, 2003.
15. Freestone JF, Thomas WP, et al: Idiopathic effusive pericarditis with tamponade in the horse, *Equine Vet J* 19:38, 1987.
16. Long MT, Foreman JH, et al: Hypertrophic osteopathy characterized by nuclear scintigraphy in a horse, *Vet Radiol Ultrasound* 34:289, 1993.
17. Marr CM, Reef VB, et al: Aortico-cardiac fistulas in seven horses, *Vet Radiol Ultrasound* 39:22, 1998.
18. Sleeper MM, Durando MM, et al: Aortic root disease in four horses, *J Am Vet Med Assoc* 219:491, 2001.
19. Derkson FJ, Reed SM, Hall CC: Aneurysm of the aortic arch and bicarotid trunk in a horse, *J Am Vet Med Assoc* 179:692, 1981.
20. Lester GD, Lombard CW, Ackerman N: Echocardiographic detection of a dissecting aortic root aneurysm in a Thoroughbred stallion, *Vet Radiol Ultrasound* 33:202, 1992.
21. Sage AM: Cardiac disease in the geriatric horse, *Vet Clin N Am Equine Pract* 18:575, 2002.
22. Dixon PM, Nicholls JR, et al: Chronic obstructive pulmonary disease: anatomical cardiac studies, *Equine Vet J* 14:80, 1982.
23. Sage A: Cardiac disease in the geriatric horse. *Vet Clin N Am Equine Pract* 18:575, 2002.

SECTION VII

The Abdomen



Chapter 41

Peritoneum and Peritoneal Cavity

PERITONEAL RADIOGRAPHY

Single-Target Protocol (STP)

Abbreviated sonographic examination of the peritoneal cavity for the express purpose of detecting and sampling fluid, also known as *focused assessment with sonography for trauma*, or FAST, was initially developed to detect hemoperitoneum in humans and was later modified for more general use in dogs.[1,2] Designed to rapidly examine four or more high-probability sites for the presence of fluid, this method appears to be applicable to horses, in particular those exhibiting signs of colic where peritonitis is suspected or requires exclusion. However, unlike with dogs and humans, the FAST protocol remains unproven in horses.

Peritonography (Celiography)

Abdominal contrast can be enhanced with the instillation of either gas or diagnostic iodine solution into the abdominal cavity, procedures termed *positive-* and *negative-contrast peritonography*, respectively.

Lloyd and co-workers reported the radiographic appearance of *negative contrast peritonography* in normal adult horses.[3] Using a pump, medical-grade carbon dioxide was gradually instilled into the abdomens of six standing horses until they began to show signs of discomfort (about 36 L). The animals were then radiographed (140 kVp and 40 mAs) and the carbon dioxide vented through the previously installed catheter and three-way stopcock.

The added carbon dioxide provided improved visceral clarity, but only in the dorsal part of the abdomen. Organs and tissues showing better contrast or detail included (1) the dorsal portions of the diaphragmatic crura, (2) the dorsal aspect of the gastric fundus, (3) both kidneys, (4) the dorsal and caudal margins of the spleen, and (5) the region of the mesenteric root. The appearance of the middle and ventral portions of the abdomen failed to improve. No harmful effects were observed.

The authors theorized that gas peritonography could improve the appearance of an excretory urogram or, when used in combination with angiography, aid in detecting lesions in the cranial mesenteric artery caused by *Strongylus vulgaris*.

Carbon dioxide was chosen over other gases because it offered the following advantages: it (1) is less flammable than oxygen, (2) is more quickly absorbed and eliminated than room air, and (3) has less potential for diffusion and gas trapping within the lumen of the colon than nitrogen.

Caution: *It is possible to accidentally perforate the intestine with the catheter used for insufflating the carbon dioxide, especially if the bowel is distended because of blockage.*

▮▮▮ PERITONITIS

Peritonitis associated with a large volume of pleural fluid can be radiographically detected in a small or medium-sized foal. The major radiographic observations are increased abdominal density and decreased visceral detail (Figure 41-1). If the foal is imaged while standing, the air-filled portions of the intestine will be situated dorsally as a result of *flotational effect*. If free air is present, one or more fluid levels may be evident.

Sonographically, peritonitis varies according to its etiology. Chemical peritonitis is usually associated with clear fluid, whereas the fluid found with bacterial peritonitis usually contains particulate matter. Fibrin tags often accompany chronic peritonitis of whatever cause.

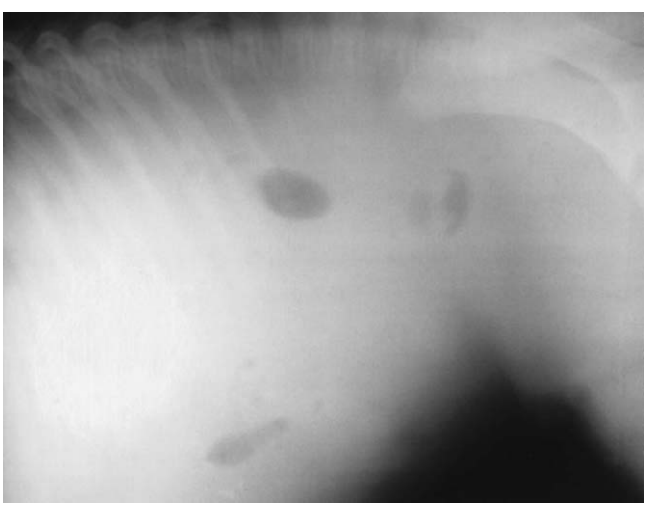


Figure 41-1 • Lateral abdominal radiograph of a colicky foal shows increased density and decreased detail characteristic of a large volume of peritoneal fluid, which in this case proved to be a chemical peritonitis resulting from a ruptured bladder.

▮▮▮ HEMOPERITONEUM

In its simplest form, hemoperitoneum is an expression of severe abdominal injury, such as a ruptured liver or spleen, but disease is rarely simple. Thus hemoperitoneum may be caused by a wide variety of abdominal disorders, including abdominal abscess, abdominal tumor, ruptured mesenteric aneurysm, or visceral torsion. In a foal, ruptured umbilical blood vessels are a prime consideration.

Green and co-workers reported hemoperitoneum caused by rupture of a juvenile granulosa cell tumor in a 12-hour-old Thoroughbred filly hospitalized for colic, depression, pale mucous membranes, and abdominal distension presumed to be the result of fluid.[4] Gatewood and co-workers reported a similar occurrence in a 9-year-old mare.[5]

▮▮▮ CHYLOPERITONEUM

May and co-workers reported chyloperitoneum in a 3-year-old miniature horse, presumably resulting from abdominal adhesions. Chyloperitoneum most often develops in newborn foals as a result of lymphatic dysplasia or congenital lymphangiectasia. Lymphangitis, both the necrotic and nonnecrotic forms, may be associated with a chylous peritoneal effusion. Intestinal obstruction usually leads to lymphatic obstruction, backup, and leakage. Chyloabdomen has also been reported in association with abdominal abscesses.[6] Hanselaer and Nyland reported the sonographic features of a large, multicompartmented mesenteric abscess in a 5-month-old American Saddlebred filly hospitalized for chyloperitoneum.[7]

▮▮▮ FREE ABDOMINAL AIR

The radiographic or sonographic detection of free peritoneal air is a most serious matter, one that should be treated as an emergency. The implications of such a finding, in the absence of a penetrating wound, are that an air-containing organ, such as the stomach or intestine, has perforated, for example, a gastric ulcer in a foal.

Free abdominal air is far easier to recognize radiographically than sonographically. Air may accumulate in various portions of the abdomen, signaling its presence by outlining adjacent viscera. Alternatively, small gas pockets may lie against the surface of one or more organs, creating distinctive crescent-shaped shadows rarely seen under other circumstances.

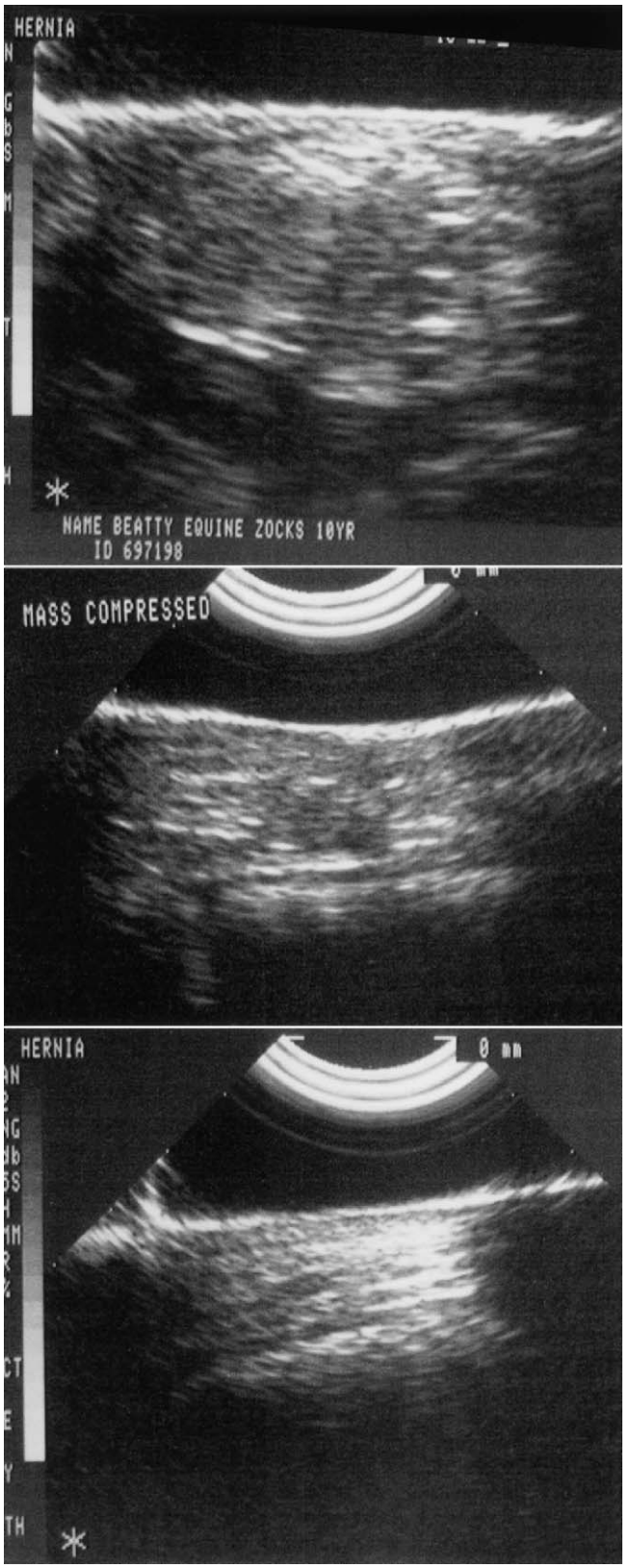


Figure 41-2 • Close-up cross-sectional sonogram of an umbilical hernia scanned first with only light pressure **(A)** and subsequently **(B)** with forceful pressure. In the lightly scanned image, the hernial content is plainly visible, appearing as a compressed oval of mixed echogenicity. In the second, forcefully scanned image, the abdominal wall appears nearly normal except for a small hypoechoic area centrally. A normal abdominal wall is provided for comparison **(C).**

▮▮▮ ABDOMINAL ABSCESS, TUMOR, ENCAPSULATED FOREIGN-BODY SPONGES

The radiographic detection of abdominal masses or mass effects is directly proportional to the size of the lesion and its density; location is of relatively less importance. The identification of an abnormal abdominal shadow may be direct or indirect. The concept of direct mass identification is straightforward and needs no explanation.

The Concepts of Direct and Indirect Mass Identification

Indirect mass identification is predicated on *inferring* the presence of a mass based on its presumed effect on its surroundings. The larger the mass or mass effect, the greater the likelihood it will affect its surroundings to the extent that it can be identified radiographically. For example, a large central abdominal mass or mass effect will displace or *clear* the adjacent viscera, especially the bowel, from the immediate area, which it is hoped would arouse the diagnostic suspicion of the viewer.

Abdominal fluid observed in association with abdominal tumors or abscesses can be sampled with ultrasound guidance, but these two potential sources can be difficult to distinguish from one another using only laboratory resources.[8]

▮▮▮ UMBILICAL HERNIA

Congenital umbilical hernias differ in sonographic appearance, in part because of the way they are scanned. For example, when only light pressure is placed on the surface of a hernia, its content is likely to remain just beneath the skin. Conversely, when a hernia is forcefully scanned, often in an attempt to obtain maximal skin contact, its content is often forced fully or partially back into the abdomen. Furthermore, forceful compression is likely to obscure the opening in the abdominal wall through which peritoneal content has passed, whatever its nature (Figure 41-2). The sonographic sequence of *appearance-disappearance-reappearance* is the hallmark of a reducible umbilical hernia.

References

1. Singh G, Arya N, et al: Role of ultrasonography in blunt abdominal trauma, *Injury* 28:667, 1997.
2. Boyson SR, Rozanski EA, et al: Evaluation of a focused assessment with sonography for trauma protocol to detect free abdominal fluid in dogs involved in motor vehicle accidents, *J Am Vet Med Assoc* 225:1198, 2004.
3. Lloyd KC, Kerr LY, et al: Negative contrast peritonography in the horse, *Vet Radiol* 30:28, 1989.

4. Green SL, Specht TE, et al: Hemoperitoneum caused by rupture of a juvenile granulosa cell tumor in an equine neonate, *J Am Vet Med Assoc* 193:1417, 1988.
5. Gatewood DM, Douglas JP, et al: Intra-abdominal hemorrhage associated with a granulosa-thecal cell neoplasm in a mare, *J Am Vet Med Assoc* 196:1827, 1990.
6. May KA, Cheramie HS, Prater DA: Chyloperitoneum and abdominal adhesions in a miniature horse, *J Am Vet Med Assoc* 215:676, 1999.
7. Hanselaer JR, Nyland TG: Chyloabdomen and ultrasonic detection of an intra-abdominal abscess in a foal, *J Am Vet Med Assoc* 183:1465, 1983.
8. Zicker SC, Wilson WD, Medearis I: Differentiation between intra-abdominal neoplasms and abscesses in horses, using clinical and laboratory data: 40 cases (1973-1988), *J Am Vet Med Assoc* 196:1130, 1990.

Chapter 42

The Gastrointestinal Tract

THE STANDARD GASTROINTESTINAL SERIES

In our hospital we radiograph only the abdomen of foals. Most can be imaged with one or at most two 14- by 17-inch films. All images are made with the foals in the erect position, if at all possible. I often use a horizontal x-ray beam to obtain a ventrodorsal view in foals that are unable to stand, which also allows for the assessment of intraluminal and extraluminal fluid levels, something that is not possible using a vertically directed beam.

SOME GENERAL CONSIDERATIONS

Decreased Fat Equals Decreased Detail

Foals, like all immature animals, possess little peritoneal fat and thus little intraabdominal contrast. What is visible for the most part are the portions of the stomach and bowel that contain gas. As might be expected, the distribution of fluid and gas within the stomach and intestine is individually quite variable; it is this variability that often renders abdominal examinations inconclusive, especially where obstruction is suspected.

Fluid Levels and Patient Positioning

Gastrointestinal fluid levels are a normal occurrence but are apparent only in *standing* images and require careful interpretation. In this latter regard, it is often wise to repeat any questionable film within a short time to see whether there have been any changes. Generally speaking, *a static bowel is potentially more serious than a dynamic one.*

Variations in the Stomach Related to Alternate-side Radiography

As described previously in dogs and cats, the positions of gas and fluid within the stomach are determined by a combination of *patient position* and *gravity.* In the *left lateral* position, fluid predictably drops in the *dependent* portions of the stomach—the fundus and left lateral aspect of the body—while air rises into the right lateral aspect of the body and antrum. When the right side of the animal is down, the situation is reversed, with the air moving to the left side and the fluid to the right.

ABDOMINAL TOPOGRAPHY

Stomach

The stomach occupies various amounts of the cranial half of the abdomen, depending on how full and thus how large it becomes. The stomach is composed for the most part of the *body,* with the far right and left sides containing the *pyloric antrum* and *fundus*, respectively. The pylorus is too small to visualize, but its probable location can sometimes be estimated, depending on what other parts of the stomach and duodenum are visible. It is a common mistake to refer to the antrum—the muscular portion of the stomach on the far right side of the body—as the pylorus.[1]

The Bowel Mass in General

Like most animals, horses have a bowel comprising three major elements: (1) the small intestine, (2) the cecum, and (3) the large intestine. The small intestine is quite lengthy (about 70 feet long in an adult) and arranged in a serpentine fashion; its diameter is similar throughout. It is entered cranially through the pylorus and exits caudally into the cecum. The capacity of the intestine is estimated to be between 40 and

50 L. For an overall radiographic perspective on the gastrointestinal tract of a young foal, see Figure 42-8.

Small Intestine

The small intestine is initially divided into two parts: a fixed portion, termed the *duodenum;* and a mesenteric portion, made up of the jejunum and ileum. The bulk of the small intestine normally resides in the *dorsal part of the left half of the abdomen* in close association with the small colon, but it is by no means confined to this location. For example, when the cecum is empty, parts of the small bowel may extend as far ventrally as the abdominal floor or as far laterally as the right flank. Thus *some degree of normal small intestinal displacement must be anticipated when assessing abdominal radiographs.*

Cecum

The cecum of the horse is made up of three parts: (1) a bulbous base, (2) an elongated body, and (3) an apex. Although relatively short (only about 4 feet long), the cecum has a large capacity (25 to 30 L), in large part because of its multiple rows of outpouchings, or haustra. Both its tapered and blunted extremities are blind, with sphincter-controlled entrance and exit openings (*ileocecal* and *cecocolic orifices*) situated side by side on the lesser curvature of the base. Most of the cecum lies on the floor of the abdomen, its body attached dorsolaterally to the first part of the colon by the *cecocolic fold*, its tapered end pointing cranially.

Large Intestine

The large intestine is divided into two parts: (1) a thick, double-looped, proximal part, the *large colon* (also referred to as the *great colon*); and a shorter, much smaller, distal segment, the *small colon.*

Large Colon. The dorsal and ventral portions of the large colon loosely resemble a partially inflated inner tube folded over on itself, with its convex surfaces facing the diaphragm. The two principal loops are divided into four sections according to their location within the abdomen: (1) *right dorsal colon,* (2) *left dorsal colon,* (3) *right ventral colon,* and (4) *left ventral colon.* There are also three designated curvatures, two cranially and one caudally, respectively named the (1) *diaphragmatic flexure,* (2) *sternal flexure,* and (3) *pelvic flexure.*

Small Colon (Descending Colon). The small colon appears insignificant compared with the anatomic grandeur of its larger "brother." As mentioned earlier, the small colon is often intermingled with the small intestine in the left upper part of the abdomen.

Rectum

The cranial half of the rectum, or the peritoneal portion, is little more than a continuation of the small colon. The caudal half of the rectum, situated in the retroperitoneum, normally contains a flask-shaped dilation termed the *ampulla recti.*

▮▮▮ BARIUM EXAMINATION

Gastroenterography

Barium, or better, barium and air combined, *may* be able to identify some intragastric lesions, depending on their size, shape, location, and contrast volume and concentration. The type and number of radiographic projections employed and the position of the animal while being radiographed also bear strongly on the likelihood of finding a particular kind of lesion. The probability of radiographically identifying any lesion in the stomach of a foal is much better than identifying a similar lesion in an adult.

Double-contrast examination of foals suspected of having gastric ulcers can *potentially* identify one or more of the following: (1) localized thickening or other wall deformities; (2) large and, less often, medium-sized ulcer craters; and (3) various types of filling defects.

If only the *location* of the stomach is being sought, so-called *barium marking* is adequate for the job, although a large volume of undiluted barium is required.

Campbell and co-workers described the technique and normal radiographic anatomy of gastrointestinal barium examination in young foals.[2] Using a commercial 30% wt/vol barium suspension, administered at 5 ml per kilogram of body weight, five normal foals were radiographed in the standing right lateral, recumbent right and left lateral, and ventrodorsal positions. Barium reached the large colon by 8 hours. Recumbent views were deemed superior to standing projections but not by a great deal. Pertinent radiographic findings are listed in the following section (Boxes 42-1 and 42-2).

Colonography

Fisher and Yarbrough described the technique and advantages of retrograde barium examination (colonography) in young colicky foals suspected of having obstruction.[3] Although both sensitivity and specificity were said to be 100 percent *(the perfect test),* the small number of animals examined (i.e., 25) probably makes such claims premature although certainly promising.

Technique. The following is a combination of Fisher and Yarbrough's technique and my own method of performing colonography in young foals suspected of having a large intestinal obstruction:

- Unless extremely weak, the foal should be sedated using drugs that have the least effect on intestinal motility.

Box 42-1
Salient Features of Barium Gastroenterography in Normal Foals

STOMACH

The stomach appeared larger in younger animals because of a smaller cecum and large colon. As the size of the cecum and large colon increased, they displaced the stomach dorsally.

The axis of the stomach was tipped cranioventrally in the standing lateral view, which falsely suggested a small liver.

On average, the height of the stomach was twice its craniocaudal width unless it was distended.

In right lateral recumbency, the pyloric antrum filled with barium; in left lateral position, the barium moved into the fundus.

DUODENUM

The duodenum could be identified only in the standing right lateral and ventrodorsal views immediately after the barium was given.

JEJUNUM AND ILEUM

The bowel mass was relatively evenly distributed on either side of the midline, and air-fluid levels were scant. The small intestine was rapidly opacified with barium but not beyond 3 hours.

CECUM

The cecum, characterized by its distinctive pleats (*haustra*) and often a basilar gas cap, became visible within 1 and 2 hr.

The cecocolic junction was seen most regularly in the recumbent right lateral view, but the ileocecal junction could not be identified consistently.

Superimposition of the cecum and ventral colon in the standing position often made for confusing imagery.

LARGE COLON

Colonic visibility was a function of size, which in turn was a function of age; in other words, the older the foal, the greater the likelihood of seeing the large colon. Sand or feed did not adversely affect visibility.

Like the cecum, the ventral part of the large colon contained haustra.

The right half of the large colon was seen best in the recumbent right lateral view; similarly, the left half was optimally projected with the left side down.

SMALL COLON AND RECTUM

Gas was often seen in the small colon and rectum, which were typically situated in the left caudal abdomen, described by the authors as "draped ventrally to the abdominal floor."

Fluid levels were present in foals less than 2 mo old.

Box 42-2
Barium Transit Times in Foals

STOMACH AND DUODENUM

The stomach and duodenum were best imaged immediately after giving barium.

Barium had disappeared from the stomach of most foals by 2 hr after contrast administration.

CECUM

Barium reached the cecum within 2 hr in all foals.

LARGE COLON

Colonic transit was faster in younger foals (10 to 12 days old) compared with older ones (60 to 70 days old).

In the younger foals, barium was observed in the transverse colon by 3 hr; in older foals, the contrast required at least 8 hr to be consistently seen in this location. Barium reached the transverse colon by 5 hr in one 42-day-old foal.

SMALL COLON

Barium had disappeared from the terminal bowel by 36 hr in the youngest foals but remained in some of the older animals for 48 hr or more.

- Lateral and ventrodorsal survey radiographs are made to ensure proper radiographic technique; a high-contrast image is preferable.
- With the foal on its back, a Bardex rectal catheter is inflated in the rectum sufficient to prevent barium leakage.
- Five hundred milliliters of gravity-fed commercial barium suspension is slowly instilled, and a ventrodorsal radiograph is made. The resultant image is assessed for abnormality. If a clear-cut blockage is identified, a lateral and *another ventrodorsal* radiograph are made, the latter to ensure that the blockage initially seen is genuine and has not changed in any significant way. If there is no change, the examination is concluded.
- If no sign of obstruction is identified, another 500 ml of barium is given, and the previous film sequence is repeated.
- This process continues until (1) an obstruction has been identified, (2) the desired portions of the colon have been assessed, or (3) barium begins to leak from the anus as a result of pressure-induced rectal distension and loosening of the catheter cuff.

Barium Flow Path. From the point of administration, that is, the rectum, barium travels the following route through the large intestine as seen in a ventrodorsal radiograph:

- Rectum
- Small colon (configured in a series of loops)
- Transverse colon
- Right dorsal colon
- Left dorsal colon
- Left ventral colon

Pneumogastrography

Dik and Kalsbeek described pneumogastrography in 3 normal and 23 abnormal horses.[4] The horses were examined after 24 hours without feed, without drugs, and in the standing position. Pneumogastrograms or

fluoroscopy or both identified gastric tumors and gastric parasites, and they served to distinguish gastric from perigastric masses. When one reads this account, it appears the authors relied heavily on fluoroscopy in addition to a very powerful, ceiling-suspended x-ray machine. In my experience, gastrointestinal studies in adult horses have for the most part been unrewarding.

▮▮▮ THE TERMINOLOGY OF GASTROINTESTINAL DISEASE

Some confusion exists regarding the precise meaning of many of the terms used to describe gastrointestinal disease in the horse. In an effort to alleviate this problem, I have listed the terms that I will subsequently use in this chapter, obviously my preferences, along with their definitions.

- *Ileus:* This term means *obstruction,* not excessive intestinal gas; it is typically inferred from radiographs based on intestinal dilation.
- *Obstructive Pattern:* An imprecise but clearly evocative clinical term describing an abnormal-appearing intestine, which, in the opinion of the observer, is obstructed.
- *Surgical or Nonsurgical Abdomen:* Highly subjective terms implying that a particular horse does or does not require surgery, based solely on radiographic appearances and, to a large extent, the opinion of the person interpreting the radiographs.
- *Intestinal Segment:* Preferred over the term *intestinal loop* because most areas of radiographic concern are not actually looped; rather, they are configured in a variety of forms, including straight lines. If a questionable bowel segment is actually looped or folded, then describe it as such; otherwise use the more general term, *intestinal segment.*
- *Segmental Dilation:* Dilation of a single bowel segment.
- *Regional Dilation:* Dilation of a single bowel region or section.
- *Generalized Dilation:* Dilation of most or the entire visible portion of the intestine.
- *Abnormal Bowel Distribution Pattern:* An abnormal intestinal arrangement.
- *Intestinal Displacement:* A specific displacement of some or most of the bowel.
- *Intestinal Entrapment:* A portion of the intestine that is abnormally situated and unable to move.
- *Intestinal Torsion:* Bowel that is abnormally twisted, usually in at least two locations. In most cases, the most serious implication of such disfiguration is the associated vascular obstruction, which if not relieved will eventually lead to bowel necrosis and perforation.
- *Intussusception:* The telescoping of one bowel segment into another. As with torsion, the associated vascular compromise is the most serious aspect of the condition.
- *Gastric or Intestinal Atony:* A noncontractile, relatively stationary stomach or bowel frequently associated with serious intestinal disorder or systemic disease. Also known as a *functional ileus* or a *static* or *fixed intestine.* Serial radiographs featuring one or more unchanging elements are required to substantiate gastric or intestinal atony.

▮▮▮ RADIOGRAPHIC APPEARANCE OF THE NORMAL STOMACH

The stomach is situated just behind the diaphragm, appearing as a vertically oriented, compressed oval. In a standing image, a fluid level frequently marks its location (Figure 42-1). If entirely fluid filled or empty, the stomach may be difficult or impossible to locate (Figure 42-2). When only small amounts of gas are present, the stomach may resemble the intestine. There is a great deal of variability.

▮▮▮ THE DILATED STOMACH

Normal Variation

The presence of mild to moderate gastric dilation in a young foal may or may not be diagnostically important. For example, I have often radiographed the abdomen of a colicky foal that initially showed gastric distension, but in progress films made later the same day, the stomach appeared normal. The point is that there is no way of knowing how long the stomach has been distended, nor how long it will persist—thus the enormous value in making progress films in such circumstances.

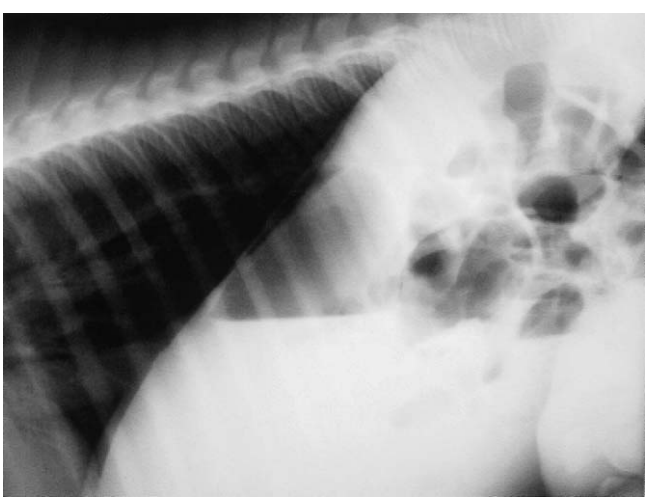


Figure 42-1 • Normal abdomen in a day-old foal in which the stomach (located immediately caudal to the diaphragm) appears as a dark half-circle, the result of a fluid level.

With regard to how large the stomach of a normal foal should appear, I have not found the published normal **2-to-1 ratio** (gastric height compared with gastric width) to be reliable, at least as far as employing it as the principal means of diagnosing gastric obstruction in a foal (although an abnormal ratio has some merit as supporting evidence).

Gastric Dilation Secondary to Mechanical Ventilation

Secondary gastric distension has been reported in association with mechanical ventilation in a foal, where an inadequately inflated fitted endotracheal tube leaked air into the throat, which eventually found its way to the stomach.

▮▮▮ GASTRIC ULCER

Foals

The disease most responsible for gastric dilation in older foals is gastric ulcer. In such cases, the distended stomach is usually filled with a combination of gas and fluid. If the ulcer is bleeding, a portion of the fluid will be blood. Depending on where and how the stomach is being obstructed, there may be gas in the biliary system of the liver. If *gastroesophageal reflux* is present, there may be *megaesophagus* and related *aspiration pneumonia*.

Phenylbutazone is known to cause gastric ulcers in the glandular portion of the stomach of foals. Traub and co-workers reported the radiographic appearance of experimentally induced gastric ulcers in foals between 3 and 10 months of age. Seen in double-contrast gastrograms, the ulcers appeared as either relatively discrete filling defects surrounded by barium or, alternatively, as small circular or oval-shaped barium accumulations.[5]



Figure 42-2 • Normal abdomen in a day-old foal in which the stomach (located immediately caudal to the diaphragm) is fluid filled and thus is indistinguishable from the adjacent liver.

Rebhun and Power described naturally occurring gastric ulcers in both foals and adult horses, reporting that such lesions may be incidental findings found at necropsy, or they may be the source of clinically evident disease.[6]

Gastric ulcers are not visible radiographically, nor can they be readily identified with diagnostic opaques (water-soluble diagnostic iodine solutions). Generally the best that can be hoped for is circumstantial evidence of the kind described previously.

Caution: *Do not use barium in an effort to detect gastric ulcers if there are signs of peritonitis or a pneumoperitoneum on survey radiographs, either of which suggests perforation.*

If an ulcer perforates, there are at least three potential consequences: (1) an omental seal may form with little or no leakage of stomach content; (2) a chemical or bacterial peritonitis may develop; or, (3) in the case of large, unsealed ulcers, a pneumoperitoneum may occur (Figure 42-3).

Adults

Gastric ulceration has been reported as a common occurrence in racehorses, with a prevalence range of 55 to 100 percent. Rabuffo and co-workers reported a prevalence rate of 87 percent in racing Standardbreds, with older castrated males at greatest risk.[7] As with foals, there are no lesion-specific radiographic disease indicators.

Obstructed Cardia (Gastric Inlet Obstruction)

Peterson and co-workers described the fluoroscopic appearance of an incomplete obstruction in the gastric cardia of an 11-year-old Morgan stallion, which also caused dilation of the adjacent esophagus. When barium was given, it temporarily pooled in the distal esophagus before spilling into the stomach in a manner resembling a *cascade stomach*, as described in people.[8]

Pyloric Stenosis (Gastric Outlet Obstruction)

Pyloric obstruction may be due to a variety of physical causes: congenital or acquired pyloric hypertrophy, feed impaction, pyloric ulceration with associated swelling, pyloric scarring secondary to ulceration, tumor, obstructive cholangitis, and foreign body (including some fruits and vegetables). Atony of the stomach results in stasis or "functional obstruction" but is not nearly as serious with respect to potential rupture. Proximal duodenal blockage is difficult or impossible to distinguish from pyloric obstruction. For an in-depth discussion on the treatment and diagnosis

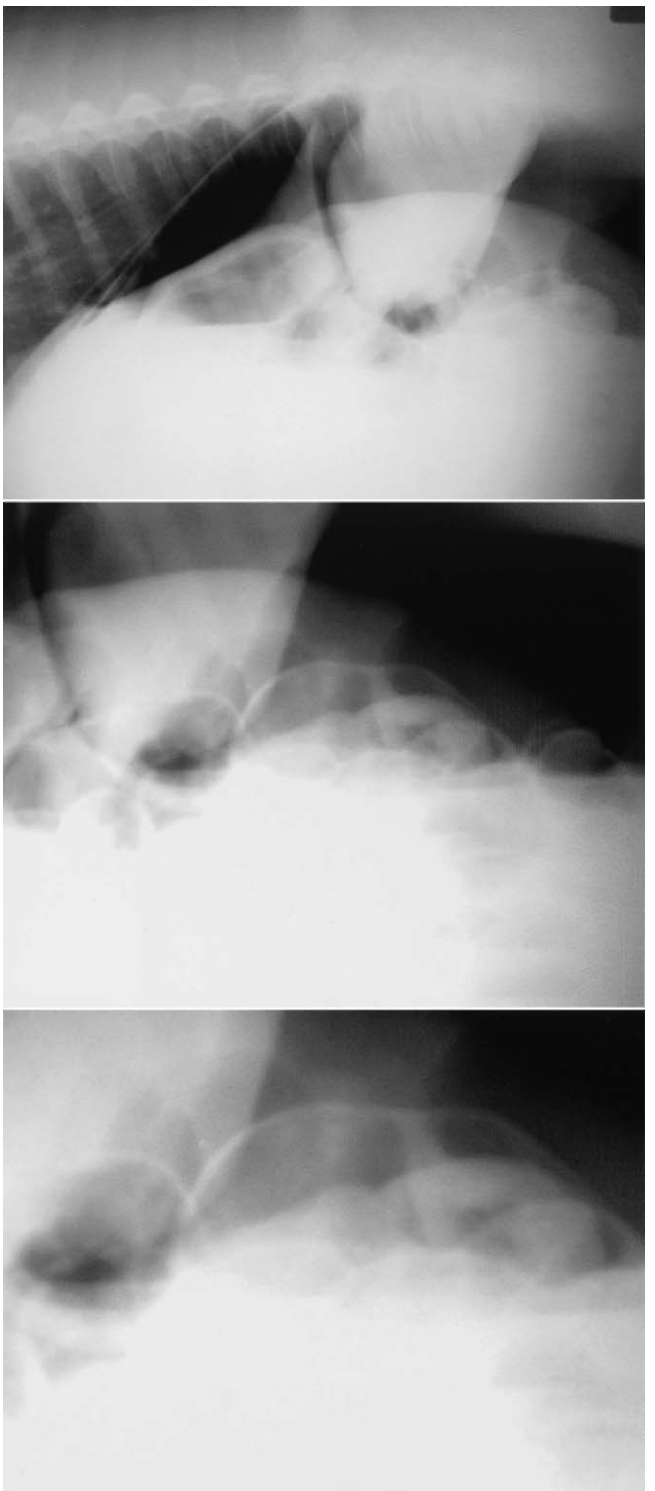


Figure 42-3 • Lateral view **(A)** of the craniodorsal abdomen of a young foal with a perforated stomach ulcer shows a large-volume pneumoperitoneum tracing portions of the cranial viscera, particularly the gas-filled intestine as seen in close **(B)** and ultra-close-up **(C)** views.

of pyloric ulcers in foals, I recommend the clinical case conference by Aronoff and discussants.[9]

Gastric enlargement is the only radiographic abnormality I have seen with this disorder, but it is an inconsistent, nonspecific finding. Gastrography is probably the easiest way to determine whether the stomach is capable of emptying, usually within an hour. If perforation or rupture is suspected, the barium should be replaced with a diagnostic iodine solution, keeping in mind that most such contrast media are hyperosmolar and will result in a transient but substantial fluid shift into the stomach.

▮▮▮ GASTRIC TUMOR

Tennant and co-workers reported six cases of squamous cell carcinoma of the stomach of the horse.[10] Aronoff and co-workers reported a gastric squamous carcinoma in a 20-year-old gelding. Thanks to a large volume of air in the stomach and the size and dorsal location of the tumor, it was possible to make a tentative diagnosis from plain films.

Gardiner and co-workers reported a leiomyosarcoma in a 12-year-old Thoroughbred gelding hospitalized because of chronic weight loss and inappetence. Neither sonography nor radiography was able to provide a diagnosis. At necropsy an invasive leiomyosarcoma was found in the caudal portion of the thoracic esophagus, the abdominal esophagus, the stomach, and the adjacent surface of the liver.[11]

Leiomyoma and leiomyosarcoma occur most commonly in the large and small intestine rather than in the stomach or esophagus of horses. Other abdominal tumors causing weight loss include lymphosarcoma, malignant melanoma, granulosa cell tumor, and transitional cell carcinoma.

▮▮▮ TRANSFORMATIVE GASTRIC FOREIGN BODIES

Persimmon Obstruction

Ripe persimmons undergo an unusual, and potentially dangerous, transformation once within the gastrointestinal tract.[12] Specifically, persimmons undergo a hardening process, initiated by a polymerization of tannin and followed by coagulation once the fruity mass becomes saturated by stomach acid. The resultant coagulum then progressively hardens as it slowly reacts with cellulose, hemicellulose, and protein.

Gastric Rupture

Gastric rupture is usually fatal as a result of septic peritonitis and related shock, although survival has been reported.[13] Kiper and co-workers described gastric rupture in 50 horses.[14] No association was found between gastric rupture and any of the following

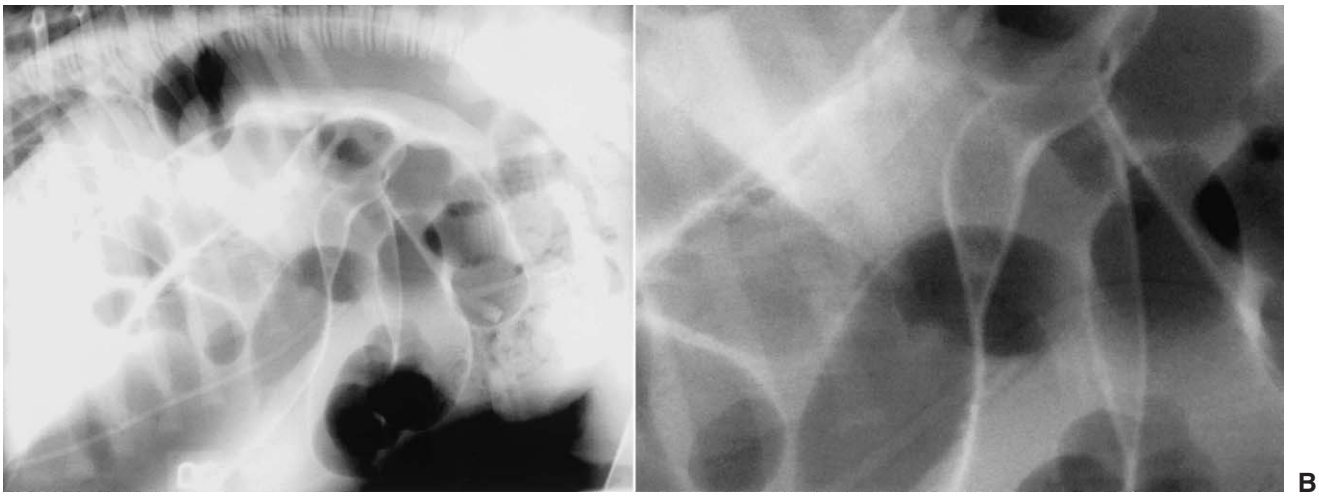


Figure 42-4 • Lateral **(A)** and lateral close-up **(B)** views of the abdomen of a foal with a torsed stomach show much of the intestine outlined by air as a result of a large-volume pneumoperitoneum caused by gas leaked from a ruptured stomach.

factors: time of year, age, gender, and breed. Other than perhaps the severity and rapidity of the resultant illness, there was nothing to distinguish a ruptured stomach from a perforated intestine.

To date, all the foals I have seen with ruptured stomachs have had a large-volume pneumothorax as identified in abdominal radiographs and a large volume of peritoneal fluid as seen sonographically. Most also have intestinal dilation and atony as determined by a minimally changing or static bowel pattern over an 8- to 12-hour period.

▮▮▮ GASTRIC TORSION

The true incidence of gastric torsion in foals and horses is not known. As in dogs with twisted stomachs, equine torsions lead initially to blockages of the cardia and pylorus, but also to serious vascular compromise, which is of even greater pathophysiologic significance.

Radiographically, the appearance of a torsed stomach depends on its size, its shape and position, and its physical influence on the nearby viscera, in particular the intestine. A typical scenario unfolds as follows: the stomach rotates on its long axis, blocking its entrance and exit, in the process creating a closed compartment. Through a combination of events—the accumulation of internal secretions such as stomach acids and massive transudation resulting from vascular strangulation—the stomach swells, displacing the adjacent viscera caudally. Because of its gas content, the displaced bowel mass is usually most evident.

The stomach, because it has been deprived of much or all of its blood supply, slowly begins to die: anoxia, ischemia, and finally necrosis, eventually resulting in one or more perforations, which in turn leads to chemical and bacterial peritonitis. Perforation also allows gas to escape the stomach and accumulate in the abdominal cavity. Depending on the volume of pneumoperitoneum, the exterior surfaces of portions of the bowel (as well as other organs) may become visible (Figure 42-4).



Figure 42-5 • Lateral thoracic view of the foal shown in Figure 42-4 shows an opaque stomach tube extending no farther than the diaphragm because of secondary esophageal obstruction.

As an initial test of the patency of the cardia, an opaque stomach tube can be passed and a full-length lateral radiograph made to determine whether the tube enters the stomach (Figure 42-5). If it does, or appears to do so, then this should be verified with an injection of a small amount of water-soluble diagnostic opaque. Great care must be taken not to force the tube once resistance is encountered; otherwise, the esophagus may be punctured.

▮▮▮ RADIOGRAPHIC APPEARANCE OF THE NORMAL SMALL INTESTINE

There is no single radiographic appearance that depicts a normal intestine in a foal. Rather, there are a variety of appearances, which are for the most part variations on a single radiographic theme. Accordingly, diagnosis must be of a cautious nature, particularly when attempting to diagnose intestinal obstruction.

The Dilated Small Intestine

Small intestinal disorders are estimated to account for about half of all cases of colic, with about 70 percent of these being strangulating lesions, 40 percent of which involve the ileum.[15] Armed with such knowledge, it is not surprising that intestinal distension is considered by many to be the gold standard of small intestinal obstruction of whatever cause.

In my opinion, nothing could be farther from the truth. Colicky foals usually feature some degree of fluid or gaseous bowel distension, which is frequently of a *highly labile* nature, changing from day to day (Figure 42-6) and sometimes hour-by-hour (Figure 42-7). Thus there are few radiographic appearances that consistently and reliably portray an obstructive bowel pattern.

Small Intestinal Radiometrics

As with dogs and cats, efforts have been made to diagnose abnormal small intestinal dilation in horses by comparing the suspicious intestinal segment to the

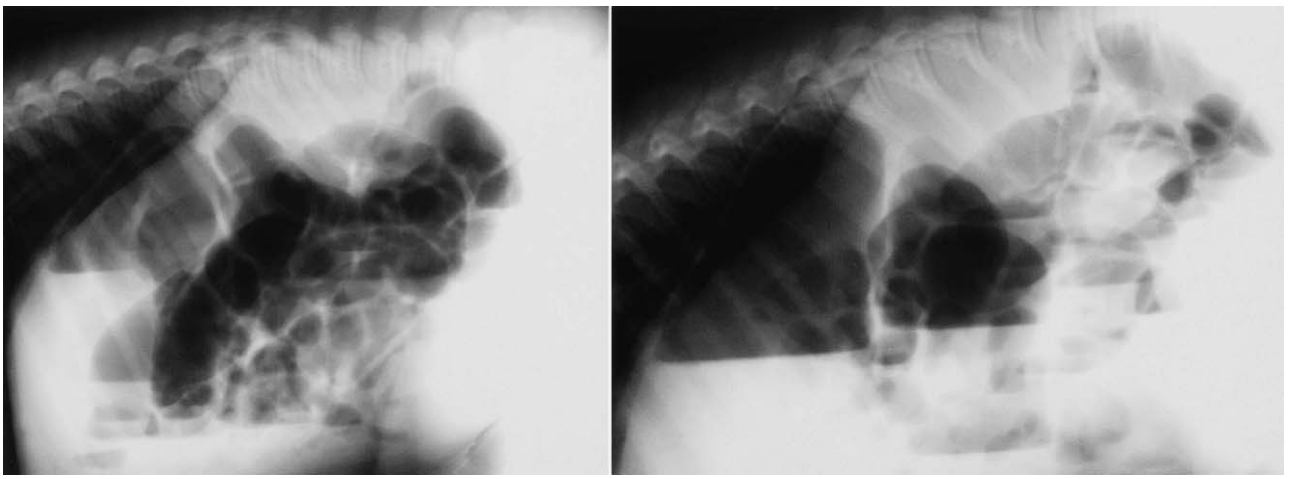


Figure 42-6 • A, Lateral abdominal image of a colicky foal shows mild to moderate intestinal distension cranially with a small amount of air and fluid in the stomach. **B,** A day later, the appearance of the gastrointestinal tract has changed decidedly, featuring a greater amount of air and fluid in the stomach. Note the fluid level and much less bowel gas. The foal fully recovered by the following day.

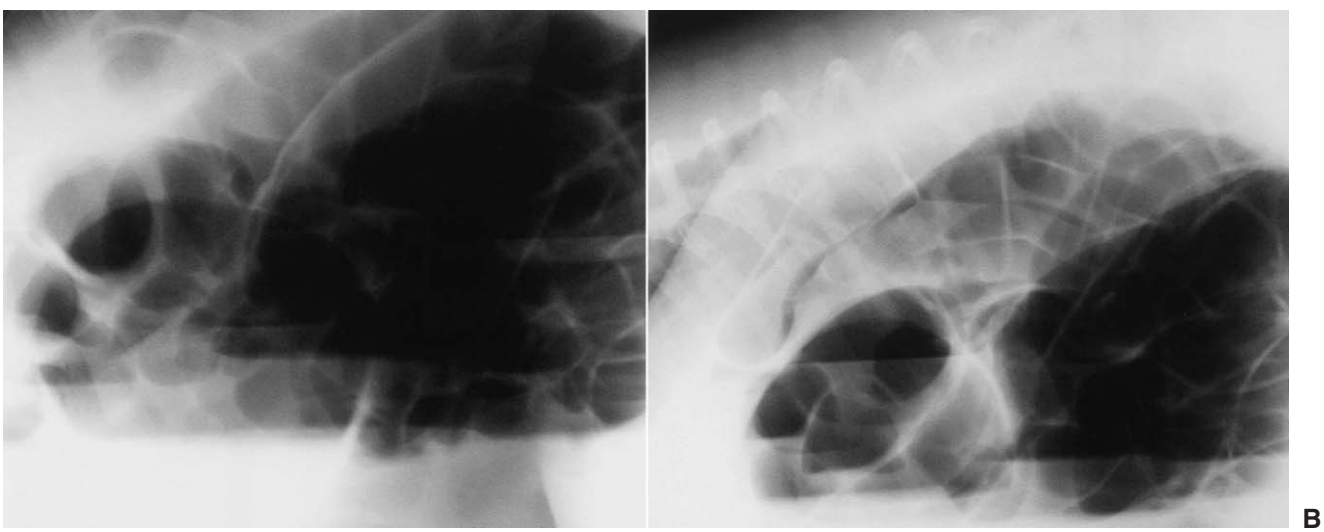


Figure 42-7 • Close-up lateral abdominal images of a 3-week-old colicky foal made 30 minutes apart: the initial film **(A)** shows an air-distended small and large intestinal fluid level; the second image **(B)** reveals less distension and a different distribution. The foal fully recovered with only supportive treatment.

length of a specific lumbar vertebra. In this regard, Fischer determined that the normal small intestinal diameter should not exceed *1.1 times the length of the first lumbar vertebra* (L1).

Measurements notwithstanding, it is probably true that the greater the degree of small intestinal distension, especially when it reaches the point of being indistinguishable from the large colon, the greater the probability of a significant blockage, a view strongly supported by Fischer and co-workers in their report on radiographic diagnosis of gastrointestinal disorders in foals.[16]

Sources of Small Intestinal Dilation

There are many sources of small intestinal dilation; normal variation and enteritis are the most common. The small intestine often appears radiographically dilated with unrelated pulmonary diseases such as pneumonia (Figure 42-8) or respiratory distress syndrome. Diseases reported to be associated with moderate to severe intestinal dilation include those listed in Box 42-3.

Diagnostic Axiom: *Strictly on a probability basis, excessive abdominal gas in foals is more likely to be abnormal than not; and, if accompanied by distension, it is more likely to be the result of obstruction (mechanical or functional) than enteritis.*

Small Intestinal Fluid Levels: How Many Is Too Many?

In a standing lateral or decubital radiograph of a foal's abdomen, fluid levels are the single most outstanding feature. Attempting to capitalize on this fact, some authors, apparently influenced by similar speculation

Box 42-3
Disorders Associated With Moderate to Severe Small Intestinal Dilation

- Intestinal foreign body (e.g., enterolith, fecalith)
- Congenital malformation of the intestine (e.g., atresia coli, atresia ani)
- Intestinal impaction (meconium impaction in foals)
- Proximal intestinal ulcer
- Intestinal and paraintestinal abscess
- Intestinal tumor
- Intestinal entrapment (incarceration) (e.g., by mesodiverticular band or gastrosplenic ligament)
- Intestinal volvulus
- Mesenteric thrombosis
- Intestinal adhesion (often postsurgical)
- Intestinal agangliosis
- Serious bacterial enteritis *(Clostridia, Salmonella)*
- Moderate to severe peritonitis (functional ileus)
- Diaphragmatic hernia with intestinal displacement
- Secondary intestinal atony related to any of the above disorders

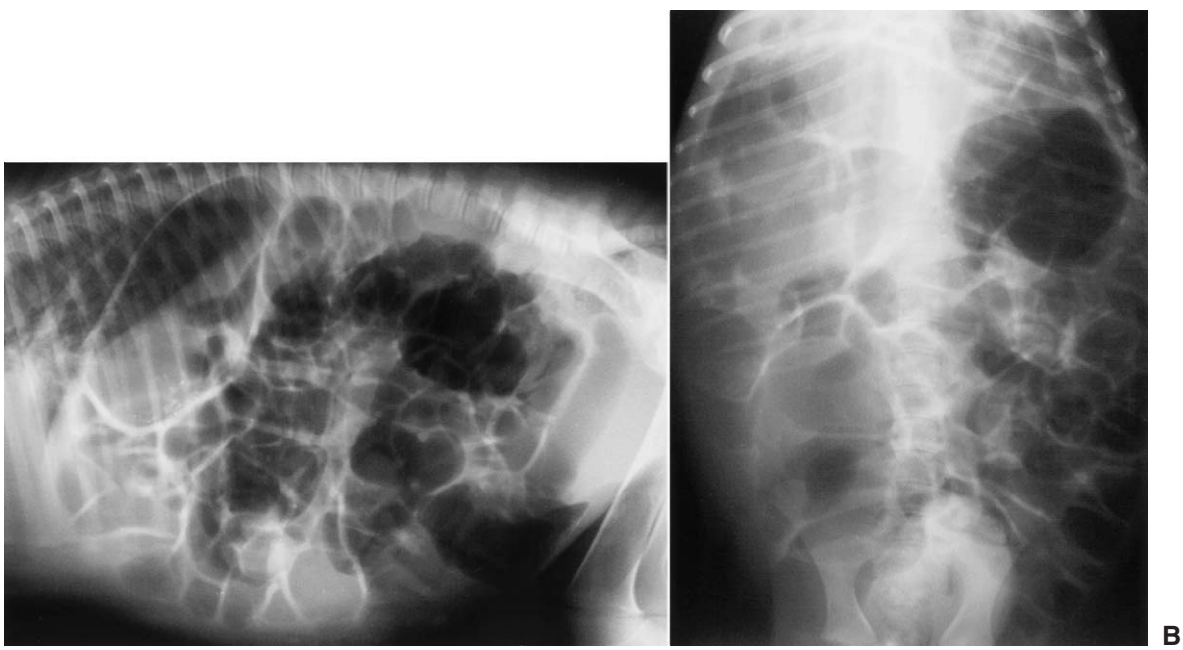


Figure 42-8 • Lateral **(A)** and ventrodorsal **(B)** abdominal images of a seriously ill pneumonic foal show gaseous distension of the entire gastrointestinal tract as the result of secondary atony. The foal eventually recovered.

in people and dogs, have tried to relate the *number* of visible fluid levels to the probability of intestinal obstruction.[17] To my knowledge, no specific cutoff point has been determined. Others have suggested that when multiple fluid levels lie at the *same height*, the probability of obstruction is greater than if they are unevenly distributed. In my experience, neither of these diagnostic predictors has proven consistently reliable (Figure 42-9).

Consequences of Small Intestinal Dilation

Severe or prolonged small intestinal dilation can lead to transudation and eventually to bacterial and chemical peritonitis. Under such circumstances (as well as others), small gas bubbles may accumulate in the intestinal wall, a condition termed *pneumatosis intestinalis.*

Prolonged dilation also causes varying degrees of vascular and lymphatic stasis, functional blockages that in turn can lead to intestinal anoxia, ischemia, and ultimately necrosis.

Severe enteritis also may adversely affect the normal balance between intestinal absorption and secretion, leading to a net fluid loss and, in the process, further intestinal distension.

Small Intestinal Intussusception

Although a consistent association between enteritis and intussusception has long been sought, as far as I am aware, none has yet been found. This contradicts the widely held belief among veterinarians that intestinal intussusception is caused by an inflamed, hyperactive bowel. Two other possibilities mentioned in the literature include general anesthesia and drugs that increase intestinal motility, although they too are unproven.

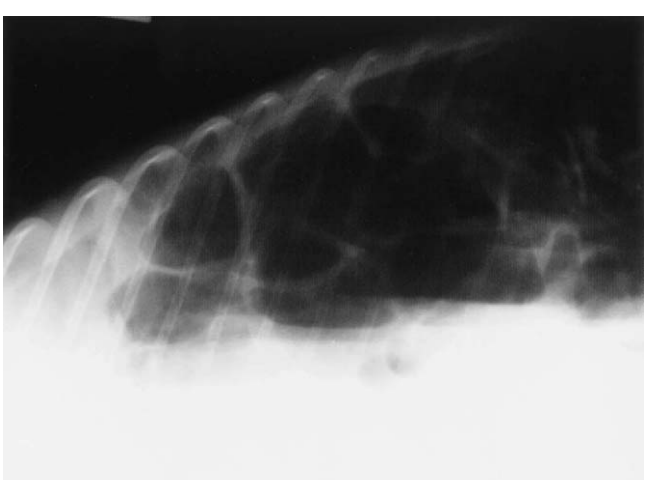


Figure 42-9 • Decubital view of the abdomen of a colicky foal shows multiple small and large intestinal fluid levels, most of which lie along the same line. The foal was treated supportively and discharged 2 days later.

Although theoretically possible, I have not been able to consistently diagnose intussusception in foals using plain films. However, others and I have sonographically diagnosed intussusception. Small intestinal intussusception in foals appears as it does in pet animals: *concentric rings* or *cylinders,* depending on whether the affected bowel is being scanned in cross section or in long section. Theoretically, in a recently formed intussusception, the adjacent bowel should appear distended and hypermotile, whereas in a chronic intussusception, the bowel would more likely appear atonic.

Depending on how proximal the obstruction is, the stomach may also appear distended. The presence of peritoneal fluid suggests intestinal transudation and possibly peritonitis. A pneumoperitoneum suggests related intestinal perforation and occasionally traumatic perforation of the abdominal portion of the esophagus or stomach by a feeding tube.

▮▮▮ RADIOGRAPHIC APPEARANCE OF THE NORMAL CECUM AND COLON

Dilated Cecum and Colon

Colonic torsion is rare in young foals and, when present, is difficult or impossible to distinguish from other forms of large colon disease.

Radiology of Nonobstructive Colic in Foals

Clearly, nonobstructive colic in foals lacks any sort of signature appearance, although some might argue otherwise, particularly with respect to gaseous distension of the bowel.

▮▮▮ INTESTINAL OBSTRUCTION

Mechanical obstruction, regardless of the species in which it is found, is usually accompanied by intestinal distension. Unfortunately, from a diagnostic perspective, distension may also be found with a wide variety of nonobstructive disorders, including some forms of enteritis. Intestinal atony, also known as *paralytic or functional ileus,* may be difficult or impossible to differentiate radiographically from a physical blockage of the bowel.

Breeds reported to be at increased risk for small colon obstruction include Arabians, ponies, and American miniature horses[18] (Box 42-4).

Radiographic Disease Indicators of Mechanical Intestinal Obstruction in Foals and Adult Horses

Distension of the small intestine is the radiographic hallmark of intestinal obstruction, although, as mentioned previously, it may also be found with non-

obstructive bowel disease. The large bowel may or may not be distended with small intestinal obstruction, depending on where and how the small bowel is blocked. In general, the longer an obstruction exists, the more extensive the distension. In some instances, the small bowel may become so distended that it resembles the colon.

Fisher and Yarbrough proposed comparing the diameter of a suspicious small intestinal segment (as seen radiographically) with the length of the first lumbar vertebra (L1). If the diameter of the bowel is greater than 1.1 times the length of L1, it is considered distended (but not necessarily obstructed).[19] In my experience, measurements of this sort, termed *radiometrics*, are most reliable in identifying marked intestinal distention (Figure 42-10), but they often fall short when it comes to lesser degrees of enlargement. A similar comparative measurement has been used with mixed success in dogs and cats.

Once obstructed, the intestine reflexively and persistently attempts to move its contents beyond the point of blockage, eventually becoming fatigued and dilated. In addition to losing its peristaltic capacity, the obstructed bowel also ceases its mixing and pendular activity. The resultant atony leads often leads to a near-complete stasis of the bowel as depicted radiographically by a minimally changing bowel pattern as seen in two or more sequential radiographs (Figure 42-11).

The radiographic disease indicators and causes of intestinal obstruction and atony in foals and adult horses are summarized in Boxes 42-5 through 42-11.

Box 42-4
Causes of Intestinal Obstruction in Foals

Single or multiple intestinal foreign bodies
Intestinal impaction (especially meconium)
Intestinal entrapment (intestinal incarceration)
Intestinal strangulation (intestinal volvulus, mesenteric volvulus)
Intussusception
Congenitally incomplete intestine
Congenitally interrupted intestine

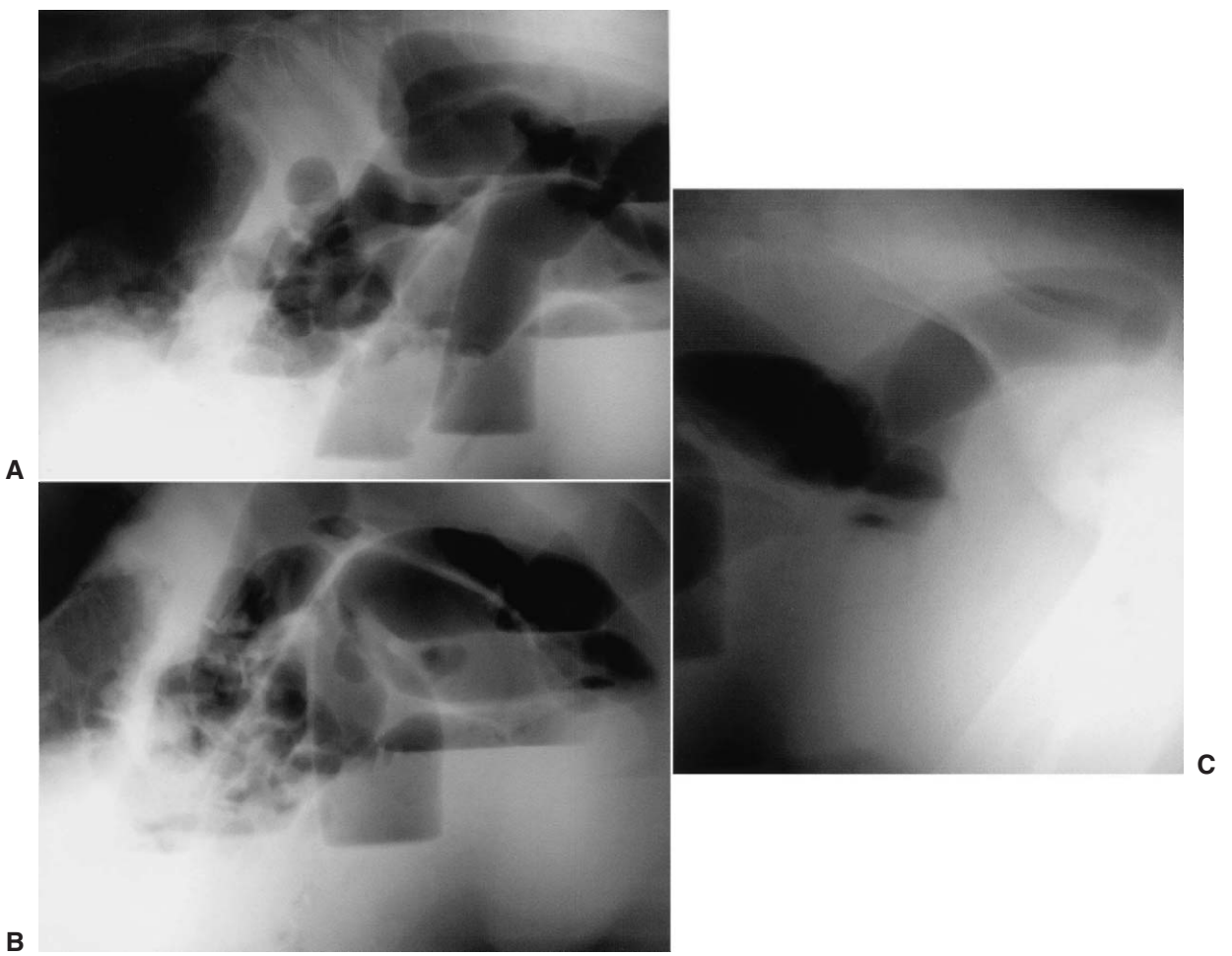


Figure 42-10 • Close **(A)** and ultra-close-up **(B)** views of an entrapped small intestine in a foal show multiple fluid levels within a markedly distended small intestine. A third close-up view **(C)** shows a dilated small intestinal segment looped into the abdomen.



Figure 42-11 • Lateral abdominal radiograph of a colicky foal with a meconium impaction shows gaseous distension of portions of both the large and small intestines. The appearance persisted in progress films until the blockage was relieved.

Box 42-5
Radiographic Disease Indicators (RDIs) of Intestinal Obstruction in Foals

Small intestinal distension
Large intestinal distension
Intestinal atony
Intestinal stasis
Abrupt change in intestinal diameter

Box 42-6
Causes of Intestinal Atony in Foals

Intestinal trauma
Peritonitis
Systemic infection
Intestinal fatigue following prolonged colic
Mesenteric infarction
Some forms of severe enteritis (necrotizing enteritis, ulcerative or necrotizing colitis)
Intestinal wall infection (inferred from the presence of gas bubbles in the intestinal wall, *pneumatosis intestinalis*)

Box 42-7
Radiographic Disease Indicators (RDIs) of Atony in Foals

Generalized intestinal distension
Regional intestinal distension gradually becoming generalized
Regional intestinal distension rapidly becoming generalized
Many fluid levels that fail to change in subsequent examinations

Box 42-8
Causes of Intestinal Obstruction in Foals

Single or multiple intestinal foreign bodies
Intestinal impaction (especially meconium)
Intestinal entrapment (intestinal incarceration)
Intestinal strangulation (intestinal volvulus)
Intussusception
Congenitally incomplete intestine
Congenitally interrupted intestine

Box 42-9
Radiographic Disease Indicators (RDI) of Intestinal Obstruction in Adult Horses

Small intestinal distension
Large intestinal distension
Intestinal atony
Intestinal stasis
Abrupt change in intestinal diameter
Visible enterolith

Box 42-10
Causes of Intestinal Atony in Adult Horses

Severe trauma
Systemic infection
Intestinal fatigue following prolonged colic
Mesenteric infarction secondary to endocarditis
Some forms of severe enteritis

Box 42-11
Radiographic Disease Indicators (RDIs) of Atony in Adult Horses

Generalized intestinal distension
Regional intestinal distention gradually becoming generalized
Regional intestinal distention rapidly becoming generalized
Many fluid levels that fail to change in subsequent examinations

From Orsini JA: Abdominal surgery in foals, *Vet Clin N Am Equine Pract* 13:393, 1997.

Box 42-12
Causes of Small Intestinal Strangulation in Horses

Pedunculated lipomas
Epiploic foramen entrapment
Volvulus
Internal herniation
Adhesions
Diaphragmatic hernia
Inguinal hernia
Scrotal hernia
Umbilical hernia
Intussusception

Box 42-13
Sonographic Findings Found With Intestinal Obstruction Caused by Strangulating Pedunculated Lipoma

Variable amount of fluid-distended intestine
Involved bowel has thickened wall due to edema
Affected bowel fails to contract, and thus content appears static (intestinal stagnation)
An abnormal amount of peritoneal fluid is present

Strangulating Obstruction of the Small Intestine

Strangulating small intestinal obstructions not only block the intestinal lumen but also obstruct the associated vasculature, leading to intestinal anoxia and ischemia and, if unrelieved, bowel necrosis and perforation.

Causes of Small Intestinal Strangulation

Mair and Edwards described the causes and consequences of strangulating obstructions of the small intestine (Box 42-12).[21]

Gayle described strangulation of the small intestine in 15 horses caused by mesenteric tears.[22] Fatalities were associated with three occurrences: (1) lengthy sections of trapped bowel, (2) the inability to relieve the entrapment, and (3) associated bleeding. Moll and co-workers reported strangulation of the small intestine in 14- and 20-year-old geldings by components of the spermatic cord.[23]

Vascular Intestinal Injury

Reperfusion Injury. *Intestinal reperfusion injury* refers to the damage that occurs to strangulated bowel *following* surgical relief, injury that is presumably related to restoration of blood flow. It is estimated that up to 25 percent of horses sustain such an injury, an injury that hinders reepithelialization of the intestinal lining and potentially allows bacteria and endotoxins access to the systemic circulation.

Blikslager and co-workers studied the relative importance of intestinal reperfusion injury in the horse, particularly with respect to the amount of xanthine oxidase and neutrophils contained within the microvascularity of the intestinal epithelium combined with low-flow ischemia. They concluded that reperfusion injury is of genuine concern and is potentially treatable.[24]

Thrombosis and Intestinal Infarction. White described 18 horses with intestinal infarction resulting from cranial mesenteric arterial thrombosis but without intestinal strangulation, a condition also termed *thromboembolic colic*.[25-27] Minimal distension of the small intestine in most of these cases (verified at surgery) suggested that the absence of radiographic or sonographic intestinal enlargement—common in strangulating lesions—may serve to distinguish one disorder from the other.

▮▮▮ PEDUNCULATED LIPOMAS

Edwards and Proudman reported the clinical features of intestinal obstruction caused by lipomas in 75 horses.[28] Templer and co-workers described the sonographic findings associated with jejunal obstruction caused by a strangulating lipoma in a mare (Box 42-13).[29]

▮▮▮ ILEOCECAL INTUSSUSCEPTION

Ford and co-workers reported the clinical features and surgical outcome of ileocecal intussusception in 26 horses.[30] Two types of ileocecal intussception were described: acute and chronic. Most of the horses were young. Those with the acute form of the disease had severe abdominal pain over some part of the previous 24 hours; those with the chronic form suffered from a less painful, episodic type of colic for three or more weeks. On average, the acute lesions were longer and more easily reduced than the chronic ones.

Radiographically, ileocolic intussusceptions are difficult or impossible to identify as such but occasionally may be suggested by an abnormal bowel distribution pattern or area of intestinal clearance. Sonographically, ileocecal intussusceptions, like intestinal intussusceptions elsewhere, are typically characterized by concentric, alternating light and dark rings, or so-called *target lesions*.[31]

▮▮▮ CECOCOLIC INTUSSUSCEPTION

Gaughan and Hackett reported 11 cases of equine cecocolic intussusception in a group of 842 horses undergoing exploratory surgery for colic.[32] Ileocecocolic intussusception was also reported as a postsurgical complication in a 4-year-old Thoroughbred.[33]

▮▮▮ COMBINED CECAL/LARGE COLON VOLVULUS

Ross and Bayha reported a rare case of combined cecal/large colon volvulus in a 2-year-old Standardbred colt; at surgery this volvulus was attributed to multiple mesenteric defects.[34]

▮▮▮ COLONIC INTUSSUSCEPTION

Large-colon intussusception is rare in horses.[35] When intussusceptions do occur, they have no specific radiographic disease indicators, but they may cause sufficient backup of intestinal gas and fluid that obstruction is suggested. A visible mass is rarely present.

Colonography is capable of demonstrating a colonic intussusception in the form of a unique accumulation of barium situated between the two involved bowel segments and intervening mesentery, termed a *coiled spring sign*.

Sonographically, the situation is far different: a highly characteristic *concentric circle lesion* is created by the telescoping of one bowel segment into another, as viewed in cross-section.

▮▮▮ COLITIS

Ultrasound

Jones and co-workers reported the sonographic appearance of right dorsal colitis in five horses.[36] The major sonographic abnormality was hypoechoic thickening of the intestinal wall as observed through the right 11th, 12th, and 13th intercostal spaces. The diseased dorsal colon was about three times thicker than the normal bowel (in round numbers, about 1.5 cm compared with 0.5 cm). The thickened, hypoechoic appearance of the bowel was thought to be due to submucosal edema, accumulation of inflammatory cells, and granulation tissue.

There have been numerous reports of intestinal disease in horses causing subclinical or overt disseminated intravascular coagulation.[37-39]

Ulcerative Colitis

East and co-workers reported the use of radioisotope-labeled leukocytes to aid in the diagnosis of ulcerative colitis in two horses.[40]

▮▮▮ INTESTINAL ULTRASOUND

Normal Duodenum

Kirberger and Van Den Berg reported the sonographic appearance of the normal duodenum in the adult horse.[41] The duodenum was consistently identified in the right 16th and 17th intercostal spaces, ventral to the right kidney, traveling along an imaginary line connecting the olecranon and sacral tuberosity. The duodenal wall was 3 to 4 mm thick and featured five distinct layers (from inside out): (1) mucosal surface, (2) mucosa, (3) submucosa, (4) muscle, and (5) serosa. Contractions were observed periodically; luminal content varied with diet and when the animal had last eaten.

Enteroliths

Enteroliths, of whatever composition, may or may not cause pain and discomfort, largely depending on their capacity to obstruct the bowel. Even when enteroliths do cause colic, it is less severe than intestinal pain caused by other causes, although it is likely to last longer.[42]

Using x-ray diffraction, Blue and Wittkopp described the chemical composition of a group of enteroliths obtained from the intestinal tracts of 11 horses suffering from colonic obstruction or perforation. Most were composed of ammonium magnesium phosphate. Enteroliths of similar composition were also obtained from a farm with a history of enterolith obstruction and well water high in magnesium content.[43]

In an interesting historical aside, the authors pointed out that the word *bezoar* was derived from the Persian word *padzahr*, meaning "antipoison," coined during the Middle Ages when enteroliths were kept as charms and remedies against disease or used as drinking vessels.

Peloso and co-workers reported the radiographic appearance of an enterolith in an 11-month-old miniature horse. Surgery and later necropsy confirmed the presence of an enterolith in the proximal part of the small colon. Subsequent chemical analysis showed the stone to be composed primarily of magnesium phosphate.[44]

In my experience, enteroliths are often difficult to locate precisely with either radiography or ultrasound in anything but young foals. Even when isolated bowel specimens containing multiple enteroliths are radiographed, it can be hard to distinguish stones from high-density stools (Figure 42-12). Intestinal dilation is often quite variable. Barium examination following earlier plain-film identification often reveals only partial (as opposed to complete) obstruction. A medium-sized enterolith is shown in Figure 42-13.

Fecaliths and Fecalith Impaction. Fecaliths are often attributed to excessively coarse, high-bulk, difficult-to-digest grass or feed and typically cause blockage of the small colon.[45] McClure and co-workers reported the plain-film appearance of fecalith impaction of the small colon in two miniature foals.[46] Those were radiographed, and all exhibited some degree of intestinal dilation, although there was no consistent pattern or any clear indication as to the specific nature of the animal's colic.

Foreign Material Impaction

Boles and Kohn reported on a variety of foreign materials that can lead to impaction of the small colon in young horses, including fabric, cord, rope, and rubber, typically bound up with ingesta.[47]

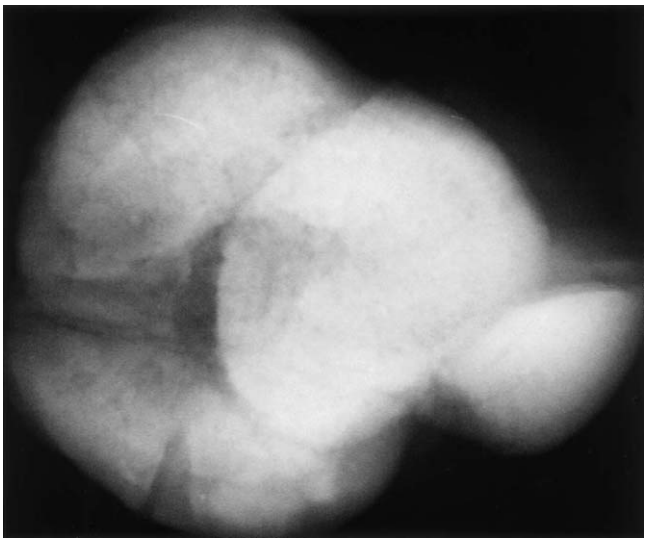


Figure 42-12 • A surgically removed segment of necrotic intestine containing multiple enteroliths.



Figure 42-13 • A resident demonstrates an enterolith she recently removed from an adult horse.

Nephrosplenic Entrapment of the Large Colon

The task of medical imaging in confirming a presumptive diagnosis of nephrosplenic entrapment typically falls to ultrasound rather than radiography. Where surgical correction is required, usually only a single preoperative examination is required; however, when postural manipulation or "rolling" is performed, a second ultrasound examination is needed to confirm that the large colon has been freed from its entrapment by the nephrosplenic ligament.[48,49]

The likelihood that a particular horse will have a sonographically demonstrable nephrosplenic entrapment generally hinges on the results of rectal palpation.[50] The possibility of colonic entrapment increases in animals that have undergone previous abdominal surgery, which may result in adhesions between the spleen and previous incision site and a resultant increase in the nephrosplenic space.[51]

▮▮▮ INTESTINAL SAND

Ramey, and later Bertone, reported the radiographic appearance of intestinal sand in four horses with chronic diarrhea and weight loss.[52,53] The intestinal sand was radiographically outstanding, situated in the ventral aspect of the cranioventral abdomen, as seen in a lateral abdominal radiograph. Typically the intestinal sand resembles a bowel seen in lateral profile, with its bottom toward the ventral abdominal wall. Although the sand is readily discernible, its precise location within the intestinal tract is not.

▮▮▮ INTESTINAL FIBROSIS

Traub-Dargatz and co-workers described intestinal fibrosis causing partial intestinal obstruction in five horses and two ponies.[54] There were no characteristic radiographic or sonographic features. Necropsy showed dilated, thick-walled intestines with diminished longitudinal folds. In four of the animals, the small intestine was only half the normal length. Gastric enlargement and ulcers were found in two animals. Microscopic assessment revealed that much of the intestinal thickening was due to submucosal fibrosis (10 times thicker than normal). As a result of their findings, the authors proposed that intestinal fibrosis be considered a potential cause of intestinal colic and weight loss.

▮▮▮ COLONIC ADENOCARCINOMA

East and co-workers described an obstructive colonic adenocarcinoma in a 15-year-old Arabian stallion. Among the many tests performed on the horse to determine the source of its illness, nuclear imaging revealed rib and sternal metastases.[55]

References

1. Lester GD, Lester NV: Abdominal and thoracic radiography in the neonate, *Vet Clin N Am Equine Pract* 17:19, 2001.
2. Campbell ML, Ackerman N, Peyton LC: Radiographic gastrointestinal anatomy of the foal, *Vet Radiol* 25:194, 1984.

3. Fisher T, Yarbrough TY: Retrograde contrast radiography of the distal portions of the intestinal tract in foals, *J Am Vet Med Assoc* 207:734, 1995.
4. Dik KJ, Kalsbeek HC: Radiography of the equine stomach *Vet Radiol* 26:48, 1985.
5. Traub JL. Gallina AM, et al: Phenylbutazone toxicosis in the foal, *Am J Vet Res* 44:1410, 1983.
6. Rebhun WC, Turner HT: Gastric ulcers in foals, *J Am Vet Med Assoc* 180:404, 1982.
7. Rabuffo TS, Orsini JA, et al: Associations between age or sex and prevalence of gastric ulceration in Standardbred racehorses in training, *J Am Vet Med Assoc* 221:1156, 2002.
8. Peterson FB, Donawick WJ, et al: Gastric stenosis in a horse, *J Am Vet Med Assoc* 162:328, 1972.
9. Aronoff N, Keegan KG, et al: Management of pyloric obstruction in a foal, *J Am Vet Med Assoc* 210:902, 1997.
10. Tennant B, Keirn DR, et al: Six cases of squamous cell carcinoma of the stomach of the horse, *Equine Vet J* 14:238, 1982.
11. Boy M, Palmer JE, et al: Gastric leiomyosarcoma in a horse, *J Am Vet Med Assoc* 200:1363, 1992.
12. Kellum LL, Johnson PJ, et al: Gastric impaction and obstruction of the small intestine associated with persimmon phytobezoar in a horse, *J Am Vet Med Assoc* 216:1279, 2000.
13. Steenhaut M, Vlaminck K, Gasthuys F: Surgical repair of a partial gastric rupture in a horse, *Equine Vet J* 18:331, 1986.
14. Kiper ML, Traub-Dargatz, Curtis CR: Gastric rupture in horses: 50 cases (1979-1987), *J Am Vet Med Assoc* 196:333, 1990.
15. Loesch DA, Rodgerson DH, et al: Jejunal anastomosis following small intestinal resection in horses: seven cases (1999-2001), *J Am Vet Med Assoc* 221:541, 2002.
16. Fischer AT, Kerr LY, O'Brien TR: Radiographic diagnosis of gastrointestinal disorders in the foal, *Vet Radiol* 28:42, 1987.
17. Fluckiger MA, Kaegi B, et al: What is your diagnosis? *J Am Vet Med Assoc* 191:1139, 1987.
18. Dart AJ, Snyder JR, et al: Abnormal conditions of the equine descending (small) colon: 102 cases (1979-1989), *J Am Vet Med Assoc* 200:971, 1992.
19. Fischer AT, Yarbrough TY: Retrograde contrast radiography of the distal portions of the intestinal tract in foals, *J Am Vet Med Assoc* 207:734, 1995.
20. Orsini JA: Abdominal surgery in foals, *Vet Clin N Am Equine Pract* 13:393, 1997.
21. Mair TS, Edwards GB: Strangulating obstructions of the small intestine, *J Equine Vet Educ* 15:192, 2003.
22. Gayle JM, Bliksslagger AT, Bowman KE: Mesenteric rents as a source of small intestinal strangulation in horses: 15 cases (1990-1997), *J Am Vet Med Assoc* 216:1446, 2000.
23. Moll HD, Howard RD, et al: Small intestine strangulation by components of the spermatic cord in two geldings, *J Am Vet Med Assoc* 215:824, 1999.
24. Bliksslager AT, Roberts MC, et al: How important is intestinal reperfusion injury in horses? *J Am Vet Med Assoc* 211:1387, 1997.
25. White NA: Intestinal infarction associated with mesenteric vascular thrombotic disease in the horse, *J Am Vet Med Assoc* 178:259, 1981.
26. Klohnen A, Vachon AM, Fisher AT: Use of diagnostic ultrasonography in horses in horses with signs of acute abdominal pain, *J Am Vet Med Assoc* 209:1597, 1996.
27. Fontaine GL, Rodgerson DH, et al: Ultrasound evaluation of equine gastrointestinal disorders, *Comp Cont Educ Pract Vet* 21:253, 1999.
28. Edwards GB, Proudman CJ: An analysis of 75 cases of intestinal obstruction caused by lipomas, *Equine Vet J* 26:18, 1994.
29. Templer AS, Garcia-Seca O, et al: Ultrasonic findings in a mare with strangulating jejunal obstruction associated with pedunculated lipomas, *Equine Vet J* 15:52, 2003.
30. Ford TS, Freeman DE, et al: Ileocecal intussusception in horses: 26 cases (1981-1988), *J Am Vet Med Assoc* 196:121, 1990.
31. Dowling PM, Todhunter P: What is your diagnosis? *J Am Vet Med Assoc* 205:39, 1994.
32. Gaughan EM, Hackett RP: Cecocolic intussusception in horses: 11 cases (1979-1989), *J Am Vet Med Assoc* 197:1373, 1990.
33. Erkert RS, Crowson CL, et al: Obstruction of the cecocolic orifice by ileocecocostomy in a horse, *J Am Vet Med Assoc* 222:1743, 2003.
34. Ross MW, Bayha R: Volvulus of the cecum and large colon caused by multiple mesenteric defects in a horse, *J Am Vet Med Assoc* 200:203, 1992.
35. Robertson JT, Tate LP: Resection of intussuscepted large colon in a horse, *J Am Vet Med Assoc* 181:927, 927.
36. Jones SL, Davis J, Rowlingson K: Ultrasonographic findings in horses with right dorsal colitis: five cases (2000-2001), *J Am Vet Med Assoc* 222:1248, 2003.
37. Dolente BA, Wilkins PA, Boston RC: Clinicopathologic evidence of disseminated intravascular coagulation in horses with acute colitis, *J Am Vet Med Assoc* 220:1034, 2002.
38. Morris DD, Beach J: DIC in six horses, *J Am Vet Med Assoc* 183:1067, 1983.
39. Welch RD, Watkins JP, Taylor TS: Disseminated intravascular coagulation associated with colic in 23 horses (1984-1989), *J Vet Intern Med* 6:29, 1992.
40. East LM, Trumble TN, et al: The application of technetium-99mTc-HMPAO labeled white blood cells for the diagnosis of right dorsal ulcerative colitis in 2 horses, *Vet Radiol Ultrasound* 41:360, 2000.
41. Kirberger RM, Van Den Berg JS: Duodenal ultrasonography in the normal adult horse, *Vet Radiol Ultrasound* 36:50, 1995.
42. Cohen ND, Vontur CA, Rakestraw PC: Risk factors for enterolithiasis amoung horses in Texas, *J Am Vet Med Assoc* 216:1787, 2000.
43. Blue MG, Wittkopp RW: Clinical and structural features of equine enteroliths, *J Am Vet Med Assoc* 179:79, 1981.
44. Peloso JG, Coatney RW, et al: Obstructive enterolith in an 11-month-old miniature horse, *J Am Vet Med Assoc* 201:1745, 1992.
45. Meagher DM, Bugreff SE: Surgical conditions of the small colon and rectum in the horse in proceedings, *Am Assoc Equine Pract* 71, 1989.
46. McCure JT, Koblik C, et al: Fecalith impaction in four miniature foals, *J Am Vet Med Assoc* 200:205, 1992.
47. Boles CL, Kohn CW: Fibrous foreign body impaction colic in young horses, *J Am Vet Med Assoc* 171:193, 1977.
48. Sivula NJ, Trent AM, Kobluk CN: Displacement of the large colon associated with nonsurgical correction of large-colon entrapment in the renosplenic space in a mare, *J Am Vet Med Assoc* 197:1190, 1990.
49. Sivula NJ: Renosplenic entrapment of the large colon in horses: 33 cases (1984-1989), *J Am Vet Med Assoc* 199:244, 1991.

50. Baird AN, Cohen ND, et al: Renosplenic entrapment of the large colon in horses: 57 cases (1983-1988), *J Am Vet Med Assoc* 198:244, 1990.
51. Moll HD, Schumacher J, et al: Left dorsal displacement of the colon with splenic adhesions in three horses, *J Am Vet Med Assoc* 203:425, 1993.
52. Ramey DW, Reinertson EL: Sand-induced diarrhea in a foal, *J Am Vet Med Assoc* 185:537, 1984.
53. Bertone JJ, Traub-Dargatz JL : et al: Diarrhea associated with sand in the gastrointestinal tract of horses, *J Am Vet Med Assoc* 193:1409, 1988.
54. Traub-Dargatz JL: Schultheiss PC, et al: Intestinal fibrosis with partial obstruction in five horses and two ponies. *J Am Vet Med Assoc* 201:603, 1992.
55. East LM, Steyn PE, et al: Occult osseous metastasis of a colonic adenocarcinoma visualized with technetium Tc 99m hydroxymethylene diphosphate scintigraphy in a horse, *J Am Vet Med Assoc* 213:1167, 1998.

Chapter 43

Liver and Spleen

LIVER

Radiographing the liver to determine whether or not it is diseased "boils down" to three things: it is too large, too small, or misshapen. Occasionally density discrepancies—gas, mineral, metal—suggest disease, but such findings are rare. In short, hepatic radiology is for the most part unrewarding.

Hepatic ultrasound, on the other hand, can be quite revealing, although as with any examination of something as large as the liver, it is often time consuming and technically challenging. As in the case of pet animals, the diagnostic benefits of ultrasound in foals and horses tend to be exaggerated. Although few will dispute the capability of ultrasound to identify a large hepatic mass, such as an abscess or tumor or a cirrhotic liver bathed in peritoneal fluid, it is quite another proposition to diagnose a diffuse liver disease like hepatitis, at least with any degree of certainty (Figure 43-1).

This is not to say that hepatic ultrasound is a waste of time—hardly—but one's diagnostic expectations should be realistic: localized and regional liver diseases are detectable, provided the available equipment is capable of clearly detecting them and the examiner has the ability to recognize the diseased portion of the liver once it is encountered. Second, all but the most severe of diffuse liver diseases are very difficult to recognize sonographically.

SPLEEN

Like the liver, the radiographic pursuit of splenic disease is often an exercise in futility; but the sonographic search for disease can be quite rewarding, given the close proximity of much of the spleen to the surface of the left paralumbar fossa.

NONSPECIFIC SONOGRAPHIC FINDINGS IN HORSES WITH LIVER DISEASE

Durham and co-workers reported multiple, nonspecific sonographic findings in horses with a variety of liver diseases, including those that caused one or more of the following pathologic abnormalities: (1) moderate fibrosis, (2) moderate or severe biliary hyperplasia, and (3) severe hemosiderosis (Box 43-1).[1]

Hepatic Abscess

Sellon and co-workers reported liver abscesses in three horses.[2] Clinically, the animals had histories of weight loss, fever, inappetence, and depression. Sonographically, there was no characteristic appearance. The observed lesions were of mixed echogenicity, with or without gas and fluid pockets. Other hepatic diseases, including (1) tumor, (2) granuloma, (3) infarction, and (4) hemorrhage, also share some of these sonographic features.

Cholelithiasis

Cholelithiasis is more common in horses than in any other domestic species and is the leading cause of biliary obstruction. Traub and co-workers described cholelithiasis in four horses, two of which were examined sonographically because of abdominal pain and laboratory evidence of biliary obstruction. The other two cases were incidental necropsy findings.[3] Brandon and Stanley also reported the sonographic diagnosis of bile stones *(choleliths)* in an icteric 9-year-old Quarter Horse.[4] Reef and co-workers reported cholelithiasis in eight horses, emphasizing the sonographic aspects of the disease, particularly the biliary congestion that often accompanies cholelithiasis.[5]

Assessing Bile Flow (Biliary Kinetics)

Hornof and Baker described the scintigraphic technique and normal values for evaluating biliary kinetics in the horse[6] (Table 43-1).

Hepatic Tumor

Lennox reported the sonographic appearance of a hepatoblastoma in a $2\frac{1}{2}$-year-old Thoroughbred filly hospitalized for lethargy, anorexia, and weight loss. Sonographically, the lesion was characterized by numerous closely packed, echogenic foci, which obliterated the normal echotexture of the liver.[7]

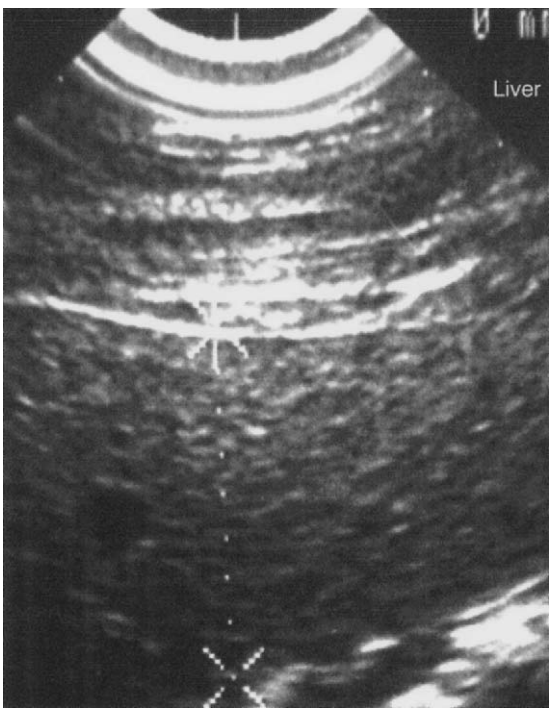


Figure 43-1 • Normal-appearing hepatic sonogram in a horse with diffuse hepatitis illustrates the limitations of ultrasound in diagnosing diffuse liver disease.

Pyrrolizidine Alkaloid Poisoning

In the Pacific Northwest, consumption of *Senecio* plant species, which contain pyrrolizidine alkaloids, can cause liver failure in horses.[8] Unfortunately there are no consistently reliable sonographic disease indicators.

▮▮▮ SPLEEN

Nephrosplenic (Renosplenic) Entrapment

The sonographic diagnosis of nephrosplenic entrapment is different from most other methods because a positive diagnosis is predicated on what is *not* seen rather than what is. The scan necessary to confirm or deny the presence of nephrosplenic entrapment is performed high in the left paralumbar fossa. A positive diagnosis is based on the absence of either the spleen or left kidney and, in its stead, reverberation artifact caused by gas-filled intestine (Figure 43-2). A negative examination is heralded by the presence of a normal spleen and left kidney (Figure 43-3).

Although some published reports describing the sonographic features of nephrosplenic entrapment leave the impression that the diagnosis is quite straightforward, this is not always the case. For example, either the spleen *or* the kidney may appear in the left lumbar fossa but without its companion organ, suggesting, but failing to confirm, the diagno-

Box 43-1
Nonspecific Sonographic Abnormalities Found in Horses With Diseased Livers

Generalized increased echogenicity
Focal increase in echogenicity
Generalized decreased echogenicity
Focal decrease in echogenicity
Decreased size (hepatic atrophy)
Increased size (hepatomegaly)
Increased vascular size (vascular congestion)
Rounded or blunted liver margins

Table 43–1 • NORMAL BILIARY ACTIVITY LEVELS*

Parameter	Fed Horses	Unfed Horses
Maximum **hepatic** activity	Reached within 10 min in all instances. In fed horses, reached 50% of maximum activity in 26 min ± 5 min	In unfed horses, reached 50% of maximum activity in 36 min ± 14 min
Maximum activity within **bile duct**	Reached within 15 min in fed horses, ± 4 min	Reached within 18 min in unfed horses ± 6 min
Time from injection to 50% maximum activity	21 min in fed horses ± 5 min	30 min in unfed horses ± 7

*As determined using ^{99m}Tc-labeled disofenin.

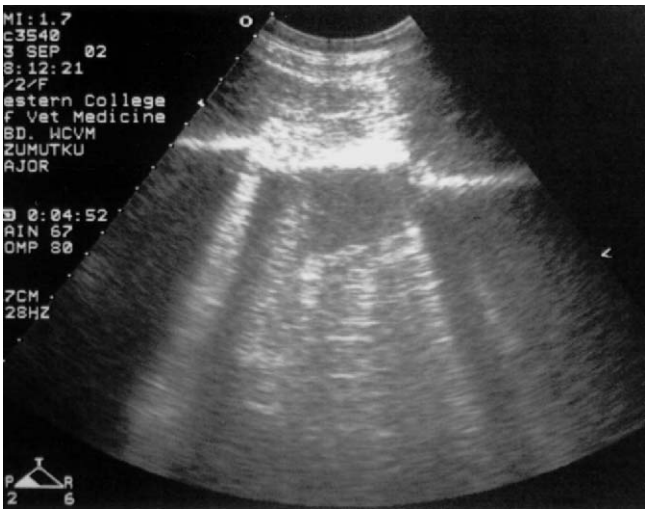


Figure 43-2 • Sonogram obtained from the left paralumbar fossa of a horse with nephrosplenic entrapment shows characteristic reverberation artifacts caused by an air-filled bowel segment.

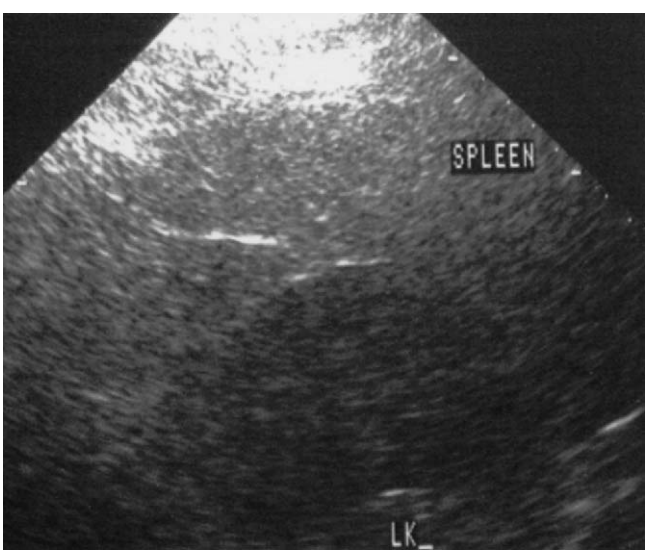


Figure 43-3 • Sonogram obtained from the left paralumbar fossa of a horse with suspected nephrosplenic entrapment shows a normal spleen and left kidney, which denies the diagnosis.

sis (Figure 43-4). I encounter this sort of diagnostic ambiguity with regularity, perhaps as much as 20 to 25 percent of the time, particularly after a horse has been rolled in an effort to correct an entrapment.

In instances in which there is a discrepancy between what was palpated and what was seen sonographically, I recommend that the left paralumbar fossa be rescanned while the horse is being repalpated. The palpater's moving fingers can be seen readily in the ultrasound beam, often clarifying any question about what is being palpated.

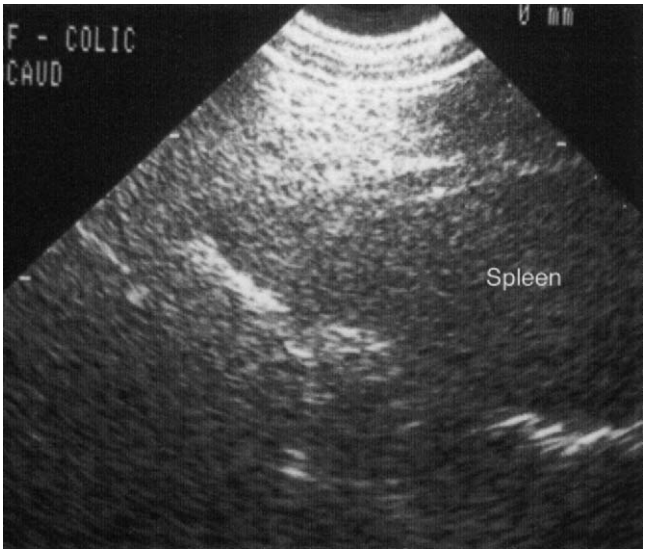


Figure 43-4 • Sonogram obtained from the left paralumbar fossa of a horse with suspected nephrosplenic entrapment shows the cranial aspect of the spleen surrounded by air-filled bowel segments on three sides.

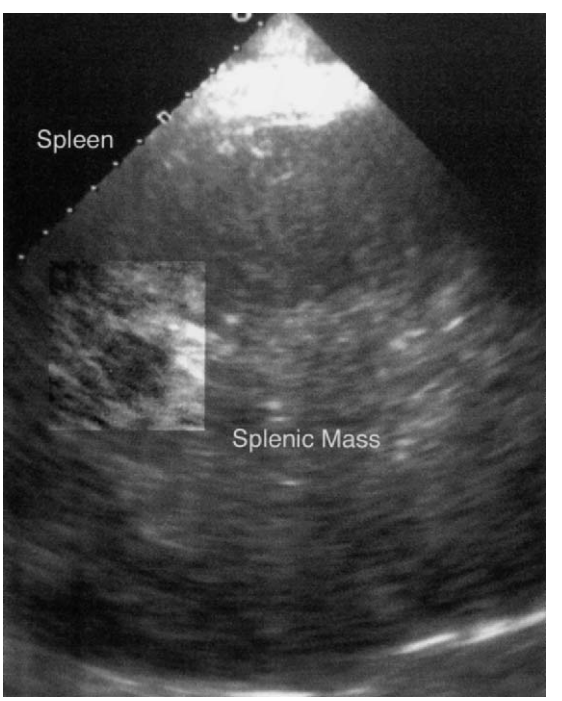


Figure 43-5 • Sonogram from a horse with hemangiosarcoma shows characteristic cavitary lesion *(emphasis zone)* within a larger splenic mass.

Splenic Tumors

Splenic hemangiosarcoma usually appears as one or more variably marginated cavitary masses, often accompanied by peritoneal hemorrhage (Figures 43-5 and 43-6).

Hance and co-workers described the sonographic appearance of presumed metastatic lymphosarcoma in

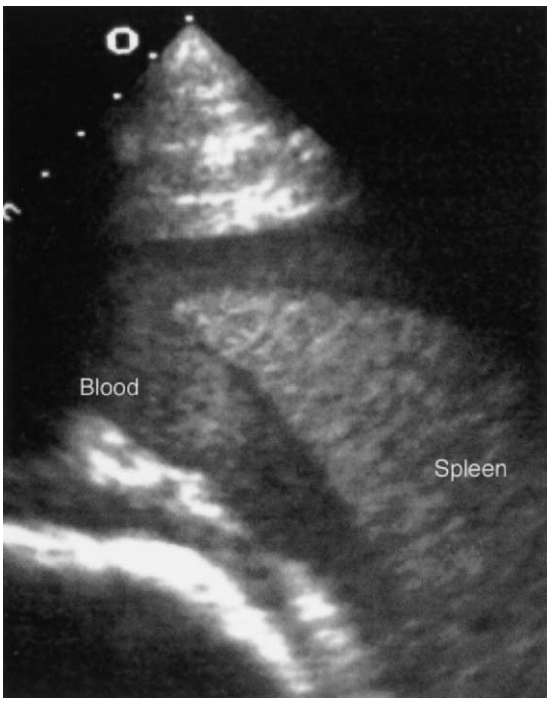


Figure 43-6 • Sonogram obtained from the horse shown in Figure 43-5 shows a normal portion of the animal's cancerous spleen surrounded by blood leaked from the tumor.

the spleen of a 4-year-old Quarter Horse gelding.[9] The splenic lesions appeared raised, well circumscribed, and hypoechoic. The spleen was enlarged overall, and there was a small volume of clear peritoneal fluid.

References

1. Durham AE, Newton JR, et al: Retrospective analysis of histological, clinical, ultrasonographic, serum biochemical, and hematological data in prognostic evaluation of equine liver disease, *Equine Vet J* 35:542, 2003.
2. Sellon DC, Spaulding K, et al: Hepatic abscesses in three horses, *J Am Vet Med Assoc* 216:882, 2000.
3. Traub JL, Rantanen N, et al: Cholelithiasis in four horses, *J Am Vet Med Assoc* 181:59, 1982.
4. Brandon B, Stanley C: What is your diagnosis? *J Am Vet Med Assoc* 222:289, 2003.
5. Reef VR, Johnston JK, et al: Ultrasonic findings in horses with cholelithiasis: eight cases (1985-1987), *J Am Vet Med Assoc* 196:1836, 1990.
6. Hornof WJ, Baker DG: Biliary kinetics of horses as determined by quantitative nuclear scintigraphy, *Vet Radiol* 27:85, 1986.
7. Lennox TJ, Wilson JH, et al: Hepatoblastoma with erythrocytosis in a young female horse, *J Am Vet Med Assoc* 216:718, 2000.
8. Pearson EG: Liver failure attributable to pyrrolizidine alkaloid toxicosis and associated with inspiratory dyspnea in ponies: three cases (1982-1988), *J Am Vet Med Assoc* 198:1651, 1991.
9. Hance SR, Shiroma JT, Bertone JJ: Ultrasonic diagnosis, *Vet Radiol* 33:101, 1992.

Chapter 44

Urinary Tract

RENAL SONOGRAPHY

Normal Sonographic Anatomy

Penninck and co-workers reported the sonographic appearance of the kidneys in three normal horses and a single case of a calcified renal adenoma.[1] As in pet animals, the renal cortex of the horse appears relatively bright compared with the medulla but relatively dark compared with the nearby spleen. The deep renal interior is composed of an anechoic pelvis and pelvic recesses, interspersed with echogenic foci corresponding to intrapelvic fat and fibrous tissue. Unlike that of the dog and cat, the equine kidney has a distinctly triangular shape featuring rounded corners.

Renal Biopsy

Percutaneous renal biopsy is ideally performed with sonographic assistance. Barratt-Boyes and co-workers have reported their experience obtaining renal biopsies (primarily right-sided) from seven normal horses using both full sonographic guidance and preprocedural renal localization.[2] Sonographic localization followed by "blind biopsy" was preferred over constant sonographic surveillance because it required fewer people. The preferred route to the lateral aspect of the right kidney was a transverse approach through the 17th intercostal space. Biopsy of the left kidney proved potentially more hazardous, twice requiring penetration to access underlying kidney.

Renal Dysplasia

Ramirez and co-workers reported the sonographic appearance of renal dysplasia in a 3-month-old Quarter Horse colt.[3]

Ectopic Ureter

Congenital and acquired ureteral ectopia has been described in foals.[4,5] Blikslager and co-workers described the sonographic and urographic appearance of bilateral ectopic ureter in an incontinent 7-week-old Appaloosa filly.[6] Urography was performed under anesthesia, using 300 ml of diagnostic organic iodine solution (Renografin 76, Amfac, Shawnee Mission, Kansas 66203). Distal ureteral contrast was enhanced by catheterizing the bladder, removing as much of the urine as possible and replacing it with air. Films were made at 5, 15, and 40 minutes post injection.

The collecting systems of both kidneys were dilated, along with their respective ureters. The bladder failed to opacify, but contrast was observed in the vagina, strong circumstantial evidence of ureteral displacement, which necropsy later confirmed.

Tomlinson and co-workers described the use of percutaneous ultrasound-guided pyelography to diagnose hydronephrosis and ectopic ureter in a 3-week-old filly.[7]

Renal Calculi (Nephrolithiasis, Kidney Stones)

Wooldridge and co-workers described the sonographic appearance of renal dysplasia in a 2-year-old Quarter Horse, leading to hydronephrosis, hydroureter, renal and ureteral calculi, and eventually renal failure.[8] Ehnen and co-workers described renal and ureteral obstruction caused by kidney stones.[9] Common clinical signs in the eight horses included weight loss, poor performance, and decreased appetite. Diagnosis was made with a combination of sonography and rectal palpation. As might be anticipated, the obstructed ureters were urine distended. When identified, the ureteral stones appeared as discrete echogenic objects.

Hydronephrosis

The most common cause of acquired hydronephrosis in horses is nephrolithiasis or ureterolithiasis. Less often, hydronephrosis is caused by infection, tumor, postinflammatory adhesion, or injury related to surgery. Congenital ureteral ectopia is usually associated with hydronephrosis and often infection.

Jones and co-workers reported unilateral hydronephrosis in a 4-month-old foal hospitalized because of hematuria. Transabdominal sonography revealed an enlarged, hydronephrotic right kidney, but the ureter and retroperitoneal cavity could not be identified.

Nephritis

Kisthardt and co-workers reported the sonographic appearance of pyelonephritis in seven horses initially seen because of hematuria.[10] One or more of the following sonographic abnormalities characterized renal infection:

- Decreased length
- Increased echogenicity
- Abnormal contour
- Poor or absent corticomedullary junction
- Dilated or distorted renal pelvis and pelvic recesses
- Focal hypoechoic or hypoechoic cortical defects

Renal Carcinoma (Renal Adenocarcinoma)

Ramirez and Seahorn described the sonographic appearance of a renal carcinoma in a 15-year-old Tennessee Walking Horse mare.[11] The tumor appeared as a large, eccentric, relatively hyperechoic mass protruding from the caudal pole. Other than some distortion at the junction between the tumor and kidney, the latter appeared sonographically normal, with a discrete cortex and medulla.

In their discussion, the authors point out that renal tumors occur rarely in horses and do not show any gender preference. Renal carcinomas develop in the polar cortex within the tubular epithelium and gradually expand, often leading to adhesions. The tumor eventually spreads via the lymph or blood systems to the regional lymph nodes and lungs. The presence of renal carcinoma is often signaled clinically by polyuria and polydipsia combined with an abnormal urine/creatinine ratio. There is no cure.[12]

Ureteral Stenosis

Morisset and co-workers reported a case of congenital ureteral stenosis in a 2-day-old foal with uroperitoneum.[13] Sonographically, the left renal pelvis appeared dilated, but retrograde urography failed to determine the cause. Guided by ultrasound, diagnostic iodine solution was injected directly into the left renal pelvis (*unilateral antegrade urography*), eventually revealing distal ureteral stenosis. The procedure was repeated on the opposite kidney, which showed leakage of contrast from a dilated proximal ureter.

After ureteral repair and relocation, postoperative urine leakage, and infection, the foal eventually recovered. The histologic appearance of the resected portion of the left ureter was considered consistent with ureteritis, although there was no proof of infection. The authors did not speculate about how the proposed ureteritis was able to develop so rapidly after birth or whether this might have been an in utero infection.

Umbilical Evagination of the Urinary Bladder

Textor and co-workers reported the displacement of the urinary bladder into the umbilicus in an 8-hour-old Standardbred filly; this was diagnosed sonographically[14] (Box 44-1).

Ruptured Urinary Bladder

Bladder rupture in adult horses has been attributed to a variety of causes, including (1) dystocia in the mare, (2) urethral obstruction due to calculi, (3) urethral hematoma, (4) structural weakening subsequent to surgery, (5) infectious perforation related to umbilical infection, (6) torn bladder adhesions, (7) blunt trauma, and (8) iatrogenic rupture: overdistension during endoscopy or catheter perforation (Figure 44-1).[16]

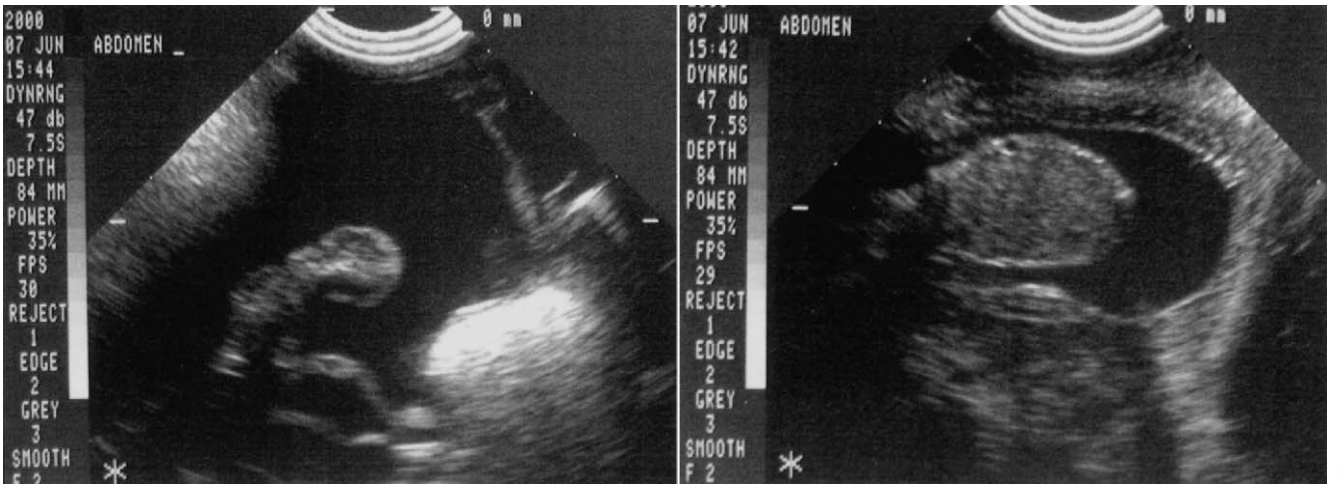
Bladder Tumor

Lymphosarcoma. Sweeney and co-workers described a large pelvic lymphosarcoma that infiltrated the wall of the urinary bladder, obstructing a ureter and causing hydronephrosis. The tumor also invaded the uterus.[17] The renal lesion was detected with transabdominal ultrasound; the bladder lesion was identified using rectal sonography.

Adrenal Glands. Johnson described pheochromocytoma in two horses, a 12-year-old Standardbred and

Box 44-1
Causes of Urinary Outflow Obstruction in Horses

Neurologic	Cauda equina syndrome
	Equine protozoal myeloencephalitis
	Herpes myeloencephalitis
Nonneurologic	Urolithiasis
Neoplastic	Tumors
Parasitic	Habronemiasis
Inflammatory/infectious	Nonspecific inflammatory swelling (urethritis)
	Inflammatory urethral webs[15]
Congenital	Congenital urethral webs
	Congenital longitudinal and fenestrated transverse urethral partitions



A B

Figure 44-1 • A, Abdominal sonogram shows a large volume of clear peritoneal fluid, the result of a perforated urinary bladder and resultant chemical peritonitis. **B,** A second sonogram shows fluid surrounding a testicle.

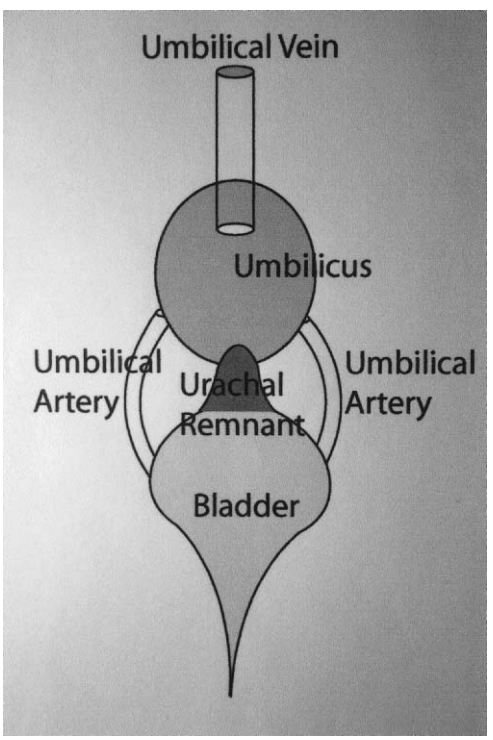


Figure 44-2 • Umbilical diagram showing essential anatomic elements and their spatial relationships.

a 21-year-old Quarter Horse. Common clinical signs included excessive sweating, muscle tremors, tachycardia, tachypnea, hyperglycemia, azotemia, colic, and hemoperitoneum. Retroperitoneal swelling, detected on rectal palpation, was the result of bleeding from the tumor.[18]

Table 44–1 • NORMAL UMBILICAL AND UMBILICAL VASCULAR MEAN DIAMETERS IN 1- AND 7-DAY-OLD FOALS

Umbilical Element	1-Day-Old Foal	7-Day-Old Foal
Umbilical vein	8.3 mm (±3.0)	5.8 mm (±1.5)
Umbilical stump	15.5 mm (±2.7)	12.5 mm (±2.3)
Urachus plus arteries	17.7 mm (±2.7)	17.8 mm (±2.6)
Umbilical arteries	7.8 mm (±1.7)	6.4 mm (±1.5)

Modified from Levan RP, Craychee T, Madigan JE: Practical method of umbilical ultrasonic examination of one-week old foals: the procedure and the interpretation of age-correlated size ranges of umbilical structures, *Equine Veterinary Sci.*

▮▮▮ SONOGRAPHIC ASSESSMENT OF THE SUSPECT UMBILICUS

Sonographic Examination

Routine sonographic examination of the foal umbilicus consists of four parts (Figure 44-2):

1. Examination of the umbilicus
2. Examination of the umbilical vein
3. Examination of the umbilical arteries and urachal remnant
4. Examination of the umbilical arteries and bladder

Several authors have published normal sonometrics for the foal umbilicus and related vasculature, including the (1) umbilical vein, (2) umbilical stump, (3) urachus plus arteries, and (4) umbilical arteries. Lavan and co-workers have provided normal values for both 1- and 7-day-old foals (Table 44-1).[19]

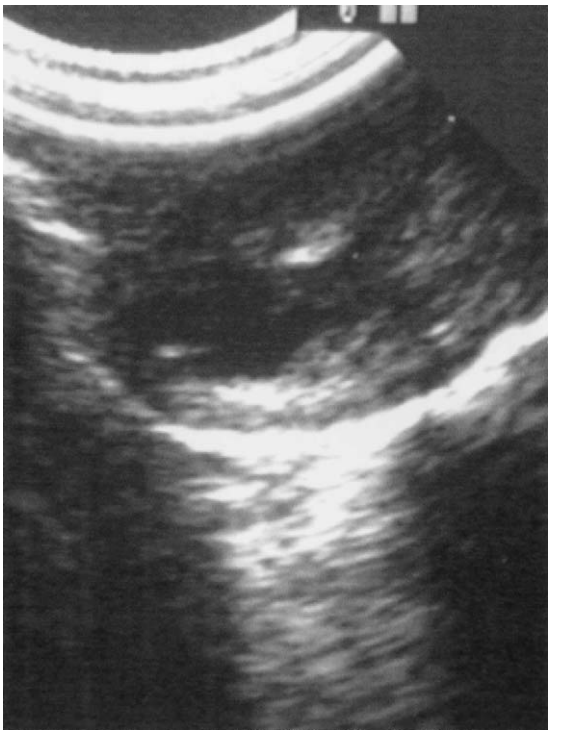


Figure 44-3 • Abscessed umbilicus with cavitation and a pair of small air pockets featuring strong through transmission, indicating the fluid nature of the cavity.

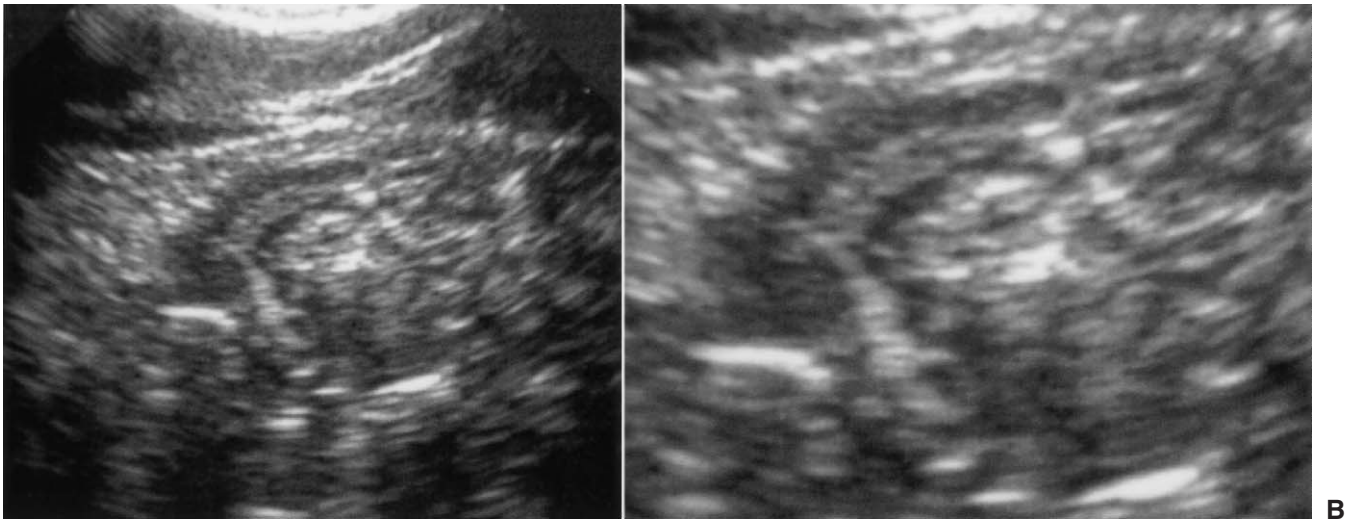


Figure 44-4 • A, Sonographic cross-section of an abscessed umbilical vein and its infected surroundings *(center).* **B,** A close-up view of the umbilical vein shows the classic features of severe phlebitis: (1) luminal enlargement, (2) wall thickening, (3) a septic thrombus, and (4) gas.

Umbilical Infection

Umbilical infection in young foals can assume a variety of forms: (1) generalized inflammation (*omphalitis*), (2) abscessation, (3) inflammation of the umbilical vein (*ompalophlebitis*), (4) inflammation of the umbilical arteries (*omphaloarteritis*), (5) septicemia, and (6) urachal patency. Contrary to some published reports, most of the examinations performed in our hospital are prompted by a swollen, nonreducible umbilical swelling. Drainage and pain may also be associated with umbilical infection but are inconstant features. A number of examples follow (Figures 44-3 through 44-5).

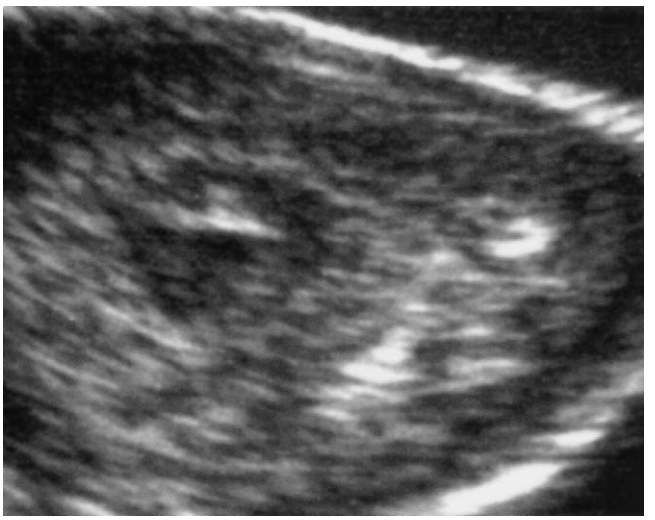
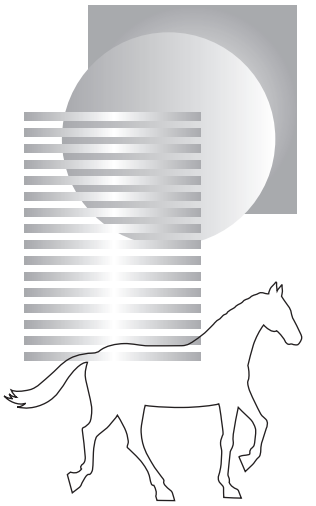


Figure 44-5 • Sonographic oblique section of an infected umbilical vein *(left center)*, umbilical artery *(far right center)*, and surrounding tissues.

References

1. Penninck DG, Eisenberg HM, et al: Ultrasonography: normal and abnormal, *Vet Radiol* 27:81, 1986.
2. Barratt-Boyes SM, Spensley MS, et al: Ultrasound localization and guidance for renal biopsy in the horse, *Vet Radiol Ultrasound* 32:121, 1991.
3. Ramirez S, Williams J, et al: Ultrasound-assisted diagnosis of renal dysplasia in a 3-month-old Quarter Horse colt, *Vet Radiol Ultrasound* 39:143, 1998.
4. Stickle RL, Wilcock BP, Huseman H: Multiple ureteral defects in a Belgian foal, *Vet Med Small Anim Clin* 70:819, 1975.
5. Jean D, Marcoux M, Louf C-E: Congenital bilateral distal defect of the ureters in a foal, *Equine Vet Educ* 10:17, 1998.
6. Blikslager AT, Green EM, et al: Excretory urography and ultrasonography in the diagnosis of bilateral ectopic ureters in a foal, *Vet Radiol Ultrasound* 33:41, 1992.
7. Tomlinson JE, Farnsworth K, et al: Percutaneous ultrasound-guided pyelography aided diagnosis of ectopic ureter and hydronephrosis in a 3-week-old filly, *Vet Radiol Ultrasound* 42:349, 2001.
8. Wooldridge AA, Seahorn TL, et al: Chronic renal failure associated with nephrolithiais, ureterolithiasis, and renal dysplasia in a 2-year-old Quarter Horse gelding, *Vet Radiol Ultrasound* 33:121, 1992.
9. Ehnen SJ, Divers TJ, et al: Obstructive nephrolithiasis and ureterolithiasis associated with chronic renal failure in horses: eight cases (1981-1987), *J Am Vet Med Assoc* 197: 249, 1990.
10. Kisthardt KK, Schumacher J, et al: Severe renal hemorrhage caused by pyelonephritis in 7 horses: clinical and ultrasonic evaluation, *Can Vet J* 40:571, 1999.
11. Ramirez S, Seahorn TL: Ultrasonography as an aid to diagnosis of renal cell carcinoma in a horse, *Vet Radiol Ultrasound* 37:383, 1996.
12. Traub-Dargatz JL: Urinary tract neoplasia, *Vet Clin N Am Equine Pract* 14:495, 1998.
13. Morisset S, Hawkins JF, et al: Surgical management of a ureteral defect with ureterorrhaphy and of ureteritis with ureteroneocystostomy in a foal, *J Am Vet Med Assoc* 220:354, 2002.
14. Textor JA, Goodrich L, Wion L: Umbilical evagination of the urinary bladder in a neonatal filly, *J Am Vet Med Assoc* 219:953, 2001.
15. Blikslager AT, Tate LP, Jones SL: Neodymium:yttrium-aluminum-garnet laser ablation of a urethral web to relieve urinary outflow obstruction in a horse, *J Am Vet Med Assoc* 218:1970, 2001.
16. Walesby HA, Ragle CA, Booth LC: Laparoscopic repair of ruptured urinary bladder in a stallion, *J Am Vet Med Assoc* 221:1737, 2002.
17. Sweeney RW, Hamir AN, Fisher RR: Lymphosarcoma with urinary bladder infiltration in a horse, *J Am Vet Med Assoc* 199:1177, 1991.
18. Johnson PJ, Goetz GL, et al: Pheochromocytoma in two horsers, *J Am Vet Med Assoc* 206:837, 1993.
19. Lavan RP, Craychee T, Madigan JE: Practical method of umbilical ultrasonic examination of one-week old foals: the procedure and the interpretation of age-correlated size ranges of umbilical structures, *Equine Vet Sci* 21:100, 2001.



Index

A

Abdomen
  abscess of, 525
  encapsulated foreign body sponges, 525
  free air in, 524
  topography, 527-528
    of bowel mass, 527-528
    of cecum, 528
    of large intestine, 528
    of rectum, 528
    of small intestine, 528
    of stomach, 527
  tumor of, 525
Abscesses
  of abdomen, 525
  of brain, 402
  Brodie's, 252-253
  of epiglottis, 419
  of fibula, 252-253
  hepatic, 544
  of lungs
    pneumonia and, 486-487, 487f, 488f
  of mediastinum, 491
  of pelvis, 214, 215f
  solar, thermography for, 30
  of spine, 458
  of teeth, 370
Accessory fractures
  of carpus, 160-161, 170f
Acetabulum
  fractures of, 216, 220-223f
Actinobacillus lignieresii, 377
Acute flexor tendon
  injury to
    radiography, 316
    sonography of, 313-316
    tendography, 316-317, 317b
Adamantinoma
  of mandible, 344, 346f
  of teeth, 369, 369f
Adaptive stress remodeling, 30
Adenocarcinoma
  of gastrointestinal tract, 541
Adrenal glands
  tumors of, 549-550
Adult respiratory distress syndrome (ARDS), 488, 501
Ameloblastic odontoma
  of teeth, 369-370
Ameloblastoma
  of teeth, 368-369
Anatomic restoration, 23
Anesthesia
  carotid blood flow and, 403
  regional perineural, 30
Aneurysmal bone cyst, 344-345
Angiography
  of foot, 28
  of tarsus, 294-295
Angular limb deformity, 10, 13-15f
  Nancy view of, 15-16, 16f, 17f
  recumbent views of, 16, 18f
Antebrachial flexor compartment syndrome, 191-192
Aorta
  aneurysm of
    thrombosis and, 515, 516f
  root disease of, 515
Aortic arch
  of cervical esophagus, 428
  interruption of, 508
Apical granulomas, 357
Apical infections
  of mandible, 357
  of maxilla, 357
Apophysis
  development of, 6, 6f
Arch fractures
  of cervical spine, 434, 436, 439f
ARDS. *See* Adult respiratory distress syndrome
Arterial duct
  persistent, 506-507, 508f
Arthritis
  of carpus, 163-164
    carpal canal syndrome, 164
    experimental, 164
Arthritis (*Continued*)
    radiographical detection of, 163-164
  septic
    of tarsus, 269, 271-274f, 274
Arthrography, 53
  of carpus, 175, 178
  of fetlock joint, 128
  of shoulder, 206-207
    femoral head fracture, 207, 208f, 209f
    greater tubercle fracture, 207
    technique of, 206
Articular fractures
  of fibula, 251
Arytenoid chondritis, 414
  of epiglottis, 418, 419f
Aspergillus, 485
Aspiration
  of trachea, 424-425
Aspiration pneumonia, 486, 531
Atheroma. *See* Epidermal inclusion cyst
Atony
  causes of, 539b
  of esophagus, 497
  radiographic disease indicator, 538b
Atrial fibrillation, 512
Axial osteochondral fragments, 103

B

Back. *See* Spine
Bacterial endocarditis, 512-513, 513f
Bacterial infections
  of orbit, 387, 389, 391f, 392f
Bacterial pneumonia
  in adults, 482-484
Bacteroides, 484
Barium swallow
  cervical esophagus and, 426
Basilar fractures
  of skull, 396-398
    basisphenoid-basioccipital, 396-397, 397f, 398f, 399f
    presphenoid, 397
    temporal, 397-398

Page numbers followed by "f" refer to illustrations; page numbers followed by "t" refer to tables; page numbers followed by "b" refer to boxes.

Basisphenoid-basioccipital fractures, 396-397, 397f, 398f, 399f
Biarticular fractures
of carpus, 156-157, 160f
Biceps brachii muscle, 200
Bicipital tenosynovitis
of shoulder, 208
Bilateral stress fractures, 251
Bile, flow of
liver disease and, 545, 545t
Biliary kinetics, 545
Biopsy
of urinary tract
sonography and, 548
Bipartite proximal sesamoid bones, 109
Bladder
rupture of
sonography and, 549
tumors of, 549-550
Body fractures
displaced
of fibula, 250, 251f
nondisplaced
of fibula, 245, 247, 250, 250f
of radius, 181-182, 184f
Bone spavin
tarsus, 280-284
atypical, 282, 282f, 283f
fusion of, 282, 284, 284f, 285f
posttraumatic osteoarthritis and, 284, 286f
radiographic progression of, 282-284, 284f, 285f
typical, 282, 283f
where and what principle of, 281, 281f, 282f
Bone windows, 31
Bones
abscesses of, chronic
of fibula, 252-253
adult *vs.* newborn, 1, 2f, 3f
angulation of, 10, 13-15f
cannon
fractures of
of growth plate, 134
incomplete dorsal metacarpal stress, 135
proximal palmar stress, 134-135
carpal, fracture of, 17, 20f
carpus, 150-151, 153-154f
palmar carpal ossicle, 153-154
radiocarpal joint fat deposits, 154, 155f
vestigial (accessory), 150, 153, 154f
cartilage space, 7, 9f
curvature of, 10, 13-15f
cutback zones, 1, 5f, 6f
cysts of
aneurysmal, 344-345
of condylar, 225
femoral, 239, 240f
of mandible, 344-345
P3, 52
dysplastic, 17, 20f
fractures of
age of, 23
cannon bone, 134-135
Bones (*Continued*)
carpal, 17, 20f
concomitant injury, 23
healing of, 23-25
location of, 23
open, 23
postoperative care, 23
repair method, 23
severity of, 23
surgical skill, 23
transport, 23
grafts, 25
growth plates, 1, 5f, 6f
hypoplastic, 17, 20f
immaturity of, 7, 10, 11f, 12f, 15t
long
growth of, 6-7, 10f
prematurity of, 7, 10, 11f, 12f, 15t
radiometrics and, 10-11, 15
remodeling, 25-27
accommodative, 25-26f, 27
exercise induced, 25-27
traumatically induced, 27
scar. *See* Traumatic exostosis
separate ossification centers, 4, 4t, 5f, 6
splint
of metacarpus, 132f
active *vs.* inactive, 130
fractures of, 130, 133-134f
irradiated, radiographic evaluation of, 131
spur
of tarsus, 266
tarsal, fracture of, 17, 20f
tubulation, 1, 5f, 6f
tumors of
multiple hereditary exostoses, 21
polydactylism, 21
volume loss, 7, 9f
Bowel mass
abdominal topography of, 527-528
Brachygnathia
of mandible, 348
Brain
abscess of, 402
magnetic resonance imaging of, 402
standard imaging of, 402
trauma to, 402
Branchial cysts
of throat, 415, 416b
Brodie's abscess, 252-253
Bronchiectasis, 493-494
Bronchitis, 493
Bronchography, 493
Bronchus
anatomy of, 493
bronchiectasis, 493-494
bronchography of, 493
compensatory dilation of, 493
cross-sections, 462, 467f
heaves, 494
inflammation of, 493
of neck, 431
thickening, 462-463, 467f
Bruising
of lung, 475
of tarsus, 261-262, 262f
Bucked shins, 135
Bulla
infection of, 398-400, 400f, 401f
traumatic, 477, 478f
Bursitis
of carpus, 174
Bursography, 53

C

Cable cerclage system, 180
Calcaneus
fractures of, 265, 266f
infection of, 275-278, 276f, 277f
sequestra, 276-277, 278f
Calcification
of larynx
dystrophic, 415, 415f
metaplasia, 415
mineralization, 415, 415f
Calculi
sonography and, 548
Cancer
of bladder, 549
of eye, 391
of gastrointestinal tract, 541
of pharynx, 413
Candida, 485
Cannon bones
fractures of
of growth plate, 134
incomplete dorsal metacarpal stress, 135
proximal palmar stress, 134-135
Capillary-failure theory, 499
Caps
teeth and, 367, 367f, 368f
Capsular tear
of tarsus, 263-264
Carcinoma. *See* Cancer
Cardiac hypoplasia, 508
Cardiac tamponade, 314-315
Carotid artery
blood flow in, 403
of neck
Doppler of, 424
Carpal canal syndrome, 164
Carpal spavin
of carpus, 173-174, 177f
of metacarpus, 142, 145-146f
Carpitis syndrome, 163
Carpus
arthritis of, 163-164
carpal canal syndrome, 164
experimental, 164
radiographical detection of, 163-164
arthrography of, 175, 178
beam angle, radiographic variation of, 154-155, 156-157f
bones of, 150-151, 153-154f
palmar carpal ossicle, 153-154
radiocarpal joint fat deposits, 154, 155f
vestigial (accessory), 150, 153, 154f
bruising of, 168, 172
bursitis of, 174
carpal spavin of, 173-174, 177f

Carpus (*Continued*)
cavography of, 174f, 178
computed tomography of, 178
contracture of, 18
cuboidal bones of, 149-150, 151f
customized views of, 149
deep cuts of, 172, 174-176f
deformity of
blood-borne infection, 168, 173f
osteochondritis of, 168, 172f
valgus/varus angulation and, 167
draining sinuses, 172, 174-176f
foreign body of, 174-175
fractures of
accessory, 160-161, 170f
biarticular, 156-157, 160f
chip, 155-156, 159f
corner, 156, 159f
fragment source, 157, 159, 160f
fresh (acute) injury, 155, 157f
incidence/location of, 159-160, 159t, 161-170f
intermediate (subacute) injury, 155, 158f
kissing lesions, 161
old (chronic) injury, 155, 155t, 158f
radiographical prediction of, 161
slab, 156-157, 160f
types of, 155-161
hematoma of, 172, 173f
hygroma of, 172, 173-174f
magnetic resonance imaging of, 178
puncture wounds of, 172, 174-176f
rows of, 150-151
sinography of, 178
skin markers of, 172, 176-177f
skyline projections of, 149, 152f
sonography of, 178
sprains of, 162, 170-171f
standard series of, 149, 150-152f, 153t
steroid arthropathy, 164, 166
strains of, 162
subluxation of, 162-163, 171f
synovioma of, 174
tendonitis, 172
Cartilage space, 7, 9f
Cascade stomach, 531
Catheter
intravascular, unknotting heart, 505
jugular vein and, 422-423, 424b
Caudal cruciate, 229
Caudal heel pain syndrome, 62, 67, 74
thermography for, 30
Caudal lumbosacral spinal region
standard series of, 211, 213f
Caudal synovial pouch, 228
Cavography
of carpus, 174f, 178
of eye, 393, 394f
of parotid duct, of mandible, 349, 351
of salivary glands, 405
Cecum
abdominal topography of, 528
dilated, 536
nonobstructive colic, 536
Celiography, 523-524
Cellulitis
of cervical spine, 452-453
of guttural pouches, 407
Cementoma
of teeth, 369
Cervical esophagus
aortic arch of, 428
barium swallow and, 426
choking, 427, 427b, 427f, 428f
complications of, 429, 430f
esophagostomy, 429, 430f
feeding tubes and, 429, 430f
cysts of, 429-430
dilation of, 427-428, 429f
diverticula, 428-428
esophagography of, 426
fistula of, 430
obstruction of, 427, 427b, 427f, 428f
phytobezoar, 429
pressure and, 426
radiography of, 426, 426b
rupture of, 430
stricture, 429
tumors of, 430, 431b
vascular ring anomaly, 428
Cervical spine
cellulitis of, 452-453
congenital malformation of, 450-452
injury and, 451-452
radiometrics, 450-451
diskospondylitis, 453
dislocation of, 436-437, 438-440f
fractures of, 434
arch, 434, 436, 439f
body, 434
compression, 434
dorsal element, 434, 436, 439f
growth plate, 434, 437f
ventral element, 434
fusion of, 453
meningomyelocele, 452
occipitoatlantoaxial dysplasia, 452
osteoarthritis of, 439-440, 441f
congenital facetal joint asymmetry and, 440-441
protozoal myeloencephalitis, 450, 451f
ruptured intervertebral disk, 452
spina bifida, 452
spondylitis, 453
spondylosis, 453
standard series of, 433-434, 434-436f
torticollis of, 437, 439
tumors of, 452
vertebral instability of
causes of, 442t
myelographic assessment of, 443-447
plain-film assessment of, 442-443, 442b, 444-445f
radiography of, 442, 442f, 443f
Chest wall
diaphragmatic hernia, 479-480
hydropneumothorax, 479, 479f
injury to, 475-477
emphysema, 475
Chest wall (*Continued*)
lung bruising, 475
pneumothorax, 475, 476b, 476t, 477, 477f, 478f
rib fractures, 475, 476f
wound penetration, 475
pleural fluid, 477, 479, 479b, 479f
pneumomediastinum, 479, 479f
traumatic bulla, 477, 478f
Chip fractures
of carpus, 155-156, 159f
navicular disease, 71, 71b
osteochondral, 155-156
Choking, 427, 427b, 427f, 428f
Cholelithiasis
liver disease and, 544
Chondroma
of ulna/radius, 188, 191
Chondrosarcoma
of ulna/radius, 191
Chronic obstructive pulmonary disease (COPD), 495f, 496-495
Chyloperitoneum, 524
Chylothorax, 501, 501b
Circulation, persistent fetal pulmonary, 499
Clubfoot, 58, 59f, 60f, 74, 358
Coccidioides, 485
Coiled spring sign, 540
Colitis
ulcerative, 540
ultrasound of, 540
Collateral ligament, 229
sprain-avulsion-fractures of, 235
Colon
dilated, 536
nonobstructive colic, 536
Colonography
gastrointestinal tract barium examination, 528-529
Communicating bursal infections
of elbow, 196-197
Compartment syndrome, 191-192
Compound fracture. *See* Open fracture
Compression fractures
of cervical spine, 434
Computed radiography
of foot, 28, 30b, 31
Computed tomography (CT)
of carpus, 178
of face, 372-374, 374f
adult, 372-373
foal, 372-373
therapeutic outcome with, 374
of mandible
infections, 362
of maxilla
infections, 362, 365f
of secondary sinusitis, 377-378
of sinonasal disease, 382, 384f, 385f
of skull, 330, 332f
of tarsus, 261
Condylar
bone cyst, 225
flattening of, 236-237
fracture of, 220, 225, 225f
Condylar-glenoid overlap, 348, 350f

Congenital bronchopulmonary dysplasia, 499
Congenital sustentacular hypoplasia
  tarsus and, 293
Congestive heart failure, 520-521
COPD. *See* Chronic obstructive pulmonary disease
Cor pulmonale, 519-520, 522f
Corner fractures
  of carpus, 156, 159f
Corner sign, 84
Corns
  thermography for, 30
Coronary region
  tumors of, 53, 58
Corynebacterium equi. *See* Rhodococcus equi
Corynebacterium pseudotuberculosis, 199
Coxal joint
  dislocation of, 216
Cranial cruciate ligament, 229
  sprain-avulsion-fractures of, 234
Cranial synovial pouch, 228
Cranium
  fractures series of, 396, 397f
Crena, 32, 33, 33f
Crushing
  of tarsus, 261-262, 262f
Cryptococcus, 485
CT. *See* Computed tomography
Cuboidal bones
  of carpus, 149-150, 151f
Cutback zones, 1, 5f, 6f
Cyanotic heart disease, 509-510
  intrapulmonary shunting, 509-510
  right-to-left shunt, 509, 509b
  truncus arteriosus, 509
Cysts
  bone
    aneurysmal, 344-345
    of condylar, 225
    femoral, 239, 240f
    of mandible, 344-345
    P3, 52
  branchial, 415, 416b
  of cervical esophagus, 429-430
  dentigerous, 363, 366, 366f, 382
  epidermal inclusion, 378
  of epiglottis, 418, 419f
  follicular, 368-368
  of guttural pouches, 408
  interosseous epidermoid cyst, of mandible, 345
  of mandible, 344-345
  of neck, cervical esophagus, 429-430
  paranasal sinus, 378-380, 378b, 379f
  of pharynx, 413
  of thyroglossal duct, 413

D

Dacryocystitis, 383
Dacryocystorhinography
  of nasolacrimal duct obstruction, 384
Deep-muscle abscess infections
  of elbow, 197, 199
Degenerative valvular disease, 516-519
  inflow insufficiency, 516-518, 517f, 518f
  outflow insufficiency, 518-519, 519-522f
Dental lamina dura, 353
Dental. *See* Teeth
Denticles, 366
Dentigerous cyst, 363, 366, 366f, 382
Desmitis, 312-313
  causes of, 312-313
  diffuse, 313
  imaging of, 313
  localized, 313
  susceptibility of, 312-313
  terminology of, 312
Diaphragmatic hernia, 479-480
Diastema, 367
DIC. *See* Disseminated intravascular coagulation
Diffuse maxillary alveolar periostitis, 357
Digital flexor tendons
  anatomy of, 305, 308f, 309f
Dilation
  of cervical esophagus, 427-428, 429f
  of esophagus, 497
Discyocaulus arnfieldi, 488
Diseases
  of epiglottis, 413, 413f, 414f
    abscess of, 419
    age-related, 416
    arytenoid chondritis of, 418, 419f
    cysts of, 418, 419f
    dysfunction, 416, 417f
    dysplasia, 417, 417f, 418f
    entrapment of, 417-418
    foreign bodies of, 419, 420f
    hypoplasia, 417, 417f, 418f
    inflammation of, 419, 420b
    radiometrics, 416-417
  of larynx
    arytenoid chondritis, 414
    calcification, 415, 415f
    collapse, 413
    congenital web, 414
    epiglottis, 413, 413f, 414f
  of liver
    abscesses, 544
    bile flow assessment, 545, 545t
    cholelithiasis, 544
    pyrrolizidine alkaloid poisoning, 545
    sonography of, 544, 545b
    tumors, 545
  of lungs
    in adults, 462, 466f, 467f
    bronchial cross-sections and, 462, 467f
    bronchial thickening, 462-463, 467f
    in foals, 462
    industrial, 487
    radiographic indicators of, 468
  navicular
    avulsion, 71, 73
    body, 70-73
Diseases (*Continued*)
    chip, 71, 71b
    pathologic, 70, 72f
  of pharynx, 411-412
    abscessation, 412, 412f
    palatal, hypoplasia of, 411
Disk, rupture of, 452
Diskospondylitis, 453
  of spine, 458
Dislocations (subluxation)
  of cervical spine, 436-437, 438-440f
  of coxal joint, 216
  of distal phalangeal, 46, 48f
  of hip, 216
  of patella, 233, 233f, 234f
  of radius, 186-187, 191f
  of shoulder, 207
  of tarsus, 266, 267f
  of temporomandibular joint, 347-348, 350f, 351f
Disseminated intravascular coagulation (DIC), 501
Distal flexor tendon sheath
  sonography of, 95
Distal interphalangeal joint
  contracture of, 18
Diverticula, 428-428
Diverticulum
  pulsion, 429
  traction, 429
Doppler
  of carotid artery, 424
Dorsal element fractures
  of cervical spine, 434, 436, 439f
Dropped hip, 211
Drowning, near, 501
Ductal atresia, 405
Duodenum
  ultrasound of, 540
Dynamic laryngeal evaluation, 417
Dysplasia
  of epiglottis, 417, 417f, 418f
  sonography and, 548
Dyspnea
  postanesthesia, 420

E

Ear
  infection of, 398-400, 400f, 401f, 402
  infection of, middle guttural pouches and, 410-411
Ear tooth, 363, 366, 366f, 382
Ectopia
  of teeth, 363, 366, 366f
Ectopic ureter
  sonography and, 548
Eikenella corrodens, 453
Elbow
  anatomic variation of, 193
  fractures of
    olecranon, 193, 195, 196f, 197f
    physeal, 195
    sprain-avulsion, 195-196, 198f
  infection of
    communicating bursal, 196-197
    deep-muscle abscess, 197, 199

Elbow (*Continued*)
epicondylar abscess, 199
postoperative, 199
olecranon hygroma of, 193
standard series of, 193, 194f, 195f
supplementary views of, 193, 195f
Emphysema, 475
Empyema, 378, 378f
of guttural pouches, 407, 407f
Enteroliths
ultrasound of, 540, 541f
Enthesiophytes, 326
Enthesitis, 326
Epicondylar abscess infections
of elbow, 199
Epidermal inclusion cyst, 378
Epiglottis
disease of, 413, 413f, 414f
abscess of, 419
age-related, 416
arytenoid chondritis of, 418, 419f
cysts of, 418, 419f
dysfunction, 416, 417f
dysplasia, 417, 417f, 418f
entrapment of, 417-418
foreign bodies of, 419, 420f
hypoplasia, 417, 417f, 418f
inflammation of, 419, 420b
radiometrics, 416-417
Epiglottitis, 419, 420b
Epiphysis
closure of, 6
development of, 6, 6f
inflammation of, 6
Epiphysitis, 6
Equine nigropallidal encephalomalacia, 403
Escherichia coli, 418, 488
Esophagography, 426
Esophagostomy
cervical esophagus and, 429, 430f
Esophagus. *See also* Cervical esophagus
acquired stricture of, 497
atony of, 497
congenital stenosis of, 497
dilation of, 497
foreign body in, 497, 498f
Ethmoid hematoma, 380-381, 381f
Eye
cavography of, 393, 394f
imaging of, 387
radiologic, 387, 388f, 389f
sonometrics, 387, 389f, 390t
ultrasound, 387
injuries to, 387-391, 390f
foreign body, 389
fracture, 387, 391f, 392f
infection, 387, 389
retrobulbar abscessation, 389
retrobulbar hematoma, 389
sequestra, 391, 393f
nasolacrimal duct obstruction in, 393, 395
anatomy of, 393
causes of, 393, 395, 395f
sinography of, 393
Eye (*Continued*)
tumors of, 391-393
primary, 391
secondary, 391, 393
squamous cell carcinoma, 391, 393

F

Face
computed tomography of, 372-374, 374f
adult, 372-373
foal, 372-373
therapeutic outcome with, 374
deformity of, 333
fractures of, 333, 335f, 336f
magnetic resonance imaging of, 374
Facial osteodystrophia fibrosa, 333
Facial tunnel, 372, 374f
False thoroughpin, 267
Fatigue fractures
of fibula, 245, 247, 250, 250f
FCD. *See* Fractured caudal eminence
Fecaliths
ultrasound of, 540
Feeding tubes
cervical esophagus and, 429, 430f
Femoral head
fracture of
growth plate, 216, 219f, 220f
Femoral shaft
of fracture of, 219-220, 224f, 225f
Femoropatellar joint, 228
Femorotibial joint, 228
Fetlock joint
anatomic variants of, 96
arthrography of, 128
comparable anatomic specimens of, 99-110f
contracture of, 18
diagnostic approach to, 96-97
dislocations
metacarpophalangeal/metatarsophalangeal, 105, 109
distal sheath
swelling of, 128
fractures of
caudal eminence, 101-103, 105-107f
distal metacarpal/metatarsal, 105
dorsal eminence, 97-98, 100-101, 101-104f
growth plate, 103, 105, 108-109f
longitudinal, 105
plantar fragments, 103, 107f
proximal phalanx, 97
infection of
of distal metacarpal/metatarsal growth plate, 123
of P1, 125, 126-127f
of sesamoid, 123, 125
magnetic resonance imaging of, 96
osteoarthritis of
capsular region, 115
cartilage space, 120, 124f
cranial aspect, 116
O'Brien's five region strategy to, 115
Fetlock joint (*Continued*)
osteophytes, 120, 124f
palmar/plantar aspect, 116
sesamoid bones, 116
osteochondritis of
metacarpus/metatarsal III, 116, 117-118f
P1, 116, 116t
proximal sesamoid, 109-113, 110f
fractures of, 109-113
primary injury mechanisms of, 109
sesamoiditis, 118, 119-122f, 120
sprain-avulsion-fractures of, 120, 122-123f
sprains of, 120, 122-123f
standard views of, 96, 97-99f, 98t
synovioma of, 120, 123, 125f
Fibroma
nonossifying
of coronary region, 58
of pastern joint, 94
of tendon sheath, 326
Fibrosarcoma
of lungs, 490-491
Fibula
chronic bone abscess of, 252-253
fracture of, 245, 250f
articular, 251
body, displaced, 250, 251f
body, nondisplaced, 245, 247, 250, 250f
fatigue, 245, 247, 250, 250f
stress, 245, 247, 250, 250f
limb angulation of, 252f, 253
misdiagnosis and, 245, 247f, 248f
osteochondritis of, 253
physeal growth of, 252f, 253
sonography of, 253
standard series of, 245, 246f
Fistula
of cervical esophagus, 430
of jugular vein, 423-424
Fistulous withers
of spine, 457f, 458
Fluoride osteosclerosis, 21
Fluorosis
teeth and, 370
Foals
face, computed tomography of, 372-373
gastrointestinal tract ulcer of, 531
lung disease of, 462
P3 anatomic variations of, and adults, 32
pneumonia in
interstitial, 481-482, 483f
newborn and, 481, 482f
pneumocystis carinii, 482
thorax
standard series of, 461-462
Follicular cysts, 368-369
Foot
computed radiography of, 28, 30b, 31
MRI, nuclear medicine of, 31-32
radiography of
preparation for, 35-36, 36f

Foreign bodies
of carpus, 174-175
encapsulated sponges
in abdomen, 525
of epiglottis, 419, 420f
of esophagus, 497, 498f
in eye, 389
of gastrointestinal tract, 532-533
of nose, 382, 383f
of pharynx, 412
of sinuses, 382, 383f
soft-tissue
of metatarsus, 297, 301f
Foreign material
impaction of, ultrasound of, 540
Fractured caudal eminence (FCD), 101-103, 105-107f
Fractures
of acetabulum, 216, 220-223f
articular, 242, 243f
basilar
of skull, 396-398
of basisphenoid-basioccipital, 396-397, 397f, 398f, 399f
biarticular phalangeal, 89, 90-91f
of bone
age of, 23
concomitant injury, 23
healing of, 23-25
location of, 23
open, 23
postoperative care, 23
repair method, 23
severity of, 23
surgical skill, 23
transport, 23
of cannon bones
of growth plate, 134
incomplete dorsal metacarpal stress, 135
proximal palmar stress, 134-135
of carpus
accessory, 160-161, 170f
biarticular, 156-157, 160f
chip, 155-156, 159f
corner, 156, 159f
fragment source, 157, 159, 160f
fresh (acute) injury, 155, 157f
incidence/location of, 159-160, 159*t*, 161-170f
intermediate (subacute) injury, 155, 158f
kissing lesions, 161
old (chronic) injury, 155, 155t, 158f
radiographical prediction of, 161
slab, 156-157, 160f
types of, 155-161
caudal eminence, 85, 88-89f, 89
of cervical spine, 434
arch, 434, 436, 439f
body, 434
compression, 434
dorsal element, 434, 436, 439f
growth plate, 434, 437f
ventral element, 434
chip
osteochondral, 155-156
Fractures (*Continued*)
complete (articular), 43
of condylar, 220, 225, 225f
of elbow
olecranon, 193, 195, 196f, 197f
physeal, 195
sprain-avulsion, 195-196, 198f
extensor process, 45
eye, 387, 391f, 392f
of face, 333, 335f, 336f
femoral shaft, 219-220, 224f, 225f
of fetlock joint
caudal eminence, 101-103, 105-107f
distal metacarpal/metatarsal, 105
dorsal eminence, 97-98, 100-101, 101-104f
growth plate, 103, 105, 108-109f
longitudinal, 105
plantar fragments, 103, 107f
proximal phalanx, 97
of fibula, 245, 250f
articular, 251
body, displaced, 250, 251f
body, nondisplaced, 245, 247, 250, 250f
fatigue, 245, 247, 250, 250f
stress, 245, 247, 250, 250f
glenoid, 204, 205f, 206f
of growth plate
distal femoral, 220, 225, 225f
femoral head, 216, 219f, 220f
healing, 84-85, 87f
nonhealing, 84-85, 87f
humeral stress, 208
of humerus, 209
of hyoid bone, 415-416
of mandible, 339, 342
healing of, 243f, 339, 342, 342f
postoperative radiographs of, 339, 342f
posttraumatic sequestration of, 342, 343f
radiographic detectability of, 339, 341f
of maxillary, 333, 336f
medial epicondylar, 209
of metatarsus, 299, 301-303f, 302
navicular disease
avulsion, 71, 73
body, 70-73
chip, 71, 71b
pathologic, 70, 72f
nonfracturing, 89-90
of nose, 333, 334f
occipitalcondylar, 398, 399f
of orbit, 387, 391f
palmar, 44-47f
of pastern joint, atypical
configuration of, 84, 86f
of pastern joint, growth plate, 83-84, 84-85f
closure time, 83
configuration of, 84-85f
of patella, 232-233
pathologic, 45
of pelvis, 211, 213f, 214f
phalangeal, 38
Fractures (*Continued*)
phalangeal, distal, 42-46
classification of, 43, 44t
complete (articular), 43
differential diagnosis of, 43b
healing of, 45-46
marginal sequestrum, 44
radiographic assessment, 45-46
scintigraphic assessment, 45-46
solar margin (marginal), 43-44
standard P3 series, 43
toe, 43-44
phalangeal, middle, 42
pile-driver, 434
of presphenoid, 397
of proximal sesamoid, 109-113
atypical, 109-110, 110-111f
avulsion, 112-113
basilar, 111-112, 112-114f
body, 110-111, 111f
classification of, 109-110, 110-111f
distal metacarpal stress, 113, 115
of radius, 180
body, 181-182, 184f
growth plate, 182-183, 186f
growth scar, 184, 186f
nuclear medicine and, 180-181
pseudofractures, 182-183, 185f
stress, 181
of ribs, 475, 476f
saucer, 44
of scapula/shoulder
blade, 202, 204f
glenoid, 204, 205f, 206f
supraglenoid tubercle, 202, 204f
of spine, 455-457
sprain-avulsion
of tarsus, 262, 263-265f
of stifle
articular, 242, 243f
patella, 232-233
sprain-avulsion, 234-235
stress
bilateral, 251
of tarsus, 264-266
calcaneal, 265, 266f
palmar process, 266
talar, 265-266
of teeth, 363, 366f
of temporal, 397-398
of temporomandibular joint, 347
of tibia, 245, 248f, 249f
of toe, 43-44
transport, 155
of ulna, 184, 186, 187-190f
plating, 186
wing, 44-47f
Free air
in abdomen, 524
Fungal pneumonia
in adults, 485
Fusion
of cervical spine, 453
Fusion myth, 284

G

Gastric inlet obstruction, 531-532
Gastric outlet obstruction, 531-532

Gastroenterography
gastrointestinal tract barium examination, 528, 529b
Gastrointestinal tract
abdominal topography, 527-528
of bowel mass, 527-528
of cecum, 528
of large intestine, 528
of rectum, 528
of small intestine, 528
of stomach, 527
adenocarcinoma of, 541
barium examination, 528-530
colonography, 528-529
gastroenterography, 528, 529b
pneumogastrography, 529-530
terminology of, 530
cancer of, 541
cecal/large colon volvulus, 539
cecocolic intussusception, 539
cecum
dilated, 536
nonobstructive colic, 536
clonic intussusception, 540
colitis
ulcerative, 540
ultrasound of, 540
colon
dilated, 536
nonobstructive colic, 536
dilated, 530-531
mechanical ventilation and, 531
fat and, 527
fibrosis, 541
fluid levels, 527
foreign bodies of, 532-533
ileocecal intussusception, 539
intestinal sand, 541
obstructions of, 536-539, 537b
causes of, 539b
radiographic indicator of, 536-537, 537f, 538b
strangulating, 538b, 539
vascular intestinal injury, 539
patient position and, 527
pedunculated lipomas, 539, 539b
persimmon obstruction, 532
radiographic appearance of, 530, 530f, 531f
rupture of, 532-533
small intestine
dilated, 534-536, 534f, 535b, 535f
fluid levels in, 535-536, 536f
intussusception, 536
radiographic appearance of, 534
radiometrics, 534-535
standard series of, 527
torsion of, 533, 533f
tumors of, 532
ulcer of
in adults, 531
cardia obstruction, 531
in foals, 531, 532f
pyloric stenosis, 531-532
ultrasound of, 540-541
duodenum, 540
enteroliths, 540, 541f
fecaliths, 540
Gastrointestinal tract (*Continued*)
foreign material impaction, 540
nephrosplenic entrapment and, 541
Glenoid cavity, 200
Glenoid fractures, 204, 205f, 206f
Glenoid notch, 200
Gluteal region
abscess of, 214, 215f
Grafts
bone, 25
Granulomatous infections
of orbit, 389
Granulomatous pneumonia, 486
Greater trochanter, 218-219, 224f
Greater tubercle, 200
Growth plate, 1, 5f, 6f
closure
of radius, 180, 181b, 181f, 182f
fractures of
of cervical spine, 434, 437f
distal femoral, 220, 225, 225f
femoral head, 216, 219*f*, 220f
of radius, 182-183, 186f
infection of
radius, 187-188
Growth scar fractures
of radius, 184, 186f
Gunshots, 381-382, 382f
Guttural pouches, 406-411
abscessation, 407
cellulitis, 407
cysts of, 408
deformity of, 409, 410f
ear infection, middle, 410-411
empyema, 407, 407f
fistulation, 407-408
gaseous distention of, 409-410, 410f, 411f
hemorrhage, 408-409
manta ray sign, 407, 407f
masses of, 408
mycosis, 408-409
perforation, 408-409, 409f
pharyngeal compression, 407
radiographic anatomy of, 406-407, 406f
radiographic examination of, 406
retropharyngeal adenopathy and, 409, 410f
tumors of, 408
tympany, 409-410, 410f, 411f

H

Halicephalobus gingivalis, 389
Heart
congenital anomalies of, multiple, 508
intravascular catheter unknotting, 505
murmurs of, 512
radiographic exam of, 503
size of, 506
sonography of, 503-504
anatomic assessment of, 504
color mapping, 504
spectral Doppler, 504
stress echocardiography, 504-505, 505b
Heaves
of bronchus, 494
Hemangiosarcoma
of lungs, 490
Hematoma
of carpus, 172, 173f
ethmoid, 380-381, 381f
retrobulbar, 389
of spine, 458-459, 458f
Hemoperitoneum, 524
Hemorrhage
exercise-induced pulmonary, 499, 500f
of guttural pouches, 408-409
Hernia
diaphragmatic, 479-480
pericardioperitoneal, 508-509
umbilical, 525, 525f
Herniated disk. *See* Disk, rupture of
Heterotopic polyodontia, 363, 366, 366f
Hilary step, 219
Hip
acetabulum fracture, 216, 220-223f
dislocation of, 216
femoral head fracture, 216
infection of, 218, 233f
osteochondritis of, 218
standard series of, 216, 217f, 218f
Histoplasma, 485
Hock stress radiography
of innjuries
soft-tissue, of tarsus, 262-263
HPOA. *See* Hypertrophic pulmonary osteoarthropathy
Humeral stress fracture
of shoulder, 208
Hyaline membrane disease, 500
Hydronephrosis
sonography and, 549
Hydropneumothorax, 479, 479f
Hygroma, of carpus, 172
Hyoid bone fracture, 415-416
Hyperflexion
acquired, 74
congenital, 74
distal phalangeal, 74
Hypersensitivity pneumonia, 487
Hyperthermia
exercise-induced intratendinous, 310
Hypertrophic pulmonary osteoarthropathy (HPOA), 501
pericarditis and, 515
Hypoplasia
of epiglottis, 417, 417f, 418f
Hypoplastic left heart syndrome, 508

I

Idiopathic tenosynovitis, 128
Ileocecal intussusception, 539
Immunopneumonia, 487
Industrial lung disease, 487
Infections
of bulla, 398-400, 400f, 401f
of calcaneus, 275-276, 276f, 277f
of ear, 398-400, 400*f*, 401f, 402
of ear, middle
guttural pouches and, 410-411

Infections (*Continued*)
of elbow
communicating bursal, 196-197
deep-muscle abscess, 197, 199
epicondylar abscess, 199
postoperative, 199
of fetlock joint
of distal metacarpal/metatarsal growth plate, 123
of P1, 125, 126-127f
of sesamoid, 123, 125
of hip, 218, 233f
of mandible, 342-343, 344f, 356-363
apical, 357
clinical presentation of, 356
computed tomography of, 362, 365f
foreign body, 343, 345f
nuclear imaging of, 363
progression of, 358, 363-365f
pulpitis, 357
radiographic appearance of, 357-358, 359-362f
sequestration, 342-343
ultrasound of, 358, 362
of maxilla, 333, 337f, 356-363
apical, 357
clinical presentation of, 356
computed tomography of, 362, 365f
nuclear imaging of, 363
progression of, 358, 363-365f
pulpitis, 357
radiographic appearance of, 357, 358f, 359f
ultrasound of, 358, 362
of metacarpus
physeal, 140, 141-142f
surgical, 145, 147f
navicular disease, 69-70, 71-72f
of orbit, 387, 389
bacterial, 387, 389, 391f, 392f
granulomatous, 389
of P3
bone cysts, 52
coffin joint dislocation, 51-52, 58f
drainage, 50, 50f
focal marginal bone loss, 51, 53-55f
foreign bodies, 51, 52-53f
gas, 48f, 49, 49f
marking studies, 50, 50f
osteitis, 46
osteochondritis, 52
osteomyelitis, 46, 51-52
periosteal difference, 46, 49
periostitis, 46
points of attack, 49
radiographic indicators, 48f, 49, 49f
septic arthritis, 51-52
sequestration, 51, 56f
sinography, 50, 50f
soft-tissue defects, 51, 51f
of pastern joint, 90, 93-94f, 93-95
of patella, 234, 234f
of pelvis, 211, 213, 214f
Infections (*Continued*)
physeal, of metacarpus, 140, 141-142f
of spine
abscess, 458
diskospondylitis, 458
fistulous withers, 457f, 458
hematoma, 458-459, 458f
spondylitis, 457-458, 458
supraspinatous bursitis, 458
surgical
of calcaneus, 277-278
of metacarpus, 145, 147f
of sustentaculum tali, 274-275, 276f
of tarsus, 267-274
inoculation-type joint, 267-268, 271f
septic arthritis, 269, 271-274f, 274
septicemia joint, 267-268, 269f, 270f
of tendon
lacerations and, 325, 326
of thyrohyoid, 399-400, 400f, 401f
of umbilicus, 551, 551f, 552f
Inferior check ligaments
anatomy of, 305, 308, 308f, 309f
Inflammatory pericardial disease, 514
Inhalation pneumonia, 486
Injuries
catastrophic, 97, 101f
to chest wall, 475-477
emphysema, 475
lung bruising, 475
pneumothorax, 475, 476b, 476t, 477, 477f, 478f
rib fractures, 475, 476f
wound penetration, 475
to eye, 387-391, 390f
foreign body, 389
fracture, 387, 391f, 392f
infection, 387, 389
retrobulbar abscessation, 389
retrobulbar hematoma, 389
sequestra, 391, 393f
soft-tissue, of tarsus, 261-264
bruising, 261-262, 262f
capsular tearing of, 263-264
crushing, 261-262, 262f
hock stress radiography, 262-263
lacerations, deep, 262
nuclear scintigraphy of, 263
puncture wounds, 262
ruptured peroneus tertius, 262
sprain, 262, 263-265f
sprain-avulsion fracture, 262, 263-265f
strain, 262
to spine
fractures, 455-457
lumbar, 457
thoracic, 455, 457
to trachea, 424, 424f, 425f
Inoculation-type joint infection
of tarsus, 267-268, 271f
Intercondylar eminence
fragmentation of, 239-240, 241f, 242f
Interosseous epidermoid cyst
of mandible, 345
Interstitial pneumonia
in adults, 484, 485f
in foals, 481-482, 483f
Intertarsal drilling, 284-286, 286f, 287f
Intervertebral disk
rupture of, 452
Intestines
large. *See* Large intestine
small. *See* Small intestine
Intussusception, 536, 539
Invasive pulmonary aspergillosis. *See* Pulmonary aspergillosis
Involucrum, 277
Ischial tuberosity
abnormal uptake patterns of, 213-214
nuclear imaging of, 213-214
uptake ratio of, 213

J

Joint(s)
coffin, 51-52, 73
congenital facetal joint asymmetry and osteoarthritis of, 440-441
coxal, 216
dislocation
coffin joint, 51-52
of coxal joint, 216
of temporomandibular joint, 347-348, 350f, 351f
distal interphalangeal, 73-74
contracture of, 18
femoropatellar, 228
femorotibial, 228
fetlock
anatomic variants of, 96
arthrography of, 128
comparable anatomic specimens of, 99-110f
contracture of, 18
diagnostic approach to, 96-97
dislocations
metacarpophalangeal/metatarsophalangeal, 105, 109
distal sheath
swelling of, 128
fractures of
caudal eminence, 101-103, 105-107f
distal metacarpal/metatarsal, 105
dorsal eminence, 97-98, 100-101, 101-104f
growth plate, 103, 105, 108-109f
longitudinal, 105
plantar fragments, 103, 107f
proximal phalanx, 97
infection of
of distal metacarpal/metatarsal growth plate, 123
of P1, 125, 126-127f
of sesamoid, 123, 125
magnetic resonance imaging of, 96
osteoarthritis of
capsular region, 115
cartilage space, 120, 124f

Joint(s) (*Continued*)
cranial aspect, 116
O'Brien's five region strategy to, 115
osteophytes, 120, 124f
palmar/plantar aspect, 116
sesamoid bones, 116
osteochondritis of
metacarpus/metatarsal III, 116, 117-118f
P1, 116, 116t
proximal sesamoid, 109-113, 110f
fractures of, 109-113
primary injury mechanisms of, 109
sesamoiditis, 118, 119-122f, 120
sprain-avulsion-fractures of, 120, 122-123f
sprains of, 120, 122-123f
standard views of, 96, 97-99f, 98t
synovioma of, 120, 123, 125f
inoculation-type joint, tarsus infection, 267-268, 271f
pastern, 94
abnormal width of, 77
arthrodesis, 94
cuts of, 90, 93-94f, 93-95
fractures of, growth plate, 83-84, 84-85f
closure time, 83
configuration of, 84-85f
infections of, 90, 93-94f, 93-95
narrowing of, 77, 79f
osteochondritis, 93-94
punctures of, 90, 93-94f, 93-95
ringbone of, 78-83
deep punctures, 83
definition of, 78, 80, 80f, 81f
high/low, 81
implant dislocation, 82-83
infection, postoperative, 82-83
lacerations, 83
phalangeal lateral ridges, 83
primary, 80, 81f
screw breakage, 82-83
secondary, 80, 82f
sprains, 83-84f
surgical fusion attempt of, 81-83, 83f
types of, 80-81
standard series of, 77, 78-79f, 78t
tumors of, 94
widening of, 77, 78f, 80f
sacroiliac, 211
septicemia joint, tarsus infection, 267-268, 269f, 270f
temporomandibular (TMJ), 345-347, 347f
angle-dependent variation, 346-347, 349f
customized views of, 347, 350f
dislocation of, 347-348, 350f, 351f
fractures of, 347
radiographic sensitivity of, 345-346, 348f
Joint laxity, 16, 19f
Joint mice, 290
Jugular vein
catheter and, 422-423, 424b
fistula of, 423-424
Jugular vein (*Continued*)
sonography of, 422, 423f
thrombi classification of, 422
thrombophlebitis of, 422
thrombosis of, 422
venography of, 422, 423f

K

Keratoma
of coronary region, 53, 58
of pastern joint, 94
Kidney stones
sonography and, 548

L

Lameness
duration of, 39
Laminitis, 36, 36f, 37f
advanced age and, 41
blood supply in, 41-2, 42t
corrective shoeing, 39, 41
development of, in opposite foot, 39, 39b
pituitary disease and, 41
radiographic prognosis in, 39
thermography in, 30
trimming, 39, 41
Large intestine
abdominal topography of, 528
Larynx
disease of
arytenoid chondritis, 414
calcification, 415, 415f
collapse, 413
congenital web, 414
epiglottis, 413, 413f, 414f
Leaning off, 57f, 77
Leiomyosarcoma
of mandible, 344
Lesser trochanter, 218-219
Ligaments
anatomy of, 309, 309t
classification of
lesion echogenicity and, 312
lesion location and, 312
lesion pattern and, 312
lesion severity and, 312
injuries
classification of, 311-312
descrption of, 311-312
experimental, 311
nonlacerative, 309, 310t
sonography of, 321-324323f, 324t
spine and, 455
nuclear imaging of, 318-319
sonography of, 312f, 319-320, 319b, 320f, 322f
thermography of, 318-319
Limbs
angulation, 10, 13-15f
curvature of, abnormal, 10, 13-15f
causes of, 16-17, 19f, 20f
Linford method, 38
Lipomas
pedunculated, 539, 539b
Liver
disease of
abscesses, 544
bile flow assessment, 545, 545t
cholelithiasis, 544
pyrrolizidine alkaloid poisoning, 545
sonography of, 544, 545b
tumors, 545
Loculated fluid
of mediastinum, 491
Long digital extensor tendon
sprain-avulsion-fractures of, 235
Lumbar spine
injuries of, 457
Lungs
abscess of
pneumonia and, 486-487, 487f, 488f
bruising of, 475
cancer of
pleural fluid and, 491
diseases of
in adults, 462, 466f, 467f
bronchial cross-sections and, 462, 467f
bronchial thickening, 462-463, 467f
in foals, 462
industrial, 487
radiographic indicators of, 468
tumors of
fibrosarcoma, 490-491
hemangiosarcoma, 490
mediastinal, 491
pleural, 491
primary, 490
radiographic appearance of, 490-491
secondary, 490
Lungworm, 488
Lymphedema
of metatarsus, 303
Lymphoid hyperplasia
of pharynx, 412-413
Lymphosarcoma
of bladder, 549
of mediastinum, 491

M

Magic-angle effect, 31
Magnetic resonance imaging (MRI)
of brain, 402
of cadaver feet, 31
of carpus, 178
of face, 374
of live horses, 32
nuclear medicine
of foot, 31-32
of tarsus, 261
of tendons injuries, 311
Magnetography. *See* Magnetic resonance imaging (MRI)
Mandible
brachygnathia of, 348
congenital malformation of, 348
dental infection of, 356-363

Mandible (*Continued*)
apical, 357
clinical presentation of, 356
computed tomography of, 362, 365f
nuclear imaging of, 363
progression of, 358, 363-365f
pulpitis, 357
radiographic appearance of, 357-358, 359-362f
ultrasound of, 358, 362
examination of, 339, 340f, 341f
fractures of, 339, 342
healing of, 243f, 339, 342, 342f
postoperative radiographs of, 339, 342f
posttraumatic sequestration of, 342, 343f
radiographic detectability of, 339, 341f
infection of, 342-343, 344f
foreign body, 343, 345f
sequestration, 342-343
parotid duct of
atresia, 348-349, 351
cavographic diagnosis of, 349, 351
obstruction, 348-349, 351
temporomandibular joint, 345-347, 347f
angle-dependent variation, 346-347, 349f
customized views of, 347, 350f
dislocation of, 347-348, 350f, 351f
fractures of, 347
radiographic sensitivity of, 345-346, 348f
tumors of, 343-344
adamantinoma, 344, 346f
bone cysts, 344-345
interosseous epidermoid cyst, 345
leiomyosarcoma, 344
ossifying fibroma, 344, 347f
osteosarcoma, 343-344, 345f, 346f
Manta ray sign, 407, 407f
Mare reproductive loss syndrome, 514
Marie's disease, 501
Masses
of guttural pouches, 408
of sinus, 378-380, 380f
Maxilla
dental infection of, 356-363
apical, 357
clinical presentation of, 356
computed tomography of, 362, 365f
nuclear imaging of, 363
progression of, 358, 363-365f
pulpitis, 357
radiographic appearance of, 357, 358f, 359f
ultrasound of, 358, 362
fractures of, 333, 336f
infection of, 333, 337f
tumors of, 333, 337f, 338
Medial epicondylar fracture
of shoulder, 209
Mediastinum
tumors of
abscess, 491
loculated fluid, 491
lymphosarcoma, 491
Megaesophagus, 427-428, 429f, 531
Melanoma, malignant
of coronary region, 58
of pastern joint, 94
Meningomyelocele, 452
Menisci, 229
Mesothelioma
malignant, 491
Metacarpus
cannon bones, fractures of
of growth plate, 134
incomplete dorsal metacarpal stress, 135
proximal palmar stress, 134-135
carpal spavin of, 142, 145-146f
curvature of, in adult horses, 146-147, 147f
imaging findings of, 136f
arterial injury, 135
collateral circulation, 135
complete metacarpal fracture, 135, 136f
metacarpal fracture healing, 135, 137-138f
osselets, 146, 147f
osteomyelitis *vs.* periostitis, 140, 141-142
physeal infection of, 140, 141-142f
sequestration of, 140, 142-143f
sonography of, 305, 306f
splint bones, 132f
active *vs.* inactive, 130
fractures of, 130, 133-134f
irradiated, radiographic evaluation of, 131
sprains
presentation of, 309-311, 309f
standard series of, 130, 131-132t, 131f
strains
presentation of, 309-311, 309f
surgical infections of, 145, 147f
traumatic exostosis of, 135, 138-139f
wounds of
drainage of, 139-140, 140f
gas pockets, 138-139, 139f
periosteal new bone, 139
swelling, 138
tissue defects, 138
Metatarsus
fracture of, 299, 301-303f, 302
lymphedema of, 303
soft-tissue foreign body of, 297, 301f
sonography of, 305, 306, 307f
sprain of, 297, 299
presentation of, 309-311, 309f
standard series of, 297, 298f, 300b
strains
presentation of, 309-311, 309f
strategic facts about, 297, 299f, 300f
tumors of, 302-303, 303f
Metrizamide myelography, 443
Monteggia fracture, 199
Multiple hereditary exostoses, 21
Murmurs, of heart, 512
Mycetoma, 486
Mycosis
of guttural pouches, 408-409
Mycotic pneumonia
in adults, 485
Myelography
vertebral instability and
cord angulation, 446-447, 449f
cord lift, 446, 448f
diagnosis of, 445-447
diskal indentation, 445-446, 448f
dural pinching, 445
flow failure, 448, 451f
image quality, 443-444
lesion probability, 444
metrizamide, 443
misdiagnosis of, 448, 449b
nonstress, 444-445, 446f, 447f
risk of, 444, 446f
standing, 450
Myocardial disease
ventricular tachycardia and, 512

N

Nancy view
of angular limb deformity, 15-16, 16f, 17f
Nasolacrimal duct obstruction, 382-384
anatomy of, 382
radiographic, 383-384
dacryocystorhinography of, 384
in eye, 393, 395
anatomy of, 393
causes of, 393, 395, 395f
Navicular disease
anatomic variations of, 58-60, 59b, 61-63f
bipartite deformities, 73, 73f
bursa, distal interphalangeal joint and, 73-74
caudal heel pain syndrome, 62
chip fractures, 71, 71b
coffin joint, 73
congenital multipiece, 73, 73f
fractures
avulsion, 71, 73
body, 70-73
chip, 71, 71b
pathologic, 70, 72f
gross view, 62-63, 65f
high coronary view of, 65, 67f, 68f
infection, 69-70, 71-72f
lateral view of, 65, 68f
low coronary view of, 67
projectional variations of, 60, 62, 63-65f
radiographic indications of, 63-65, 64t, 66f
scintigraphic diagnosis of, 68-69
skyline view of, 65, 67, 69-71f
soft-tissue mineralization, 73
standard series, 58, 59t, 61f
thermography for, 30

Navicular disease (*Continued*)
tripartite deformities, 73, 73f
vascular channel redux, 67-68
Neck
bronchus, 431
carotid artery
Doppler of, 424
cervical esophagus
aortic arch of, 428
barium swallow and, 426
choking, 427, 427b, 427f, 428f
complications of, 429, 430f
cysts of, 429-430
dilation of, 427-428, 429f
diverticula, 428-428
esophagography of, 426
fistula of, 430
obstruction of, 427, 427b, 427f, 428f
phytobezoar, 429
pressure and, 426
radiography of, 426, 426b
rupture of, 430
stricture, 429
tumors of, 430, 431b
vascular ring anomaly, 428
jugular vein
catheter and, 422-423, 424b
fistula of, 423-424
sonography of, 422, 423f
thrombi classification of, 422
thrombophlebitis of, 422
thrombosis of, 422
venography of, 422, 423f
sinuses
drainage of, 431, 431b
trachea, 424f
aspiration of, 424-425
collapse of, 425
injury to, 424, 424f, 425f
tracheostomy and, 425, 425f
Nephritis
sonography and, 549
Nephrolithiasis
sonography and, 548
Nerve injury
pelvis and, 214
Nose
foreign bodies of, 382, 383f
fractures of, 333, 334f
gunshot to, 381-382, 382f
standard views of, 371
Nuclear imaging. *See also* Radionuclide imaging
of mandible
infections, 363
of maxilla
infections, 363
of pelvis, 213-214
of sacroiliac joint, 211
of suspensory ligaments, 321
of tendons, 318-319
of thorax, 468
Nuclear medicine. *See also* Radionuclide imaging
of foot
computed tomography, 31
Nuclear medicine (*Continued*)
magnetic resonance imaging, 31-32
thermography, 30-31
radius fractures and, 180-181
Nuclear scintigraphy
of tarsus, 263

O

O'Brien, T.R., 115
Occipitalcondylar fracture, 398, 399f
Occipitoatlantoaxial dysplasia, 452
OCD. *See* Osteochondritis dissecans
Odontoma
of teeth, 369
Olecranon fractures
of elbow, 193, 195, 196f, 197f
Olecranon hygroma
of elbow, 193
Open fracture, 23
Orbit. *See also* Eye
fracture of, 387, 391f
infection of, 387, 389
bacterial, 387, 389, 391f, 392f
granulomatous, 389
Ossification centers, separate
appearance of, 4, 4t, 5f
disappearance of, 4, 4t, 5f
Ossification fronts, 4, 5f, 6
Ossified collateral cartilages. *See* Side bones
Ossifying fibroma
of mandible, 344, 347f
Osteoarthritis
of cervical spine, 439-440, 441f
congenital facetal joint asymmetry and, 440-441
of fetlock joint
capsular region, 115
cartilage space, 120, 124f
cranial aspect, 116
O'Brien's five region strategy to, 115
osteophytes, 120, 124f
palmar/plantar aspect, 116
sesamoid bones, 116
of tarsus, 266-267, 268f
Osteochondral chip fractures, 155-156
Osteochondral lesions
formation of, 235-236
Osteochondritis, 20-21, 168, 172f
cystic femoral, 239
femoral, 236
of fetlock joint
metacarpus/metatarsal III, 116, 117-118f
P1, 116, 116t
of fibula, 253
fractured caudal eminence *vs.*, 101-103, 105-107f
of hip, 218
of pastern joint, 93-94
of patellar, 236, 237f
of shoulder, 208, 210f
of tarsus, 286-290
distal talar tuberosity, 290, 291f
distal tibial epiphysis, 286
Osteochondritis (*Continued*)
sagittal ridge, 286, 288, 288f
third bone of, 290, 292f, 293f
tibial malleolus, 288, 289f
trochlear ridges, 288, 289-291f
Osteochondritis dissecans (OCD). *See* Osteochondritis
Osteochondrosis, 20
zinc-induced, 21
Osteochondrositis. *See* Osteochondritis
Osteoma
of teeth, 369
Osteomyelitis, 241-242, 242f, 243f
of tarsus, 267-274
inoculation-type joint, 267-268, 271f
septic arthritis, 269, 271-274f, 274
septicemia joint, 267-268, 269f, 270f
Osteopetrosis, 21
Osteosarcoma
of mandible, 343-344, 345f, 346f
of ulna/radius, 191
Otitis media, 398-400, 400f, 401f

P

P3
absence of, 52-53
anatomic variations of
cortical thickness of, 33
degree of arch of, 33
extensor process, 33-34, 35f
foals *vs.* adults, 32
frontal profile, 32
lateral profile, 32
rotation of, 33
side bones, 33, 34f
simulated lesions, 33-34, 35f
solar margin, 33, 33f
trabeculation of, 33, 34f
vascular channels, 33, 33f
vascularity of, 32, 32f
hypoplasia of, 53
infection of
bone cysts, 52
coffin joint dislocation, 51-52, 58f
drainage, 50, 50f
focal marginal bone loss, 51, 53-55f
foreign bodies, 51, 52-53f
gas, 48f, 49, 49f
marking studies, 50, 50f
osteitis, 46
osteochondritis, 52
osteomyelitis, 46, 51-52
periosteal difference, 46, 49
periostitis, 46
points of attack, 49
radiographic indicators, 48f, 49, 49f
septic arthritis, 51-52
sequestration, 51, 56f
sinography, 50, 50f
soft-tissue defects, 51, 51f
Pain
caudal heel pain syndrome, 30, 62, 67, 74

Pain (*Continued*)
palmar heel pain syndrome, 30
spine and
ligament injury and, 455
overuse, 455
sprain, 455
Palatal myositis, 413
Palate
hypoplasia of, 411
displacement of, 411-412
Palmar heel pain syndrome
thermography for, 30
Palmar process fractures
of tarsus, 266
Paracoxal foreign body, 225-226, 226f
Paranasal sinus cysts, 378-380, 378b, 379f
Paranasal sinusography, 372
Parasitic pneumonia, 487
Parotid duct
of mandible
atresia, 348-349, 351
cavographic diagnosis of, 349, 351
obstruction, 348-349, 351
Pastern joint
abnormal width of, 77
arthrodesis, 94
cuts of, 90, 93-94f, 93-95
fractures of, growth plate, 83-84, 84-85f
closure time, 83
configuration of, 84-85f
infections of, 90, 93-94f, 93-95
narrowing of, 77, 79f
osteochondritis, 93-94
punctures of, 90, 93-94f, 93-95
ringbone of, 78-83
deep punctures, 83
definition of, 78, 80, 80f, 81f
high/low, 81
implant dislocation, 82-83
infection, postoperative, 82-83
lacerations, 83
phalangeal lateral ridges, 83
primary, 80, 81f
screw breakage, 82-83
secondary, 80, 82f
sprains, 83-84f
surgical fusion attempt of, 81-83, 83f
types of, 80-81
standard series of, 77, 78-79f, 78t
tumors of, 94
widening of, 77, 78f, 80f
Patella
congenital, 233-234
congenital absence of, 234
dislocation of, 233, 233f, 234f
fracture of, 232-233
infection of, 234, 234f
osteochondritis of, 236, 237f
standard series of, 227, 231f
Patellar ligament
sprain-avulsion-fractures of, 235
Pedal osteitis, 36
Pelvis
abscess, 214, 215f
fracture of, 211, 213f, 214f
Pelvis (*Continued*)
infection of, 211, 213, 214f
ischial tuberosity
abnormal uptake patterns of, 213-214
nuclear imaging of, 213-214
uptake ratio of, 213
nerve injury, 214
standard series of, 211, 212f
thigh
strain of, 214
third trochanter
abnormal uptake patterns of, 213-214
nuclear imaging of, 213-214
uptake ratio of, 213
vascular disease and, 215
Pericardioperitoneal hernia, 508-509
Pericarditis
classification of, 513
constrictive, 514
effusive, 513-514
fibrinous, 513
hypertrophic pulmonary osteoarthropathy and, 515
restrictive, 513
Periodontal membrane, 353
Periosteal osteosarcoma, 204
Peritoneum
inflammation of, 524, 524f
radiography of, 523-524
celiography, 523-524
peritonography, 523-524
single-target protocol, 523
Peritonitis, 524, 524f
Peritonography, 523-524
Peroneus tertius
rupture of
of tarsus, 262
Peroneus tertius tendon
sprain-avulsion-fractures of, 235
Phalangeal
displacement, 38
distal
dislocation (subluxation), 46, 48f
fractures of, 42-46
hyperflexion of, 74
estimation lines, 37-38
foundered, 38-39, 39-42f
fractures, 38
of distal, 42-46
of middle, 42
gas, 38, 38f
hoof wall, 38
laminitis, 39-42
middle
fractures of, 42
new bone, 38
radiometrics, 7f, 36-37
rotation, 36-37
sinking, 38
Pharyngeal
compression
guttural pouches and, 407
Pharynx
cancer of, 413
collapse of, 413
Pharynx (*Continued*)
cysts of, 413
diseases of, 411-412
abscessation, 412, 412f
palatal, hypoplasia of, 411
foreign body of, 412
lymphoid hyperplasia of, 412-413
palatal myositis, 413
Physeal fractures
of elbow, 195
Phytobezoar
cervical esophagus, 429
cervical esophagus and, 429
Pile-driver fracture, 434
Pituitary disease
laminitis and, 41
Pleura
malignant mesothelioma, 491
tumors of, 491
Pleural fluid, 477, 479, 479b, 479f
causes of, 469, 470b
consequences of, 469
lung cancer and, 491
radiographic appearance of, 469-470
sonographic appearance of, 471, 473f, 474, 474f
Pleuritis
sonographic appearance of, 471, 472
Pleuropneumonia, 482-483. *See also* Pleural fluid
Pneumatosis intestinalis, 536
Pneumoconiosis, 487
Pneumocystis carinii
in foals, 482
Pneumogastrography
gastrointestinal tract barium examination, 529-530
Pneumomediastinum, 479, 479f
Pneumonia
in adults
bacterial, 482-484
fungal, 485
interstitial, 484, 485f
mycotic, 485
septicemia, 484-485
sonology, 483-484, 484f, 485f
toxemia, 484-485
aspiration, 486
in foals
interstitial, 481-482, 483f
newborn, 481, 482f
Pneumocystis carinii, 482
granulomatous, 486
hypersensitivity, 487
inhalation, 486
lung abscess, 486-487, 487f, 488f
parasitic, 487
pneumomediastinum, 488
radiographic appearance of, 481
Rhodococcus equi, 481
viral, 486
Pneumothorax
injury to, 475, 476b, 476t, 477, 477f, 478f
Podotrochlear apparatus, 28

Poisoning
pyrrolizidine alkaloid, 545
yellow-star thistle, 403
Polydactylism, 21
Positive silhouette sign, 506
Presphenoid fractures
of skull, 397
Protozoal myeloencephalitis, 450, 451f
Proximal interphalangeal joint. *See* Pastern joint
Proximal sesamoid
fetlock joint, 109-113, 110f
fractures of, 109-113
primary injury mechanisms of, 109
fractures of
atypical, 109-110, 110-111f
avulsion, 112-113
basilar, 111-112, 112-114f
body, 110-111, 111f
classification of, 109-110, 110-111f
distal metacarpal stress, 113, 115
Pseudofractures
of radius, 182-183, 185f
Pthium, 485
Pulmonary aspergillosis, 486
Pulmonary blastomycosis, 486
Pulmonary coccidioidomycosis, 485
Pulmonary infarction, 488
Pulmonary osteopathy, 501
Pulmonary thrombosis, 488
Pulpitis
of mandible, 357
of maxilla, 357
Pyrrolizidine alkaloid poisoning
liver disease and, 545

R

Racehorses
heart murmurs in, 512
Radiographic appearance of
pleural fluid, 469-470
Radiographic disease indicator (RDI)
of atony, 538b
intestinal obstruction and, 538b
vertebral instability and, 443, 444-445f
Radiography. *See also* Computed radiography
of acute flexor tendon, 316
of angular limb deformity, 17, 20b
of arthritis of carpus, 163-164
atony, radiographic disease indicator, 538b
of bones splint, metacarpus, 131
of carpus
arthritis, 163-164
beam angle, 154-155, 156-157f
fractures, 161
of cervical esophagus, 426
of cervical spine, vertebral instability of, 442, 442f, 443f
in focal marginal bone loss, 53-55f
of foot, 28, 29f, 30t
preparation for, 35-36, 36f
of fractures
of carpus, 161
Radiography (*Continued*)
of mandible, 339, 341f, 342f
phalangeal, distal, 45-46
of gastrointestinal tract
appearance of, 530, 530f, 531f
obstructions of, 536-537, 537f, 538b
small intestine, 534
of guttural pouches, 406-407
of heart, 503
of infections
of mandible, 357-358, 359-362f
of maxilla, 357, 358f, 359f
of P3, 48f, 49, 49f
of injuries
soft-tissue, of tarsus, 262-263
of laminitis, 39
of lungs, 468
diseases of, 468
tumors of, 490-491
of mandible
dental infection of, 357-358, 359-362f
fractures of, 339, 341f, 342f
temporomandibular joint, 345-346, 348f
of maxilla
dental infection of, 357, 358f, 359f
of metacarpus, splint bones, 131
of nasolacrimal duct obstruction, 383-384
of navicular disease, 63-65, 64t, 66f
of neck, cervical esophagus, 426, 426b
of P3 infection, 48f, 49, 49f
of peritoneum, 523-524
celiography, 523-524
peritonography, 523-524
single-target protocol, 523
of pleural fluid, 469-470
diaphragmatic slope, 470, 470f
level of, 469, 470f
zone of, 469-470, 471f
of pneumonia, 481
of shoulder, 200, 202f, 210f
of sinonasal disease, 317, 375, 375t
of sinusitis, secondary, 377, 377f
of skull, 329-332, 330-332f
of small intestine, 534
of soft-tissue injury of tarsus, 262-263
of spine, 455
thoracolumbar, 455, 456f
of splint bones, of metacarpus, 131
of squamous cell carcinoma, 490
of stifles, lesions of, 230-232
of suspensory ligaments, 320-321, 321b, 321t
of tarsus
bone spavin, 282-284, 284f, 285f
injury, soft-tissue, 262-263
of teeth, 355, 357f, 358f
of temporomandibular joint (TMJ), 345-346
of thoracolumbar spine, 455, 456f
of thorax and lung disease, 468
Radiography (*Continued*)
of throat, guttural pouches, 406-407, 406f
of tumors, of lungs, 490-491
of ulna, 180, 183f
of vertebral instability, of cervical spine, 442, 442f, 443f
Radionuclear compartmental syndrome, 191-192
Radionuclide imaging
of foot, 28
Radiopharmaceutical uptake patterns
abnormal radiographs findings and, 30
age and, 29
breed and, 29
nerve block and, 30
usage and, 29
Radius. *See also* Ulna
dislocation of, 186-187, 191f
fractures of, 180
body, 181-182, 184f
growth plate, 182-183, 186f
growth scar, 184, 186f
nuclear medicine and, 180-181
pseudofractures, 182-183, 185f
stress, 181
growth plate closure, 180, 181f, 182f
times of, 180, 181b
growth plate infection, 187-188
fractures and, 187-188
osteochondritis of, 192, 192f
standard series of, 180
tumors of, 191f
chondroma, 188, 191
chondrosarcoma, 191
osteosarcoma, 191
Radon seeds
tarsus and, 293, 294f
RDI. *See* Radiographic disease indicator
Rectum
abdominal topography of, 528
Respiratory distress syndrome, 500
adult, 501
Retrobulbar abscessation, 389
Retrobulbar hematoma, 389
Retropharyngeal adenopathy
of guttural pouches, 409, 410f
Retropharyngeal lymph node
abscessation of, 416
Rhinitis
sinonasal disease and, 376-377, 376f
Rhinosinusitis, 377
sinonasal disease and, 377
Rhodococcus, 487
Rhodococcus equi, 211, 241, 481
Ribs
fracture of, 475, 476f
Ringbone
of pastern joint, 78-83
deep punctures, 83
definition of, 78, 80, 80f, 81f
high/low, 81
implant dislocation, 82-83
infection, postoperative, 82-83

Ringbone (*Continued*)
lacerations, 83
phalangeal lateral ridges, 83
primary, 80, 81f
screw breakage, 82-83
secondary, 80, 82f
sprains, 83-84f
surgical fusion attempt of, 81-83, 83f
types of, 80-81
Roman-nosed, 32, 60f
Rostrocaudal
view of, 371

S

Sacroiliac joint
nuclear imaging of, 211
standard series of, 211, 213f
Salivary glands
cavography of, 405
congenital defects, 405
tumors of, 405-406
Sarcocystis neuroma, 402, 450
Scapula blade fractures, 202, 204f
Scapular fracture
of shoulder
blade, 202, 204f
glenoid, 204, 205f, 206f
supraglenoid tubercle, 202, 204f
Scapular pitfall, 200, 203f
Scapular tumors, 204
Scintigraphy
in diagnosis of navicular disease
bone-phase, 68
force-plate analysis, 68-69
soft-tissue, 68
Secondary bronchiectasis, 493
Septal deviation, 382
Septic arthritis, 241-242, 242f, 243f
of tarsus, 269, 271-274f, 274
Septic cordal, rupture of, 513, 513f, 514f
Septic physitis, 187-188
Septicemia, 484-485
Sequestra, 44
Serous arthritis, 163
Serratia marcescens, 513
Sesamoiditis
of fetlock joint, 118, 119-122f, 120
Sharpey's fibers, 353
Shoeing, corrective
for laminitis, 39, 41
Shoulder
arthrography, 206-207
femoral head fracture, 207, 208f, 209f
greater tubercle fracture, 207
technique of, 206
bicipital tenosynovitis, 208
dislocation of, 207
foreign bodies in, 205-206
humeral fracture, 209
humeral stress fracture, 208
medial epicondylar fracture, 209
ossification centers, 200, 203f
osteochondritis of, 208, 210f
radiographic strategy, 200, 202f, 210f
Shoulder (*Continued*)
scapular fracture
blade, 202, 204f
glenoid, 204, 205f, 206f
supraglenoid tubercle, 202, 204f
scapular pitfall, 200, 203f
scapular tumors, 204
sequestra of, 205-206
sinography of, 205, 206f, 207f
sinus tracts of, 205-206
sonography of, 205-206, 207f
appearance of, 201-202
Shunt
intrapulmonary, 509-510
right-to-left, 509, 509b
Side bones
P3, anatomic variations of, 33, 34f
Single-target protocol (STP)
peritoneum and, 523
Sinography
of carpus, 178
of eye, 393
of shoulder, 205, 206f, 207f
of tarsus, 78f, 278-279, 279f
Sinonasal disease
abnormalities causing, 375-377, 375b
congenital/developmental, 375-376
rhinitis, 376-377, 376f
clinical signs of, 374, 375b
computed tomography of, 382, 384f, 385f
dentigerous cyst, 382
differential radiographic diagnosis of, 375, 375t
empyema, 378, 378f
ethmoid hematoma, 380-381, 381f
foreign bodies of, 382, 383f
masses, 378-380, 380f
nasolacrimal duct obstruction and, 382-384
anatomy of, 382
dacryocystorhinography, 384
paranasal sinus cysts, 378-380, 378b, 379f
prevalence of, 374, 375b
radiographic diagnosis of, 371
rhinosinusitis, 377
septal deviation, 382
series of, 371
sinusitis, 377
primary, 377
secondary, 377-378, 377f
tumors, 378-380, 380f
unilateral epistaxis, cause of, 374-375
Sinuses
drainage of, 431, 431b
foreign bodies of, 382, 383f
gunshot to, 381-382, 382f
standard views of, 371, 372-374f
Sinusitis, 377
primary, 377
secondary, 377-378, 377f
computed tomography of, 377-378
radiographic findings in, 377, 377f
Skull
basilar fractures of, 396-398
basisphenoid-basioccipital, 396-397, 397f, 398f, 399f
occipitalcondylar, 398, 399f
presphenoid, 397
temporal, 397-398
radiographic examination of, 329-332, 330-332f
computed tomography, 330, 332f
sarcoids of head, 330, 332
Skyline view
of navicular disease, 65, 67, 69-71f
Slab fractures
of carpus, 156-157, 160f
Slipped capital physis, 216
Slow flow theory, 187
Small intestine
abdominal topography of, 528
dilated, 534-536, 534f, 535b, 535f
fluid levels in, 535-536, 536f
intussusception, 536
radiographic appearance of, 534
radiometrics, 534-535
Soft callus, 27
Soft-tissue injury
of tarsus, 261-264
bruising, 261-262, 262f
capsular tearing of, 263-264
crushing, 261-262, 262f
hock stress radiography, 262-263
lacerations, deep, 262
nuclear scintigraphy of, 263
puncture wounds, 262
ruptured peroneus tertius, 262
sprain, 262, 263-265f
sprain-avulsion fracture, 262, 263-265f
strain, 262
Soft-tissue windows, 31
Solar abscess
thermography for, 30
Sonography
of acute flexor tendon, 313-316
echogenicity, 314
edema and, 314
effusion, 31f, 314, 316, 318f
hemorrhage and, 314
interior changes, 314
regional hyperemia, 314
shape, abnormal, 313-314
size, 313
strains, 314-317f
of carpus, 178
of digital flexor tendon sheath, 95
of fibula, 253
of heart, 503-504
anatomic assessment of, 504
color mapping, 504
spectral Doppler, 504
of jugular vein, 422, 423f
of liver disease, 544, 545b
of metacarpus, 305, 306f
of metatarsus, 305, 306, 307f
pleural fluid appearance and, 471, 473f, 474, 474f
pleuritis and, 471, 472

Sonography (*Continued*)
regional nerve blocks and, 326
of shoulder, 201-202, 205-206, 206f, 207f
of tarsus, 293-294
of tendon injuries, 321-324323f, 324t
of tendons injuries, 311
of umbilicus, 550-551, 550f, 550t
infection, 551, 551f, 552f
of urinary tract, 548-550
biopsy, 548
bladder rupture, 549
calculi, 548
carcinoma, 549
dysplasia, 548
ectopic ureter, 548
hydronephrosis, 549
kidney stones, 548
nephritis, 549
nephrolithiasis, 548
tumors, 549-550
umbilical evagination, 549, 549b
ureteral stenosis, 549
Sonology
adult pneumonia and, 483-484, 484f, 485f
Sonometrics
of eye, 387, 389f, 390t
Sphenooccipital suture, 396
Spina bifida, 452
Spine
infection of
abscess, 458
diskospondylitis, 458
fistulous withers, 457f, 458
hematoma, 458-459, 458f
spondylitis, 457-458, 458
supraspinatous bursitis, 458
injuries to
fractures, 455-457
lumbar, 457
thoracic, 455, 457
pain and
ligament injury and, 455
overuse, 455
sprain, 455
radiography of, 455
thoracolumbar
radiographic anatomy of, 455, 456f
tumors of, 459
Spleen, 544
nephrosplenic entrapment, 545-546, 546f
tumors of, 546-547, 546f, 547f
Splint bones
of metacarpus, 132f
active *vs.* inactive, 130
fractures of, 130, 133-134f
irradiated, radiographic evaluation of, 131
Spondylitis, 453
of spine, 457-458, 458
Spondylosis, 453
Sprain-avulsion fractures
of collateral ligament, 235
of cranial cruciate ligament, 234
Sprain-avulsion fractures (*Continued*)
of elbow, 195-196, 198f
of fetlock joint, 120, 122-123f
of long digital extensor tendon, 235
of patellar ligament, 235
of peroneus tertius tendon, 235
of stifle, 234-235
of tarsus, 262, 263-265f
Sprains
of carpus, 162, 170-171f
of fetlock joint, 120, 122-123f
of metacarpus, 309-311, 309f
of metatarsus, 297, 299
ringbone of pastern joint, 83
spine and, 455
of tarsus, 262, 263-265f
Squamous cell carcinoma
of eye, 391, 393
radiographic appearance of, 490
Staphylococcus aureus, 418, 484
Steroid arthropathy, 112, 284
Stifle
anatomic features of, 227-229
arthrography, 229
fractures of
articular, 242, 243f
patella, 232-233
sprain-avulsion, 234-235
interior anatomy of, 228-229, 232f
lameness of, 232, 232b
lesions of
radiographic detection of, 230-232
magnetic resonance of, 232
regional swelling of, 241
sonography of, 230-231
standard series of, 227, 228-231f
Stomach
abdominal topography of, 527
cascade, 531
STP. *See* Single-target protocol
Straight sesamodian ligament
desmitis of, 94-95
Strains
of acute flexor tendon, 314-317f
of carpus, 162
of metacarpus, 309-311, 309f
of metatarsus, 309-311, 309f
of tarsus, 262
of thigh, 214
Strangles, 416
Street nail, 69-70, 71-72f, 74
Streptococcus equi, 402, 407, 512
Streptococcus zooepidemicus, 487
Stress fracture
humeral
of shoulder, 208
Stress fractures
bilateral, 251
of fibula, 245, 247, 250, 250f
of radius, 181
Stricture
cervical esophagus, 429
of cervical esophagus, 429
Strongyloides, 241
Strongylus vulgaris, 524
Supraglenoid tubercle fractures, 202, 204f
Supraglenoid tuberosity, 200
Supraspinatous bursitis
of spine, 458
Suspensory ligaments
anatomy of, 305, 308, 308f, 309f
chronic desmitis and, 321
nuclear imaging of, 321
radiography of, 320, 321b
stress, 320-321, 321t
Synovial chondromatosis, 191
Synovial invagination, 67
Synovial osteochondromatosis, 162, 240
Synovioma
of carpus, 174
of fetlock joint, 120, 123, 125f

T

Talar fractures
of tarsus, 265-266
Tarsus
anatomic facts about, 257
anatomy of, 257, 260f, 261f
angiography of, 294-295
bone spavin, 280-284
atypical, 282, 282f, 283f
fusion of, 282, 284, 284f, 285f
posttraumatic osteoarthritis and, 284, 286f
radiographic progression of, 282-284, 284f, 285f
typical, 282, 283f
where and what principle of, 281, 281f, 282f
bone spur of, 266
bone tumors of, 290, 293, 294f
calcaneus
infection of, 275-276, 276f, 277f
infection of, surgical, 277-278
sequestra, 276-277, 278f
surgical infection of, 277-278
computed tomography of, 261
congenital sustentacular hypoplasia, 293
contracture of, 20
development of, 257-261
dislocation of, 266, 267f
drilling of, 284-286, 286f, 287f
false thoroughpin, 267
fractures of, 264-266
calcaneal, 265, 266f
palmar process, 266
talar, 265-266
infection of, 267-274
inoculation-type joint, 267-268, 271f
septic arthritis, 269, 271-274f, 274
septicemia joint, 267-268, 269f, 270f
sustentaculum tali, 274-275, 276f
injury, soft-tissue, 261-264
bruising, 261-262, 262f
capsular tearing of, 263-264
crushing, 261-262, 262f
hock stress radiography, 262-263
lacerations, deep, 262
nuclear scintigraphy of, 263

Tarsus (*Continued*)
puncture wounds, 262
ruptured peroneus tertius, 262
sprain, 262, 263-265f
sprain-avulsion fracture, 262, 263-265f
strain, 262
magnetic resonance imaging of, 261
osteoarthritis of, 266-267, 268f
osteochondritis of, 286-290
distal talar tuberosity, 290, 291f
distal tibial epiphysis, 286
sagittal ridge, 286, 288, 288f
third bone of, 290, 292f, 293f
tibial malleolus, 288, 289f
trochlear ridges, 288, 289-291f
osteomyelitis of, 267-274
inoculation-type joint, 267-268, 271f
septic arthritis, 269, 271-274f, 274
septicemia joint, 267-268, 269f, 270f
probed-based marking studies of, 279-280, 280f
radon seeds and, 293, 294f
sequestration of, 280, 280f, 281f
sheath swelling, 267
sinography of, 78f, 278-279, 279f
soft-tissue tumors of, 290, 293, 294f
sonography of, 293-294
standard series of, 254, 255f, 256f
flexed lateral, 254, 259f
immature, 254, 256f, 257f
sentinel bones, 254, 258f
skyline calcaneus, 254, 259f
sustentaculum tali
infection of, 274-275, 276f
tumors of, 290, 293, 294f
ultrasound of, 261, 261b
Teeth
abscess of, 370
anatomic facts of, 354b
anatomy of, 353
radiographic, 355, 357f, 358f
angulation of, excessive, 366-367
caps, 367, 367f, 368f
developmental facts of, 354b
ectopia of, 363, 366, 366f
eruption dates of
canine, 353
cheek, 353, 354t
incisors, 353
mechanism, 353
roots, 353, 354t
fluorosis, 370
formula, 353
fractures of, 363, 366f
malocclusion of, 363, 367-368, 368f, 369f
malpositioning of, 363
patient-tailored examination of, 355
projections, 354-355
radiographic anatomy of, 355, 357f, 358f
root apex radiolucent area, 353
spacing of, abnormal, 367
standard series of, 354, 355f, 356f
Teeth (*Continued*)
supernumerary cheek, 355-356, 355b
tumors of, 368-370
adamantinoma, 369, 369f
ameloblastic odontoma, 369-370
ameloblastoma, 368-369
cementoma, 369
odontoma, 369
osteoma, 369
Temporal fractures
of skull, 397-398
Temporal teratoma, 363, 366, 366f
Temporohyoid osteoarthropathy, 398-400, 400f, 401f
Temporomandibular joint (TMJ), 345-347, 347f
angle-dependent variation, 346-347, 349f
customized views of, 347, 350f
dislocation of, 347-348, 350f, 351f
fractures of, 347
radiographic sensitivity of, 345-346, 348f
Temporomandibular osteoarthropathy, 402
Tendography, 316-318
acute flexor tendon injury and, 316-317, 317b
techniques of, 317-318
types of, 317
Tendonitis, 312-313
carpus, 172
causes of, 312-313
diffuse, 313
imaging of, 313
localized, 313
susceptibility of, 312-313
terminology of, 312
Tendons
anatomy of, 309, 309t
classification of
lesion echogenicity and, 312
lesion location and, 312
lesion pattern and, 312
lesion severity and, 312
injuries
classification of, 311-312
description of, 311-312
experimental, 311
histology and, 311
magnetic resonance imaging of, 311
nonlacerative, 309, 310t
sonography of, 311, 321-324323f, 324t
lacerations of, 324-326
dorsally situated, 325, 325f
flexor, 325
healing of, 324
infections and, 325, 326
nuclear imaging of, 318-319
sonography of, 312f, 319-320, 319b, 320f, 322f
thermography of, 318-319
tumors of
sheath, 326
Thermography
for caudal heel pain syndrome, 30
for corns, 30
of distal limb, 30-31
foot, 31
joints, 30-31
ligaments, 31
long bones, 31
muscles, 31
tendons, 31
in laminitis, 30
for navicular disease, 30
for palmar heel pain syndrome, 30
for solar abscess, 30
Thigh
strain of, 214
Third trochanter, 218-219, 223f
abnormal uptake patterns of, 213-214
nuclear imaging of, 213-214
uptake ratio of, 213
Thoracic spine
injuries of, 455, 457
Thoracolumbar spine
radiographic anatomy of, 455, 456f
Thorax
imaging of, 461
lung disease and
in adults, 462, 466f, 467f
bronchial cross-sections and, 462, 467f
bronchial thickening, 462-463, 467f
in foals, 462
radiographic indicators of, 468
nuclear imaging and, 468
pulmonary pattern recognition, 463, 466
standard series of, 461-462, 462-465f
adults, 462, 463-465f
foals, 461-462, 462f
ultrasound and, 466, 468
Thoroughpin, 267
Three-dimensional reconstruction, 31
Throat
branchial cysts of, 415, 416b
examination of, 405, 406f
guttural pouches, 406-411
abscessation, 407
cellulitis, 407
cysts of, 408
deformity of, 409, 410f
ear infection, middle, 410-411
empyema, 407, 407f
fistulation, 407-408
gaseous distention of, 409-410, 410f, 411f
hemorrhage, 408-409
manta ray sign, 407, 407f
masses of, 408
mycosis, 408-409
perforation, 408-409, 409f
pharyngeal compression, 407
radiographic anatomy of, 406-407, 406f
radiographic examination of, 406

Throat (*Continued*)
retropharyngeal adenopathy and, 409, 410f
tumors of, 408
tympany, 409-410, 410f, 411f
hyoid bone fracture, 415-416
postanesthesia dyspnea, 420
retropharyngeal lymph node abscessation, 416
salivary glands
cavography of, 405
congenital defects, 405
tumors of, 405-406
Thrombi
jugular vein
classification of, 422
Thrombophlebitis
of jugular vein, 422
Thrombosis
of jugular vein, 422
Thyroglossal duct cysts, 413
Thyrohyoid
infection of, 399-400, 400f, 401f
Tibia
fracture of, 245, 248f, 249f
misdiagnosis and, 245, 247f, 248f
standard series of, 245, 246f
Tibial tuberosity
fragmentation of, 240
TMJ. *See* Temporomandibular joint
Topography, abdominal, 527-528
of bowel mass, 527-528
of cecum, 528
of large intestine, 528
of rectum, 528
of small intestine, 528
of stomach, 527
Torticollis
of cervical spine, 437, 439
Toxemia, 484-485
Toxic shock syndrome, 484-485
Trachea, 424f
aspiration of, 424-425
collapse of, 425
injury to, 424, 424f, 425f
tracheostomy and, 425, 425f
Tracheostomy, 425, 425f
Transpastern arthrodesis, 89
Transport fracture, 23
Transtarsal drilling, 284-286, 286f, 287f
Trauma
to brain, 402
ventricular tachycardia and, 512
Traumatic exostosis, 135, 138-139f
Tricuspid artresia, 507-508
Tricuspid valve
closure of, 507-508
congenital absence of, 507-508
Trimming
for laminitis, 39, 41
Trochlear ridge
osteochondritis of, 236, 237f, 238f
Trough
lesions of, 237, 239f
Truncus arteriosus, 509
Tubulation, 1, 5f, 6f
Tumoral calcinosis, 240
Tumors
of abdomen, 525
of bladder, 549-550
of bone
multiple hereditary exostoses, 21
polydactylism, 21
of cervical esophagus, 430, 431b
of cervical spine, 452
of coronary region, 53, 58
fibroma, 58
keratoma, 53, 58
melanoma, 58
of eye, 391-393
primary, 391
secondary, 391, 393
squamous cell carcinoma, 391, 393
fibroma
of pastern joint, 94
of gastrointestinal tract, 532
of guttural pouches, 408
hepatic, 545
keratoma
of pastern joint, 94
of lungs
fibrosarcoma, 490-491
hemangiosarcoma, 490
mediastinal, 491
pleural, 491
primary, 490
radiographic appearance of, 490-491
secondary, 490
of mandible, 343-344
adamantinoma, 344, 346f
bone cysts, 344-345
interosseous epidermoid cyst, 345
leiomyosarcoma, 344
ossifying fibroma, 344, 347f
osteosarcoma, 343-344, 345f, 346f
of maxillary, 333, 337f, 338
of mediastinum
abscess, 491
loculated fluid, 491
lymphosarcoma, 491
melanoma
of pastern joint, 94
of metatarsus, 302-303, 303f
of pastern joint, 94
of pleura, 491
of radius/ulna, 191f
chondroma, 188, 191
chondrosarcoma, 191
osteosarcoma, 191
of salivary glands, 405-406, 549-550
of scapula, 204
of sinus, 378-380, 380f
of spine, 459
splenic, 546-547, 546f, 547f
of tarsus, 290, 293, 294f
of teeth, 368-370
adamantinoma, 369, 369f
ameloblastic odontoma, 369-370
ameloblastoma, 368-369
cementoma, 369
odontoma, 369
osteoma, 369
of tendon sheath, 326
Tumors (*Continued*)
fibroma, 326
lipoma, 326
of ulna, 188, 191, 191f
Tympany
of guttural pouches, 409-410, 410f, 411f

U

Ulcerative colitis, 540
Ulna. *See also* Radius
fractures of, 184, 186, 187-190f
plating and, 186
osteochondritis of, 192, 192f
radiographic variation of, 180, 183f
standard series of, 180
tumors of, 191f
chondroma, 188, 191
chondrosarcoma, 191
osteosarcoma, 191
Ultrasound
of eye, 387
of foot, 28
of gastrointestinal tract, 540-541
duodenum, 540
enteroliths, 540, 541f
fecaliths, 540
foreign material impaction, 540
nephrosplenic entrapment and, 541
of mandible
infections, 358
of maxilla
infections, 358, 362
of tarsus, 261, 261b
of thorax, 466, 468
Umbilical evagination
sonography and, 549, 549b
Umbilical hernia, 525, 525f
Umbilicus
sonography of, 550-551, 550f, 550t
infection, 551, 551f, 552f
Unilateral epistaxis
cause of
sinonasal disease and, 374-375
Uremic encephalopathy, 402-403
Ureteral stenosis
sonography and, 549
Urinary tract
sonography of, 548-550
biopsy, 548
bladder rupture, 549
calculi, 548
carcinoma, 549
dysplasia, 548
ectopic ureter, 548
hydronephrosis, 549
kidney stones, 548
nephritis, 549
nephrolithiasis, 548
tumors, 549-550
umbilical evagination, 549, 549b
ureteral stenosis, 549

V

Valves, 516-519
inflow insufficiency, 516-518, 517f, 518f

Valves (*Continued*)
outflow insufficiency, 518-519, 519-522f
regurgitation of, 516-519
inflow insufficiency, 516-518, 517f, 518f
outflow insufficiency, 518-519, 519-522f
Vascular channel redux
navicular disease, 67-68
Vascular channels, 32, 33, 33f
traumatic dilatation of, 109
Vascular disease
pelvis and, 215
Vascular ring anomaly, 428
Vegetative endocarditis, 512-513, 513f
Venography
of jugular vein, 422, 423f
Ventral element fractures
of cervical spine, 434
Ventricular septal defect (VSD), 506, 507f
Ventricular tachycardia, 512
Vertebral instability
of cervical spine
causes of, 442t
Vertebral instability (*Continued*)
myelographic assessment of, 443-447
plain-film assessment of, 442-443, 442b, 444-445f
radiography of, 442, 442f, 443f
myelography and
cord angulation, 446-447, 449f
cord lift, 446, 448f
diagnosis of, 445-447
diskal indentation, 445-446, 448f
dural pinching, 445
flow failure, 448, 451f
image quality, 443-444
lesion probability, 444
metrizamide, 443
misdiagnosis of, 448, 449b
nonstress, 444-445, 446f, 447f
risk of, 444, 446f
standing, 450
Videoendoscopy
tracheal collapse and, 425
Villonodular synovitis, 120, 123, 125f
Viral arteritis, 486
Viral pneumonia, 486
VSD. *See* Ventricular septal defect

W

Wind puffs, 128
Wobbler. *See* Cervical spine, vertebral instability of
Wounds
chest wall, 475
gunshot
sinonasal disease, 381-382, 382f
of metacarpus
drainage of, 139-140, 140f
gas pockets, 138-139, 139f
periosteal new bone, 139
swelling, 138
tissue defects, 138
puncture
carpus, 172
soft-tissue, of tarsus, 262
Wyoming strangles, 199

X

Xerography
of foot, 28

Y

Yellow-star thistle poisoning, 403